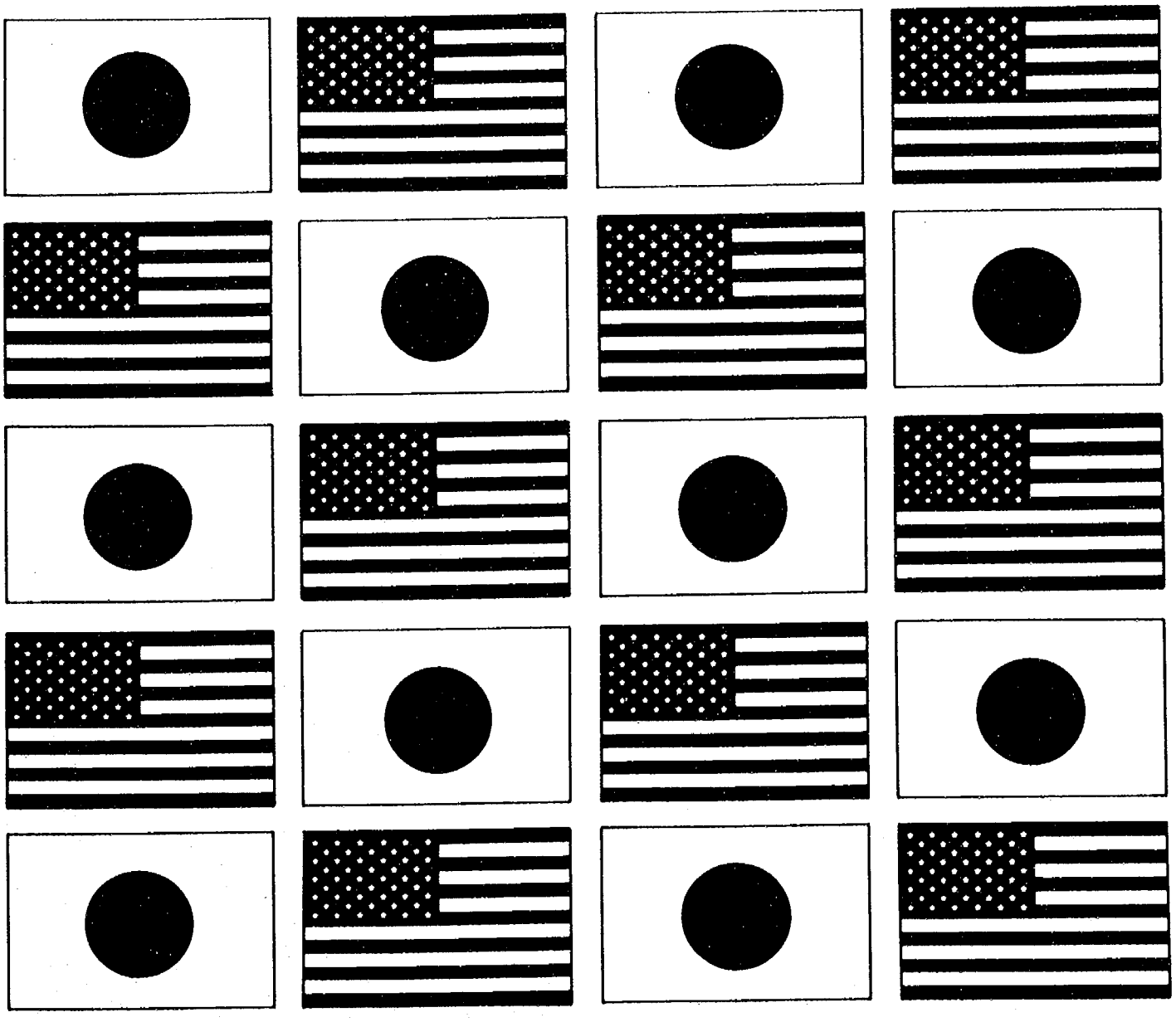
ISSN 0386-5878
Technical Memorandom
of PWRI No.3217

Wind and Seismic Effects

Proceedings of the 25 th Joint Meeting

UJNR



May, 1993

Copyright © (1993) by P.W.R.I.

All rights reserved. No part of this book may be reproduced by any means, nor transmitted, nor translated into a machine language without the written permission of the Director General of P.W.R.I.

この報告書は、土木研究所長の承認を得て刊行したものである。したがって、本報告書の全部又は一部の転載、複製は、土木研究所長の文書による承認を得ずしてこれを行ってはならない。

Wind and Seismic Effects

PROCEEDINGS OF
THE 25TH JOINT
MEETING OF
THE U.S.-JAPAN
COOPERATIVE PROGRAM
IN NATURAL RESOURCES
PANEL ON WIND AND
SEISMIC EFFECTS

CONTENTS

PREFACE ——— 9
AGENDA OF JOINT TECHNICAL MEETING AND SITE VISITS ——— 1
LIST OF PANEL MEMBERS ——— 13
LIST OF TASK COMMITTEE MEMBERS ——— 27
RESOLUTIONS ——— 33
PAPERS ——— 39

_____ denotes presenter

THEME 1. Wind Engineering

Features of Surface Winds Associated with Typhoon 9119 (Mirelle), ——— 43
Fumiaki Fujibe and Tokunosuke Fujitani

Damage of Buildings Caused by Typhoon 9119, ——— 51
Hisashi Okada

Offshore Platform Damage Assessment in the Aftermath of Hurricane Andrew ——— 65
Charles E. Smith

Wind-Induced Vibrations of Super Long-Span Suspension Bridge in Turbulent Wind, ——— 81
Hiroshi Sato, Ryuichi Toriumi and Masahiko Yasuda

Improved Analytical Procedure for Predicting Flutter Response of Long Span Bridges, ——— 95
Chunsheng Cai and Harold R. Bosch
(Presented by James D. Cooper)

THEME 2. Kushiro-oki Earthquake, Cairo Earthquake, Flores Island Earthquake and Landers Earthquake

Outline of Strong-Motion Records on the Off Kushiro Earthquake in 1993, ——— 109
Osamu Nakano, Toshio Yamauchi, Manabu Kaneko and Yuuji Ono

Damage to Infrastructures Caused by the 1993 Kushiro-oki Earthquake, ——— 121
Takashi Iijima, Yutaka Iida, Yasuyuki Koga, Kazuhiko Kawashima and Kenichi Tokida

Damage to Buildings and Housing Lots Caused by the Kushiro-oki Earthquake, 1993, ——— 149
Tatsuo Murota, Yoshikazu Kitagawa and Mikio Futaki

Damage of Buildings due to The Flores Island Indonesia Earthquake of December 12, 1992, ——— 169
Shinsuke Nakata

Characteristics of Earthquake-Induced Landslide Sites : Case of the Flores Island Earthquake of 1992, ——— 183
Takekazu Akagiri and Yohta Kumaki

Field Observation on Damages due to Flores Island Earthquake Tsunami of December 12, 1992, ——— 199
Takaaki Uda

Infrastructures Damege by Cairo, Egypt, Earthquake of October 1992 and Flores Island, Indonesia, Earthquake of December 1992, ——— 205
Tomomitsu Fujii and Kazuhiko Kawashima

Recorded Ground Motions from the MS=7.5 Landers, California, Earthquake of June 28, 1992, ——— 227
A. Gerald Brady

THEME 3. Earthquake Engineering

CORPS of Engineers Research Program on Concrete Dams, ——— 237
Robert L. Hall and William E. Roper

Stiffness of Rockfill Materials in Laboratory and In-situ Test, ——— 253
Akira Nakamura and Nario Yasuda

Strengthening Methodology for Lightly Reinforced Concrete Frames, ——— 265
L. T. Phan, D. R. Todd, H. S. Lew

Guideline for Evaluating Design Earthquake Ground Motion for Dynamic Analysis of Buildings, ——— 273
Yoshikazu Kitagawa, Izuru Ohkawa, Toshihide Kajima and Shin Koyama

The Coordinated U.S.A. Research Program on Structural Control for Safety, Performance, and Hazard Mitigation, ——— 285
Robert D. Hanson and T. T. Soong

Integrated Approach to Structural Control for Seismic Hazard Mitigation, ——— 327
Masanobu Shinozuka, R. Ghanem and M. Constantinou

Shaking Table Test of Building Model with Seismic Response Control by Fuzzy Optimal Logic, ——— 343
Yoshikazu Kitagawa, Mitsumasa Midorikawa, Masanori Iiba,

Hideo Fujitani and Toshihide Kajima

Structural Impedance Modification and Energy Consideration for Structural Control, ——— 355
Craig A. Rogers

Studies at PWRI on Mitigation Works against Liquefaction of Sandy Ground, ——— 381
Yasuyuki Koga, Osamu Matsuo and Junichi Koseki

Liquefaction Susceptibility of Fine-Grained Soils, ——— 389
J. P. Koester and A. G. Franklin

Application of Soil Liquefaction Potential to Seismic Design of Civil Engineering Structures in Japan, ——— 405
Kenichi Tokida and Yoshio Ninomiya

Deformation Analysis of Quay Walls due to Liquefaction, ——— 417
Susumu Iai and Tomohiro Kameoka

Progress of Civil Engineering, Including Wind and Seismic Engineering, and Its Contribution to Economic and Social Development in Modern Japan, ——— 431
Yukihiko Sumiyoshi

Performance Based Seismic Design and Evaluation Criteria, — 463
James R. Hill, Robert P. Kennedy, Stephen A. Short, Thomas A. Nelson and Robert C. Murray

Guidelines for Disaster Information Systems for Important Infra-Structures, ——— 475
Kazuhiko Kawashima, Kenichi Tokida, Hideki Sugita, Hideo Matsumoto and Tomoru Nakajima

Civil Infrastructure Systems Research : Intelligent Materials and Natural Hazard Mitigation, ——— 487
Shih-Chi Liu and Ken P. Chong (Presented by Robert D. Hanson)

Evaluation of Ground Displacement and Its Effect on Lifeline Performance, ——— 491
Steven Glaser (Presented by H. S. Lew)

New Developments in Analyzing Ground Motion and Structural Recordings : Site Amplification and Soil-Structure Interaction, ——— 503
Erdal Safak (Presented by A. Gerald Brady)

Present Situation and Possibility of Constructing Bridge Foundations in Deep Water in Japan, ——— 523
Michio Okahara, Jiro Fukui and Tomohiro Fujimura

THEME 4. Storm Surge and Tsunamis

Numerical Simulation by Multi-level Model for Storm Surge Generated by Ise-wan Typhoon, ——— 541
Chiaki Goto, Hidenori Shibaki and Tomotsuka Takayama

Storm Surge Assessment for Hurricanes Andrew and Iniki, ——— 547
William E. Roper and Andrew W. Garcia

THEME 5. U.S.-Japan Cooperative Research Program

General Concept of Japan Connection Design Manual for Precast Seismic Structural Systems, ——— 569
Fumio Watanabe, Hitoshi Shiohara and Shinsuke Nakata

PRESSS - A Coordinated U.S./Japan Research Program on the Design of Precast Seismic Structural Systems, ——— 579
Nigel Priestly, UCSD and H. S. Lew

U.S.-Japan Cooperative Earthquake Research Program on Composite and Hybrid Structures, ——— 585
Hiroyuki Yamanouchi, Stephen A. Mahin, Subhash C. Goel and Isao Nishiyama

Seismic Response Control of Highway Bridges by Variable Damper, ——— 593
Kazuhiko Kawashima and Shigeki Unjo

MANUSCRIPTS AUTHORED FOR THE PANEL MEETING BUT NOT PRESENTED ORALLY

Wind Resistant Design of Light-Frame Buildings ——— 615
Ronald W. Wolfe

Loss Experience from Wind and Earthquakes in the Department of Energy ——— 635
James R. Hill

Reconstruction of Erzincan(Turkey) Following the 13 March, 1992 Earthquake ——— 645
Mehmet Celebi

DOE NPH Mitigation Policy and Standards Program ——— 655
James R. Hill, Robert C. Murray

Effect of Dynamic Loads on Lateral Strength of Nail Connections for the Manufactured/Modular Housing Industry 665
Steve G. Winistorfer, Lawrence A. Soltis

The Offshore Nicaraguan Earthquake and Tsunami of September 2, 1992 ——— 693
Mehmet Celebi, David Harlow

U.S. Coordinated Program for Masonry Building Research: Eighth Year Status ——— 701
James L. Noland

Mount Pinatubo Eruption : A Review ——— 711
C. S. Barrientos

Concept Behind Ultimate Strength Design Guidelines for Reinforced Concrete Buildings in Japan ——— 715
S. Otani, M. Teshigawara, S. Nakata, T. Murota

IDNDR SYMPOSIUM
- Symposium for Celebrating the 25th Anniversary of the Panel -

Earthquake Engineering - Stepping into the Next Century — 727
Keizaburo Kubo

ASCE's Contributions toward Technology for Disaster Mitigation ——— 741
Edward O. Pfrang

Cooperation on Research and Technological Development in Wind and Earthquake Engineering between U.S.A. and Japan in the last 25 Years ——— 749
- Activities on the Panel on Wind and Seismic Effects, UJNR -
Yukihiko Sumiyoshi

Lessons from the Loma Prieta Earthquake ——— 769
Richard N. Wright

Damages and Lessons Learned from Hurricane Hugo and Andrew
G. Robert Fuller ——— 787

APPENDIX
TASK COMMITTEES REPORTS ——— 811
TECHNICAL SITE VISITS
Noel J. Raufaste

PREFACE

This publication is the proceedings of the 25th Joint Meeting of the U.S.-Japan Panel on Wind and Seismic Effects. The meeting was held at the Public Works Research Institute, Tsukuba, Japan, during May 17-20, 1993. The 25th Anniversary Panel Symposium was held in Tokyo on May 21, 1993. The proceedings include the program, list of members, panel resolutions, task committee reports and technical papers presented at the Joint Panel Meeting and at the 25th Anniversary Panel Symposium, 9 technical papers that are not orally presented at the Joint Panel Meeting, and summary of the technical site visits.

BACKGROUND

The U.S.-Japan Cooperative Program in Natural Resources(UJNR) was created in January 1964. It is part of the U.S.-Japan Cooperative Science Program. The objective of UJNR is to exchange information on research results and exchange scientists and engineers in the area of natural resources for the benefit of both countries. The UJNR is composed of 16 Panels each responsible for specific technical subjects.

The Panel in Wind and Seismic Effects was established in 1969. Seventeen U.S. and seven Japanese agencies participated with representatives of private sector organizations, to develop and exchange technologies aimed at reducing damage from high wind, earthquakes, storm surge, and tsunamis. This work is produced through collaboration between U.S. and Japanese member researchers working in 10 task committees. Each committee focuses on specific technical issues, e.g., strong motion data and application. The Panel provides the vehicle to exchange technical data and information in design and construction of civil engineering lifelines, buildings and water front structures, and to exchange high wind and seismic measurement records. Annual meetings alternate between Japan and United States(odd numbered years in Japan; even numbered years in U.S.). These 1-week technical meeting provide the forum to discuss ongoing research and research results; 1-week technical study tours follow the meeting.

The National Institute of Standards and Technology (NIST) provides the U.S.-side chairman and secretariat. The Public Works Research Institute (PWRI), Japan, provides the Japan-side chairman and secretariat.

Direct communication between counterpart country organizations is the cornerstone of the Panel. Effective information exchanges and exchanges of personnel and equipment have strengthened domestic programs of both countries. There are opportunities for experts in various technical fields to get to know their foreign counterparts, conduct informal exchanges, bring their respective views to the frontiers of knowledge, and advance knowledge of their specialities.

The Panel's results have supported improvement in practices in both countries. They have:

1. Created and exchanged digitized earthquake records used as the basis of design and research.
2. Produced data that advanced retrofit techniques for bridge structures.
3. Developed field test data for use in aerodynamic retrofit of bridge structures.
4. Produced full-scale test data that advanced seismic design standards for buildings.
5. Advanced technology for repairing and strengthening reinforced concrete, steel, and masonry structures.
6. Improved in-situ measurement methods for soil liquefaction and stability under seismic loads.
7. Created a database comparing Japanese and US standard penetration test to improve prediction of soil liquefaction.
8. Created a database on storm surge and tsunamis and verified mathematical models of tsunami and storm surge warning systems.
9. For use by seismically active countries, e.g., Australia, Canada, Italy, Mexico, Peru, Taiwan, Turkey, and North Africa, the Panel has transferred its findings on earthquake engineering information and strong-motion measurement techniques.

HIGHLIGHTS OF THE 25th JOINT PANEL MEETING

The 38 papers presented at the Joint Meeting were organized into five themes: Wind Engineering; Earthquake Engineering; Storm Surge and Tsunami; U.S.-Japan Cooperative Research Program; Reconnaissance Reports on the Kushiro-oki, Cairo, Flores Island, and Landers Earthquakes.

Highlights include:

- Technical presentations:
  - highlighted important work by the U.S. and Japan Panel.
  - important knowledge was exchanged for research and practice, e.g., analytical and experimental research results on wind engineering; Ministry of Construction's real time disaster information system; integrated, practical approach to active and passive control of structural response; recommendations for seismic design of waterfront structures; procedures for development of seismic time histories for inelastic design; model for seismic soil-structure interaction; procedure for investigation of liquefaction susceptible sites; rational and empirical methods for estimating liquifaction displacement; improved two-layer model for storm surge; and guide for design and construction on houses to resist extreme winds.

- information was exchanged about extensive U.S. and Japanese public works projects and civil engineering research and their applications into practice.

- Excellent projects are being performed by both sides in intelligent and active materials and systems technologies. Panel participants advance their competence by becoming more familiar with these research projects and through direct participation in appropriate research.

- Reports on reconnaissance of recent earthquakes shows again the need to address the vulnerability of non-ductile concrete and masonry buildings.

- Task Committee activities grow in strength. The T/C structure is an extremely effective vehicle to explore in depth the technologies and methods being used by both countries.

  - Six Task Committee workshops/conferences were held in the past year and seven workshops are planned for the coming year.
  - Four Task Committees were consolidated into two new Task Committees:
    - New Task Committee A on Strong Motion Data and Applications, created by merging former Task Committees A and E.
    - New Task Committee C on Design, Evaluation and Improvement of Structures, created by merging Task Committees C and D.
  - Created a new Task Committee D on Dam Earthquake Engineering.
  - Revised mission objectives of two Task Committees:
    - Task Committee B focuses on Testing and Evaluation Procedures for Building Systems.
    - Task Committee G focuses on Structural Control and Intelligent Material Systems.

- Cooperative Research Programs continue to be productive. Since the 24th Joint Panel Meeting cooperative research has led to Japan-side publications of:
  - Precast Connection Design Manual, and
  - Design Guidelines for New Precast Concrete Systems.

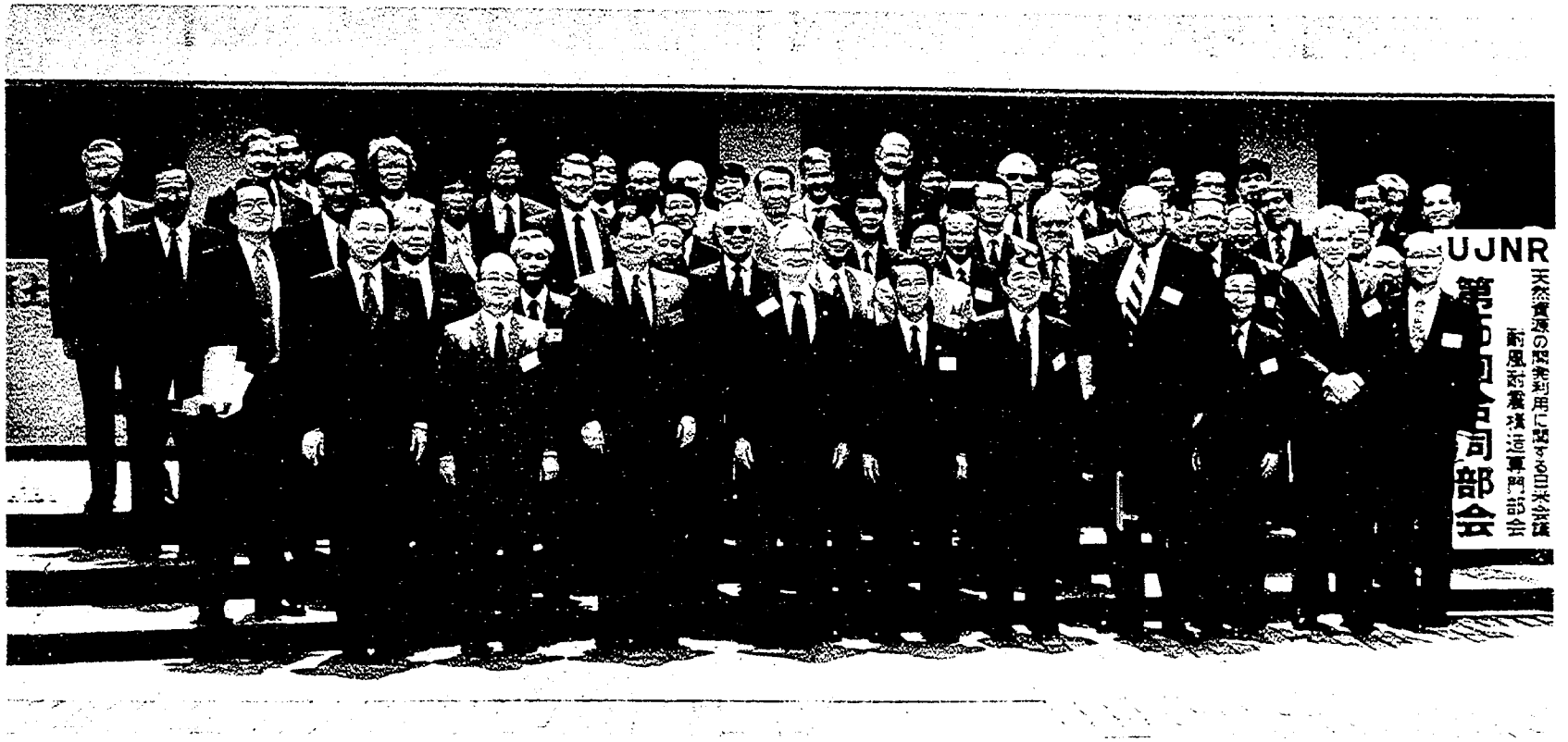
  A new Cooperative Research Program was approved on Seismic Performance of Composite and Hybrid Structures.

25th ANNIVERSARY PANEL SYMPOSIUM

To commemorate its 25th Joint Meeting, the Panel held a symposium in Tokyo on Friday 21 May 1993, "Toward Development of Future Technology for Disaster Mitigation" as a contribution to the International Decade for Natural Disaster Reduction. Over 200 engineers attended. Papers dealt with accomplishments of the Panel and the state of research and practice

in wind and seismic effects. Four of the five technical talks were presented by Panel Members. A Poster Session highlighted the work of the Joint Panel's activities, featured its members agencies, and chronicled the history of Japan's severe earthquakes. The five papers presented are included in the Section, IDNDR SYMPOSIUM of this proceedings.

Takashi Iijima, Secretary-General
Japan-Side Panel on Wind and Seismic Effects



U.S. Side and Japan Side Attendance
25th Joint Meeting of the U.S.-Japan Panel on Wind and Seismic Effects

Agenda of Joint Meeting and Site Visits

AGENDA OF JOINT TECHNICAL MEETING AND SITE VISITS

TECHNICAL MEETING

May 17 (Mon)

10:30 OPENING CEREMONIES
(8TH Floor Conference Room, Main Building)

Call to order by Takashi Iijima, Secretary-General, Japan Side

Opening remarks by Toru Kondo, Vice-Minister of Construction for Engineering Affairs

Remarks by Edward M. Malloy, Minister-Counselor for Environmental, Scientific and Technological Affairs, Embassy of the United States of America

Remarks by Shinichiro Ogawa, Director, International Affairs Division, Science and Technology Promotion Bureau, Science and Technology Agency

Remarks by Yukihiko Sumiyoshi, Chairman JAPAN-Side, Panel on Wind and Seismic Effects, Director-General, Public Works Research Institute, Ministry of Construction

Remarks by Richard N. Wright, Chairman U.S.-Side, Panel on Wind and Seismic Effects, Director, Building and Fire Research Laboratory, National Institute of Standards and Technology, Department of Commerce

Introduction of JAPAN Members by Japan Panel Chairman

Introduction of U.S. Members by U.S. Panel Chairman

Elect Joint Meeting Chairman

Adopt Agenda

Adjourn

11:45 Group Photograph

12:00 Lunch (Hosted by Port and Harbour Research Institute, Ministry of Transport and Meteorological Research Institute, Japan Meteorological Agency)
[1F Conference Room]

13:00 Session 1 (Theme I Wind Engineering) Chairman - R. N. Wright

13:00 Features of Surface Winds Associated with Typhoon 9119 (Mirelle),
Fumiaki Fujibe and Tokunosuke Fujitani, MRI

13:20 Damage of Buildings Caused by Typhoon 9119,
Hisashi Okada, BRI

13:40 Offshore Platform Damage Assessment in the Aftermath of Hurricane Andrew
Charles E. Smith, MMS

14:00 Discussion

14:20 Break

14:35 Session 2 (Theme I Wind Engineering) Chairman - R. N. Wright

14:35 Wind-Induced Vibrations of Super Long-Span Suspension Bridge in Turbulent Wind,
Hiroshi Sato, Ryuichi Toriumi and Masahiko Yasuda, PWRI

14:55 Improved Analytical Procedure for Predicting Flutter Response of Long Span Bridges,
Chunsheng Cai and Harold R. Bosch, FHWA (Presented by James D. Cooper)

15:15 Discussion

15:30 Break

15:45 Task Committee Meetings

A: Strong-Motion Instrumentation Arrays and Data, and
E: Ground Motion and Seismic Design Forces
[5F Room 524]

B : Large-Scale Testing Programs,
C : Repair and Retrofit of Existing Structures, and
D : Evaluation of Performance of Structures
[5F Room 526]

F : Disaster Prevention Methods for Lifeline Systems
[5F Room 531]

I : Storm Surge and Tsunamis [6F Room 627]

17:15 Adjourn

18:00 Reception Hosted by Vice-Minister of Construction for Engineering Affairs (Hotel Tsukuba Sun-Route, Hou-Ou Hall, Tel. 0298-52-1151)

_____ denotes presenter

MAY 18 (TUE)

9 : 0 0 Session 3 (Theme II Kushiro-oki Earthquake)
Chairman - Yukihiko Sumiyoshi

9 : 0 0 Outline of Strong-Motion Records on the Off Kushiro Earthquake in 1993,
Osamu Nakano, Toshio Yamauchi, Manabu Kaneko and Yuuji Ono, CERI

9 : 1 5 Damage of Infrastructures Caused by the 1993 Kushiro-oki Earthquake,
Takashi Iijima, Yutaka Iida, Yasuyuki Koga, Kazuhiko Kawashima and Kenichi Tokida, PWRI

9 : 3 0 Damage to Buildings and Housing Lots Caused by the 1993 Kushiro-oki Earthquake,
Tatsuo Murota, Yoshikazu Kitagawa and Mikio Futaki, BRI

9 : 4 5 Discussion

1 0 : 0 5 Break

1 0 : 2 0 Session 4 (Theme II Cairo Earthquake, Flores Island Earthquake and Landers Earthquake)
Chairman - Yukihiko Sumiyoshi

1 0 : 2 0 Damage of Buildings due to The Flores Island Indonesia Earthquake of December 12, 1992,
Shinsuke Nakata, BRI

1 0 : 3 5 Quake-Triggered Landslide Caused by the Flores Island Earthquake of 1992,
Takekazu Akagiri and Yohta Kumaki, GSI

1 0 : 5 0 Guidelines for Disaster Information Systems for Important Infra-Structures,
Kazuhiko Kawashima, Kenichi Tokida, Hideki Sugita, Hideo Matsumoto and Tomoru Nakajima, PWRI

1 1 : 1 0 Recorded Ground Motions from the M=7.5 Landers, California, Earthquake of June 28, 1992,
A. Gerald Brady, USGS

1 1 : 2 5 Discussion

1 2 : 0 0 Lunch (Hosted by National Research Institute For Earth Science and Disaster Prevention, Science and Technology Agency) [1F Conference Room]

1 3 : 0 0 Session 5 (Theme III Earthquake Engineering)
Chairman - Yukihiko Sumiyoshi

1 3 : 0 0 CORPS of Engineers Research Program on Concrete Dams,
Robert L. Hall and William E. Roper, CORPS

1 3 : 2 0 Stiffness of Rockfill Materials in Laboratory and In-situ Test,
Akira Nakamura and Nario Yasuda, PWRI

13:40 Discussion

14:00 Break

14:15 Session 6 (Theme III Earthquake Engineering)
Chairman - Yukihiko Sumiyoshi

14:15 Strengthening Methodologies for Light Frame Buildings,
H. S. Lew, NIST

14:35 Guideline on Evaluation of Design Earthquake Ground Motion for Building,
Yoshikazu Kitagawa, Izuru Ohkawa, Toshihide Kajima and Shin Koyama, BRI

14:55 Discussion

15:15 Break

15:30 Task Committee Meetings

G : Passive, Active and Hybrid Control [5F Room 524]
H : Soil Behavior and Stability during Earthquakes [5F Room 526]
J : Wind and Earthquake Engineering for Transportation Systems [5F Room 531]
K : Wind and Earthquake Engineering for Offshore Structures [6F Room 627]
Dam Earthquake Engineering [8F Conference Room]

17:00 Adjourn

18:30 Reception Hosted by Director-General of Public Works Research Institute (Ushiku-Chateau, Tel.0298-73-3151)

MAY 19 (WED)

9 : 0 0 Session 7 (Theme III Earthquake Engineering)
Chairman - R. N. Wright

9 : 0 0 The Coordinated U.S.A. Research Program on Structural Control for Safety, Performance, and Hazard Mitigation, Robert D. Hanson and T. T. Soong, Univ. of Michigan

9 : 2 0 Integrated Approach to Structural Control for Seismic Hazard Mitigation, Masanobu Shinozuka, Princeton Univ., R. Ghanem and M. Constantinou, State Univ. of New York at Buffalo,

9 : 4 0 Shaking Table Tests of Building Model with Seismic Response Control System by Fuzzy Optimal Logic, Yoshikazu Kitagawa, Mitsumasa Midorikawa, Masanori Iiba, Hideo Fujitani and Toshihide Kajima, BRI

1 0 : 0 0 Structural Impedance Modification and Energy Consideration for Structural Control, Craig A. Rogers, Virginia Polytechnical Institute and State Univ.

1 0 : 2 0 Discussion

1 0 : 4 0 Break

1 0 : 5 5 Session 8 (Theme III Earthquake Engineering)
Chairman - R. N. Wright

1 0 : 5 5 Studies at PWRI on Mitigation Works against Liquefaction of Sandy Ground, Yasuyuki Koga, Osamu Matsuo and Junichi Koseki, PWRI

1 1 : 1 5 Liquefaction Susceptibility of Fine-Grained Soils, J. P. Koester and A. G. Franklin, CORPS

1 1 : 3 5 Application of Soil Liquefaction Potential to Seismic Design of Civil Engineering Structures in Japan, Kenichi Tokida and Yoshio Ninomiya

1 1 : 5 5 Deformation Analysis of Quay Walls due to Liquefaction, Susumu Iai and Tomohiro Kameoka, PHRI

1 2 : 1 5 Discussion

1 2 : 3 5 Lunch (Hosted by Geographical Survey Institute, Ministry of Construction) [1F Conference Room]

1 3 : 3 5 Session 9 (Theme III Earthquake Engineering)
Chairman - R. N. Wright

1 3 : 3 5 Progress of Civil Engineering, Including Wind and Earthquake Engineering, and Its Contribution to Economic and Social Development in Modern Japan, Yukihiko Sumiyoshi, PWRI

13:55 Performance Based Seismic Design and Evaluation Criteria, James R. Hill, Robert P. Kennedy, Stephen A. Short, Thomas A. Nelson and Robert C. Murray, DoE

14:15 Damage and Importance of Countermeasure Learned from the 1992 Cairo, Egypt Earthquake and the 1992 Flores, Indonesia Earthquake, Tomomitsu Fujii and Kazuhiko Kawashima, NLA

14:35 Civil Infrastructure Systems Research : Intelligent Materials, and Natural Hazard Mitigation, Shih-Chi Liu and Ken P. Chong, NSF (Presented by Robert D. Hanson)

14:55 Discussion

15:15 Break

15:30 Session 10 (Report of Workshops)

Chairman - R. N. Wright

15:30 F : 5th U.S.-Japan Workshop on Earthquake Disaster Prevention for Lifeline Systems

15:40 G : 2nd U.S.-Japan Workshop on Earthquake Protective Systems for Bridges

15:50 J : 9th Bridge Workshop

16:00 K : U.S.-Japan Workshop on Wind and Earthquake Engineering for Offshore Structures

16:10 C, D and G : Smart and High Performance Material/System Workshop

16:20 Discussion

16:40 Adjourn

18:00 Individually Hosted Dinner

MAY 20 (THU)

9 : 0 0 Session 11 (Theme III Earthquake Engineering)
Chairman - R. N. Wright

9 : 0 0 Evaluation of Ground Displacement and Its Effect on Lifeline Performance,
Steven Glaser, NIST (Presented by H. S. Lew)

9 : 2 0 New Developments in Analyzing Ground Motion and Structural Recordings : Site Amplification and Soil-Structure Interaction,
Erdal Safak, USGS (Presented by A. Gerald Brady)

9 : 4 0 Present Situation and Possibility of Constructing Bridge Foundations in Deep Water in Japan,
Michio Okahara, Jiro Fukui and Tomohiro Fujimura, PWRI

1 0 : 0 0 Discussion

1 0 : 2 0 Break

1 0 : 3 5 Session 12 (Theme IV Storm Surge and Tsunamis)
Chairman - R. N. Wright

1 0 : 3 5 Numerical Simulation by Multi-level Model for Storm Surge Generated by Ise-wan Typhoon,
Chiaki Goto, Hidenori Shibaki and Tomotsuka Takayama, PHRI

1 0 : 5 5 Storm Surge Assessment for Hurricanes Andrew and Iniki,
William E. Roper and Andrew W. Garcia, CORPS

1 1 : 1 5 Field Observation on Damages due to Flores Island Earthquake Tsunami of December 12, 1992,
Takaaki Uda, PWRI

1 1 : 3 0 Discussion

1 1 : 5 0 Lunch (Hosted by Building Research Institute, Ministry of Construction [1F Conference Room]

1 2 : 5 0 Session 13 (Theme V U.S.-Japan Cooperative Research Program)
Chairman - R. N. Wright

1 2 : 5 0 General Concept of Japan Connection Design Manual for Precast Seismic Structural Systems,
Fumio Watanabe, Hitoshi Shiohara and Shinsuke Nakata, BRI

1 3 : 1 0 U.S.-Japan Cooperative Research in Precast Seismic Structural Systems (PRESSS) Program - Status Report,
Nigel Priestly, UCSD and H. S. Lew, NIST

1 3 : 3 0 U.S.-Japan Cooperative Earthquake Research Program on Composite and Hybrid Structures,
Hiroyuki Yamanouchi, Stephen A. Mahin, Subhash C. Goel and Isao Nishiyama, BRI

1 3 : 5 0 Seismic Response Control of Bridges by Variable Dampers,
Kazuhiko Kawashima and Shigeki Unjo, PWRI

1 4 : 1 0 Discussion

14:30 Break

14:45 Reports of Task Committees
- A : Strong-Motion Instrumentation Arrays and Data
- B : Large-Scale Testing Programs
- C : Repair and Retrofit of Existing Structures
- D : Evaluation of Performance of Structures
- E : Ground Motion and Seismic Design Forces
- F : Disaster Prevention Methods for Lifeline Systems
- G : Active, Passive and Hybrid Control
- H : Soil Behavior and Stability during Earthquakes
- I : Storm Surge and Tsunamis
- J : Wind and Earthquake Engineering for Transportation Systems
- K : Wind and Earthquake Engineering for Offshore Structures

16:00 Break

16:10 Adoption of Final Resolution

16:50 Break

17:00 Closing Ceremony
Call to Order by Takashi IIJIMA, Secretary-General, Japan-Side Panel

Closing Remarks by Richard N. WRIGHT, Chairman U.S.- Side Panel

Closing Remarks by Yukihiko Sumiyoshi, Chairman JAPAN - Side Panel

18:30 Reception Hosted by U.S. Members (Techno-Hall, Tsukuba Research Support Center, Tel. 0298-58-6080)

IDNDR SYMPOSIUM

(SYMPOSIUM FOR CELEBRATING THE 25TH ANNIVERSARY OF THE PANEL at Star Room, 5th Floor of Main Building, Tojoh Kaikan, Tokyo)

May 21 (Friday)

13:00 Opening Session

Remarks by Toru Kondo, Vice-Minister of Construction for Engineering Affairs

Remarks by Edward M. Malloy, Minister-Counselor for Environmental, Scientific and Technological Affairs Embassy of the United States of America

13:20 Earthquake Engineering Stepping in the Second Century
Keizaburo Kubo, Professor Emeritus of University of Tokyo

14:00 ASCE's Contributions toward Technology for Disaster Mitigation
Edward O. Pfrang, Executive Director of American Society of Civil Engineers, the First U.S.-Side Chairman of the UJNR Wind and Seismic Effects Panel

14:50 Cooperation on Research and Technical development in Wind and Earthquake Engineering between U.S.A. and Japan in the Last 25 Years
-Activities of the Panel on Wind and Seismic Effects, UJNR-
Yukihiko Sumiyoshi, Japan-Side Chairman of the UJNR Wind and Seismic Effects Panel, Director-General of PWRI

15:20 Break/Poster Session (U.S. and Japan Panel Members)

16:00 Lessons from the Loma Prieta Earthquake
Richard N. Wright, U.S.-Side Chairman of the UJNR Wind and Seismic Effects Panel, Director of Center for Building and Fire Research Laboratory, NIST

16:50 Damages and Lessons Learned from Hurricane Hugo and Andrew
G. Robert Fuller, UJNR Wind and Seismic Effects Panel Member, HUD

17:40 Closing Remarks

18:00 Reception (Kokonoe Room, 6th Floor, New Building of Tojoh Kaikan, Tokyo)

TECHNICAL STUDY TOUR

May 22 (Saturday)

Visit to Miyagase Dam Construction Site(Kanagawa Prefecture)

May 23 (Sunday)

Fly from Tokyo to Matsuyama
(Ehime Pref. Shikoku Island)
Visit to Matsuyama City and the Matsuyama Castle
Dinner (hosted by Ehime Prefectural Government)

May 24 (Monday)

Visit to Amagogawa Bridge(Ehime Pref.)
Visit to Kanpuzan Tunnel Construction Site
(Ehime Pref. & Kochi Pref.)
Dinner (hosted by Kochi Prefectural Government)

May 25 (Tuesday)

Visit to Konpira Shrine, Kabuki Theatre and Mannoh National Park(Kagawa Pref.)
Visit to Tadotsu Research Institute(kagawa Pref.)
Visit to Yoshima Parking Area, Honshu-Shikoku Bridge
(Kagawa Pref.)
Visit to Korakuen Park(Okayama Pref.)
Dinner (hosted by Honshu Shikoku Bridge Authority)

May 26 (Wednesday)

Visit to the Site of Automatic Construction of Building (Smart System)(Nagoya City)
Visit to Passively Controlled Building(Tokyo)
Dinner (hosted by ASCE, Sasano-Yuki)

May 27 (Thursday)

Visit to Minato-Mirai 21 Construction Site
Visit to Common Utility Ducts Construction Site of Yoshino-Isoko Local Government(Kanagawa Pref.)
Visit to Yokohama Bay Bridge and Tsurumi Cable Stayed Bridge(Kanagawa Pref.)
Dinner(hosted by U. S. members, New Sanno Center)

May 28 (Friday)

Visit to Extension of Runway of Haneda Airport and National Highway Route #357 (Tokyo Bay)
Visit to Trans-Tokyo Bay Highway Construction Site (TTB)
Dinner (hosted by Trans-Tokyo Bay Highway Co. Ltd.)

May 29 (Saturday)

U.S. Members Leave Japan

List of Panel Members

JAPAN-SIDE PANEL ON WIND AND SEISMIC EFFECTS MEMBERSHIP LIST

Mr. Yukihiko Sumiyoshi
Chairman, Japan-side
Panel on Wind and Seismic Effects,
UJNR
Director-General
Public Works Research Institute
Ministry of Construction
1, Asahi, Tsukuba-shi,
Ibaraki-ken 305

Dr. Takashi Iijima
Secretary-General, Japan-side
Panel on Wind and Seismic Effects,
UJNR
Assistant Director-General
Public Works Research Institute
Ministry of Construction
1, Asahi, Tsukuba-shi,
Ibaraki-ken 305

Dr. Tokunosuke Fujitani
Chief, The Second Research
Laboratory
Applied Meteorology Research
Division
Meteorological Research Institute
Japan Meteorological Agency
1-1 Nagamine, Tsukuba-shi,
Ibaraki-ken 305

Dr. Minoru Fujiwara
Director, Structure and Bridge
Department
Public Works Research Institute
Ministry of Construction
1, Asahi, Tsukuba-shi,
Ibaraki-ken 305

Mr. Tadao Hoya
Head, Geographic Department
Geographical Survey Institute
Ministry of Construction
1, Kitazato, Tsukuba-shi
Ibaraki-ken 305

Dr. Susumu Iai
Chief, Geotechnical Earthquake
Engineering Laboratory
Port and Harbour Research Institute
Ministry of Transport
3-1-1, Nagase, Yokosuka
Kanagawa-ken 239

Mr. Yutaka Iida
Director, Earthquake Disaster
Prevention Department
Public Works Research Institute
Ministry of Construction
1, Asahi, Tsukuba-shi,
Ibaraki-ken 305

Dr. Takamasa Inatomi
Chief, Structural Dynamics
Laboratory
Structural Engineering Division
Port and Harbour Research Institute
Ministry of Transport
3-1-1, Nagase, Yokosuka
Kanagawa-ken, 239

Dr. Kazuhiko Kawashima
Secretary, Japan-side
Panel on Wind and Seismic Effects,
UJNR
Head, Earthquake Engineering
Division
Earthquake Disaster Prevention
Department
Public Works Research Institute
Ministry of Construction
1, Asahi, Tsukuba-shi,
Ibaraki-ken 305

Dr. Yoshikazu Kitagawa
Director, International Institute of Seismology and Earthquake Engineering
Building Research Institute
Ministry of Construction
1, Tatehara, Tsukuba-shi,
Ibaraki-ken 305

Mr. Osamu Matsuo
Head, Soil Dynamics Division
Earthquake Disaster Prevention Department
Public Works Research Institute
Ministry of Construction
1, Asahi, Tsukuba-shi,
Ibaraki-ken 305

Dr. Chikahiro Minowa
Cooperative Research Officer
National Research Institute for Earth Science and Disaster Prevention
3-1, Tennodai, Tsukuba-shi,
Ibaraki-ken, 305

Mr. Hatsukazu Mizuno
Head, Large-Scale Structure Testing Division
Production Department
Building Research Institute
Ministry of Construction
1, Tatehara, Tsukuba-shi,
Ibaraki-ken 305

Mr. Tatsuo Murota
Director, Structural Engineering Department
Building Research Institute
Ministry of Construction
1, Tatehara, Tsukuba-shi,
Ibaraki-ken 305

Mr. Akira Nakamura
Head, Fill Type Dam Division
Public Works Research Institute
Ministry of Construction
1, Asahi, Tsukuba-shi,
Ibaraki-ken 305

Mr. Masanori Nakano
Head, Foundation Engineering Division
Structure and Bridge Department
Public Works Research Institute
Ministry of Construction
1, Asahi, Tsukuba-shi,
Ibaraki-ken 305

Dr. Osamu Nakano
Head, Structures Section
Civil Engineering Research Institute
Hokkaido Development Bureau
Hokkaido Development Agency
1-3, Hiragishi, Toyohira-ku
Sapporo, Hokkaido, 062

Dr. Shinsuke Nakata
Director,
Testing and Evaluation Department
Building Research Institute
Ministry of Construction
1, Tatehara, Tsukuba-shi,
Ibaraki-ken 305

Mr. Kazuhiro Nishikawa
Head, Bridge Division
Structure and Bridge Department
Public Works Research Institute
Ministry of Construction
1, Asahi, Tsukuba-shi,
Ibaraki-ken 305

Dr. Setuo Noda
Director, Structural Engineering Division
Port and Harbour Research Institute
Ministry of Transport
3-1-1, Nagase, Yokosuka,
Kanagawa-ken 239

Dr. Shigeyuki Noto
Director, Structures Division
Civil Engineering Research Institute
Hokkaido Development Agency
1-3, Hiragisi, Toyohira-ku
Sapporo, Hokkaido, 062

Dr. Nobuyuki Ogawa
Head, Earthquake Engineering Laboratory
National Research Institute for Earth Science and Disaster Prevention
Science and Technology Agency
3-1, Tennodai, Tsukuba-shi,
Ibaraki-ken 305

Mr. Keiichi Ohtani
Director, Disaster Prevention Research Division
National Research Institute for Earth Science and Disaster Prevention
Science and Technology Agency
3-1, Tennodai, Tsukuba-shi,
Ibaraki-ken, 305

Dr. Hisanori Ohtsuka
Head, Ground Vibration Division
Earthquake Disaster prevention Department
Public Works Research Institute
Ministry of Construction
1, Asahi, Tsukuba-shi,
Ibaraki-ken 305

Mr. Shin Otsuka
Head, Typhoon Research Division
Meteorological Research Institute
Japan Meteorological Agency
1-1, Nagamine, Tsukuba-shi
Ibaraki-ken 305

Dr. Shin Okamoto
Director-General, Building Research Institute
Ministry of Construction
1, Tatehara, Tsukuba-shi,
Ibaraki-ken 305

Dr. Hiroshi Sato
Secretary, Japan-side
Panel on Wind and Seismic Effects, UJNR
Head, Structure Division
Structure and Bridge Department
Public Works Research Institute
Ministry of Construction
1, Asahi, Tsukuba-shi,
Ibaraki-ken 305

Dr. Masaki Seino
Head, Seismology and Volcanology Research Division
Meteorological Research Institute
Japan Meteorological Agency
1-1, Nagamine, Tsukuba-shi
Ibaraki-ken 305

Dr. Tomotsuka Takayama
Director, Hydraulic Engineering Division
Port and Harbour Research Institute
Ministry of Transport
3-1-1, Nagase, Yokosuka,
Kanagawa-ken 239

Mr. Shigenobu Tanaka
Head, Coastal Engineering Division
River Department
Public Works Research Institute
Ministry of Construction
1, Asahi, Tsukuba-shi,
Ibaraki-ken 305

Dr. Hiroyuki Yamanouchi
Special Researcher for
INternational Standard
Planning Department
Building Research Institute
Ministry of Construction
1, Tatehara, Tsukuba-shi,
Ibaraki-ken 305

Dr. Tatsuo Uwabe
Chief, Disaster Prevention
Laboratory
Structural Engineering Division
Port and Harbour Research Institute
Ministry of Transport
3-1-1, Nagase, Yokosuka-shi
Kanagawa-ken 239

Dr. Yutaka Yamazaki
Director, Production
Department
Building Research Institute
Ministry of Construction
1, Tatehara, Tsukuba-shi,
Ibaraki-ken 305

UNITED STATES-SIDE PANEL ON WIND AND SEISMIC EFFECTS MEMBERSHIP LIST

Dr. Richard N. Wright
Chairman, U.S. Side
Panel on Wind and Seismic Effects, UJNR
Director, Building and Fire Research Laboratory
National Institute of Standards and Technology
U.S. Department of Commerce
Gaithersburg, MD 20899
U.S.A.
TEL. 301-975-5900 FAX. 301-975-4032

Mr. Noel J. Raufaste
Secretary-General, U.S. Side
Panel on Wind and Seismic Effects, UJNR
Head, Cooperative Research Programs Building and Fire Research Laboratory
National Institute of Standards and Technology
U.S. Department of Commerce
Gaithersburg, MD 20899
U.S.A.
TEL. 301-975-5905 FAX. 301-975-4032

Dr. Kharaiti L. Abrol
Acting Director
Structural Engineering Service (088C1)
Department of Veterans Affairs
810 Vermont Avenue, NW
Washington, DC 20420
U.S.A.
TEL. 202-233-7179 FAX. 202-233-2115

Dr. John Ake
Geophysicist
Seismotectonics and Geophysics Section
P.O. Box 25007
Bureau of Reclamation
U.S. Department of the Interior
Denver, CO 80225
U.S.A.
TEL. 303-236-4195 FAX. 303-236-6763

Dr. S. T. Algermissen
Research Geophysicist
Hazard and Risk Assessment Group
MS 966, POB 25046
Denver Federal Center
Geological Survey
U.S. Department of the Interior
Denver, CO 80225
U.S.A.
TEL. 303-273-8557 FAX. 303-273-8600

Mr. Charles E. Anderson
Seismic Safety Coordinator
P.O. Box 25007 (D-3130)
Bureau of Reclamation
U.S. Department of the Interior
Denver, CO 80225
U.S.A.
TEL. 303-236-9114 FAX. 303-236-6763

Dr. Celso S. Barrientos
Supervisory Physical Scientist
National Environmental Satelite Data
Information Service-Code E/RA28
National Oceanic and Atmospheric Administration
U.S. Department of Commerce
5200 Auth Road
Camp Springs, MD 20746
U.S.A.
TEL. 301-763-8102 FAX. 301-763-8108

Dr. Eddie N. Bernard
Director, Pacific Marine Environmental Laboratory
National Oceanic and Atmospheric Administration
U.S. Department of Commerce
7600 Sand Point Way, NE
BIN C15700/Building 3
Seattle, WA 98115-0070
U.S.A.
TEL. 206-526-6239 FAX. 206-526-6815

Dr. Roger D. Borcherdt
Branch of Engineering Seismology
and Geology
U.S. Geological Survey
U.S. Department of the Interior
345 Middlefield Road, MS 977
Menlo Park, CA 94025
U.S.A.
TEL. 415-329-5619 FAX. 415-329-5163

Dr. A. Gerald Brady
Research Civil Engineer
Branch of Engineering Seismology
and Geology
Geological Survey
U.S. Geological Survey
U.S. Department of the Interior
345 Middlefield Road, MS 977
Menlo Park, CA 94025
U.S.A
TEL. 415-329-5664 FAX. 415-329-5163

Mr. H. Lee Butler
Chief, Research Division
Coastal Engineering Research
Center
U.S. Army Engineer Waterways
Experiment Station
Office CEWES-CR
3909 Halls Ferry Road
Vicksburg, MS 39180-6199
U.S.A
TEL. 601-634-2405 FAX. 601-634-4314

Dr. Ken P. Chong
Program Director
Structural Systems and
Construction Processes
Directorate of Engineering
National Science Foundation
1800 G Street, N.W., Room 1108
Washington, DC 20550
U.S.A.
TEL. 202-357-9542 FAX. 202-357-0167

Dr. Riley M. Chung
Group Leader
Earthquake Engineering
Structures Division
Building and Fire Research
Laboratory
National Institute of Standards
and Technology
U.S. Department of Commerce
Gaithersburg, MD 20899
U.S.A.
TEL. 301-975-6056 FAX. 301-975-4032

Mr. James D. Cooper
Deputy Chief, Structures Division
HNR-10
Federal Highway Administration
U.S. Department of Transportation
6300 Georgetown Pike
McLean, VA 22101
U.S.A.
TEL. 703-285-2060 FAX. 703-285-2379

Dr. A. G. Franklin
Chief, Earthquake Engineering
and Geophysics Division
CEWES-GH Geotechnical Laboratory
U.S. Army Engineer Waterways
Experiment Station
3909 Halls Ferry Road
Vicksburg, MS 39180-6199
U.S.A.
TEL. 601-634-2658 FAX. 601-634-4134

Mr. G. Robert Fuller
Acting Director
Manufactured Housing and
Construction Standards Division
Room 9152 HSMM
U.S. Department of Housing
and Urban Development
Washington, DC 20410-8000
U.S.A.
TEL. 202-755-7430 FAX. 202-755-7445

Mr. James H. Gates
Caltrans-Structures
P.O. Box 942874
Sacramento, CA 94274
U.S.A.
TEL. 916-227-8773 FAX. 916-323-2259

Mr. Peter E. Gurvin
Director, Building Design and
Engineering Division
Foreign Building Operations
Building SA-6, Room 335
U.S. Department of State
Washington, DC 20520
U.S.A.
TEL. 703-875-6117 FAX. 703-875-6204

Dr. Walter W. Hays
Deputy for Research Applications
Office of Earthquake
Volcanoes and Engineering
905 National Center
U.S. Geological Survey
U.S. Department of the Interior
Reston, VA 22092
U.S.A.
TEL. 703-648-6711 FAX. 703-648-6717

Mr. Barry Heyman
Director, Prevention, Mitigation,
and Preparedness Division
Office of Foreign Disaster
Assistance
N/S Room 1262A
Department of State
320 21st Street, NW
Washington, DC 20523
TEL. 202-647-7544 FAX. 202-647-0776

Mr. James R. Hill
Manager, Natural Hazards
Mitigation Programs
Office of Safety
Health and Quality Assurance
U.S. Department of Energy
Washington, DC 20545
U.S.A.
TEL. 301-903-4508 FAX. 301-903-5285

Mr. Larry C. Hultengren
Senior Structural Engineer
Office of Civil/Structural
Engineering
Foreign Building Operations
U.S. Department of State
Washington, DC 20520
U.S.A.
TEL. 703-875-6194 FAX. 703-875-6204

Dr. Dov Jaron
Director
Division of Biological and Critical
Systems
National Science Foundation
1800 G Street, NW
Washington, DC 20550
U.S.A
TEL. 202-357-9500 FAX. 202-357-7636

Dr. William B. Joyner
Geophysicist
Branch of Ground Motion
and Faulting
U.S. Geological Survey
U.S. Department of the Interior
345 Middlefield Road, MS 977
Menlo Park, CA 94025
U.S.A.
TEL. 415-329-5640 FAX. 415-329-5163

Dr. Michael G. Katona
Chief Scientist
Air Force Civil Engineering
Laboratory
Headquarters Air Force Civil
Engineering Support Agency
U.S. Department of the Air Force
Tyndall AFB, FL 32403-6001
U.S.A
TEL. 904-283-6274 FAX. 904-283-6064

Mr. Roger M. Kenneally
Structural Engineer
Structural and Seismic Engineering Branch
Mail stop NL / S - 217A
U.S. Nuclear Regulatory Commission
Washington, DC 20555
U.S.A.
TEL. 301-492-3893 FAX. 301-492-3696

Dr. H. S. Lew
Chief ,Structures Division
Building and Fire Research Laboratory
National Institute of Standards and Technology
U.S. Department of Commerce
Gaithersburg, MD 20899
U.S.A.
TEL. 301-975-6061 FAX. 301-975-4032

Dr. Shih-Chi Liu
Program Director
Structural Systems
Division of Biological and Critical Systems
National Science Foundation
1800 G Street, N.W., Room 1132
Washington, DC 20550
U.S.A.
TEL. 202-357-9780 FAX. 202-357-7636

Dr. Steve D. Markwell
Chief
Geotechnical and Geology Division
Code D-3600-P.O. Box 25007
Bureau of Reclamation
U.S. Department of the Interior
Denver, CO 80225
U.S.A.
TEL. 303-236-9329 FAX. 303-236-6763

Dr. Francis G. McLean
Chief
Geotechnical Engineering and Embankment Dams Branch
P.O. Box 25007
Bureau of Reclamation
U.S. Department of the Interior
Denver, CO 80225
U.S.A.
TEL. 303-236-3854 FAX. 303-236-6763

Mr. Herbert Meyers
Chief, Earth Geophysics
National Geophysical Data Center
National Oceanic and Atmospheric Administration
U.S. Department of Commerce
325 Broadway
Boulder, CO 80303-3328
U.S.A.
TEL. 303-497-6521 FAX. 303-497-6513

Mr. Ugo Morelli
Policy Manager for Seismology
Federal Emergency Management Agency
500 C Street, SW
Washington DC 20472
U.S.A
TEL. 202-646-2810 FAX. 202-646-3041

Mr. Howard D. Nickerson
Earthquake Engineering and Weapons Specialist
Naval Facilities Engineering Command
Hoffman Building #2, Room 12S63,
Code 04B2
200 Stovall Street
Alexandria, VA 22332
U.S.A.
TEL. 202-433-8599 FAX. 202-433-8777

Dr. William E. Roper
Assistant Director
Research and Development
(Civil Works)
U.S. Army Corps of Engineers
20 Massachusetts Avenue, N.W.
Washington, DC 20314-1000
U.S.A.
TEL. 202-272-0257 FAX. 202-272-0907

Dr. John B. Scalzi
Program Director
Structures and Building Systems
National Science Foundation
1800 G Street, N.W.- Room 1108
Washington, DC 20550
U.S.A.
TEL. 202-357-9542 FAX. 202-357-7636

Dr. Erwin L. Schaffer
Assistant Director
Wood Products Research
Forest Products Laboratory
Forest Service
U.S. Department of Agriculture
One Gifford Pinchot Drive
Madison, WI 53705-2398
U.S.A.
TEL. 608-231-9272 FAX. 608-231-9592

Mr. Charles E. Smith
Research Program Manager
Offshore Minerals Management
Technology Assessment
and Research Branch
Minerals Management Service
U.S. Department of the Interior
381 Elden Street, MS 4800
Herndon, VA 22070-4817
U.S.A.
TEL. 703-787-1559 FAX. 703-787-1010

Dr. T. T. Soong
Samuel P. Capen Professor
Department of Civil Engineering
National Center for Earthquake
Engineering Research
State University of New York
at Buffalo
212 Ketter Hall
Buffalo, NY 14260
U.S.A.
TEL. 716-645-2469 FAX. 716-645-3733

Alternate Members

Dr. Clifford J. Astill
Program Director
Division of Biological and Critical
Systems
National Science Foundation
1800 G Street, N.W.- Room 1132
Washington, DC 20550
U.S.A.
TEL. 202-357-9500 FAX. 202-357-9803

Dr. Mehmet K. Celebi
Research Civil Engineer
Branch of Engineering Seismology
and Geology
Geological Survey
U.S. Department of the Interior
345 Middlefield Road, MS 977
Menlo Park, CA 94025
U.S.A.
TEL. 415-329-5623 FAX. 415-329-5163

Mr. Michael J. Changery
Chief, Global Analysis Branch
National Climatic Data Center
National Oceanic
and Atmospheric Administration
U.S. Department of Commerce
Federal Building
Ashville, NC 28801
U.S.A.
TEL. 704-259-0765 FAX. 704-259-0246

Mr. C. Y. Chen
Senior Civil/Geotechnical Engineer
Office of Foreign Buildings
U.S. Department of State
Code SA-6, Room 327
Washington, DC 20520
U.S.A.
TEL. 703-875-6207 FAX. 703-875-6204

Mr. Vincent P. Chiarito
Research Structural Engineer
Structural Mechanics Division
Structures Laboratory
U.S. Army Engineer Waterways
Experiment Station
3909 Halls Ferry Road
Vicksburg, MS 39180-6199
U.S.A.
TEL. 601-634-2714 FAX. 601-634-3412

Dr. James F. Costello
Senior Structural Engineer
Structural and Seismic Engineering
Branch
Structural Section
Office of Nuclear Regulatory
Research
U.S. Nuclear Regulatory Commission
Mail Stop 007NL
Washington , DC 20555
U.S.A.
TEL. 301-492-3818 FAX. 301-492-3696

Mr. Lucian G. Guthrie
Structural Engineer
Office of Chief of Engineers
Headquarters U.S. Army Corps of
Engineers
Corps of Engineers Civil Works
Engineering Div.
U.S. Department of the Army
20 Massachusetts Avenue, N.W.
Washington, DC 20314-1000
U.S.A.
TEL. 202-272-8673 FAX. 202-272-1485

Dr. Robert L. Hall
Chief, Structural Analysis Group
U.S. Army Engineer Waterways
Experiment Station
3909 Halls Ferry Road
Vicksburg, MS 39180-6199
U.S.A.
TEL. 601-634-2567 FAX. 601-634-3412

Dr. James R. Houston
Chief, Coastal Engineering
Research Center
U.S. Army Engineer Waterways
Experiment Station
3909 Halls Ferry Road
Vicksburg, MS 39180-6199
U.S.A.
TEL. 601-634-2000 FAX. 601-634-2655

Mr. James F. Lander
Geophysicist
Cooperative Institute for Research
in Environmental Sciences
University of Colorado
Campus Box 449, Room 152 RL3
3100 Marine Street
Boulder, CO 80309
U.S.A.
TEL. 303-497-6446 FAX. 303-497-6513

Mr. Robert R. Ledzian
Senior Staff Assistant for
Research
Office of Liaison - Engineering
Research, Coad 3020
Bureau of Reclamation
U.S. Department of the Interior
1849 C Street, N.W.
Washington, DC 20240
U.S.A.
TEL. 202-208-3432 FAX. 202-208-6252

Mr. Tingley K. Lew
Research Structural Engineer
Structures Division
Naval Civil Engineering Laboratory
560 Laboratory Drive-Suite L51
Port Hueneme, CA 93043-4328
U.S.A.
TEL. 805-982-1234 FAX. 805-982-1418

Mr. Michael Mahoney
Physical Scientist
Federal Emergency Management
Agency
500 C Street, SW
Washington, DC 20472
U.S.A
TEL. 202-646-2810 FAX. 202-646-3041

Dr. J. Eleonora Sabadell
Director, Natural and Manmade
Hazards Mitigation Program
Directorate of Engineering
National Science Foundation
1800 G Street, N.W. - Room 1132
Washington, DC 20550
U.S.A.
TEL. 202-357-9780 FAX. 202-357-9803

Dr. Erdal Safak
Research Structural Engineer
U.S. Geological Survey
U.S. Department of the Interior
922 National Center
Reston, VA 22092
U.S.A.
TEL. 703-648-6534 FAX. 703-648-6717

List of Task Committee Members

TASK COMMITTEE MEMBERSHIP LIST

Task Committee	U.S. Side	Japanese Side
A. Strong Motion Data and Applications	* A.G. Brady	* S. Noda
	C.J. Astill	Y. Kitagawa
	R.D. Borcherdt	K. Ohtani
	M.K. Celebi	M. Seino
	A.G. Franklin	H. Ohtsuka
	W.B. Joyner	H. Mizuno
	R.B. MacDonald	S. Iai
	F.G. McLean	K. Mimura
	H. Meyers	
	J.R. Hill	
	S.T. Algermissen	
	C.S. Barrientos	
	G.R. Fuller	
	J. Hunt	
	J. Kimball	
	T.K. Lew	
	E. Safak	
B. Testing and Evaluation Procedures for Building Systems	* H.S. Lew	* K. Ohtani
	V.P. Chiarito	O. Matsuo
	J.E. Sabadell	H. Mizuno
	C.E. Smith	S. Noda
	J. Beavers	Y. Yamazaki
	S. Sweeney	H. Sato
C. Design, Evaluation and Improvement of Structures	* K.P. Chong	* H. Yamanouchi
	P.A. Brady	S. Nakata
	G.E. Freeland	M. Fujiwara
	J.O. Jirsa	S. Okamoto
	H.S. Lew	Y. Iida
	T.K. Lew	Y. Yamazaki
	H.D. Nickerson	T. Fijitani
	D.H. Oh	M. Nakano
	M.A. Phipps	S. Ohtauka
	J.B. Scalzi	H. Sato
	D. Jones	
	D. Eagling	
	S. Woodson	
	S.A. Asar	
	M.K. Celebi	
	G.R. Fuller	
	E.L. Schaffer	
	R.L. Hall	
	J.R. Hill	
	J. Hunt	
	D. Ellsworth	

Task Committee	U.S. Side	Japanese Side
D. Dam Earthquake Engineering	* W.E. Roper R.M. Chung	* A. Nakamura H. Ohtsuka K. Kawashima
F. Disaster Prevention Methods for Lifeline Systems	* R.M. Chung C.J. Astill M.K. Celebi J.D. Cooper G. Al-Chaar T.K. Lew J.B. Scalzi J.S. Spencer S. Wu	* Y. Iida K. Kawashima N. Ogawa H. Ohtsuka T. Uwabe S. Noto M. Sato
G. Structural Control and Intelligent Material Systems	* S.C. Liu V.P. Chiarito K.P. Chong J.R. Hayes L.C. Hultengren T.T. Soong	* Y. Kitagawa K. Kawashima N. Ogawa H. Yamanouchi H. Sato C. Minowa
H. Soil Behavior and Stability during Earthquakes	* A.G. Franklin C.J. Astill R.D. Borcherdt C.Y. Chen F.G. McLean C.E. Smith	* H. Ohtsuka A. Nakamura O. Matsuo H. Mizuno S. Iai Y. Iida S. Noto T. Inatomi M. Nakano
I. Storm Surge and Tsunamis	* H. Meyers C.J. Astill C.S. Barrientos E.N. Bernard L. Butler C.F. Jelesnianski J. Lander W.E. Roper	* S. Tanaka M. Seino S. Ohtsuka T. Takayama
J. Wind and Earthquake Engineering for Transportation Systems	* J.D. Cooper A.G. Franklin J.H. Gates J.B. Scalzi H.S. Lew	* M. Fujiwara T. Fujitani K. Kawashima K. Nishikawa Y. Iida H. Ohtsuka H. Sato M. Sato M. Nakano

Task Committee	U.S. Side	Japanese Side
K. Wind and Earthquake Engineering for Offshore and Coastal Facilities	* C.E. Smith	* T. Uwabe
	C.S. Barrientos	T. Fujitani
	W.E. Roper	S. Noda
	J.E. Sabadell	T. Inatomi
	M.C. Miller	S. Iai
	M.K. Celebi	M. Nakano

* Chairman of Task Committee

Resolutions

RESOLUTIONS

RESOLUTIONS OF THE TWENTY-FIFTH JOINT MEETING U.S.-JAPAN PANEL ON WIND AND SEISMIC EFFECTS (UJNR)

Public Works Research Institute
Tsukuba, Japan
May 17-20,1993

The Following resolutions are hereby adopted:

1. The Twenty Fifth Joint Panel Meeting provided an opportunity to exchange valuable technical information which was beneficial to both countries. In view of the importance of cooperative programs on the subject of wind and seismic effects, the continuation of Joint Panel Meetings is considered essential.

2. The following activities have been conducted since the Twenty-Fourth Joint Meeting:

a. Two PWRI researchers (Y. Yamaguchi and J. Koseki) worked in the USA (WES and MIT) to promote and conduct research that advanced the state-of-the-art in earthquake and wind engineering; two PWRI researchers visited NIST to exchange information on wind and seismic effects.

b. Technical documents, research reports, and proceedings of workshops were exchanged.

c. Six Significant conferences were held:

a) The Third U.S.-Japan Joint Technical Coordinating Committee on Precast Seismic Structural Systems Program, Task Committee (B), at San Diego, U.S.A., November 18-20, 1992.

b) The Fifth Workshop on Earthquake Disaster Prevention for Lifeline Systems, Task Committee (F), at Tsukuba, Japan, October 26 and 27, 1992.

c) The Second Workshop on Earthquake Protective Systems of Bridges, Task Committee (G), at Tsukuba, Japan, December 7 and 8, 1992.

d) The Workshop on Smart and High Performance Materials and Structures, Task Committees (G), (C) and (D), at Tsukuba, Japan, May 14 and 15, 1993

e) The Ninth Bridge Workshop, Task Committee (J), at Tsukuba, Japan, May 10 and 11, 1993.

f) The First Workshop on Wind and Earthquake Engineering for Offshore and Coastal Facilities, Task Committee (K), at Yokosuka, Japan, May 12 and 13, 1993.

3. The Panel in celebration of its 25th Anniversary, will hold jointly with the IDNDR Promotion Section of the Ministry of Construction, a one-day Symposium on the International Decade for National Disaster Reduction (IDNDR), in Tokyo on May 21, 1993. The purpose of the Symposium is to increase the awareness of the people of Japan about the disastrous effects from strong winds and earthquakes. The UJNR Panel will present four of the five presentations. Dr. E. O. Pfrang, Executive Director of the American Society of Civil Engineers, the first U.S.-side Chairman of the Panel, was invited by the Japan-side Panel to make a presentation.

4. The Panel will continue to seek methods to contribute to the International Decade of Natural Disaster Reduction (IDNDR) such as exchanging Proceedings of Joint Panel Meetings and Task Committee Workshops with their respective country's National Committees of IDNDR.

5. The Panel endorsed the consolidation of T/C (A) "Strong Motion Instrumentation Arrays and Data" with T/C (E) "Ground Motion and Seismic Design Forces" into a new T/C (A) "Strong Motion Data and Application." The Panel endorsed the consolidation of T/C (C) "Repair and Retrofit of Existing Structures" with T/C (D) "Evaluation of the Performance of Structures" into a new T/C (C) "Design, Evaluation and Improvement of Structures." The Panel endorsed the name change of T/C (B) "Large-Scale Testing Programs" to "Testing and Evaluation Procedure for Buildings Systems" to reflect its expanded role. Also, the Panel endorsed the revision of the name of T/C (G) to reflect its expanded scope: "Structural Control and Intelligent Material Systems."

6. The Panel endorsed the creation of a new T/C (D) on Dam Earthquake Engineering. Its objective was reviewed and approved by the Panel. Its mission statement will be developed by both side T/C chairmen and will be approved by both sides Panel Chairmen.

7. The Panel approved the Task Committee reports developed and presented during the Twenty-Fifth Joint Meeting. Each report includes objectives and scope of work, accomplishments, future plans and other information.

8. The Panel endorsed the following proposed Task Committee Workshops during the coming year.

a. Task Committee (A) plans a Workshop on Strong Earthquake Motions, March 1994, Menlo Park, U.S.A.

b. Task Committee (B) plans a Fourth Joint Technical Coordinating Committee Meeting on Precast Seismic Structural Systems Program, November 1993, Japan.

c. Task Committee (F) plans a 6th Workshop on Earthquake Disaster Prevention for Lifeline Systems before the 26th Joint Meeting, U.S.A.

d. Task Committee (G) in cooperation with T/C (J) plans a 3rd Workshop on Earthquake Protective Systems of Bridges, February 1994, U.S.A.

e. Task Committee (G) plans a Workshop on Structural Control and Intelligent Material Systems before or after the 26th Joint Meeting, U.S.A.

f. Task Committee (I) plans a 3rd Tsunami Workshop, August 28, 1993, Osaka, Japan.

g. Task Committee (J) plans a 10th Bridge Workshop before the 26th Joint Meeting, Lake Tahoe, U.S.A.

Task Committee (H) is planning a Third Workshop on Remedial Treatment of Potentially Liquefiable Soils at Tsukuba, Japan in summer 1994. Task Committee (K), in cooperation with T/C (I), is planning a Second Workshop on Wind and Earthquake Engineering for Offshore and Coastal Facilities in U.S.A. in fall, 1994.

Scheduling for the workshops shall be performed by the U.S. and Japan Chairmen of the respective Task Committees with concurrence of the Joint Panel Chairmen. Results of each activity conducted before the 26th Joint Meeting shall be presented at the 26th Joint Meeting.

9. The Panel recognizes the importance of the work by both sides in the U.S.–Japan Joint Research Program on Composite and Hybrid Structures.

10. The Panel plans to publish "Newsletters", to disseminate the Panel's activities and accomplishments. Both side Secretaries will identity an appropriate method to collect information so the first Panel Newsletter can be published during the summer of 1993.

11. The Panel recognizes the importance of continued exchange of personnel, technical information, research results, and recorded data that lead to mitigating losses from strong winds and earthquakes. The Panel also recognizes the importance of using available large-scale testing facilities in both countries. Thus, these activities should continue to be strengthened and expanded and, as appropriate, share Task Committee activities at other meetings that have technical relevance to the Task Committee activities. The Panel will provide official endorsement to facilitate these exchanges.

12. The Twenty-Sixth Joint Meeting of the UJNR Panel on Wind and Seismic Effects will be held at NIST, Gaithersburg, MD, May 1994. Specific dates, program, and itinerary will be proposed by the U.S.-Side Panel with concurrence of the Japan-Side Panel.

Papers

Theme 1

Features of surface winds associated with Typhoon 9119 (Mirelle)

by

F. Fujibe and T. Fujitani*

ABSTRACT

Typhoon 9119 (Mirelle) hit the mainland Japan on 27–28 September 1991 with extensive wind damage in Kyushu and Honshu. This report describes surface wind fields during its passage in northern Kyushu by using data from an automated observation network of the Japan Meteorological Agency. Winds were strongest just to the right and 50–100km in the left-rear quadrant of the center, but were relatively weak (<10ms^{-1}) in the left-front quadrant and just to the left-rear of the center. The weak wind area in the left-rear quadrant was bounded by a mesoscale cold front accompanied by strong wind and heavy rain. Similar wind fields are found for several other typhoons in the past.

KEYWORDS: Asymmetric wind fields, Kyushu, Surface winds, Typhoon 9119

1. INTRODUCTION

The mainland Japan is often hit by typhoons in summer and autumn, especially in August and September. The frequency of landfall onto the four major islands (Kyushu, Shikoku, Honshu and Hokkaido) is ~3/year on the average.

Many typhoons which hit the mainland Japan are distorted due to topography and/or entering a frontal zone, so that a well-defined eye and eyewall clouds may be lost and the temperature fields may be highly nonuniform. However, mesoscale wind fields for such typhoons have been rather poorly documented in contrast to detailed researches on the structure of mature typhoons and hurricanes.

Typhoon 9119 (Mirelle, 27–28 September 1991; hereafter T9119) was the severest typhoon that hit the mainland Japan in the last thirty years. It caused extensive wind damage and recovered public attention to wind disasters due to typhoons. This report outlines the severe surface winds due to T9119, and describes the surface wind and temperature fields in northern Kyushu during its passage.

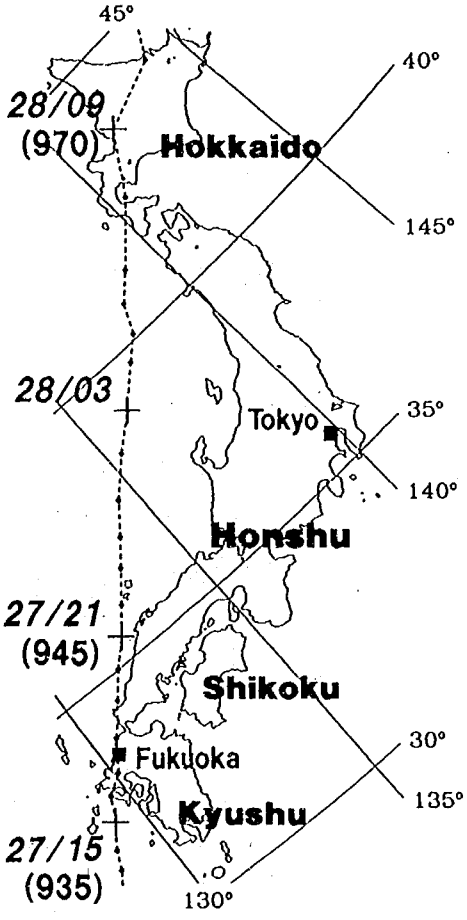


Fig.1 Track of Typhoon 9119 on 27–28 September 1991. Hourly positions of the center are shown in dots and six-hourly positions are shown in "+" with central pressure in hPa and time in JST.

* Meteorological Research Institute, Tsukuba 305, Japan.

2. OUTLINE OF T9119

Figure 1 shows the track of T9119. The typhoon reached the northwestern coast of Kyushu (near Sasebo) at around 1630 JST (0730 UTC) 27 September and moved northeastward at a speed of 60–70kmh^{-1}. Then it passed the Sea of Japan with increasing speed (80–100kmh^{-1}) and reached Hokkaido at around 0730 JST 28 September.

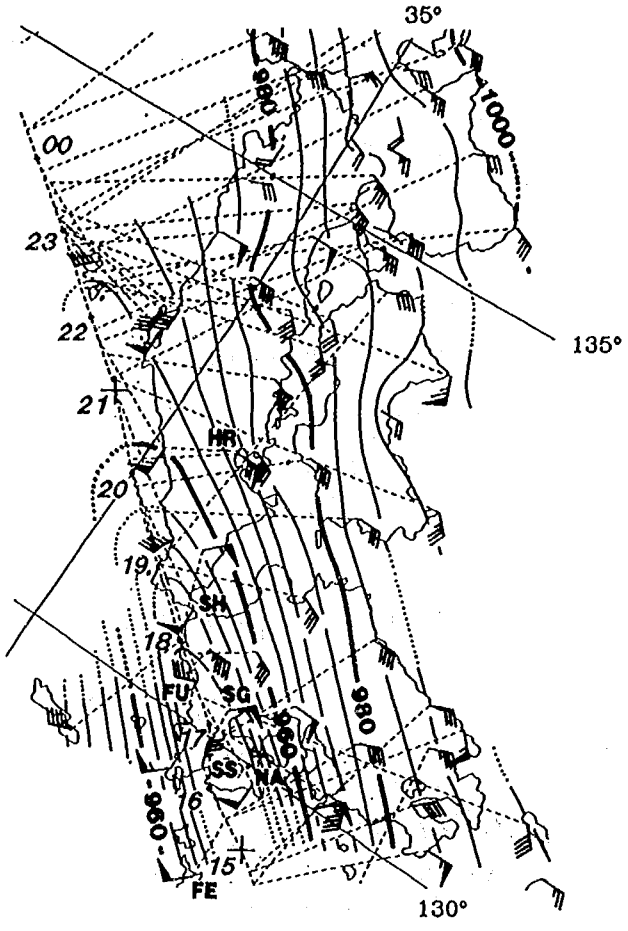


Fig.2 Distribution of minimum sea-level pressure (solid lines; every 4hPa) and maximum sustained wind along the track of T9119. Full barbs indicate 5ms^{-1}, pennants indicate 25ms^{-1}. Hourly positions of the typhoon center (JST) are shown in italics. For stations at which maximum wind exceeded 15ms^{-1}, the positions of the typhoon center at the time of its occurrence are shown in thin dashed lines. FE=Fukue, NA=Nagasaki, SS=Sasebo, SG=Saga, FU=Fukuoka, SH=Shimonoseki and HR=Hiroshima.

Figure 2 shows the distribution of minimum sea-level pressure and maximum sustained wind (ten minute averages) at observatories of the Japan Meteorological Agency (JMA) along the track of T9119. Minimum pressure was 941.1hPa at Sasebo, 942.8hPa at Saga and Fukuoka, and 947.0hPa at Shimonoseki. Thus the typhoon maintained central pressure lower than 950hPa for a few hours during its passage across northern Kyushu. The central pressure rose above 970hPa by the time it reached Hokkaido, but severe winds were maintained in the southeastern quadrant where winds were intensified due to the fast movement of the typhoon.

Maximum sustained winds exceeded 20ms^{-1} and peak gusts exceeded 50ms^{-1} at many stations in Kyushu and Honshu. Former records of sustained wind were renewed at seven stations and those of peak gusts were renewed at 27 stations. The records of peak gusts were renewed at more stations than those of sustained winds partly because of the high sensitivity of the new-type anemometer.

Wind damage occurred in a wide area from Kyushu to northern Honshu. More than 120 thousand houses were damaged and 371 houses totally collapsed. The total damage in crops and forests is estimated to amount to 600–700 billion yen. In particular, more than 15 million cedars are estimated to have been blown down in Kyushu, and apples were blown off at a percentage of nearly 100% in some regions in northern Honshu. On the other hand, widespread floods were prevented in spite of the storm surge reaching 285cm at the highest. The number of casualties was 62, which was much smaller than those caused by many intense typhoons before the 1960's.

3. SURFACE WIND AND TEMPERATURE FIELDS IN NORTHERN KYUSHU

(1) Meso-α-scale features

Figure 3 shows the wind and equivalent potential temperature (Θe) fields at 0900 JST (=0000 UTC) 27 September 1991. At 09 JST, the center of the typhoon was covered with warm air of Θe>340K, while cold air of Θe<320K existed along the east coast of China corresponding to northerly winds. The region of cold air spread over the Yellow Sea by 2100 JST with a zone of sharp Θe gradient just to the northwest of the typhoon, although warm air around the center was still maintained.

Figure 4 shows radar echo maps in and around Kyushu at 1500, 1715 and 1900 JST 27 September 1991. At 1500 JST, which is about an hour before landfall, the typhoon had a well defined eye surrounded by concentric cloud bands. However, the cloud bands around the center began to lose its concentric disposition after landfall, and the eye was almost covered with clouds by 1715 JST. The concentric cloud pattern was largely disturbed by 1900 JST. Satellite imagery (not shown) indicates that convective clouds disappeared rapidly in the central region after the typhoon had passed northern Kyushu.

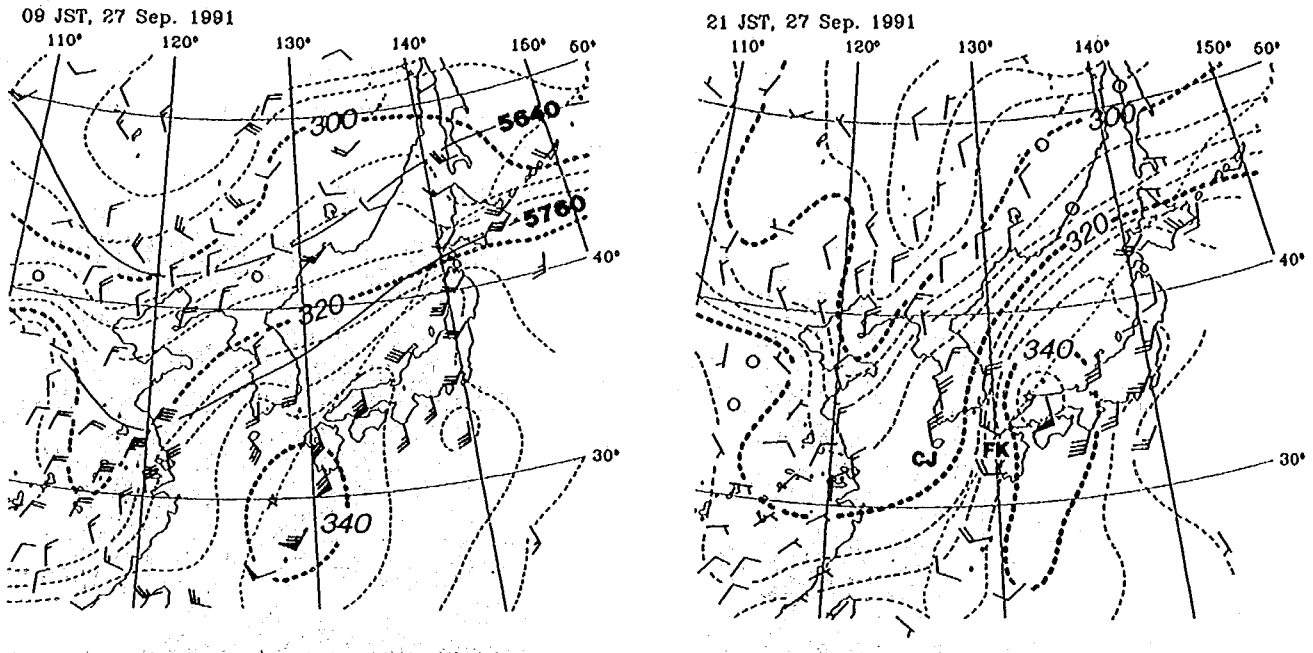


Fig.3 Distribution of wind and equivalent potential temperature (dashed lines; every 5K) at the 850hPa level at (a) 0900 JST (=0000 UTC) and (b) 2100 JST 27 September 1991. Contours of 5640m and 5760m at the 500hPa level are also shown in (a). Winds are shown in the same way as in Fig.2 with circles indicating calm. The center and track of T9119 are shown in "☆" and a thin dashed line. FU=Fukuoka, CJ=Cheju Island.

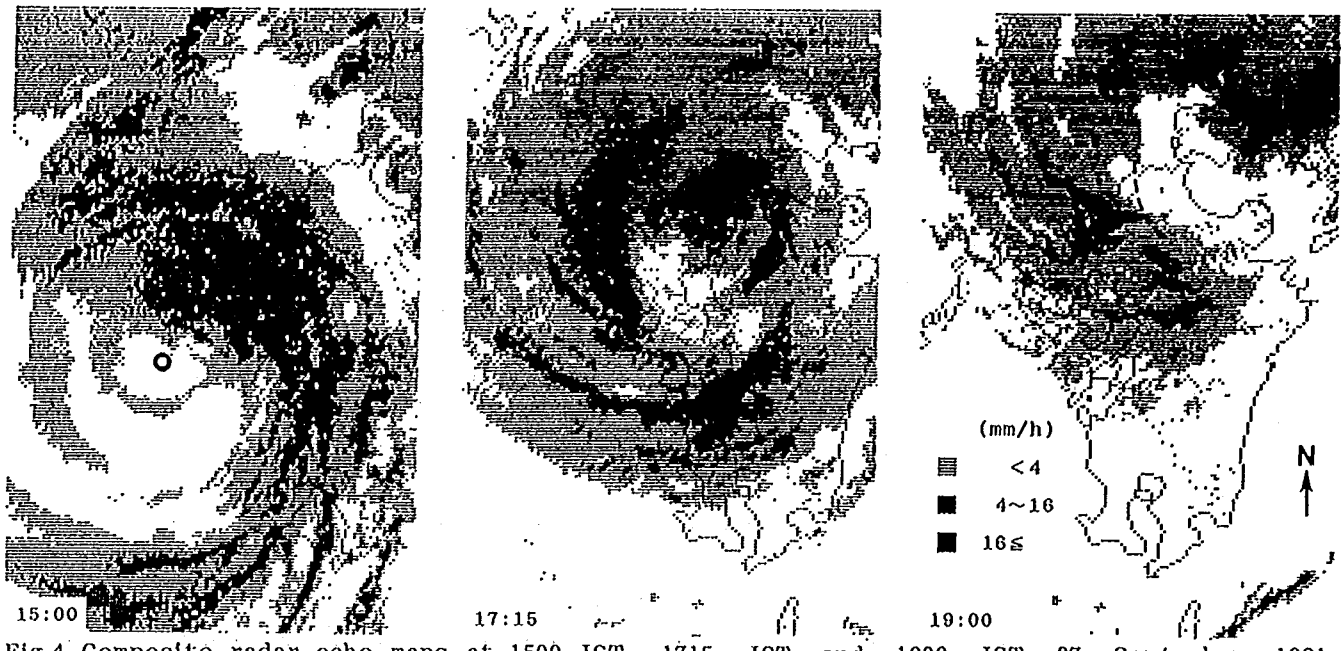


Fig.4 Composite radar echo maps at 1500 JST, 1715 JST and 1900 JST 27 September 1991. Positions of the typhoon center are shown in "○", and the positions of Sasebo and Fukuoka are shown in "+" and "×", respectively.

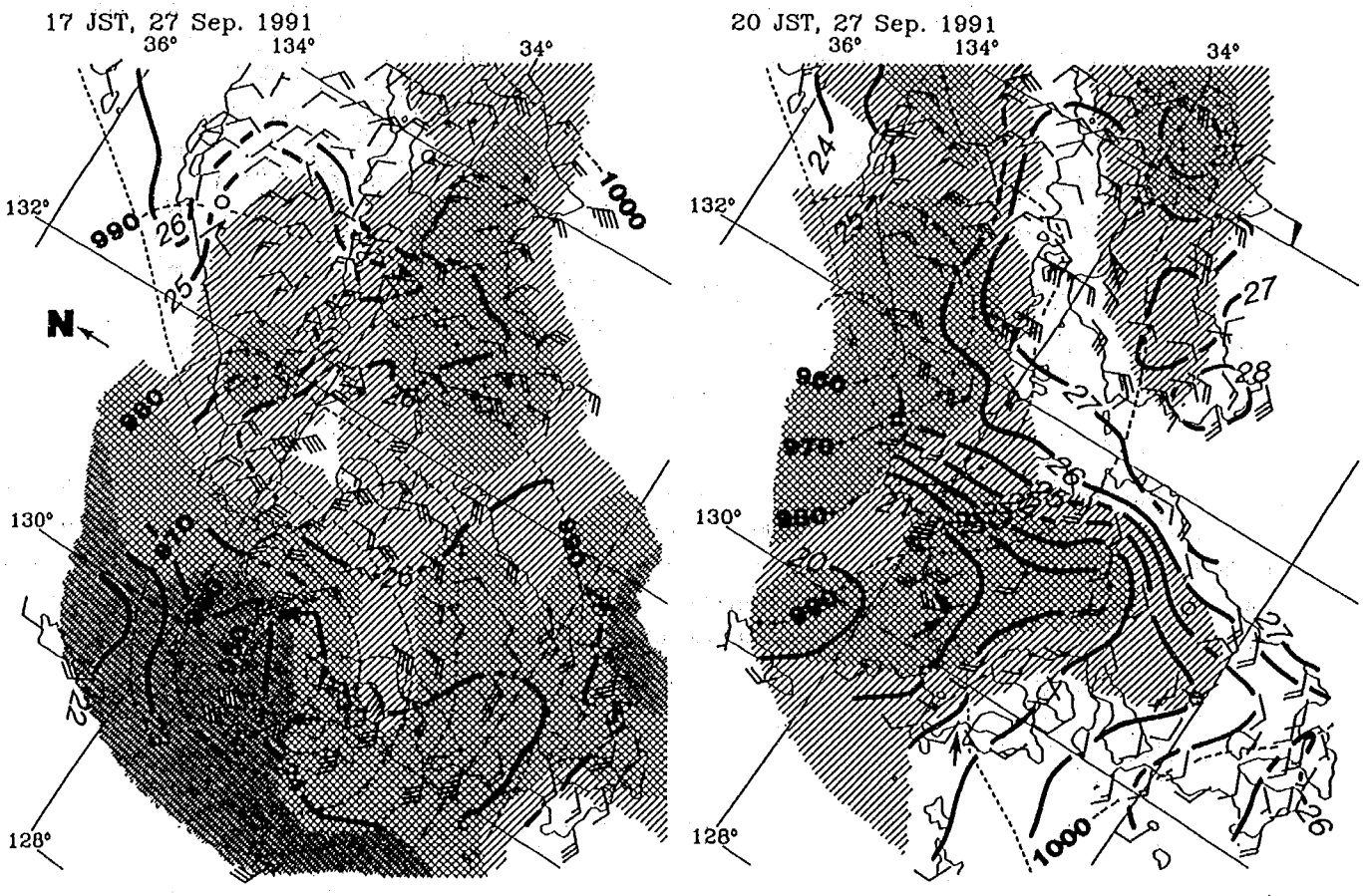


Fig.5 Distribution of surface wind and temperature (heavy solid lines; °C) at 1700 and 2000 JST 27 September. Winds are shown in the same way as in Fig.2. Temperature is adjusted to the sea level with a lapse rate of 5Kkm^{-1}. Hatching indicates area in which precipitation in the preceding hour exceeded 1mm, 4mm and 16mm with increasing tones. Positions of Fukuoka and Sasebo are indicated in arrows.

Figure 5 shows the surface wind and temperature fields at 1700 and 2000 JST obtained from the AMeDAS (Automated Meteorological Data Acquisition System) network. Strong southerly winds dominated over the southeastern quadrant of the typhoon with wind speed exceeding 10ms^{-1} at many stations as fas as 500km distant from the center. In comparison, northwesterly winds in the southwestern quadrant were relatively weak, but a region of northwesterly winds of 10–20ms^{-1} can be observed in a tongue-shaped region of low temperature (20–24°C) 100–200km to the southwest the center. This cold zone was not present before landfall according to the self-recording chart at Fukue (100km southwest of Sasebo), where temperature did not fall below 22°C during the passage of the typhoon.

Figure 6 shows the vertical sounding data at Fukuoka and the Cheju Island (400km west of Fukuoka; Fig.3) at 2100 JST. The middle troposphere over the Cheju Island was very dry with relative humidity below 20%. Since the tongue-shaped cold zone agreed with the area of heavy rain corresponding to the rainband behind the typhoon (Fig.4), it is likely that the cold air at surface was generated by evaporation of rain drops as a result of advection of dry air from the northwest.

Thus wind and temperature fields in T9119 were rapidly becoming asymmetric as the typhoon passed northern Kyushu. Asymmetry in pressure fields also became manifest with time with a trough stretching northeastward from the center (Fig.5).

(2) Meso-β-scale wind fields near the center of T9119

In order to observe the surface fields near the track of the typhoon in detail, a composite analysis was made by using ten minute records at AMeDAS stations in northern Kyushu. Data from 20 minutes before to 30 minutes after each hour were composed by adjusting the movement of the typhoon. For wind and precipitation, which are ten minute averages or totals, the observation time was regarded to be five minutes earlier than the record time. Figure 7 shows the composite fields for 1600–1900 JST obtained in this way. For the sake of comparison, self-recording charts at Sasebo and Fukuoka are shown in Fig.8.

At 1600 JST, the typhoon center was

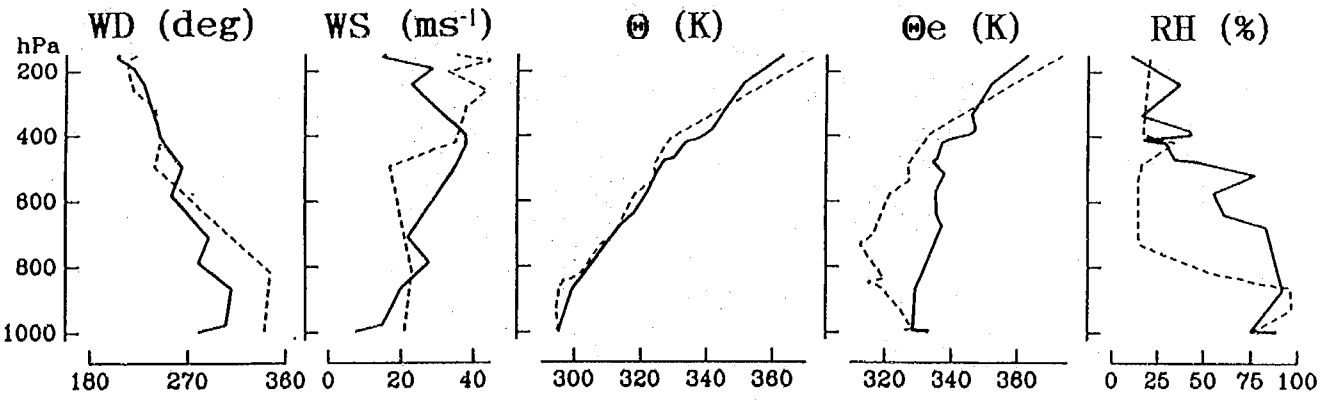


Fig.6 Vertical sounding data at Fukuoka (solid lines) and the Cheju Island (dashed lines) at 2100 JST 27 September. WD=wind direction, WD=wind speed, Θ=potential temperature, Θe=equivalent potential temperature and RH=relative humidity.

just offshore Sasebo. The low wind region around the center was surrounded by strong wind regions with wind speed exceeding 15ms^{-1}, although a region of weak wind extended in the left-front quadrant. The detailed wind field near the center is not certain because of lacking data on the sea, but the sudden reversal of wind direction coinciding with the minimum pressure at Sasebo (Fig.8a) indicates the existence of a low wind zone corresponding to the pressure center.

After landfall (1700–1900 JST), surface wind and temperature fields showed following features.

(A) The vortex center defined from the distribution of wind direction roughly agreed with or was only slightly behind the pressure center.

(B) The distribution of wind speed shows a higher degree of asymmetry with regions of strong wind ~30km to the right of the center and 50–100km in the left-rear quadrant. Winds were relatively weak (<10ms^{-1}) in the left-front quadrant and within 50km of the center in the left-rear quadrant.

(C) Temperature was above 24°C to the right of the center, with no or weak rain. On the other hand, a region of low temperature (<22°C) and strong rain spread in the left-rear quadrant. This cold area nearly agreed with the strong wind area mentioned in (B). The front edge of this area had the character of a mesoscale cold front with a temperature gap of 2-3°C in a width of 20-30km.

(D) These features were maintained during the three hours 1700–1900 JST, but the region of weak wind tended to spread backward from the center with time. At 2000

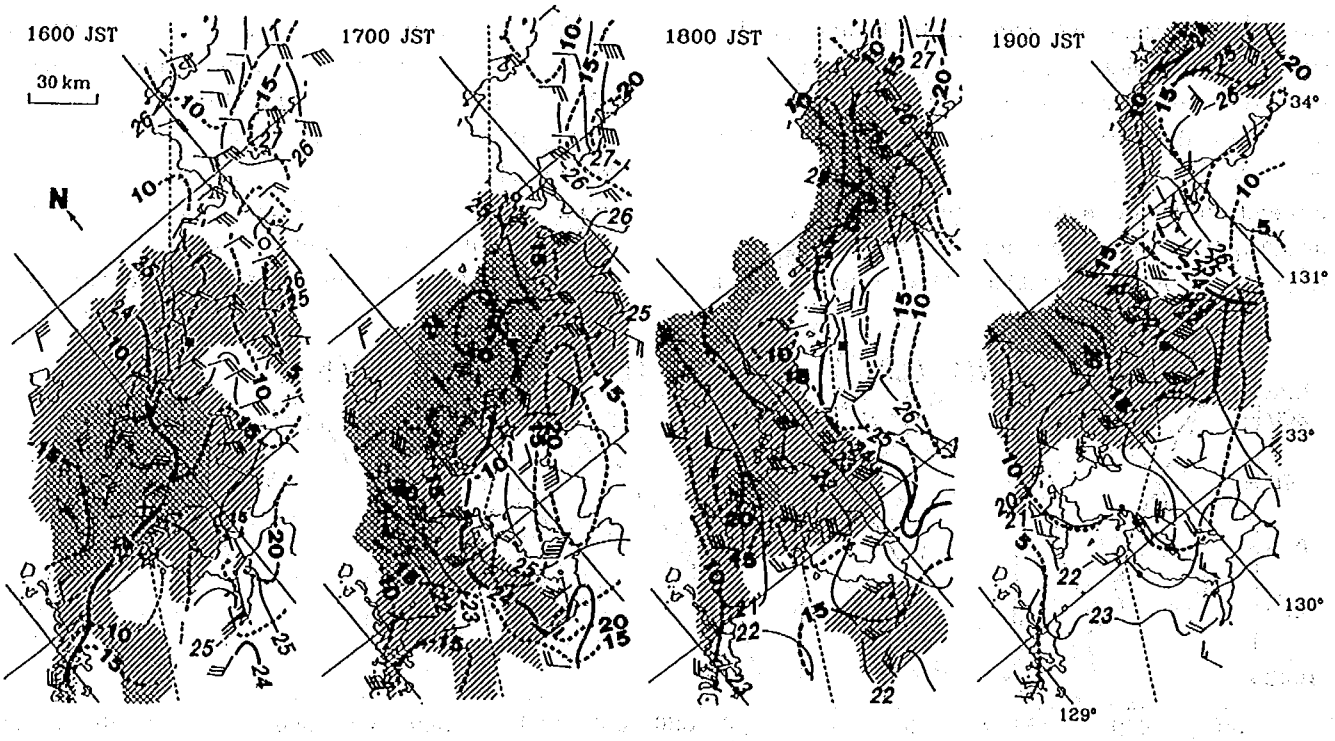


Fig.7 Composite fields of wind vectors (arrows), wind speed (heavy dashed lines; every 5ms^{-1}) and temperature (solid lines, °C) for 1600–1900 JST 27 September. Hatching indicates area in which precipitation in the preceding ten minutes exceeded 1mm and 4mm with increasing tones. The position of Fukuoka is shown in "■" (near the center of each map), and that of Sasebo is shown in "+" in the map for 1600 JST.

JST, the region of strong northwest winds lay 100–200km away from the center as shown in Fig.5.

The self-recording chart at Fukuoka (Fig.8b) indicates that (1) the easterly wind ahead of the typhoon was relatively weak, (2) wind direction shifted from east to west at almost the same time as the pressure minimum, although not so sharply as at Sasebo, (3) the wind speed was at the minimum after 1800 JST, which is more than half an hour later than the wind direction shift, and then (4) increased suddenly at 1825 JST accompanied by a temperature fall (3.5°C by 1900 JST) and heavy rain. The changes in (4) correspond to the passage of the mesoscale cold front mentioned above, and were observed at most stations along the track except for those on the west coast.

4. COMPARISON WITH OTHER TYPHOONS

For typhoons in the 1940's and 1950's, in which typhoons often caused great damage, many reports were issued by the JMA (Central Meteorological Observatory until 1956) including detailed description of surface wind fields. Figure 9 shows the composite wind field for T5029 (Kezia) which passed northward through Kyushu on 13–14 September 1950 (Ishimaru et al., 1951). The weak wind area in the pressure center (☆) extended for several tens of kilometers in the left-rear quadrant, and was surrounded by a strong wind area spreading from ~30km right of the center to 50–100km in the left-rear quadrant. On the other hand, the distribution of wind directions was nearly symmetric, although the vortex center lagged behind the pressure

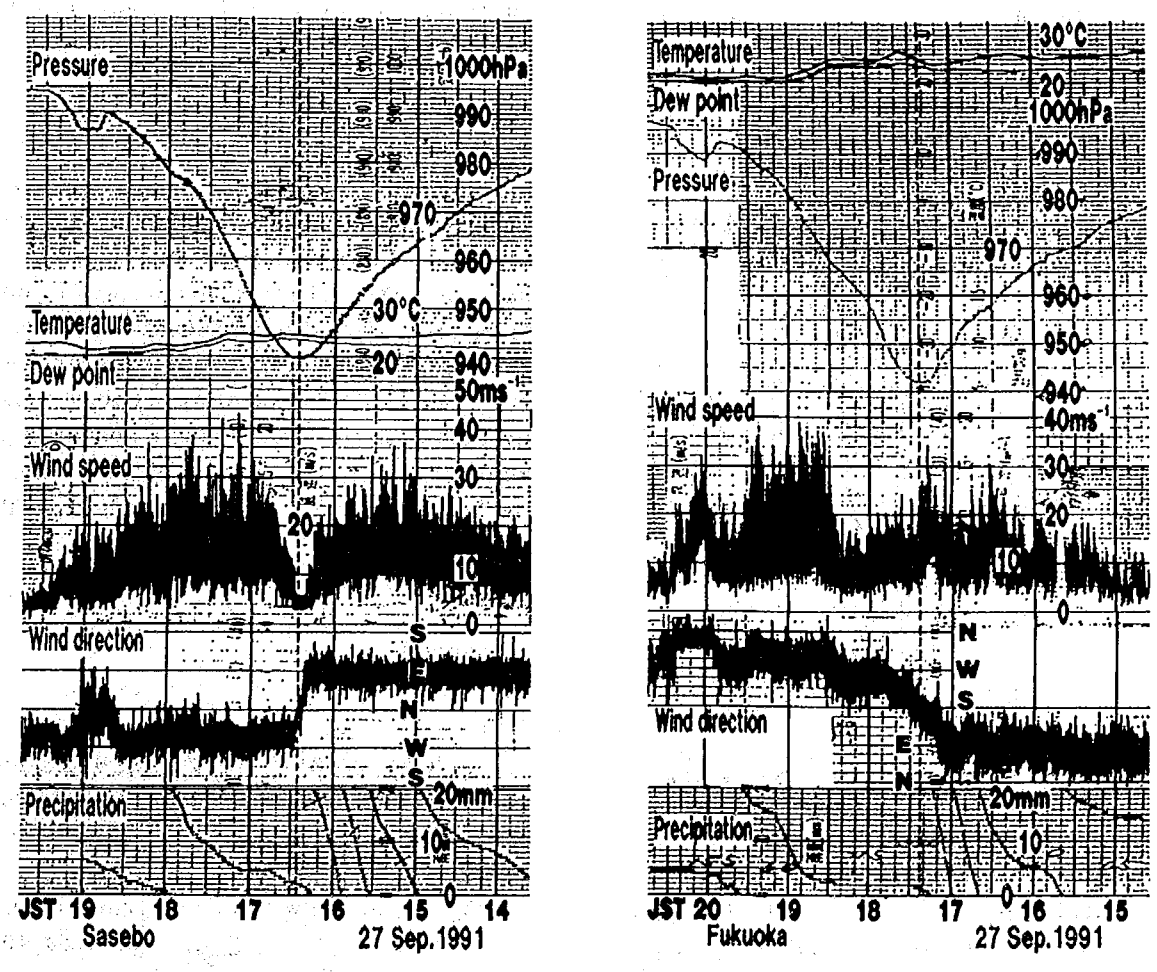


Fig.8 Self-recording charts at Sasebo and Fukuoka.

center by about 20km. These features are similar to those for T9119. Moreover, the strong wind area in the left-rear quadrant was associated with heavy rain as in the case of T9119, although the temperature drop with it was at most 1°C.

The weak wind area in the left-rear quadrant is found also in composite wind fields in other typhoons such as T5415 and T5822, and also can be recognized from self-recording charts near the track of many others. It appears to be general that this weak wind area becomes obvious with time, and is often associated with the formation of a mesoscale cold front.

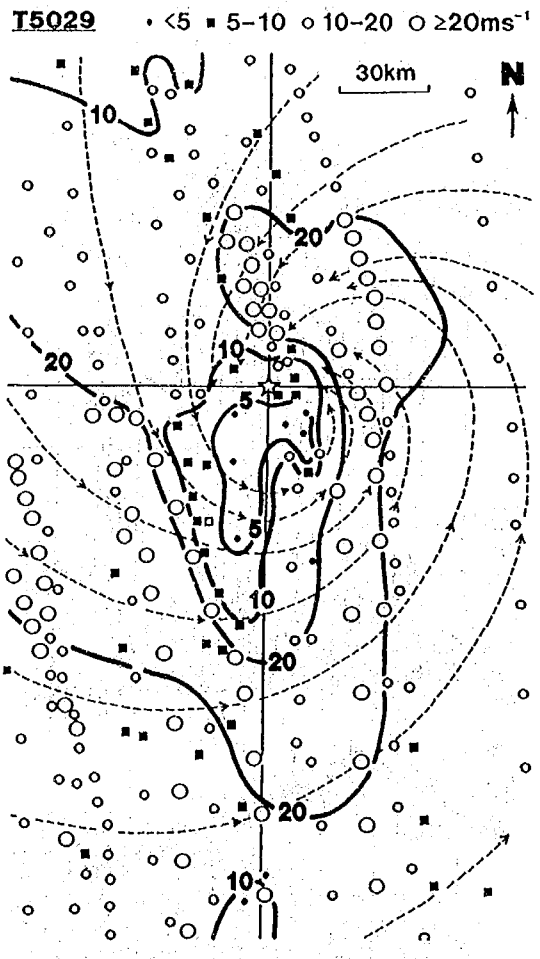


Fig.9 Composite fields of wind speed for T5029 (Kezia) passing northward through Kyushu. Dots, squares and circles indicate hourly observations of wind speed at JMA observatories, and thick solid lines indicate smoothed isotachs.

5. CONCLUDING REMARKS

The distribution of surface wind in T9119 was asymmetric with a weak wind area extending from the left-front quadrant to the left-rear quadrant of the center. This weak wind area was bounded by a mesoscale cold front followed by strong winds and low temperature. Similar features are found for many typhoons in the past.

From the standpoint of disaster prevention, it should be kept in mind that winds may be weak for an hour or so after the passage of the typhoon center, and then intensify suddenly.

Shapiro (1983) produced a weak wind area in the left-rear quadrant of a hurricane in a simple diagnostic model incorporating surface friction. However, further observational and theoretical studies will be required before relating his results to nonuniform wind fields in actual typhoons.

ACKNOWLEDGMENTS

Ten minute data at AMeDAS stations were collected with the aid of the Fukuoka District Meteorological Observatory. Hourly data at JMA observatories were obtained from data files in charge of the computer room of the Meteorological Research Institute (MRI). Self-recording charts were used by courtesy of the Typhoon Research Department of the MRI. This study was supported by "Special Coordination Funds for Promoting Science and Technology" of the Science and Technology Agency of Japan.

REFERENCES

Ishimaru, Y. et al., 1951: Report of the typhoon "Kezia". Mem. Cent. Meteorol. Obs., 35, 295–511 (in Japanese with English abstract).

Shapiro, L. J., 1983: The asymmetric boundary layer flow under a translating hurricane. J. Atm. Sci., 40, 1984–1998.

Damage of Buildings caused by Typhoon 9119

by
Hisashi Okada* and Tatsuo Murota**

Abstract

Typhoon 9119 caused severe damage to dwelling houses etc. in 1991. 1,056 houses were completely destroyed and 13,483 were partially destroyed. The casualties were 62 killed and 2,837 wounded. There were no typhoons caused such sever damage and injury in the these ten years.
This paper describes the records of wind speed of typhoon 9119 and the damage of buildings caused by typhoon 9119. A guide book for home builders and a pamphlet for the residents which were made after typhoon 9119 is introduced here.

KEYWORD: airborne debris
building damage ; gust factor ; typhoon

1. Introduction

Typhoon 9119 passed through the north-east side of Japan from September 27 to 28 in 1991, causing much damage in almost all parts of Japan. The numbers of completely and partially destroyed houses were 1,056 and 13,483 respectively. There were no typhoons caused such severe damage in these ten years. The casualties were 62 killed and 2,837 wounded. Power transmission towers and poles, forests, fruit trees and etc were also received sever damages.
In the damage of buildings, blown-off of roof tiles on dwelling houses attracted much attention. Authors surveyed the building damage in the north of Kyusyu and found about 80% of dwelling houses received damage on their roofing.
It was remarkable that the almost damage was caused not by flood and/or ground collapse but strong wind.
This paper describes the results of damage survey on the buildings.
A guide book for home builders and a pamphlet for residents, which were made after Typhoon 9119, will be briefly introduced here.

2. Meteorological records

2.1 History of Typhoon 9119

The track of typhoon 9119 are shown in fig.1. A tropical depression formed over the tropical South Pacific Ocean on the east of Marshal Islands on 13 September. Moving westward, the depression grew stronger. On 16 September, the central barometer became 1,000 hPa, maximum wind speed 18m/s. The transition from tropical depression to typhoon took place at that time. The definition of typhoon with the maximum wind speed is shown in Table 1, with the one of hurricane.
The typhoon turned to north-west on the east of Philippine Islands. Passing on the east of Miyako-jima Island, it turned to north-east. The typhoon continued growing on that way. The central barometer on the east of Philippine Islands was 925 hPa that was the lowest value on its life. The maximum wind speed was 50m/s at that time.
It landed on the south of Sasebo, Nagasaki, past 16 o'clock on 27 September. The central barometer was 940 hPa at landfall. The maximum wind speed was 50m/s, the area where wind speed was more than 25m/s having 300 km radius.
After crossing the north of Kyusyu, it moved through the Sea of Japan with rapid speed. It landed on Toshima peninsula, Hokkaido before 8 on 28 September. The central barometer was 955 hPa at re-landfall, the maximum wind speed was 40m/s and the area where wind speed was more than or equal 25m/s had 370 km radius. Typhoon 9119 moved to the Sea of Okhotsk after 10 on 28 September. It weakened to extratropical cyclone around 15 o'clock near the Kuril Islands.

2.2 Wind Speeds

Wind speed is measured in Japan by propeller type anemometer which has 8m distance constant. Therefore instantaneous wind speed is about 1 second average wind

* Head of Aerodynamics Section, Structural Engineering Department, Building Research Institute, Ministry of Construction
** Director of Structural Engineering Department, Building Research institute, Ministry of Construction

speed. Wind speed is required as 10 minute average wind speed.
Maximum wind speeds and maximum instantaneous wind speeds of typhoon 9119 were recorded at the all meteorological observation stations in Japan. The height of anemometers are different from each meteorological observation stations. Then maximum wind speeds at 10 m high above the ground were estimated by using the following equation.

$$U(10) = U(Z)\left(\frac{10}{Z}\right)^{0.2} \quad (1)$$

where,
U(10) = wind speed at 10 m high
U(Z) = wind speed at Z
Z = the height of anemometer.
Fig. 2 shows the distribution of maximum wind speeds at 10m high.

2.3 Gust Factors of Wind

Table 2 shows maximum wind speeds, maximum instantaneous wind speeds and wind speeds at the time recorded the maximum instantaneous wind speeds at meteorological observation stations in Kyushu. The ratios of maximum instantaneous wind speeds to wind speeds at the time recorded the maximum instantaneous wind speeds or gust factors of wind were required by Maeda [1]. Fig. 3 shows relation between the gust factor and wind speed. The gust factor shows decreasing inclination with increasing of wind speed. Gust factors of extra-tropical winds are said to be around 1.5. Based on the records of typhoon 9119, gust factors of typhoon are greater than those of the extra-tropical winds just as hurricanes' [2].

3. Building Damage and Injury

3.1 Statistics of Building Damage and Injury

Table 3 shows the statistics of damage and injury in every prefecture. Building damage was classified into following three levels.
Completely destroyed:
Floor area of damaged part of the building is more than or equal 70 % of the whole, or the cost of damaged main flame is more than and equal 50 % of the current price of the building.
Partially destroyed:
Floor area of damaged part of the building is less than 70 % and more than or equal 20% of the whole, or the cost of damaged main flame is less than 50% of the current price of the house.
Slightly damaged:
The damage is less than the state of partial destruction.
Following three rates expressing damage amount of buildings were required in each prefectures by Hayashi [3].

$$R.C = \frac{C.D}{T.H} \quad (2)$$

$$R.P = \frac{P.D}{T.H} \quad (3)$$

$$R.D = \frac{C.D+P.D+S.D}{T.H} \quad (4)$$

where,
R.C, R.P and R.D.= rates of Complete destruction , partial destruction and damage of houses, respectively
C.D., P.D. and S.D = numbers of houses completely destroyed, partially destroyed and sightly damaged, respectively
T.H. = number of households
The results are shown in table 2 and in Fig.3. The figure shows the north of Kyusyu and the north of Tohoku received sever damage.
The casualties were 61 killed and 2,837 wounded. Katsura[3] surveyed the causes to the death. The results shows in table 4. Attention should be paid to the result showing many people were blown off to death by strong wind and killed by airborne debris.

3.2 Building damage

Authors surveyed the building damage in the north of Kyusyu. The details of the survey results are described here.
The most remarkable damage on buildings was the one on roofings of dwelling houses. Photos 1 to 3 show the damage on roofings. Around 80% of dwelling hoses in the survey area received damage on their roofings. The popular roofings in the north of Kyusyu are cement roof tiles and clay roof tiles. Many of them were brown off by strong wind. Some of them were broken by attacking something airborne debris. Vinyl sheets were covered on the damaged roof as temporary measures. It took long period, from a few months to about one year, to restore them
Photos 4 and 5 shows dwelling houses whose roof frame works were broken. The dwelling houses received such damage were generally old. And many of them stood in the area where the wind seemed to be strengthened by the terrain. Followings are also considered to be the reason why the roof

frameworks were blown off; The blown-off of roofings leaded to the reduction of roof weight. Increasing in internal pressure occurred by the breakage of windows and/or external walls.
Public buildings like gymnasiums of schools were received their metal sheet roofings shown in photos 6 and 7. They were made from long sheets of metal. Once a part of them was lifted up, wind easily blew in the underneath of them. This resulted in the failure of the whole sheets.
Photos 8 and 9 show the damage on external walls and eaves soffits. The breakage of them often resulted in the increasing of internal pressures.
Photo 10 shows the damage of roof deck. In this case, supporting cantilever beams were rather long. Their fixed ends did not have adequate stiffness and strength. Therefore the beams largely deflected. This resulted in the damage of roof deck.
Photos 11 and 12 show the roof framework destruction. The roofings were light metal sheets and the joints of roof framework had not enough strength to resist wind lift forces.
Light steel frames for car ports and etc. were widely observed to have been destroyed as shown in photo 13.
Photos 14 and 15 show the damage caused by airborne debris. The debris were roof tiles, metal sheet roofings and etc.

4. A guide book and a pamphlet

A guide book and a pamphlet for the measure to the damage of dwelling houses due to strong winds were made after typhoon 9119. The work was done by the committee organized in the Building Center of Japan sponsored by prefectures in the north of Kyusyu. The guide book is for the home builders. Information on damage of dwelling houses due to strong winds, measures to airborne debris, design and execution to wind loads and etc. are summarized in it. Following is its content.

1. Damage of dwelling houses due to strong winds
2. Measures to airborne debris
3. Philosophy of the design to wind loads
4. Design and execution of dwelling houses
5. Maintenance

Appendix

·Examples of Design of dwelling houses to Wind loads

·Summary results of damage survey on dwelling houses and behaviors of residents in typhoon 9119

The pamphlet is for the residents. It gathers the information on measures and behaviors they should take before and during strong winds.

Concluding Remarks

1.Typhoon 9119 caused severe damage on buildings.
2.Damage on roofings were especially serious.
3. Damage of roofings produced much airborne debris. And airborne debris promoted to cause further damage.
4. A guide book and a pamphlet were made after typhoon 9119. They are expected to defuse the information on appropriate design of housing to wind loads and actions before and during strong winds.

Reference

[1] "Survey report on typhoon 9119 damage" ,all in Japanese, Building Center of Japan, 1993
[2] "Gust Factors Applied to Hurricane Winds", W.R.Krayer and R.D.Marshall, Bulletin American Meteorological Society, Vol. 73, No.5, May 1992
[3] "Study on Wind Damage and Injury caused by Typhoon 9119", all in Japanese, Study Group on Natural disaster, August 1992

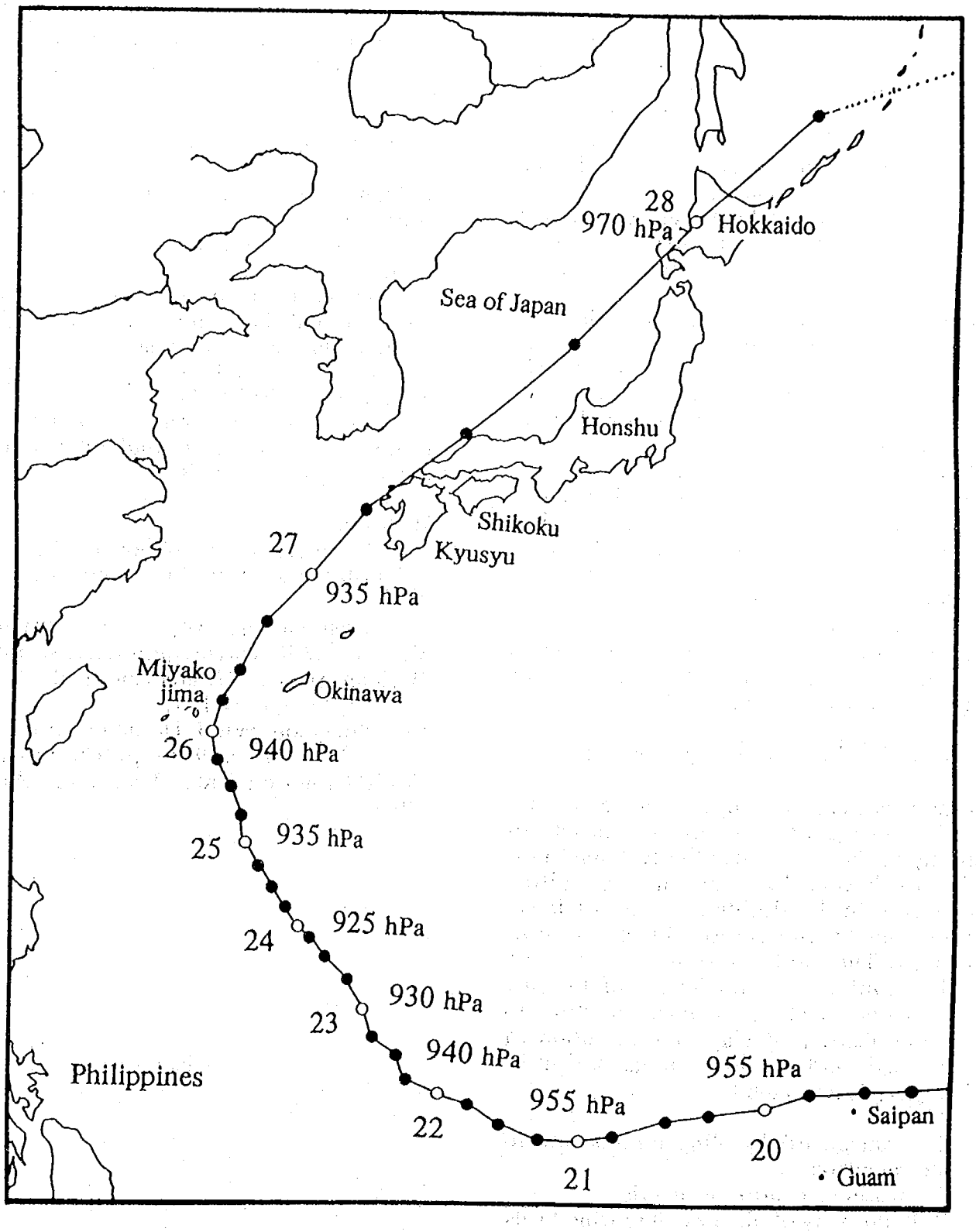


Fig.1 The track of Typhoon 9119

Table 1 Wind Speeds of Typhoon and Hurricane

	Maximum wind speed (m/s)											
	9		17		25		35		45		55	
Typhoon	Tropical depression	Weak tropical storm	Typhoon									
			weak		medium		strong		very strong		violent	
Hurricane	Tropical depression	Weak tropical storm	Topical storm				Hurricane					

Table 2 Maximum Wind Speeds and Maximum Instantaneous Wind Speeds in Kyusyu

No.	Observation. station	Meas. height	Maximum wind			Maximum instantaneous wind speed			Mean wind at the max. of ins.wind s.	
		(m)	Speed (m/s)	Dir.	D/Time. d. h. m	Speed (m/s)	Dir.	D/Time d. h. m	Speed (m/s)	Dir.
837	Tanega-shima	10.6	19.4	SW	27 17 20	35.7	S	27 14 10		
836	Yaku-shima	9.9	12.8	S	27 13 10	34.8	SSW	27 14 35	12.6	SSW
831	Makurazaki	10.4	27.1	S	27 14 30	49.9	SW	27 15 25	21.8	SW
827	Kagoshima	22.0	19.3	SE	27 14 40	44.5	S	27 15 21	17.7	SSW
823	Akune	13.4	23.0	WSW	27 17 0	42.0	WSW	27 16 59	23.0	WSW
829	Miyako-nojo	11.7	17.0	SSE	27 12 30	39.0	SSE	27 12 26	17.0	SSE
835	Aburatsu	19.0	27.7	SW	27 15 30	41.5	S	27 13 34	24.5	SSW
830	Miyazaki	21.2	16.0	SSE	27 14 40	33.1	SSE	27 14 35	16.0	SSE
822	Nobeoka	13.2	19.0	S	27 16 40	40.0	S	27 16 32	19.0	S
838	Ushibuka	20.6	27.0	SE	27 14 30	52.1	SW	27 16 16	23.8	SW
824	Hitoyoshi	12.1	21.1	SSE	27 15 30	48.8	SSE	27 15 27	21.1	SSE
819	Kumamoto	14.8	25.8	S	27 16 50	52.6	S	27 16 52	23.3	S
821	Mt. Aso	10.2	30.2	S	27 16 20	60.9	SW	27 18 25	28.2	SW
817	Nagasaki	18.7	25.6	W	27 17 20	54.3	SW	27 16 41	21.5	WSW
843	Fukue	10.3	24.7	NNW	27 15 30	47.5	NNW	27 15 28	24.7	NNW
812	Sasebo	13.1	17.6	ENE	27 15 40	42.1	W	27 17 20	16.5	W
805	Hirado	11.0	26.8	NW	27 17 30	49.5	NW	27 17 16	26.4	NW
800	Iwahara	12.9	22.5	NNW	27 18 0	42.6	NNW	27 17 57	22.5	NNW
813	Saga	25.5	29.1	SE	27 16 40	52.6	SSE	27 16 46	26.7	SSE
807	Fukuoka	24.5	18.3	NNW	27 20 10	44.6	WNW	27 18 47	18.3	WNW
809	Iizuka	11.1	22.3	S	27 17 40	48.3	SSE	27 17 37	22.3	S
814	Hita	10.6	16.7	SSW	27 17 50	44.4	SSW	27 17 58	15.5	SSW
815	Ohita	19.8	18.3	SSW	27 18 50	38.3	SSE	27 17 14	17.3	SSE
762	Shimonoseki	30.6	24.0	W	27 19 50	45.3	ESE	27 17 42	21.4	ESE

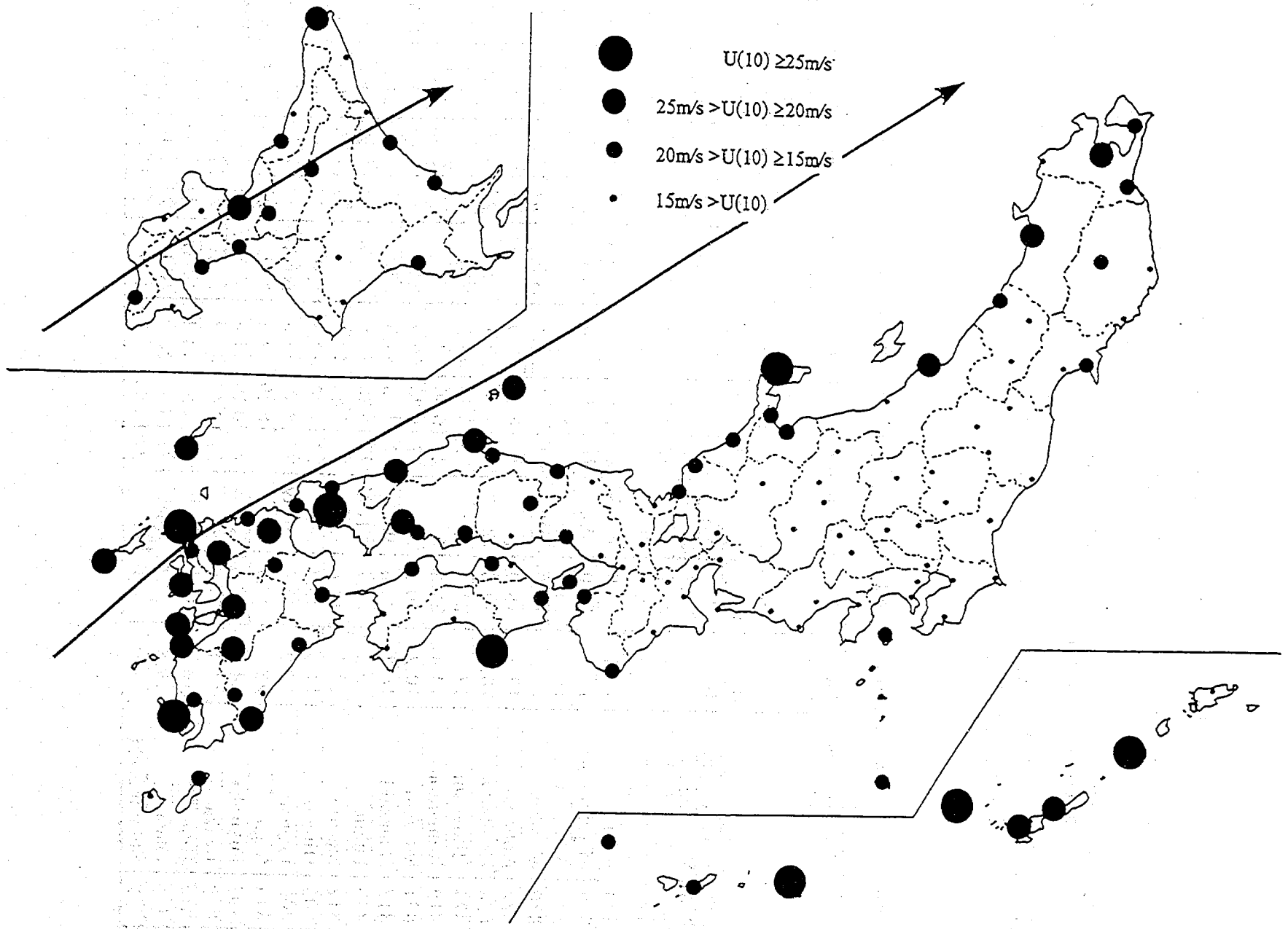


Fig.2 The distribution of maximum wind speed at 10 m high

Table 3 Casualties and Damage of Houses

Prefecture	Dea-th	Injury		Number of household	Number of damage houses			Damage ratio of houses (%)		
		serious	slight		C.D.	P.D.	S.D.	R.C	R.P	R.D
Hokkaido	1	0	6	2,166,723	0	0	104	0.00	0.00	0.00
Aomori	9	41	213	453,251	110	1,716	12,844	0.02	0.38	3.24
Iwate	0	2	24	438,671	0	37	353	0.00	0.01	0.09
Miyagi	0	1	0	718,111	0	0	2	0.00	0.00	0.00
Akita	5	33	133	358,644	55	385	14,878	0.02	0.11	4.27
Yamagata	1	2	4	344,285	0	8	367	0.00	0.00	0.11
Fukushima	0	0	1	615,544	0	0	30	0.00	0.00	0.00
Ibaraki	0	1	0	853,852	0	0	27	0.00	0.00	0.00
Tochigi	0	0	0	587,180	0	0	1	0.00	0.00	0.00
Gunma	0	0	0	615,480	0	0	0	0.00	0.00	0.00
Saitama	0	0	0	2,154,794	0	0	18	0.00	0.00	0.00
Chiba	0	0	0	1,864,062	0	0	0	0.00	0.00	0.00
Tokyo	0	0	0	4,949,217	0	0	2	0.00	0.00	0.00
Kanagawa	0	0	0	2,916,732	0	0	4	0.00	0.00	0.00
Niigata	1	2	29	707,779	1	27	5,152	0.00	0.00	0.04
Toyama	0	4	8	319,297	1	4	132	0.00	0.00	0.73
Ishikawa	1	14	40	360,841	7	86	11,747	0.00	0.02	3.28
Fukui	0	3	14	234,234	2	11	1,694	0.00	0.00	0.73
Yamanashi	0	0	0	272,194	0	0	6	0.00	0.00	0.00
Nagano	0	0	0	658,283	0	5	55	0.00	0.00	0.01
Gifu	0	0	4	607,269	1	0	59	0.00	0.00	0.01
Shizuoka	0	0	0	1,145,896	0	0	0	0.00	0.00	0.00
Aichi	0	0	1	2,224,209	0	0	2	0.00	0.00	0.00
Mie	0	0	0	556,919	0	0	19	0.00	0.00	0.00
Shiga	0	0	0	369,731	0	0	3	0.00	0.00	0.00
Kyoto	0	0	15	911,474	1	2	1,020	0.00	0.00	0.11
Osaka	2	1	10	3,126,952	0	1	14	0.00	0.00	0.00
Hyogo	0	13	53	1,825,580	3	47	5,527	0.00	0.00	0.31
Nara	0	0	0	441,888	0	0	1	0.00	0.00	0.00
Wakayama	0	0	0	351,463	0	0	1	0.00	0.00	0.00
Tottori	3	0	0	191,294	2	48	453	0.00	0.03	0.26
Shimane	1	21	81	235,014	10	176	29,878	0.00	0.07	12.79
Okayama	0	5	13	640,388	6	49	3,932	0.00	0.01	0.62
Hiroshima	6	4	45	1,024,211	50	442	22,661	0.00	0.04	2.26
Yamaguchi	6	30	209	534,584	35	650	36,018	0.01	0.12	6.87
Tokushima	0	0	2	262,082	1	4	107	0.00	0.00	0.04
Kagawa	0	0	7	327,100	0	0	91	0.00	0.00	0.03
Kochi	1	0	0	293,742	1	3	16	0.00	0.00	0.01
Ehime	1	2	47	512,715	64	158	4,406	0.01	0.03	0.90
Fukuoka	11	97	669	1,693,032	263	4,042	180,544	0.02	0.24	10.92
Saga	0	18	68	253,555	23	673	34,208	0.01	0.27	13.77
Nagasaki	5	43	214	503,328	158	2,453	87,955	0.03	0.49	17.99
Kumamoto	4	391		578,862	172	1,408	147,280	0.03	0.24	25.72
Oita	1	13	103	416,600	78	942	56,532	0.02	0.23	13.81
Miyazaki	0	1	15	397,000	1	2	206	0.00	0.00	0.05
Kagoshima	2	11	54	664,767	10	100	7,239	0.00	0.02	1.11
Okinawa	0	0	2	378,741	1	4	43	0.00	0.00	0.01
Total	61	2,837		42,057,570	1,056	13,483	665,631	0.00	0.03	1.62

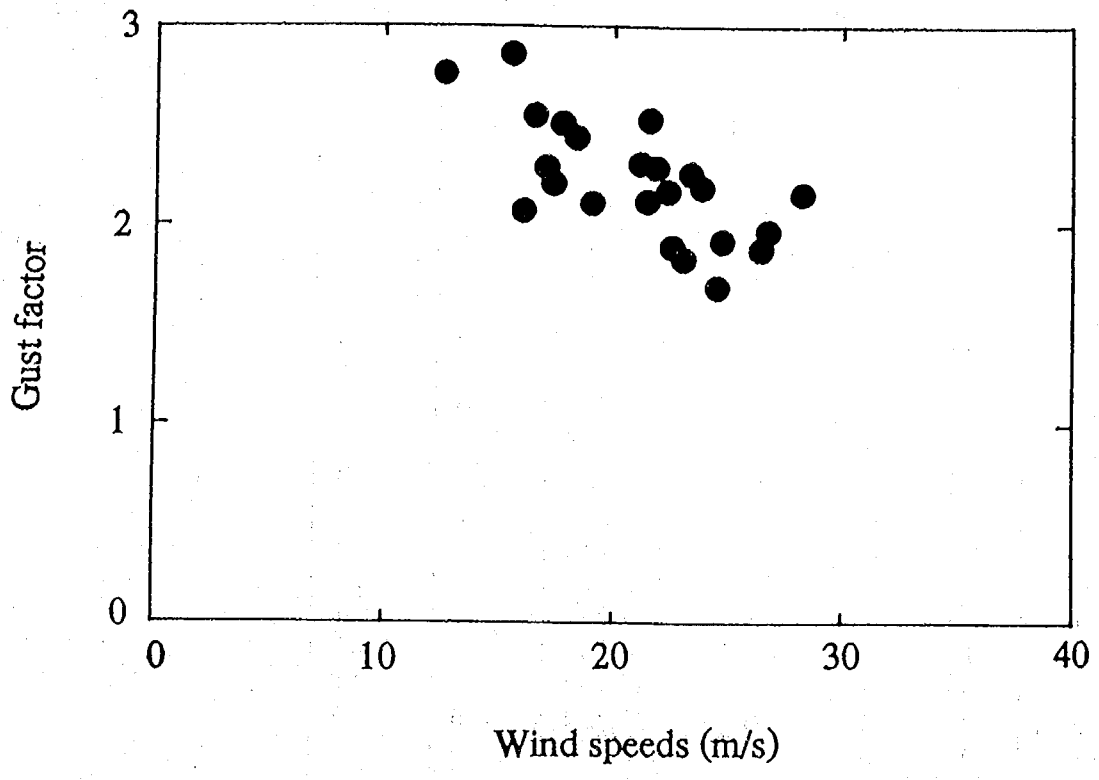
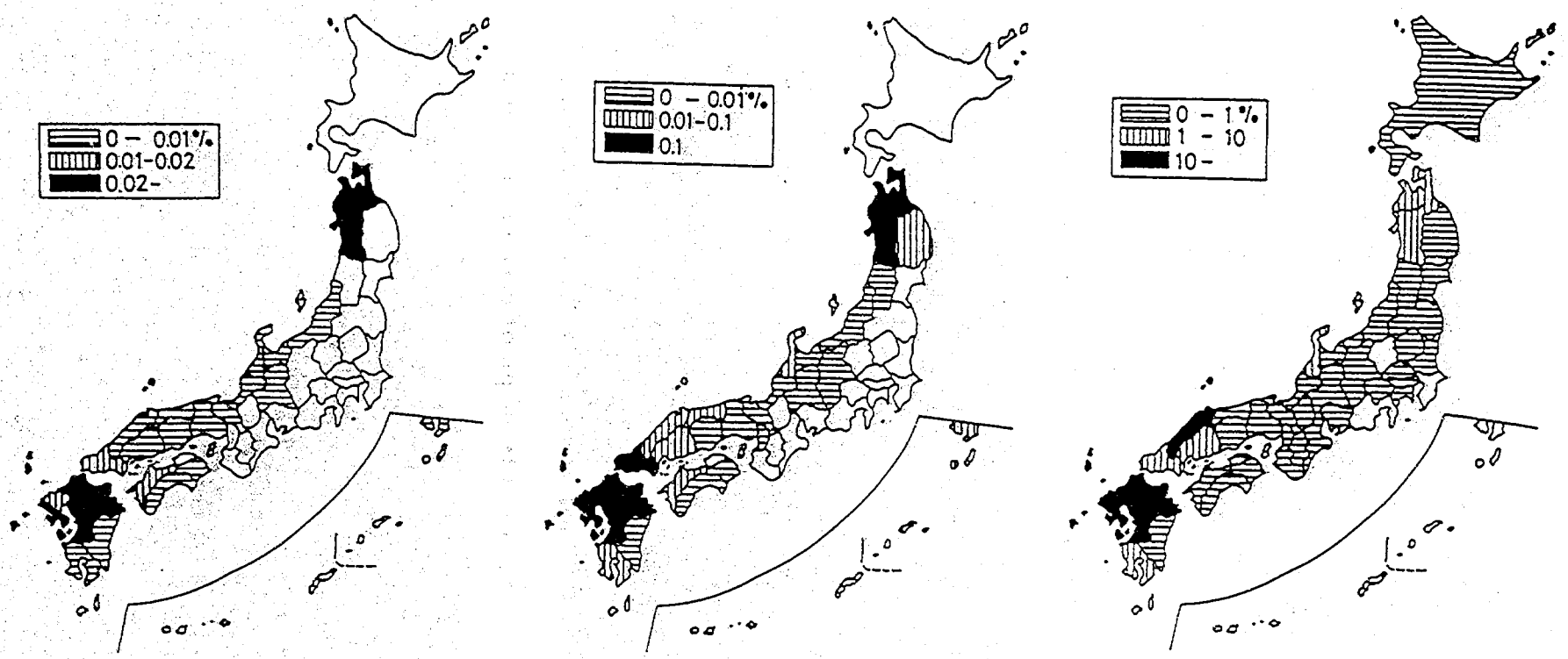


Fig.3 Relation between gust factors and wind speeds

Table 4 Causes of the Death

Cause	Number
fall and drowned in the sea	10
hit by airborne debris	14
clashed under buildings etc.	18
blown-off by strong wind	19



(a) rate of complete destruction (b) rate of partial destruction (c) rate of damage

Fig.4 Distribution of damage rates of houses



Photo. 1 Damage site in Nagasaki;
The roofs damaged are covered with vinyl sheets



Photo. 2 Damage of cement roof tiles

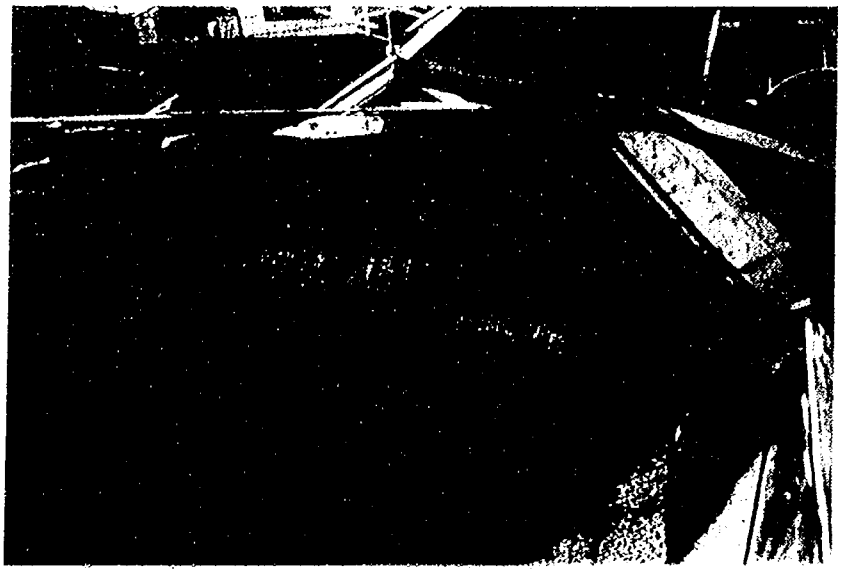


Photo. 3 Damage of asphalt singles

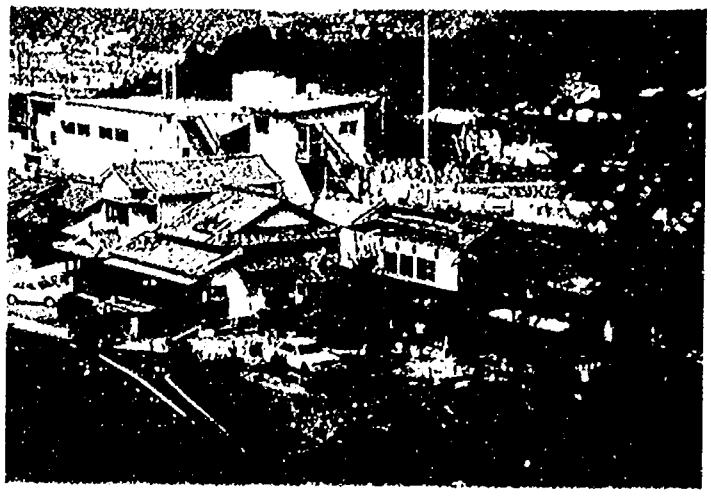


Photo. 4 Roof framework was destroyed.



Photo. 5 Old house received serious damage.

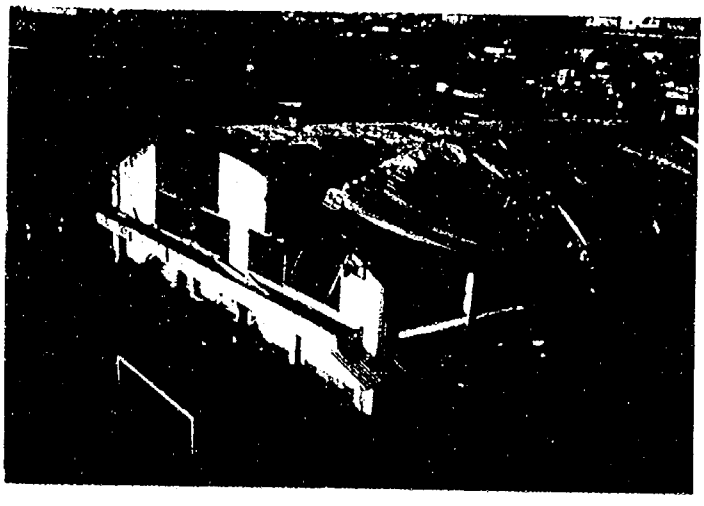


Photo. 6 Steel roofings on barrel roof were removed.

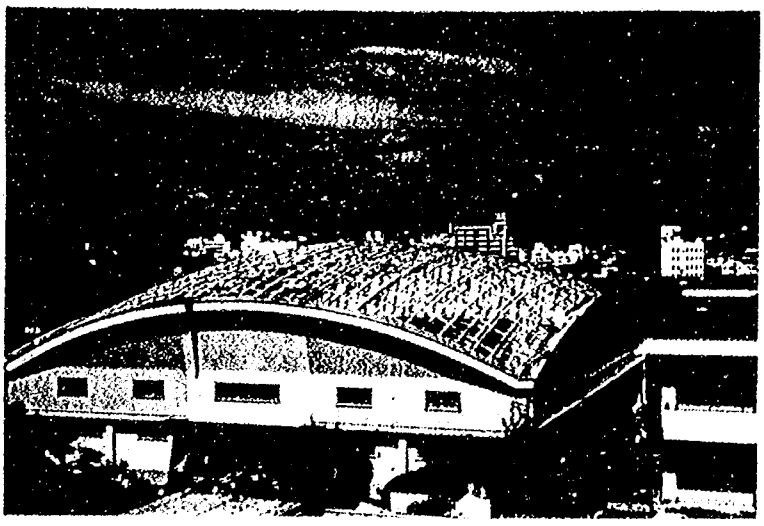


Photo. 7 Roofings were completely blown off.



Photo. 8 External walls were removed.



Photo. 9 Wind blows into the roof framework through the damage eaves

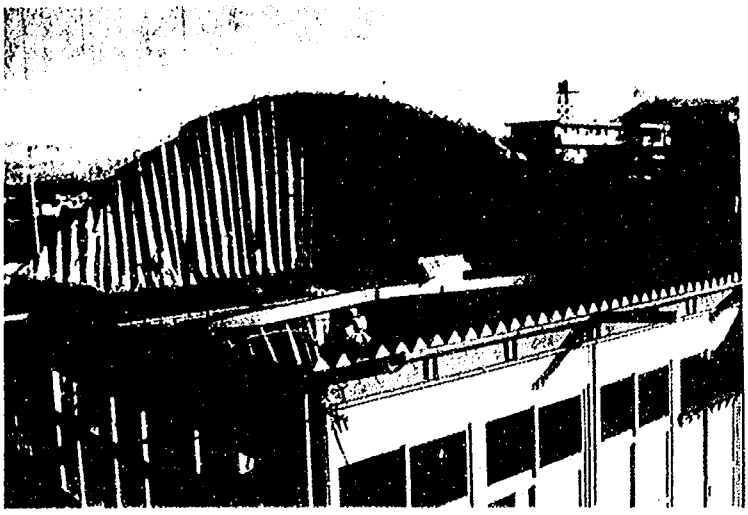


Photo. 10 Metal roof deck was lifted.



Photo. 11 Destruction of roof with metal roofing.

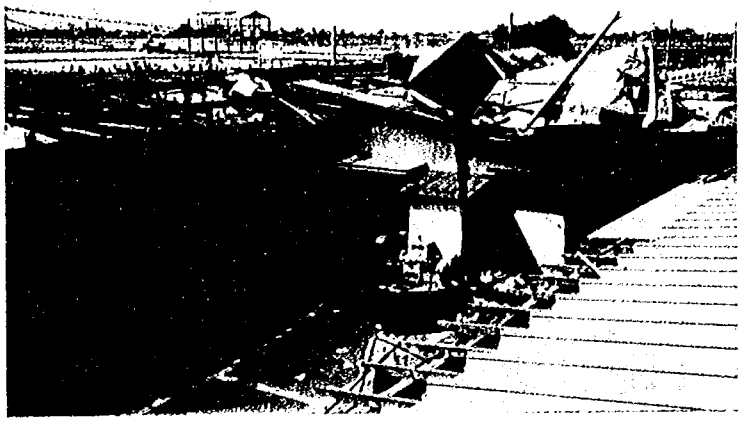


Photo. 12 Roof framework were blown off.



Photo. 13 Destruction of light frame car port



Photo. 14 Breakage of the external wall due to airborne debris



Photo. 15 Metal roofings attacked windows.

Offshore Platform Damage Assessment in the Aftermath of Hurricane Andrew

by

Charles E. Smith*

ABSTRACT

During the period of August 24-26, 1992, Hurricane Andrew, a storm with sustained wind velocities over 145 mph, caused extensive damage to offshore oil and gas facilities in its path through the Central Gulf of Mexico (GOM). Approximately 2000 of the 3852 structures in place on the U.S. Outer Continental Shelf (OCS) were exposed to hurricane force winds. One hundred sixty-four structures were toppled, are leaning, or were condemned. Many more suffered some form of structural damage to the topsides.

The intent of this paper is to document damage to OCS structures in the aftermath of Hurricane Andrew and to assess the important engineering aspects relative to the storm. Damage will be correlated with platform characteristics such as wind, water depth, and distance to shore, as well as data from environmental hindcast studies. Although no offshore fatalities were attributed to the storm, more than one-third of the oil and one-fifth of the gas production in the GOM were shut-in.

KEYWORDS: Gulf of Mexico; hurricane damage; offshore platforms; oil and gas operations; wind; wind speed.

1. INTRODUCTION

Hurricane Andrew's passage through the center region of the GOM in late August 1992, wrecked unprecedented damage to oil and gas structures and pipelines located on the OCS off Louisiana. The range of damaged facilities include mobile drilling rigs, offshore platforms and satellite wells, topside systems including well heads and production handling and processing equipment, risers, and pipelines. Reference 1 provides an overview of the damage and the impact of the storm on offshore oil and gas operations. In all, one hundred sixty-four structures were toppled, are leaning, or were damaged to such a degree they have been condemned. Many more suffered some form of structural damage. Three hundred ninety-six segments of pipeline were reported damaged. Seven pollution events and two fires occurred, and five mobile drilling rigs were set adrift.

Despite the damage encountered in the direct path of the hurricane, the evacuation of

*Research Program Manager
Technology Assessment and
Research Branch
Minerals Management Service
Herndon, Virginia 22070-4817

employees from installations and the shuting-in of operations in advance of the storm saved lives and helped to minimize any environmental pollution. Although no offshore fatalities were reported, more than one-third of the oil, 270,000 barrels of oil per day (BOD), and one-fifth of the natural gas capacity, 2.75 billion cubic feet of gas per day (BCFGD), were temporarily lost. Prior to the hurricane, GOM facilities produced approximately 750,000 BOD and about 17.5 BCFGD. To date, all but 2 percent of the oil and gas production has been restored. Some production will be lost permanently due to the prohibitive costs associated with replacing or repairing structures on marginal or near-depleted reservoirs.[1]

The storm struck the South Timbalier, Ship Shoal, South Pelto, and Eugene Island regions the hardest. Figure 1 shows the general track of Andrew through these regions. These regions are some of the oldest producing areas in the Gulf with the older platforms dating back to the late 1940's. These tracks are covered with numerous platforms and single-well caissons installed at a time when design criteria were evolving by trial and error. Figure 2 provides a breakdown of the number of toppled or leaning structures. The term structure, in the context of this paper, refers to either a platform or satellite facility. A platform is defined as a steel jacket structure which would support a multi-well complex with major production processing capabilities. A satellite structure is usually classified as a single-well caisson or a very small structure supporting one or two wells with very limited production processing capabilities. Figure 3 illustrates a slightly damaged satellite structure, and Figure 4 shows major damage to a platform. A leaning caisson is shown in Figure 5 and represents a typical failure pattern to a single well satellite facility.

The response of the structures subjected to the might of Hurricane Andrew's forces are and will remain of great interest to the oil and gas industry and to relevant government regulatory agencies. It is estimated that 2000 of the approximately 4000 GOM structures were exposed to hurricane force winds. Of these 2000, eight hundred were designed and installed before 1976, after which the API developed more stringent design criteria. Before this time, many structures were designed for the 1 in 25-year storm as opposed to the currently used 100-year criterion. Also, of particular importance was the assessment of deck heights above the mean water level. The newer standards call for a five-foot air gap above the design wave crest to prevent water impacting the deck structure. Table 1 provides a brief update on changes in the API RP 2A which have occurred and are of significance to the assessment of integrity of older platforms. A preliminary assessment of the structures that failed indicated that if they had been designed to current standards, most would have survived the storm.

2. STRUCTURAL DAMAGE

Figure 6 shows the distribution of damaged platforms and satellites versus water depth, and Figure 7 shows the

distribution versus year installed. Sixty-eight percent of the platforms and ninety-eight percent of the satellites which failed were in less than 100 feet of water. This reflects somewhat on the age of the structures (i.e., earlier exploration was in shallow water) as well as the type of structure used to produce the field (i.e., the satellite structures are very economical for shallow water locations).

Figure 7 indicates that the majority of the platforms which failed were installed before 1976. As stated previously this is about the time that industry standards were improved. For example, during the period 1955-1964, the maximum design wave was felt to be approximately 59 feet with a drag coefficient of 0.5. The water current velocity was not included with wave water particle velocity in determining the force on the structure. In 1965, the maximum design wave was still felt to be about the same; however, it was recommended that the current should be included in determining the force on the structure. In 1976, based on research and observed failures in other hurricanes, the reference wave was increased to 72 feet and the drag coefficient was raised to 0.6. These requirements produced a much stronger structure. But more importantly, it raised the decks of the structures to prevent the dramatic increase in loading due to the crest of the wave inundating the lower decks. To further mitigate this concern, the API later adopted a standard calling for a 5-foot air gap above the wave crest elevation and included a provision for a reference level storm tide.[2]

Figure 7 would seem to dispute the early age argument as far as satellite structures are concerned. However, single-well caissons were very popular for developing small reservoirs in shallow water in the late 1970's to mid-1980's. Standards for the installation of caisson-type structures were not developed until 1987, and the lack of design guidelines could account for the greater number of failures of structures installed before this date. The Minerals Management Service (MMS) issued a policy statement in 1989 which provided basic guidelines regarding the design and installation of such structures.[3] It stated that since permanent freestanding caissons serve as well protectors and/or small platforms for producing wells, and as such, must be designed in accordance with the applicable provisions of 30 CFR 250, Subpart I, "Platforms and Structures." The geotechnical requirements were relaxed somewhat so that a soil boring taken within a one-mile radius of the site could be acceptable as being representative of a boring taken at the site.

Figure 8 shows the distribution of failed structures versus the distance in miles from shore. The majority of failed structures are within 25 miles of the shore. Again, this is indicative of the age of the platforms and the use of satellite facilities in shallow water. The Mississippi Delta region of the GOM is very shallow out to the Continental Slope. The engineering geology on the slope is among the most complex of any offshore area in the world where mudflows present major hazards to exploration and

production activities. Lacking the current technology to meet these problems, the older platforms were placed on sites in the more secure shelf region (i.e., closer to shore). Satellite structures proved to be the most economical method of developing shallow water areas, and platforms were moved into deeper waters.

3. ENVIRONMENTAL CONDITIONS

Andrew originated as a tropical depression on August 16, 1992, in the South Atlantic and began a northwesterly track toward North America. The storm grew in intensity and on the morning of August 22, 1992, it was officially classified as the first hurricane of the 1992 season. Andrew continued on a northwesterly course and wrecked widespread destruction across the Bahamas and the southern Florida peninsula where wind speeds in excess of 160 mph were recorded.[4] The storm lost some intensity passing over land, but it regained force as it advanced westward over the warm waters of the GOM before hitting the heart of the U.S. offshore oil and gas operations.

Table 2 provides a comparison between Hurricane Andrew's characteristics and those of several other major hurricanes as they came ashore along the Gulf Coast.[5] As a category 4 hurricane on the Saffir/Simpson Scale, Andrew probably approached the conditions of a 200-year design storm as it passed over the deeper waters of the Grand Isle Area. Losing strength as it made landfall, Andrew's intensity was probably less than the specified 100-year event for the shallow water sites in the GOM.

Since very little information is available from actual storm measurements, the industry has had to rely on data developed from reliable hindcast studies to obtain values of surface winds, waves, currents, and surges within the track of the storm. Figure 9 is a sample of the results for the maximum significant wave height developed by a confidential industry study for the purpose of evaluating the performance of offshore facilities.[6] To protect the confidentiality of the data, the numerical values of the contours have been removed. It is of interest to note that the hindcast study predicted the highest load intensities to the east of the storm track in the exact areas where the largest number of damaged and/or toppled structures occurred. The light and dark dots in Figure 10 represent heavily damaged or collapsed structures.

The chart shown in Figure 11 provides the distribution of the number of leaning or toppled structures versus the significant wave height predicted from the hindcast study conducted in Reference 6. The data reflect the same general distribution as that found in Figure 6 depicting the correlation between failures and water depths. One conclusion which might be drawn from these data is that as the large waves moved into shallower waters they started "feeling" the seafloor, grew steeper and broke against the structures in their path. The tremendous forces generated by the breaking waves, especially if they were high enough to inundate the decks, could account for the large number of failures in the 25-75 foot water depth.

4. CURRENT EFFORTS

The damage considered thus far has all been observed from the water surface. There is a strong possibility that major underwater damage exists, especially on some of the older, less-maintained steel jacket platforms. As a result of these concerns, the MMS issued Notice to Lessees and Operators (NTL) No. 92-07 to require companies with platforms in the path of the hurricane to conduct underwater inspections of those structures to determine whether any damage exists.[7]

The mandatory inspections are required on all platforms located within 50 miles northeast of the path of the eye of Hurricane Andrew and within 35 miles on the southwest side. In all, about 700 platforms will be inspected. To date (May 1993), the inspections have not been completed. However, the results obtained thus far have indicated that underwater damage is very light and not of the magnitude as first thought.

To better understand the performance of OCS facilities during a major storm event, the MMS initiated an in-house study to assess the impact of Hurricane Andrew. The information to be gathered and analyzed will be vital for evaluating past and present platform design criteria, topside facility designs, and current regulatory requirements for safety and pollution prevention systems on OCS facilities. The project will consist of the following major subsets as shown in Figure 12:

- *Loss and damage assessment ;*
- *Oceanographic and meteorological forcing functions and hindcast studies;*
- *Failure analyses, modeling, and reporting; and*
- *Design and inspection criteria, operational findings, and recommendations.*

The industry, in a like manner, initiated a joint industry project (JIP) to amass the information gained from platform failures as well as survivals during Hurricane Andrew and apply that knowledge base in the management of existing platforms. The main objectives of the JIP are as follows:[8]

- *Provide comprehensive documentation on the platforms affected (survived, damaged, or failed) by Hurricane Andrew;*
- *Provide an evaluation of how and why platforms survived;*
- *Provide an assessment of methods that can be used to forewarn of similar problems in future large storms; and*
- *Perform a calibration, using a reliability format to update and adjust, where necessary, current practiaces for assessing the intensity of existing platforms.*

Figures 13 and 14 show, in simple terms, how the calibration wil be performed. The project should improve industry's ability to make informed decisions concerning the structural integrity of platforms, thereby improving the cost-effectiveness and safety measure for future operations. It will enable the operators to anticipate future standards and

regulations in reference to any proposed platform reassessment process. The MMS is participating in this project as a member of the JIP.

Also, on behalf of the industry, the API, through the Fixed Criteria Subcommittee, has initiated a significant effort to establish a section in RP 2A covering the topic of "Assessment of Existing Structures for Determination of Fitness." As part of this initiative, API held a workshop to address the response of structures to Hurricane Andrew. It is envisioned that provisions providing guidance on the assessment of existing structures will be incorporated into API standards in the near future.

5. CONCLUSIONS

Hurricane Andrew caused an unprecedented amount of damage to offshore oil and gas facilities in the GOM. The monetary damage to offshore operations as a result of the storm could well be in excess of $1 billion. Approximately 14 platforms and 28 satellite structures were toppled, and many more are leaning, some to the extent that they will be removed from service. Many other platforms experienced some form of damage to their topside facility. A complete tally of damaged platforms will not be possible until the underwater inspections have been conducted and the data analyzed. Major failures which did occur were predominantly on platforms installed before 1976 or to satellite structures installed before 1987. In both instances, failures occurred before significant improvements were made in their respective design standards.

The fact that many of the older structures withstood a near direct hit from the storm, yet suffered little or no damage, provides considerable confidence as to their integrity, even though they do not meet today's design criteria. The MMS and the industry are jointly studying damages associated with the Andrew experience in order to assess the impact on and to calibrate future reassessment methods. Due to the preventive measures taken by the industry, no loss of life was contributed to offshore operations; and even though some release of products occurred, the amount of pollution was held to a minimum.

6. REFERENCES

1. Smith, C.E., "Effects of Hurricane Andrew on Offshore Oil and Gas Facilities," Proceedings, International Workshop on Wind and Earthquake Engineering for Offshore and Coastal Facilities,Yokosuka, Japan, May 12-13, 1993.

2. American Petroleum Institute Recommended Practice for Planning, Designing and Constructing Fixed Offshore Platforms, API Recommended Practice 2A (RP2A).

3. "Conditions for Approval of Freestanding Caissons Application," Minerals Management Service Memorandum, New Orleans, August 30,1989.

4. Reinhold, T.A., Vickery,

P.J., and Powell, M.D., "Wind Speeds in Hurricane Andrew: Myths and Reality," American Concrete Institute, San Juan, Puerto Rico, October 1992.

5. Structure Response Due to Hurricane Andrew," Open Meetin Organized by the API Offshore Standardization Committee and the Fixed System Criteria Subcommittee, Houston, Texas, October 1992.

6. Cardone, V. J. and Cox, A.T., "Hindcast Study of Hurricane Andrew (1992) Offshore Gulf of Mexico," Oceanweather Inc., November 1992 (Confidential Study until October 31, 1994).

7. "Structural Damage Caused by Hurricane Andrew" Notice to Lessees and Operators; No. 92-07; Minerals Management Service,New Orleans September 17, 1992.

8. "Hurricane Andrew Effects on Offshore Platforms; Proposal for a Joint Industry Project," PMB Engineering, Inc., San Francisco, California, September 1992.

TABLE 1. UPDATES OF API RP 2A
SIGNIFICANT TO PLATFORM ASSESSMENT
(Taken from Reference 5)

DATE	EDITION	CHANGE
1969	1st	o Note: Drag and mass coefficient minimums of 0.5 and 1.3
1971	2nd	o Minimum mass coefficient raised to 1.5
1/72	3rd	o Punching shear equation introduced for simple joints o Fatigue first addressed by limiting nominal brace stress to 20 ksi
10/72	4th	o Punching shear equations expanded to address design rigorously and to include all joint types. T, K&Y and Cross joints are designed identically
1975	6th	o Minimum drag coefficient raised to 0.6 o First addressed axial and bending interaction. Introduced chart of "k" and "Cm" factors
1976	7th	o Included reference level wave height for GOM
4/77	8th	o First reference to API-2H steel for consideration in joint cans o First specific recommendations when a detailed fatigue analysis is needed
11/77	9th	o Included reference level wave height for areas on East and West Coast o Updated punching shear equations o Differentiated performance of T, K&Y and Cross joints. Included non-linear interaction of axial and bending forces
1980	11th	o Included steel groups and classes. First specific recommendation to use "Class A" steels in joints
1986	16th	o Required a 5 ft. air gap and included reference level storm tide
1993	20th	o Drag and mass coefficients respectively set to 0.7 and 1.6 for smooth cylinders and to 1.05 and 1.2 for rough cylinders

Table 2. Comparison of Hurricane Andrew to Historical Hurricanes from Galveston to Mobile Bay (Taken from Reference 5)

Storm		Pressure differential Ap(mb)	Radius to Maximum Wind Rmax(n.mi.)	Storm forward speed Vf(kts)	Peak wind speed Wm(kts)
Camille	1969	105	12	14	111
Betsy	1965	72	40	17	95
Andrew	**1992**	**78**	**16**	**11**	**94**
SEP	1900	76	14	10	93
SEP	1915	78	31	12	93
Carmen	1974	76	15	10	93
Carla	1961	75	30	7	87
Hilda	1964	73	21	6	85
Frederic	1979	65	25	11	85
Alicia	1983	50	20	7	74

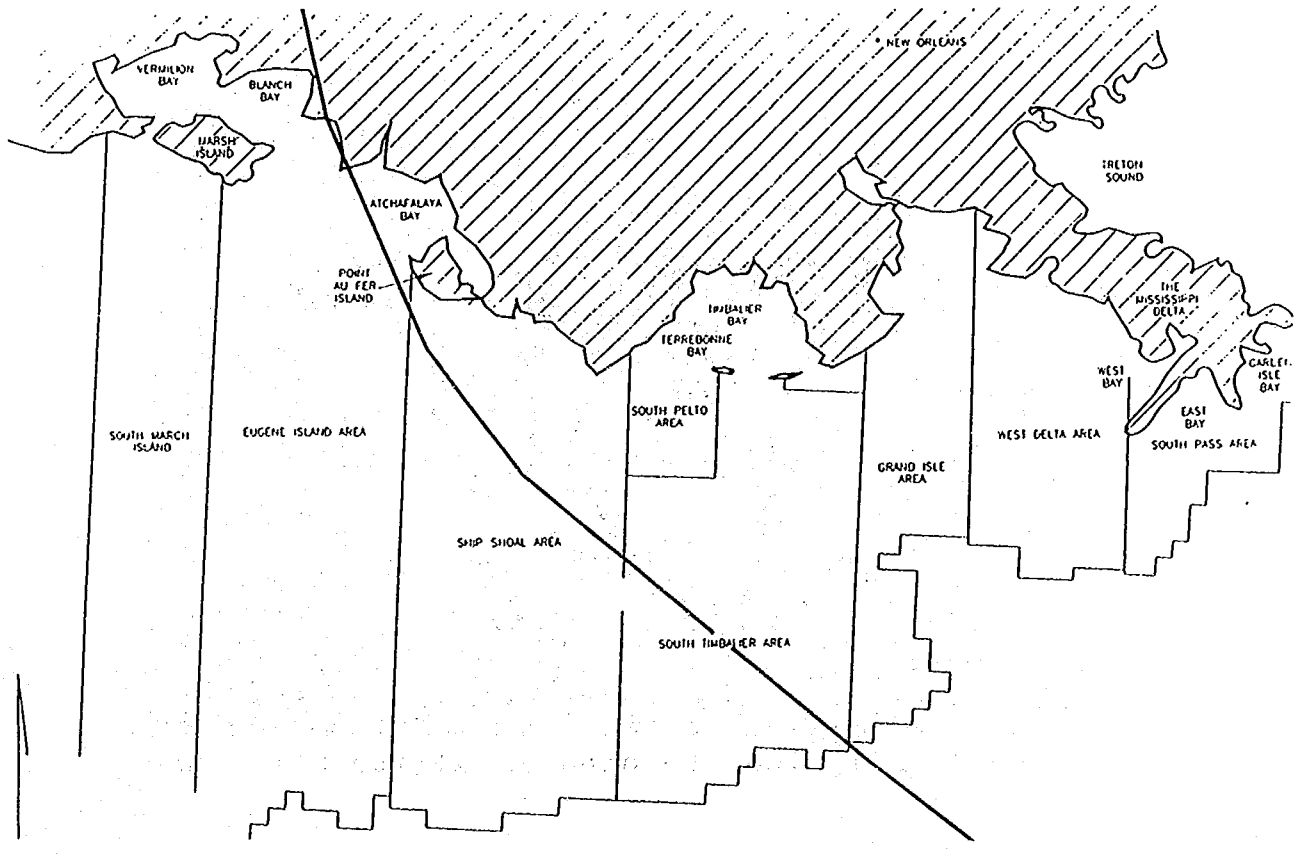


Figure 1. Storm Track Through the Oil and Gas Production Areas in the Gulf of Mexico

PLATFORMS		SATELLITES	
Toppled	14	Toppled	28
Leaning	8	Leaning	114
Subtotal	22	Subtotal	142

TOTAL 164

Figure 2. Major Structural Damage from Hurricane Andrew

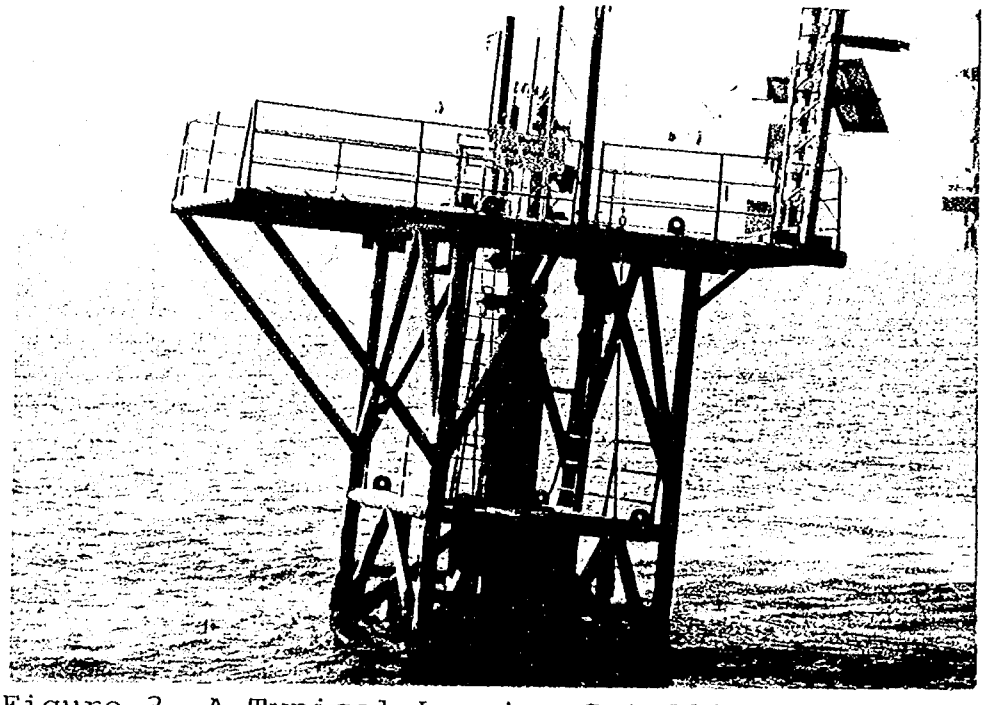


Figure 3. A Typical Leaning Satellite Structure

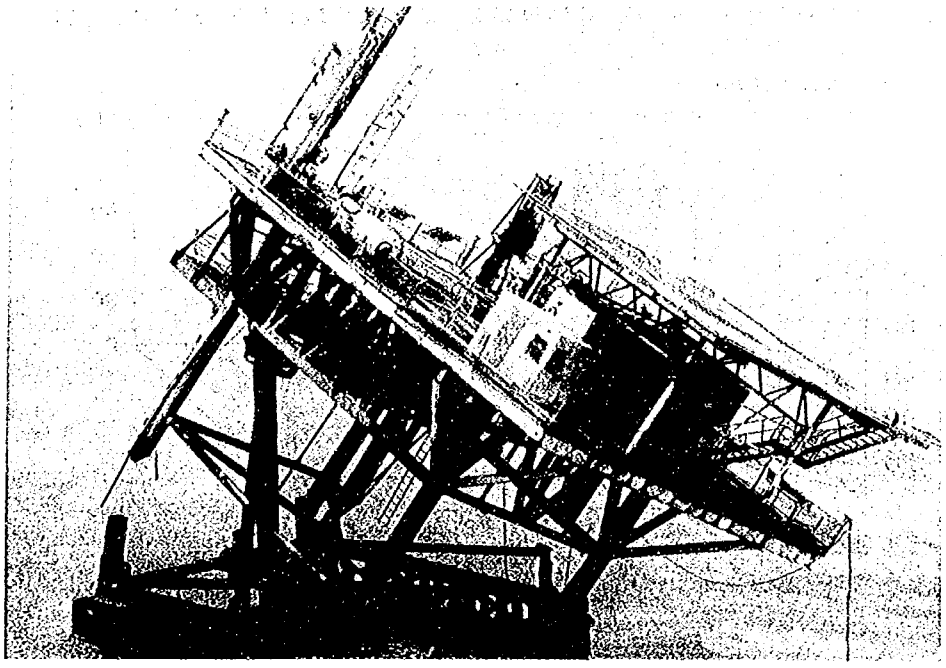


Figure 4. Major Damage to a Platform Structure

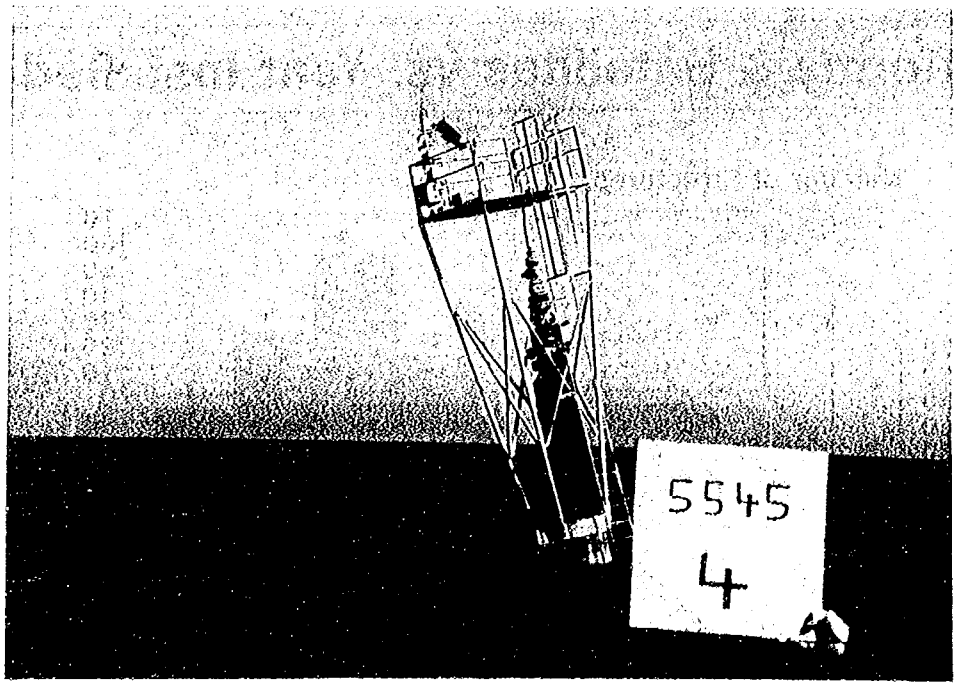


Figure 5. A Damaged Single-Well Caisson

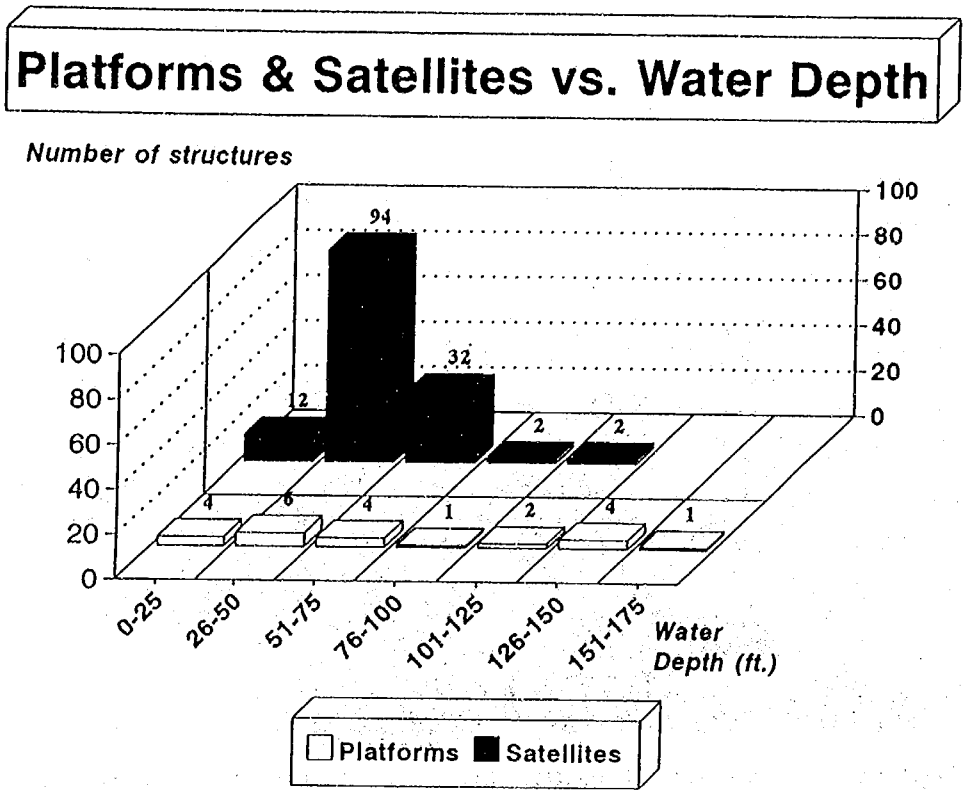


Figure 6. Platform and Satellite Distribution by Water Depth

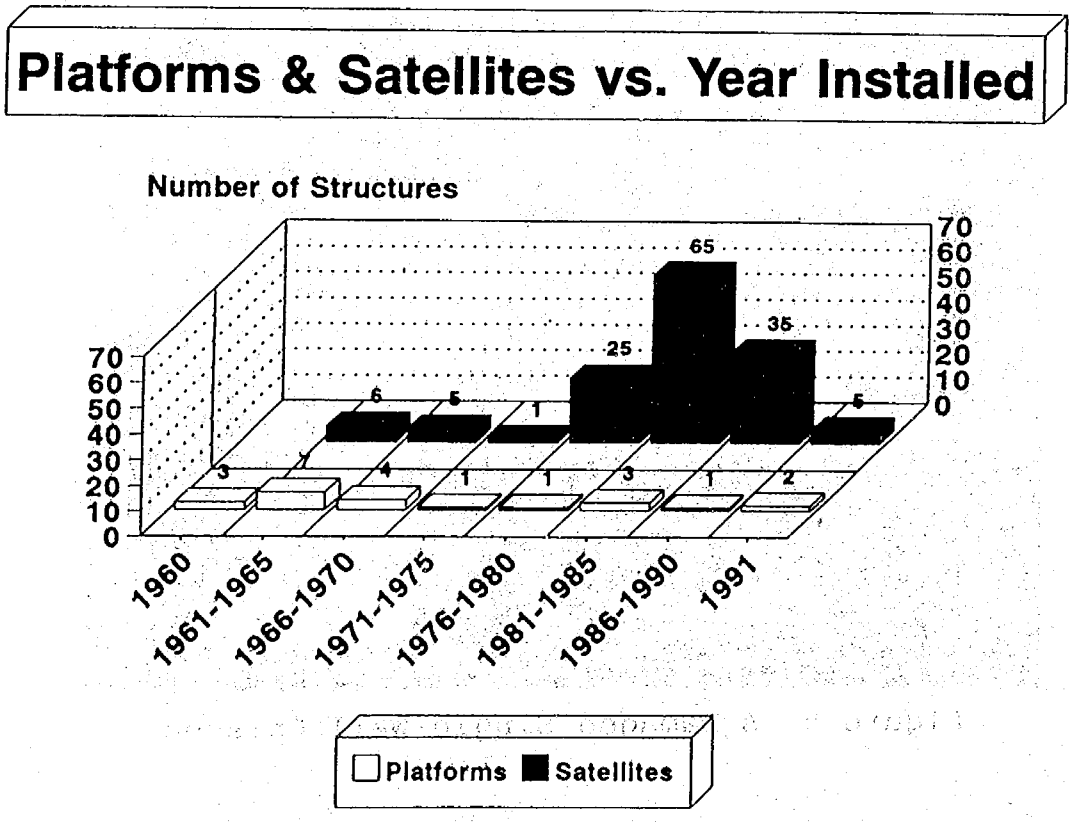


Figure 7. Platform and Satellite Distribution by Year Installed

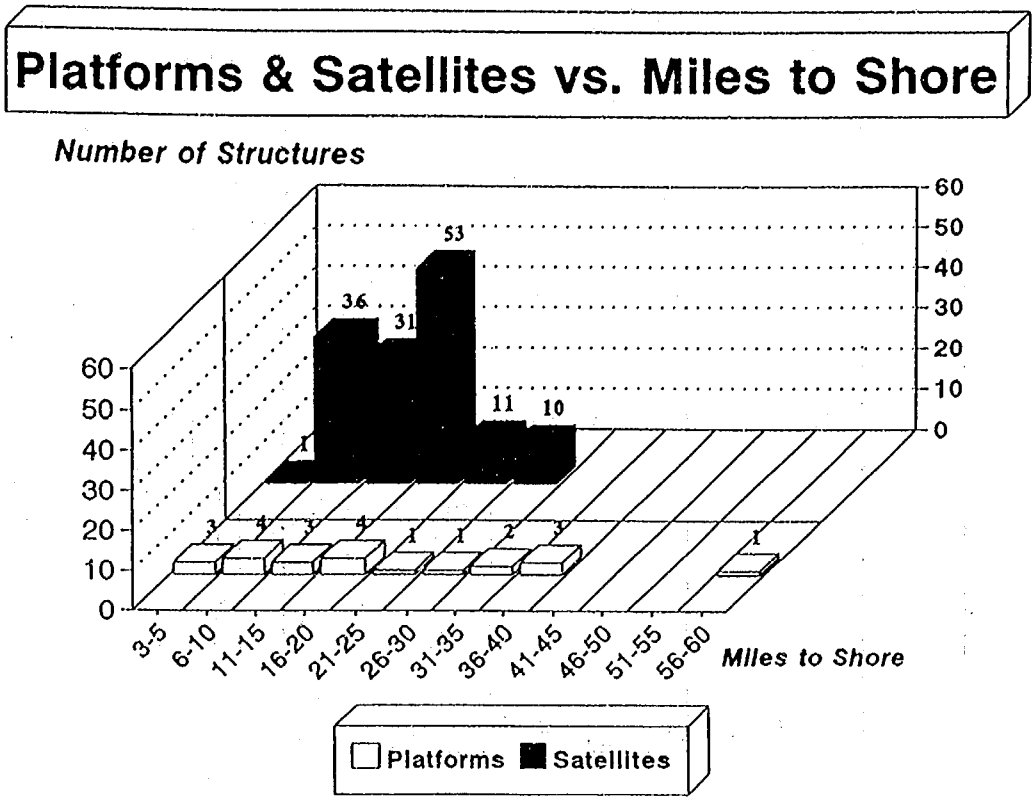


Figure 8. Platform and Satellite Distribution by Miles to Shore.

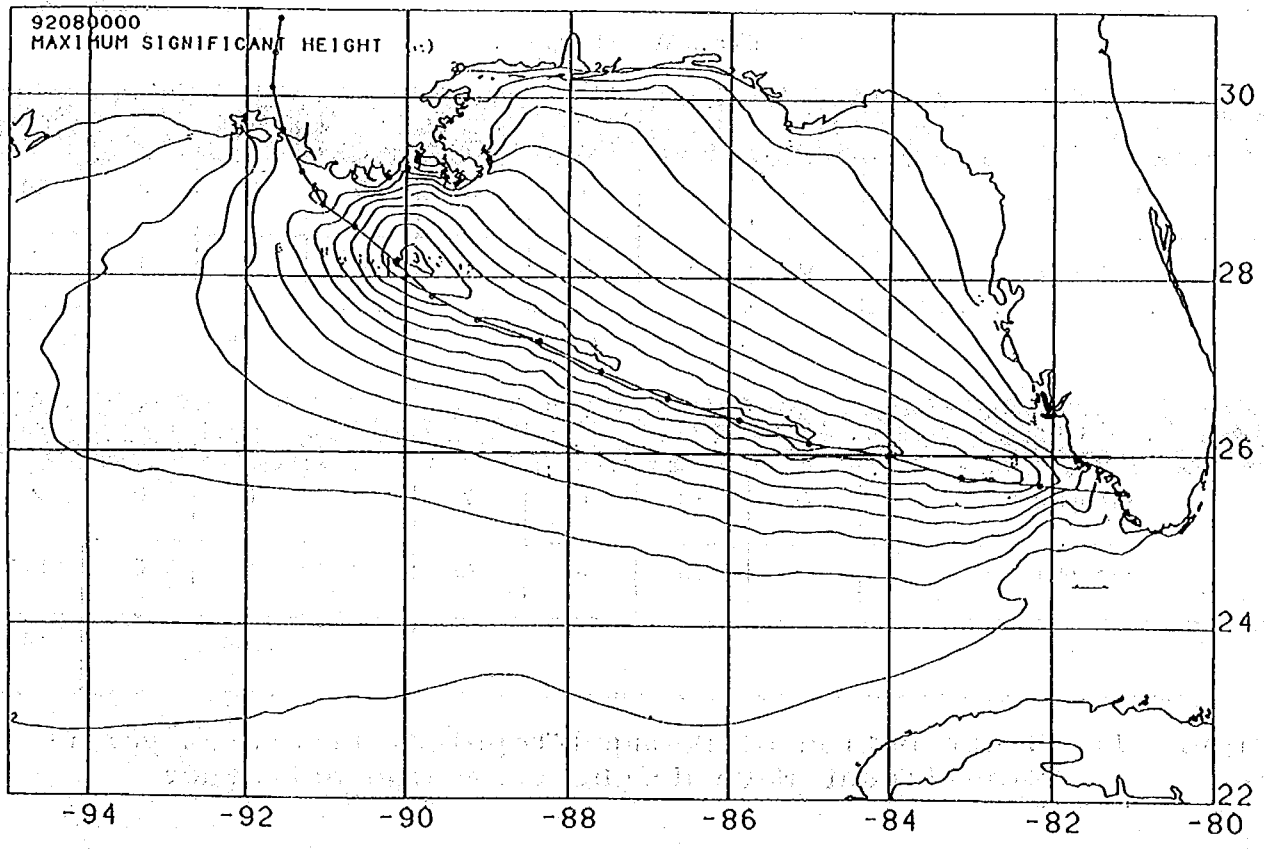


Figure 9. Hindcast for Maximum Significant Wave Height

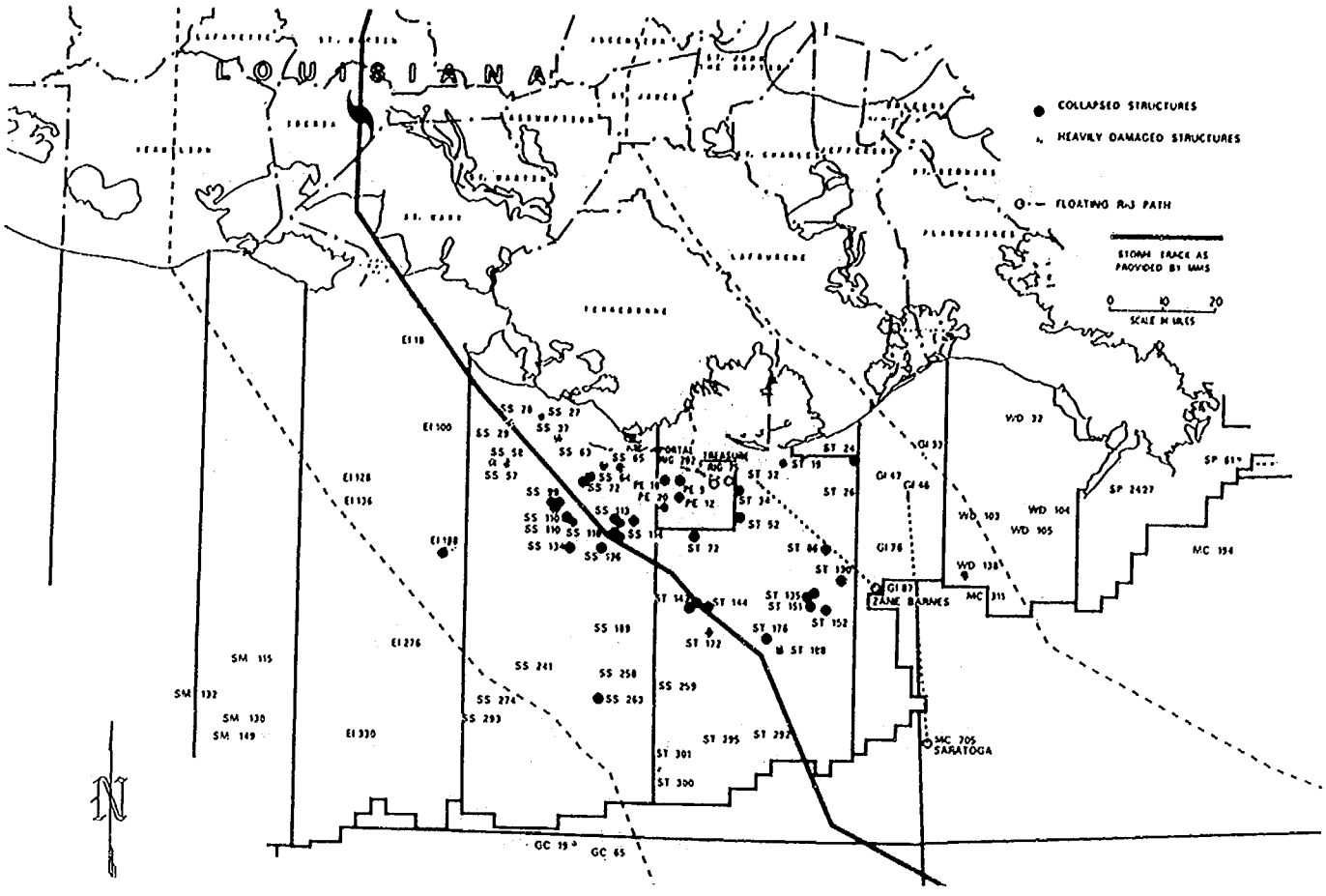


Figure 10. Location of Heavily Damaged (Light Dots) and Collapsed (Dark Dots) Structures

Significant Wave Height (M)								
Platform								
• Toppled	3	3	2	3	0	0	3	14
• Leaning	0	3	2	1	0	1	1	8
						Total		22
Satellite								
•Toppled	0	13	6	7	2	0	0	28
• Leaning	0	58	36	20	0	0	0	114
						Total		142

Figure 11. Distribution of Damaged/Toppled Structures versus Significant Wave Height from Hindcast Study

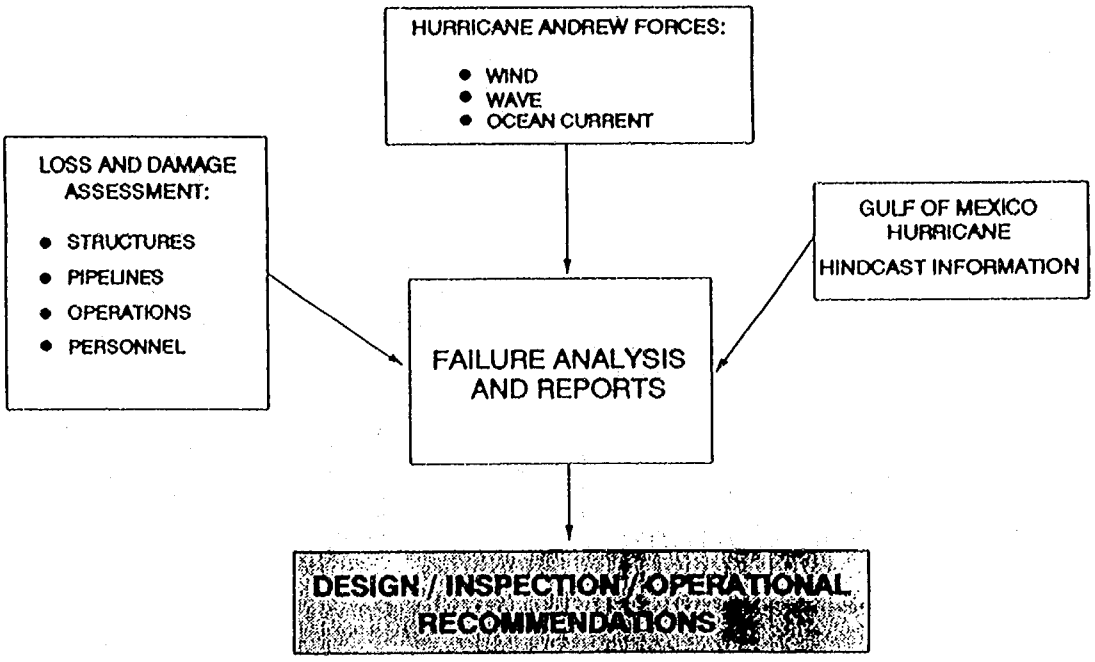


Figure 12. Subsets of the MMS Damage Assessment Study

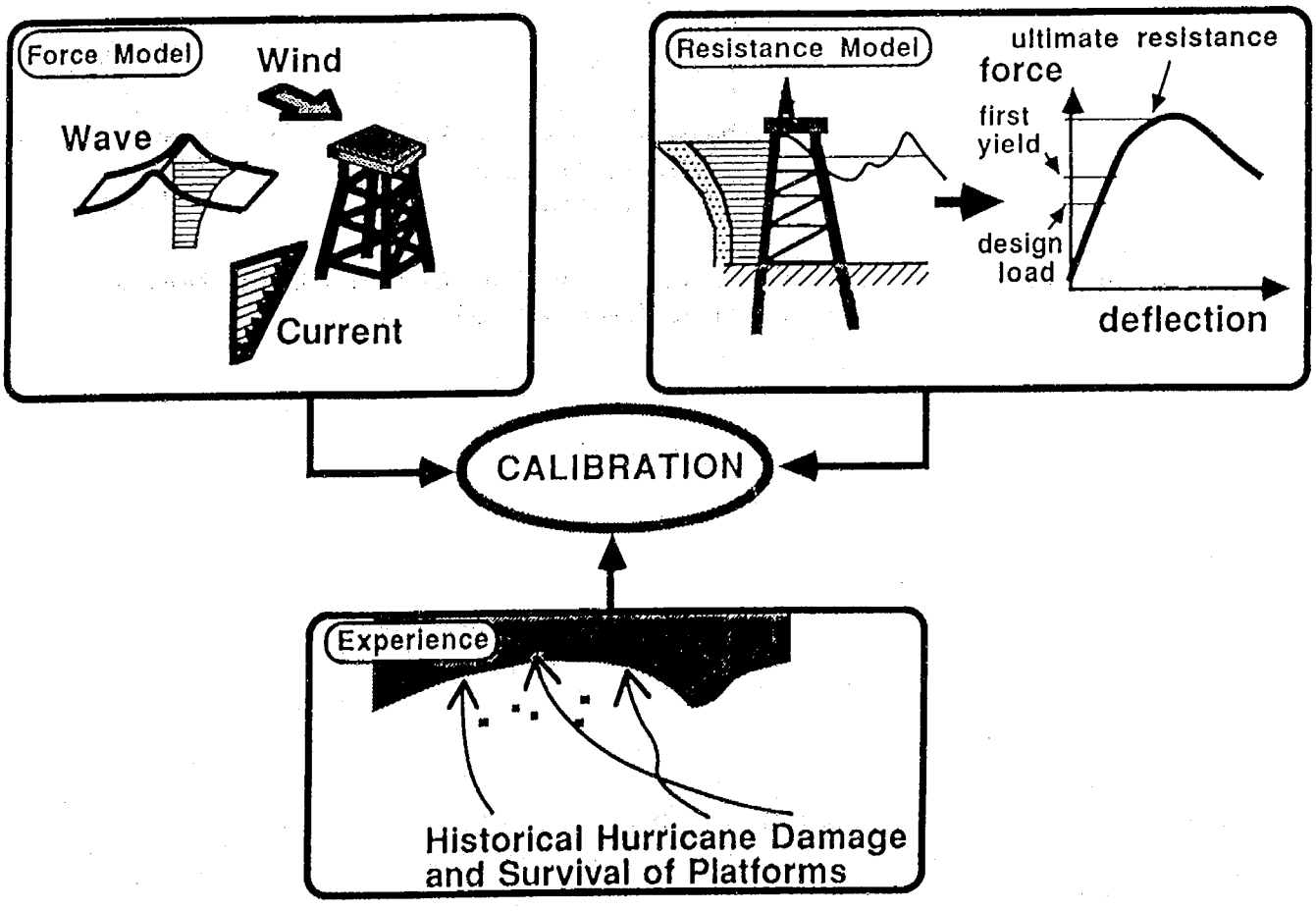


Figure 13. Input to the Joint Industry Calibration Study (Taken from Reference 8)

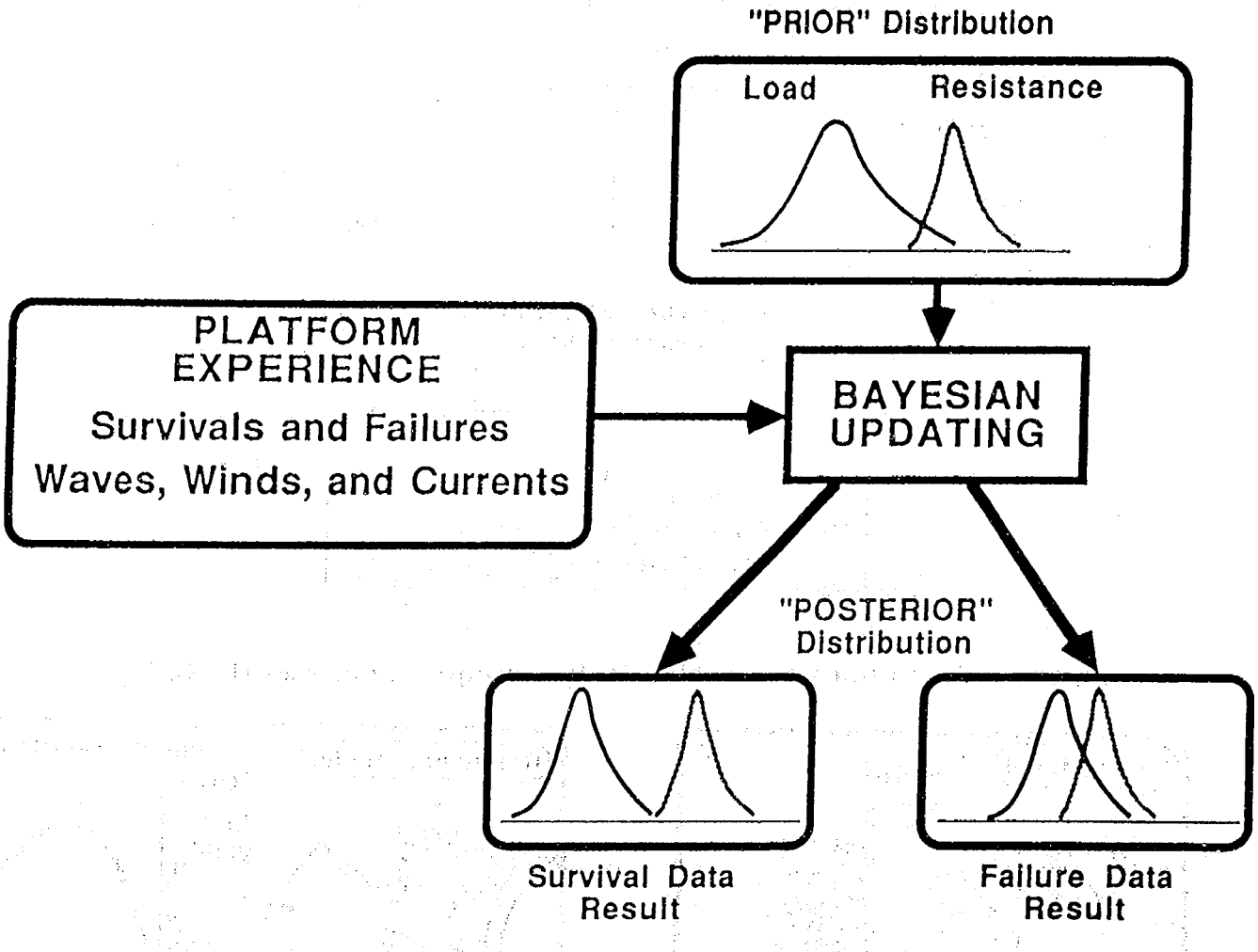


Figure 14. Bayesian Updating to Redefine Calibration Model
(Taken from Reference 8)

Wind-Induced Vibrations of Super Long-Span Suspension Bridge in Turbulent Wind

by

Hiroshi Sato[1], Ryuichi Toriumi[2], and Masahiko Yasuda[3]

ABSTRACT

Wind-induced vibrations of the super long-span bridge in turbulent flow were studied using aeroelastic full model at the Large Boundary Layer Wind Tunnel.

Random vibrations caused by turbulence (gust responses) were observed in horizontal bending, vertical bending and torsional mode. As wind speed increases, the vibration of torsional 1st mode becomes dominant, and apparent damping becomes smaller. This seems to be the effect of flutter.

In order to investigate the effect of turbulence on flutter, apparent damping in turbulent flow was compared with that in smooth flow. It was found that the effect of turbulence on flutter was small for this bridge model.

The observed gust responses were compared with the calculated ones. As for vertical bending and torsional responses, the agreement was fairly good, however, the agreement was poor for horizontal bending responses. The more accurate estimation of aerodynamic admittance or space correlation seems to be required.

KEYWORDS

Wind, Super long-span suspension bridge, Flutter, Gust response, Turbulence

1. INTRODUCTION

Long-span bridges such as suspension bridges have lower natural frequencies than medium-span bridges. It means that aerodynamic instabilities such as flutter may happen to long-span bridges at lower wind speed. Therefore, the safety of long-span bridges to wind should be investigated before their construction.

Since natural frequencies becomes lower as span length becomes longer, the study on wind effects on super long-span bridges is very important. The Akashi Kaikyou Bridge, which is now under construction, will have the main span length of 1990m, which is 580m longer than the Humber Bridge, the longest bridge in the world at present.

In Japan, the safety of proposed design of long-span bridges to wind-induced instabilities has been confirmed mainly by spring-mounted rigid sectional model test in smooth laminar flow. Since the span length of the Akashi Kaikyou Bridge (Fig. 1) is much longer than the existent longest bridge in the world, it was thought that the wind-induced instabilities should be confirmed by more accurate wind tunnel study, namely full aeroelastic model study.

From these reasons, cooperative study on wind resistant design of super long-span bridges was started in 1989 by Public Works Research Institute, Ministry of Construction and Honshu Shikoku Bridge Authority. The Large Boundary Layer Wind Tunnel (Fig. 2) was constructed at PWRI in 1991 (ref. 1), and flutter characteristics were investigated in smooth flow using the full aeroelastic model, whose scale ratio was 1/100 (ref. 2).

The wind speed of natural wind changes in time and in space. The wind-induced vibrations of long-span bridges are different in turbulent flow from in smooth flow, whose wind speed is almost constant in time and space. It was reported that random vibrations due to gust were observed in turbulent flow, and that the characteristics of flutter, galloping, and vortex-induced vibrations were changed due to effects of turbulence (ref. 3, 4, 5, 6). The wind-induced vibrations of long-span bridges can be predicted more accurately if the model is tested in turbulent flow, whose

---

1 Dr. Eng., Head, Structure Division, Structure and Bridge Department, Public Works Research Institute, Ministry of Construction

2 M. Eng., Senior Research Engineer, ditto

3 M. Eng., Director, Tarumi Construction Office, The First Construction Bureau, Honshu-Shikoku Bridge Authority

characteristics are similar to those of natural wind at erection site.

In this paper described are the wind tunnel study on the Akashi Kaikyou Bridge in turbulent flow using the full aeroelastic model. Flutter characteristics in turbulent flow are compared with those in smooth flow. Observed gust responses are compared with calculated ones.

2. PURPOSE OF THE STUDY

The purpose of the study is to make clear the wind-induced vibrations of super long-span bridges in turbulent flow. Effect of turbulence on flutter, and gust response are focused.

3. TEST CONDITION

3.1 BRIDGE MODEL

The same aeroelastic full model as was used in smooth flow test (ref. 2) was used. The scale ratio was 1/100. The general view of the model and cross section of the stiffening truss are shown in Fig. 3 and 4, respectively. The natural frequency and mode shape of the model are summarized in Table 1.

3.2 TURBULENT FLOW

The turbulent flow was generated by spires and roughness. In the simulation of turbulent flow, it was thought that turbulent intensity and integral scale of turbulence were the most important parameters to be similar to natural wind. The intensity of turbulence Iu for main wind direction at the deck height was assumed to be 10%. Several spires and some arrangements of roughness blocks were tested, and the most suitable spires and roughness blocks were selected. They are shown in Fig. 5.

The main properties of the turbulent flow, such as mean wind speed distribution, turbulence intensity distribution, integral scale of turbulence, power spectral density functions of wind speed, and space correlation of wind speed are shown in Figures 6 to 10, respectively. Although the power extent of vertical distribution of mean wind speed was a little larger and the integral scale of turbulence was a little smaller, the properties of the simulated turbulent flow were thought to be fairly satisfactory.

4. TEST RESULTS

The relationship between mean wind speed at the deck height and displacement of the deck at mid-span are shown in Fig. 11. In the figures, the maximum displacement, maximum vibrational amplitude and root mean square of the vibrational displacement are shown in each direction such as horizontal bending, vertical bending and torsion. Typical time history records and power spectral density functions of vertical displacement at downstream chord at mid-span are shown in Fig. 12.

It seems obvious that the random vibrations observed at relatively low wind speeds were caused by approaching turbulence. As wind speed increases, however, characteristics of the vibration changes. The power near the torsional 1st mode becomes dominant at higher wind speeds as shown in Fig. 12. The increase rate of the vibrational amplitude with wind speed becomes larger at higher wind speed. It can be seen clearly in Fig. 13, where displacement and wind speeds were plotted in logarithmic scales. These changes in vibrational characteristics seem to be caused negative aerodynamic damping, which result in flutter. The apparent damping of the model in wind, which is sum of structural damping and aerodynamic damping, was estimated by random decrement method (ref. 7), and is shown in Fig. 14. It is clear that the apparent damping becomes small at high wind speeds.

5. DISCUSSION

5.1 EFFECT OF TURBULENCE ON FLUTTER

The vibrations of the bridge model at high wind speed in turbulent flow were caused by both gust and negative aerodynamic damping. It can be said that the observed vibrations are mixture of gust response and flutter. It is difficult to separate vibrational amplitude caused by flutter from that caused by gust. Therefore, the effect of turbulence on flutter were discussed on damping rather than vibrational amplitude.

The relationship between wind speed and apparent damping of torsional vibration in turbulent flow is shown in Fig. 15, compared with that in smooth flow. Since the difference in apparent damping between in turbulent flow and in smooth flow is small, it can be said that the effect of turbulence on flutter is small in case of the Akashi Kaikyou

Bridge.

5.2 COMPARISON BETWEEN CALCULATED GUST RESPONSES AND OBSERVED ONES

(a) Calculation Method

For comparison, gust responses of horizontal bending, vertical bending and torsion were calculated according to the ordinary methods in frequency domain (ref. 8). In the calculation of torsional gust responses, the effect of horizontal bending modes were considered.

As for wind and structural properties, the observed data were used. As for coefficients of drag, lift and aerodynamic moment, the data measured in sectional model test in smooth flow were used. Aerodynamic forces caused by gust were calculated according to quasi-steady theory, corrected by aerodynamic admittance and space correlation as follows.

aerodynamic admittance for drag (ref. 8)

$$X_u^2(f_d)=2[kf_d-1+\exp(-kf_d)]/(kf_d)^2$$

aerodynamic admittance for lift and moment (ref. 9)

$$X_w^2(f_b)=(a+\pi f_b)/[a+(\pi a+1)\pi f_b+2\pi(\pi f_b)^2]$$

space correlation (ref. 10)

$$R(f_b)=\exp(-kf_b \mid x_1-x_2 \mid /B)$$

where,
a : constant (=0.1811)
B : width of stiffening truss
D : depth of stiffening truss
f : frequency
$f_b=fB/U$
$f_d=fD/U$
k : decay factor (assumed to be 8)
U : mean wind speed
x_1, x_2 : coordinate along bridge axis

Aerodynamic damping for horizontal and vertical bending vibration was calculated according to quasi-steady theory. As for torsion, aerodynamic damping was assumed to be zero.

(b) Comparison

The gust responses calculated at the design wind speed are shown in Table 2, compared with the responses observed in experiment. The agreement in vertical bending and in torsion is fairly good, however, the agreement in horizontal bending is poor.

At present, the cause of the discrepancy is not clear. But it may be said that aerodynamic forces caused by gust should be estimated more accurately. More accurate aerodynamic admittance or space correlation seems to be required.

6. CONCLUDING REMARKS

Wind-induced vibrations of the super long-span bridge in turbulent flow were studied using aeroelastic full model at the Large Boundary Layer Wind Tunnel. The main findings are as follows.

(1) Random vibrations caused by turbulence (gust responses) were observed in horizontal bending, vertical bending and torsional mode. As wind speed increases, the vibration of torsional 1st mode becomes dominant, and apparent damping becomes smaller. This seems to be the effect of flutter.

(2) In order to investigate the effect of turbulence on flutter, apparent damping in turbulent flow was compared with that in smooth flow. It was found that the effect of turbulence on flutter was small for this bridge model.

(3) The observed gust responses were compared with the calculated ones. As for vertical bending and torsional responses, the agreement was fairly good, however, the agreement was poor for horizontal bending responses. The more accurate estimation of aerodynamic admittance or space correlation seems to be required.

REFERENCES

1) Yokoyama K., Kanazaki T. and Yasuda M., Boundary layer wind tunnel study on full aeroelastic long span bridge model, Proc. 23rd Joint Panel Meeting on Wind and Seismic Effects, UJNR, 1991

2) Yokoyama K., Kanazaki T. and Yasuda M., Flutter characteristics of super long-span suspension bridge, Proc. 24th Joint Panel Meeting on Wind and Seismic Effects, UJNR, 1992

3) Davenport A.G., Isymov N. and Miyata T., The experimental determination of the

response of suspension bridges to turbulent wind, Proc. 3rd Int. Conf. on Wind Effects on Bldgs. and Sts., 1971

4) Melbourne W.H., West Gate Bridge wind tunnel tests, 1973

5) Irwin H.P.A.H. and Schuyler G.D., Experiments on a full aeroelastic model model of Lions' Gate Bridge in smooth and turbulent flow, Laboratory Technical Report, National Research Council Canada, 1977

6) Narita N., Yokoyama K., Sato H. and Nakagami Y., Aerodynamic characteristics of continuous box girder bridges relevant to their vibrations in wind, Proc. 7th Int. Cong. on Wind Engineering, 1987

7) Technical Comittee on the Wind Resistant Design of the Honshu-Shikoku Bridge, Final reports on the observation of large scale bridge model (Part 2), JSCE, 1978 (in Japanese)

8) Davenport A.G., Buffeting of a suspension bridge by storm winds, Proc. ASCE, Vol. 88, ST3, 1962

9) Fung, Y.C., An Introduction to the Theory of Aeroelasticity, John Wiley & Sons, 1955

10) Davenport A.G., The spectrum of horizontal gustiness near the ground in high winds, Q.J. Roy. Met. Soc., Vol. 87, 1961

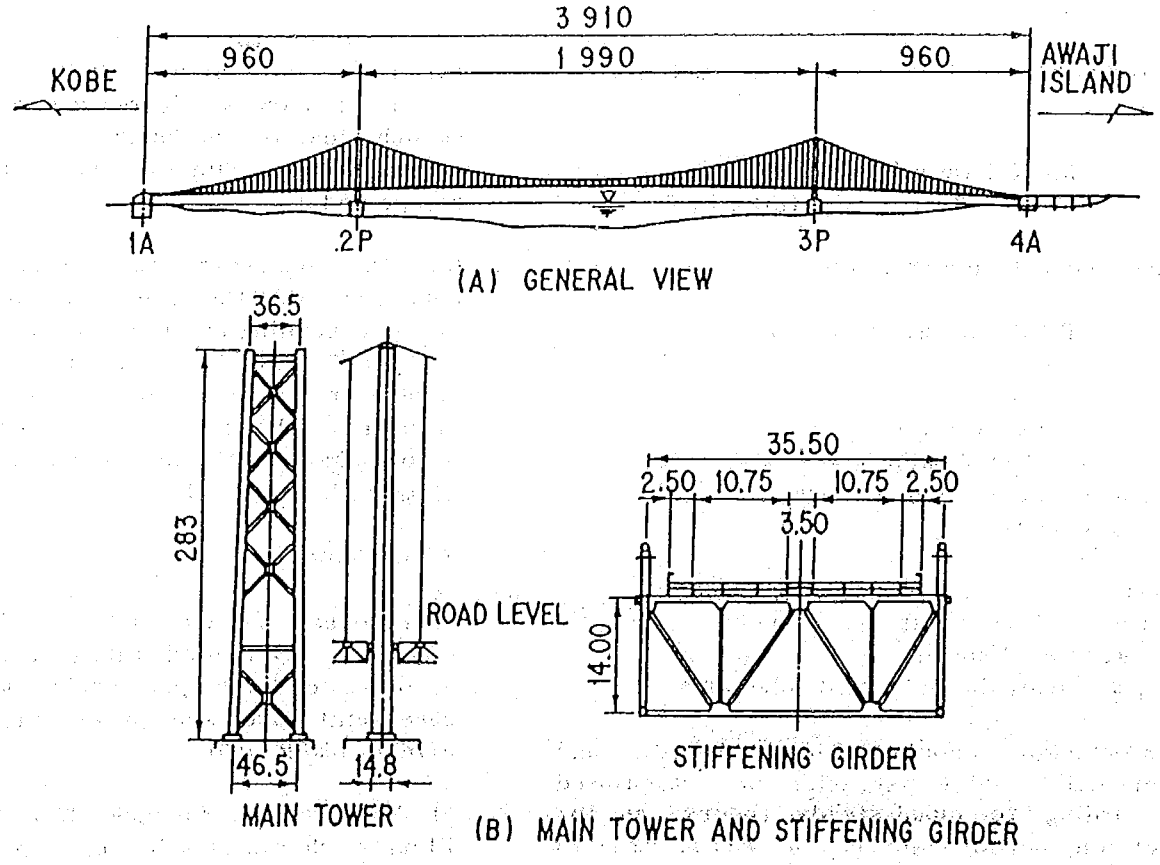


Fig.1 General View of the Akashi Kaikyo Bridge (unit:m)

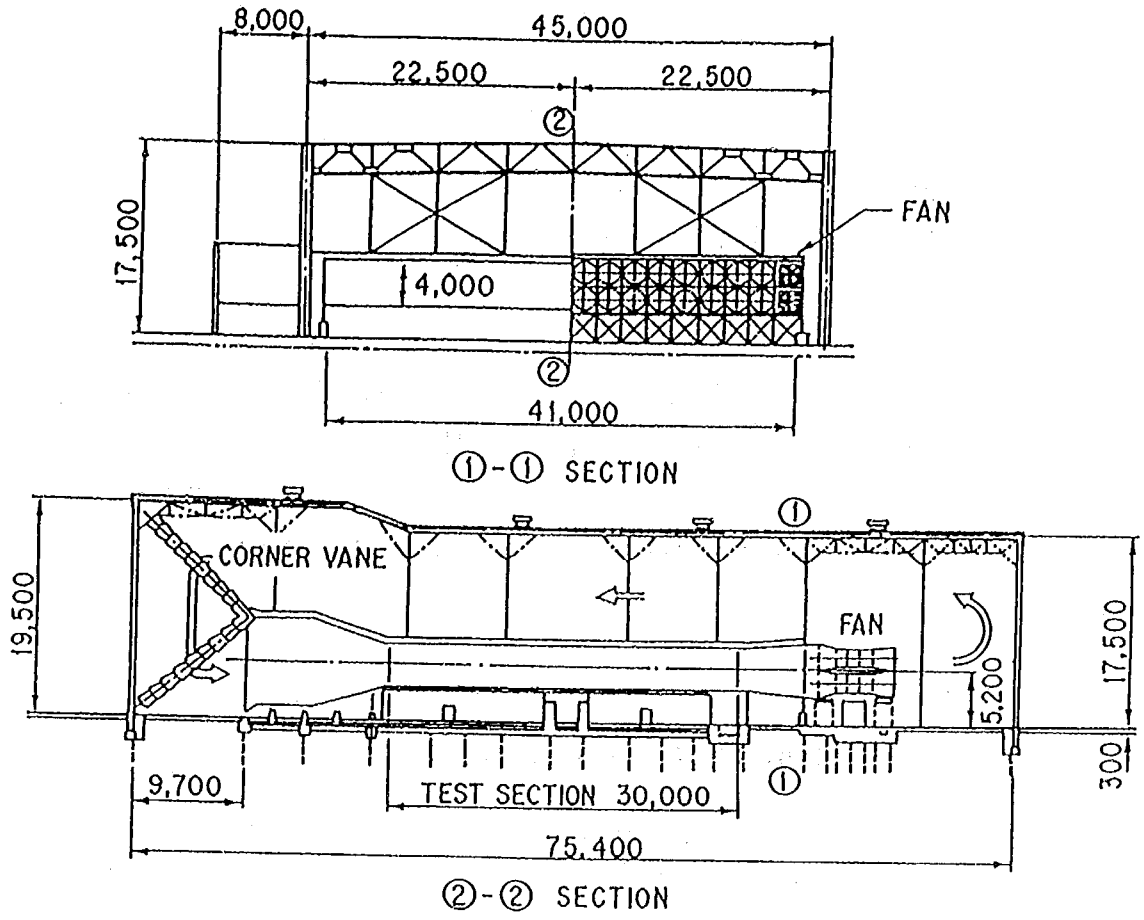


Fig.2 General Layout of Large Boundary Layer Wind Tunnel (unit:m)

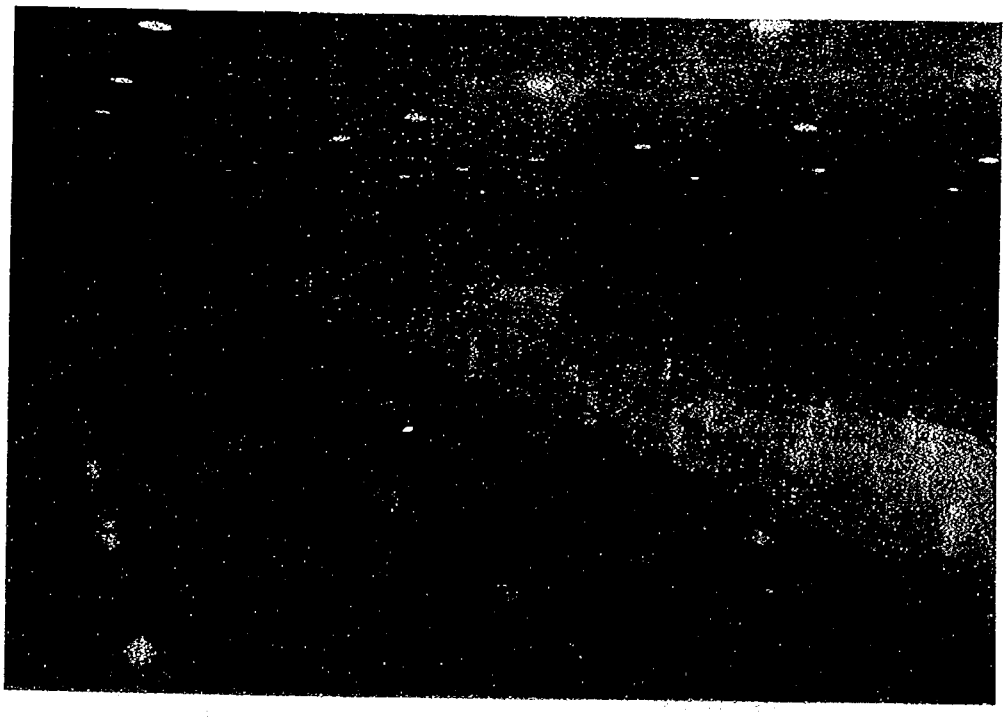


Fig.3 Full Bridge Model of the Akashi Kaikyo Bridge

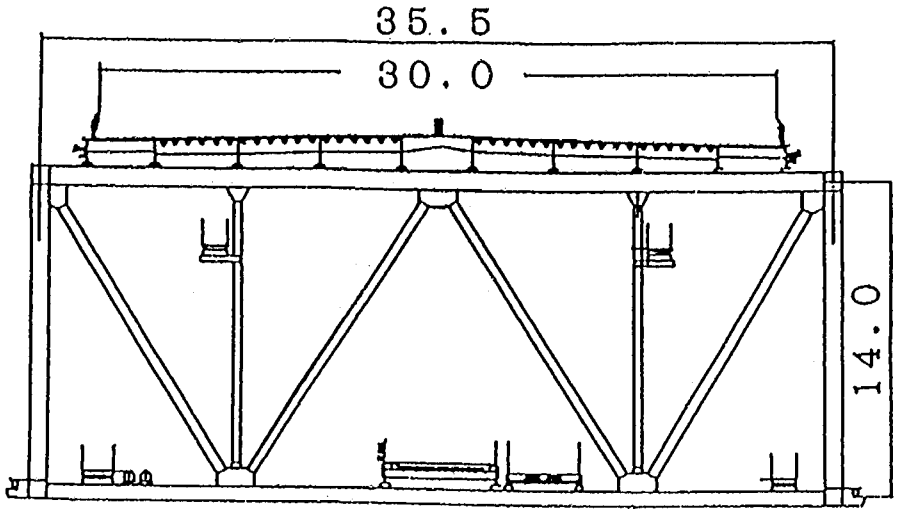


Fig.4 Cross Section of Truss Stiffening Girder (unit:cm)

Table 1 Natural Frequency of the Model

Mode #	Mode Shape	Natural Frequency (Hz)	
		Calculated	Measured
1	Vertical bending	0.638	0.635
2	Vertical bending	0.745	0.732
3	Vertical bending	0.835	0.830
4	Vertical bending	1.213	1.221
5	Torsional	1.497	1.550
6	Torsional	2.077	2.075
7	Horizontal	0.387	0.391
8	Horizontal	0.775	0.781

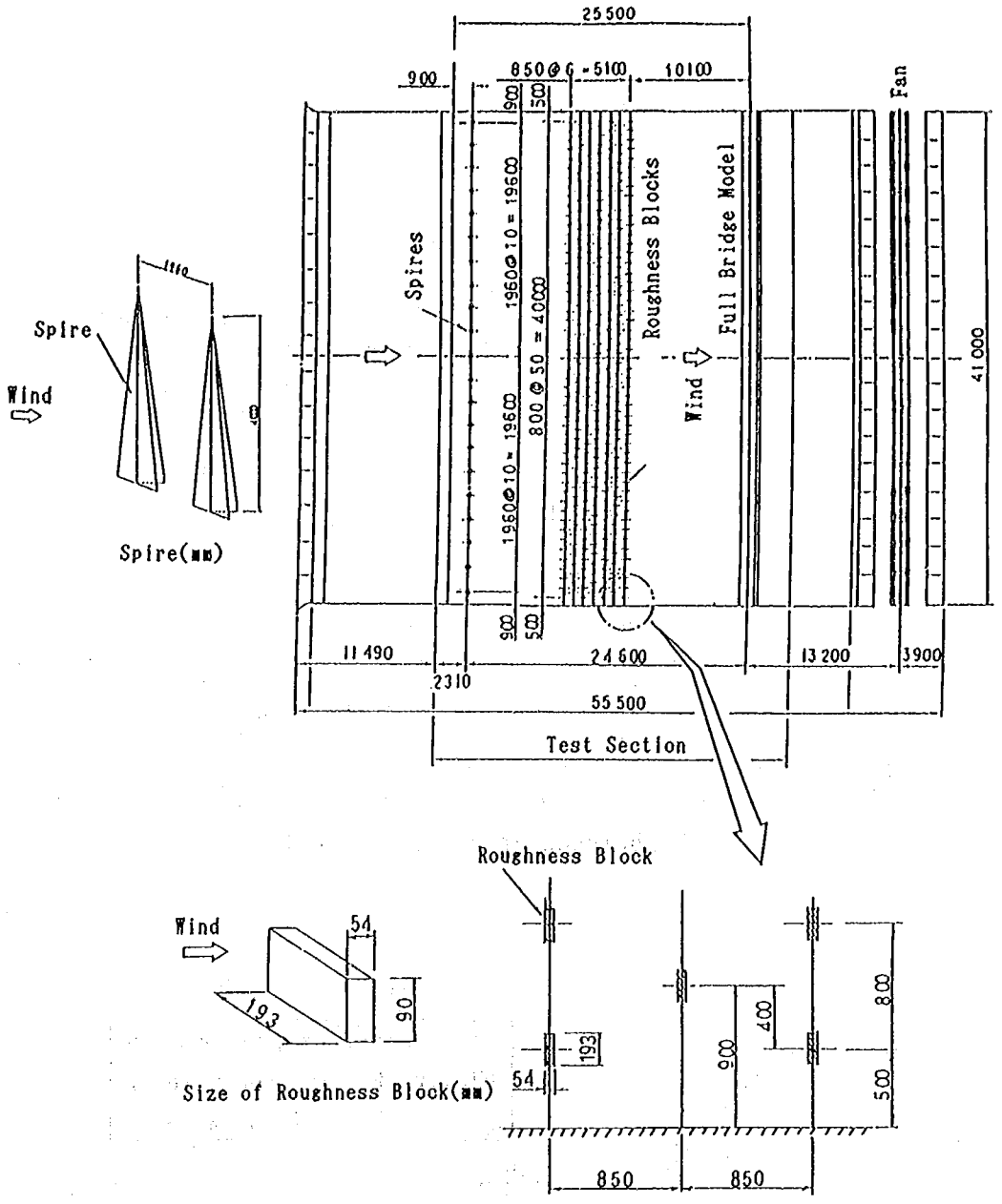


Fig.5 Spires and Roughness Blocks

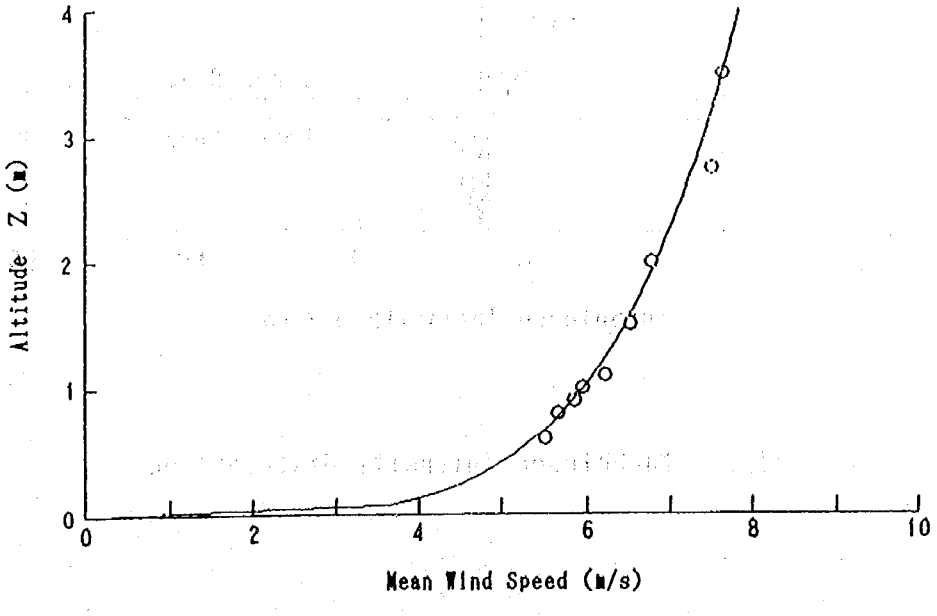
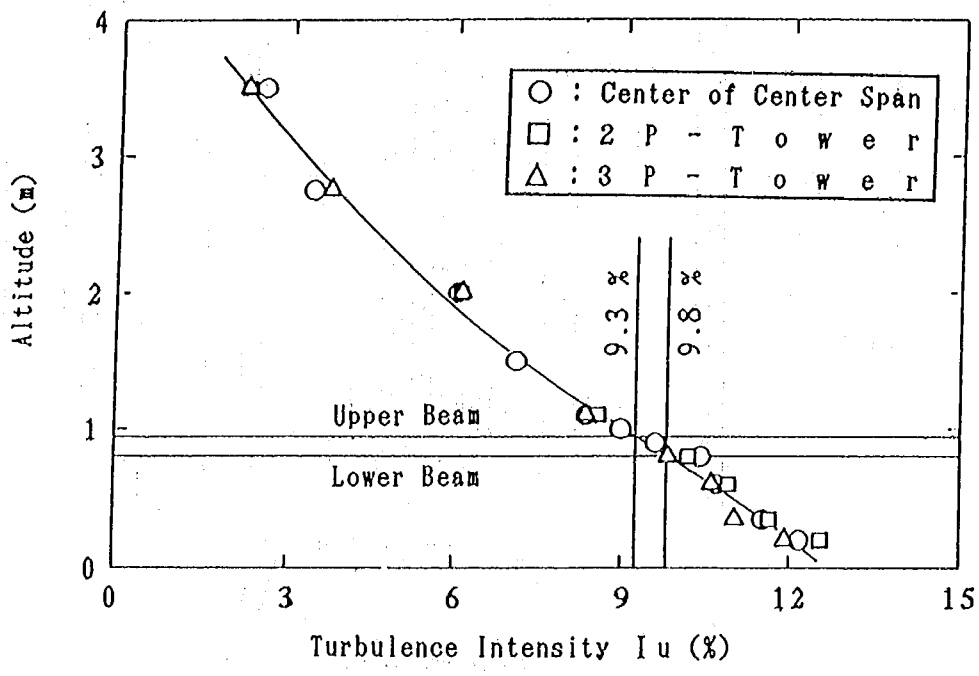


Fig.6 Mean Wind Speed Distribution



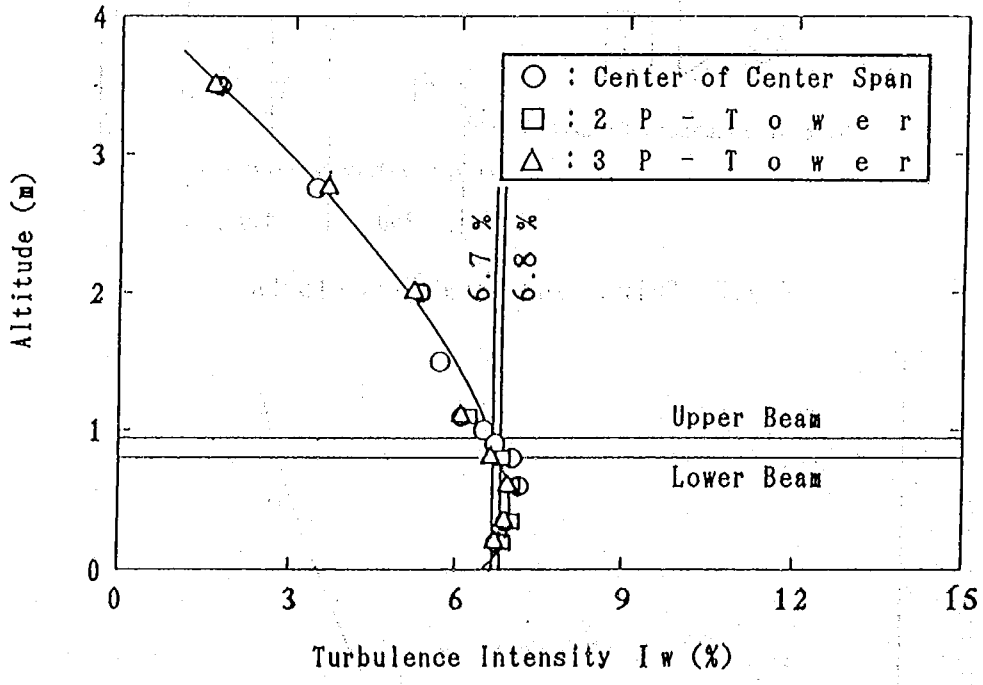
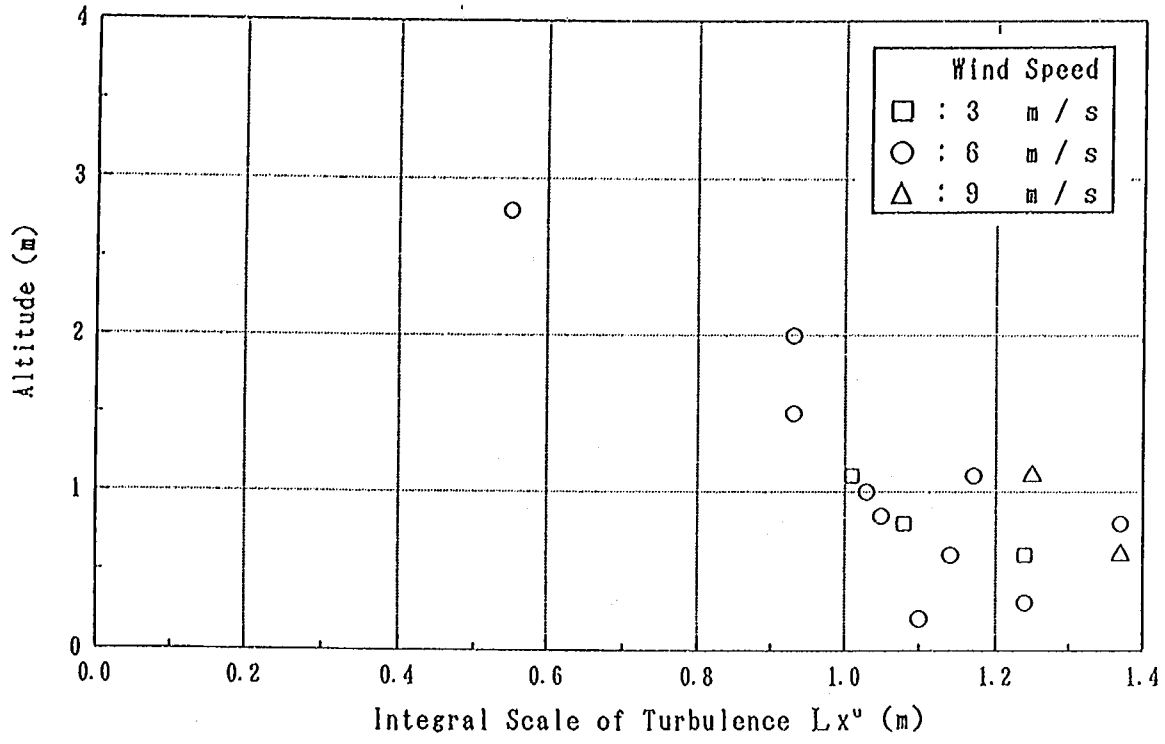


Fig.7 Turbulence Intensity Distribution



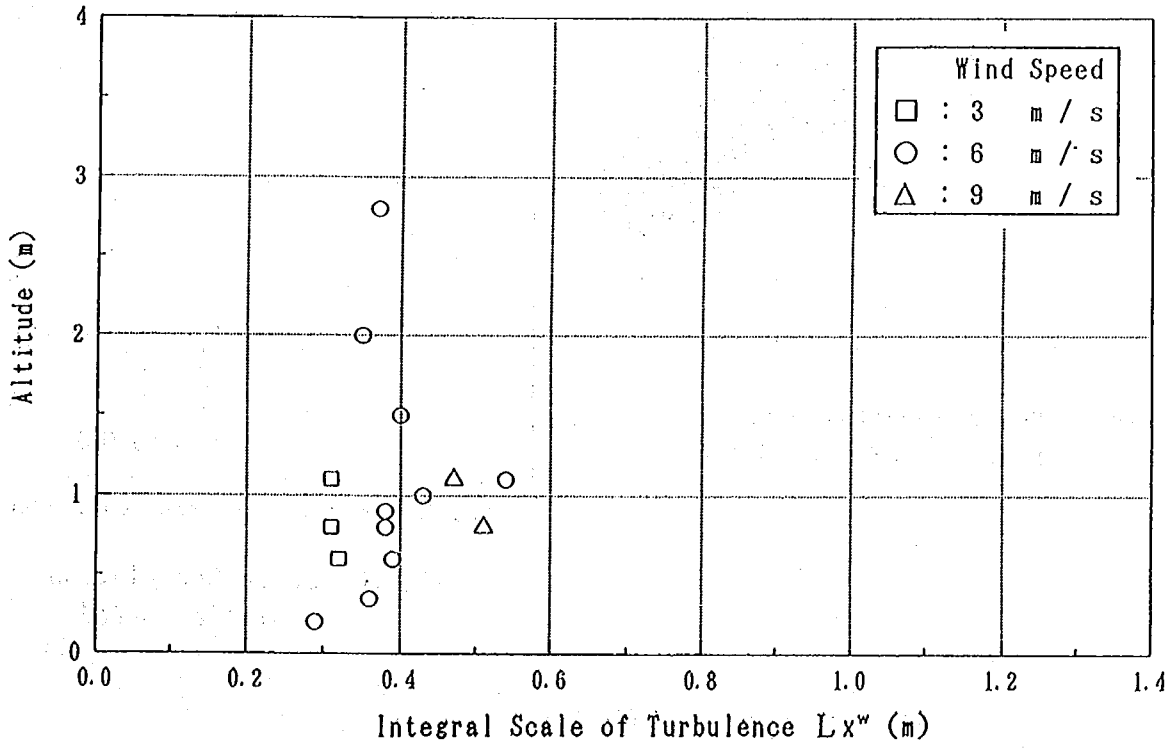
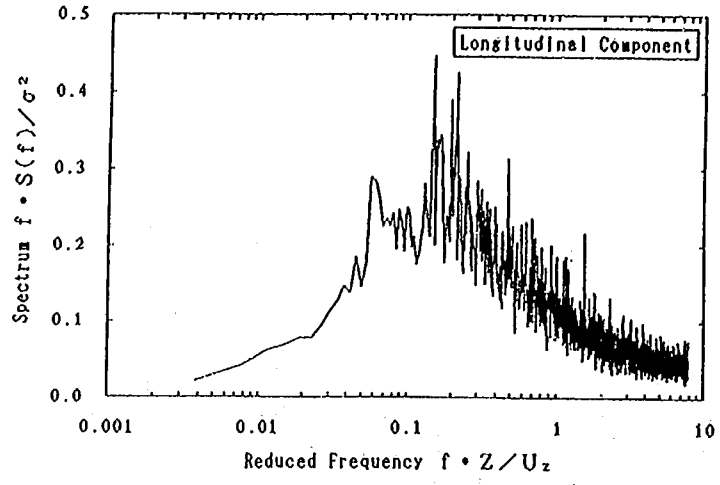


Fig.8 Integral Scale of Turbulence



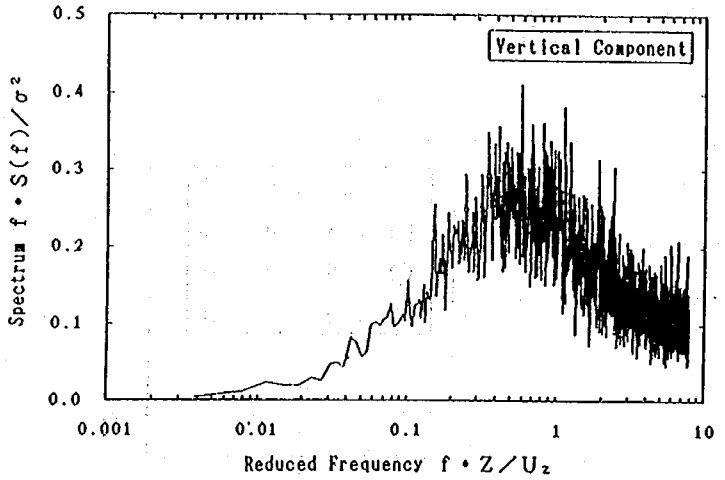
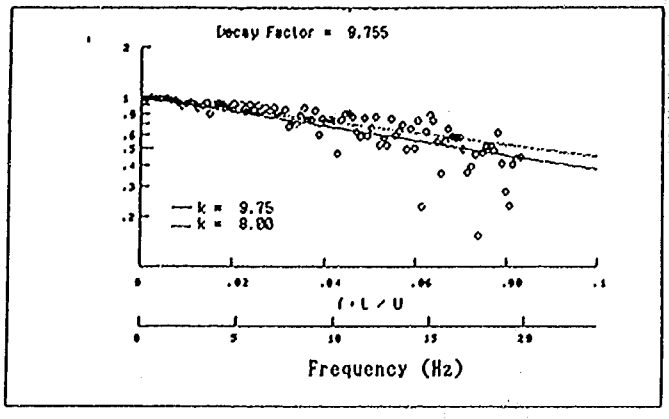
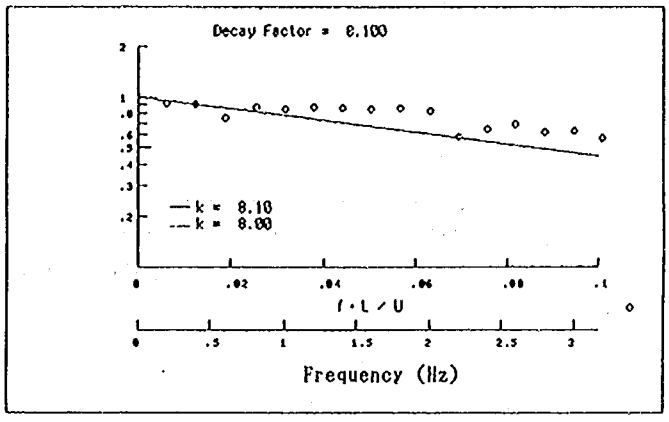


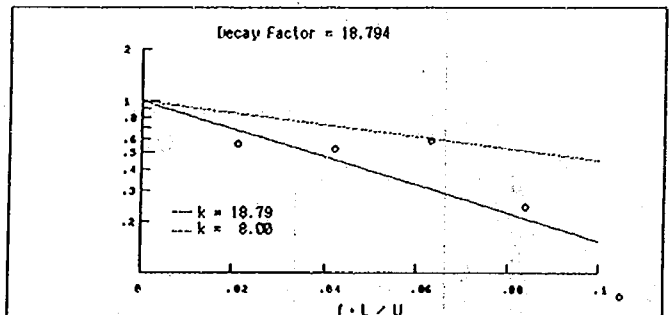
Fig.9 Power Spectral Density Function of Wind Speed



(a) Distance between two measurement points (20mm)



(b) Distance between two measurement points (150mm)



(c) Distance between two measurement points (500mm)

Fig.10 Space Correlation of Wind Speed

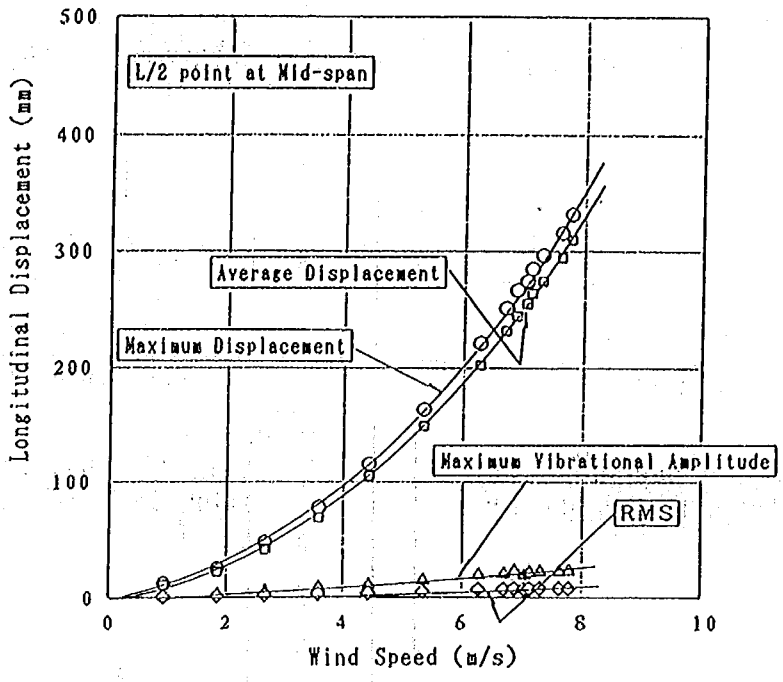


Fig.11(a) Displacement in Turbulent Flow

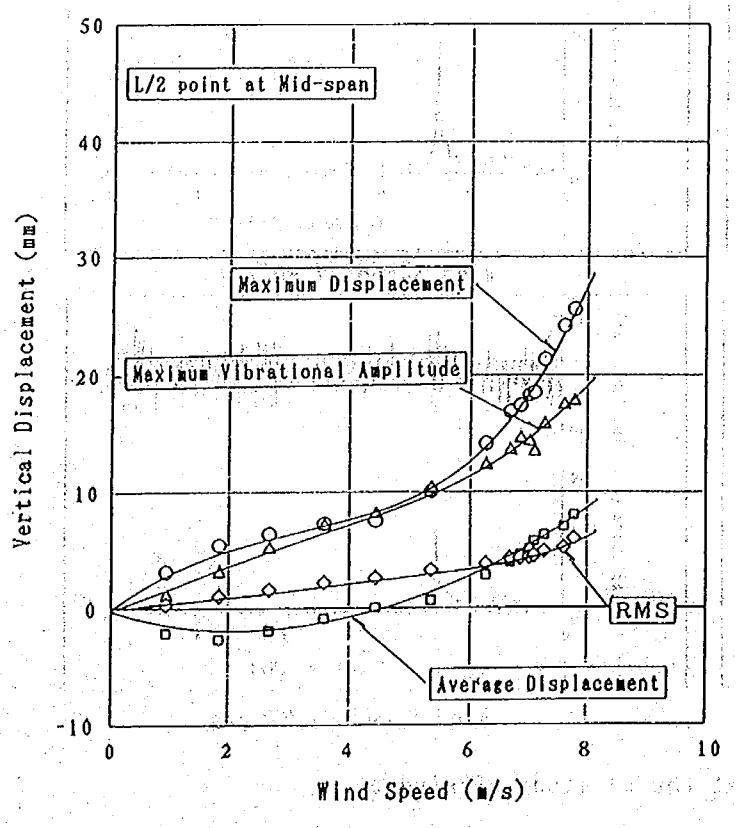


Fig.11(b) Displacement in Turbulent Flow

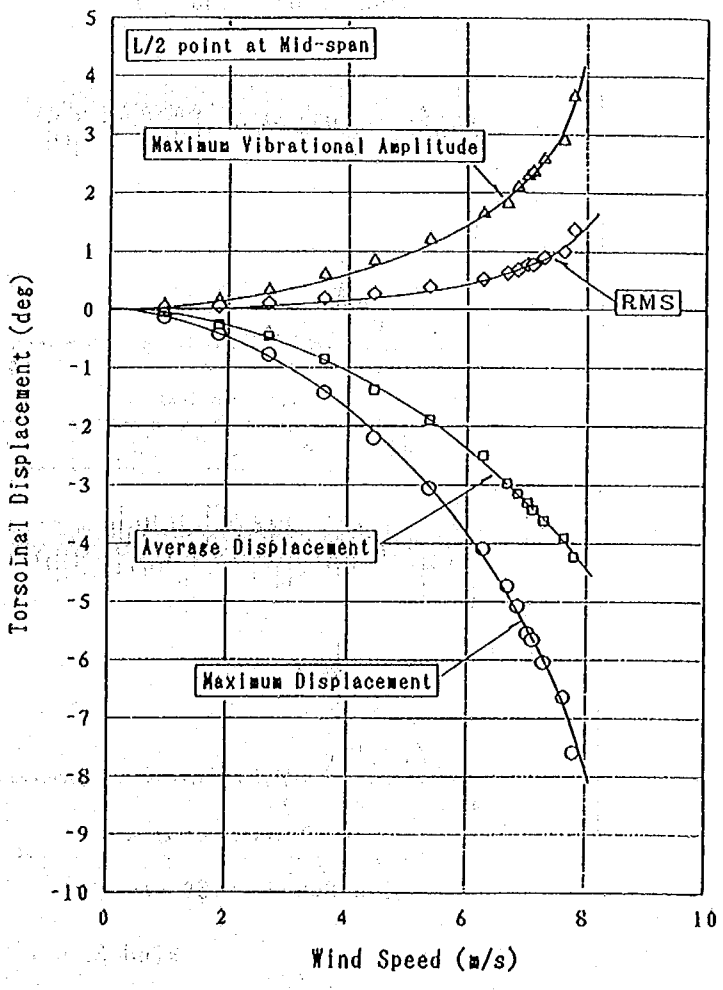
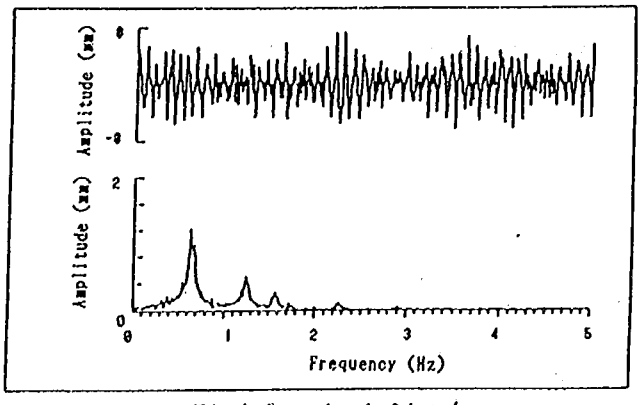
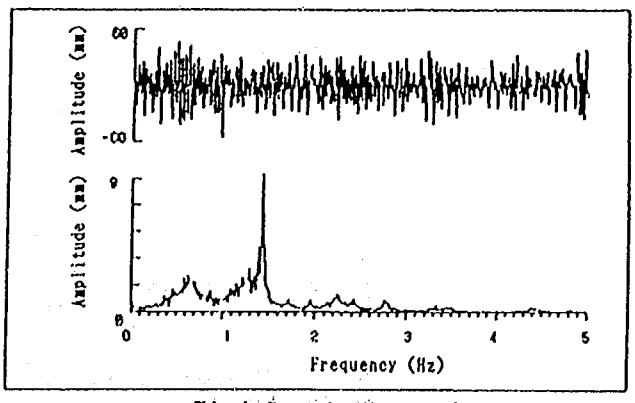


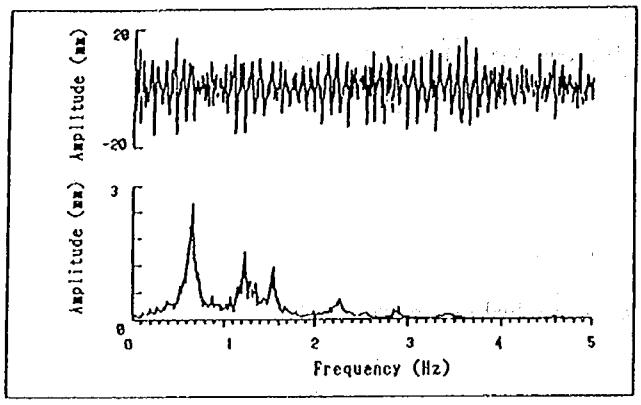
Fig.11(c) Displacement in Turbulent Flow



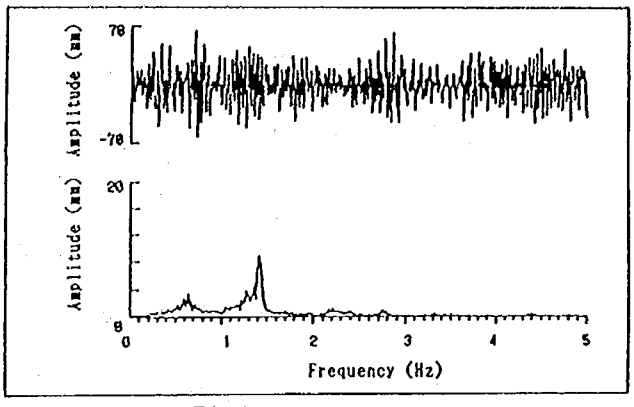
Wind Speed 1.84 m/s



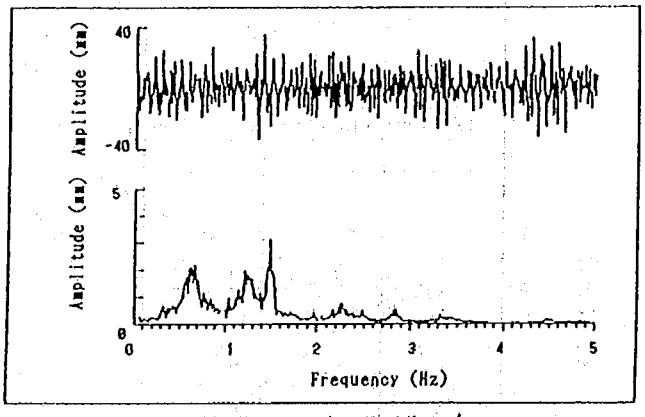
Wind Speed 7.02 m/s



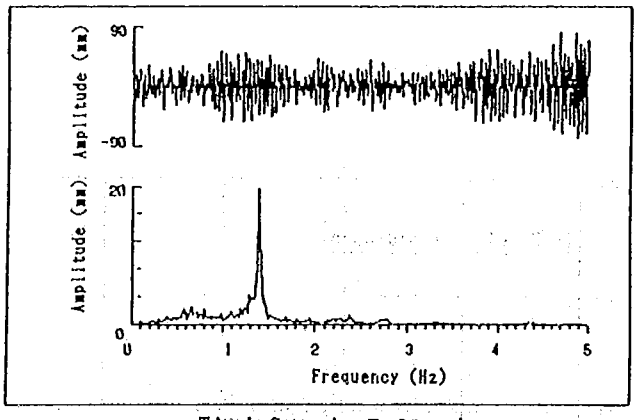
Wind Speed 3.59 m/s



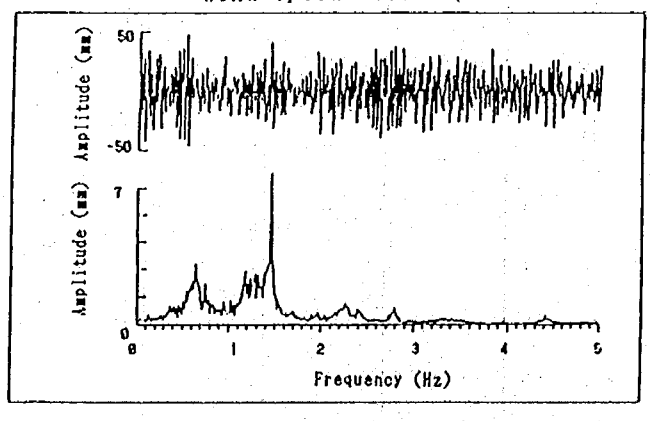
Wind Speed 7.27 m/s



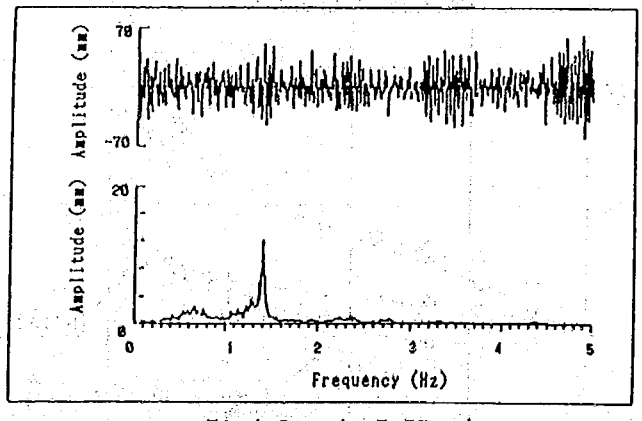
Wind Speed 5.35 m/s



Wind Speed 7.60 m/s



Wind Speed 6.68 m/s



Wind Speed 7.77 m/s

Wind Speed : at the altitude of girder

Fig.12 Power Spectral Density of Response

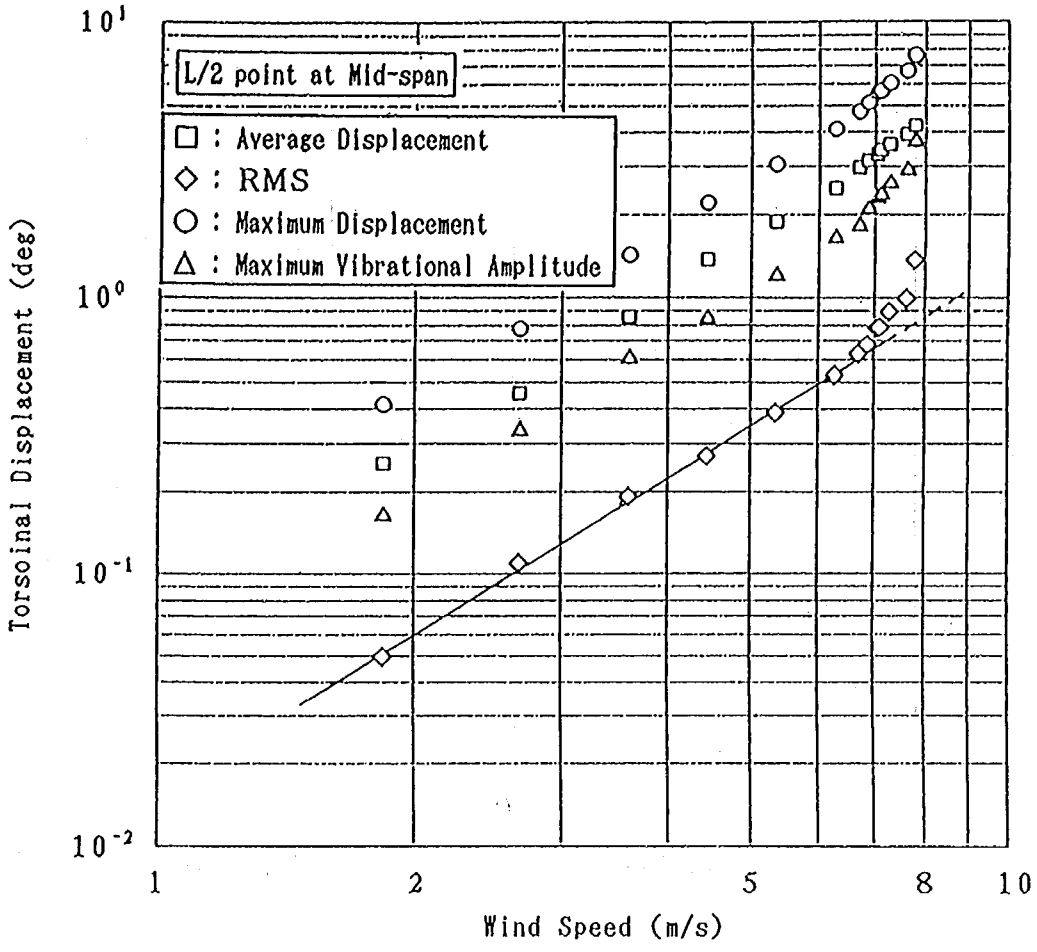


Fig.13 Displacement in Turbulent Flow (logarithmic scales)

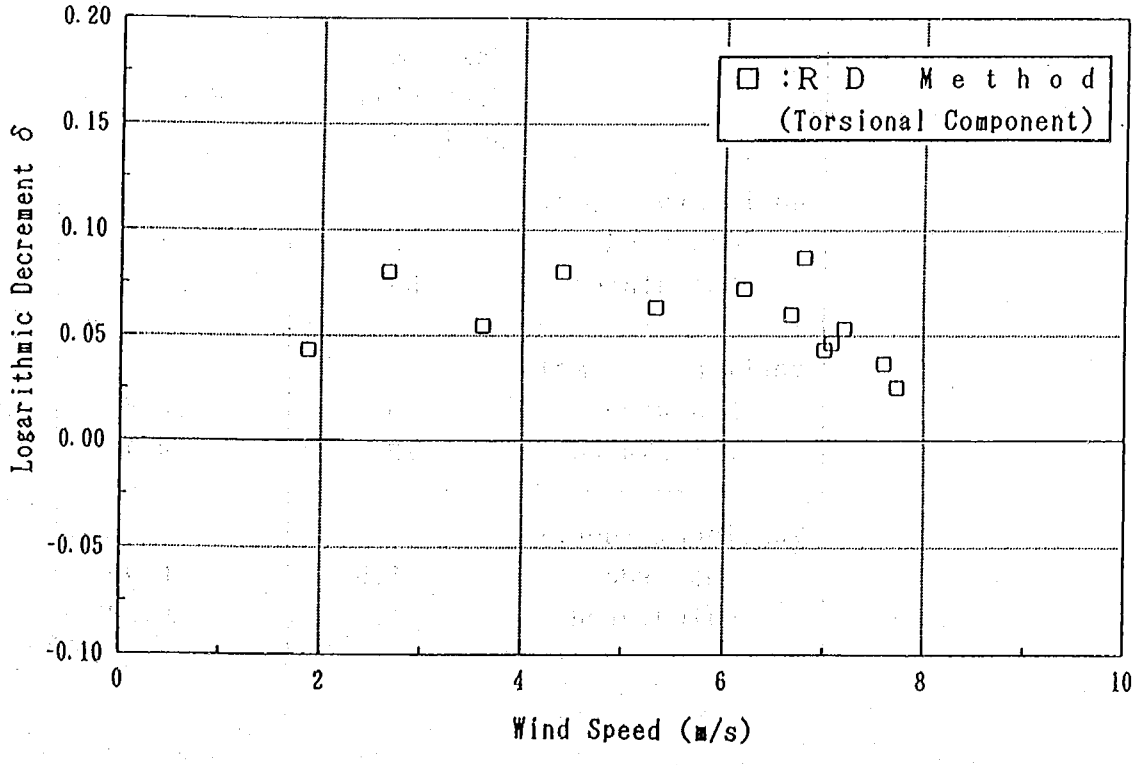


Fig.14 Damping of the Model Turbulent Flow

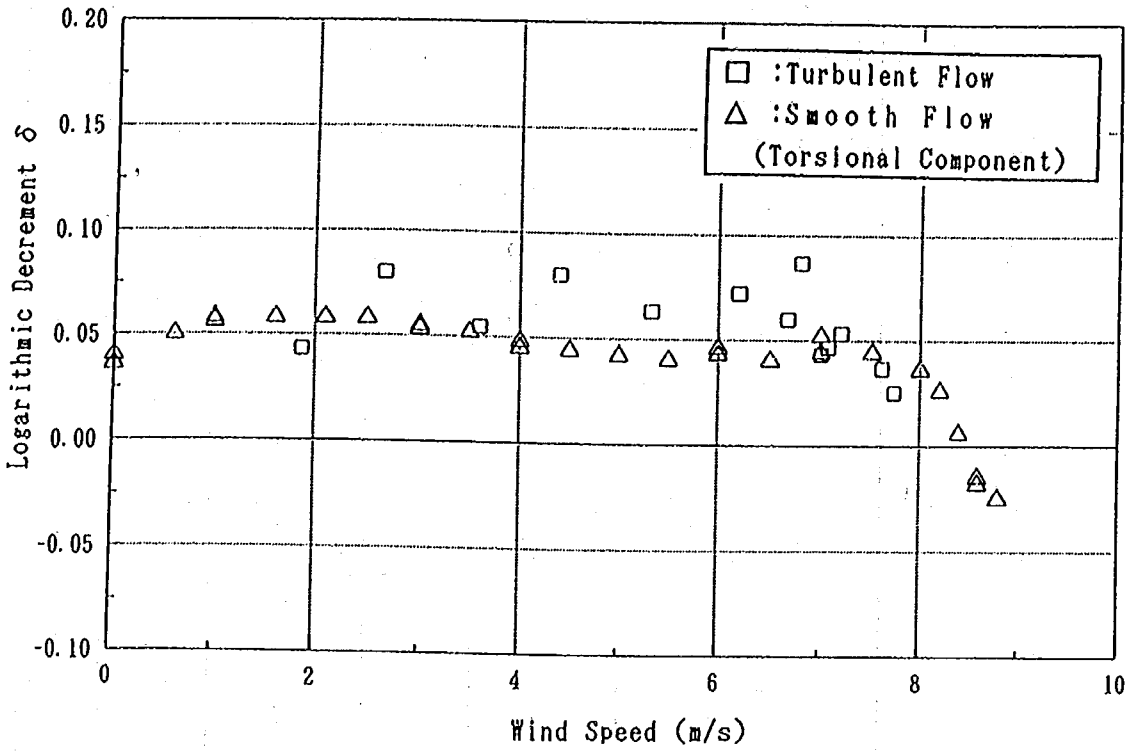


Fig.15 Damping of the Model (Turbulent Flow,Smooth Flow)

Table 2 Gust Responses

	Maximum Vibrational Amplitude	R.M.S.
Horizontal (mm)		
Measured	22	7
Calculated	56	21
Vertical (mm)		
Measured	13	3.6
Calculated	12	4.1
Torsional (deg.)		
Measured	1.9	0.49
Calculated	1.7	0.53

Improved Analytical Procedure for Predicting Flutter Response of Long-Span Bridges

by

Chunsheng Cai* and Harold R. Bosch**

ABSTRACT

An analytical procedure to investigate flutter instability of long-span bridges under turbulent wind excitation is developed. Using flutter derivatives from the laboratory, finite element methods make possible the formulation of a general aerodynamic equation of motion. Based upon this formulation, the flutter behavior of bridges under both laminar and turbulent wind excitations can be evaluated, and computational effort can be reduced by employing a random parametric excitation analysis. Flutter analysis of the Luling bridge is conducted and the proposed analysis is proven to be efficient.

KEYWORDS: flutter; bridge; wind; instability; vibration

1. INTRODUCTION

Flutter is a self-excited aerodynamic instability which can result in the collapse of bridges. A number of publications have dealt with both theories and tests relative to the flutter of long-span bridges. For the reasons of both mathematical complexity and technical difficulty, most previous theoretical and experimental works were conducted in laminar winds (Scanlan 1978a; Namini 1989; Scanlan and Jones 1990). By means of a random parametric excitation method, Lin (1979) made the theoretical analysis of turbulent wind effects on flutter instability possible. In his work, Lin observed that turbulence can sometimes have a destabilizing influence rather than the favorable stabilizing effect commonly assumed. Similar observations were made in the experimental work of Huston (1986). Lin's analysis is mathematically complex and requires considerable computational effort when multimode analysis is conducted (Bucher and Lin 1988). Therefore, approximate or simplified methods have to be used (Bucher and Lin 1989). Since the indicial function is used for wind force models in the previous parametric excitation analysis, it is difficult to implement an efficient and practical analysis procedure using finite element methods.

The objective of the present study is to develop a procedure to investigate the flutter instability of long-span prototype bridges under either laminar or turbulent wind excitations. Using flutter derivatives from the laboratory, finite element methods make possible the formulation of a general aerodynamic equation of motion. Based upon this formulation, computational effort can be reduced by employing a random parametric excitation analysis. Flutter analysis of the Luling bridge is conducted and the proposed analysis is proven to be efficient.

2. AERODYNAMIC MOTION EQUATION

Wind loading is separated into self-excited loads and buffeting loads. The former may cause instability of bridges while the latter causes random vibration. For the purpose of finite element analysis, the self-excited loads (Scanlan 1978a), denoted by subscript *se*, on a unit length of deck are expressed in the following matrix forms:

---

* Graduate Research Fellow, FHWA Turner-Fairbank Highway Research Center, 6300 Georgetown Pike, McLean, VA 22101.
** Research Structural Engineer, FHWA Turner-Fairbank Highway Research Center, 6300 Georgetown Pike, Mclean, VA 22101.

$$\{F_{se}\} = U^2 [F_d] \{q\} + U^2 [F_v] \{\dot{q}\} \quad (1)$$

where U is wind velocity which is interpreted, in this study, as mean wind velocity in laminar flow, or, mean wind velocity plus a turbulent component in turbulent flow; $[F_d]$ and $[F_v]$ which are functions of flutter derivatives H_i^*, P_i^*, and A_i^* are called *flutter derivative matrices* corresponding to displacement $\{q\}$ and velocity $\{\dot{q}\}$ respectively.

Similarly, the buffeting loads (Scanlan 1978b), denoted by subscript b, on a unit length is

$$\{F_b\} = \bar{U}^2 [C_b] \{\eta\} \quad (2)$$

where $\bar{U}$ is mean wind velocity, $[C_b]$ is steady-state force coefficient matrix; and $\{\eta\}$ is normalized turbulent wind component vector, i.e., the turbulent wind components divided by mean wind velocity.

Space frame elements are used to model the bridge deck system. By extending the force vectors in Eqs. 1 and 2 into six degrees of freedom, i.e., three translations and three rotations, and expressing the displacements $\{q\}$ in terms of displacements at nodes $\{y_e\}$ through shape function $[N]$, i.e., $\{q\} = [N]\{y_e\}$, the equivalent self-excited node forces can be obtained by means of the equivalent virtual work principle:

$$\begin{aligned}\{F_{se}^e\} &= \int_0^L [N]^T \{F_{se}\}\, dx \\ &= U^2 \int_0^L ([N]^T [F_d] [N] \{y_e\} \\ &\quad + [N]^T [F_v] [N] \{\dot{y}_e\})\, dx \\ &= U^2 [AS_e] \{y_e\} + U^2 [AD_e] \{\dot{y}_e\}\end{aligned} \quad (3)$$

where $[AS_e]$ and $[AD_e]$ are called the aerodynamic stiffness matrix and aerodynamic damping matrix of the element, respectively. Similarly, the equivalent buffeting node forces can be obtained:

$$\begin{aligned}\{F_b^e\} &= \int_0^L [N]^T \{F_b\}\, dx \\ &= \bar{U}^2 \int_0^L [N]^T [C_b]\, dx \{\eta\} \\ &= \bar{U}^2 [f_b^e] \{\eta\}\end{aligned} \quad (4)$$

Then, the node forces in the local coordinate system can be transformed to the global coordinate system. The total self-excited node forces can be assembled from element forces:

$$\begin{aligned}\{F\}_{se} &= \sum_e \{F_{se}^e\} \\ &= U^2 ([AS] \{y\} + [AD] \{\dot{y}\})\end{aligned} \quad (5)$$

where the structure matrices $[AS]$ and $[AD]$ result from the contribution of element matrices $[AS_e]$ and $[AD_e]$ respectively.

Similarly the total buffeting node forces can be obtained:

$$\{F\}_b = \sum_e \{F_b^e\} = \bar{U}^2 [f_b] \{\eta\} \quad (6)$$

Once the self-excited and buffeting forces are obtained, the following general aerodynamic motion equation can then be derived:

$$\begin{aligned}&[M] \{\ddot{y}\} + [D] \{\dot{y}\} + [K] \{y\} = \\ &U^2 ([AS] \{y\} + [AD] \{\dot{y}\}) + \bar{U}^2 [f_b] \{\eta\}\end{aligned} \quad (7)$$

where $[M]$, $[D]$, and $[K]$ are mass, damping, and stiffness matrices, respectively.

Introducing the modal analysis method and pre-multiplying both sides of Eq.7 by the mode

shape matrix $[\Phi]^T$, the general motion equation in the mode space can be obtained:

$$[M^*]\{\ddot{\xi}\} + [D^*]\{\dot{\xi}\} + [K^*]\{\xi\} = U^2 * ([AS^*]\{\xi\} + [AD^*]\{\dot{\xi}\}) + \bar{U}^2 [f_b^*]\{\eta\} \quad (8)$$

where $[M^*]$, $[D^*]$, and $[K^*]$ are generalized mass, damping, and stiffness matrices, respectively; and $\{\xi\}$ is generalized coordinate vector.

The flutter derivative matrices $[F_d]$ and $[F_w]$ in Eq.1 are functions of reduced frequency $k=(b\omega)/\bar{U}$. In flutter analysis, ω is oscillating circular frequency which can be determined by the condition of non-trivial homogenous solution of Eq.8 (Namini 1989). In buffeting analysis, natural circular frequency can be used in each corresponding mode (Scanlan 1978b, 1988).

3. PARAMETRIC RANDOM VIBRATION

In Eq.8, if the wind velocity U is treated as the mean value and the buffeting force is dropped, the flutter analysis becomes a deterministic eigenvalue problem as was done in Namini (1989). However, if the U is treated as two parts, a mean value and a random (turbulent) component, then Eq.8 is a parametric random excitation problem, and a knowledge of stochastic differential equations is thus needed. Lin (1979) is the first to treat Eq.8 as a parametric random excitation problem. By use of the approximation:

$$U^2(t) = (\bar{U} + u(t))^2 \sim \bar{U}^2 + 2\bar{U}u(t) \quad (9)$$

where $u(t)$ is the along-wind turbulent component of wind, Eq.8 is expressed in the first-order form to conduct the analysis with the parametric random excitation method:

$$\{\dot{X}\} = \left([A] + [B]\frac{u(t)}{\bar{U}}\right)\{X\} + [C]\{\eta\} = [A]\{X\} + ([B]\{X\}\{\delta\}^T + [C])\{\eta\} \quad (10)$$

where $\{\delta\}^T = [1,0]$; $\{X\}$ = state-space vector; and $[A]$, $[B]$, and $[C]$ are matrices introduced for convenience.

Approximating the physical state-space vector $\{X\}$ as a Markov process, using Ito's stochastic differential equation, Ito's differential rule, as well as stochastic ensemble average, the moments for different order can be obtained. The readers are referred to (Ibrahim 1985) for more details. For engineering purposes, only the first and second moments are generally needed.

The first moment $\{\mu\}$ is derived as:

$$\{\dot{\mu}\} = [F]\{\mu\} + \{R\} \quad (11)$$

where $\{\mu\} = E(\{X\})$, E = ensemble average. $\{R\}$ results from buffeting force. The second moment $\{\nu\}$ is:

$$\{\dot{\nu}\} = [H]\{\nu\} + \{Q\} \quad (12)$$

where $\{Q\}$ results from buffeting force.

In the above formulation, if three natural modes are considered, then the size of state-space vector $\{X\}$ will be six. Therefore, the size of matrix $[H]$ will be 21 by 21. If the indicial function is used in the wind force model, $[H]$ will be 210 by 210 (Bucher and Lin 1988, Bucher and Lin 1989). This means that 210 simultaneous algebraic equations need to be solved for buffeting analysis and the eigenvalues of a 210 by 210 matrix need to be obtained at every wind velocity to identify flutter instability in flutter analysis. If more modes are used, the size of the matrix $[H]$ will increase rapidly and

simplification has to be used as shown in (Bucher 1989). The formulation of this study can significantly reduce the computational effort.

4. FLUTTER INSTABILITY

Since the inhomogeneous term (buffeting force) doesn't affect flutter instability, the general approach is to drop it and solve the homogeneous equation to identify the critical flutter speed. In turbulent wind, system instability is interpreted as the moment instability in this study, and the corresponding wind velocity is identified as the flutter speed (Lin 1979). Conceptually, if the real part of one of the eigenvalues of *[F]* or *[H]* becomes positive, then the first moment or the second moment become unstable. The following procedure is used to identify the flutter speed.

4.1 First Moment Instability

In Eq.11, if the inhomogeneous term *{R}* is dropped, then the motion equation reduces to the flutter problem described by first moment. If we set $\{\delta\}^T = [0,0]$, it can be shown from Eq.10 that the equation reduces to that of the flutter problem in the deterministic case (in laminar flow) expressed in the form of the state-space vector.

The oscillating circular frequency and critical flutter speed for the first moment can be identified by the pK-F method used in laminar flow (Namini 1989). In the deterministic case, the oscillating frequency is the motion frequency of the generalized coordinates. For the indeterministic case, i.e., in turbulent flow, the oscillation frequency is the motion frequency of the mean value of the generalized coordinates.

4.2 Second Moment Instability

The successful use of the Pk-F method is based on the understanding that the natural frequencies are not strongly changed by aerodynamic force when wind velocity is low. Therefore, the eigenvalues of the flutter matrix can be initialized by the natural frequencies and then a trial-and-error method can be used to find the true eigenvalues.

For the second moment instability, it is hard to give an appropriate initial value which will guarantee the convergence of the trial-and-error process. Therefore, all the eigenvalues of matrix *[H]* in Eq.12 need to be identified. The size of *[H]*, (modes*(2*modes+1)) by (modes*(2*modes+1)), increases quickly as the number of modes increases. Solution of the eigenvalues of a large non-symmetric matrix is quite labor intensive. Further, since we must judge the flutter instability based upon the fact that the real part of one of the eigenvalues transitions from negative to positive, we need to obtain very accurate solution of each eigenvalue, at least one of which is very small (close to zero). This makes the numerical process still more difficult. In addition, we need to repeat the above process for many wind velocities or turbulence intensities to identify the critical flutter speed. The whole process requires prohibitive computational effort.

The second moment of the stationary buffeting response can be obtained from Eq.12 as follows

$$\{v\} = -[H]^{-1}\{Q\} \qquad (13)$$

Lin (1979) pointed out that the buffeting response *{v}* tends to become infinite when the wind velocity increases close to flutter speed. Tsiatas (1988) used this idea to identify the flutter speed based on buffeting prediction. In this study, it is found that the buffeting mean-square response in Eq.13 may become negative, which is physically impossible. Therefore, instability of the second moment will be declared when buffeting mean-square response becomes either negative or infinite. This numerical process significantly reduces computational effort compared to that of finding the eigenvalue of *[H]* as discussed above.

5. NUMERICAL EXAMPLE

The Luling bridge is a cable-stayed bridge which spans the Mississippi River connecting the towns of Luling and Destrehan in St. Charles Parish, about 12 miles (19.3 kilometers) west of New Orleans, Louisiana. It has a total length of 2745 feet (836.7 meters) which is divided into five spans with the center span being 1235 feet (376.4 m) meters) between tower piers. The cables are arranged as a double-plane fan with 12 cables in each plane. The readers are referred to (Bosch 1978) for detailed information.

A nonlinear static analysis to determine the deformed configuration, and linear dynamic analysis to obtain natural frequencies and natural modes was conducted using the LEAF program developed by (Namini 1989). The first vertical, second vertical and first torsional modes are used in the following analysis. These modes are referred to as mode 1, mode 2, and mode 3 with natural frequencies 0.43 (Hz), 0.63 (Hz), and 1.22 (Hz), respectively.

5.1 Flutter in Laminar Flow

To compare the results of this study with those of (Namini 1989) and to verify the programming of this study, the authors conducted the flutter study in laminar flow with wind attack angles of zero and six degrees.

In the process of measuring the flutter derivatives from experiments, the displacement $\{q\}$ and self-excited force $\{F_{se}\}$ in Eq.1 are taken to be along the center line of deck. For finite element simulation, the displacement $\{q\}$ in the self-excited force model and all the wind forces should be, therefore, referred to the center of deck for consistency with experiments. In Namini's (1989) analysis, the section was divided into two lines of elements coincident with the two box girders. The displacements along these elements, instead of along the center line of the deck, were used in the finite element simulation of the self-excited forces. This is not conceptually consistent with experiments. This can be corrected by putting one additional line of elements along the center line of the deck, and the wind forces are applied to these elements. Alternatively, the relationship between the displacements along the center line of deck and those along the girder lines is derived based on a rigid body assumption, and then the forces can be equivalently distributed along the two girder lines. This is conveniently done by modifying some of the flutter derivatives (Cai 1993). This wind distribution method is denoted as *Present Study*[3] in Table 1. Another study denoted as *Present Study*[2] in Table 1, using the same wind force distribution as that of Namini (1989), is also conducted for comparative purposes. The influence of flutter derivatives H_1^* and A_3^* on flutter speed is investigated. The results are presented in Table 1.

Namini (1989) used a "lumped" aerodynamic element formulation. This formulation ignores the aerodynamic bending moment which is generally of second order importance to the torsional instability, but may be important to vertical instability. In this study, the consistent finite formulation described in Eqs. 3 and 4 is used. When H_1^* equals zero, *Present Study*[2] has not only the same wind force distribution, but also the same finite element formulation as those of Namini (1989). In this case, the two approaches give almost exactly the same results as shown in Table 1. However, when H_1^* is considered, results from the two models are somewhat different. Since H_1^* is negative as shown in Fig.1, it represents positive aerodynamic damping, which should enhance the resistance to flutter. For this reason, the flutter speeds in the third column in Table 1 should be larger than those in the fourth column. The lumped formulation in (Namini 1989) does not reflect this tendency.

The damping ratios in all the above studies were 0.207 % for bending and 0.08% for torsion modes. These numbers are the existing damping ratios for the section model (Namini 1989). The actual damping of the prototype bridge should be higher than the section model. Therefore, the

results given in Table 1 are conservative.

From section model tests, Bosch (1978) conservatively predicted that the prototype Luling bridge has a flutter speed of 190 km/h (118 m.p.h) for a six degree attack angle, and greater than 402 km/h (250 m.p.h.) at zero degrees. If damping ratios of 1.3% for bending and 0.5% for torsion modes are assumed, this study predicts a flutter speed of 207 km/h (129 m.p.h.) for six degree attack angle and greater than 402 km/h (250 m.p.h) for zero degrees. The validity of the present program can be demonstrated by all the above results.

5.2 Flutter in Turbulent Flow

After verification of the program in the laminar flow, the flutter analysis in turbulent flow is conducted.

The first moment instability can be identified by the Pk-F method as used in the case of laminar wind. The instability of the second moment is observed when the mean square of the generalized coordinate becomes infinite or negative, both being physically impossible. The results for the first and second moment instabilities are summarized in Figs.2 and 3.

It can be seen from the figures that the turbulent component of wind does not significantly change the stability of the first moment unless the controlling mode changes. If the flutter control mode does change due to the influence of turbulent components, then a sharp change in slope occurs in the curve and the flutter speed can vary significantly when compared with laminar flow (with spectral density being Zero). This sharp change in slope was also found in (Bucher 1989) when controlling mode changes.

When the spectral density is larger than 0.2, the influence of turbulent component on the second moment instability is significant. It should be noted that white noise input is assumed in the parametric random excitation analysis. If the instability boundaries shown in Figs. 2 and 3 are to be used for engineering applications, it is necessary to determine first the spectral density of the actual wind, and then convert it into the spectral density of equivalent white noise to judge the influence of the turbulent wind component on flutter. Bucher and Lin (1989) suggested using the spectral density at zero frequency as the spectral density of the equivalent white noise. This represents a value of about 0.2 for Simiu's wind spectrum if the wind velocity is 60 m/s, the height of bridge is 50 m and the turbulence intensity is 0.12. Very high normalized spectral density is unrealistic. The dramatic reduction of the flutter speed at very high spectral densities shown in Figs. 2 and 3 are, therefore, more academic than practical.

6. CONCLUSIONS

A finite element procedure which is suitable for flutter analysis in both laminar and turbulent winds is developed. By use of a parametric excitation method, the effects of turbulence on flutter instability are investigated for the existing Luling bridge. The flutter of the bridge in laminar wind is treated as a special case of turbulent wind with zero turbulence intensity. The influence of the turbulence intensity on the first moment is very small which agrees with previous general conclusions (Lin 1979; Tsiatas and Sarkar 1988). However, this conclusion only holds true when mode 3 (torsional mode) controls the flutter. From the parametric excitation analysis, mode 1, which is ever-stable in the laminar flow, appears to be unstable when the turbulence intensity is quite large, though this is an unrealistic condition. If the flutter is controlled by mode 1, then turbulence intensity does exhibit a large influence on first moment.

Although the influence of turbulence intensity on the second moment stability is large for the Luling bridge when wind spectral density is high, the design requirement for flutter speed of 240 km/h at zero degree attack angle can still be met for a realistic level of normalized spectral density which is generally less than 0.2.

7. REFERENCES

Cai, C.S. (1993). "Prediction of Long-Span Bridge Response to Turbulent Wind." Interim Report to Federal Highway Administration.

Bosch, H.R.(1978). "Aerodynamic Investigation of the Luling, Louisiana Cable-Bridge." Report No. FHWA-RD-77-161, Federal Highway Administration, Offices of Res. and Development, Washington, D.C.

Bucher, C. G., and Lin, Y. K. (1988). "Stochastic Stability of Bridges Considering Coupled Modes." *Journal of Engineering Mechanics*, ASCE, 114(12), 2055-2070.

Bucher, C. G., and Lin, Y. K. (1989). "Stochastic Stability of Bridges Considering Coupled Modes: II." *Journal of Engineering Mechanics*, ASCE, 115(2), 384-400.

Huston, D. R. (1986). *The Effects of Upstream Gusting on the Aeroelastic Behavior of Long Suspended-Span Bridges*. A Dissertation Presented to the Faculty of Princeton University in Candidacy for the Degree of Doctor of Philosophy, Recommended for Acceptance by the Department of Civil Engineering.

Ibrahim, R. A. (1985). *Parametric Random Vibration*. Research Studies Press LTD., Letchworth, Hertfordshire, England.

Lin, Y. K. (979). "Motion of Suspension Bridges in Turbulent Winds." *Journal of the Engineering Mechanics Division*, ASCE, 105(6), 921-932.

Lin, Y. K., and Ariaratnam, S. T. (1980). "Stability of Bridge Motion in Turbulent Winds." *Journal Of Structural Mechanics*, 8(1), 1-15.

Namini, A. (1989). *The Aerodynamic Stability of Cable-Stayed Bridges*. Dissertation Submitted to the Faculty of the Graduate School of the University of Maryland in Partial Fulfillment of the Requirements for the Degree of Doctor of Philosophy.

Scanlan, R. H., Beliveau, J. G., and Budlong, K. S. (1974). "Indicial Aerodynamic Functions for Bridge Decks." *Journal of Engineering Mechanics Division*, ASCE, 100(4), 657-672.

Scanlan, R. H. (1978a). "The Action of Flexible Bridges under Wind, I: Flutter Theory." *Journal of Sound and Vibration*, 60(2), 187-199.

Scanlan, R. H. (1978b). "The Action of Flexible Bridges under Wind, II: Buffeting Theory." *Journal of Sound and Vibration*, 60(2), 202-211.

Scanlan, R. H. (1978c). "Effects of Turbulence on Bridge Flutter Derivatives." *Journal of the Engineering Mechanics Division*, ASCE, 104(4), 719-733.

Scanlan, R. H. (1984). "Role of Indicial Functions in Buffeting Analysis of Bridges." *Journal of Structural Engineering*, ASCE, 110(7), 1433-1446.

Scanlan, R. H. (1987a). "Interpreting Aeroelastic Models of Cable-Stayed Bridges." *Journal of Engineering Mechanics*, ASCE, 113(4), 555-575.

Scanlan, R.H. (1988). "On Interpreting Model and Prototype Responses of Suspended-Span Bridge to Wind." *Proc. 19th Joint Meeting of the U.S.-Japan Cooperative Program in Natural Resources Panel on Wind and Seismic Effects.*

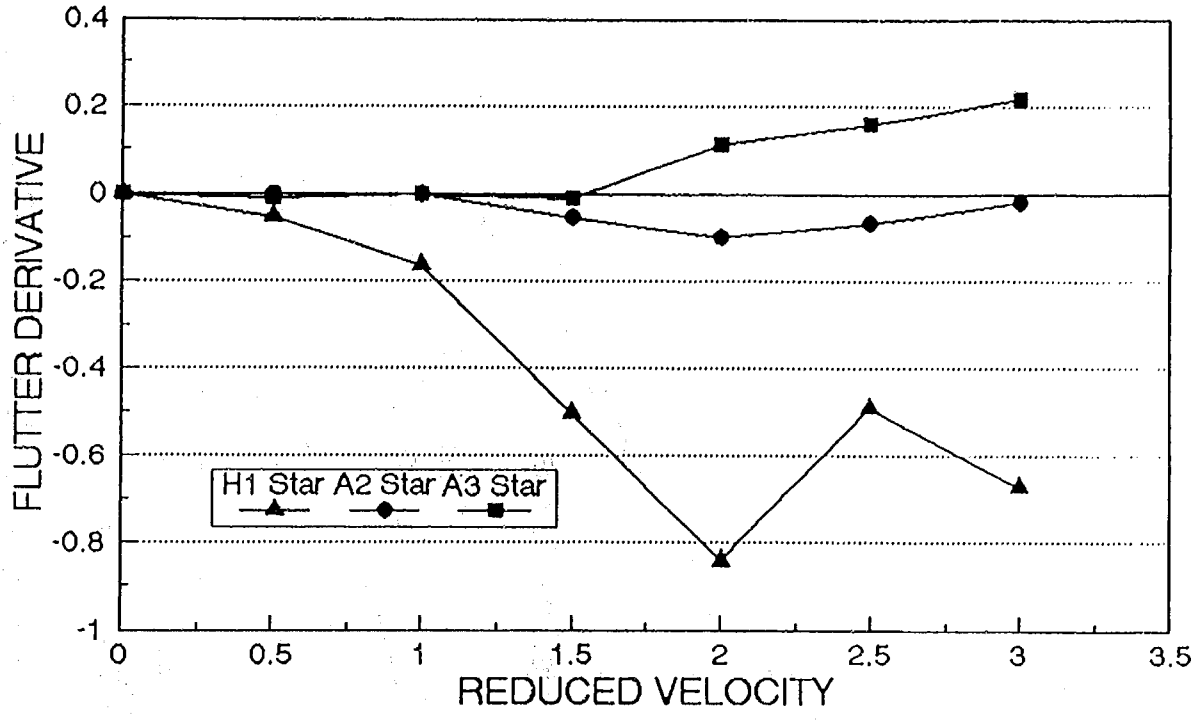
Scanlan, R. H., and Jones, N. P. (1990b). "Aeroelastic Analysis of Cable-Stayed Bridges." *Journal of Structural Engineering*, ASCE, 116(2), 279-297.

Tsiatas, G., and Sarkar, P. P. (1988). "Motion Stability of Long-Span Bridges under Gusty Winds." *Journal of Engineering Mechanics*, ASCE, 114(2), 257-277.

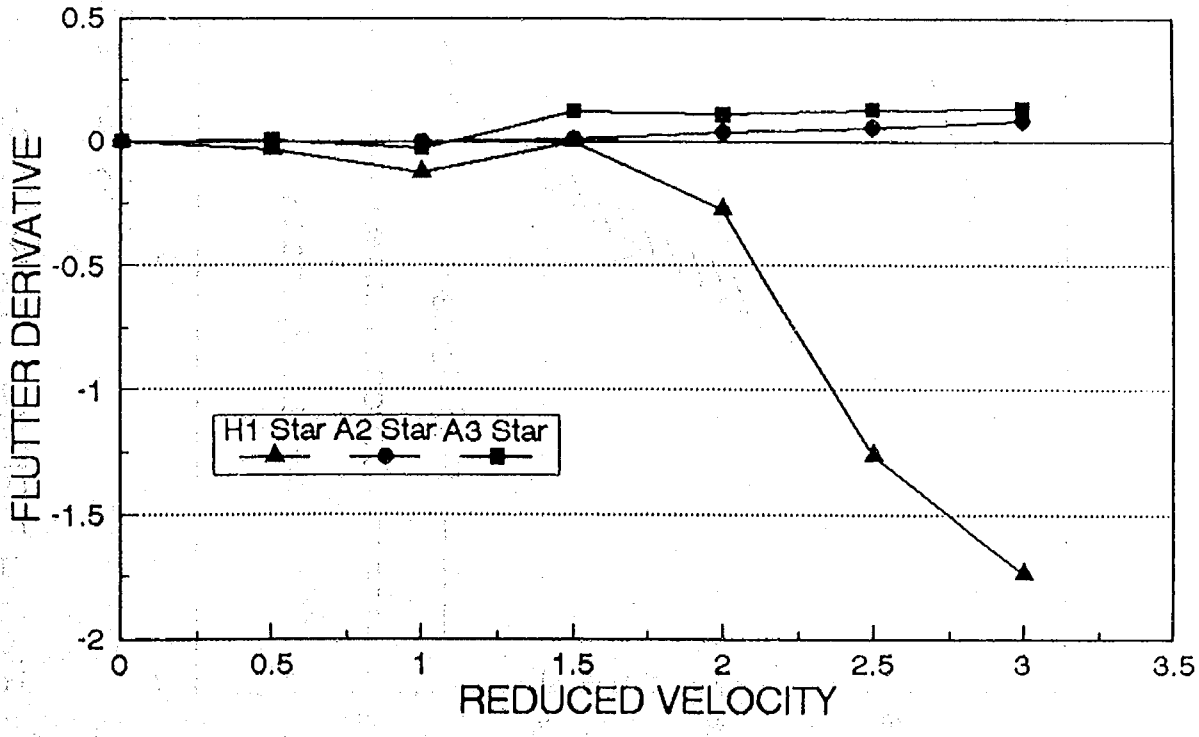
Table 1 Flutter speed of Luling Bridge in Laminar Flow

Angle of Attack (deg)	Analysis Methods	$H_1^*, A_2^* \& A_3^*$ (km/hr)	$A_2^* \& A_3^*$ (km/hr)	A_2^* only (km/hr)
0	Namini (1989)[1]	342	344	389
	Present Study[2]	395	344	389
	Present Study[3]	402	365	390
6	Namini (1989)[1]	139	134	133
	Present Study[2]	158	133	133
	Present Study[3]	158	141	141

1. Lumped self-excited force applied at nodes along girder center lines
2. Consistent self-excited force applied at nodes along girder center lines
3. Consistent self-excited force applied at nodes along bridge center line



(a) Angle of Attack at Zero Degree



(b) Angle of Attack at Six Degrees

Figure 1 Flutter Derivatives of Luling Bridge

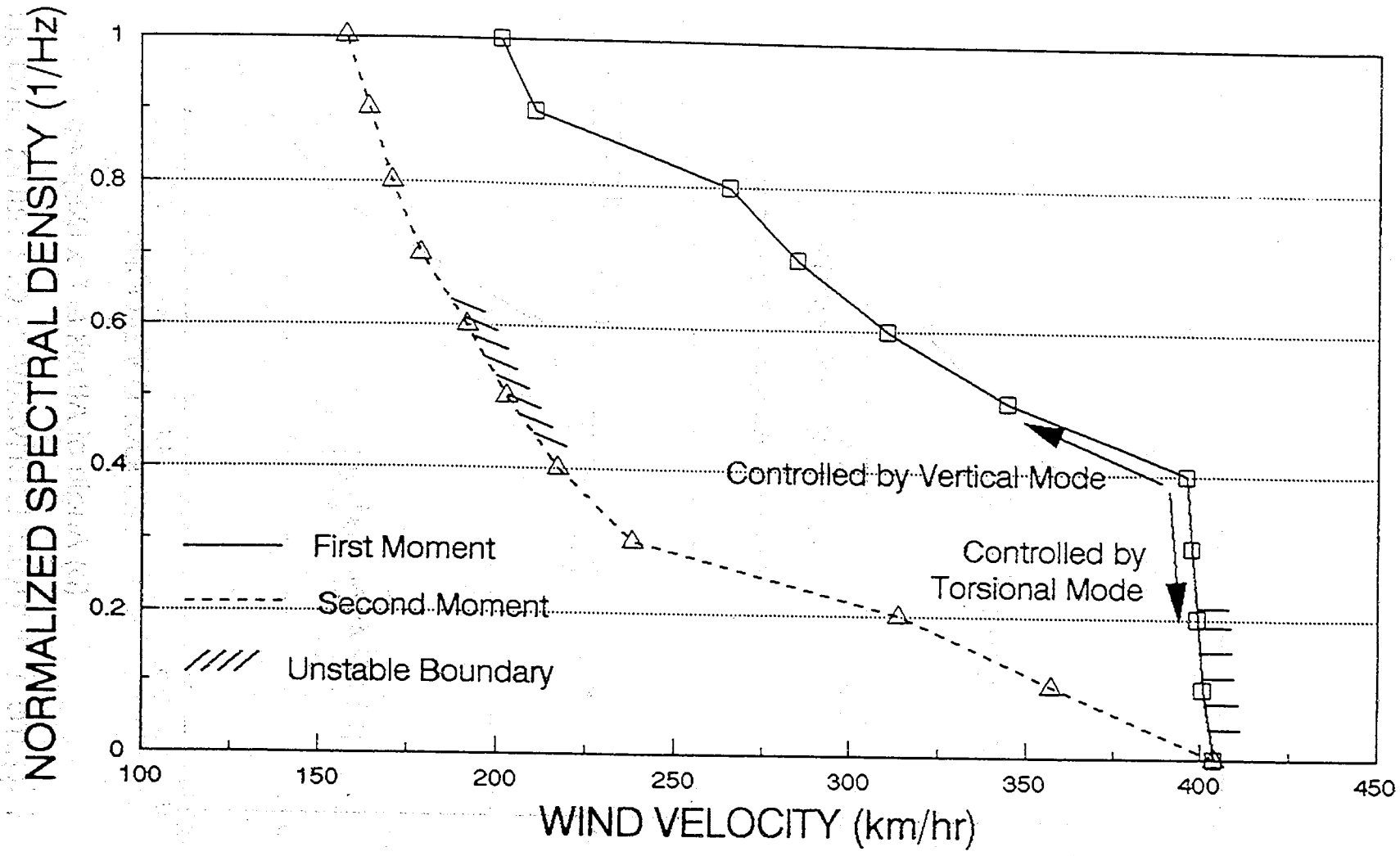


Figure 2 Flutter Intability Boundary (Angle of Attack at Zero Degree)

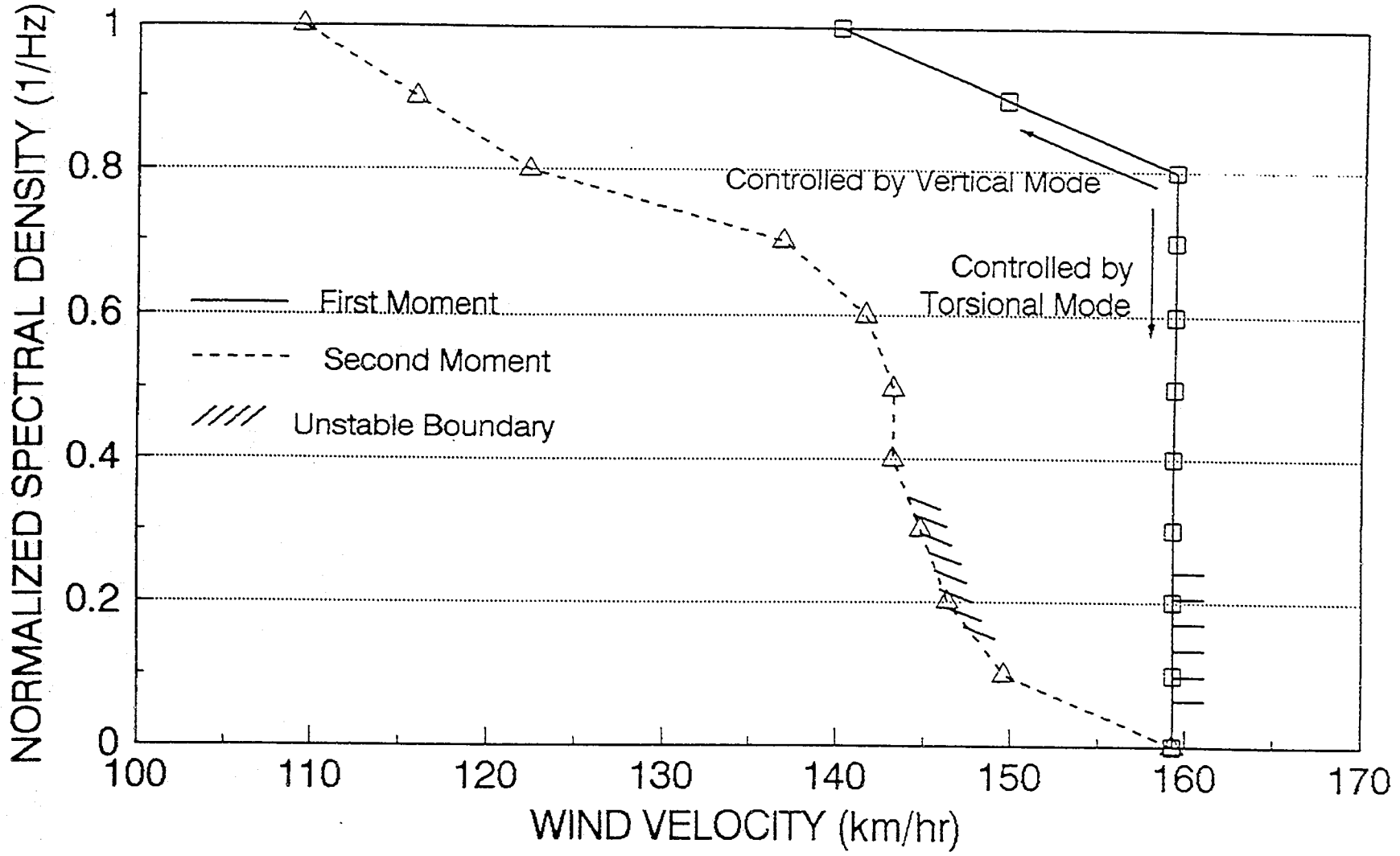


Figure 3 Flutter Instability Boundary (Angle of Attack at Six Degrees)

Theme 2

Outline of Strong-motion Records on the Off Kushiro Earthquake in 1993

Osamu NAKANO[1], Toshio YAMAUCHI[2]
Manabu KANEKO[3] and Yuji ONO[3]

ABSTRACT

Presented are the results of an investigation in which collected strong-motion records on the 1993 Off Kushiro Earthquake were digitized and wave analyses including power spectrum, acceleration response spectrum and so on were performed.

On roads, there was little damage to bridges except bridges with poor substructure, but much damage to earth works in cuts and embankments

After conducting power spectrum analysis of strong-motion record at some seismic stations, it was clarified that wave period of about 2-seconds was predominent in the principal waves in the 1993 Off Kushiro Earthquake.

KEYWORDS: the 1993 Off Kushiro Earthquake; strong-motion record; strong-motion seismograph; polarization analysis

1. INTRODUCTION

A major earthquake that hit extensive areas in northeasten Japan took place at 8:06 p.m., January 15, 1993 with its hypocenter off Kushiro, located in the eastern part of Hokkaido. The quake measured 7.8 on the magnitude by the Japan Meteorological Agency (JMA) scale, comparable in magnutude to the 1923 Great Kanto Earthquake which registerd 7.9. It was later designated the "1993 Off Kushiro Earthquake" by the JMA according to a traditional manner.

A strong tremor rumbled through the Pacific coast region of Hokkaido. Six on the seismic intensity scale of the JMA with up to seven was registered in Kushiro City, which is located very near to the epicenter and 5 in Obihiro City, Hiroo Town and Urakawa Town.

The powerful earthquake caused heavy damages to roads, embankments of rivers and port facilities mainly in eastern Hokkaido.

Restoration was difficult due to frozen soil peculiar to cold regions such as Hokkaido. For example, it took as much as three weeks to resume gas supply service among key lifelines in the city of Kushiro because many gas leaks happened underground.

The Structures Section of the Civil Engineering Research Institute began strong-motion observation at the Chiyoda Bridge on Octoeber of 1966. As of March, 1993, 28 seismic stations with strong-motion seismographs are open at bridges on national highways in Hokkaido under the control of the Structures Section.

Out of which, the strong-motion records on the 1993 Off Kushiro Earthquake were collected from 20 bridges including the Chiyoda Bridge and the Tokachi-Kakoh (the Tokachi estuary) Bridge. Wave analysis was carried out with spectrum analysis after digitizing the records.

This report will present the results of an investigation on the strong-motion records at stations, located relatively close to the epicenter.

2. DETAILS OF THE EARTHQUAKE

The 1993 Off Kushiro Earthquake was the first temblor, which was registered 6 in the seismic intensity scale of the JMA with up to 7, since the 1982 Off Urakawa Earthquake

1) Dr., Head, Structures Section, Civil Engineering Research Institute
2) Deputy Head, ditto
3) Research Engineer, ditto

which registerd 7.1.

Table-1 summarizes the outline of the 1993 Off Kushiro Earthquake and the damages caused by the earthquake in which the casualty toll does not include one person who was killed by a gas leak after the earthquake. Table-2 lists up major earthquakes which occured in Japan in the past.

For the magnitude, the 1993 Off Kushiro Earthquake got the fifth position, in the wake of the 1923 Great Kanto Earthquake in the Taisyo era, the Nankai Earthquake, and the two earthquakes of Off Takaichi after the Second World War.

The 107km focal depth is also characteristic of this earthquake, different from other major earthquakes in which the depth of the focus were relativly shallow..

Besides the damages in Table-1, some national trunk roads were forced to stop daily service immediately after emergency check by the Hokkaido Development Bereau as road administrator: on Route 44 between Miyazono-machi, Akkeshi Town and the Kumaushi plain, Hamanaka Town; Route 240 between Shitakara plain, and Teshibetsu plain, Akan Town; and Route 272 between Arekinai and Tohro, Shibecha Town. The suspension of traffic on Route 240 was due to damages to the substructure of the Matsunoe Bridge, and for the others collapse of earth works.

Prefectural roads also were closed as of 5:00 p.m. on January 18 on 11 sections of 11 roads.

Railway service by Hokkaido Railway Co. was suspended on two lines as well: the Nemuro and Senmo Main Lines. Normal service was resumed on February 1. It was reported by the company that the total damage amounted to about 1.5 billion yen, including running losses due to suspension of services.

Many traces of soil liquefaction due to the earthquake remained in extensive areas; On Route 44 between Kiba and Kashiwagi in Kushiro Town, manholes of sewer buried in the walkways were lifted about 1.5m high, and in the West Port of Kushiro, concrete slabs on wharves were disrupted

Fortunately, there were no major fire disasters and though heaters like oil stove were used in the severe Hokkaido winter, only seven fires broke out.

3. SEISMIC STATIONS AND STRONG-MOTION RECORDS

Strong-motion records on the earthquake were obtained at 20 seismic stations. Figure-1 describes our own network of strong-motion observation. Figure-2 represents the location of the stations relatively close to the epicenter, and Table-3 gives the names of bridges, ground classifications, the types of strong-motion seismographs installed, and distances from the epicenter.

The new Onnetoh Bridge, first base-isolated bridge in Hokkaido, was completed last year next to the present Onnetoh Bridge which has been installed strong-motion seismographs since 1974. As the strong-motion records on the ground, a pier and an abutment were able to collect in this time, these data are the first ones obtaind from the place very close to a base-isolated bridge in the case of a major earthquake in Japan. We hope that these will contribute to the further development of base-isolated designs.

Digital-type strong-motion seismographs produced by Rion Co. were installed on the Tokachi-Kakoh Bridge, the most modern bridge, completed at the end of last year. For dealing with the digital data, we faced serious difficulties with sampling frequency of the data and a mismatch between hardware and software. Therefore, it appears that further investigations will be necesarry with this seismograph.

All strong-motion records except at the Tokachi-Kakoh Bridge were in analog

form, on stylus paper (SMAC-B_2) or scratch record film (SMAC-Q), they were digitalized by applying corrections for time, centeral axis, circular arc, and instrument characteristics during A/D conversion based on a control system[1] for strong-motion records developed by the Structures Section.

Table-4 shows the list of the maximum acceleration of strong-motion records by each component.

Records at the Otanoshike Bridge, obtained near the epicenter of the powerful earthquake, are very valuable data. The maximum acceleration is very large, 372 gal on a horizontal component in the bridge longitudinal direction. Data obtained from the four other bridges are also very important to seismic engineering.

The maximum acceleration indicates that both two horizontal motion were very powerful and large the same as the past major earthquakes. In addition, it should be took note that the vertical movement were very large as well.

4. ANALYSIS OF STRONG-MOTION RECORDS

Strong-motion records were analyzed using data at the following three bridges in this investigation: Otanoshike Bridge on Route 38, Chiyoda Bridge on Route 242, and Tokachi-Kakoh Bridge on Route 366. The three-conponent seismograms recorded at the bridges are shown in Figures-3,-4, and -5, respectively.

First of all, the 3-component seismograms of the Tokachi-Kakoh Bridge was diveded into two parts: 1) the 10 seconds from the start of recording, corresponding to the P-wave, and 2) the 16-48 seconds corresponding to the S-wave, to clarify predominant period of each case after calculating power spectrum and acceleration response spectrum.

Figure-6 describs a soil boring log near the Tokachi-Kakoh Bridge, and Figure-7 is one example of case-2 on the power spectrum analysis in the longitudinal direction. The result indicates that long-periodic waves of about 2 seconds were predominent in the main quake motion.

A 3-component seismograph was placed at 50m below the ground surface at this bridge as well, and the underground accelerations were compared with those on the ground to investigate an amplification ratio by the frequency components. Figure-8 shows the result of comparison in the longitudinal direction. The predominant period at 50m below the ground surface was also about 2 seconds. Furthermore, it was clarified that the wave with 2 second-period was amplified as much as three times between -50m depth and the ground surface.

Figures-9 and -10 show the power spectrum of principal waves at the Otanoshike and the Chiyoda Bridge like at the Tokachi-Kakoh Bridge.

They also have predominent natural periods of around 2 seconds.

It is clear that wave periods of about 2-seconds were predominent in the principal waves in the 1993 Off Kushiro Earthquake. The results show the characteristics of damages by the earthquake: on roads, there was little damage to bridges except bridges with poor substructure, but much damage to earth works in cuts and embankments; rever dikes on poor ground suffered considerably.

5.POLARIZATION ANALYSIS

For backazimuth estimates, a time-domain non-linear polarization filter analysis, originally proposed by Flinn[2] has been used. In this study, "Rectilinear Motion Detector Filter Analysis" was adopted, which is widely used to emphasize the phase difference in a direction of seismic waves. The characteristics of this analytical method are expressed by the dual parameters of the rectilinearity of

the elliptic, particle orbital motion in a three dimensional space and in the direction of polarization. A data set was built from the analysis of three-conponent recordings from seimic stations at the Tokachi-Kakoh Bridge and the Otanoshike Bridge. This technique, however, was used for calculating an acceleragram in a given direction.

Results of the analysis of seismic waves by directions are illustrated in Figure-12. In case of the Tokachi-Kakoh Bridge, they indicated 241 gal in the east-west direction and 168 gal in the north-south direction. Other strong-motion records also indicated the similar trend of the direction. These results have good agreement with the report by Hokkaido University that the Pacific plate fractured in the north-south and horizontal directions in the 1993 Off Kushiro Earthquake.

6. CONCLUSIONS

The characteristics of the 1993 Off Kushiro Earthquake are:

1) The first one which has the hypocenter of as deep as 107 km below the sea level among major earthquakes in Japan.
2) With magnitude of 7.8, the 5th largest after 1923.
3) The casualty toll, in particular the death toll was very small.
4) Only seven fires broke out in spite of the sever winter season in Hokkaido
5) Vertical motion was considerably large according to the collected data.
6) Analysis of the strong-motion records showed that long-periodic wave of about 2-seconds were predominent among the secondary waves.
7) For azimuth, the component of the north-south direction in the horizontal motion was larger than that of the east-west direction.

REFERENCES

1) "Control System of Strong-motion Records" ; Civil Engineering Institute Monthly Reports, No.466, 1992.3.
2) Flinn, E.A.: Signal Analysis using Rectilinearity and Direction of Particle Motion.

Table-1 Outline of the 1993 Off Kushiro Earthquake

Date	January 15, 1993
Time	8:06 p.m.
Magnitude on the JMA scale	7.8
Hypocenter	Long.144°23′E., Lat.42°51′N.
Depth of the focus	107km
Killed	1person
Wounded	933persons
Damage to buildings (half to full)	84 houses
Damage to bulidings (less than half)	3387 houses
Total amount of damage	About one hundred billion yen

Table-2 Details of Recent Major Earthquakes

Date	Name	M_j	Focal Depth
September 1, 1923	Great Kanto Earthquake	7.9	—
December 21, 1946	Nankai Earthquake	8.0	20km
March 4, 1952	Off Tokachi Earthquake	8.2	0
August 12, 1961	Off Kushiro Earthquake	7.2	80
June 16, 1964	Niigata Earthquake	7.5	40
May 16, 1968	Off Tokachi Earthquake	7.9	0
June 17, 1973	Off Nemuro Peninsula Earthquake	7.4	40
June 12, 1978	Off Miyagi Prefecture Earthquake	7.4	40
March 21, 1982	Off Urakawa Earthquake	7.1	40
May 26, 1983	Off Akita Prefecture Earthquake	7.7	14
January 15, 1993	Off Kushiro Earthquake	7.8	107

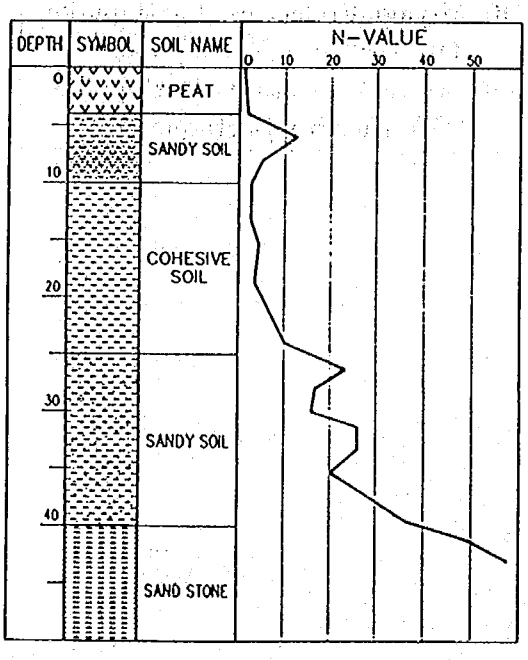
Table-3 Ground and Other details of Seismic Stations

Bridge Name	Ground Classification	Type	Distance
Otanoshike	2nd class	SMAC-B_2	21km
Tokachi-Kakoh	3rd class	SM-12	65
Chiyoda	3rd class	SMAC-B_2	82
Onnetoh	3rd class	SMAC-Q	100
Hiroo	1st class	SMAC-Q	109

Table-4 Maximum Accelerations

Bridge Name	Latitude	Longitude	Acceleration (gal)		
			LG	TR	UD
Otanoshike	43.01°	144.25°	372	352	118
Tokachi-Kakoh	42.74°	143.60°	234	183	144
Chiyoda	42.92°	143.39°	244	244	70
Onnetoh	43.25°	145.48°	341	363	114
Hiroo	42.27°	143.32°	584	325	178

LG : Longitudinal Direction
TR : Transversal Direction
UD : Up and Down



Fugure-6 Soil Boring Log at the Tokachi-Kakoh Bridge

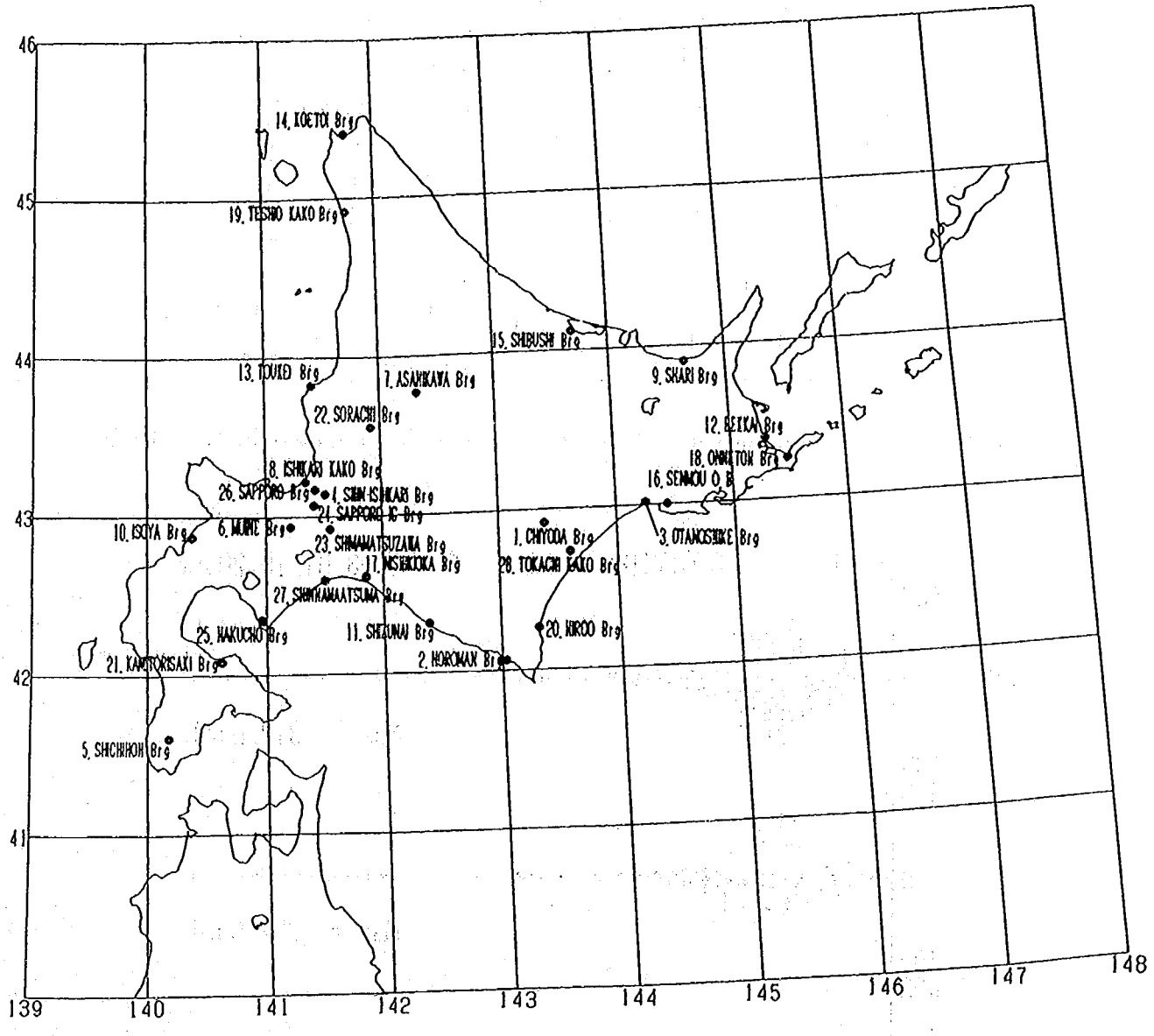


Figure-1 Location of Seismic Stations of the Structures Section

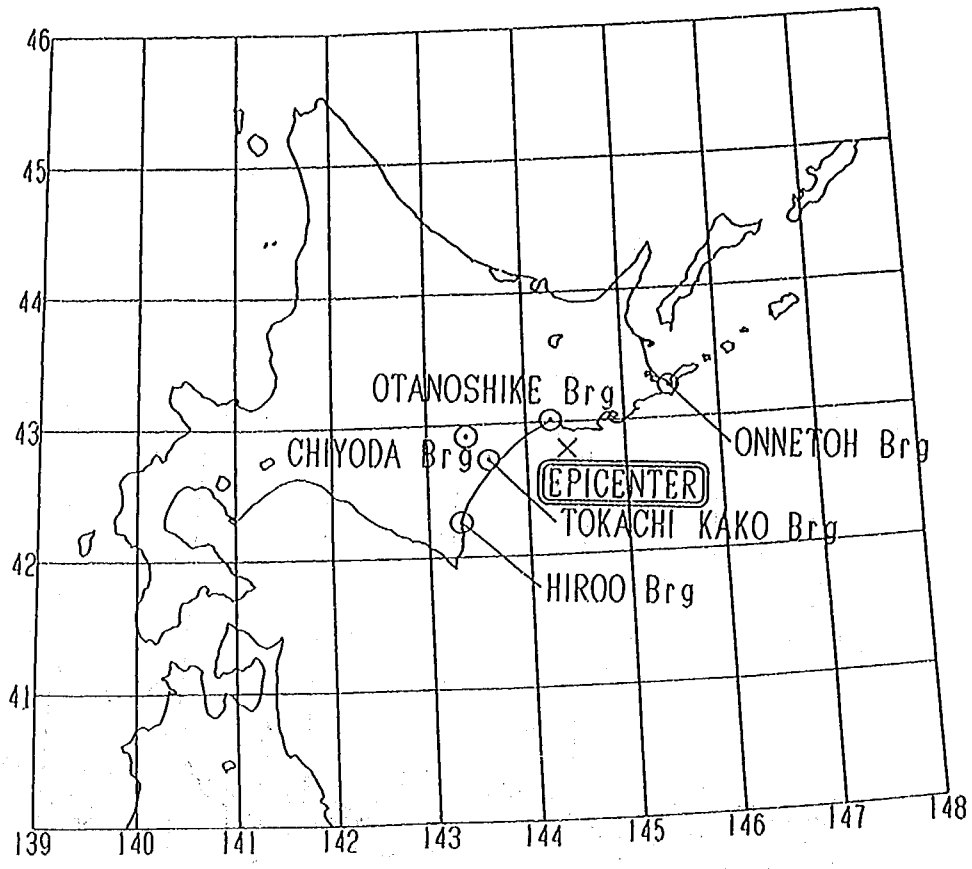


Figure-2 Epicenter and Location of Seismic Stations investigated in this Study

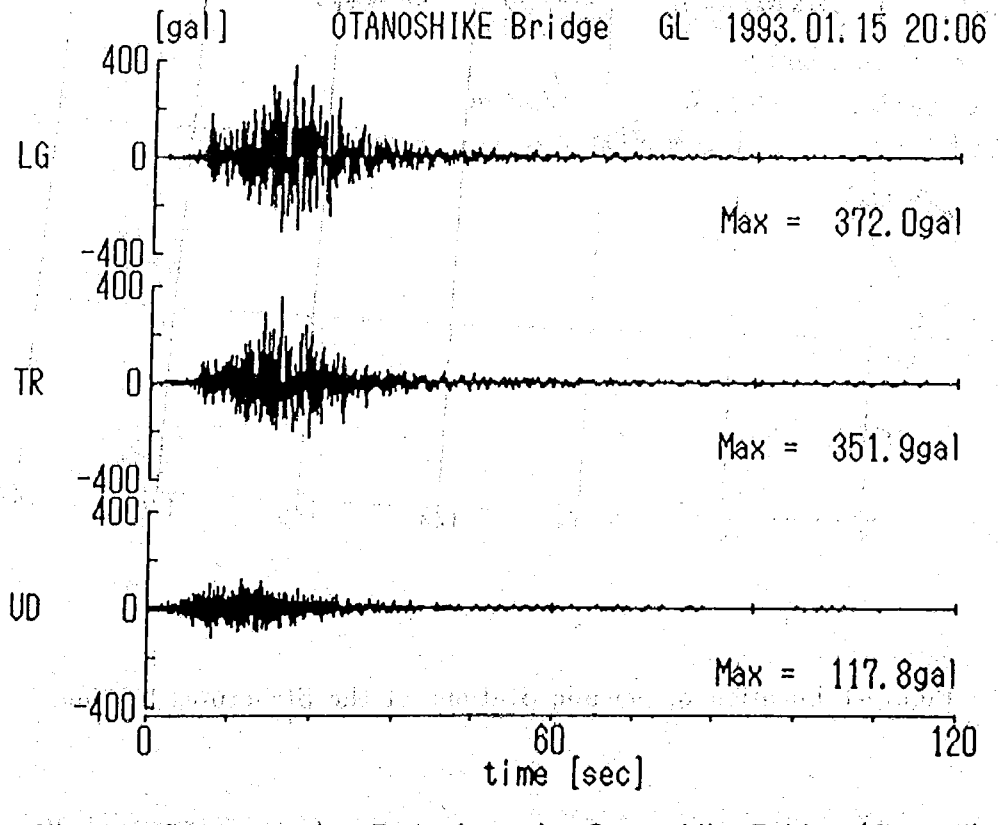


Figure-3 Strong-motion Record at the Otanoshike Bridge (Ground)

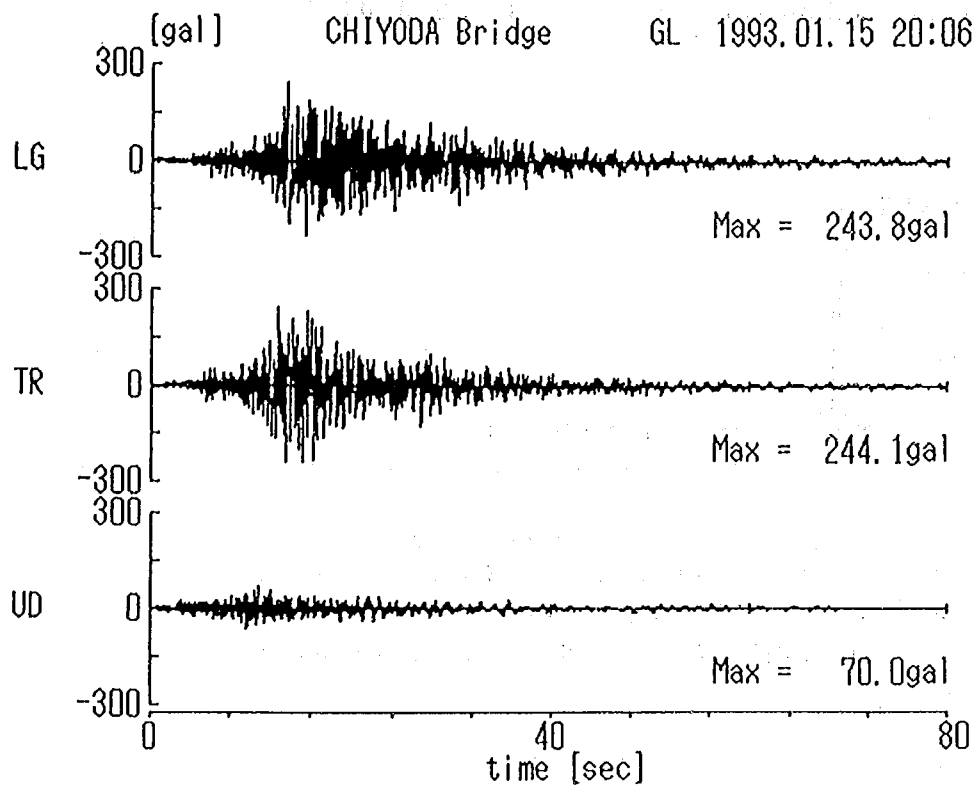


Figure-4 Strong-motion Record at the Chiyoda Bridge (Ground)

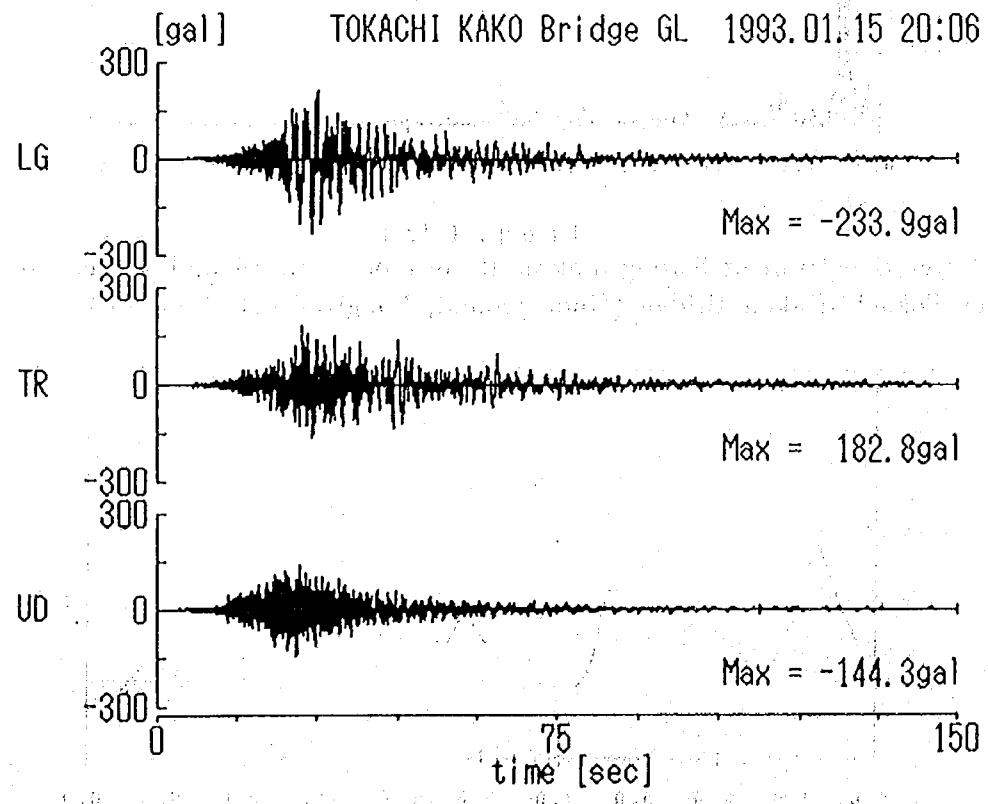


Figure-5 Strong-motion Record at the Tokachi-Kakoh Bridge (Ground)

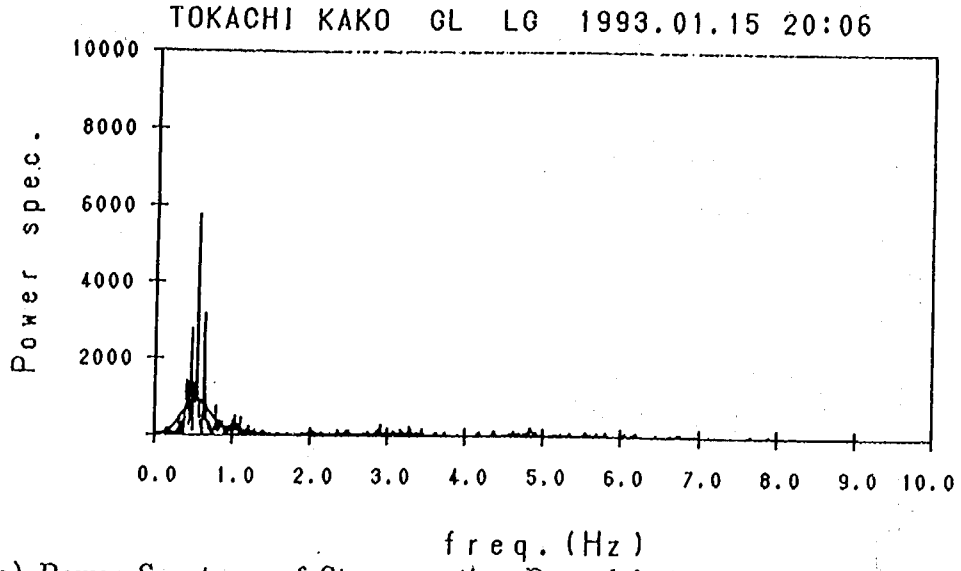


Figure-7(a) Power Spectrum of Strong-motion Record between 16 and 48 seconds at the Tokachi-Kakoh Bridge (Ground, Longitudinal Direction)

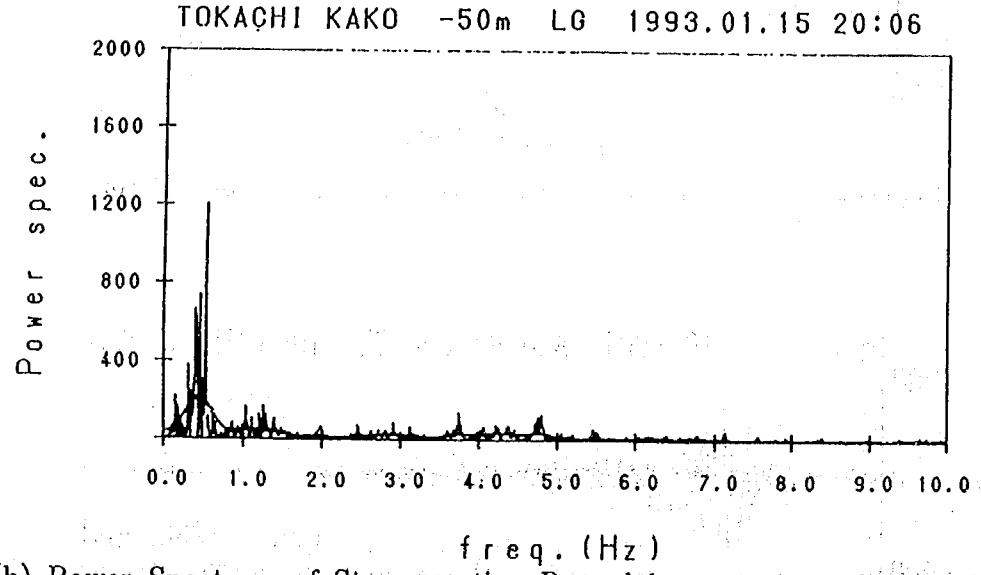


Figure-7(b) Power Spectrum of Strong-motion Record between 16 and 48 seconds at the Tokachi-Kakoh Bridge (Underground, Longitudinal Direction)

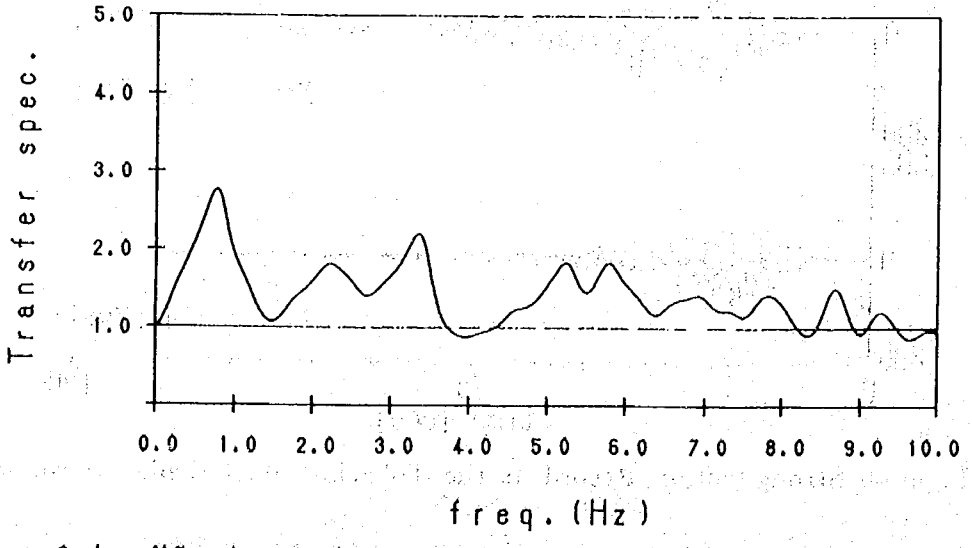


Figure-8 Amplification Ratio between Ground Surface and -50m Depth at the Tokachi-Kakoh Bridge (Longitudinal Direction)

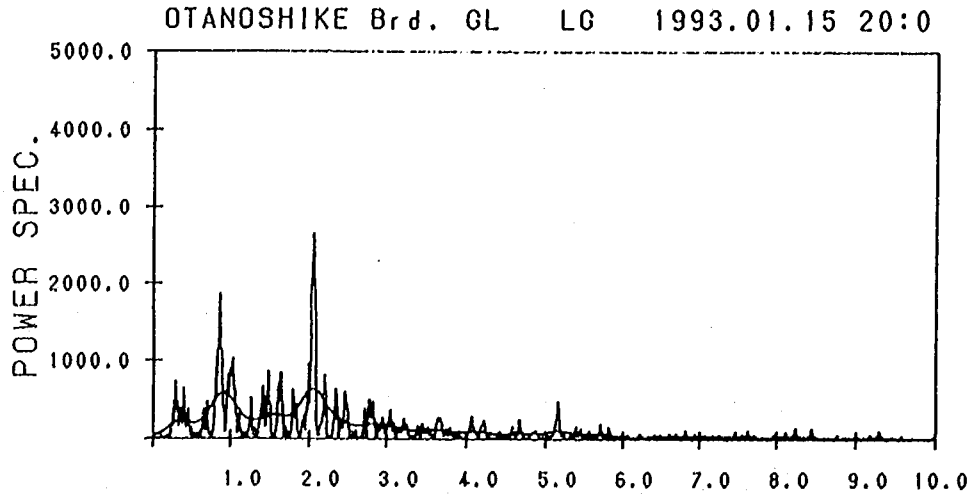


Figure-9 Power Spectrum of Strong-motion Record at the Otanoshike Bridge (Ground, Longitudinal Direction)

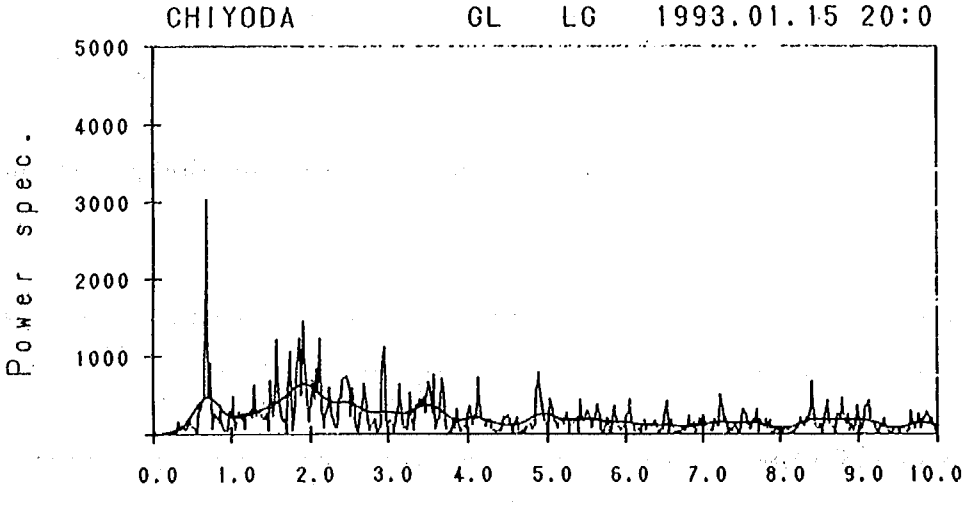


Figure-10 Power Spectrum of Strong-motion Record at the Chiyoda Bridge (Ground, Longitudinal Direction)

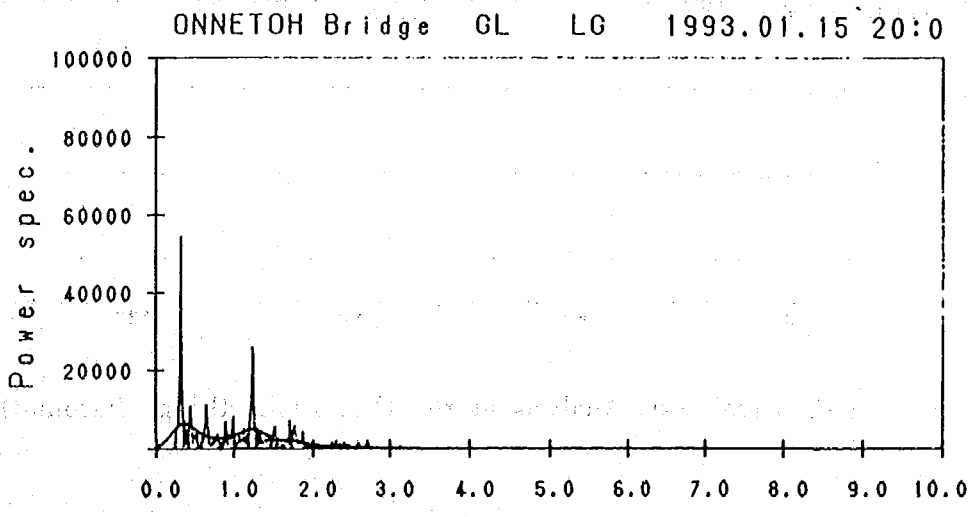


Figure-11 Power Spectrum of Strong-motion Record at the Onnetoh Bridge (Ground, Longitudinal Direction)

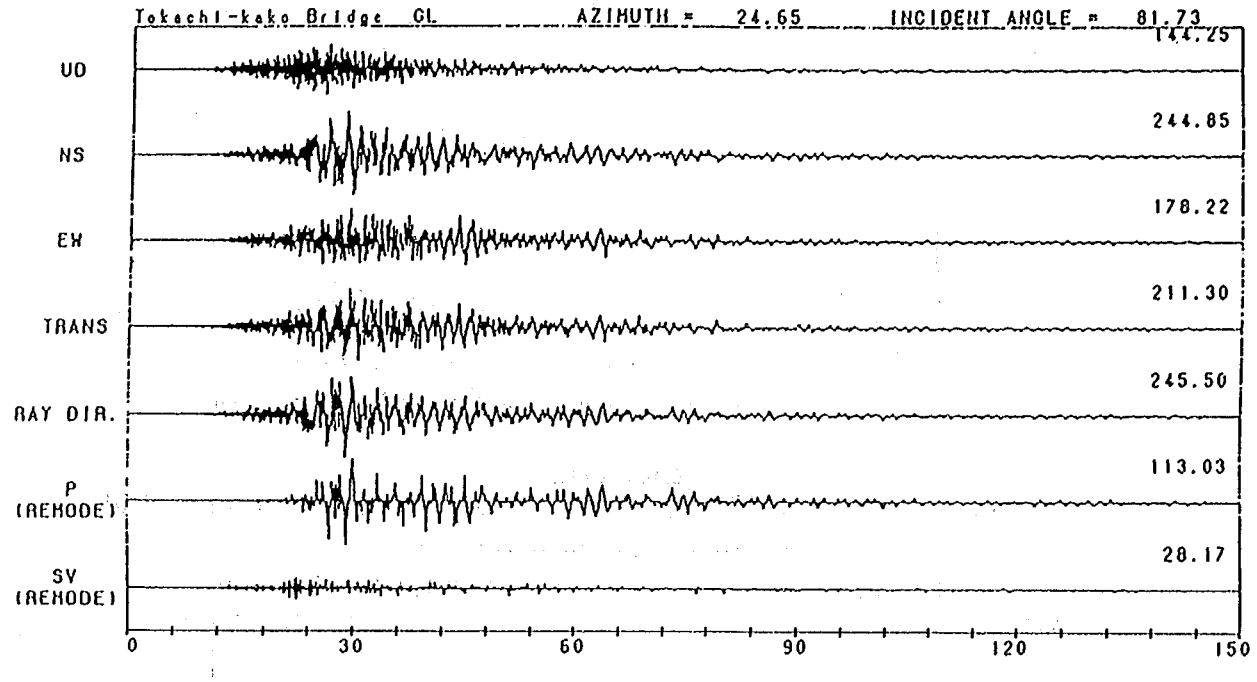


Figure-12(a) Principal Axis Analysis at the Tokachi-Kakoh Bridge (Ground)

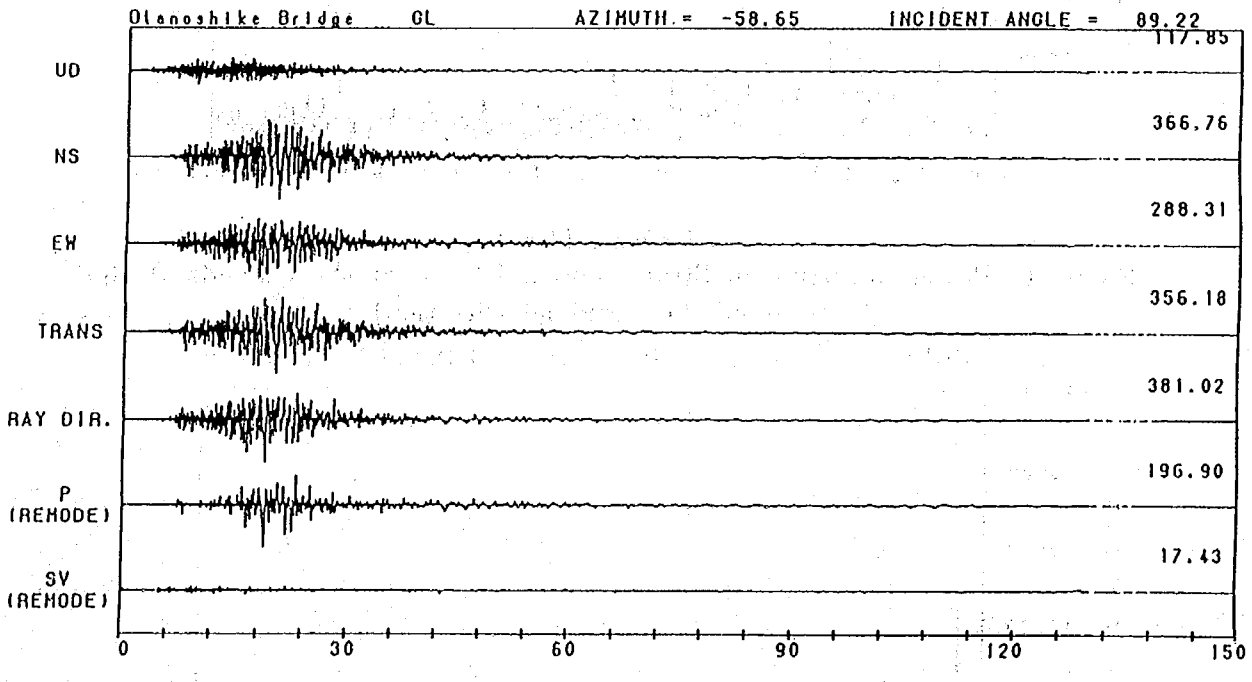


Figure-12(b) Principal Axis Analysis at the Otanoshike Bridge (Ground)

Damage to Infrastructures Caused by the 1993 Kushiro-oki Earthquake

by
Takashi IIJIMA[1], Yutaka IIDA[2], Yasuyuki KOGA[3], Kazuhiko KAWASHIMA[4] and Ken-ichi TOKIDA[5]

ABSTRACT

Introduced is the outline of the results of the investigation done by the PWRI teams, focusing on damage to infrastructures caused by the 1993 Kushiro-oki Earthquake.

KEY WORD

Earthquake, Damage, Infrastructure.

1. INTRODUCTION

In Japan after the Nagano-ken-seibu Earthquake on September 14, 1984, no earthquake had caused fatalities for more than 8 years. At 8:06 p.m. on January 15, Coming-of-Age Day, 1993, an earthquake with a magnitude of 7.8 on the Richter scale occurred, with its epicenter located off-Kushiro in the eastern part of Hokkaido.
The earthquake caused serious damage to infrastructures and lifeline facilities and exerted large influence on civic life and economic activities.
The Public Works Research Institute sent investigation teams to Kushiro and Obihiro areas in Hokkaido and to the Tohoku region, where a lot of damage was reported, between January 17 and February 3, in order to investigate the status of damage to infrastructures and lifeline facilities and to collect fundamental information concerning factors of the cause of damage.
The following is the outline of the results of the investigation focusing on damage to infrastructures.

2. OUTLINE OF THE EARTHQUAKE

The hypocenter of the earthquake was located at ten and a few kilometers off the shore of Kushiro city. The Richter magnitude was nearly equal to that of Kanto earthquake of 1923, 7.9. The damage caused by the earthquake, however, was not as severe. The main reason would be that the depth of the hypocenter was large. The distribution of seismic intensities reported by the Japan Meteorological Agency on the JMA scale is shown in Figure 1. The intensity at Kushiro city is VI and those at the eastern part of Hokkaido and at the Pacific Ocean side of the Tohoku region are more than IV.

The Public Works Research Institute observes strong seismic motions at the facilities of the Ministry of Construction. In Hokkaido, the Civil Engineering Research Institute, and the River Control Sections of Development and Construction Divisions of the Hokkaido Development Bureau observe strong seismic motions. Strong motion records were collected to the Public Works Research Institute soon after the earthquake. The detailed characteristics of the earthquake ground motion will be analysed after the records are digitized. The peak ground accelerations, namely the maximum amplitudes of acceleration wave records, are shown in Figure 2.

---

1)Assistant Director General, PWRI, MOC
2)Director, Earthquake Disaster Prevention Dept., PWRI, MOC
3)Research Coordinator for Underground Development, PWRI, MOC
4)Head, Earthquake Engineering Div., Earthquake Disaster Prevention Dept., PWRI, MOC
5)Director, Kanazawa Work Office, Hokuriku Regional Construction Bureau, MOC

The Strong-Motion Earthquake Observation Council publishes prompt reports of strong-motion records in Japan. According to these records the attenuation characteristics of peak ground accelerations in horizontal two components are shown in Figure 3. The attenuation curves in the figure are drawn with use of a formula obtained from strong-motion records of past earthquakes whose focuses were shallower than 60 kilometers. It is inappropriate to compare the records with the curves, because of the large depth of the hypocenter, 107 kilometers. The observed values show a tendency to be generally greater than that on the curves at the intermediate range of 50-150 kilometers.

The damage was not so severe in spite of the magnitude of seismic ground motion in this earthquake. In order to investigate the cause for this into the characteristics of ground motion, response acceleration spectrum ratio is calculated with use of the strong motion record on the ground of the Ohtsu Dike (not damaged) near the mouth of the Tokachi River. According to this, the predominant period of this seismic strong motion is around 0.15-0.35 seconds: the short-period component is predominant. Furthermore, the elapsed time of primary part in acceleration wave is about 25-30 seconds: it is relatively short. These matters should be examined in detail in the future.

3. OUTLINE OF DAMAGE

Table 1 shows the outline of damage caused in both Hokkaido and Aomori prefectures by the Kushiro-oki Earthquake. Earthquake disaster was developed not only in Hokkaido but also in the Tohoku region. Since the amount of the direct damage in Aomori prefecture which was most damaged in the Tohoku region comes only 2.6% of that in Hokkaido, most of the damage is concentrated in Hokkaido. The total amount of the direct damage is estimated to be ¥46.3 billion which is 6.3 times as large as that induced in Hokkaido by the 1982 Urakawa-oki Earthquake.

The total number of casualties in Hokkaido was 933 including 1 person killed (excluding 1 person killed by gas poisoning), 113 persons deadly injured and 819 persons slightly injured. Casualties in Kushiro city, Shiranuka town and Obihiro city were 444, 91 and 65 persons respectively. The casualties here amounted to 64% of those in Hokkaido. Casualties were caused by tumbling and falling down of furniture, scatter of window glasses and getting scalded by hot water and oil.

The total number of damaged houses in Hokkaido was 3,471 with 12 completely destroyed (including 2 destroyed by land slide and 2 destroyed by the earth and sand), 72 partially destroyed and 3,387 slightly destroyed. Out of them 2,552 of house damages were in Kushiro city, which were 75% of those in Hokkaido. Because the damage ratio (84 completely and partially destroyed houses/ total 78,000 houses in Kushiro city) is calculated as 0.09%, the amount of house damage was rather small in the area affected by strong ground motion of VI in JMA scale. As the area had experienced seven earthquakes which caused strong ground motion greater than IV in the past 30 years, they had much empirical knowledge concerning earthquake countermeasures in Kushiro city. For this reason fires caused by the earthquake were only 9, in spite of the fact that the earthquake occurred

just after dinner time.

As to civil engineering structures, various types of infrastructures such as road, river and sewerage facilities and lifeline facilities such as water, electricity, telephone and gas facilities were affected by the earthquake. Figure 4 shows the locations where major damages were developed. The details of damage will be described in the following chapters. Damage outlines of each type of facilities are as follows.

Concerning road facilities, earthquake disaster was developed both to road embankments and to highway bridges. Major types of damage to road embankments were cave-in, subside, cracks along embankments and collapse of the shoulder of road. The suspension of traffic due to a large scale cave-in was made at 7 locations such as Itoizawa (National Highway Route 44), Higashi-Arekinai (National Highway Route 272) and Arekinai (Prefectural Road, Toro-Akkeshi Line). Major types of damage on highway bridges were crack of piers, damage of bearing supporting and damage of upper girders at supporting sections. The suspension of traffic due to significant damage on piers was made at Matsunoe-bashi Bridge (National Highway Route 240), Shintawa-bashi Bridge (Prefectural Road, Nakashibetsu-Shibecha Line), Hatsune-bashi Bridge (Prefectural Road, Honryu-Onbetsu Teishajo Line) and Yoda-bashi Bridge (Prefectural Road, Horoyakanto Line).

Concerning river facilities, earthquake disaster was developed on embankments, shore protection and sluiceway. Major types of damage on river facilities were partial cave-in of embankments caused with cracks on the top and slope, and whole collapse in which the original shape do not remain itself. In and around Kushiro city, 32 rivers of 11 water systems were affected by the earthquake. Significant damage was developed in the Kushiro river system and in the Tokachi river system.

Concerning sewerage facilities, damage of the fundamental treatment facilities, breakage and weaving of sewage pipes and projection of man-holes were developed. As the major damage to the fundamental treatment facility was breakage of pipes at the connections to sedimentation basins, influence on treatment function was rather small. Investigation into sewage pipes were conducted with use of micro video cameras.

Concerning lifeline facilities, damage to water and gas facilities most affected civic life. The major type of damage to water and gas facilities was breakage of underground pipelines. Due to the damage to water pipelines, water supply was suspended to about 3,560 houses around Shibecha town. Water supply was recovered on January 28. As gas leakage had been reported in and around Midorigaoka and Musa areas in Kushiro city, gas supply was cut off to about 9,300 houses. Gas supply was recovered on February 4.

Concerning electricity, due to the breakage and inclination of electric poles and falling-off of transformers from poles, electric power supply was suspended to about 56,000 houses in and around Kushiro city. Electric power supply was recovered within 24 hours after the earthquake.

Concerning telephone facilities, the emergency circuit control resulted in

heavy congestion of the telephone network around the eastern part of Hokkaido. But normal telephone services were recovered no later than January 16.

4. DAMAGE TO FACILITIES

4.1 Damage To Roads

Major damage to roads was concentrated on road embankments which experienced failure, settlement, longitudinal cracks on road surfaces, and collapse of shoulders. Cut slopes and natural slopes did not cause any damage to roads in the investigated area. (Damage to road bridges are reported in 4.2.)

Large scale failure of road surfaces occurred at Itoizawa in Atsukeshi Town on National Highway Route 44 (the cross section was a half-bank and half-cut, and a half-bank), at Higashi-Arekinai in Shibecha Town on National Highway Route 272 (a half-bank and half-cut, and a half-bank section), at Toridoshi in Kushiro Town on National Highway Route 391 (a half-bank section), at Pashukuru in Shiranuka Town on National Highway Route 38 (a both-bank section), and at Arekinai in Shibecha Town on Prefectural Road Toro-Atsukeshi Line (a both-bank section). In each case a high-raised embankment adjoining a cut section or filled on a transversely inclined concave ground such as a valley suffered sliding failure. The prominent feature was that the collapsed soil moved to a long distance and reached very far. At Itoizawa and at Higashi-Arekinai several cars accidentally fell into the damaged part of the embankment.

Settlement and longitudinal cracks of road surfaces took place near the Gojukoku Bridge in Shibecha Town on National Highway Route 391 (a half-bank and half-cut, and a both-bank section), at Fukayama in Kushiro Town on National Highway Route 44 (a both-bank section), near Hikari Bridge in Tsurui Village on Prefectural Road Tsurui-Teshikaga Line (a half-bank and half-cut section) and at other sections. Similar to the severely damaged sections as already mentioned, most of the damaged sections were adjoining a cut section or filled on a concave ground. In the latter case sliding failure of slopes on the downstream side caused longitudinal cracks of road surfaces.

Collapse of shoulders occurred at many sites including low embankments. In each case a deep crack was made in the boundary between the road surface and the slope, and the whole slope slid down as a block toward the toe. This feature could be associated with the frozen slope surface.

Figure 5 shows the cross section of the damaged embankment at Itoizawa on National Highway Route 44. This figure corresponds to a half-bank section although the damaged part includes a half-bank and half-cut section adjoining a cut section. An estimated soil profile is also shown in the figure. The toe of the slope borders on soft soil in damp ground, but the embankment itself is appeared to be located on scree sediment which has a large bearing capacity. This estimation coincides with the fact that the section had performed without any trouble such as settlement. There are embankments directly filled on the damp ground near the damaged section, but no damage has been reported. Accordingly the damp ground is not considered the direct cause of the

failure.

The filled material at Itoizawa is volcanic sandy soil with a small amount of fine content. Water was observed to spring out from the lower part of the damaged embankment although the water content at the upper part was not high. Therefore it is estimated that ground water had existed in the embankment at a certain level. Incidentally no drainage work had been installed in the damaged embankment.

The collapsed soil at Itoizawa appears to have flowed easily, because it moved to a long distance and formed a very gentle slope as shown in Figure 5. As a consequence it is considered one of the cause of the failure that the fill material with high water content due to poor drainage in ordinary condition liquefied by the earthquake motion.

On the whole the water content of soil which consists of embankments adjoining a cut section or filled on a concave ground sometimes increases due to permeation of water from the original ground. Therefore it is possible that other damaged embankments were in the same condition as Itoizawa was. For example, at Higashi-arekinai on National Highway Route 272 the most severely damaged part was a half-bank section between half-bank and half-cut sections and was filled on a small valley. At Arekinai on Prefectural Road Toro-Atsukeshi Line the damaged part adjoined a cut section, and the neighboring embankment on the opposite side of the cut section experienced no damage. At Toridoshi on National Highway Route 391 and at Pashukuru on National Highway Route 38 the damaged embankments were filled on a concave ground, where a local amplification of the earthquake motion may have affected the initiation of the failure.

At Chobushi in Toyokoro Town on National Highway Route 336 four pipe culverts were reported to have been damaged due to settlement of a both-bank type embankment which was filled on damp ground with a height of 2m. At Higashi-arekinai on National Highway Route 272 a vertical crack was made on the upper part of a downstream wing of a pipe culvert located near the damaged embankment.

The traffic was suspended at many sites immediately after the earthquake, and it was still suspended at seven sites on the 19th of February, 1993 which include Itoizawa on National Highway Route 44, Higashi-arekinai on National Highway Route 272, and Arekinai on Prefectural Road Toro-Atsukeshi Line.

4.2 Damage to Highway Bridges

15 bridges administered by Kushiro Development and Construction Department, Hokkaido Development Bureau, 5 bridges by Obihiro Development and Construction Department, ditto, 10 bridges by Kushiro Construction Office, Hokkaido Prefectural Government, 28 Bridges by Obihiro Construction Office, ditto and 1 bridge by Kushiro City, totally 59 bridges were damaged by the earthquake. Immediately after the earthquake, suspension of traffic of all or heavier buses and trucks was made on 6 bridges which were judged to be unstable by the cracks of piers or damages of bearing supportings. Among 8 bridges in which approach embankments were damaged, 4 bridges in which cave-in of approach embankment occurred were opened to

alternate traffic with lane control after filling up the embankment.

Investigation on the site was made on 13 bridges which were reported to be suffered major damages. Table 2 shows the major damages occurred on those bridges.

With regard to substructures, medium to extensive damage occurred at Matsunoe-bashi bridge(National Highway Route 240), Hatsune-bashi bridge(Prefectural Road, Honryu-Onbetsu Teishajo Line) and Shintawa-bashi bridge(Prefectural Road, Nakashibetsu-Shibecha Line). Residual movement of abutment was occurred at Chokubetsu-bashi bridge(National Highway Route 38). With regard to bearing supportings, rupture of anchor bolts and pins were occurred at Gojukoku-bashi Bridge(National Highway Route 391) and Ikeda-ohashi Bridge(National Highway Route 242) respectively. With regard to shoe pedestal, cracks of shoe pedestal concrete were occurred at Matsunoe-bashi Bridge and Asahi-Kosenkyo Bridge. Although our field survey had not be made, extensive damage of pier was occurred at Yoda-bashi Bridge(Prefectural Road, Horoyakanto Line Route 881).

With regard to superstructures, damage of upper girder at supporting section was occurred at Matsunoe-bashi Bridge and Gojukoku-bashi Bridge.

Photo 4 shows the extensive damage occurred at P4 pier of Matsunoe-bashi Bridge. Matsunoe-bashi Bridge is 5-span simple supported PC girder bridge with length of 157 meter. It is a first grade bridge constructed in 1963 over Kushiro River. Subsurface layer consists of both gravel and tuff deposit, and bed rock is gravel deposit about 6 meter from ground surface. The type of abutment, pier and foundation are inverted T-type, T-type with round section and open caisson respectively.

Horizontal cracks were occurred at 3 piers among 4 piers. X shaped shear crack was occurred at the P4 pier which suffered the most extensive damage. According to the falling off of concrete, main reinforcement and tie hoop was exposed at the section. Based on the swelling of main reinforcements, horizontal displacement developed at P4 pier during earthquake should exceed the displacement at which the pier shows maximum strength, and the residual strength of the pier should already be less than yielding strength. With regard to abutments, cracks of shoe pedestal mortar, cracks of shoe pedestal concrete and damage of upper girder at edge section were occurred.

Concerning the damage of highway bridge, features obtained from the field survey are as follows;

(1) At 4 bridges among 5 bridges which suffered damage on piers, the damage was developed by shear at the mid-height of piers where main reinforcements were terminated. The reason of this damage should be the shortage of bond length of main reinforcement. Though the bond length was revised in the 1980 design specifications, bridges designed along the specifications prior to 1980 have some possibility to be suffered this type of damage. Piers with small sectional area ought to be paid special attention.

(2) With regard to the sectional shape of piers, 3 bridges with round section piers and 1 bridge with ellipse

section piers were damaged. No damage was occurred at bridges with rectangle section piers. The reason why so many damages were developed at piers with round section should be studied.

(3) At 5 bridges among 12 bridges which suffered major damage, cracks of ground surface and slit between ground and pier/abutment could be seen. It can be pointed out that these traces show the movement of ground surface toward the river. At Tsuruatsunai-bashi Bridge(Prefectural Road, Akan-shibecha Line), because sand boil on ground surface could be seen, the sand liquefaction should be occurred. At 4 bridges among 5 bridges, cave-in of approach embankment were occurred.

(4) Most of damages were developed at bearing supportings and its circumference. Though they are small damages, design and retrofitting of bearing supportings should be improved.

4.3 Damage to River Facilities

4.3.1 General

Damage to river facilities is summarized in Table 3. The damaged sites were distributed among 32 rivers in 11 river systems, and they amounted to 114 sites and 30.552 kilometers in length. (These figures are subject to change depending on the result of future investigations.)

The total number of damaged levees was 71 and was the largest among river facilities. They were 25.4 kilometer in total length and the damage can be classified into three types: (1) longitudinal crack on the crest and on the slope, and partial settlement of the crest, (2) uniform settlement of the whole crest, (3) total alteration of the original cross section. Major damage corresponds to either (1) or (3). The damaged levees were supported by a soft peat layer on an alluvial sand or gravel. Although reduction of strength of the soft layer due to the earthquake motion and liquefaction of the sand may have occurred, detailed investigations are needed to explain the failure mechanism. Sand boils were observed on several sites. As temporary repair the cracks were filled and the damaged slopes were covered with vinyl sheets or sandbags. Permanent repair will be made by a partial or a total cutback and refill depending on the degree of the damage.

Damage to the revetments amounted to 13 sites and 2.07 kilometers in length. Concrete block covering works slid down as a whole, and revetments with wet masonry slope covering works tilted forward. Two stair- shaped embankments for water friendly improvement were damaged although adjoining connected-concrete block covering works were without damage.

Damage to sluice gates, sluice pipes and other structures amounted to 30 sites. Sluice gates, sluice pipes and downstream drain works were damaged by expansion of bonds of the main structure and the underground structure such as pipes, and tunneled rivers were damaged by opening of cracks. Other damage includes different displacement of stairs to approach revetments for water friendly improvement, forward tilt of falling works, and blockage of a river by failure of neighboring embankment constructed as a residential land.

In the followings the principal damage in the Kushiro river system and in the

Tokachi river system are described.

4.3.2 Damage in the Kushiro river system

River facilities in the Kushiro river system were damaged at 20 sites (8.27 kilometers in total length) along the Kushiro River which is the main stream and at 9 sites (0.28 kilometer in total length) along 4 branch streams such as the Setsuri River. They include 19 damaged embankments along the Kushiro River, and the other sites were structures such as revetments, sluice gates, sluice pipes and tunneled rivers.

Damage to an embankment on the left side of a retarding basin was prominent and is described herein.

The embankment stretches for 3.8 kilometer upstream from a cross levee of the basin. It was damaged at 6 sites for the total length of 2.29 kilometer. Figure 6 shows the cross section of the most severely damaged part. The damage corresponds to the type (3) as already mentioned, that is total alteration of the original cross section. The original section had been approximately 8 meters in crest width, 7 meters in height and 50 meters in base width. The earthquake caused a settlement of the crest about 2.8 meters at the largest part accompanied by longitudinal or transversely inclined cracks, and different displacement due to the cracks was about 2.0 meters. The waterside slope experienced several longitudinal cracks and collapsed outward in a sliding mode.

4.3.3 Damage to the Tokachi river system

Damages to the Tokachi river system amounted to 42 sites including 24 levees, 7 revetments, 10 sluice gates and sluice pipes, and 1 falling work. Figure 7 shows the cross section of an embankment on the right side at Tounai located 31.5 to 33.0 kilometers upstream from the river mouth, which was the most severely damaged. The damage corresponds to the type (3) as is similar to the case of the embankment on the left side of the retarding basin on the Kushiro River. The original section had been approximately 12 meter in crest width, 7 meter in height and 70 meters in base width. The earthquake caused an outward collapse of the shoulder in a sliding mode, and the crest settled down about 2 meter which was accompanied by longitudinal cracks of approximately 1 meter in width and 2 meter in depth.

4.4 Damage to Dams

The investigation was requested for the dams which are located in the seismic intensity of over V on JMA scale by Tohoku Regional Construction Bureau, Hokkaido Development Bureau, and the Hokkaido Government Office. As the result of the investigation, all the dams have not had the changes in the surface (ex. crack, slide etc.). After the thaw, we need to investigate dam bodies, hydraulic structures, and the connections between dam bodies and abutments again.

(1) Tokachi Dam (rock fill dam)
The maximum acceleration at the crest was equal to 118gals. The amount of leakage increased from 110 ℓ /min to 170 ℓ /min by the earthquake. It had returned in 130 ℓ /min on February 1.

(2) Nilkappu Dam (rock fill dam)
The maximum acceleration at the crest was equal to 193gals. After the earthquake, the leakage contained

muddy water. It is supposed because of measuring the mud which precipitate in the gutter. The amount of underseepage decreased from 290.3 ℓ /min to 278.5 ℓ /min by the earthquake. It increased in 326.8 ℓ /min on January 20. And it had returned in 278.5 ℓ /min on January 26. Neither horizontal nor vertical displacement was observed at the crest.

(3) Takami Dam (rock fill dam)
The maximum acceleration at the crest was equal to 222gals. The amount of leakage increased from 306 ℓ /min to 312 ℓ /min. But it has decreased to 299 ℓ /min on January 21.

(4) Samani Dam (gravity dam)
The maximum acceleration at the crest was equal to 139gals. By the earthquake, some repaired concrete in the joints of gallery was separated. The leakage contained muddy water, but it had returned on February 3. The amount of the leakage and the uplift pressure increased at a few drain pipes, but after a while they have become constant or decreasing.

(5) Senganishi Dam (earth fill dam)
The overflow of the spillway (side overflow type) was blurred with water. As the water level was lowered from EL.199.0 to EL.197.4, the blur disappeared. Because the joints of the overflow (the joint interval of 11meters) were opened with 7 ~ 8 millimeters width at maximum, water blurred above the level of the sealing strip made from vinyl chloride. Consequently, it is not definite whether the joints opened due to the earthquake.

(6) Ninokura Dam (asphalt facing dam)
The amount of the leakage at the gallery remained at 1.3 ℓ /min after the earthquake.

(7) Matakido Dam (earth fill dam)
The amount of the leakage remained at 60 ℓ /min.

(8) Taki Dam (gravity dam)
The maximum acceleration at the crest was equal to 136gals. The amount of the leakage remained at 25 ℓ /min.

(9) Yukiyagawa Dam (gravity dam)
The amount of the leakage remained at 620m ℓ /min.

As a result, it was confirmed that the dams which were built on rock foundation with the modern design and construction were safe for the earthquake.

4.5 Damage to Sewage Works

The following is a report on damage to sewage works. Field trips for this report were made on Kushiro City, Kushiro Town, Shibecha Town and Shibetsu Town from January 27 to January 28 and from January 29 to February 1. According to a summary made by Hokkaido prefectural government, however, damage on sewage works has also been reported in other cities and towns. In order to investigate the inside of sewer systems, video cameras are commonly used, but it takes time. At the time we made our trips, the investigation was still unfinished. This paper, therefore, does not report the whole damage.

4.5.1 Kushiro City

Damage was reported at three treatment plants, five pumping stations and many sewers in Kushiro City. At Furukawa Treatment Plant, wastewater was spilled out onto ground surface because of the damage at expansion joint of the concrete conduit which connects the

preaeration tank to the primary settling tank. Also, wastewater was spilled out onto ground surface because of the damage at expansion joint of concrete conduit which connects discharge tanks of pumping facility and preaeration tanks. Air was released because of the damage at a flexible joint of the pipe which delivers air to aerator. The standby generator slipped out of the position from its foundation and was damaged. Ground subsidence was observed at a part of its site.

At Shirakaba Treatment Plant, an expansion joint was broken at the pipe gallery and the pipe gallery slipped out of the position at this joint, making a 10cm-high step. A lot of ground water and sand entered the pipe gallery. Ground subsidence was observed around this pipe gallery and control building.

At Otanoshike Treatment Plant, preaeration tanks leaned. Also, an expansion joint was split out about 2.5 centimeters at the pipe gallery.

All treatment plants in this city were damaged. The damage, however, was not so serious at any treatment plants as to affect their basic function. Treatment of wastewater was continued without any great difficulties at each treatment plant.

Ground subsidence was observed at Hamamachi Pumping Station, Minamihama Pumping Station, Ohkawa Pumping Station, Kashiwagi Pumping Station and Asahimachi Pumping Station.

13 sites were found to be seriously damaged on sewers by the time of Jan. 26. At 3 sites out of 13, temporary submersible pumps were installed in order to bypass the damaged sections. At Furukawa- No.30-main sewer which is one of these 3 sites, it was difficult to investigate the inside of the pipe by video camera because of the large amount of inflow. At the other 10 sites, the increase of water level in the manholes was observed. They were left as they were, however, because there seemed to be very small possibility that the wastewater in the manholes would overflow onto the ground surface.

Almost all sewers are hume concrete pipes. Damage was done by breakdown of pipes, disconnection of joints, displacement of pipes and inflow from pipes or manholes. It is reported that the TV camera which can measure the amount of pipe displacement easily should be developed.

4.5.2 Kushiro Town

23 sites were found to be seriously damaged on sewers in Kushiro Town because of breakdown of pipes, disconnection of joints and so forth. Among them, it should be noted that total of 18 manholes were lifted into the air from ground along National Highway Route 44. We consider it was caused by liquefaction. This area, which is at 1-chome, Kiba, 2-chome, Kiba and 1-chome, Katsuragi, was improved by sand from the Old-Kushiro River nearby. Therefore, we consider liquefaction is easy to be occurred in this area. Detailed study on the cause of this damage should be done.

The main sewer which crosses National Highway Route 44 had been jammed. A temporary sewer was set to divert wastewater.

4.5.3 Shibecha Town

14 sites were found to be seriously damaged on sewers in Shibecha Town including five sites of inflow caused

by cracks on manholes. Damage has not been reported at the treatment plant except slight ground subsidence.

It was observed that sewers between manholes bend over upwards. This was the typical type of damage on sewers in this area. Sewers are PVC pipes and mostly egg-shaped. We consider this area has poor subsoil since the Kushiro River flows nearby and since it run through this area before.

4.5.4 Shibetsu Town

14 sites were found to be damaged on sewers in Shibetsu Town. The damage was same type as that in Shibecha town. At first, damage was not observed from the outside. Afterwards, investigators went into manholes to see directly the inside of the pipes and they found damage. The water level in some manholes went up, but sewers were still working on without any serious problems. Damage does not have been reported on the treatment plant.

4.6 Damage to Lifeline Facilities

Damage investigation of lifeline facilities was carried out mainly through hearing to managers of the authorities concerned and through field trips.

4.6.1 Damage to Water Distributing Facilities

Water supply failed at about 260 houses in Kushiro city, 1,000 houses in Kushiro town and 2,300 houses in Shibecha town because of damage to water distributing facilities. Damage almost developed from pipelines, partly from pumping facilities. Most of damaged pipelines were made of asbestos-cement. Types of damage were separation and snap of pipeline at joints. Water system for agriculture required a little long time for repair, however all facilities were repaired perfectly by January 28. During repairing, water was supplied by neighbor municipalities and the Self-Defence Forces.

4.6.2 Damage to Electric Power Facilities

After the earthquake, the electric supply failed at about 37,000 houses in Kushiro area and 19,000 houses in Obihiro area. All-night repair was carried out, then electricity was recovered at 8:06 p.m. on January 16. Damage to electric power facilities are shown in Table 4.

Collapse of electric poles was concentrated at Midorigaoka town, which was due to failed embankment. Snap of electric poles concentrated at Sakai town, which was due to collapse of chimney, and at Midorigaoka town, which was due to failed embankment. Therefore these damage are judged to have occurred not directly but indirectly.
Inclination of transformers was concentrated mainly at Showa town. Some transformers at Onbetsu town fell off on account of looseness of steel wire connecting transformers with poles.

4.6.3 Damage to Telecommunications Facilities

After the earthquake, general call was restricted in order to keep the line for emergency call, so the telephone call was congested at the east of Hokkaido. However recovery of telecommunication completed by noon on January 16.

Damage to telecommunications

facilities are shown in Table 5. The damage which produced an evil effect on telecommunications was only the cutting of glass fiber cable laid underground due to failure of road.

4.6.4 Damage to Gas Facilities

Damage to gas facilities was concentrated at Midorigaoka town and Takesa town in Kushiro city, which was due to pipelines failure. Gas leakage occurred at these town, so gas supply was cut off at 9,300 houses about 90 minutes after the earthquake occurrence. In order to prevent the gas leakage accident, repair was carried out after the stopcock was confirmed to be closed at every house. Because excavated soils were frozen, repair did not get along smoothly, therefore about 700 workers gathered from all over the country to assist repair.
At Otanoshige town,which was located to the west of Kushiro city, one person was killed by gas leakage.

4.7 Damage to Housing Lots

Damage to the housing lots consists mainly of such cases in which houses slid together with the ground because of collapse of steep slope or were destroyed by colluvial deposits. Most forms of collapse were landslides. 11 places were damaged (7 houses completely destroyed, 7 half destroyed, 1 partly destroyed) including those where cracks occurred (Table 6). Housing lots by slope collapse were centered in the outlying area of the uplands to the east of Kushiro City. In most cases, it is reported that the soil of the slopes consists of sandy volcanic ash, built with embankments. Some are on high ground water level. The following are outlines of the damage, focusing on two typical cases in Midorigaoka 6 chome and Zaimoku-cho.

1)Midorigaoka 6 chome
The collapse here occurred on a slope with an embankment in the green area around the uplands. The slope is about 11 meters high, at an incline of 32 to 38 degrees, and faces south. The housing lots were located on the top of it, while roads and housing lots were located at the bottom. Vegetation or trees covered the surface of the slope, with no artificial buildings being located there.

The nature of the soil of the sliding cliff is un-consolidated, fine-grained volcanic ash soil of loess color, which is the embankment. Experienced drilling near the uplands shows volcanic ash soil (embankment) belo N-value from surface course to 5.2 meters in depth.

The collapse spread over an area 11 meters high and 70 meters wide. Its shoulders collapsed from 5 to 12 meters behind. The sliding cliff is about 4 meters in relative height, at an incline of 70 to 90 degrees. The sliding surface is considered to be circular.

The colluvial deposit expands southeast, crossing the obliquity a little to reach horizontally the maximum point about 40 meters from the end of the slope.

As for damage to the houses, on the top, 2 were completely destroyed (including one washed away) and 2 half destroyed, while a workman's hut completely destroyed.

2)Zaimoku-cho
It is reported that a circular slip occurred on the bottom of the slope, and the colluvial deposit assumes a stepped landscape. It destroyed the

concrete retaining wall at the end of the slope, and then spread into the road, flowing about 5 meter ahead, and finally stopped, destroying part of a house. The width of the collapse was about 20 meters. The slope is 8.2 meters high, at an incline of 35 degrees, located in the outlying area of the uplands. It consists of surface soil (10 to 30 centimeters) and sandy volcanic ash with some pumice.

4.8 Ground Damage (Liquefaction)

Kushiro area damaged by the earthquake is famous for its marsh in Japan. In this area, peat layer is deposited widely. In some part of the area, low N-value sandy soil was deposited and liquefied during the earthquake. But it was difficult to verify the occurrence of liquefaction, because it snowed after the earthquake. The points of liquefaction verified by the investigation were the points near Tsuruatsunai Bridge on Prefectural Road Akan-Shibecha, Chokubetsu Bridge and Shoro Bridge on National Highway Route 38, and Katsuragi and Kiba areas in Kushiro town. In each case, the occurrence of liquefaction was verified by sand boils on the ground and the deformation of structures obviously judged to be induced by liquefaction. Sizes of the liquefaction were relatively small.
The distinguished case damaged by liquefaction is uplift of a sewage manhole at Katsuragi and Kiba areas on National Highway Route 44 at Kushiro town. The manhole at this point was uplifted about 1.5 meters. Figure 8 shows grain size distributions of sands boiled at this point, and Figure 9 shows liquefaction resistance factor F_L calculated. This figure indicates that 5-10 N-value sand layer is below about 3.5 meters from the ground surface, F_L-value at this layer is smaller than that at surface layer. Furthermore, it seems reasonable to suppose that the manhole buried at a depth of about 4.5 meters was damaged easily by liquefaction in comparison with facilities buried at more shallow depth such as electric cables and street inlets.

5. CONCLUSIONS

Damage to various public works facilities caused by Kushiro-oki Earthquake which occurred on January 15, 1993 was preliminarily reported based on the reconnaissance survey result conducted by PWRI. The general feature was roughly grasped although the information was limited due to lack of survey time. Various types of damage such as urban type damage in Kushiro city and damage to highway embankment and bridge in rural areas were observed. The investigation and analysis of the causes of the damage will be continued at PWRI as in previous earthquakes for the reduction of earthquake disaster.

Acknowledgement

The authors would like to express their heartiest appreciation to the cooperation from Construction Department, Civil Engineering Research Institute, Obihiro Development and Construction Department, Kushiro Development and Construction Department of Hokkaido Development Bureau, Department of Public Works, Department of Housing and Urban Development, Obihiro District Public Works Management Office, Kushiro District Public Works Management Office of Hokkaido Government, Kushiro City, Kushiro Town, Shibecha Town, NTT, Hokkaido Electricity Co., Kushiro Gas Co., Kushiro District Truck Association,

Kushiro District Meteorological Observatory.

[REFERENCES]

(1) Japan Road Association: Guide Specifications for Earthquake Hazard Mitigation for Transportation Facilities - Post-Earthquake Countermeasures -, 1987(in Japanese)

Table 1 Damage Statistics

Category	(Unit)	Hokkaido *1	Aomori pref. *2
Fatality	(Person)	1	0
Serious Injury	(Person)	113	1
Slight Injury	(Preson)	819	0
Damage to Residential Houses	(House)	3,471	3
Damage to Non-residential Houses	(House)	48	2
Damage Cost to Agricultural Products	(Thousand Yen)	2,908,820	996,000
Damage Cost to Public Works	(Thousand Yen)	18,800,300	0
Damage Cost to Fishery	(Thousand Yen)	1,607,639	130,000
Damage Cost to Forestry	(Thousand Yen)	1,290,558	0
Damage Cost to Sanitation	(Thousand Yen)	949,557	2,500
Damage Cost to Commerce and Industry	(Thousand Yen)	14,704,912	44,277
Damage Cost to Education	(Thousand Yen)	1,130,218	8,382
Others	(Thousand Yen)	2,461,272	0
Total Damage Cost	(Thousand Yen)	46,332,769	1,185,027

*1 After Fire and Disaster Prevention Division, Hokkaidou Government, As of February 17, 1993

*2 After Fire and Disaster Prevention Division, Aomori Prefecture Goverment, As of February 22, 1993

Table 2 Major Damage Developed at Highway Bridges

DAMAGE / NAME	LINE	LENGTH (m)	ADMINISTRATOR	TYPE	A	B	C	D	E	F	G	H	I	J	TRAFFIC CONTROL
Matsunoe-bashi	National Highway Route 240	157	A	5-span Simple Supported PC Girder Bridge	○	○			○	○					Passing Prohibited(1/16)
Tsuruatsunai-bashi	Estate Road, Akan-shibecha Line	13	C	2-span Simple Supported Steel Girder Bridge									○	○	Lane Limit(1/16)
Hikari-bashi	ditto	42	C	ditto				○		○	○		○	○	ditto
Shintawa-bashi	Estate Road, Nakashibetu-shibecha Line	60.3	C	3-span Simple Supported Steel Girder Bridge		○				○	○			○	Passing Prohibited(1/16)
Gozyukoku-bashi	National Highway Route 391	249	A	7-span Simple Supported PC Girder Bridge	○	○		○		○	○				None
Gozyukoku-kosenkyo	ditto	15	A	Simple Supported Steel Bridge						○					None
Parumai-bashi	Estate Road, Shoro-akeshi Line	14	C	ditto						○			○	○	Passing Prohibited(1/15) Lane Limit(1/25)
Asahi-kosenkyo	Estate Road, Kushiro-tsurui-teshikaga Line	215	C	Multi-span Simple Supported Steel Bridge					○					○	None
Chokubetu-bashi	National Highway Route 38	42	B	Simple Supported Steel Bridge			○	○		○	○		○	○	Passing Prohibited(1/16) Weight Limit(4tf, 1/18)
Hatsune-bashi	Estate Road, Honryu-Onbetu-teishajo Line	172	C	6-span Simple Supported Steel Bridge		○				○		○			Lane and Weight Limit (4tf, 1/16)
Tokachi-kakokyo	Natioal Highway Route 336	928	B	12-span PC Box-girder Bridge						○	○				None
Ikeda-ohhashi	Estate Road, Obihiro-Urahoro Line	412	B	2-span Simple Supported Truss Bridge				○		○					Passing Prohibited(1/16) Weight Limit(7tf, 1/26)
Yoda-bashi	Estate Road, Horoyakanto Line Route 3881	70	D	3-span Simple Supported Steel Bridge		○				○	○				Passing Prohibited(1/16)
Total	———	—	———	———	2	5	1	4	2	11	6	1	4	6	———

ADMINISTRATOR: A: Kushiro Development and Construction Department, Hokkaido Development Bureau
B: Obihiro Development and Construction Department, ditto
C: Kushiro Construction Office, Hokkaido Prefectural Government
D: Obihiro Construction Office, ditto

TYPE OF DAMAGE: A: Damage of Upper Girder
B: Damage of Pier
C: Damage of Abutment
D: Damage of Bearing Supporting
E: Damage of Shoe Pedestal Concrete
F: Damage of Shoe Pedestal Mortar
G: Damage developed at stopper of Bearing Supporting
H: Damage of Connection between Girders
I: Cave-in of Embankment
J: Crack of Ground Surface, Sand Boil

Table 3 Damage to River Facilities

As of February 20, 1993

Name	(Administrator)	Number of Site	Length*(Km)
Kushiro-gawa	(Nation)	20	8.27
	(Hokkaido Government)	9	0.28
Tokachi-gawa	(Nation)	9	11.67
	(Hokkaido Government)	33	1.869
Watenbetsu-gawa	(ditto)	12	1.33
Onbetsu-gawa	(ditto)	1	2.0
Cyokubetsu-gawa	(ditto)	2	0.55
Cyaro-gawa	(ditto)	1	—
Syoro-gawa	(ditto)	4	1.5
Cyorobetsu-gawa	(ditto)	3	0.06
Yuudo-gawa	(ditto)	11	0.388
Shibetsu-gawa	(ditto)	4	2.62
Nishibetsu-gawa	(ditto)	5	0.015

* The sum total length of damage sites of embankments and revetments

Table 4 Damage to Electric Power Facilities

Types of Damage	Nuber of Damage
Inclined Utility Pole	135
Sunken Utility Pole	-
Collapsed Utility Pole	6
Broken Utility Pole	7
Fallen Transformer	2
Inclined Transformer	6,000
Broken Pipeline	1
Broken Pipeline laid along Bridge	1

Table 5 Damage to Telecommunications Facilities

Types of Damage	Nuber of Damage
Cut-off Glass Fiber	1 (Shiranuka)
Movement of Pipeline with Metal Cable	2
Damaged Manhole	270
Cracked Pipeline	50
Slide of Pipeline laid along Bridge	25
Broken Telegraph Pole	5(Midorigaoka)
Inclined Telegraph Pole	Many (Showa-kita)

Table 6 The General Condition of the Damaged Housing Lots

	Location	Condition of Damage
1	Midorigaoka 6 chome, Kushiro City	-collapse of a slope with embarkment -4 house completely destroyed -2 half destroyed, 1 partly destroyed
2	Midorigaoka 5 chome, Kushiro City *No. 2, 3, 4 are series of areas	-1 house completely detroyed -2 half destroyed, 2 partly destroyed -crack in the housing lots on the cliff of areas -piled blocks at the bottom of the slope partly destroyed
3	Midorigaoka 5 chome, Kushiro City	-1 house completely destoryed -1 half destroyed, 4 partly destroyed -crack and subsidence on the cliff due to landslide -head of the barrier works transformed -drainage damaged -wall on the stepped dam damaged
4	Midorigaoka 5 chome, Kushiro City	-1 house completely destroyed -1 half destroyed -cracks on the cliff and some expansion on the surface of the slope
5	Midorigaoka 5 chome, Kushiro City	-cracks on the cliff expanding in width -shape of slope transformed
6	Yayoi-cho , Kushiro City	-cracks on upper part of slope -head of the retaining wall altered in shape
7	Zaimoku-cho 2, Kushiro City	-collapse of slope -1 house half destroyed, 1 partly destroyed
8	Miyamoto-cho 2 chome, Kushiro City	-cracks and subsidence on top of slope -1 house partly destroyed
9	Kashiwagi-cho, Kushiro City	-cracks and subsidence on top of slope -top of the drainage partly altered in shape
10	Zaimoku-cho, Kushiro City	-cracks on slope and on crown of piled blocks which had been there since construction of housing lots
11	Zaimoku-cho 1, Kushiro City	-head of retaining wall altered in shape

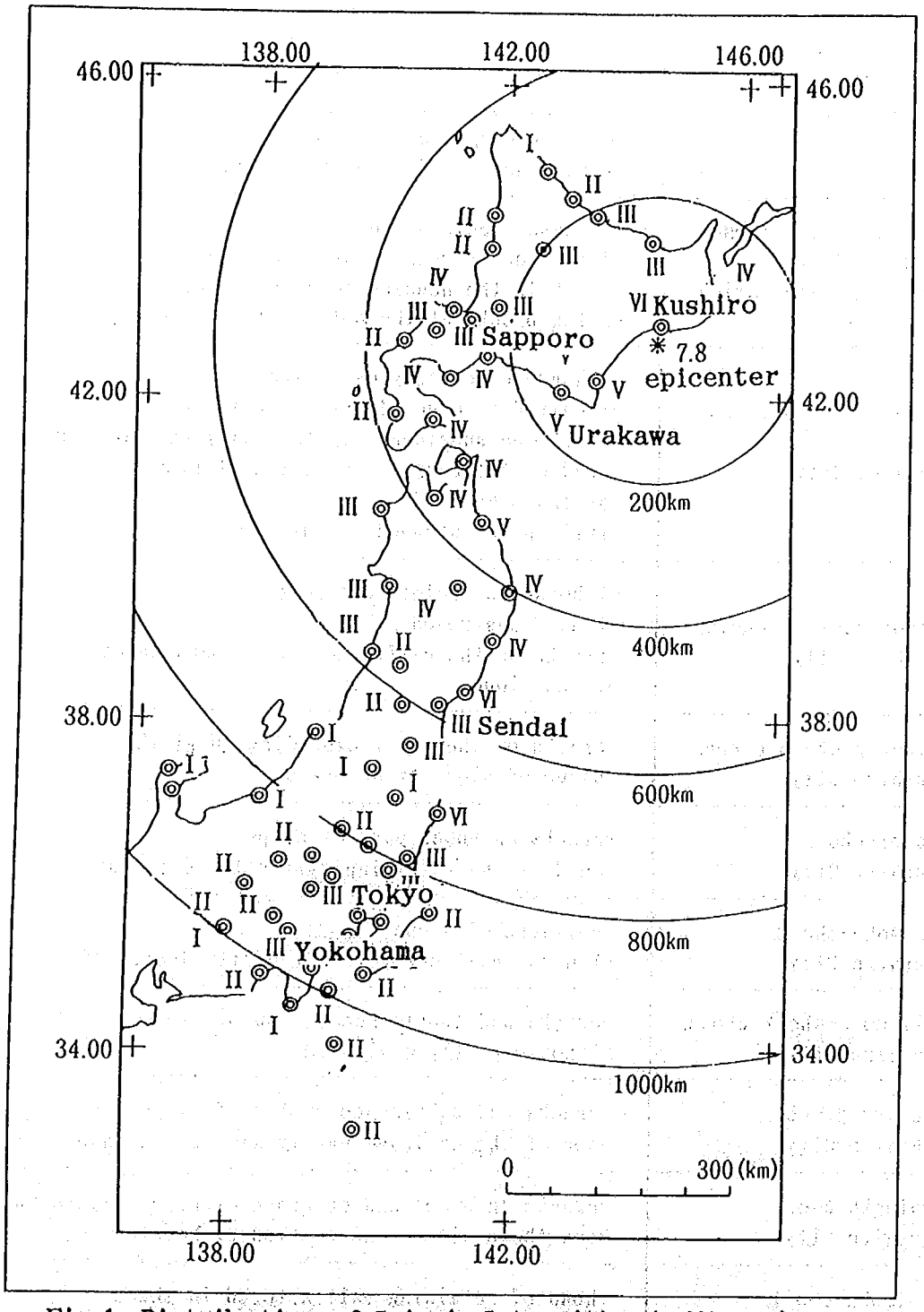


Fig 1 Distribution of Seismic Intensities in MA scale.
(MA scale ranges from 0 to Ⅶ)

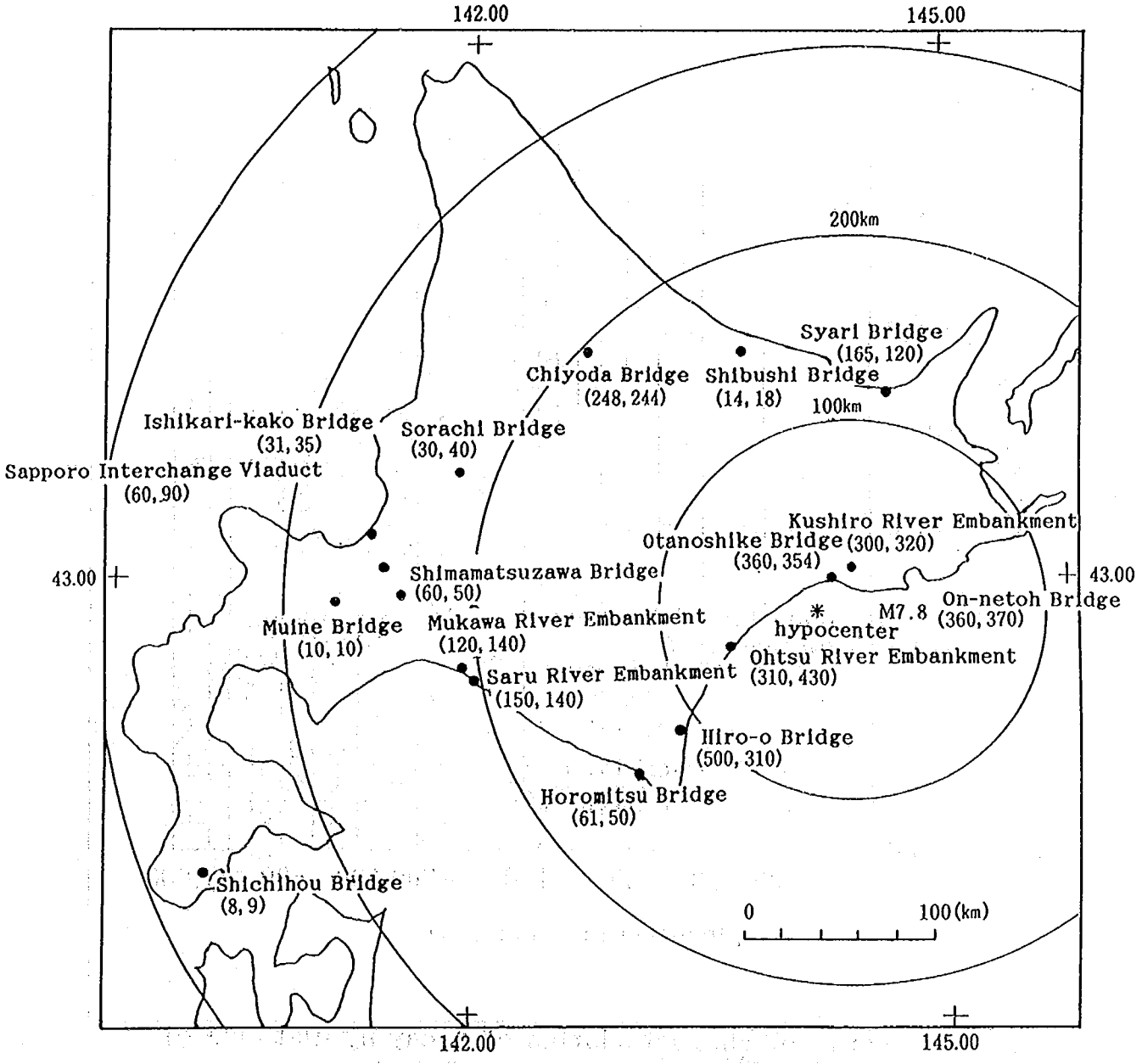


Fig 2 Distribution of Maximum Acceleration on Ground Surface by Strong Motion Observation.

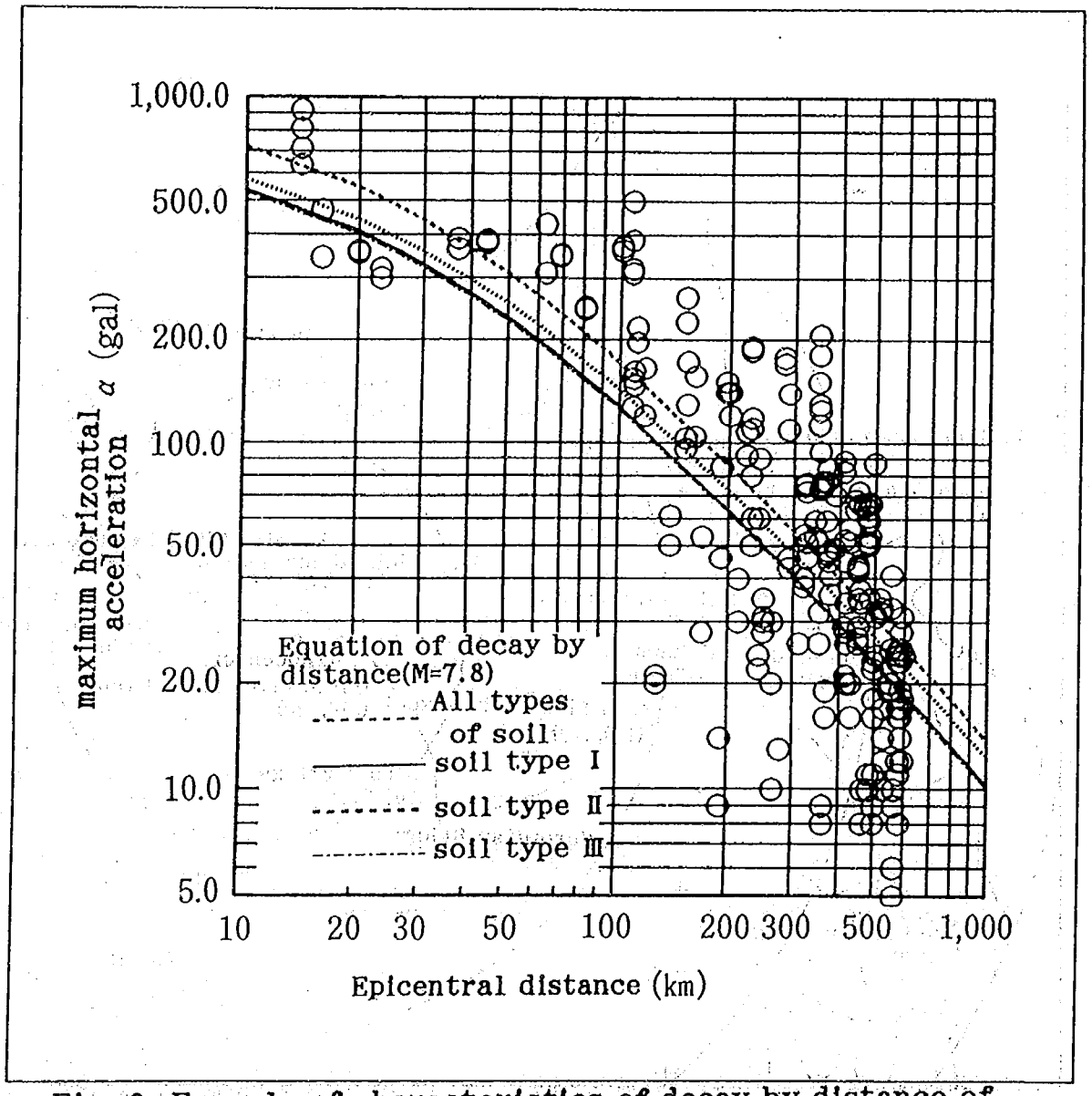


Fig 3 Example of characteristics of decay by distance of maximum acceleration at ground surface
(116Points、△≦600km)

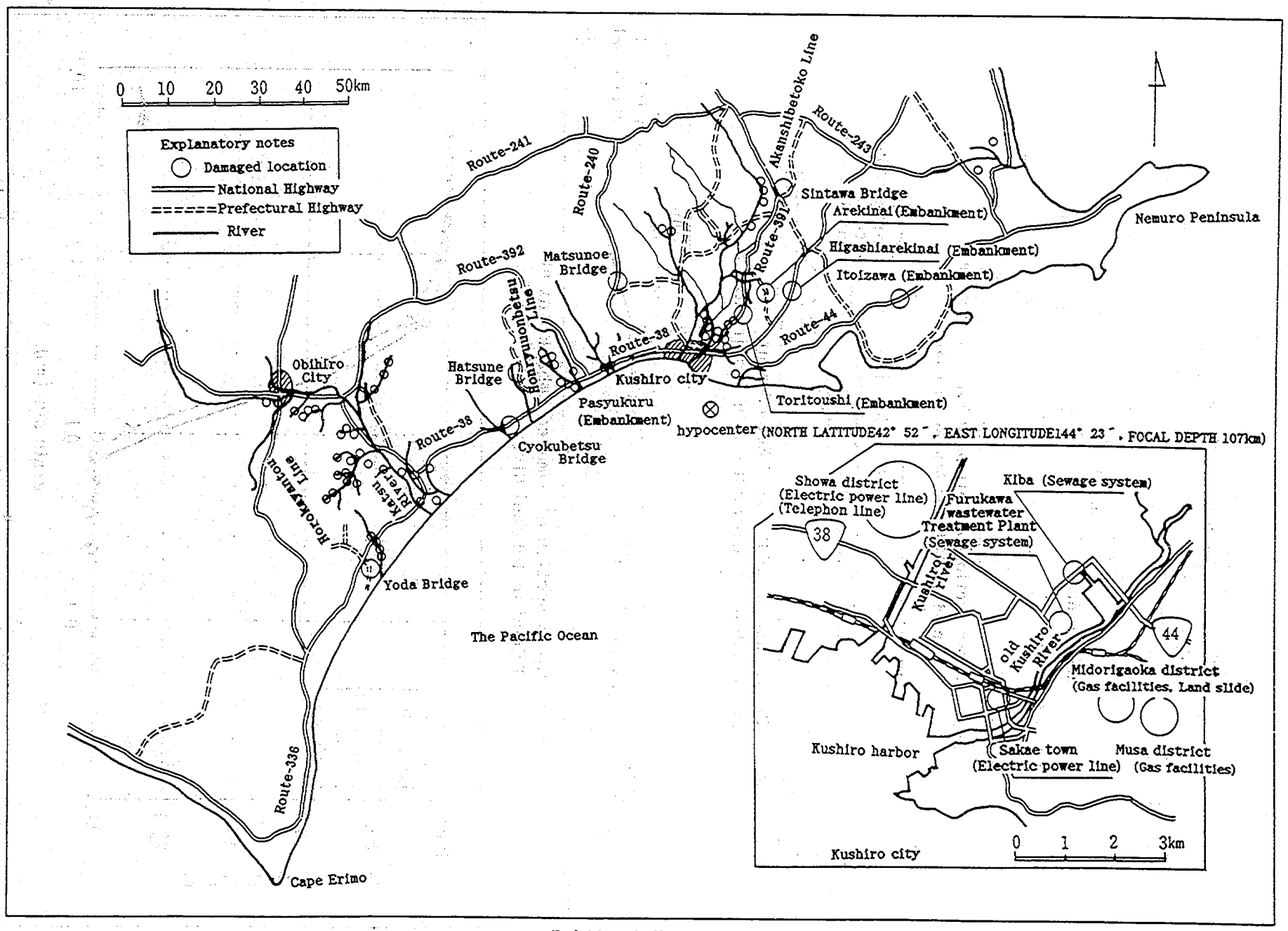


Fig 4 Public civil engineering and construction facilities damage position picture

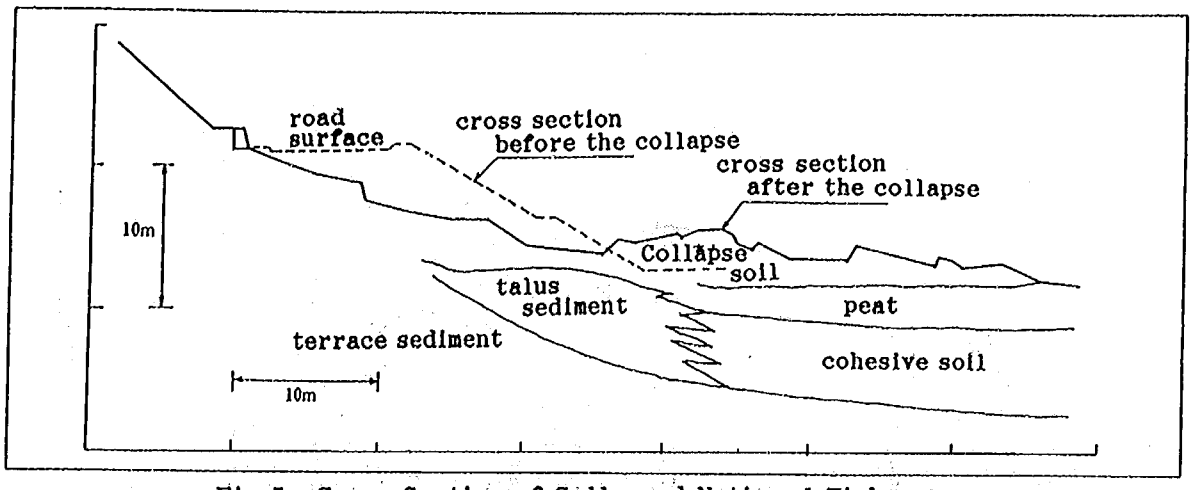


Fig 5 Cross Section of Collapsed National Highway Route 44 at Itoizawa,Atsukeshi town.

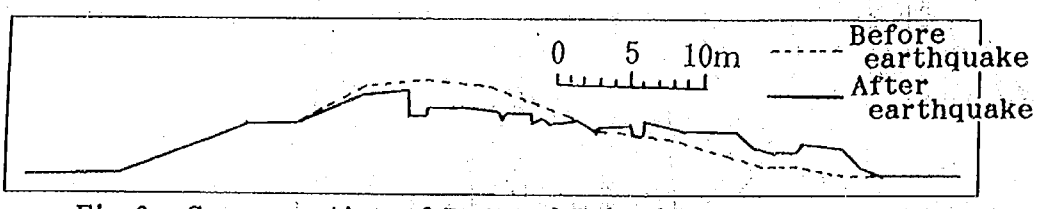


Fig 6 Cross section of Damaged Embankment Surrounding Retarding Basin in Kushiro River.

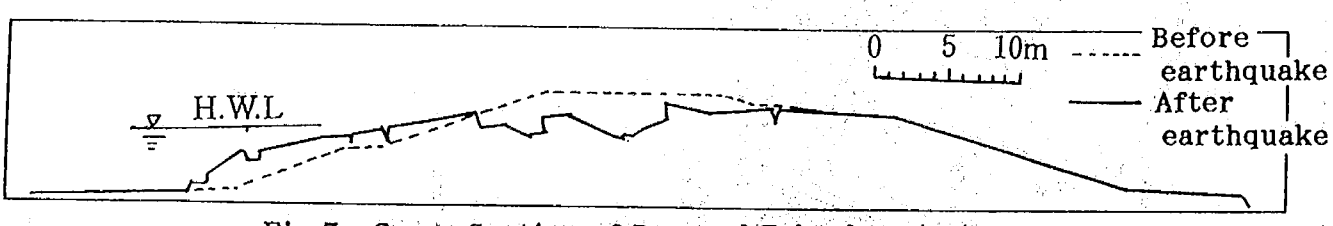


Fig 7 Cross Section of Damaged Embankment at Tohnai in Tokachi River.

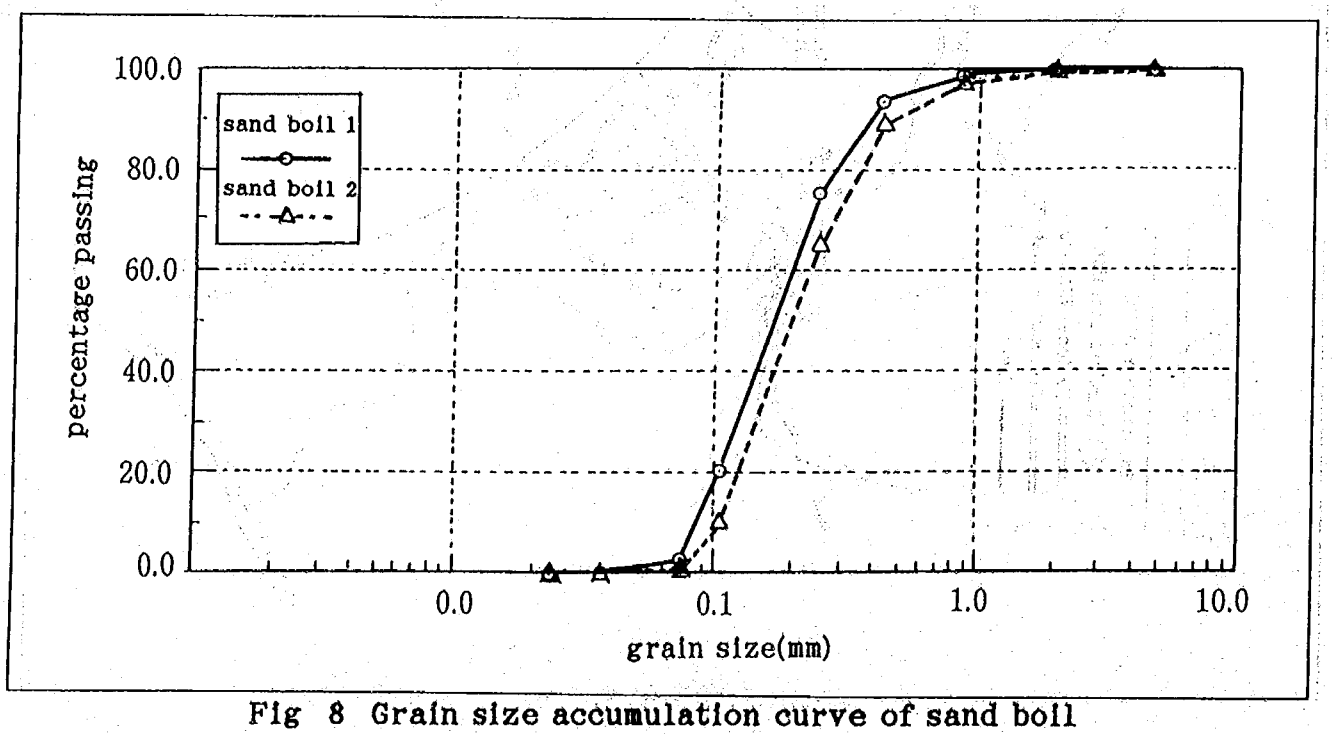


Fig 8 Grain size accumulation curve of sand boil at Katsuragi,Kushiro town

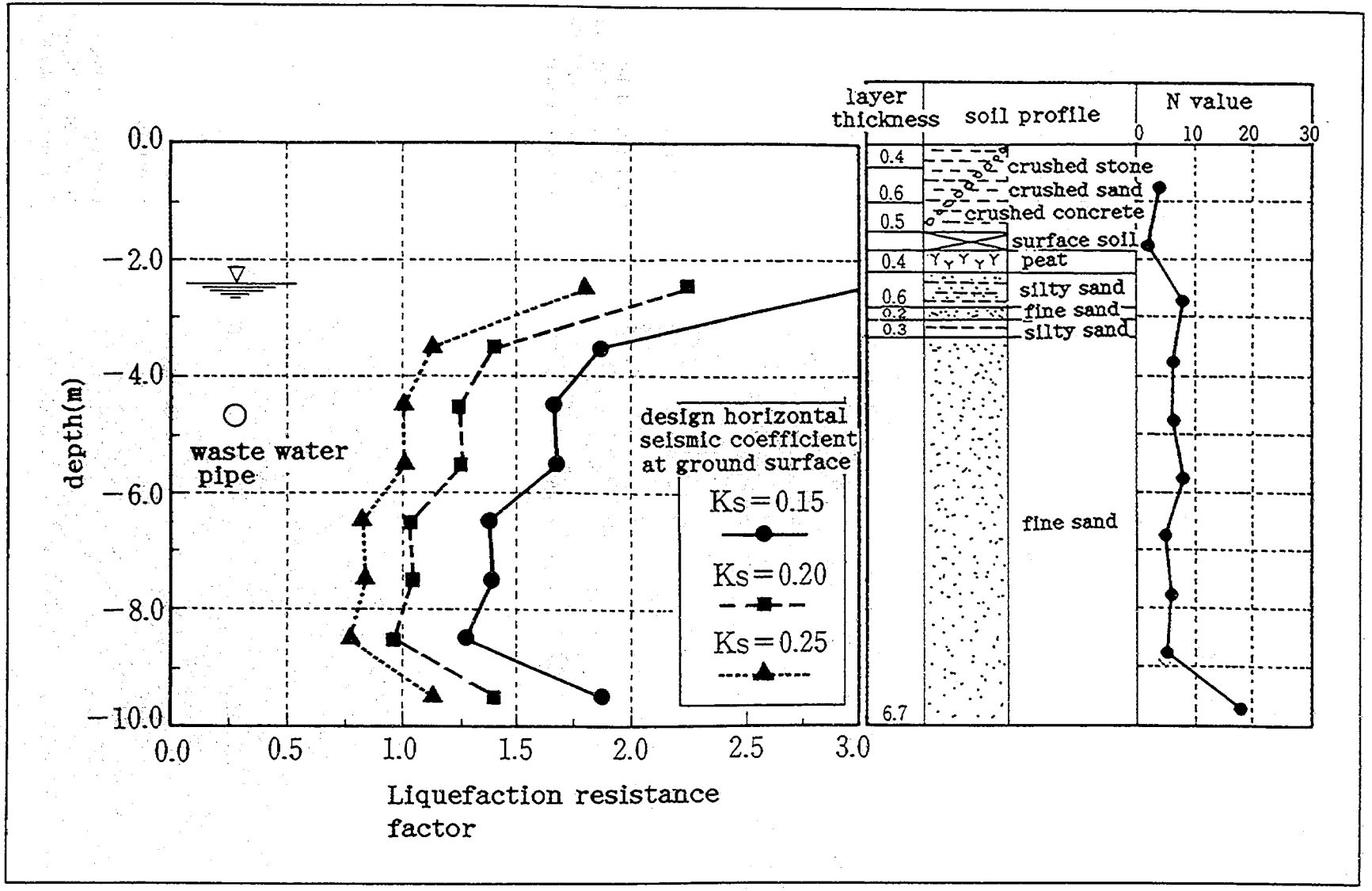


Fig 9 Liquefaction Resistance Factor(F_L) and Soil Boring Log at Katsuragi,Kushiro town.

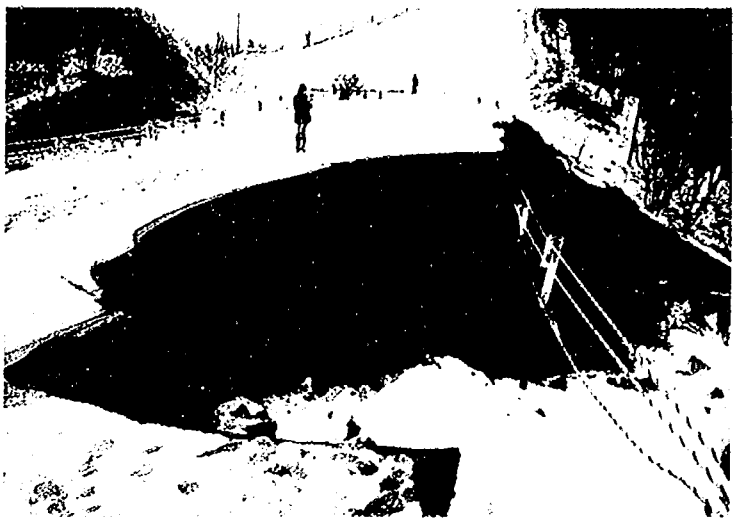


Photo 1.

Collapse of Road Embankment
in Prefectural Road
Touro-Akkeshi Line.
(Arekinai, Shibecha town)



Photo 2.

Collapse of Road Embankment
in National Highway Route-391.
(Near the Gojukoku Bridge,
Shibecha town)



Photo 3.

Collapse of Road Embankment
in National Highway Route-44.
(Itoizawa, Atsukeshi town)

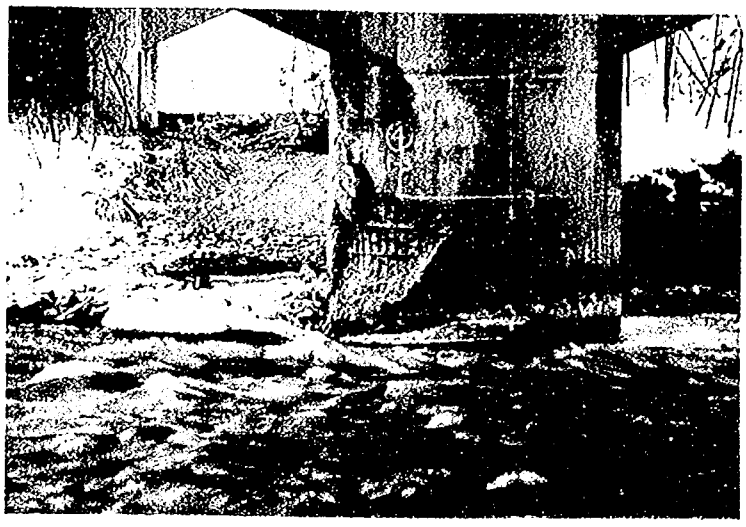


Photo 4.

Damage to Pier No.4 in Matsunoe-bashi Bridge, National Highway Route-240.

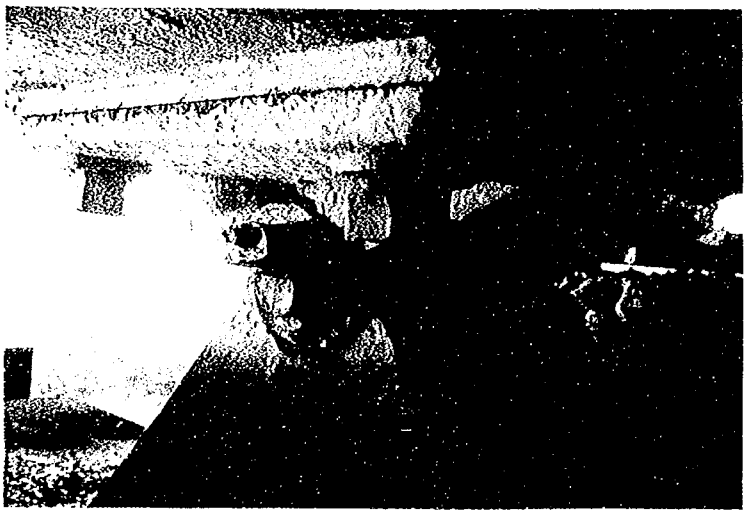


Photo 5.

Damage to Pin in Hinge Support on Pier No.3 Ikeda-oohashi Bridge, in National Highway Route-242.

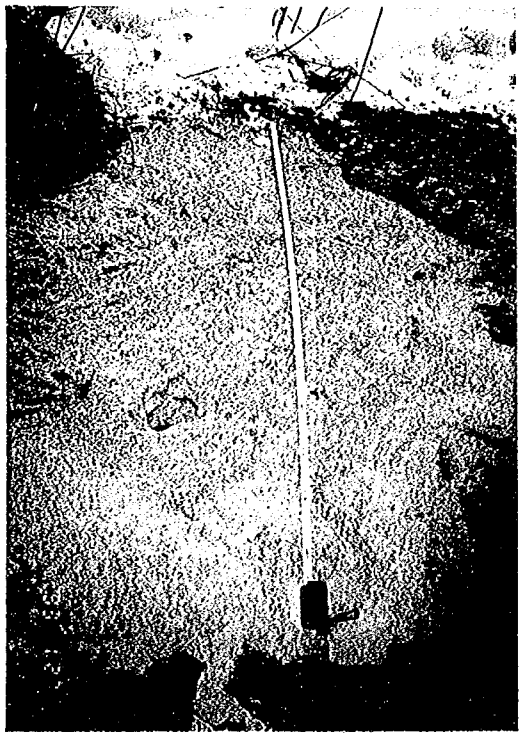


Photo 6.

A trace of Boiling, in front of Abutment of Tsuru-atsunai Bridge.



Photo 7.

Damage to Embankment of Kushiro River.



Photo 8.

Damage to Embankment of Tokachi River.



Photo 9.

Up-lift of Manhole for Waste Water System by Soil Liquefaction.
(Katsuragi, Kushiro town)

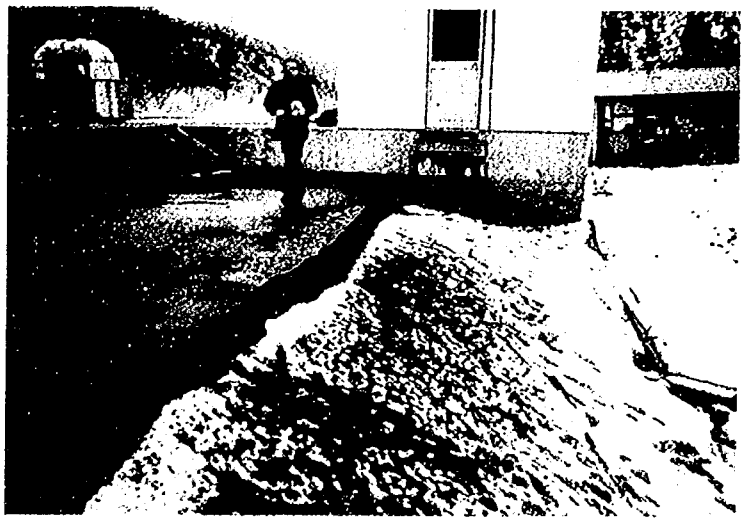


Photo 10.

Settlement of Soil at Waste Water Treatment Plant. (Shirakaba, Kushiro city)

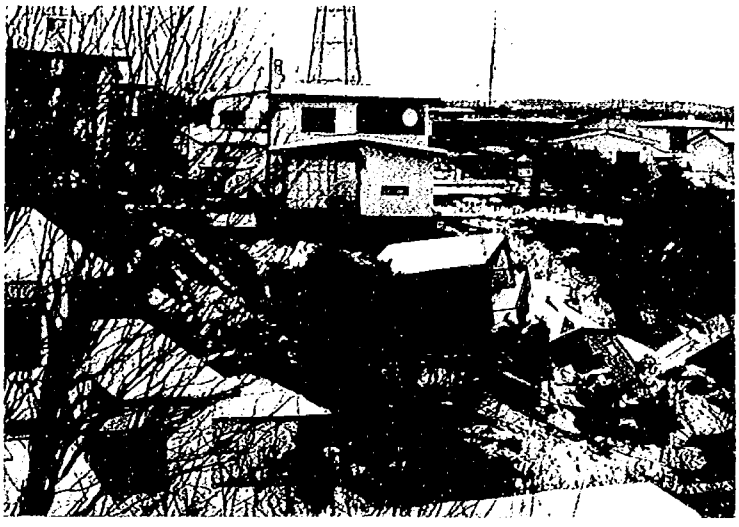


Photo 11.

Slope Failure at Midori-ga-oka in Kushiro city.

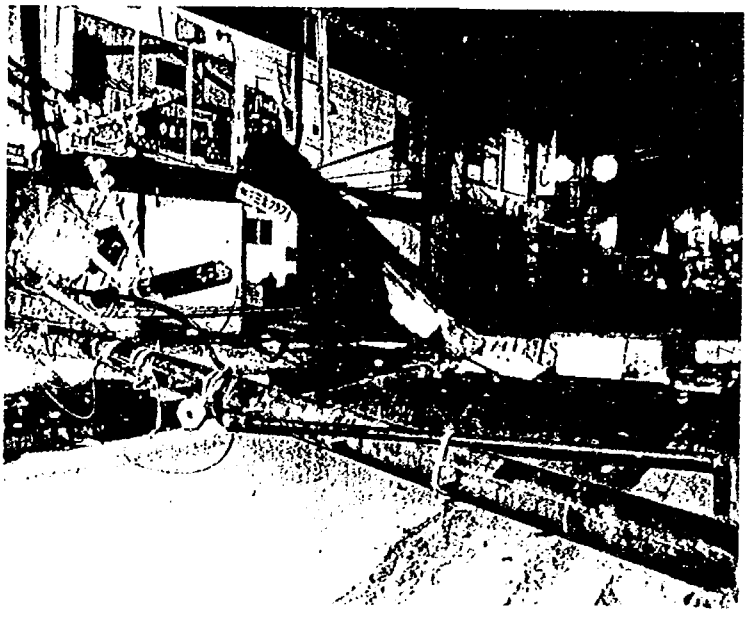


Photo 12.

Collapse of Electric Light Poles and Chimneies.

Damage to Buildings and Housing Lots Caused by the Kushiro Earthquake, 1993

by
Tatsuo Murota*, Yoshikazu Kitagawa**
and
Mikio Futaki***

ABSTRACT

This paper describes the results of a survey made by the Building Research Institute and Housing Bureau of the Ministry of Construction on the damage to buildings and housing lots caused by the Kushiro Earthquake, 1993. Seismological dimnsions of the earthquake and the characteristics of the ground motion which was observed at a point near the epicenter are presented. Also presented are statistics of damage to buildings and persons, outline of the damage to buildings, houses and housing lots and also the occurrence of fires.

1. INTRODUCTION

On January 15, 1993, a destructive earthquake with Richter magnitude 7.8 occurred near the coast of Kushiro City, Hokkaido, Japan. The Housing Bureau and the Building Research Institute dispatched a team to Kushiro City from January 18 to 20. The team investigated the damage to buildings and housing lots at and around Kushiro City. This paper describes the results of the investigation.

2. DESCRIPTION OF THE EARTHQUAKE AND GROUND MOTION

The Kushiro Earthquake, 1993 with magnitude 7.8 occurred on January 15, 1993 at 8:06 P.M. local time, with its hypocenter at a depth of 107km at latitude 42° 51'N, longitude 144° 23'E. Ground motion caused by the earthquake was felt widely in northern and central Japan. Seismic intensities (JMA intensity) observed in Hokkaido and Tohoku areas by the Japan Meteorological Agency are shown in Fig.1.

Ground motions caused by the earthquake were recorded at about 70 observation stations by SMAC- or DC-type strong motion seismographs set in Hokkaido and eastern Japan.

The Building Research Institute has a 200km-mesh seismic strong motion observation network and it recorded ground motions caused by this earthquake at 11 points. At two of those points, one at Kushiro Meteorological Observatory (epicentral distance 14km) and the other at Hiroo Town Office (epicentral distance 108km), large accelerations exceeding 100 cm/sec^2 were observed. Figs 2 and 3 show the accelerograms and Figs 4 and 5 show the pseudo velocity response spectra corresponding to those accelerograms.

The maximum ground motions at the site of Kushiro Meteorological Observatory which were estimated from the accelerograms are shown in Table 1.

Looking at Fig.2, it is observed that strong horizontal ground motions with acceleration of 600 to 700 cm/sec^2 continued for

Table 1 Maximum ground motions observed at Kushiro Meteorological Observatory

	N-S comp.	E-W comp.
Max. accel. (cm/sec^2)	637	711
Max. vel. (cm/sec)	42.3	33.5
Max.disp. (cm)	7.3	4.9

* Director, Structural Engineering Department, Building Research Institute, Tsukuba - shi, Ibaraki-ken, Japan 305

** Director, International Institute for Seismology and Earthquake Engineering, BRI

*** Head, Housing Construction Div., Production Department, BRI

about 20 seconds in Kushiro area. And it is inferred from Fig.4 that the seismic response is expected to be large for structures with fundamental periods of 0.2 to 1.0 second; in case of 5% damping, the maximum response velocity will be as much as 100 cm/sec.

3. STATISTICS OF DAMAGE

According to data compiled by the Kushiro District Government as of 3P.M. on January 17, numbers of deaths and injuries from the earthquake was 2 and 420, respectively, and also 489 housings were damaged in the Kushiro district. Table 2 is the statistics of damage from the earthquake.

4. CAUSES OF DEATHS AND INJURIES

Causes of two deaths were as follows:

(1) A 65 year old man died in the living room of his house under a lighting facility which fell down on him from the ceiling. The facility was of 1m diameter and 18kg weight.

(2) A 76 year old woman was discovered dead in the next morning of the earthquake. The cause of her death was judged as CO gas poisoning after the judicial dissection. Her room was on the first floor of a five-storied reinforced concrete apartment. Around the apartment had been observed gas leakage soon after the earthquake and so residents including her evacuated for four hours until the midnight when the gas cock was shut on the street main gas supply line. It is inferred that gas which collected under the first floor (wood construction) during the evacuation might diffuse into her room during her sleep and cause the poisoning.

According to building officials of Kushiro District Government, half of injuries scalded with hot water in kettles which had been put on room-heating stoves for supplying moisture. Fig.6 shows kettles put on a kerosene stove in an ordinary dwelling in Kushiro area.

5. OUTLINE OF DAMAGE TO BUILDINGS

5.1 Housings

A major cause of wholly destruction of five dwellings in Kushiro City and three in Shibecha Town was landslides or subsidence of housing lots. In towns of Shiranuka and Onbetsu about 40km west of Kushiro City, seven dwellings were wholly destructed. All of them were of two-storied wooden construction and they collapsed or inclined at the first story. A major cause of them was insufficient amount of shear walls and poor construction in the first story. Fig.7 and Fig.8 show typical examples of those destructions.

Major causes of partial destruction or partial damage to housings were falling-off of exterior wall claddings (Fig.9) and breakage of chimneys (Fig.10). Most housings in Kushiro

Table2 Damage from Kushiro Earthquake, 1993 compiled by Kushiro District Government as of 3P.M. on January 17, 1993

Item	Quantity		
	Kushiro City	Other Area	Total
1. Dead	2	0	2
2. Injured	314	106	420
3. Housings	210	279	489
Wholly destroyed	5	9	14
Partially destroyed	4	17	21
Partially damaged	201	253	454
4. Non-residential buildings	no data	100	100
5. Primary and middle schools	39	73	112
6. Social education facilities	no data	29	29
7. Health and welfare facilities	no data	25	25
8. Suspension of water supply*	no data	3862	3862
9. Stoppage in power supply*	no data	3030	3030
10. Gas leakage*	123	------	123

* number of households suffered

area do not have tile roofs but have galvanized iron sheet roofs. So, no serious damage was observed on roofs.

5.2 Non-residential buildings

(a) Steel construction

Two gymnasia of steel construction suffered serious damage from the earthquake. Major causes of the damage were breakage of bracings in ceiling plane (Fig.11), falling-off of exterior wall claddings (Fig.12) and breakage of window panes (Fig.13).

(b) Mixed brick masonry and heavy timber construction

A few warehouses of mixed brick masonry and heavy timber construction suffered partial collapse to brick walls in Kushiro City (Fig.14).

(c) Reinforced-concrete construction

The Kushiro Fire Station is in a three-storied reinforced-concrete building, which has a fire watch tower of about 40m high above the ground. The watch room at the tower top fell down by about 30m on a roof of the three-storied building and caused a serious damage there (Fig.15). The watch room was of steel construction and had not been used for the last 20 years.

Damage to reinforced-concrete buildings except the Kushiro Fire Station was not so serious as anticipated from the very large ground motion accelerations recorded at the Kushiro meteorological Observatory. Many of reinforced-concrete buildings suffered damage such as shear cracks on walls (Figs 16 and 17), breakage and separation in expansion joints (Fig.18), etc., which suggested unusual strong effects of the earthquake.

5.3 Furnitures

Effects of ground motion of the earthquake were observed more clearly and strongly in the damage to furnitures. Even in dwellings or buildings which suffered no serious damage to structures, furnitures and/or their contents fell over or were spilled violently on floors, causing numbers of injuries and, in some cases, fires.

6. OUTLINE OF DAMAGE TO HOUSING LOTS

6.1 Geologic setting (Fig.19)

The downtown Kushiro City is located on a low land called Kushiro Plane. South-eastern part of the plane continues to the Kushiro Terrace (S.L. + 30 to 60m) and the Nemuro Terrace (S.L. + 70 to 140m). Sediments in the upper part of those terraces are volcanic clay and pumice tuff.

Urban areas of Kushiro City are expanding onto the Kushiro Terrace for the last two decades and many housing lots has been developed there. The Kushiro Meteorological Observatory is also located on this terrace.

6.2 Damage to housing lots

Many housing lots in Midori-ga-oka (Green Hill) area on the Kushiro Terrace suffered damage seriously or less in the earthquake. Major causes of the damage were sliding of earth banks, slopes or retaining walls and subsidence of fill-up ground. Figs 20 to 22 show typical land slide damage and Figs 23 to 25 show damage caused by sliding of earth bank.

7. FIRES AND THEIR CAUSES

In Kushiro City nine fires occurred from the earthquake under the following circumstances:

(1) Dwelling #1; a kerosene stove fell over.
(2) ditto #2; a kimono cabinet fell over a kerosene stove.
(3) ditto #3; a book shelf fell over a coal stove.
(4) ditto #4; a heat-stock type electric heater fell over a carpet.
(5) Combined restaurant and dwelling #1; cloths fell over a gas stove.
(6) ditto #2; an electric stove fell over a carpet.
(7) Restaurant; Brick walls of a furnace collapsed and made burning charcoal scatter on floor.
(8) Ten-storied restaurant building; fire occurred at the 8th floor because of the shortage of power lines.
(9) Charcoal distillation cottage; a wood distillation chamber collapsed.

The cottage (9) burnt down but there were no effect on urban areas because it was located in the suburbs. Fires of (3), (4), (6) and (7) were extinguished by residents themselves. Fires (1), (2) (5) and (8) were extinguished by fire-fighters until 9:30 P. M. on the day.

8. CONCLUDING REMARKS

In the Kushiro Earthquake, 1993, most buildings and housings could resist with no serious damage under the action of very strong ground motions. Any knowledge in the current

earthquake engineering can not explain this fact reasonably. This is the most important question raised on us by this earthquake. We should hereafter tackle this problem to refine and correct the current knowledge on the seismic damage to structures.

Casualties caused by the down-fall of lighting facilities or by gas-poisoning and earthquake-triggered fires which occurred in a winter season of a cold district, gave us very valuable information for sophisticating seismic disaster mitigation measures.

Overturning of furnitures and damage to artificial fill ground are well-known and important issues to be solved for mitigating loss of personnel and properties. The Kushiro Earthquake has recalled us the necessity of finding some realistic solutions for these issues.

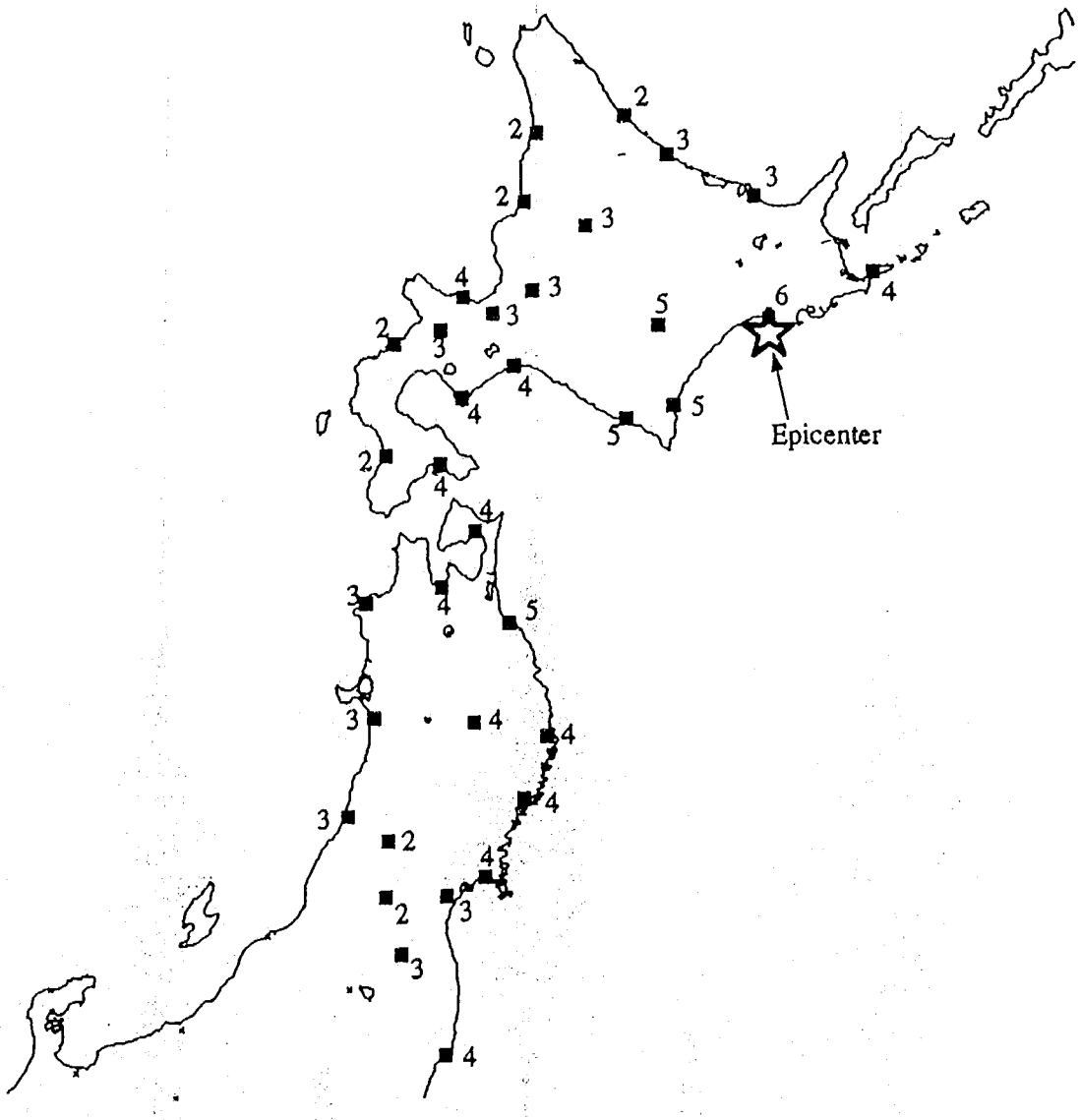


Fig.1 Seismic intensity map

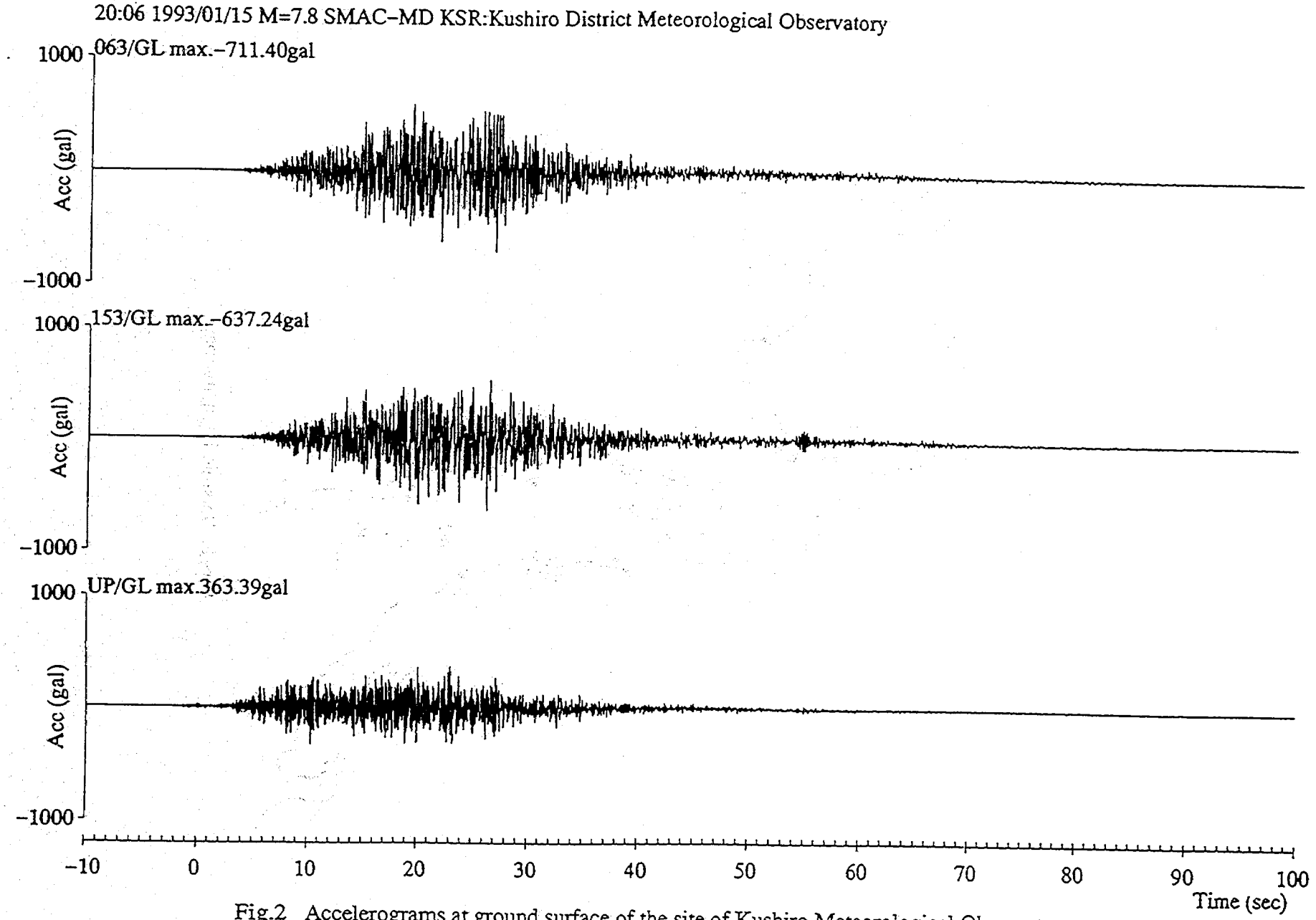


Fig.2 Accelerograms at ground surface of the site of Kushiro Meteorological Observatory

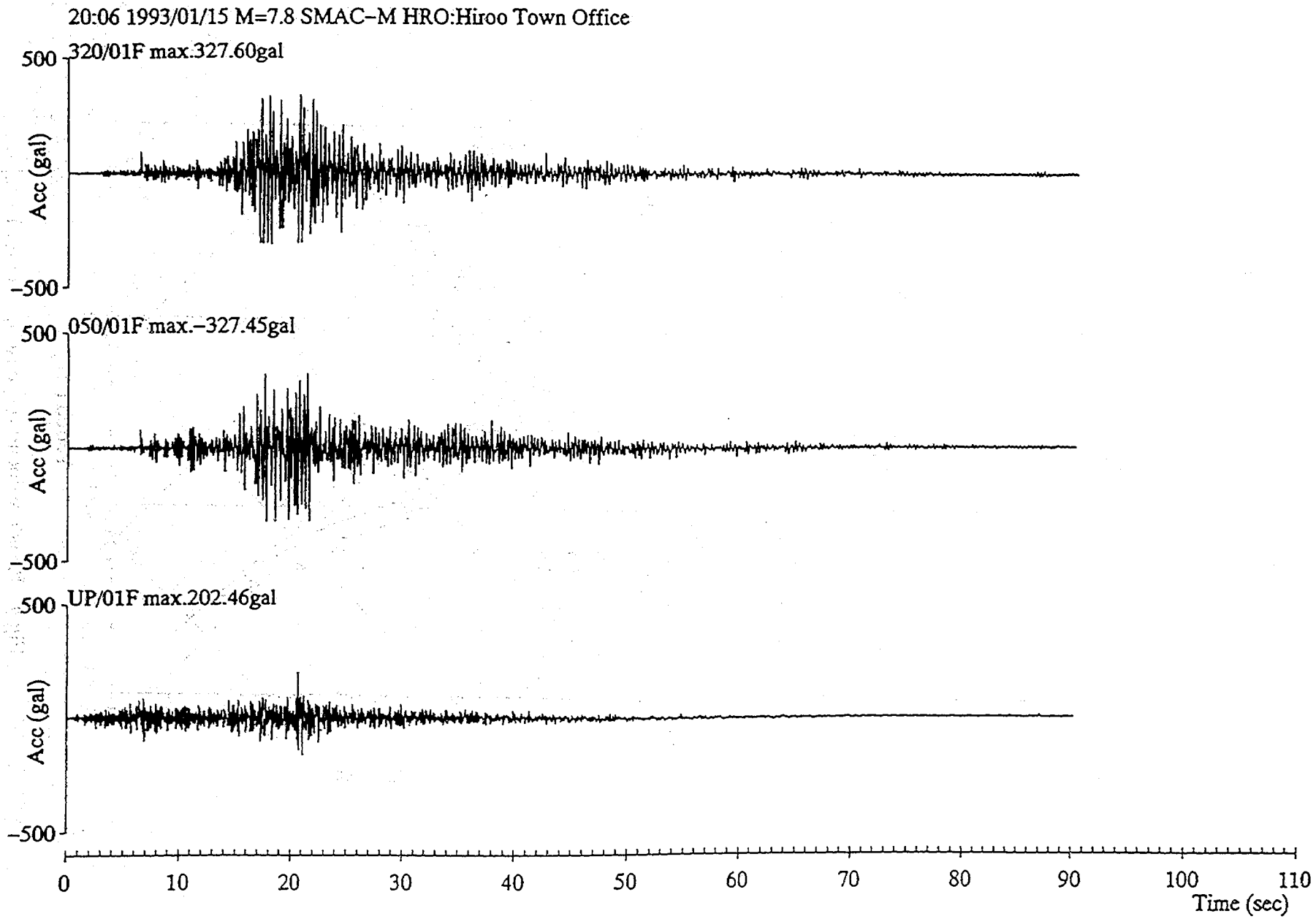


Fig.3 Accelerograms at the first floor of Hiroo Town Office

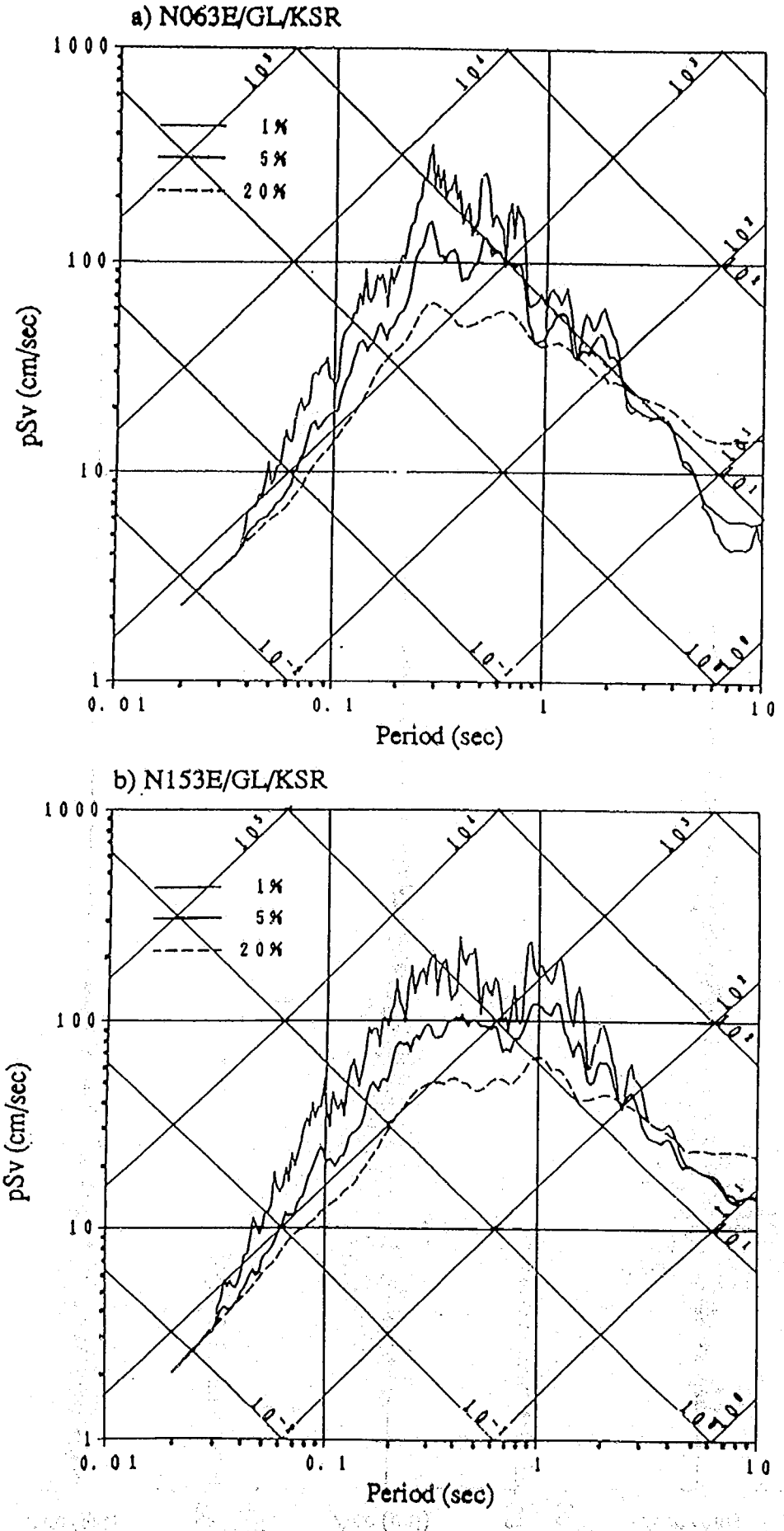


Fig 4 Pseudo velocity response spectra for Kushiro

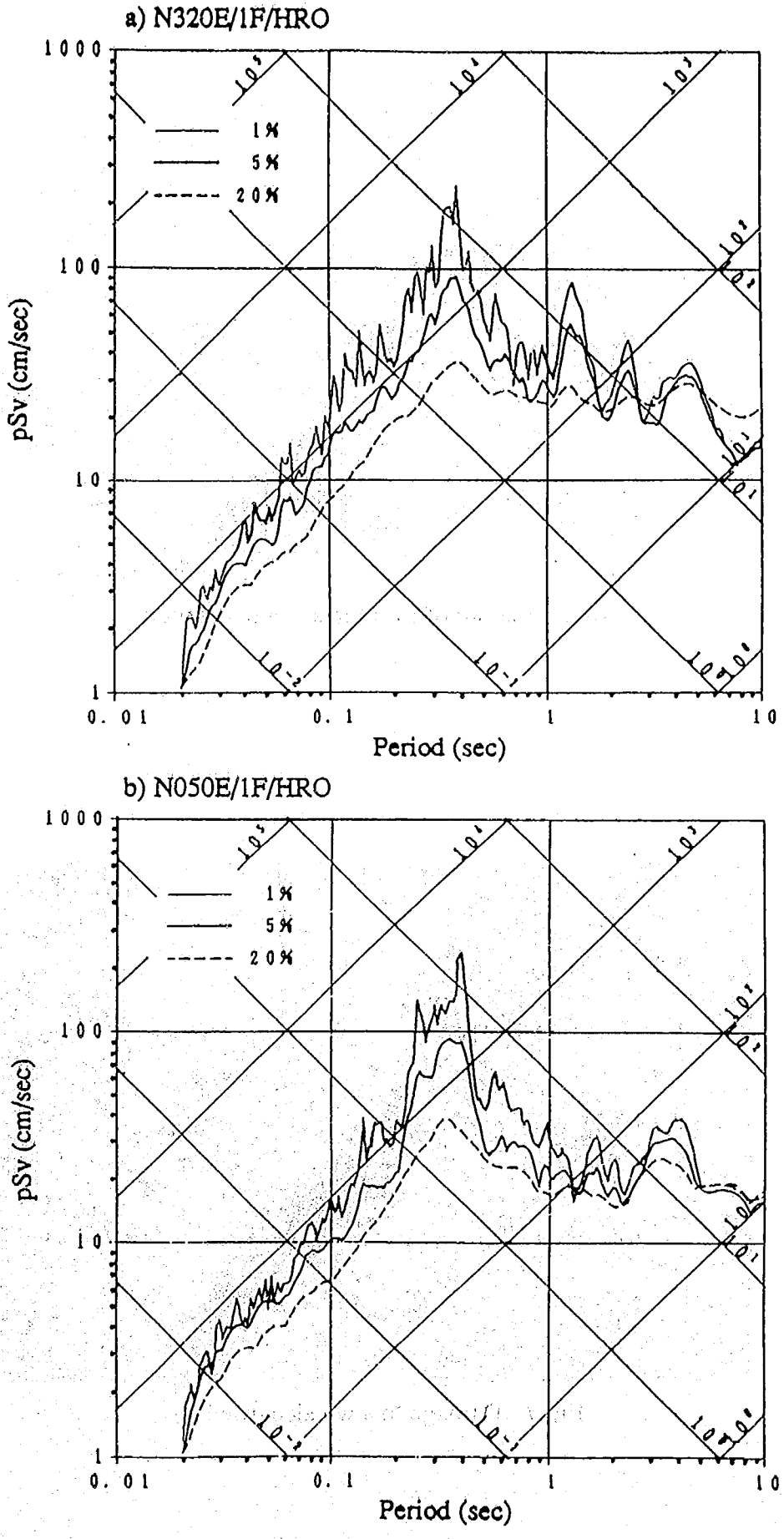


Fig.5 Pseudo velocity response spectra for Hiroo

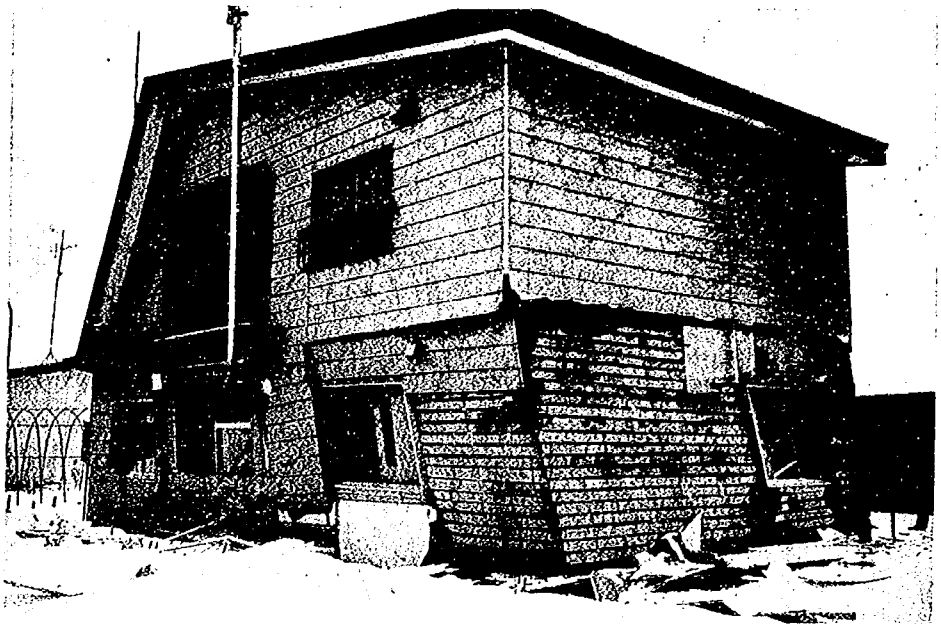


Fig.6 Layout of furnitures in a living room

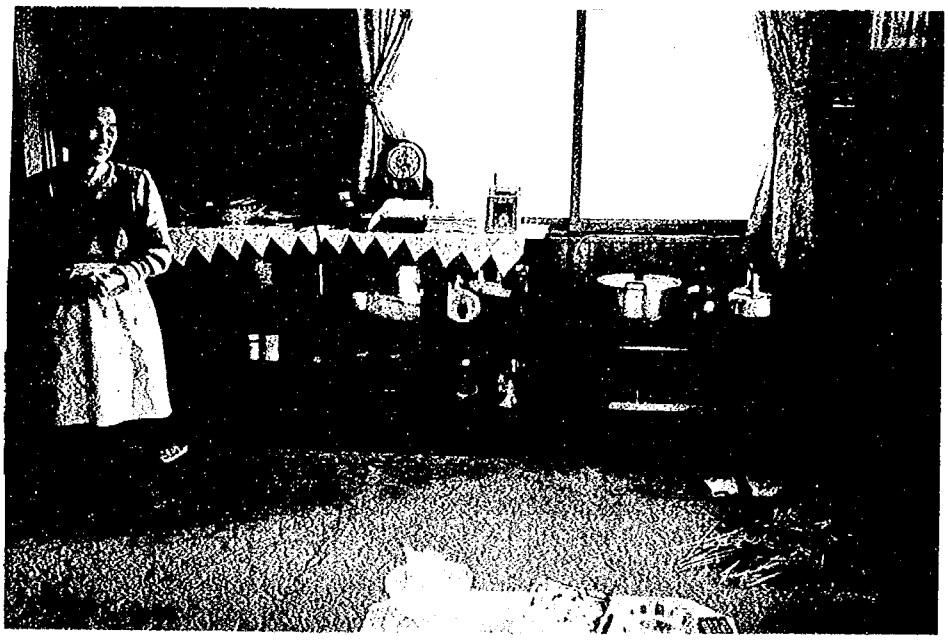


Fig.7 Damage to a wooden dwelling



Fig.8 Damage to a wooden building

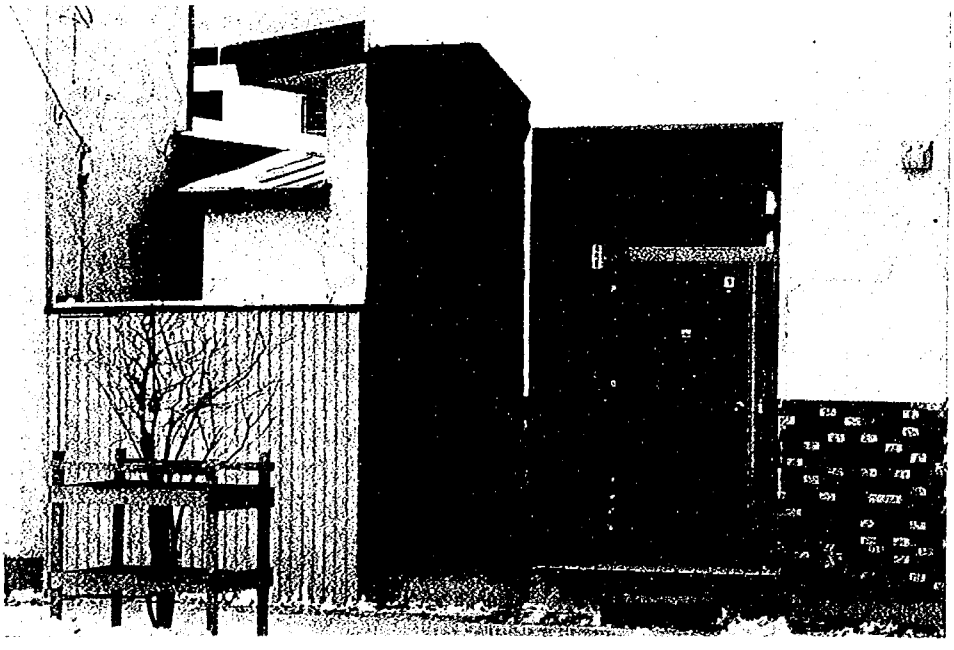


Fig.9 Damage to exterior wall claddings

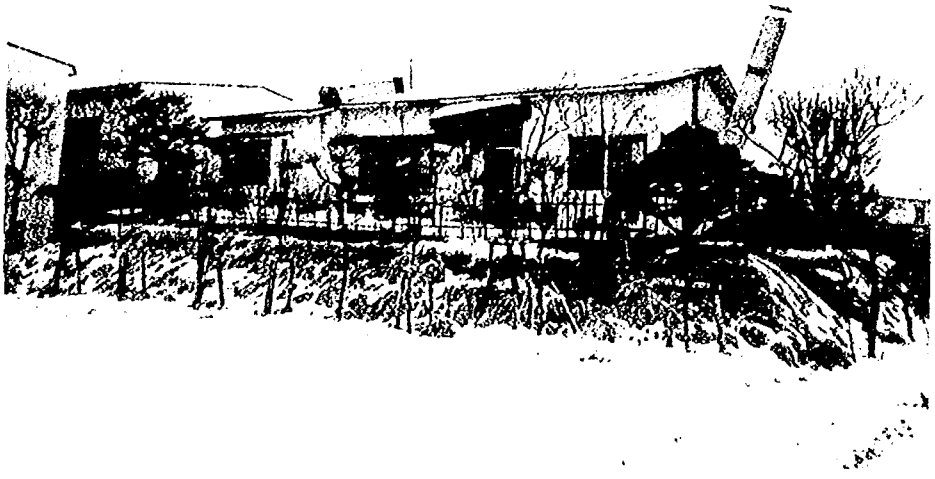


Fig.10 Inclination of a chimney

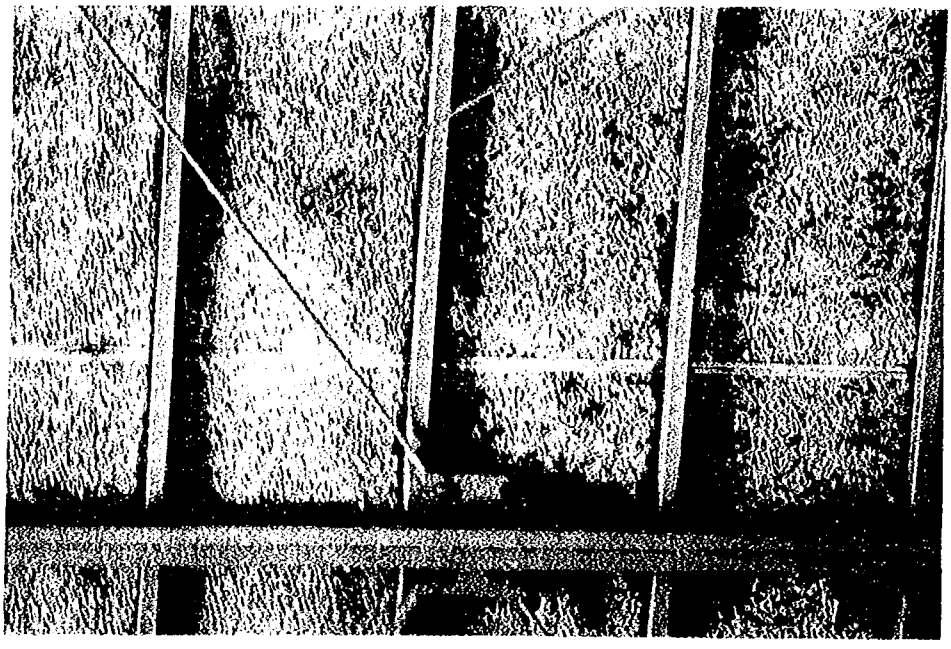


Fig.11 Damage to a horizontal bracing



Fig.12 Destruction of exterior wall claddings



Fig.13 Damage to window panes

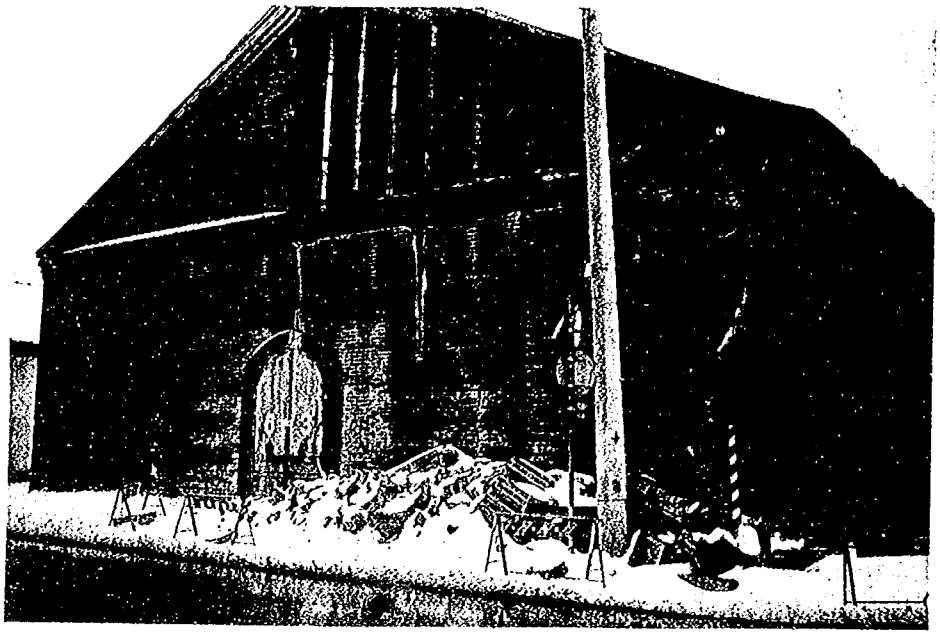


Fig.14 Partial collapse of brick masonry walls

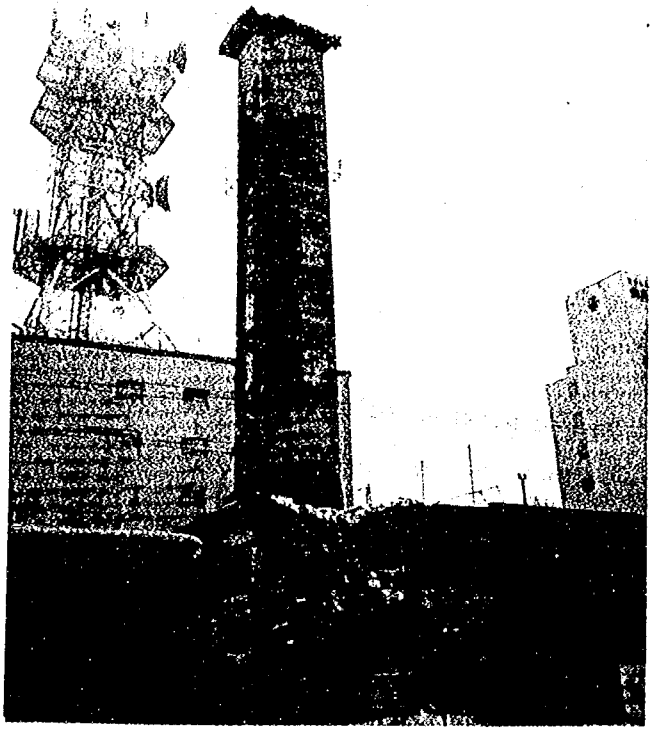


Fig.15 Kushiro Fire Station. Watch room at the top of 40m high tower fell down onto a roof of three-storied building.

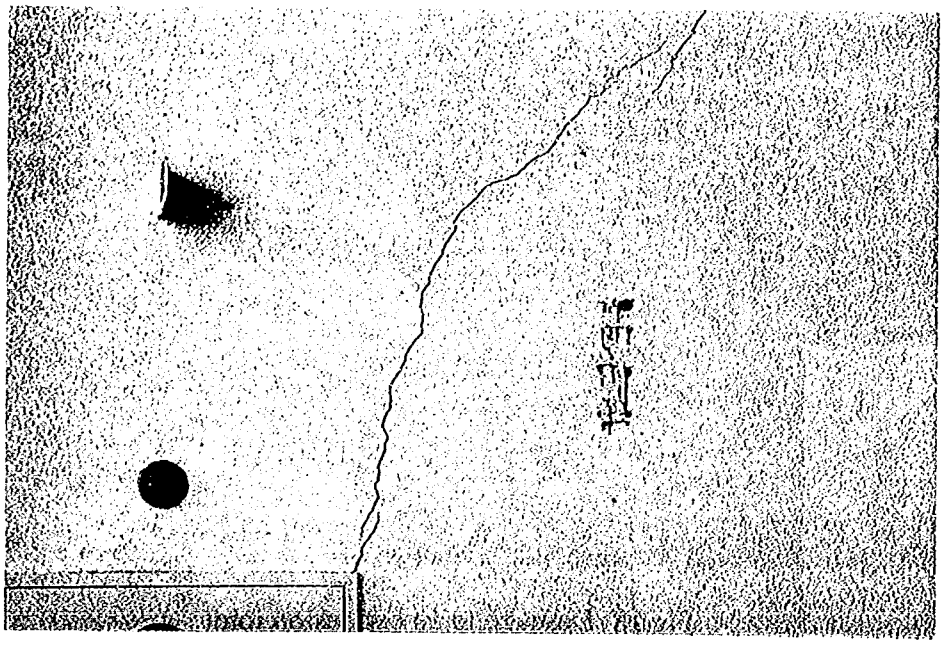


Fig.16 Shear crack in a RC wall

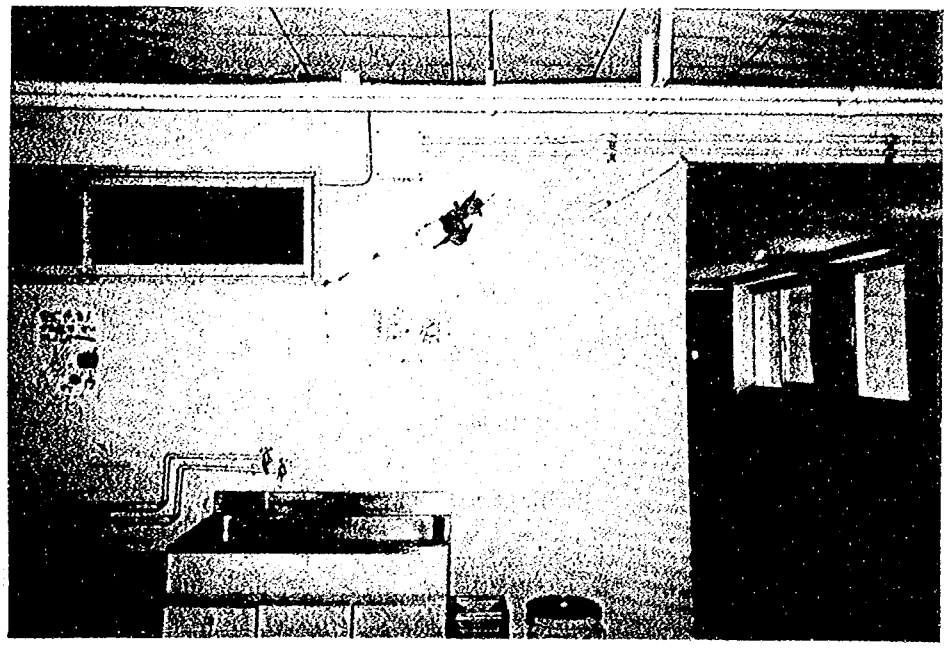


Fig.17 Shear crack in a RC wall

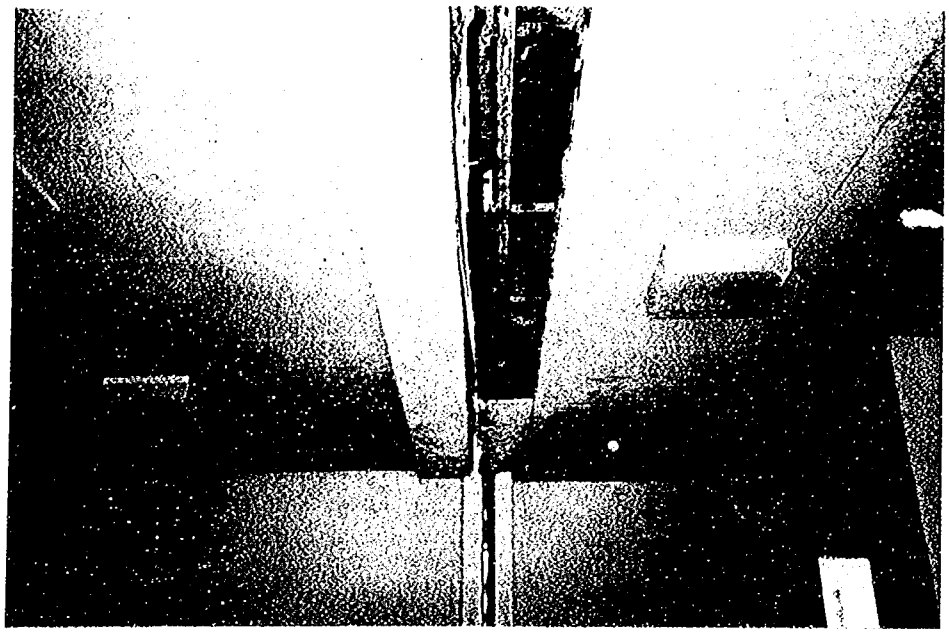


Fig.18 Damage to an expansion joint

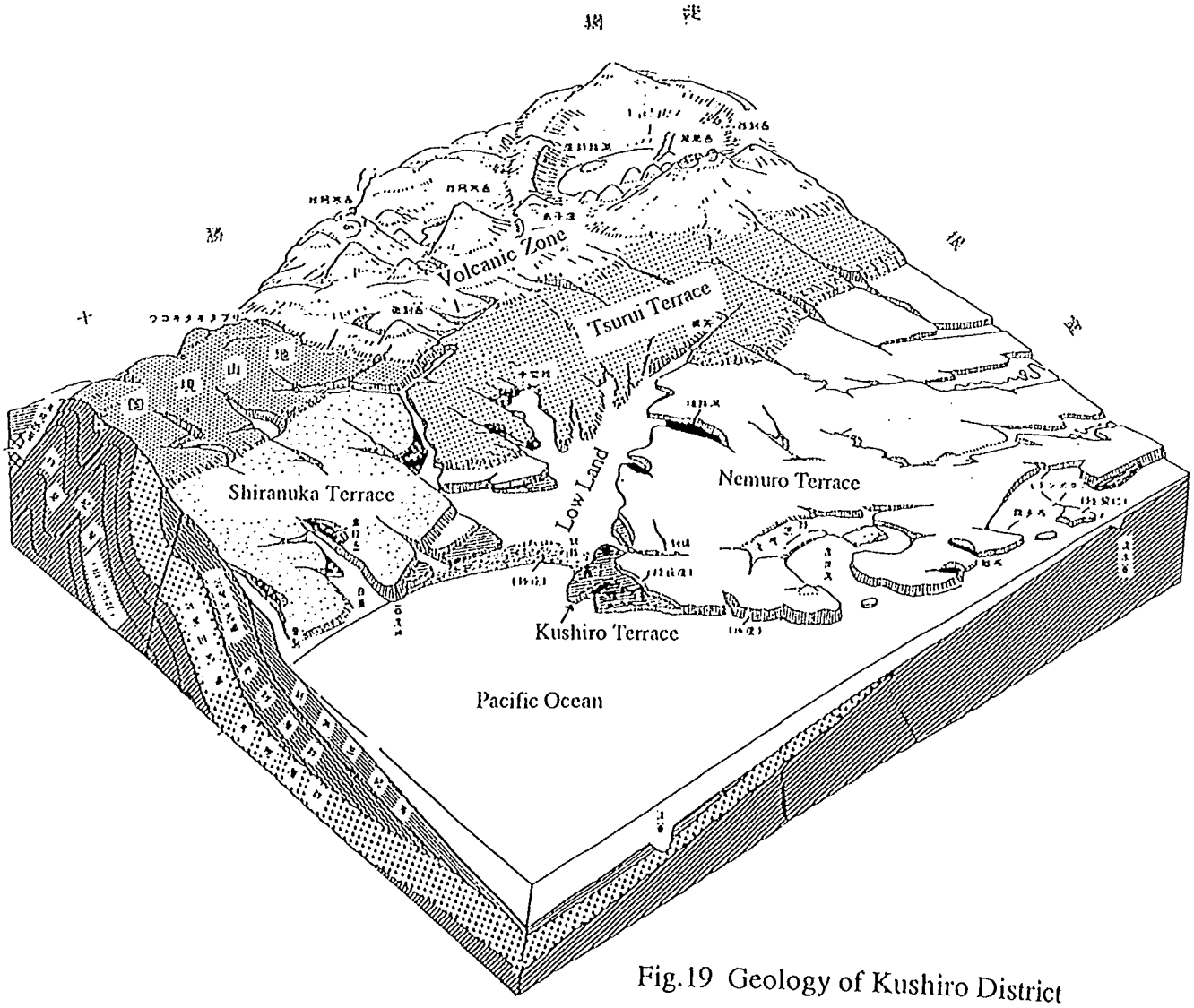


Fig.19 Geology of Kushiro District

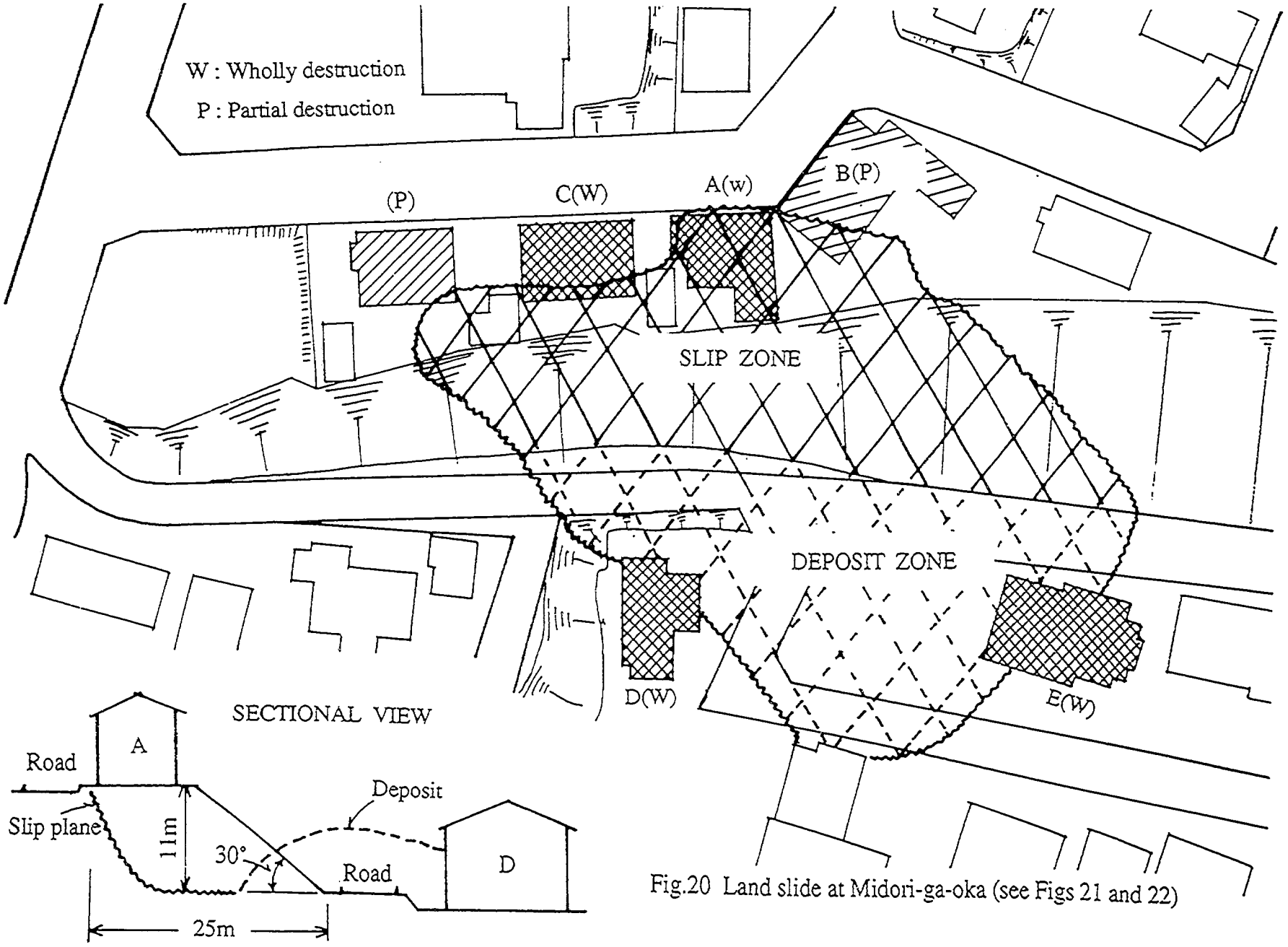


Fig.20 Land slide at Midori-ga-oka (see Figs 21 and 22)





Fig.21 Fig.22 Land slide at Midori-ga-oka

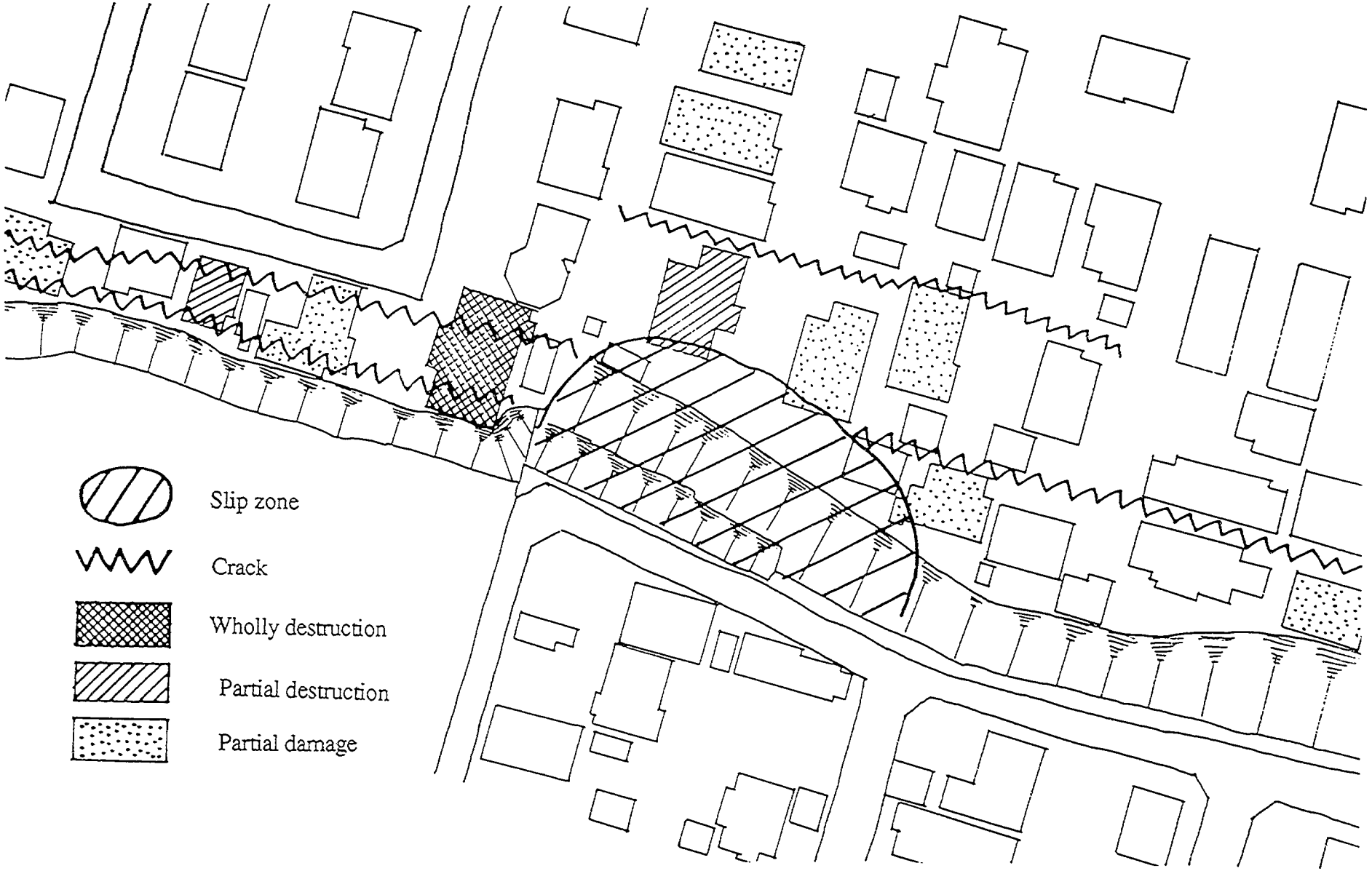


Fig.23 Damage to fill bank at Midori-ga-oka



Fig. 24 Slip and subsidence of housing lots



Fig.25 Inclination of dwellings

DAMAGE OF BUILDINGS DUE TO THE FLORES ISLAND INDONESIA EARTHQUAKE OF DECEMBER 12, 1992

by

Shinsuke NAKATA

ABSTRACT

This report briefly describes the reconnaissance activities of the Japanese Building Expert Team dispatched by the Japanese Government through the Japan International Cooperation Agency (JICA) to cooperate with organizations related to earthquake and tsunami hazard in Republic of Indonesia in estimating the effects of the Flores Island,Indonesia earthquake of December 12,1992 in the rehabilitation and recommendation of damaged structures. Damage due to earthquake vibration was concentrated to brick masonry buildings . Building team reconnaissanced Ende city ,Maumere city and Babi Island in east side of the Flores Island. The improvement of seismic performance of masonry buildings is also discussed in this paper.

KEYWORD : earthquake damage ; brick masonry building; seismic performance ; international corporation

1. INTRODUCTION

The main shock of the Indonesia Flores Island earthquake occurred at 1:29 P.M. (local time) on December 12, 1992, having a surface-wave magnitude of 7.5 (Ms) which caused much damage;around 2,000 people died due to collapse of buildings and tsunami. The epicenter was located about 40 km west northwest of Maumere, Flores Island, the Republic of Indonesia. According to aftershock data, the rupture zone is inferred to extend about 100 km to the east of Flores Island.

In view of the heavy damage from the earthquake, the Japanese government decided to offer a financial aid of U.S.$ one million, and immediate relief supplies worth U.S.$ 0.5 million through Japan International Cooperation Agency (JICA). The Indonesia government requested Japan to dispatch an expert team mainly specialized emergency measures, in which Japan, one of the most earthquake stricken countries, has the most advanced earthquake in the world.

In response to this request, the Japanese government immediately started the selection of experts in cooperation with Ministry of Construction, National Land Agency, Ministry of Education and other agencies concerned, and decided to dispatch immediately a Japan Disaster Relief Team (Expert Team) through JICA during a period from December 20 to 30. This decision was made under the Law concerning the Dispatch of the Japan Disaster Relief Team. The team consists of 8 experts covering fields of seismology, building and civil engineering and emergency countermeasures.

The quick response team, collected information from Indonesian sources and took field survey in Flores Island. The meetings were held with rehabilitation activity leaders in disaster stricken areas.

The recommendations from the Japan Disaster Relief Team showed briefly in the following ;

1. Strengthening of high-gain seismograph and strong-motion accelerograph observations
2. Planning of emergency evacuation from tsunamis in potentially dangerous areas
3. Planning of measures against tsunami hazard
4. Immediate opening of schools
5. Reinforcement of brick-frame structure and earthquake-proof test
6. Strengthening of existing masonry buildings
7. Repair of damaged bridges and earthquake-proof test of existing bridges
8. Reinforcement of mountain roads and planning of road networks

Director , Testing & Evaluation Department
Building Research Institute
Ministry of Construction

9. Planning of measures against liquefaction in port area
10. Planning of measures against landslides
11. Urgent planning of restoration of damaged areas
12. Planning of public education of earthquake and tsunami disaster to people from a very young age

2. EARTHQUAKE SOUCE MECHANISM

A very large earthquake occurred near Flores Island, Indonesia, on December 12, 1992. The hypocentral parameters given by U.S. Geological Survey are the followings; the origin time, 03: 20:28.1 in UT (01:29 P.M., in local time); location, 8.482s, 121.030E, depth. 36 km,; and surface-wave magnitude Ms, 7.5. The epicenter is about 40 km WNW of Maumere, near the northern coast of central Flores Island. The earthquake is the largest event since the 1977 Sumba earthquake (Ms 7.9, Mw 8.3).

The aftershock area extends as long as 100 km in the direction of ENE (Fig.1). This indicates that the initial rupture started at the west end of aftershock area and the rupture propagated 100 km toward the east-northeast.

3.DAMAGE SITUATION

Flores Island locates 1,600 kilometers far to the east side of Jakarta,capital city of Indonesia ,of which east side four prefectures ; Sikka,Ende,Ngada and East Flores were severely damaged. Width of this island is about 450 kilometers and its length in north-south direction is about 50 kilometers at maximum. The geology of the east side of this island is almost volcanic feature, where was much suffered by the earthquake this time. The mountainous and valley area are exposed with steep rocky surfaces. The height of mountains is about 2,000 meters. Some of them are active volcanoes. The land usage in Flores Island is as follows; rice fields and orchard : 15 percent, forest: 53 percent and savanna: 32 percent. The population of this island is around one million , and main industry is agriculture and miners are fishery and sightseeing. Farm products are cocoa,coconuts,coffee and corns besides rice.

The damage of housing is concentrated to the east area of Flores Island and it was caused by earthquake vibration and tsunami. Damage distribution map was reported as shown in Fig.1 from the Ministry of Public Works. The army headquarter for the damage measures reported the damage statistical data as shown in Table 1. Around 2,000 people were killed and a half of them were dead by tsunami. Especially damage of buildings were concentrated to Ende city (population :seventy thousands) and Maumere city (fifty thousands) . The greater part of damaged buildings due to earthquake are brick or "adobe" masonry structures without or with a few reinforcements. Our reconnaissance was done in these two cities.

3.1 Damage in Ende City

Ende city locates in the central area of Flores Island and face to Savu Sea. Building team surveyed fortyfour buildings in this city area for two hours guided by the staff of Ende prefecture office. Fig.2 shows the outline of Ende city map. The numerals in this figure are the buildings which we reconnaisanced. Photo 1-Photo10 are picked up pictures of buildings in this city.

Among fortyfour buildings, twentyfive buildings were collapsed. It was very difficult to find out non-damaged buildings. Many of buildings are first storied brick masonry structures. Such structures have double stack of masonry brick as popular as in the world.

According to the interview of the engineer in Sikka prefecture, weight mixing ratio of portland cement, sand and lime is respectively 1.0:3.0:10.0 used in the mortal of masonry structure. Buildings of concrete block masonry were also observed, and many of them were severely damaged. Newly constructed buildings were used reinforced concrete frame with masonry wall The collapse ratio of such buildings is not so higher than that of pure masonry buildings. However their sizes of sections of columns and beams were much smaller than those as usual in Japan. Reinforced concrete columns are about 15cm x 15cm in sections and used longitudinal reinforcement was 13 millimeter diameter plain bars. Little of deformed bars were utilized in the reinforced concrete structures.

3.2 Damage of Maumere City

Maumere city faces to Flores Sea.Damage situation of it's buildings are shown in Photo 11-Photo 24. This city is beautiful city-covered with green color trees and about three kilometer width in east - west direction and around two kilometers length in north-south direction. It was also severely damaged. Fig.3 shows the sketch of this city. It's east part was not so severely damaged. However, first story reinforced concrete buildings of the airport

facilities and army forces base camp were severely damaged in this area. Almost of all buildings were brick masonry and first storeyed. Their roofing is timber structure covered with clay tiles or tin therefore roofing is not heavy. Many of masonry buildings were much damaged in the central area. In this city around three hundred people were dead due to the collapse of such buildings by earthquakes.

As shown in Fig.3, central area of this city was much damaged. Buildings along the coast area were tilted and settled due to liquefaction of foundation soil. In the central area, reinforced concrete water tank structure was found to be almost non-damaged. It's height is around fifteen meters. The section size of its four columns were 30cm by 30cm. Considering that this type of reinforced concrete water tank tower was not damaged so severely, input earthquake was estimated not to be so large; 0.1g - 0.2g. Typical masonry structural walls which are often observed in this city, were estimated the lateral load carrying capacity of more than 0.2g base shear coefficient from very lough assumptions and calculation. However, the lateral load carrying capacity of masonry wall system in out-of-plane direction was much smaller than that of in-plane shear capacity of masonry wall as mentioned above.

Especially along Radjacentis Street which is main commercial area in this city, more detailed damage survey was conducted. Such results are shown in Fig.4 The classification of damage grade was defined by outside observation of buildings.

Among thirty two brick masonry buildings (M), fifteen buildings were collapsed (47%). Two reinforced concrete framed masonry wall buildings (RC+M) were collapsed among twenty-two same types buildings (9%). sixteen (RC+M) buildings were severely damaged (73%). Twenty seven M structures were also severely damaged (84%). Many of photographs showed such traces of " out-of-plane " collapse of masonry buildings.

3.3 Analysis of Damage

From two days reconnaissance of damaged buildings, the followings are summarized as features of buildings damage

1) Many brick masonry buildings with wooden roofings were collapsed, which have non-seismic reinforcements. It was considered that the cause of such damage shall be based on the out-of-plane collapse of masonry wall segment.
2) In the down town area, some of buildings were more than two storeyed reinforced concrete frame structure with brick masonry walls. Their collapse ratio to total numbers of reinforced concrete buildings was smaller than that of masonry structures, and many of them remained in medium damage grade.
3) Damage of reinforced concrete buildings which were considered to be recently constructed was quite slight. The section sizes of their columns and beams were much smaller than those used in Japan.
4) Construction method of foundations and footings seemed to be poor for the out-of-plane resistance of masonry wall to earthquake force.

4. SEISMIC REGULATIONS

According to the Indonesian Seismic Code of Ministry of Public Works, design seismic coefficient; Cd is defined as equation (1).

$$Cd = C\ I\ K \qquad (1)$$

where

C ; base design shear coefficient, six categories are defined in all of Indonesia Republics. In each zone, two values are defined by the soil condition Flores Island is classified in Zone 2, as shown in Fig.5

I ; importance factor

general building	: 1.0
important facility	: 1.5
important and dangerous facility	: 2.0

K; structural coefficient

reinforced concrete	: 1.0
prestressed concrete	: 1.4
steel	: 1.0

From Fig.5 , assuming I=1.0 and K=1.0, design base shear coefficient Cd's values is 0.09 in hard soil and 0.07 in soft soil in zone 2 for the short natural period of structures.

Seismic shear coefficient calculated from ultimate shear capacity of in-plane masonry wall system is far larger than this design coefficient. However its out-of-plane capacity was evaluated as about 0.1g. It is easily realized that the responsed earthquake force to the structure exceeds 0.1g, then many masonry structure collapsed in out-of-plane direction . Considering these earthquake damage, design base shear coefficient Cd should be discussed more in detail especially on the matter of out-of-plane direction of wall system .

5 RECOMMENDATION

For the countermeasure of safer masonry building due to earthquake, much more improved device is indispensable to the seismic strength against out-of-plane falling down of brick masonry wall system.

In order to start such device development, following items will be effective;

a) to strengthen more the rotation resistance of foundation system.
b) to strengthen out-of-plane wall system

As long as masonry structure is low rise building, in-plane shear strength of masonry wall may be enough to such level of earthquake as occurred this time. However the out-of-plane bending resistance is very small. It is required some reinforcement using reinforcing bars, wires and bamboos, which should be installed in masonry walls with enough anchorage to concrete foundation systems. Bamboo is useful as reinforcement, which is available in Sikka Prefecture, it's Young's modulus and tensile strength are respectively $1.25\text{-}1.55 \times 10^5 kg/cm^2$ and $1700\text{-}2400 kg/cm^2$. So, bamboo can be much effective for strengthening wall system by intelligent and careful device of construction. Such detailed construction manual for local people should be based on the test results which shall be planned and conducted in Research Institute of Human Settlements, Ministry of Public Works, Bandung. From now the education system for such seismic proof construction workmanship should be widely distributed to local people by video tape and demonstration of model construction and so on.

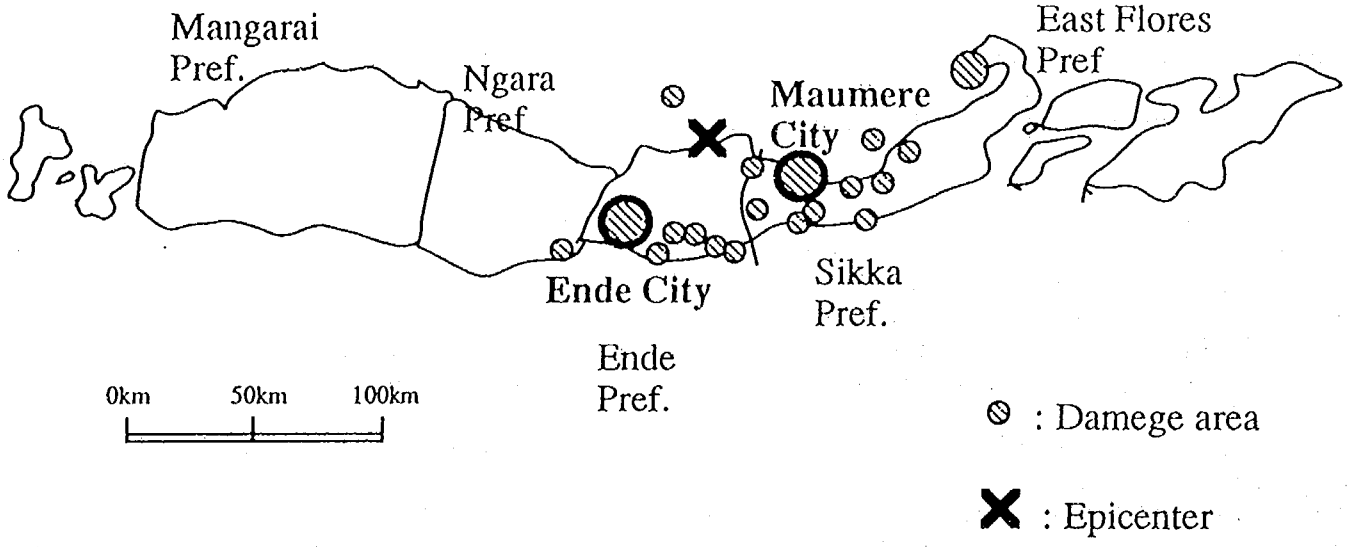


Fig.1 Map of Flores Island

Table 1 Overall Damage

26 Dec. 1992

Regency	Population ('85)	Area	Human Damage				Building Damage				
			Dead	Injured		Missing	Office	Church Mosk	People House	School	others
				Heavy	Light						
	(Prs)	(km²)	(Prs)	(Prs)	(Prs)	(Prs)	(house)	(house)	(house)	(house)	(house)
Sikka	236,691	1,731.9	1,457	252	1,256	8	56	47	10,200	324	4
Ende	212,349	2,046.6	229	106	227	-	344	193	13,804	281	154
Ngada	188,353	3,037.9	18	2	4	-	67	45	1,194	100	68
Flores Timur	267,295	3,079.2	376	15	241	61	26	22	2,920	80	50
Total	904,688	9,895.6	2,080	375	1,728	69	493	307	28,118	785	276

Notice 1. Human damage (Dead) in Flores Timur includes about 200 victims by Tsunami.
2. Building damage (Housing) includes figures of houses partially damaged.

Source : Army's Headquarters for Emergency Activities in WAIOTI Airport in Maumere.
(Figures table which was prepared for the review to President in 23 Dec. 1992.)

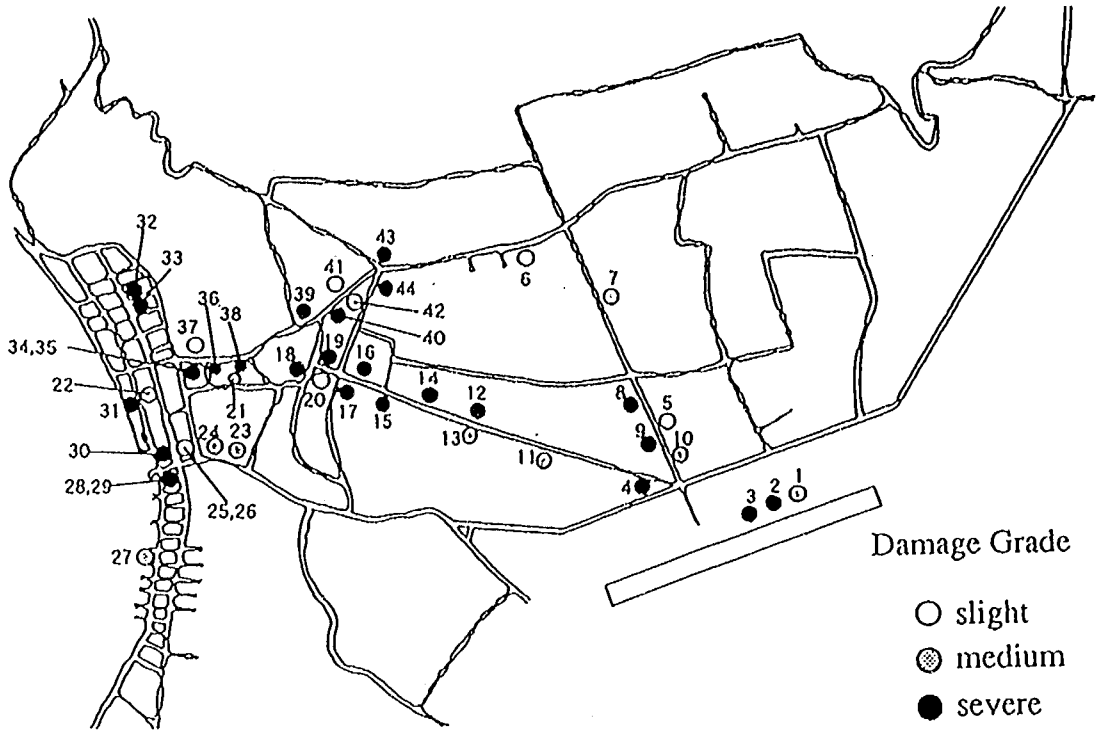


Fig.2. Ende City Map

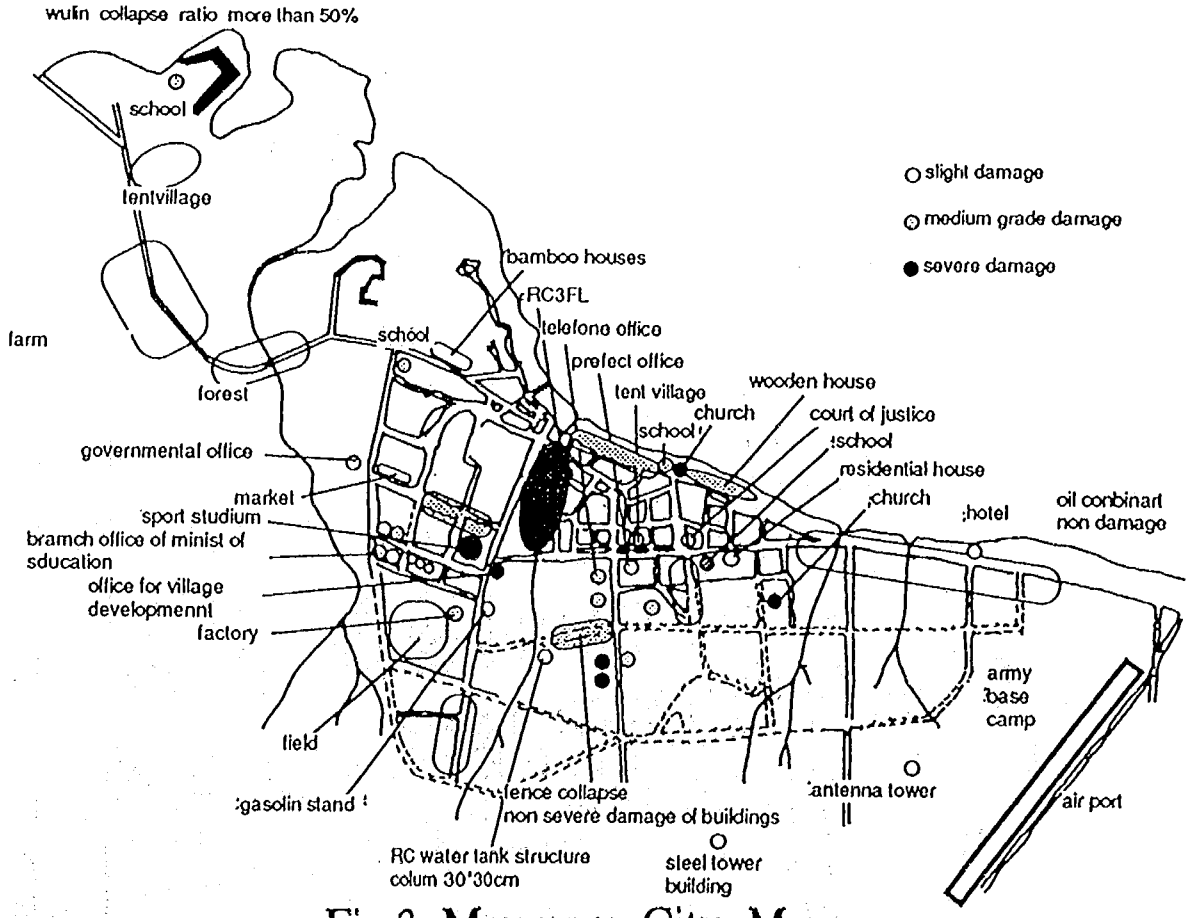


Fig.3 Maumere City Map

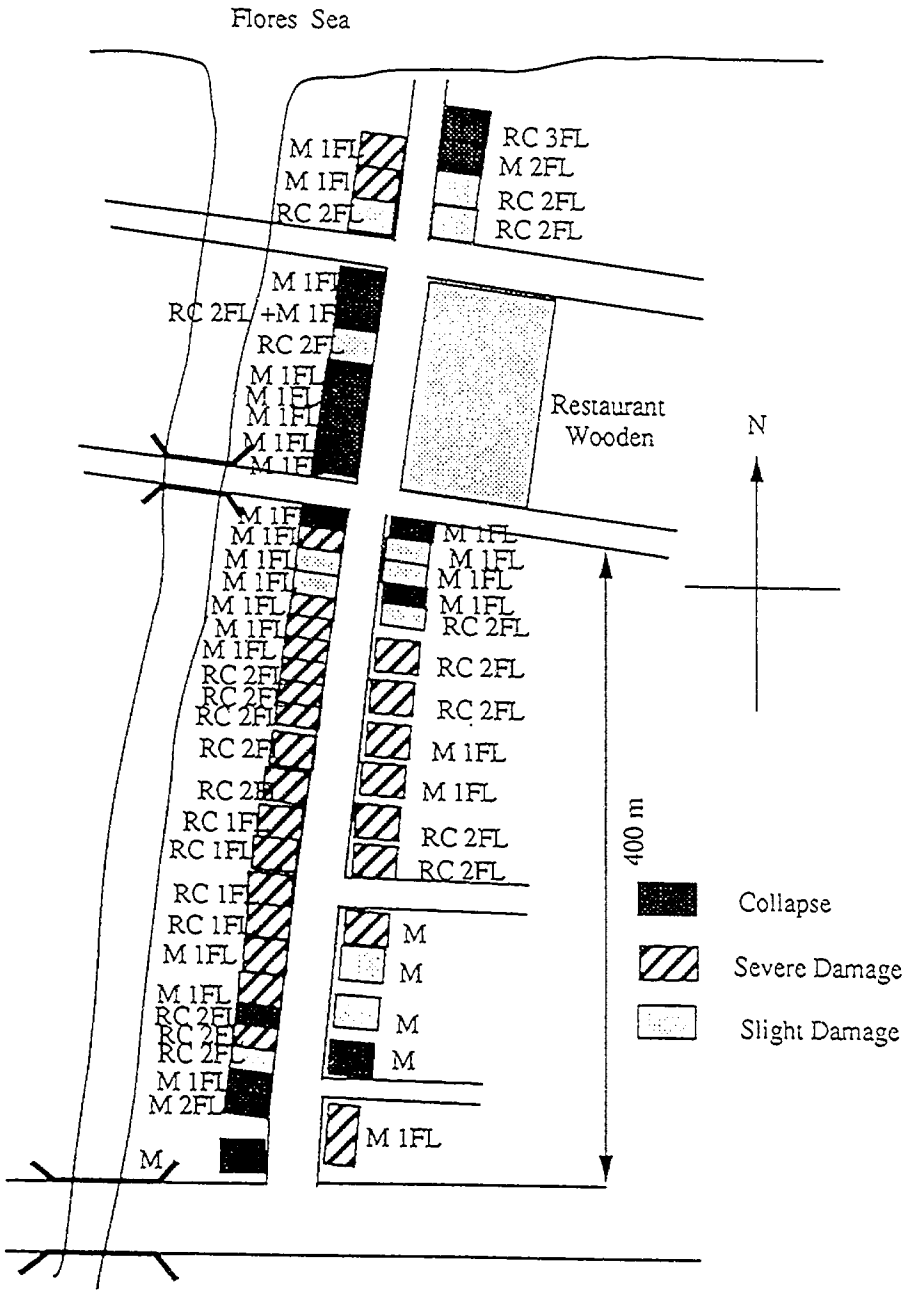


Fig.4 Maumere City Commercial Area

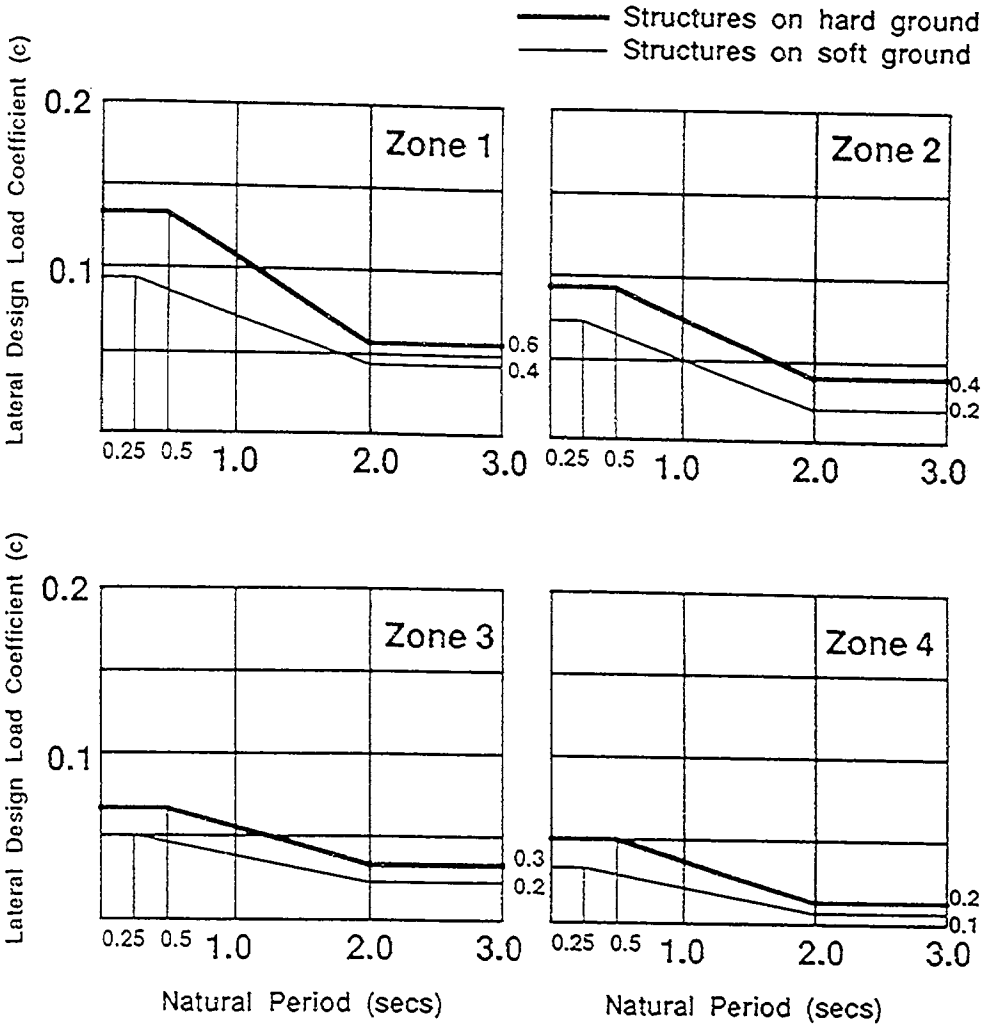


Fig. 5 Unmodified C Values

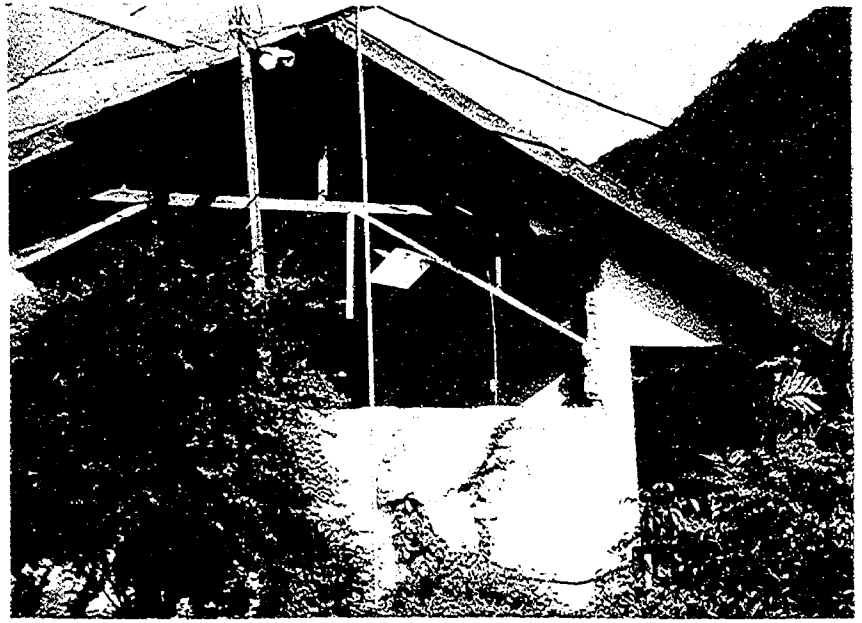


Photo 1 masonry building in Ende airport, falling down of side wall

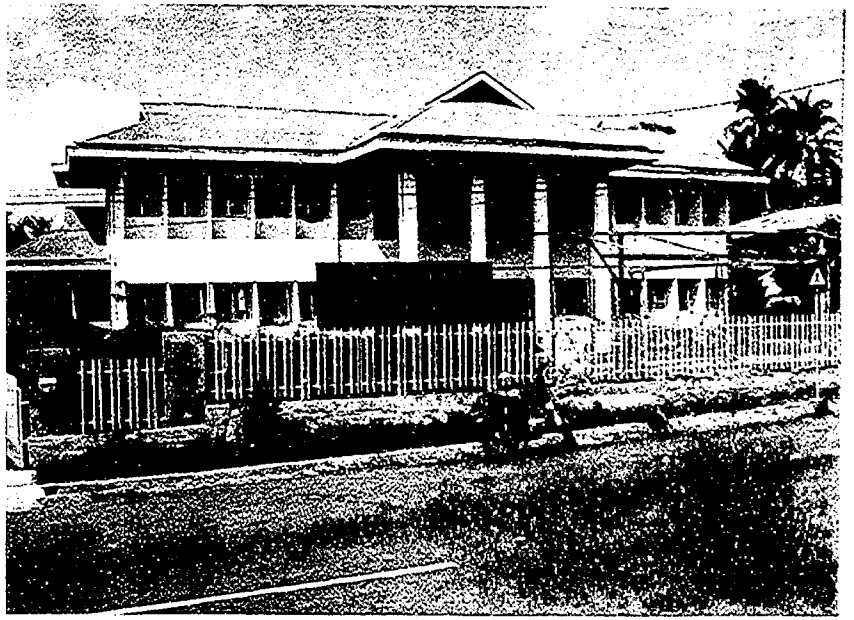


Photo 3 Ende city office , severe damage , remaining story drift 10 cm

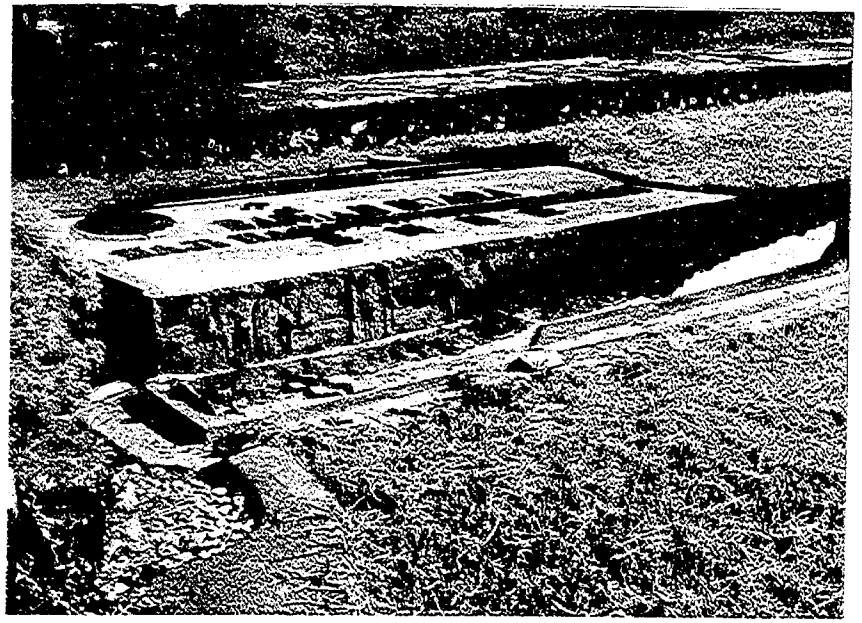


Photo 2 airport name plate wall panel ,falling down , no reinforcing



Photo 4 Ende city office , close up

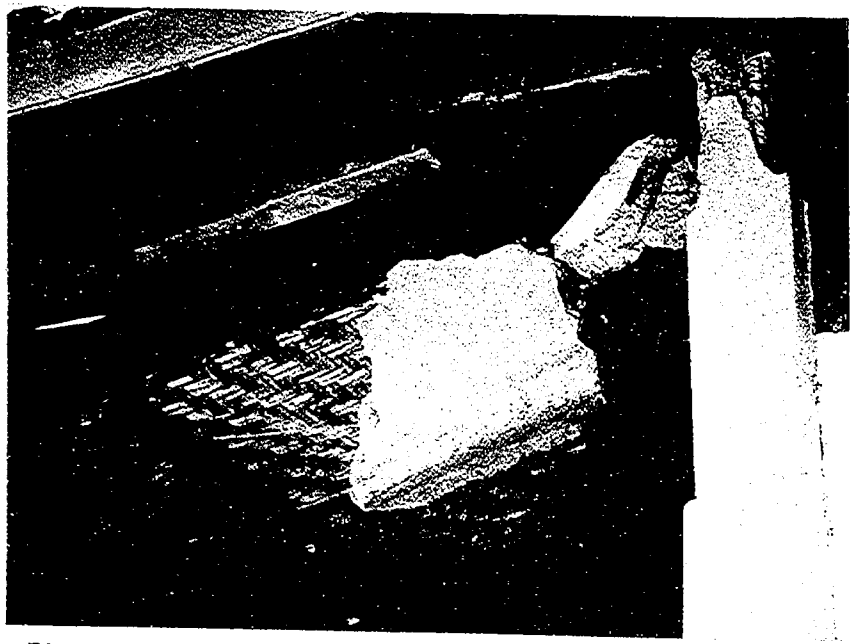


Photo 5 close up of this school building ; column top and ceiling



Photo 6 adobe one storey house, severe damage

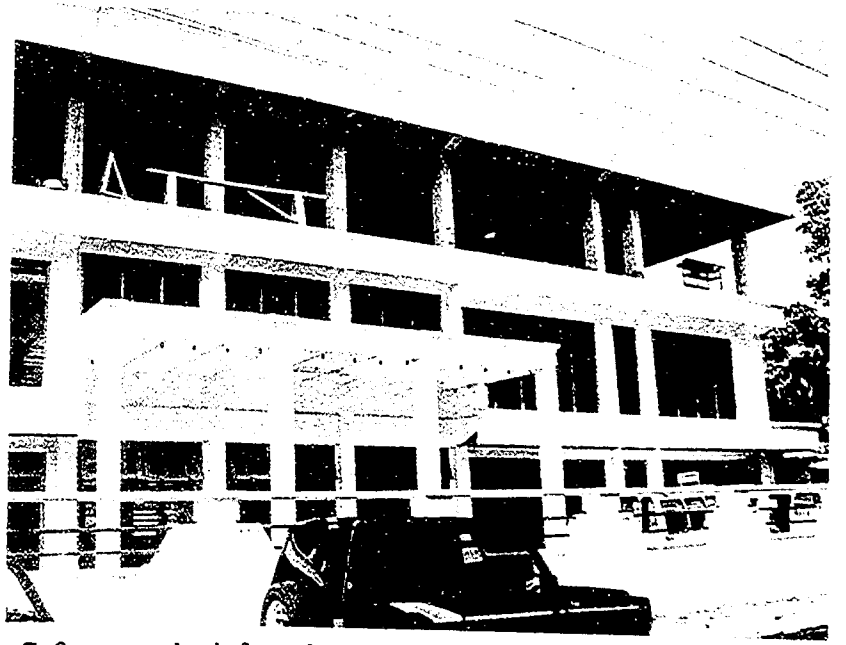


Photo 7 3 storeyed reinforced concrete building; slight damage, under construction

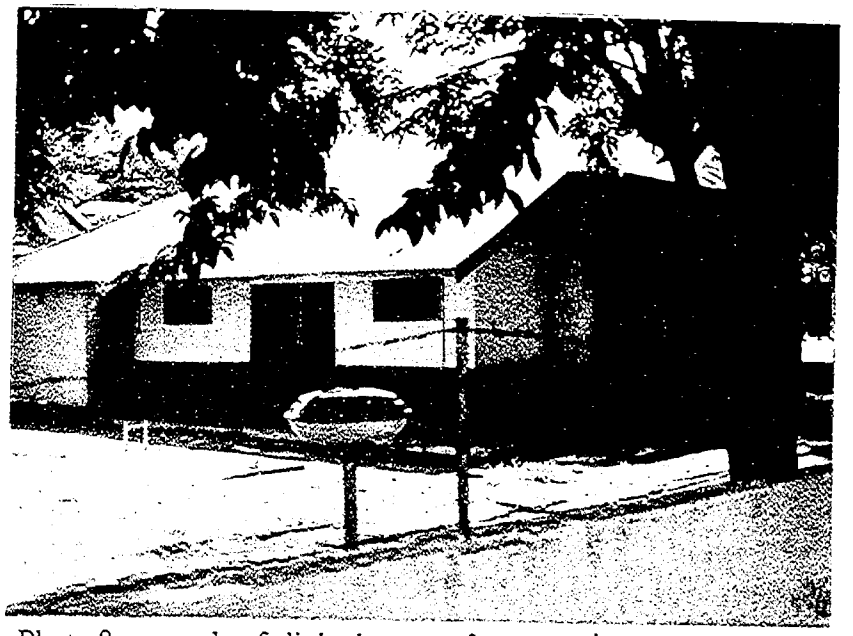


Photo 8 example of slight damage of masonry house



Photo 9 3-storeyed reinforced concrete frame + masonry wall building ; collapsed

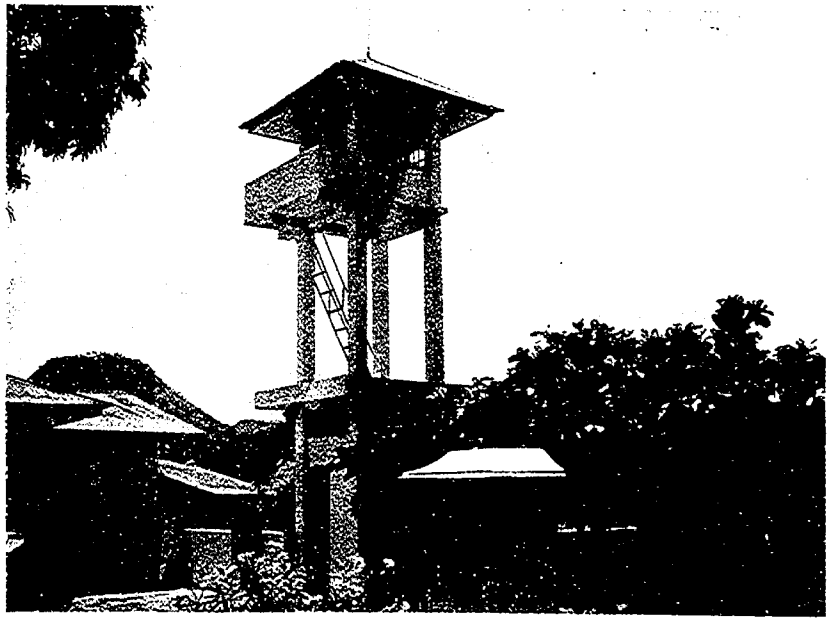


Photo 11 reinforced concrete tower building; slight damage

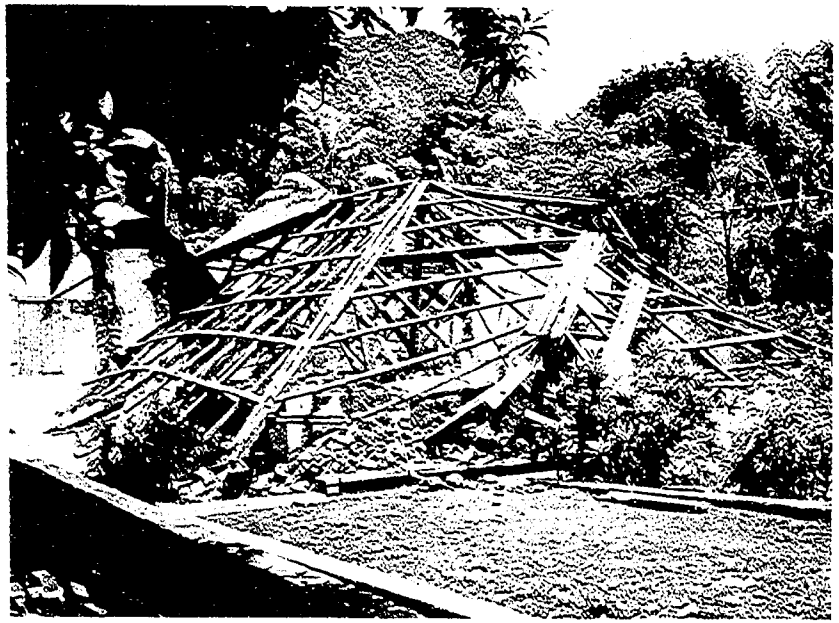


Photo 10 typical damage pattern of masonry wall building ; perfect collapse

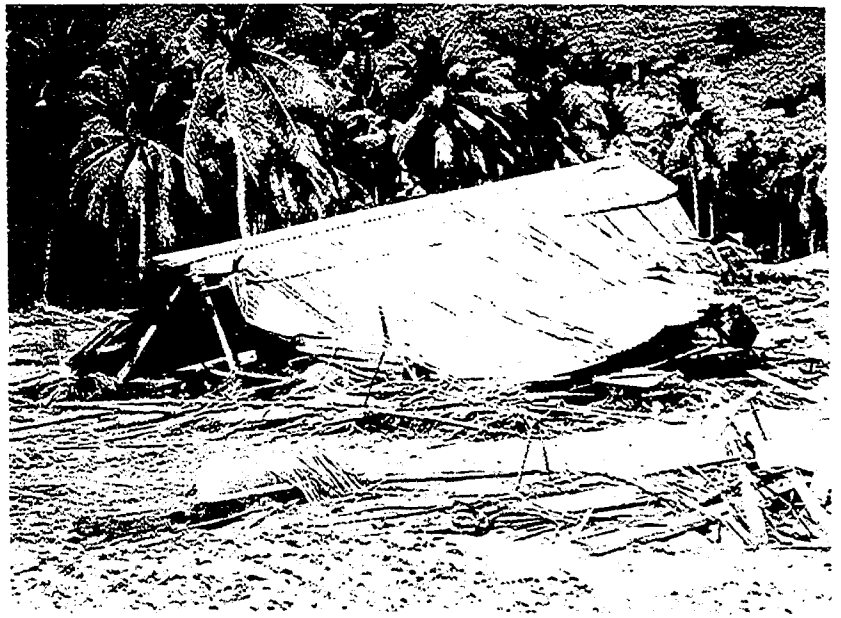


Photo 12 collapsed house due to tsunami in Babi Island 30 km from Maumere city



Photo 13 damage of Maumere port ; stranding of steamer by tsunami



Photo 15 typical collapse pattern of masonry house; many of masonry houses were collapsed like this pattern in Maumere city



Photo 14 perfect collapse of Wulin town by tsunami 3 km west of Maumere



Photo 16 collapsed mosque along sea shore street in Maumere city ; masonry wall structure, timber roofing

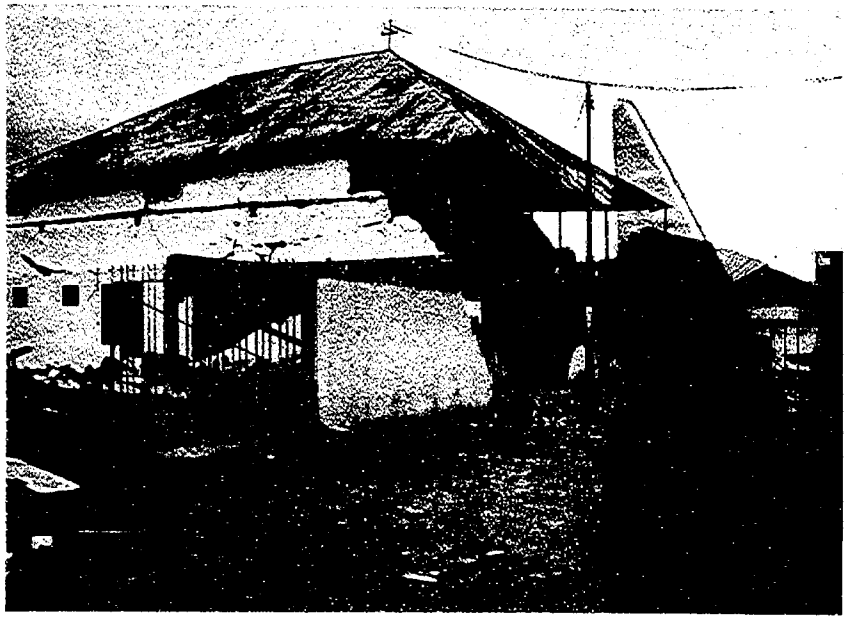


Photo 17 severe damage (out of plane break) of wall system of masonry storage building



Photo 19 timber and bamboo house in Maumere city ; no damage , timber houses were almost non damaged in Maumere city

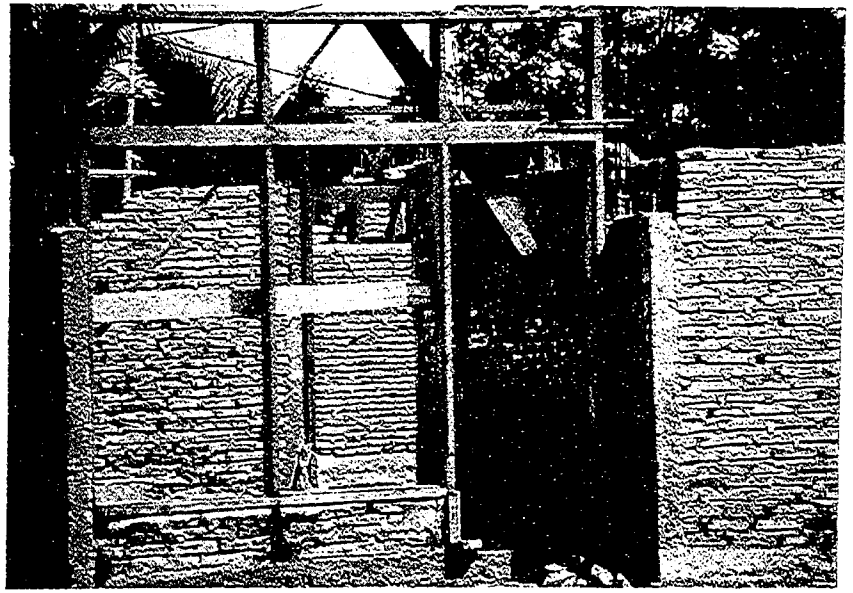


Photo 18 new type masonry wall building with reinforced concrete framing; under construction

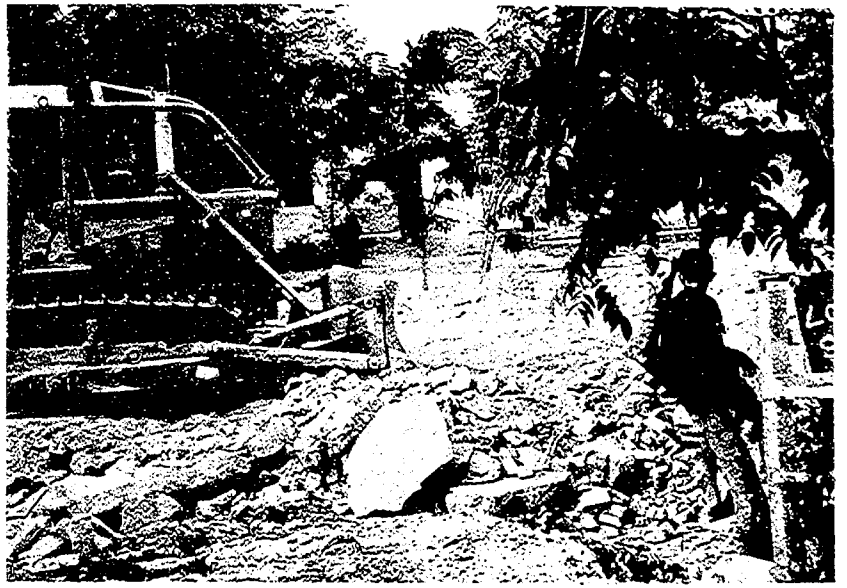


Photo 20 two storey reinforced concrete masonry building; severe damage,business work was done in temporary facilitated sheet tent

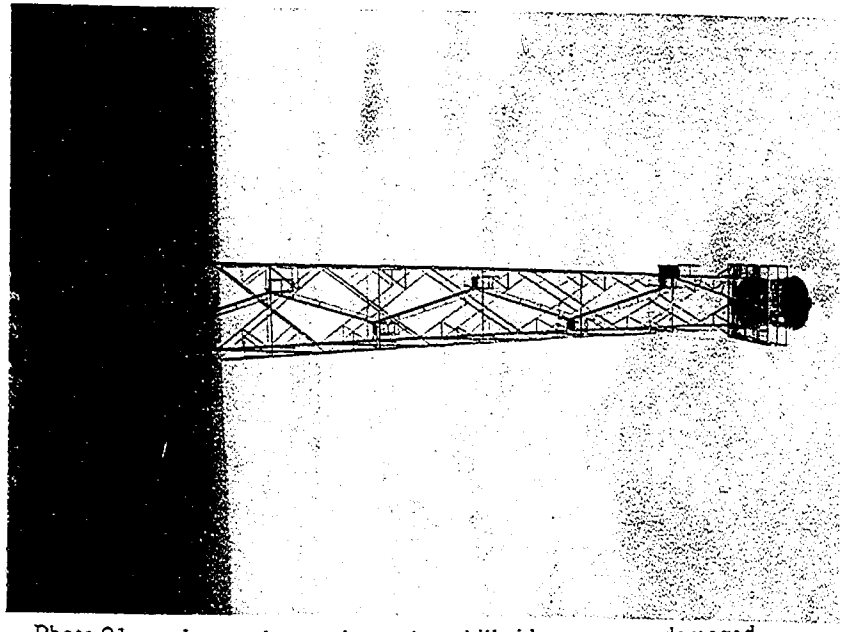


Photo 21 steel tower locates in southern hill side area ; non damaged

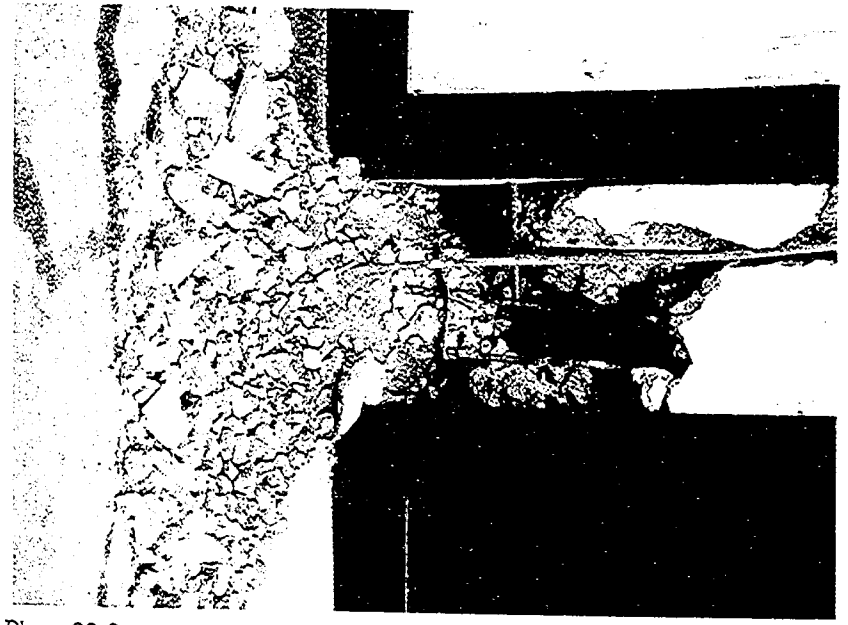


Photo 22-2 small column and small size reinforcing bars of same building



Photo 22-1 severely damaged reinforced concrete masonry wall building

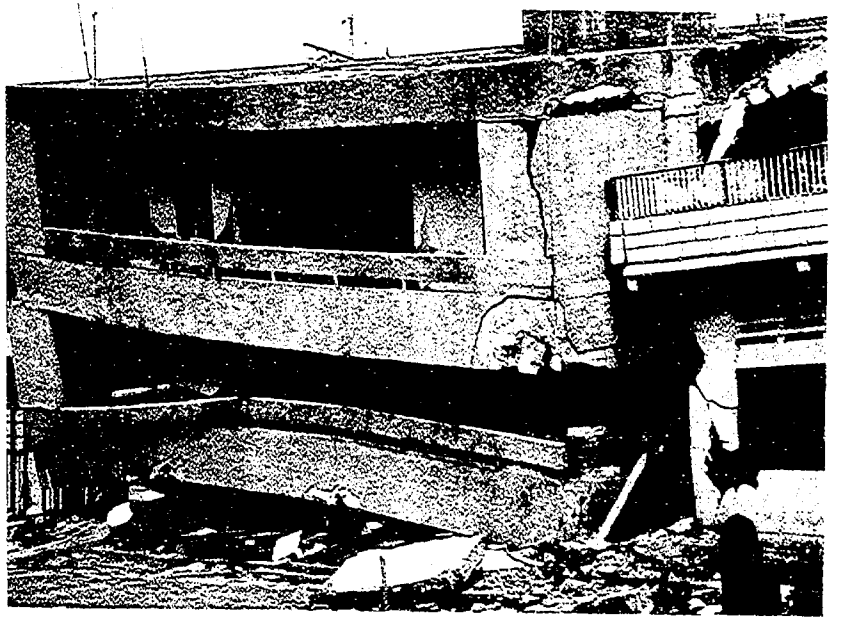


Photo 23 collapse of reinforced concrete building which seemed to be heavier



Photo 24 gasoline stand roofing at hill side area of Maumere city ; steel ,non damage

CHARACTERISTICS OF EARTHQUAKE-INDUCED LANDSLIDE SITES: CASES OF THE FLORES ISLAND EARTHQUAKE OF 1992

Takekazu AKAGIRI and Yohta KUMAKI

1.Characteristics of earthquake induced landslide sites

From the geomorphological viewpoint, mountainous region is characterized as follows (Egawa:1979, Kumaki and Suzuki: 1982, Kumaki:1988,Kumaki:1991):

1) The most important geomorphic process is the breakup of mountains by dissection. Therefore land surface is basically divided into three areas i.e. less-dissected, active dissection and after-dissection areas (Fig.1).

2) The "dissection front" i.e. the border between less-dissected and active dissection areas makes nick lines. It moves from the end of mountains towards high places. In most cases several dissection fronts are visible in a mountainous region. They are originated of different ages.

3) The movement of dissection front is intermittently caused by landsliding in general, so that landslides are tend to occur on the zone along the dissection front.

4) A dissection front can be subdivided into two parts. One is made by valley-head erosion and the other is made by the influence of lateral river erosion or coastal erosion. In the same way, slope in the active dissection area can be subdivided into valley-head slope and valley-wall slope or coastal cliff.

It is well known that rainfall-induced landslides occur more frequently in the valley-type slopes in horizontal profile than crest-type or straight-type slopes. HATANO (1974) pointed out that catchment area of the sliding point as well as slope angle is the most critical morphometric factor to the cause of landslide triggered by heavy rainfall. These mean that water percolating downward through the soil plays very important role to the sliding induced by heavy rainfall. As the result, landslide frequency in valley-head slope where water gathers is higher than that in the valley-wall slope, and dissection front on the valley-head slope moves more rapidly than that on the valley-wall slope.

On the contrary, in case of landslide triggered by earthquake, there is little relationship between sliding site and catchment area or slope type since the water effect is very small, so that slope angle is the most important factor (Fig.2). Valley-head slope is of valley-type in horizontal profile and more

---

Geographical Survey Institute
Ministry of Construction

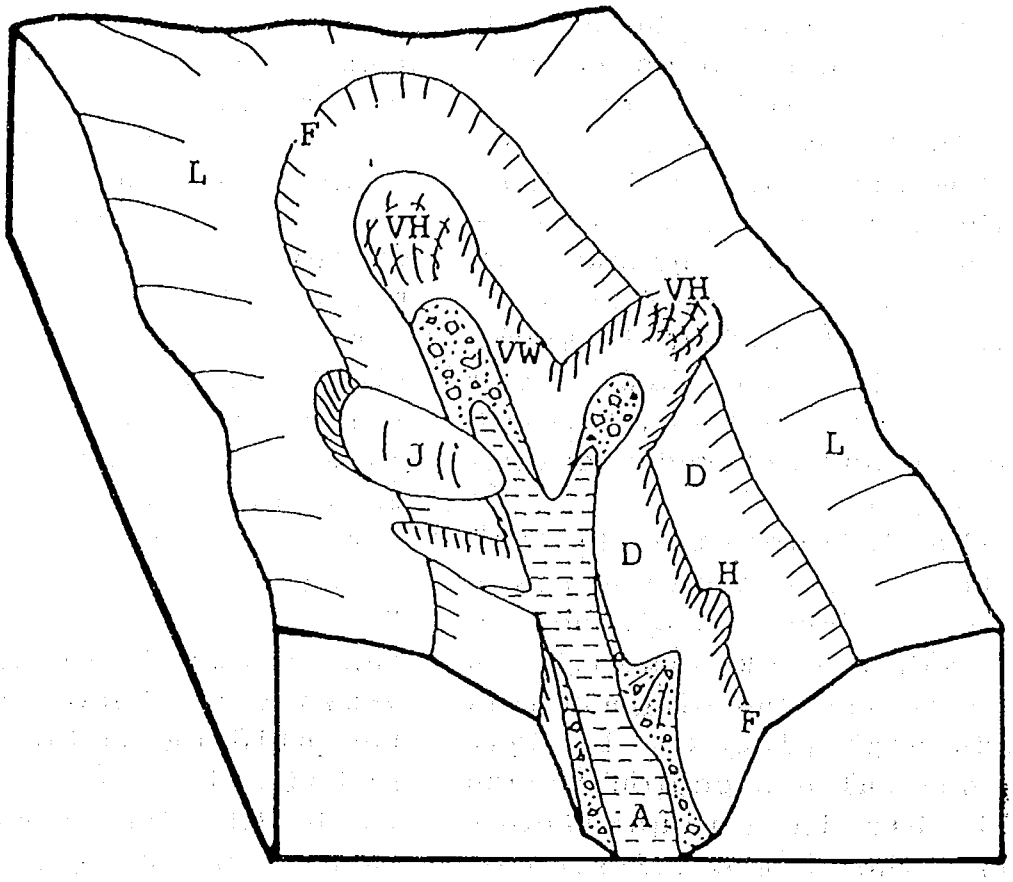


Fig.1 Schematic geomorphic feature of mountainous region (Modified from KUMAKI, 1991)
L:Less-dissected area, D:Active dissection area, A:After-dissection area, F:Dissection front, VH:Valley-head slope, VW:Valley-wall slope J:*Jisuberi* landslide, H:*Hokai* landslide

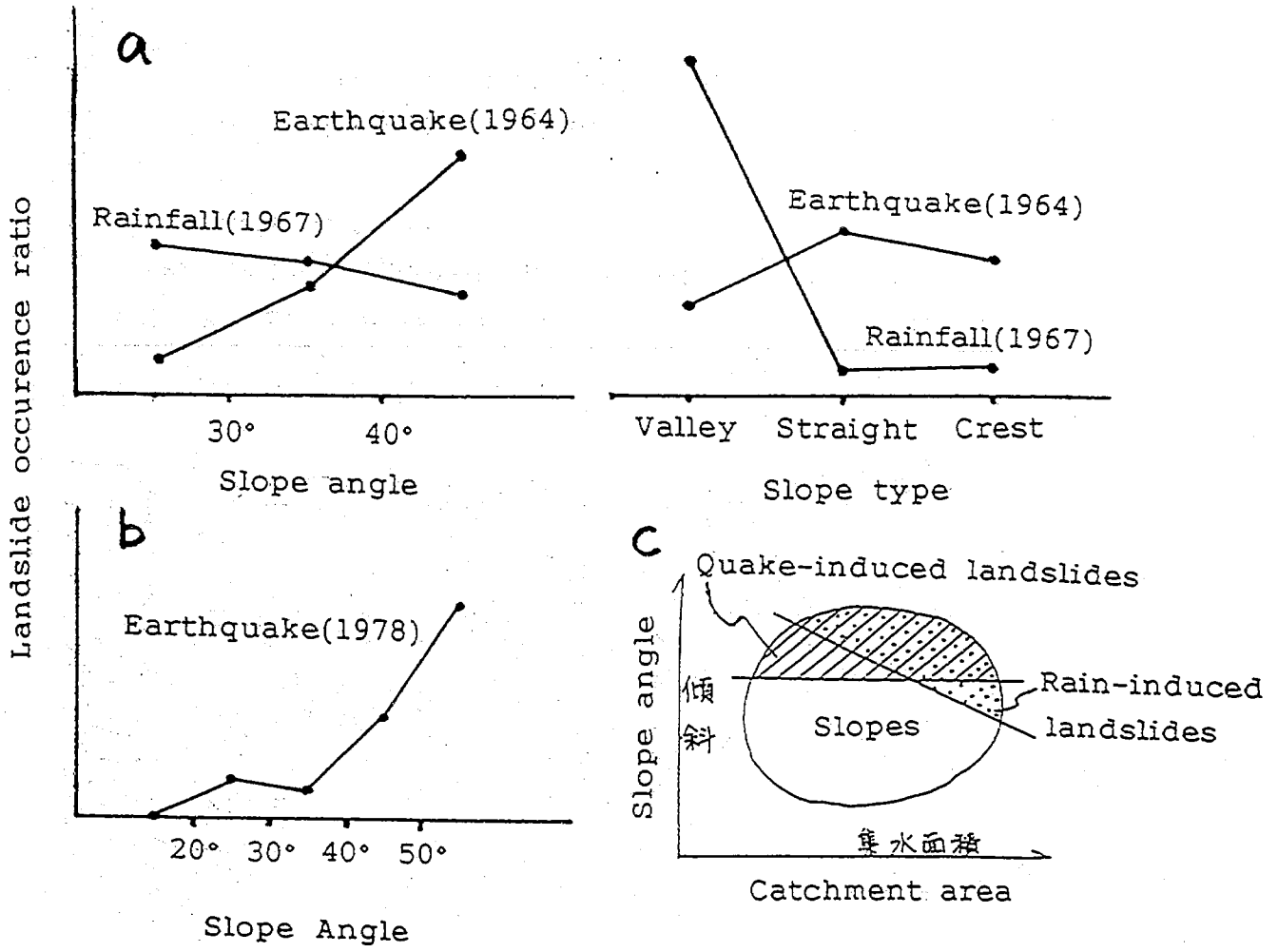


Fig.2 Site properties of quake-induced and rain-induced landslides (a:Modified from NIPPON DORO KYOKAI, 1991; b:Modified from GSI, 1979; c:TANIOKA & KANMAE, 1979)

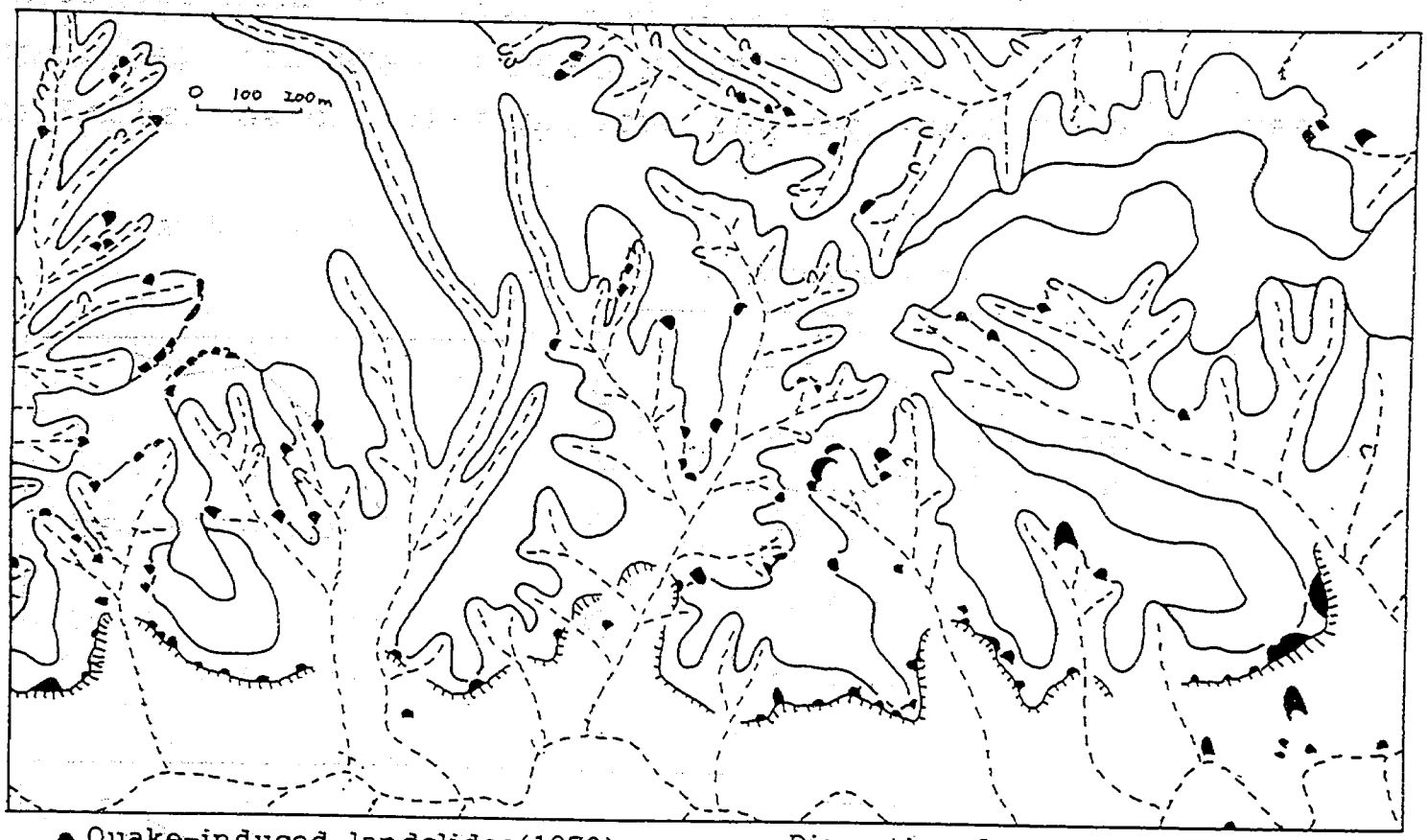


Fig.3 Distribution of landslides induced by an earthquake
(Modified from GSI, 1978)

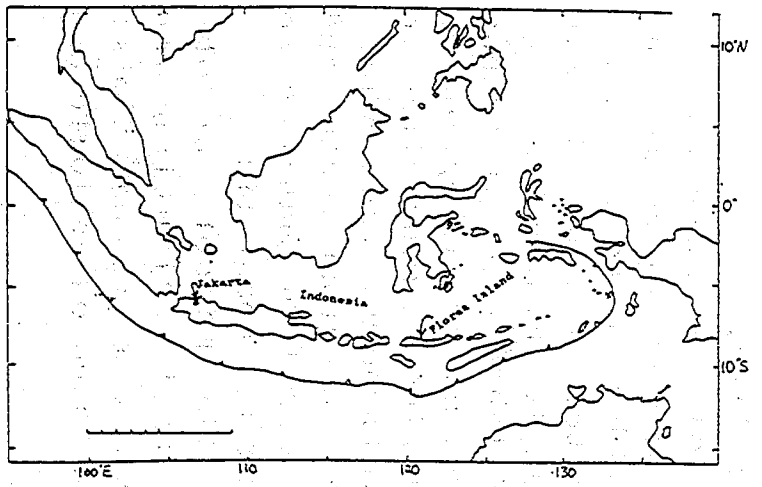


Fig.4-1 Index of Flores Island

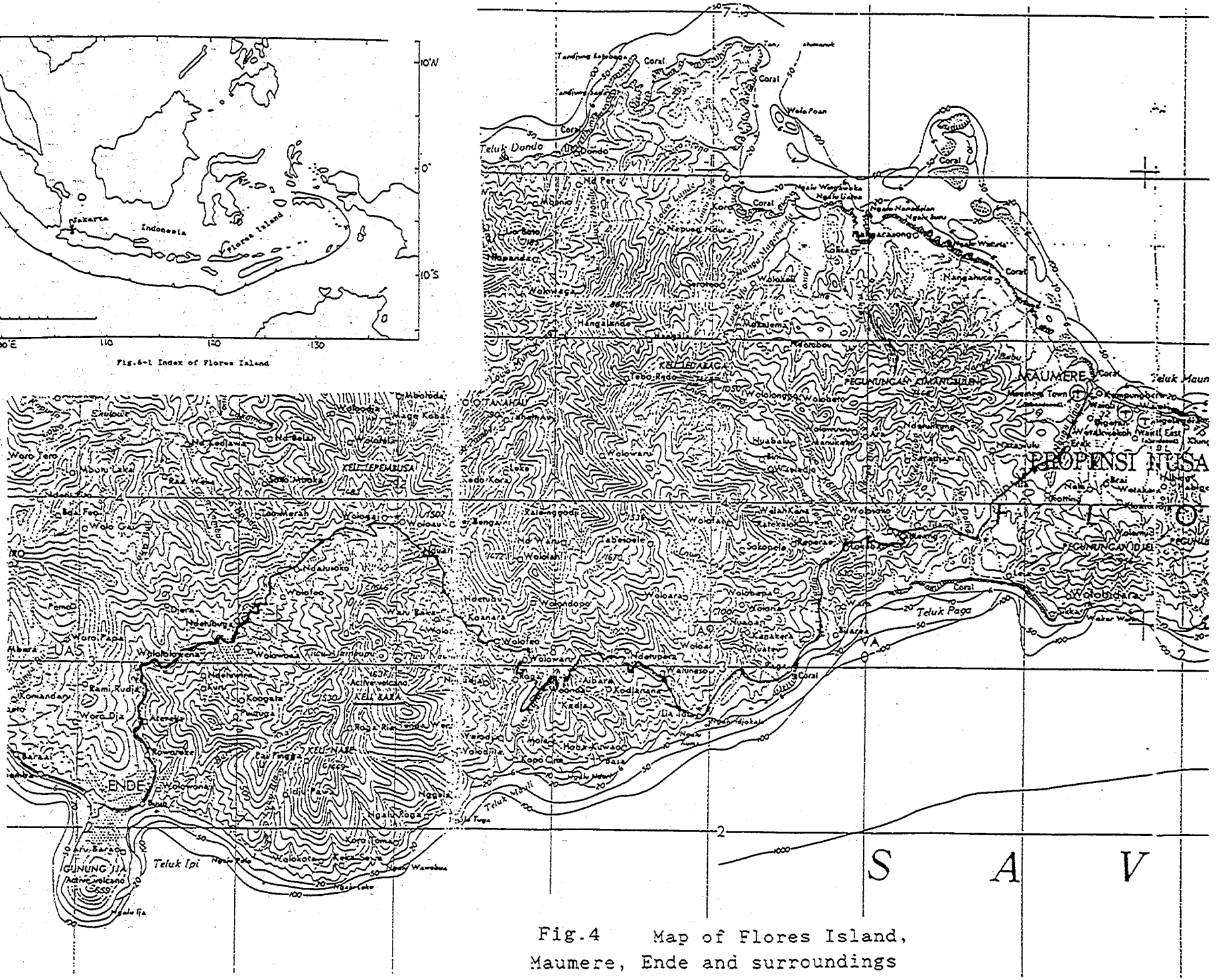


Fig.4 Map of Flores Island, Maumere, Ende and surroundings

gentle in gradient in general compared with valley-wall or coastal erosion slope. Therefore, the ratio of landsliding on the upper margin of valley-head slope is relatively low, while the ratio on the upper margin of valley-wall slope or coastal cliff is high (Fig.3). Especially slopes which has a young dissection front in the lowermost part are unstable and easy to collapse by seismic shaking. Ontake Landslide of 1984, one of the largest landslides in recent years, is an example (Nagaoka et.al., 1985; Nagaoka, 1987). It is also pointed out that valley-wall slopes tend to become such situation due to the downward or lateral river erosion, and moreover, similar condition sometimes results from artificial slope cuttings (GSI, 1978; GSI, 1979; Fig.3).

2. Flores Island

Flores Island is located in the eastern part of Indonesia. The island is located from 8~9° S, to 120~123° E. Many volcanoes are distributed beltlike in the central part of this long island. Raised and present coral reefs are distributed along the coastal area. Climate is Savanna.

Followings are evidently clear in combination with geomorphology, geological characteristeics, relief distribution, soil distribution and other natural landscapes with aerial photointerpretation.

Mountainous area consists of remarkably weathered rocks which can be easily dissected. River drainage basins have not been artificially changed remarkably. And rivers keep natural forms still in the present. It is clear that the research area is never safe from natural hazards.

3. Landslides

The term landslide includes various types of slope failures, which are landcreeps, landcollapses, big collapses of mountain body, roadside slope failures and others.

A big earthquake often causes many landslides including roadside slope failures. This time, the earthquake caused so many and various types of landslides in mountainous area. And supplementarily road side slope failures in hilly areas. Especially landslides were concentrated into the mountainous area from Maumere to Ende.

One of the authors researched the actual conditions of landslides in the area using a helicopter, because it was impossible for him to reach the sites of landslides via ground routes because of disruption of road traffics in many sites in the mountainous area where there was no detour route. And using a car from Maumere to Nebe along the coast line.

For the reason, he observed the distribution and characteristics of these phenomena based on geologic and

geomorphological approaches using oblique aerial photointerpretation taken by himself.

It was clarified that more than a few hundreds of sites of slope failures were caused. And road side slope failures were also caused in many sites from Maumere to Ende. Also the relationships between physical conditions and landslides in the mountainous area caused by the earthquake.

4. Roadside slope failures along the coast line from Maumere to the eastward route

Roadside slope failures were caused along the national route from Maumere to the eastward in several sites, and supplementarily in hilly area in the volcanic fans which is undulating near Maumere.

In these sites, road side slope failures were caused at the sites where slopes were cut or banked.

Geology of the sites consists of Tertiary limestone, which are originated from raised coral reefs and Quarternary volcanic fans including pyroclastic flows and volcanic ash. Through the whole area, it seems that geology is very weak.

In the route, there were many sites of cracks of the pavement. A few of land collapses formed deposit areas at each site which consists of volcanic pyroclastic flows and limestone. At one of them, it is evidently clear that land collapse was caused repeatedly in the past in the same site.

5. Landslides in Mountainous Area from Maumere to Ende

There is the national route from Ende to Maumere through the mountainous area. And the route was suspended in many points. The team for restoration work must work one site by one site from both sides of the route because there is no detour route to the inner damaged sites.

The researchers tried to clarify the characteristics of the whole area. Slope failures are several hundreds of sites including mountainous area. Seismic intensity is 5 to 6 in this area.

The followings were clarified. But these are the result based on preliminary observation from the helicopter. And further research must be done based on vertical aerial photographs.

This area consists of volcanic area, hilly land of summit recordance, which consists of land surface of the former erosion cycle and large scales of complex volcanic fans. Drainage patterns are pinnate type, dendritic type and radiation type in the mountainous area.

The earthquake caused many and various types of landslides. These were caused in the mountainous slopes and at roadsides slopes. These consist of two groups. One is newly failured ones. Another is repeated ones.



Photo 1
Road side collapse
in the hilly land

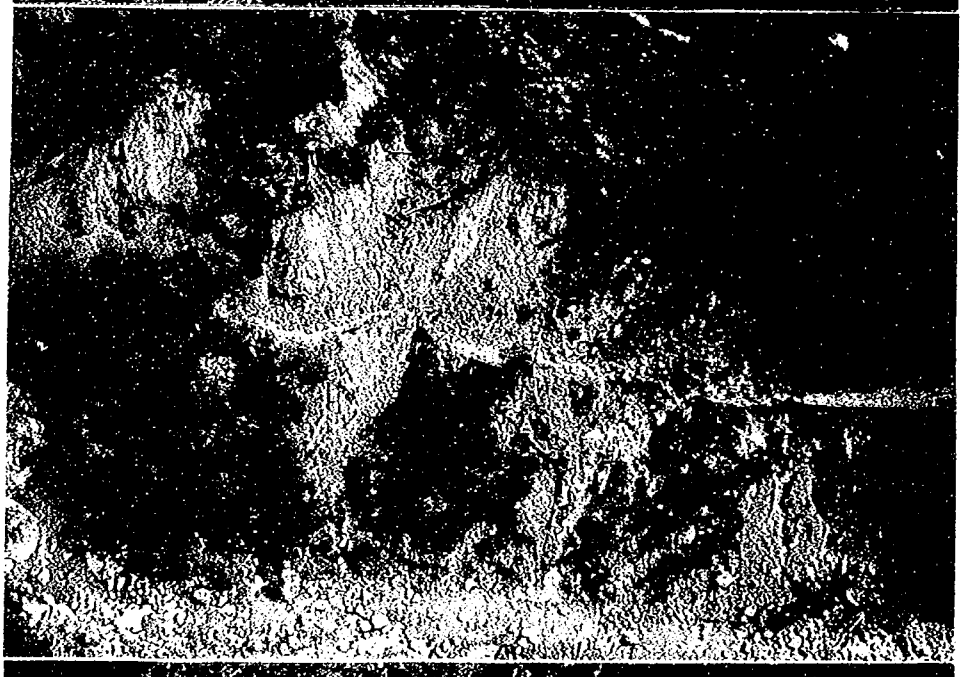


Photo 2
Road side collapse
beside the river

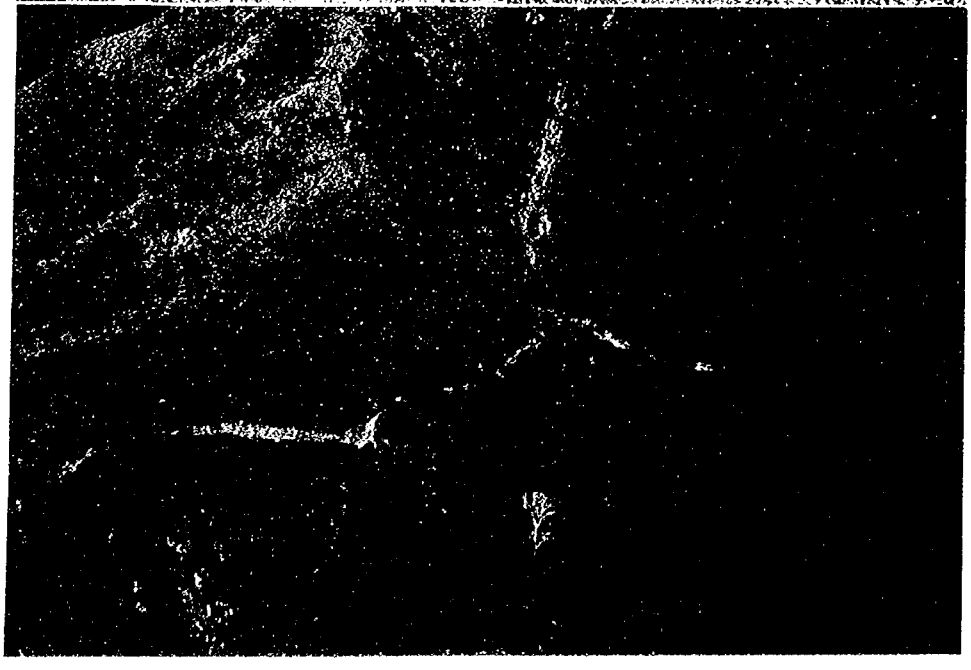


Photo 3
Intersection with
road 0 or 1st order
valley





Photo 4 and 5
Valley wall type slopes
Collapses were caused at upper break line.



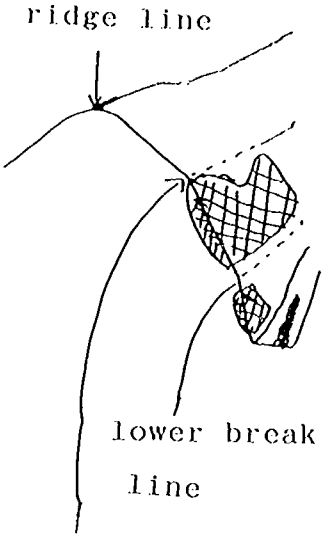


Photo 6
Valley wall slope
Collapses were caused at lower break line.

breka line=
dissection front

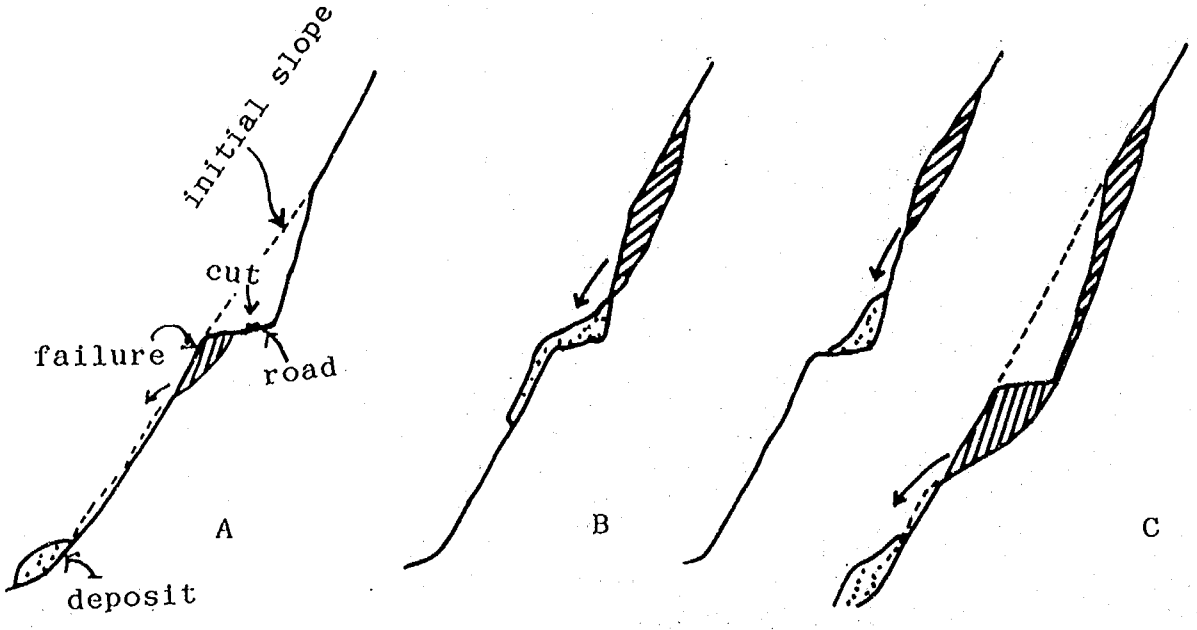


Fig.5 Types of road side slope failures

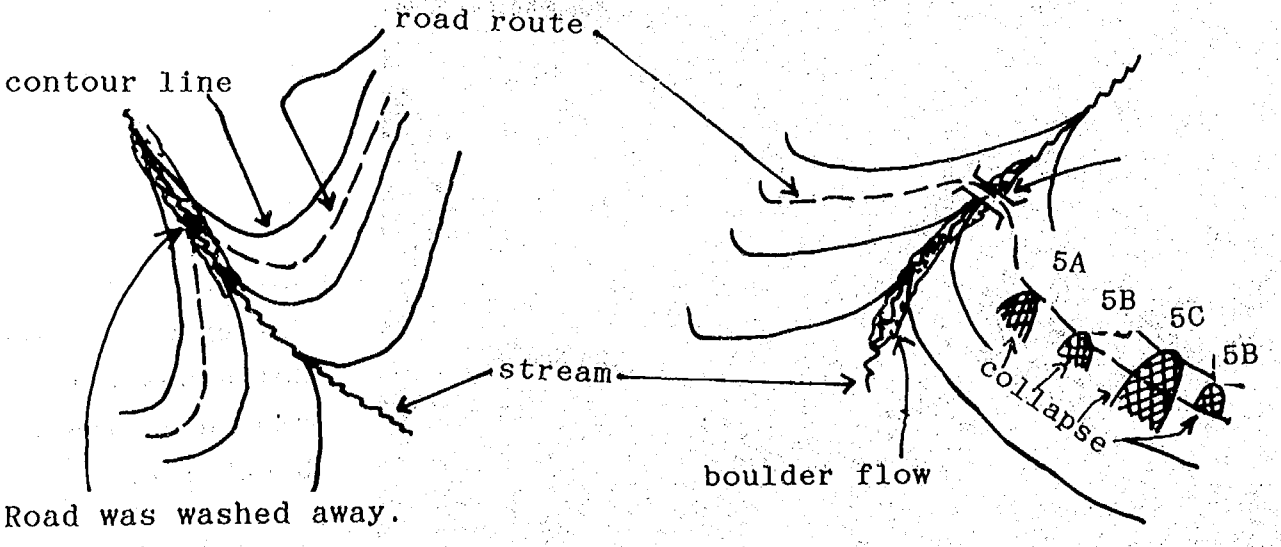


FIg.6 Explanation of road side slope failure

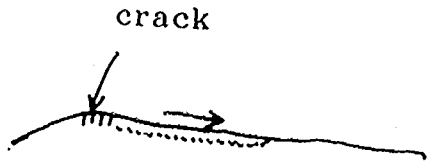


FIg.7 Creep

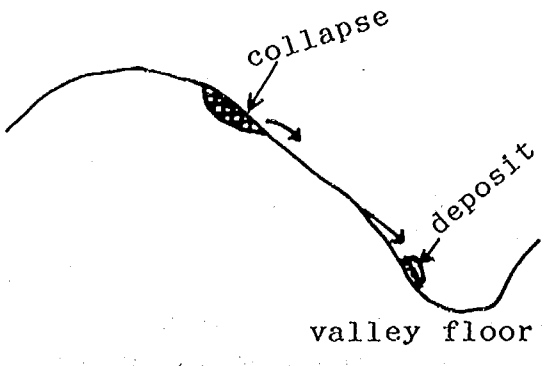


Fig.8 Single collapse

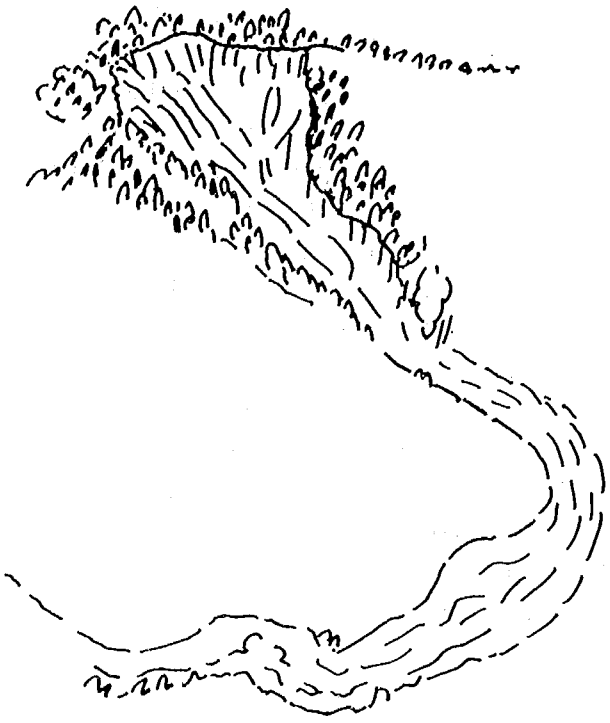


Fig.10 Deep and big collapse

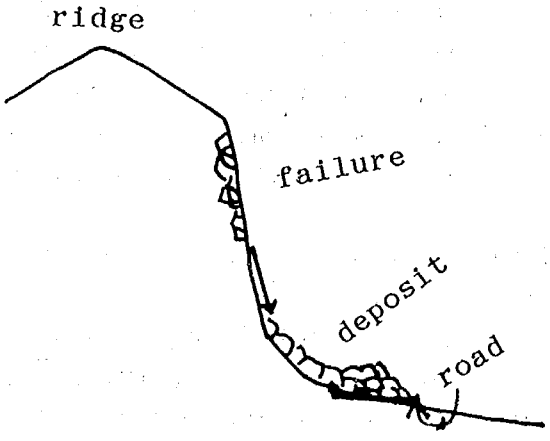


Fig.9 Rockwall failure

6. Characteristics of landslides and roadside failures

Landslides and roadside slope failures are classified into several groups as shown in the followings. (2) to (7) were caused without any relation to roads.:(1) roadside slope failures, (2) surface collapses caused just under the break line of ridges, single, (3) surface collapses caused just under the break line of ridge, complex slides or collapses with broad width, (4) large collapses which forms a long tail with deposit of reddish brown boulder flows, (5) small collapses with a head to tail, (6) landslides with many cracks at the top of collapses. (7) rock wall failures

(1) Roadside slope failures:

Many small slope failures were caused at roadsides from Maumere to Ende.

This type is classified into three.

1) Slope failures at mountain side of the road side,

2) Slope failures including mountain side of the roadside slope and valley side through the roadbed,

3) Slope failures at valley side of roadside slope.

And the type can be classified into another two groups.

4) Road side slopes, which were formed by cut and bank, were failured by the earthquake. Previous 1) to 3) are classified into this group.

5) Geomorphologically and geologically, slope failures are easily caused in specified sites. If the road crosses the site, naturally, the road is damaged. In the research area, there are many sites of this kind. Type 2) can be interpreted systematically.

Using aerial photointerpretation, it is evidently clear whether the collapsed sites are active or not in most cases.

(2)and (3) Surface collapses in mountain slopes:

Many landslides were caused in mountain slopes without any relations to roads. These were caused just under break lines of each ridge. Most of surfaces were collapsed, subsequently reddish soil came out in broad area in the mountinous area. And these types are repeated types of collapses. These are caused at steep slopes of pinnate river drainage systems in mountainous area with summit recordance.

(4)Deep and large scale of collapses:

Deep and large scales of collapses were caused in the surroundings of the volcano. There is an active volcano with three craters on the top. The surrounding area is covered by thick accumulative material supplied from the volcano. This type of collapse has a large head (collapsed area) and a long tail (transportation

route with deposit, and deposit area).

(5) A single collapses in a dendritic drainage system:

This type of landslides were caused in steep slopes on the mountain ridges. In the research area, 0-order streams in a dendritic(=tree) type. This type has a small head and very long and fine tail.

(6) Landcreeps:

This type of landslidese were caused at the top of a little gentle ridges. There are many cracks at the top of the landslides. This is a kind of landcreeps. Slope steak is available to monitor the behavior of this type of landslides whether the landslides may move soon or not.

(7) Rock wall failures:

Rock slopes were collapsed at the slopes of rocky mountains. Under the vertical cliffs, there are deposits rocks.

7. Conclusions

1)Page 2, 3 and 4 show that collapses in slopes are more easily caused by eathquake if the slope angle is steeper.

2)Fig.5 to 9 of page 10 and 11 show that quake-induced landslides were caused often at the break lines (dissection front) which consists of upper dissection front and artificial dissection front (road side cut slopes).

3)The idea of this report is based on geomorphological approach which is geomorphological mapping with idea of geomorphological process.

Already we have manuals for prediction of landslides which will be caused by heavy rainfalls. Through this study, it can be said that these manuals can be available for prediction of landslides which will be caused by earthquakes in future.

It can be said that so many and various types of landslides were caused by the earthquake. These were caused at or near break line (artificial, natural) in the valley-wall slopes or steep slopes. It is clear that these landslides were caused inspecified sites geomorphologically.

References:

K.Abe(1993):The leader's report of Indonesia earthquake diasters urgent relief specialists team. 1993.1.12. JICA.

I.Doi,N.Ukon(1983):Disasters caused in 1983 heavy rainfall in Shimane pref. Shinsabo vol.36, No.2, p39-43.

EGAWA,Y.(1979): Studies on the classification of landslides. Shin-Sabo, No.112, 10-18.

GEOGRAPHICAL SURVEYINSTITUTE (1978)! Disaster Situation Map of the Izu-Oshima Kinkai Earth quake of 1978"

GEOGRAPHICAL SURVEY INSTITUTE (1979):"Research Report on

the Disaster of the IzuOshima Kinkai Earthquake of 1978", 56p.

Geographic department and Photogrammetric department (1984): Big Mountain Failures Caused in 1984 Western part of Nagano Pref. Bul.of GSI.

HATANO, S. (1974): Collapse landforms (Part 2) Tsuchi-to-Kiso, Vol.22, No.11, 85-93.

Hokubu forestry office, Sanbu civil engineering office (1988):Disasters in the mountainous area caused by the Chibaken east off earthquake and measurement. Jisuberi. vol.24, No.4, p35-38.

Japan Expert Team as dipatched by the Japanese Government through Japan International Cooperation Agency (1992): Preliminary Report, Flores Island, Indonesia Earthquake of December 12,1992. --Preliminary Investigation and Recommendations --.

Japan Survey Engineering Society (Nihon Sokuryou Chousa Gijutu Kyoukai) (1984): Practical Research Method and Procedures of Landslides Using Aerial Photographs. Kajima Shuppankai.

Japan Road Society (Nihondouro kyoukai) (1988): References on Road Disasters Caused by Earthquake.

E.K.Kertapati, A.Soehaimi and A.Djuhanda(1992): Seismotectonic Map of Indonesia.

KUMAKI, Y. (1988): An attempt of multi-purpose geomopholo-gical mapping. Chiri,Vol.33, No.6, 34-39.

KUMAKI,Y. (1991): Mass movement. Journal of the Japan Society of Engineering Geology, Vol.32, 188-195.

KUMAKI,Y. and SUZUKI,M.(1982): A tentative plan on the land-form classification of the mountainous area. Jour.of the Japan Cartographers Association, Vol.30, No.2, 9--17.

NAGAOKA, M. (1987): Geomorphological characteristics and causal factors of the 1984-Ontake Landslide caused by the Naganoken-seibu Earthquake. Transactions, Japanese Geomorphological Union,Vol.8, 95-112.

NAGAOKA,M., HOSHINO,Y., TAKEI, Y.,ICHIKAWA,S,SAITOH,F.(1985) :Geomorphological characteristics and factors of the large-scale landslide and debris flow on the south slope of Ontake volcano caused by the Naganoken seibu Earthquake, 1984. The 17th Joint Meeting, Panel on Wind and Seismic Effects, UJNR.

NIPPON DORO KYOKAI (1991): Research Report on the Earthquake Disaster Measures of Roads, 219p.

Y.Nakayama (1988): Slope failures caused in Chiba pref. east off earthquake. Jisuberi. vol.24, No.4, p33-35.

M.Oya(1983):Application to slope failure disasters -- detailed geomorphological mapping based on aerial photointerpretaion-. by Ohmori. in "Method and application of geomorphological mapping". Kokon-shoin. Tokyo.

K.Seo(1983): On the boulder

flow disasters caused by the Nihon-kai-chubu earthquake (Japan Sea Middle Area Earthquake. Shinsabo. vol.36-No.2, p31-37

Specialists team of the Ministry of Construction (1992): References for JDR team 1992. 12 JICA Indonesia office

N.Suwarna,S. Santosa dan and S.Koesoemadinata(1989):Geological Map of the Ende Quadangle, East Nusa Tenggara.

PH.Tambunan, MH.Thamrin, Sutikno(1981): Peta Geologi Teknik Untuk Pengembangan Wilayah Maumere, Kabupaten Sikka, Flores Nusa Tenggara Timur.

TANIOKA,S. and KANMAE,W.(1979) :A comparison of geomorphic condition between earthquake-induced and rainfall-induced landslides. Abstracts of Papers Presented at the Annual Meeting of the Association of Japanese Geographers, Vol.16,78-79.

Touhoku District bureau of Construction (1986): '83 Japan sea middle area earthquake damage report.

N.Uehara, S.Aoyama, Imam Soeparm (1992):Actual conditions of earth- quake damages in Maumere of Flores Island, JDR reference report for discussion 1992.12.18.

Warren Hamilton(1979):Geology of Indonesia. Iwanami-koza. Chikyu kagaku 16 "Sekaino Chishitu (world geology)" p399-425. Iwanami shoten.

T.Yasue, 3 others(1983):On the mechanism of slope failures caused by earthquake. Doboku gijutu shiryou No.1948.

H.Yoshimatu and others (1990): Research on slope failures caused by the Chibaken east off earthquake. Dobokugijutu shiryou.No.2824.

Field observation on damages due to Flores Island Earthquake Tsunami of December 12, 1992

by

Takaaki UDA*

ABSTRACT

The tsunami damage in Indonesia is reported in this paper. This tsunami was generated by an earthquake of Magnitude 7.5 occured off the Flores Island in Indonesia at 13:29 on December 12 in 1992. Most characterisitic damages due to the tsunami were observed in Babi Island and Wuring area. Babi Island is of circular shape and its diameter is about 2.5km, and it islocated about 38km northeast of Maumere Port. Tsunami front invaded this island from south, where water depth is very deep since the coral reef does not exist. By this tsunami attack all buildings on this island were destroyed and 750 people out of 950 living were killed. Wuring is located about 2km northwest of Maumere Port. In this area vast amount of sea water invaded land from the shoreline with keeping strong energy compared with the wave overtopping at a rough wave condition. Everything including houses is destroyed and carried away in a mess, and 79 people were killed. This report is based on the investigation of International Urgent Relief Team including this author in response to the request of Indonesia Goverment.

KEYWORDS: tsunami damage; Flores Island; International Urgent Relief Team; field observation.

1. Introduction

Large tsunami was generated by an earthquake of Magnitude 7.5 occurred off the Flores Island in Indonesia at 13:29 on December 12 in 1992. Extensive coastline near Maumere on Flores Island was damaged by this tsunami. Particularly on Babi Island located about 10km east of Besar island, 750 people were killed out of total population (950) of the village and the village was totally destroyed by this tsunami. The author had an opportunity to visit Flores Island right after the earthquake in order to conduct the urgent investigation of tsunami damages for a member of International Urgent Relief Team (headed by Prof. K. Abe in Earthquake Res. Inst., Univ. of Tokyo) in response to the request of Indonesian Government. This report summarizes the results of the field observation of tsunami inundation height at several locations, tsunami damages in Babi Island, Wuring area and Maumere Port, where severe damages were observed. Furthermore, some considerations on the causes of damage will be made.

2. Geographical Features of the Damaged Area

The Flores Island, damaged by an earthquake, is located about 1300 km east of the center of Java Island and about 680 km east of Bali Island (Fig.1). Due to the analysis of the worldwide seismic observation data collected by United States Geological Survey the epicenter of the earthquake is located in Lat. 8.482°S and Long. 121.930°E, and the depth is 36 km. The scale of the earthquake is Maginitude 7.5. The center of the earthquake is located at about 40 km NNW of Maumere in Flores Island.

3. Investigation of Tsunami Inundation Height

Field observation on tsunami inundation height was carried out between Dec.23 and Dec.25 along the coastline of Flores Island as well as the Babi Island. The inundation height was measured by a staff and a handlevel. Since the reference level of the ground was not known, vertical height of the inundation was measured with reference to the sea level at the measuring time. After the field investigation, the inundation height above the mean sea level at Maumere Port was calculated based on the astronomical tide at Maumere Port predicted by JODC of the Maritime Safety Agency, Ministry of Transport in Japan.

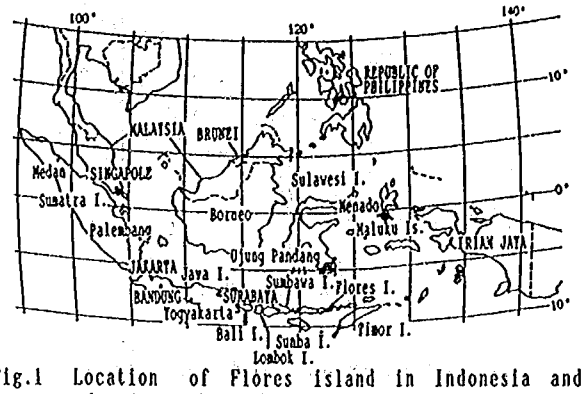
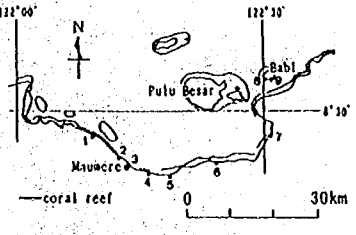


Fig.1 Location of Flores Island in Indonesia and epicenter of earthquake.

The mark of the tsunami inundation was clearly read on the outside wall of houses at many locations in Flores Island. On the other hand, on Babi Island the inundation height was measured based upon the height where floating debris attached to the trees, since all houses were destroyed by tsunami.

Figure 2 shows the location map of the observation sites and the measured inundation height in meter. Maximum inundation height of 2.45m was measured at Wuring area in Flores Island.



Location	Inundation height(m)
① Nangahure	2.28
② Paring	2.45
③ Maumere Port	2.25
④ Kajoli	2.28
⑤(east of)Kalpore	1.66
⑥ Kalgate	2.22
⑦ Nangobrok	1.93
⑧ (west)Babi	3.66,3.48,3.28 2.88,3.26
⑨ (east)Babi	3.68,3.51,3.19

Fig.2 Location map around Maumere and tsunami inundation height.

Tsunami height decreases from this area to east because of the sheltering effect of Besar island and to west due to the existence of the offshore coral reef as shown in Fig.3. In Babi island maximum inundation height was about 3.7m, and it is about 1.2m larger than that at Wuring area.

* Dr. Eng., Head, Coastal Eng. Div., Public Works Res. Inst., Ministry of Construction, Ibaraki 305 Japan.

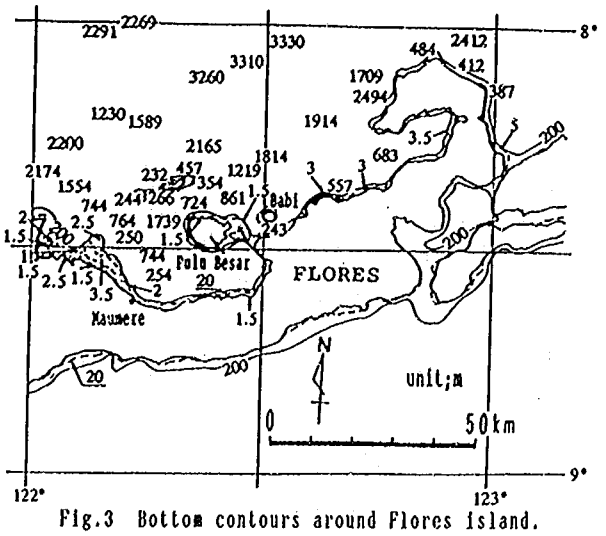


Fig.3 Bottom contours around Flores island.

4. Tsunami Damages

Although tsunami brought many casualties in widespread area, most characteristic damages due to tsunami can be observed in Babi island and Wuring area. In Babi island 750 people died out of 950 living in this small island and only 200 were able to escape from tsunami. Similarly, death toll of 79 was confirmed at Wuring area. In the following tsunami damages at two locations are discussed as well as the case in Maumere Port.

(1) Maumere Port

Port facilities were severely destroyed not only by tsunami but also the liquefaction damage of the ground associated with the earthquake. Photo 1 shows a ship raised over the quay in Maumere Port.

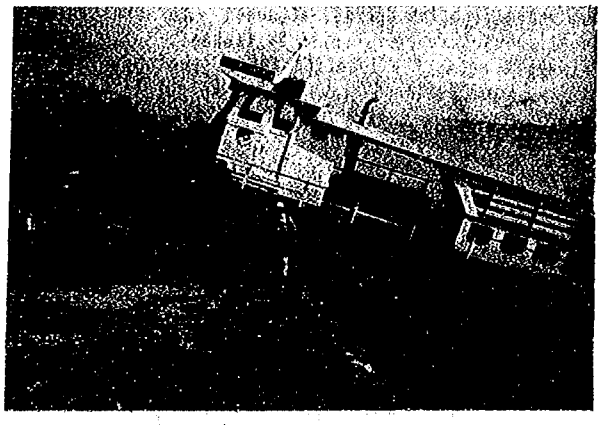


Photo 1 A ship raised over the quay in Maumere Port.

The height of the quay wall at this time was about 1.5m above the sea level. Taking account of the draft of this boat, tsunami wave height at this location is considered to be about 1m over the present ground level. At a location east of this point, the quay was destroyed by both the earthquake and tsunami as shown in Photo 2, and a truck was carried away toward the tip of the pier by the returning current of tsunami. Photo 3 shows the inundation height left at the outside wall of the house. The height pointed out by the right hand shows the inundation level and maximum depth at the side wall was about 50cm.

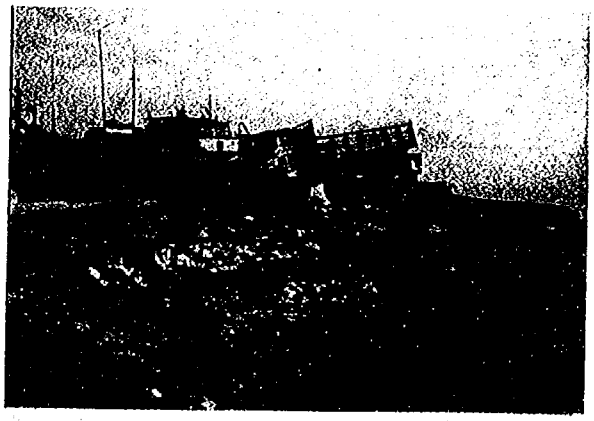


Photo 2 Damaged pier of Maumere Port and a truck carried by tsunami.



Photo 3 Inundation height in Maumere Port.

(2)Wuring area

Wuring is located about 2km northwest of Maumere Port. Tsunami can be characterized by the phenomena that vast amount of sea water invade land from the shoreline with keeping strong energy compared with the wave overtopping at a rough wave condition. This means that the damaged area due to tsunami is totally different from that by the flooding with gradual increase of water level. Everything including houses is destroyed and carried away in a mess. Furthermore near the fishery port fishing boats floating with tsunami often corride with the houses and thus enlarge the destruction of houses. Photo 4 shows the disastrous situation of Wuring area. It is seen from this picture that vast amount of debris were scattered and a fishing boat was also carried. Photo 5 shows the situation at a location further seaward from Photo 4. Here many houses of raised floor were destroyed and many boats were scattered on land. In photo 4 some buildings were left since the position was located considerably landward from the shoreline, but at the location shown in Photo 5 houses were further destroyed. Photo 6 shows the disastrous situation at further seaward location and here the houses were destroyed much severely. At Wuring area many houses of raised floor had been built and almost all these houses were destroyed. In photo 6 the inundation height can be clearly read at the white wall of the building, of which ground level is about 1m, and

It is seen that the height between the mark and the present ground level i s 1.6m. This means that tsunami wave of the height of a man ran up in this area. Similarly Photo 7 shows the inundation height at Wuring area. Since this point is located landward of the location shown in Photo 8 and the ground elevation of the house is higher, the inundation height read from the glass window is about 0.8m, which is lower than that in Photo 8.



Photo 4 Tsunami disaster at Wuring area (landward side from the center of the village).



Photo 5 Tsunami disaster at Wuring area(Center of the village).



Photo 6 Tsunami disaster at Wuring area (Seaward side from the center of the village).



Photo 7 Inundation height at Wuring area (1).



Photo 8 Inundation height at Wuring area (2).

In this area final death toll was 79. The causes of tsunami disaster at Wuring area can be summarized as follows:

1) This area is located outside of the shelter zone by Besar island.
2) It was not protected by shallow coral reef as the coastline west of this location.
3) This village is located at the western shore of U-shaped bay, where generally tsunami height increases by Green's effect.
4) Many houses of raised floor were built in the low land.

(3)Babi Island Babi island is located about 38km northeast of Maumere Port. This island is of circular shape and its diameter is about 2.5km. Coral reef well develops around this small island as shown in Fig.4.

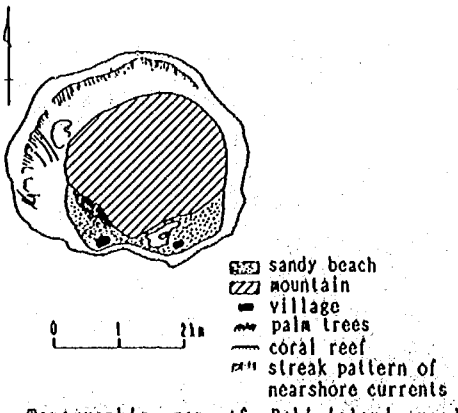


Fig.4 Topographic map of Babi island read from aerial photograph.

Off the north shore of this island wide reef develops due to the incidence of wind waves, whereas it is narrow off the south shore. In addition, two large cuspate forelands develop on the south side of the island. These geomorphological features imply that the location receiving the most severe action by wind waves are north and northwest shores, and two cuspate forelands were formed by the depositional effect of the coral debris produced near the reef edge by the action of breaking wave and carried by the longshore currents around this island. Accordingly, the foreshore and backshore height of the sandy beach in two cuspate forelands are of the order(1-1.5m) of the run-up height of diffracted waves in the leeside of the island. Tsunami front invaded these sandy beaches from south, where water depth is very deep since the coral reef does not exist. The direction of the tsunami movement can be confirmed to be from south to north by the following observations: 1)Debris of the houses were scattered in the palm trees north of the original positions as shown in Fig.4. 2)Palm trees were fallen down by tsunami with their roots heading south. 3)An eyewitness from this disaster pointed out that the tsunami came form south. By this tsunami attack all buildings of this village were destroyed. Photo 9 shows the oblique picture of the village devastated by the tsunami taken in the southwest direction from the middle of the mountain. Since tsunami attacked the village from south, debris of houses were carried northward and scattered inside the palm trees. For instance, from Photo 10 showing the situation inside the palm trees, it is observed that vast amount of debris were scattered. The village located on the sandy beach was totally demolished. Photo 11 shows the concrete basement of the destroyed school building.

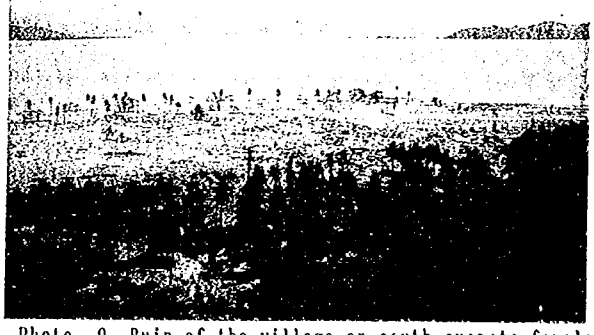


Photo 9 Ruin of the village on south cuspate foreland

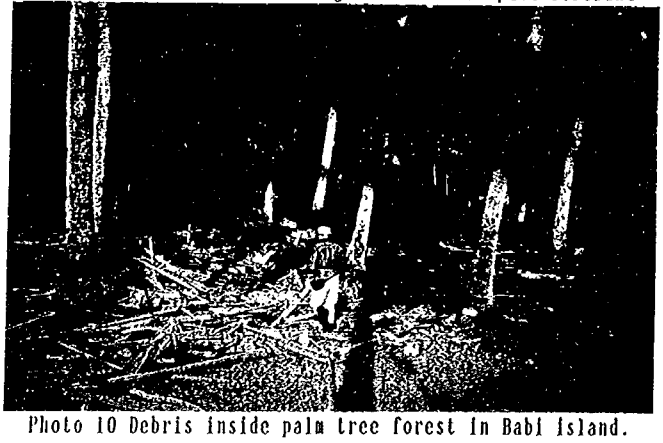


Photo 10 Debris inside palm tree forest in Babi island.



Photo 11 Damaged school buildings.

In the observation of the inundation height of tsunami on Babi island, the height was read from the mark where some debris were attached to the trees (Photo 12). It was difficult to read the inundation mark from the side wall of the houses because every house had been totally destroyed. Since the pole is fixed 1m above the ground level, the upper level of the attached debris becomes about 2.5m. The ground level of this sandy beach is approximately equal to about 1m, and this means that the inundation height with reference to the sea level attains to about 3.5m. One of the characteristics found in this field observation is that many palm trees fell down with their heads directing north or toward the center of the island as shown in Photo 13.



Photo 12 Inundation height on foreshore of Babi island.



Photo 13 A palm tree being collapsed by tsunami and heading north on the south shore of Bali island.

This implys that palm trees were fallen down by the wave force of tsunami attacked from south. As mentioned above, wide reef develops on the north shore of Babi island with poor development of coral reef on the south shore. In addition to this the bottom slope of the south shore is very steep. Since the cuspate foreland protrudes and wind waves incident from north are well protected by the island itself, the leeside of the island has been used for the anchoring harbor. However, since the wave length of tsunami is much longer than that of wind waves and therefore tsunami energy can reach the lee side of the relatively small scale island, the safety zone against wind waves does not necessarily mean the same zone against tsunami. If shore protection facilities had been built around the village on the sandy shore, it is considered that tsunami disaster did not take place. In fact, the village was totally devastated because of the lack of the shore protection facilities. This is the same condition of the complete destruction of Taro village in Iwate Prefecture in Japan due to the Sanriku Tsunami occured in 1933. Above mentioned three examples can be summarized as follows. Generally speaking,tsunami damages are not large in the coastal zone of relatively high ground elevation. In the case of the Babi island, the ground elevation was low as 1-1.5m, originally formed by the depositional effect of wind waves on the foreshore, so that large damages were observed. Similarly, at Wuring area many houses were built on the ground elevation lower than 1m. This again caused severe damages.

5. Some Considerations

After the tsunami all inhabitants on Babi island evacuated to Flores island, and no one lives on this island at present. However the number of the people returning to the island will increase with time, since many people on this island have been living by fishery. And in the long-term a village will be formed again. Thus the generation of tsunami causes the same disaster on this island. In order to solve this problem without the abandonment of this island, it is necessary to build coastal dike along the shoreline. The construtlon cost of coastal protection facilities against tsunami such as a coastal dike is usually considerably expensive. In addition, the probability of the reoccurrence of the earthquake tsunami is considered to be very low. Furthermore, in Indonesia there are so many islands having the same natural conditions as Bali island and this country's national economy is in developing state. Taking these points into account, it may be difficult to build coastal protection facilities in a small island of Babi. From this point of view, many problems were remained to be solved regarding future planning for preventive works against tsunami at the disscussion with the Indonesian Government. Further consideration is necessary to solve these problems.

6. Concluding Remarks

Urgent investigation of tsunami disaster was made in Flores island in Indonesia. Since the duration of the field observation was limited to be only three days, the measurement of tsunami height at sufficiently many points was impossible, and therefore, tsunami nundation height in rather narrow coastal zone was reported in this paper. Fortunately a study team of Ministry of Education in Japan further investigated tsunami inundation height in the more extensive areas and thus detailed information can be obtained by the report to be published later. The author would like to thank JODC of the Maritime Safety Agency, Ministry of Transport in Japan for the permission of utilizing the predicted tide level in Maumere Port. In addition, he would like to thank Associate Prof. Yoshinobu Tsuji of Earthquake Res. Inst. of Univ. of Tokyo for many discussions on the prediction of tide level and the cause of the tsunami.

INFRASTRUCTURES DAMAGE BY CAIRO, EGYPT, EARTHQUAKE OF OCTOBER 1992 AND FLORES ISLAND, INDONESIA, EARTHQUAKE OF DECEMBER 1992

by Tomomitsu FUJII[1] and Kazuhiko KAWASHIMA[2]

ABSTRACTS

Presented in this paper is the damage of infrastructures caused by the Cairo, Egypt Earthquake of October 12, 1992 and the Flores Island, Indonesia Earthquake of December 12, 1992. Ground motion estimation, damage feature, liquefaction, tsunami and earthquake preparedness are described. Importance of training and education as well as damage information dissemination are also presented.

KEY WORDS : Cairo Earthquake, Flores Island Earthquake, Ground Motion, Damage Feature, Liquefaction, Tsunami, Earthquake Preparedness

1 INTRODUCTION

Although earthquake preparedness is extremely important for preventing damages due to an earthquake, it is generally quite difficult in the areas where frequency of occurrence of earthquakes is low. In such areas, the accumulation of scientific knowledge on an earthquake and earthquake damage has not been made, and this sometimes amplifies the damage.

In late 1992, the Cairo, Egypt, Earthquake and Flores Island, Indonesia, Earthquake occurred. For cooperating disaster mitigation and restoration, the Japan International Cooperation Agency dispatched the Japan Disaster Relief Team to Egypt and Indonesia. The mission dispatched to Egypt was consisted of 9 members and was headed by Professor Tsuneo Okada, Institute of Industrial Science of University of Tokyo. The mission dispatched to Indonesia included 8 members and was headed by Professor Katsuyuki Abe, Earthquake Research Institute of University of Tokyo. Because two authors of this paper joined into the two missions, summary of the damage[1,2] and lessons learned from the two earthquakes are presented.

2 CAIRO, Egypt, EARTHQUAKE

2.1 Outline of the Cairo Earthquake

An earthquake with moment magnitude of 5.8 occurred at 15:09 (local time) on October 12, 1992 at about 30 km south-west of Cairo city as shown in Fig. 1. Because Egypt has long history, the data on historical earthquakes can be traced as old as B.C. 2,800[3]. Fig. 2 shows the epicenters of the earthquakes which occurred around Cairo. The epicenters of historical earthquakes which were determined from old documents are included in Fig. 2. The latest earthquake which hit the Cairo area occurred on August 7, 1847 at Faiyum[4]. About 185 persons were killed by this earthquake. There have been no disastrous earthquakes around Cairo for about 150 years till the Cairo Earthquake of October 12, 1992.

Fig. 3 shows the accumulated number of earthquake vs. earthquake magnitude within 300 km around the north Cairo from 1952 to 1985[5]. It is seen from Fig. 3 that the averaged annual number of an earthquake with magnitude of 6 or larger is 0.05. The maximum credible earthquake is said about 6.8. On the other hand, Fig. 4 shows the same relation within 300 km around the Tokyo Bay, Japan from January 1885 to December 1979[6]. The averaged annual number of an earthquake with magnitude of 6 or larger is about 3. This means that the frequency of occurrence of an earthquake in Egypt is about 1/69 of that in Tokyo, Japan. As can be anticipated from this evidence, it has been believed by public that no earthquake occurs in Egypt.

The main damage by the Cairo Earthquake is summarized as shown in Table 1. The casualties and injured were mostly developed in Cairo, Giza and Faiyum. Almost 200 students were killed in panicked stampede rather than by the collapse of school buildings. 73 peoples were killed at Heliopolis by a collapse of an apartment building in which number of story was illegally increased from 8 to 14. Photos 1 and 2 show the damaged building soon after the collapse and the foundation after debris was removed. Because no evidence showing failure of the foundation and surrounding soils were seen, it is considered that the damage was developed due to inadequate strength of the building.

Fire by the earthquake did not fortunately occurred.

Damage mostly occurred at old un-reinforced masonry and adobe housings as shown in Photos 3 and 4. Damage to new buildings was generally small. Damage to infrastructures was also limited.

1) Director of Earthquake Disaster Countermeasures Division, Disaster Prevention Bureau, National Land Agency
2) Head of Earthquake Engineering Division, Earthquake Disaster Prevention Department, Public Works Research Institute, Ministry of Construction

2.2 Ground Motion and Soil Condition

Because no strong motion accelerographs were installed in the vicinity of Cairo and the epicentral area, strong motion records were not obtained. Because evaluation of the intensity of ground shaking at the damaged area is difficult based on the instrumental records, it was made based on the empirical attenuation equation.

Based on the analysis of 394 components of free field strong motion records, the peak ground acceleration may be estimated as[7] :

$$a_{max} = 233 \times 10^{0.313M} \times (R + 30)^{-1.218} \quad (1)$$

where

a_{max} : peak ground acceleration (cm/sec2)
M : earthquake magnitude
R : epicentral distance (km)

Assuming the surface magnitude of 5.3, the attenuation of peak ground acceleration is predicted by Eq.(1) as shown in Fig. 5. Because the epicentral distance is ranging from 30 km to 40 km at Giza and Cairo area, respectively, the peak ground acceleration a_{max} predicted by Eq. (1) is about 70 cm/sec^2 at Giza and 60 cm/sec^2 at Cairo. These values provide the preliminary insight for the ground acceleration developed at the damaged areas. It should be however noted that Eq.(1) gives the mean value of the measured acceleration, and has a large scatter around the mean value. When one considers one standard deviation from the mean value, the value predicted by Eq. (1) has to be multiplied by 1.7 and 1/1.7.

Fig. 6 shows a soil condition at Cairo city across the Nile River. Cairo city is located on the river terrace and soft alluvial deposits along the river.

2.3 Seismic Codes

Because of low frequency of occurrence of an earthquake, no seismic design seems to be presently made in Egypt for infrastructures. However design and construction of infrastructures are apparently better than those for ordinary buildings which suffered destructive damages due the the earthquake.

An example of the better design and construction is seen for road bridges. Comprehensive descriptions on loads, materials and allowable stress are specified in the Egyptian Code of Practice for Steel Constructions and Bridges (Ministerial Decree, No. 451-1989) and the Egyptian Code of Practice for Soil Mechanics and Foundation (Part 1 - Part 10, Ministerial Decree, No. 451-1989). Descriptions on seismic effects are few, and only some descriptions on soil liquefaction are provided in the Egyptian Code of Practice for Foundations Subjected to Vibrations and Dynamic Loads (Ministerial Decree, No. 449-1991). The treatment of the liquefied soil in design is not precisely stipulated.

However according to the General Authority of Roads and Bridges, various considerations which are effective for increasing seismic safety of bridges have been implemented as :

1) In-situ loading test is generally made for at least two piles per site for studying the load bearing capacity in vertical direction. Piles are subjected to vertical loading up to 2 times and 3 times of the design loading for the bearing piles and the friction piles, respectively, so as to confirm the yielding load. For example, a pile as shown in Photo 5 was subjected to 480 tf, which is twice as large as the design loading, at Faraskour Bridge.

2) Soils up to 8 m below the river bottom is generally disregarded in design of pile foundations as a design measure against scouring effect. Although the effect of soil liquefaction is not considered in design, such consideration is effective for increasing lateral stiffness of piles.

2.4 Damage of Roads and Bridges

Damage survey was made for Zamalek Overcrossing (Photo 6), Beni Suef Bridge, Faraskour Bridge (Photo 7) and Dessuk Bridge. No seismic damage was observed at those bridges. As was described in 2.3, design and construction seem conservative although seismic effects are not considered.

2.5 Damage of Lifelines

A visit to Rod El Farag Water Plant, Greater Cairo Water Supply Authority was made. No serious damage so as to affect the water supply was not developed by the earthquake. Only minor damage was developed at :

a) Cracks at masonry wall of a finished water pump station.
b) Increase of water leakage at a duct in the filters.
c) Offset and dislocation of a concrete wall of the clarifier (Photo 8).

2.6 Soil Liquefaction

Soil liquefaction was observed at Barmasht - El Aiyat area. Several sand blow holes with a diameter as large as 4 m and a depth of 2 m were developed as shown in Photo 9. The sand spread over a paddy field. Fig. 7 shows the grain size accumulation curve of the sand. The average grain size D_{50} is 0.17 mm - 0.25 mm.

Although soil boring data at the site is not available, it is considered from the site inspection that the soil consists of saturated loose fine sand overlaid by cohesive clay with thickness of 1 - 2 m. Because the cohesive soil prevented the blow-up of water associated with the increase of pore-water pressure of sandy layer, the diameter of sand blow became quite large.

According to the eyewitnesses, the water and sand blew up as high as 3 m, and it continued about 45 minutes.

Based on the past experiences, it is known that the soil liquefaction tends to be developed in the area with a radius R from the epicenter as[8]

$$\log R = 0.77 M - 3.6 \quad (2)$$

where

R : radius (epicentral distance, km)

M : earthquake magnitude

Fig. 8 shows the relation predicted by Eq. (2) as well as the observed data at Barmasht - El Alyat (M = 5.3, R = 19 km). It is clearly seen that during the Cairo Earthquake the liquefaction occurred far from the threshold predicted by Eq. (2). This may be attributed to the fact that the sand at Barmasht area is extremely loose.

2.7 Restoration and Education on Earthquake

The Civil Defense Department, Ministry of Interior is responsible for rescuing victims under collapsed buildings by various disasters such as an earthquake and fire. The equipments in the department seem to be well maintained and the moral of the rescue team is excellent. Training for rescuing victims have been occasionally made.

Education on disaster to the public is also made in a room of the Public Relations Section of the Department, using video equipment. This kind of rooms are located in some other places. Even before the Cairo Earthquake, education and drill were made to the public in consideration of their importance.

However, panic of citizens in fear of the earthquake unfortunately occurred widely in Cairo and its vicinity. Especially, at scholar students panicked and many of them were injured or pressed to death when they tried to evacuate from the school buildings. For preventing such panic, public education and information dissemination in proper way are essential. Taking into account the evidence of the earthquake that affected variety of citizens in wide area, earthquake preparedness is very important not only at the central government but at local governments, schools and other agencies.

Because strength of buildings is not the same, it can not be compared in general sense, but it is educated in Japan through daily training not to evacuate confusedly from school buildings to outside but to keep staying underneath stable desks when an earthquake occurs. Because it is very important to respond without confusion against an earthquake, educations and training are repeatedly made through various opportunities and methods including dissemination of information by pamphlets which can be easily understood by the public. And also because the Great Kanto Earthquake which caused more than 140, 000 victims occurred on September 1, 1923, this day is designated as a special day for Disaster Prevention. Various trainings are made nation-widely on the Disaster Prevention Day so that citizens can have experience and training against disasters.

A number of persons who lost their housings stayed in tents provided by the Government as shown in Photo 10. At the area where aid could not be provided, people lived in a private tent as shown in Photo 11. Many people lived in tents not only because they lost their housing but because they had strong feared of the occurrence of aftershocks.

Egyptian people had been in fear of aftershocks for long time since October 12. Every time when a small aftershock occurred many people evacuated from housings, and some of them stayed outside in fear of possible collapse of the housings.

Furthermore the Japan Disaster Relief Team members had many inquiries from individuals and mass-media on the potential occurrence of a next large earthquake. Some peoples were in fear of occurrence of volcanic eruption.

The NRIAG (National Research Institute of Astronomy and Geophysics) immediately determined, on the basis of available seismic data in Helwan Station, the preliminary epicenter of the mainshock and sent this information to the Ministry of Scientific Research. And the NRIAG reports the number of aftershock twice a day at 9:30 and 15:30 to the Ministry. The earthquake information on the mainshock was officially announced on October 14.

There is no section responsible for releasing earthquake information to press and citizens in NRIAG nor in the Egyptian Government Offices. Thus, seismologists and researchers in NRIAG are faced to respond to various inquiries from press and citizens.

When a large earthquake occurs, it is extremely important to provide fast and accurate information about the earthquake not only to

administrative organizations but to public for mitigating earthquake disaster. In Japan, the Japan Meteorological Agency is responsible for this task, and reliability of the Agency is well recognized.

Timely and proper dissemination of the information on evaluation of future seismic activities based on scientific basis is very important together with public education. However, improvident information dissemination, to the public without enough scientific knowledge on the earthquake activity, based only on pure seismological point of view may cause panic. On the other hand, lack of information causes unnecessary fear among the public. It is therefore important to disseminate the earthquake information so that the public easily understands it and so that it is consistent with various aid activities. It is essentially important to disseminate scientific information on an earthquake, volcanic eruption and disasters before disasters occur.

3 FLORES ISLAND, INDONESIA, EARTHQUAKE

3.1 Outline of the Flores Island Earthquake

An earthquake with surface magnitude of 7.5 occurred at 13:29 (local time) on December 12, 1992 at north coast of the Flores Island, Indonesia as shown in Figs. 9 and 10. The epicenter is 8.48 ° S and 121.93° E.

The Flores Island has the length of about 360 km and width of 12 - 70 km. There are 19 volcanoes in the island. The Flores Island, which is a part of Nusatenggara Timur Province, is of Manggarai, Ngade, Ende, Sikka Flores Timur Regency.

Table 2 shows the human and building damage. Major damage was developed at Sikka, Ende, Ngada and Flores Timur Regency. Number of death was 2,080, and about 70 % of the total death concentrated at Sikka Regency. Damage was especially destructive at Maumere city which is on the alluvial fan deposit formed by the River Kalimati.

Tsunami damage was destructive, and occurred extensively over at least 100 km along the cost of Flores Sea. About 50 % of the death was caused by tsunami. Major tsunami damage was developed at Babi Island and Wuring area near Maumere.

Building damage concentrated on unreinforced masonry buildings as shown in Photo 12.

3.2 Ground Motion

Although it is said that 57 strong motion accelerographs are installed in Indonesia, no information regarding the location of the accelerographs and the strong motion records by the earthquake was obtained.

Assuming that the earthquake magnitude M of 7.5, the peak ground acceleration predicted by Eq. (1) attenuates as shown in Fig. 11. Because the sites are so close with the fault, it was assumed that the epicentral distance in Eq. (1) be measured from the center of the fault zone instead of the epicenter. The distance at Maumere and Ende is then approximately 25 km and 80 km, respectively. The peak ground acceleration from Eq. (1) is therefore evaluated as 0.4 g at Maumere and 0.2 g at Ende.

3.3 Damage by Tsunami

Extensive damage was developed due to tsunami along the coast of Flores Sea. In particular, damage at Babi Island and Wuling was destructive. At Babi Island, a village with population of about 950 was completely damaged as shown in Photos 13, 14 and 15. About 750 were killed by the tsunami at this island. The tsunami height is estimated as high as 3.7 m.

Photos 16, and 17 show the destructive damage at Wuling. The maximum tsunami height is estimated as 2.45 m.

3.4 Damage of Roads and Bridges

Extensive damage was developed in roads and bridges in Flores Island. Fig. 12 shows the major National Roads and Provincial Roads in the damaged area. Major damage was concentrated on the National Road connecting Ende and Maumere, National Road connecting Maumere and Larantuka, and the Provincial Road connecting Maumere and Magapanda.

The most serious damage was developed at National Road between Ende to Maumere which crosses in mountainous area. Because Ende and Maumere are the two major cities in the island, suspension of traffic between the two cities cause various problems for transportation in the island. As shown in Fig. 13 the road was suspended at 18 sites between Ende and Maumere.

Major damage at this route was developed by slope failure as shown in Photo 18. Fig. 14 classifies the type of failures. At the site where one side was cut and the other side was embanked (cut and filled embankment), the filled embankment often settled and this caused extensive cracks on the pavement. Failure also occurred at cut slopes and natural slopes. Destructive failure in which not only the cut slope but the natural slope failed as shown in Photo 19 were also observed at several sites.

Stone falling as shown in Photo 20 was observed

at several sites.

Extensive damage of pavement and bridges were developed by soil instability along the Flores Sea. Single span or two span simply supported girder bridges, which were probably constructed before the Second World War, often suffered settlement and tilting of abutments and back soils as shown in Photo 21. The settlement was as large as 1m. Such settlement and tilting of abutments were mostly caused by sliding of surrounding soils as shown in Fig. 15.

There are several new steel truss girders supported by reinforced concrete single columns or frame piers as shown in Photo 22. Damage was generally less in the truss bridges. The rubber cushion as shown in Photo 23 placed at the end of the deck behaved quite well for reducing the impact between the deck and the abutment wall.

3.5 Damage of Irrigation Facilities

A water barrier on a river near Nebe suffered damage on the parapet wall of water gate as shown in Photos 24 and 25. The parapet wall tilted with the back side being apart from the soil. Large settlement was developed at the back soils along the wall. Leakage of water from the parapet wall was seen. Photo 26 shows damage of the water gate.

3.6 Damage of Ports

The Maumere Port as shown in Photo 27 suffered extensive damage due to tsunami and soil liquefaction in addition to the ground shaking. The quay wall and retaining wall for the apron overturned toward sea side and was badly damaged as shown in Photo 28.

Photo 29 shows a boat and a truck attacked by the tsunami.

3.7 Damage of Airport

The Control Tower of the Maumere Airport and the Ende Airport was badly damaged. The Control Tower at the Maumere Airport is four story masonry building, and was subjected to extensive shear failure at the wall with the glass being broken. The control Tower at Ende Airport is three story masonry building, and was suffered significant shear failure at the wall as shown in Photo 30. The damage was so extensive that they could not be used. The apron and run-way suffer no damage at both Airports.

3.8 Damage of Lifelines

Water supply was interrupted at wide area in Flores Island. In Maumere a number of main wells were badly damaged due to the earthquake. This caused suspension of water supply for three days after the earthquake. Although the damage was repaired, amount of the supply was still about 50 % of the normal supply even two weeks after the earthquake. The water was delivered by water-tank vehicles as shown in Photo 31.

At Ende, the electricity is generated by 7 diesel engine generators as shown in Photo 32. They did not suffer damage. Masonry wall of the building storing the generators fell down at two locations. Because cables distributing electricity were ruptured at several sites, the electricity was suspended for two days after the earthquake. This caused problems for water supply.

3.9 Soil Liquefaction

Soil liquefaction was developed extensively along the coast of Flores Sea.

Fig. 16 shows a soil profile at Maumere. The ground condition is of sandy soils with the thickness of about 30 m - 50 m overlaid by top soil with about 5 m thickness. Because water table is shallow, the sand at Maumere is quite vulnerable to liquefaction.

Fig. 17 shows the grain size accumulation curve for the three specimens obtained at three sites along the Flores Sea. The averaged grain size D_{50} is 0.15 - 0.44 mm.

From Fig. 8 which shows the empirical relation by Eq. (2), it is anticipated that liquefaction occurred as far as 150 km from the epicenter.

Special interest was large soil settlement and lateral soil movement developed widely along the coast of Maumere city as shown in Photo 33. At this site large settlement probably as large as 1 $\sim$ 2 m was developed along the coast. Photo 34 shows the settlement of storage yard. Several cracks on soils and road pavement were seen as shown in Photo 35 parallel to the coast. It is considered that the lateral spreading due to liquefaction caused such large settlement and lateral movement of top soils.

3.10 Restoration and Rehabilitation

Emergency activities were made based on the Declare of the President of Republic of Indonesia under the cooperation of central government, province, regency, sub-regency and Armed Forces as shown in Fig. 18. Because the regency office suffered damage, the Chief of the regency took command of the Headquarters for Disaster Countermeasures at the Governor's official residence.

The first-aid stations were placed in Maumere to

provide the first-aid treatment. Fortunately hospitals were functional after the earthquake, and medical care could be made as shown in Table 3. There were sufficient supply for medical and pharmaceutical products in Maumere. But at Ende, the relief supplies were not enough because road transportation between Maumere and Ende was interrupted.

There were no serious trouble for daily living at Maumere because business service was resumed soon after the earthquake and relief supplies were provided. At Ende, however, the relief supplies were not enough because of road damage between Maumere and Ende. Although helicopters were used for distributing supplies, the amount of distribution was limited.

Many peoples stayed in tents after the earthquake. Lack of tents made many peoples be accommodated in open space like the military camp. Approximately 100 tents were pitched as shown in Photo 36 in a park near the official residence at Maumere. Because almost 10 families were accommodated in a large tent, there seems to be approximately 3,000 - 4,000 peoples in the tents.

It was planned to complete the emergency actions and the rehabilitation works by the early January 1993 and the end of March 1993, respectively. The rehabilitation of public facilities such as roads had the highest priority. It was planned to complete the repair of the National Road connecting Maumere and Ende by the early January, 1993. Many heavy construction machines such as bulldozer were transported from main island. The rehabilitation of public facilities and schools need the high priority. The target date for resuming schools was the early January 1993.

Because there are no major cities and sufficient road network in Flores Island, materials required for restoration and daily living needed to be supplied by sea and air transportation from Jawa Island. This resulted in two weeks for initiating the full restoration. It is learned from the evidence that active support of the central and regional governments is inevitable for prompt restoration. For such purpose, it is of great importance to evaluate damage degree immediately after an earthquake based on close collaboration among related ministries, and to restore the damage under clear strategy.

4 CONCLUDING REMARKS

Damage feature of infrastructures in the Cairo, Egypt, Earthquake of October 1992 and the Flores Island, Indonesia, Earthquake of December 1992, were briefly described. Based on the survey on the damage and earthquake preparedness in Egypt and Indonesia, the following conclusions may be pointed out :

1) Design and construction of infrastructures are far better in both countries than those for private buildings. Seismic damage of important infrastructures was limited.

2) Because infrastructures which have been so far constructed are small in size, seismic damage developed was limited in the two earthquakes even if seismic effects were not considered. But seismic effects are required to be considered in design for constructing modern infrastructures with large size.

3) Damage of roads caused serious problems in wide areas in Flores Island. Because damage of infrastructures considerably affects function of the region, significant attention needs to be paid for preventing damage of infrastructures.

4) Tsunami caused destructive damage along coastal areas. Education on tsunami behavior and training for evacuation are extremely important as well as appropriate tsunami warning systems and countermeasures for mitigating propagation of tsunami.

5) Improvident information dissemination to the public on future earthquake activities may cause panic when the public does not have enough scientific knowledge on an earthquake. It is important to disseminate the information so that it can be easily understood and that it is consistent with the aid-activities.

6) There are no special advises for two countries for mitigating seismic damage. Because earthquakes repeat in the future, it is the only way to provide appropriate preparedness. It includes seismic design, seismic evaluation, seismic strengthening, disaster information systems, and education and dissemination on damage of disaster. A standard procedure for evaluating vulnerability of exiting structures needs to be established with the highest priority.

7) If one classifies the earthquake environment in terms of the frequency of occurrence and the earthquake magnitude, a matrix such as the one presented in Table 4 may be obtained. It is generally difficult to take an appropriate measure against earthquakes at the areas where frequency of occurrence of earthquakes is low as shown in Table 5. Special attention needs to be paid in such areas for preventing seismic damage.

Because safety of structures is a matter to be evaluated from economic and benefit point of view, relative importance between economy and safety of structures needs to be carefully

considered. For example, in designing nuclear power stations, the highest priority is placed on safety of the facilities. They are designed against the maximum credible earthquakes at the site. On the other hand, ordinary infrastructures and buildings are designed so that essential function be maintained for JMA (Japan Meteorological Intensity) intensity V, and fatal damage be prevented even for JMA Intensity VI. It is often evaluated that JMA Intensity V and VI is referred to the peak ground acceleration of 0.08 - 0.25 g and 0.25 - 0.4 g, respectively, although it is very rough because such intensity depends both on strength of ground motion and strength of structures. This is concept that structures need to keep their function against the earthquakes with high probability to occur within the structures lifetime, and to prevent collapse even against the larger earthquakes.

8) Avoiding unreinforced brick and adobe structures is the most essential measure for preventing seismic damage of structures developed in the two earthquakes. This is true for reducing structural damage by an earthquake all over the world. In Japan, construction of unreinforced brick structures which was imported from European countries after the Meiji Restoration in 1867 was prevented after the destructive damage developed in Nohbi Earthquake in 1892 and the Kanto Earthquake in 1923. If brick structures continue to be constructed, destructive damage may be developed still now. Because it is generally difficult in low seismic areas to consider seismic effect in design, technical development which enables to adopt more ductile materials is required. Because Japanese did not have an impression that wooden housings are poor construction, it was not so difficult to avoid the brick constructions. Because wooden constructions are vulnerable to fires, various countermeasures for preventing spread of fires such as an increase of road apace and adoption of fire-proof sidings and walls are being made. It is also repeatedly educated to extinguish fires at kitchen and stoves for preventing fire ignition.

ACKNOWLEDGEMENTS

The authors would like to express their sincere appreciation to the invaluable supports provided by various governmental organizations of Arab Republic of Egypt and Republic of Indonesia. Without supports provided by the Japanese Embassy and JICA Office in Egypt and Indonesia, survey could not be made so smoothly. Voluntary effort by the Japanese who were in Egypt and Indonesia is also greatly appreciated. Special appreciation also goes to the kind cooperation and assistance of the members of Japan Disaster Relief Team of the Japan International Cooperation Agency.

References

1) Japanese Expert Team as Dispatched by the Japanese Government through Japan International Cooperation Agency : Preliminary Report on Cairo, Egypt Earthquake of October 12, 1992, October 1992
2) Japanese Expert Team as Dispatched by the Japanese Government through Japan International Cooperation Agency : Preliminary Report on Flores Island, Indonesia Earthquake of December 12, 1992, December 1992
3) Kebeasy, R. M. : Seismicity of Egypt, Proc. Workshop on the Broad-band Seismic Network for the Mediterranean, CCSEM, September 1990
4) Ibrahim, E. M. : Seismic Activity in the Different Techtonic Provinces of Egypt, 4th Egyptian Training Course on Earthquake Engineering, Egyptian Society for Earthquake Engineering, November 1990
5) Albert, R. N. H. : Seismicity and Earthquake Hazard at the Proposed Site for a Nuclear Power Plant in the Anshars Area, Nile Delta, Acta Geophysica Polonia, Vol. 35, No. 4, 1987
6) Kawashima, K. : Seismic Damage of the Cairo, Egypt Earthquake of October 1992, Civil Engineering Journal, Vol. 35-3, March 1993
7) Kawashima, K. and Aizawa, K. : Attenuation of Peak Ground Acceleration, Velocity and Displacement Based on Regression Analysis of Japanese Strong Motion Records, Earthquake Engineering and Structural Dynamics, Vol. 14, pp.199-215, 1986
8) Kuribayashi, E. and Tatsuoka, F. : History of Earthquake Induced Soil Liquefaction in Japan, Bulletin of Public Works Research Institute, Vol. 31, 1977
9) Kawashima, K. and Uda, T. : Seismic Damage of Flores Island, Indonesia Earthquake of December 12, 1992, Civil Engineering Journal
10) Fujii, T. and Kawashima, K. : Seismic Damage of Cairo, Egypt Earthquake of October 1992 and the Flores Island, Indonesia Earthquake of December 1992, Journal of the Japan Society of Civil Engineers

Table 1 Major Damage by the Cairo Earthquake

(1) Human Damage	Casualty	561
	Injured	12,192
	Needs treatment in Hospital	2,270
	No needs treatment in Hospital	9,922
(2) Damage to Educational Facilities	Major Repair	2,301
	Minor Repair	3,569
	No use	1,087
(3) Damage to Mosque	Major Repair	211
	Minor Repair	544
(4) Damage to Monuments	Major Repair	14
	Minor Repair	104
(5) Damage to Homes and Houses	Major Repair	4,395
	Minor Repair	22,235
	No use	7,796

Table 2 Main Damage of the Flores Island Earthquake

Regency	Population ('85) (Prs)	Area (km^2)	Human Damage				Building Damage				
			Dead (Prs)	Injured		Missing (Prs)	Office (house)	Church Mosk (house)	People House (house)	School (house)	Others (house)
				Heavy (Prs)	Light (Prs)						
Sikka	236,691	1,731.9	1,457	252	1,256	8	56	47	10,200	324	4
Ende	212,349	2,046.6	229	106	227	—	344	193	13,804	281	154
Ngada	188,353	3,037.9	18	2	4	—	67	45	1,194	100	68
Flores Timur	267,295	3,079.2	376	15	241	61	26	22	2,920	80	50
Total	904,688	9,895.6	2,080	375	1,728	69	493	307	28,118	785	276

Note : 1) Human damage (Dead) in Flores Timur includes about 200 victims by Tsunami.
2) Building damage (Housing) includes partially damaged houses.
Souse : Army's Headquarters for Emergency Activities in WAIOTI Airport in Maumere on December 26, 1992.

Table 3 Number of Injured Who Had Medical Care at a hospital in Maumere

Date	Persons Who Visit Hospital	Persons in Hospital	Persons Who Took Medical Care	Dead	Persons Discharged From Hospital
12 Dec.'92	128	82	10	36	—
13	68	46	20	2	15
14	39	23	16	—	30
15	287	27	260	—	21
16	222	25	197	—	28
17	205	6	199	—	3
18	229	5	224	—	3
19	322	3	319	—	4
20	154	5	149	—	—
21	225	6	219	—	—
Total	1,879	228	1,613	38	104

Source : Army's Headquarters for Emergency Activities in WAIOTI Airport in Maumere.

Table 4 Classification of Earthquake Environment in terms of Frequency of Occurrence and Magnitude of Earthquakes

		MAGNITUDE OF EARTHQUAKE		
		Small ($M \leqq 7$)	Medium ($7 < M < 8$)	Large ($M \geqq 8$)
FREQUENCY	Low	Egypt Spain	Canada, Philippines, Indonesia	U.S.A. (Central and South)
	Medium	Armenia	Turkey	U.S.A. (West), New Zealand, China, India Mexico
	High			Japan, Chile Peru

Table 5 Difficulty of Preparedness against Earthquakes Depending on Frequency of Occurrence and Magnitude of Earthquakes

		MAGNITUDE OF EARTHQUAKE		
		Small ($M \leqq 7$)	Medium ($7 < M < 8$)	Large ($M \geqq 8$)
FREQUENCY	Low			
	Medium			
	High			

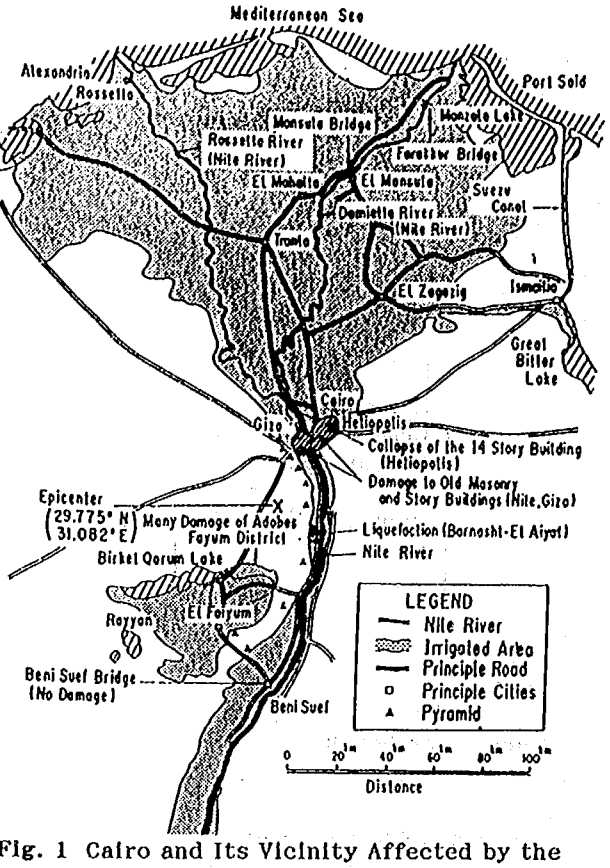


Fig. 1 Cairo and Its Vicinity Affected by the Cairo Earthquake

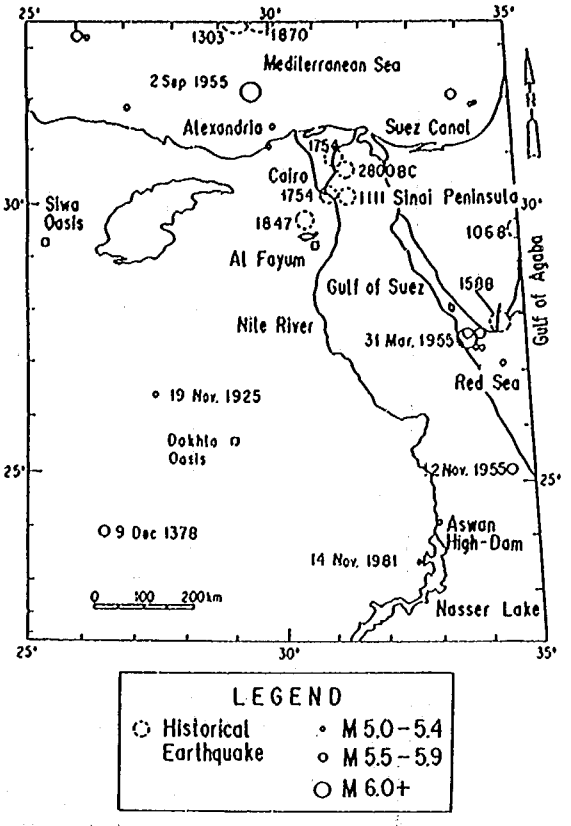


Fig. 2 Epicenter of the Past Earthquakes around Cairo

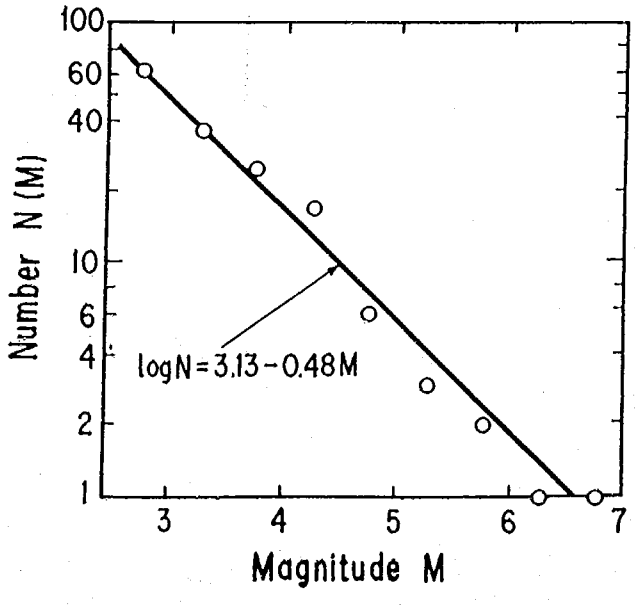


Fig. 3 Accumulated Number of Earthquakes within 300 km around north Cairo between 1952 and 1985[6]

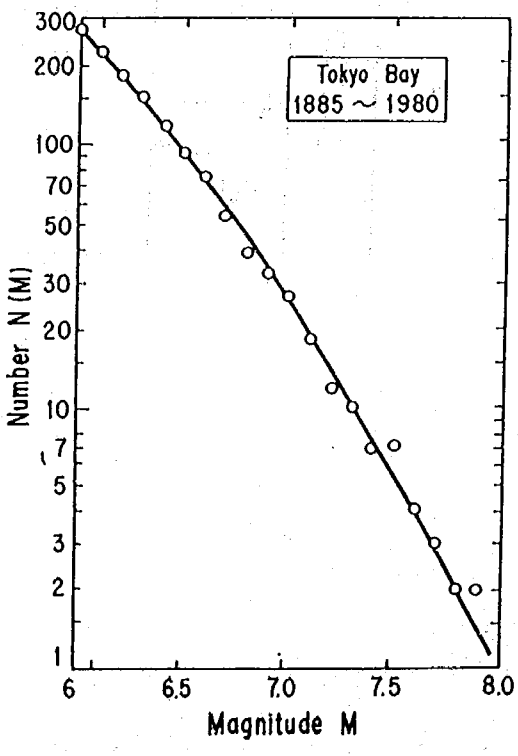


Fig. 4 Accumulated number of Earthquakes within 300 km around Tokyo Bay between 1885 and 1979

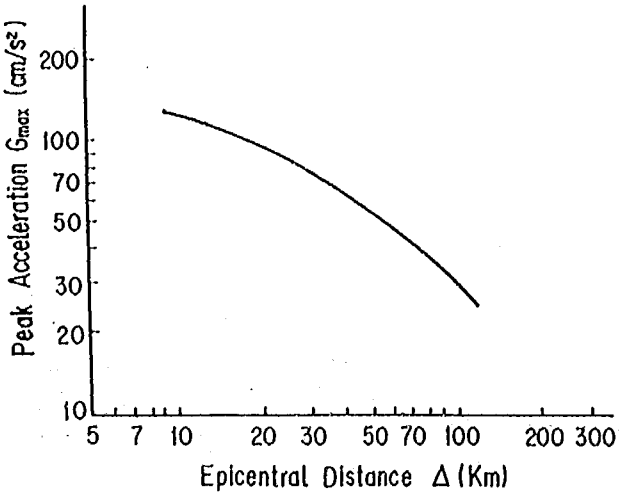


Fig. 5 Attenuation of Peak Ground Acceleration Predicted by Eq. (1)

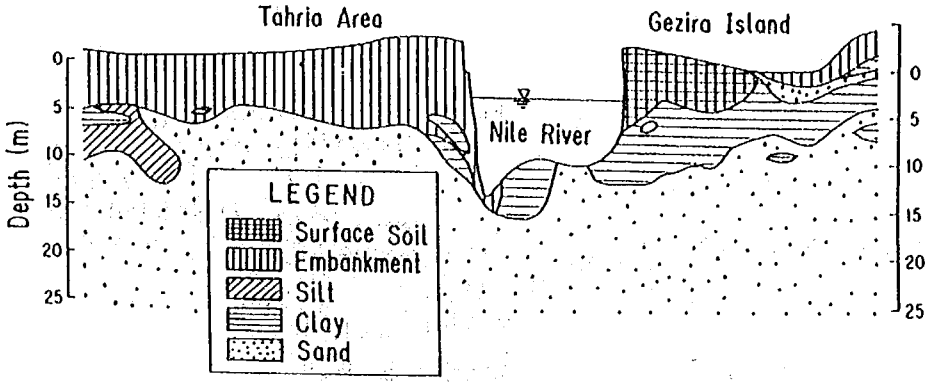


Fig. 6 Soil Condition at Cairo city

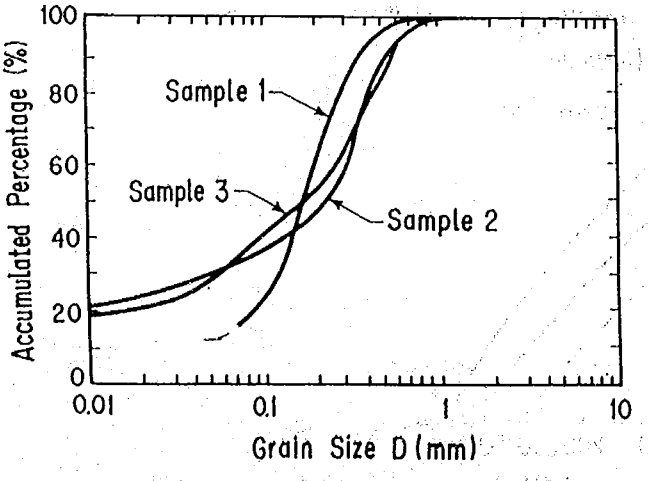


Fig. 7 Grain Size Accumulation Curve of the Liquefied Sand at Barmasht - El Alyat Area

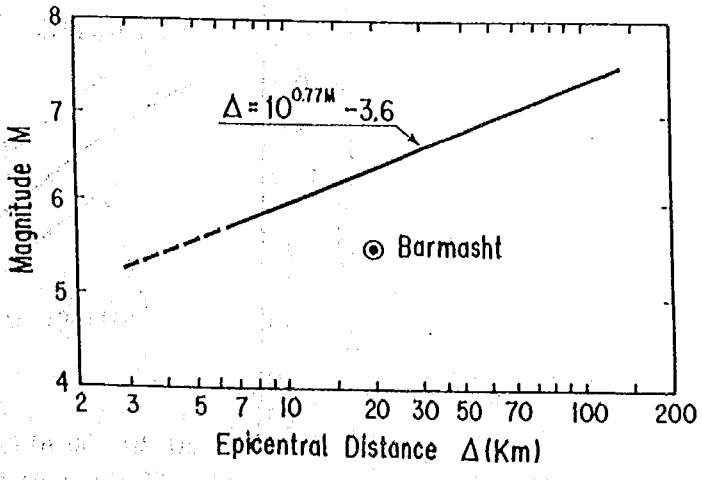


Fig. 8 Threshold for Causing Liquefaction

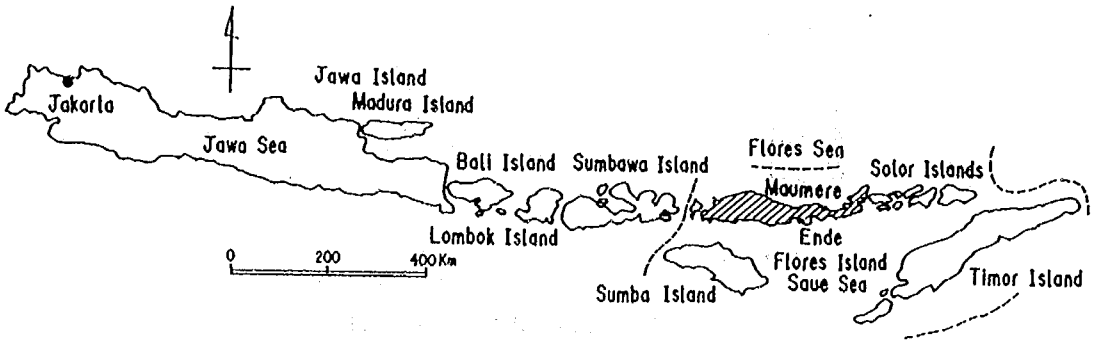


Fig. 9 Flores Island

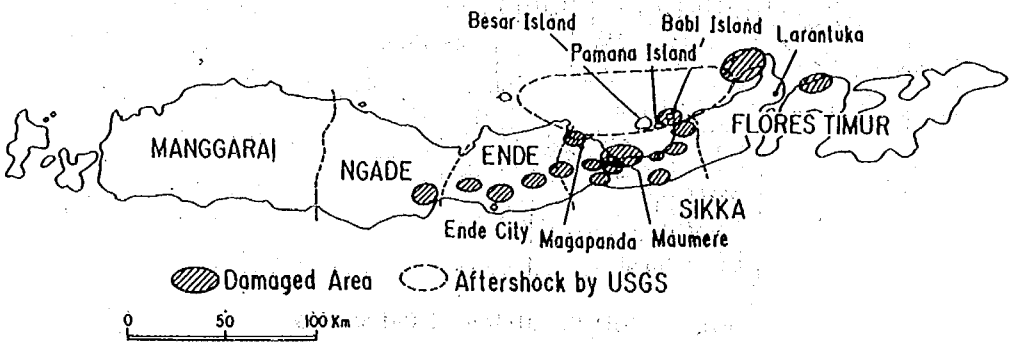


Fig. 10 Damaged Region and Aftershock Area

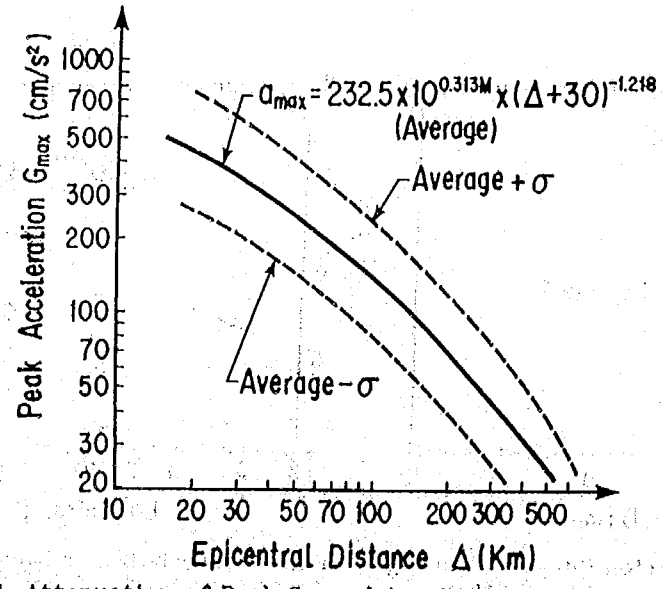


Fig. 11 Attenuation of Peak Ground Acceleration Predicted by Eq. (1)

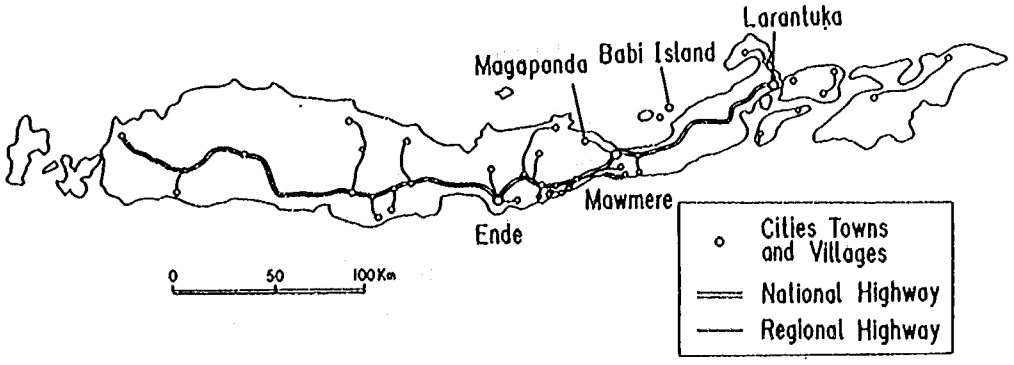


Fig. 12 Major National Roads and Provincial Roads in Flores Island

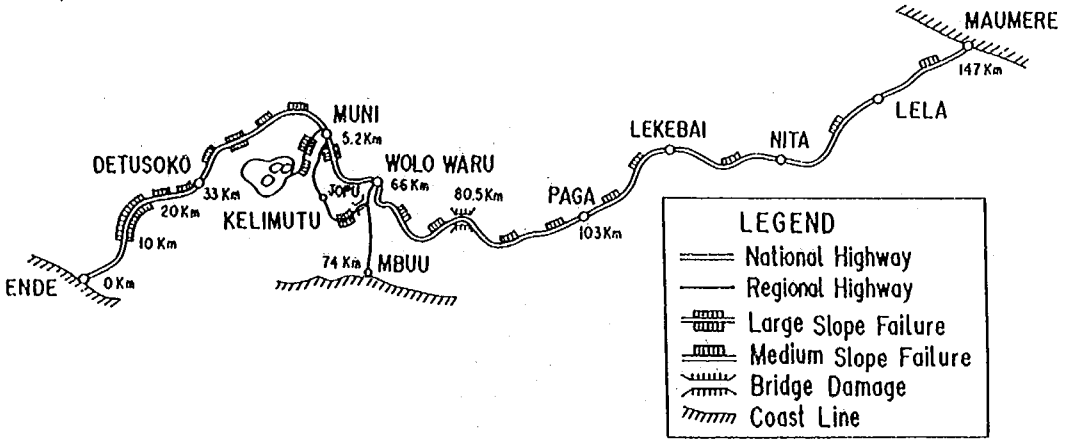


Fig. 13 Major Damage on National Road from Ende to Maumere

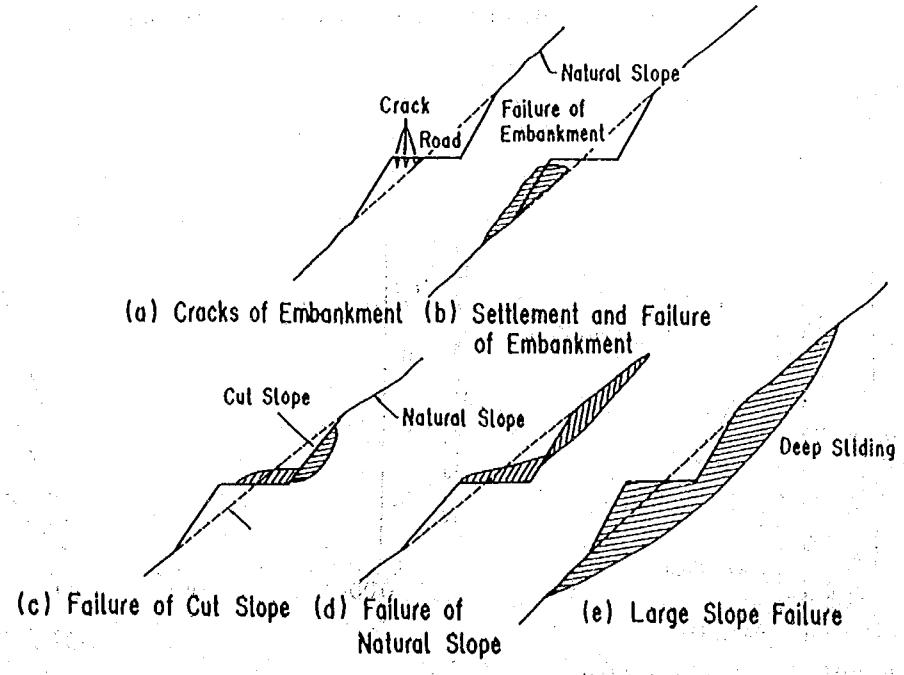
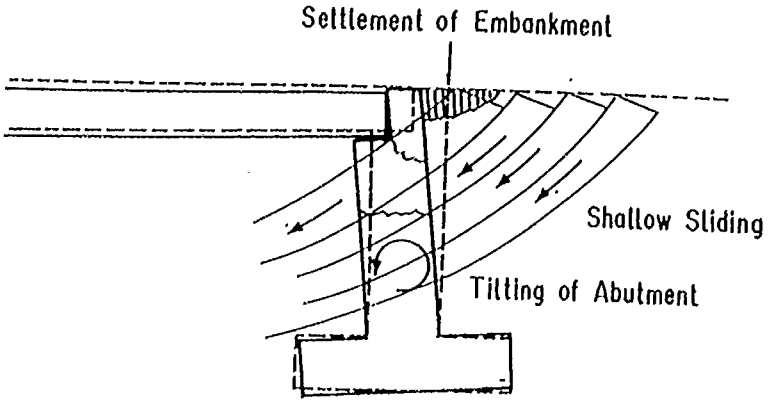
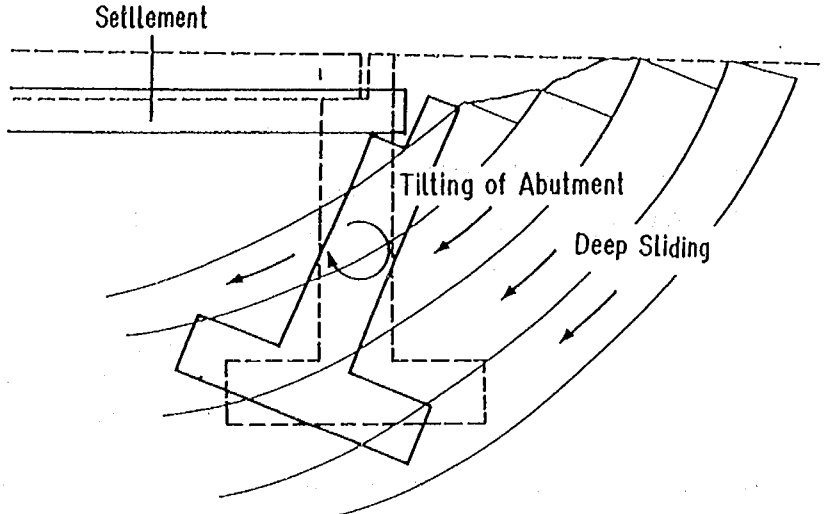


Fig. 14 Types of Slope Failure



(a) Shallow Soil Failure



(2) Deep Soil Failure

Fig. 15 Damage of Bridge Abutments due to Soil Instability

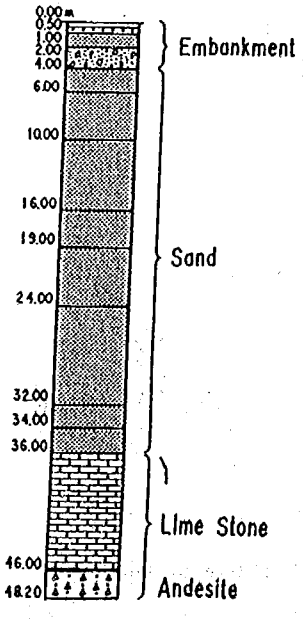


Fig. 16 Soil Profile at Maumere City

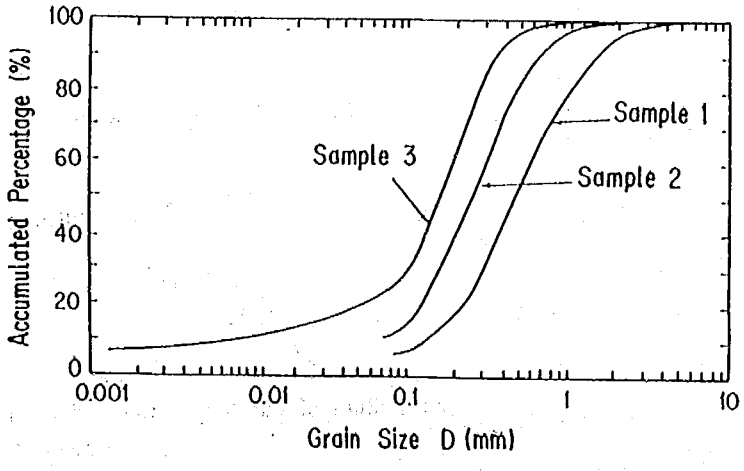


Fig. 17 Grain Size Accumulation Curve of Sand

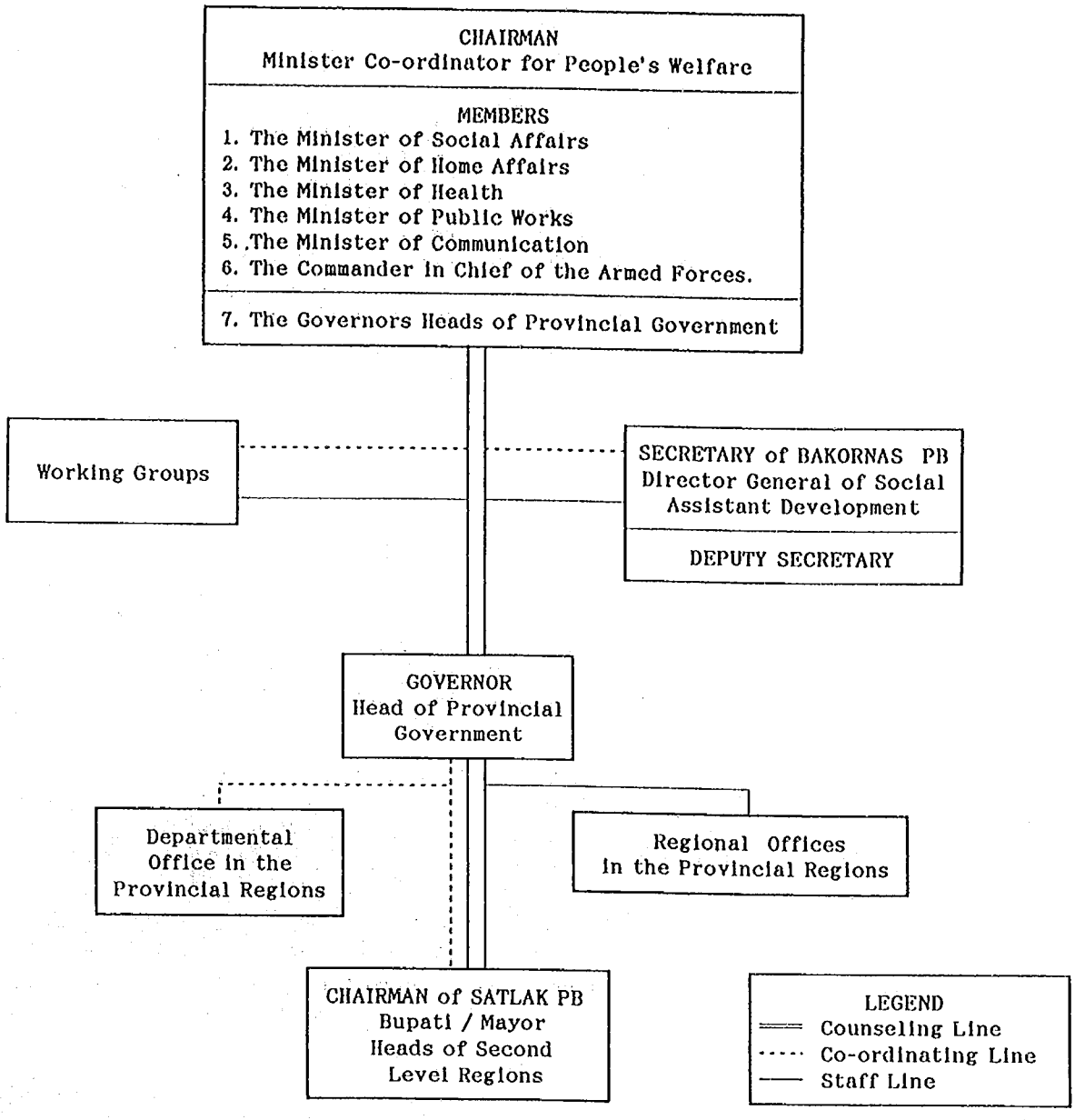


Fig. 18 Structure of Bakornas

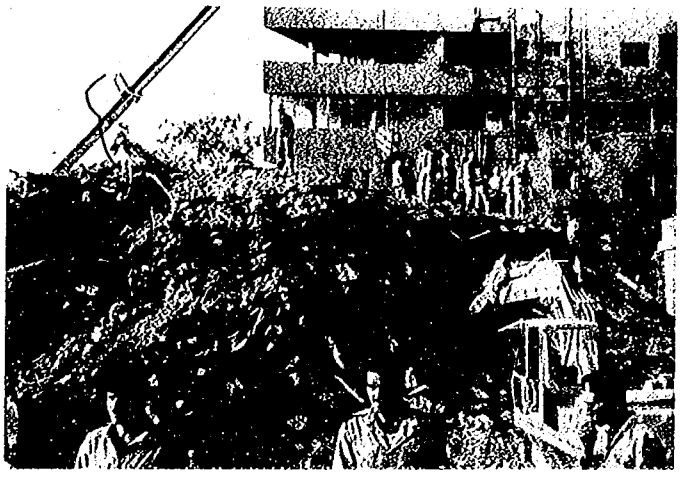


Photo 1 Collapse of 14-story Building at Hellopolis

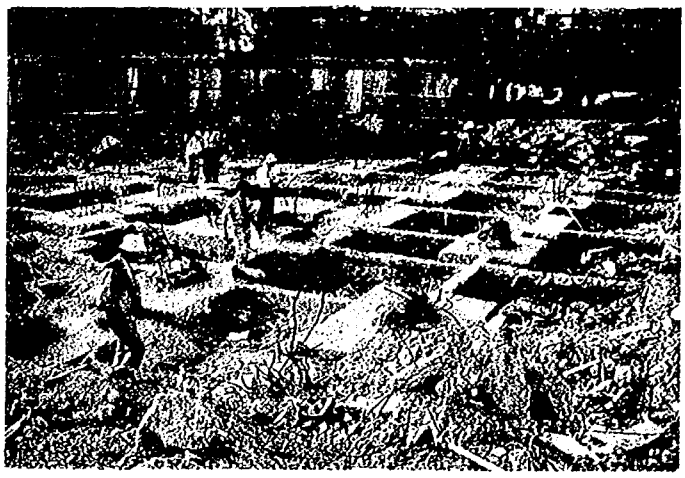


Photo 2 Foundation of 14-story Building



Photo 3 Damage of Adobe Housing at Faiyum



Photo 4 Damage of Unreinforced Masonry Buildings at Downtown Cairo

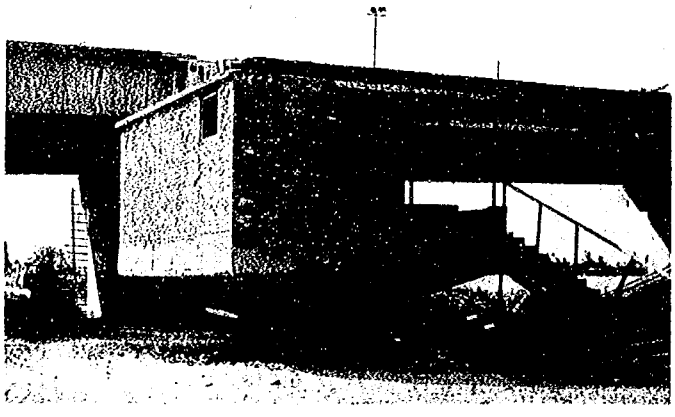


Photo 5 Test Pile Subjected to 480tf Loading (now used for Controlling House for the Site)



Photo 6 Zamalek Overcrossing (No Damage)



Photo 7 Fsaraskour Bridge (No Damage)

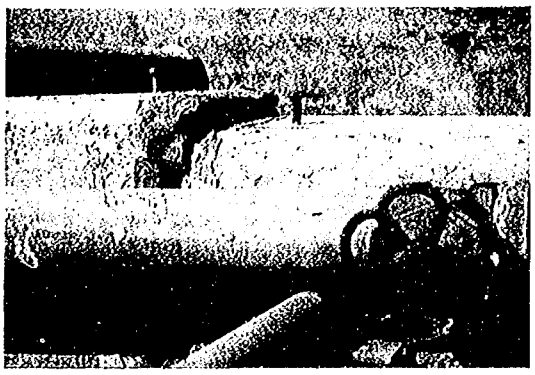


Photo 8 Offset of Concrete Wall of Clarifier



Photo 9 Sand Blow Hole due to Liquefaction at Barmasht - El Alyat



Photo 10 Emergency Tents

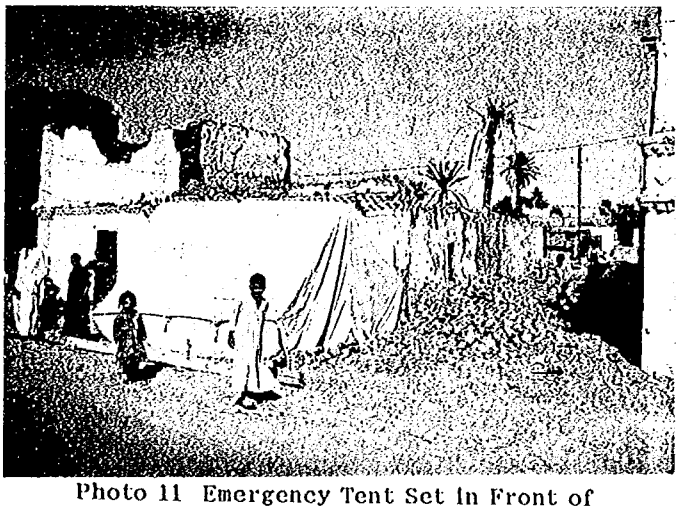


Photo 11 Emergency Tent Set In Front of Housing



Photo 12 Damage of Masonry Building



Photo 13 Damage of Babi Island due to Tsunami



Photo 14 Damage of Babi Island due to Tsunami



Photo 15 Damage of Babi Island due to Tsunami



Photo 16 Tsunami Damage at Wuling



Photo 17 Tsunami Damage at Wuling



Photo 18 Large Slope Failure



Photo 19 Destructive Slope Failure Including Cut Slope and Natural Slope



Photo 20 Stone Falling

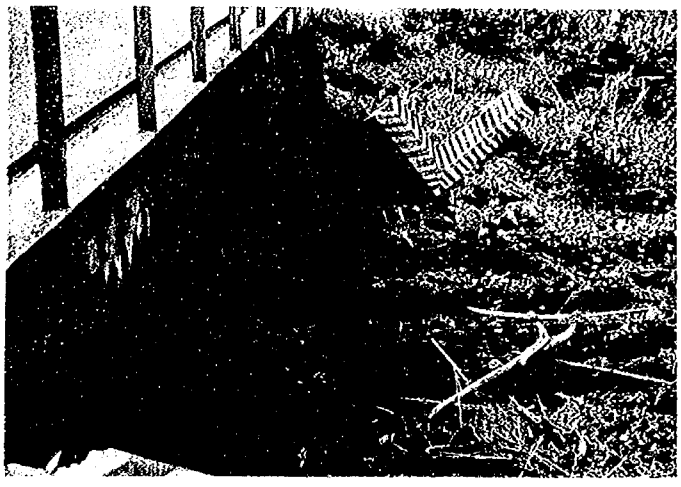


Photo 21 Settlement of Bridge Abutment and Back-Fill



Photo 22 Truss Bridge

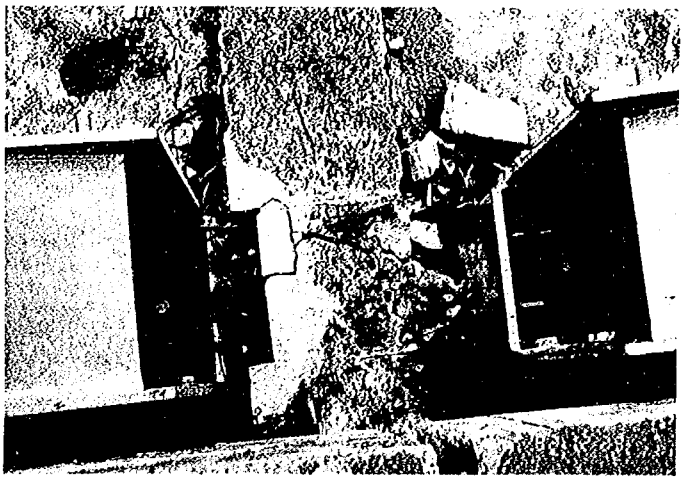


Photo 23 Longitudinal Stopper with Rubber Cushion

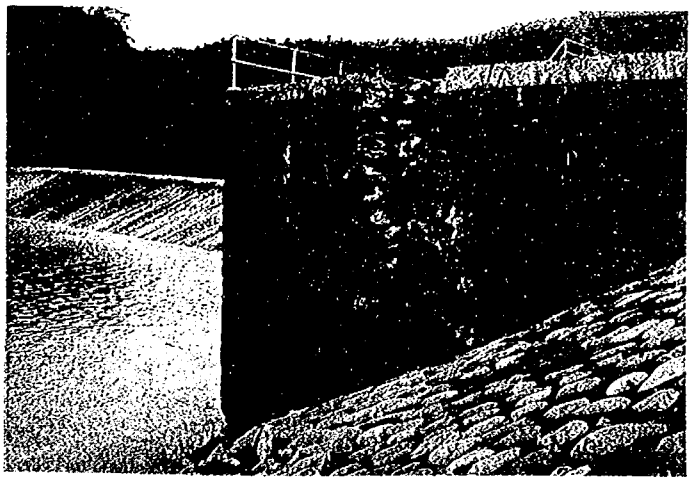


Photo 24 Damage of Concrete Block Cover along Water Barrier

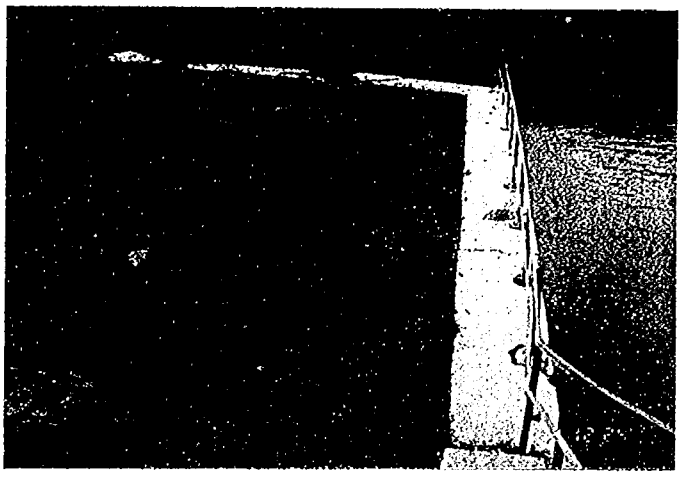


Photo 25 Tilting of Parapet Wall and Settlement of Back-fill



Photo 26 Cracks of Water Gate



Photo 27 Maumere Port



Photo 28 Tilting of Retaining Wall and Settlement of Back-Fill

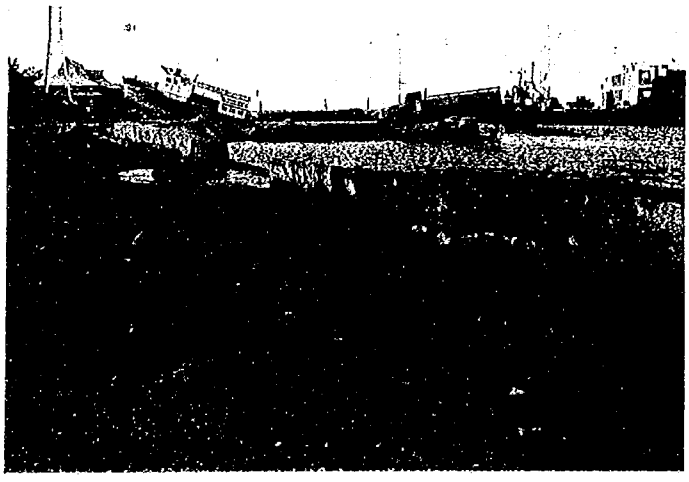


Photo 29 Settlement of Apron and Failure of Wall (A Ship and A Boat which were surged by the Tsunami could be seen)



Photo 30 Damage of Control Tower at Ende Airport

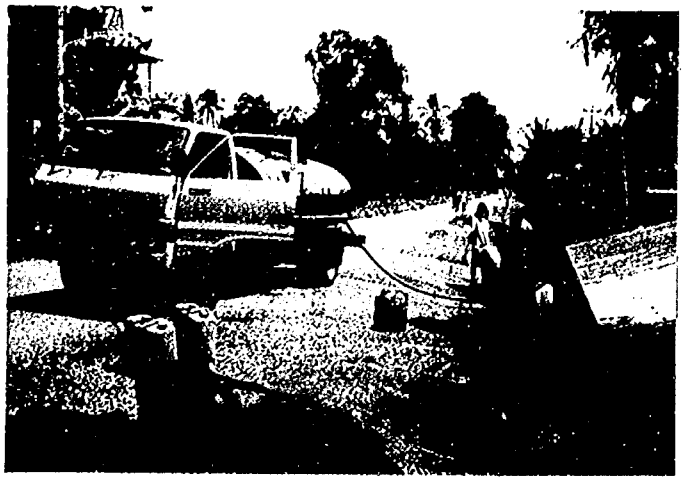


Photo 31 Emergency Water Supply by Water-Tank Vehicle near Ende

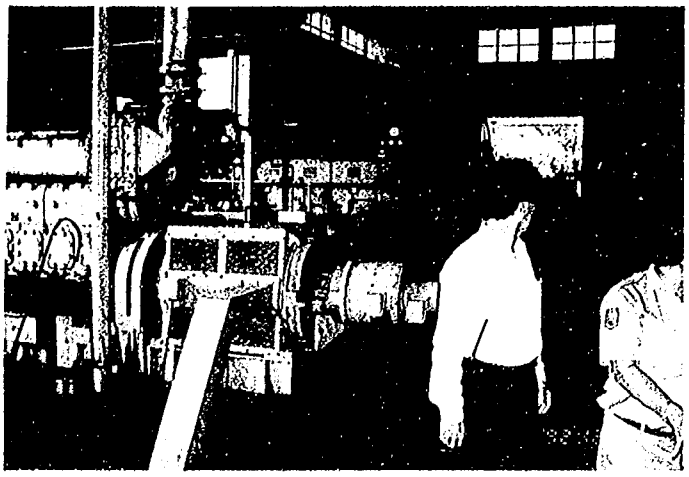


Photo 32 Diesel Generator for Electricity at Ende



Photo 33 Settlement and Lateral Soil Movement Developed around Maumere City



Photo 34 Settlement of Coast Line and Settlement of Storage Yard along the Coast



Photo 35 Cracks on Ground Surface along the Coast (Maumere city)

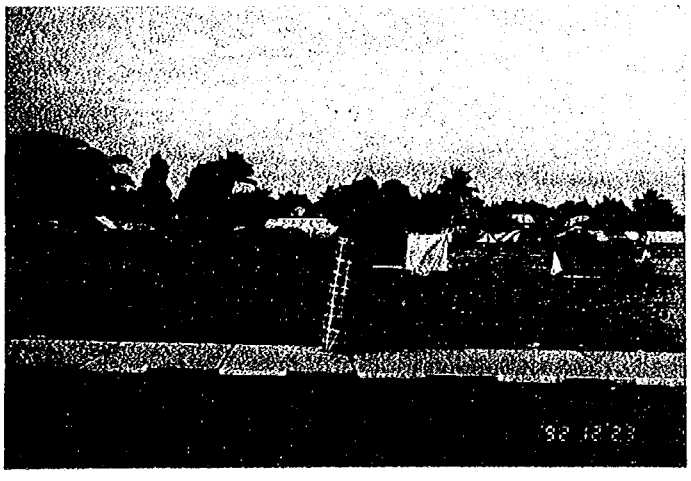


Photo 36 Emergency Tent Camp

Recorded Ground Motions from the MS=7.5 Landers, California, Earthquake of June 28, 1992.

by

A. Gerald Brady*

ABSTRACT

Southern California seismicity increased significantly during April and June of 1992, with the ML6.1 Joshua Tree earthquake on April 22, 1992, the MS7.5 Landers earthquake on June 28, 1992, and the ML6.5 Big Bear earthquake on the same date. More than 300 strong-motion stations produced records from the Landers earthquake, from networks operated by the California Division of Mines and Geology, the US Geological Survey, and others. The Landers earthquake is the largest in California since the MS7.7 1952 Kern County earthquake. The large number of recording stations is more a function of the density of instrumentation in southern California than it is an indication of the engineering significance of the data. The epicenter location and rupturing detail combined to provide few records of potentially damaging ground motion.

KEYWORDS: accelerograms; earthquakes; engineering; ground motion; networks.

1. INTRODUCTION

The epicenter of the Landers earthquake was located close to the small California town of Landers, 80 km east of San Bernardino, and 160 km east of Los Angeles. A series of faults were involved with the rupture, which commenced close to the southern end of the series. Here, the faults strike in the northerly direction, but finish, after several steps to the east, striking more to the northwest. A total rupture length of 85 km was determined during field investigations by geologists from the U.S. Geological Survey, the California Division of Mines and Geology, and various universities and consulting firms. The surface wave magnitude of 7.5, the largest in California since the MS7.7 Kern County earthquake of 1952, gave promise, unfulfilled, of a significant set of strong-motion records from permanently-installed southern California instrumentation.

2. SUMMARY OF NETWORKS IN SOUTHERN CALIFORNIA

2.1 Networks

The California Strong-Motion Instrumentation Program (CSMIP) operates a network of accelerographs throughout the state, within the Office of Strong-Motion Studies, Division of Mines and Geology, Department of Conservation, the Resources Agency, of the State of California. Instrumented stations are concentrated in the urban areas centered in Los Angeles, San Francisco and other earthquake-prone cities; on, or close to, the important California earthquake faults; and in other regions of interesting seismicity.

The U.S. Geological Survey (USGS) operates, under the National Strong-Motion Program (NSMP), a network of stations throughout the US (including Alaska and Hawaii), and Puerto Rico. These stations include a significant number of cooperative installations maintained by the NSMP for the US Army Corps of Engineers, the Metropolitan Water District of Southern California, the US Department of Veterans Affairs, and for numerous private building owners as required by the City of Los Angeles building code.

Smaller networks are maintained in southern California for specific purposes. The University of Southern California maintains an 80-station network throughout the Los Angeles basin. The Southern California Edison Company (SCE), a power utility, has a network covering its operating area. One specific record from the SCE network, at Lucerne

* USGS, Menlo Park, California, 94025

Valley, close to the rupture, is of wide interest to the engineering community. The SMA-2 instrumentation is currently being evaluated with a view to recovering more long-period content than was contemplated in the original design. Numerous universities, private companies and building owners have small networks.

2.2 Lack of Coverage for Potentially Damaging Motion

The maps of Figures 1, 2 and 3 indicate the coverage of the far-field and epicentral regions where it might have been expected that potentially damaging ground motions would occur. The epicenter lies close to the southern extremity of the set of ruptured faults. The rupture travelled north, meeting with delays each time it side-stepped to the east to continue its generally northward progress (Toppozada, 1993). These delays in the rupture travel ensure that records from all stations will have a longer duration than if the delays had not occurred. They also ensure that the buildup of amplitudes of transverse shear waves ahead of the rupture front cannot occur to the same extent as would happen if the rupture front travelled at close to the shear wave velocity. At stations in the direction opposite to the motion of the rupture front, that is, towards the south, the amplitudes of the expected motions from the receding source are not likely to be significantly affected by delays in the source movement.

The urban centers of Los Angeles and San Bernardino lie to the west of the epicenter, from where the rupture proceeded northwards. Stations associated with the San Andreas and San Jacinto fault zones lie generally in the southwest quadrant with respect to the epicenter and the ruptured faults. None of the NSMP stations, and only two of the CSMIP stations lie to the north or northwest of the set of ruptured faults. The two CSMIP stations are 84 km from the epicenter and 23 km from the northwest extremity of the faulting. It is almost as though the earthquake chose to occur in the most tantalizing part of the state, causing hundreds of triggers, but leaving any potentially damaging motions unrecorded.

3. CSMIP AND USGS RECORDS

3.1 CSMIP Strong-Motion Data

The following highlights of the CSMIP strong-motion data are abstracted from Shakal and others (1992). A total of 144 stations were triggered, ranging in complexity from three-component triaxial ground response accelerographs to a curved concrete bridge with 36 sensors. The closest station, with an epicentral distance of 14 km, is Joshua Tree Fire Station to the southeast, where the peak acceleration was 0.29 g. There are 88 ground response stations and 56 extensively instrumented structures (including 47 buildings, 6 dams, the major freeway interchange, an airport control tower and a power plant). However, the limited usefulness of the data set from an engineering standpoint is borne out by the few ground response records with significant horizontal peak values. There are only two stations having peaks between 0.29 and 0.20 g, the second being at Yermo to the northwest; six between 0.20 and 0.15 g; and 19 between 0.15 and 0.10 g. The closest structure with extensive instrumentation, a Palm Springs 4-story hospital to the south, is 43 km distant and has a ground level peak of 0.07 g. The structure with the highest ground level peak, 0.18 g, is the freeway interchange to the west at a distance of 81 km. As is the case with all extensive structures having an obvious tendency to resonate readily, it can be assumed that this ground motion peak is affected by the motions of the associated structure.

The CSMIP records are placed geographically with a bias towards the southwest quadrant, but provide a very useful dataset for those seismologists concerned with details of the fault rupture. Digital TERRAscope recordings have already been used to derive the distribution of slip along the fault to compare with observable surface slip (Kanamori and others, 1992). Processing of

the CSMIP records is under way, and the first 22 ground response records are available on floppy disk. An attempt is currently under way to reassess the long-period capability of the recording, digitizing and processing techniques, because interesting long-period content, outside the current range, is clearly present in some records. (Information: CDMG, OSMS, 801 K St, Mail 13-35, Sacramento, CA95814-3531; ph 916-322-3105)

3.2 USGS/NSMP Strong-Motion Data

The following information on NSMP data is abstracted from a letter sent to the NSMP mailing list within a few days of the earthquake, and from Etheredge and others (1993). A total of 111 stations covering a wide range of complexity and local substation geographical extent was triggered by the Landers event (see Table 1). Ground sites consisting of single 3-component triaxial accelerometers numbered 48. Two buildings with extensive instrumentation, in the adjacent cities of Loma Linda and San Bernardino, 80 km to the west, have ground level accelerations close to 0.1 g. The 4-story Loma Linda VA Hospital has 15 channels, 11 of which are at ground level for an extensive investigation of rotational input. The highest acceleration in the structure is 0.27 g, and structural accelerations exceeded 0.1 g for 27 seconds. The 6-story San Bernardino County Government Center has 18 channels, three of which are at an adjacent ground site. Structural peaks reached 0.34 g, and accelerations exceeded 0.1 g for more than 30 seconds.

The four temporary GEOS sites (Borcherdt and others, 1985) in Table 1 were established as part of an investigation of aftershocks of the M6.1 Joshua Tree, California earthquake of April 22, 1992, two months earlier. GEOS at these four stations, ranging in epicentral distance from 23 to 37 km, were still in place at the time of the Landers earthquake. Data from the USGS-designed GEOS were provided by S. Hough of USGS, Pasadena.

One NSMP station, Tripp Flats, at a distance of 75 km due approximately south, is a digital recorder connected by modem and phone lines to Menlo Park, where the data were received shortly after the earthquake. This represents a first for NSMP, where less than 2% of the network is recording digitally, and only a few have phone access.

Processing of the NSMP analog film records has not yet commenced as personnel and fiscal restraints require that we first study the feasibility of having it done on a 600 dots-per-inch flat bed scanner.

4. PEAK VALUE ANOMALIES AND IMPLICATIONS FOR PEAK PREDICTIONS

Two important factors contribute to the peak ground acceleration attenuation for this earthquake. First, the average rupture speed was low because the rupturing was delayed every time the rupture jumped eastward onto a fresh fault. These delays probably ensured that the buildup of transverse shear wave amplitudes ahead of the rupture did not occur, and that the normal patterns of P-, S-, and surface waves in all quadrants of the fault geometry did not appear. In a general sense, it is clear that if the strain energy release in an MS7.5 event can be spread out over a longer period of time than normal, that is, corresponding to the rupture travelling the length of the fault at close to the velocity of the shear wave, then individual peak ground motion values, acceleration, velocity and displacement, will generally be less. On the other hand, the number of well-recorded MS7.5 events is not high, and current attempts to predict peak motion attenuation already require sufficient extrapolation from the experience of lesser events that this delay factor is possibly a non-issue at the present time.

Secondly, almost all the stations within 50 km of the epicenter are within the southwest quadrant with respect to the epicenter. At further epicentral distances, out to 200 km and more, the stations spread wider than this southwest quadrant,

but not by much. At the end of the rupturing, as the faults strike more to the northwest, the same station bias to the southwest prevails, although two CSMIP stations, at Yermo and Barstow, become prominent, straight ahead of the stopping rupture and 23 and 33 km, respectively, from it. Although one quadrant is as interesting as the other three for ground motions from an infinitesimal slip on a vertical strike-slip fault, the southwest quadrant is at a serious disadvantage from the ground motion aspect if the rupture is declining in influence as it disappears from view to the north on a north-striking fault. The Yermo record is reproduced in Fig. 4.

Almost all the strong-motion records from this event consequently bear little resemblance to what we had hoped to see from an MS7.5 event in the well-instrumented southern California seismic environment. The disappointment is alleviated somewhat by the recognition that official groups having the responsibility of estimating the probability of large events on the southern section of the San Andreas fault are reassessing this probability upwards.

5. CONCLUSIONS

Although more than 300 stations produced records recovered from the Landers earthquake, this number is more indicative of the instrumentation density in southern California than the usefulness to the engineering community, considering the 7.5 surface wave magnitude. Processing is under way at CSMIP for the significant records, and is expected to commence at NSMP. Both the seismological, and, to a lesser extent, the engineering communities, will be interested in the analyses possible with this dataset.

6. REFERENCES

Borcherdt, R.D., J.B. Fletcher, E.G. Jensen, G.L. Maxwell, J.R. VanSchaack, R.E. Warrick, E. Cranswick, M.J.S. Johnston and R. McClearn, 1985, A general earthquake observation system (GEOS), Bull Seis Soc Am. 75, 6, 1783-1825.

CSMIP, 1992, Release Nos. 1, 2 and 3 - Processed strong-motion data from the Landers earthquake of June 28, 1992: fliers from CDMG, see Shakal and others, 1992.

Etheredge, E., R. Maley, R. Porcella, A. Acosta, E. Anjal, L. Foote, D. Johnson, W. Jungblut, T. Noce, M. Salsman, and J. Switzer, 1993, Strong-motion accelerograph records from the M=7.5 Landers, California earthquake of June 28 1992: U.S. Geological Survey Open-file Report, in preparation.

Kanamori, H., H.K. Thio, D. Dreger, E. Hauksson, and T. Heaton, 1992, Initial investigation of the Landers, California earthquake of 28 June 1992 using TERRAscope: Geoph. Res. Letters, 19, 22, 2267-70.

Shakal, A., M. Huang, T. Cao, R. Sherburne, R. Sydnor, P. Fung, P. Malhotra, C. Cramer, F. Su, R. Darragh, and J. Wampole, 1992, CSMIP strong-motion records from the Landers, California earthquake of 28 June 1992: Calif. Div. of Mines and Geol. Report No. OSMS 92-09.

Toppozada, T.R., 1993, The Landers-Big Bear earthquake sequence and its felt effects: California Geology, Jan/Feb 1993.

TABLE 1

NSMN STATIONS, BY TYPE

Ground site or small building	48
Large or multi-story building	35
Dam or reservoir facility	15
Pump or filter plant	6
Base-isolated bridge	1
Base-isolated building	1
Down-hole array	1
Temporary GEOS site	4

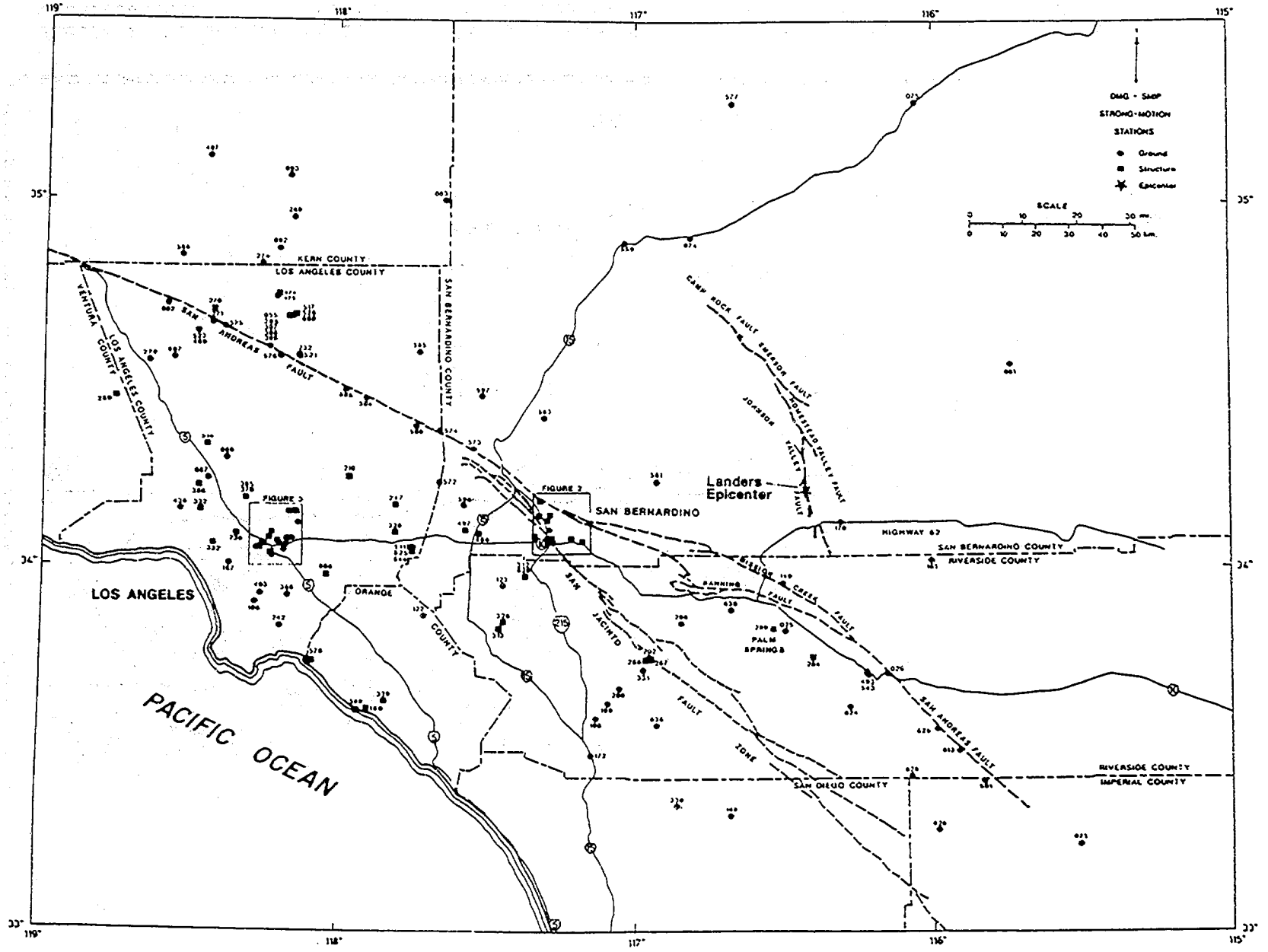


Figure 1. CDMG-CSMIP stns recording the Landers earthquake. Boxes surround the Los Angeles and San Bernardino stns. (Details in Shakal and others (1992), from which this map is taken).

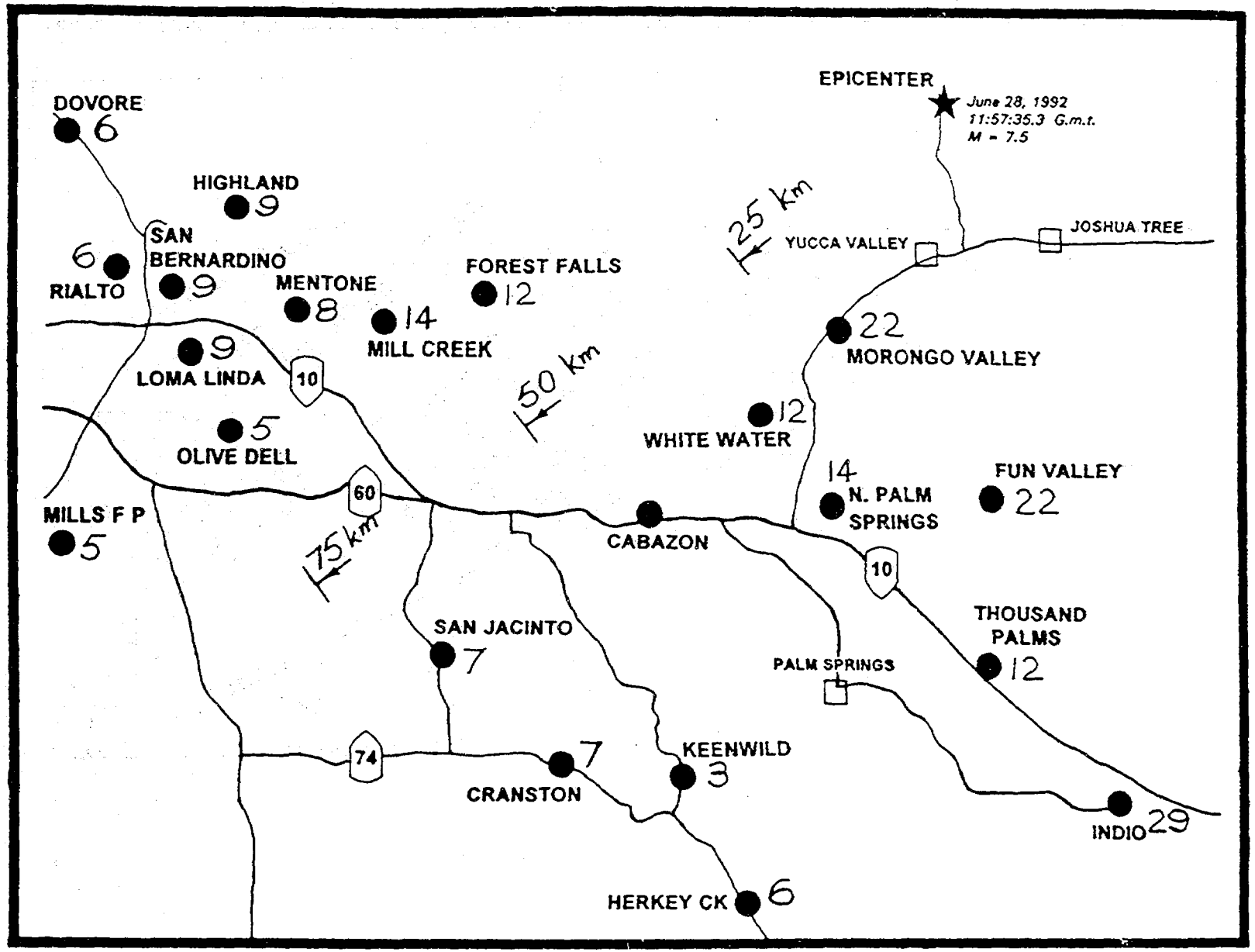


Figure 2. USGS-NSMP stations within 75 km recording the Landers earthquake. Peak horizontal accelerations in % g are shown if 5% or greater (from Etheredge and others, 1993).

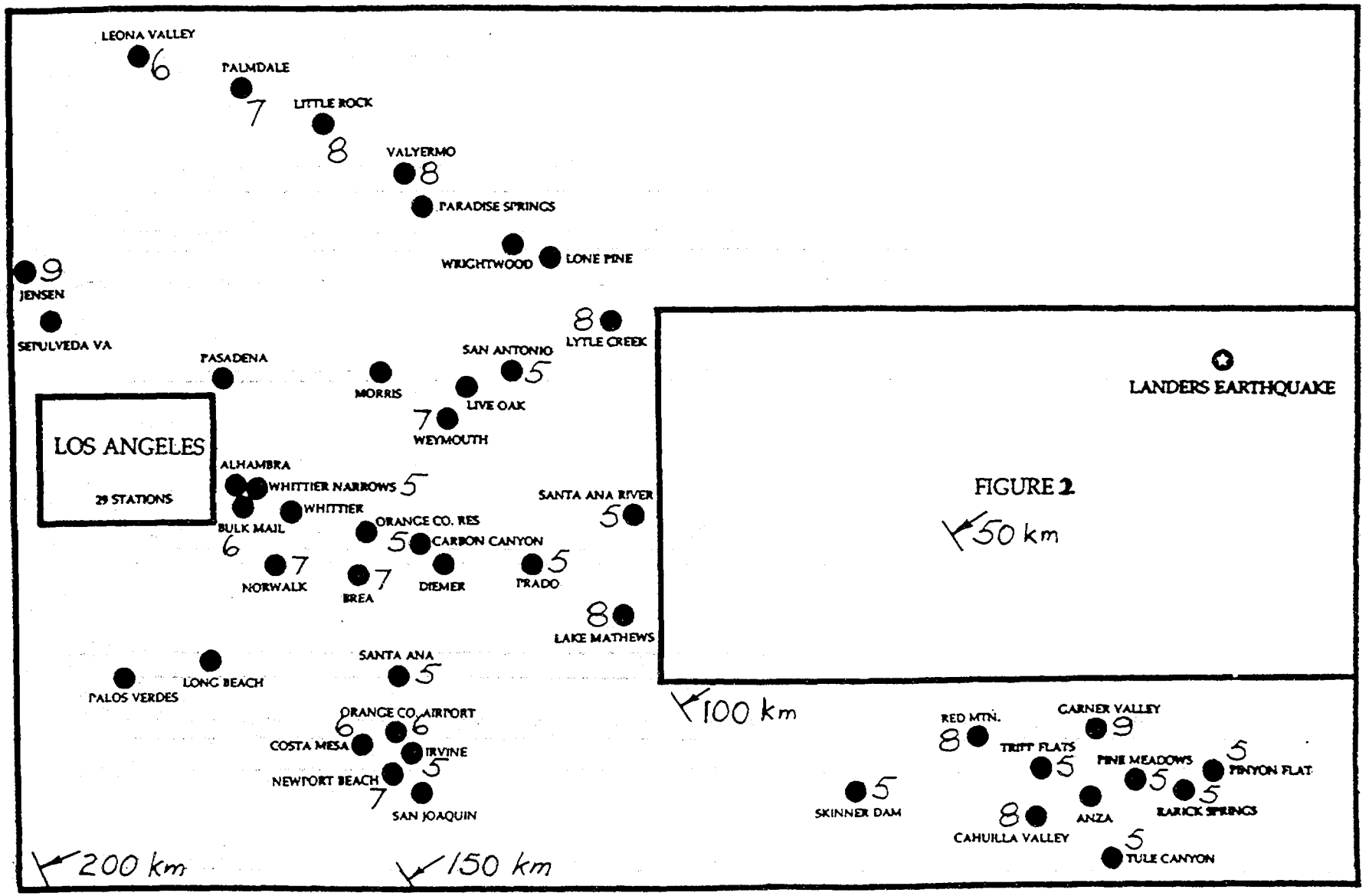


Figure 3. USGS-NSMP stations recording the Landers earthquake. Peak horizontal accelerations in % g are shown if 5% or greater. See Fig. 2 for the close stations. Details for the boxed Los Angeles stations are in Etheredge and others (1993), the source of the map.

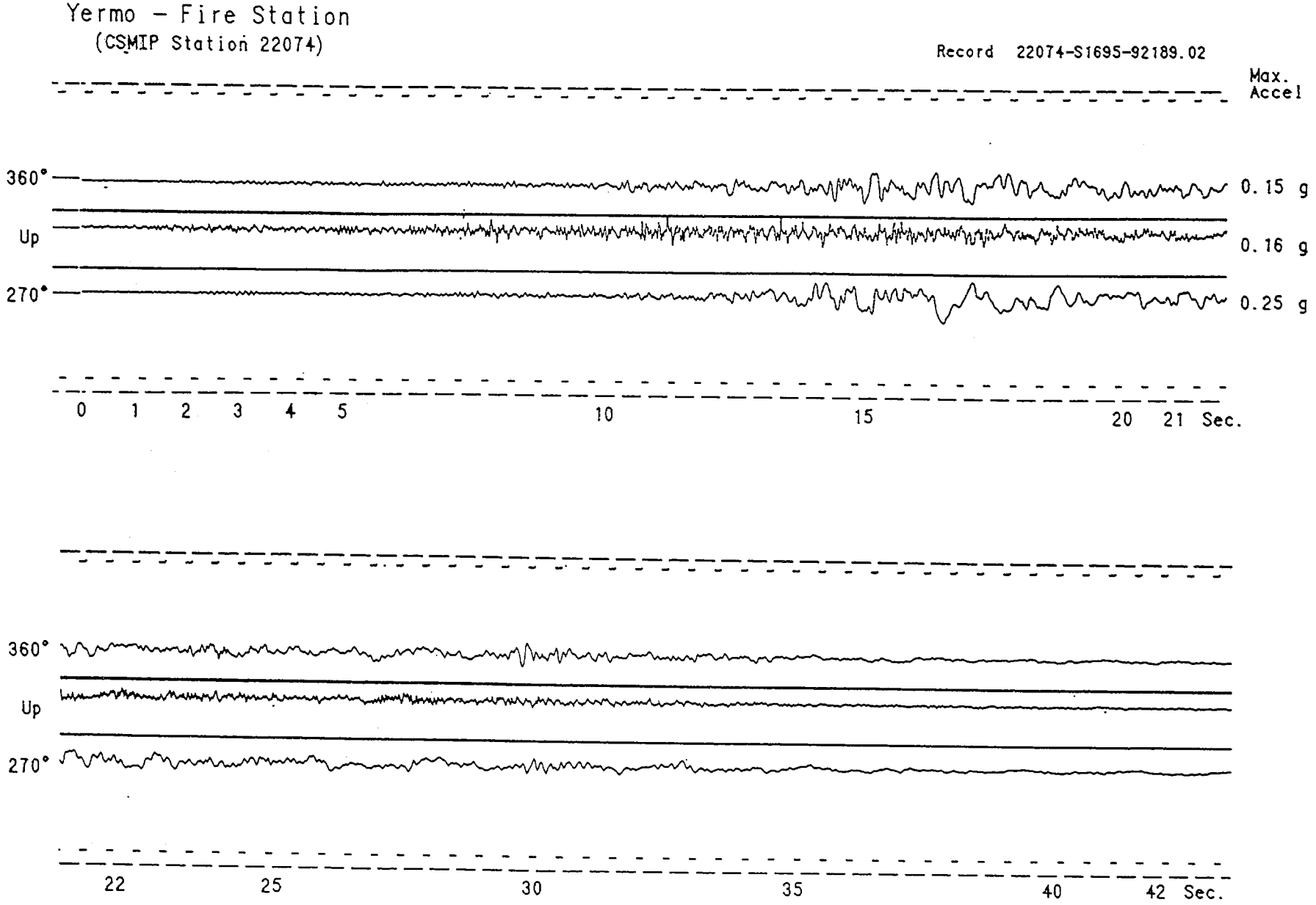


Figure 4. CSMIP record from Yermo station, No. 074 in Fig. 1, (from Shakal and others (1992).

Theme 3

Corps of Engineers Research Program on Concrete Dams

by

Robert L. Hall, Ph.D.* and
William E. Roper, Ph.D., P.E.**

ABSTRACT

The Corps of Engineers is scheduled to begin an earthquake engineering research and development effort called the Earthquake Engineering Program (EEP) in September of 1994. The EEP will address needs in the general areas of earthquake ground motions and site characterization, material behavior, and the seismic response of concrete dams. The priorities of the EEP have been established by both structural and geotechnical field review groups consisting of the Corps' premier engineers who are actively designing new facilities or the remediation of existing facilities. The EEP will use research from other Government organi- zations, universities, or agencies involved in seismic research. The objectives of the program are to: (1) develop practical, more effective seismic design procedures where they are now missing, (2) reduce the uncertainty in our seismic safety assessments and avoid costly defensive design, (3) reduce the risk of catastrophic failure of Corps hydraulic structures, primarily dams, and (4) save money on new construction and remediation efforts. This paper describes the Corps' recent experiences in designing a criterial hydraulic structure, identifying the remediation of an existing dam, and investigating the importance of nonlinear responses.

KEYWORDS: concrete dams; earthquake engineering program; nonlinear response; reservoir bottom absorption.

1. INTRODUCTION

The Corps of Engineers, as well as other organizations, has sponsored only limited research in the area of earthquake engineering. The majority of the Corps' research has historically been in support of specific research to assist in a particular project. This procedure has resulted in delays of current projects in order to conduct the necessary research to properly address critical technical seismic needs. This method of funding seismic research resulted in the field offices recommending the funding of a new research and development program. The EEP will allow us to develop the necessary analytical tools to support the design and analysis of new hydraulic projects or the remediation of existing structures.

The EEP research and development effort (Roper, et al, 1992) addresses both the geotechnical and structural aspects of the

* U.S. Army Engineer Waterways Experiment Station, Vicksburg, MS 39180-6199
** U.S. Army Corps of Engineers, Washington, D.C. 20314-1000

seismic engineering of the Corps' hydraulic structures. Therefore, two field review groups were established to review the proposed programs developed by the Corps' Structures and Geotechnical Laboratories at the U.S. Army Engineer Waterways Experiment Station in Vicksburg, Mississippi. Each field review group consisted of engineers from field offices involved in the current design or remediation of the Corps' critical hydraulic structures. The research laboratories used their experience and contacts with other Government agencies and universities to ensure that the program would not duplicate any ongoing or planned research projects. The field review groups established priorities and identified other areas of needed research for both the structures and geotechnical areas. The field review group established the highest priority as research supporting the needs for reservoir dams.

The EEP was also closely coordinated with representatives from the Office of Chief of Engineers in Washington, D.C. The structures group solicited the assistance of the Civil Engineering Research Foundation (CERF), which is part of the American Society of Civil Engineers (ASCE). CERF's role was to ensure that the proposed structural research was a well-developed program which would develop the state-of-the-art design and analysis tools dealing with all aspects of concrete dams and appurtenant structures, would identify any ongoing or planned research which would either duplicate or complement the Corps' planned research, and would identify any possible opportunities to develop partnerships with the Corps to meet the objectives of the planned research program. The CERF report verified that the Corps program for concrete dams was a well-developed program that would generate new tools for design and analysis of concrete dams and would provide major accomplishments which would influence the U.S.'s ability to evaluate structures representing an important part of our infrastructure.

This paper presents the Corps' experiences and corresponding research needs in designing an inclined intake tower, remedying a concrete gravity dam, and developing guidance for nonlinear analysis of concrete dams.

2. REMEDIATION

The Folsom Project was designed and built by the Corps of Engineers during the period from 1948 to 1956. The concrete gravity section of the dam is located on the America River about 32.2-km upstream from the city of Sacramento, California, and serves as a drainage area of approximately 4,856 square km. A vicinity map of the Folsom Project is shown in Figure 1. The original controlling criterion used for establishing the section of the overflow concrete section was that the static resultant fall within the central 50 percent of the base and the sliding ratio not be greater than 0.85 under the extreme operating conditions and earthquake pseudo-static acceration of 0.05 g acting upstream. Tierra Engineering Consultants, Inc. (1983) performed a seismological study and determined that the maximum credible earthquake (MCE) for the project is an earthquake of Local Magnitude 6.5 at a distance of 15 km of the East Branch of the Bear Mountains fault zone. A

seismic stability study was performed to evaluate the dynamic response of Folsom Dam in the event of an MCE.

The seismic analyses of the critical cross section of the dam were conducted using the two-dimensional finite-element program, EAGD-84 (Fenves and Chopra, 1984). This program determines the time-history response of the dam from specified earthquake ground motions with the simultaneous effects of dam-water interaction, dam-foundation rock interaction, and reservoir bottom absorption included. Water compressibility is also included since this component can have a significant effect on the earthquake response of a concrete dam. The dam monolith is idealized using four-node nonconforming planar finite elements, while the foundation rock supporting the dam is represented as a homogeneous, isotropic, viscoelastic half-plane. Dissipation of strain energy in the concrete is modeled with a constant hysteretic damping factor. The viscous damping ratio for all natural vibration modes of the concrete dam, on a rigid foundation with no reservoir, is taken as a constant hysteretic damping factor of twice the viscous damping ratio. The frequence-dependent stiffness matrix for the foundation rock, idealized as a viscoelastic half-plane, is defined at the nodal points of the dam. The ground motions are input at the base of the dam. The resulting solutions provide a reliable estimate of the maximum principal stresses of the concrete dam.

Ground motions representative of earthquakes that might occur near Folsom Dam were defined by two horizontal accelerograms, both having peak acceleration of 0.35 g. Vertical accelerograms were generated from the horizontal components by increasing the frequency constant by 1.5, and multiplying the amplitudes by 0.6. All analyses used gross or normal maximum reservoir pool elevations. The calculated stresses are most dependent on the foundation modulus and assumption of reservoir bottom absorption.

For a value of 0.78 for the reservoir bottom absorption and foundation modulus of 68.9 x 10^3 kp, an overall maximum principal stress of 6.01x10^3 kp was calculated to occur on the downstream face (Hall, et al, 1989). This stress state is located about where the vertical downstream face begins its transition to the inclined slope, and exceeds the maximum apparent dynamic tensile strength of 5.79 x 10^3 kp by 3.9 percent. To investigate the depth to which cracking may penetrate, envelope values of the maximum principal were prepared (Figure 2). For the worst case, the maximum apparent dynamic tensile strength is exceeded to a depth of about 0.7 m. For the conditions, it is concluded that the dam will maintain its structural integrity during and after a major earthquake.

However, if effects of reservoir bottom absorption are not included in the analysis, an overall maximum principal stress of 7.5 x 10^3 kp was calculated to occur on the downsteam face and exceed the maximum apparent dynamic tensile strength through the entire cross section. These results demonstate the importance of including the effects of reservoir bottom absorption. Current values of reservoir bottom absorption are based on the mis-

match of impedance, assuming a one-dimensional wave propagation between the reservoir and the reservoir bottom material. Further research is required to better define the effects of the reservoir bottom absorption and procedures to determine values to model the interaction between the reservoir and the reservoir bottom material.

3. NONLINEAR BEHAVIOR

The Corps of Engineers' Engineer Technical Letter (ETL) 1110-2-303 outlines a sequence of analyses of concrete gravity dams subjected to the MCE. The first step is a two-dimensional (2-D) linear-elastic response spectrum or time-history analysis with 5 percent of critical viscous damping. This analysis may include the effects of hydrodynamic loads, foundation flexibility, and absorption of the reservoir bottom. The stresses from this analysis are used for design or remediation unless the tensile stresses exceed 15 percent of the ultimate compressive strength of the concrete. If tensile stresses exceed this state of stress, adjustments are made in the assumed damping to account for some cracking of the concrete. These different levels of damping are assumed to account for the nonlinear material behavior of concrete and to produce a conservative result (Hall, 1990).

Mlakar (1986) evaluated this procedure by performing a material nonlinear analysis of three different dams of different heights subjected to two different earthquake records. The ground motions and the reservoir-structure dynamic interaction were modeled with the ADINA 84 general-purpose, finite-element program. The N65W and vertical components of the 1966 Parkfield, California, earthquake recorded at Temblor No. 2 Station were used for each analysis. The records from this earthquake were chosen because the peak ground accelerations and frequency content are representative of strong ground motions. The nonoverflow cross sections selected were characteristic of the Corps' population of concrete gravity dams. All foundations were assumed rigid. The shortest section analyzed represented the Richard B. Russell Dam on Savannah River in Georgia. This structure is 56.4 m high and has a modulus of elasticity of 20.6×10^6 kp. The finite-element grid contains 65 elements and 247 nodes, providing 594 degrees of freedom. The 2-D cross section experienced no nonlinear behavior when subjected to the Parkfield ground motions. The magnitude of the ground motions was tripled in order to determine the nonlinear response of this gravity dam. Figure 3 shows the cracked regions of the dam due to the tripled Parkfield accelerations. The second gravity dam modeled has a height of 91.4 m, but it is not representative of a particular dam. The previous finite-element grid was modified to model this geometry. The nonlinear analysis showed two cracked zones on the downstream surface at the elevation of slope change and at a slightly lower elevation (Figure 4). These cracks progress to the upstream face. An examination of the elastic ETL procedure for this situation reveals no indication of cracking above the base of the dam. The third dam analyzed was the Dworshack Dam on the Clearwater River in Idaho. This gravity dam is 194.5 m high and it has an estimated modulus of elasticity of 34.5×10^6 kp. This structure was chosen to represent the tallest dam

owned by the Corps of Engineers. The finite-element model of this dam has 80 elements and 363 nodes, with 726 degrees of freedom. The nonlinear analysis indicates a cracked zone which transcends the cross section of the elevation of the change in downstream slope (Figure 5). Cracking was also indicated at the upstream edge of the base.

Fenves performed a nonlinear seismic analysis of the tallest (122 m) nonoverflow monolith of the Pine Flat Dam. The finite-element model of the structure consists of 162 nodes, comprising 136 quadrilateral elements with a total of 315 degrees of freedom. The finite-element model of the impounded reservoir water extends upstream 365 m from the dam and consists of 224 constant-pressure elements. By modeling the reservoir, the analysis accounts for the interaction between the reservoir and dam. Stiffness proportional damping was used to provide 5-percent critical damping of the fundamental frequency, and a modulus of elasticity of 22.4 x 10^6 kp was used. The S69E component of the 1952 Taft ground motion was taken as a horizontal component acting in the upstream-downstream direction. The peak ground acceleration from these ground motions was 0.18 g.

When the reservior was empty, the Taft ground motion had to be scaled up by a factor of 2.5 to an acceleration of 0.45 g in order to initiate cracking. However, when the reservoir was assumed full (116 ft), the nonlinear analysis indicated cracking from unscaled Taft ground motions. The cracking occurred at the head of the dam where a stress concentration existed because of the assumed rigid foundation. When ground motions were scaled to 0.27 g, cracks were shown to propagate further along the base. When ground motions were scaled to 0.36 g, cracking also occurred on the downstream slope where the change in the slope occurred. The extensive cracking led to a numerically unstable solution, which indicates that stability analyses are needed.

These nonlinear analyses clearly indicate the importance of the nonlinear material response of the Pine Flat Dam to these ground motions. The ETL criteria appeared to be reasonably accurate for these five analyses. However, the procedure needs further investigation because there is no theoretical basis for assuming that tensile cracking results in increased energy dissipation, which is implied by greater damping ratios.

The Panel of Earthquake Engineering for Concrete Dams Committee on Earthquake Engineering, Division of Hazard Mitigation, through the National Research Council, has completed a publication entitled "Earthquake Engineering for Concrete Dams: Design, Performance, and Research Needs" (NCR, 1990). This publication presents details for needed research in the nonlinear seismic response of concrete dams.

Nonlinear capabilities are important in determining the seismic stability of concrete gravity dams. The capability to develop a complete program as described above is beyond the single capability of the Corps of Engineers. However, the Corps can strategically use the research being performed through other organizations to answer these complex issues and develop the necessary tools and

criteria. Nonlinear analysis will provide the necessary insight for the development of reliable cost-saving earthquake-resistant designs.

4. INCLINED INTAKE TOWER

The proposed Seven Oaks Project will be located in the Upper Santa Ana River Basin with the primary purpose of flood control. It is a part of the Santa Ana River (California) Mainstream Project (Figure 7). The dam is to be located 56.3 km upstream from the existing Prado Dam. The project will consist of a 182.9-m-high earth- and rock-fill dam and a complex outlet system consisting of an inclined intake structure, a regulating outlet gate chamber encased in the rock abutment, and adjoining tunnels which will carry the water through the abutment. The intake structure has an inclined geometry due to the severe seismic threat in this area. The dam will be constructed in a region of high seismicity between the two branches of the San Andreas Fault. The site is located approximately 2 km upstream from the mouth of the Santa Ana River Canyon near the South Branch of the San Andreas Fault. According to the Corps of Engineers assessment, the North Branch of the Fault crosses the future reservoir about 1 km upstream from the dam site.

The outlet works for the Seven Oaks project consist of an inclined intake structure, a pressurized conduit leading to the regulating outlet gate chamber (which includes a vertical air shaft), a downstream (unpressurized) tunnel consisting of a channel and access system downstream of the gate chamber, and the plunge basin. This system is designed to pass regulated flows ranging from 0.085 cubic meters per second (cm/s) to 198 cm/s and diversion flows up to 36.8 cm/s. The intake structure has a vertical height of over 60.96 m. This structure will be inclined against the rock abutment at an angle of approximately 14 degrees from the vertical. The structure foundation measures approximately 17.45 m in the upstream-downstream direction by 20.12 m in the cross-stream direction. The base is to be completely embedded in the rock foundation.

The seismicity for the proposed site of the Seven Oaks Dam is described in Reference 2.

Both response spectra and time-history calculations were conducted. The structure and rock are represented by a three-dimensional (3-D) finite-element model shown in Figure 6. The model consists of two primary parts, the structure model and the rock model. These two models have common nodes at the interface. The forces at these nodes are assumed to be the forces which would be required to restrain the structure and prevent separation from the rock. The model consists of a total of 6,108 nodes, having a total of 15,585 degrees of freedom. The intake structure portion of the model contains 2,545 3-D solid elements and 190 beam elements. Due to the very complex nature of the structure/rock system, it is difficult to fully understand the interaction of the two. Prior analyses using a nonlinear contact surface between the structure and a rock continuum model have shown that there is the likelihood of at least some separation of the structure and rock if the structure is not rigidly attached. Any appreciable

separation should be considered dangerous due to the enormous masses involved. The conclusion is that the structure should be rigidly tied to the rock abutment (Johnson and Hall, 1992).

For a free-standing tower, effects of water in the reservoir can be very significant. For the situation represented by the Seven Oaks system (water on three sides), the contribution to structure response of the surrounding reservoir water is much less understood. The general Westergaard procedure was initially used in determining added water masses.

The analyses to date have included a very in-depth study of structure response for both response spectra calculations and time-history analyses. The initial studies using Westergaard added mass approach resulted in an overly conservative design for the required anchorage necessary to connect the tower to the rock abutment. By developing a finite-element model of the reservoir to solve the reservoir-structure interaction problem, forces were determined which allowed the design of this critical hydraulic structure.

This analysis demonstrated the need for the following:

- Finite-element grid generation tools specifically for intake tower.
- Research in modeling the contact surface between the structure and rock abutment.
- Easy-to-use tools for determining hydrodynamic force.
- Research to develop procedures to model 3-D ground motion.
- Research to study ductility of reinforced hydraulic structures.
- Research to study the nonlinear behavior of these critical structures that are subjected to the MCE.

5. CONCLUSION

The seismic analysis of concrete dams and their appurtenant structures has progressed to use elastic-numerical modeling. It is critical that research be performed to include the effects of both material and geometric nonlinearity in order to predict the response of these structures subjected to ground motions from an MCE. The formalization of national and international partnerships is needed to perform the necessary material testing, structural model testing, prototype testing, and development of numerical procedures and probability-based design criteria. The research resulting from the partnerships would produce the knowledge and tools necessary to accurately evaluate the seismic performance and safety of concrete dams and their appurtenant structures.

6. REFERENCES

1. Bolt, Bruce A. (1987). "Seismological Report for Seven Oaks Dam for Santa Ana River Basin, California, for Geotechnical Branch, Los Angeles District Corps of Engineers," Contract Report DACW 09-87-M-1734.

2. Fenves, G. (1987). "Earthquake-Induced Cracking in Concrete Gravity Dams," American Society of Civil Engineers.

3. Fenves, G., and Chopra, A. K. (1984). "EAGD-84: A Computer Program for Earthquake Analysis of Concrete Gravity Dams," Report No. UCB/EERC-84-11, Earthquake Engineering Research Center, University of California, Berkeley, CA.

4. Fenves, G., and Chopra, A.K. (1984). "Earthquake Analysis and Response of Concrete Gravity Dams," Report No. UCB/EERC-84/10, Earthquake Engineering Research Center, College of Engineering, University of California, Berkeley, CA.

5. Hall, R. L. (1990). "Nonlinear Seismic Response of Gravity Dams," Eighth ASCE Structures Congress.

6. Hall, R. L., Woodson, S. C., and Nau, J. M. (1989). "Seismic Stability Evaluation of Folsom Dam and Reservoir Project Report 3, Concrete Gravity Dam Report," GL-87-14, p 214, U.S. Army Engineer Waterways Experiment Station, Vicksburg, MS.

7. Johnson, W. G., and Hall, R. L. (Draft). "Seismic Analysis of Seven Oaks Inclined Intake Tower," SL-92, p 491, U.S. Army Engineer Waterways Experiment Station, Vicksburg, MS.

8. Mlakar, P. F. (1986). "Nonlinear Response of Concrete Gravity Dams to Strong Earthquake-Induced Ground Motion," Technical Report SL-87-7, U.S. Army Engineer Waterways Experiment Station, Vicksburg, MS.

9. National Research Council (1990). Earthquake Engineering for Concrete Dams: Design, Performance, and Research Needs, National Academy Press, Washington, D.C.

10. Tierra Engineering Consultants, Inc. (1983). "Geological and Seismologic Investigations of the Folsom, California, Area," Contract Report DACW 05-82-C-0042, U.S. Army Engineer District, Sacramento, CA.

11. Roper, W. D., Hynes, M. E., and Davidson, R. F. (1992). "U.S. Army Corps of Engineers Earthquake Engineering Research Program," Wind and Seismic Effects Proceedings of the 24th Joint Meeting.

12. U.S. Army Corps of Engineers, "Earthquake Analysis and Design of Concrete Gravity Dams," ETL No. 1110-2-303, Washington, D.C.

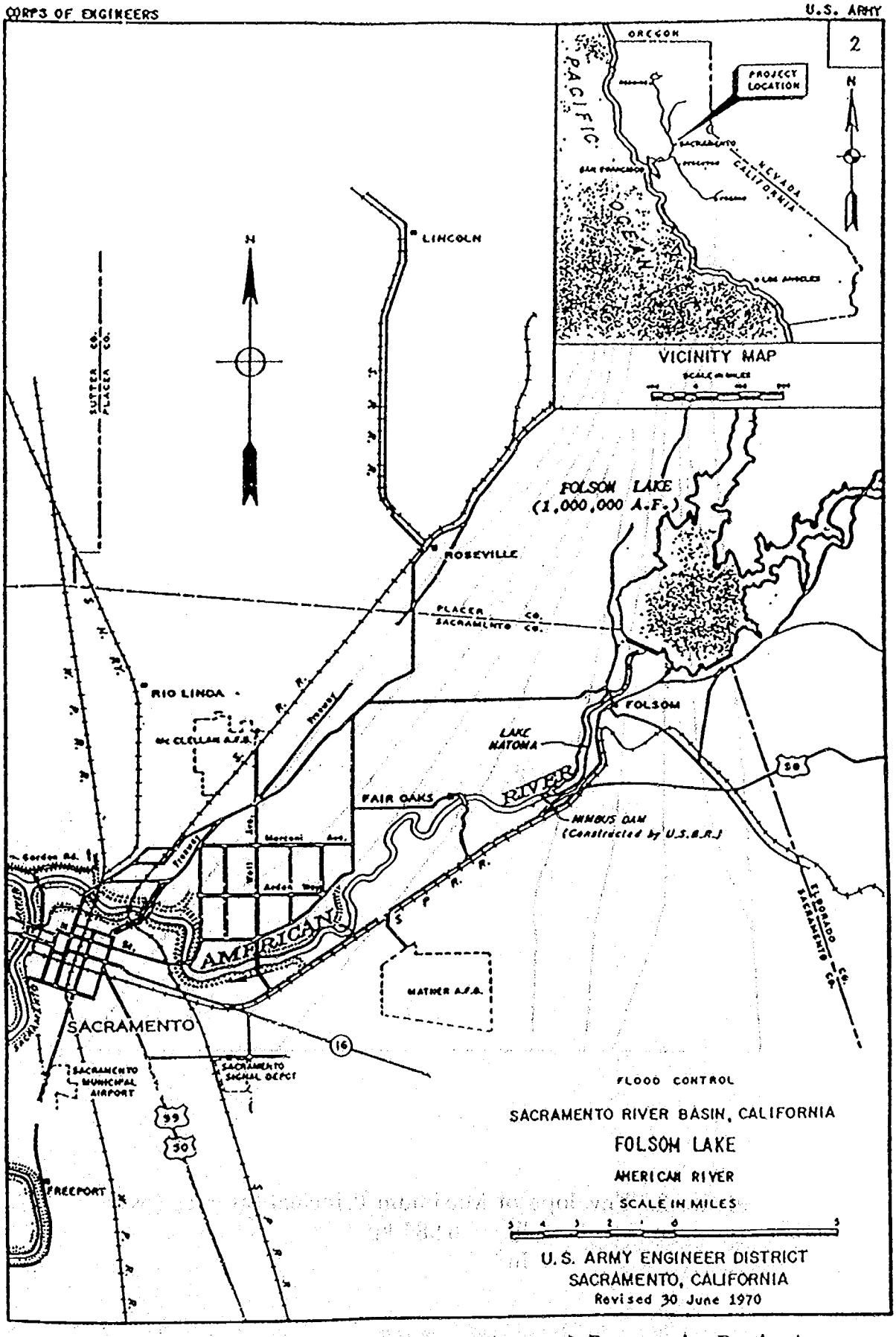


Figure 1. Location of Folsom Dam and Reservoir Project

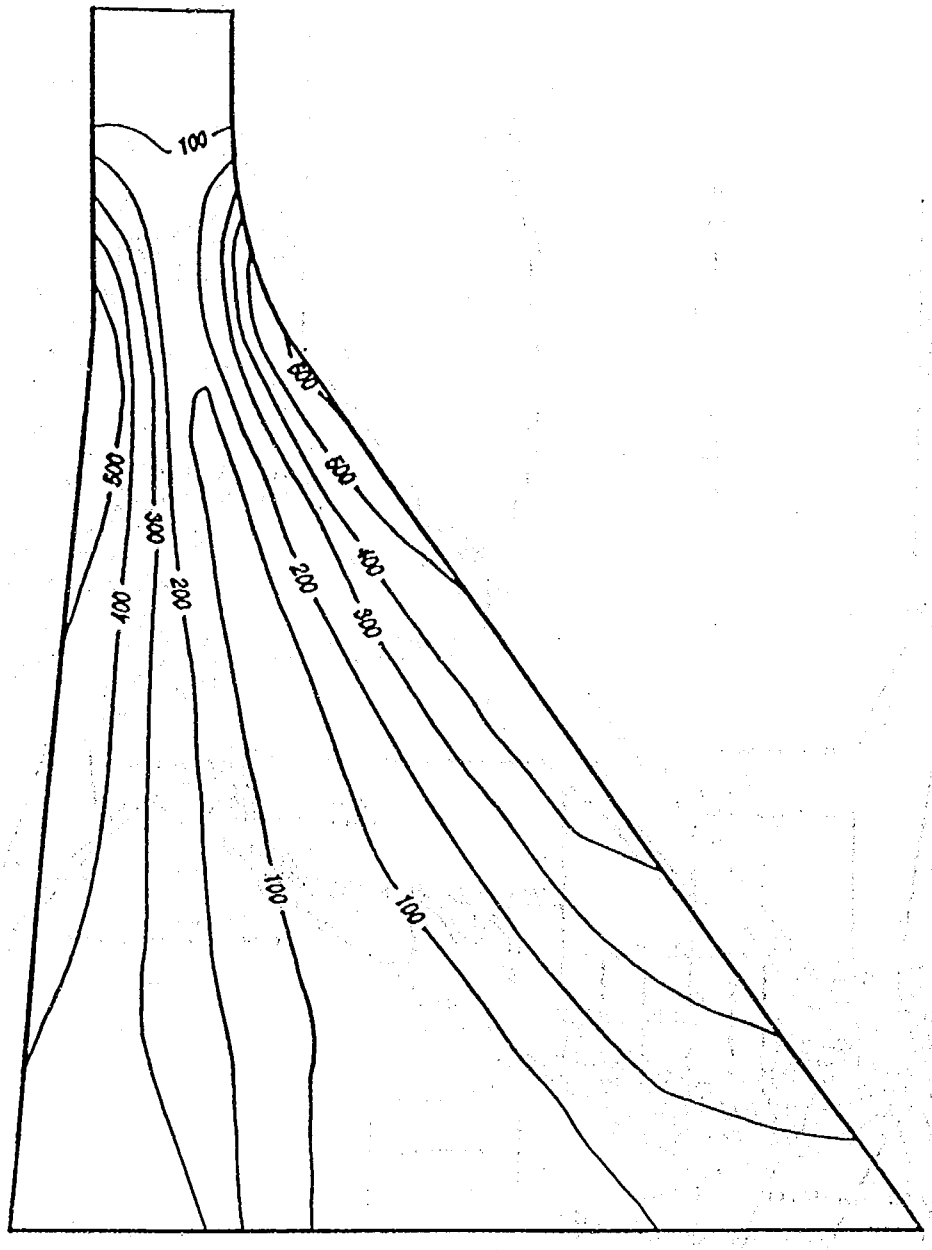
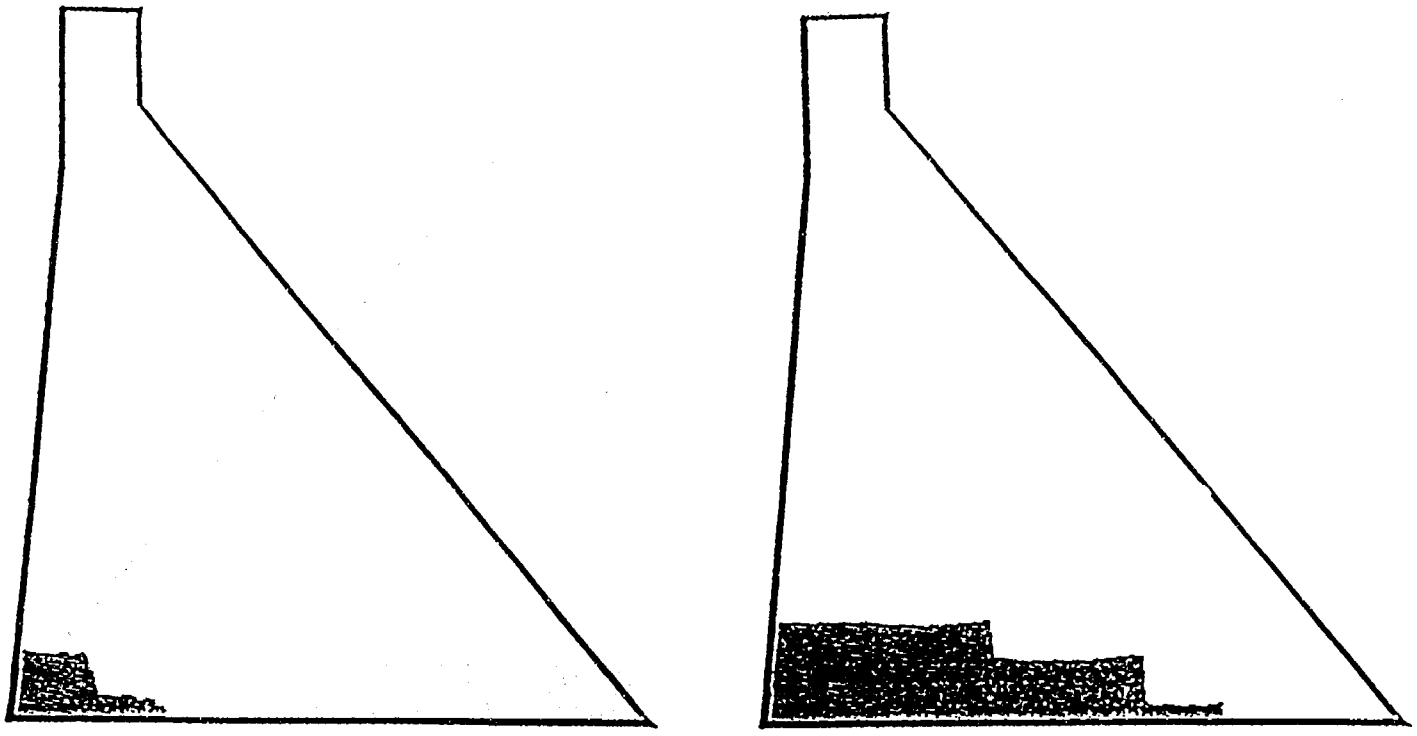


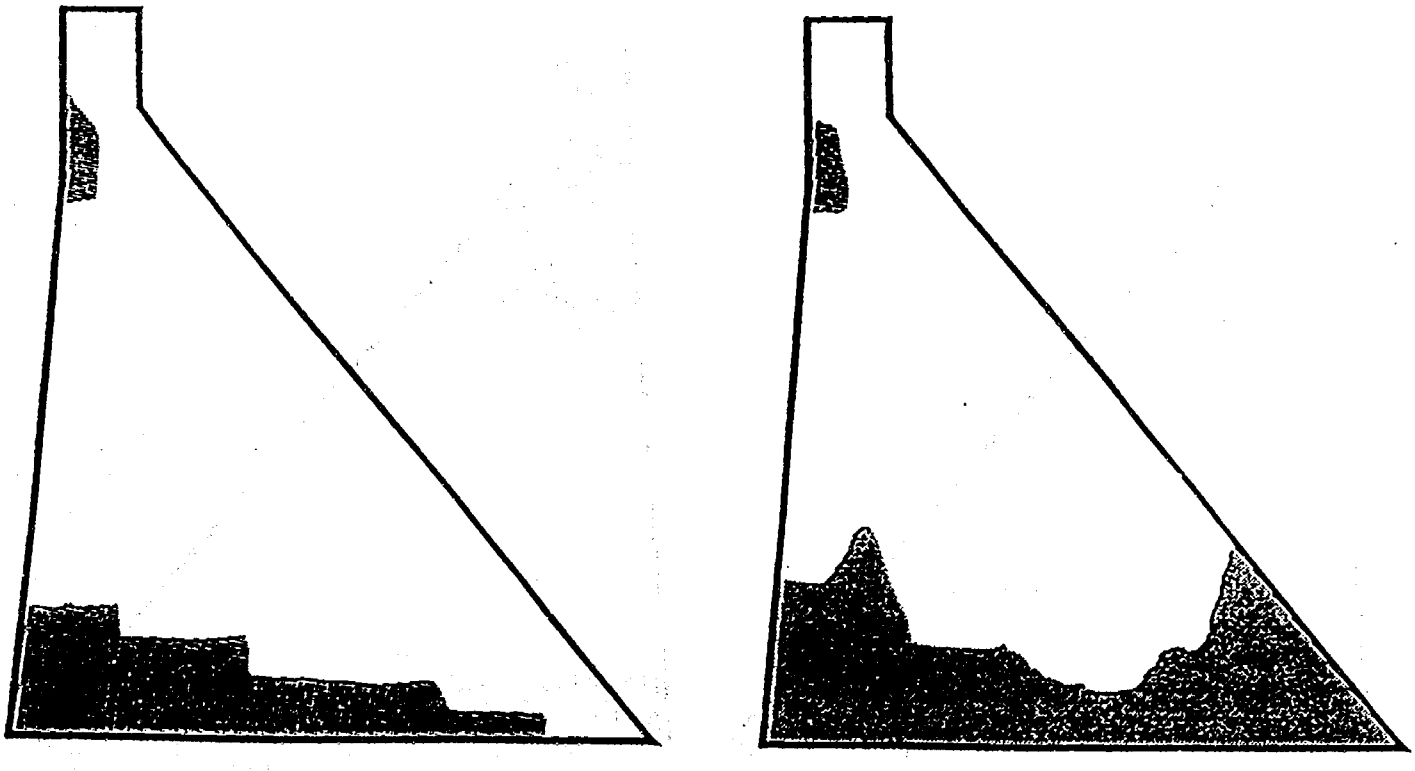
Figure 2. Envelope of Maximum Principal Stresses (psi)

$\frac{lb}{in.^2}$ = 6.984 kp



(a) t = 3.84 sec.

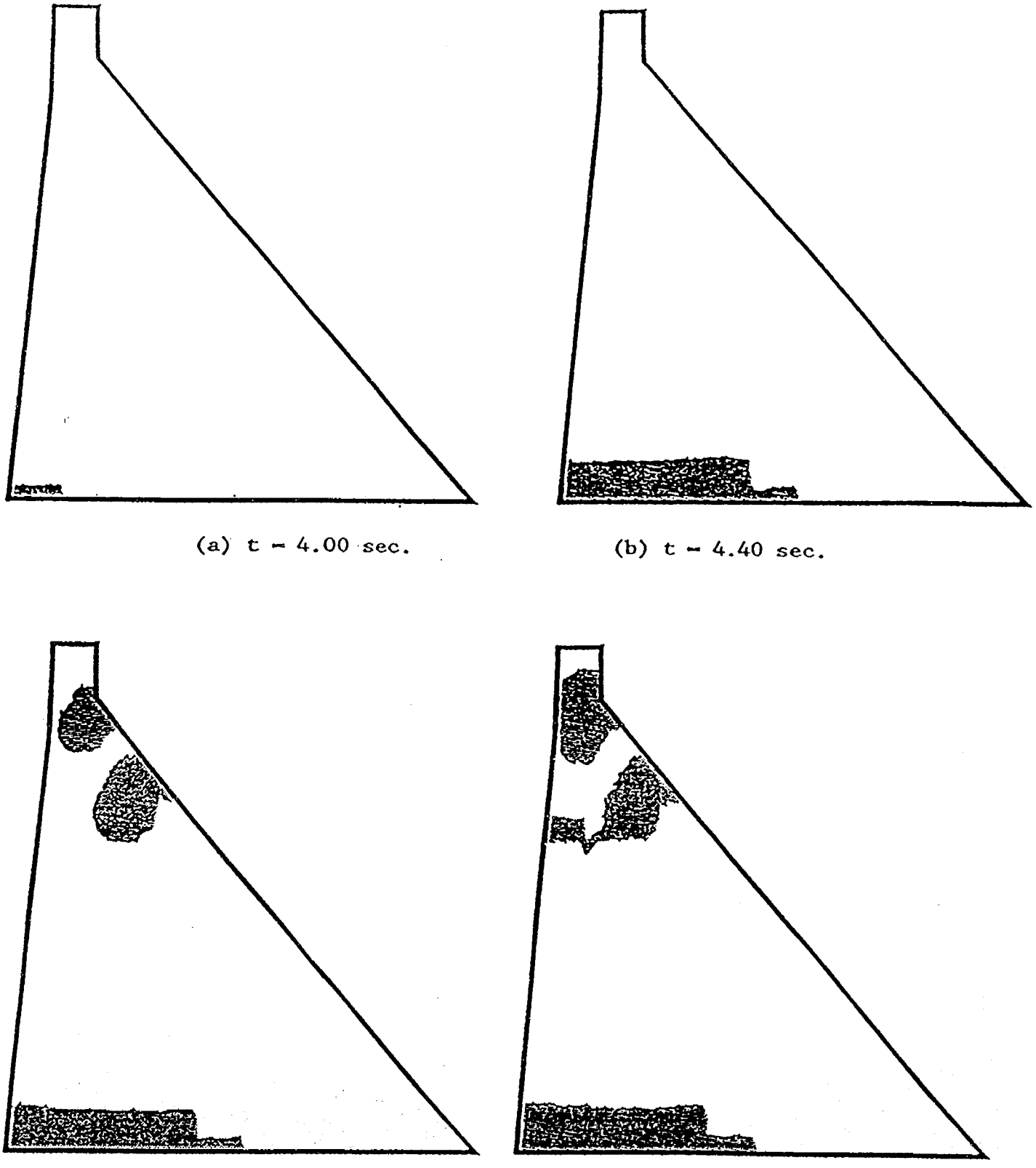
(b) t = 3.92 sec.



(c) t = 4.02 sec.

(d) t = 4.04 sec.

Figure 3. Cracked zones of Russell Dam with tripled Parkfield loading



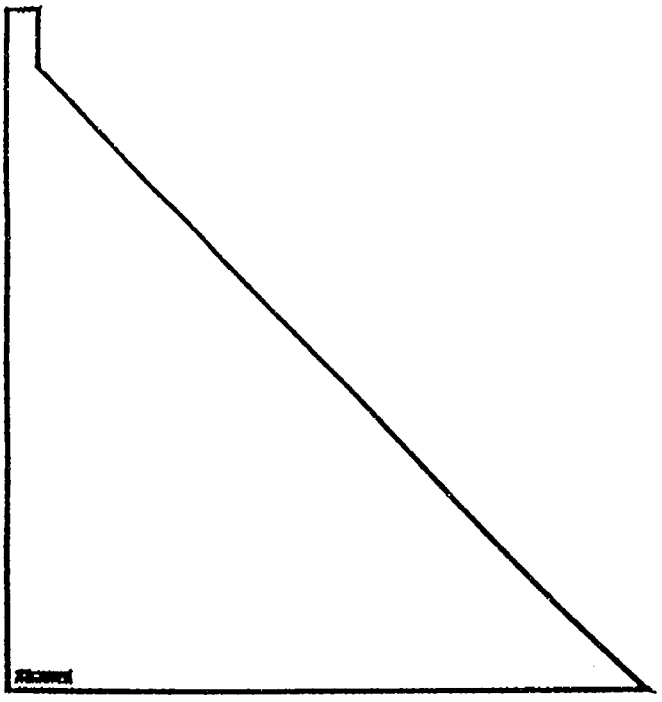
(a) t = 4.00 sec.

(b) t = 4.40 sec.

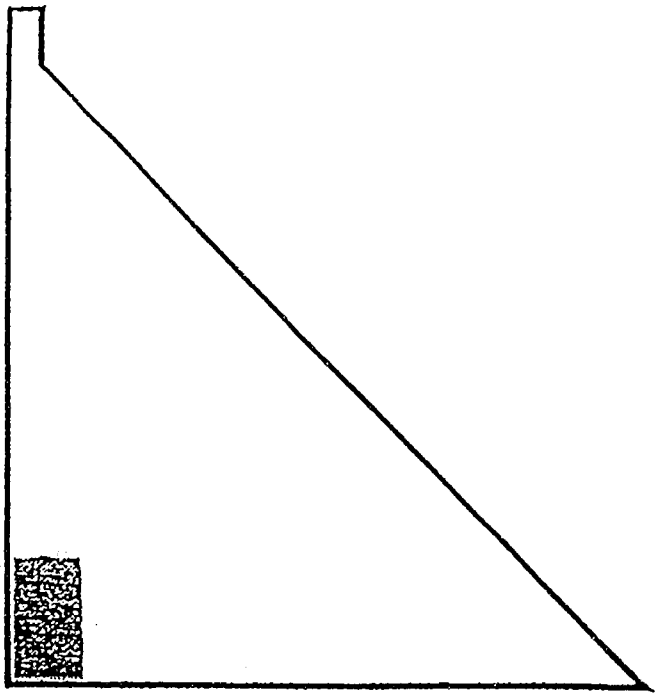
(c) t = 4.48 sec.

(d) t = 4.56 sec.

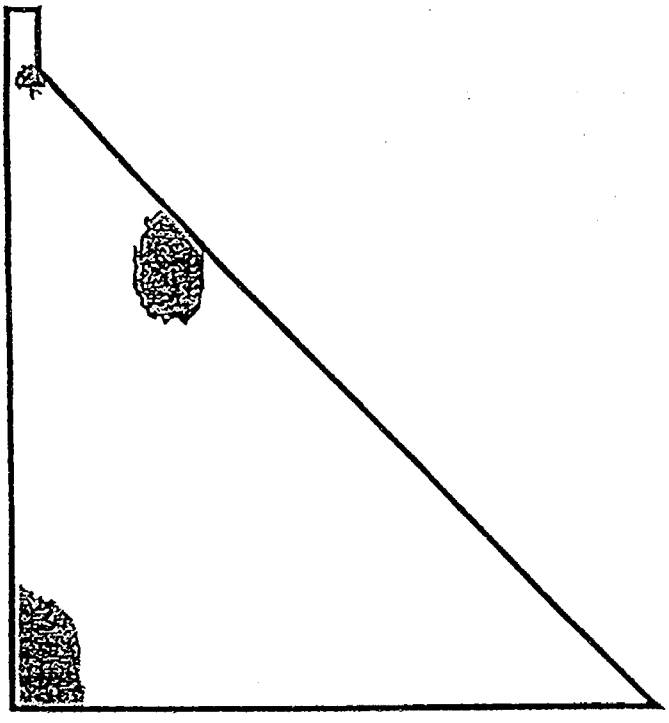
Figure 4. Cracked zones of Standard Dam



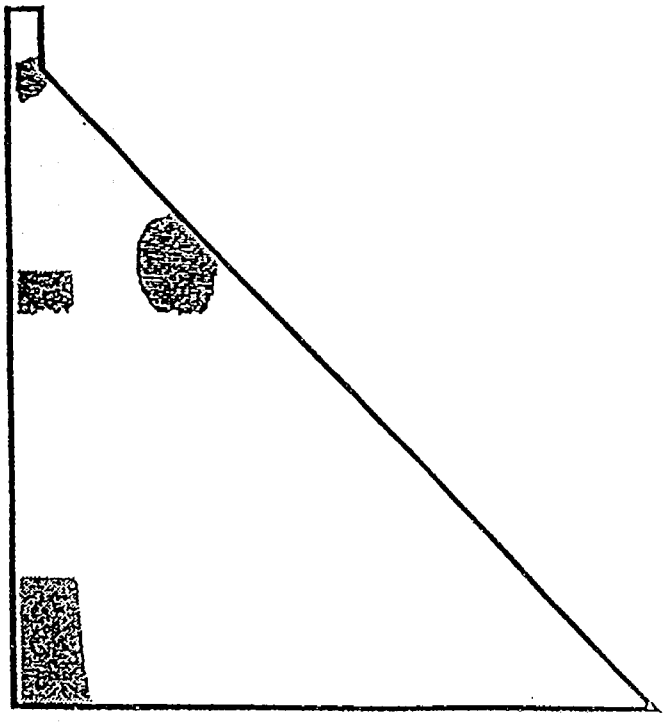
(a) t = 4.04 sec.



(b) t = 4.16 sec.



(c) t = 4.24 sec.



(d) t = 4.40 sec.

Figure 5. Cracked zones of Dworshak Dam

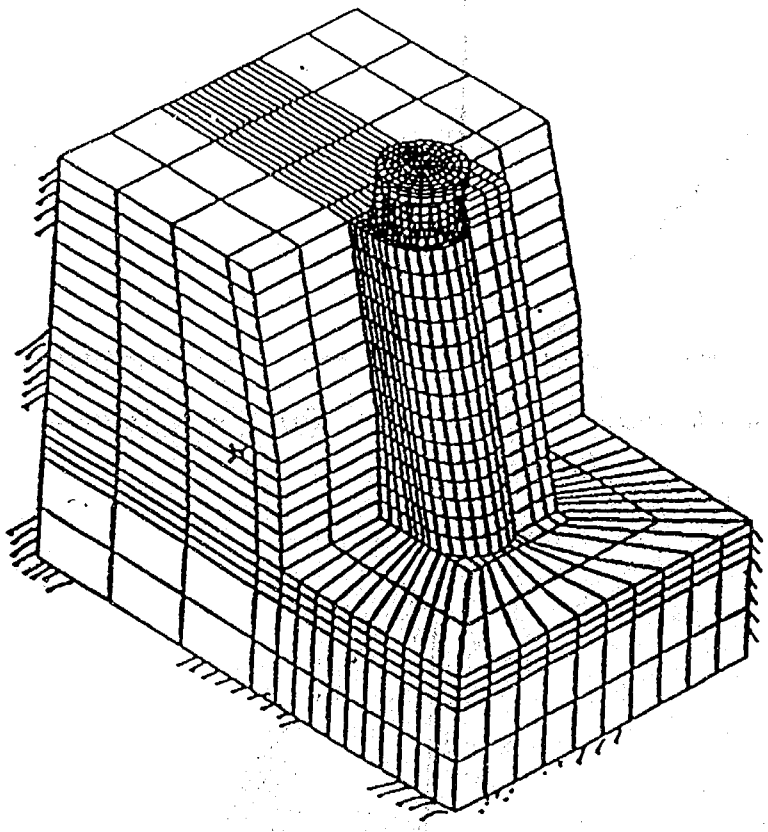


Figure 6. Finite element model

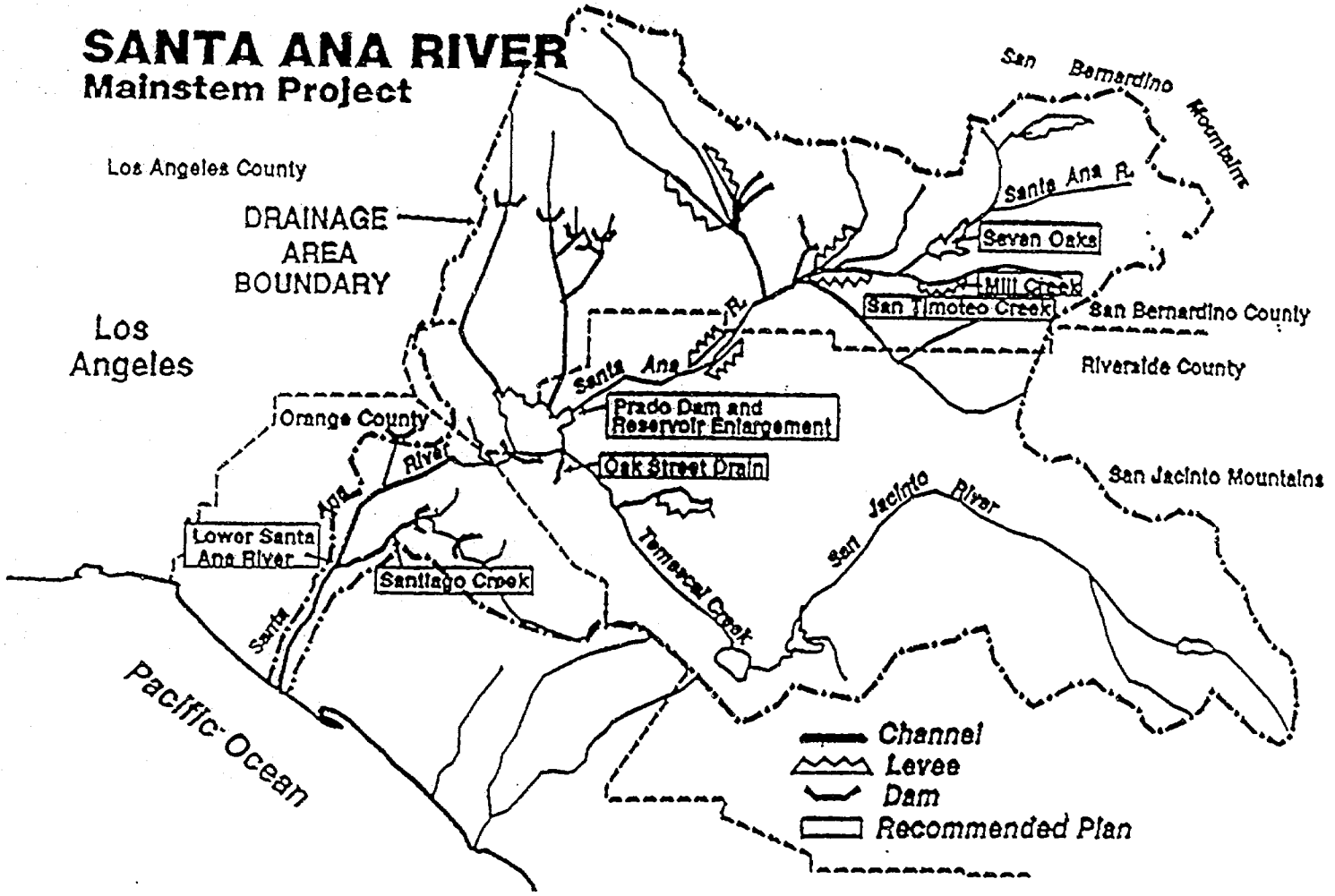


Figure 7. Santa Ana River Mainstream Project

STIFFNESS OF ROCKFILL MATERIALS IN LABORATORY AND IN-SITU TESTS

by
Akira NAKAMURA*1
Nario YASUDA*2

ABSTRACT

Stiffness of rockfill materials in very small strain range was investigated by comparing the results obtained from monotonic and cyclic loading laboratory tests, and those obtained from geophysical exploration and PS-logging in the field. Using a precision linear variable differential transformer (LVDT) for displacement, elastic moduli in very small strain ranges of rockfill materials were measured in monotonic and cyclic loading triaxial tests. It was found that the test results showed a high degree of correspondence. Shear modulus of rockfill materials, which was obtained from a monotonic loading torsional simple shear test, and that from a cyclic loading torsional simple shear test also showed good correspondence. Furthermore, the stiffness from in-situ tests in rockfill dams nearly corresponded with the stiffness from a large-scale triaxial tests in the laboratory.

KEYWORDS; Stiffness, embankment dam, rockfill materials, laboratory test, in-situ test

1. INTRODUCTION

For analysis of the behavior of soil structures using coarse grained granular materials (rockfill material), such as rockfill dams and reclaimed islands during earthquakes, the dynamic physical properties of rockfill materials in very small strain range must be known. Evaluation of deformation characteristics and understanding of the stiffness of in-situ ground in minute strain ranges are especially necessary for the design of soil structures (Burland 1989). However, in order to obtain the dynamic physical properties of rockfill materials from laboratory tests, highly precise and large-scale apparatus for cyclic loading tests are required. The number of cases studied is less than that of laboratory tests using sandy soil. This paper will examine the dynamic deformation characteristics of rockfill materials by laboratory tests and it is assumed to be a profitable for dynamic analyses of soil structures.

Monotonic loading tests are conducted on regions of elastic to plastic states attended the state of failure (axial strain ε_a = 0 - 0.15). Monotonic loading tests may include cyclic loading tests on very small strain ranges. As Teachavorasinskun *et al.*(1990,1991) have pointed out, the correspondence in the results of monotonic and cyclic loading tests in minute strain ranges is noticeable. This signifies that not only the strength property of a material but also its dynamic physical property is obtainable by a monotonic loading test alone, leading to simplification of laboratory tests.

This paper will introduce methods of cyclic and monotonic loading tests in the laboratory, focusing on the physical properties of rockfill materials at very small strain ranges. Comparative studies which have been pursued on the deformation characteristics of rockfill materials at very small strain ranges will also be examined.

Comparison on shear moduli for very small strain ranges from laboratory and in-situ experiments is important in conventional and precise investigation of ground stiffness by laboratory tests. Powell *et al.*(1991) obtained the stiffness at very small strain by laboratory and in-situ tests using undisturbed specimens for six sites of cohesive soil ground and indicated that both values show very good correspondence.

When the maximum shear modulus at a very small strain range, G_{max} (G_o), derived from a laboratory test, and the shear modulus G_f, derived from in-situ elastic wave velocity, are compared, G_{max} was estimated to be smaller than G_f due to inevitable turbulence in specimens at the time of sampling from sand and cohesive soils. Kokusho (1989) reported that this tendency increased in proportion to the increment of G_f. However, Tatsuoka *et al.* (1990) attributed the difference of the results of the in-situ and laboratory tests to the inaccurate measurement of the very small axial strain, deformation characteristics being defined at too a large strain level, and the non-negligible effect of bedding errors during the preparation of the specimen. They proposed a new method for measuring axial strain, conducted laboratory and in-situ tests using a sedimentary soft rock, and reported that the shear moduli at very small strain in both tests showed correspondence.

*1 Head, Fill-type Dam Division Dam Department, Public Works Research Institute, Ministry of Construction, Tsukuba City, 305 Japan
*2 Chief Research Engineer, ditto

In this study, the relation between G_{max} and G_f of rockfill materials was investigated, since construction procedures of in-situ structures and preparation procedures of specimens were estimated to be equal in rockfill dams. As a rockfill dam is compacted by heavy machinery, a laboratory specimen was tamped by an electric vibratory hammer. First, in-situ geophysical exploration for two rockfill dams were made, and elastic wave velocities for each depth were obtained. Secondly, large-scale cyclic triaxial tests, in which the deformation property at a very small strain range is measurable, were conducted for rockfill materials brought into the laboratory from quarry sites of these dams. Then, elastic wave velocity obtained from G_{max} in a cyclic loading test was compared with the in-situ elastic wave velocity.

2. RELATIONSHIP BETWEEN MONOTONIC AND CYCLIC LOADING TESTS

2.1 laboratory test apparatus

The specimen size of a large-scale triaxial testing apparatus is 30 cm in diameter and 60 cm in height as shown in Fig.1. Its loading method adopts the electric hydraulic servo system, which allows for normal monotonic and cyclic loading tests by strain and stress control condition. Friction around loading rod for axial load was reduced by a bearing guide between a bearingstand and the rod. By using a compensation chamber for the section-area of a loading rod, the prevention of rod floating and compensation for penetration volume of a rod during consolidation are possible.

Axial compression and extension loads were measured by a waterproof load cell which was attached to the cap of the specimen. Micro axial strain was measured, as shown in Fig.2, by a waterproof linear variable differential transformer for displacement (Matsumoto *et al.* 1991). Axial displacement was derived by averaging values measured by displacement transformers installed diagonally at two points on a specimen cap. This procedure can eliminate errors due to mechanical friction, hysteresis and the specimen's eccentricity, which appear in conventional displacement transducers, and highly precise minute displacement could be measured. In monotonic loading tests, besides minute displacement, large strain extending to failure was measured by a displacement transformer with a large capacity set on a piston rod outside of a triaxial cell.

Analog signals from each transducer passed through amplifiers, were converted to digital signals after they passed through a low-pass filter of 10 Hz, and were entered into a personal computer at 100 Hz for cyclic loading tests and 500 Hz for monotonic loading tests. High-speed sampling of at least 100 Hz is necessary for measuring the very small strain. Specifications for main transducers are shown in Table 1.

2.2 Materials and testing methods

Materials with the maximum grain size D_{max} = 63.5 mm used for tests were sandstone (angular material) and riverbed gravel (round material) and were adjusted so as to be similar to the grain size distributions in the field. A grain size distribution curve is shown in Fig.3, while the physical properties of the materials are shown in Table 2. Specimens were prepared by dividing samples into 6 layers, the grain size distribution of which was adjusted to be the same for each layer, spreading the air-dried materials uniformly into a mold for depolarization of grain size and then compacting the materials using an the electric vibratory hammer (950 blows/min., weight 320 N, diameter of loading plate 29 cm) to reach specified relative densities (Dr = 70 and 90 %). Two membranes with 4mm thickness were used in this study.

All tests were conducted in non-saturated (air-dried) conditions and consolidated drained states under the conditions shown in Table 3. The procedure of cyclic loading tests is shown in Fig.4 (stage test). Specimens were consolidated under the specified confining stress. After the completion of consolidation, cyclic load of 0.2Hz was increased in stages (cyclic loading was repeated 12 times for each step and the 10th data were adopted as the result). When the generated strain reached a level of around 5 x 10^{-4}, the next confining stress was applied to the specimen and the same procedure was repeated.

In monotonic loading tests, failure strength was confirmed by continuous shearing force up to 15 % of axial strain.

2.3 Discussion

Since monotonic loading tests are conducted on subjects ranging from elastic regions to plastic regions (axial strain ε_a = 0 - 0.15), which extend to failure, and deformation characteristics from cyclic loading tests are concerned with very small strain ranges (ε_a = 10^{-6} - 10^{-3}), the monotonic loading test may include the cyclic loading tests. Therefore, if a relationship is found to exist between monotonic and cyclic loading tests in the strain ranges where they overlap,

testing can be simplified by estimating the dynamic physical property of the materials from monotonic loading tests alone. Therefore, the results of monotonic and cyclic loading tests were compared with each other by focusing on deformation characteristics of rockfill materials at very small strain ranges.

(1) Relation of deformation characteristic from monotonic and cyclic loading tests

According to Kondner (1963), a stress and strain relationship (see Fig.5) derived from a monotonic loading test can be approximated by the following hyperbolic curve:

$$[1]\quad \sigma_1-\sigma_3 = \varepsilon_a/(a + b\,\varepsilon_a)$$

Here, the values of a and b are constants depending on the type of soil material and axial strain velocities during a monotonic loading compression test.

Hardin and Drnevich (1972) used hyperbolic curve of Eq.1 by Kondner as a skeleton curve in modeling a stress and strain relationship obtained from a cyclic loading test. As shown in Fig.5, both the maximum elastic moduli E_o from monotonic loading test and elastic moduli E_A at an axial strain ε_A obtained from cyclic loading tests are estimated to agree with each other. Here, the results of two tests are compared on E_o and E_A.

(2) Results of comparison

The increase of cyclic number of loading at a shear strain level accompanying dilatancy in volumetric strain (over 1 x 10^{-3}) caused compaction of specimens with dry sand and increased the values of elastic modulus E and shear modulus G (Ishihara (1976)). This is called a stress history. In the cyclic loading tests conducted in this study, the maximum strain occurred was around the level of 5 x 10^{-4}, while the changed values of void ratios before and after the test were less than 0.01. Hence, compaction of specimens by cyclic loading did not appear to influence E and G values. Therefore, rockfill materials were estimated not to receive the influence of stress history in cyclic loading tests as well as in monotonic loading tests.

With a larger number of sampled data (one datum per 1/500 second), the comparison of the results from monotonic and cyclic loading tests was conducted on Toyoura sand, the initial void ratio e_o of which was equal to 0.65, as shown in Fig. 6.

The aforementioned maximum elastic modulus E_o at ε = 1 x 10^{-6}, calculated from the a value indicated by a section of a longitudinal axis of the relation curve of $\varepsilon_a/(\sigma_1 - \sigma_3)$ and ε_a, were obtained from a monotonic loading test. By increasing the sample number of data, elastic moduli E from a monotonic loading test were obtained up to a minute strain range less than ε_a = 2 x 10^{-6}. The E values from monotonic and cyclic loading tests showed good correspondence in the axial strain range 10^{-6} to 5 x 10^{-5} under confining stress σ_c = 0.2 and 0.4 MPa.

The comparisons of monotonic and cyclic loading test results on rockfill materials are described as follows.

A stress and strain relationship at a micro strain range in a monotonic loading test is shown in Fig.7. Precise values for elastic moduli were calculated for axial strain of around 1 x 10^{-6}, which shows a linear relation in strain range less than 1 x 10^{-5}. The maximum elastic modulus E_o was obtained by the least square method from the linear relation of $\varepsilon_a/(\sigma_1 - \sigma_3)$ and ε_a.

Incidentally, Duncan and Chang's method (1970) is known to obtain a maximum elastic modulus E_o, which is one of the influential physical property values of an embankment analysis of a filldam body. In this method, E_o is obtained from a linear section of a curve, in which the relationship between axial strain and the inverse numbers of elastic moduli (from a monotonic loading triaxial test) is plotted as shown in Fig.8.

Since E_o was obtained against a linear section of initial stress and strain relation, E_o values fluctuate greatly depending on axial strain range. The stress and strain relation obtained by measurement of very small strain shows a convex curve, and as Tatsuoka et al.(1992) have indicated, Duncan and Chang's method was not appropriate for calculating the maximum elastic modulus E_o at an very small axial strain range. In particular, caution is necessary to evaluate deformation characteristics E_o of soft rock foundation and improved soil with cement at very small strain, because E_o of these materials is very dependent on axial strain.

The relationship between shear strength $\tau_f(=(\sigma_1-\sigma_3)_{max}/2)$ at failure in a monotonic loading triaxial test and E_o is shown in Fig.9. The triangular symbols in the figure represent crushed angular rockfill materials, while the solid black circles illustrate round gravel materials. Linear correlation was seen between τ_f and E_o independent of initial void ratio and confining stress. As for the same shear strengths, the E_o value of round gravel materials was smaller than that of angular rockfill materials. As a cause, the effect of the difference in grain size distribution cannot be

neglected; furthermore, when specimens of similar relative densities and confining stresses were compared, shear strengths of both angular and round materials coincide with each other, leading to the assumption that differences in the particle shape were influenced by the differences in elastic moduli.

The relation between elastic moduli and axial strain obtained from monotonic and cyclic loading tests for angular rockfill materials and round gravel materials is shown in Fig.10, as illustrated in their relationship for Toyoura sand in Fig.6. For both materials, elastic moduli of monotonic and cyclic loading tests at minute axial strain show good coincidence regardless of confining stress.

A torsional simple shear test is one of the tests which simulate the stress and strain conditions in the field. From an engineering standpoint the in-situ stress and strain condition can be simplified by assuming that the magnitudes of shear stresses changes due to the earthquake loading with a) the rotation of principal stress axes and b) the cyclic simple shear deformation which is distributed uniformly in the height direction such as shear strain.

A static stress and strain relation within the dam body is a plane strain condition in which the strain in the direction of the dam axis is zero and the angle between the principal stress at the center of a dam body and a horizontal banking surface is in a state of flux (Matsumoto *et al.* 1990).

As in a triaxial test, the relationship between shear strain and shear stress in the monotonic loading test using a large-scale torsional simple shear testing apparatus is shown in Fig. 11. The cylindrical specimen has an outer diameter of 80 cm, an inner diameter of 40 cm and a height of 80 cm. The material used is gabbro rock from the quarry site of Sagurigawa Dam which was completed in 1992. The relative density of specimen is 85 % with grain size distribution indicated in Fig.3. Relationships of stress and strain in very small strain range were obtained with high precision for each confining stress and also showed a convex curve for strain ranges less than 4 x 10^{-5}. The relation between shear moduli G and shear strain γ_{at}, whose values were derived from both cyclic and monotonic loading tests, is shown in Fig. 12. A degree of correspondence was noted for shear strains less than 1 x 10^{-4}.

Teachavorasinskun *et al.* (1991) reported correspondence between shear moduli derived from monotonic and cyclic loading torsional simple shear tests using Toyoura and Hamaoka sands.

Fig.13 shows the relationship between the maximum elastic modulus E_o from the aforementioned monotonic loading test and the maximum elastic modulus E_{max} from a cyclic loading test. Relative densities were adjusted to 70 and 90 % for both angular and round rockfill materials. The figure shows that E_o and E_{max} nearly correspond with each other in the specimens of rockfill materials with 70 % of relative density, regardless of the shape of particle and the level of compaction. Fig.14 shows E_0 and E_{max} for monotonic and cyclic loading tests at axial strain of 2.0 x 10^{-4} respectively, E_{mono} and E_{cycl} are normalized at E_o and E_{max} for each confining stress. Specimens are angular rockfill materials with relative densities of 70 and 90%. As confining stress increased, the effect of stress history appeared more intensively, and E_{cycl} became larger than E_{mono}.

As mentioned above, in a minute strain range, elastic modulus from a monotonic loading triaxial test corresponds well with one from a cyclic loading triaxial test. This was also confirmed by shear moduli from a torsional simple shear test. Therefore, regardless of testing methods and the shape of particle, the elastic moduli obtained from a cyclic loading test can be estimated to a certain extent from the elastic moduli of monotonic loading tests.

3. COMPARISON BETWEEN LABORATORY TESTS AND IN-SITU TESTS

3.1. Shear wave velocity obtained by a laboratory test

Tests were conducted with a large-scale cyclic triaxial testing apparatus.

Specimen sizes are 30 cm in diameter and 60 cm in height as shown in Fig.1. Grain size distribution of specimens was regulated so as to be similar to that of the rock materials used for each embankment dam. Specimen preparation and testing were conducted as previously described.

Axial strain was measured by LVDT for displacement with 5 mm in measuring length and stress by a 19.6 kN load cell. Shear strain and maximum shear modulus G_{max} were obtained from axial strain ε_a and maximum elastic modulus E_{max}, through Poisson's ratio ν as shown in Eq.2.

$$[2a] \quad \gamma = (1 + \nu) \cdot \varepsilon_a$$

$$[2b] \quad G_{max} = E_{max} / \{ 2 \cdot (1 + \nu) \}$$

From test results, relation between G_{max} and mean principal effective stress σ_m' of rockfill materials of Miho and Shichigashuku Dams could be expressed by the following equations

(see Fig.15).

(Miho Dam)

$$[3a]\quad G_{max} = 558\,\frac{(2.17 - e)^2}{1 + e}\,(\sigma_m')^{0.88}$$

(Shichigashuku Dam)

$$[3b]\quad G_{max} = 947\,\frac{(2.17 - e)^2}{1 + e}\,(\sigma_m')^{0.62}$$

Here, e is the void ratio of rockfill materials of dam bodies. Quality control tests conducted during construction of each dam indicated that the e value was 0.25 for Miho Dam and 0.27 for Shichigashuku Dam respectively. If the deformation of a dam body is assumed to be two-dimensional with plane strain condition, σ_m' represents the stress at the depth D (unit;m) and can be expressed by Eq.4.

$$[4]\quad \sigma_m' = 1/30\cdot(1 + \nu)\cdot(1 + K)\cdot\rho_t\cdot D$$

Here, ν is Poisson's ratio, K is principal stress ratio, and ρ_t is density of wet soil (Miho Dam; 23 kN/m³, Shichigashuku Dam; 21 kN/m³ by quality control tests).

Shear wave velocity V_s was calculated from G_{max} using the following equation:

$$[5]\quad V_s = (10\cdot g\cdot G_{max}/\rho_t)^{0.5}$$

Here, g is gravitational acceleration (9.8 m/sec²).

In this manner, the relation between depth D and V_s is calculated from G_{max} which is derived from a laboratory test.

3.2 In-situ geophysical exploration test

(1) Miho Dam

Miho Dam is a 95 m high rockfill dam with a central impervious core as shown in Fig.16. Elastic wave velocity was measured by small-scale blasting at intervals of 2.5m utilizing gauge holes for internal movement measuring system and through reception points at intervals of 2.5m established on two sidings, A and B, shown in Fig.17. The length of A siding was 250m along the stream axis, while the B siding measured 200m along the dam axis. The gauge holes for the internal movement measuring system used for small-scale blasting were located at 288m in the elevation and 116m from the upper end of the A siding. The resulting velocity distributions within the dam body classified by depth are shown in Fig.18. Since the reservoir is at the upstream side of the dam body, V_s distribution was not obtained for upstream points. Also shown here are average V_s values for Japanese rockfill dams reported by Sawada *et al.*(1978), which were slightly higher than those derived from this study. Results of a triaxial test in the laboratory are also shown in this figure and correspond well with the results of geophysical exploration. V_s/V_p was 0.48 independent of the depth. Poisson's ratio calculated from Eq.6 was 0.35 as shown in Fig.19.

$$[6]\quad \nu = \frac{1 - 2\cdot(V_s/V_p)^2}{2\cdot\{1 - (V_s/V_p)^2\}}$$

Here, V_p is the velocity of the primary wave.

(2) Shichigashuku Dam

Shichigashuku Dam is also a 93m high rockfill dam with a central impervious core, as shown in Fig.20. Elastic wave velocity was measured through observation holes on the up and downstream slopes of the dam body along the depth direction. The plank hammering method in which a thick board established next to observation holes is strongly hit measured primary wave velocity, and the heavy weight dropping method in which a weight is dropped was used for measurement of secondary wave velocity as illustrated in Fig.21. A pick-up with geophones made up of three components was lowered from the upper end of an observation hole downward, measuring the traveling time of trigger for every 1m in depth. A pick-up was fixed to a hole wall by expanding a rubber tube inside, using compressed air supplied from the outside. Four series of measurements were conducted at various stages of the embankment (see Fig.22). V_s values classified by depth for the third and fourth exploration of a downstream slope are shown in Fig.23. The fourth exploration was conducted after the completion of embankment, and a larger V_s value was shown due to the progress of embankment at the inner part of the dam body. These values were larger than the values which Sawada *et al.* indicated at shallow points. In the figure, results of a cyclic loading triaxial test are also shown (a solid line) and closely correspond with results of an in-situ exploration at deep points.

A torsional simple shear test is estimated to simulate the in-situ stress condition very well. Concerning mean principal effective stress, Matsumoto *et al.*(1990) confirmed that shear modulus obtained from a cyclic loading torsional simple shear test was 10% larger than that from a cyclic loading triaxial test. Therefore, the curves for the results of laboratory tests in Figs.18 and 23 are estimated to shift slightly to the right side. Poisson's ratios in Shichigashuku Dam distribute from 0.27 to 0.35 as shown

in Fig.24 and indicated an increasing tendency with depth.

4. CONCLUSIONS

In an effort to simplify tests, the relationship between monotonic and cyclic loading tests was investigated with triaxial specimens. The results are summarized as follows:

By setting up a precision linear variable differential transformer on the cap of the specimen, elastic moduli of very small strain range between 10^{-6} and 10^{-4} were obtained through high velocity data samplings. With the focus on deformation characteristics in a very small strain, results of a monotonic loading test were compared with those of a cyclic loading test for Toyoura sand, and correspondence was observed in elastic moduli from the two tests. Elastic moduli for rockfill materials, which were obtained from monotonic and cyclic loading tests, showed correspondence in very small strains less than 1×10^{-5} level. However, strain dependency of elastic modulus in the monotonic loading test indicated a larger decreasing ratio according to the increasing of strain than in the cyclic loading test.

This indicated that it is possible to estimate the physical property values at very small strain for dynamic analysis from the results of a monotonic loading test alone without conducting cyclic loading tests, and also accumulation of much data is necessary for certification. However, hereafter the standardization of measuring methods for minute strain range in laboratory tests can therefore be expected.

For rockfill dams, the stiffness obtained by the in-situ tests (geophysical exploration and PS-logging) and the laboratory test were confirmed to show near correspondence with each other. It can be said that the similarity between construction conditions of the rockfill dams and the specimen preparation in laboratory tests (which use reconstructed materials) can explain the high degree of correspondence between the respective test results. However, since the stress and strain relation of the real dam body is in the condition of simple shear stress, further investigation such as torsional simple shear test is necessary to confirm the stiffness of the body of rockfill dams.

NOTATION

D; Depth
E; Elastic modulus
E_0; Maximum elastic modulus in monotonic triaxial test
E_{max}; Maximum elastic modulus in cyclic triaxial test
E_{cycl}; Elastic modulus in cyclic triaxial test
E_{mono}; Elastic modulus in monotonic triaxial test
G; Shear modulus
G_0; Maximum elastic modulus in monotonic loading test
G_{max}; Maximum shear modulus in cyclic loading test
G_f; Shear modulus by in-situ geophysical exploration
g; Gravitational acceleration
LVDT; Linear variable differential transformer
TSS; Torsional simple shear test
TX; Triaxial test
V_p; Velocity of primary wave
V_s; Velocity of secondary wave
ε_a; Axial strain
γ ;Shear strain
γ_{at}; Shear strain in torsional simple shear test
σ_m'; Mean principal effective stress
ν;Poisson's ratio
τ_f; Shear strength
τ_{at}; Shear stress in torsional simple shear test

REFERENCES

Burlad, J.B.(1989), "'Small is beautiful'-the stiffness of soils at small strains", Canadian Geotechnical Journal. 26, pp.499-516

Duncan,J.M. and Chang, C.Y.(1970), "Nonlinear Analysis of Stress and strain in Soils", Proc. of the ASCE, Vol.96, SM5, pp.1629-1653

Hardin ,B.O. and Drnevich, V.P.(1972), "Shear modulus and Damping in Soils; Design Equations and Curves", Jour. of SMFD, Proc. of ASCE, Vol.98, No.SM7, pp.667-692

Ishihara, K.(1976), "The Basis on Soil Dynamics", Kajima Press(in Japanese)

Kokusho, T.(1989), "In-Situ dynamic soil properties and their evaluations", The state of-the-Art Paper,Proc.of the 8th ARC, SMFE, Vol.2, pp.215-240

Kondner, R.L.(1963), "Hyperbolic Stress-strain Response; Cohesive Soils", Proc.ASCE, Vol.89, No.SM1, pp.115-143

Matsumoto, N., Yasuda, N. and Ohkubo, M.(1986), "Dynamic shear modulus, damping ratio and Poisson's ratio of coarse grained granular materials", Civil Engineering Journal, Vol.28, No.7, pp.44-49, (in Japanese)

Matsumoto, N., Yasuda, N., Ohkubo, M. and Kinoshita, Y.(1990), "Shear strength and Dynamic Deformation Characteristics of Gravels", Proceedings of JSCE, No.424 III-14, pp.95-104, (in Japanese)

Matsumoto, N., Yasuda, N., Yoshioka, R. and Ohkubo, M.(1991), "Cyclic and monotonic triaxial tests of gravels in micro-strain range", Symposium on triaxial testing methods, JSMFE,

pp.169-172,(in Japanese)
Powell, J.J.M and Butcher, A.P.(1991), "Assessment of ground stiffness from filed and laboratory tests", Deformation of Soils and Displacements of Structures, Proceedings 10th European Conference on soil mechanics and foundation engineering, Vol.1, pp.153-156
Sawada, Y., Takahashi, T.,Sakurai, A. and Yajima, H.(1977), "The distribution characteristics of the material properties and the dynamic behaviors of rockfill dams", Electric Power Central Research Institute, No.377008 (in Japanese)
Tatsuoka, F. and Shibuya, S.(1991), "Relationship of the deformation properties of soils and rocks between the triaxial tests", Symposium on triaxial testing methods, JSMFE, pp.39-84,(in Japanese)
Tatsuoka, F. and Shibuya, S.(1992), "Deformation characteristics of soils and rocks from field and laboratory tests", Report of the Institute of Industrial Science, The University of Tokyo, Vol.37, No.1, Serial No.235
Teachavorasinskun, S., Park. C. S., Katoh, S., Shibuya, S. and Tatsuoka, F.(1990), "Deformation and strength characteristics of sand in monotonic and cyclic Torsional Shear" The 25th Japan National Conference on Soil Mechanics and Foundation Engineering, JSMFE, pp.461-464,(in Japanese)
Teachavorasinskun, S., Shibuya, S. and Tatsuoka, F.(1991), "Stiffness of Sands in Monotonic and Cyclic Torsional Shear", Geotechnical Engineering Congress 1991, Vol.2, Geotechnical special publication No.27, pp.863-878

Table 1 Main features of transducer

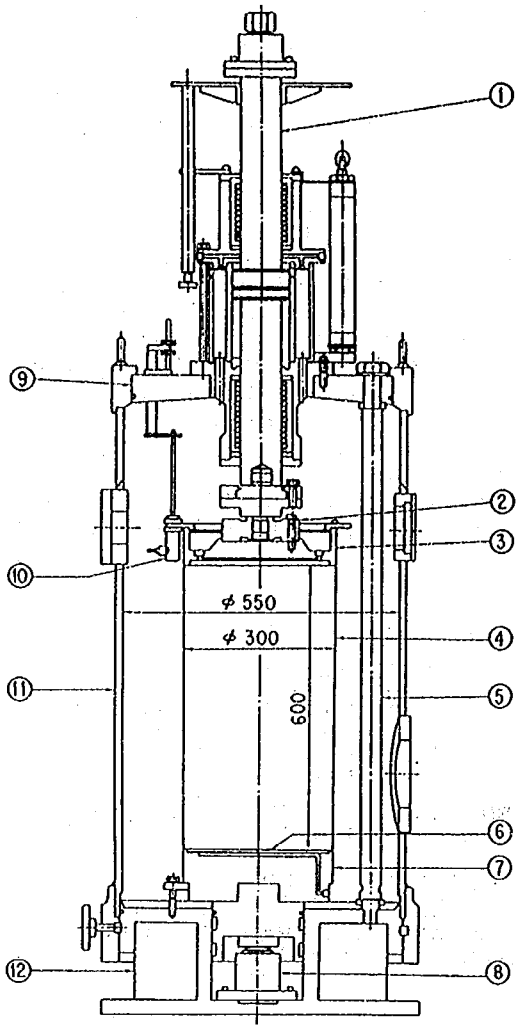
	CAPACITY	MAIN FEATURE		
		TYPE	ACCURACY	RESOLUTION
AXIAL LOAD	COMPRESSION(19.6kN) EXTENSION(9.8kN)	STRAIN GAUGE	LESS THAN ± 0.5 %	0.06 kPa
INTERNAL AXIAL DISPLACEMENT	5 mm	DIFFERENTIAL TRANSFORMER	LESS THAN ± 0.5 %	1 x 10^{-5} %
EXTERNAL AXIAL DISPLACEMENT	150 mm	DIFFERENTIAL TRANSFORMER	LESS THAN ± 0.5 %	1 x 10^{-3} %
EXTERNAL VOLUME CHANGE	± 66.5 cc	DIFFERENTIAL MANOMETER	LESS THAN ± 0.5 %	0.03 cc

Table 2 Physical properties of testing materials

		SAND STONES (ANGULAR ROCK)	RIVER BED GRAVEL (ROUND ROCK)
UNIFORMITY COEFFICIENT	U_c	7.0	14.7
SPECIFIC GRAVITY	G_s	2.65	2.62
WATER CONTENT	W %	0.65	2.08
ABSORPTION	Q %	0.99	3.28
MAXIMUM VOID RATIO	e_{max}	0.72	0.55
MINIMUM VOID RATIO	e_{min}	0.23	0.27

Table 3 Test conditions of monotonic and cyclic loading tests

CONSOLIDATION AND DRAINAGE CONDITIONS	ISOTROPIC CONSOLIDATION AND DRAIN	
INITIAL VOID RATIO	ANGULAR	e_0 = 0.38 , 0.28
	ROUND	e_0 = 0.36 , 0.30
CONFINING STRESS	σ_3=0.1,0.2,0.4 MPa	
CONTROL CONDITION	MONOTONIC	1.0 %/min : STRAIN CONTROL
	CYCLIC	0.2 Hz (SINUSOIDAL) : STRESS CONTROL



① LOADING ROD
② LOAD CELL FOR CYCLIC LOADING TEST
③ LOADING CAP
④ SPECIMEN
⑤ SUPPORT
⑥ POROUS METAL DISK
⑦ PEDESTAL
⑧ LOAD CELL FOR MONOTONIC LOADING TEST
⑨ UPPER PLATEN
⑩ LINEAR DISPLACEMENT TRANSDUCER
⑪ TRIAXIAL CELL
⑫ LOWER PLATEN

Fig.1 Schematic view of large-scale triaxial testing apparatus

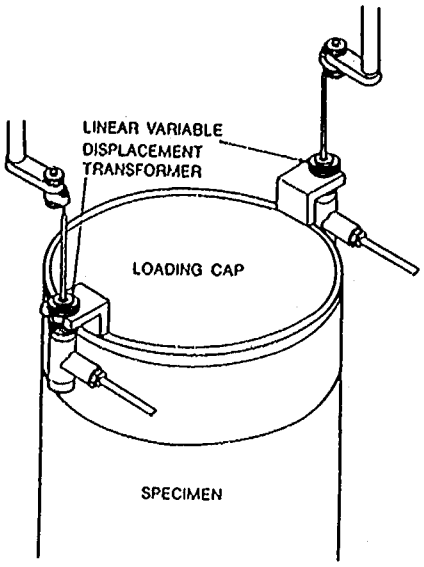


Fig.2 Detailed view of linear displacement transformer

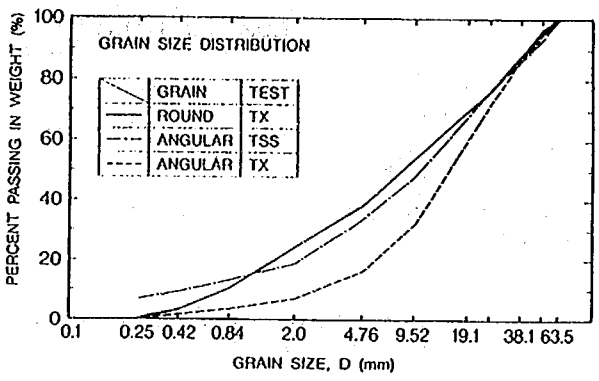


Fig.3 Grain size distribution of materials

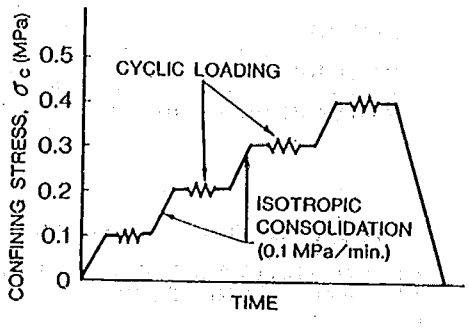


Fig.4 Process of cyclic loading test

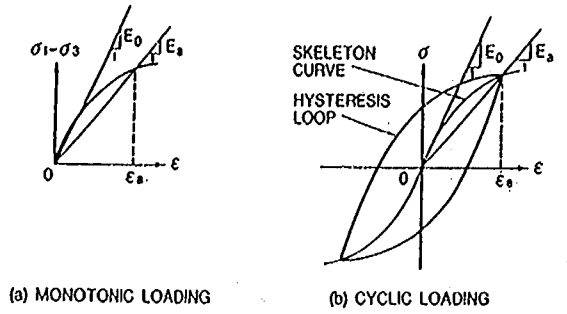


Fig.5 Stress and strain relationship

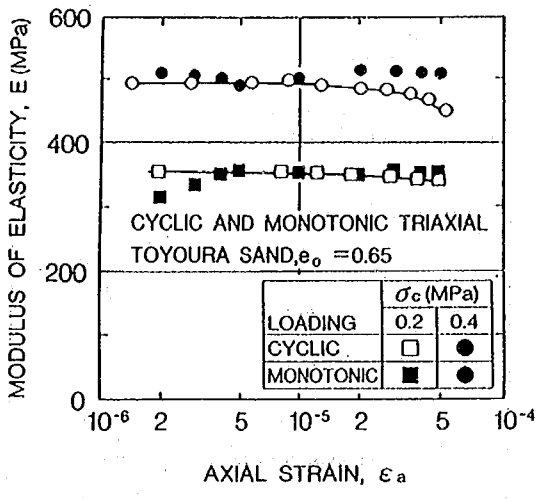


Fig.6 Comparison of monotonic and cyclic loading tests of Toyoura sand

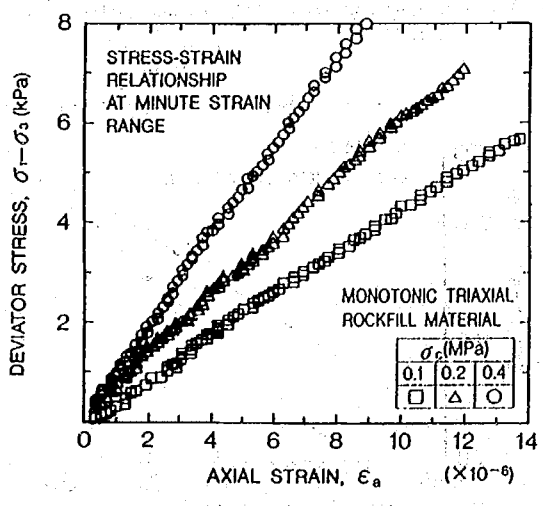


Fig.7 Stress and strain relationship in triaxial test at minute strain range

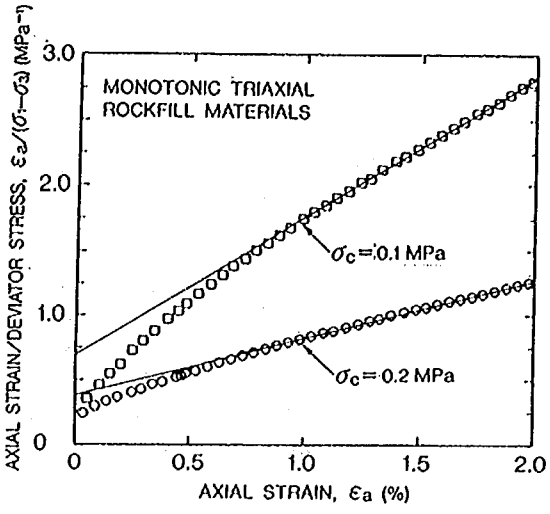


Fig.8 Relationship between $\varepsilon_a/(\sigma_1 - \sigma_3)$ and ε_a

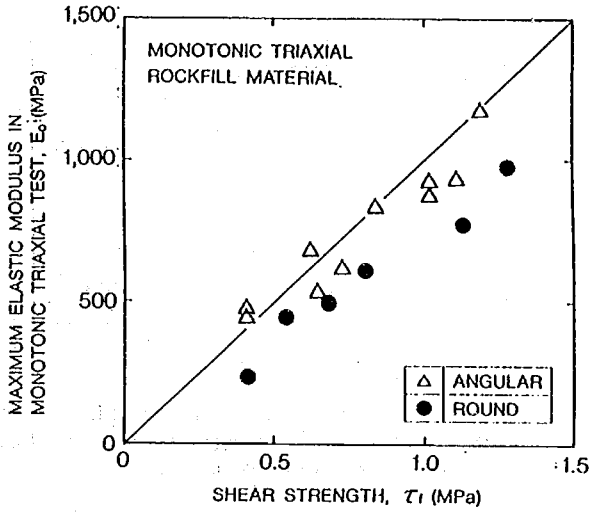


Fig.9 Relationship between shear strength and he maximum elastic modulus in monotonic loading test

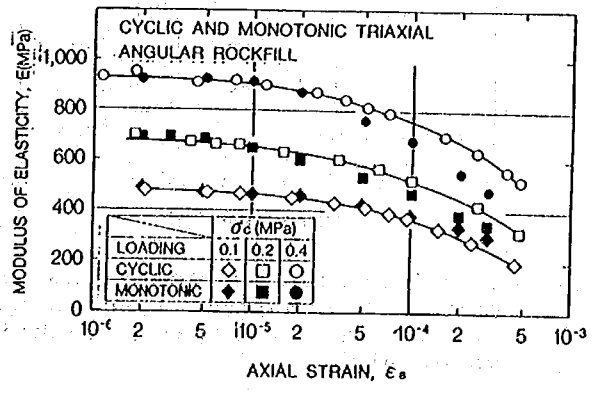


Fig.10(a) Comparison of monotonic and cyclic loading triaxial tests of angular rockfill materials

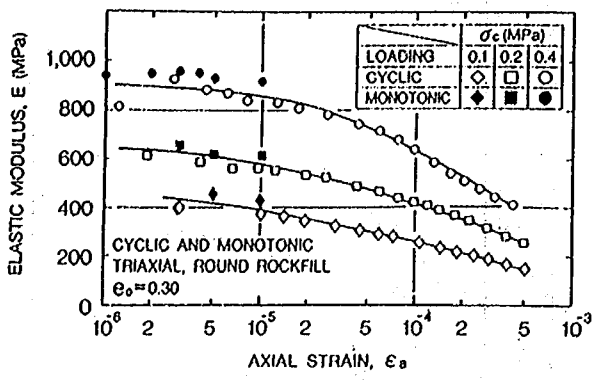


Fig.10(b) Comparison of monotonic and cyclic oading triaxial tests of round gravels

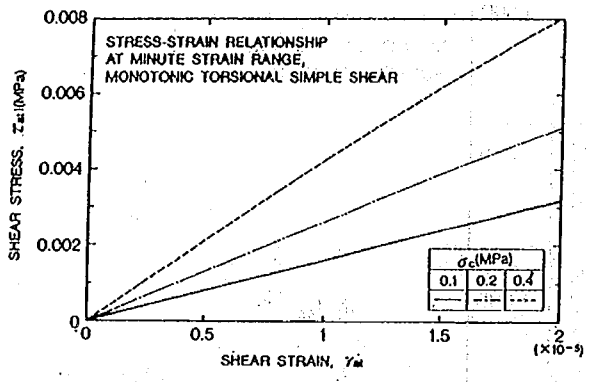


Fig.11 Stress and strain relationship in torsional simple shear test at minute strain range

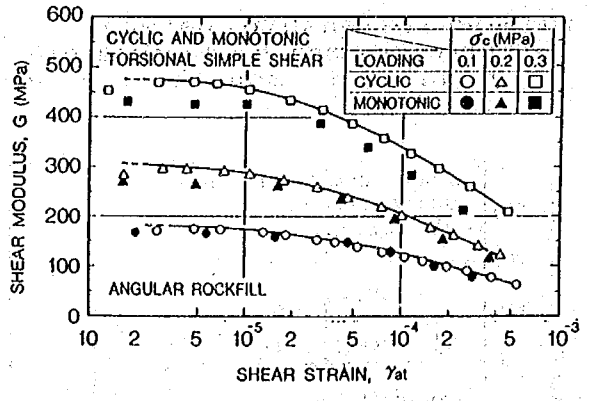


Fig.12 Comparison of monotonic and cyclic loading torsional simple shear test of angular rockfill materials

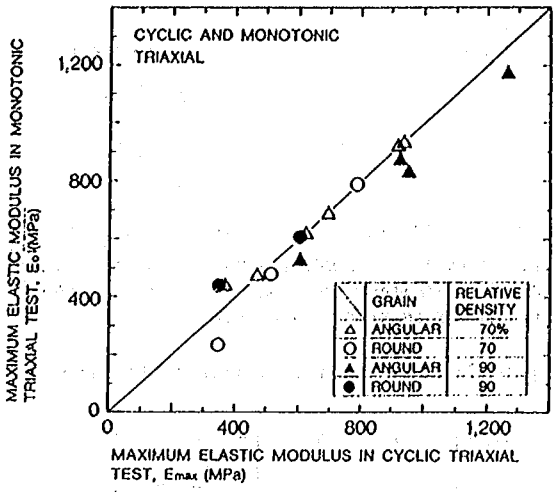


Fig.13 Relationship of E_o and E_{max} in triaxial tests

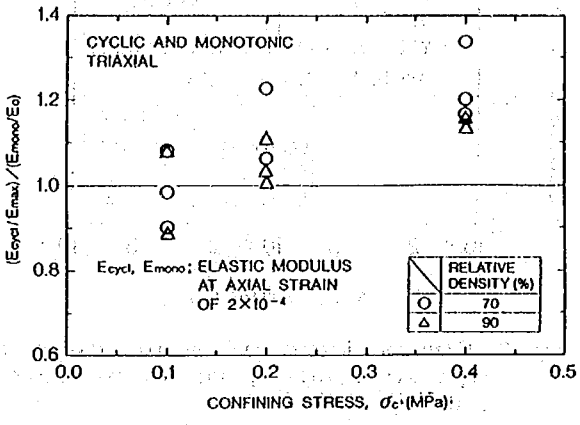


Fig.14 Comparisons of E_{mono} and E_{cycl} at $\varepsilon_a=2\times10^{-4}$

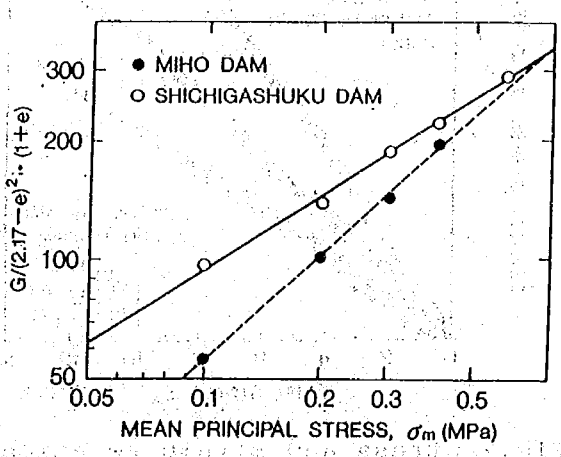


Fig.15 Relationship of $G/(2.17-e)^2\cdot(1+e)$ and mean principal stress

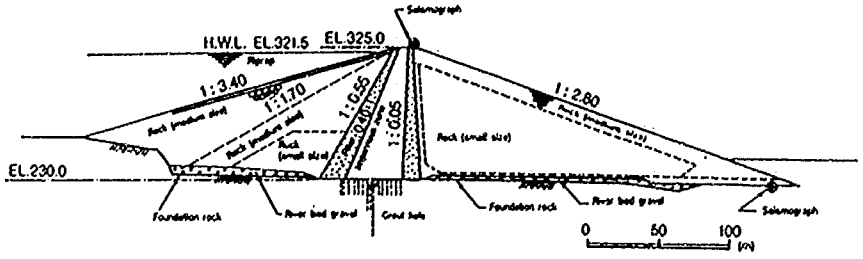


Fig.16 Cross section of Miho Dam

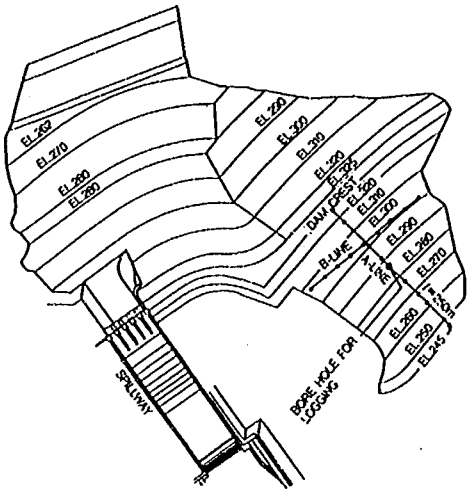


Fig.17 Location of A and B sidings in Miho Dam

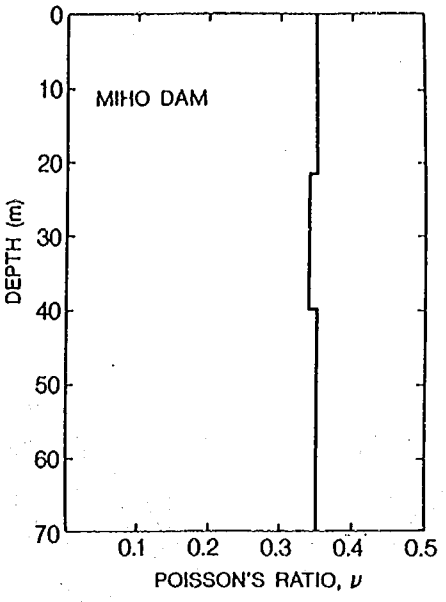


Fig.19 Distribution of Poisson's ratios at each depth (Miho Dam)

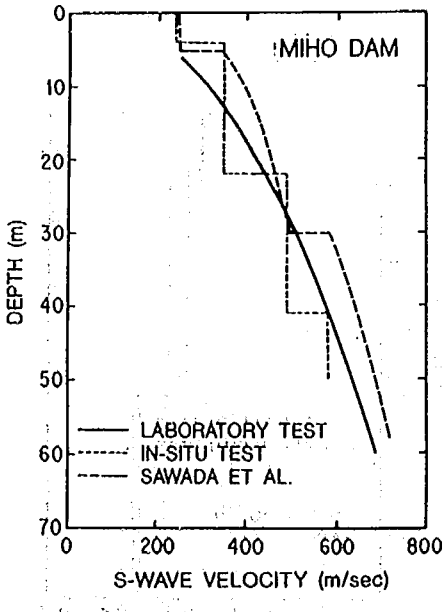


Fig.18 Distribution of shear wave velocity at each depth (Miho Dam)

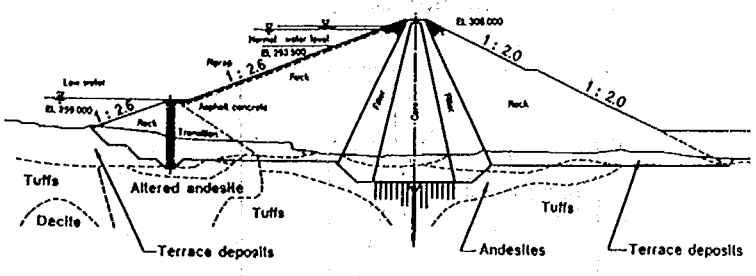


Fig.20 Cross section of Shichigashuku Dam

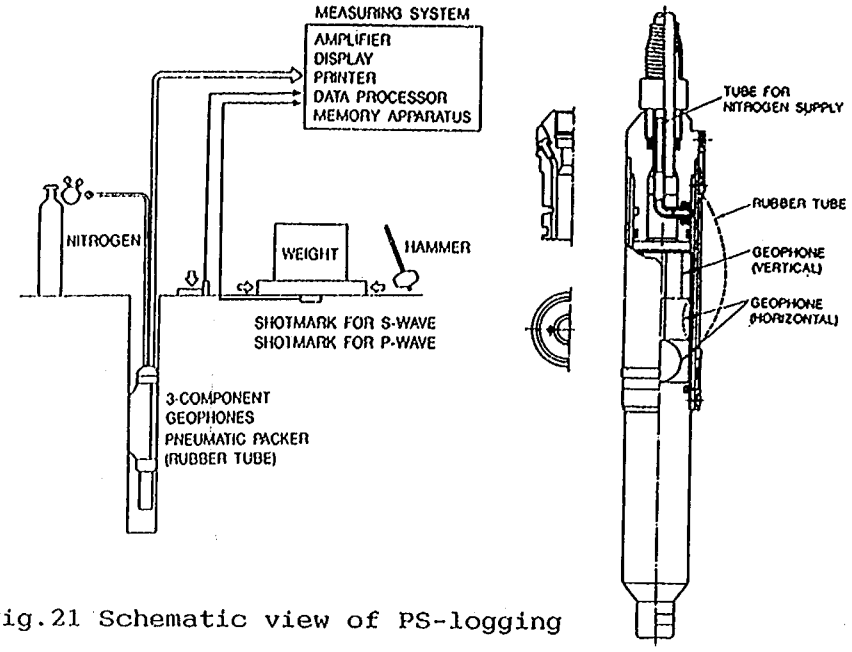


Fig.21 Schematic view of PS-logging

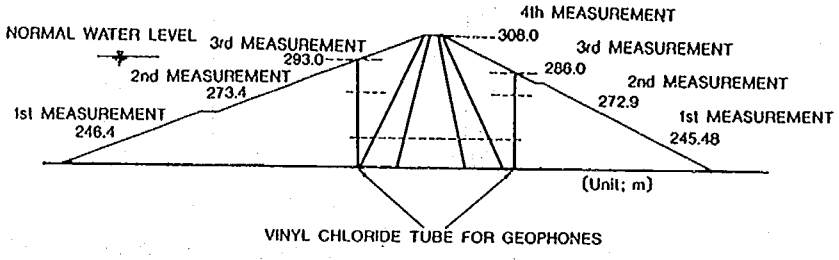


Fig.22 Measurement of elastic waves at four elevations of the banking (Shichigashuku Dam)

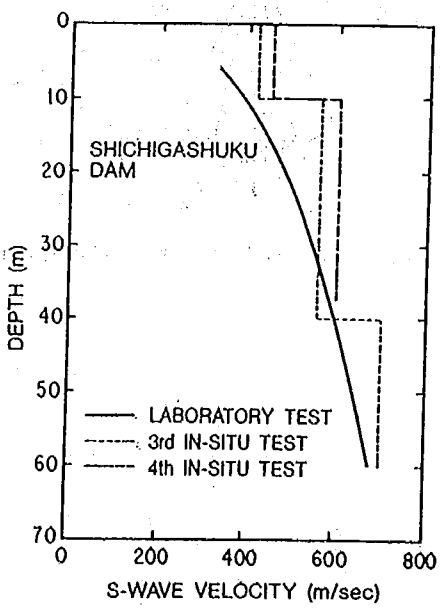


Fig.23 Distribution of shear wave velocity at each depth (Shichigashuku Dam)

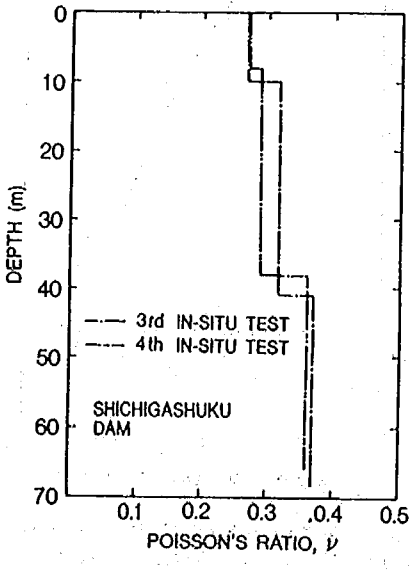


Fig.24 Distribution of Poisson's ratios at each depth (Shichigashuku Dam)

Strengthening Methodology For Lightly Reinforced Concrete Frames

by

L.T. Phan[1], D.R. Todd[1], and H.S. Lew[2]

ABSTRACT

An analytical method for evaluating the inelastic dynamic structural response of lightly reinforced concrete (RC) frames strengthened by infilled shear walls was developed. This method involved the development of hysteresis failure models for existing and strengthened RC frames and the incorporation of the models into the computer program IDARC for analysis. The hysteresis models were developed in terms of the stiffness degradation parameter α, the strength degradation parameter β, and the pinching parameter γ. The models were validated by analyzing a one-story, one-bay infilled frame, tested by Aoyama et al., and a three-story, one-bay infilled frame tested by Higashi et al. The results of the analyses showed that (1) hysteresis models developed using one-story, one-bay frames can be incorporated into IDARC for the analysis of frames with more than one-story height, and (2) reasonable predictions of structural behavior, both in terms of ultimate load capacity and in absorbed energy on a per cycle basis, can be determined using the hysteresis models.

KEYWORDS: Building technology; dynamic analysis; earthquake; frames; hysteresis models; infilled walls; reinforced concrete; system identification.

1. INTRODUCTION

Unless properly designed and detailed, reinforced concrete (RC) buildings are vulnerable to earthquake ground shaking. The relatively large mass of concrete buildings creates high inertial forces. Catastrophic failures that occurred in the 1971 San Fernando, 1985 Mexico City, and 1988 Armenia earthquakes, among others, illustrate the vulnerability and potential for large loss of life in older or poorly designed and built RC buildings. In order to reduce the risk associated with such RC structures that were designed and built without adequate consideration of seismic safety, an accurate understanding of the behavior of such structures under seismic loads is needed. Although experimental studies provide valuable information, analytical and computational methods are the most time and cost effective methods for assessing large numbers of structures and strengthening schemes.

During the past decade sophisticated nonlinear dynamic analysis programs capable of analyzing the performance of RC structures under seismic loads have been developed. Improvements to these programs are still being developed. To obtain sufficiently accurate analyses of actual behavior, the hysteresis rules which characterize the behavior of RC structures under cyclic loads must be identified and incorporated into the analysis programs.

This paper presents the development of hysteretic models using existing experimental data to describe the actual behavior under cyclic loads of existing RC frames with and without strengthening elements.

[1] Research Structural Engineer, Structures Division, National Institute of Standards & Technology, Gaithersburg, MD 20899, U.S.A.
[2] Chief, Structures Division, National Institute of Standards & Technology, Gaithersburg, MD 20899, U.S.A.

2. INELASTIC ANALYSIS OF REINFORCED CONCRETE FRAMES

The program IDARC (Inelastic Damage Analysis of Reinforced Concrete Frame-Shear Wall Structures) was developed by Park, Reinhorn, and Kunnath [1]. IDARC performs static analysis of inelastic behavior and failure mode under monotonic loading, and a step-by-step inelastic dynamic response analysis using the Newmark-β method. The program also performs a damage analysis, calculating damage indices for individual members, and for the entire building. IDARC uses two-dimensional analysis to evaluate the behavior of three-dimensional structures; transverse beam elements are used to model the effects of slabs and beams connecting parallel frames. Identical frames can be lumped together. Other elements available for modeling structures include beams, columns, shear walls, and edge columns.

The accuracy of any dynamic inelastic response analysis is heavily dependent on the correctness of the model used to describe the hysteretic behavior of the components. For analysis of reinforced concrete, the model must be able to describe stiffness degradation, strength deterioration, pinching behavior, and unsymmetric hysteresis. However, the model must also be simple since every additional parameter used to refine complex hysteresis loop shapes adds to computational time and complexity. The parameters α, β, and γ determine the stiffness degradation, strength deterioration, and pinching behavior, respectively. Figure 1 and the descriptions below, taken from Park et al.,[1] describe the effects of the three parameters on a trilinear skeleton curve.

α - "The stiffness degradation is introduced by setting a common point on the extrapolated initial skeleton curve line, and assumes that the unloading lines aim at this point until they reach the x-axis. The parameter α specifies the degree of stiffness degradation, and, more importantly, the area enclosed by the hysteresis loops."

β - "The parameter β specifies the rate of strength degradation."

γ - "The pinching behavior is introduced by lowering the target maximum point (A in Figure 1) to a straight level of γP_y (B in Figure 1) along the previous unloading line. Reloading points aim this new target point 'B' until they reach the crack closing deformation. The stiffness of reloading paths is changed at this point to aim the previous target maximum point 'A'. The introduction of such a pinching behavior also leads to a reduction of hysteresis loop areas and indirectly, the amount of dissipated energy."

In order to accurately analyze existing or strengthened reinforced concrete frame structures, it is necessary to obtain parameters (α, β, γ) which have been calibrated by experimental results. The hysteresis models developed in this study include the following types of construction:

- bare frames
- monolithic wall-frame constructions
- frames strengthened by CIP infilled walls, with and without wall openings
- frames strengthened by multiple precast concrete panels, with and without wall openings.

3. THREE-PARAMETER HYSTERESIS MODELS

The procedure used for the development of the empirical three-parameter hysteresis models involves the following two main tasks:

1. Determine the values for three parameters α, β, and γ which best fit the experimental hysteresis loops. In this study fifty five test results were used to calibrate these parameters.

2. Based on the fifty five sets of α, β, and γ, multiple-variable regression analysis was performed to obtain empirical expressions

for α, β, and γ in terms of the physical properties of the test specimens.

The system identification procedure was used to identify hysteresis parameters of the fifty-five test results selected for this study. In this procedure cumulative errors between the predicted and measured total absorbed hysteretic energy were minimized. Examples of the match between the predicted and measured hysteresis responses of four specimens are shown in Figures 2 a to h. In Figures 2 a, c, e, and g, the dashed lines represent the experimental results and the solid lines are the predicted hysteresis responses corresponding to the estimated hysteresis parameters α, β, γ obtained from system identification. Figures 2 b, d, f, and h are histograms of the measured and predicted absorbed energy for the four specimens. As can be seen from Figure 2, the three parameters α, β, and γ identified for each test specimen were able to predict reasonably well the load-deformation hysteresis behavior of the test specimens. They also predict the absorbed energy of the specimen on a per cycle basis. Empirical expressions for the hysteresis parameters for different structural systems are given in Phan, Todd, and Lew[2]. The hysteresis models for different structural systems include

- bare frames,
- monolithic wall-frame systems,
- frames strengthened by CIP infilled wall, and
- frames strengthened by multiple precast concrete panels.

4. VALIDATION OF HYSTERETIC MODELS FOR USE WITH IDARC

The validity of using these models to predict the behavior of actual structures using IDARC is presented.

Two frames were analyzed, a one-story one-bay frame tested by Aoyama et al. [3,4,5,6] (specimen C2005-I), and a three-story one-bay frame specimen tested by Higashi et al [7] (specimen 78-3PW). For each frame, two IDARC analyses are performed, one using the IDARC recommended default values for hysteresis parameters α, β, and γ, and the other using hysteresis parameters obtained from the hysteresis models developed in this study. The results of these analyses are shown in Figures 3 and 4.

5. CONCLUSIONS

The empirical hysteresis models developed in this study are capable of providing reasonable estimates of the hysteresis performance of reinforced concrete frames. The results of this study showed that the hysteresis performance of one-bay one-story reinforced concrete bare frames, monolithic wall-frame constructions, frames infilled by CIP concrete walls, and frames infilled by precast concrete panels can be reasonably predicted. Furthermore, the same model development approach presented in this study can be used in developing hysteresis models for beam-column joints and column strengthening techniques to provide more analytical options for the selection of other strengthening schemes for existing RC frames.

6. REFERENCES

1. Y.J. Park; A.M. Reinhorn; S.K. Kunnath, "IDARC: Inelastic Damage Analysis of Reinforced Concrete Frame-Shear Wall Structures", National Center for Earthquake Engineering Research, Technical Report NCEER-87-0008, July 1987.

2. L.T. Phan; D.R. Todd; H.S. Lew, "Strengthening Methodology for Lightly Reinforced Concrete Frames-I", NISTIR 5128, National Institute of Standards and Technology, Gaithersburg, Maryland, February, 1993.

3. H. Aoyama; D. Kato; H. Katsumata; Y. Hosokawa, "Strength and Behavior of Postcast Shear Walls for Strengthening of

Existing Reinforced Concrete Buildings" List of Manuscripts Submitted to Eighth WCEE in San Francisco 7/1984, Aoyama Laboratory, Department of Architecture, University of Tokyo, Hongo, Bunkyo-ku, Tokyo 113, Japan.

4. H. Aoyama, "Seismic Strengthening of Existing Reinforced Concrete Buildings in Japan", Department of Architecture, Faculty of Engineering, The University of Tokyo, Japan, September, 1986.

5. H. Shiohara; Y. Hosokawa; T. Nakamura; H. Aoyama, "Earthquake Strengthening Method of Existing Reinforced Concrete Buildings", Transactions of the Japan Concrete Institute, Volume 6, p. 725-732, 1984.

6. H. Shiohara; Y. Hosokawa; T. Yamamoto; H. Aoyama, "Shear Stress Distribution in Earthquake Strengthening Post-Cast Reinforced Concrete Shear Wall", Transactions of the Japan Concrete Institute, Volume 7, 1985.

7. Y. Higashi; T. Endo; Y. Shimizu, "Experimental Studies on Retrofitting of Reinforced Concrete Structural Members", Proceedings of the Second Seminar on Repair and Retrofit of Structures, pp. 126-155, University of Michigan, Ann Arbor, MI, May 1981.

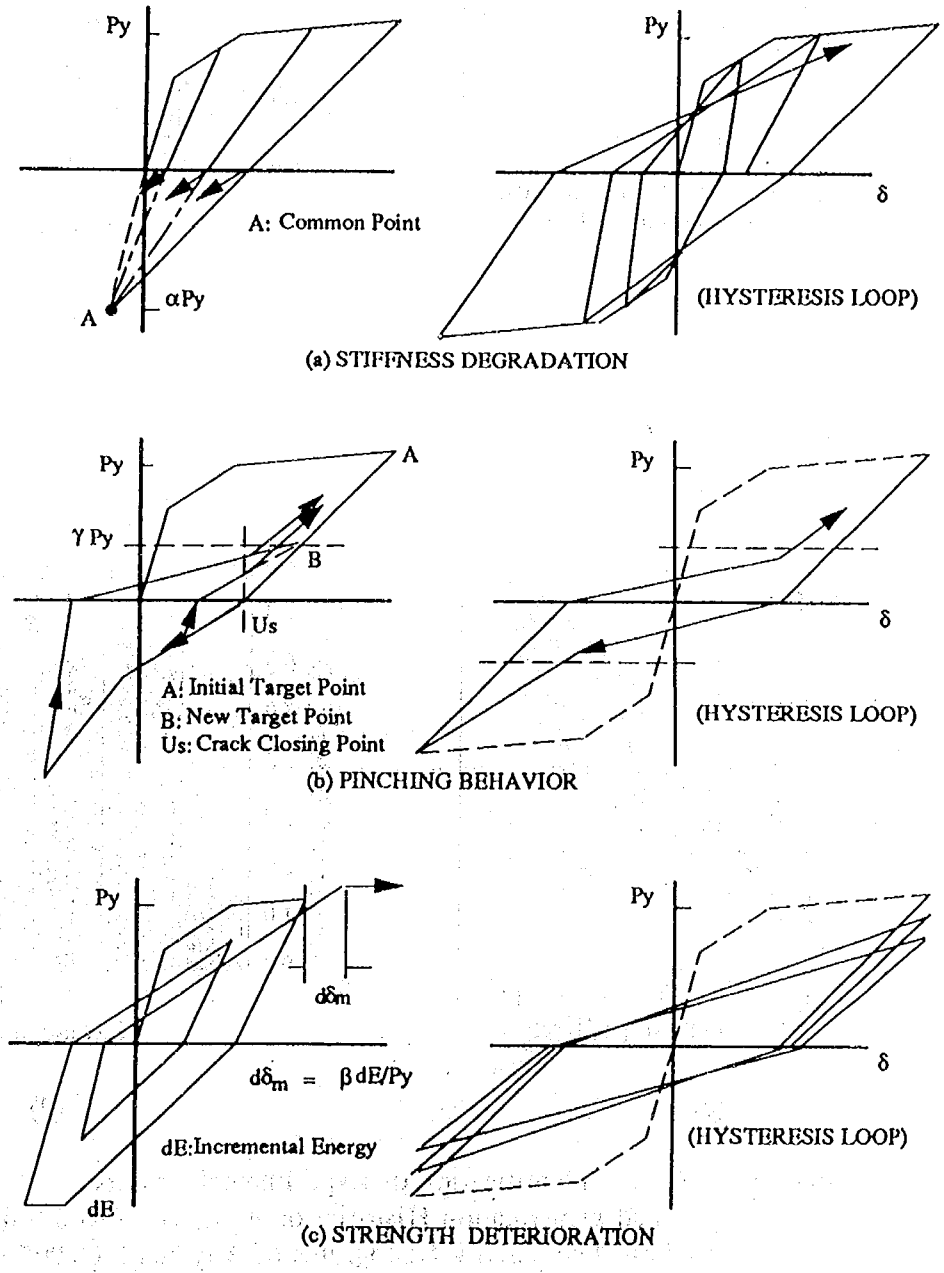
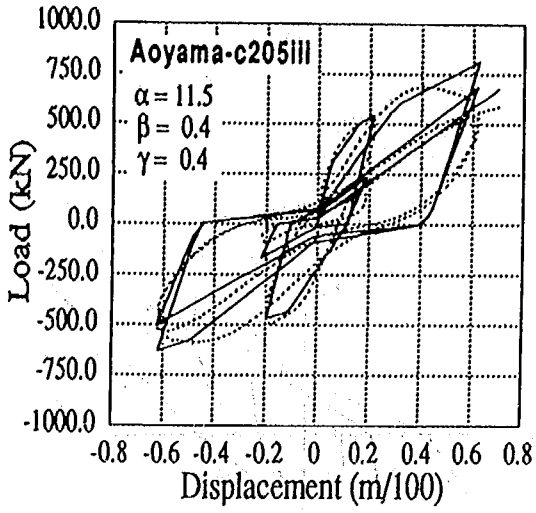
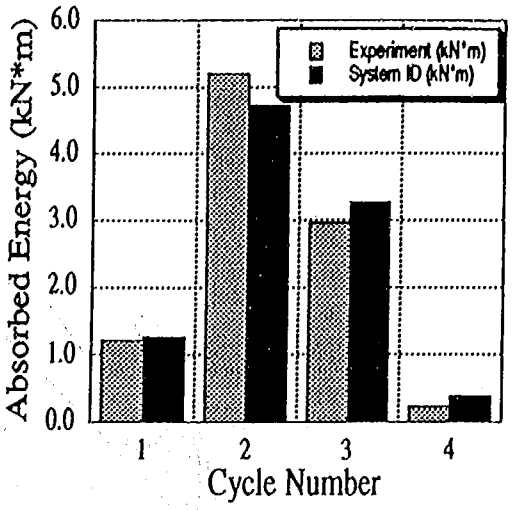


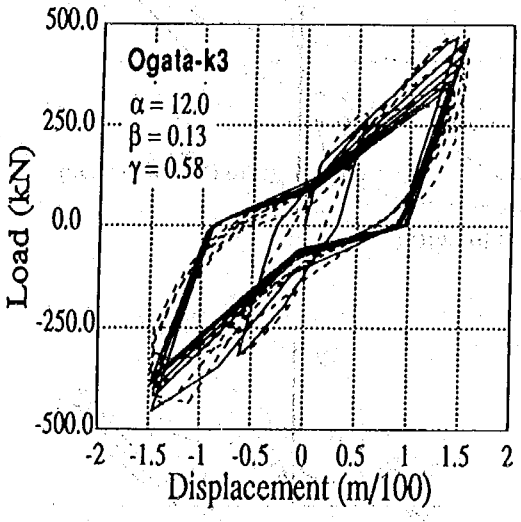
Figure 1. Three-Parameter Hysteresis Models
(After Park, Reinhorn, and Kunnath [1])



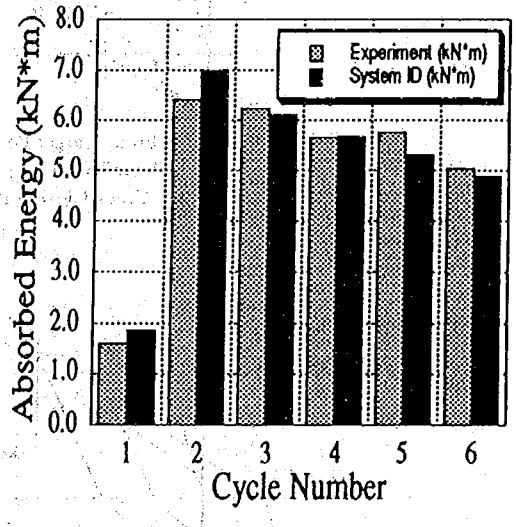
(a)



(b)

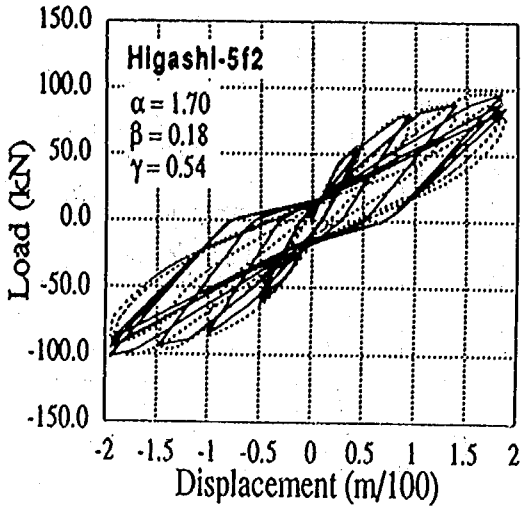


(c)

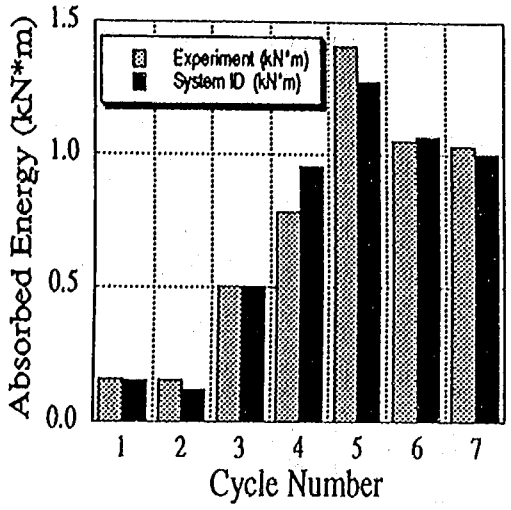


(d)

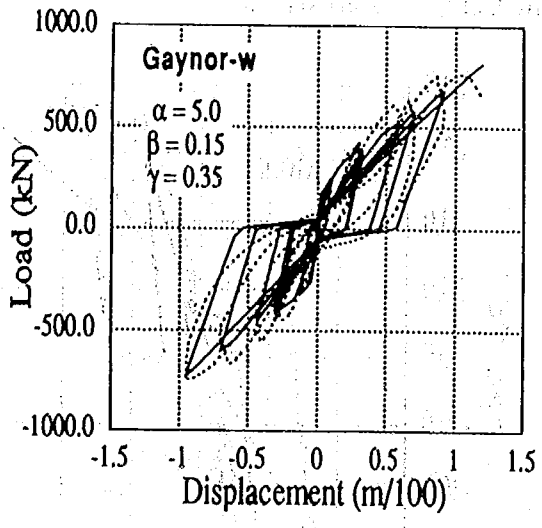
Figure 2. System Identification of Experimental Results
(a) Load-Deformation Histories of Aoyama's C2005-iii
(b) Absorbed Energy Histograms of Aoyama's C2005-iii
(c) Load-Deformation Histories of Ogata's K3
(d) Absorbed Energy Histograms of Ogata's K3



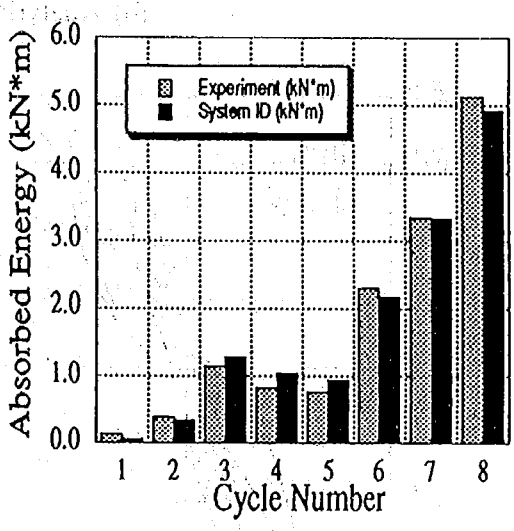
(e)



(f)



(g)



(h)

Figure 2. System Identification of Experimental Results (continued)
(e) Load-Deformation Histories of Higashi's 5-F2
(f) Absorbed Energy Histograms of Higashi's 5-F2
(g) Load-Deformation Histories of Gaynor's W
(h) Absorbed Energy Histograms of Gaynor's W

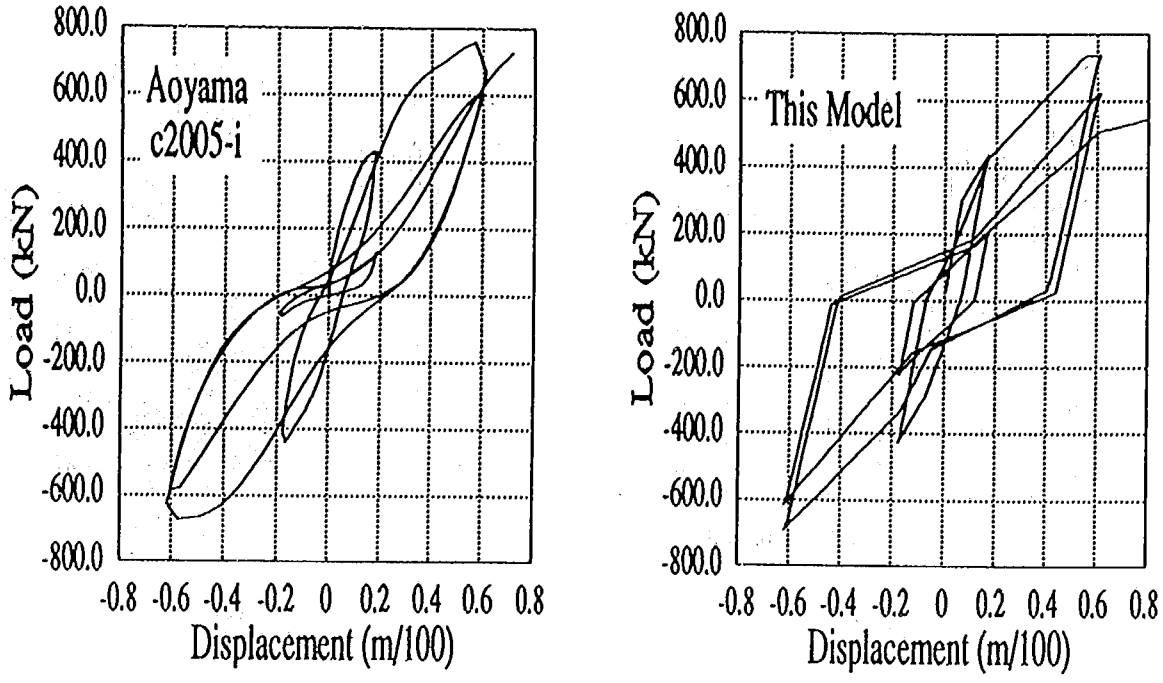


Figure 3. Comparison of Experimental and Analytical Hysteresis Behavior for Aoyama's One-Story, One-Bay Frame C2005-i
(a) Experimental Result
(b) Analytical Result Using Hysteresis Model

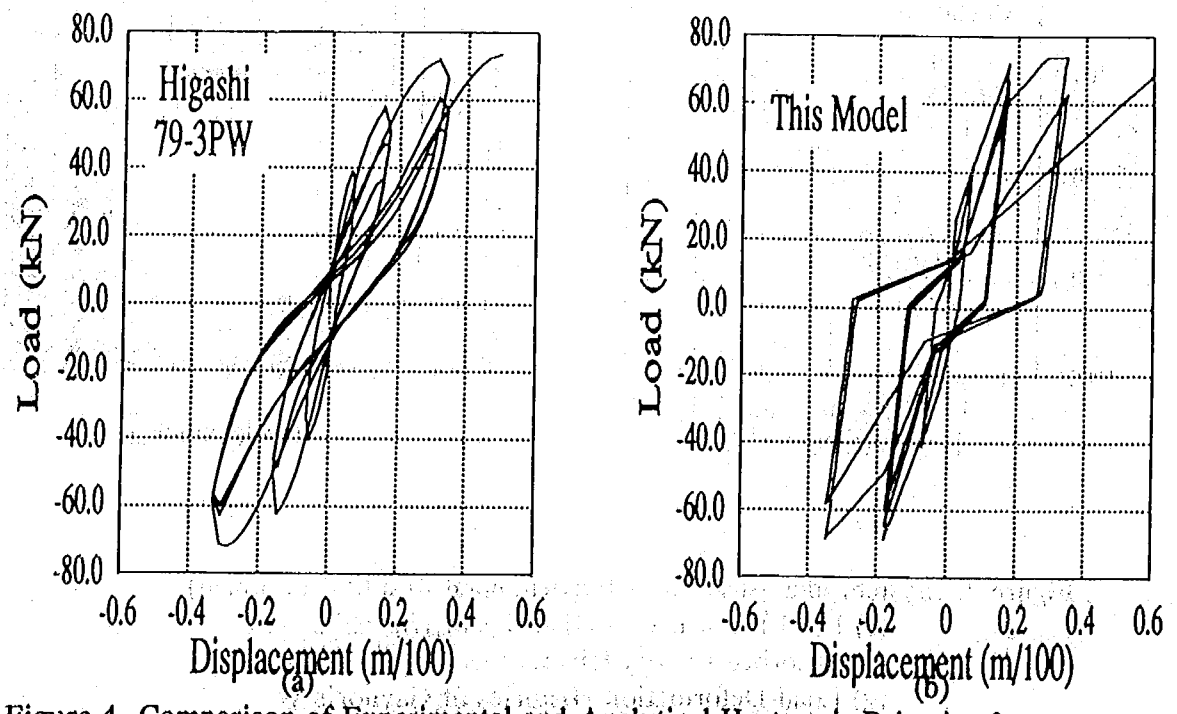


Figure 4. Comparison of Experimental and Analytical Hysteresis Behavior for Higashi's Three-Story, One-Bay Frame 79-3PW
(a) Experimental Result
(b) Analytical Result Using Hysteresis Model

A GUIDELINE FOR EVALUATING DESIGN EARTHQUAKE GROUND MOTION FOR DYNAMIC ANALYSIS OF BUILDINGS

by

Yoshikazu KITAGAWA*, Izuru OKAWA*
Toshihide KASHIMA*, and Shin KOYAMA*

ABSTRACT

We propose a guideline for evaluating design earthquake ground motion used in the dynamic analysis of buildings. The guideline includes methodologies to construct the design response spectrum, to generate the time history of design earthquake ground motion. It also includes usage of the generated motion for analysis as design procedure and examples of the design spectrum applied to cases of design.
These methodologies presented here are mainly for high-rise buildings and base-isolated buildings that require dynamic analysis in the seismic design. Those can, however, be applied to other classes of buildings.

Key Words

Guideline, Base layer, Design earthquake ground motion, Longer period component, Soil amplification, Liquefaction, Topographical effect, Envelope function, Duration

INTRODUCTION

The Building Code of Japan, amended in 1981, regulates that specific buildings, such as high-rise buildings taller than 60 meters or buildings with base-isolated devices, must be licensed by the Minister of Construction (MOC). Any such building conforming to the law shall be subjected to a structure evaluation for seismic safety using dynamic response analysis by the Appraisal Committee, in the Building Center of Japan (BCJ).
In these cases, the earthquake motion used as design input motion for dynamic analysis should be chosen considering the following possibilities:

- Using actual recorded data of past strong earthquake motion (e.g., El Centro 1940 NS, Taft 1952 EW, Hachinohe 1968 NS, EW)
- Using actual recorded data of past strong earthquake motion with the amplitude and frequency characteristics modified
- Using specific artificial earthquake motions (i.e., simulated earthquake motions)

Up to the present time, the design seismic load can be represented by the following peak amplitudes:

For elastic response:
Max.Acc.=150-250 gal,
Max.Vel.=25 cm/sec
For elastoplastic response:
Max.Acc.=300-500 gal,
Max.Vel.=50 cm/sec

Most of the behaviors of building can be elucidated by structural experiments. However, despite advances in theoretical modeling and analytical techniques, earthquake motions themselves have been collectively treated on the safe side due to difficulties with recurrence and scarce opportunities for actual proof.

Currently, there are no standardized earthquake wave forms used as fundamental data in the dynamic response analysis. Therefore, a special examination is conducted in the design phase on what type of earthquake wave form should be used for the structure design built on various ground types from actual earthquake wave forms.

Generally, the response of a structure during earthquake is associated with the following five characteristics:
(1) Earthquake source
(2) Propagating path of seismic wave
(3) Ground surrounding the structure
(4) Soil-structure interaction
(5) Characteristics of structure

* Building Research Institute, MOC
Tatehara-1, Tsukuba, Ibaraki 305, JAPAN

Thus, the seismic behavior of a structure is affected by both the ground and earthquake motion characteristics. The converse is also true: the earthquake motion at a structure site is affected by the characteristics of the structure. Therefore, a proper evaluation methodology for design input earthquake motion for buildings considering the site specific properties is needed rather than representative actual recorded data of the past strong earthquake motion.

On the premise of these conditions, the Research Committee for Design Earthquake Ground Motion has been organized in BCJ to carry out the cooperative research project between BRI (Building Research Institute) and BCJ. As a final outcome of this 4-year research program that began in 1989, a guideline for evaluating design earthquake ground motion for buildings incorporating the latest research results on ground motions was proposed.

The guideline is briefly presented in this paper

A Guideline for Evaluating Design Earthquake Ground Motion for Dynamic Analysis of Buildings

1. General considerations

1.1 Scope of application

This guideline is applicable to the seismic design of buildings that require dynamic analysis.

The implementation of this guideline may be excluded in part in case where appropriate extra investigation and/or research is made.

(Commentary)

In Japan, the buildings that require a dynamic analysis are high-rise buildings with heights of more than 60 meters and base-isolated buildings. The guideline presented here is applicable to any other building that has a natural period between 0.1 and 8 seconds.

1.2 Terminology

Design earthquake ground motion -- Generic name of ground motion that is used for dynamic analysis in the seismic design of a building and is herein defined as motion at the ground surface

Design response spectrum - Design earthquake ground motion defined in terms of the response spectrum

Basic response spectrum - Response spectrum prescribed at the exposed engineering-oriented base layer

Engineering-oriented base layer -- Base layer that is set up for design purposes. The shear wave velocity of the layer is herein defined to be greater than approximately 400 meters per second

Exposed engineering-oriented base layer - An engineering-oriented base layer which is exposed on the free surface

Design earthquake ground motion time history -- Design earthquake ground motion defined in terms of time history with which a step-by-step dynamic analysis is executed

Longer period component of earthquake ground motion - Components of waves with approximately 2 to 10 seconds of period contained in earthquake ground motion

Level 1, Level 2 - Dually defined intensity levels for design prescribed by amplitudes of the motion and/or preferable seismic performance of the buildings against seismic load

Liquefaction - A form of ground failure whereby a cohesionless soil loses strength as a result of an increase in pore pressure due to earthquake ground motion

Seismic bedrock -- A layer whose shear wave velocity is more than approximately 3 kilometer per second and broadly exists around and beneath the construction site concerned

Acceleration response spectrum -- Maximum absolute acceleration response of the single degree of freedom system to earthquake ground motion given as a function of the period and the damping factor of the system.

Pseudo velocity response spectrum -- Velocity response spectrum herein defined as the acceleration response spectrum divided by the natural circular frequency

Envelope function -- A function that defines time variation of the amplitude level of the design earthquake ground motion time history

Surface soil -- Soil deposits existing above the engineering-oriented base layer

Amplification property -- A property where the soil deposit enlarges the amplitude of specific components of ground motion

Seismic activity -- Potential susceptibility to earthquake motions at the construction site depending upon the frequency of earthquake occurrences and the closeness to the source region

Topographical effect -- Influence of surficial land form and/or geological formation on the surface motion

Spectral modal analysis -- Analytical technique for obtaining maximum responses to a specified input motion. The response computation is based on the summation of modal responses.

Magnification in acceleration response -- Acceleration response spectrum normalized by the maximum input acceleration

(Commentary)

The above are the specific terms used as key words in this document and the definitions of some of these terms may be valid only for this guideline.

1.3 Symbols

The symbols used in this guideline are summarized as follows.

T -- Period (sec)

ζ -- Seismic activity coefficient

Z -- Seismic zoning factor

T_i -- the i-th period that defines the amplification property of soil layers (sec)

Tg -- Fundamental period of surface soils (sec)

V_e -- Average shear wave velocity of surface soils

V_b -- Shear wave velocity

V_i -- Shear wave velocity of the i-th soil layer consisting of surface soils

h_i -- Thickness of the i-th soil layer consisting of surface soils

ΔV -- Variation of shear wave velocities of surface soil deposits

α -- Coefficient of soil amplification in shorter period

β -- Maximum coefficient of soil amplification

$_H$S(T) -- Design response spectrum for horizontal motion (cm/s)

$_H$S'(T) -- Modified design response spectrum for horizontal motion (cm/s)

$_H$B(T) -- Basic response spectrum for horizontal motion (cm/s)

$_H$G(T) -- Coefficient of soil amplification for horizontal motion

$_H$L(T) -- Coefficient of the longer period component for horizontal motion

$_H$P(T) -- Coefficient of liquefaction for horizontal motion

$_H$I(T) -- Coefficient of topographical effect for horizontal motion

$_V$S(T) -- Design response spectrum for vertical motion (cm/s)

$_V$S'(T) -- Modified design response spectrum for vertical motion (cm/s)

$_V$B(T) -- Basic response spectrum for vertical motion (cm/s)

$_V$G(T) -- Coefficient of soil amplification for vertical motion

$_V$L(T) -- Coefficient of the longer period component for vertical motion

$_V$P(T) -- Coefficient of liquefaction for vertical motion

$_V$I(T) -- Coefficient of topographical effect for vertical motion

2. Basic Philosophy

The evaluation of design earthquake ground motion is prescribed as follows.

(1) Design earthquake ground motion shall be determined considering the seismic activity around the construction site, the properties of ground motion at the engineering-oriented base layer, the longer period components of the earthquake ground motion, and the amplification characteristics of the surface soil.

(2) Design earthquake ground motion shall be determined for the following two design levels.

Level 1 - A level of earthquake ground motion that is expected to occur more than once during the service period of the building

Level 2 - A level of the maximum ground motion which has been experienced in the past or is expected to occur in the future around the site

(3) Design earthquake ground motion shall be set up for horizontal and vertical motions

(4) Design earthquake ground motion shall be firstly set up as design response spectrum in the following form;

i) Acceleration response spectrum or pseudo relative velocity response spectrum with 5 % damping

ii) Valid for the period range between 0.02 and 10 sec

(5) Design earthquake ground motion time history is subsequently generated based on the design response spectrum

(Commentary)

The design response spectrum is defined on the ground surface. The engineering-oriented base layer (hereafter referred to as EOBL) is defined as a soil layer with more than approximately 400m/sec of shear wave velocity as mentioned in section 1.2 Terminology.

The dually defined design levels correspond to the following conditions, which are identical to the specification of the design earthquake motion for high-rise buildings in Japan. The response of a building to Level 1 design motion is that the building incurs no damage and that the main structure behaves elastic. The response of a building against to Level 2 design motion is that danger to human life, such as a collapsing outer wall, is avoided.

The earthquake ground motion is generally expressed as three components, i.e., two perpendicular horizontal components and one vertical component. The guideline shows how to determine a single component of motion. The horizontal component can be applied to any direction of loading.

3. Procedures for generating the design earthquake ground motion

The design earthquake ground motion is evaluated with the following procedure.

(1) Evaluate the basic response spectrum.
(2) Compute the dynamic characteristics of the surface soil.
(3) Set up the design response spectrum.
(4) Generate the design earthquake ground motion time history, if necessary.

(Commentary)

In this guideline, the design earthquake ground motion is defined as both of the design response spectrum and the design earthquake ground motion time history. Both are based on the basic response spectrum defined on the engineering-oriented base layer. It is also assumed that the design response spectrum is computed on the ground surface. The concept is shown in Fig.1.

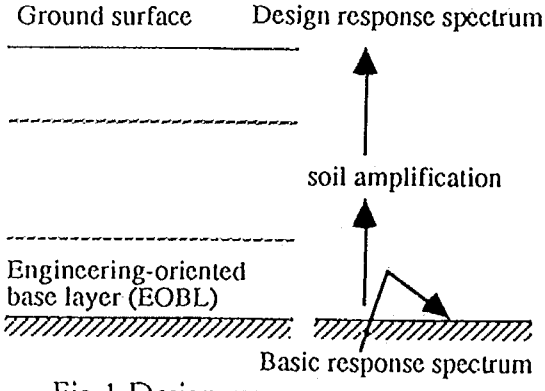


Fig.1 Design response spectrum

4. Design Response Spectrum

The design response spectra determined shall be those of the horizontal and/or vertical components for two design levels. Design response spectrum shall be computed with a seismic activity coefficient, a standard response spectrum, coefficients of both the longer period component and soil amplification. Furthermore, coefficients of both liquefaction and topographical effect shall apply when those effects can not be ignored.

(Commentary)

It is generally recognized that an earthquake is caused by the rupture of a seismic fault. The earthquake ground motions expected at a site vary with the properties of the seismic source, the propagating path, and the surface soil. There are many factors involved when determining the earthquake ground motion. We chose such factors that truly have significant influence on the ground motion from an engineering point of view and that can be evaluated not only qualitatively but also quantitatively.

In this guideline, the design response spectrum is evaluated using the following items.

- Seismic activity coefficient
- Basic response spectrum
- Coefficient of the longer period component
- Coefficient of soil amplification
- Coefficient of liquefaction
- Coefficient of topographical effect

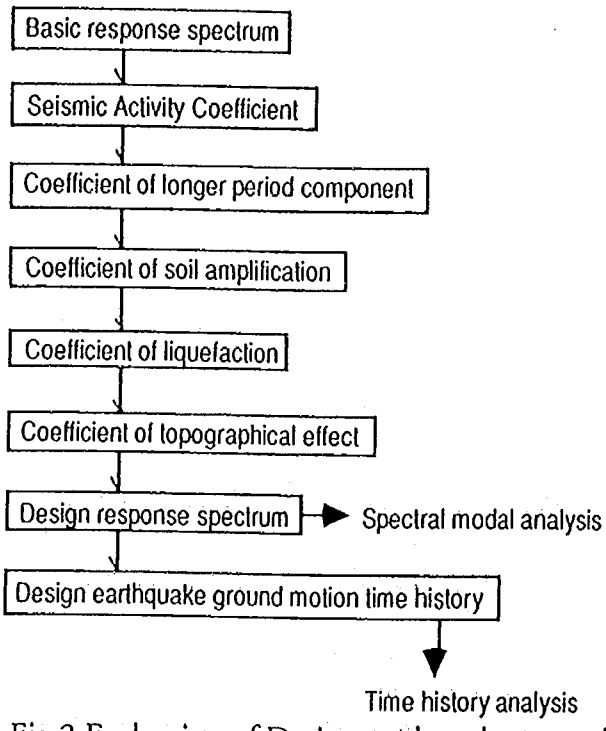


Fig.2 Evaluation of Design earthquake ground motion

4.1 Seismic activity coefficient ζ

The seismic activity coefficient (ζ) introduces regional information of the seismic activity.
The seismic zoning factor that is used in the current seismic design code may be used for this coefficient..

(Commentary)

The intensity of seismic motion at a location primarily depends upon the earthquake magnitude and the distance to epicenter

(hypocenter). It is well-known that in Japan earthquake occurs in specific areas such as along the Pacific coast. Consequently, intensity of seismic motion which a building experiences during its service period varies with the region in which the building stands. The seismic activity coefficient is introduced to consider such regional gaps in the expected values of ground motion intensity.

The basic response spectrum in this guideline is based on the data obtained in and around the Kanto area located in eastern Japan. Therefore, the seismic activity coefficient for sites in the Kanto area may be 1.

According to research on the regional gap with respect to the peak amplitudes, the gap may be 1 to 10 in some cases. Similar studies for spectral values are not sufficient, however, since the data in areas other than the Kanto area is limited.

The seismic zoning factor Z in the current seismic code of Japan can be alternatively used for the seismic activity coefficient.

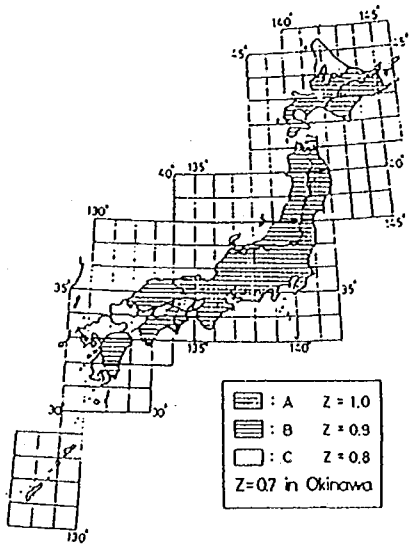


Fig.3 Seismic zoning factor Z

4.2 Design response spectrum for horizontal motion ${}_{H}S(T)$

The design response spectrum for horizontal motion ${}_{H}S(T)$ is computed using the following expression.

$$ {}_{H}S(T) = \zeta \cdot {}_{H}B(T) \cdot {}_{H}L(T) \cdot {}_{H}G(T_i) $$

where ζ : Seismic activity coefficient
${}_{H}B(T)$: Basic response spectrum for horizontal motion
${}_{H}L(T)$: Coefficient of the longer period component for horizontal motion
${}_{H}G(T_i)$: Coefficient of soil amplification for horizontal motion

The computed spectrum is further modified with the coefficients of both liquefaction and topographical effect, when the possibility of liquefaction in sandy soil is high, and/or when the effect of surficial land form can not be ignored. The expression is thus.

$$ {}_{H}S'(T) = {}_{H}S(T) \cdot {}_{H}P(T) \cdot {}_{H}I(T) $$

where ${}_{H}P(T)$: Coefficient of liquefaction for horizontal motion
${}_{H}I(T)$: Coefficient of topographical effect for horizontal motion

When the design response spectrum is required at the EOBL, the following expression is used.

$$ {}_{H}S(T) = \zeta \cdot {}_{H}B(T) \cdot {}_{H}L(T) $$

The magnification in acceleration response spectra shall not exceed 4 for design response spectra.

4.2.1 Basic response spectrum for horizontal motion ${}_{H}B(T)$

The basic response spectrum for horizontal motion ${}_{H}B(T)$ is defined as the response spectrum on the EOBL and is provided in Fig.4.

(Commentary)

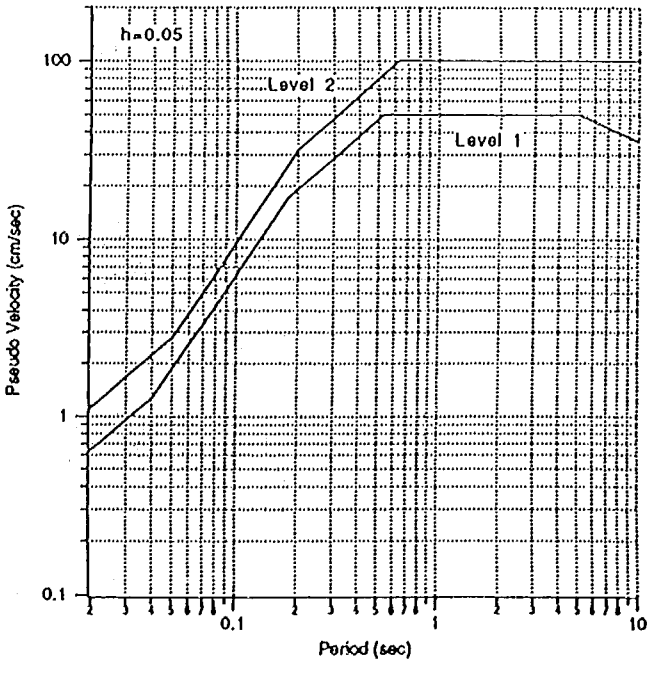


Fig.4 Basic response spectrum for horizontal motion

4.2.2 Coefficient of the longer period component for horizontal motion $_HL(T)$

The coefficient of the longer period component for horizontal motion introduces the regional gap into the amplitude of the longer period components. The coefficient for three regions in Japan are as follows.

Area 1 - Tokachi plain, Aomori plain, Kitakami basin, Akita plain, Shonai plain, Kanto plain, Niigata plain, Nagano basin, Saku basin, Nobi basin, Osaka plain, Kumamoto plain, Oita plain, Area surrounding Kagoshima city

Area 2 - Ishikari plain, Sendai plain, Area surrounding Shirakawa city, Toyama plain, Kofu basin, Coast of Suruga-bay area, Area surrounding Hamamatsu city, Ohmi basin, Nara basin, Kochi plain, Area surrounding Nobeoka city, Miyazaki plain, and its equivalents in scale

Area 3 - Areas other than the above, and hard rock areas

(Commentary)

The coefficient of the longer period component for horizontal motion $_HL(T)$ evaluates the regional gap in amplification property of longer period components caused by the geologic formation of the underground structure as deep as the seismic bedrock, and considers the difference in the property between 2 and 10 seconds. The coefficients are shown in Fig.5, for the three areas, and are specified for the central part of each location.

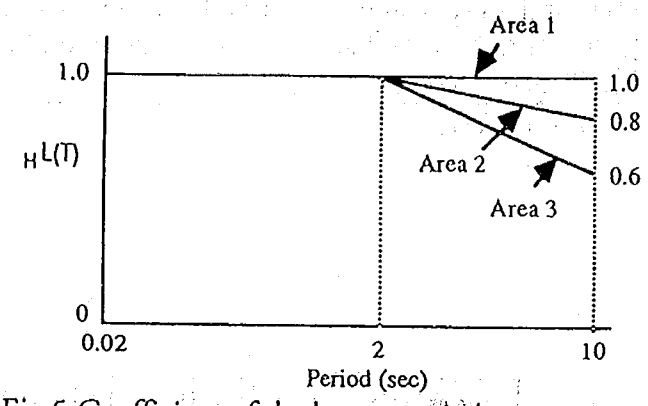


Fig.5 Coefficient of the longer period component for horizontal motion

4.2.3 Coefficient of soil amplification for horizontal motion $_HG(T_i)$

The coefficient of soil amplification for horizontal motion $_HG(T_i)$ introduces the amplification characteristics of the soil deposit above the EOBL and is prescribed for the classifications of surface soils and two design levels.

(Commentary)

The surface soils are classified into two categories: uniform type and non-uniform type. The non-uniform type is assigned when $\Delta V/V_e$ is larger than or equal to 0.2 and V_e/V_b is larger than or equal to 0.25, otherwise the uniform type is assigned. ΔV and V_e are defined as follows.

$$V_e = \sum_i V_i \cdot h_i / \sum_i h_i$$

$$\Delta V = \sum_i (|V_i - V_e| \cdot h_i) / \sum_i h_i$$

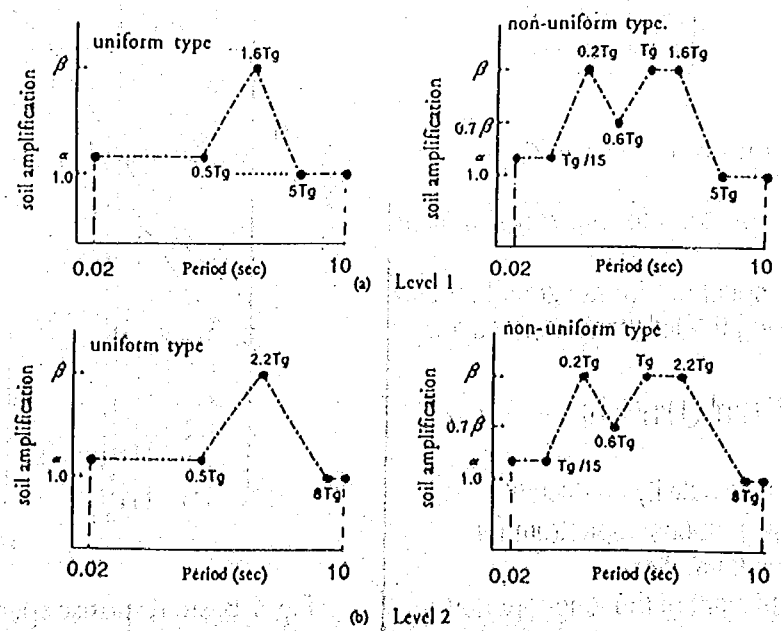


Fig.6 Coefficient of soil amplification for horizontal motion

where, h_i is the thickness of the i-th layer and V_i is the shear wave velocity of the i-th layer.
The coefficients of soil amplification for horizontal motion ${}_HG(T_i)$ are given as shown in Fig.6.The variables T_g, α, and β are given as follows.

$$T_g = 4\sum_i h_i / V_s$$

For level 1

For the uniform type,

$$\alpha = 1.5 - 0.5T_g \text{ and } T_g \geq 0.5$$
$$\beta = 2.6 - 1.6(V_s / V_b)$$

For the non-uniform type,

$$\alpha = 1.9 - 0.9T_g \text{ and } T_g \geq 0.5$$
$$\beta = 3.2 - 2.2(V_s / V_b)$$

For level 2

For the uniform type,

$$\alpha = 1.0 - 0.4T_g \text{ and } T_g \geq 0.5$$
$$\beta = 2.4 - 1.4(V_s / V_b)$$

For the non-uniform type,

$$\alpha = 1.6 - T_g \text{ and } T_g \geq 0.5$$
$$\beta = 2.9 - 1.9(V_s / V_b)$$

4.2.4 Coefficient of liquefaction for horizontal motion ${}_HP(T)$

The coefficient of liquefaction for horizontal motion ${}_HP(T)$ introduces the influence of the earthquake-induced excess pore pressure on the ground motion and is prescribed according to the stages of liquefaction.

(Commentary)

When the soil deposit includes saturated sand with high liquefaction potential, another non-linearity due to increase in pore pressure, or decrease in the effective confining pressure should be considered. This is in addition to the non-linearity of the soil due to the increase of strain that is taken into account in this guideline by discriminating the amplification property with the level of the earthquake motion at the EOBL. The influence is classified into three categories according to the liquefaction potential described by a parameter such as the liquefaction resistance ratio F_L, which is commonly used in Japan.

Table 1 Classification of the Influence of Pore Pressure

Category	Influence	F_L	Correct
A	ignorable	$1.5<F_L$	No
B	exists	$1.0<F_L\leq 1.5$	Yes
C	Liquefaction	$F_L\leq 1.0$	detail*

* individual study in detail

Table 2. Coefficient of Liquefaction for horizontal motion

Design Level	Coefficient of liquefaction				
1	T(s)	0.02	$1.6T_g$	$5T_g$	$8T_g$
	${}_HP(T)$	1.0	1.0	1.2	1.0
2	T(s)	0.02	$2.2T_g$	$5T_g$	$8T_g$
	${}_HP(T)$	1.0	1.0	1.2	1.0

4.2.5 Coefficient of topographical effect for horizontal motion ${}_HI(T)$

The coefficient of topographical effect for horizontal motion ${}_HI(T)$ introduces the influence of the land forms of the site on the ground motion and is prescribed according to the degree of the surficial topography.

(Commentary)

The coefficient of soil amplification assumes that a soil deposit consists of horizontally layered soils. However, in most of the cases, the underground structure has, more or less, geological irregularities in the layering or surficial land forms. When the influence of such irregularities cannot be ignored, the effect of soil amplification should be considered according to the properties. The soil conditions with geological irregularities include cliffs, slopes, hills(ridges), embankments, valleys for surficial irregularity, and the irregularity of layer interfaces.

Since the geological conditions vary widely, a quantitative generalization of the dynamic property is still under investigation via earthquake observation and analytical examinations.

4.3 Design response spectrum for vertical motion $\nu S(T)$

The design response spectrum for vertical motion $\nu S(T)$ is computed using the following expression.

$$\nu S(T) = \zeta \cdot \nu B(T) \cdot \nu L(T) \cdot \nu G(T_i)$$

where, ζ : Seismic activity coefficient
$\nu B(T)$: Basic response spectrum for vertical motion
$\nu L(T)$: Coefficient of the longer period components for vertical motion
$\nu G(T)$: Coefficient of soil amplification for vertical motion

The computed spectrum is further modified with the liquefaction correction coefficient and the topographical effect correction coefficient, when there is a high possibility of liquefaction in sandy soil or when considering the effect of surficial land form. The expression is thus,

$$\nu S'(T) = \nu S(T) \cdot \nu P(T) \cdot \nu I(T)$$

where, $\nu P(T)$: Coefficient of liquefaction for vertical motion
$\nu I(T)$: Coefficient of topographical effect for vertical motion

When the design response spectrum is required at the level of the EOBL, the following expression is used.

$$\nu S(T) = \zeta \cdot \nu B(T) \cdot \nu L(T)$$

The magnification in acceleration response spectra shall not exceed 4 for design response spectra.

(Commentary)

The description for vertical motion is essentially identical to the horizontal motion. Compared with that for horizontal motion, however, research activity on vertical motion to date has not been so high as to provide sufficient data . Therefore, in this section, the basic response spectrum and the coefficient of soil amplification are explicitly prescribed. The coefficients of longer period, liquefaction, and topographical effect are added only to maintain consistency with the horizontal motion.

4.3.1 Basic response spectrum for vertical motion $\nu B(T)$

The basic response spectrum for vertical motion $\nu B(T)$ is defined as the response spectrum on the exposed EOBL and is provided in Fig.7.

(Commentary)

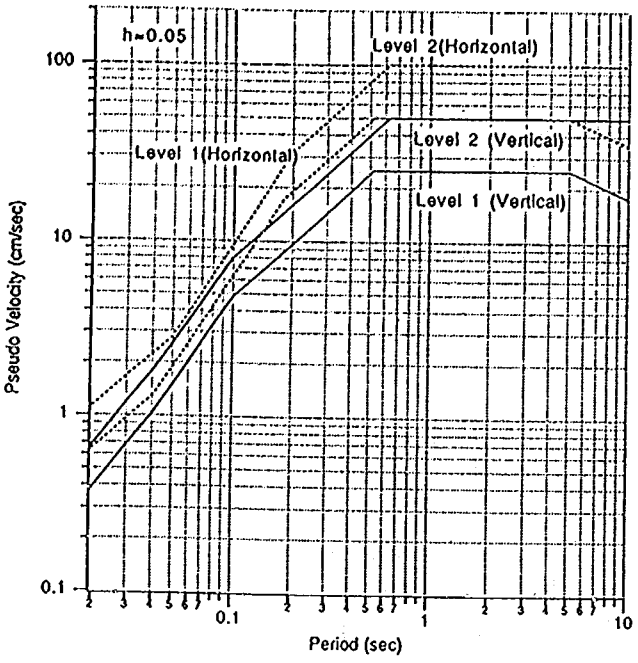


Fig.7 Basic response spectrum for vertical motion

4.3.2 Coefficient of the longer period component for vertical motion $\nu L(T)$

The coefficient of longer period component for vertical motion $\nu L(T)$ is tentatively assumed to be identical to the coefficient for horizontal motion, namely,

$$\nu L(T) = {}_H L(T)$$

4.3.3 Coefficient of soil amplification for vertical motion $\nu G(T_i)$

The coefficient of soil amplification for vertical motion $\nu G(T_i)$ introduces the amplification property of soil deposit above the base layer for vertical motion and is prescribed for classifications of surface soils and two design levels.

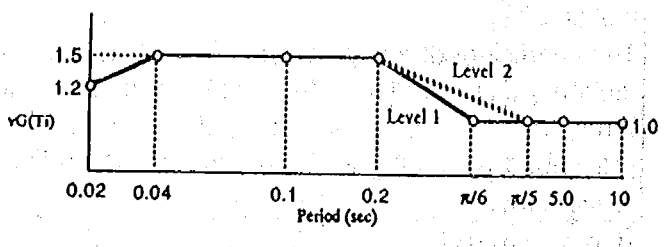


Fig.8 Coefficient of soil amplification for vertical motion

4.3.4 Coefficient of liquefaction for vertical motion γP(T)
The coefficient of liquefaction for vertical motion γP(T) introduces the influence of the earthquake-induced excess pore pressure on ground motion and is prescribed according to the stages of liquefaction.

4.3.5 Coefficient of topographical effect for vertical motion γI(T)
The coefficient of topographical effect for vertical motion γI(T) introduces the influence of the land forms around the site on the ground motion and is prescribed according to the degree of the surficial topography.

5. Generation of design earthquake ground motion time history
The design earthquake ground motion time history shall be generated for two design levels considering the frequency content and time varying property of amplitude for two design levels.
5.1 Generation of time history
The design earthquake ground motion time history shall be generated so that the response spectrum is compatible with the design response spectrum.

5.2 Duration and envelope function of the time history
The time-varying property of ground motion is prescribed by the duration and the envelope function.

(Commentary)
The time history analysis (step-by-step analysis) method is commonly used for the response analysis of a complicated structure or for nonlinear response analysis. The design earthquake ground motion time history is generated so that the response spectrum coincides with the design response spectrum.
The following is the method commonly used to generate a time history whose response spectrum is compatible with the design response spectrum.

Methodology for generating the simulated earthquake ground motion

(1) Superposition of sinusoidal waves
There are many schemes to define wave forms. Here, the acceleration wave form is expressed as a superposition of many components,

$$y(t) = e(t)\sum_i A_i \cos(\omega_i t + \phi_i)$$

where e(t) is an envelope function that provides non-stationarity of a wave, A_i is the amplitude of i-th component, w_i is the circular frequency of the i-th component, and f_i is the phase angle of the i-th component. The A_i is iteratively modified to obtain higher compatibility with the design response spectrum. In most cases, f_i is assumed to be uniformly distributed between 0 and 2π

(2) Modifying the recorded motion
There is a method in which phase angles of a recorded accelerogram are used instead of random phase angles. In such a case, it is preferable to avoid a record that has a small magnitude and short duration.

Qualification of the resulting wave form
The generated accelerogram should be qualified using criteria such as good compatibility with the design spectrum, sufficient number of frequency components, and proper values of peak velocity and peak displacement.
(1) Compatibility to the design spectrum
Three items can be considered as check points to determine the compatibility of the resulting wave form with the design response spectrum.
i) Minimum spectral ratio

$$\varepsilon_{min} = \left| \frac{S_{psv}(T_i, 0.05)}{DS_{psv}(T_i, 0.05)} \right|_{min} \geq 0.85$$

ii) Coefficient of variation (ν) of the spectral ratio

$$\nu \leq 0.05$$

iii) Deviation of average spectral ratio from 1

$$\left|1 - \varepsilon_{ave}\right| \leq 0.02$$

where S_{psv} is the calculated pseudo-velocity response spectrum, DS_{psv} is the design response spectrum (target spectrum) and T_i is the period at which compatibility is calculated, and

$$\nu = \sqrt{\frac{\Sigma(\varepsilon_i - 1)^2}{N}},$$

$$\varepsilon_{ave} = \frac{\Sigma \varepsilon_i}{N},$$

$$\varepsilon_i = \frac{S_{psv}(T_i, 0.05)}{DS_{psv}(T_i, 0.05)}.$$

In the above evaluation, the number of frequency points in which the compatibility is checked might be between 200 and 300, and it is recommended to choose a point from frequencies that are not the component frequency.

(2) Peak velocity and peak displacement
It is also recommended to show the peak values for velocity and displacement by integrating the generated accelerogram and the property of the filter used as well.

Generation of multi-component accelerograms
When time histories of two horizontal components or of three components including vertical motion are required, one of the following techniques may be used.

- Use a different set of random numbers to simulate an independent time history for uniform random phase scheme.
- Use each component time history for the phase angle scheme.

6. Usage of the design earthquake ground motion

6.1 Correction of the design response spectrum by a damping factor
When the spectral modal analysis method is used in the dynamic analysis, the design response spectrum may be corrected in accordance with each modal damping factor.

6.2 Correction of the design response spectrum with input condition
When input motion is required at ground levels other than the base layer or ground surface, design earthquake ground motion may be determined using the response analysis of the soil deposits.

(Commentary)
It is generally recognized that the duration and envelope function of earthquake ground motion reflect the process of fault rupture. Earthquakes of magnitudes 7 and 8 are assumed for design Levels 1 and 2, respectively.
Since the design earthquake ground motion for design Level 1 is used mainly for allowable stress design method, the duration of time history may be long enough to give peak response values. In addition, the coda portion of the wave should be taken into account to consider the non-linear response of structure.
The following envelope functions are recommended in this guideline.

For Level 1 -- duration of 60 seconds

$$e(t) = (t/5)^2 \qquad 0 \le t < 5$$
$$e(t) = 1 \qquad 5 \le t < 25$$
$$e(t) = \exp\{-0.066(t-25)\} \qquad 25 \le t \le 60$$

For Level 2 -- duration of 120 seconds

$$e(t) = (t/5)^2 \qquad 0 \le t < 5$$
$$e(t) = 1 \qquad 5 \le t < 35$$
$$e(t) = \exp\{-0.027(t-35)\} \qquad 35 \le t \le 120$$

EXAMPLE OF GENERATED DESIGN EARTHQUAKE GROUND MOTIONS

Construction of the design response spectra

The design response spectra $_H S(T)$ are evaluated for two sites, i.e., Site-1, Site-2; with the seismic activity coefficient of 1, the coefficient of the longer period component L(T) of 1for the period longer than 2 sec. The configuration of layers of each site is shown in Fig.9. The parameters used for evaluating $_H G(T_j)$ are summarized in Table 3.

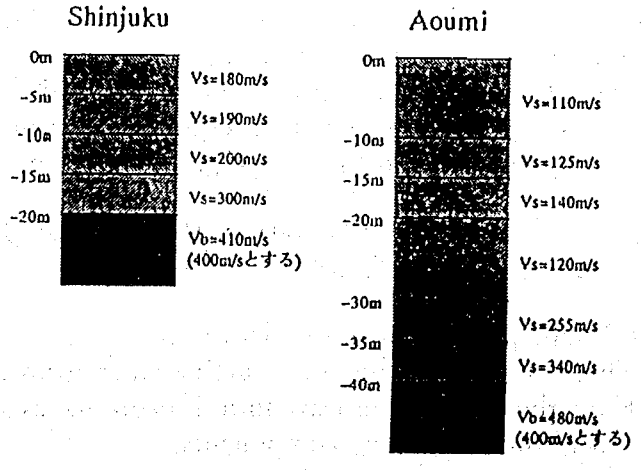


Fig.9 Soil layers of test sites

Table 3 Parameters for determining $_HG(T_i)$ for two test sites

	Site-1	Site-2
Ve(m/sec)	217.5	165
Tg(sec)	0.368	0.970
Ve/Vb	0.544	0.413
DV(m/sec)	41.25	66.25
DV/VE	0.190	0.402
Classification	Uniform	Non-uniform
α(Level-1)	1.32	1.03
α(Level-2)	0.85	0.63
β(Level-1)	1.73	2.29
β(Level-2)	1.64	2.12

The design response spectra evaluated for Site-1 and Site-2 are shown in Figs.10 and 11 for two design levels.

Example of the Generation of design earthquake ground motion time histories

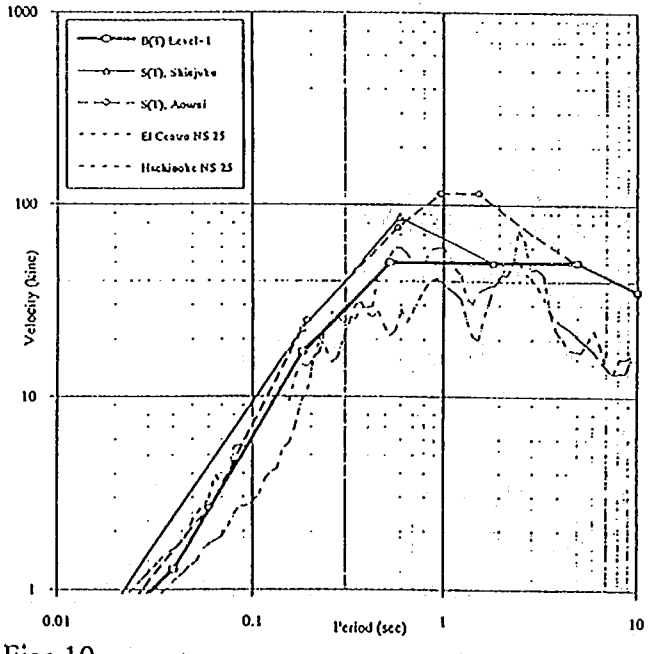
The time histories corresponding the given spectra were generated for the basic design reponse spectra. The compatibility of the computed time history to the target spectrum is shown in Figs.12 and 13. The time history is shown in Figs.14 and 15, respectively. It seems that a good compatibility is obtained in these cases.

ACKNOWLEDGEMENTS

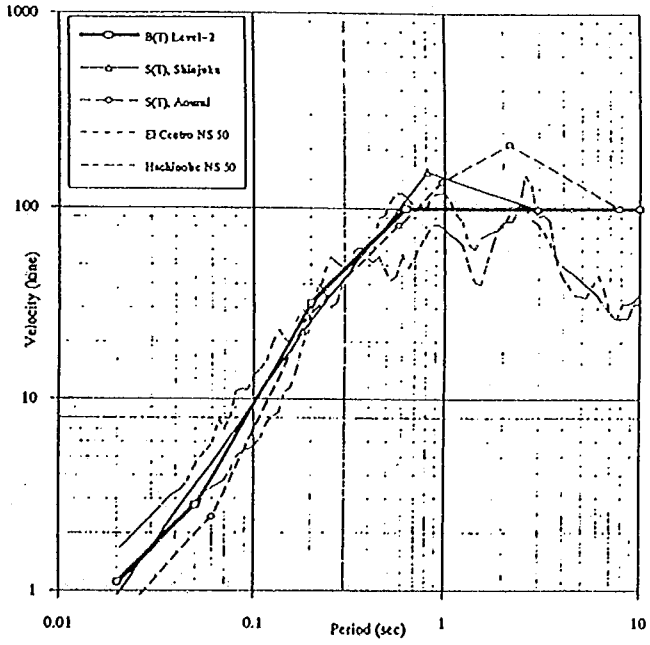
Many researchers have contributed greatly to complete the proposal of the guideline. We would like to express sincere thanks to the Committe members for their collaboration.

REFERENCES:

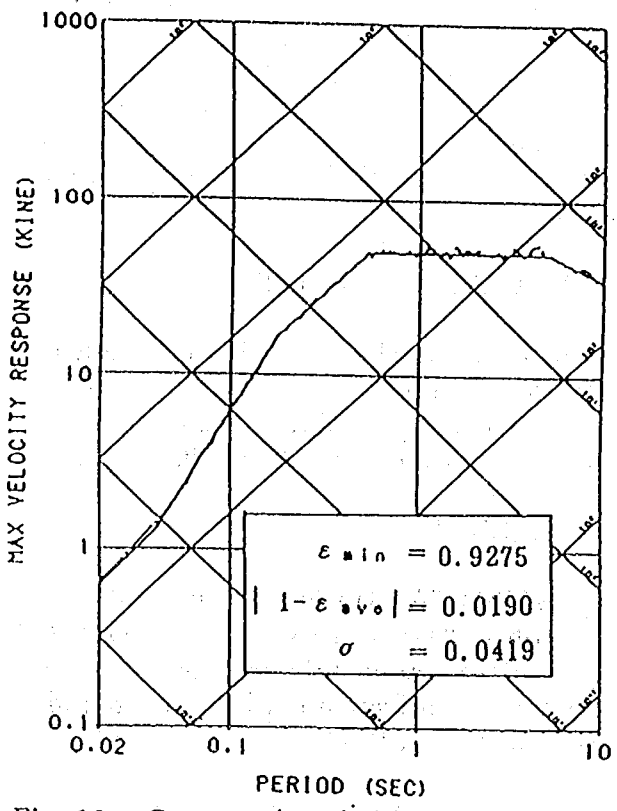
BRI & BCJ, "A GUIDELINE FOR EVALUATING DESIGN EARTHQUAKE GROUND MOTION FOR BUILDINGS", Annual Report Vol.2, Research Committee for Design Earthquake Ground Motion, March, 1992,



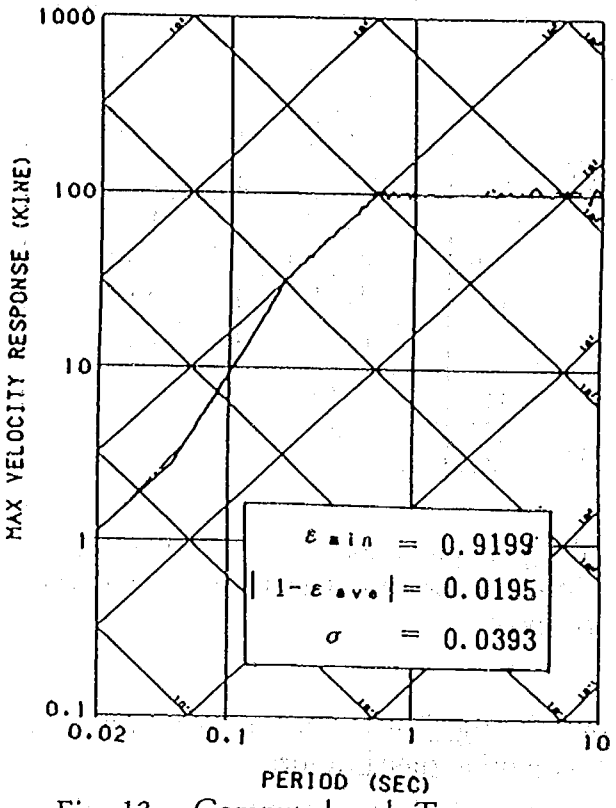
Figs.10 Design response spectra for Level-1



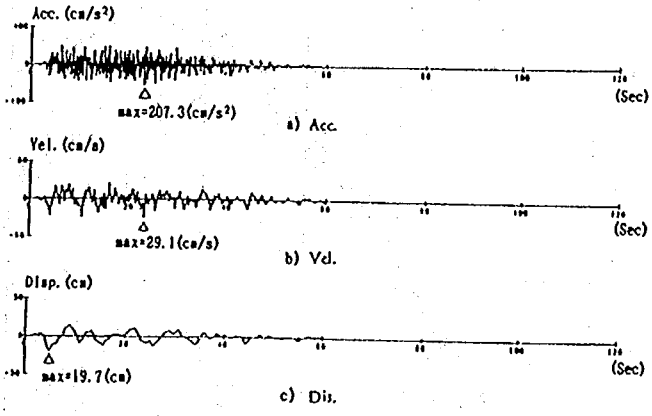
Figs.11 Design response spectra for Level-2



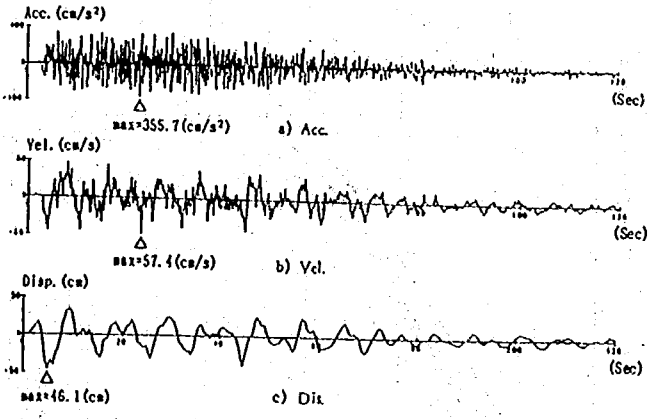
Figs.12 Computed and Target spectrum for Levels 1



Figs.13 Computed and Target spectrum for Level 2



Figs.14 Generated time histories for Level-1



Figs.15 Generated time histories for Level-2

THE COORDINATED U.S.A. RESEARCH PROGRAM ON STRUCTURAL CONTROL FOR SAFETY, PERFORMANCE, AND HAZARD MITIGATION

Robert D. Hanson[1] and T. T. Soong[2]

ABSTRACT

The coordinated USA National Science Foundation research program started in the summer of 1992. Early results from these new grants, several continuing grants, and parallel efforts funded through NCEER are summarized. The topics range from assessments of the enhanced safety and performance of structures; theoretical and experimental development of specific active, passive and hybrid devices; to full-scale implementation studies.

KEYWORDS: active control; devices; hazard mitigation; hybrid control; passive control

1. INTRODUCTION

When NSF initiated its five year research program on structural control for safety, performance, and hazard mitigation in 1992, the co-authors were asked to serve as coordinators for the program. The purpose for the coordination was to maximize the productivity of each individual effort and to speed implementation of these research results in practice. We were asked to coordinate recent past, current and near future projects funded by the NSF program with ongoing projects funded by the National Center for Earthquake Engineering Research, SUNY at Buffalo. This coordination effort will provide many challenges and opportunities over the next four years.

The remaining portion of this paper provides brief summaries of each individual research effort prepared by the principal investigator of each project. NSF projects which do not have a summary included are marked *.

2. 1992 NSF GRANTS

Ahmet E. Aktan, University of Cincinnati
Steel Highway Bridges

Alfredo H-S. Ang, Univ of California, Irvine
Safety and Performance Enhancement

Jamshid Ghaboussi, University of Illinois
Neural Networks

*Barry J. Goodno, Georgia Inst of Tech
Hybrid Control of Building Seismic Response Using Architectural Cladding

Robert D. Hanson, University of Michigan
Electrorheological Active Members

Victor C. Li, University of Michigan
Smart Cementitious Composites

Jack Y.K. Lou, Texas A & M University
Tuned Liquid Damper

*Sami F. Masri, University of Southern California, Studies of Integration and Implementation Issues in the Active Control of Lifeline Systems

Thomas M. Murray, Virginia Polytech & State Univ., Occupant Induced Motion

Ronald L. Sack, University of Oklahoma
Phase Related Input Control

Benson Shing, University of Colorado
Adaptive Hybrid Control

Jackson C. Yang, University of Maryland
Optical Fiber Sensor

3. CONTINUING PROJECTS

Billie F. Spencer, University of Notre Dame
Robust Feedback Control

Henry T. Yang, Purdue University
Control Uncertainties Under Wind Loads

Jann N. Yang, Univ of California, Irvine
Hybrid Control of Bridges

Jann N. Yang, Univ of California, Irvine
Full-Scale Control Implementation

4. NCEER PROJECTS

M.C. Constantinou, S U N Y Buffalo
Multistage Fluid Dampers

M.Q. Feng, University of California, Irvine
Hybrid Energy Dissipation

D.A. Foutch, University of Illinois
Viscoelastic Dampers

A.M. Reinhorn, S U N Y Buffalo
Secondary and Nonstructural Systems

T.T. Soong, S U N Y Buffalo
Full-Scale Building Implementation

T.T. Soong, S U N Y Buffalo
Vibration Control of Sensitive Equipment

1. University of Michigan, Ann Arbor
2. State University of New York, Buffalo

EXPLORING THE PROBLEMS IN ACTIVE STRUCTURAL CONTROL AND HEALTH MONITORING OF EXISTING CONSTRUCTED FACILITIES BY UTILIZING A DECOMMISSIONED STEEL TRUSS HIGHWAY BRIDGE.

Emin Aktan, Stuart Shelley, Kuo-Liang Lee.
University of Cincinnati.

A "real life" active vibration control system was implemented and tested on a 250 foot span steel truss highway bridge (Photo 1). Reduction in global vibration levels of up to 20db (90% reduction) were achieved during testing using random, sinusoidal and step release disturbance excitation. The control system demonstrated the ability to control response due to these large mechanically induced loads, yet was sensitive enough that vibration from human movement on the bridge was detected and attenuated. This work verified the viability of an innovative theoretical development in the field of active vibration control of structures, adaptive modal filter based modal control, and also provided a wealth of knowledge regarding the practical problems which will be experienced in actual installations which will be required to operate reliably for long periods without human intervention.

The adaptive modal filter (AMF) based active vibration control method is an innovative control approach which has been developed at the University of Cincinnati. The method is unique in that it utilizes adaptive spatial filtering to simplify the response of a complicated system into responses of individual single mode systems. This method is excellently suited to implementation on complex structures outside of the laboratory due to a number of unique characteristics:

a) It is generally very difficult to obtain an accurate and complete model of real world systems to use for control design and implementation. Very little knowledge of the system is required in order to implement the AMF based controller. The only information required is the poles of the modes to be controlled. No mode shapes are required and no information at all is required regarding uncontrolled modes.

b) The AMF control method gracefully accommodates sensor failures (and also actuator failures in the case of multi-actuator control systems) and calibration changes. Indeed, due to the inclement weather experienced during the testing, at any given time, approximately 20% of the accelerometers utilized for the control system were failed.

c) The AMF based controller is robust to varying system dynamics.

Test results demonstrating controller performance and robustness to varying system dynamics are shown in Figures 1 through 3. Figure 1 shows open and closed loop Frequency Response Functions (FRF) measured at a servo-hydraulic disturbance actuator. The response is dominated by the first bending mode of the bridge which is attenuated by a factor of 10 with active control. Figure 2 shows open loop FRFs measured 9 hours apart. Large changes in frequency and amplitude of resonant peaks are evident. Figure 3 shows that the controller performance has not deteriorated in spite of these large shifts in system properties.

A great deal was learned regarding the practical aspects of real life active vibration control implementation. The harsh winter environment experienced throughout the test period (freezing rain, snow, high winds) provided an ideal accelerated test laboratory which dramatically demonstrated the need for fault tolerance and robustness to changing system dynamics.

The work which was proposed under the investigators' one year FY92 NSF support has been accomplished and final review and documentation of results is in progress. Current goals are to secure continuing NSF support in order to implement a semi-permanent installation for active vibration control and system dynamic property monitoring. Areas of interest include multi-input control, actuator and sensor failure accommodation and detection, autonomous controller retuning and continuous monitoring of system dynamic characteristics.

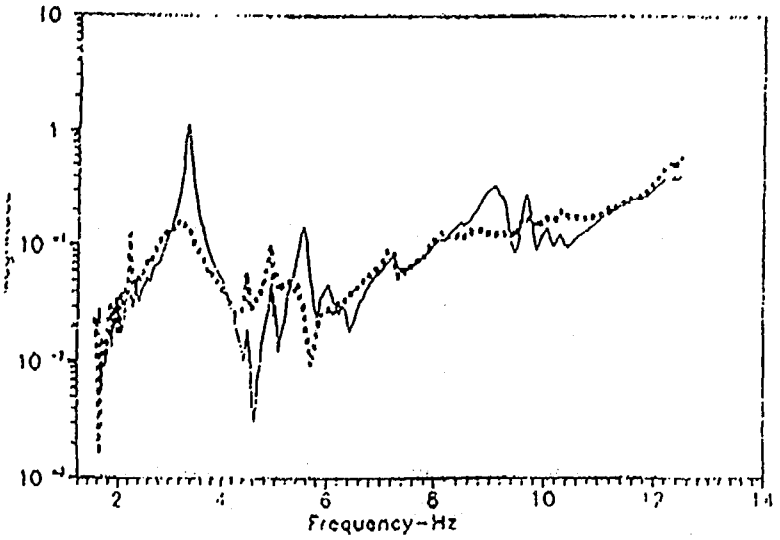


Fig.1 Open & Closed Loop Frequency Response -03/10 10PM

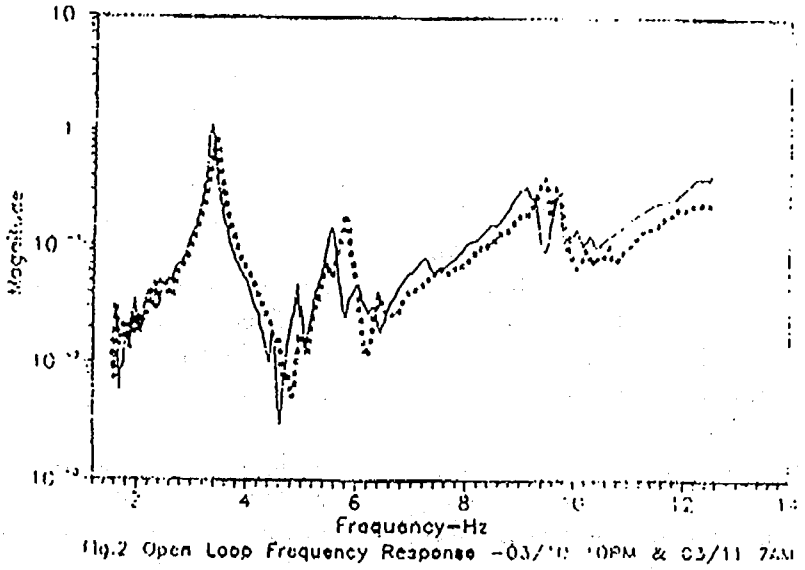


Fig.2 Open Loop Frequency Response -03/10 10PM & 03/11 7AM

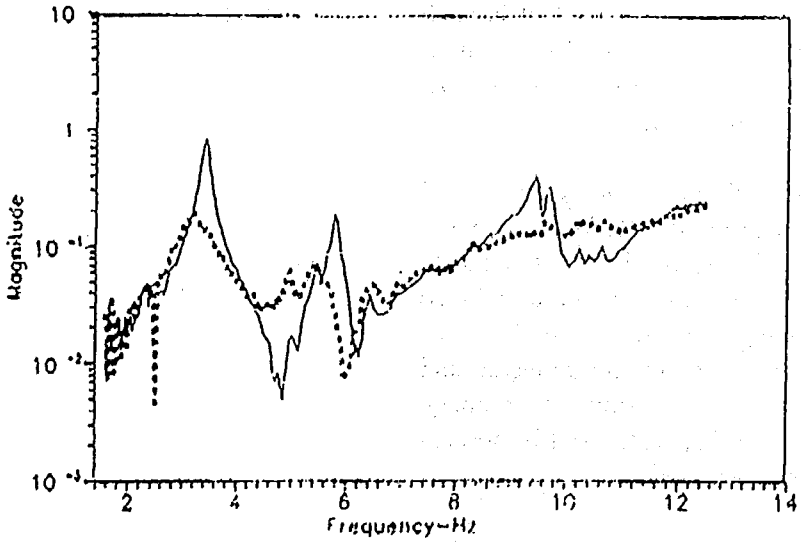


Fig.3 Open & Closed Loop Frequency Response -03/11 7AM

SAFETY AND PERFORMANCE ENHANCEMENT THROUGH STRUCTURAL CONTROL

Principal Investigator: A. H-S. Ang
University of California
Irvine, CA 92717

In order to ascertain the effectiveness of structural control as an alternative means for protection against earthquakes, more careful and complete evaluation of structural system integrity is needed. A comprehensive analysis showing the potential advantages and limitations of a structure with active, passive, or hybrid protective system can be influential in the successful implementation of control technology. Such analyses may include the following:

- assessment of probability of exceeding specified (e.g., tolerable) damage;

- assessment of probability of structural collapse.

The above assessments should cover all possible intensities of earthquake motions; i.e. respective fragility functions should be generated. Integration of these fragilities with the hazard function for the pertinent site would yield the respective expected annual and lifetime probabilities.

The economic advantage of structural control may also be an important measure of effectiveness. In particular, the reduction in the expected life-cycle damage cost relative to that of the corresponding structure without control is such a measure. To assess this cost effectiveness, however, requires information on damage cost as a function of damage level.

The studies suggested above are being performed using data for specific structures that were damaged during the Mexico City earthquake of 1985. Based on a damage model developed previously, and using data for several of the buildings in Mexico City that were damaged and subsequently repaired, a preliminary damage cost function is developed, expressed in percent (%) of replacement cost.

Two buildings (one that collapsed and the other repaired) were selected for in-depth study. Both structures were examined in terms of the potential improvement in safety and damage prevention that can be achieved through proper application of structural control; the associated cost effectiveness is also assessed. Results for one of the buildings are presented graphically in Figs. 1 through 3.

Figures 1 and 2 show the fragility curves against excessive damage and collapse, respectively, for the building without control; corresponding fragilities of the same building with active and passive controls are also shown in the figures. Fig. 3 shows the damage cost of the building as a function of the ground motion intensity. Integrating this cost function with the annual seismic hazard curve for Mexico City yields the expected annual damage cost for the building; similar integration with the lifetime hazard function would lead to the expected life-cycle damage cost.

The results have obvious implication to retrofitting of structures. Conceivably, had the above building been properly retrofitted with active or passive control, its reliability of surviving the 1985 earthquake without collapse would have been significantly enhanced - e.g. with rubber isolators, the 50-year lifetime collapse probability would be 6×10^{-6} versus 1.18×10^{-1} of the original structure. Also, the damage cost of the same building could have been much lower - e.g. the expected annual damage cost would be 0.2% versus 2.18% of replacement for the original structure.

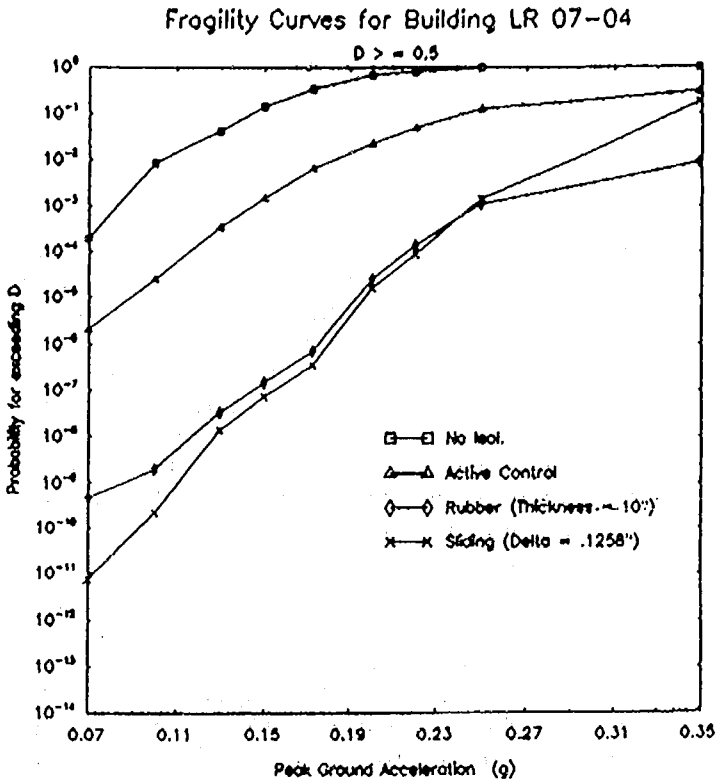


Fig. 1: Fragility Curves Against Excessive Damage

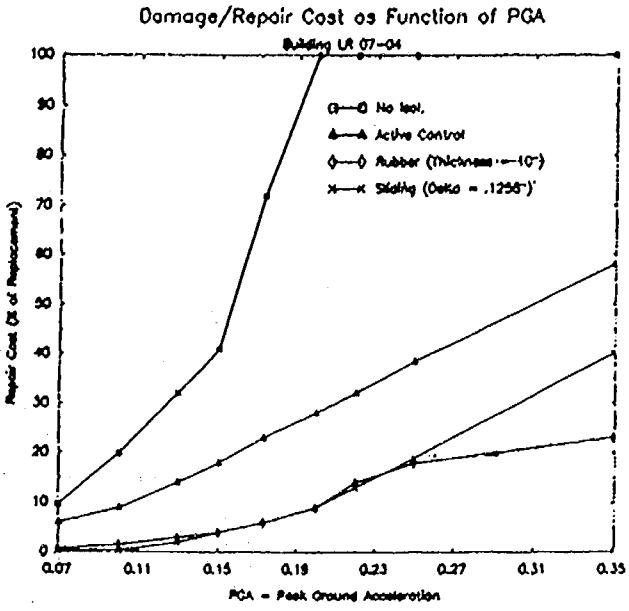


Fig. 3: Damage Costs as Function of PGA

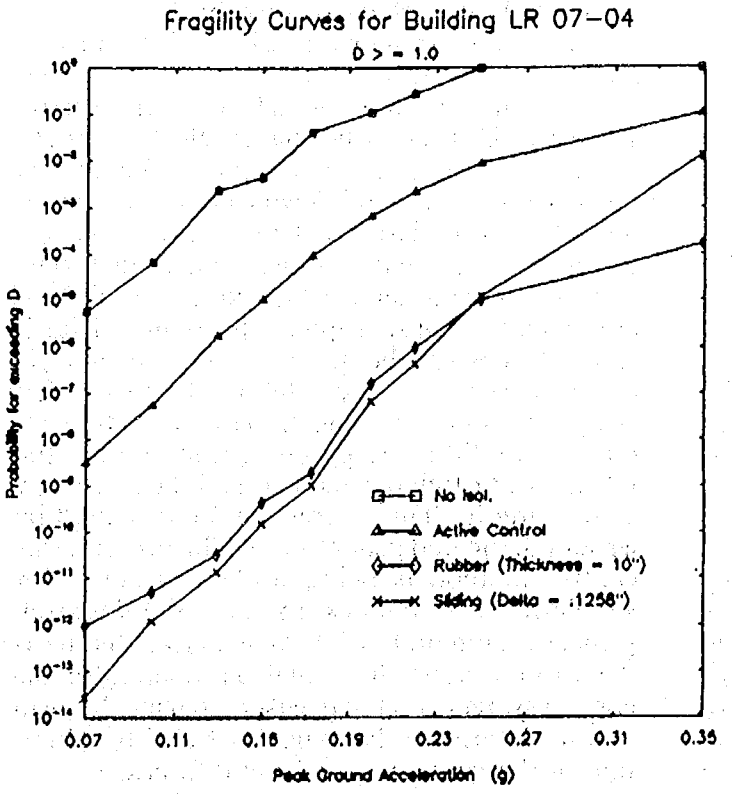


Fig. 2: Fragility Curves Against Collapse

ACTIVE CONTROL OF STRUCTURES USING NEURAL NETWORKS

J. Ghaboussi, Y. K. Wen and S. L. Paul

The overall goal of this research project is to develop the methodology for the active control of structures using neural networks. The advantages of structural control with neural networks are: adaptivity of the control system; the ability to control nonlinear structural response; and, the potential for development of systems capable of recovery from partial failure. The short term goals of the research project are to develop and test appropriate neural network structural control schemes. Currently, research is being conducted in two areas. In one research task we are developing and testing advanced neural network control methods applied to tendon control schemes. On a separate task we are working on the development of a new and innovative structural control method using suspended weights. The actual control of the structure with suspended weight will also be accomplished with the trained neural networks. Both of these research projects are in the first phase of development and testing through computer simulations. In the next phase of research, experiments will be performed in both projects.

Adaptive and Nonlinear Structural Control Using Neural Networks The neural networks structural control system being investigated in this project is schematically shown in Figs 1 and 2. The controller is trained with the aid of an emulator which itself must be trained first. The emulator network learns the transfer function between the actuator signal and the sensor readings. Consequently, the information needed for the training of the actuator can readily be obtained by sending random signals to the actuators and measuring the response of the structure at the sensors. After the training of the emulator, the controller network is trained directly on the structure by satisfying the appropriate control criteria. At the present, appropriate software have been developed for numerical simulation of the structure, the control system and the neural network simulators. A special type of neural network, in which the network architecture adaptively evolves during the training, is being used in this research project. This adaptive neural network has been developed by the Principal Investigator and his co-workers on other research projects. In the next phase of this research, the proposed neural network control system will be tested in the laboratory. For this purpose the neural network emulator and neural network controller will be trained directly on the structure in the lab. The performance of the trained neural network controller will be investigated experimentally.

Structural Control with Suspended Weights The major drawback of most of the structural control methods is that they are highly energy intensive. This is specially serious during earthquakes when the energy sources and the distribution systems are disrupted. The proposed control system uses an innovative design to avoid the high energy requirement. It uses a reserve kinetic energy to resist the earthquake forces. The proposed control system consists of large masses, possibly located underground, suspended from the structure by a cable and pulley system, as shown in Fig. 3. The masses are caused to move in the vertical direction, while producing a horizontal force couple on the structure. During the normal comfort control to reduce the wind generated motions, the masses are accelerated up and down to generate the required horizontal forces. This operation is energy intensive, similar to other control methods. However, during the earthquakes, when the energy sources are disrupted, the required horizontal forces can be generated by successively dropping the mass and catching the suspended weight, as shown in Fig. 4. This operation requires very little energy, enough to operate the release and catch mechanism and the computer controlling it. This energy can be provided by a small dedicated generator. At the present, this control method is being studied in computer simulations. In the next phase of this research project we intend to perform experiments in order to determine the actual parameters of the control system and the release/catch mechanism and to determine the magnitude and the duration of the generated horizontal forces.

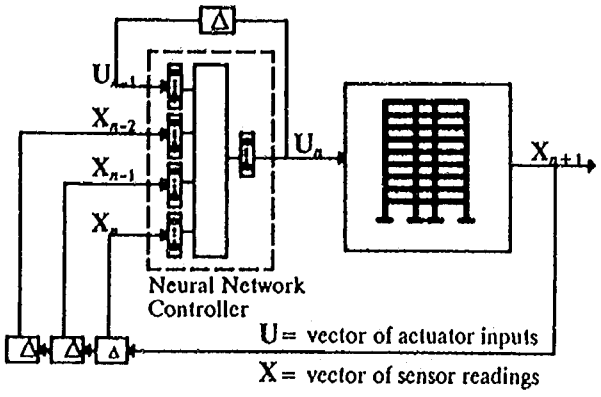


Figure 1 Neural network Controller

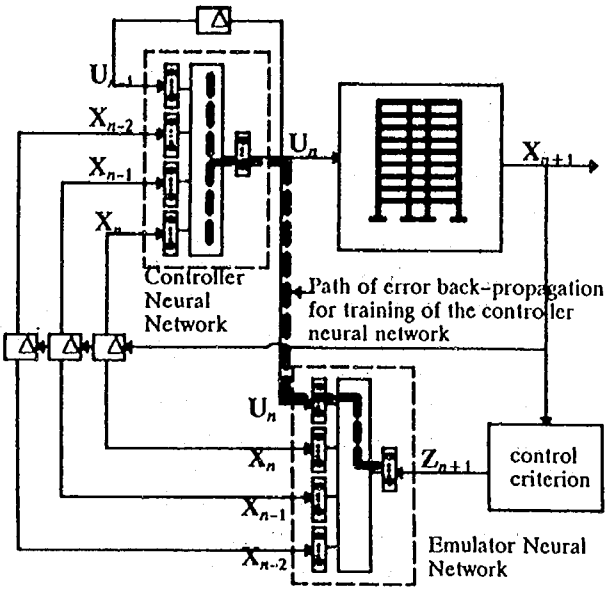


Figure 2 Training of the controller neural network with the aid of the emulator

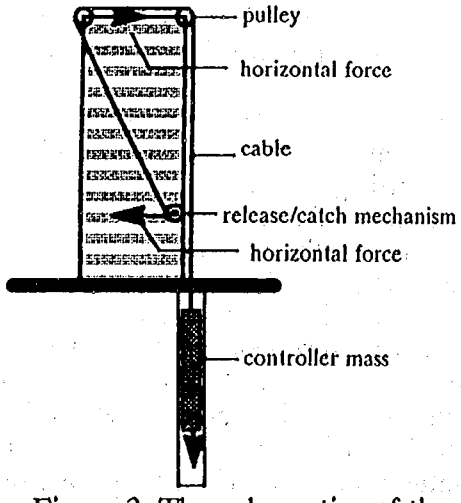


Figure 3. The schematics of the proposed structural control scheme

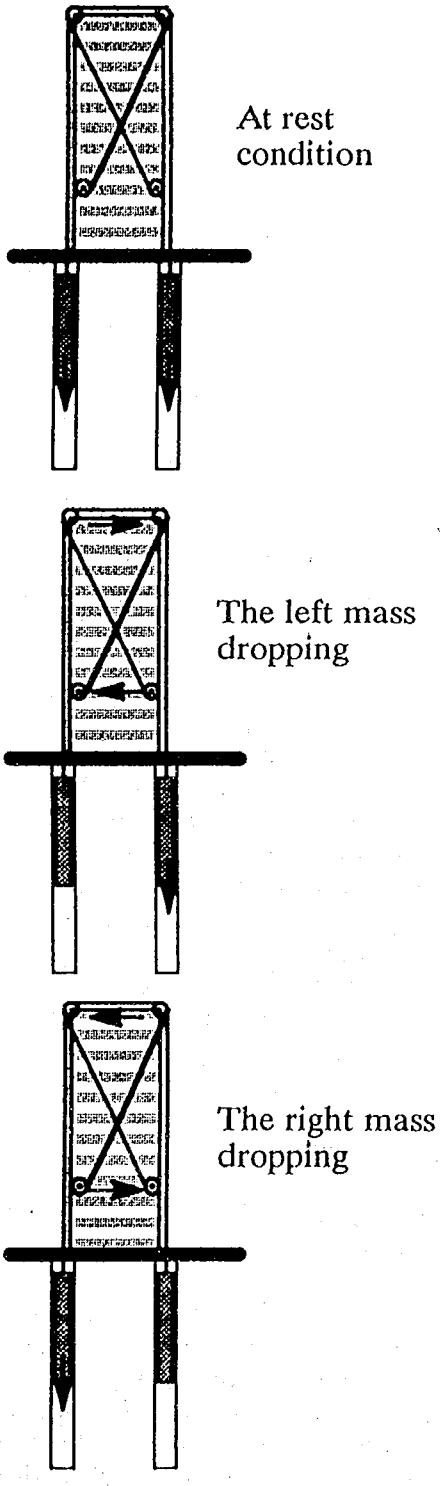


Figure 4. Generating horizontal forces by dropping the weights

ACTIVE MEMBERS FOR CONTROL OF STRUCTURES SUBJECTED TO EARTHQUAKES AND WIND STORMS

Robert D. Hanson, Frank E. Filisko, N. Harris McClamroch, Henri P. Gavin, Daniel Gamota, and David Ortiz
University of Michigan, Ann Arbor, MI

Project Description and Objectives.

The main objective of this project is to develop a control system for active structural members which requires almost no external energy to attenuate the dynamic response of buildings and bridges during earthquakes or strong wind storms. This will be accomplished through the development of active structural members whose mechanical properties can be changed nearly instantaneously by an electrical signal from a structural controller. It is proposed that the new active structural member would be constructed, at least in part, from electro-rheological materials whose stiffness and damping properties can be actively controlled. The advantage of electro-rheological materials is that their mechanical properties can be changed by over a hundred-fold by a low amperage electrical field and that these changes occur in milliseconds. The development of structural members whose dynamic properties can significantly change almost instantaneously on command provides a new opportunity for structural control. The establishment of a new structural control approach which would utilize the unique properties of active structural members requires a new philosophy for the development of control algorithms.

Project Tasks.

This objective will be realized through the successful completion of three tasks:

Task 1 is to develop an active axial structural member utilizing electro-rheological materials whose stiffness and damping properties change nearly instantaneously with an applied low amperage electrical field. Physical testing and experimental verification of the active member properties with imposed electrical field is part of this task.

Task 2 is to establish control algorithms for buildings and bridges subjected to earthquakes and strong winds. These algorithms will require a new philosophy directed toward active structural member control.

Task 3 is to verify that the established control system appropriately influences the properties of the active structural members, and that the controlled structural members produce the desired dynamic performance of the building or bridge.

Successful completion of these three tasks will result in development of active structural members with mechanical properties which can be controlled on command, and a control system which will be able to make intelligent decisions and to issue commands for member property changes. This new technology will result in buildings and bridges with variable structural properties which satisfy high performance, safety and hazard mitigation requirements, both in usual operating environments as well as in extraordinary environments during earthquakes and wind storms. It is expected that these new actively controlled structural members, together with existing passive mechanisms, can successfully mitigate the most severe environmental loads with total system reliability at a minor increase in cost.

Research Progress.

Task 1: Development of Active Structural Members with Electro-Rheological Materials

Because axial force members have the greatest influence on the structural stiffness of building frames, research and development of electro-rheological axial force members with stiffness and damping characteristics will be investigated first. The device currently being tested in the laboratory consists of a series of closely spaced parallel plates constructed in a rectangular configuration. The space between the plates is filled with a electro-rheological material manufactured at the University of Michigan.

Alternate plates are connected to an electrical ground and the others to a high voltage, low amperage power supply. From initial tests it has been determined that the prototype device is capable of even higher forces than expected, and that compact full-scale configurations are possible.

Task 2. Establish Structural Control Algorithm for Bridges and Buildings for Active Structural Members.

It is assumed that the structure, and perhaps the ground, will be instrumented with sensors or transducers to provide measurements for displacements, velocities, and accelerations at specified locations. The sensed information will be transmitted to a central computer, where real time decisions are to be made based on a control algorithm, and the control voltages applied to the electro-rheological elements are automatically adjusted. Inner and outer loop control algorithms are being studied in parallel. The outer loop algorithm uses traditional linear and nonlinear control theories adapted to the needs of the building and bridge structures under consideration. The inner loop algorithm under consideration employs a neural network to control the active member itself, which is expected to be influenced by a variety of environmental, electrical, and mechanical parameters.

A suspension bridge, Figure 1, and a base isolated building are being used as the first control models in this study because they provide simpler structures, in a control sense, than multi-story buildings. The number of control points is limited and the performance criteria can be expressed by fewer variables. Because the dominant frequencies are low and well separated, successful control should be easier.

References.

Gamota, Daniel and F. E. Filisko (1991a), "Dynamic mechanical studies of electro-rheological materials: Moderate frequencies", J. Rheol. 35(3), 399-426.

Gamota, Daniel and F. E. Filisko (1991b), "High frequency dynamic mechanical studies of an aluminosilicate electrorheological material", J. Rheol. 35(7).

Leitmann, G. and E. Reithmeier (1993), "Semi-Active Control of a Vibrating System by Means of Electrorheological Fluids", Dynamics and Control, Vol.3, pp. 7-33.

Soong, T.T.,(1990a) Active Structural Control: Theory and Practice, Longman Scientific & Technical (John Wiley & Sons, Inc., New York), Great Britain.

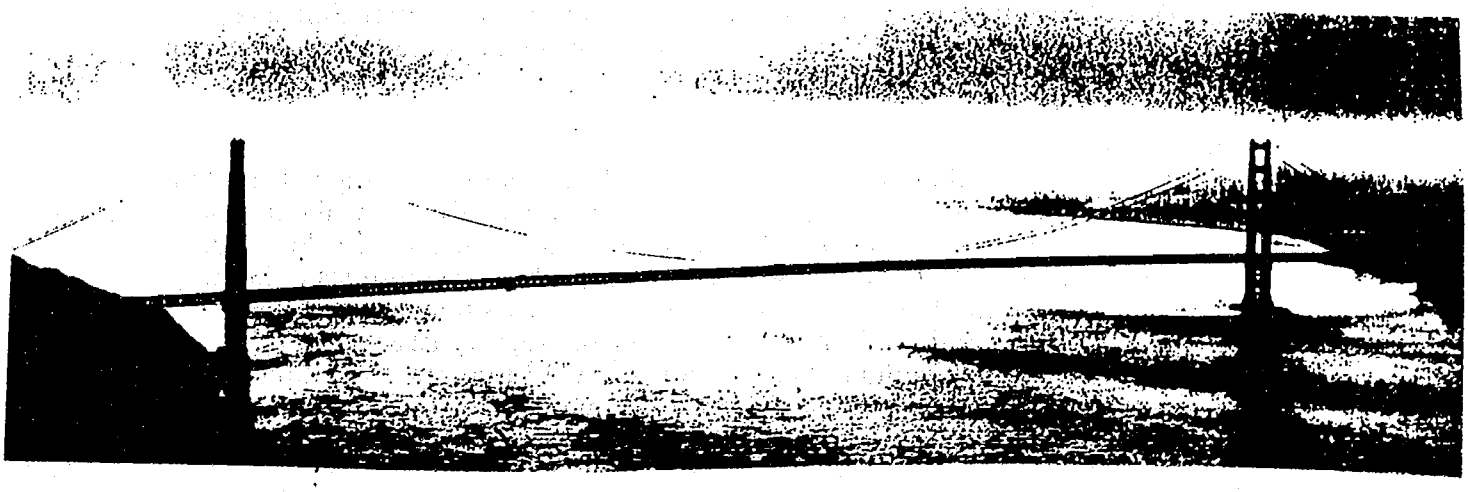


Figure 1. Golden Gate Suspension Bridge, San Francisco, California

Passive Smart Cementitious Composites With Crack Repair Capability

Victor Li
Advanced Civil Engineering Materials Research Laboratory
University of Michigan, Ann Arbor, MI 48109-2125

Project start date: September, 1992
Report date: March 19, 1993

This project represents an investigation into the feasibility of developing a smart structural composite which has a self-healing capability whenever and wherever cracks are generated as a result of seismic overloads, cyclic loading or other mechanical or environmental loads. Controlled cracking is used to activate the release of chemicals into cracks for sealing purpose. The chemicals are stored in hollow fibers which are randomly mixed into the concrete, together with crack control reinforcing fibers. Thus, the designed composite will be passive in the sense that the rehealing process does not require external intervention, but rather the sensors and actuators distributed through out the structural system are activated by each overload event.

The major elements of this project consist of
1. Feasibility studies of passive actuators and sensors: Fiber/coating/chemical/matrix combinations and release mode.
2. Studies of control system: Interfacial bond, pseudo strain-hardening, and crack width control.
3. Study of chemical release mechanisms.
4. Real time direct observation of chemical rehealing under E-SEM.

Long term goal: Analysis, design and implementation of composite system with passive rehealing capability.

Short term goal: Analysis of crack width control in order to minimize the amount of chemical that needs to be carried by the hollow fibers. Design composite system and perform tensile and fracture testing to confirm the concept of crack width control. This control system must work in order to practically implement this passive smart concept. Another immediate goal is to select a specific fiber type which will be used to carry the chemical. This fiber will be tested for its sensing capability. Our initial choice is a hollow glass fiber which utilize its own brittleness to sense matrix cracking and respond by breaking.

Research findings:
1. Composite Design: Based on micromechanical analysis, an initial composite system has been designed with neat cement reinforced by polyethylene fibers. Uniaxial test confirms that this system undergoes pseudo strain-hardening when overloaded. Even when strained beyond the elastic limit, the load carrying capacity continues to increase, up to several percent strain. Figure 1 shows the tensile stress-strain curve of this composite in comparison to that of a neat cement and an ordinary fiber reinforced concrete. The average crack width in this composite is 0.13 mm. Investigation of controlling parameters governing crack width and techniques for reducing crack width is on-going.

2. Damage Tolerance: Under extreme loading, such as that experienced by materials at the tip of a sharp notch, the designed composite is found to be much more damage tolerant than ordinary cementitious materials. Cement or concrete would fracture. Ordinary fiber reinforced concrete would fracture with fiber bridging across a single

enlarging crack. The specially designed composite was found to undergoing controlled microcracking around the notch tip, as shown in Figure 2. This characteristic should be ideal for self-healing when chemical release is activated by these microcracks.

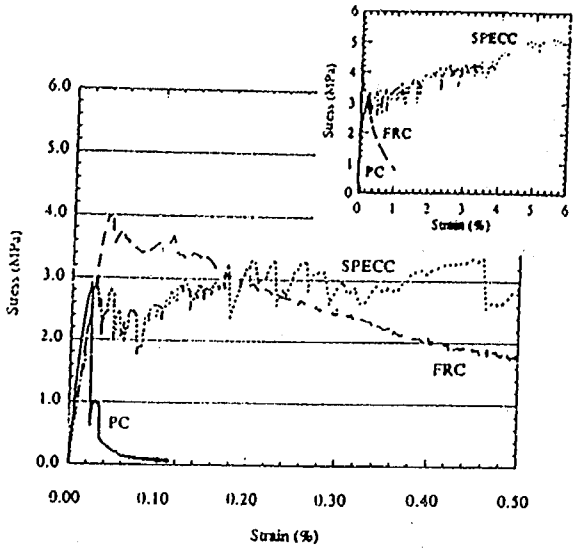


Figure 1



Figure 2

ACTIVE TUNED LIQUID DAMPER FOR STRUCTURE CONTROL

Jack Y.K. Lou, Loren D. Lutes, and Suhada Jayasuriya

PROJECT DESCRIPTION

Recently, tuned liquid dampers (TLD) have been installed in a number of buildings in Japan. Model tests have shown a reduction of RMS building motion of more than 50 percent in some cases. Furthermore, the TLD system offers many advantages for structural control as compared to other devices.

Although the effectiveness of the TLD system for control of wind-induced vibrations has been demonstrated, it may not be adequate in its passive mode for control of earthquake-induced vibrations. However, it is expected that its effectiveness could be greatly enhanced by adding active control to make it a hybrid control system.

SHORT AND LONG TERM GOALS

The objectives of the present research are: (1) to further advance the passive TLD technology, and (2) to investigate the merits of adding active control to further enhance TLD effectiveness over a wider range of frequencies.

The work is scheduled for three years. The goal for the first year work is to assess the magnitude of liquid damping as affected by various TLD parameters and motion characteristics; and to derive suitable transfer function for the liquid sloshing force.

The goals for the second year work are to assess the need of active control, using a SDOF building model with a passive TLD; to develop suitable control algorithms based on the transfer function developed; and to conduct experiments to demonstrate the feasibility of the hybrid TLD system. Stochastic methods of random vibration will be used to confirm the effectiveness, stability, and robustness of the TLD for controlling motions which are characteristic of wind and earthquake response.

During the third year, work will continue on the active control TLD system. In addition, large scale model tests will be conducted at SUNY-Buffalo using available multi-story building model to verify the effectiveness of the actively-controlled system.

The long term goals for the research will be focused on the development of design guidelines for active TLD systems and the application of active TLD for suspension bridges and offshore structures.

WORK ACCOMPLISHED DURING THE FIRST YEAR

Accomplishments during the first year were delayed by the withdrawal of a research assistant who was scheduled for the project and by the leave of absence of the Co-PI. However, rapid progress has been made since December. The test platform has been modified, needed instrumentation and apparatus designed and fabricated, and series of model tests have been conducted. This is briefly described below.

The test platform shown in Figure 1 is driven by a hydraulic actuator controlled by a MTS material testing system. Either displacement or force control of the actuator can be accomplished. Thus, both the wind- and earthquake-induced motions can be simulated.

The model TLD is supported on four specially designed and fabricated shear load cells, monitoring the total bottom shear force. Base acceleration is also monitored by a precision low frequency accelerometer. Therefore, the net bottom shear and the damping forces produced by the slosh liquid can be determined accordingly. Sample results are presented in Figure 2. Preliminary calculations indicate that for a smooth TLD tank having a mass of 1% one cannot achieve 5% damping even in the frequency range of resonance. Internal structural elements would have to be added to increase the damping. Model tests will continue in the next five months. Further evaluations and conclusions can be reported at the first PIs' Coordination Meeting in June.

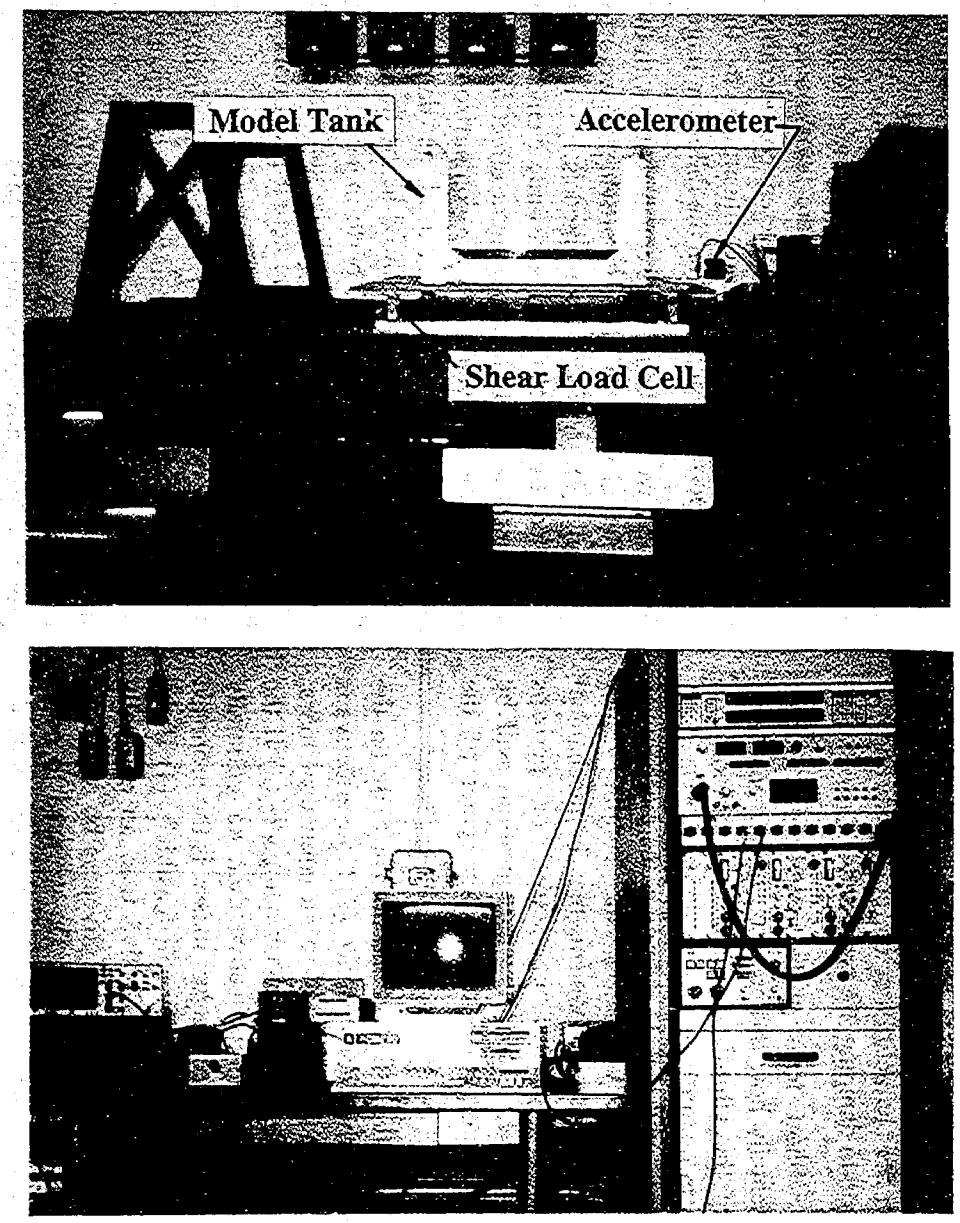


Figure 1. Test Apparatus

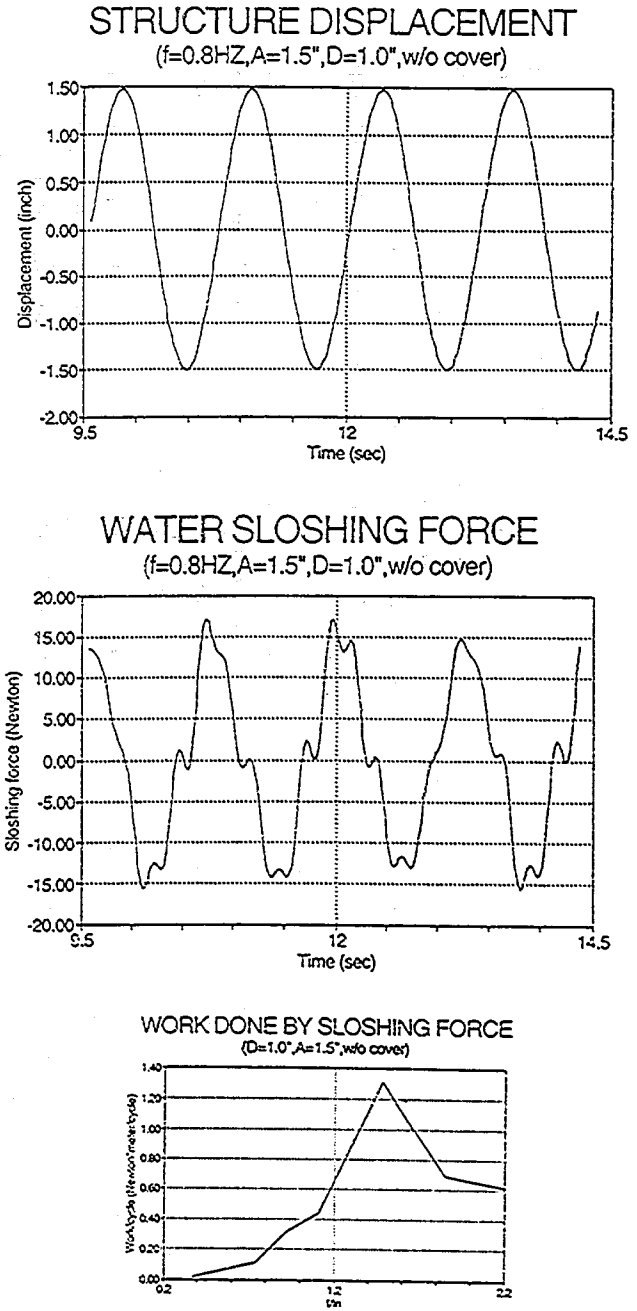


Figure 2. Sample Results

CONTROL OF OCCUPANT INDUCED FLOOR MOTION

Thomas M. Murray
Daniel J. Schneck

Project Description. The use of lightweight floor systems has increased significantly over the past several years. The primary advantage of these systems is the reduction in material costs associated with less dead weight. Also, the lighter materials are easier to ship and erect resulting in a savings in construction costs.

Although lightweight floor systems provide an economical alternative to the more expensive conventional systems, this savings is often negated by serviceability considerations relating to vibration performance.

Human vibration perception can be characterized as a function of the natural frequency, displacement amplitude, and damping of a structure. An improvement in dynamic performance can, therefore, be achieved by increasing the damping of the system by installing external damping devices.

Past attempts at artificially induced damping have produced only limited success. However, the present study focuses on a promising new approach in which the characteristics of the human body as they relate to damping are examined.

Goals. Short term goals include determining experimentally how the presence of human bodies influence the vibration response of a floor. In addition to quantifying the magnitude of effect, the experiments will seek to determine the mechanisms the human body utilizes in damping floor vibrations. These mechanisms may be mechanical or electrical, passive or active, or perhaps something else. The following questions will be addressed in order to unlock the secret of the human body.

(1) What is the effect of the human body on the frequency of the floor system? (2) How effective is the human body compared to an equivalent mass, optimally damped, tuned mass damper? (3) If the human body is less effective than an optimally designed TMD of equivalent mass, is the proposed study of the human body still feasible? (4) If the human body is more effective than an optimally designed TMD, can the effectiveness be explained by active control theories? Do we need to go to active means to have the same effectiveness as the human body? (5) Is all of the mass of the human body involved in the absorption process or is some of the mass inert? (6) At what frequencies is the human body most effective as a vibration absorber? (7) How does the human position affect the amount of damping provided by the human body? (8) Do two people weighing 200 lbs. have the same effect on the floor dynamics as one 200 lb. person? (9) Are there less sophisticated forms of life, an egg for instance, which also possess the efficient damping properties of the human body? If so, unlocking the secret here may hold some answers for designing efficient, multi-frequency, passive devices.

The long term goal is to extrapolate the information, gained from the study of the human body, to develop a device capable of controlling structural vibrations.

Progress and Preliminary Results. Progress to date has begun answering the above questions. Some of these questions are summarized below.

The human body seems to have a pure damping effect on the floor. When several humans, whose combined weight exceeded 3 times the floor weight, stood on a test floor there was no appreciable shift in natural frequency of the floor. The damping effect, however, was very high. When the same weight of inert mass was added to the floor, there were no significant changes in the damping percentage with respect to the bare floor; however the natural frequency was lowered considerably. Many of these concepts are illustrated in the sample experiment presented on the following page.

Analytical work is being done concurrently with the experimental work in order to provide answers to question (2). Test floor models are being developed, by modal testing and finite elements, to determine the theoretical maximum effect a TMD can have on a given floor for comparison with actual results from humans used as dampers. These models can also be utilized in the future for theoretical prediction of the performance of actual devices. Several models have been completed and will soon be calibrated to the actual test floors so the comparisons can be made.

The answer to question (3) is yes. Preliminary results have shown the human body to be effective over a frequency range rather than at a single frequency as in a TMD. This ability to control a range of frequencies in a passive device would provide a great advantage over a TMD.

CONTROL OF OCCUPANT INDUCED FLOOR MOTION

Thomas M. Murray
Daniel J. Schneck

SAMPLE EXPERIMENT:

A series of vibration tests were performed on a two-joist model floor located at the Virginia Tech Structures Laboratory. The floor was excited by a shaker located at midspan and the response was recorded by an accelerometer placed adjacent to the shaker. Damping was measured by using the "half power" method. Seven tests were performed in which a single person stood on the floor next to the shaker. Also, tests were performed using concrete blocks and buckets of water as added inert mass. Finally, a test was performed in which two people stood next to the shaker.

Figure 1 is a plot of added weight verses damping. As the figure shows, the concrete blocks and water had no effect on damping. The amount of damping remained slightly below 1 percent of critical for all added inert mass. The presence of a human occupant, however, had a dramatic influence on damping. Damping increased from 1 percent to over 2 percent when a 125 pound person stood on the floor and damping increased to 3 percent when a 240 pound person stood on the floor. When two people totaling 310 pounds stood on the floor, the damping increased to almost 4 percent.

Figure 2 is a plot of added weight verses fundamental frequency. As expected, the addition of inert mass reduced the fundamental frequency of the system. What is interesting is that when the added weight was that of a human body, the frequency experienced little change. Only small variations about the bare floor frequency of 9.47 hz were observed.

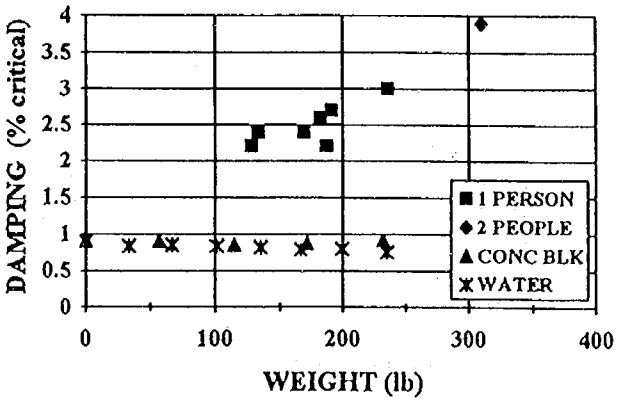


Figure 1. Weight vs Damping

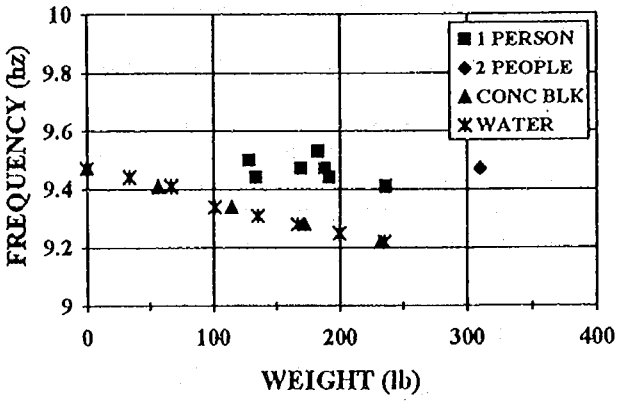


Figure 2. Weight vs Frequency

Structural Control for Phase-Related Inputs

Ronald L. Sack
William N. Patten
Univ. of Oklahoma

A. Ebrahimpour
Penn State Univ.

Humans can produce significant dynamic loads, both while remaining in place and moving. The objectives of the proposed research are to: (a) define the dynamic loads generated by activities involving motion such as walking and running; and (b) establish the benefits and efficiency of low power semiactive control technologies to mitigate excessive structural response due to phase related occupant loads.

We constructed a force platform 9.15 m long and 2.03 m wide consisting of various modules as shown in Fig. 1. The platform is designed so that the subjects have 1.83 m of acceleration ramp to achieve their steady-state motion before encountering the instrumented module. The instrumented force platform is composed of 6 independent plates (81 cm by 91 cm) constructed of 2.5 cm aluminum honeycomb material, each supported by four short instrumented cantilever beams. The natural frequency of each panel is greater than 100 Hz.

We measured loads imposed by one and two people moving across the force platform. A typical force-time history plot with a subject walking totally on the instrumented platform is shown in Fig. 2. Each participant traverses the platform by walking (slow, medium and fast), running and marching. Using the descriptive parameters as functions of several independent variables (e.g., weight and body type), we formulated a regression model for an individual's load history.

Loads imposed by two people traversing the platform were also measured. If two people walk or run with no prompt, the phase lag between their foot strikes is random. But, if two people march across the platform in response to a prompt signal, the phase lag between the two responses is small and can be statistically related (via an exponential distribution). We measured the phase lag between two individuals by conducting a sufficient number of tests where the subjects moved to a prompt. Using temporal summation of two individual histories we can generate the load-time histories for two people. Crowd coherency is governed by auditory and visual effects. We will obtain the total imposed loads by mathematically extrapolating from single foot strikes of participants moving side by side in two or more rows. The experimental information will be extrapolated for loads by large groups of various sizes using simulation, along with the descriptive parameter statistics and the phase lag distribution for two individuals. Loading spectra will be obtained for various activities.

Vibrations of the lightweight floor system will be mitigated using semi-active control. The controlled inputs will be provided by tunable hydraulic dampers. These low-power actuators, which resemble the common hydraulic shock absorber, typically include a motorized internal valve, or pressure actuated servo valve. The power required by the process is that necessary to position the valve.

In order to demonstrate the concept of applying semiactive damping to structures, a preliminary experiment was conducted. The natural frequency of the structure (without the damper attached) was 4 Hz. A commercially available controllable semiactive damper was then affixed to the midspan (see Fig. 3). A small brushed DC motor was used to provide modulation of a hydraulic by-pass valve that is mounted internal to the damper. Bench testing revealed that the motor was able to move the valve from a full open to a full closed position in approximately 10 ms. A PC based data acquisition system was utilized to acquire the amplified accelerometer output. A sample rate of 2 KHz hardware filter was used to eliminate high frequency noise from the data. Updates of the actuator occurred at 1 KHz.

An individual jumped on and off the walkway to test the response of the system. Figure 4 shows the controlled and uncontrolled acceleration frequency response. The results make it clear that the activation of the damper attenuates the magnitude of the response. Also the frequency content of the controlled response is generally higher than the resonant frequency of the structure. Preliminary results indicate that a semiactive structural damper can affect a significant change in the way a structure responds to loads imposed by pedestrians.

The material is based upon work supported by the U.S. National Science Foundation under Grant MSS-9202731. Any opinions, findings and conclusions or recommendations expressed are those of the writers and do not necessarily reflect the views of the National Science Foundation.

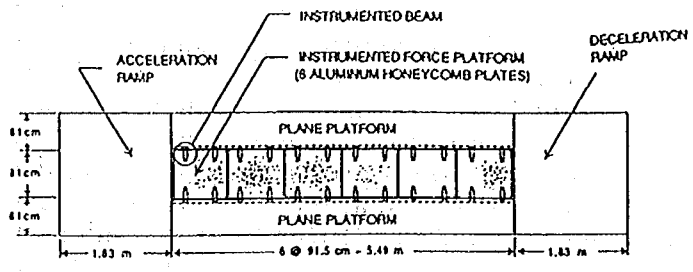


Figure 1. The force platform for measuring moving loads

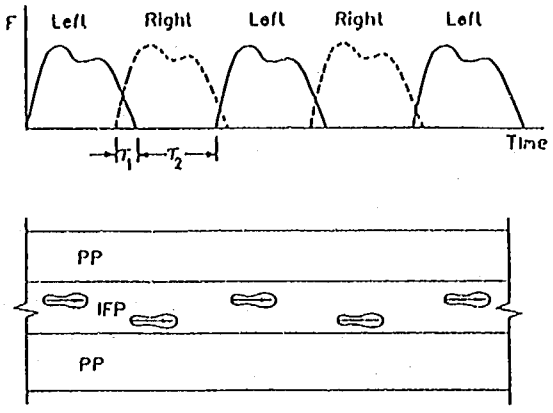


Figure 2. Force-time plot of a subject walking

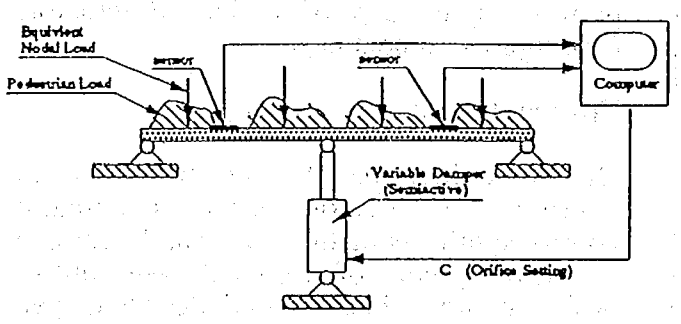


Figure 3. Floor system with semiactive damper

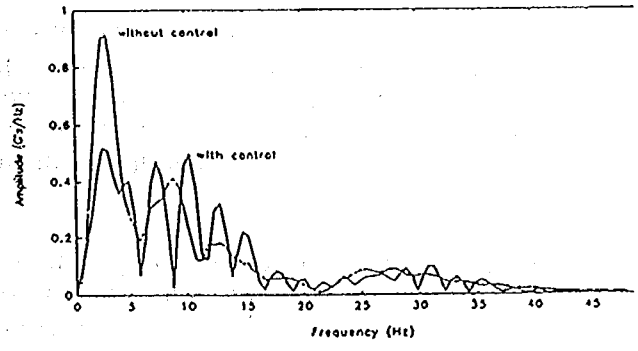


Figure 4. FFT of the Beam Vibration

DEVELOPMENT OF ADAPTIVE HYBRID CONTROL TECHNIQUES FOR BUILDING STRUCTURES

Benson Shing, Renjeng Su, Dan Frangopol, and Martin Mikulas
University of Colorado at Boulder

Objective

Our research investigates a new concept of hybrid control. It focuses on a hybrid actuator which can be used as either a passive damper or an active device. It is a screw-jack and shock-absorber type of actuator. The device can be installed in structural braces with collocated sensors and control electronics. The system based on such a distributed control system will be easy for reconfiguration and continuous tuning of control logic. It therfore offers great potential for adaptive control.

Research Tasks

Three research tasks will be conducted under this project. The first task is the development of control algorithms. We first review existing methods for designing control laws active control of buildings under earthquakes. Our emphasis in the review is to evaluate the techniques in the light of safety, robustness, and the potential for adaptive control. Next, adative control techniques will be developed to cope with realistic changes in structrural dynamics. Furthermore, the issue of reliability associated with the active control of buildings will also be examined.

The second task is the hardware development of the hybrid actuator. In the first year, mechanical design of the hybrid actuators will be conducted. Electronics for controlling the acturtor prototype will be developed in the second year.

The final task is to conduct experimental verification of the adaptive hybrid control concept. An experimental test bed will will be set up which includes a model structrure and the actuators. The control design procedures for both hardware and control laws will be tested. The issue of time delay will also be evaluated.

Research Progress From July 1992 to March 1993

Design of Active Control Laws

We have examined the conventional linear quadratic regulator (LQR) approach and the instantaneous optimal control approach with a six-story building investigated by Yang, et. al. We have analyzed the robustness of LQR controllers with a sample El Central ground excitation with its phases shifted by all-pass filters. In summary, our research findings are:

1) The objective of LQR design does not cover well the overall building control objectives. For example, the displacement limits which are crucial to the building safety can not be systematically handled in the control logic design. 2) The conventional optimal control method or instantaneous optimal control method does not give systematic consideration to the nature of the earthquakes such as their frequency content and randomness. 3) Due to the variation of phases of ground excitation, a building under active control may experience up to 15 per cent variation in its maximum displacement and 20 per cent in maximum control force.Therefore, the benefit of one control logic over another must be considered in the context of such large performance deviations. (See figures on next page.)

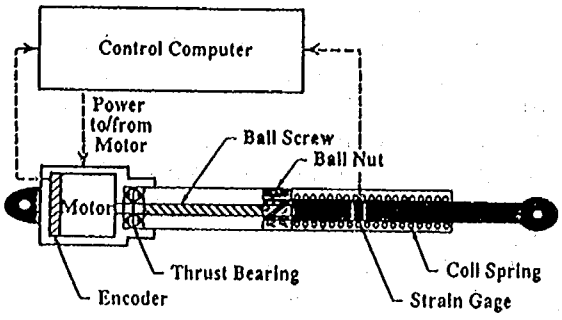
Developement of Hybrid Actuator

Dynamical analysis has be performed on a preliminary concept of the hybrid actuator. (See figures on next page.)

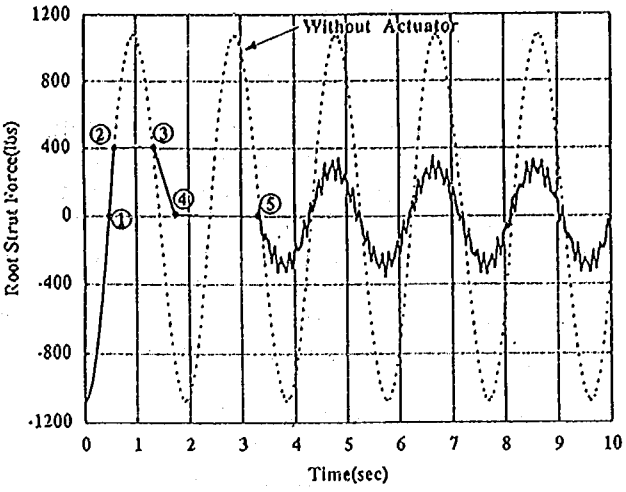
Future Goals

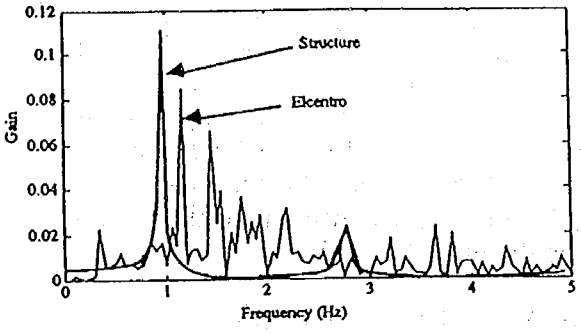
Our immediate goals for this project are to continue the development of systematic control synthesis method. We shall continue the development of a closed-loop control design method which incorporates the known information of ground excitation such as frequency content and amplitudes. We also intend to investigate the balance between frequency shifting and additive damping to achieve the control objectives. The development of the actuator will also continue as planned.

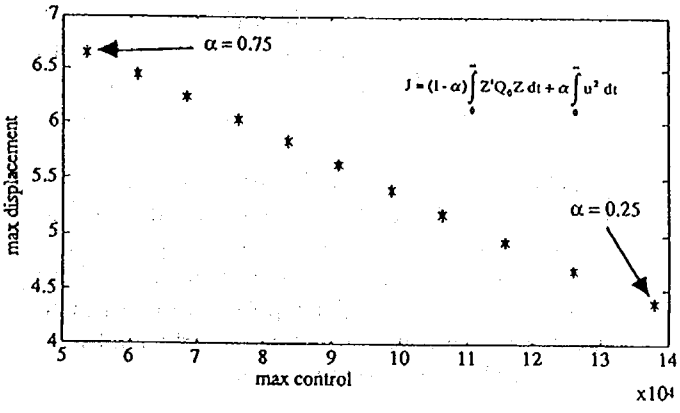
LINEAR LOAD CONTROL ACTUATOR
(Energy Absorbing Strut)

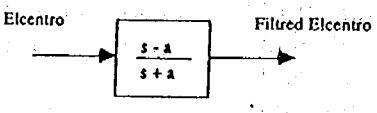


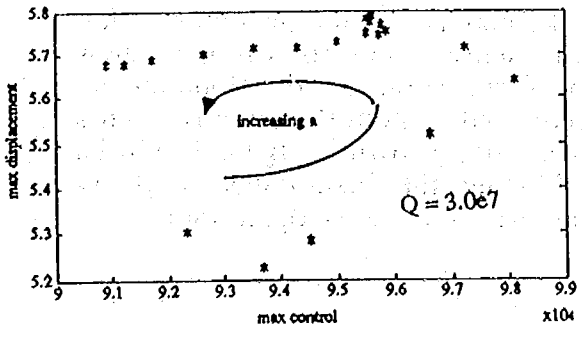
ROOT STRUT FORCE WITH AND WITHOUT ACTUATOR
(Spring Preload = 400 lbs)

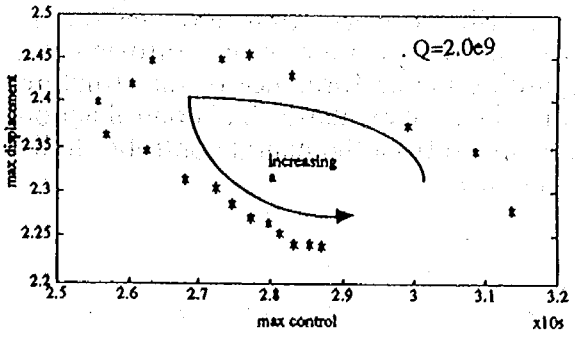












ACTIVE CONTROL OF STRUCTURE INSTRUMENTED WITH OPTICAL FIBER SENSOR UNDER EARTHQUAKE LOADING

J.C.S. Yang, F. Amini, J.S. Sirkis and G.Z. Qi

Project Scope:

This is a three years project including two tasks: (1) development of a neural network control scheme for structures subjected to earthquake loading; (2) shake table experimental test of a scaled structural model instrumented with optical fiber sensors to verify the neural network control approach to be developed in this research.

Neural Network Controller:

Due to the attributes of the neural network, such as massive parallelism, adaptability, robustness and inherent ability to handle the nonlinearity, in this research project, we propose to develop a neural network approach for structural control. There are two steps involved in the development. A Backpropagation Through Time (BTT) neural controller would be developed first. The BTT neural controller is trained based on the instantaneous minimization of the performance index of the structure and may not ensure the optimization in the global sense. Therefore, in next step, a new component, Critic neural network, will be implemented to the BTT neural controller to reinforce the training process and to achieve the global control optimization.

Experimental Testing

The structure control experiments will be carried out in the laboratory using a scaled model structure. The model structure will be a 1:8 scaled 3-story steel frame of a prototype structure modeled by the method of artificial mass simulation and the lumped mass approach. In addition to the accelerometers and strain gauges, the optical fiber sensors will be mounted on the structure to provide more information regarding the performance of the structure under the base excitation and control action determined from the neural controller to be developed.

Summary of Progress to Date:

Up to date, most of the research efforts are focused on the development of the neural network control scheme for structures subjected to earthquake loadings. The BTT neural network controller has been developed and presented in the US/China/ Japan Joint Workshop on Structural Control held in Shangshai, China, Oct. 5-7, 1992. The BTT neural network controller as shown in figure 1 consists two components: (1) a neural network (NN) emulator to model the structure; (2) a control action neural network trained by using the BTT method and used to determine the control actions.

Neural Network Emulator

The neural network emulator is a required component in the BTT neural controller, in order to train the control action neural network. As shown in figure 1, the utility function $U_m(t+1)$ is calculated from the difference between the outputs of the emulator and the real structure. By minimizing the $U_m(t+1)$ the neural network emulator can be trained to reach the desired accuracy representing the real structure. In this project, a 10-story San Jose apartment building is modeled by a 3-layer neural network. Three earthquake records (M_L= 6.1, 5.8 and 7.0) are used to trained and examine the model.

Control Action Neural Network

After the neural network emulator is obtained the control action network can then be trained (figure 1). As an example, figure 2 shows the performance of the San Jose building subjected to the Loma Prieta earthquake before and after the newly developed BTT neural controller is applied.

Adaptive Critic Neural Network

Since the performance index is minimized for instantaneous time t, the BTT neural controller may not ensure the optimization in global sense. The efforts in next steps will be focused on the development an adaptive critic neural network. This adaptive critic, shown in figure 3, will be trained using the instantaneous utility function to achieve global optimization.

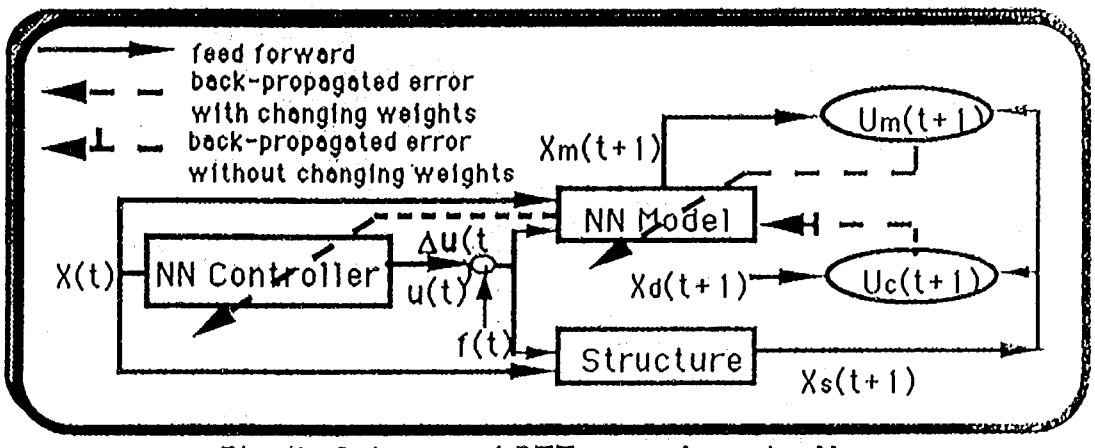


Fig. 1 Scheme of BTT neural controller

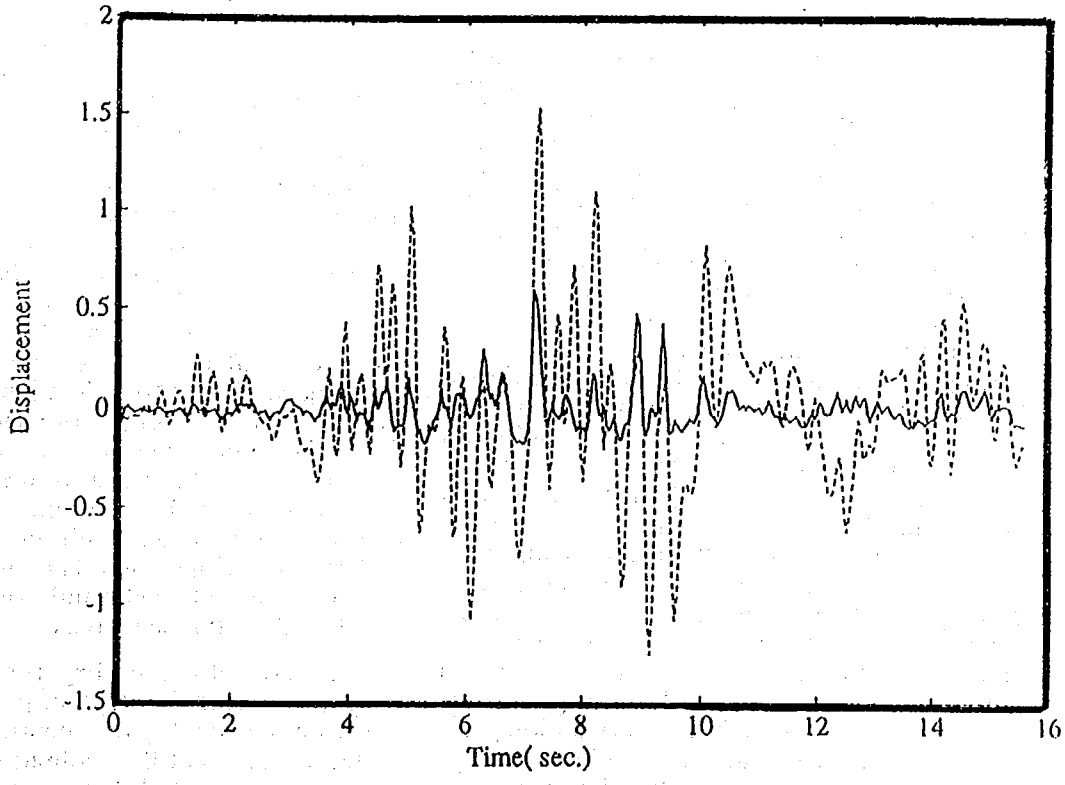


Fig 2 Relative Response of apartment building before (dashed) and after (solid) control (unit: cm)

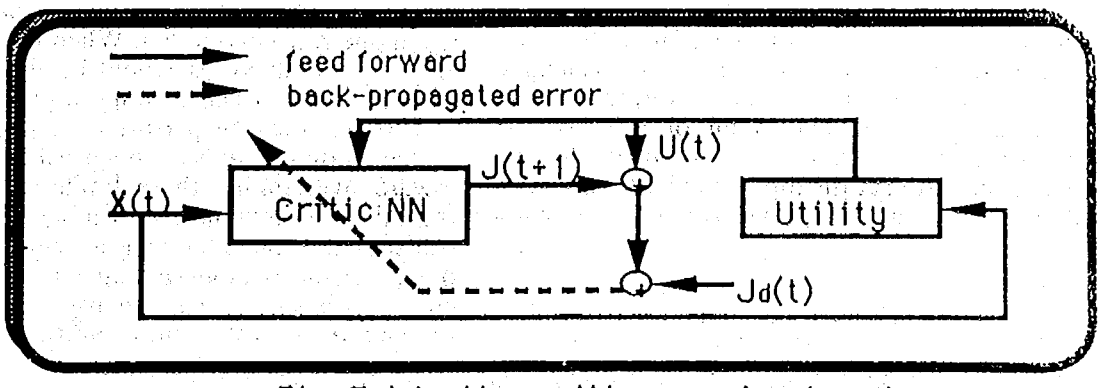


Fig. 3 Adaptive critic neural network

ROBUST FEEDBACK CONTROL OF STRUCTURES FOR EARTHQUAKE HAZARD MITIGATION

B. F. Spencer, Jr.[1] and Michael K. Sain[2]
University of Notre Dame
Notre Dame, IN USA 46556

Project Description

The objective of National Science Foundation Grant BCS-90-06781 has been to develop control strategies for earthquake-excited structures in such a way that the controlled structures have robust performance and wide stability margins. Significant advances have been achieved toward the grant goals during its two years of activity; and the results have been documented in the publications, which are listed at the end of this report. A summary of portions of the work is provided in the next few paragraphs.

Optimization methods in the frequency domain have been applied to the active control of civil engineering structures. The research has made it clear how a number of attractive features inherent in frequency domain control approaches can be exploited for this class of applications. Frequency domain optimal control strategies allow the designer to deal directly with natural representations of the structural model and its excitation. Moreover, they permit a specification of disturbance attenuation over a desired frequency range, and a roll-off of the control action at high frequencies where measurement noise may otherwise cause difficulties. Application of the technique to an eight-story structure under seismic excitation, with an active mass damper as control mechanism, has been achieved. Measurements were ground, floor, and damper accelerations. In contrast to reported studies employing time domain control techniques, the frequency domain controller was shown to be capable of reducing the building's response in both the first and second modes using the active mass damper. Control of a 60-story building under along-wind excitation has also been studied. A procedure to account for the frequency dependent nature of the wind excitation in optimal control design was established through factorization of the cross spectral density matrix of the wind fluctuation. In this example, floor accelerations were measured and used to calculate the optimal control force. However, rather than minimizing the displacement or velocity, the controller was designed to minimize directly the acceleration at the top of the building. It has thus been established that frequency domain optimal control techniques provide a good match with engineering practice.

A significant development is associated with new approaches to the time delay problem in controller implementations for civil engineering structures. The question of time delay in the loop, from sensing, from computing, and from actuating, is an important target of research in structural control. In the past, difficulties with such delay have led to loop instability and reduced performance. Work under this grant has reported substantial increases in stability margin over existing techniques, while demonstrating a capability to improve performance in the process. The approach is clear and algorithmic, and should be easy to use and understand for those working in this area.

When a stochastic formulation of the structural control problem has been undertaken, a great deal of interest has centered on the use of quadratic performance criteria and linear structural models, whether in the time domain with the Linear Quadratic Gaussian methods or in the frequency domain with H_2 methods. Among the many reasons for this interest are the facts that the optimal controller is linear, the controlled structural system is stable, and the frequency domain language can be used. Work carried out under this grant has shown that it is possible to enlarge the family of such desirable linear controllers by broadening the type of performance under consideration. Studies with such new measures of performance have established the remarkable fact that previous linear designs for structural control may have placed the operation of the controlled building in a highly sensitive range, with regard to such parameters as stiffness and damping coefficients. The new and enlarged family of controllers is able to reduce this sensitivity.

Studies have also been begun on probabilistically quantifying the effect of parameter uncertainty on the stability of a controlled structure, on the variances of floor vibrations, and on the variances of control forces required on the building. Most non-probabilistic approaches to the parameter robustness issue are conservative in nature, as a result of using worst case scenarios in one form or another. When many parameters are involved, as would be the case in a large building, it can be quite difficult to get a realistic estimate of performance failures. The probabilistic methods have a great deal to offer toward overcoming these limitations. Results from this research have shown that certain control strategies have far superior performance to others when random parameters are considered. Such studies can be used to focus research efforts on structural control issues which

1. Assoc. Prof., Dept. of Civil Engrg. and Geo. Sci.
2. Freimann Prof., Electrical Engrg.

will reap the most benefits. They also provide objective measures for comparing the performance of different structural control strategies.

The hysteresis-type of nonlinearity is of interest in the structural control problem, for instance in the case of sliding bearings. Over the last 25 years, little has been done on the control of such devices, although considerable effort has gone into modelling. Recently, we made use of the Chua-Stromsmoe hysteresis model to set up a class of nonlinear, dynamical, hysteretic plants. Then we applied a servomechanism architecture originating in gas turbine engine control to demonstrate the possibility of high performance applications in the case of such behavior.

Progress has continued with the use of tensor expansion solutions of the nonlinear optimal regulator problem. This approach has been applied to a tension leg platform, a Duffing system, and to an inverted pendulum. Additionally, to better understand the behavior of the nonlinear dynamical systems to be controlled, the finite element method has been applied to the solution of the Fokker-Planck equation for several important nonlinear stochastic systems, thereby giving accurately, for the first time, the joint probability density function of the response for a given initial distribution.

Finally, an earthquake simulator has been designed, constructed and installed at the University of Notre Dame using grant funds. The goal of having such a facility is to provide an opportunity to examine a wide variety of issues pertinent to implementation of the proposed control strategies for larger, more complex structures. Additionally, a three-story scale model building has been constructed, and control strategies are currently being implemented and tested. The experimental verification of acceleration feedback control for this model is underway, and will be presented in video form at the American Control Conference, San Francisco, 1993. Nonlinear optimal control techniques for generating accurate replicas of well known quakes are in an advanced stage of development.

Publications

1. J. Suhardjo, B.F. Spencer, Jr. and M.K. Sain, "Nonlinear Optimal Control of a Duffing System," *Int. J. of Nonlinear Mech.*, Vol. 27(2), pp. 157-172, 1992.

2. J. Suhardjo, B.F. Spencer, Jr. and Ahsan Kareem, "Frequency Domain Optimal Control of Wind Excited Buildings," *J. of Engrg. Mech., ASCE*, Vol. 118(12), pp. 2463–2481, 1992.

3. B.F. Spencer, Jr., M.K. Sain, J.C. Kantor and C. Montemagno, "Probabilistic Stability Measures for Controlled Structures Subject to Real Parameter Uncertainties," *Smart Materials and Structures*, 1993, in press.

4. J. C. Kantor and B. F. Spencer, Jr., "On Real Parameter Stability Margins and Their Computation," *Int. J. of Control*, Vol. 57(2), pp. 453-462, 1993.

5. J. Suhardjo, B.F. Spencer, Jr. and Ahsan Kareem, "Active Control of Wind Excited Buildings: A Frequency Domain Based Design Approach," *J. of Wind Engrg. and Industrial Aerodynamics*, Vol. 41–44, pp. 1985–1996.

6. B.F. Spencer, Jr. and L.A. Bergman, "On the Numerical Solution of the Fokker-Planck Equation for Nonlinear Stochastic Systems," *Nonlinear Dynamics,* in press.

7. M. K. Sain, C-H. Won and B. F. Spencer, Jr., "Cumulant Minimization and Robust Control", in *Stoch. and Adaptive Control*, Tyrone E. Duncan and Bozenna Pasik-Duncan, Editors. New York: Springer-Verlag Lecture Notes in Control and Information Sciences, Vol. 184, pp. 411-425, 1993.

8. B.F. Spencer, Jr., J. Suhardjo and M.K. Sain, "Frequency Domain Optimal Control Strategies for Aseismic Protection," *J. of Engrg. Mech.*, in press.

9. P.M. Sain, M.K. Sain and B.F. Spencer, Jr., "Design of Actively Controlled Structures with Time Delays," *J. of Engrg. Mech.*, submitted.

10. B. F. Spencer, Jr. and J. Suhardjo, "Recent Theoretical Developments in Active Structural Control," *Proc. 1991 ASCE Struct. Congress*, Indianapolis, April/May 1991, pp. 129-132.

11. L.A. Bergman and B.F. Spencer, Jr. "Robust Numerical Solution of the Transient Fokker-Planck Equation for Nonlinear Dynamical Systems," *Proc. IUTAM Symp. Nonlinear Stoch. Mech.*, Torino, Italy, 1991, pp. 49-60.

12. B.F. Spencer, Jr. and L.A. Bergman, "Solution of the Transient Fokker-Planck Equation by the Finite Element Method," *Proc., 1st Int. Conf. on Comp. Stoch. Mech.*, Corfu, Greece, Sept. 17-19, 1991, pp. 359-370.

13. P. M. Sain, M. K. Sain and A. N. Michel, "Nonlinear Model-Matching Design of Servomechanisms", *Proc., First Symp. on Design Methods for Control Systems, IFAC*, Zurich, Switzerland, pp. 594-599, September 1991.

14. B.F. Spencer, Jr., J. Suhardjo and M.K. Sain, "Frequency Domain Control Algorithms for Civil Engineering Applications," *Proc., Int. Workshop on Tech. for Hong Kong's Infrastructure Development*, Hong Kong, Dec. 19-20, 1991, pp. 169-178.

TITLE: ACTIVE AND PASSIVE CONTROLS OF COMPLEX STRUCTURES WITH UNCERTAINTIES UNDER WINDS LOADS
NSF Grant No. BCS-9022714
Principal Investigator: Henry T. Yang

It was proposed to develop a hybrid (combined active and passive) control system incorporating a refined stochastic finite element method for optimal control of tall buildings, bridges, and other complex structures, with uncertain structural parameters subjected to random dynamic wind loads. The structural uncertainties such as initial geometric imperfections, material properties, boundary conditions, and structural damping coefficients, etc. were assumed as random in space. The wind loads were assumed as random in both time and space. This development may also be applicable to earthquake loads.

The short term goals of this project are: (1) to develop an optimal hybrid control law for uncertain general and complex structures subjected to deterministic and stochastic wind loads, with applicability to structures under earthquake type of loads as well; (2) to study and compare the dynamic transient response behaviors of uncontrolled, actively controlled, passively controlled, and hybridly controlled general and complex structures due to the effects of each and combined structural uncertain parameters, with emphasis on the assessment of the effects of such structural parametric uncertainties on the performance of the control system proposed; (3) to study and compare the characteristics of structural safety and reliability of the uncontrolled, actively controlled, passively controlled, and hybridly controlled uncertain general and complex structures under random wind excitations, with applicability to structures with earthquake type of loads as well.

The long term objectives of this project is to develop a hybrid structural control system to significantly improve the reliability and safety of realistic and practical structures such as buildings, bridges, and complex shells with a combination of several structural uncertainties subjected to random wind (primarily) and earthquake loads.

The progress we have made during the first year of the project includes the following

- An active control algorithm based on an optimal independent modal space control theory has been developed for high-rise buildings with incomplete measured data. Examples of optimal active control of a two-floor and an eight-floor building modeled by simple shear beams, without and with passive base-isolation devices, were performed to demonstrate the efficiencies of various control designs. (See "Simple Model for Optimal Control of Tall Buildings" by Yang, et al. in the Journal of Structural Engineering, ASCE, Vol. 119, No. 3, March, 1993, pp. 902-919)
- The active control of a tall building modeled as a cantilever subjected to random wind loadings using Monte Carlo simulation method has been studied. The building was assumed to be controlled by using five active tendons. The wind velocity was assumed to be random in both space and time domains generated using the Davenport spectrum together with local average technique (Figs. 1 and 2).
- A control algorithm based on the instantaneous optimal closed-loop control technique has been developed for the control of buildings subjected to deterministic earthquake excitations. The building frame was modeled using a two-node, six-degree-of-freedom planar frame element as a basic tool for the analysis. Examples of optimal control of a three-bay, ten-story steel building frame were illustrated using base isolators and active tendons (Figs. 3 and 4).

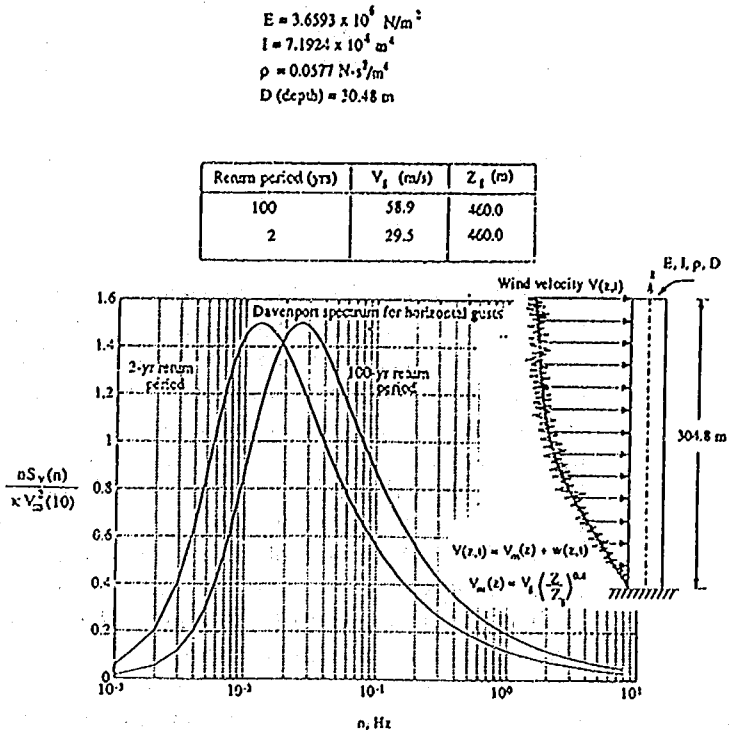


Fig. 1: Modeling of a building and wind loads using ten beam element

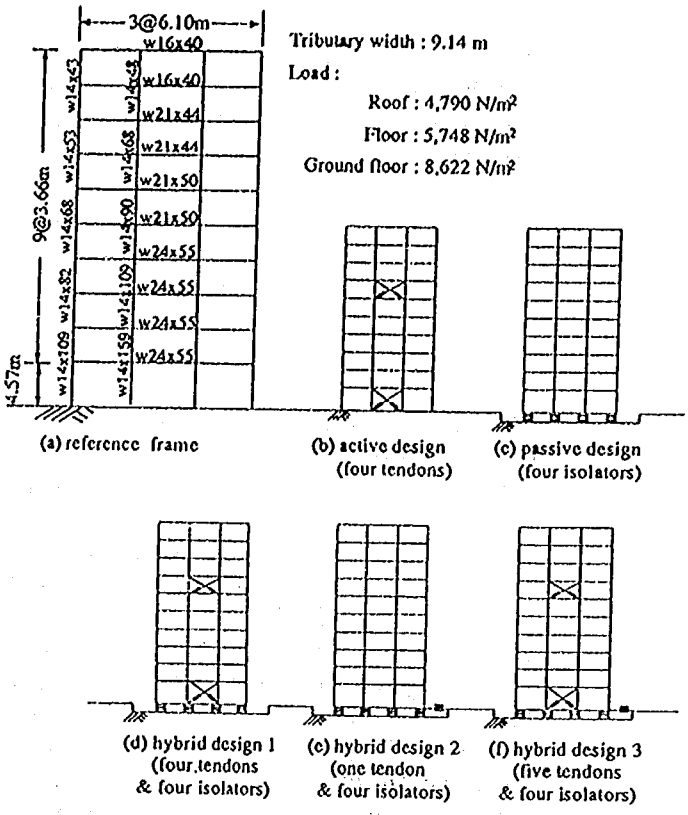


Fig. 3: A 10-story 3-bay steel frame with various control designs

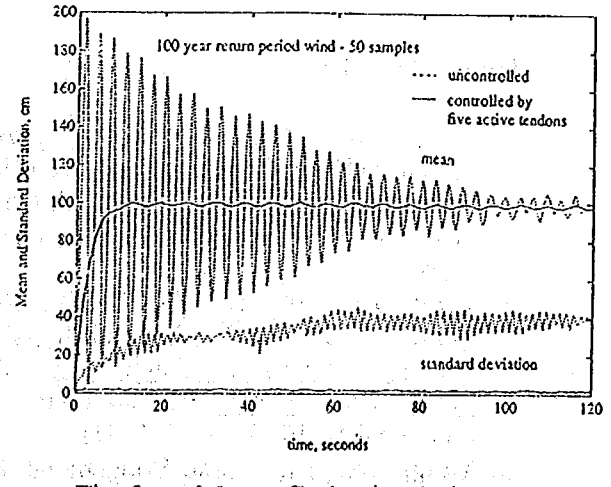


Fig. 2: Monte Carlo simulations of mean and standard deviation of displacement at the top floor of the building subjected to the hundred year return period wind loads

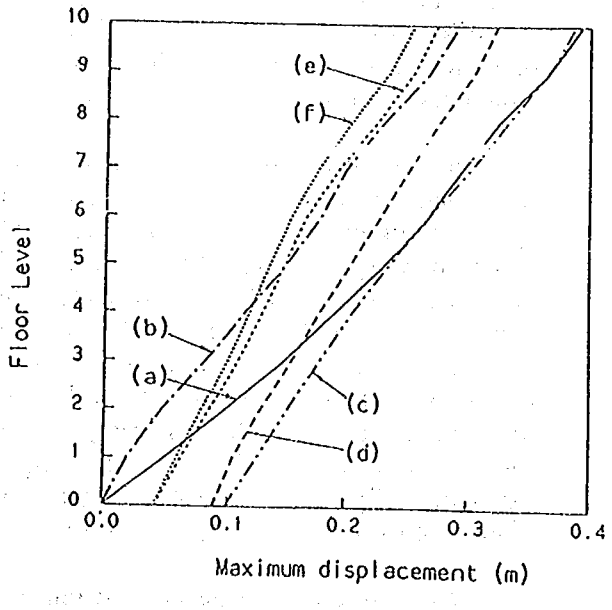


Fig. 4: Maximum floor displacements for the six design cases

HYBRID CONTROL OF SEISMIC RESPONSE OF BRIDGE STRUCTURES: A COORDINATED EFFORT BETWEEN THE U.S. AND JAPAN

Principal Investigator: Jann N. Yang
University of California
Irvine, CA 92717

This project is to conduct collaborative research on aseismic hybrid control of bridge structures between the University of California, Irvine (UCI), and the Public Works Research Institute (PWRI), Ministry of Construction, Japan.

The main objective is to carry out in-depth theoretical/numerical studies of aseismic hybrid control systems for bridge structures. In particular, control algorithms will be developed for various types of hybrid control systems for bridge structures currently being developed at PWRI. These hybrid systems include a combination of rubber bearings and variable dampers, rubber bearings and actuators, as well as possible combinations of sliding bearings and variable dampers or sliding bearings and actuators. Hybrid control systems, which consist of a combination of passive and active control devices have been shown by K. Kawashima et al at PWRI to be more effective and practical in reducing the response of long-span bridge structures subjected to strong earthquakes.

Aseismic hybrid control systems are often inelastic (such as active rubber-bearing isolation systems), highly nonlinear (such as active sliding isolation systems and variable stiffness devices), or time-variant (such as variable viscous dampers). The short-term goal is to develop control algorithms which could be incorporated into computer/processor and control hardware for aseismic hybrid control of bridge structures. The long-term goal is to implement experimentally demonstrated aseismic hybrid systems on full-scale bridge structures.

Theoretical studies will be carried out at UCI, whereas hardware developments and experimental tests will be conducted at PWRI. Various control algorithms developed at UCI will be used in the experimental tests. Results of the experimental tests obtained at PWRI will be correlated with the corresponding theoretical/numerical solutions obtained at UCI. Discrepancies between experimental and theoretical results will be examined, investigated and corrected.

The progress during the first year research has been very satisfactory. The LQR control theory is generalized to include the effect of actuator dynamics and a minimization of the acceleration response. Thus, the adverse effect of a system time delay due to the slow reaction of actuators can be removed and the acceleration of the bridge deck can be minimized. A nonlinear control method is proposed for aseismic hybrid control systems and its performance is shown to be better than that of the linear control law. A nonlinear discontinuous control method is established, which is applicable to nonlinear and inelastic systems as well as other types of aseismic hybrid control systems. The main feature of such a control method is to design controllers to drive the response trajectory into the switching surface on which the response trajectory moves stably toward the equilibrium position. The method provides an effective and robust means of controlling bridge structures. Preliminary results indicate that the control performance is remarkable. A typical bridge structure investigated is schematically shown in Fig. 1. Publications resulting from the research project are listed in the following:

Publication List:

1. Yang, J.N., et al, "Control of Hysteretic System Using Velocity and Acceleration Feedbacks", J. of Eng. Mech., ASCE, Vol. 118, No. 11, November 1992, pp. 2227-2245.
2. Yang, J.N. and Li, Z., "Active Stiffness Control of Seismic-Excited Buildings", Proc. 3rd Pan American Congress of Applied Mechanics-PACAM III, Sao Paulo, Brazil, January 4-8, 1993, pp. 568-571.
3. Yang, J.N., Li, Z. and Vongchavalitkul, S., "A Generalization of the Theory of Optimal Control", paper presented at the US-China-Japan Workshop on Structural Control, October 5-7, 1992 (proceedings in press).

4. Yang, J.N., Li, Z., and Vongchavalitkul, "Nonlinear Control of Buildings Using Hybrid Systems", Proc. of Seminar on Seismic Isolation, Passive and Energy Dissipation and Active Control, ATC-17-1, Vol. 2, pp. 811-822, Applied Technology Council, San Francisco, CA, March 11-12, 1993.
5. Yang, J.N. and Li, Z., "Hybrid Control of Seismic-Excited Bridge Structures Using Variable Dampers", paper to be presented at the ASCE Structures Congress to be held in April, 1993, Irvine, CA.
6. Yang, J.N., Li, Z. and Vongchavalitkul, S., "Stochastic Hybrid Control of Hysteretic Structures", paper submitted for publication in Journal of Probabilistic Engineering Mechanics, 1992.
7. Yang, J.N. and Li, Z., "Application of VSS Control Theory to Civil Engineering Structures", paper to be presented at the 9th VPI&SU Symposium on Dynamics and Control of Large Structures, May 10-12, 1993.
8. Young, D.K. and Yang, J.N., "Discontinuous Active Stiffness Control for Civil Structures", paper to be presented at the 9th VPI&SU Symposium on Dynamics and Control of Large Structures, May 10-12, 1993.
9. Yang, J.N., Li, Z. and Vongchavalitkul, S., "A Generalization of Optimal Control Theory: Linear and Nonlinear Structures", National Center for Earthquake Engineering Research Technical Report, NCEER-92-0026, October, 1992.

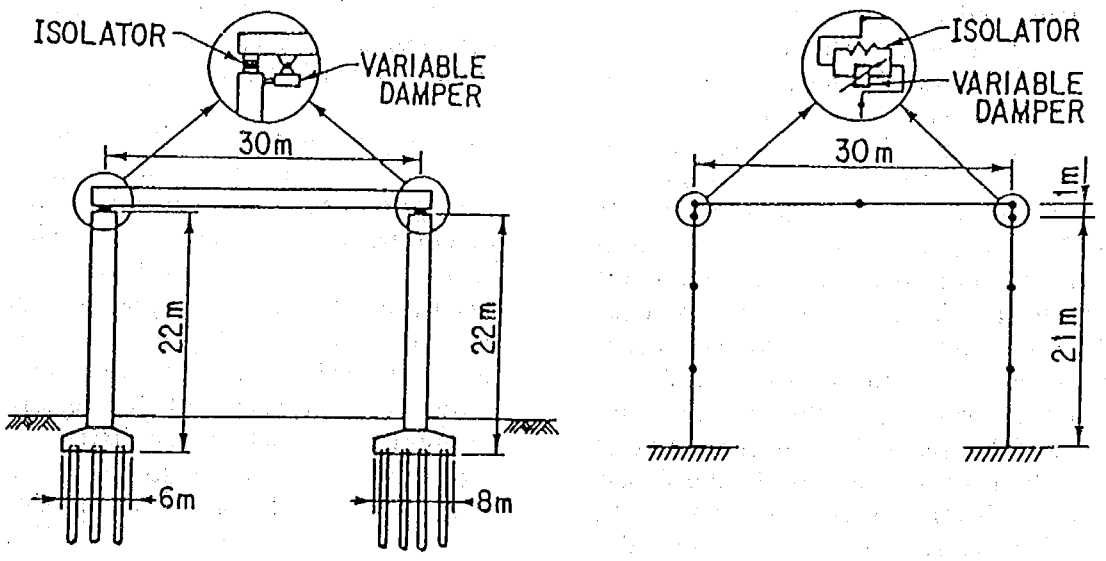


Fig. 1: Highway Bridge With Rubber-Bearing Isolators and Variable Dampers

FULL-SCALE ACTIVE CONTROL RESEARCH AND IMPLEMENTATION

Principal Investigator: Jann N. Yang
Co-Principal Investigators: W. Schmitendorf
F. Jabbari
University of California, Irvine, CA 92717

This project concerns research, development, design and implementation of a large-scale active control structural system. Several full-scale prototype active control systems have been built and tested in Japan in recent years, but no full-scale research and state-of-the-art system of this important new technology has been developed to date in the U.S.

The proposed system comprises a 150-foot high tower research structure to be built at the National Inventor's Hall of Fame in Akron, Ohio. The tower will be capable of dynamic excitations by (i) simulated earthquakes, (ii) natural winds, and (iii) other types of motions by mechanical means. The design will be flexible, permitting the dynamic properties and control configuration of the tower to be varied for research use, and will incorporate features to enable state-of-the-art active control techniques to be developed and tested. The tower would serve the following functions: (a) a showcase of the Inventor's Hall of Fame as a research effort that represents the first full-scale structure in the U.S. incorporating the innovative active structural control technology; (b) a test facility for researchers working in the area of active control; and (c) a research product used as an educational tool for students, professionals and visitors to the Inventor's Hall of Fame. The project will be carried out by a collaborative industrial and academic based research team from the following organizations: University of California, Irvine; National Center for Earthquake Engineering Research; Ove Arup and Partners (Consulting Engineers, New York); National Invention Center; MTS Systems Corporation; and JSPolshek and Partners (Architects, New York). In addition, a Project Advisory Committee consisting of nine experts was formed to provide guidance throughout the project. The entire project will be conducted jointly by all participants of the team. However, responsibilities to manage and lead parts of the project are assigned as follows: (a) development and research of control strategies to be implemented and adapted to the demonstration structure - UCI/J.N. Yang; (b) development, integration and testing of control components and structure -NCEER SUNY/A. Reinhorn; and (c) design and construction management of actively controlled test facilities - OAP/G. Nordensen.

The entire project consists of three phases: (a) research, development and design of the structure; (b) fabrication and installation; and (c) field testing and research demonstration. The cost of executing this project (excluding construction costs of the base structure) is estimated to be 1.5 million over a three-year period. The cost sharing is outlined as follows: (a) National Invention Center 50%; (b) NSF 25%; and (c) NCEER 25%. In addition, the National Invention Center will erect a base tower at a cost of $250,000-$400,000. MTS Systems Corporation is expected to provide technical assistance, consultation and financial support in hardware development.

The progress during the first year at UCI and NCEER has been satisfactory. Various control strategies to be implemented and adapted to the demonstration tower have been evaluated. The recently matured H_∞ control theory, that has not been explored for civil engineering applications to date, has been demonstrated to be quite effective and robust for the demonstration structure. The results of this research will be published (see publication list). Preliminary alternative designs of the tower have been made and scaled model testings on the shaking table have been prepared at NCEER, SUNY/Buffalo. An alternative design of the tower is shown schematically in Fig. 1.

After one year effort, this project is now temporarily on hold because the National Invention Center has not been able to raise its target funding. Due to the current economical situation, the National Invention Center was not able to contribute its share of the first year funding. Critical evaluations of the funding situation are being made by the National Invention Center and its final decision will be made in May, 1993.

Publication List

1. Schmitendorf, W., Jabbari, F. and Yang, J.N., "Robust Control of Buildings Under Earthquake", paper to be presented at the ASCE Structures Congress to be held in April, 1993, Irvine, CA.

2. Schmitendorf, W.E., Jabbari, F. and Yang, J.N., "Robust Control Techniques for Buildings Under Earthquake Excitation", paper accepted for publication in Journal of Earthquake Engineering and Structural Dynamics.

3. Schmitendorf, W.E., Jabbari, F. and Yang, J.N., "Active Control Techniques for Buildings: Reducing Acceleration and Deformation", paper to be presented at the 9th VPI&SU Symposium on Dynamics and Control of Large Structures, May 10-12, 1994, Blacksburg, VA.

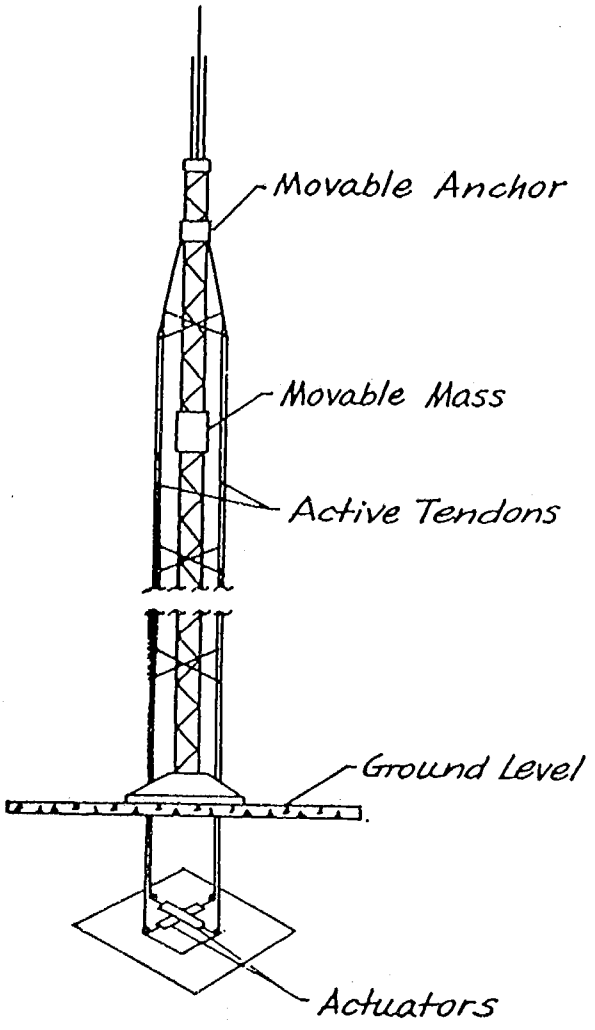


Fig. 1: Actively Controlled Tower of Invention (Alternative Form)

DEVELOPMENT OF MULTISTAGE FLUID DAMPERS

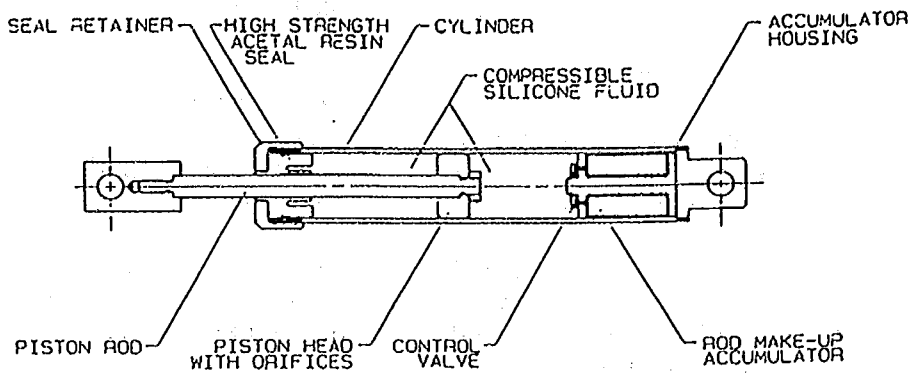
Michael C. Constantinou, Dept. of Civil Engineering, State University of New York, Buffalo, NY.
Douglas P. Taylor, Taylor Devices, Inc., N. Tonawanda, NY.

This project represents part of an on-going research project on the adaptation and use of advanced military-related technology in applications of seismic hazard mitigation. Already, experimental and analytical results have been generated which demonstrate that advanced fluid dampers and fluid damping/restoring force devices can substantially improve the seismic performance of structural systems to which they are attached. Characteristics of these devices which are of interest in structural applications are insensitivity of mechanical properties to significant temperature changes, small size in comparison to output force and stroke capability, low cost and longevity and reliability as demonstrated by over 20 years of use in military and aerospace applications.

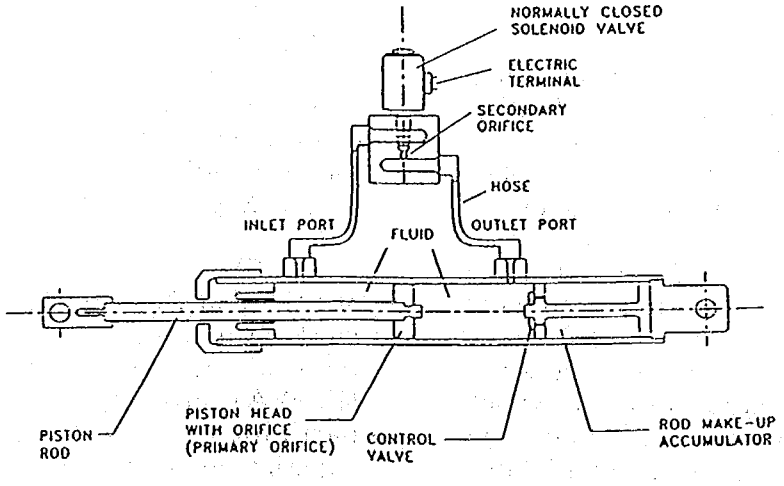
This particular project concentrates on the development of semi-active multistage fluid dampers and fluid damping/restoring force devices. These devices, as their already studied passive counterparts, produce control forces which are induced by the motion of the structure itself, and do no require external power. Rather they use multiple orifices and simple accumulators which are activated or de-activated by solenoid valves. The valves themselves are activated by electric signals supplied by a battery. The devices behave as active multistage damping and stiffness elements.

The first year of this research project concentrates on the design, construction, testing and mathematical modeling of a multistage fluid damper. The device is an adaptation of a large scale active vibration/shock isolation strut developed by Taylor Devices, Inc., for the U.S. military. As of February 1993, the device has been constructed and tested for verification of its basic design. Comprehensive testing is scheduled to start in March 1993.

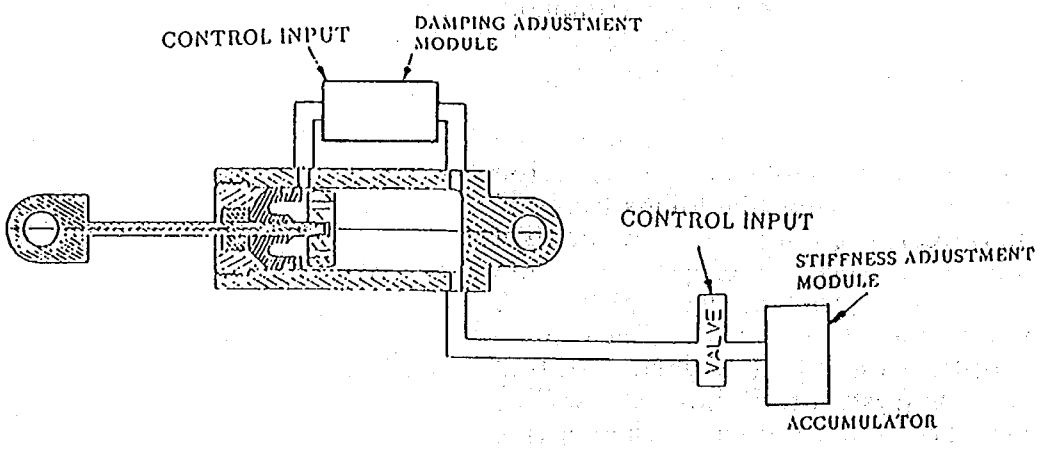
Long-term goals of the project are: (a) Develop and construct a multistage damping/restoring force fluid device. (b) Develop control algorithms in cooperation with other NCEER investigators in Intelligent and Protective Systems. (c) Implement the hardware and control algorithms in shake table testing of a model structure.



Construction of Passive Fluid Damper



Construction of Two-stage Semi-active Fluid Damper



Construction of Semi-active Stiffness/Damping Fluid Device

ENERGY DISSIPATION SYSTEMS, HYBRID CONTROL SYSTEMS, AND ELASTOMERIC ISOLATION SYSTEMS

Maria Q. Feng

The objective of this research is to further develop and apply friction controllable sliding isolation systems for hybrid control of structures under seismic loads. Under a Year 6 NCEER Grant (915411A), the PI worked with Professor M. Shinozuka at Princeton and developed a prototype friction controllable sliding isolation system and verified its effectiveness through preliminary shaking table tests. During 1992-1993, the PI has accomplished the following analytical and experimental research.

1) Through Monte Carlo simulation, the behavior of the friction controllable sliding isolation system has been studied under various earthquakes (with different spectral shapes, dominant frequencies, intensities and duration of motion). It is demonstrated that the friction controllable system indeed more effectively isolates structures than its passive counterparts. Figure 1. shows an example of simulation results in which passive and hybrid systems are compared. The results of this research were summarized in a paper entitled "Seismic Response Variability of Bridges on Friction controllable Isolators" and presented at the Second US-Japan Workshop on Earthquake Protective Systems for Bridges held December 7-8, 1992, in Tsukuba, Japan.

2) The application of the friction controllable sliding isolation system to multistory buildings has been analytically examined. A control algorithm was developed and the overturning problem was solved. A paper based on this research - "Application of a Hybrid Sliding Isolation System to Buildings" - will be published in the Journal of Engineering Mechanics, ASCE. and a paper entitled "An Innovative Base Isolation System for Buildings" will be presented at the ASCE Structures Congress '93 to be held April, 1993 in Irvine, CA.

3) Collaborating with Taisei Corporation, a new version of the friction controllable sliding isolation system has been developed which has many features of practical importance, such as a monitoring and protective device for overturning problem of the sliding bearing, a more efficient and practical pressure control system, etc. Figure 2 conceptually shows the new friction controllable bearings.

In the future, the PI plan to conduct the following work.

1) In the summer of 1993, shaking table tests will be carried out with a multistory building model equipped with the new friction controllable sliding isolation system at the Technology Research Center of Taisei Corporation, Japan.

2) To assist M. Constentinou at SUNY at Buffalo and M. Shinozuka working on protective systems under a Federal Highway Administration (FHWA) project, the PI will also participate in the shaking table experiments on passive sliding isolation systems for bridges which are scheduled in June, 1993, at the Public Works Research Institute, Ministry of Construction, Japan.

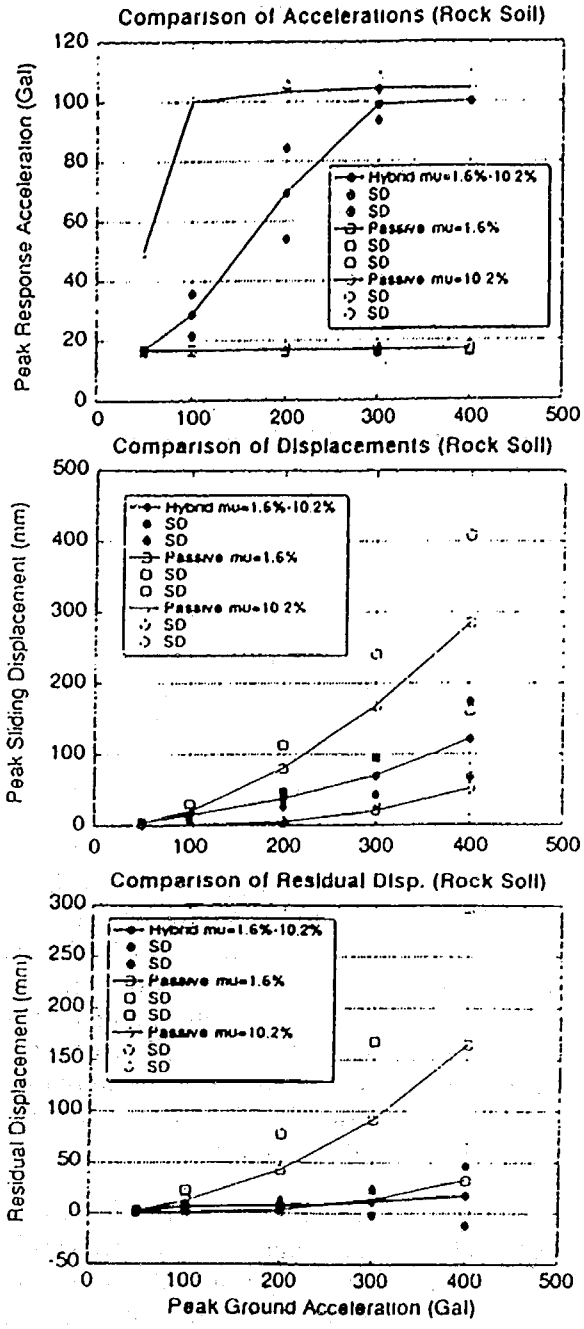


Fig. 1: Simulation Results (Still Soil)

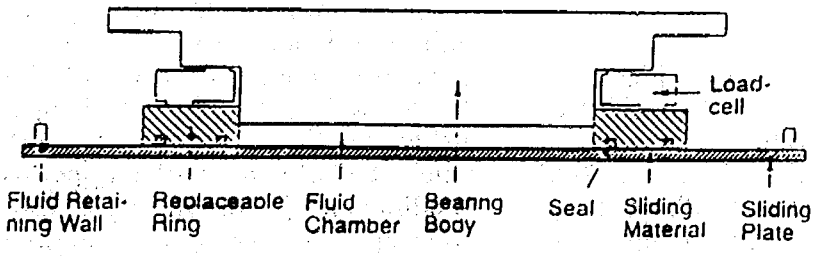


Fig. 2: New Sliding bearing

SEISMIC RETROFIT OF NONDUCTILE REINFORCED CONCRETE FRAMES USING VISCOELASTIC DAMPERS

D. A. Foutch, P. A. Brady, and S. L. Wood
Department of Civil Engineering
University of Illinois at Urbana-Champaign
Urbana, Illinois

Project Description

Existing nonductile reinforced concrete frame buildings pose a serious threat to human life in regions of high and moderate seismicity. These buildings possess very little ductility and often fail in a brittle manner when subjected to strong earthquake ground motions. One method of retrofitting existing steel buildings that has shown great promise is the use of supplemental dampers made of viscoelastic and other materials.

The objective of this research project is to investigate the effectiveness of using passive supplemental dampers to reduce the seismic vulnerability of nonductile reinforced concrete frame (NDCF) buildings. This type of building generally performs unsatisfactorily during a strong earthquake because critical members lack the reinforcement details required to ensure ductile response. Passive supplemental damper technology may provide a method to improve the seismic performance of these structures, thereby protecting the lives of the occupants and reducing the extent of property damage.

Nonductile reinforced concrete frame buildings are inherently more complex both statically and dynamically than steel frame buildings. The concrete structures are stiffer, heavier and generally much less ductile in nature. New VE damper technology will be investigated in this project as an efficient repair technique for existing NDCF buildings.

The research project has been divided into three phases. In Phase I, the feasibility of using VE dampers was evaluated using subassembly tests. A scale model of a NDCF building will be constructed in Phase II to investigate the influence of VE dampers on global structural response. Design guidelines and a full-scale implementation will be developed during Phase III. Phase I has been completed and the model for Phase II has been designed.

Four 6/10-th scale models have been tested as part of the Phase I studies. Two of the models were identical beam-slab-column subassemblies and two were identical slab-column (flat plate) subassemblies. Each of the models represents the critical second floor joint region of a three story NDCF building that was built in California in the 1950's. Geometric similitude was maintained between the prototype structures and the models. For each type of model, one specimen was tested without VE dampers and one was tested with them.

The first model, BSC1, was tested without dampers. The second model, BSC2, was tested with two sizes of dampers. Four of the larger dampers (5 in. long) were installed first as shown in Figure 1. After testing this model, the dampers were replaced by smaller (2-1/2 in. long) ones and another sequence of tests was run. An elevation view of BSC1 with and without dampers is shown in Figure 1.

The relative displacement of the total slab level shear force vs. slab relative displacement are shown in Figure 2. The hysteresis curves are exceptionally pinched and anemic for the undamped model. The undamped structure is clearly in trouble during this test. The damped model, on the other hand, exhibits very full and stable hysteresis behavior. The effects of the added VE dampers are dramatically shown in these figures.

The results of the tests reported herein clearly demonstrate the feasibility of adding viscoelastic passive dampers to nonductile concrete frame buildings to improve their performance during strong earthquakes. A great deal of research remains to be done, however, before full-scale implementation may be undertaken with confidence. Some of the problems that need to be addressed are as follows: (1) the design methodology for VE dampers for use in highly nonlinear structures; (2) the most efficient deployment of dampers in a NDCF building; and (3) the most cost effective design philosophy for using VE dampers in existing NDCF buildings.

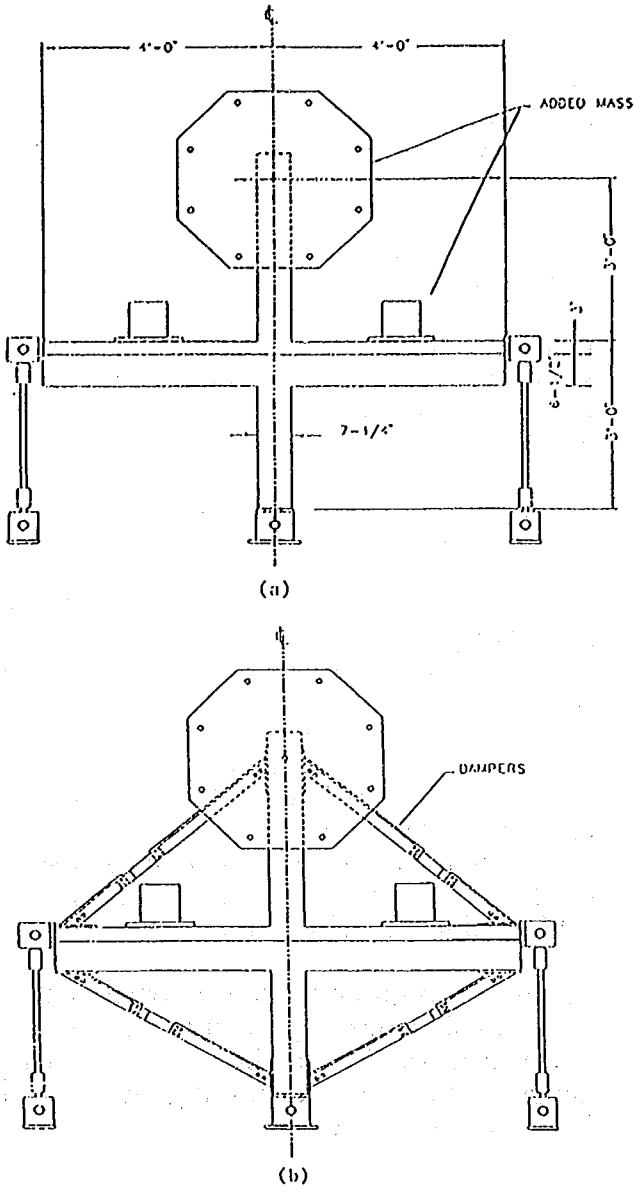


Fig. 1. Elevation views of (a) Model BSC1 without dampers and (b) Model BSC2 with VE dampers.

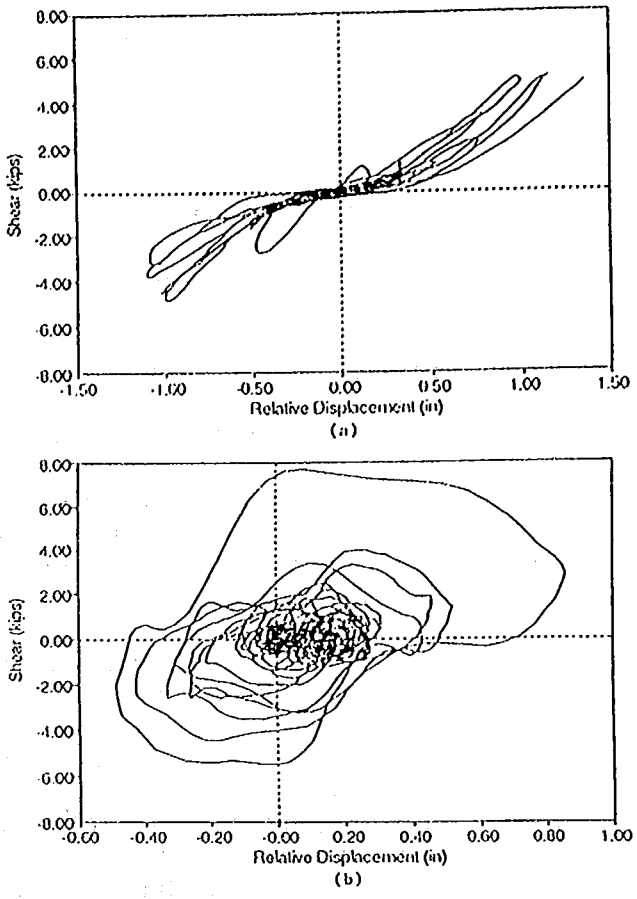


Fig. 2. Slab level relative displacement vs. total shear force for (a) BSC1 without dampers and (b) BSC2 with 5 inch dampers for El Centro with 30% span setting.

INNOVATIVE SUPPORT METHODS FOR STRUCTURES, SECONDARY SYSTEMS AND NONSTRUCTURAL COMPONENTS

A.M. Reinhorn, S. Nagarajaiah, T.T. Soong
Department of Civil Engineering
State University of New York at Buffalo
Buffalo, NY 14260

PROJECT DESCRIPTION

This project has been devoted to the development of hybrid control techniques for support of structures and equipment subjected to base motion. The intention of the project was development of a realistic model for application of control techniques, development of several theoretical techniques, and finally experimental verification and development of practical techniques for reduction of energy input in isolated-controlled systems.

The hybrid system proposed (see Figs. 1 and 2) includes: (i) a series of low friction sliding bearings using highly pressurized teflon interface sliding against stainless steel, (ii) a low capacity servocontrolled hydraulic actuator with an inner analog controller and, (iii) a digital controller (microcomputer) using various control algorithms to reduce the absolute acceleration of the foundation, of the structure and/or the equipment.

The system was developed to test three different control algorithms: (i) a **friction force control algorithm** which minimizes the friction force transmitted to the foundation using a minimum difference of measured control force versus an assumed friction force; (ii) an **absolute acceleration control algorithm** using an instantaneous optimal feedback scheme based on minimizing locally a cost function that considers both actuator consumption and response parameters; (iii) a **fuzzy sets control algorithm** using a schematic of reducing the absolute acceleration in total force or incremental force formulations.

The first two series of algorithms (mentioned above) were verified analytically and experimentally using a 5.5 kips actuator and a 4.9 kips model (foundation). The schematic of the control system and the results of the experiments using four different earthquake excitations are shown in Table 1. Although the experimental results of the hybrid system show some improvement over the passive system, the results were not satisfactory, as anticipated by analysis. The reasons for such reduced efficiency were identified and a new experimental set-up was redesigned (a) to reduce support friction, (b) to provide real restoring force versus a virtual actuator spring, (c) to refine time delay compensation using a predictive scheme (d) to improve actuator fixture.

Finally the highly nonlinear controller that controls the response of the nonlinear sliding system has been improved using a **new fuzzy sets logic**. The analytical results obtained simulating system imperfections and delayed response, shown in Table 1, indicate substantial improvements over the other controllers. The experimental study, (currently in progress) was designed to verify implementational issues of on-line computations and adaptive computations. Additional nonlinear control algorithms based on the fuzzy logic are currently developed and subjected to experimentation.

The results obtained to date show that hybrid systems using fuzzy logic can be implemented and use a fraction of the energy of a fully active system while aiming to superior improved response.

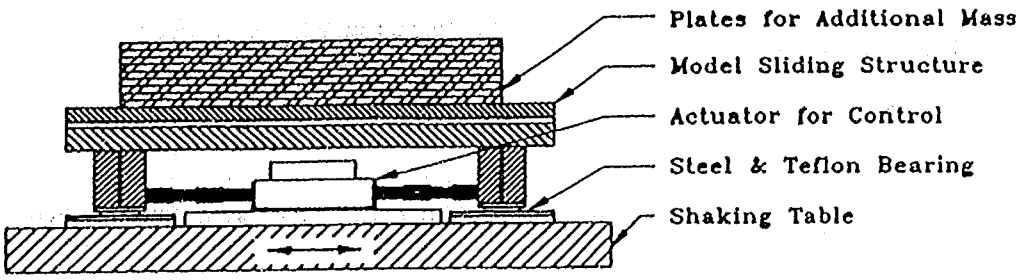


Fig. 1 - Hybrid system assembly.

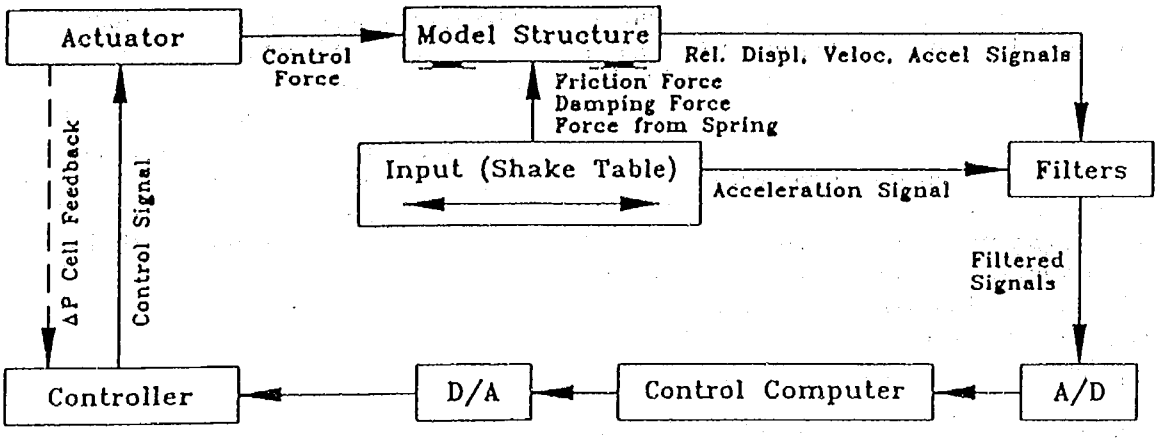


Fig. 2 - Block diagram of control system.

Table 1. Response of Experimental Model

Name (1)	Base Fixed (Experiment) Peak (2)	RMS (3)	Passive Isolation (Analytical) Peak (4)	RMS (5)	Instantaneous Acceleration Control (Experiment) Peak (6)	RMS (7)	Friction Force Control (Experiment) Peak (8)	RMS (9)	Fuzzy Control (Analytical) Peak (10)	RMS (11)
Basemat Acceleration (G's)										
El Centro S00E	0.327	0.051	0.192	0.061	0.175	0.044	0.201	0.033	0.133	0.052
Taft 200%	0.357	0.062	0.188	0.074	0.151	0.053	0.245	0.039	0.123	0.060
Hachinohe EW	0.195	0.041	0.180	0.050	0.134	0.039	0.141	0.031	0.121	0.045
Artificial Motion	0.416	0.060	0.230	0.069	0.175	0.052	0.207	0.041	0.139	0.058
Absolute Basemat Displacement (inches)										
El Centro S00E	1.77	0.37	2.03	0.49	1.92	0.40	1.65	0.34	1.92	0.38
Taft 200%	2.19	0.41	2.04	0.48	1.98	0.45	1.88	0.38	2.39	0.55
Hachinohe EW	3.74	1.03	3.77	1.01	3.68	1.04	3.70	1.06	3.96	1.03
Artificial Motion	3.49	0.70	4.71	0.79	3.16	0.68	3.24	0.64	2.74	0.71
Relative Basemat Displacement (inches)										
El Centro S00E	-	-	0.53	0.318	0.76	0.199	0.76	0.184	1.72	0.164
Taft 200%	-	-	0.46	0.277	0.45	0.166	0.46	0.175	1.02	0.338
Hachinohe EW 100%	-	-	0.18	0.130	0.77	0.176	0.84	0.316	0.80	0.172
Artificial Motion	-	-	0.64	0.299	1.40	0.195	1.30	0.324	2.08	0.384

FULL-SCALE IMPLEMENTATION OF STRUCTURAL CONTROL

T.T. Soong and A.M. Reinhorn
Department of Civil Engineering
State University of New York at Buffalo,
Buffalo, NY 14260

PROJECT DESCRIPTION

This project has been devoted to the design, development and fabrication of a full-scale active bracing system (ABS), and the installation of this system in a dedicated test structure in Japan. The effectiveness of this system under actual wind loads and seismic ground motions can thus be realistically assessed, leading to a better understanding of the workings of this control mechanism and to the formulation of design guidelines.

The system was installed in 1990 and has experienced several earthquake episodes. During 1992-93, the primary research task was to process and evaluate observed data, to compare observed data with the estimated analytical results, and to verify the system's capability to operate or shutdown under prescribed conditions.

The structure is a symmetric two-bay six-story building constructed of rigidly connected steel frames of rectangular tube columns and W-shaped beams with reinforced concrete slabs at each of the floors. Weighing 600 metric tons, the structure was designed as a relatively flexible structure with a fundamental period of 1.1 sec in the strong direction and 1.5 sec in the weak direction, in order to simulate a typical high-rise building. The structure has low damping in the dominant modes (between 0.5% and 1% of critical).

The ABS consists of diagonal tube braces attached to the first story of the building. The control system enables longitudinal expansion and contraction of the braces by means of hydraulic servocontrolled actuators attached along the braces. The control system includes also a hydraulic power supply, an analog and digital controller, and analog sensors as shown schematically in Fig. 1.

As mentioned earlier, the structure has been subjected to several recent earthquake motions and its response was recorded while the control system was automatically activated during each of these episodes. The ground motion was simultaneously recorded and was used with an analytical model to estimate the probable response of the structure in the uncontrolled mode. The peak and RMS responses at two locations of the structure and the control force requirements during two recent earthquakes are summarized in Table 1. The observed response was compared with that estimated using the time step analysis and the identified properties of the system. They show very good agreement.

While several active mass dampers have been implemented in full-scale structures over the last few years, the active bracing system reported here represents the first full-scale active system of this type developed and tested under actual ground motions. The results obtained to date demonstrate that the concept of an active tendon or bracing system, originated almost 20 years ago, has led to the successful development of the device for civil engineering structural control. Furthermore, the ABS can be implemented with existing technology under practical constraints such as power requirements and under stringent demands of reliability.

Table 1. Peak and RMS Responses during Recent Earthquakes

Response	Floor	X Direction				Y Direction			
		April 10,92		April 14,92		April 10,92		April 14,92	
		Control		Control		Control		Control	
		ON	OFF	ON	OFF	ON	OFF	ON	OFF
(1)	(2)	(3)	(4)	(5)	(6)	(7)	(8)	(9)	(10)
(a) Peak response									
Acceleration	6	11.36	15.30	15.25	19.50	15.66	15.46	11.50	15.03
(cm/sec/sec)	Base	7.36	7.36	8.93	8.93	11.77	11.77	9.24	9.24
Velocity	6	0.74	1.16	1.06	1.66	1.27	1.55	1.53	1.58
(cm/sec)	Base	0.23	0.23	0.37	0.37	0.74	0.74	0.49	0.49
Displacement	6	1.00	1.51	1.45	1.97	1.70	1.70	1.96	2.44
(mm)	Base	0.30	0.30	0.40	0.40	0.78	0.78	0.55	0.55
Control Force (kN)		64.0		82.7		143.2		88.6	
Control Force/Weight		1.06%		1.38%		2.38%		1.48%	
(b) RMS response									
Acceleration	6	1.89	3.39	2.28	3.51	1.97	4.67	1.91	4.14
(cm/sec/sec)	Base	1.04	1.04	1.30	1.30	1.02	1.02	1.11	1.11
Velocity	6	0.19	n/a	0.26	n/a	0.20	n/a	0.25	n/a
(cm/sec)	Base	0.04	n/a	0.06	n/a	0.05	n/a	0.06	n/a
Displacement	6	0.29	0.77	0.42	0.69	0.33	1.08	0.46	0.86
(mm)	Base	0.11	0.11	0.12	0.12	0.06	0.06	0.08	0.08
Control Force (kN)		17.2		21.7		16.3		16.9	
Control Force/Weight		0.29%		0.36%		0.27%		0.28%	

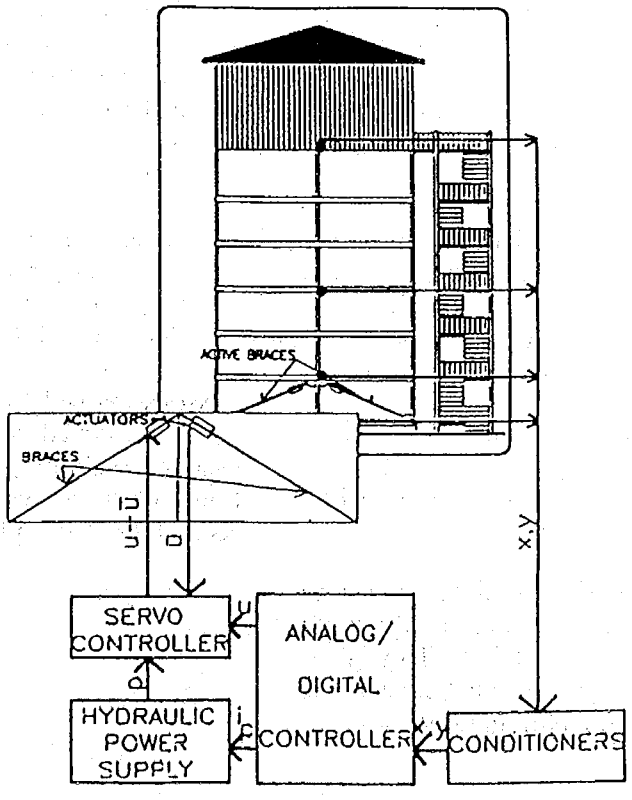


Fig. 1. Block Diagram of ABS

VIBRATION CONTROL OF SENSITIVE EQUIPMENT

T.T. Soong
Department of Civil Engineering
State University of New York at Buffalo,
Buffalo, NY 14260

PROJECT DESCRIPTION

Equipment such as data processing installations, intelligent workstations, and personal computers are vital to successful operation of business and industry. Any interruption in the operation of these systems can lead to total chaos if they fail due to earthquakes and vibrational effects.

As a joint research program with IBM, this research program places emphasis on the following issues: (1) Seismic vulnerability and performance of computer and data processing equipment, (2) Performance evaluation of existing methods of installation and restraining devices, and (3) Innovative installation methodology and performance verification.

During 1992-93, a variety of data processing equipment such as those shown in Fig. 1 were evaluated to determine effects on equipment function and safety concerns. The methods selected represented a cross section of typical installations and covered the range from free casters to innovative passive dissipation devices.

1. Free casters (free to roll with no locking devices) are a normal installation method for many DP devices.

2. Locked casters provide a friction lock on the caster and thus reduce the amount of free motion. Higher energies are coupled into the equipment and there is increased exposure to tipping of units with a high center of gravity.

3. Flexible restraints such as "bungee" cords (rubber shock cords) or springs were evaluated as a possible means of restricting free motion while providing some decoupling.

4. A method that provides good resistance to overturning, yet also provides a limited amount of decoupling is the "toggle bar" This is essentially a steel rod in tension between the equipment base and the building floor.

5. Several innovative isolation/damper units utilizing coiled wire ropes and viscoelastic damping material were evaluated for both displacement and acceleration reductions. A typical viscoelastic damper installation is shown in Fig. 2.

The following are preliminary test results based n observations made during the test runs.

1. The freely rolling or locked caster, bungee cord and spring restraint installation methods all allowed excessive machine motion when installed in mid and upper stories of buildings. This motion sometimes resulted in damage to external channel and power cables.

2. Several isolation techniques (viscoelastic dampers and coiled wire rope dampers) tested showed promise, but require additional development to provide practical installation methods.

3. Both toggle bars and the fixed method prevented excessive motion and provided resistance to overturning, and also did not cause any system hard failures.

4. Most installation methods tested were satisfactory for the ground floor or first floor of a building.

5. Any installation method (such as toggle bars, isolation dampers, or fixed) that severely restricts the movement of the machine must be tied to the sub-floor or a braced raised floor in order to resist the resultant overturning moments.

6. A variation of the toggle bar installation method, using a neoprene bushing to fill the space between the toggle bar and the clearance hole in the raised floor gave satisfactory results.

Lessons learned from these initial tests have produced improved designs of innovative restraining systems, including semi-active and active systems. Some of these systems will be tested during the second test series planned for the summer of 1993.

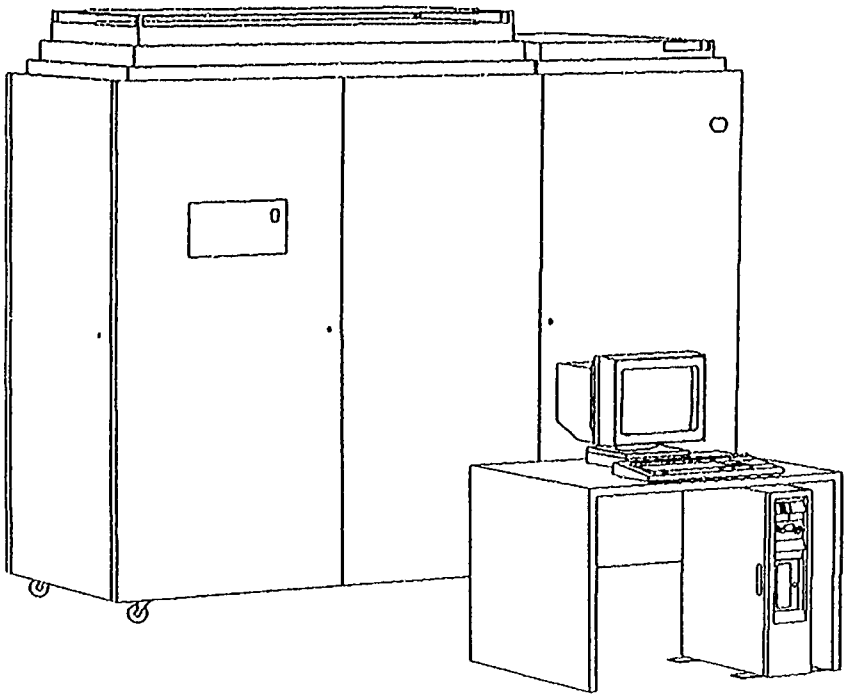


Fig. 1. Typical Data Processing Equipment Studied in the Test Program

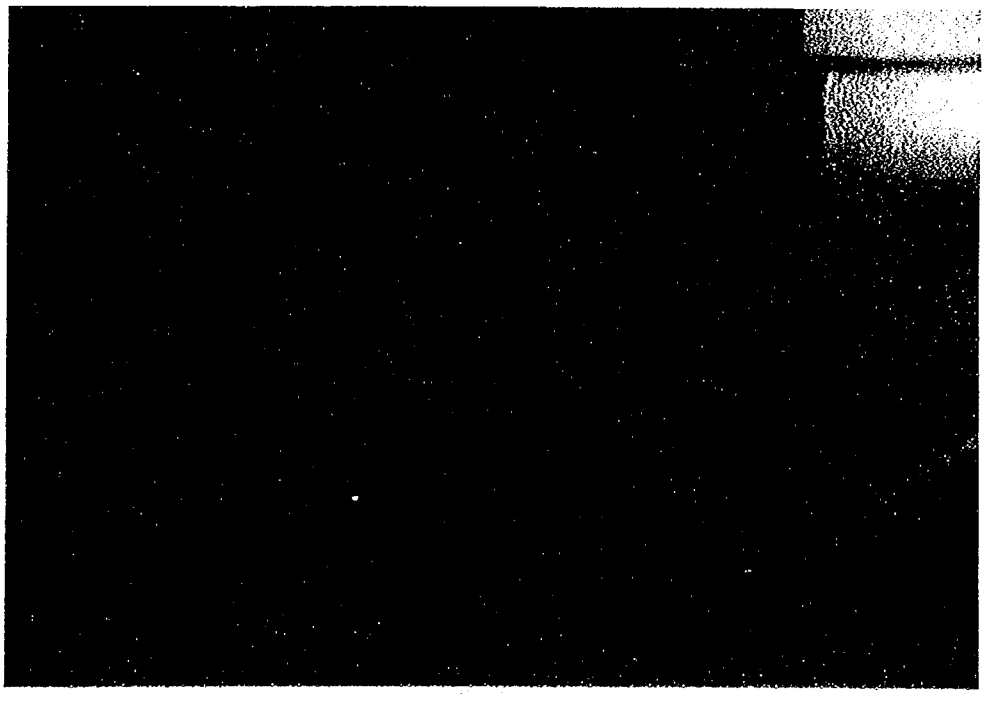


Fig. 2. IBM 9370 Viscoelastic Damper Installation



Integrated Approach to Structural Control for Seismic Hazard Mitigation

M. Shinozuka*, R. Ghanem† and M. Constantinou‡

1 Introduction

Startling advances in electronics hardware over the last decade have spawned a wealth of scientific investigations into controlling the interaction of constructed facilities with their environment. In particular, vibration control of buildings and bridges under various dynamical loads has occupied a prominent place in these research endeavors. The purpose of this control application is to minimize the damage sustained by a structure during its vibration. While the definition of damage itself, as well as its diagnosis, remain quite elusive, control strategies have been compared based on their ability to reduce the maximum value of displacement and base shear. It should be noted that this criterion may be far from adequate, especially if fatigue is a potential failure mode. In that case, the frequency content of the response may be a more appropriate measure of performance. The advances in hardware technology have permitted the development of related control concepts along different paths. The first such concept has relied on the ability of modern technology to feedback measurements from the structural system to high precision actuators which could then be utilized to produce a force that modifies the dynamics of the structure in a desirable fashion. A number of difficult issues are involved in this approach to control. Firstly, this approach is borrowed from the aerospace industry where the dynamics of the structures involved are usually well known, and gravity is not of major concern. In civil engineering structures, on the other hand, the dynamical behavior of the structures involved is quite complex, thus jeopardizing the ability to predict their behavior. Furthermore, the nature of external forces involved in civil engineering structures is such that they are not known in advance. In particular when ground motion due to an earthquake is involved, these forces can be realizations from non-stationary random processes which cannot be adequately modeled. The ability to perform optimal open loop control seems therefore to be limited by the inability to properly model the dynamics of the structure as well as the inability to anticipate the magnitude of the external excitation. These factors contribute greatly to the issue of control reliability and accuracy. They can be partially remedied by relying on adaptive control, whereby a predictive model of the dynamical system is continuously updated. This model update reduces the effect of modeling errors since the prediction horizon of the model need not be further away than the observations time interval. The issue remains, however, of not being able to anticipate the external load. Another complication associated with the open loop control of civil engineering structures, is the magnitude of force required to achieve a desired level of control. A cap on the level of available force can, of course, be embedded into the optimality criterion for the control. This could, however, severely restrict the achievable performance of the control algorithm. To these issues is added the issue of hardware reliability under emergency conditions.

The second control concept that has been pursued in parallel with open loop control is that of closed loop control. In this configuration, no external force is added to the system, and the control force is achieved using the dynamics of the system

*Department of Civil Engineering, Princeton University Princeton, NJ, USA, 08544.

†Department of Civil Engineering, SUNY, Buffalo, NY, USA, 14260.

‡Department of Civil Engineering, SUNY, Buffalo, NY, USA, 14260.

itself. This mode of control has also been referred to as semi-active, and passive. Usually, this type of control is achieved by modifying the dynamical properties of the structure being controlled. Most commonly, this achieved in a passive manner by increasing the level of damping in the structure, or modifying the stiffness of the structure prior to the application of the external load. A generalization of this idea involves the implementation into the structure of variable energy dissipation and restoring force devices. Recent research efforts have aimed at implementing variable damping and variable stiffness into structural models subjected to earthquake excitations[3, 1, 4, 2]. Specifically, two alternatives are being pursued at the State University of New York (SUNY) Structures Laboratory. These involve continuously variable damping devices such as available through electro-rheological (ER) fluids[7], and multistage variable dampers, providing a discrete number of damping levels.

The advantage of closed loop control over open loop control seems to be mainly one of reliability and implementation. In fact, open loop control relies on external sources of power and energy, without which it cannot provide any level of support for the structure being controlled. Furthermore, the amount of power required for the optimality criteria to be achieved may be prohibitively large. Closed loop control on the other hand, relies on the dynamics of the structure itself to generate the control force. This ensures an intrinsic reliability of the control strategy.

In this paper, two closed loop control strategies are compared. These consist of the passive damping approach, and the variable damping approach. It is demonstrated, using numerical simulation that for a multi-degree-of-freedom system, the utilization of variable damping enhances the ability of the dynamical system to respond to external excitation while satisfying strict performance criteria. This advantage over constant passive damping disappears when the structure involves a single-degree-of-freedom system. The variable damping component utilized in the simulations involves a nonlinear damping device such as encountered in ER fluids. Its behavior could be approximated using a multi-stage variable damper which under construction at SUNY.

2 Simulation of Dynamical Systems

Two simplified models of dynamical systems incorporating variable damping are analyzed in this section. The first model represents a single-degree-of-freedom (SDOF) system subjected to an earthquake excitation. The second system corresponds to a two-degree-of-freedom model of a dynamical system, subjected to an earthquake base excitation. Vibration suppression in both systems is sought in two ways. First by increasing the level of passive damping, then by incorporating a variable damping device into the dynamics of both systems. Since the two-degree-of-freedom model is assumed to represent a primary-secondary assemblage, the variable damping was implemented at the connection between the primary and secondary systems, in an attempt to control the vibration of the secondary system.

Figures (1)-(4) show the results from the SDOF system. Figure (1) depicts the behavior of the oscillator when subjected to El-Centro excitation in the presence of only nominal passive damping. Both the displacement and normalized base shear are shown as a function of time. Figures (2) and (3) correspond to the same oscillator with a value of passive damping equal to twice the nominal previous value, and to ten times that value, respectively. Note that although the displacement was substantially reduced due to the presence of additional damping, the base shear was not affected. In fact, higher order oscillations in the base shear appear with the addition of passive damping. Figure (4) shows the behavior of the oscillator with the introduction of a variable damping device. The high frequency component in the base shear is eliminated, but so is the reduction in displacement levels. It seems therefore, that under most circumstances, a variable damping device of the form tried here can be outperformed using an appropriate passive damping device. These results reinforce the results from a previous investigation [4][6] where the vibration control associated with various forms of variable damping was analyzed.

It was found that a certain level of passive damping could always be found that matched the performance of the variable damping device.

The recommendation from the SDOF does not extend to the two-degree-of-freedom model. In fact, the difference between the passive and variable dampers on the two-degree-of-freedom system is qualitatively different from the SDOF. Figure (5) shows the time variation for the displacement of the secondary system, as well as the combined linear restoring force (spring plus nominal damping), under the condition of nominal passive damping and no control force. Increasing the level of passive damping substantially reduces the maximum displacement (Figures (6) and (7)), without however affecting the overall behavior of the system, such as the magnitude of the other peaks, or the spectral content. A side effect of the increased damping is a substantial increase in the base shear of the secondary system. Not only is the maximum base shear increased, but the whole character of the base shear is affected, as reflected by the higher frequency content, and the generally higher levels of base shear, seen throughout the duration of the earthquake, and not only at the maximum level. This global change in the base shear can be detrimental if fatigue is a potential failure mode.

The introduction of variable damping into the restoring force mechanism of the secondary system induces desirable changes in both displacement and base shear levels. Indeed, as shown in Figure (8), the introduction of a variable damper having the form $F_d = 30\dot{v}|\dot{v}|$ into the system eliminates the high frequency components of the base shear, while at the same time reducing its magnitude. Furthermore, the level of displacement of the secondary system is also reduced. It seems therefore that the introduction of variable damping into the system has succeeded in eliminating, simultaneously, high levels of base shear, and high levels of displacement. Also, it is noted that the added variable damping has filtered out the high frequency content in the base-shear, thus further reducing the risk of excessive stresses in the isolation devices.

3 Implementation of Variable Damping and/or Restoring Force

A major issue in the incorporation of variable damping and restoring force in the design of structural systems is probably related to its actual implementation. This issue is currently being addressed at SUNY-Buffalo, and satisfactory solutions have been obtained. With the declassification of various military applications, a large number of innovative and high-tech designs have been made available to civilian use. A number of these applications involve variable dampers and/or restoring stiffness devices that are capable of delivering a discrete number of damping levels and/or restoring force in a very efficient and reliable manner. Due to their stringent design specifications, these devices are highly reliable, and rely in a minimal fashion on moving mechanical parts. Instead, they utilize novel orifice design, valves, and accumulators to deliver the required level of damping and restoring forces. Figure (9) illustrates the construction of such a device which is capable of delivering two levels of damping. Figure (10) shows a modification of this device which allows for the development of stiffness in addition to a damping force. Figure (11) shows a further modification of this device that is capable of delivering a variable stiffness in addition to the variable damping force. Furthermore, these two forces can be adjusted independently. Variations of these devices found numerous applications in the U.S. military. Examples of applications are in the suspension system of armored vehicles, in the suspension system of self-propelled Howitzers and the Sikorsky Flying Crane Helicopter.

During the 1960's, the Sikorsky CH-54 Flying Crane Helicopter used an adjustable stiffness fluid device to isolate the lifted load from the airframe. This device was considered adaptive in that it accepted sensor inputs and altered its output to suit different loads and load environments. This device was entirely successful, but relatively few aircrafts were quickly built to meet the needs of the Vietnam conflict. Today, many of these helicopters are still in service with the Air National Guard

and various commercial construction firms. Since the Flying Crane semi-active fluid device was concealed within the air frame on a low visibility program, few people are aware of its success.

In addition to these devices, components that feature smart materials are currently being investigated for their variable damping and stiffness capabilities. Indeed, the variable damping used in the simulations of the previous section has been suggested as representative of the behavior of Electro-Rheological fluids. Other forms have also been suggested that have, however, similar phenomenological behavior as the model utilized here. Other smart materials that are being investigated for their potential use in vibration control and suppression include Electro-Rheological Magnetic Fluids[5], and Piezoelectric materials.

4 Conclusions

Based on the simplified analysis presented herein, it is suggested that variable damping devices can be quite useful for applications involving the vibration isolation and control of secondary components in a dynamical system, while having a negligible impact on the behavior of the primary component. Taking into consideration the issue of reliability and cost, the advantages of variable damping make it a strong candidate for the suppression of excessive structural vibrations.

Bibliography

[1] Constantinou, M.C., "NCEER-Taisei research on sliding isolation systems for bridges," *NCEER Bulletin*, Vol. 6, No. 3, pp. 1-4, 1992.

[2] Constantinou, M.C., Symans, M.D., and Taylor, D.P., "Fluid viscous dampers for improving the earthquake resistance of buildings," *Structures Congress, ASCE*, April 1993, Irvine, CA.

[3] M.Q. Feng, and M. Shinozuka, "Control of seismic response of bridge structures using variable dampers," *Journal of Intelligent Material Systems and Structures*, (to appear) 1992.

[4] Ghanem, R. and Shinozuka, M., "Development of vibration suppression devices using variable dampers," *NCEER Bulletin*, Vol. 6, Number 3, et.alpp.5-8, July 1992.

[5] Pinkos, A., Shtarkman, E., and Thomas, F., "An actively damped passenger car suspension system with low voltage electro-rheological magnetic fluid," SAE Technical Paper Series 930268, 1993.

[6] Shinozuka, M., Constantinou, M., and Ghanem, R., "Passive and active fluid dampers in structural applications," U.S./China/Japan Workshop on Structural Control, October 1992, Shanghai, China.

[7] Weiss, K., Carlson, J.D., and Coulter, J.P., "Material aspects of electrorheological systems," *Journal of Intelligent Materials Systems and Structures*, Vol. 4, pp. 13-34, 1993.

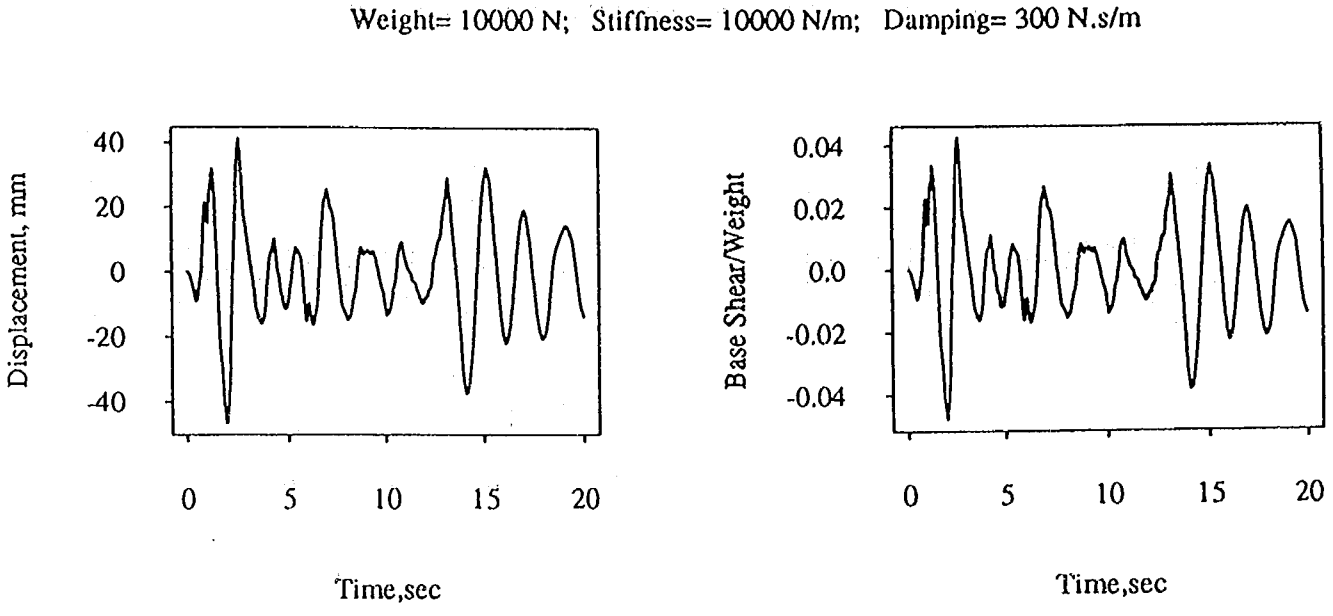


Figure 1: Response of the SDOF with Nominal Passive Damping - Displacement vs. Base-Shear.

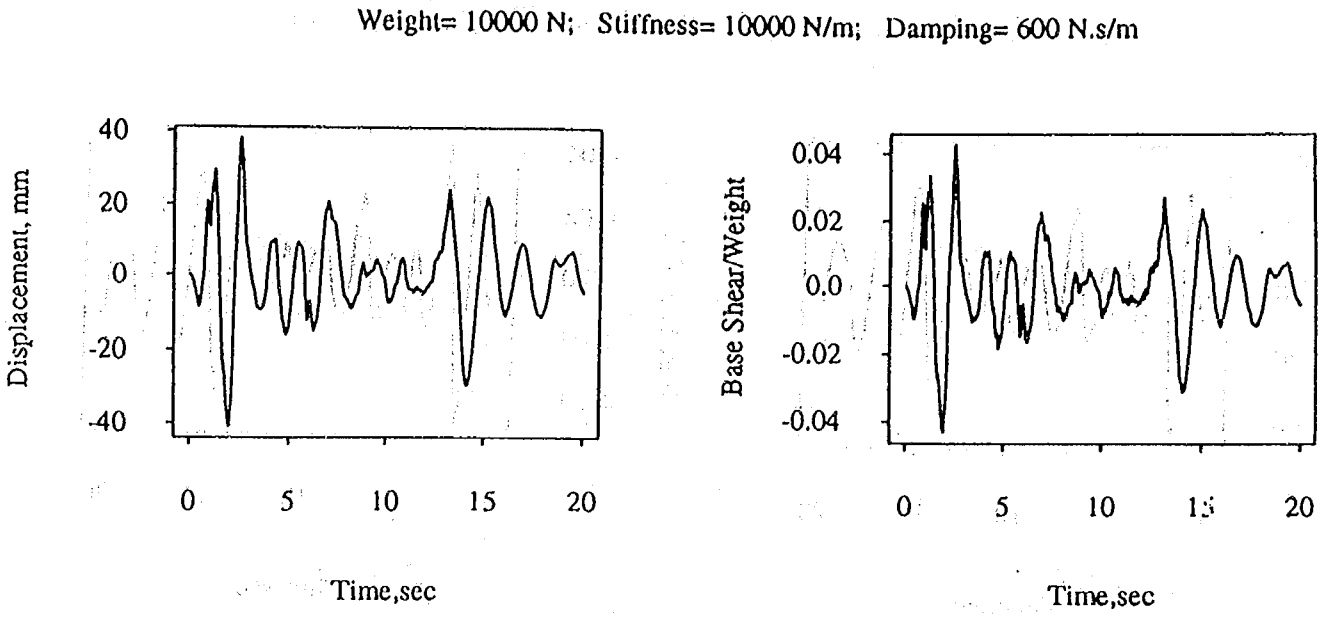


Figure 2: Response of the SDOF with Passive Damping Equal to Twice Nominal - Displacement vs. Base-Shear.

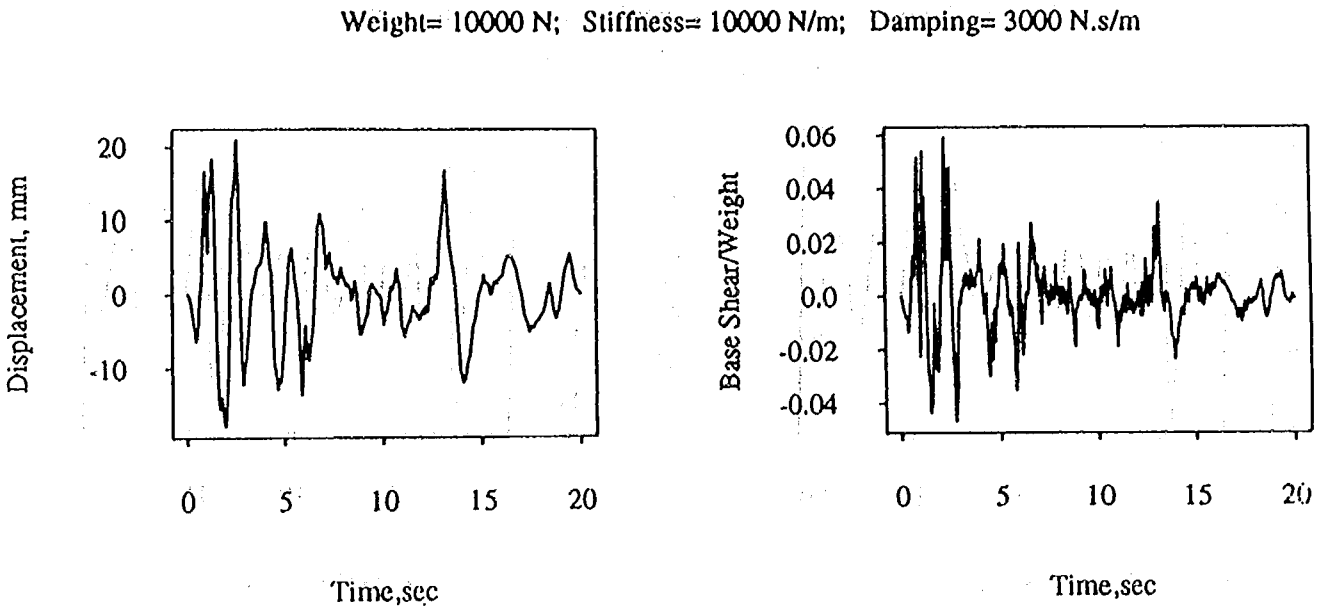


Figure 3: Response of the SDOF with Passive Damping Equal to Ten Times Nominal - Displacement vs. Base-Shear.

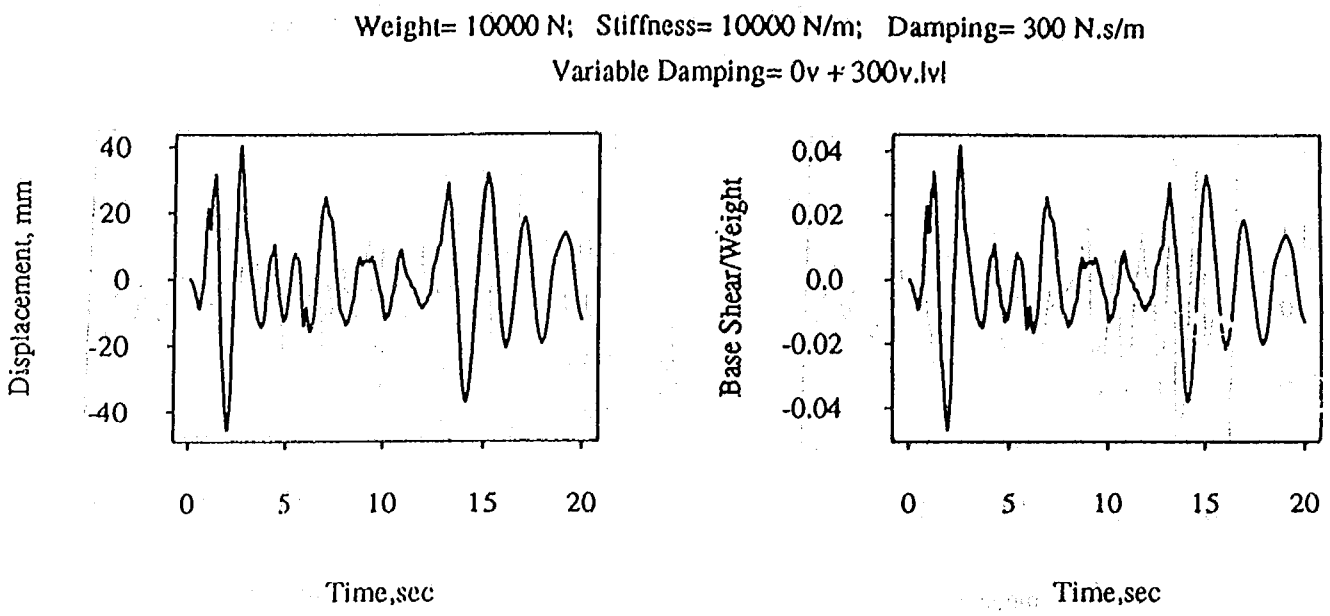


Figure 4: Response of the SDOF with Nominal Passive Damping and Variable Damping - Displacement vs. Base-Shear.

W1= 10000 N; W2= 100 N; K1= 10000 N/m; K2= 250 N/m; C1= 300 N.s/m; C2= 30 N.s/m

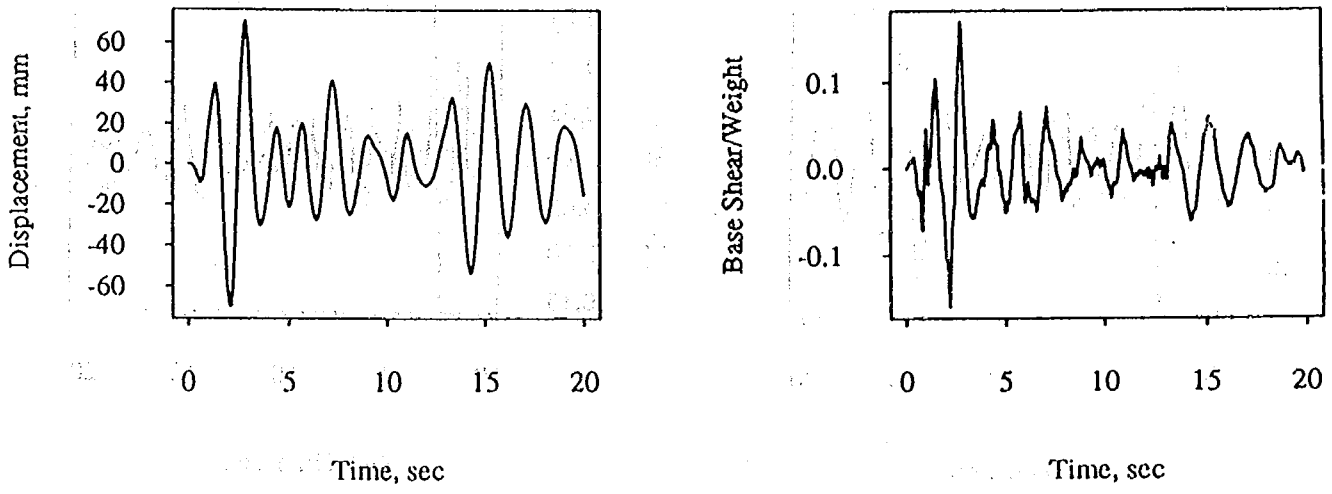


Figure 5: Response of the MDOF with Nominal Passive Damping - Displacement and Base-Shear of Secondary System.

W1= 10000 N; W2= 100 N; K1= 10000 N/m; K2= 250 N/m; C1= 300 N.s/m; C2= 60 N.s/m

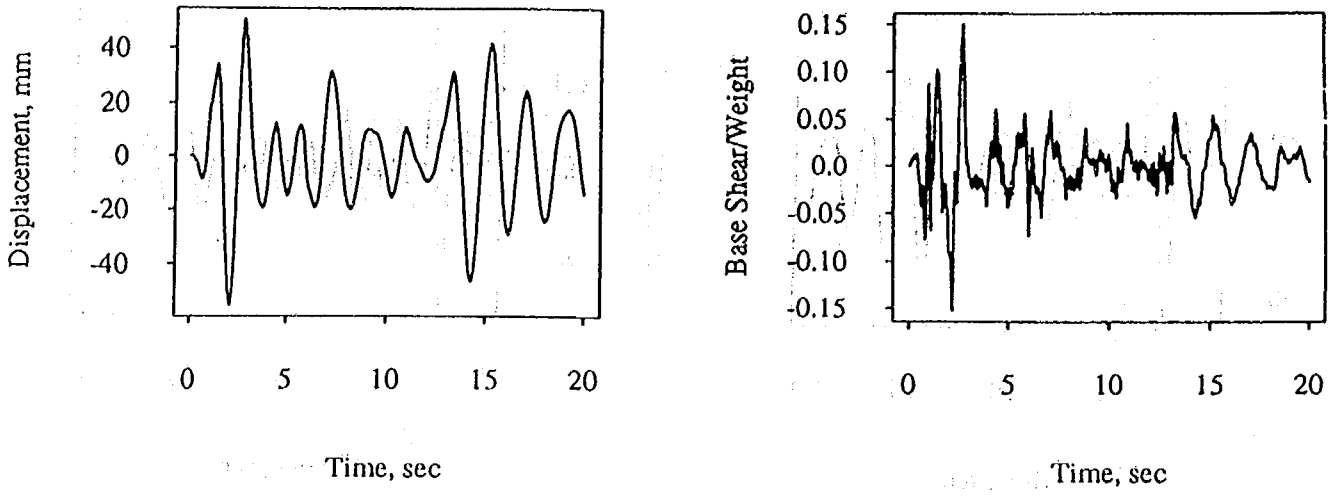


Figure 6: Response of the MDOF with Passive Damping Equal to Twice Nominal - Displacement and Base-Shear of Secondary System.

W1= 10000 N; W2= 100 N; K1= 10000 N/m; K2= 250 N/m; C1= 300 N.s/m; C2= 300 N.s/m

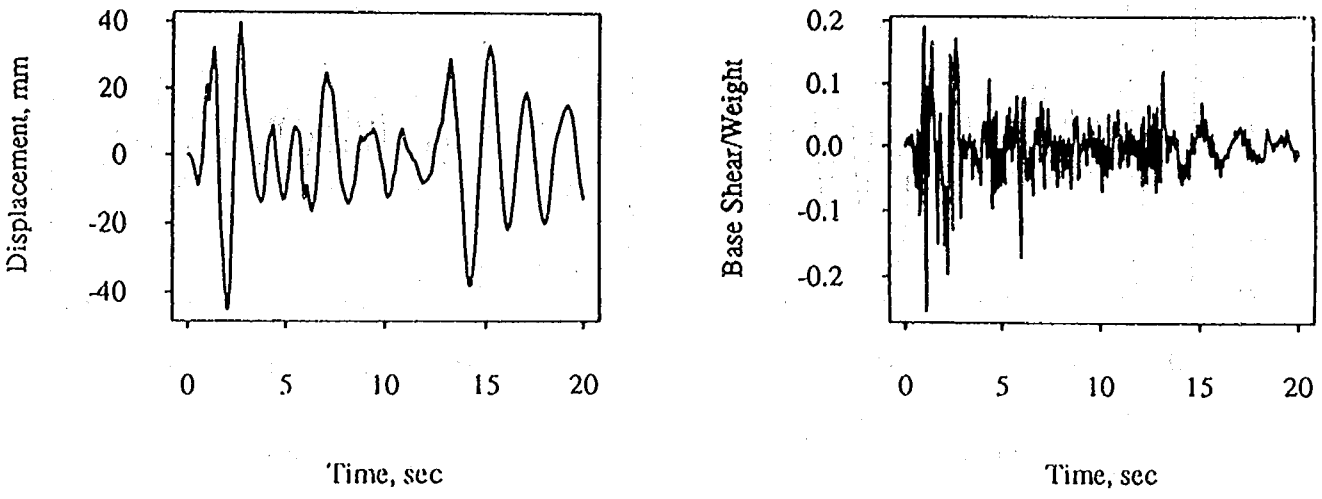


Figure 7: Response of the MDOF with Passive Damping Equal to Ten Times Nominal - Displacement and Base-Shear of Secondary System.

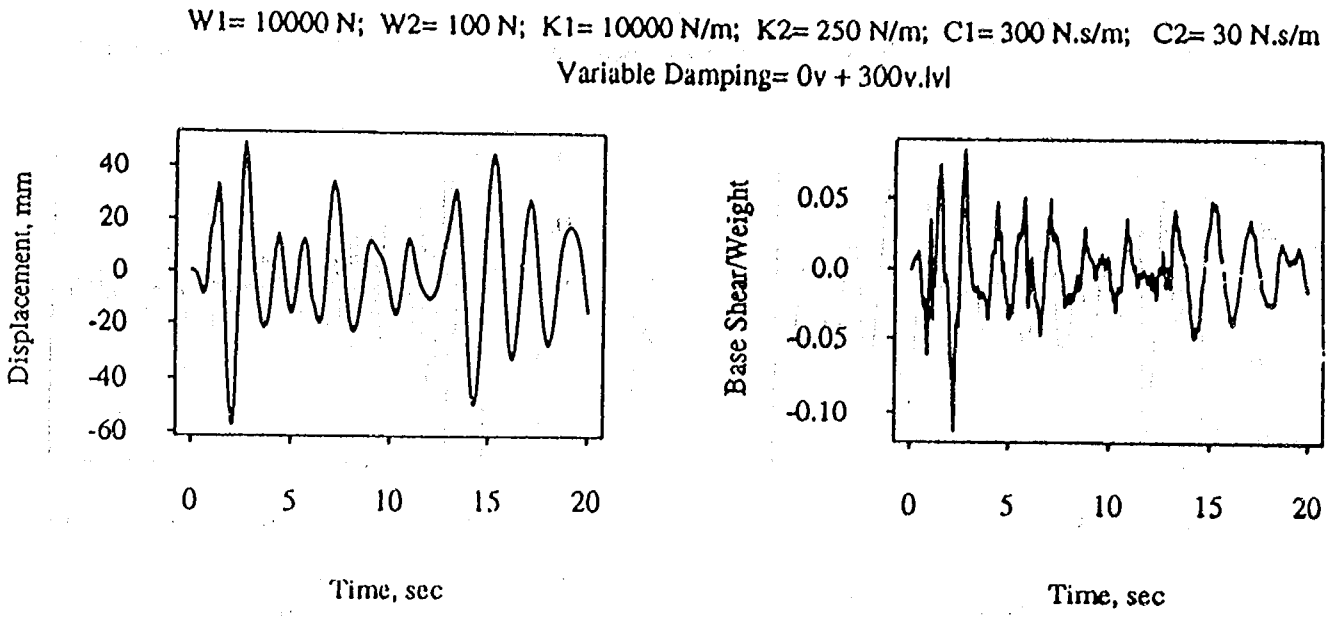


Figure 8: Response of the MDOF with Nominal Passive Damping and Variable Damping - Displacement and Base-Shear of Secondary System.

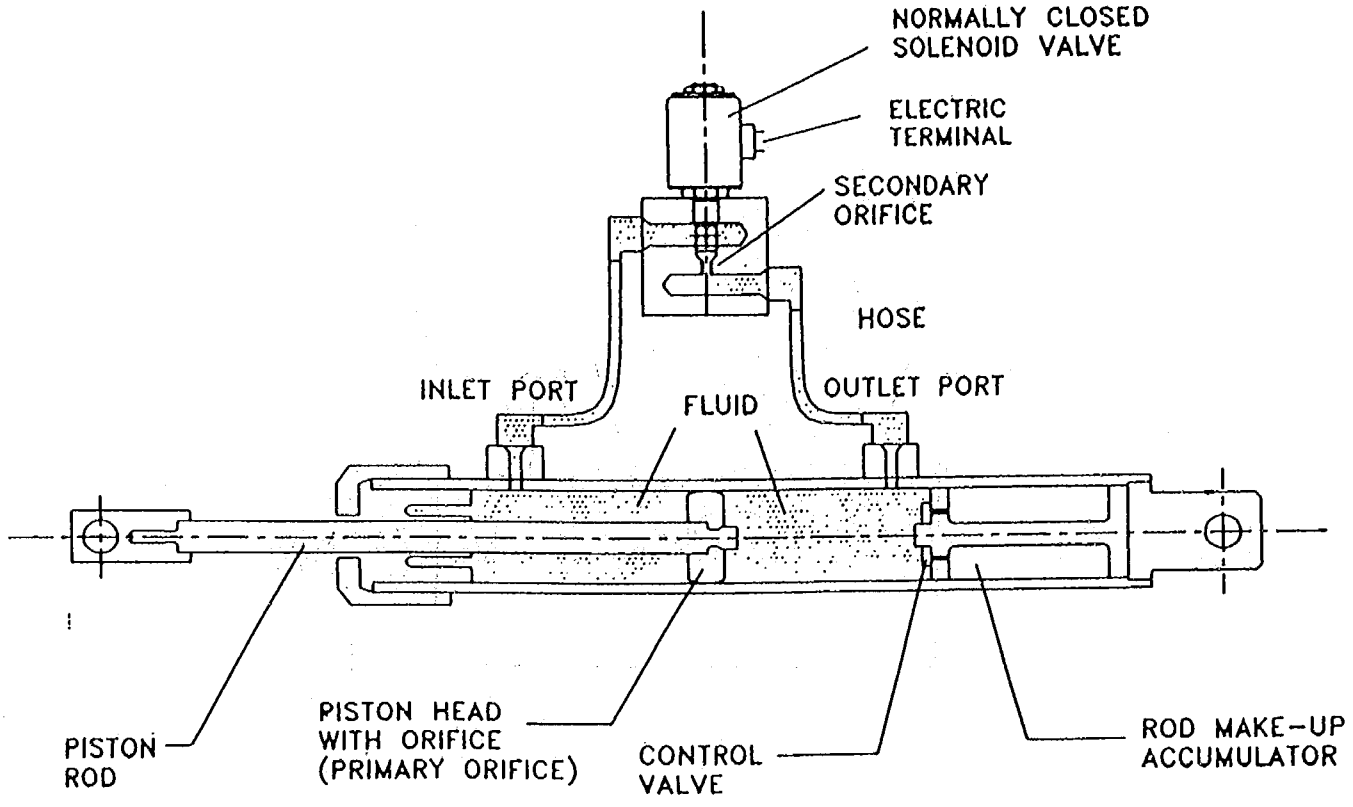


Figure 9: Construction of a Two-Stage Fluid Damping Device.

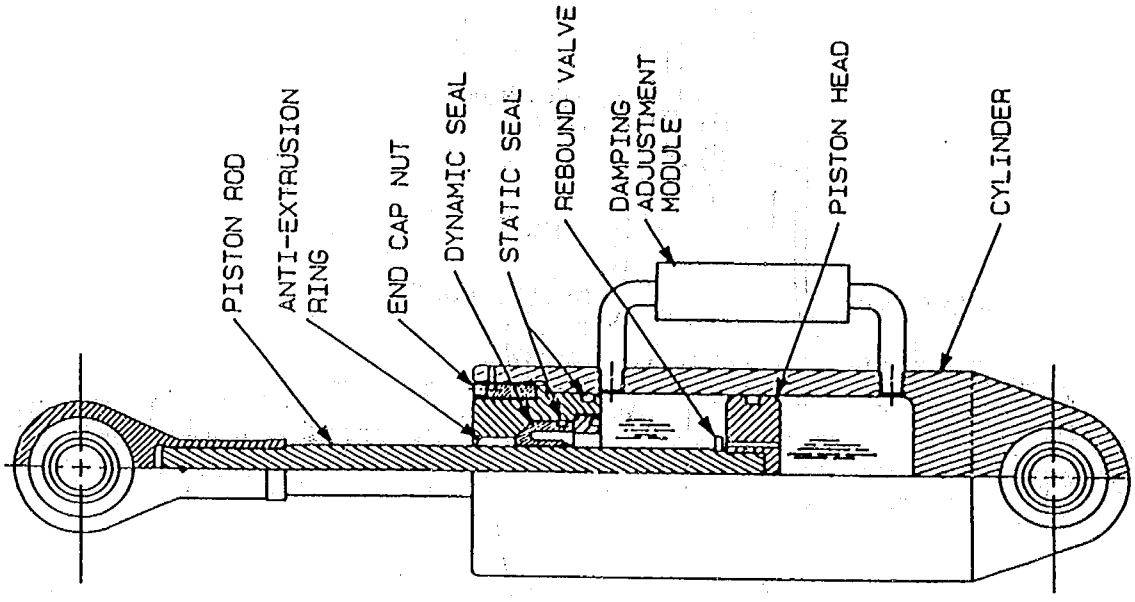


Figure 10: Construction of a Two-Stage Fluid Damping Device with Stiffness.

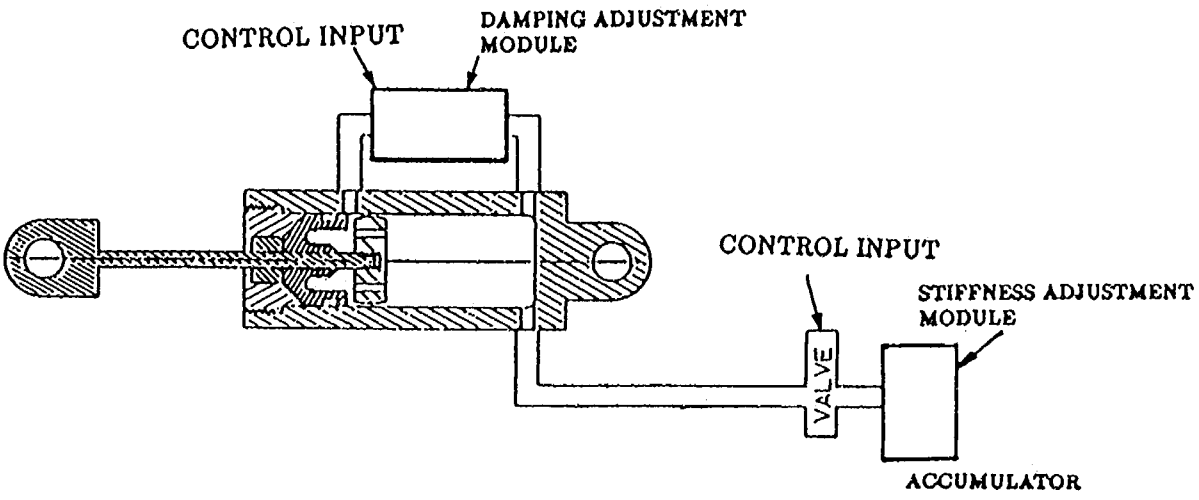


Figure 11: Construction of a Variable Damping and Stiffness Device.

Shaking Table Test of a Building Model with Seismic Response-Control by Fuzzy Optimal Logic

Yoshikazu Kitagawa[1], Mitsumasa Midorikawa[2],
Masanori Iiba[3], Hideo Fujutani[3], and Toshihide Kashima[4]

ABSTRACT

This paper presents the outline of shaking table tests for an active seismic response-control system that uses fuzzy optimal control and their results. The specimen was modeled mathematically and the response of the model was simulated numerically. The test results confirmed the validity of the vibration control effect of the seismic response-control system. As a result, it is pointed out that the effectiveness of this control system can be increased by modifying the membership function and the initial value, and that the results of seismic response-control tests can be qualitative evaluated by a rather single simulation method.

KEYWORDS: seismic response-control, shaking table test, fuzzy optimal logic, building model, simulation

1. INTRODUCTION

In building structures, it is generally difficult to construct a control system since there are many unknown variables such as the type of structure, material, and construction, and the deterioration of the structural performance with passage of time. In case of controlling the vibration of a structure subjected to earthquakes, it is critical that the response of a control system be quick enough to include time from sensing external turbulence to putting actuators in operation. There are, however, uncertainties in input signals to a control system caused by many factors such as the direction of input ground motions and the location of sensors. For dealing with these vague and uncertain problems, further development and application are needed on an intelligent control system that uses fuzzy optimal logic or neural networks.

On the premise of these conditions, a series of studies was conducted to evaluate the effectiveness of a seismic response-control system that uses fuzzy optimal logic[1) 2)]. To verify the validity and applicability of such a control system, a series of shaking table tests was conducted using a model specimen. The specimen was modeled mathematically and the response of the model was simulated numerically. This paper presents the outline of these tests and their results.

2. SEISMIC RESPONSE-CONTROL SYSTEM

2.1 Outline of Control System

Figure 1 shows flow of the seismic response-control system used in this study which predicts input earthquake motion, identifies the structure of the building in real time, and optimizes control variables accordingly[1)]. The algorithm used in the system incorporates fuzzy logic into the earthquake motion prediction and optimization so that uncertain, or fuzzy, phenomena can be handled rationally[3)]. The system uses an active seismic response-control method that combines the equivalent variable mass method, where the controlling force acts against the inertia force, and the equivalent variable viscosity method, where the controlling force is due to viscous damping. The former method reduces the influence of input earthquake motion, and the latter increases the damping by viscosity.

1)Director, Building Research Institute, Ministry of Construction, Tsukuba, Japan
2)Head, BRI
3)Senior Research Engineer, BRI
4)Research Engineer, BRI

2.2 Equations of Motion

The following equations of motion were used.

$$m_2\ddot{y}_2+c_2\cdot(\dot{y}_2-\dot{y}_1)+k_2\cdot(y_2-y_1)+u_d-u_m=-m_2\cdot\ddot{z}_0 \quad \cdots(1)$$

$$m_1\ddot{y}_1+c_1\cdot\dot{y}_1-c_2\cdot(\dot{y}_2-\dot{y}_1)+k_1\cdot y_1-k_2\cdot(y_2-y_1)=-m_1\cdot\ddot{z}_0 \quad \cdots(2)$$

$$u_d=\Delta c_2\dot{y}_2 \quad \cdots(3)$$

$$u_m=\alpha\cdot m_2\cdot\ddot{z}_2 \quad \cdots(4)$$

where u_d is the controlling force due to viscous damping, ΔC the coefficient of additional viscous damping, u_m the controlling force acting against external inertia force, and α the reduction factor.

Earthquake response was analyzed by solving the above equations of motion by the linear acceleration method.

2.3 Control Algorithm

2.3.1 Structural identification

In our control system, the maximum value of response displacement Y of the uppermost floor (considered to maximum absolute value during the control period Δt_i) is determined by a trade-off between the controlling forces Um_i and Ud_i (considered the maximum absolute values during Δt_i).

In the structural identification, the following equations are used:

$$y_{i-1}=a_{i-1}\cdot(1-\alpha_{i-1})\cdot x_{i-1}/\Delta c_{i-1} \quad \cdots(5)$$

$$y_i=a_i\cdot(1-\alpha_i)\cdot x_i/\Delta c_i \quad \cdots(6)$$

$$\dot{y}_{i-1}=b_{i-1}\cdot(1-\alpha_{i-1})\cdot x_{i-1}/\Delta c_{i-1} \quad \cdots(7)$$

$$\dot{y}_i=b_i\cdot(1-\alpha_i)\cdot x_i/\Delta c_i \quad \cdots(8)$$

Where a_{i-1}, a_i, b_{i-1} and b_i are calculated from the responses for the ith-1 and ith control periods. From the values thus obtained, predicted values of the maximum response displacement and maximum response velocity (y_{i+1} and $\dot{y}_{i+1}$) for the ith+1 control period are calculated using the following equations:

$$a_{i+1}=(a_{i-1}+a_i)/2 \quad \cdots(9)$$

$$b_{i+1}+(b_{i-1}+b_i)/2 \quad \cdots(10)$$

$$y_{i+1}=a_{i+1}\cdot(1-a_{i+1})\cdot x_{i+1}/\Delta c_{i+1} \quad \cdots(11)$$

$$\dot{y}_{i+1}=b_{i+1}\cdot(1-a_{i+1})\cdot x_{i+1}/\Delta c_{i+1} \quad \cdots(12)$$

where x_{i+1} is the predicted maximum value of input earthquake motion for the ith+1 control period. The predicted maximum values, Um_{i+1} and Ud_{i+1}, for controlling forces for the ith+1 control period can be calculated as follows:

$$Um_{i+1}=\alpha_{i+1}m_2x_{i+1} \quad \cdots(13)$$

$$Ud_{i+1}=\Delta c_{i+1}Y_{i+1}=b_{i+1}(1-\alpha_{i+1})X_{i+1} \quad \cdots(14)$$

The right-hand side of Eq. (14) can be derived using Eq. (12).

2.3.2 Maximizing decision

The maximizing decision uses the membership function (see Fig. 6) defined for the maximum response displacement Y and the controlling force U. With respect to the controlling force, the maximum value U'_{i+1} in the control period Δt_{i+1} is defined in the following equation.

$$U'_{i+1}=\sqrt{Ud^2_{i+1}+Um^2_{i+1}} \quad \cdots(15)$$

The values of α and ΔC need to be decided simultaneously using the membership function (MF) for Y, shown in Fig. 6(a) and Eq. (11), and the membership function for U, shown in Fig. 6(b) and Eq. (15). By using Eqs. (11)-(15), Y_{i+1} and U'_{i+1} are transformed into α_{i+1} (or Δc_{i+1}) plane. Values of U and α (or ΔC) are determined as the optimal membership degree and the optimal control variable.

3. EXPERIMENTAL PROCEDURE

3.1 Flow of Control Signals

Figure 2 shows the testing device used and the

positions of the sensors. The testing device consists mainly of a model, a reaction frame, an actuator, and personal computers. The actuator was installed between the uppermost floor of the model and the reaction frame.

Figure 3 shows the flow of control signals. Signals from the sensors installed on the model are input into personal computers (PC) 1 and 2. PC2 predicts input earthquake motion, performs structural identification, and optimizes the reduction factor (α) and the coefficient of additional viscous damping (ΔC). Both α and ΔC are necessary for calculating the controlling force (Um) acting against inertia force and for the controlling force (Ud) due to viscous damping, from the membership function for the response displacement and controlling force at the uppermost floor. The values of α and ΔC are sent to PC 1 at intervals of 1.2 seconds, which calculates the required controlling force and sends control signals to the actuator.

3.2 Specifications of Model

The model is a two-story steel structure consisting of floors and columns (see Fig. 1). Table 1 shows the specifications of the model.

3.3 Control Facilities

Table 2 shows the types of sensors, personal computers used, and the specifications of the actuator, which are the major components of the vibration control system.

3.4 Procedure of Response Control

To obtain the characteristics and responses of the building model and to compare between the responses under controlled and uncontrolled situations, the following conditions were defined.

a)Uncontrolled condition

The actuator was not activated. Dynamic characteristics and responses of the model alone were obtained.

b)Pseudo-uncontrolled condition

The actuator was activated. To simulate the responses of the uncontrolled model, signals were sent to the actuator.

c)Response control condition

Signals for controlling the response of the model were sent to the actuator.

As kinds of the testings, free vibration testing and shaking table testing were carried out. Four kinds of earthquake motions were used: 1940 El Centro NS, 1952 Taft EW, 1968 Hachinohe NS and EW. The maximum acceleration was approximately 30 and 60 gals.

3.5 Dynamic Characteristics of Model without Response Control

3.5.1 Dynamic characteristics and response of model alone

The natural frequency and the damping ratio obtained from the free vibration test of the model (i.e., not controlled) were 1.312 Hz and 0.211%, respectively. Figure 4 compares the observed displacement response with the calculated values. These calculated values used a spring constant of 0.3685 t/cm (for all stories) for the column determined from the natural frequency.

3.5.2 Response of the model under pseudo-uncontrolled condition

In order to make the dynamic characteristics of the model equipped with the actuator (under a pseudo-uncontrolled condition) simulate those of the model alone, command signals for the actuator were designed and generated to reproduce the characteristics of the first mode vibration of the model. Figure 5 compares the observed displacement response of the model under this pseudo-uncontrolled condition with the calculated values, confirming that the response of the model under the pseudo-uncontrolled condition accurately reproduced the response of the model alone.

4. EXPERIMENTAL RESULTS

4.1 Determination of Test Parameters

The membership function was defined as shown in Figs. 6(a) and (b). The values of D1 and D2 in the membership function for response displacement were varied as shown in Table 3, while the member-

ship function for the controlling force was fixed. The ordinate μ of the membership function (i.e., degree of satisfaction) shows that if μ=1, both the response displacement and the controlling force are at acceptable levels, and that they become less acceptable as μ approaches zero. In our experiments, the initial values of α for the first and second control periods were set at 0.00 and 0.99, respectively. The reason for using α=0.99 was to reduce the inertia force due to the input of the initial earthquake motion.

4.2 Effects of Seismic Response-Control

4.2.1 Effect of response control at the initial α value of 0.00

Table 4 shows the maximum ratio of the relative displacement at the uppermost floor under the pseudo-uncontrolled condition to that under the controlled condition that used earthquake motion and a membership function. Figures 7(a) and (b) show the time history of the relative displacement at the uppermost floor under the pseudo-uncontrolled condition (thin line) and the controlled condition (thick line) for Cases 18 and 47 shown in Table 3. As seen in these Figures, the response was dramatically reduced after about 15 seconds. Figures 8(a) and (b) show the time history of ΔC for Cases 18 and 47. As the figures indicate, the additional damping required for response control increased after about 10 seconds. In the case where the additional damping increased after the response at the uppermost floor was maximized, this maximum response did not become much smaller than that for the simulated uncontrolled condition, even though the response decreased after the occurrence of the additional damping .

4.2.2 Influence of membership function

Examination of the test cases for all input earthquake motions revealed that the maximum response in Experiment 3, in which response conditions were more severe than in Experiments 1-1 and 2-1 as shown in Table 4, was reduced to a greater degree. On the other hand, response reduction in Experiment 5, in which response conditions were less severe, was small. In Experiment 4, which was conducted under the severest response conditions, control became completely ineffective. In this experiment, the second-mode-like vibration (i.e., approximately 3 Hz) occurred that involved the resonance of the second floor. This is thought to be because only the first mode was considered in the control system.

4.2.3 Effect of the initial value of α

In Experiments 1-1 and 1-2 and in 2-1 and 2-2, the same membership function but different initial values of α, respectively, were used. The time history of the relative displacement of the uppermost floor at the initial α value of 0.99 for Cases 53 and 50 is shown in Figs. 7(c) and (d), respectively, and the time history of the additional damping for the same cases is shown in Figs. 8(c) and (d). As seen in these figures, the inertia force was reduced at the initial α value. The additional damping of 20-30 times the viscous damping of the model occurred early in the response process, causing the response to converge. This damping effect is particularly pronounced in Case 50. At the initial α value of 0.00, response control is shown to be less effective. Figures 9(a) and (b) show the time history of the controlling force at the initial α values of 0.00 (Case 18) and 0.99 (Case 53), respectively. Figure 9 corresponds to the patterns of change in the additional damping shown in Figs. 8(a) and (c). From these results, we conclude that when α=0.99, additional damping is high and response control is effective.

5.RESULTS AND DISCUSSION OF NUMERICAL SIMULATION

5.1 Maximum Response Displacement

Numerical simulation of the response analysis for both controlled and uncontrolled conditions was carried out. In the simulation, the accelerograshs of the shaking table recorded in different test cases were used as input earthquake motions with a maximum acceleration of 30 gals.

Table 5 compares the measured and calculated

maximum response displacements for the controlled condition where A and B represent the ratio of these measured and calculated values to those for the uncontrolled condition, respectively, and C is the ratio A/B. That the values of A and B are greater than 1.00, shows that the reducing effect of the calculated results tends to be greater than the measured results.

5.2 Time History of Response

Figure 10 compares the time histories of the measured and calculated responses for both controlled and uncontrolled conditions, Figure 11 shows the maximum response displacement for control period Δt. The measured and calculated values, both of which are for Case 53, showed a reduction in the inertia force due to the use of the initial α value of 0.99. Throughout the time history, the experiment and the simulation showed similar tendencies with each other.

5.3 Degree of Satisfaction in Response Displacement

Figure 12 shows the membership function for the response displacement Y at the uppermost floor defined for Case 53, and the frequency distribution of the maximum response displacement for control period Δt (normalized by maximum frequency=1). Values corresponding to amplitudes of 0.10 cm or less were ignored. As seen in Fig.12, both the measured and calculated frequencies of the response displacement in the lower range were higher in the controlled condition than in the uncontrolled condition. When vibration was controlled, the frequency distribution and the membership function showed similar tendencies with each other, indicating that the membership function simulating the controlled response had the intended control effect.

6. CONCLUSION

This paper outlined the shaking table tests for an active seismic response-control system that uses fuzzy optimal control and reported on the test results. The test results confirmed the validity of the vibration control effect of the seismic response-control system. The effectiveness of this control system can be increased by modifying the membership function and the initial value of α. Because seismic response-control became ineffective under certain conditions, there is a need for improvement, such as incorporating the response of the first floor to handle higher mode vibration.

It was also demonstrated that the results of seismic response-control tests can be qualitatively evaluated by a rather simple method of simulation.

ACKNOWLEDGMENT

This study was planned by a committee for research on seismic response-control structural systems (chaired by Hiroshi Kawamura) organized in the Japan Association for Building Research Promotion as part of a government and private sector joint research program of the Ministry of Construction. We would like to express sincere thanks to the Committee members for this collaboration.

REFERENCES

1)TANI, A. and H. KAWAMURA, "Fuzzy Optimal Seismic Control System of Building - In case of Active Equivalent Variable Mass System -", Proc. of the Second International Symposium on Uncertainty Modeling and Analysis, Apr. 1993, pp. 611-618

2)KITAGAWA, Y., H. KAWAMURA, A. KOIKE, and et al., "Seismic Response Control System by Fuzzy Optimal Logic (Part 1 - Part4)", Summaries of Technical Papers of Annual Meeting Architectural Institute of Japan, Structures I, August 1992, pp. 845-852 (in Japanese).

3)KAWAMURA, H. and J.T.P. Yao, "Application of Fuzzy Logic to Structural Control Motion of Civil Engineering Structures", Proc. of NAFIPS '90, Quarter Century of Fuzziness, Tront, Vol.1, June 1990, pp. 67-70

Table 1 Specification of Model

Component	Specification
Floors	·Composed of steel plates, H-shaped steels and additional weights ·Dimension of Plan : about 1580x1080 mm ·Weight of 2F : 2.027 tonf ·Weight of RF : 2.030ton
Columns	·Four Columns for Each Story ·Dimension of Cross Section : 19x235mm ·Height : 1500mm

Table 2 Control Facilities

Component	Types or Specification
Sensor	Accelerometer(Strain Gage and Servo Type) Velocity Transducer(Servo Type) Displacement Transducer(Inductance Type) Load Cell(Electrical Charge Type)
Computer	PC-9801FS with Math Coprocessor(NEC)
Actuator	Hydraulic Type Capacity : 300kgf Stroke : ±100mm Max. Velocity : 100kine Frequency : 0.5～10Hz

Table 3 Experimental series

Exp. No.	D 1 (cm)	D 2 (cm)	Initial Value of α	Earthquake motion (Maximum Acc-gal) Experimental Case NO.
1-1	0.9	1.5	0.00	EL-CENTRO NS(30)-Case17, (60)-Case21 TAFT EW(30)-Case31, (60)-Case33 HACHINOHE NS(30)-Case37, (60)-Case43 HACHINOHE EW(30)-Case46
1-2	0.9	1.5	0.99	EL-CENTRO NS(30)-Case56
2-1	0.6	1.2	0.00	EL-CENTRO NS(30)-Case18, (60)-Case22 TAFT EW(30)-Case27, (60)-Case34 HACHINOHE NS(30)-Case38, (60)-Case44 HACHINOHE EW(30)-Case47
2-2	0.6	1.2	0.99	EL-CENTRO NS(30)-Case53, (60)-Case54 TAFT EW(30)-Case52 HACHINOHE NS(30)-Case51 HACHINOHE EW(30)-Case50
3	0.3	0.9	0.00	EL-CENTRO NS(30)-Case19, (60)-Case23 TAFT EW(30)-Case29 HACHINOHE NS(30)-Case39, (60)-Case45 HACHINOHE EW(30)-Case48
4	0.15	0.75	0.00	TAFT EW(30)-Case30 HACHINOHE NS(30)-Case40
5	1.2	1.8	0.00	EL-CENTRO NS(60)-Case26 TAFT EW(60)-Case35 HACHINOHE NS(30)-Case42
6	0.6	1.5	0.00	EL-CENTRO NS(60)-Case25 TAFT EW(60)-Case36
7	0.3	1.5	0.00	EL-CENTRO NS(30)-Case20, (60)-Case24 TAFT EW(30)-Case32 HACHINOHE NS(30)-Case41

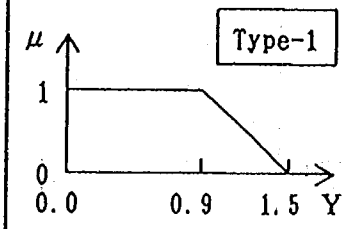
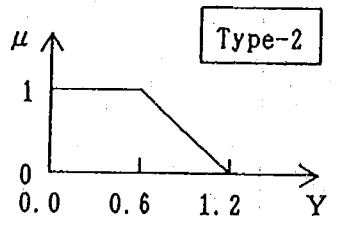
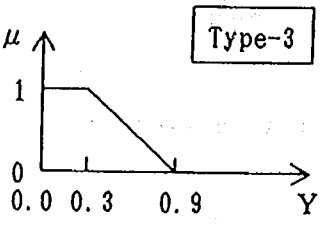
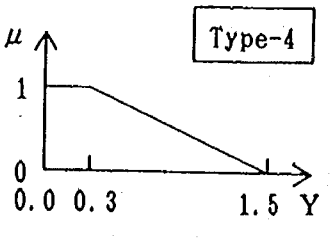
Note: The membership function of controlling force is constant.
(U_1 = 50 kgf, U_2 = 400 kgf)

Table 4 Maximum Relative Displacement

Exp. NO.	Maximum Relative Displacement of Uppermost Story Ratios of Response (Controlled / Uncontrolled) Input Earthquake							
	EL-CENTRO NS		TAFT EW		HACHINOHE NS		HACHINOHE EW	
	30gal	60gal	30gal	60gal	30gal	60gal	30gal	60gal
1 − 1	1.386 0.796	1.968 0.695	1.278 0.908	2.236 0.905	0.963 0.967	1.861 1.032	2.379 1.000	
1 − 2	1.051 0.603							
2 − 1	1.296 0.744	2.030 0.717	1.332 0.947	2.132 0.862	0.950 0.954	1.790 0.993	2.301 0.967	
2 − 2	0.900 0.517	1.366 0.482	0.632 0.449		0.770 0.773		0.601 0.253	
3	1.273 0.731	＊1	1.193 0.848		0.956 0.960	1.783 0.989	1.807 0.760	
4			＊1		＊1			
5		2.351 0.830		2.298 0.930		1.815 1.007		
6		2.008 0.709		2.086 0.844				
7	1.269 0.728	＊1	1.212 0.861		0.951 0.955			＊2
Pseudo Uncntled	1.742	2.833	1.407	2.472	0.996	1.803	2.379	

NOTE:＊1 Control is impossible.
＊2 Slanted lines means that experiment is not carried out.

Table 5 Comparison of Test and Numerical Simulation

Membership function for response displacement Y(cm) of uppermost floor	Initial values of reduction factor α	Maximum response displacement Y(cm) of uppermost floor (controlled / uncontrolled)			
		El Centro NS	Taft EW	Hachinohe NS	Hachinohe EW
	0.00	(Case17) ← Simulation Case			
		1.386 (0.796) ← Test results (maximum response disp.) / A:Controlled / Uncontrolled (test: max. resp. disp.)			
		0.798 (0.475) ← Calculated results (maximum response disp.)			
		1.68 ← B:Controlled / Uncontrolled (simulation: max. resp. disp.) / C=A/B			
	0.99	(Case56)			
		1.051 (0.603)			
		0.741 (0.441)			
		1.37			
	0.00	(Case18)	(Case27)	(Case38)	(Case47)
		1.296 (0.744)	1.332 (0.947)	0.950 (0.949)	2.301 (0.967)
		0.807 (0.480)	0.631 (0.436)	0.456 (0.476)	0.988 (0.409)
		1.55	2.17	1.99	2.36
	0.99	(Case53)	(Case52)	(Case51)	(Case50)
		0.900 (0.517)	0.632 (0.449)	0.770 (0.773)	0.601 (0.253)
		0.870 (0.518)	0.574 (0.397)	0.463 (0.484)	0.755 (0.313)
		1.00	1.13	1.60	0.808
	0.00	(Case19)	(Case29)	(Case39)	
		1.273 (0.731)	1.193 (0.848)	0.956 (0.960)	
		0.765 (0.455)	0.674 (0.466)	0.470 (0.491)	
		1.61	1.82	1.96	
	0.00	(Case20)	(Case32)	(Case41)	
		1.269 (0.728)	1.212 (0.861)	0.951 (0.955)	
		0.752 (0.447)	0.650 (0.450)	0.456 (0.476)	
		1.63	1.91	2.01	
Uncontrolled (pseudo-uncontrolled)	Test	1.742	1.407	0.996	2.379
	calculated	1.681	1.446	0.957	2.416

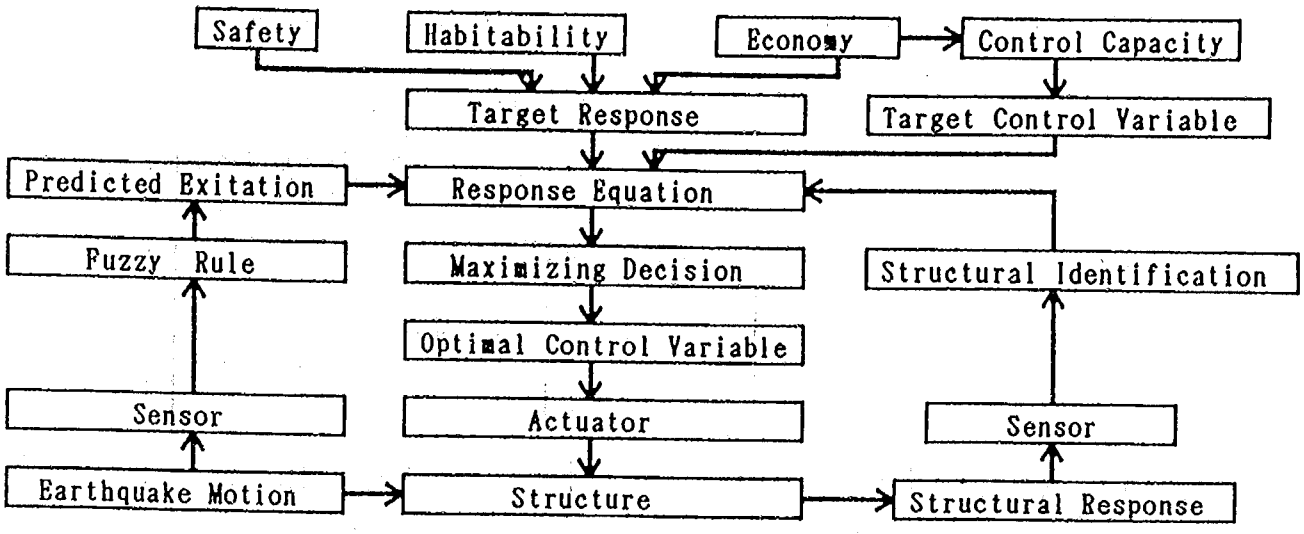


Fig. 1 Flow of Seismic Response Control System

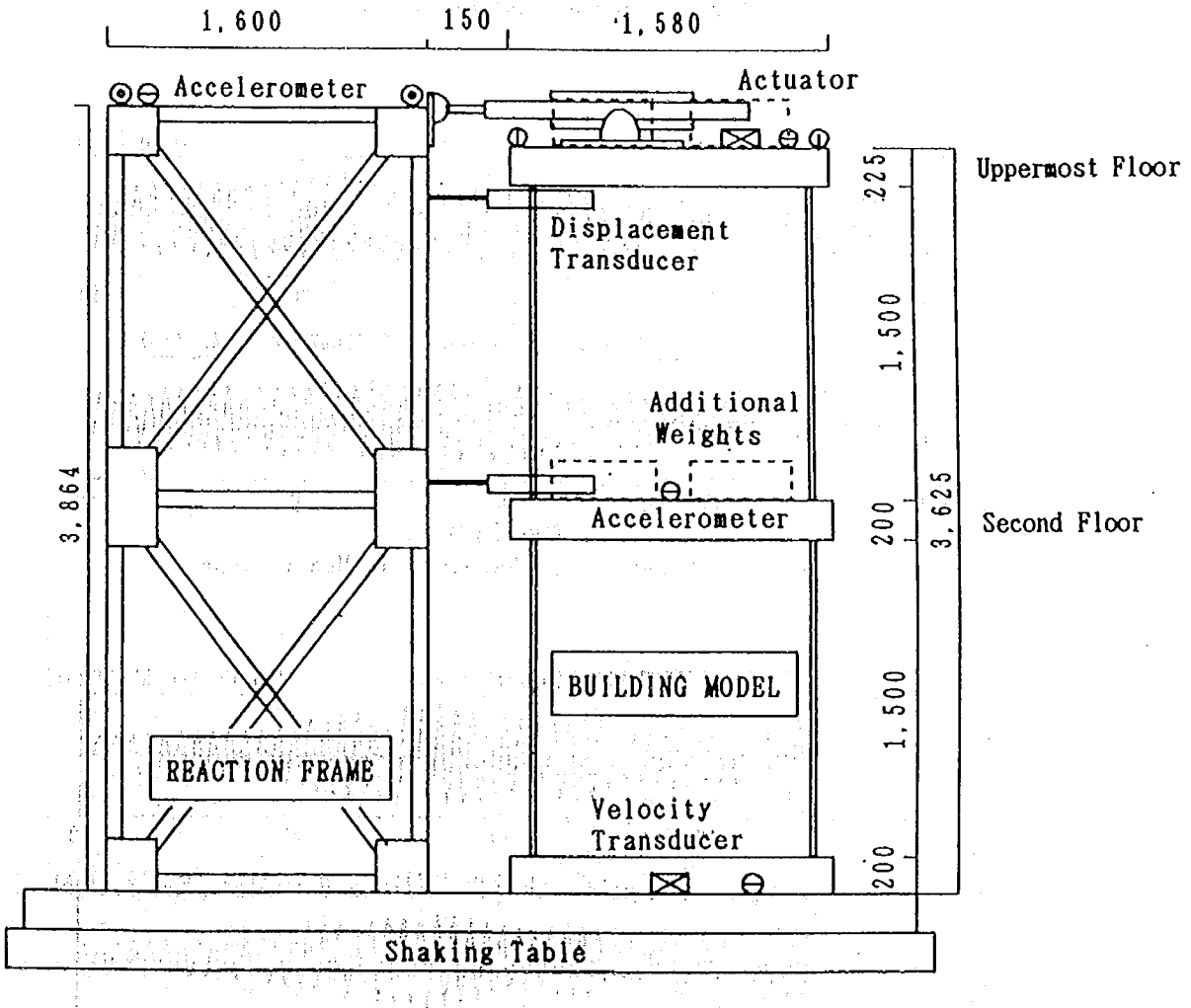


Fig. 2 Model Setup and Instrumentation

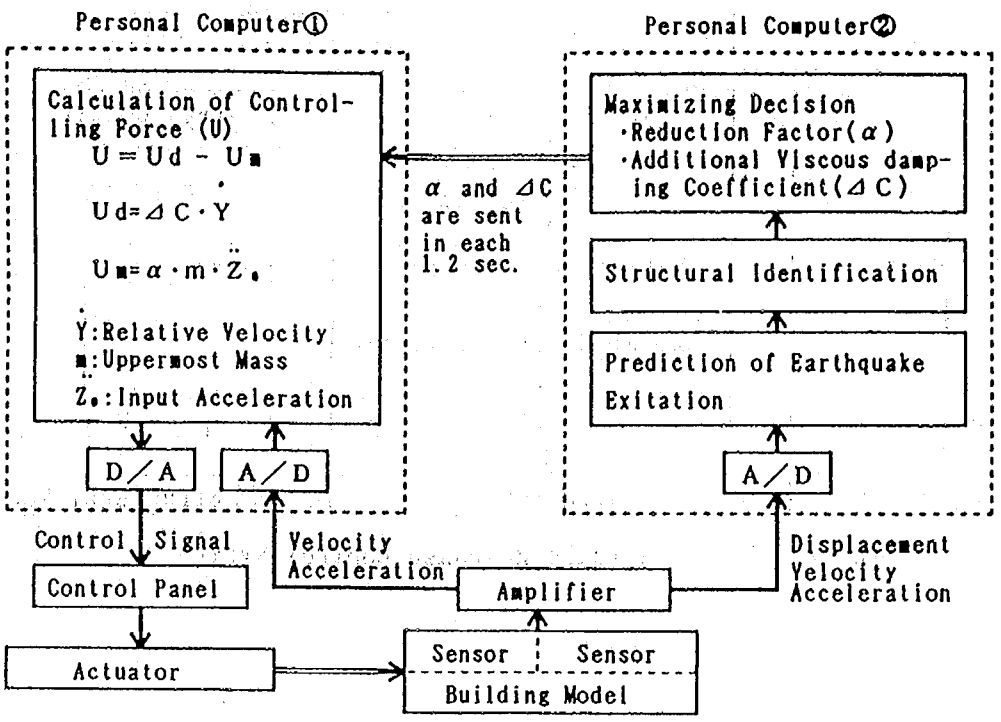


Fig. 3 Flow of Control Signals

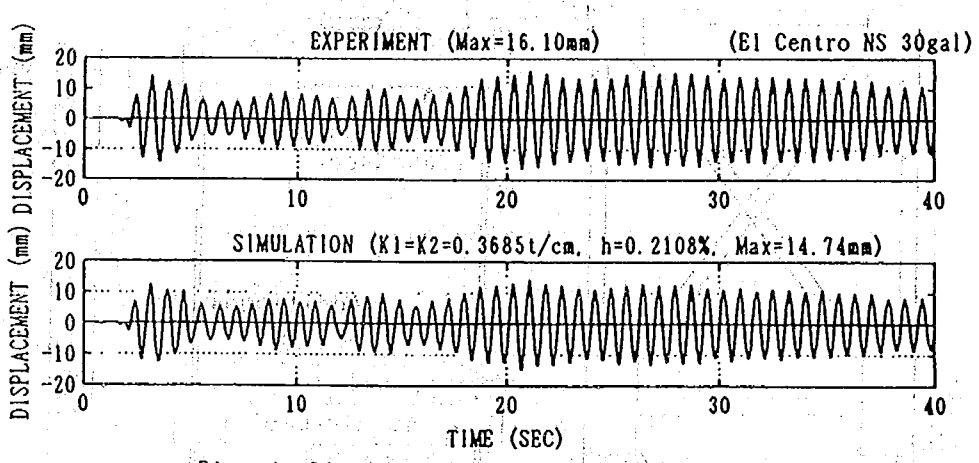


Fig. 4 Displacement Response in Model Alone

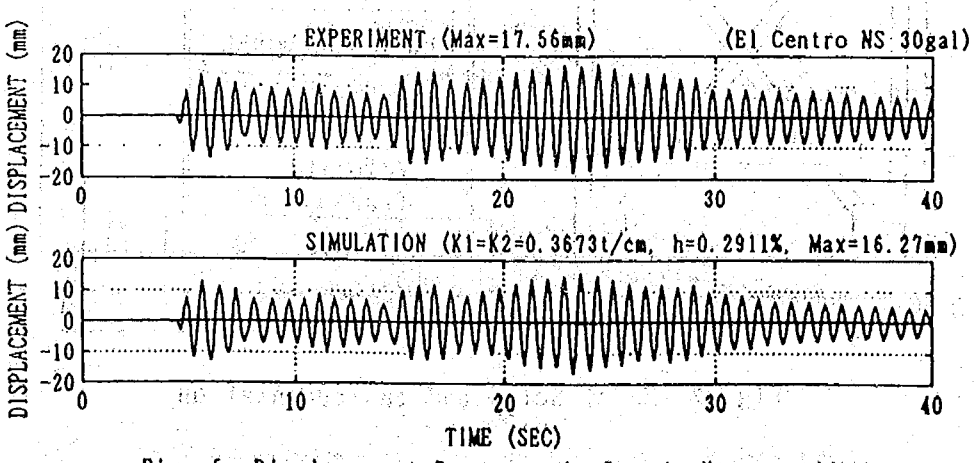
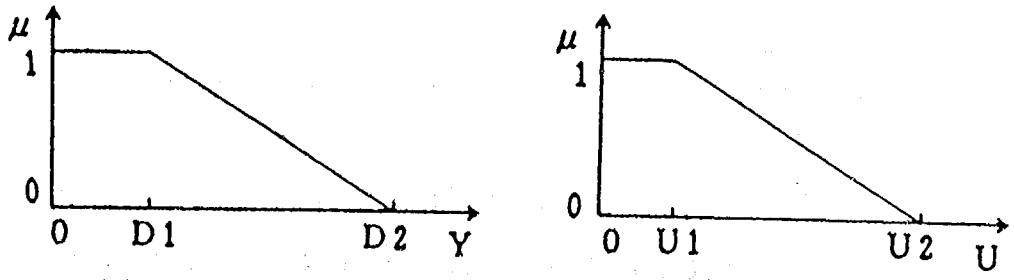
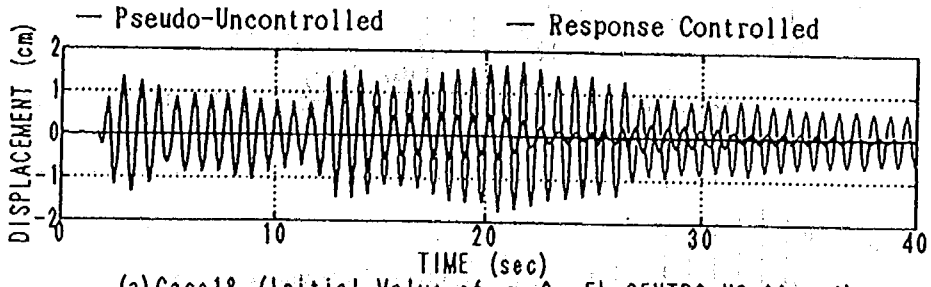


Fig. 5 Displacement Response in Pseudo-Uncontrolled

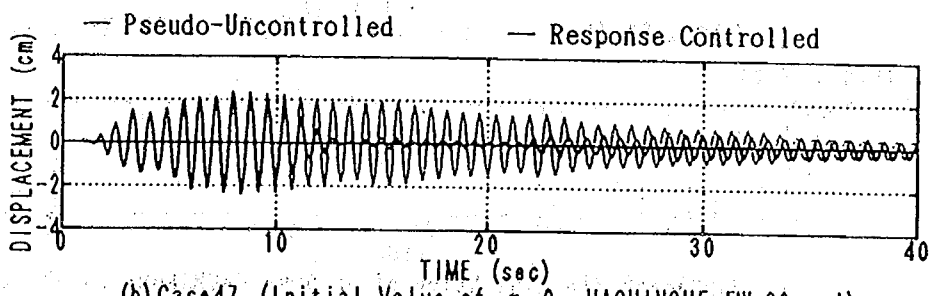


(a) Relative Displacement of Uppermost Story (b) Controlling Force

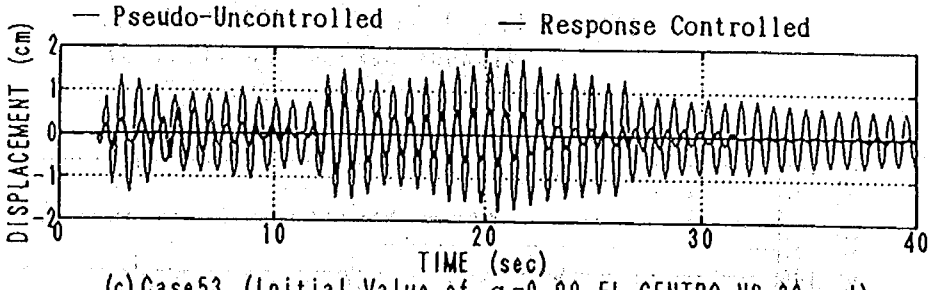
Fig. 6 Membership Functions



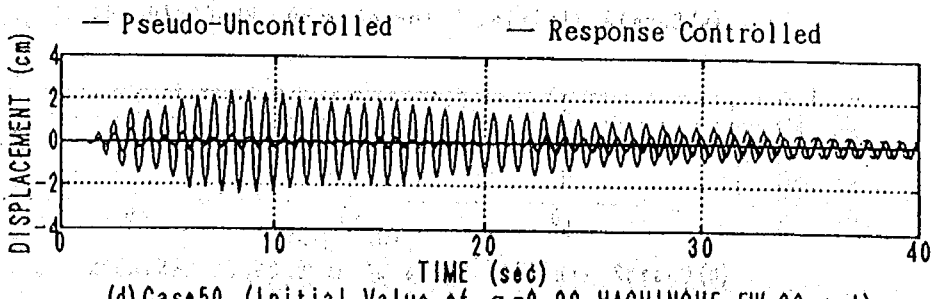
(a) Case18 (Initial Value of α=0 , EL-CENTRO NS 30 gal)



(b) Case47 (Initial Value of α=0 , HACHINOHE EW 30 gal)

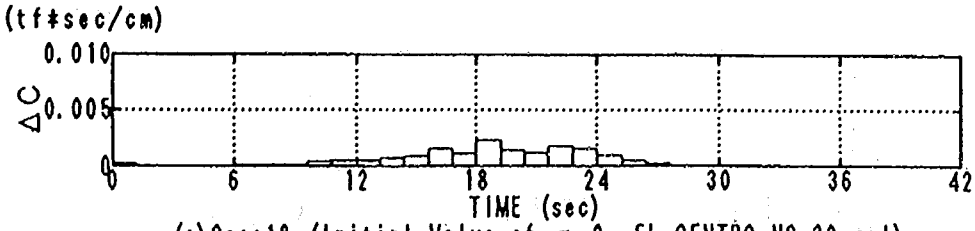


(c) Case53 (Initial Value of α=0.99, EL-CENTRO NS 30 gal)

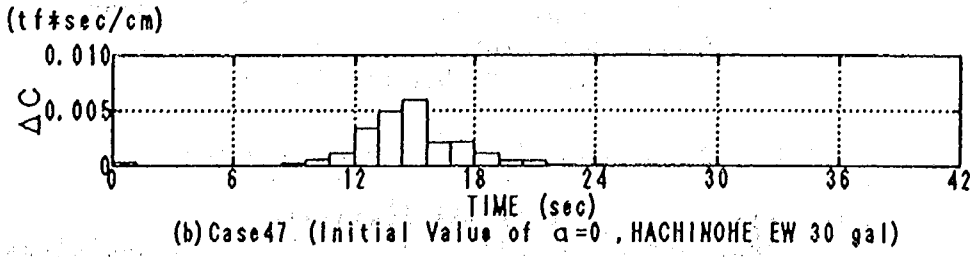


(d) Case50 (Initial Value of α=0.99, HACHINOHE EW 30 gal)

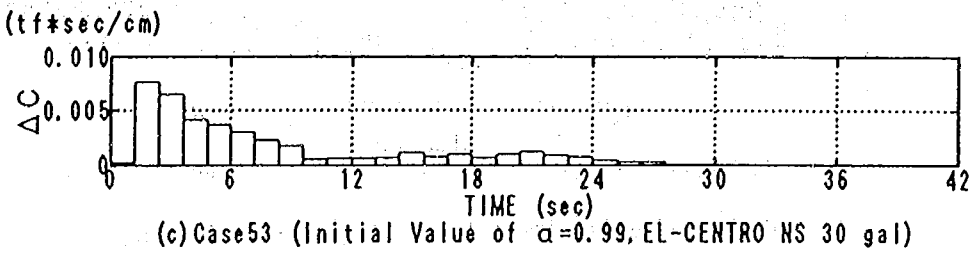
Fig. 7 Effect of Response Control on Relative Displacement of Uppermost Story



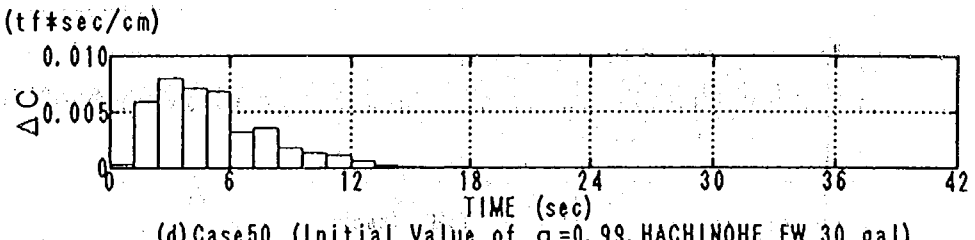
(a) Case18 (Initial Value of α=0 , EL-CENTRO NS 30 gal)



(b) Case47 (Initial Value of α=0 , HACHINOHE EW 30 gal)

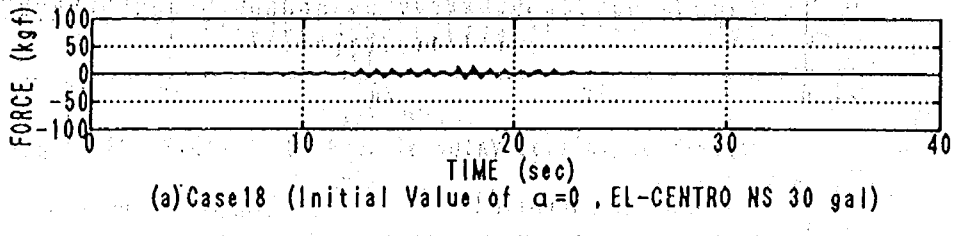


(c) Case53 (Initial Value of α=0.99, EL-CENTRO NS 30 gal)

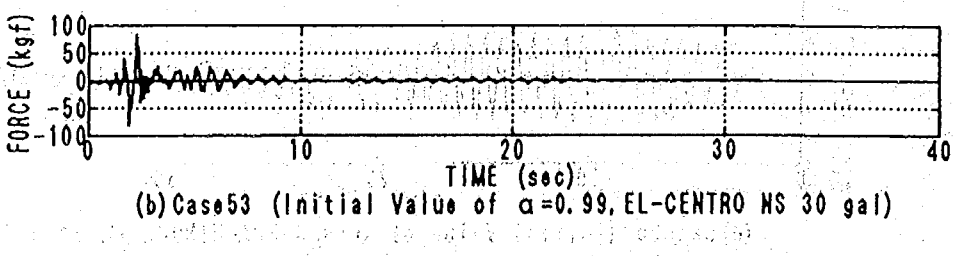


(d) Case50 (Initial Value of α=0.99, HACHINOHE EW 30 gal)

Fig. 8 Time Histories of Additional Viscous Damping Coefficient



(a) Case18 (Initial Value of α=0 , EL-CENTRO NS 30 gal)



(b) Case53 (Initial Value of α=0.99, EL-CENTRO NS 30 gal)

Fig. 9 Time Histories of Controlling Force

Structural Impedance Modification and Energy Consideration for Structural Control

Craig A. Rogers
Center for Intelligent Material Systems and Structures
Virginia Polytechnic Institute and State University
Blacksburg, VA 24061-0261

Abstract

Actively controlled structures consist of a hydro-mechanical or an electro-mechanical actuator and the structure to be controlled. In such a system, the interaction between the actuator and the structure is governed by the structural as well as the actuator impedance. In this paper, a generic impedance-based approach to facilitate the analysis of an actively controlled structure is presented. The approach is presented via an example involving an electromechanical (piezoelectric) actuator driven one-degree-of-freedom spring-mass-damper system. This method captures the physics of interaction between actuator and structure in an actively controlled structure, which is the impedance match between various active components and host-structures. Its utility and importance is illustrated by means of an experimental example and a numerical case study.

The conventional static and dynamic finite element approaches used for PZT-driven structures are briefly summarized. The impedance methodology is then discussed in comparison with the static approach. The basic elements of the impedance method, i.e., the structural impedance corresponding to actuator loading and the dynamic output characteristics of PZT actuators, are addressed. The advantages of using the impedance approach over conventional approaches are discussed using a simple numerical example.

Introduction

There are two approaches currently used in the dynamic analysis of active material systems, one is referred to as a static approach and the other is dynamic finite element approach. Both of these approaches have some drawbacks in analyzing the dynamic response of active material systems resulting from the activation of integrated induced strain actuators, such as PZT patches. A brief review of these two approaches is given below.

Static Approach

The static approach refers to the method of using a statically determined equivalent force or moment as the amplitude of the forcing function to determine the dynamic response due to the activation of integrated induced strain actuators. There are several approaches to determining

the equivalent force or moment from bonded PZT actuators. One widely used approach is the pin force model. In the pin force model (Crawley and Deluis, 1989), it is assumed that the mechanical interaction between a bonded actuator and its host structure occurs at the ends of the actuator in the form of concentrated forces. This concentrated force can be determined based on the strain compatibility and *static* force equilibrium between the actuator and structure. This concentrated force or moment is then used to represent the effect of the induced strain actuator in static and dynamic analyses by assuming that the resultant "pin-force" is frequency independent.

Another widely used approach for determining the static equivalent force or moment uses Euler-Bernoulli beam equations (Crawley and Deluis, 1989) or consistent plate equations which are fundamentally the same as the pin force models except for a variation in the assumed strain field. The equivalent force or moment determined from Euler-Bernoulli beam theory is also more accurate than the pin force model because it includes the mechanical stiffening and the bending of the bonded PZT actuators. Once again, the force or moment is calculated based on the stiffness of the structure at the point where the actuators are attached and the resultant induced force or moment is independent of frequency, even for dynamic analysis.

The static approach, as will be discussed in this paper, should be avoided in the dynamic analysis of active material systems as a result of these obvious shortcomings.

Dynamic Finite Element Approach

The electrically induced strain from any induced strain actuator (i.e., PZT or PMN) has the same effect as thermal expansion on the structural response. When using the dynamic finite element approach to determine the dynamic response of an active material system, the actuators are treated as regular integral structural components with associated mass, stiffness, and damping. The equivalent excitation forces of the actuators (the forcing terms in the finite element equation, $[M]\{\ddot{u}\} + [C]\{\dot{u}\} + [K]\{u\} = \{F_{eq}\}$) are equal to the actuator blocking forces (Liang and Rogers, 1989; Hagood et al., 1990; Sung et al., 1992).

The dynamic finite element analysis can provide correct prediction of the dynamic response. However, there are some drawbacks associated this approach. For example, extremely fine finite element mesh around an actuator is needed in order to provide satisfactory convergence. It is also difficult to customize a commercially available finite element program to deal with the harmonic dynamic thermal expansion needed to model the induced strain effect of actuators. This approach does not capture the physical essence of the dynamic interaction between the actuator and structures. For example, the forcing terms in the dynamic finite element analysis is frequency independent (blocking forces of the actuators). This may create a false impression that the force exerted on a structure by an actuator is its blocking force, which is not true as will be discussed in this paper.

In this paper, an impedance approach for dynamic analysis of active material systems will be presented. Numerical results of the dynamic response of a beam excited by a PZT actuator

based on various approaches discussed will be provided. Experimental validation of the approach will be provided. This paper will also provides a comparison between static, dynamic finite element, and impedance approaches.

Impedance Methodology

The impedance method of analyzing the dynamic response of active material systems can be simply described: the interactions between actuators and structures are governed by the dynamic output characteristics of the actuators and the dynamic characteristics of the structure, i.e., the structural impedance. To begin, we shall study the basic elements of this approach by examining the following example, a PZT actuator-driven one-degree-of-freedom spring-mass-damper (SMD) system and review the static approach as well.

The static response of a PZT/structure interaction (Fig. 1) is determined by coupling the constitutive relations of PZT and structure with their equilibrium and compatibility conditions. The force-displacement relation for the PZT actuator can be expressed as:

$$F=K_A(x-x_{in}) \ , \qquad (1)$$

where x is the displacement, F is the force exerted by the actuator, and K_A is the static stiffness of the PZT given by $Y_{22}^E w_A h_A/l_A$ where w_A, h_A, and l_A are the width, thickness, and length of the PZT actuator, respectively. x_{in} is the free induced displacement of the actuator given by $d_{32}El_A$ where d_{32} is the piezoelectric constant and E is the electric field. The force and displacement relation for the spring is given by:

$$F=-K_S x \ , \qquad (2)$$

where K_S is the spring constant. Equations (1) and (2) describe the force and displacement relations of the PZT actuator and spring. The force given by both equations is the force within the components. The force and displacement convention is positive for tension and negative for compression. If the induced displacement of the PZT actuator, x_{in}, is in the positive direction (also positive x direction as shown in Fig. 1), the resulting force in the spring is negative as expressed by Eq. (2).

Figure 2 illustrates the force-displacement relations of both the PZT actuator and spring. The intersection determines the static equilibrium of the actuator and spring system. A so-called "equivalent force" can be determined as:

$$F_{eq}=\frac{K_A K_S}{K_S+K_A}x_{in} \ . \qquad (3)$$

The "equivalent force" is used to represent the presence and activation of the PZT actuator in

the static approach. To determine the dynamic response of a mechanical system, as shown in Fig. 3, with the static approach, the governing equation is expressed by: $m\ddot{x} + c\dot{x} + K_s x = F_{eq}\sin(\omega t)$, where F_{eq} is determined from Eq. (3). Notice that the stiffness of the PZT is not included and this "equivalent force" is independent of frequency or constant over the entire frequency range of possible excitation.

The impedance approach will treat the problem differently. As an example of how the impedance approach is used to determine the dynamic response of an actuator-driven system, consider the PZT-driven one-degree-of-freedom spring-mass-damper (SMD) system shown in Fig. 3. In a dynamic scenario, the following relation based on the concept of mechanical impedance should be utilized for the structure (the spring-mass-damper system):

$$F = -Z\dot{X}\,, \tag{4}$$

where $\bar{Z}$ is the mechanical impedance of the SMD system given by:

$$Z = c + m\frac{\omega^2 - \omega_n^2}{\omega} i\,, \tag{5}$$

where i is $(-1)^{1/2}$, c the damping coefficient, m the mass, and ω the excitation frequency. The reason for the negative sign in Eq. (4) is the same as in Eq. (2). The resonant frequency of the SMD system, ω_n, is given by:

$$\omega_n = \sqrt{K_S/m}\,. \tag{6}$$

Assuming a harmonic steady state excitation, recall

$$\dot{x} = \omega i x\,. \tag{7}$$

The force-displacement for the SMD can now be expressed as:

$$F = -K_D x = -[c\omega i - m(\omega^2 - \omega_n^2)]\,x\,, \tag{8}$$

where K_D is called the dynamic stiffness.

In static analysis, the force-displacement relation of PZT, according to the constitutive equations, is given by Eq. (1). In the dynamic analysis, Eq. (1) is no longer adequate, the dynamic output characteristics of PZT actuators must be used, which can be determined based on a coupled electro-mechanical analysis.

Dynamic Output Characteristics of PZT Actuators

Consider the PZT actuator shown in Fig. 3. The electric field is applied in the z-direction, and

it is assumed that the PZT expands and contracts only in the y-direction. The constitutive relation of the PZT of the (T, E)-type (stress and electric field as independent variables) may be expressed as follows:

$$S_2=\bar{\bar{s}}_{22}^{E}T_2+d_{32}E \tag{9}$$

and

$$D_3=\bar{\epsilon}_{33}^{T}E+d_{32}T_2\,, \tag{10}$$

where S_2 is the strain, T_2 the stress, $\bar{s}_{22}^{E}$ the complex compliance at zero electric field, d_{32} the piezoelectric constant, $\bar{\epsilon}_{33}^{T}$ the complex dielectric constant at zero stress given by $\epsilon_{33}^{T}(1-\delta i)$, δ the dielectric loss factor, and D_3 the electric displacement.

The equation of motion for a PZT vibrating in the y-direction may be expressed as follows:

$$\rho\frac{\partial^2 v}{\partial t^2}=\bar{Y}_{22}^{E}\frac{\partial^2 v}{\partial y^2}\,, \tag{11}$$

where v is the displacement in the y-direction, ρ is the density of the PZT, $\bar{Y}_{22}^{E}=Y_{22}^{E}(1+i\eta)$, is the complex modulus of PZT at zero electric field, and η is the mechanical loss factor of PZT.

Solving Eq. (11) by separating the displacement v into time and spatial domain solutions yields:

$$v=\bar{v}e^{i\omega t}=(A\sin ky+B\cos ky)\,e^{i\omega t}\,, \tag{12}$$

where

$$k^2=\omega^2\rho/\bar{Y}_{22}^{E}\,. \tag{13}$$

The PZT is connected to a structure which is represented by its impedance, Z. The equilibrium and compatibility relation between the structure and the PZT can be described by:

$$T_{2_{y=l_A}}=\bar{T}_{2_{y=l_A}}e^{i\omega t}=-\frac{Z\bar{V}_{y=l_A}i\omega}{w_A h_A}e^{i\omega t}\,. \tag{14}$$

The simplest expression for structural impedance is the one given by Eq. (5) for a one-degree-of-freedom SMD system.

Equation (14) provides one boundary condition for Eq. (12). Another boundary condition is given by $\bar{v}_{y=0}=0$, which leads to B=0.

Substituting Eq. (14) into Eq. (9) yields:

$$\bar{S}_2=\frac{d\bar{V}}{dy}\Big|_{y=l_A}=-\bar{s}_{22}^{E}\frac{Z\bar{V}_{y=l_A}i\omega}{w_A h_A}+d_{32}\bar{E}\,. \tag{15}$$

Note: a bar over a variable indicates its spatial component except in the case of complex material properties, such as $\bar{s}_{22}^{E}$ and $\bar{Y}_{22}^{E}$. The coefficient, A, in Eq. (12) can be solved from Eq. (15) as:

$$A=\frac{d_{32}\bar{E}}{k\cos(kl_A)+\frac{\bar{s}_{22}^{E}Zi\omega}{w_A h_A}\sin(kl_A)}\,. \tag{16}$$

In order to further simplify the derivation and help us to explain the physics from a point of view of impedance matching, the mechanical impedance of the PZT actuators is introduced here. If a constant force excitation is applied to a PZT actuator, such as the one shown in Fig. 3, the actuator response can be determined following the same derivation outlined in Eqs. (12) to (16). The mechanical impedance of the PZT actuator defined, as the ratio of the excitation force to the velocity response, may be expressed as:

$$Z_A=-\frac{K_A(1+\eta i)}{\omega}\frac{kl_A}{\tan(kl_A)}i\,. \tag{17}$$

Note: the mechanical impedance of the actuator defined above is the short-circuit actuator impedance.

The coefficient, A, given by Eq. (16) can then be simplified as:

$$A=\frac{Z_A d_{32}\bar{E}}{k\cos(kl_A)\,(Z_A+Z)}\,. \tag{18}$$

It is necessary to mention here that the second constitutive relation of PZT given by Eq. (10) is not used. Physically, this indicates that the power supply always satisfies the current requirement of the PZT actuators.

The output displacement of the PZT actuator and the strain and stress field, as well as the electric displacement field can then be solved as follows:

$$\bar{X}=\bar{V}_{y=l_A}=\frac{Z_A d_{32}\bar{E}l_A}{Z_A+Z}\frac{\tan(kl_A)}{kl_A}\,, \tag{19}$$

and the strain:
and the stress:

$$\overline{S}_2=\frac{Z_A d_{32}\overline{E}}{Z_A+Z}\frac{\cos(ky)}{\cos(kl_A)}\ , \tag{20}$$

$$\overline{T}_2=\left(\frac{Z_A}{Z_A+Z}\frac{\cos(ky)}{\cos(kl_A)}-1\right)d_{32}\overline{Y}_{22}^{E}\overline{E}\ , \tag{21}$$

and the electric displacement field:

$$\overline{D}_3=\frac{Z_A\overline{Y}_{22}^{E}d_{32}^2\overline{E}}{Z_A+Z}\frac{\cos(ky)}{\cos(kl_A)}+(\overline{e}_{22}^{E}-d_{32}^2\overline{Y}_{22}^{E})\overline{E}\ . \tag{22}$$

The force output from the actuator (within the actuator) can be obtained from Eq. (21) as:

$$\overline{F}=w_A h_A \overline{T}_{2_{y=l_A}}=-\frac{Z}{Z_A+Z}d_{32}\overline{E}\overline{Y}_{22}^{E}w_A h_A\ . \tag{23}$$

The output characteristics of an excitation device, such as a shaker, are usually expressed in terms of its free stroke and dynamic blocking force. The free stroke of a PZT actuator, $\overline{x}_f$, can be calculated from Eq. (19) by assuming the mechanical impedance, Z, to be zero, yielding:

$$\overline{x}_f=d_{32}\overline{E}l_A\frac{\tan(kl_A)}{kl_A}\ . \tag{24}$$

The dynamic blocking force, $\overline{F}_b$, can be determined from Eq. (23) by assuming an infinite mechanical impedance, Z, yielding:

$$\overline{F}_b=-\overline{Y}_{22}^{E}d_{32}\overline{E}w_A h_A\ . \tag{25}$$

Equations (24) and (25) provide the dynamic output characteristics of PZT actuators. Based on Eq. (25), the dynamic blocking force of a PZT actuator is frequency independent, which is superior to shakers whose dynamic blocking force is constant in only a limited frequency range (Ewins, 1984). However, it is necessary to state that although a PZT actuator has a "constant" dynamic blocking force, the forces acting on a structure from integrated PZT actuators are not necessarily constant. The interaction forces from the integrated actuators are functions of the structural impedance, as will be discussed later.

The free stroke of a PZT actuator is a function of frequency. At the resonance of the PZT actuator corresponding to $kl_A=(n-1/2)\pi$, where n can be any positive integer, the displacement output for a PZT can be infinite if there is no damping (the tangent function is infinite at these values). However, as a low frequency transducer, the operating frequency range should be far below its first resonant frequency, for example, below 1/5 of the resonant frequency as a rule-of-thumb (Thomson, 1981). Thus, a PZT actuator may be treated as a constant displacement

output device ($d_{32}\overline{E}l_A$). This approximation causes less than 3% error. For example, if the length of an actuator is 0.05 m, the Suggested Operation Frequency Range (SOFR), which is 1/5 of the first resonant frequency of the PZT actuator, will be from DC to around 2.8 kHz.

If a PZT actuator is driving a mechanical system, the output force and displacement of the PZT actuator are related. This relation can be determined by combining Eq. (19) and (23) to eliminate the structural impedance term, Z, yielding:

$$\overline{F}=K_A(1+i\eta)\frac{\tan(kl_A)}{kl_A}\overline{X}+\overline{F}_b \,. \qquad (26)$$

Compared with the static force-displacement relation given by Eq. (1), Eq. (26) includes structural damping and the dynamics of the actuator. If the frequency is within the SOFR, $\tan(kl_A)/kl_A$ is about 1. A PZT actuator may be treated as a linear output device independent of frequency.

Determination of Actuator/Structure Dynamic Interaction

If the dynamic characteristics of the structure and the actuators are known, the dynamic interaction between the structure and actuator can be determined from the Dynamic Actuator/Structure Interaction Chart (DASIC), as shown in Fig. 4. In Fig. 4, the dynamic output characteristics of a PZT actuator given by Eq. (26) are independent of frequency if the frequency is within the SOFR. The dynamic characteristics of the mechanical system as given by Eq. (8) are represented by a group of rotating lines, as shown in Fig. 4. The intersection of the rotating lines with the output characteristics of the PZT determines the dynamic response, e.g., force and stroke. Note that the damping is not included in the DASIC. When the excitation frequency is zero, the intersection of the dynamic force-displacement lines of the SMD and PZT is the same as the static response determined in Fig. 2. When the frequency increases, the F-D lines of the SMD system rotate counter-clockwise around the origin of the coordinate system. The new intersection point of the F-D lines of the SMD system (non-zero frequency) and PZT actuator determines the dynamic response of the system. When the excitation frequency is the same as the resonant frequency of the SMD system, ω_n, the F-D line of SMD is coincident with the displacement axis. This indicates that the PZT actuator is free to expand and contract and the stress inside the actuator is zero, which implies that the induced force of the actuator is zero. When the excitation frequency is greater than ω_n, the mechanical displacement of the PZT actuator is larger than the free stroke, x_{in}. This indicates that the PZT actuator is stressed and deformed by the inertia of the mass and the recovery of the spring. If the excitation frequency is equal to the resonant frequency of the entire system (PZT + SMD), $\overline{\omega}_n$, which corresponds to the line parallel to the F-D relation of the PZT, the force and displacement within the actuator and spring are infinite. $\overline{\omega}_n$ can be approximated from the following expression:
where m_A is the mass of the actuator.

If the excitation frequency is greater than $\overline{\omega}_n$, the displacement response is out-of-phase with

$$\overline{\omega}_n = \sqrt{\frac{K_A + K_S}{m_A + m}} \quad , \tag{27}$$

respect to the displacement response before the frequency reaches $\overline{\omega}_n$. The dynamic equilibrium is in the third quadrant as shown in Fig. 4. If the frequency is infinite, the F-D line of the SMD is coincident with the force axis, which means that the SMD is dynamically rigid. The force provided by the actuator is the dynamic blocking force, $\overline{F}_b$. However, it is necessary to remember that the excitation frequency needs to be within the SOFR in order to use this chart. If the excitation frequency is greater than the SOFR, the variation of the actuator output characteristics needs to be considered. This can be done by rotating the F-D line of the PZT actuator clockwise around the point corresponding to the blocking force.

The actuator/structure interaction can also be explained using the concept of mechanical impedance matching in Eq. (23). If the impedance of the mechanical system is at its lowest, which corresponds to its resonance, the force provided by the PZT actuator is at its lowest. This corresponds to the case where the F-D line rotates to coincide with the displacement axis. If the structural impedance matches the actuator impedance, the actuator provides the maximum force and power. In DASIC, actuator and structure impedance matching is represented by parallel F-D lines. It is necessary to state that impedance matching between an output device and its load means that both impedances are complex conjugate.

Calculation of Structural Impedance

In order to use the impedance approach, the structural impedance corresponding to actuator loading must be calculated first. The excitation force provided by integrated actuators can be very complicated. For example, the actuation provided by a PZT actuator bonded on a beam is shear force and its distribution may be expressed with a hyperbolic tangent function (Lin and Rogers, 1992). Determination of the structural impedance corresponding to a distributed actuator can be very difficult. In this paper, the structural impedance of beams corresponding to two types of actuator excitation will be discussed.

Consider a beam structure with a complex modulus of elasticity $\overline{Y}_B$, mass density ρ_B, and moment of inertia over area K^2. The equation of motion for the transverse deflection y(x,t) is: where p(x,t) is the external dynamic loading, 'a' is the cross-sectional area of the beam, and $\overline{c}$

$$\frac{\partial^2 y}{\partial t^2} = -\overline{c}^2 K^2 \frac{\partial^4 y}{\partial x^4} + \frac{p(x,t)}{\rho_B a} \quad , \tag{28}$$

is the complex wave speed of the beam given by:

$$\overline{c}^2 = \frac{\overline{Y}_B}{\rho_B} \quad , \tag{29}$$

The governing Eq. (28) is solved by expanding the transverse displacements and external loads in terms of the eigenfunctions, $\chi_m(x)$, of the beam. The applied forcing function is harmonic and can be expressed as:

$$p(x,t) = \sum_{m=1}^{\infty} P_m \chi_m(x) \exp(i\omega t) , \qquad (30)$$

where ω is the driving frequency and $\chi_m(x)$ can be determined based on the boundary conditions of the beam. The transverse displacements can also be expressed in terms of the eigenfunctions of the beam as:

$$y(x,t) = \sum_{m=1}^{\infty} W_m \chi_m(x) \exp(i\omega t) . \qquad (31)$$

The modal amplitudes, W_m, can then be solved by substituting Eqs. (30) and (31) into Eq. (28). For example, if the boundary condition of the beam is simply-supported, the modal amplitude may be determined as:

$$W_m = \frac{P_m / \rho_B a}{\overline{c}^2 k^2 \left(\frac{m\pi}{L}\right)^4 - \omega^2} , \qquad (32)$$

where L is the length of the beam.

Consider a beam with two PZT actuators bonded on top and bottom. The actuators are activated out-of-phase, resulting in a pure bending excitation. The effect of the actuators can be represented by a pair of bending moments, M. If the two ends of the actuators are at ξ_1 and ξ_2, respectively, the external moment distribution may be expressed as follows using the Delta functions:

$$M(x) = M[\delta(x-\xi_2) - \delta(x-\xi_1)] . \qquad (33)$$

The pressure function, p(x), can be expressed with the following function as:

$$p(x) = \frac{d^2 M(x)}{dx^2} = M[\delta''(x-\xi_2) - \delta''(x-\xi_1)] . \qquad (34)$$

The modal amplitudes for the pressure expression, P_m, can be calculated using the following expression:

$$P_m = \frac{\int_0^L p(x)\,\chi_m(x)\,dx}{\int_0^L \chi_m^2(x)\,dx} \quad . \tag{35}$$

The modal amplitudes for the displacement expression can be calculated from Eq. (32). The equivalent rotational structural impedance corresponding to the pure bending moment of the actuators is defined to be:

$$Z_R = M/(\dot{\theta}_2 - \dot{\theta}_1) = M/(\theta_2 - \theta_1)\,i\omega \quad , \tag{36}$$

where θ_1 and θ_2 are the rotation angles at ξ_1 and ξ_2, respectively, which are found by differentiating the transverse deflection with respect to x:

$$\begin{aligned} \theta_1 &= \sum_{m=1}^{\infty} W_m \chi_m' \big/_{x=\xi_1} \\ \theta_2 &= \sum_{m=1}^{\infty} W_m \chi_m' \big/_{x=\xi_2} \quad . \end{aligned} \tag{37}$$

The equivalent structural impedance given by Eq. (36) needs to be modified in order to be used in Eqs. (19) to (23). The interaction between the beam and actuator previously discussed may be represented by a simple system of two actuators creating pure bending moment to drive a rotational mass-spring-damper system having the same rotational impedance as given by Eq. (36), as shown in Fig. 5. The two actuators have the same length l_A, width w_A, and thickness h_A, and they are h_B apart, where h_B is the thickness of the beam. If the rotation of mass is θ, the axial displacement of either of the actuators, x, will be $\theta h_B/2$ (assuming small deformation). The dynamic force equilibrium and geometrical compatibility together may be expressed as:

$$F = [2Z_R/(h_B + h_A)^2]\dot{x} = Z\dot{x} \quad . \tag{38}$$

The equivalent mechanical impedance determined from Eq. (38) can be directly used in Eqs. (19) to (23) to determine the stress, strain, force, displacement, and electric displacement of the PZT actuators. It is also necessary to mention that the mechanical impedance of the actuator, Z_A, used in those equations needs to be doubled since the thickness of the equivalent actuator has been doubled considering two actuators on the top and bottom of the beam.

For an actuator whose effect can be represented with a point loading, such as a stacked PZT actuator used in truss structures and a magnetostrictive actuator, as shown in Fig. 6, the definition of corresponding structural impedance to actuator loading can be expressed as:

$$Z = \frac{F}{\dot{x}} \quad . \tag{39}$$

This impedance is usually determined by calculating the structural response, $\dot{x}$, corresponding

to an arbitrary force, F, at the actuator location.

When calculating the structural impedance, the influence of the actuator stiffness and damping should not be included because they have been included in the impedance model through the short-circuit actuator impedance. The mass loading of the actuator, however, needs to be included in the calculation of structural impedance for surface bonded actuator configuration. This requires to solve a set of linear equations to determine the modal amplitude, W_m. The derivation of modal amplitude here (Eq. (28) to Eq. (32)) ignores the effect of mass loading on the transverse vibration.

Determination of Structural Dynamic Response

Once the structural impedance corresponding to the actuator load is calculated, the stress within the actuators can be determined from Eq. (21). The actuator excitation, whether it is a moment or force, can then be determined. For example, if the actuators create pure bending, the excitation moment can be determined as:

$$M_A = \bar{T}_2 w_A h_A h_B \,. \qquad (40)$$

If the magnitude of moment in Eq. (33) is assumed to be unity, the corresponding modal amplitudes can be found to be $\bar{W}_m$ from Eq. (32). The actual dynamic response of the beam can then be determined based on the following modal amplitude:

$$W_m = M_A \bar{W}_m \,. \qquad (41)$$

Numerical Example

Figure 6 shows a cantilever beam with a PZT actuator support vertically at 0.025 m away from its root. The d_{32} effect of the actuator is utilized to generate a vertical excitation. The beam is made of aluminum with a density $\rho_B = 2700$ kg/m^3, elastic modulus $Y_B = 60$ GPa, length $l_B = 0.25$ m, width $w_B = 0.02$ m, and thickness $h_B = 2$ mm. The loss factor for the aluminum is assumed to be 0.005. The PZT actuator has a width $w_A = 2$ mm, length $l_A = 0.05$ m, and thickness $h_A = 0.25$ mm. The basic material properties for the PZT material (G1195) are listed in Table 1.

Table 1: Material Properties of G1195 PZT (from Piezo System, Inc.)

d_{32} (m/volt)	Y_{22}^E N/m^2	ρ kg/m^3	ϵ_{33}^T Farads/m	δ	η
-166×10^{-12}	6.3×10^{10}	7650	1.5×10^{-8}	0.015	0.001

Assuming the electric voltage applied to the PZT actuator is 100 volts, the dynamic response of the beam at a point 0.1 m from the root of the beam is calculated using the static, dynamic finite element, and impedance methods, and is illustrated in Fig. 7. The solid line is from the impedance approach, which is completely coincident with the dashed line predicted using the dynamic finite element approach. The response predicted by the static approach is given by the dash-dotted line. It is apparent that the static approach fails to include the stiffening of the PZT actuator, which in this case is significant.

The electro-mechanical power can also be calculated based on the electric displacement given by Eq. (22). The resistive and reactive power of the coupled electro-mechanical system can then be determined, as shown in Fig. 8. The resistive power represents the actuator power consumption due to the mechanical damping of the PZT actuator and the beam, as well as the dielectric loss of the PZT actuator. The reactive power reflects the transfer of the kinetic or potential energy of the entire mechanical system as well as the reactive electric field energy. Detailed discussion of power consumption and energy transfer can be found in previous work (Liang et al., 1992, 1993).

Experimental Validation

Rossi et al. (1993) have applied the impedance approach presented in this paper to study the dynamic response of one-dimensional cylindrical ring structures. It is very convenient to apply the impedance method to study the structural dynamic response if the structural impedance of the ring, which is similar to the impedance defined by Eqs. (36) and (38), is determined from the equation of motion of cylindrical structures. Experiments have also been conducted to verify the utility of the impedance model for shell structures. A brief discussion of the experimental results is provided here.

The test article is an aluminum ring with two bonded curved PZT actuators, as shown in Fig. 9. The out-of-plane displacements at point 1, 2, 3, and 4 are measured using a VPI (vibration pattern image) laser system. The measured velocity response and the theoretical prediction based on the impedance and static approaches at point #4 is plotted in Fig. 10. In Fig. 10, the solid line is the experimental results, the prediction using the impedance approach is given by the dashed line, and the results obtained with the static model similar to the pin-force model given by Crawley and deLuis (1989) are illustrated by the dash-dotted line. It is apparent that the results by the impedance approach agree extremely well with the experimental results while the static approach failed to accurately predict the dynamic response around the second and the forth mode. The physical explanation of this phenomena can be found from the point of actuator mass loading and stiffening. Detailed discussion of these experimental results can be found in the paper by Rossi et al. (1993) as well as in the following discussion.

Discussion of the Numerical Results

What are the dynamic mechanics of active material systems? The following discussion of the simple example above will establish an understanding of the dynamic interaction between actuators and their host structures. Figure 11 shows the mechanical impedance of the cantilever beam at the point of PZT actuator support (dashed line). The mechanical impedance of the PZT actuator according to Eq. (14) is also calculated (dash-dotted line). The valleys of the mechanical impedance curve of the beam correspond to the resonances of the cantilever beam, which indicates that at the resonance, the beam is dynamically very soft. This is the reason why the force output from the PZT actuator is the lowest at the resonance of the beam, as shown by the solid line in Fig. 11. When the impedance of the actuator matches the impedance of the beam, the force output of the PZT actuator is maximum. Note: there are two intersections between the mechanical impedance curves of the PZT actuator and the beam around each peak; only the first intersection which corresponds to the complex conjugates of the impedances is physically meaningful. The frequency corresponding to the first intersection is also the resonant frequency of the entire mechanical system (beam and PZT support) as explained in DASIC.

The stiffening effect on the resonant frequency due to the extra stiffness of the PZT actuator can be determined based on the actuator and structural impedance match. If the width of the actuator in the above numerical example increases, the mechanical impedance of the PZT actuator also increases. The frequency corresponding to the first intersection around every peak of the beam impedance curve will increase, as can be seen in Fig. 11. A higher resonant frequency indicates more stiffening from the PZT actuator. When the stiffness or impedance of the PZT actuator is so high that the actuator behaves like a rigid support, the resonant frequencies are those corresponding to the peak frequencies of the beam impedance curve. This happens when the actuator impedance curve intersects at the peak or is completely above the beam impedance curve.

The force applied to the beam by the actuator, referred to as the actuator force output in this paper (which is actually the force within the actuator), is apparently not a constant, as illustrated by the solid line in Fig. 11. The lower dotted line is the equivalent force used in static analysis, as determined from Eq. (3). The difference between the two clearly indicates the incorrect physical representation of the static model. The higher dotted line in Fig. 11 is the dynamic blocking force used in the dynamic finite element approach. Using this constant force as the excitation may create confusion in explaining the physics of the dynamic interaction between actuator and structure. Notice that around the resonances of the entire system (PZT actuator and beam), which correspond to the peaks of the PZT force curve predicted based on the impedance approach, the force inside the actuator (or the force acting on the beam provided by the actuator) can be larger than the dynamic blocking force illustrated by the higher dotted line. This has been observed experimentally and is due to the reactive nature of a vibrating system, and is clearly illustrated in DASIC. Another interesting thing to notice in Fig. 11 is that at the anti-resonant frequencies of the beam, the actuator output force is the same as the dynamic blocking force. This is shown in Fig. 9 by the second intersection point between the higher dotted line and the solid line around each peak of the force curve.

The impedance approach to determining the dynamic response is very different from the other

two approaches. In experimental modal analysis, the resonance of a system is determined by the frequency response function which is the ratio of the response to the excitation force. This is simply because the excitation force provided by most excitation devices, such as shakers, is not a constant for the same reason stated in this paper. Using a response resulting from a variable force tends to provide misleading results. For example, if the excitation device is a shaker, the frequency corresponding to a peak of the response curve is not the actual resonant frequency of that mode because of the extra mass loading from the shaker. Similarly, if the excitation device is a PZT actuator which has one end fixed as in the numerical example in this paper, the peak frequencies are higher than the corresponding resonant frequencies of the original mechanical system, such as the cantilever beam in the numerical example, because of the stiffening effect. Only when the excitation force is a constant are the resonant frequencies determined from the peak frequencies equal to the true resonance frequency. In the impedance approach, the frequency response function is first calculated by using a constant unit force, the dynamic response is then determined by multiplying the frequency response function and the actual actuator force output determined from the impedance approach. This is why the response predicted by the impedance approach can accurately reflect the mechanical stiffening of the actuators. It is necessary to say that induced strain actuators do not always stiffen the original mechanical system, even in the case where bonded PZT actuators are used to excite a structure. In this case, the impedance approach can still accurately predict the influence of actuator mass loading.

To further illustrate how the impedance approach predicts dynamic response, let us examine Fig. 12 which shows the actuator force output (dashed line), the beam response (dash-dotted line) resulting from a unit force excitation (frequency response function), and the actual dynamic response (solid line) of the entire mechanical system (PZT actuator and cantilever beam). We already know from the force analysis above that the valleys of the force curve correspond to the resonant frequencies of the cantilever beam, while the peaks correspond to the resonant frequencies of the actuator and beam system. It is very clear that when multiplying the dashed line and dash-dotted line to yield the solid line, the peaks of the solid line will represent the resonance of the actuator and beam system.

Conclusions

The contribution of this paper is to introduce the impedance approach, which has been well studied in the modal analysis field, to the area of active material systems. This approach, compared with the static approach and the dynamic finite element approach, has many advantages. The most important advantage of the impedance approach is that it reflects the physical essence of the mechanics of active material systems.

The work presented in this paper provides a methodology for analyzing the dynamics of active material systems with actuators. This methodology can be used with any actuators, any material systems, and any structures as long as the structural impedance corresponding to the actuator loading and the dynamic output characteristics of the actuators can be determined. This paper

has also provided an approach to determining the structural impedance corresponding to two types of actuator loading. The concept of DASIC can virtually be used to describe any linear actuator/structure interaction.

Acknowledgment

This work is supported partially by Air Force Office of Scientific Research, Grant # AFOSR-91-0416 and Office of Naval Research, Grant ONR 00014-92-1170. The authors would like to thank Dr. Jim Chang from AFOSR and Dr. K. Ng from ONR for their kind assistance. The authors would also like to thank Dr. Z. Chaudhry for his valuable suggestions.

References

Crawley, E. F. and deLuis, J., 1989, "Use of Piezoelectric Actuators as Elements of Intelligent Structures", AIAA J. 25(10).

Ewins, D. J., 1984, Modal Testing: Theory and Practice, John Wiley & Sons Inc., NY.

Ha, S. K., Keilers, C., and Chang, F. K., 1992, "Finite Element Analysis of Composite Structures Containing Distributed Piezoelectric Sensors and Actuators," AIAA Journal, Vol. 30, No. 3, March 1992, pp. 772-780.

Hagood, N. W., Ching, W. H., and von Flotow A., 1990, "Modeling of Piezoelectric Actuator Dynamics of Active Structure Control, " Proceedings, 31st SDM Conference, Long Beach, CA, AIAA-90-697-CP.

Liang, C and Rogers, C. A., 1989, "Behavior of Shape Memory Alloy Actuators Embedded in Composites," Proceedings of the 1989 International Composite Conference, Beijing, China, 1-4 Aug. 1989, pp. 475-482.

Liang, C., Sun, F. P., and Rogers, C. A., 1993, "Coupled Electric-Mechanical Analysis of Piezoelectric Ceramic Actuator Driven Systems - Determination of the Actuator Power Consumption", Proceedings, SPIE Smart Structures and Materials'93, Albuquerque, NM, 31 Jan to 4 Feb., 1993, in press.

Liang, C., Sun, F. P., and Rogers, C. A., 1992, "Investigation of the Energy Transfer and Consumption of Adaptive Structures," Proceedings, IEEE Tucson Conference, Tuscon, AZ, Dec. 1992, in press.

Pan, J, Hansen, C. H., and Snyder, S. D., 1991, "A Study of the Response of a Simply-Supported Beam to Excitation by a Piezoelectric Actuator, "Proceedings, Recent Advances in Active Control of Sound and Vibration," Blacksburg, VA, 15-17 April, 1991, Technomic

Publishing Co., Inc, Lancaster, PA.

Wang, B. T., 1991, "Active Control of Sound Transmission/Radiation from Elastic Plates Using Multiple Piezoelectric Actuators", Ph.D. Dissertation, Dept. of Mech. Eng., Virginia Polytechnic Institute and State University, June.

Rossi, A., Liang, C., and Rogers, C. A., 1993, "A Coupled Electro-mechanical Analysis of PZT Actuator Driven Structures - An Application to Cylindrical Structures," Proceedings, 34th SDM Conference, LaJolla, CA, April 19-21, 1993; in press.

Thomson, W. A., 1981, Theory of Vibration with Application, Prentice-Hall, Inc., Englewood Cliffs, New Jersey.

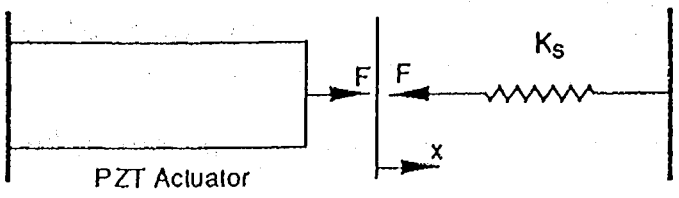


Figure 1. A spring driven by a PZT actuator.

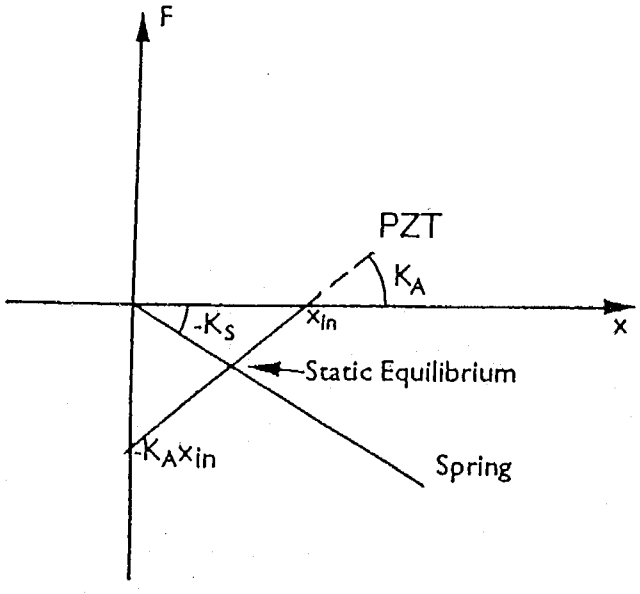


Figure 2. Determination of static equilibrium.

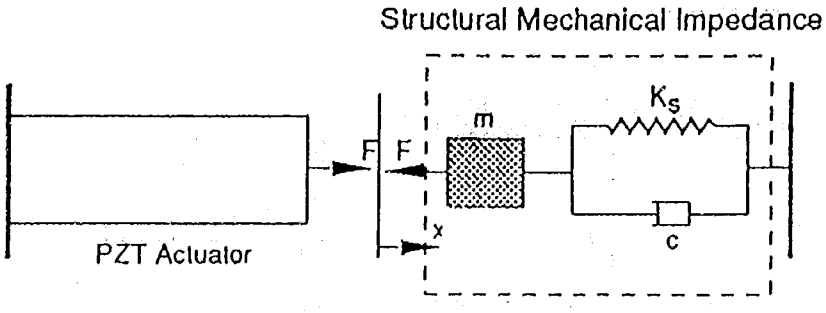


Figure 3. A schematic representation of the dynamic interaction between an actuator and its host structures illustrated by a PZT actuator-driven one-degree-of-freedom spring-mass-damper system.

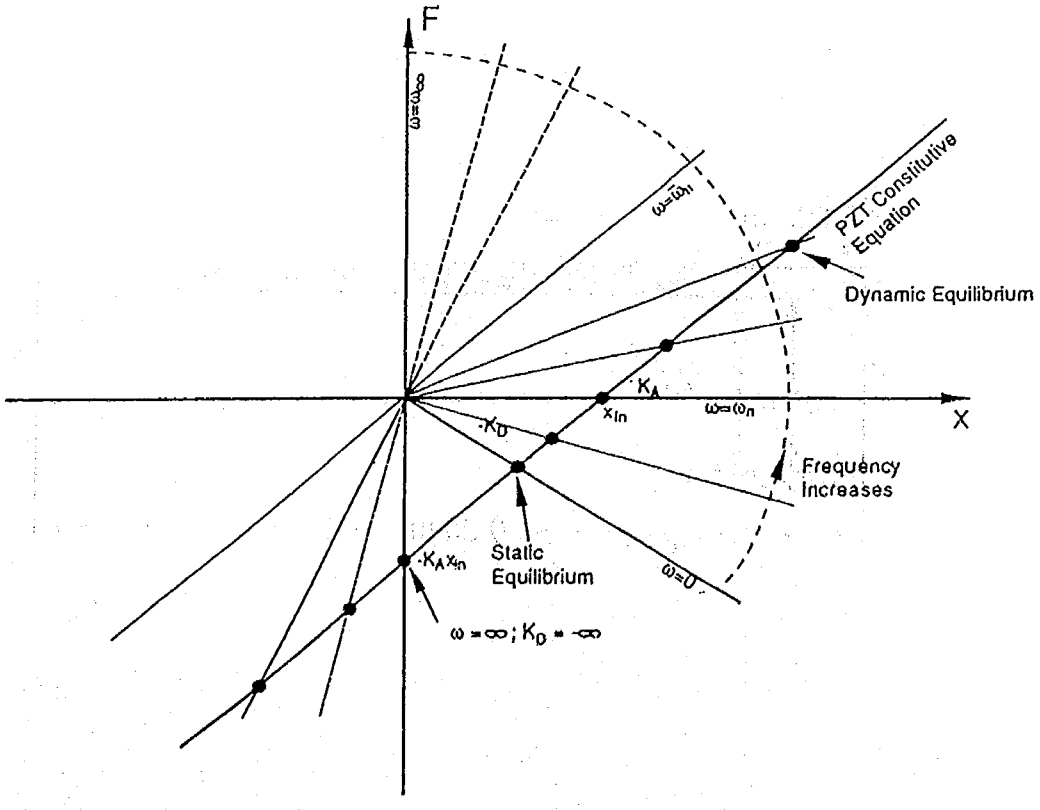


Figure 4. The dynamic actuator and structure interaction chart (DASIC).

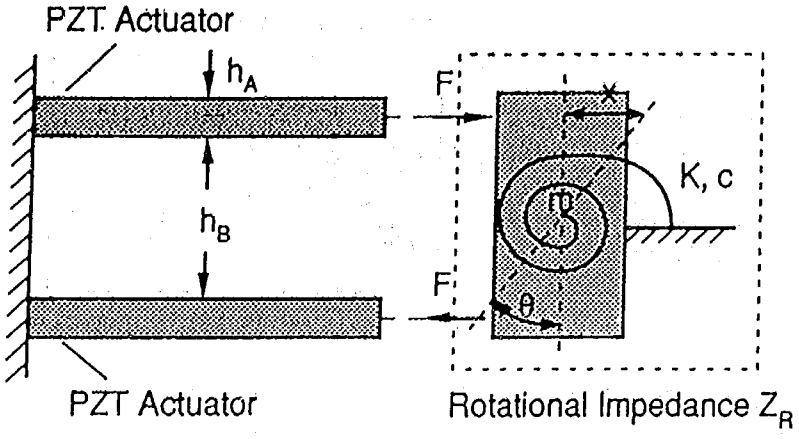


Figure 5. A simplified model for PZT actuators bonded on beam structures.

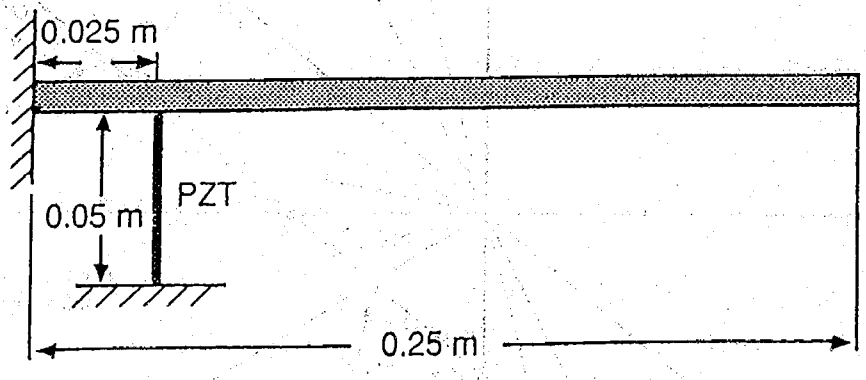


Figure 6. A cantilever beam excited vertically by a PZT actuator with one end fixed.

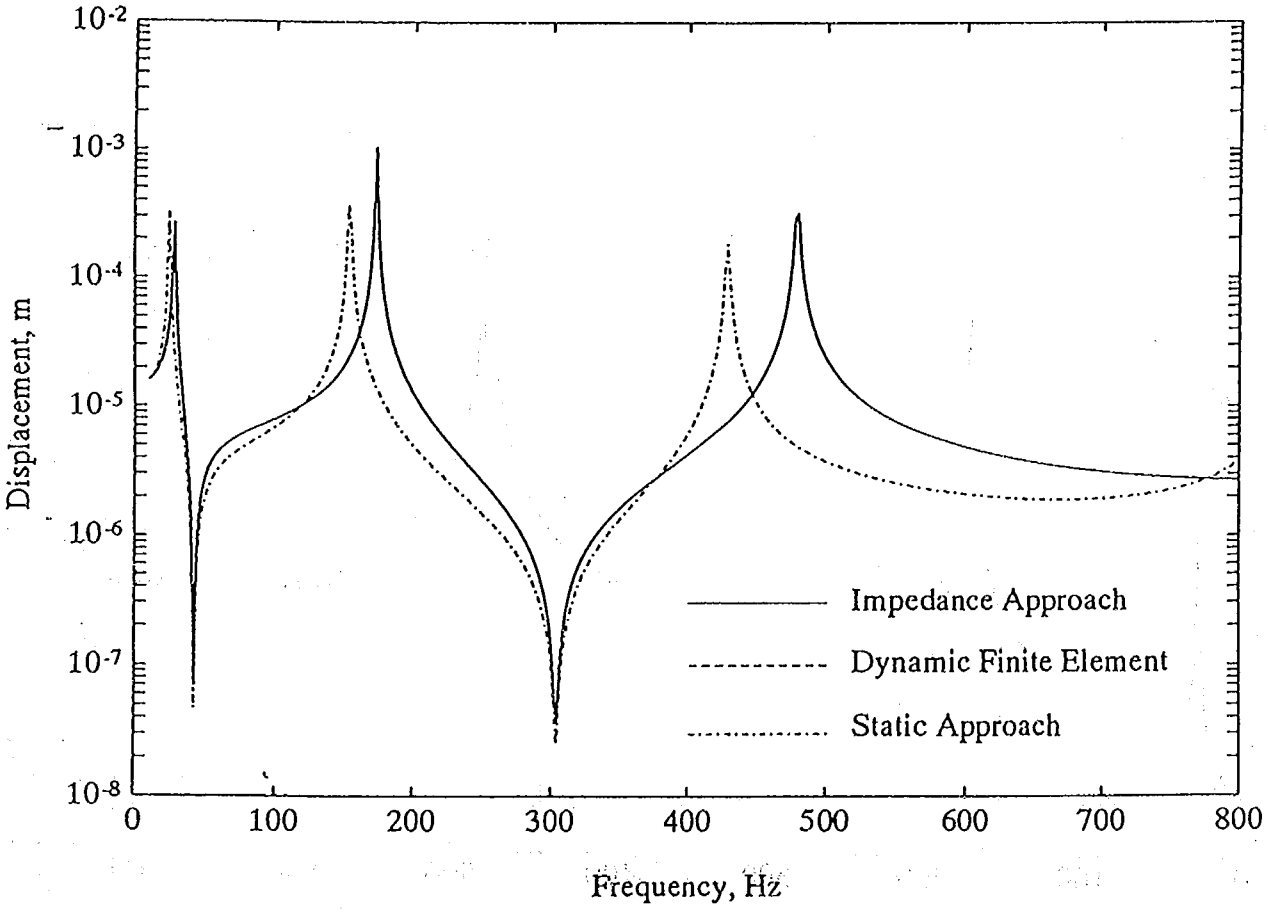


Figure 7. The dynamic response of a cantilever beam at 0.1 m from its root. The solid line is predicted by the impedance approach. The dashed line, which is completely coincident with the solid line, is predicted by the dynamic finite element approach. The dash-dotted line is predicted by the static approach.

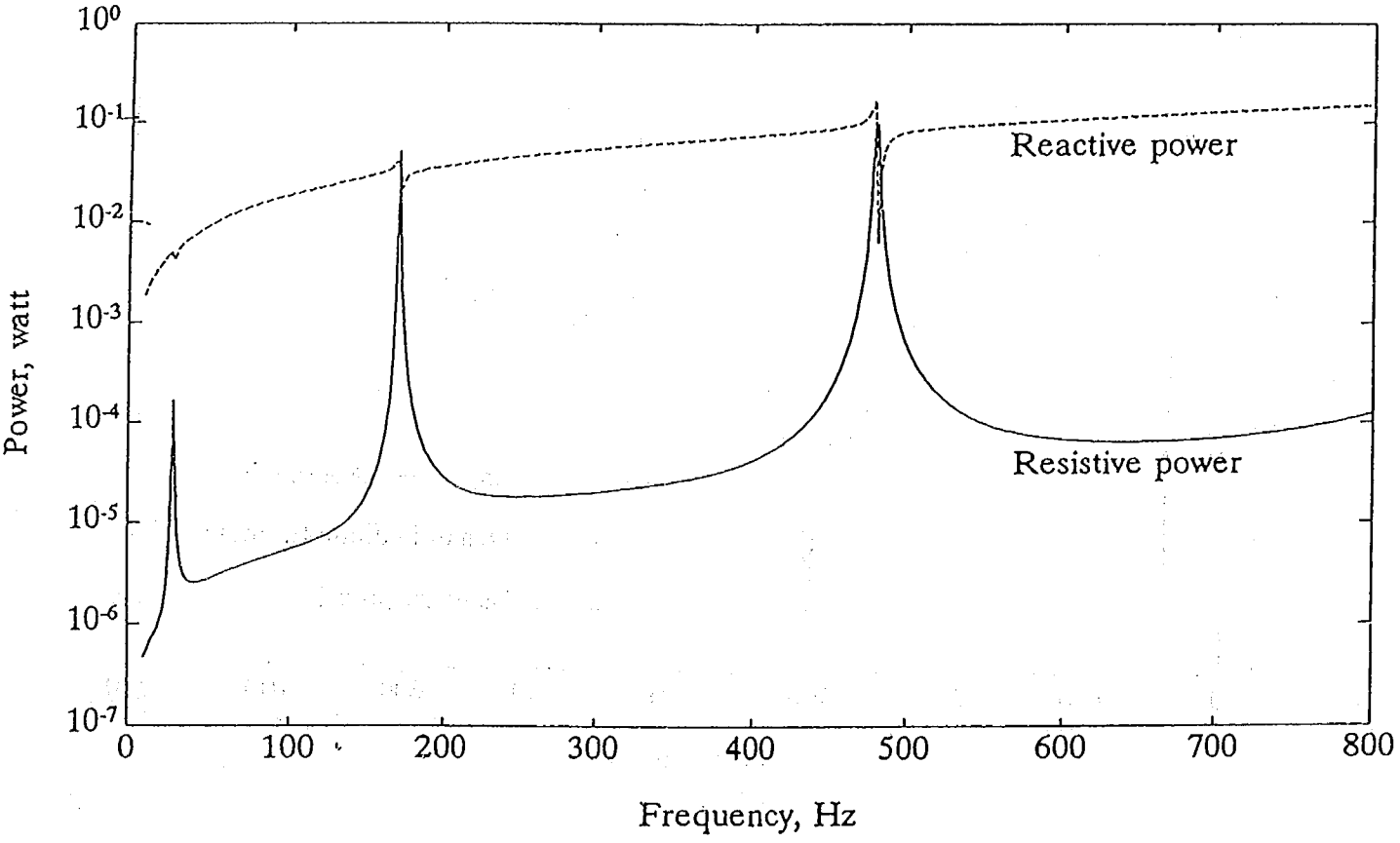


Figure 8. Resistive (solid line) and reactive power (dashed line) supplied to the PZT actuator.

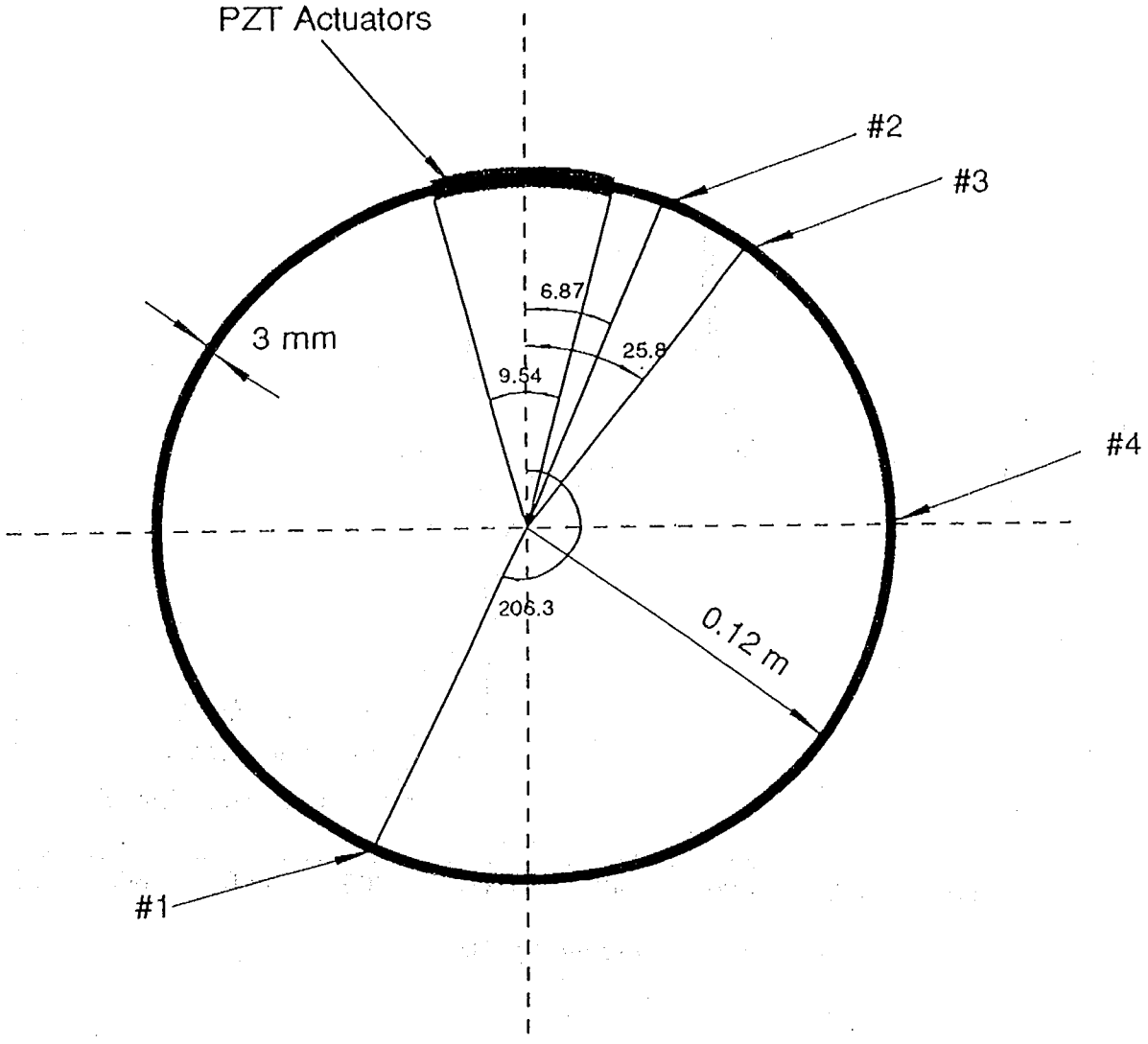


Figure 9. An aluminum ring excited by two PZT actuators. The velocity response of the ring is measured at point #1, #2, #3, and #4 (Rossi et al., 1993).

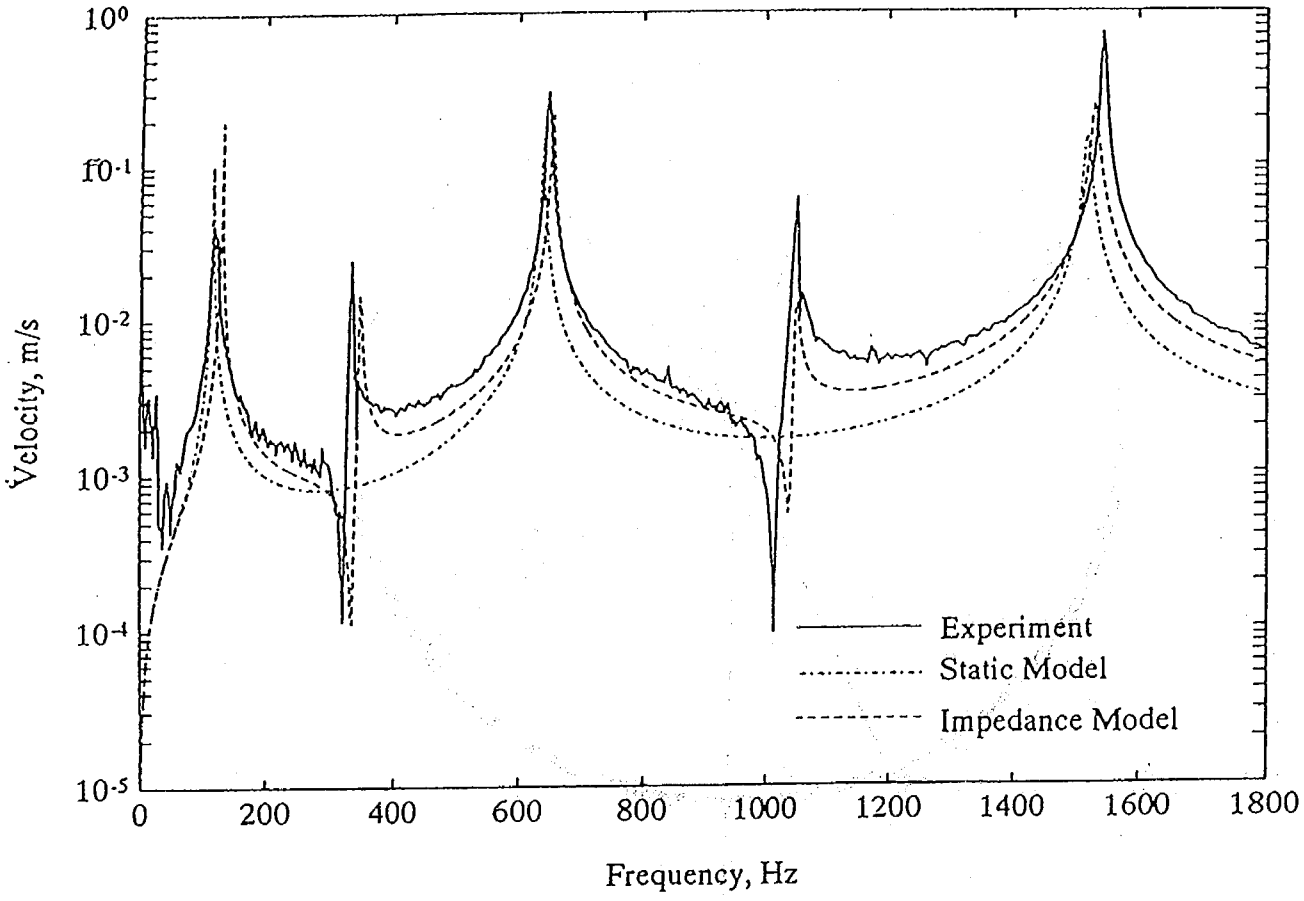


Figure 10. Experimental measurement and theoretical prediction of the velocity response of the aluminum ring at point #4 (Rossi et al., 1993).

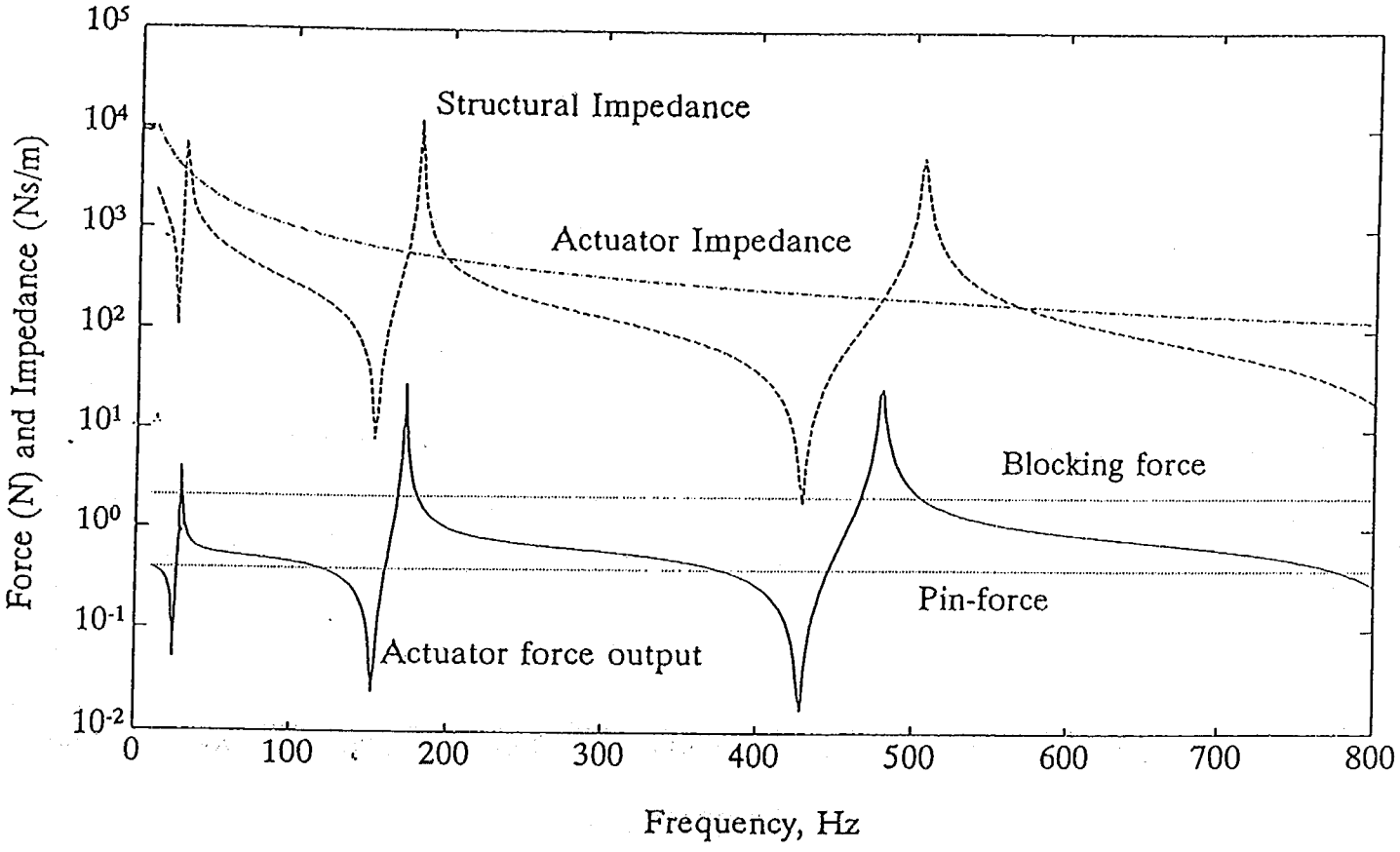


Figure 11. Mechanical impedance of the beam at 0.1 m from the root (dashed line); mechanical impedance of the PZT actuator (dash-dotted line); force output from the PZT actuator (solid line); equivalent force used by the static approach (lower dotted line); excitation force used by the dynamic finite element approach (upper dotted line).

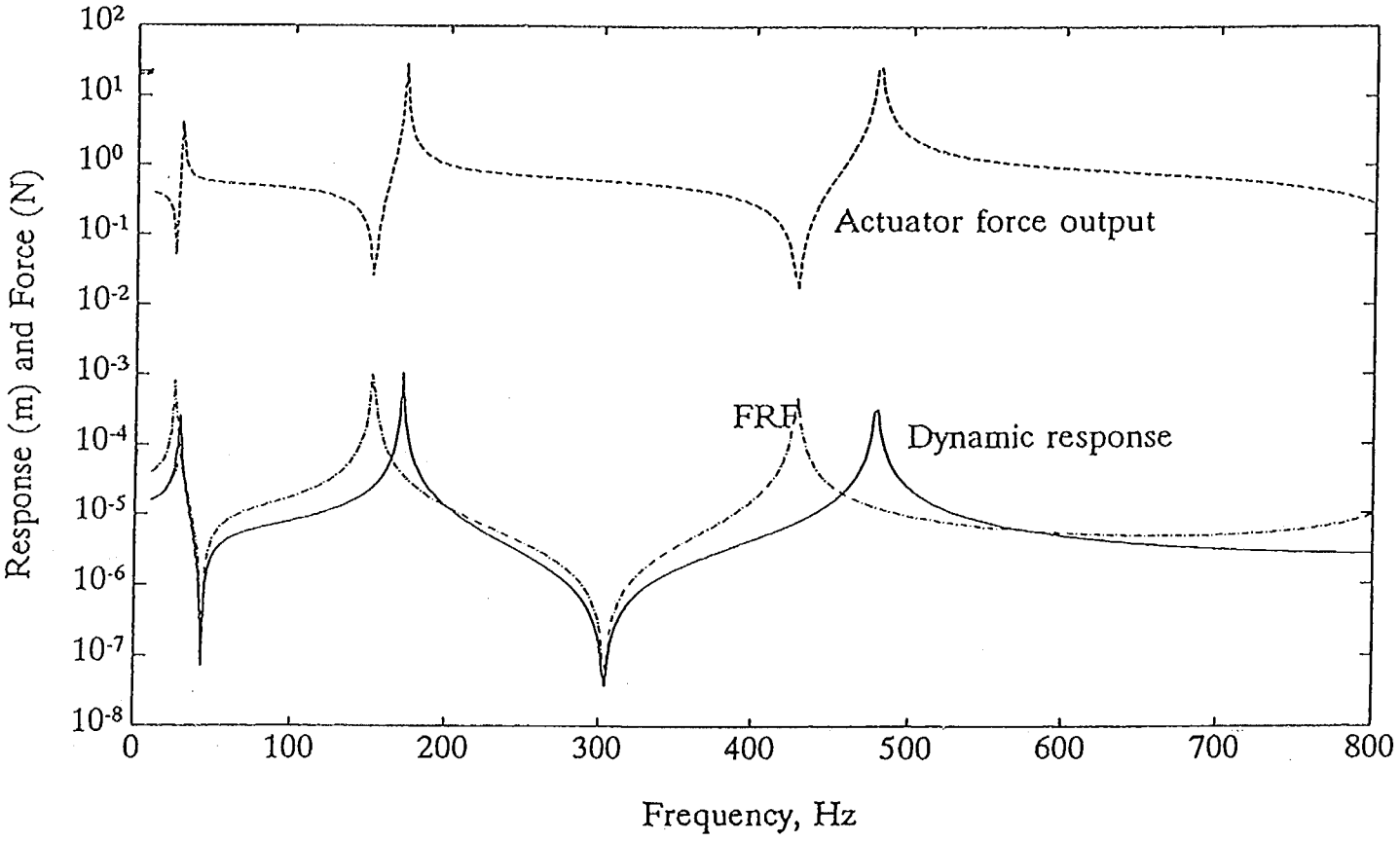


Figure 12. Determination of the dynamic response based on the frequency response function and actuator force output. Dashed line is the actuator force output, dash-dotted line is the frequency response function (or response under unit force excitation), and the solid line is the true dynamic response predicted by the impedance approach (actuator force output times the frequency response function).

Studies at PWRI on Mitigation Works against Liquefaction of Sandy Ground

by

Yasuyuki Koga[1], Osamu Matsuo[2] and Jun-ichi Koseki[3]

ABSTRACT

This paper presents current research activities on mitigation works against liquefaction of sandy ground at Public Works Research Institute.

KEYWORDS: liquefaction, mitigation works, engineering structure

1. INTRODUCTION

It has been well recognized that liquefaction of sandy ground can cause large damage to various engineering structures since the Niigata and Alaska earthquakes in 1964. Since then a great amount of studies has been conducted on the mechanism of liquefaction or its evaluation method in quite a few earthquake-prone countries, especially in USA and Japan. As a next stage of the study, practical and efficient methods to mitigate damage due to liquefaction are now demanded. This paper presents current research activities at PWRI focusing on mitigation methods against liquefaction and briefly refers to the history of research at PWRI on liquefaction as well.

2. PREVIOUS STUDIES AT PWRI ON THE MITIGATION WORKS AGAINST LIQUEFACTION

2.1 Studies on Liquefaction at PWRI

Research on liquefaction of sandy ground at PWRI started since the Niigata earthquake, 1964. Among various types of damage to many civil engineering structures, the falling down of girders of newly built Showa Ohashi Bridge manifested the necessity of critical review of the knowledge of bearing capacity of sandy ground during earthquakes. Through intensive surveys at the damaged sites during the Niigata(1964) and Tokachi-Oki(1968) earthquakes and a great amount of field and laboratory tests, it was found that the penetration resistance by SPT and gradation of the ground are the main factors to evaluate the liquefaction susceptibility (or resistance) of sandy ground. The result was incorporated into "Specifications of Earthquake-Resistant Design of Highway Bridges" in 1971.

Related research fulfilments have been presented in past UJNR meetings, which can be summarized as follows:

1) Past experience of liquefaction in Japan was comprehensively reviewed by Kuribayashi and Tatsuoka(1). The features of the liquefaction occurrence were successively reported for Miyagiken-Oki, Nihonkai-Chubu, Chibaken-Toho-Oki earthquakes(2,3,4).
2) The characteristics of the liquefied ground and structures on it was experimentally investigated. Settlement of liquefied ground and uplift of lightweight buried structures were presented by Sawada and Koga(5). The uplift of the buried structures was continued subject(6,7). The behavior of embankments resting on liquefied sand layer was another important subject(8,9,10,11).
3) Lateral flow of a wide area caused by the liquefaction has been a new and important theme(12,13).
4) Assessing the liquefaction potential in-situ has been a demanded subject and were discussed in several papers(14,15,16,17,18).

2.2 Studies at PWRI on Mitigation Works against Liquefaction

Studies to develop effective mitigation techniques against liquefaction started rather recently. A gravel drain method was applied to lightweight buried structures(5). This method was intensively studied by Sasaki and Taniguchi(19,20,21). Moreover several other mitigation methods for embankments resting on liquefied ground were experimentally examined(22).

2.3 Joint Studies on Countermeasures against Liquefaction between PWRI and Private Sector (Part I)

Several methods to mitigate liquefaction-induced damage were studied in the joint study program (1985-1990) between PWRI (Soil Dynamics Division) and the private sector including six construction firms. The main objective structures were embankments such as road embankments and river dykes, and semi-buried roads which are constructed on/in liquefiable sandy ground. The techniques studied were 1)sand compaction pile method, 2)gravel drain method, 3)deep mixing method(23,24) and 4)drainage- and-reinforcing pile method. As a consequence of the studies, a provisional design guideline of the mitigation techniques considering the conditions of structures and ground was published(25). One of the proposed design flow is illustrated in Fig.1.

---

[1]Research Coordinator for Underground Development, Planning and Research Administration Department, Public Works Research Institute, Ministry of Construction, Japan. (Formerly Head of Soil Dynamics Division) [2]Head, Soil Dynamics Division, Earthquake Disaster Prevention Department, do. [3]Researcher, do.

3. CURRENT RESEARCH PROGRAM AT PWRI ON COUNTERMEASURES AGAINST LIQUEFACTION

3.1 Research & Development Program on Earthquake Disaster Prevention in Urban Districts (EDPUD)

To integrate and develop technologies for earthquake disaster prevention in urban districts, a research and development program has been under way for the period from 1992 to 1997 at the Ministry of Construction (MOC). In this program PWRI is in charge of developing seismic hazard mitigation technologies for civil engineering structures such as roads, river works and other lifeline facilities, (while Building Research Institute (BRI) is in charge of developing those technologies mainly for buildings and its related structures). Research subjects are summarized in Table 1.

In Subject II of the table, development of new countermeasures against liquefaction and improvement of existing methods are conducted.

For this study, an advisory committee chaired by Professor Kazuya Yamamura, Nihon University was organized at the Technology Research Center for National Land Development.

1) Background for the research needs

In urban districts in Japan, typically in Greater Tokyo area and in Osaka, many urban structures and facilities are situated in the area of soft alluvial ground and in the newly developed waterfront area of recently reclaimed land. The foundation in such area often includes loose, saturated, cohesionless deposits that is susceptible to liquefaction during earthquakes. Once a strong earthquake hits the area, there may be tremendous damage to structures and facilities which may cause highly publicized economic loss and loss of life or injury. This situation requires that the soil or the foundation at the site be improved to ensure satisfactory performance.

2) Specifications for the liquefiable ground in relevant technical guidelines

The Ministry of Construction has so far provided technical specifications or guidelines for embankment structures and subsurface structures within its administration.

As for road embankment and river dykes, the guidelines state that soft foundation, loose sand deposits in particular, should be paid attention prior to construction of embankment. The remedial measures, however, are just briefly mentioned, and the details are not described in the guidelines.

As for the subsurface structures including semi-buried road and common utility duct which are usually lighter than the soil of equivalent bulk, evaluation of the stability against uplift due to soil liquefaction is specified in the relevant guidelines. But details on countermeasures are not shown as well.

There are several reasons for these guidelines not specifying countermeasures in detail. The primary reasons are:

(a) Pre-earthquake measures are usually costly, and it is generally considered that post-earthquake measures including restoration and rehabilitation are less expensive.
(b) Methods for selection, design and utilization of the countermeasure techniques are not yet fully established.

3) Current state of related existing techniques

Existing countermeasures against liquefaction of soil can be summarized in Table 2. Among these techniques some methods like sand compaction pile method(stone column method) have already been adopted at many sites and have proven to be effective during past earthquakes. These techniques, however, cannot always be applied to a variety of site conditions and different types of objective structures. Therefore, it is required to review the applicability of these existing techniques and to identify their research needs. Table 3 is the summary of the review, where the techniques are arranged according to the following aspects.

(1) Types of objective structures

The objective engineering structures are categorized into five groups. Each has different structural characteristics and liquefaction-induced failure modes. Therefore, mitigation techniques should be appropriately selected so as to prevent anticipated failure modes of the structures.

(2) Site conditions of objective structures

An appropriate mitigation techniques should also be selected considering the existence of open space at the site, and the existence of adjacent sensitive structures which do not allow construction noise or vibration. From this viewpoint, the existing techniques cannot always be applied to various site conditions, especially to remediation of existing structure foundation.

Based on such arrangement new (or recently proposed) techniques were incorporated in the table, which might be suitable for the remediation with appropriate research and development efforts. The underlined techniques in the table are those now studied under the R&D programme mentioned above.

3.2 Joint Studies on Countermeasures against Liquefaction between PWRI and Private Sector (Part II)

In order to enhance and support the R&D project mentioned above, Joint Studies between PWRI and seventeen private firms started in 1992. Five study groups in the Joint Studies are organized as shown in Table 4.

The main target of Group I is to develop new measures which has been of little practical use. Groups II to IV examine the applicability of several measures to the respective structures and aim at establishing reliable design methods. The objective structures are embankment structures including highway embankments and river dykes for Group II, linear subsurface structures including

semi-buried road, common utility duct and sewage pipes for Group III, and flat-type subsurface structures including sewage treatment pond and underground parking lot for Group IV. Group V is studying techniques suitable for improvement of wide area ground. Its primary target is a reclaimed land in which it might be more efficient to improve gross foundation than to improve foundation of each structure within the area. The possible technique presently in consideration is dewatering.

Both the R&D Programme and the Joint Studies have just started their research activities. It is expected that they coordinate with each other and efficiently proceed the activities through exchange of fruitful information.

3.3 Illustration of Several New Techniques

(1) Compaction by expansive lime pile

This technique is one of the densification methods. The most significant difference from the existing densification techniques is that this technique does not generate unallowable noise and vibration during its works. In this technique, a casing shaft with a spiral fringe is driven in the foundation, and a mixture of sand, hard burnt lime and two other chemical additives, is poured in the casing. Then the casing is gradually pulled out, and the mixed soil is placed in the depth. The lime absorbs the water in the surrounding soil and the mixed soil hardens and expands. Then it is expected that the expanded soil displaces and compacts the surrounding soils, and also increases the lateral earth pressure at rest. The detail of this technique can be seen elsewhere(26).

(2) Sheet/cylinder pile with drain

New type sheet or steel piles are used in this technique, where drain channels which has holes with mesh are attached to conventional piles. It is expected that the lateral deformation resistance of the soil surrounding the piles are retained by dissipating excess porewater pressure in sand deposits during earthquakes. The effectiveness of the technique was shown experimentally in (27).

(3) Permeation grouting

Most of previous grouting methods were used as tentative soil improvement to ensure the soil to retain by itself during excavation, or as auxiliary work at marginal sites where large equipment for soil improvement cannot be placed. In order to ensure the durability of the improved soil against dissolving, the permeation grouting technique under the study uses as injection material particulate grouts, including micro-fine cement, fly ash and clay. It is intended that the particulate grouts permeate to a distance without clogging the pores, under relatively low injection pressure.

4. RECENT APPLICATION OF MITIGATION TECHNIQUES TO SITES

Although there have been many experiences of conventional mitigation techniques in use in Japan, it is rather recent that they were applied to public works including highway embankments, river dykes and common utility ducts. Some of the projects were conducted by the Local Construction Bureaus, MOC on their own initiatives, and others were adopted by them with the technical advice of PWRI.

Following are examples of mitigation techniques recently applied to sites.

(1) Deep mixing method to a river dyke

In 1991, the deep mixing method was applied to improve the foundation of a part of a river dyke. It is located near the mouth of the Shinano River and suffered severe damage due to liquefaction of foundation soil at the Niigata Earthquake, 1964.

In order to minimize the improvement volume of soil grid-type improvement was adopted as shown in Fig.2, and the design was performed according to the design method developed by the Joint Study mentioned in 2.3 and published in (25).

(2) Cut-off sheet piles with drain to a common utility duct

A common utility duct which installs electricity transmission line, telecommunication line, gas and water pipelines was constructed in the subsurface of Ohgishima Reclaimed Island, which was constructed at off-Kawasaki sea shore about two decades ago. As shown in Fig.3, cut-off sheet pile method was adopted as a countermeasure against liquefaction of the soil. The sheet piles with drain was introduced in one section as a trial practice, where the effect of drain was not considered in the design. Instead, accelerometers and porewater pressure transducers were embedded in the soil at two adjacent locations where conventional sheet piles and piles with drain were used respectively, in order to verify the effect of drain during earthquakes.

5. SUMMARY AND CONCLUSIONS

This paper reviewed briefly the previous research activities on liquefaction of sandy ground which had been conducted at Public Works Research Institute, and presented the current research activities focusing on mitigation works against liquefaction. Among the latter, the two research projects are comprehensive and deal with various types of mitigation techniques, which are existing, newly developed or proposed. Although existing mitigation techniques have been adopted at many sites, they are still empirical. A review of them indicated that further research is required to understand their physical mechanisms and to rationalize their design methods, and that new mitigation techniques are required to meet various site conditions, especially in case of improving the soil beneath existing structures.

It is expected that the results of the research projects will lead to more widespread acceptance of the mitigation techniques against liquefaction and to more reliable economical use of them.

REFERENCES

1) Kuribayashi,E. and Tatsuoka,F. : Brief Review on Liquefaction during Earthquakes in Japan, 7th UJNR Joint Meeting, 1975.
2) Ohkubo,T., et al. : Damage Features of Civil Engineering Structures due to the Miyagi-Ken-Oki Earthquake of 1978, 11th UJNR Joint Meeting, 1979.
3) Iwasaki,T., et al. : Report on Damages to Civil Engineering Structures due to the Nihonkai-Chubu Earthquake of 1983, 16th UJNR Joint Meeting, 1984.
4) Sasaki,Y., et al. : Damage by the Chiba-ken Toho-Oki Earthquake, 21st UJNR Joint Meeting, 1989.
5) Sawada,K. and Koga,Y. : Vibration Test on Settlement of Submerged Sand Layer, 7th UJNR Joint Meeting, 1975.
6) Koseki,J. and Koga,Y. : Uplift of Semi Buried Structures in Liquefiable Sands during Earthquake, 8th Japan Earthquake Engineering Symposium, 1990.
7) Koga,Y. and Koseki,J. : Seismic Stability of Structures Buried in Liquefiable Sands against Uplift, 3rd UJNR Workshop of T/C "H" (International Workshop on Remedial Treatment of Potentially Liquefiable Soils), 1991.
8) Koga,Y. and Koseki,J. : Dynamic Centrifugal Model Tests of Embankments on Liquefiable Grounds, 22nd UJNR Joint Meeting, 1990.
9) Koga,Y. et al. : Dynamic Centrifugal Model Tests of Embankments on Liquefiable Grounds (part 2), 24th UJNR Joint Meeting, 1992.
10) Koga,Y. and Matsuo,O. : Shaking Table Tests of Embankments Resting on Liquefiable Sandy Ground, Soils & Foundations, Vol.30, No.4, pp.162-174, 1990.
11) Koga,Y., et al. : Influence of Embankments on the Liquefaction of Ground, 23rd UJNR Joint Meeting, 1991.
12) Sasaki,Y., et al. : Experimental Study on Lateral Flow of Ground Induced by Soil Liquefaction, 22nd UJNR Joint Meeting, 1990.
13) Tokida,K., et al. : Study on Prediction of Lateral Ground Flow by Soil Liquefaction and Its Influence on Piles, 24th UJNR Joint Meeting, 1992.
14) Ohashi,M., et al. : A Practical Procedure for Assessing Earthquake-Induced Liquefaction of Sandy Deposits, 10th UJNR Joint Meeting, 1978.
15) Ishihara,K. and Koga,Y. : Case Studies of Liquefaction in the 1964 Niigata Earthquake, Soils & Foundations, Vol.21, No.3, pp.35-52, 1981.
16) Iwasaki,T., et al. : Estimation Procedures of Liquefaction Potential and its Application to Earthquake Resistant Design, 14th UJNR Joint Meeting, 1982.
17) Sasaki,Y., et al. : In-Situ Test for Assessing Liquefaction Potential Using Vibratory Cone Penetrometer, 17th UJNR Joint Meeting, 1985.
18) Koga,Y., et al. : Field Investigation of Seismically Damaged Sites by Use of Vibratory Cone Penetrometer, 18th UJNR Joint Meeting, 1986.
19) Sasaki,Y. and Taniguchi, E. : Shaking Table Tests on the Countermeasure to Liquefaction by Gravel Drains, 13th UJNR Joint Meeting, 1981.
20) Sasaki,Y. and Taniguchi,E. : Gravel Drains as a Countermeasure to Liquefaction of the Ground, 14th UJNR Joint Meeting, 1982.
21) Sasaki,Y. and Taniguchi,E. : Shaking Table Tests on Gravel Drains to Prevent Liquefaction of Sand Deposits, Soils & Foundations, Vol.22, No.3, pp.1-14, 1982.
22) Sasaki,Y. and Matsuo,O. : Shaking Table Tests on the Remedial Measures to Improve Seismic Stability of Embankments, 15th UJNR Joint Meeting, 1983.
23) Koga,Y. et al. : Experimental Study on the Deep Mixing Method as a Countermeasure against Liquefaction, 2nd UJNR Workshop of T/C "H", 1988.
24) Koga,Y. et al. : Applicability of the Dynamic Centrifuge Model Test Method in Developing Countermeasure against Soil Liquefaction, Proc. International Conference Centrifuge 1991, pp.431-438, 1991.
25) PWRI, et al. : Joint Study Report on Countermeasures against Liquefaction (Part VI), PWRI, 1992 (in Japanese).
26) Mitsunari,T., et al. : A Use of Super Lime Pile Method for Improvement of Saturated Loose Sandy Soils, Proc. of ISOPE-93, International Society of Offshore and Polar Engineers, 1993 (to be published).
27) Kita,H., et al. : Experimental study on countermeasures for liquefaction by steel piles with drain, Proc. 10th WCEE, 1992.

Table 1 Overview of Research Subjects on "R&D Program on EDPUD"

I. Development of Assessment Techniques of Seismic Resistance of Soft Ground	
	1. Estimation of Ground Motion Intensity
	2. Evaluation of Seismic Resistance of Soft Ground
	3. Seismic Hazard Zoning of Soft Ground
II. Development of Seismic Hazard Mitigation Techniques for Soft Ground	
	1. Seismic Hazard Mitigation Techniques for Post-construction Sites
	2. Seismic Hazard Mitigation Techniques for Pre-construction Sites
III. Development of Seismic Design Techniques of Engineering Structures	
	1. Seismic Design Methods of New Type Structures
	2. Seismic Safety Inspection Methods of Pile Foundation

Table 2 Existing Countermeasures Against Liquefaction

Mechanism of Improvement	Techniques
Densification	Compaction ·Sand Compaction Piles ·Rod Compaction Piles ·Vibro Flotation ·Dynamic Compaction ·Vibro Tamper ·Others
Drainage, Dissipation of Excess Pore Water Pressure	·Gravel Drain ·Artificial Drain
Physical Modification	Replacement
	Pre-Soil Mixing
Chemical Modification (Hardening)	Deep Soil Mixing
	Grouting
	Compaction Grouting
Lowering of Saturation Ratio, Increase of Effective Stress	Dewatering
	Interception
Confinement of Shear Deformation	Cut-off Sheet Piles
	Subsurface Concrete Wall
	Deep Soil Mixing Wall

Table 3 Applicability of Existing and New Countermeasures Against Liquefaction

Objective structures	Typical damage modes due to liquefaction	Pre-construction site :without any restriction on site conditions		Pre-construction site adjacent to buildings :with restriction on vibration, noise and displacement		Post-construction site :improvement beneath the structures is generally difficult	
		Existing techniques	New techniques	Existing techniques	New techniques	Existing techniques	New techniques
Reclaimed land, Wide fill area	Settlement, Sliding, Lateral flow	• Use of well grained soil • Compaction	• Pre-soil mixing with cement	———	———	• Surcharge	• Dewatering
Pile foundation (of bridges, buildings)	Lateral displacement, Failure of piles or superstructures	• Use of larger foundation • Compaction	• Steel pile with drain	• Low-level vibration pile driving	• Deep mixing method	• Additional piles	• Permeation grouting • Steel pile with drain
Direct foundation	Settlement, Lateral displacement, Tilting, Failure of superstructure	• Compaction • Use of pile foundation	———	• Deep mixing method • Compaction by low-level vibration • Low-level vibration pile driving	• Compaction by expansive lime pile	• Cutt-off wall	• Permeation grouting • Compaction grouting
Underground structures • linear structures (e.g. common utility duct) • flat-type structures (e.g. underground parking lot)	Uplift, Lateral displacement, Failure of structure or joint	• Compaction • Pile foundation • Flexible joint • Cut-off wall • Gravel drain	• Wick drain, • Sheet pile with drain	• Cut-off wall formation by deep mixing method • Gravel drain • Low-level vibration pile driving • Flexible joint	• Sheet pile with drain • Compaction by expansive lime pile	• Cutt-off wall • Gravel drain • Cut-off wall formation by deep mixing method	• Permeation grouting • Sheet pile with drain
Embankment (e.g. river dyke, road)	Settlement, Sliding, Lateral flow	• Compaction		• Press-in sheet pile • Deep mixing method	• Compaction by expansive lime pile	• Cutt-off wall • Cut-off wall formation by deep mixing method	• Permeation grouting

(Remark) Countermeasures with underline are those to be studied in the ongoing research project.

Table 4 Structure of the Joint Study with Private Sector

Study Groups	Objectives
Group I	: Development of Countermeasures against Liquefaction
Application to	
Group II	: Embankment Structures
Group III	: Linear Subsurface Structures
Group IV	: Flat-type Subsurface Structures
Group V	: Wide Area Ground

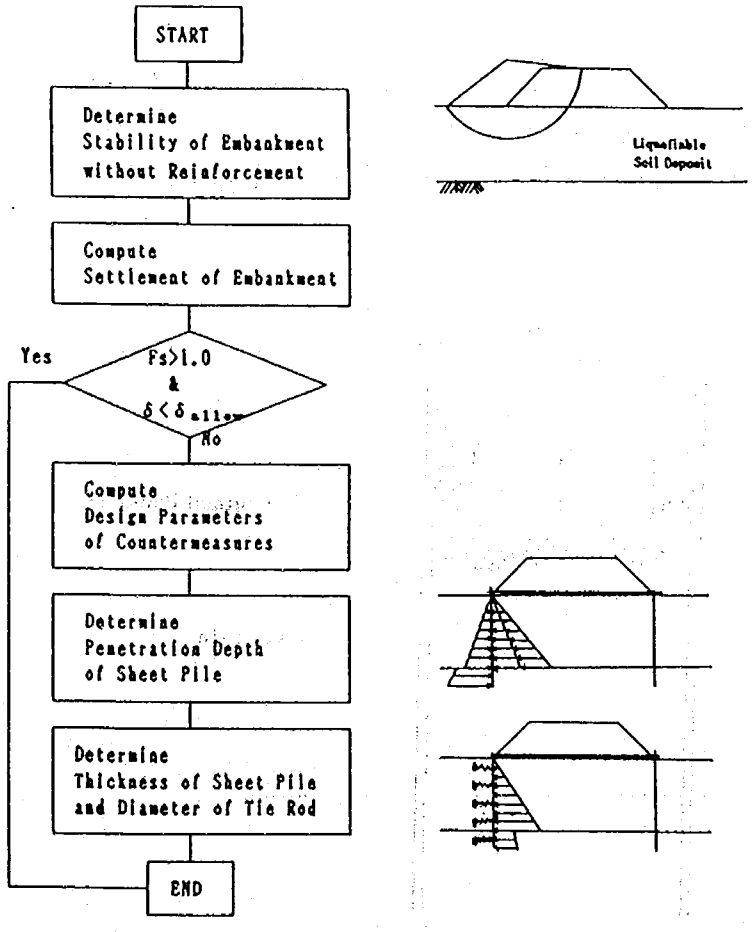


Fig.1 Design Flow Chart of Cut-off Sheet Pile Method when applied to Embankment

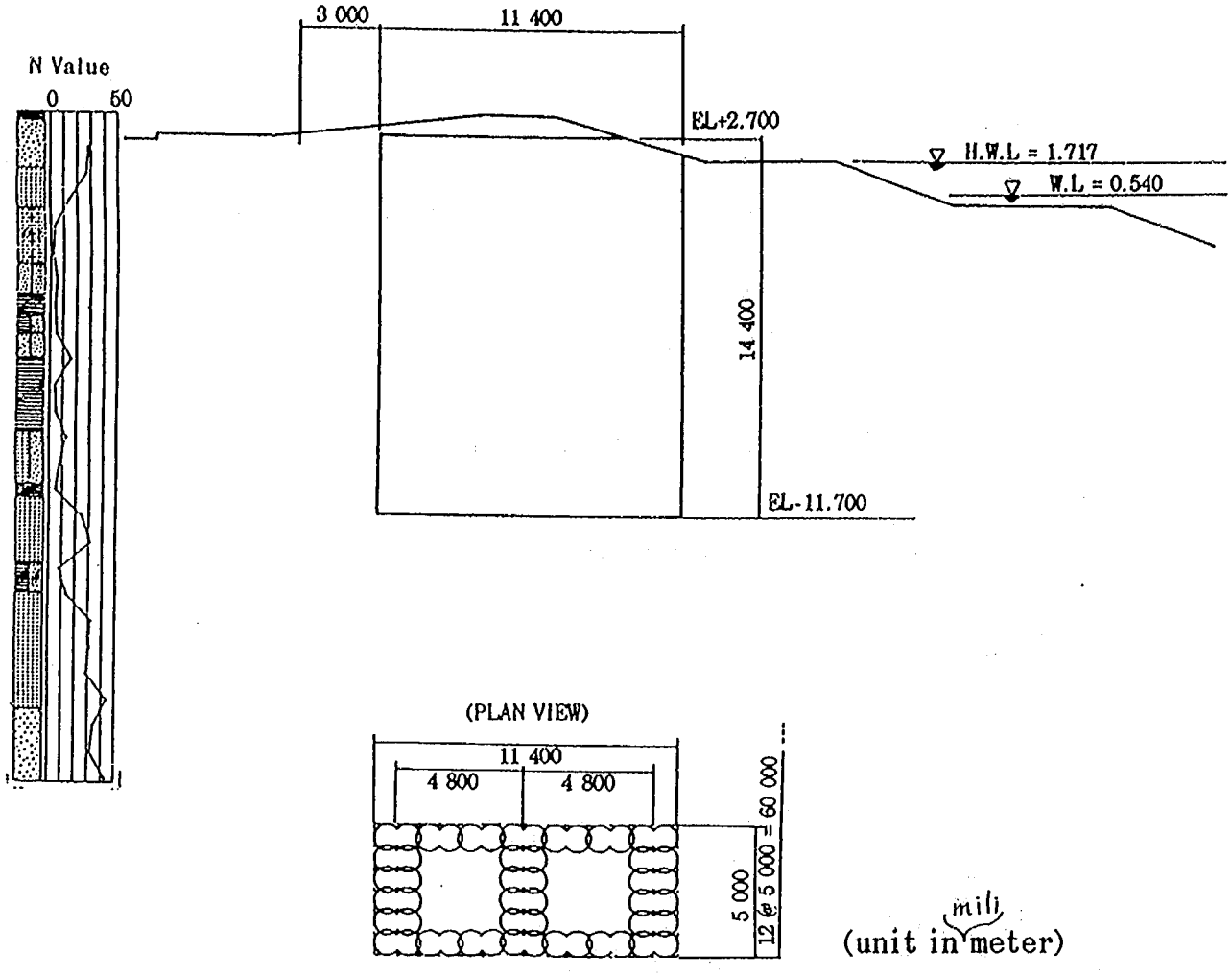


Fig.2 Deep Mixing Method applied to
Left Side Levee of Shinano River, Niigata

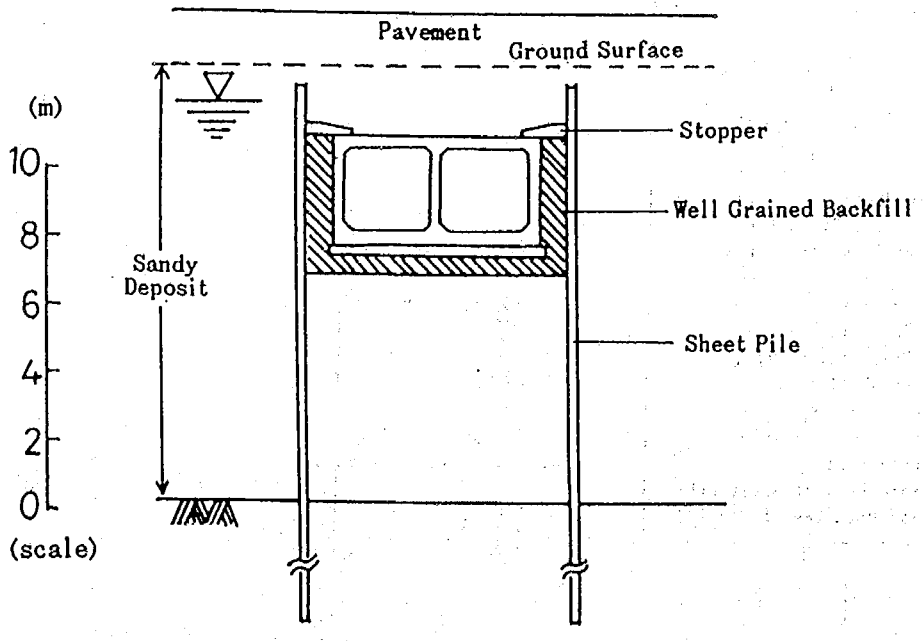


Fig.3 Sheet Piles (with Drain) applied to
Common Utility Duct,
Ohgishima Reclaimed Land, Off-Kawasaki

Liquefaction Susceptibility of Fine-Grained Soils

by

J. P. Koester*
A. G. Franklin*

ABSTRACT

Most past efforts in evaluating liquefaction potential of soils has been directed to clean or silty sands. Around 1980 evidence began to accumulate that both coarser and finer-grained soils have undergone liquefaction when shaken by strong earthquakes. Largely as a result of the publication of data from PRC earthquakes by Wang (1979) and Japanese field experience by Tokimatsu and Yoshimi (1983), fine-grained, low- to medium-plasticity soils are no longer assumed to be non-liquefiable, and it is generally accepted that they must be accounted for in seismic stability evaluations. Field data on past occurrences (and non-occurrences) of liquefaction during earthquakes provide valuable guidance on the probable limits of grain-size and plasticity ranges of soils that may be susceptible to liquefaction during earthquakes. In applying this experience, the effects of varying test methods should be taken into account. A study was done to compare liquid limit values obtained by the PRC standard test method with those obtained by the US standard method. It showed that indicated values by the PRC method are about 4.4 points higher.

KEYWORDS: earthquake; soil; liquefaction.

1. INTRODUCTION

Liquefaction potential of various types of soils has received a great deal of research attention in the geotechnical earthquake engineering community over the last three decades. Dramatic occurrences of liquefaction (defined in a broad sense as the total, or near total, loss of shear strength of a saturated soil in response to cyclic loading) in recently deposited, saturated, fine, generally uniformly-graded sands beneath the Japanese city of Niigata and in surrounding areas accompanied ground shaking during the June 16, 1964 earthquake (Japan National Committee on Earthquake Engineering, 1965). The pervasive destruction caused by loss of bearing capacity and lateral spreading in Niigata motivated extensive studies to develop method of assessing the potential for liquefaction of similar soils throughout Japan and worldwide.

Research emphasis was primarily on cyclic strength of clean sands until reports surfaced (notably Wang, W. S., 1979, 1981) in the geotechnical engineering literature of liquefaction in other types of soils, including "somewhat cohesive" soils that liquefied as a result of strong earthquakes in the People's Republic of China (PRC). Other recent research findings and re-evaluation of historical data have also shown that liquefaction occurrence is not restricted to clean, uniform, loose deposits of saturated sand. A wide range of soil gradations and consistencies, including gravels, may be associated with severe shear strength loss on undrained cyclic loading. The effects of gradation and other engineering properties on soils containing fines has not been extensively researched.

2. FACTORS AFFECTING LIQUEFACTION POTENTIAL

A monograph on the subject of ground motions and soil liquefaction by Seed and Idriss (1982) provides a comprehensive list of the factors most often studied as influential on cyclic strength of soils, divided into three categories: (1) *soil properties*, including dynamic shear modulus and damping characteristics, unit weight, grain

* U.S. Army Engineer Waterways Experiment Station, Vicksburg, Mississippi 39180

characteristics, relative density (of granular, cohesionless soils), and soil structure (fabric); (2) *environmental factors*, such as mode of soil deposition, seismic history (prior shear straining), geologic history (aging), coefficient of lateral earth pressure at rest, K_o, overconsolidation ratio, depth to water table, and effective confining pressure; and (3) *earthquake characteristics*, specifically ground shaking intensity and duration.

The effects of such soil particle characteristics as angularity, sphericity, and surface texture on liquefaction potential of granular soils are not well understood; shape and texture considerations for silt and clay particles are not discernable except by their collective influence on soil behavior through consistency effects. The grain size distribution of a soil deposit is important to consider from both its direct implications on the capacity for soil to densify and in recognition of membrane penetration compliance effects on undrained laboratory test results. Finn (1981) comments that the influence of grain size as observed by Lee and Fitton (1969) (specifically that increased mean grain size was associated with increased liquefaction resistance) may in fact be a result of the latter. Mean grain size may, in view of this consideration, be an unconservative delimiter of liquefaction susceptibility.

Tsuchida (1970) observed typical gradation curves associated with soils that liquefied during several previous Japanese earthquakes and those exhibiting similar response in laboratory shake table tests. The boundaries he proposed to distinguish liquefiable and non-liquefiable deposits under a variety of conditions are shown in Figure 1. According to this figure, fine-grained soils (silts and finer) whose mean grain size is at least 0.02 millimeters are potentially vulnerable to liquefaction under some unspecified level of shaking. In fact, Figure 1 indicates liquefaction potential in soils which are entirely composed of silt-and-finer particles (that is, particles smaller than 0.074 millimeters, which would pass through the openings in a US Standard No. 200 sieve).

Ishihara, et al. (1980) contend that the Tsuchida (1970) chart is based on performance of soils of alluvial, diluvial, or volcanic origin, and that the boundaries of "most liquefiable soils" may be unconservative with regard to soils containing a still higher fraction of low plasticity clay-size particles such as are present in mine tailings. Tokimatsu and Yoshimi (1983) compiled field performance data from Japanese earthquakes and correlated observed ground behavior with gradation characteristics; soils containing up to 60 percent by weight silt-size particles and 12 percent clay-size particles (that is, particles smaller than 0.005 millimeters) exhibited moderate-to-extensive liquefaction (in terms of affected land area). Their compilation did not catalog soil index properties, for example, Atterberg limits, which have been shown to influence cyclic strength (see, e.g., Ishihara et al, 1980, and Ishihara, 1991).

A few studies have attempted to isolate the influence of plasticity on liquefaction susceptibility. Ishihara (1991) carried out a cyclic triaxial test program to compare plasticity index to resistance against development of 5% double amplitude cyclic axial strain in 20 cycles, in specimens prepared using various types of clay and mine tailings. The results indicated a 75% increase in cyclic strength as the plasticity index increased from 5 to 40. Fines contents were not reported to support the data, but the implications are that: (1) cyclic strength is not influenced by PI in soils with PI less than about 5; and (2) cyclic strength increases strongly with PI beyond a value of 5.

3. FIELD OCCURRENCE OF EARTHQUAKE-INDUCED LIQUEFACTION IN FINE-GRAINED SOILS

3.1 People's Republic of China

Chang (1987, 1990) reports from preliminary inquiries into the PRC data base on earthquake response that active faulting is prevalent in northeastern China (PRC), resulting in frequent strong ground shaking. Four major earthquakes of magnitude 6 or greater struck the region during the period from 1967 to 1976: the 1967

Hejian earthquake (225 Km southwest of Tangshan, M=7.4); the 1975 Haicheng earthquake (400 Km east of Tangshan, M=7.3); the 1976 Horinger earthquake (550 Km west of Tangshan, M=6.3); and the 1976 Tangshan earthquake (M= 7.8) that was followed by a magnitude 7.1 aftershock.

A strong earthquake (Richter magnitude 7.8) struck the city of Tangshan on July 29, 1976 (Wang, 1979); the magnitude 7.1 aftershock occurred later that same day. The effects of liquefaction were observed throughout the region (areas totaling over 20,000 km^2) southeast of Tangshan city (Figure 2). The recent alluvial fan of the Ruan river experienced the most severe liquefaction (Figure 3); damage and other surface manifestations of liquefaction became progressively less intense toward older deltaic courses. Young alluvial deposits near Loutian and Luanan experienced the most severe liquefaction effects, at an epicentral distance between 60 km and 80 km. Chang (1987) gives a detailed account of ground failure phenomena associated with this earthquake.

Wang (W. S., 1979, 1981) catalogued the occurrence of liquefaction in soils containing fines and soils exhibiting cohesion during both the 1975 Haicheng and 1976 Tangshan events, developing charts showing grain size distribution, plasticity, and liquid limits versus water content in soils that were associated with field evidences of liquefaction. Wang found that soils which liquefied had clay content less than 15%, liquid limit less than 35%, and natural water contents greater than 90 percent of their liquid limit (by the PRC test method). These values have become known informally in the United States as the "Chinese criteria."

3.2 Japan

Japan has experienced strong earthquakes and related damage more often during the past century than has perhaps any other area in the world. Japanese geotechnical researchers have been afforded an unpleasant wealth of field occurrence data against which to evaluate the seismic response of soil deposits, with concomitant experience in liquefaction investigation. Iwasaki (1985) expanded the compilation of Kuribayashi, Tatsuoka, and Yoshida (1974) and Kuribayashi and Tatsuoka (1975) of earthquakes causing liquefaction in Japan to 50 such events, beginning with the 1872 Hamada earthquake and ending with the Nihonkai Chubu (Japan Sea) earthquake of 1983. Dramatic occurrences of liquefaction and the damaging effects thereof were observed in saturated deposits of fine, uniformly graded sands in the Japanese city of Niigata and surrounding areas resulting from ground shaking during the June 16, 1964 earthquake (Japan National Committee on Earthquake Engineering, 1965). This event, more than perhaps any other, was responsible for the rapid development of methods for assessing the potential for liquefaction of similar soils throughout Japan and worldwide.

Koester and Tsuchida (1988) reviewed laboratory and field studies by Japanese researchers that assess the influence of variations in grain size distribution and soil index properties on liquefaction potential of fine-grained soils. The geomorphology of Japan has produced predominantly uniform sand deposits that typically contain less silt and clay than those found in the peneplain and coastal regions of the PRC (Chang, 1987). Tohno and Shamato (1986) studied deposit stratigraphy and soil properties observed at liquefied and non-liquefied sites within the wide geographic region affected by the 1983 Nihonkai-Chubu (Japan Sea) earthquake and support this observation. Mine tailings and other man-made fine-grained deposits such as some compacted sand fills, however, often do contain appreciable fine grain size fractions and are important to the industry and economy of Japan. The cyclic strength of these soils has been extensively studied to develop seismic design criteria (Ishihara, et al. 1980, and Tatsuoka, Ochi, and Fujii, 1984).

3.3 United States

The upstream flow slide failure of the Lower San Fernando Dam consequent to the 1971 San Fernando earthquake has been attributed to

liquefaction of "very silty" hydraulic fill sands (Marcuson, Hynes, and Franklin, 1990, Seed, et al. 1989, Vasquez-Herrera and Dobry, 1989, and Castro, Keller and Boynton, 1989). The low residual strength and associated deformability of these low-plasticity fine-grained soils has captured the attention of earthquake engineers in the United States. This interest is perhaps due to the growing realization that a potentially pervasive hazard to critical structures (e.g., dams, locks, power generation facilities) built on alluvial soils was given insufficient attention as concern was directed to liquefaction susceptibility of loose, clean, uniform sands.

Liquefaction in soils containing silty or clayey fines is likely, though not well documented, to have occurred as a result of the 1886 Charleston, South Carolina earthquake and other events indicated by liquefaction recurrence features in the same area (Obermeier, et al. 1985) due to similarities between the peneplain deposits of the PRC and the piedmont geomorphology in the southeastern region of the US. The material now infilling liquefaction features is not necessarily representative of the soil transported upward during the release of excess pore water pressures. It is believed that the presence of clay-bearing layers confined the source stratum sands and contributed to the development of the sand boils in this area (Obermeier, et al. 1989).

Alternating layers of silty or clayey, or both, glaciomarine sand deposits have been judged to have liquefied during several northeastern US earthquakes (e.g., Tuttle and Seeber, 1989). Clayey glacial soils abound throughout the region and are often sedimented with fine sands.

The New Madrid, Missouri seismic zone (Figure 4) experienced a series of very strong earthquakes during the period December 1811 to January 1812. Wesnousky, Schweig, and Pezzopane (1989) detail a comprehensive evaluation of geologic evidence of extensive liquefaction and massive sliding of loessial bluff soils throughout the Mississippi embayment as a result of these events. Clay layers are again implicated in the impedance of excess pore pressure drainage; the investigators stop short of defining gradational and index properties of the liquefied materials due to disturbance of the original content, but it is certain that clean, uniform sand deposits are too sparsely distributed in the Mississippi River floodplain to account for the profusion of liquefaction evidence.

3.4 USSR

Ishihara, et al. (1990) report that an earthquake of magnitude 5.5 shook the Dushanbe region of the Tadjikistan Republic in the (then) USSR on January 23, 1989, whereupon wetted, low-plasticity silts (80% silt, 15% clay, liquid limit = 30, plastic limit = 20, natural water content = 40%) slumped and flowed as far as 2 km. The back-calculated residual strengths of these soils ranged from 2 to 15 kPa (42 to 313 psf). Loessial soil deposits of similar characteristics, ranging in thickness from 3 to 100 feet, are widespread over the Mississippi River valley of the central United States.

4. MEASUREMENT OF PLASTICITY

While the results of Wang's observations on liquefaction occurrence in the PRC have become widely known in the United States, it is less well known that the methods of measuring plasticity indices, which differ between countries, can significantly affect the values obtained. The senior author studied this question in order to determine how the results of Chinese experience should be applied to evaluation of liquefaction susceptibility of soils in the United States.

Soil engineers in the United States generally follow the procedures prescribed by the American Society for Testing and Materials (ASTM, 1991) for the performance of laboratory Atterberg limits tests. The ASTM procedure (ASTM D4318-84) specifies that only the fraction of a soil passing the US Standard No. 40 sieve (i.e., soil finer than 0.425 mm) be tested and uses the controlled percussion technique introduced by Atterberg and later refined by Casagrande (1932, 1958). Test specimens are prepared in essentially the same

manner as prescribed by the US Army Corps of Engineers (1970).

The liquid limit of a soil is defined by ASTM as the water content at which a V-shaped groove cut to completely divide a soil specimen placed in the hemispherical brass bowl of the Casagrande device flows together along 1/2 inch (13 mm) of the bottom of the groove when the cup has been dropped 25 times from a height of 10 mm. The percussion test is most often used worldwide, has likely produced most liquid limit data published to date, and is considered applicable to a wide range of soil types.

Silty soils, or those containing large percentages of fine sand, are difficult to properly groove for the test and exhibit wetted surfaces as the hemispherical bowl is dropped onto the hard base of the device prescribed by the ASTM Standard. The wetted surface of the test soil tends to flow while the overall water content of the specimen is yet lower than the correct liquid limit. The soil specimen may also slide along the bowl surface rather than flow as a plastic. Casagrande (1958) conceded that his liquid limit device was a dynamic test, and that the difficulties posed by silty soils might be avoided by the use of either a direct shear test or some sort of static penetration test. Sherwood and Ryley (1970) found that the use of a laboratory cone penetrometer test for liquid limit of silty or sandy soils indeed avoided grooving and sliding problems; striking excess soil to level the top of a silty or sandy specimen in the test container still wetted its surface in many cases.

In several countries, determination of liquid limit by means of a fall-cone test is preferred. The first such test, to the authors' knowledge, was introduced in 1915 by the Geotechnical Commission of the Swedish State Railways. Others have been adopted or recommended in France, India, the United Kingdom, the United States, and the countries of the former communist bloc. Test procedures and apparatus vary somewhat; for descriptions see Hansbo (1957), Karlsson (1961), Laboratoire Central des Ponts et Chaussees (1966), Sowers, Vesic, and Grandolfi (1960), Uppal and Aggarwal (1958), British Standards Institution (1975), Vasilev (1949), Stefanov (1958), Bozinovic (1958), Matschak and Rietschel (1965). Comparisons of liquid limits determined by these methods with those by the US standard method were made by Wasti (1986) and Wasti and Bezerci (1986), and presented by Koester (1992 b).

In the PRC, both liquid and plastic limits are determined using a laboratory fall cone test, in which a 76-gram, 30 degree apex angle cone is released to fall from a position in which its vertex is just touching the surface of the soil sample (Figure 5). PRC Soil Testing Standard SD128-007-84 defines the liquid limit as the water content corresponding to 17 mm penetration of the cone in five seconds (Ministry of Water and Electric Power Conservancy, People's Republic of China, 1989). The PRC Standard requires that liquid limit tests be performed on fine-grained soils with particle size finer than 0.500 mm. At least three separate batches of soil are mixed to water contents that are expected to produce penetrations of 4-5 mm, 9-10 mm, and 16-18 mm, respectively. Depth of penetration in 5 seconds is plotted against water content on a logarithmic plot, from which the liquid limit is picked. The plastic limit is defined as the water content that would produce 2 mm penetration in 5 seconds, and is obtained by extrapolation of the plot; no actual tests are attempted at water contents around the plastic limit.

Plasticity index is therefore determined using a single test procedure. The PRC standard procedure may be unique in this regard; other proponents of the fall-cone technique for liquid limit measurement use methods similar to that prescribed by ASTM to measure plastic limit (i.e., rolling moist soil on a flat surface with the fingers to determine the water content at which one-eighth inch diameter rods so formed exhibit a general tendency to crumble).

To examine the effect of the PRC test method, a series of tests was performed on twenty-seven soils, including both natural fine-grained soils and artificial mixtures of fine sand, low-plasticity silt, and plastic clay (Koester,

1992a,b). Tests were performed using the US standard procedure and a simulation of the PRC test using a Wykeham-Farrance fall-cone apparatus, with a 30 degree cone modified to have 76 grams mass.

All tested soils passed the US No. 40 sieve (i.e., they were finer than 0.425 mm), as specified by US and British testing standards. The PRC standard procedure calls for soils finer than 0.500 mm; no tests were actually performed to evaluate the differences in measured liquid or plastic limits resulting from inclusion of soil particles passing a 0.500 mm sieve and retained on a 0.425 sieve. Larger particles are non-plastic, thus their presence would be expected to lower the plasticity of the test specimens.

Figure 6 is a summary plot of liquid limit comparisons for all soil types tested. The regression equation obtained for a linear best fit of the data was

$$w_{L(PRC)} = 0.955\ w_{L(US)} + 4.41 \qquad (1)$$

The percussion ("Corps" method) and PRC fall-cone liquid limits would be essentially equivalent over the range of values encompassed by the study if the percussion limits were increased by about 4.4 (percent water content). While this offset seems small for large values of liquid limit, it can be significant in the range of plasticities important in liquefaction consideration.

Plastic limit values measured using the US standard rod-rolling method (Corps of Engineers values) are compared to those determined graphically by PRC procedures in Figure 7. The data suggest no systematic offset, but are quite scattered, more toward the lower values.

5. CONCLUSION

As the data base on field occurrence continues to grow, it is becoming increasingly evident that liquefaction may be induced by earthquakes in soils containing particles passing the US Standard No. 200 sieve, (i.e., particles finer than 74 micrometers). Largely as a result of the publication of data from PRC earthquakes by Wang (1979) and Japanese field experience by Tokimatsu and Yoshimi (1983), fine-grained, low- to medium-plasticity soils are no longer assumed to be non-liquefiable, and it is generally accepted that they must be accounted for in seismic stability evaluations.

Field data on past occurrences (and non-occurrences) of liquefaction during earthquakes provide valuable guidance on the probable limits of grain-size and plasticity ranges of soils that may be susceptible to liquefaction during earthquakes. In applying this experience, the effects of varying test methods should be taken into account. In applying the so-called "Chinese criteria," in particular, it should be noted that the test method used in the PRC produces liquid limit values about 4.4 percentage points above those obtained by US standard test methods.

6. ACKNOWLEDGEMENTS

The data presented and analyses described, unless otherwise noted, were obtained from research conducted by the US Army Engineer Waterways Experiment Station under funding provided by the US Army Corps of Engineers. Permission was granted by the Chief of Engineers to publish this information.

7. REFERENCES

American Society for Testing and Materials. (1991). "Standard test method for liquid limit, plastic limit, and plasticity index of soils." Designation D4318-84, In *Annual Book of ASTM Standards*, Section 4 - Construction, Volume 04.08 - Soil and Rock; Dimension Stone; Geosynthetics (revised annually).

Bozinovic, D. (1958). "Versuch der Bestimmung der Fliessgrenze nach der Methode des Balancierkegels." Samml. Arb. montangeoligischen Fak. Univ. Belgrad (*"Test for determining the flow limit by the balancing cone method." Collected works of the geologic faculty of the University of Belgrade*), Vol. 6, 173-175.

British Standards Institution (1975). *Methods of test for soils for civil engineering purposes.* British Standard BS 1377:1975. London: BSI.

Casagrande, A. (1932). "Research on the Atterberg limits of soils." *US Bureau of Public Roads*, 13(8), 121-130, 136.

Casagrande, A. (1958). "Notes on the design of the liquid limit device." Harvard Soil Mechanics Series No. 57, Cambridge, Massachusetts.

Castro, G., Keller, T. O., and Boynton, S. S. (1989). "Re-evaluation of the Lower San Fernando Dam - Report 1: An investigation of the February 9, 1971 slide," Contract Report GL-89-2, US Army Engineer Waterways Experiment Station, Vicksburg, Mississippi.

Chang, N. Y. (1987). "Liquefaction susceptibility of fine grained soils -- preliminary study report," Miscellaneous Paper GL-87-24, US Army Engineer Waterways Experiment Station, Vicksburg, Mississippi.

Chang, N. Y. (1990). "Influence of fines content and plasticity on earthquake-induced soil liquefaction," Contract Report to US Army Engineer Waterways Experiment Station, Vicksburg, Mississippi, Contract No. DACW3988-C-0078.

Finn, W. D. L. (1981). "Liquefaction potential: developments since 1976," *Proceedings*, International Conference on Recent Advances in Geotechnical Earthquake Engineering and Soil Dynamics, St. Louis, Vol, II, 655-682.

Hansbo, S. (1957). "A new approach to the determination of the shear strength of clay by the fall-cone test." In *Proceedings of the National Swedish Geotechnical Institute*, No. 14, Stockholm.

Ishihara, K. (1991). "Evaluation of liquefaction potential and consequent deformations in sand fills," Draft paper submitted to WorldPort LA seismic workshop, San Pedro, California, 21-23 March, Vol. 3: Geotechnical/structural sessions.

Ishihara, K, Okusa, S., Oyagi, N., and Ischuk, A. (1990). "Liquefaction-induced flow slide in the collapsible loess deposit in Soviet Tajik," Soils and Foundations, 30(4), 73-89

Ishihara, K., Troncoso, J., Kawase, Y., and Takahashi, Y. (1980). "Cyclic strength characteristics of tailings materials", *Soils and Foundations*, Japanese Society of Soil Mechanics and Foundation Engineering, Tokyo, 20(4), 127-142.

Iwasaki, T. (1985). "Soil liquefaction studies in Japan - State of the art", Public Works Research Institute Technical Memorandum No. 2239, Ministry of Construction, Tsukuba, Japan, August.

Japan National Committee on Earthquake Engineering. (1965). "Niigata earthquake of 1964," *Proceedings*, Third World Conference on Earthquake Engineering, Vol. III, New Zealand National Committee on Earthquake Engineering, February, S-78 to S-108.

Karlsson, R. (1961). "Suggested improvements in the liquid limit test, with reference to flow properties of remoulded clays." In *Proceedings of the Fifth International Conference of Soil Mechanics and Foundation Engineering*, Vol. 1, 171-184, Paris.

Koester, J. P. (1992a). "The influence of test procedure on correlation of Atterberg limits with liquefaction in fine-grained soils," *Geotechnical Testing Journal*, ASTM, GTODJ, Vol. 15, No. 4, December, pp. 352-361.

Koester, Joseph Patrick. (1992b). "Cyclic strength and pore pressure generation characteristics of fine-grained soils," Ph.D.

thesis, University of Colorado.

Koester, J. P. and Tsuchida, T. (1988). "Earthquake-induced liquefaction of fine-grained soils: some considerations from Japanese research", Miscellaneous Paper GL-88-34, U.S. Army Engineer Waterways Experiment Station, Vicksburg, MS.

Kuribayashi, E., and Tatsuoka, F. (1975). "Brief review of liquefaction during earthquakes in Japan," *Soils and Foundations*, Japanese Society of Soil Mechanics and Foundation Engineering, 15(4), 81-92.

Kuribayashi, E., Tatsuoka, F., and Yoshida, S. (1974). "History of earthquake-induced soil liquefaction in Japan," *Bulletin of the Public Works Research Institute*, Ministry of Construction, Tsukuba, Japan, Vol. 30 (In Japanese), Vol. 31 (In English, January 1977).

Laboratoire Central des Ponts et Chaussées. (1966). "Determination rapide des limites d'Atterberg à l'aide d'un pénétromètre et d'un picnomètre d'air." (*"Determination of Atterberg limits using a penetrometer and an air pycnometer"*) Dossier SGR/149, Paris.

Lee, K. L., and Fitton, J. A. (1969). "Factors affecting the cyclic loading strength of soil," *Vibration Effects of Earthquakes on Soils and Foundations, ASTM STP 450*, American Society for Testing and Materials, Philadelphia, Pennsylvania, pp. 71-95.

Marcuson, W. F. III, Hynes, M. E., and Franklin, A. G. (1990). "Evaluation and use of residual strength in seismic safety analysis of embankments," *Earthquake Spectra*, 6(3), 529-572.

Matschak, H. and Rietschel, A. (1965). "Vereinfachte Fliessgrenzenbestimmungen an bindigen Bodenarten für ingenieurgeologisch-bodenmechanische Untersuchungen." Z. angew. Geol. (*"Simplified flow limit determinations on cohesive soil types for engineering-geologic/soil mechanics investigations." Journal of Applied Geology*), Vol. 3, 135-139.

Ministry of Water and Electric Power Conservancy, People's Republic of China. (1989). *Soil Testing Manual, Designation SD128-007-84* (in Chinese, translated by Zhixian You, University of Colorado at Denver).

Obermeier, S. F., Gohn, G. S., Weems, R. E., Gelinas, R. L., and Rubin, M. (1985). "Geologic evidence for recurrent moderate to large earthquakes near Charleston, South Carolina," *Science*, Vol. 227, 408-411.

Obermeier, S. F., Weems, R. E., Jacobson, R. B., and Gohn, G. S. (1989). "Liquefaction evidence for repeated holocene earthquakes in the coastal region of South Carolina," *Earthquake Hazards and the Design of Constructed Facilities in the Eastern United States*, Annals of the New York Academy of Sciences, Vol. 558, eds. Jacob, K. H. and Turkstra, C. J., 183-195.

Seed, H. B., and Idriss, I. M. (1982). *Ground motions and soil liquefaction during earthquakes*, Engineering Monographs on Earthquake Criteria, Structural Design, and Strong-Motion Records, Earthquake Engineering Research Institute, Berkeley, California.

Seed, H. B., Seed, R. B., Harder, L. F., and Jong, H. L. (1989). "Re-evaluation of the Lower San Fernando Dam - Report 2: Examination of the post-earthquake slide of February 9, 1971," Contract Report GL-89-2, US Army Engineer Waterways Experiment Station, Vicksburg, Mississippi.

Sherwood, P. T. and Ryley, M. D. (1970). "An investigation of a cone penetrometer metered for the determination of the liquid limit." *Géotechnique*, 20(2), 203-208.

Sowers, G. G., Vesic, A., and Grandolfi, M. (1960). "Penetration tests for liquid limit." American Society for Testing and Materials STP 254, 216-226.

Stefanov, G. (1958). "Discussion on liquid limit." *Proceedings of the 4th International Conference on Soil Mechanics*, Vol. 3, 97.

Tatsuoka, F., Ochi, K., and Fujii, S. (1984). "Effect of sample preparation method on cyclic undrained strength of sand in triaxial and torsional shear tests," *Bulletin of Earthquake Resistant Structure Research Center*, University of Tokyo, No. 17, March, 29-62.

Tohno, I., and Shamato, Y. 1986. "Liquefaction damage to the ground during the 1983 Nihonkai-Chubu (Japan Sea) Earthquake in Aomori Prefecture, Tohoku, Japan," *Natural Disaster Science*, 8(1), 85-116.

Tokimatsu, K. and Yoshimi, Y. (1983). "Empirical correlation of soil liquefaction based on SPT N-value and fines content," *Soils and Foundations*, Japanese Society of Soil Mechanics and Foundation Engineering, 23(4), 56-74.

Tsuchida, H. (1970). "Prediction and countermeasure against liquefaction in sand deposits," Abstract of the Seminar of the Port and Harbour Research Institute, Ministry of Transport, Yokosuka, Japan, 3.1-3.33 (In Japanese).

Tuttle, M. P., and Seeber, L. (1989). "Earthquake-induced liquefaction in the northeastern United States: historical effects and geological constraints," *Earthquake Hazards and the Design of Constructed Facilities in the Eastern United States*, Annals of the New York Academy of Sciences, Vol. 558, eds. Jacob, K. H. and Turkstra, C. J., 196-207.

Uppal, H. L. and Aggarwal, H. R. (1958). "A new method of determining the liquid limit of soils." Road Research Paper No. 19, New Delhi.

US Army Corps of Engineers. (1970). "Laboratory soils testing." *Engineer Manual 1110-2-1906*, Updated through 20 August 1986, Washington, DC.

Vasilev, A. M. (1949). "Basic principles of the methods and techniques of laboratory determination of physical soil properties." *Pochvovedenie*, Vol. 11, 675-676.

Vasquez-Herrera, A., and Dobry, R. (1989). "Re-evaluation of the Lower San Fernando Dam - Report 3: The behavior of undrained contractive sand and its effect on seismic liquefaction flow failures of earth structures," Contract Report GL-89-2, US Army Engineer Waterways Experiment Station, Vicksburg, Mississippi.

Wang, W. S. (1979). "Some findings in soil liquefaction," Research Institute of Water Conservancy and Hydroelectric Power, Beijing, China.

Wang, W. S. (1981). "Foundation problems in aseismatic design of hydraulic structures." In *Proceedings of the Joint US - PRC Microzonation Workshop*, 11-16 September, Harbin, PRC.

Wasti, Y. (1986). "Liquid and plastic limits as determined from the fall cone and Casagrande methods." unpublished report to the Soil Mechanics Division, US Army Engineer Waterways Experiment Station, Vicksburg, Miss.

Wasti, Y. and Bezerci, M. H. (1986). "Determination of the consistency limits of soils by the fall cone test." *Canadian Geotechnical Journal*, Vol. 23, 241-246.

Wesnousky, S. G., Schweig, E. S., and Pezzopane, S. K. (1989). "Extent and character of soil liquefaction during the 1811-1812- New Madrid earthquakes," *Earthquake Hazards and the Design of Constructed Facilities in the Eastern United States*, Annals of the New York Academy of Sciences, Vol. 558, eds. Jacob, K. H. and Turkstra, C. J., 208-216.

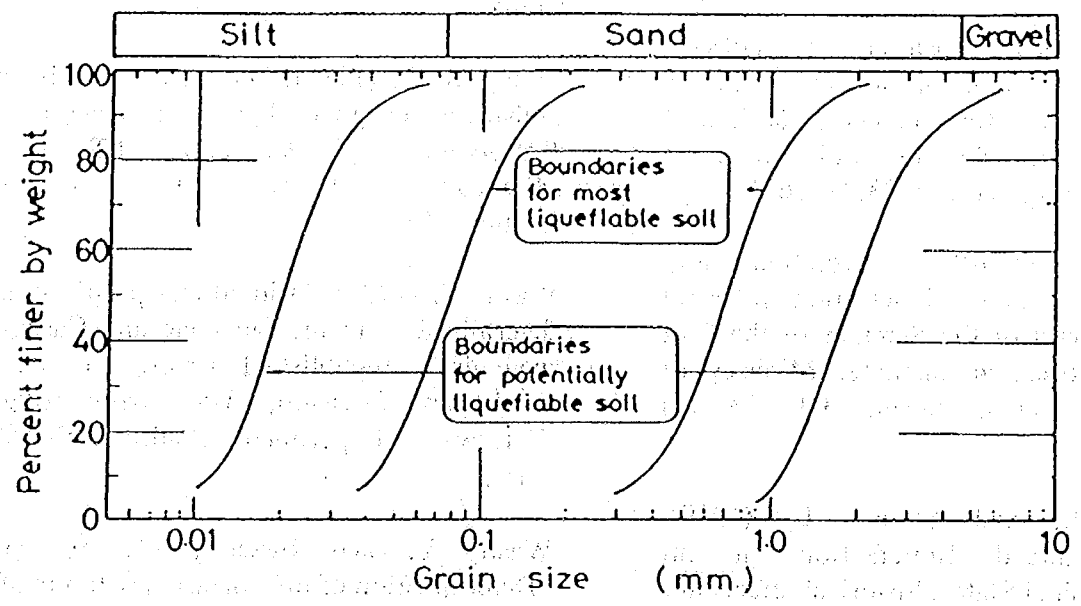


Figure 1. Gradations of liquefiable soils (Tsuchida, 1970)

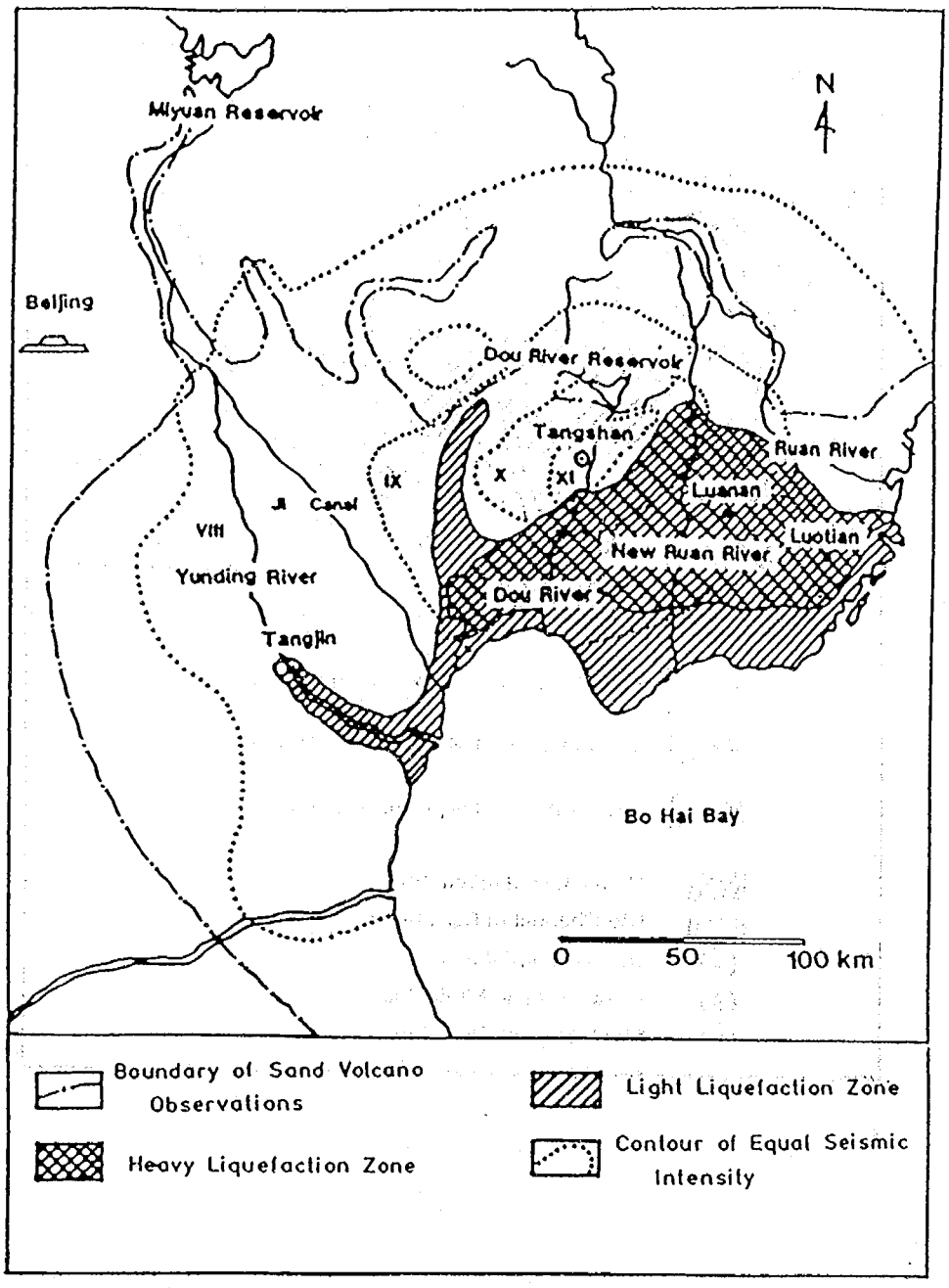


Figure 2. Liquefaction distribution, Tangshan earthquake of 1976 (Chang, 1987)

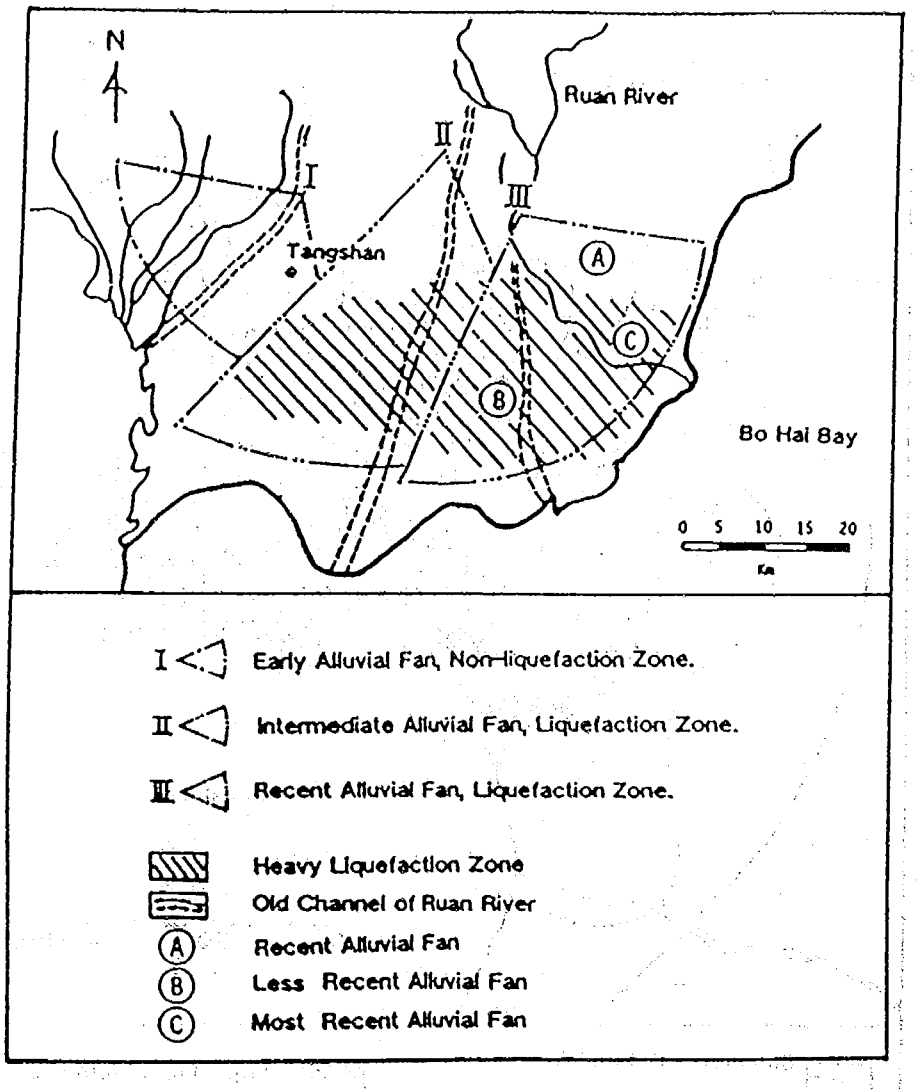


Figure 3. Migration and deposits of the Ruan River, PRC (Chang, 1987)

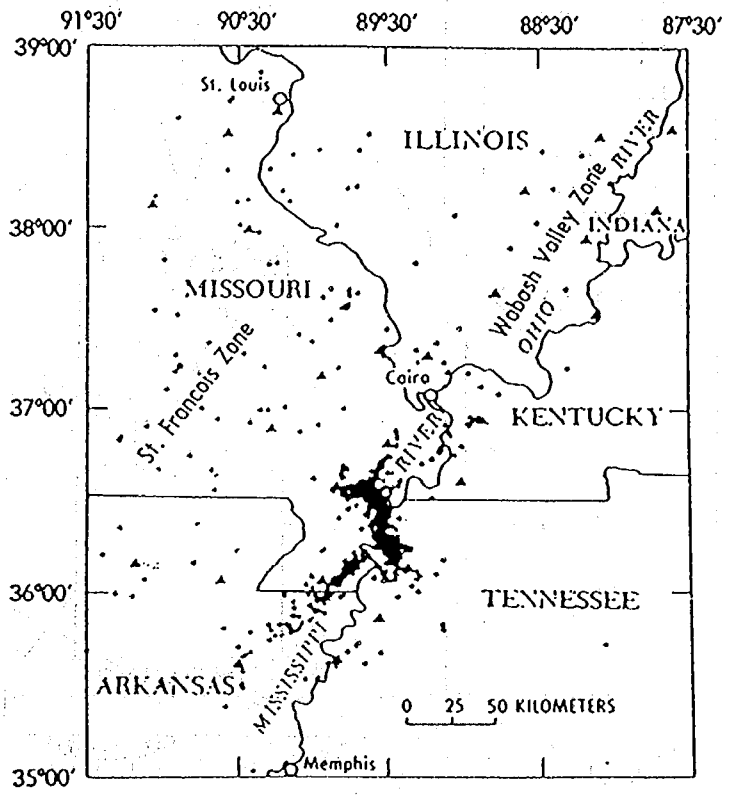
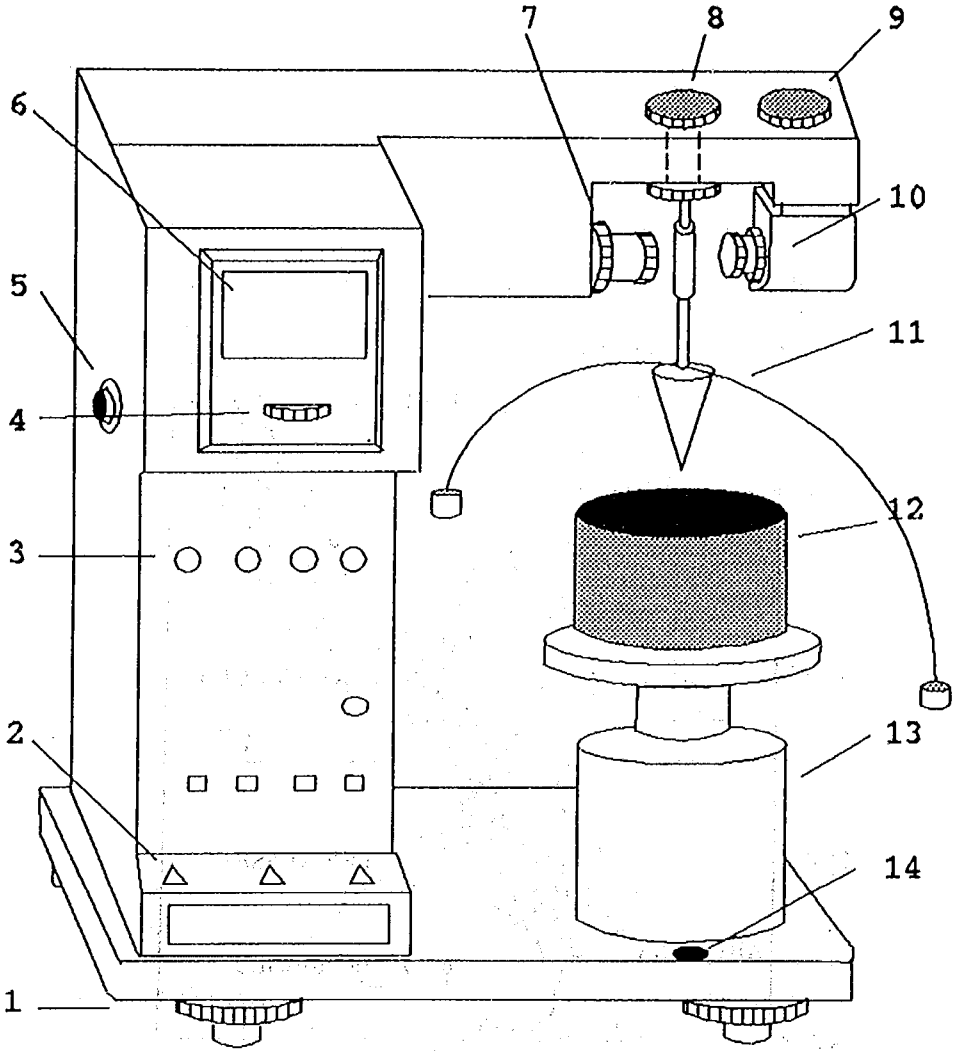


Figure 4. Earthquake epicenters along the New Madrid Seismic Zone (Wesnousky, Schweig and Pezzopane, 1989, after Stauder, 1982)



1--Level adjust
2--Control switch
3--Indicator light
4--Zero adjust
5--Reflector adjust
6--Screen
7--Objective lens adjust
8--Electromagnet
9--Light adjust
10--Light
11--Penetrometer
12--Soil specimen
13--Base
14--Leveling bulb

Figure 5. Balance cone penetrometer (after People's Republic of China soils testing standard SD128-007-84)

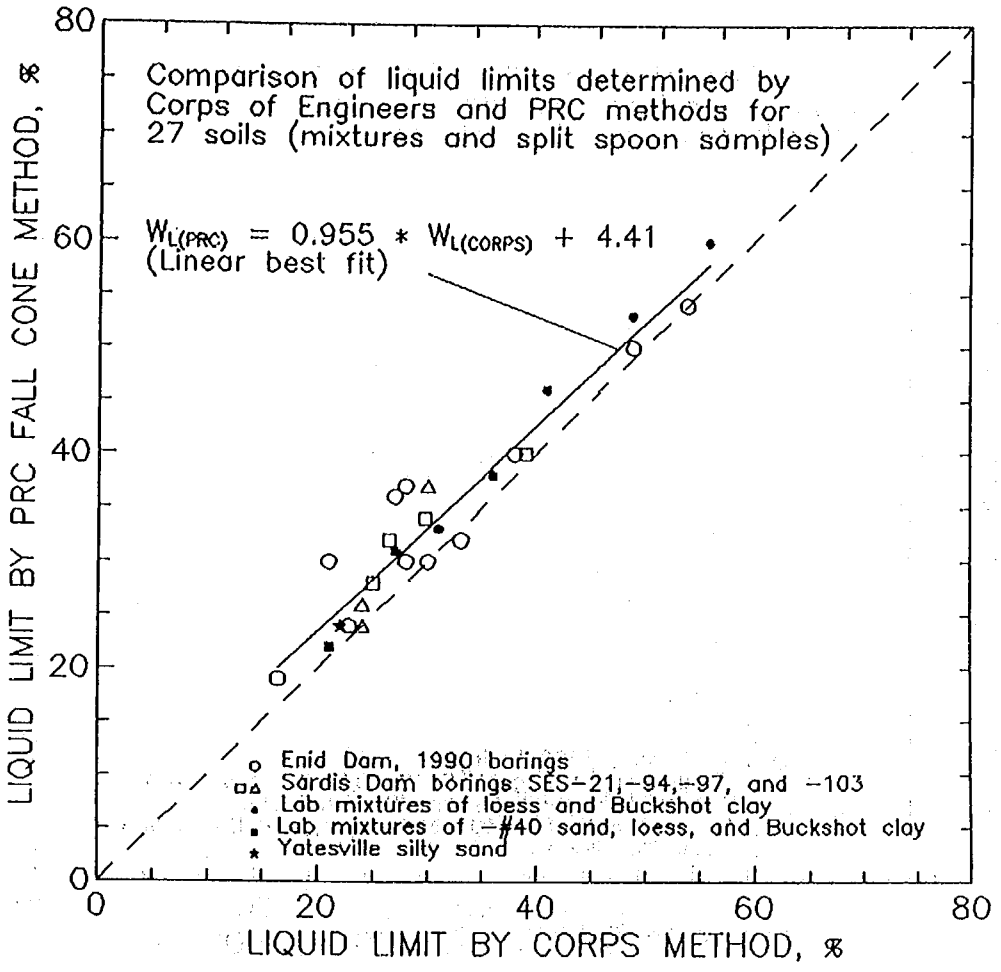


Figure 6. Liquid limit comparisons for all soil types tested

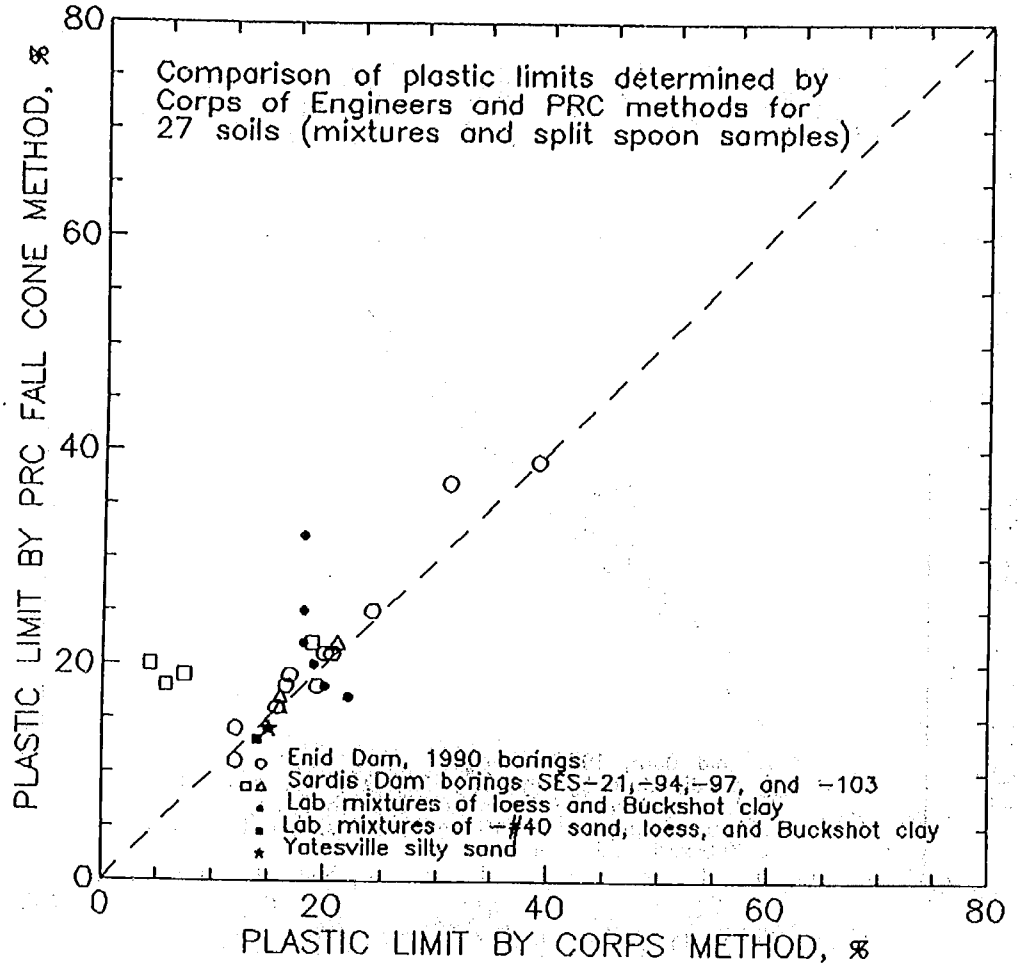


Figure 7. Plastic limit comparisons for all soil types tested

Application of Soil Liquefaction Potential to Seismic Design of Civil Engineering Structures in Japan

by

Ken-ichi Tokida[1] and Yoshio Ninomiya[2]

ABSTRACT

A number of studies and investigations on soil liquefaction have been conducted since the 1964 Niigata Earthquake in Japan. As a result of them, several simplified procedures to estimate liquefaction potential during an earthquake have been proposed, and applied in the specifications and standards for the seismic design of civil engineering structures.

This paper shows the state of practical methods for estimating soil liquefaction potential and for applying their effects to seismic design methods in the specifications of typical civil engineering structures in Japan.

KEY WORDS : Soil Liquefaction, Liquefaction Potential, Seismic Design

1. FOREWORD

A number of methods for estimating soil liquefaction potential have been studied, proposed and applied in Japan. For example, the methods can be classified into three groups as shown in **Table 1.1**: The first is empirical methods based on the liquefaction phenomena experienced in past earthquakes. The second is methods based on dynamic mechanism of soil liquefaction. The third is methods applying and combining these two methods. The details of each method will be introduced in the following sections.

2.SEISMIC DESIGN SPECIFICATIONS

2.1 Highway Bridge [1)2)]

Liquefaction potential has been considered in seismic design specifications for highway bridges since the first specification for seismic design of highway bridges was proposed in Japan, 1971. After that, the specification has been modified two times: in 1980 and 1990.

A simplified procedure has been proposed for estimating liquefaction potential and application of the effects induced by soil liquefaction against bridge foundations as follows:

1. Selection of Sandy Soil Layers Examined for Liquefaction Potential

The sandy layers with the following conditions should be considered to be liquefiable during earthquake and these liquefaction potential should

1)Director, Kanazawa Work Office,
Hokuriku Regional Construction Bureau,
Ministry of Construction .
2)Senior Research Engineer,
Ground Vibration Division,
Earthquake Disaster Prevention Department,
Public Works Research Institute,
MOC

be examined.

1)Saturated alluvial sandy layers

2)Layer's depth within 20 meter from ground surface

3)Ground water level within 10 meter from ground surface

4)D_{50} -values between 0.02 millimeter and 2.0 millimeter for grain size accumulation curve

2. Calculation of Liquefaction Potential Using Simplified Procedure

To judge whether sandy soil layers liquefy or not, a calculation of liquefaction potential should be made based on liquefaction resistance factor F_L defined by the following equation:

$$F_L = R/L \quad (2\text{-}1)$$

where F_L : Liquefaction resistance factor

R : Resistance of soil elements to dynamic loads, and

$$R=R_1+R_2+R_3 \quad (2\text{-}2)$$

$$R_1=0.00882\sqrt{N/(\sigma_v+0.7)} \quad (2\text{-}3)$$

$$R_2 = \begin{cases} 0.19 & (0.02\text{mm} \leqq D_{50} \leqq 0.05\text{mm}) \\ 0.0225\log_{10}(0.35/D_{50}) & (0.05\text{mm} < D_{50} \leqq 0.6\text{mm}) \\ -0.05 & (0.6\text{mm} < D_{50} \leqq 2.0\text{mm}) \end{cases} \quad (2\text{-}4)$$

$$R_3 = \begin{cases} 0.0 & (0\% \leqq F_c \leqq 40\%) \\ 0.004F_c-0.16 & (40\% < F_c \leqq 100\%) \end{cases} \quad (2\text{-}5)$$

L:Dynamic load to soil elements

$$L= r_d \cdot K_s \cdot (\sigma_v/\sigma_v') \quad (2\text{-}6)$$

$$r_d= 1.0-0.015 \cdot z \quad (2\text{-}7)$$

$$K_s=C_z \cdot C_G \cdot C_I \cdot Kso \quad (2\text{-}8)$$

R_1: Resistance based on relative density (see **Figure.2.1**)

R2: Resistance based on D50-values (see **Figure.2.2**)

R3: Resistance based on fines content (see **Figure.2.3**)

N : Blow count by standard penetration test

D_{50}: Mean grain size (mm)

F_c : Fines content (%)

Z : Depth from the actual ground surface(m)

K_s : Seismic coefficient for evaluating liquefaction

C_z : Seismic zone factor (see **Figure.2.4**)

C_G : Ground condition factor (see **Table 2.1**)

C_I : Importance factor (see **Table 2.2**)

K_{so}: Standard seismic coefficient (=0.15)

σ_v :Total overburden (kgf / cm^2)

σ_v': Effective overburden pressure at the static condition (kgf / cm^2)

Soil layers with liquefaction resistance factor F_L smaller than 1.0 are judged to liquefy during an earthquake. When detailed data of the soils are not obtained, the values of unit weight below and above ground water level, mean grain size and fines content of soils can be estimated roughly with soil classifications using **Table 2.3.**

3. Application of Liquefaction Potential

It is necessary to introduce the treatment of liquefiable layers judged by the former-mentioned simplified procedure for reasonable seismic design of structures. In the specifications of Highway Bridges, the bearing capacities for *liquefiable layers* should be either neglected or reduced by multiplying the original bearing capacities with the ratio of coefficient of subgrade reaction defined as the

reduction factor D_E specified as shown in **Table 2.4.** In the Specifications, the effects of liquefied layers at the depth of 10 to 20 meters are assumed to be smaller than that at the depth of 0 to 10 meters.

2.2 Common Utility Ducts [3)]

Check on Liquefaction and Uplift of Ducts.

Uplift of ducts induced by soil liquefaction should be considered for seismic design, because common utility ducts are light.

The flowchart to investigate the possibility of soil liquefaction and to check the stability of ducts caused by liquefaction is shown in **Figure 2.5.** First of all, layers needed to check liquefaction are judged with the same method as that of highway bridge.

If the ducts are predicted to be located in the liquefiable layers, a check on the stability of ducts for uplift should be made based on the equation (2-9) (refer to **Figure 2.6**)

$$F_S = \frac{W_S + W_B + Q_S + Q_B}{U_S + U_D} \qquad (2\text{-}9)$$

where, F_S is the safety factor for uplift, W_S is the weight of soils above the duct (tf /m), W_B is the body weight of duct (tf /m), Q_S is the shear resistance force (tf /m), Q_B is the friction resistance force at sides of the duct (tf /m), U_S is the uplift force by static water pressure on the base of the duct (tf /m) and U_D is the uplift force by excess pore water pressure on the base of the duct (tf /m).

The uplift force can be estimated by the equation (2-10) based on the excess pore water pressure.

$$U_D = \Delta u \cdot B = L_U \cdot \sigma_V' \cdot B \qquad (2\text{-}10)$$

where, B is the width of the duct (m), σ_V' is the effective overburden pressure at the depth of the base of duct (t /m^2), L_U is the excess pore water pressure ratio ($= \Delta u / \sigma_V'$) and Δu is the excess pore water pressure (t /m^2).

The excess pore water pressure ratio (L_U) can be estimated, as shown in **Figure 2.7,** with liquefaction resistance factor (F_L) indicated by the equation (2-1) mentioned in the Seismic Design Specifications of Highway Bridge.

2.3 Earth Structure/River Dikes

The circular arc analysis method is common to estimate the minimum safety factor for stability of river dike in Japan. In this method, a seismic coefficient and the excess pore water pressure are considered as the effects induced by earthquakes against stability of a river dike as shown in **Table 2.5 .** The seismic coefficient and excess pore water pressure are applied separately to calculate the minimum safety factor for seismic slide stability of a levee. In this paper, the former method will be called Kh-Method and the latter one called Δu-Method.

The concept of a circular arc analysis method can be shown in Figure 2.8 and the safety factor for sliding can be calculated by the following equations:

Static State:

$$F_{ss} = \frac{\Sigma \{ c \cdot l + (W - u_o \cdot b) \cos\alpha \cdot \tan\phi \}}{\Sigma (W \cdot \sin\alpha)} \qquad (2\text{-}11)$$

Seismic Analysis (Kh-Method):

$$F_{SE}(K_h) = \frac{\Sigma\{c \cdot l + \{(W - u_o \cdot b) \cdot \cos\alpha \cdot K_h \cdot W \cdot \sin\alpha\} \cdot \tan\phi\}}{\Sigma(W \cdot \sin\alpha + K_h \cdot W \cdot Y/R)} \quad (2\text{-}12)$$

Seismic Analysis (Δu -Method):

$$F_{SE}(\Delta u) = \frac{\Sigma\{c \cdot l + \{W \cdot (u_o + \Delta u) \cdot b\} \cos\alpha \cdot \tan\phi\}}{\Sigma(W \cdot \sin\alpha)} \quad (2\text{-}13)$$

where, F_{ss} is the safety factor for non-earthquakes, F_{SE} is the safety factor during earthquakes, c is the cohesion (tf /m^2), ϕ is the internal friction angle of soil, u_o is the initial pore water pressure (tf /m^2), Δu is excess pore water pressure (tf /m), α is the tilt angle of sliding surface, W is the total weight of sliced section (tf /m), K_h is the horizontal seismic coefficient, l is the length of the base of sliced section (m), b is the width of sliced section (m), R is the radius of sliding circle (m) and Y is the vertical distance between the gravity center of sliced section and the center of sliding circle (m).

Figure. 2.9 illustrates the method to estimate excess pore water pressure with use of FL-values calculated from boring data in situ.

3.FUTURE REMARKS

To judge whether sandy soil layers liquefy or not, the method to calculate liquefaction potential based on liquefaction resistance factor F_L is a valid method. However, simplified procedures to estimate Resistance of soil elements to dynamic loads, R and Dynamic load to soil elements, L shou'd be improved more reasonably in future. Furthermore, the relation between excess pore water pressure Δu and Liquefaction resistance factor, F_L should be considered more properly.

4.ACKNOWLEDGEMENTS

The authors wish to express their sincere gratitude to Mr.Takuo Azuma of P.W.R.I for his assistance to prepare this paper.

5.REFERENCE

1) Japan Road Association, "Specifications for Highway Bridges, Part V. Earthquake Resistant Design", February 1990 (in Japanese).

2) Iwasaki T., Kawashima K. and Hasegawa K., "New Seismic Design Specifications For Road Bridge in Japan", 22nd Joint Meeting of U.S.-Japan, Panel on Wind and Seismic Effects, UJNR Gaithersburg, Maryland, U.S. May 1990.

3) Japan Road Association,"Design Guideline for Common Utility Ducts (Proposal)", March, 1986 (in Japanese).

4) Taniguchi E., Koga Y. and Morishita T., "Method for Evaluating Safety Factor of Uplift of Underground Structure induced by Soil Liquefaction", 40th Annual Meeting of Japan Society of Civil Engineers, 1985 (in Japanese) .

Table 1.1 Typical Methods for Estimating Soil Liquefaction Potential

- 1. Empirical Method Based on Phenomena in Past Earthquakes (**Approach-1**)
  - 1)Maximum Epicentral Distance
  - 2)Ground Water Level / Depth of Layer
  - 3)Grain Size of Soils
  - 4)Geographical Condition
  - 5)Maximum Blow Count by Standard Penetration Test
- 2. Methods Based on Dynamic Mechanism of Liquefaction (**Approach-2**)
  - 6) Dynamic Resistance and Dynamic Load Against Soils (Ex. Liquefaction Resistance Factor : F_L)
  - 7) Pore Water Pressure and Effective Overburden Pressure
- 3. Method Applying / Combining Approach -1 and Approach -2 (**Approach-3**)
  - 8)Distribution of Liquefaction Resistance Factor (No.1) (Ex. Liquefaction Potential Index: P_L)
  - 9) Distribution of Liquefaction Resistance Factor (No.2) (Ex. Site Liquefaction Potential: I_{PL})

Table 2.1 Ground Condition Factor, CG [1)2)]

Ground Group	I	II	III
C_G	0.8	1.0	1.2

Table 2.2 Importance Factor, C_I [1)2)]

Group	C_I	Definition
1st class	1.0	Bridges on expressway (limited access highways), general national road and principal road. Important bridges on general prefectural road and municipal road.
2nd class	0.8	Other than the above

Table 2.3 Roughly Estimated Values of Unit Weight, Mean Grain Size and Fine Content of Soils [1)]

Soil Classification	Unit Weight blow Ground Water Level γ_{t1} (tf/m^3)	Unit Weight above Ground Water level γ_{t1} (tf/m^3)	Mean Grain Size D_{50}(mm)	Fines Contest FC(%)
Topsoil	1.7	1.5	0.02	80
Silt	1.75	1.55	0.025	75
Sandy Silt	1.8	1.6	0.04	65
Silty Fine Sand	1.8	1.6	0.07	50
Very Fine Sand	1.85	1.65	0.1	40
Fine Sand	1.95	1.75	0.15	30
Middle Sand	2.0	1.8	0.35	10
Coarse Sand	2.0	1.8	0.6	0
Gravel	2.1	1.9	2.0	0

Table 2.4 Reduction of Bearing Capacity of Ground According to Liquefaction Potential in the Specifications for Highway Bridge in Japan [1)]

F_L-Value	Depth of Layer Z (m)	Reduction Factor D_E
$F_L \leqq 0.6$	$0 \leqq Z \leqq 10$	0
	$10 < Z \leqq 20$	1/3
$0.6 < F_L \leqq 0.8$	$0 \leqq Z \leqq 10$	1/3
	$10 < Z \leqq 20$	2/3
$0.8 < F_L \leqq 1.0$	$0 \leqq Z \leqq 10$	2/3
	$10 < Z \leqq 20$	1

Table 2.5 Circular Arc Analysis Methods for Estimating the Seismic Slide Stability of Levee which are Common in Japan

Purpose of Estimation	Analytical Conditions
1. Stability against Inertia Load by Seismic Ground Motion (**K_h-Method**)	1) Seismic effect is considered as an inertia load. 2) Seismic cefficient should be estimated for an inertia load. 3) Only horizontal load is considered generally. 4)Minimum safety factor (Fsl) for sliding of levee is calculated.
2. Stability Against Pore Water Pressure Induced by Soil Liquefaction (Δu-Method)	1) Seismic effect is considered as excess pore water pressure induced by soil liquefaction. 2) Excess pore water pressure should be estimated properly. 3) Only horizontal load ia considered generally. 4) Minimum safety factor (F_{S2}) for sliding of levee is calculated.

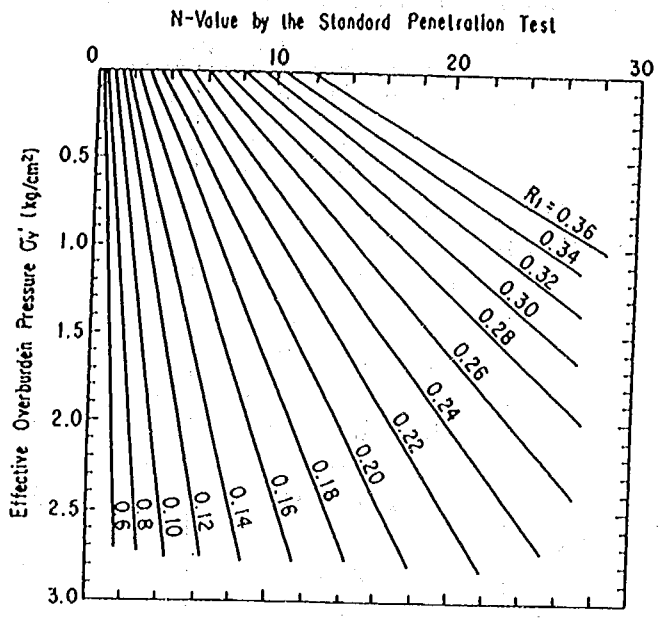


Fig.2.1 R_1-Value

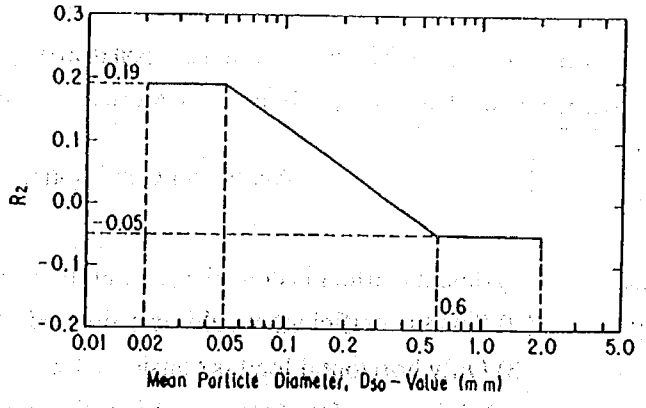


Fig.2.2 R_2-Value

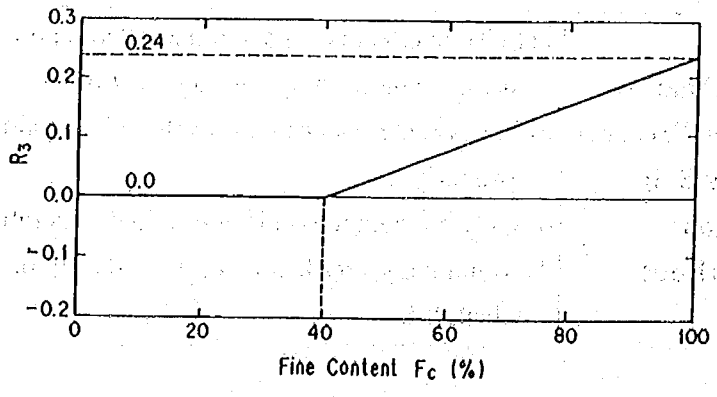


Fig.2.3 R_3-Value

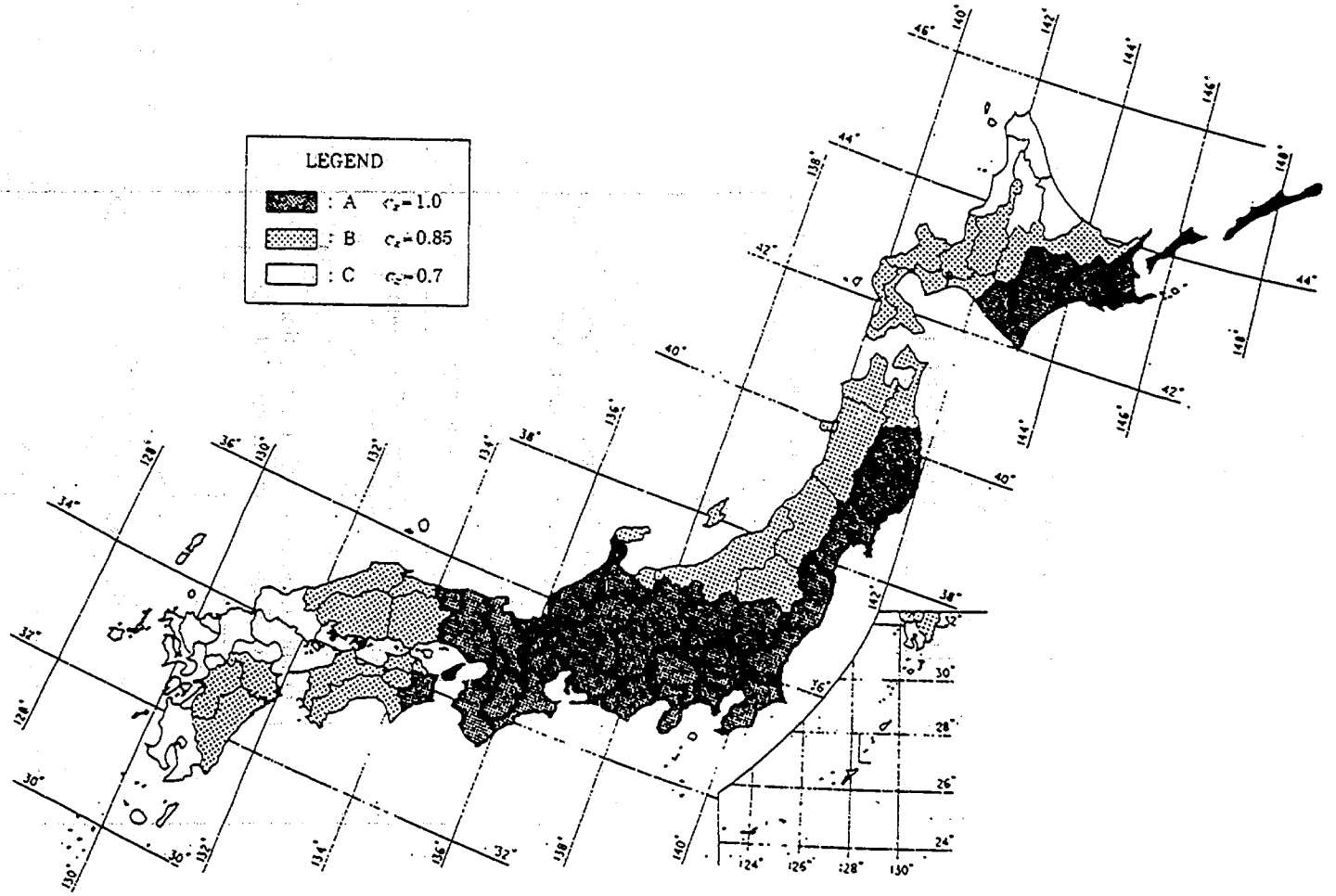


Fig.2.4 Seismic Zoning Map and Modification Coefficient, Cz

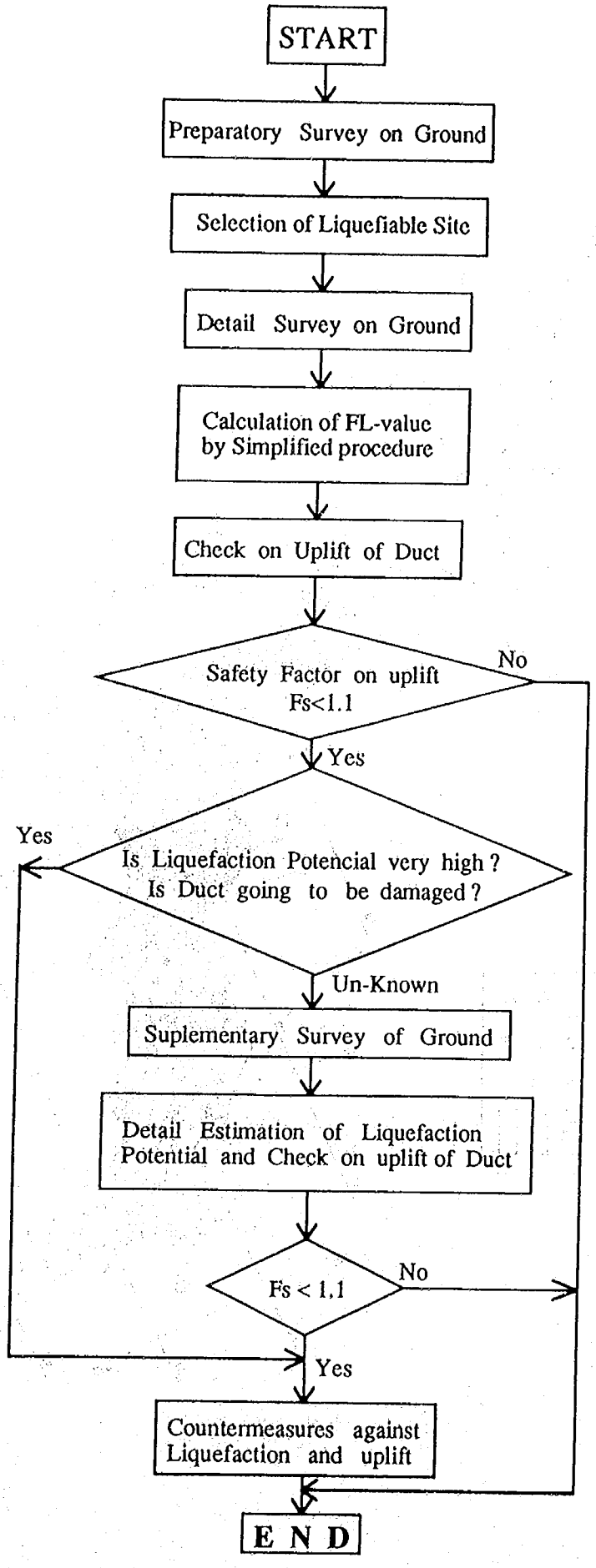


Fig.2.5 Flowchart for Uplift of Common Utility Duct

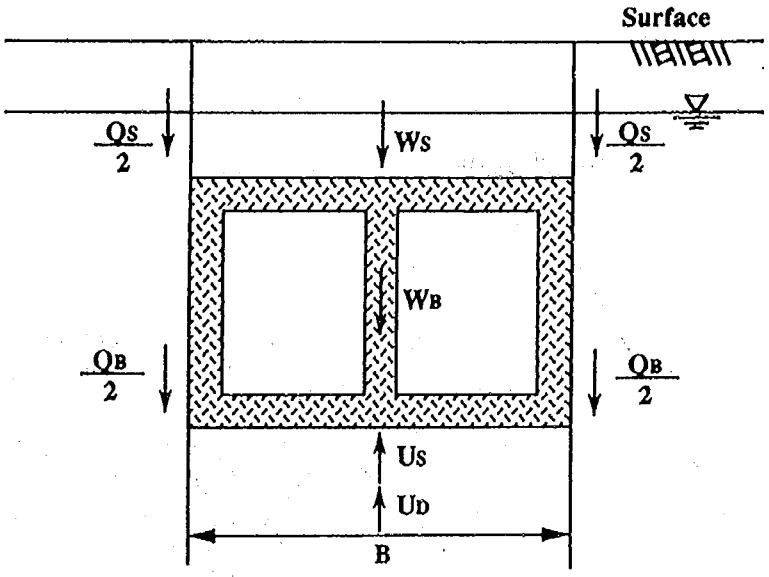


Fig 2.6 Design Force and Resistance Related to Common Utility for Checking Uplift

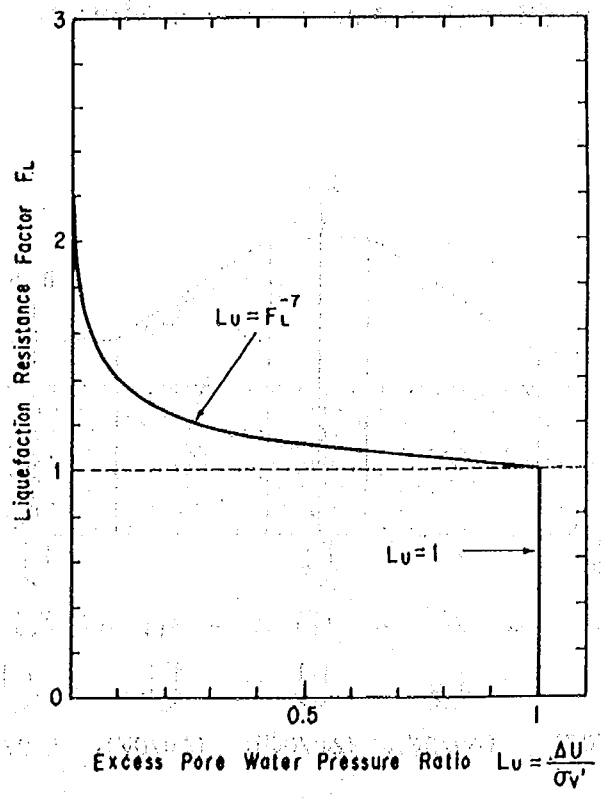


Fig 2.7 Relation between FL-value and excess pore water pressure Ratio for Design of Common Utility Duct

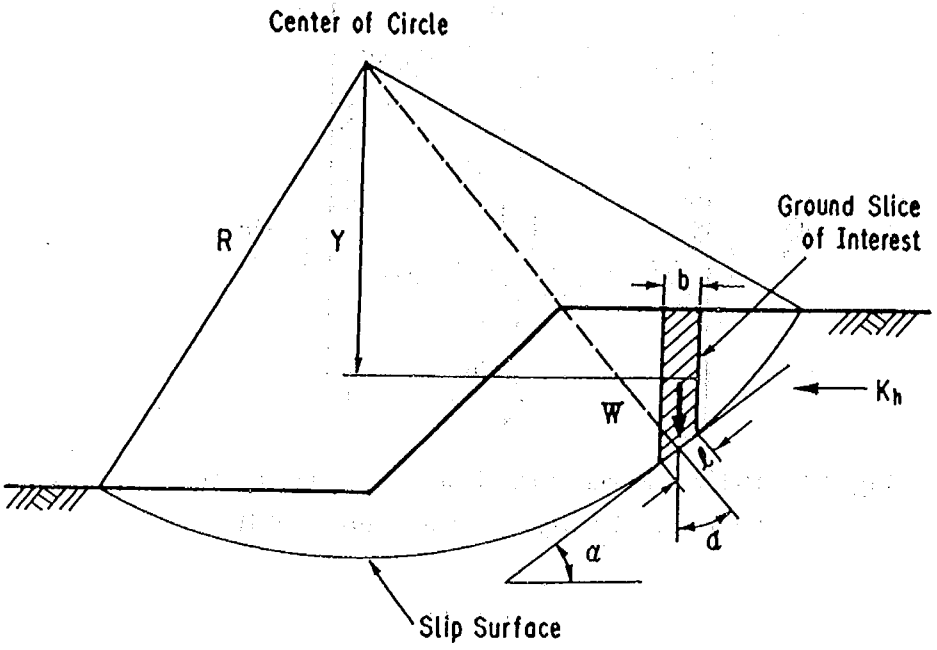


Fig2.8 Circular Arc Analysis Method

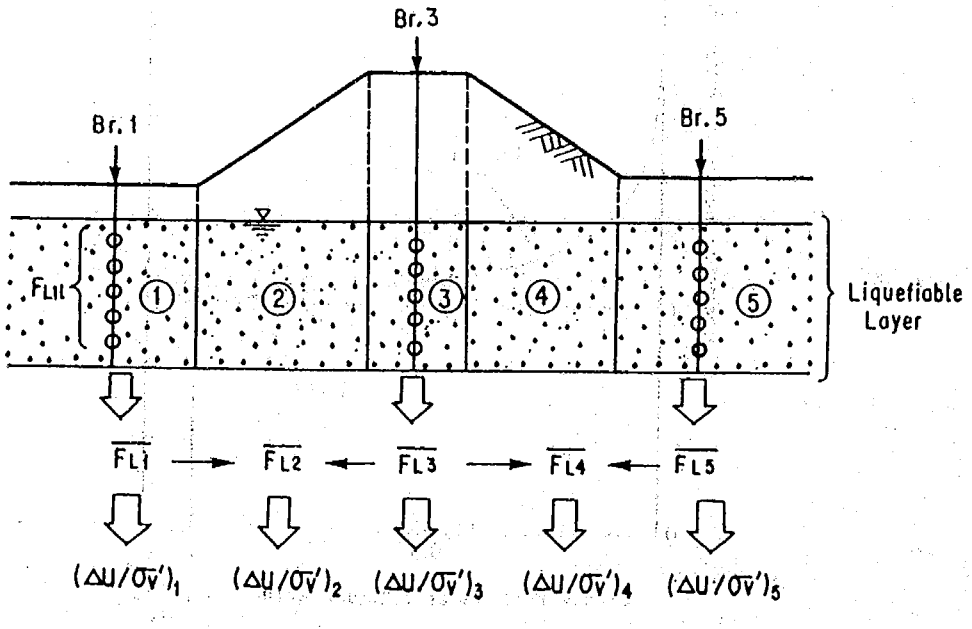


Fig 2.9 Simplified Method to Estimation Average FL-value and Excess Pore Water Pressure for Each Cell of Layers with Use of A Few Typical Boring Data

DEFORMATION ANALYSIS OF QUAY WALLS DUE TO LIQUEFACTION

Susumu IAI* and Tomohiro KAMEOKA*

ABSTRACT

In order to study the effects of liquefaction on quay walls during earthquakes, effective stress analyses are conducted on the field performance of two quay walls during an earthquake. The quay walls are of anchored steel sheet piles. Though the cross sections were similar to each other and the locations were adjacent to each other, one quay wall suffered serious damage while the other did not.

The effective stress model used in the analysis consists of a multiple shear mechanism defined in strain space. The model has the capability to represent essential features in the cyclic behavior of sand such as the effects of rotation of principal stress axis directions. For estimating the model parameters, soils were taken from the site for laboratory tests. The record of the earthquake motion was recovered from the site and digitized for the analysis.

Results of the finite element analysis are basically consistent with the observed performance of the quay walls; the model demonstrates the potential ability to differentiate between serious large deformations (i.e. damage) from negligibly small deformations (i.e. no damage) in similar types of sheet pile quay walls.

KEY WORDS : dynamic, earthquake, finite element method, harbour, liquefaction, plasticity, retaining wall, sand, sheet pile wall

1. INTRODUCTION

Past case histories during earthquakes show that quay walls often suffer significant damage if liquefaction occurs in the backfill and foundation soils. Some of the most typical examples are those observed during the Niigata Earthquake of 1964 (Ministry of Transport, 1965). Since then, extensive efforts have been made in developing methods to evaluate liquefaction susceptibility of soils and, as a result, practical means are now available to identify the conditions which lead to the occurrence of liquefaction. However, methods to evaluate effects of liquefaction on quay walls are yet to be developed.

Among the various types of retaining structures, the seismic performance of retaining structures backfilled with dry sand is relatively well understood based on the Mohr-Coulomb's failure criterion and the Newmark's sliding block concept. The recent developments in this subject can be found in the state-of-the-art report by Whitman (1991). When the sand is saturated with water, as in waterfront structures, the effect of pore water pressure becomes predominant and complicates the performance of retaining structures. Towhata and Islam (1987) offered a simplified method to incorporate the effect of pore water pressure into the sliding block concept. The method may be useful if reasonable engineering judgements are used in determining the level of excess pore water pressure and other relevant factors. Many laboratory data indicate, however, that the pore water pressure will not generally remain constant once deformation is induced in the sand nor will the deformation in the saturated sand generally be induced in such a mode of the sliding blocks as often observed in the dry sand. Effective stress analysis may be the only means for taking the complicated behavior of sand into account. In particular, a model consisting of a multiple shear mechanism (Iai et al, 1992a and b) offers the prospect of taking into account the essential features of sand under cyclic loading.

In May 1983, the Nihonkai Chubu Earthquake of magnitude 7.7 hit the northern part of Japan. The earthquake caused damage to quay walls at Akita Port located about 100 km from the epicenter. Many sand boils were observed at the quay walls. In the vicinity of one of the damaged quay walls, a quay wall survived without damage. The cross section of this wall was similar to that of the damaged quay wall, but no sand boils were observed. This case history provided a good opportunity to examine the capability of the aforementioned effective stress model to predict the effects of earthquakes on quay walls.

* Port and Harbour Research Institute
Ministry of Transport

2. AKITA PORT AND EARTHQUAKE MOTION

The epicenter of the 1983 Nihonkai Chubu Earthquake was located in the Japan Sea, called 'Nihonkai' in Japanese, as shown in Fig. 1. The seismic fault, shown by the broken lines in Fig. 1(b), dipped about 30 degrees in the east direction. With the shallow focal depth of 14 km, the earthquake caused Tsunami, killing 100 people.

As shown in Fig. 1(c), Akita Port is situated at the estuaries of the Omono and the Shinjo Rivers. Most of the quay walls were constructed along the Omono River with a backfilling method. Most of them suffered damage due to liquefaction in the backfill sand during the earthquake. The quay walls to be analyzed in the present study are located at Ohama No.2 Wharf where sand boils were observed and at Ohama No.1 Wharf where no sand boils were observed. These wharves are located near the estuary of the Shinjo River as shown in the same figure.

About 2.5 km south east of these wharves, a strong motion accelerograph was installed at the location shown in the lower right corner of Fig. 1(c). This is one of the stations deployed under the strong motion observation network of the Port and Harbour Research Institute in operation since 1963 (Kurata and Iai, 1990). The maximum accelerations recorded at Akita Port were 219, 235 and 54 Gals in NS, EW and UD directions.

The ground below the accelerograph consists of a layer of loosely deposited coarse and fine sands with thickness of about six meters and alternating layers of sandy gravel and gravel mixed with sands of about ten meters in thickness, below which lies the base of tertiary origin for the entire area of Akita Port. Contour lines of the depth of the base (Kano, 1965) are shown in Fig. 1(c) with the broken lines, indicating the accelerograph is located close to the shallowest part of the base. The soil deposit at the accelerograph site did not liquefy during the earthquake and thereby the earthquake motion recovered from the accelerograph was not affected by the soil liquefaction occurring in other parts of the area in Akita Port. The recorded time histories of the earthquake motion were digitized and corrected for the instrument response of the accelerograph through the procedure developed by one of the authors and his colleagues (Iai et al, 1978). The accelerograph was of SMAC-B2 type commonly deployed in Japan. The corrected time histories are shown in Fig. 2 (Kurata et al, 1983).

3. DAMAGED QUAY WALL

At the time of the earthquake, the quay wall at Ohama No.2 Wharf had such a cross section as shown in Fig. 3. As indicated in this figure, the quay wall was constructed with a backfilling method. The earthquake left sand boils at the quay wall, as mentioned earlier, and induced such deformations as shown in the same figure with the broken lines. An eyewitness, a truck driver who had narrowly escaped from Ohama No.2 Wharf identified that the quay wall gradually deformed during the earthquake (Tsuchida et al, 1985).

The horizontal displacements at the top of the sheet pile range from about 1.1 to 1.8 meters. The settlements at the middle part of the apron, which are indicated by the broken lines in Fig. 3, are about 1.4 meters, being almost the same as the horizontal displacements of the sheet pile wall.

Ohama No.2 Wharf consisted of such soil layers as shown in Fig. 4. The upper layer of medium sand with the mean diameter D_{50} of about 0.15 mm is originally a part of the deposit from the Shinjo River and dredged from the sea bottom for the backfilling. The lower layer of fine sand with D_{50} of about 0.4 mm is a deposit from the Omono River.

4. QUAY WALL WITHOUT DAMAGE

The quay wall at Ohama No.1 Wharf had a cross section similar to that at Ohama No.2 Wharf as shown in Fig. 5. In particular, the type of the sheet pile wall and the water depth of the quay wall at Ohama No.1 Wharf were exactly the same as those at Ohama No.2 Wharf. The ground consisted of quaternary deposits without backfilling. As shown in Fig. 6, the SPT N-values at the upper layer of medium sand with D_{50} of about 0.15 mm at Ohama No.1 Wharf are higher than those at Ohama No.2 Wharf. As partly indicated by the SPT N-values shown at the levels higher than the present ground level, the level of the original ground surface had been a few meters higher than the present level.

To summarize, the sands at Ohama No.1 Wharf are quite similar to those at Ohama No.2 Wharf except for the SPT N-values of the upper part of the ground.

5. MODELING OF SOILS

As partly mentioned earlier, the effective stress model of sands to be used in this study consists of a multiple shear mechanism (Iai et al, 1992a). With the effective stress and strain vectors written by

$$\{\sigma'\}^T = \{ \sigma_x' \ \sigma_y' \ \tau_{xy} \} \quad (1)$$

$$\{\epsilon\}^T = \{ \epsilon_x \ \epsilon_y \ \gamma_{xy} \} \quad (2)$$

the basic form of the constitutive relation is given by

$$\{d\sigma'\} = [D](\{d\epsilon\} - \{d\epsilon_p\}) \quad (3)$$

in which

$$[D] = K\{n^{(0)}\}\{n^{(0)}\}^T + \sum R_{L/U}^{(i)}\{n^{(i)}\}\{n^{(i)}\}^T \quad (4)$$

In this relation, the term $\{d\epsilon_p\}$ in Eq.(3) represents the additional strain increment vector to take the dilatancy into account and is given from the volumetric strain increment due to the dilatancy ϵ_p as

$$\{d\epsilon_p\}^T = \{d\epsilon_p/2 \ d\epsilon_p/2 \ 0 \} \quad (5)$$

The first term in Eq.(4) represents the volumetric mechanism with rebound modulus K and the direction vector is given by

$$\{n^{(0)}\}^T = \{ 1 \ 1 \ 0 \} \quad (6)$$

The second term in Eq.(4) represents the multiple shear mechanism. Each mechanism $i = 1,\ldots,I$ represents a virtual simple shear mechanism, with each simple shear plane oriented at an angle $\theta_i/2 + \pi/4$ relative to the x axis. The tangential shear modulus $R_{L/U}^{(i)}$ represents the hyperbolic stress strain relationship with hysteresis characteristics. The direction vectors for the multiple shear mechanism in Eq.(4) are given by

$$\{n^{(i)}\}^T = \{ \cos\theta_i \ -\cos\theta_i \ \sin\theta_i \} \quad (\text{for } i = 1,\ldots, I) \quad (7)$$

in which

$$\theta_i = (i-1)\Delta\theta \quad (\text{for } i = 1,\ldots,I) \quad (8)$$

$$\Delta\theta = \pi/I \quad (9)$$

The loading and unloading for shear mechanism are separately defined for each mechanism by the sign of $\{n^{(i)}\}^T\{d\epsilon\}$.

The multiple shear mechanism takes into account the effect of rotation of principal stress axis directions, the effect of which is known to play an important role in the cyclic behavior of the anisotropically consolidated sand (Iai et al, 1992b). The model has 10 parameters; two of which specify elastic properties of soil, another two specify plastic shear behavior, and the rest specify dilatancy.

In the present study, the parameters of the soils were determined from the in-situ velocity logging, the SPT N-values and the results of the undrained cyclic loading tests mentioned earlier. The details in determining the soil parameters are as follows.

In the analysis, the ground at Ohama No.2 Wharf was idealized into four kinds of soil layers as indicated in Fig. 3. Similarly, the ground at Ohama No.1 Wharf was idealized as indicated in Fig. 5. In this figure, the layer designated as Layer 2' is the combination of the upper and lower sand layers mentioned earlier. This was because the soil properties of both layers inferred from the SPT N-values were almost the same; when the SPT N-values of both layers shown in Fig. 6 were corrected to the confining pressure of 1 kgf/cm^2 (98 kPa) as often done in the liquefaction potential evaluation (Seed et al, 1985), the corrected SPT N-values became almost uniform along the depth for both of the layers.

The elastic shear modulus G_{ma} was determined based on the in-situ velocity logging at Ohama No.3 Wharf. The reference effective confining pressure of ($-\sigma_{ma}'$), which links the elastic modulus to the in-situ confining pressure in each soil layer, was determined with $K_0 = 0.5$ condition. The shear resistance angle ϕ_f' was determined by the triaxial test. The hysteretic damping factor at infinitely large shear strain H_m was determined to be 30 % by referring to the typical laboratory results summarized by Ishihara (1982).

The rebound modulus of the soil skeleton K_a was determined by assuming that Poisson's ratio is 0.3. The phase transformation angle ϕ_p', which separates the dilative and contractive zones in the stress space, was assumed to be 30 degrees by referring to the typical laboratory results. The rest of the five parameters p_1, p_2, w_1, S_1 and c_1, which specify the dilatancy, were determined by the backfitting to the liquefaction resistance curves of the sand shown in Fig. 8. The liquefaction

resistance curve for each layer shown in this figure was determined by combining the laboratory test data shown earlier and the SPT N-values at the sites for taking the in-situ conditions of soils into account. The procedure is given in the Appendix. More details of the backfitting procedure as well as the meaning of each parameter can be found in a paper by Iai et al (1990).

The soil parameters determined in this manner are summarized in Table 1. An example is given in Fig. 9 on the simulated cyclic behavior of the backfill sand computed by the present analytical model.

Among the four soil layers idealized in the analysis, there exists a layer of clayey soil designated as Layer 3 in Fig. 3. The modeling of the clayey soil needs a slight modification in the present analytical model. The modification is in fact a simplification. The authors postulate in the present analysis that the clayey soil did not significantly change the effective mean stress during the earthquake shaking and, as an approximation, kept the initial effective mean stress being constant throughout the shaking. This might be a crude approximation for a realistic behavior of the clayey soil. As a compensation, the effective angle of shear resistance of the clayey soil was so determined as to give the same undrained shear strength as measured in the laboratory with the unconfined undrained compression tests.

6. MODELING OF STRUCTURES AND SEA WATER

The quay walls at Ohama No.1 and No.2 wharves had the same type of sheet piles as mentioned earlier. The sheet piles forming the quay walls were type FSP-VI_L manufactured in Japan, having the following properties; the second moment of area 8.6×10^{-4} m^4, cross sectional area 0.0306 m^2, and density 7.5 t/m^3 (each specified per unit breadth of the beam). In the analysis, the sheet piles were simulated with linear beam elements. It is known that the displacement shape functions assumed in the commonly used beam element (e.g. Zienkiewicz, 1977) are incompatible with those of the isoparametric solid element representing the soil and hence pose a potential threat to cause an undesirable effect on the computed results of the soil-structure interaction. In the present study, more appropriate beam elements were used of which displacement shape functions are exactly compatible with those of the solid element (Hinton and Owen, 1977).

No friction was assumed to be acting between the soil and the sheet pile wall. This assumption was implemented in the analysis by imposing such a condition that the displacements of the nodal points of the soil elements and the beam elements be the same with each other in the horizontal direction but can take independent values in the vertical direction.

The tie rod was simulated by a linear beam element, mass of which was assumed to be zero, and was connected with the sheet pile and the anchor piles by hinges. No interaction was taken into account between the soil and the tie rod. This was implemented in the analysis by simply specifying the geometry of the beam element without any connection with the soil elements.

The anchor piles were idealized also by the linear beam elements. In particular, two rows of the anchor piles at Ohama No.2 Wharf were idealized by the linear beam elements, top ends of which were rigidly fixed with each other for simulating the upper concrete structure of the anchor. No friction was assumed to be acting between the soil and the anchor piles. The numerical implementation of this was done in a similar manner as mentioned earlier.

The sea water was modeled as incompressible fluid and was formulated as an added mass matrix based on the equilibrium and continuity of the fluid at the solid-fluid interface (Zienkiewicz, 1977).

7. INITIAL AND BOUNDARY CONDITIONS

(1) Initial Conditions

Before the earthquake response analysis, a static analysis was conducted with gravity to simulate the initial stresses acting in-situ before the earthquake. The same constitutive model was used as in the earthquake response analysis but with the drained condition.

Obviously a more realistic static analysis could be done by closely simulating the actual steps taken in the construction of the structures; i.e. by simulating the processes of the pile driving and the backfilling or the excavation and, if any, the effect of the pre-stress histories in the ground

due to the previous earthquakes. These steps, if taken, will be so complicated that the static analysis itself can become a major research problem. In the present analysis, such a complication was avoided because the main target is on the earthquake response analysis. The authors assumed that a simple one step loading of gravity will give a reasonable approximation of the initial stress condition. The initial earth pressures and bending moments obtained as the initial conditions will be shown later with the results of the dynamic response analysis.

(2) Boundary Conditions

During the earthquake response analysis, the seismic waves should be appropriately permitted to transmit from the domain of the analysis with the finite elements to the outside field because the boundaries of the domain fixed of the analysis do not exist in reality. In order to take this fact into account in an approximate manner, the side and bottom boundaries of the domain were simulated by viscous dampers.

The dynamic analysis should also appropriately take into account the effect of the earthquake waves transmitted from the outside field. In the present analysis, the incident wave transmitted vertically from the bottom boundary was given through the viscous dampers at the bottom. The effects of the free field motions, simulated by the one dimensional responses at outside fields, were also taken into account by transmitting them through the viscous dampers at both sides of the boundaries.

8. INPUT MOTION AND TIME INTEGRATION

With these initial and boundary conditions, the earthquake response analysis was conducted on the steel sheet pile quay walls at Akita Port. As an input motion, both of the horizontal components of the earthquake motion recorded at Akita Port, shown in Fig. 3, were at first deconvoluted by the equivalent linear method for obtaining the incident waves, and transformed into the components normal to the faces of the quay walls.

The dynamic analysis of the quay walls was conducted under the undrained conditions (Zienkiewicz et al, 1982). The numerical integration was done by the Wilson-θ method ($\theta = 1.4$) using a time step of 0.01 seconds. Rayleigh damping ($\alpha = 0$ and $\beta = 0.005$) which was proportionally decreasing with the degree of cyclic mobility was used to ensure stability of the numerical solution process.

9. ANALYSIS OF A DAMAGED QUAY WALL

(1) Earthquake Response and Deformation

The effective stress analysis of the quay wall at Ohama No.2 Wharf resulted in the deformation shown in Fig. 10; deformations towards the sea are mainly seen at the soils in front of and behind the sheet pile wall.

The maximum acceleration at the top of the quay wall was about 190 Gals as shown in the second row in Fig. 11(a). In this figure and the figures to follow, the alphabets indicate the locations shown in Fig. 10. As the shaking continues, the horizontal displacements gradually increased towards the sea as shown in Fig. 11(b). The backfill soil behind the sheet pile wall gradually settled as shown in the lower two rows in Fig. 11(c) whereas the sea bed in front of the sheet pile wall gradually swelled as shown of the top row of the same figure.

The horizontal displacement at the top of the sheet pile wall was computed being about 1.3 m at the end of the shaking whereas the observed displacements range, as mentioned earlier, from about 1.1 to 1.8 meters, indicating the computed displacement is consistent with those observed.

The settlements behind the sheet pile wall were computed being about 0.7 meters at the end of the shaking whereas the observed settlements, as mentioned earlier, were about 1.4 meters. Should the effect of yielding of the sheet pile be included in the analysis, the computed settlements would be greater and closer to those observed.

(2) Earth Pressure and Bending Moment

As shown in Fig. 12, the earth pressures (i.e. the summations of the normal effective stresses and the excess pore water pressures) acting on the sheet pile wall became greater than those before the shaking. In particular, the earth pressures behind the sheet pile after the shaking became about the same as those with the earth pressure coefficient of $K_0 = 1.0$. This is consistent with the results of the previous laboratory study on the earth

pressures acting on the fixed wall due to the liquefied soil (Tsuchida, 1968).

In accordance with those changes in the earth pressures, the bending moment of the sheet pile became greater as shown in Fig. 13. In particular, the bending moment at the level of 6 meters below the sea water level gradually increased as shown in Fig. 14.

As shown in Fig. 14, the maximum stress due to bending was computed as 500000 kPa whereas the yield strength of the steel sheet pile is 300000 kPa ($1kgf/cm^2$ = 98 kPa). This indicates that the observed phenomenon, i.e. the failure of the sheet pile, is well explained by the present analysis because, as mentioned earlier, the sheet pile was idealized in the analysis with the linear beam elements, which were assumed never to fail.

The analysis also indicates some possibility of yielding below the sea bottom. In Akita Port, a sheet pile was pulled out from the ground after the earthquake, revealing the opening of a crack at the level of 2.2 meters below the sea bottom. This is consistent with the results of the analysis.

The excess pore water pressures in the soils in front of and behind the sheet pile wall were computed as shown in Fig. 15. The excess pore water pressures rapidly increased behind the sheet pile wall at the initiation of the shaking as shown in the second and third rows. The excess pore water pressures in front of the sheet pile wall, however, fluctuated around the value of zero as shown in the top row in Fig. 15 possibly because of the high liquefaction resistance of the soil.

10. ANALYSIS OF AN UNDAMAGED QUAY WALL

(1) Earthquake Response and Deformation

The effective stress analysis of the quay wall at Ohama No.1 Wharf resulted in the deformation shown in Fig. 16. The maximum acceleration at the top of the quay wall was about 270 Gals, being much higher than in the case of Ohama No.2 Wharf, but the horizontal displacement was only about 0.2 m. The observed displacement at Ohama No.1 Wharf was about 0.05 m, indicating the analysis provided slightly conservative results, erring in the order of 0.1 to 0.2 m.

(2) Earth Pressure and Bending Moment

As shown in Fig. 17, the earth pressures acting on the sheet pile wall became greater than those before the shaking. In particular, those behind the sheet pile wall became close to those with K_0 = 1.0 condition from the ground surface to the elevation of about five meters below the sea water level, but at the lower levels the earth pressures remained very much smaller than those with K_0 = 1.0 condition.

In accordance with those changes in the earth pressures, the bending moment of the sheet pile changed as shown in Fig. 18. The maximum stress due to bending was computed as 300000 kPa as shown in Fig. 18 whereas the yield strength of the steel sheet pile is also 300000 kPa, indicating that the analysis provided slightly conservative results.

11. SUMMARY AND CONCLUSIONS

A two dimensional effective stress analysis was conducted on the behavior of the sheet pile quay walls. The results of the analysis were consistent with the observed performance of the damaged and undamaged quay walls. In the analysis, major deformations were seen in the soils in front of and behind the sheet pile wall.

With the reasonable agreement between the observed performance and the analysis, the authors draw the conclusion that the present model has the potential ability to differentiate between serious large deformations (i.e. damage) and very small deformations (i.e. no damage) in similar types of sheet pile quay walls.

REFERENCES

(1) Hinton, E. and Owen, D.R.J (1977) : Finite Element Programming, Academic Press, p.305

(2) Iai, S., Kurata, E. and Tsuchida, H. (1978) : "Digitization and correction of strong-motion accelerograms," Technical Note of the Port and Harbour Research Institute, No.286, 56p. (in Japanese)

(3) Iai, S., Tsuchida, H. and Koizumi, K. (1989) : "A liquefaction criterion based on field performances around seismograph stations," Soils and Foundations, Vol.29, No.2, pp.52-68

(4) Iai, S., Matsunaga, Y. and Kameoka, T. (1990) : "Parameter

identification for a cyclic mobility model," Report of the Port and Harbour Research Institute, Vol.29, No.4, pp.57-83
(5) Iai, S., Matsunaga, Y. and Kameoka, T. (1992a) : "Strain space plasticity model for cyclic mobility," Soils and Foundations, Vol.32, No.2, pp. 1-15
(6) Iai, S., Matsunaga, Y. and Kameoka, T. (1992b) : "Analysis of undrained cyclic behavior of sand under anisotropic consolidation," Soils and Foundations, Vol.32, No.2, pp. 16-20
(7) Ishihara, K. (1982) : "Evaluation of soil properties for use in earthquake response analysis," Proceedings of International Symposium on Numerical Models in Geomechanics, Zurich, pp.237-259
(8) Kano, T. (1965) : "On the topography and quaternary geology in the north area of Akita City, Akita Prefecture, Northeast Honshu," Report of the Research Institute of Underground Resources, Mining College, Akita University, No.33, pp.1-12 (in Japanese)
(9) Kurata, E. and Iai, S. (1990) : "Annual report of strong-motion earthquake records in Japanese ports (1989)," Technical Note of the Port and Harbour Research Institute, No.676, 324p.
(10) Kurata, E., Fukuhara, T. and Noda, S. (1983) : "Strong-motion earthquake records on the 1983 Nipponkai-Chubu Earthquake in port areas," Technical Note of the Port and Harbour Research Institute, No.458, 372p.
(11) Ministry of Transport (1965) : "Damage to port structures by the Niigata Earthquake of 1964," p.249
(12) Seed, H.B., Tokimatsu, K., Harder, L.F. and Chung, R.M. (1985) : "Influence of SPT procedures in soil liquefaction resistance evaluations," Journal of Geotechnical Engineering Division, ASCE, Vol.1-11, No.12, pp.1425-1445
(13) Tokimatsu, K. and Yoshimi, Y. (1983) : "Empirical correlation of soil liquefaction based on SPT N-value and fines content," Soils and Foundations, Vol.23, No.4, pp.56-74
(14) Towhata, I. and Islam, M.S. (1987) : "Prediction of lateral displacement of anchored bulkheads induced by seismic liquefaction," Soils and Foundations, Vol.27, No.4, pp.137-147
(15) Tsuchida, H. (1968) : "Earth pressure due to liquefied soil," Tsuchi-to-Kiso, Japanese Society of Soil Mechanics and Foundation Engineering, Vol.16, No.5, pp.3-10 (in Japanese)
(16) Tsuchida, H., Noda, S., Inatomi, T., Uwabe, T., Iai, S., Oneda, H. and Toyama, S. (1985) : "Damage to port structures by the 1983 Nipponkai-Chubu Earthquake," Technical Note of the Port and Harbour Research Institute No.511, p.447 (in Japanese)
(17) Whitman, R.V. (1991) : "Seismic design of earth retaining structures (state of the art paper)," Proceedings of the Second International Conference on Recent Advances in Geotechnical Earthquake Engineering and Soil Dynamics, St. Louis, Vol.2, pp.1767-1778
(18) Yoshimi, Y., Tokimatsu, K. and Hosaka, Y. (1989) : "Evaluation of liquefaction resistance of clean sands based on high-quality undisturbed samples," Soils and Foundations, Vol.29, No.1, pp.93-104
(19) Zienkiewicz, O.C. (1977) : The Finite Element Method, 3rd edition, McGraw-Hill Book Co.
(20) Zienkiewicz, O.C. and Bettess, P. (1982) : "Soils and other saturated media under transient, dynamic conditions," Soil Mechanics - Transient and Cyclic Loads (Pande and Zienkiewicz eds.), John Wiley and Sons, pp.1-16

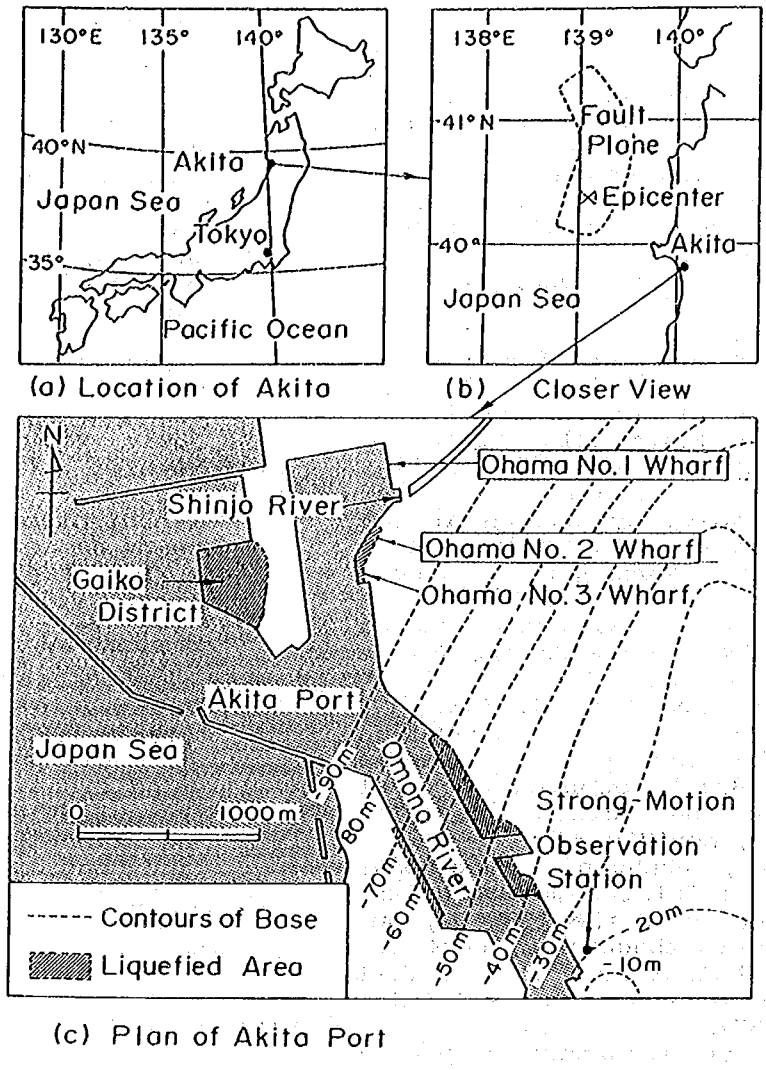


Fig. 1 Fault of the 1983 Nihonkai-Chubu Earthquake and liquefaction at Akita Port

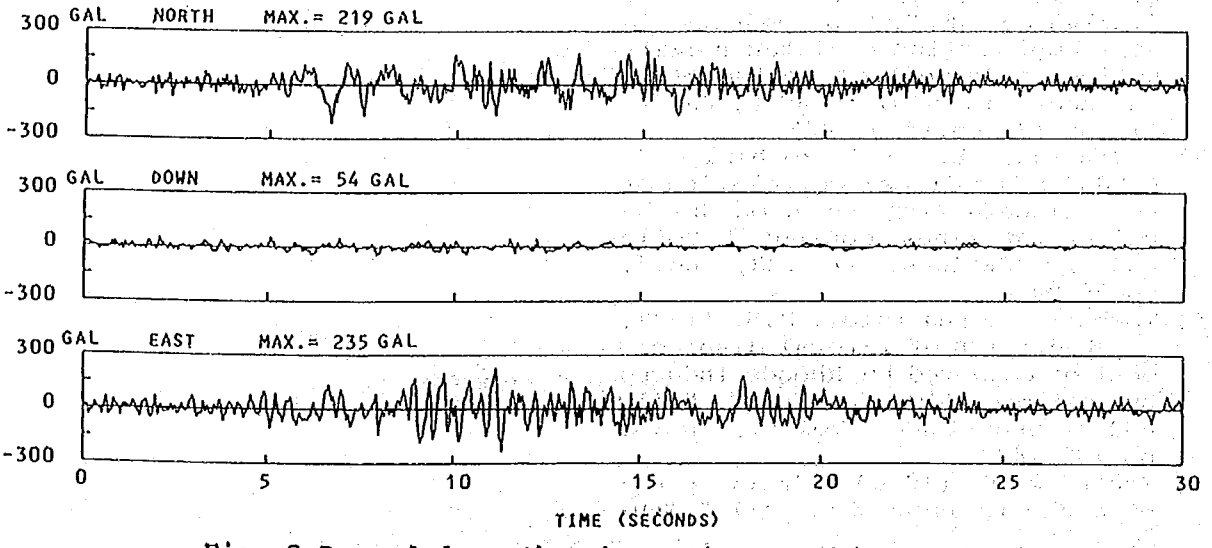


Fig. 2 Recorded earthquake motion at Akita Port

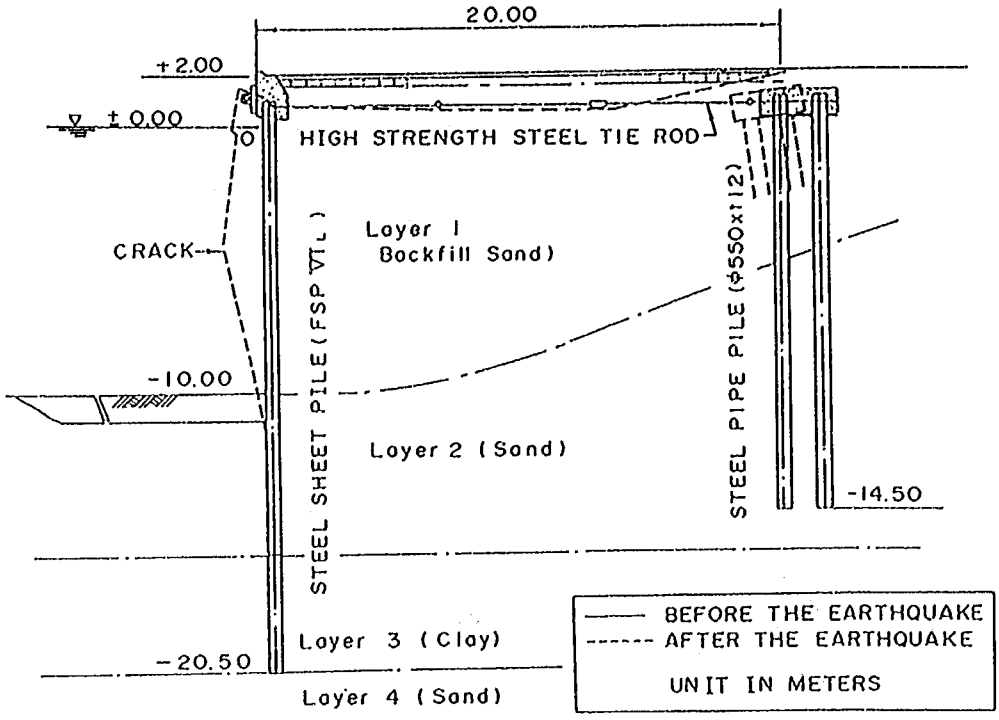


Fig. 3 Cross section of a quay wall at Ohama No.2 Wharf

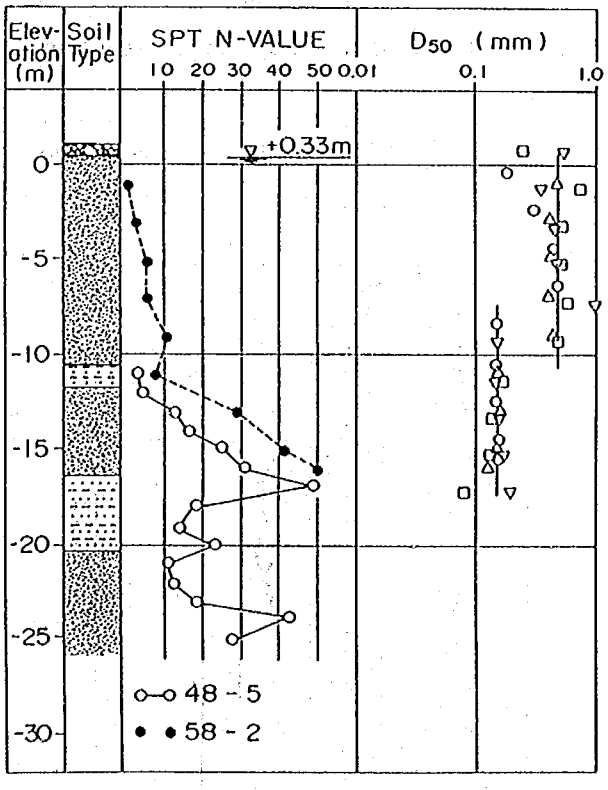


Fig. 4 Ground conditions at Ohama No.2 Wharf

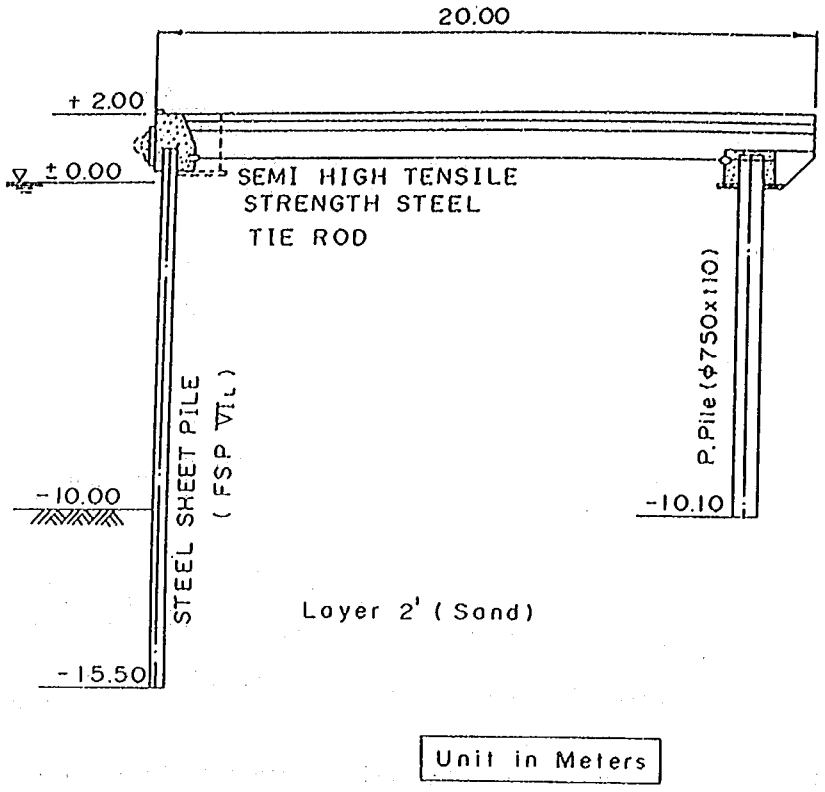


Fig. 5 Cross section of a quay wall at Ohama No.1 Wharf

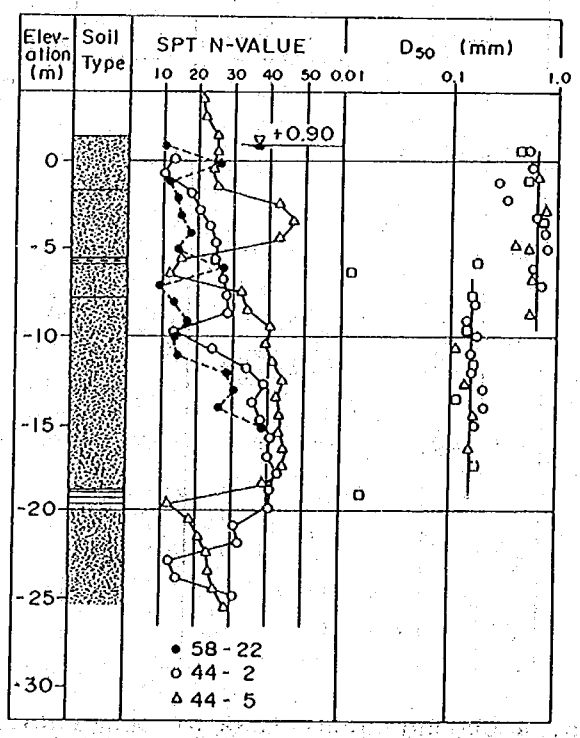
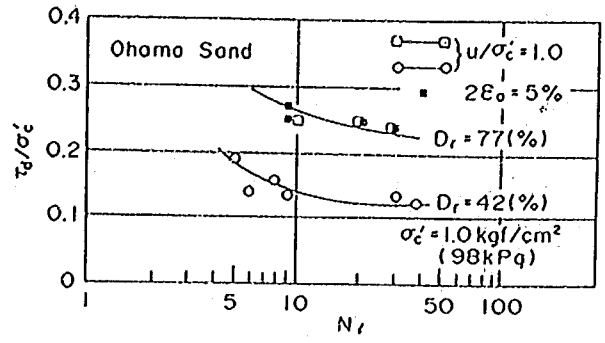
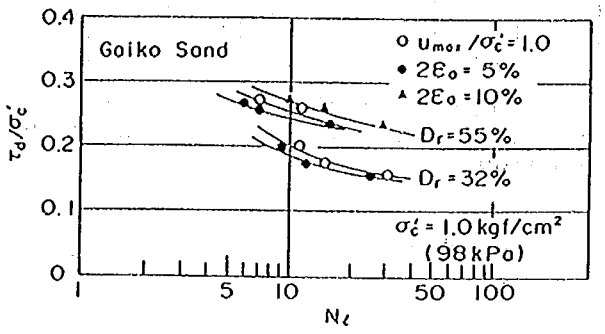


Fig. 6 Ground conditions at Ohama No.1 Wharf



(a)



(b)

Fig. 7 Liquefaction resistance curves of sands at upper and lower sand layers; (a) Backfill sand at Ohama No.2 Wharf, (b) Fill sand at Gaiko district

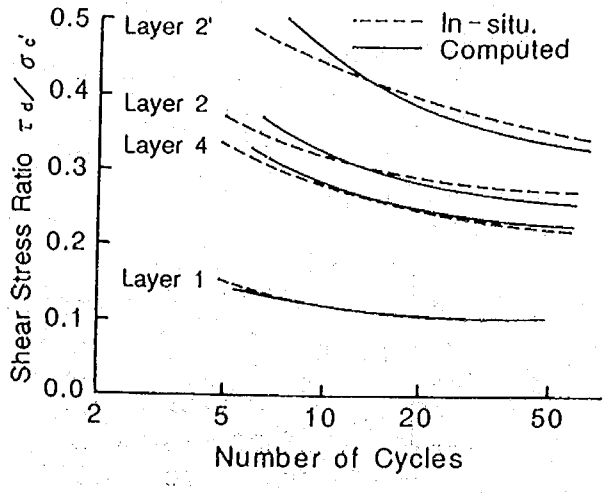
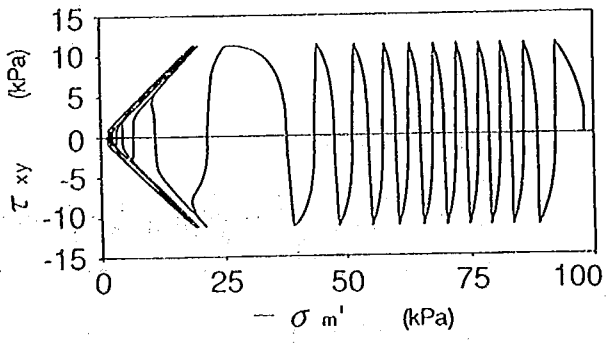


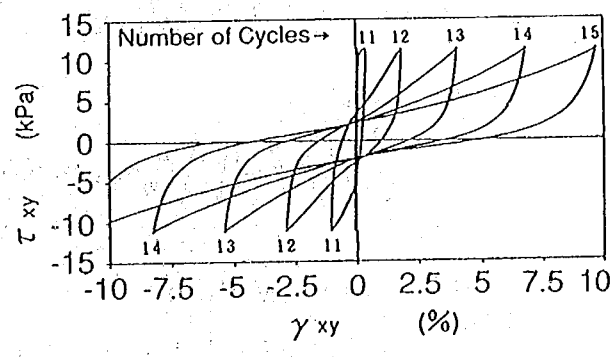
Fig. 8 In-situ and computed liquefaction resistance curves

Table 1 Soil model parameters for the analysis

	Layer 1	Layer 2	Layer 2'	Layer 3	Layer 4
G_{ma} (kPa)	33800	72200	72200	74970	168200
K_o (kPa)	89930	192100	192100	199470	447530
$-\sigma'_{ma}$ (kPa)	50	110	69	140	157
ϕ_f (deg)	37	41	43	39	44
ϕ_p (deg)	30	30	30	—	30
S_1	0.005	0.005	0.005	—	0.005
w_1	0.5	8.5	14.0	—	3.8
p_1	0.4	0.5	0.5	—	0.5
p_2	0.42	0.8	1.0	—	0.84
c_1	1.5	3.3	4.6	—	2.4



(a)



(b)

Fig. 9 Computed results of cyclic simple shearing of soil at Layer 1
(a) Effective stress path
(b) Stress strain curve

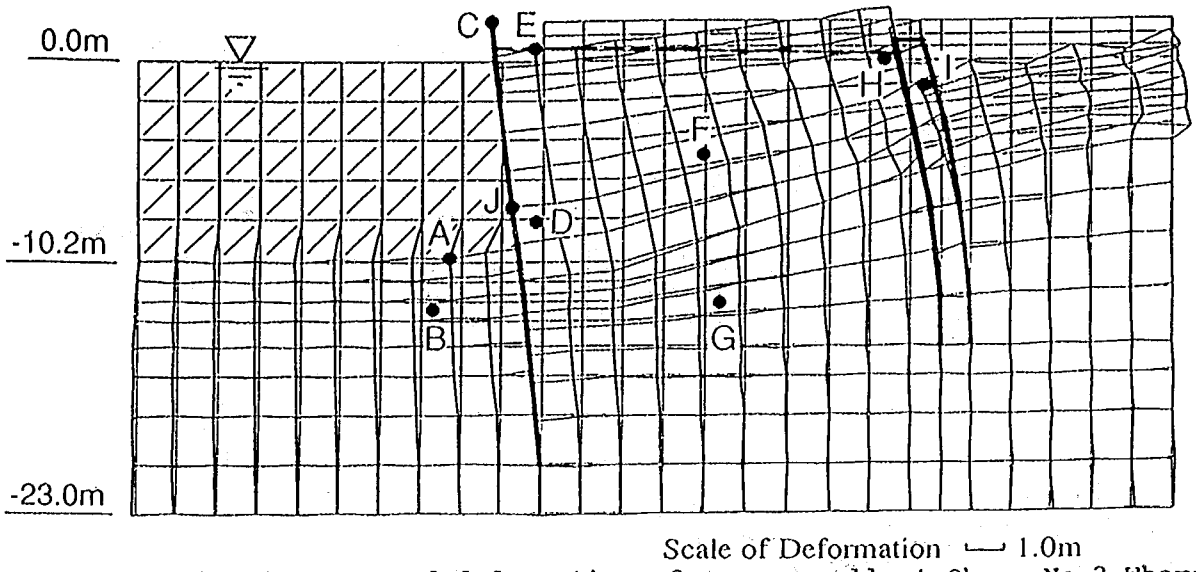


Fig. 10 Computed deformation of a quay wall at Ohama No.2 Wharf at 30 seconds of shaking

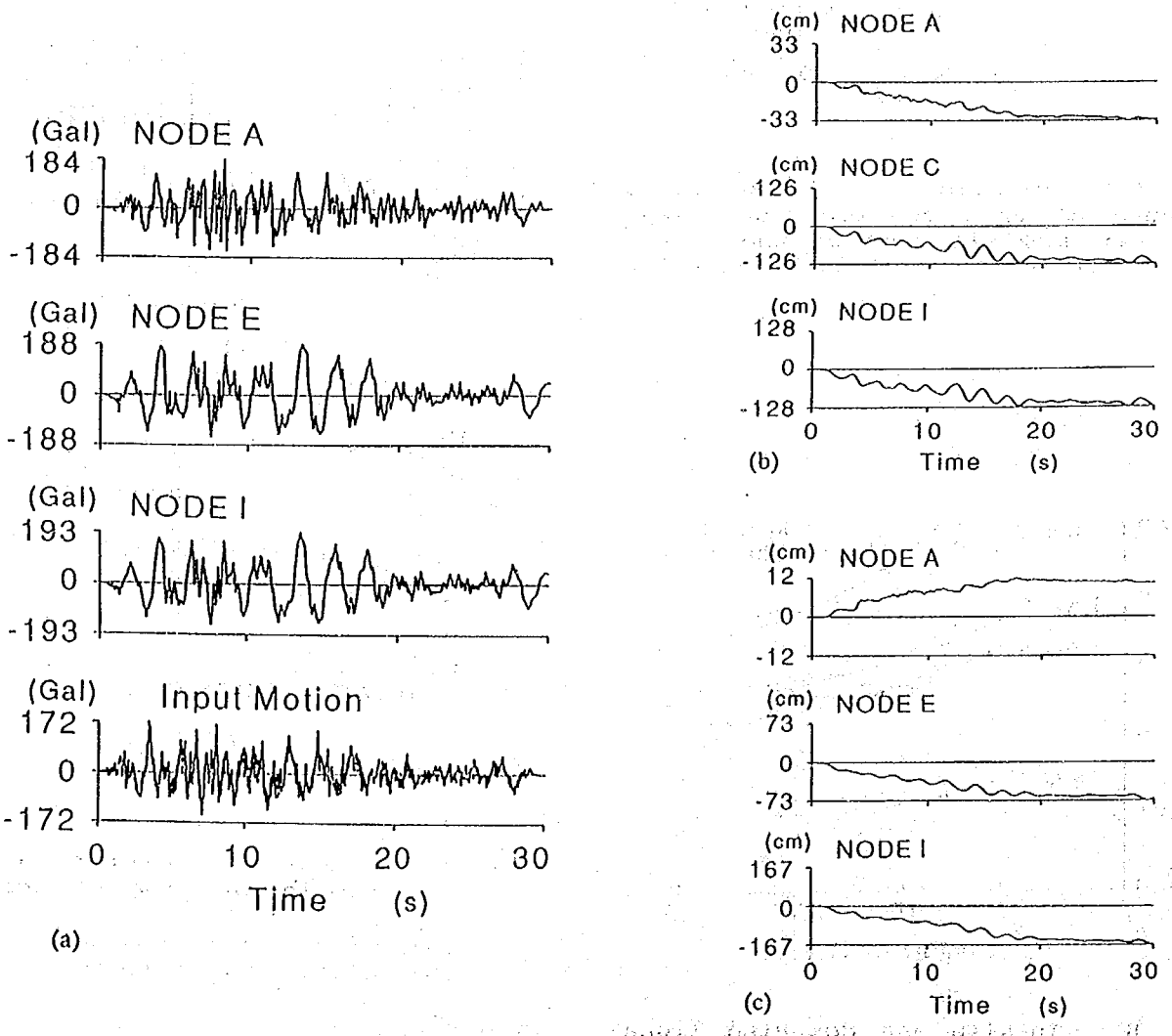


Fig. 11 Computed response accelerations and displacements at Ohama No.2 Wharf; (a) Horizontal accelerations, (b) Horizontal displacements, (c) Vertical displacements

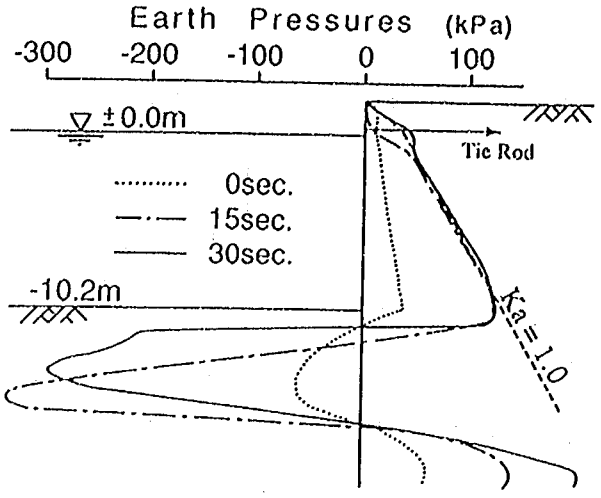


Fig. 12 Earth pressures on a quay wall at Ohama No.2 Wharf

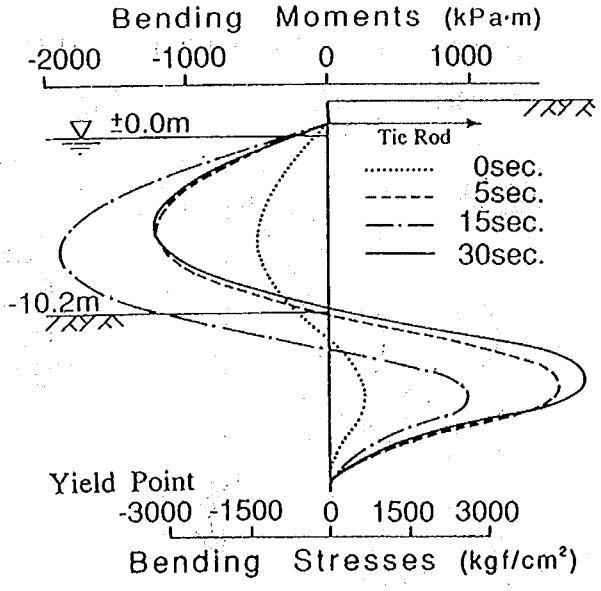


Fig. 13 Bending moments and bending stresses of a sheet pile at Ohama No.2 Wharf

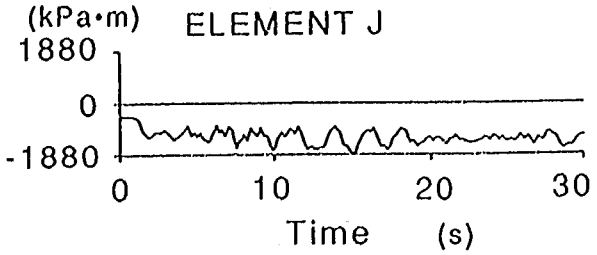


Fig. 14 Time history of bending moment of a sheet pile at the elevation of -6 m at Ohama No.2 Wharf

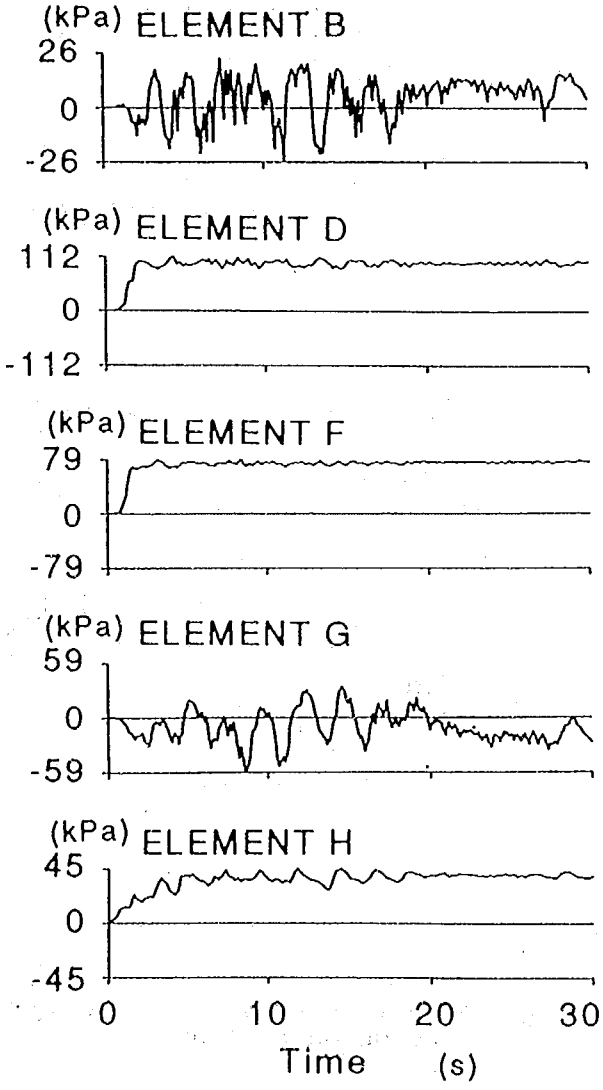


Fig. 15 Excess pore water pressures at Ohama No.2 Wharf

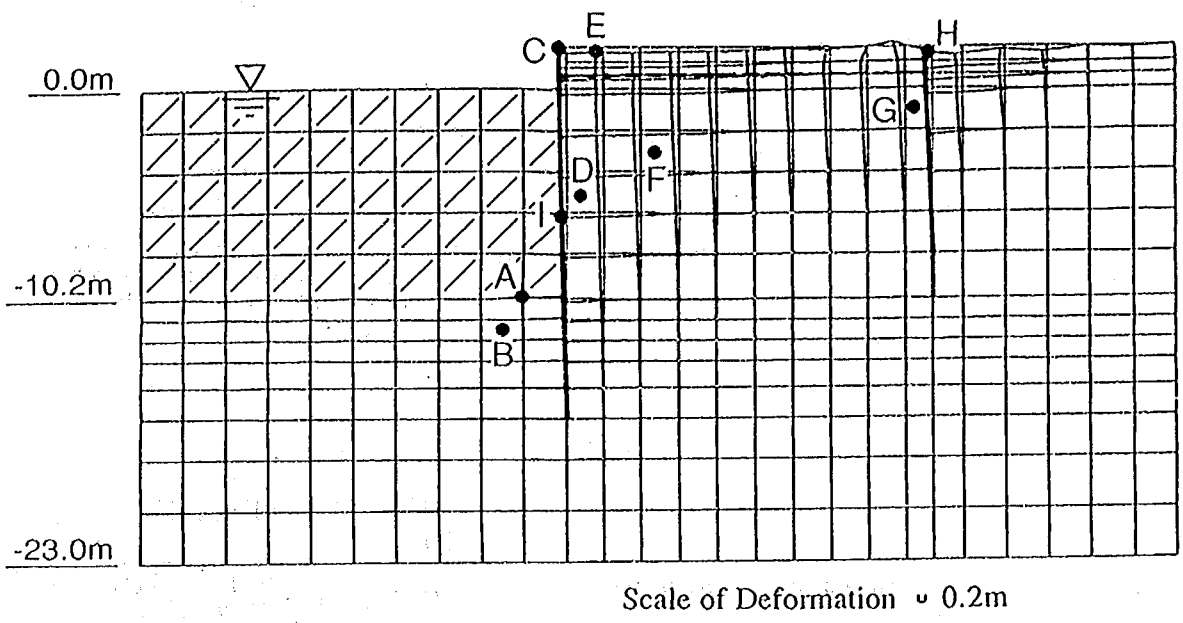


Fig. 16 Computed deformation of a quay wall at Ohama No.1 Wharf at 30 seconds of shaking

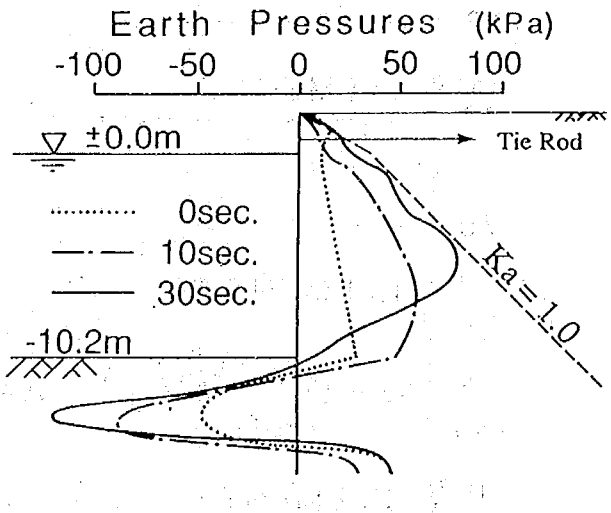


Fig. 17 Earth pressures on a quay wall at Ohama No.1 Wharf

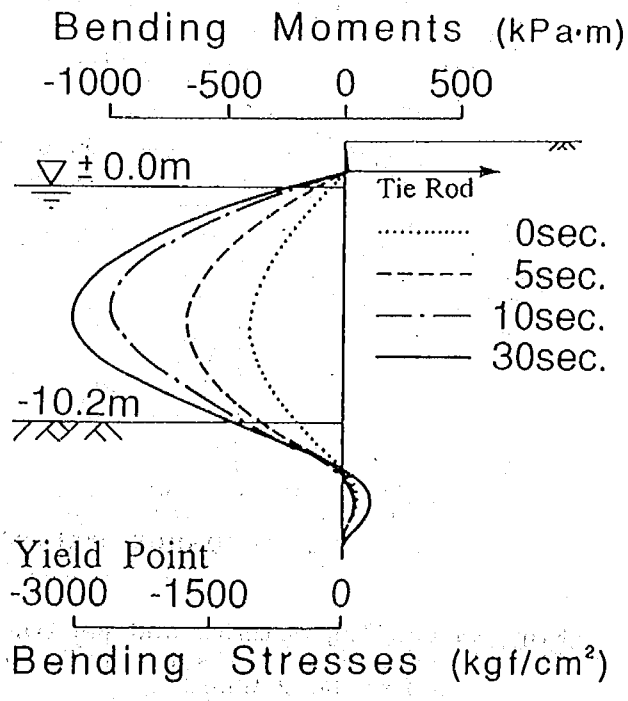


Fig. 18 Bending moments and bending stresses of a sheet pile at Ohama No.1 Wharf

PROGRESS OF CIVIL ENGINEERING, INCLUDING WIND AND SEISMIC ENGINEERING, AND ITS CONTRIBUTION TO ECONOMIC AND SOCIAL DEVELOPMENT IN MODERN JAPAN

Yukihiko SUMIYOSHI*

ABSTRACT

This paper overviews the past and future perspectives of wind and seismic engineering researches at the Public Works Research Institute. They are presented from broader view of the role of research and development for infrastructures in Japan. For this purpose, description is firstly given to the role of infrastructure investment for Japanese economy, history of progress of Civil Engineering in Japan and history of PWRI. Perspectives of the importance of wind and seismic engineering researches are then described as well as the role of PWRI based on recent trend of Japanese Society and economics.

Key Words Infrastructures, Infrastructure Investment, Civil Engineering, Public Works Research Institute, Economic Growth

1 ROLE OF INFRASTRUCTURE INVESTMENT IN JAPANESE ECONOMIC GROWTH

1.1 History of Economic Growth and Infrastructure Investment

The government of the Meiji restoration established about 125 years ago was urged to construct national traffic and communication systems and to modernize industry to centralize administrative power and encounter western countries. The government introduced western technology in various fields such as steel plants, machines and steam engines.

Fig. 1 shows the land axis of industry at the Meiji era. Before the Meiji restoration, the economic center was in Osaka while political center was in Tokyo. The line connecting from Tokyo to Osaka was the major axis in traffic and communication system. Furthermore, because the first steel plant was built in northern Kyushu island where the largest coal mine was located, the line of Tokyo-Nagoya-Osaka-Kyushu became the first Land Axis. Because there were a number of harbors along Pacific coast, the Land Axis had an advantage that the Pacific Ocean could be used as a large sea lane opened to foreign countries.

Fig. 2 shows the budget of infrastructure investment in the past. The World War I decreased the budget for infrastructure investment. This is an example of the disadvantage for excessive military spending. The Japanese economy was good during the War because of the export of war goods, however, when the War ended in 1918, a reactionary recession immediately hit the Japanese economy. Another war influence on infrastructure investment can be seen during the World War II. During and after the War, Japanese economy and infrastructure investment destructively declined.

As a whole, the growth of infrastructure investment almost followed the increase of GNP excluding in the last 10 years. In this time the growing rate of the infrastructure investment was lower than the increasing rate of GNP because of the zero-ceiling , policy in the national budget.

Fig. 3 compares the growth of infrastructure investment for railways, rivers, roads, ports and sabos before World War II. Before World War I, the major investment in traffic had been concentrated to railway development, however, wider recognition for the importance of automobile during the recovery from the Great Kanto Earthquake in 1923 and World War I urged the change from the railways to the roads. The investment to roads became larger than that of railways by the 1930s.

The world economy crisis in 1932 critically hit the Japanese economy especially at the local areas where agriculture was the major industry. The national government implemented the road and river improvement works as the countermeasure to high unemployment at the local areas.

At that time the first Road Law, the Second and the Third Flood Control Program were formulated. However, because those laws and programs could not necessarily approve the financial support, the budget in each year was unstably subjected to cut or reduction.

Fig. 4 shows the growth of infrastructure investment for railways, roads, rivers, ports and sabos after World War II. During the War, the first priority was given to the military expenditure. The industrial production became smaller than that before the War. As the result of excessive military investment, flood disasters by typhoons frequently occurred after the War. Investment for improving river facilities was increased for a while after the War for reducing

*) Director-General, Public Works Research Institute, Ministry of Construction

flood disasters. But the road investment kept the first priority as a whole.

The turning point of Japanese economic growth was the "Income-Doubling program" which was formulated in 1960. Five-year program and laws which guarantee the financial support for infrastructure investment were formulated. Extremely high increase in the infrastructure investment for all sectors is seen until 1975. It should be noted that constructions of highways and the Shin-Kansen railway was included in this program. Today, in the 11th Five-Year Road Construction Program it is planned that 14,000 km of expressway be completed.

The GNP of Japan became the second largest in the world in 1972. Although the dollar-shock in 1971 and the oil-shock in 1973 were overcome, they made the Japanese Economy to shift from the rapid growth to a state of "stable growth". Reflecting such change, the infrastructure investment also came to the moderate increase. Investment for railway declined after 1980 because the Japan National Railway was divided and transferred to private companies.

Table 1 shows the big projects which were formulated in the period of rapid economic growth. Those include the Seikan Tunnel, Honshu-Shikoku Bridges, New Kansai International Airport, Tokyo Bay Circulating Highway, Shin-Kansen Network and expressway network. Among those projects, some were already completed and now in service, and some are under construction.

In 1990, as one of the result of the Japan-US Structure Impediment Initiative (S.I.I.), the infrastructure investment in the period from 1991 to 2000 was declared to be 430 trillion Yen ($ 3.5 trillion) with emphasis on the investment for the facilities which raise the standard of living such as sewerage systems, city parks, roads and rivers facilities.

1.2 Effect of Infrastructure Investment on Economic Growth

(1) Economic Effect of Infrastructure.

Fig. 5 shows a simulation on the impact of the 10th Five-Year Road Construction Project to GNP. The model predicts the stock increase of 48 trillion Yen ($370 billion) and the flow increase of 111 trillion Yen ($850 billion) by the investment of 51 trillion Yen ($400 billion). Such increase is caused by improving the mileage, reducing travel time, increase of GNP, increase of tax and employment opportunity and low price for goods.

(2) Effect for Disaster Prevention

Reducing losses incurred by floods is one of the most major purposes of river improvement. Fig. 6 shows the ratio between the cost of damage due to disasters and GNP. It is interesting to note that although the rate was about 10% immediately after the World War II, the rate was reduced to less than 1.0% after 1965. This clearly shows the effect of implementing disaster prevention facilities such as construction of large dams and river improvements.

(3) Trigger Effect of Economic Growth

Infrastructure investments trigger economic growth. This is clearly seen in the increase of population and production at a local city. Iwate prefecture had been one of the most undeveloped region because access to major cities was limited. But the construction of the Tohoku Highway completely changed the situation. Table 2 compares population, manufacturing production and sales volume between two areas in Iwate prefecture. The area which is accessible within 30 minutes from an interchange of the Tohoku Highway could have higher increasing rate in those indices than the area which are accessible with more than 30 minutes from the interchange.

2 ADVANCES IN CIVIL ENGINEERING

2.1 History of Civil Engineering in Japan

There are 3 factors for developing civil engineering technology, i.e., research and development, engineering education, and tax law and systems which enhance the investment.

(1) Research and Development

There were 5 stages for research and development as shown in **Table 3**. The 1st stage was the period in which foreign technology was introduced by mean of inviting foreign engineers. Even before the Meiji era, there were many technologies for constructing tunnels, bridges, dams and bank protection works. However, they were not for large structures. Therefore, modern public works technologies were introduced by invited foreign engineers.

Table 4 shows the invited engineers and their contributions. Tunnel and bridge technologies were introduced from English, dam technology was introduced from U.S.A., and river and port technologies were introduced from Holland. It means that the most progressed technologies of the world at that time were introduced.

Then there was the 2nd Stage in which the introduced technologies were reformed by Japanese engineers who were educated by the invited foreign engineers. In 1880s the Japanese engineers who were educated in foreign countries

initiated to design and construct.

The 3rd stage was the technical stagnation in the period from the Taisho era to the early Showa era. The military budget and recession obstructed development of new technologies in civil engineering. Only the Kanmon Tunnel, which connects Honshu Island and Kyushu Island, was the remarkable project during this time.

4th stage was the period of 2nd introduction of foreign technologies after World War II. The rapid economic growth in 1950s required a number of construction of large tunnels, dams and bridges. Introduction of foreign technologies, especially from U.S.A., contributed to constructions of large structures. The rapid economic growth required renovation of the imported technologies so that they match with the various conditions in Japan. The renovation as well as the development of original technologies has led Japan to be one of the most advanced nation of the world in civil engineering technology today.

Remarkable construction in this period was the Sakuma Dam shown in Photo 1. Use of heavy construction machineries introduced from U.S.A. dramatically changed the existing construction process.

5th stage is the period of developing original technologies. Original technologies for constructing large structures were initiated to be developed since the late 1970s. The development of these technologies were supported by the development of other industries such as steel, machines and computers.

The most noticeable construction during this stage is the Honshu-Shikoku Bridges and the Seikan Tunnel.

The Honshu-Shikoku Bridges Project is of construction of many bridges on three routes. Photo 2 shows the Kojima-Sakaide route, completed in 1987, as the world first suspension bridge for both an expressway and a high-speed railway. Two other routes are under construction. Designs of these large bridges could be made by the precise and sophisticated analysis on seismic, wind and tidal effects. Various new technologies are being used in these bridge.

Fig. 7 shows the Akashi Strait Bridge under construction. It has a span length of 1990m, and will become the longest suspension bridge in the world when completed in 1998. Fig. 8 shows the increase of center span length in the past.

(2) History of Education in Civil Engineering

In the early Meiji era, the first civil engineering education was initiated at the College School of Engineering in 1872 based on the suggestion of Mr. Morel from England. Ministry of Education unified the high-level schools, and established the Tokyo Imperial University and the Sapporo Agricultural College. The lectures were given by the foreign engineers.

After World War II, many universities were established. These universities have educated many engineers, and it contributed to the development in civil engineering technology.

Fig. 9 shows the growth of number of students in civil engineering. Number of students including the sanitary, traffic, urban, and environmental engineering is also presented. They increased almost three times from 1960 to 1970. It means that the education system changed according to the social needs at that time.

(3) History of Financial Acts and Improvement Programs

Since the Meiji restoration, many national implementing programs were formulated to improve rivers, roads, ports and railways. But almost all the programs were reduced due to financial distress.

The government tried, therefore, to get the financial source and formulated laws for giving credit for financial support. A remarkable effort was the system of toll road and special gasoline tax exclusively used for road improvement.

Based on the financial systems and laws, various 5-year improvement programs with guarantee of budget were formulated after World War II. In addition, several public corporations were established as the organization for direct administration under the Toll System based on the Public Corporation Law. Large amount of Government Post Office Banking is financed, as a stable financial resources, to many projects of public sectors including infrastructure investment.

2.2 System for Encouraging Research and Development of Private Industries

Since the end of World War II, several foundations have been supporting the Research and Development in private companies. Tax system is one of them. Tax deduction system for the research investment was established in 1962. In this system, 20% of corporation tax can be deducted when the research investment in a fiscal year is greater than that in the preceding year. For promoting new pioneering technology, 7% of the total investment budget can be deducted in the tax.

Ministry of Construction and the Public Works

Research Institute provides support and encouraging programs for promoting research and development in civil engineering technology in private companies as shown in Table 5.

2.3 Factors Which Advances Civil Engineering

It is remarkable that it required only twenty years to digest the new technologies introduced from Western countries at the early Meiji Era. The reasons for such a fast digestion of foreign technologies may be as :

(1) In the early Meiji Era, Japan had already entered the stage of early capitalism. Therefore, it was not necessarily so difficult to import systems and technology from advanced capitalist countries.

(2) Engineers eagerly made effort to renovate introduced technology to apply to natural, economic and social conditions in Japan.

(3) Most engineers in those days were from the Samurai class. They had flourishing volunteer spirit for building a new country.

(4) Invitation of foreign engineers, establishment of Engineering College School and dispatch of young promising students to foreign countries were systematically made to absorb advanced technology and to educate engineers.

The rapid growth of economy in the 1960s allowed the large amount of money added to the national budget. Financial backing for construction projects allowed the development of new technologies and originated many large projects such as the Honshu-Shikoku Bridge, the Seikan Tunnel, and expressway network. The new movement was propelled by the general policies on technology development such as :

(1) The government supported the technical development in private industries. The government created legislation for tax deduction in technological development and joint research projects between the government and private industries. In addition, a shift of research characteristics in private companies toward applied researches allowed the government's laboratories to shift toward basic leading researches.

(2) Task committees consisting of universities, private industries and governments were often organized for large construction projects. The task committees were extremely useful for coordinating basic and practical research information.

(3) Establishment of civil engineering divisions in many national and private universities supplied many highly educated students.

(4) Many companies for steel, machinery and chemical industries developed technology related to civil engineering. This activity together with technical development of construction industry contributed for developing new materials and construction technology.

(5) Engineering researchers at universities, government and private industries often experience in actual construction process at construction sites in order to get practical way for solving problems.

3 HISTORY OF PWRI

3.1 History of PWRI

PWRI is one of the institutes with the longest long history among the national research institutes. PWRI developed a number of new technologies in 70 years. Newly developed technologies at PWRI were always characterized as "needs of times". The development of technology at PWRI has been supported by the flexibility in organization. Presently PWRI has nine Research Departments, one Center and one Branch Laboratory. Although there were only 38 staff members when it stated in 1922, there are 472 staff members presently.

In the 1920s, road construction became a very important national traffic system. Road Material Laboratory, Ministry of the Interior was built in 1921. The Laboratory became Civil Engineering Laboratory in the next fiscal year which is the origin of PWRI. Photo 3 shows the main building of Civil Engineering Laboratory at Komagome, Tokyo.

Mid noon, September 1, 1923, the Great Kanto Earthquake occurred. Magnitude of the earthquake was 7.9 on the Richter scale. Approximately 100,000 were killed, 40,000 were missing and 58,000 houses were burned. Photo 4 shows the damage at Ginza, Tokyo. The Civil Engineering Laboratory conducted extensive survey of the damage. Dr. Mononobe, Director of the Civil Engineering Laboratory, emphasized the importance for researching earthquake engineering. The achievement of the research was published as "Earthquake Study in Civil Engineering", and this report has been the base for earthquake engineering in Japan. It is worthwhile to note that the research on earthquake engineering has been the one of main roles of PWRI.

During World War II, PWRI had to conduct military-oriented researches with a small budget. Military researches conducted during this period includes reinforced concrete with bamboo reinforcement, river flashing for clearing mosquito larvas and durability of dams in the

face of bombing.

In 1948, Ministry of Construction was established and the Civil Engineering Laboratory was renamed as the Public Works Research Institute.

Allocation of the national budget to military expenditure during World War II prevented to provide countermeasures against disasters. This caused serious natural disasters after the War as shown in Table 6. Destructive damage was frequently caused due to earthquakes and typhoons.

For conducting large scale hydraulic model experiments aiming to prevent flood damage, the Shinozaki Experimental Laboratory was established. The Numazu Branch was also established in 1949 for testing construction machines and snow plow.

In 1960 the government formulated the "Income-Doubling Program". This program strengthened the economic growth and increased investment for public works. This trend produced three new branches in PWRI, i.e., the Kashima Laboratory for advancing hydraulic research in 1952, the Chiba Research Branch for advancing road research in 1960, and the Niigata Laboratory for the study of landslide and snow avalanches.

A number of new technologies developments were initiated from this period. Among them, remarkable study was the research oriented to construction of the Honshu-Shikoku Bridges, and study on soil liquefaction.

Many researches were carried out for the construction of Honshu-Shikoku Bridges. Special attention was paid to the research on seismic design and wind resistant design. New technical developments such as the application of earthquake response spectra and wind tunnel tests were made. The research greatly contributed to the success of Honshu-Shikoku Bridges Project.

Soil liquefaction caused destructive damage in Niigata Earthquake in 1964. Photo 5 shows the damage of Showa Bridge which failed due to loss of bearing capacity and permanent lateral movement of liquefied sandy soils. The damage revealed the importance for investigating soil liquefaction from its mechanism. The importance for providing the falling-down prevention devices was also widely recognized. PWRI started the research on seismic design method of bridges taking account of the effect of soil liquefaction.

In the latter half of the 1960's, the high economic growth caused various social problems such as pollution and an increase of traffic accident. The social distortion forced PWRI to build new research divisions, and 12 divisions were set from 1966 to 1975 including the Foundation Engineering Division, Ground Vibration Division, Earthquake Engineering Division and Soil Dynamics Division. Trend of researches carried out in this period changed more functionalized.

In the first half of the 1970s, the Dollar shock in 1971 and the Oil Shock in1973 discontinued the rapid economic growth in Japan. Stable economic growth has started, and deconcentration of population, particularly from metropolitan area, became an important policy. Accordingly PWRI moved to Tsukuba. Main office at Komagome and Chiba, Akabane, Shinozaki, Kashima Branches were unified to the present form.

In 1991, the Construction Management Engineering Center was established for aiming to study the construction management for activation of construction industries and the renovation of technology.

3.2 Researches on Wind and Seismic Effects at PWRI

(1) Research on Honshu-Shikoku Bridges

The Honshu-Shikoku Bridge Project is one of the most unique construction projects from various point of view. It is required to construct many types of bridges, including suspension bridges, cable stayed bridges and arch, with long span. Natural condition including wind, seismic, rock with low bearing capacity and deep sea is very strict.

Many unique technologies have been developed to realize the construction of Honshu-Shikoku Bridges. The wind and seismic effects are the core technology.

In wind engineering, the Wind Resistant Design Criteria for Honshu-Shikoku Bridges were formulated in 1967 and revised in 1976. The Criteria were the first comprehensive criteria in this field. The Criteria prescribe the design wind load including the effects of gust responses and the evaluation method of wind-induced vibrations based on wind tunnel testing.

The Criteria, together with the Guideline of Wind Tunnel Testing for Honshu-Shikoku Bridges, were applied not only for Honshu-Shikoku Bridges but also for most of the long-span bridges in Japan. While wind tunnel studies on proposed design of long span bridges were conducted according to the Criteria, new wind-induced problems, such as vortex-induced vibration of bridge deck, of bridge members, of towers at erection stage and so on, were studied and solved. Some countermeasures to increase flutter speed or to reduce amplitude of vortex-induced vibration were developed. It can be said that the Criteria

formed the basis of wind engineering on bridges in Japan.

In seismic design, the Modified Seismic Coefficient Method which modifies the lateral force depending on natural period was proposed and was put into the design. Many sophisticated computer analysis was introduced in dynamic response analysis. Dynamic overturning of rigid foundations was precisely evaluated for seismic design of Akashi Strait Bridge and Kurushima Strait Bridge.

(2) Large Boundary Layer Wind Tunnel

Safety of proposed design of long-span bridges to wind-induced instabilities has been confirmed mainly by spring-mounted rigid sectional model test in smooth laminar flow. Since the span length of the Akashi Kaikyou Bridge is much longer than the existent longest bridge in the world, it was thought that the wind-induced instabilities should be confirmed by more accurate wind tunnel study, namely full aeroelastic model study.

From these reasons, cooperative study on wind resistant design of super long-span bridges was started in 1989 by PWRI and Honshu Shikoku Bridge Authority. In order to represent the complicated geometric shape of the stiffening truss, the scale ratio of the model was thought to be at least 1/100. The main dimensions of the new Large Boundary Layer Wind Tunnel were determined from this condition, namely 41m wide, 4m high and 30m long. It was constructed at PWRI in 1991. The wind effects on the Akashi Kaikyou Bridge were studied in smooth flow and in turbulent flow using the full aeroelastic model, whose scale ratio was 1/100. Photo 6 shows the model. At present, wind tunnel study on the Tatara Bridge, which will be the longest cable-stayed bridge in the world, is in progress.

(3) Development of Seismic Design Method of Bridges

Seismic design was initiated for highway bridges in 1926 after experiencing the Great Kanto Earthquake in 1923. The importance of considering seismic effects in design of highway bridges was recognized from the extensive damage developed by the Kanto Earthquake. Various researches have been made at PWRI for developing seismic design methods since the first stage of the code enforcement.

After experiencing significant damage during strong earthquakes, seismic regulations were reviewed and amended several times as shown in Table 7. The first comprehensive seismic design stipulations were issued by the Ministry of Construction in 1971 as "Specifications for Seismic Design of Highway Bridges".

The latest specifications were issued by the Ministry of Construction in February 1990 in the form of "Part V Seismic Design " of the " Design Specifications of Highway Bridges". Major revisions introduced in the 1990 Specifications were unification of the static lateral force method (seismic coefficient method) and the modified static lateral force method (modified seismic coefficient method) including the revision of the seismic design force. It was put into Specifications based on the analysis of the data obtained from strong motion observation at PWRI.

A new method for computing inertia force for multi-span continuous bridges was also introduced based on the research at PWRI.

A ductility check for reinforced concrete piers was also newly incorporated. It was based on the recent experimental studies at PWRI as shown in Photo 7 for strength of reinforced concrete piers. Cooperative research on ductility of reinforced concrete bridge columns which was made through the Panel on Wind and Seismic Effects, UJNR, greatly contributed for legislating the ductility check of reinforced concrete columns.

(4) Strong Motion Observation

The first strong motion observation in the Ministry of Construction was initiated at Sarutani Dam in 1958. Because the importance of the observation was widely recognized at the Niigata Earthquake in 1964, the number of strong motion accelerograph increased in late 1960's. PWRI has been taking initiative in strong motion observation for infrastructures, and is presently in charge of observation at about 130 locations by about 330 strong motion accelerographs.

Dense array observation as shown in Photo 8 was initiated in 1982 for collecting data for evaluating propagation, multi-excitation and ground strain induced during an earthquake.

The strong motion records have been analyzed for various purpose. Attenuation of peak ground motions and acceleration response spectra, bracketed and normalized duration, modification of response spectra in terms of damping ratio were evaluated so far. They were incorporated in various codes and standards and have been used as the fundamental data for providing design lateral force. Soil structure interaction is also studied based on measured data.

(5) Research on Soil Liquefaction

Effect of soil liquefaction became evident when Showa Bridge fell down as shown in Photo 5 during the Niigata Earthquake 1964. Various researches were initiated after the Niigata

Earthquake. The mechanism of the liquefaction was the first target of the research, and was followed by the research for evaluating liquefaction potential. The famous F_L-Method was developed at PWRI for evaluating liquefaction potential, and it was firstly adopted in the Seismic Design Specifications of Bridges in 1980. It is now widely adopted in many codes and Standards.

Currently various researches are underway for developing seismic design method of foundation in liquefying sandy soils. Permanent deformation of liquefying soils is another important research theme. Precise model tests as shown in Photo 9 are being made with use of shaking table.

(6) Development of Seismic Vulnerability Evaluation and Seismic Strengthening

The nationwide seismic evaluation and seismic strengthening of highway bridges were made in 1971, 1976, 1979, 1986 and 1991 by the Ministry of Construction. In the 1986 evaluation, about 40,000 bridges were investigated and 11,700 bridges were found to require seismic strengthening. Most of them require installation of the device for preventing superstructure falling-down from the substructures. Evaluation of seismic vulnerability was also made for pedestrian bridges, tunnels and high embankments.

Various researches have been made at PWRI for developing rational estimation methods of seismic vulnerability and seismic strengthening methods. For example, Photo 10 shows the loading test of a reinforced concrete bridge column for developing an appropriate strengthening method. Because there are a number of reinforced concrete piers in which main reinforcements are terminated without enough splice length, an appropriate seismic strengthening method is required to be developed. The results of investigation at PWRI are being implemented for strengthening many bridge columns.

The seismic evaluation and strengthening methods of transportation facilities were compiled and published from the Japan Road Association in the form of the "Guide Specifications for Earthquake Hazard Mitigation for Transportation Facilities - Pre-Earthquake Countermeasures -" in 1987.

(7) Development of Repair Method of Seismically Damaged Structures

A comprehensive 5 year research project entitled "Development of Repair Methods for Structures Damaged by Earthquakes," was made by the Ministry of Construction between 1981 and 1986. The project is to develop post earthquake measures by providing procedures of inspection, assessment of damage extent, repair methods, and overall evaluation for repairing seismically damaged structures.

Final accomplishment of the project was compiled in 1986 in the form of " Manual for Repair Methods for Civil Engineering Structures Damaged by Earthquakes". It includes process of repair and restoration, urgent inspection and urgent treatment of damaged facilities, damage evaluation for temporary repair, temporary repair methods, and permanent repair methods. It covers various infrastructures such as roads, bridges, river hydraulic structures coastal facilities and sewage. Variety of examples of repair are also demonstrated.

Because the Manual is useful world wide, it was translated into English as an activity of the Panel on Wind and Seismic Effects, UJNR, and was published in 1988 from the National Center for Earthquake Engineering, University of New York, Buffalo.

The essence of the Manual in the area of the repair and restoration method for transportation facilities was later reorganized and published from the Japan Road Association in the form of "Guide Specifications for Earthquake Hazard Mitigation for Transportation Facilities - Pre-Earthquake Countermeasures -".

(8) Development of New Seismic Design Method for Embankment Dams

The seismic design for dams has been made by the pseudo-static method since Dr. N. Mononobe, the third Director General of PWRI, proposed it firstly in 1925. While no severe damage affecting safety of dam body itself has been experienced in dams designed by the method, strong earthquake motions greater than design seismic coefficient level were recently observed especially at crest of embankment. Some very slight damage like occurrence of cracks at dam crest was also seen in the past significant earthquakes.

Under such background, the study on the "New Seismic Design Method for Embankment Dams" was initiated at PWRI in 1986. The draft guideline was approved by a specially organized technical committee in 1991. The guideline is now applied to design practice instantly since then as tentative and supplementary to the present design method. In the process of formulating the method, the following three major points were vigorously studied.

The first is the investigation on the seismic force acting to a sliding mass in the stability calculations. The second is the examination of the input earthquake motions and the radiation damping of rock foundations in the dynamic analysis. Thirdly, the earthquake motions observed at dam foundations are arranged by the

analyses of the response spectra.

As the result, the new seismic design method has been developed as the modified pseudo-static method, which is based on the seismic characteristics of existing rockfill dams and the state-of-the-art in seismic designs. In the method, seismic forces are provided as function of the ending position of sliding circle considering the observed earthquake motions and the response of dam bodies as shown in Fig. 10. The strength of embankment material can be simultaneously evaluated in the method considering the dependency of internal friction angle on the restrained stress.

Further studies are being continued at PWRI on both dynamic characteristics of rockfill materials and dynamic analysis model to rationalize the seismic design and extend it applicable to higher rockfill dams.

(9) Development of Disaster Information Systems

A comprehensive 5 year research program entitled "Development of Disaster Information Systems" was made between 1987 and 1991. The objectives of this research project were to develop new information collection and processing systems, using advanced technology, for earthquakes, floods and debris flows. As shown in Fig. 11, key items of the research development are bird's eye information collection systems from helicopters, on-line information processing systems, and real-time digital mapping systems.

For this purpose, measuring technology of the degree of seismic damage of structures, using helicopter picture information and new media high-grade disaster prediction methods as well as planning systems for repair and restoration in the damaged area were developed. To avoid distortion of information during transferring information from the regional office to headquarters, it was aimed to develop visual motion picture systems.

The final accomplishments of the project were compiled in the form of "Guidelines of Disaster Information System" in March 1992.

(10) Passive and Hybrid Control Technologies

A comprehensive research on "Development of Base-Isolation Systems for Highway Bridges" was made from 1989 to 1992 for aiming to develop a practical design method for base-isolated highway bridges which are both safe and cost efficient. The research was conducted as a joint research between PWRI and 28 private companies. The final accomplishments were published as the Manual of Menshin Design of Highway Bridges in March 1992.

In the project, 10 new isolators and energy dissipators which have better characteristics and are superior for long-term use were developed. They were verified by the dynamic loading tests at PWRI. It was found in the project that application of the base isolation for super-long multiple-continuous highway bridges with a total length over 1 km is feasible.

Over 30 bridges were constructed or are under design presently based on the accomplishments of the research. Several bridges with the total deck Forced excitation tests with use of eccentric-mass shakers were made as shown in Photo 11. Strong motion observations are also being made for accumulating actual data.

For challenging new technology developments, hybrid control of bridge structures are being investigated as a cooperative investigation with U.S.A. research groups through the Panel on Wind and Seismic Effects, UJNR.

Among various developments, the variable damper as shown in Photo 12 is a quite unique device which varies the viscous coefficient depending on structural response so that the best energy dissipation can be made. Implementation of the variable damper for varying stiffness of bridges (variable stiffness) is also being investigated.

(11) Research on Pyroclastic Flows

Disaster caused by pyroclastic flows is one of the most destructive disasters which are accompanied with volcanic eruption. About 70 % of casualties by volcanic eruption in the world during 1900 to 1982 were killed by the pyroclastic flows and volcanic debris avalanche.

A comprehensive research on pyroclastic flows was initiated at PWRI in 1989, 2 years before the eruption of Mt. Unzen by which many people were killed. The objects of the research project were to understand the mechanism of movement of pyroclastic flows and to develop new effective countermeasures against pyroclastic flow for mitigating and preventing the disasters.

Field investigation, aerial photograph interpretation, boring excavation , soil tests and analysis of old records were made, and a lot of evidence which explain more actual condition of generation and flow-down of pyroclastic flows and the mud flows were found.

Model experiments on flow down of pyroclastic flow were initiated at PWRI since 1989 to understand the mechanism of movements of a pyroclastic flow as shown in Photo 13. More accurate model for movement of pyroclastic flows is being developed.

Actual conditions and characteristics of the

pyroclastic flows and debris flows are being studied by field observation and field investigation at Mt.Unzen-Fugen (1,359m) which began to erupt in 1990. Debris flows and pyroclastic flows have been occurring continuously from May 1991 until the present time (April 1993) as shown in Photo 14.

(12) Research on Tsunamis

Since the Meiji restoration, 6 major tsunamis hit Japan. The most destructive damage was developed by the tsunami caused by Sanriku Earthquake in 1896. At that time, 21,959 persons were killed. Most recently, 100 persons were killed by a tsunami caused by the Nihon-kai-chubu Earthquake in 1983. It took only 7 minutes for tsunami waves to propagate to the coast. Photo 15 shows the scattered concrete blocks by the tsunami at Minehama coast in Akita prefecture. Various research was made at PWRI for run-up mechanism of the tsunamis and the stability of coastal works.

Because constriction of high seawall at all the coast vulnerable to tsunami is very costly, developing appropriate systems for evacuation and information system is the important research.

4 PERSPECTIVE OF PWRI BASED ON RECENT TREND OF JAPANESE SOCIETY AND ECONOMICS

4.1 Important Trend of Japanese Society and Economy

(1)Aging and Shortening of Labour

Critical problems in Japan are aging and shortening of labors. Fig. 12 shows the population pyramid. It is clear that younger generation under 30 years old is decreasing, and labors are getting to be aged. Shortage of 1.6 million labor will take place in 2000 based on an analysis of the Ministry of Labor.

(2) Environmental Problems

Fig. 13 shows change of global temperature in the period from 1961 to 1989. Development of clean energy will be required for countermeasures of the Green-House effect. The disappearance of forests and the expansion of desert areas are one of most serious problems on the earth. This would cause shortage of rainfall and abnormal climate.

On the other hand, environmental conservation and processing urban waste are required for improving quality of life for peoples.

(3) Urban Problems

Fig. 14 compares the rate of urban population in 1950 and in 1990. Concentration of population in urban areas is increasing progressing. This causes high vulnerability for various disasters. High land price is another serious problem in urban areas.

(4) Development of Information Networks

Fig. 15 shows sales figures for the information service industry. It shows rapid growth in the market. The information industry will be more important in the future economy.

4.2 Research Theme for Needs of Time

Based on the recent trend, there are many problems to be solved immediately. Proper priority of the research direction is therefore very important for concentrating the research resources to critical problems. The following 6 research concepts which accord to "needs of times" may be essential from this point of view.

(1) Research and Development for Demands Full of Variety

It is indispensable to select the research subjects according to the needs of times.

(2) Research and Development for Advance of People's Utility

It must be noted that infrastructure implementation and R&D should always be made for users

(3) Research and Development for Environmental Prosperity

It must be noted that construction works should match with the natural condition at the sites, conserve the circumstances, and create better environment.

(4) Research and Development with International Universality

Requests to PWRI for technical cooperation from other countries are significantly increasing in recent years, therefore, it must be noted that the technology development should be the one which can be effectively used all over the world.

(5) Research and Development with Technical Originality

For coping with extremely strict natural and social conditions, such as earthquakes, typhoons and dense population, it has been important in PWRI to devote to original technology development. This is becoming more important so that PWRI can take initiative for leading other countries.

(6) Research and Development for Good

Performance and High Durability

The technical development which enables for constructing structures with superior function and high durability, which need to be left to the next generation, is particularly important.

Based on these basic concepts, there are 9 main research fields with high priority in PWRI.

(1) Effective Utilization of National Land

For achieving further economic growth, it is strongly requested to study the ways for utilizing national land more effectively. The research subjects will include ;

a) Design and construction methods for expressways, super-long bridges and tunnels which cross sea narrows and connect inner islands.
b)Utilization of large depth underground space
c)Development of new water resources and water supply systems

(2) Disaster Prevention

Large cities in Japan need to keep durability against natural disasters because it is the key for economic growth. Evaluation of vulnerability, strengthening, proper design, repair and restoration, refuge, disaster information system, and economical secondary effects need to be studied.

Traffic accidents are also serious problem in urban areas. Development of safe traffic systems is urgent issue to be solved immediately.

Aged society has already come. It is required to study for constructing roads with the function for the traffic weakling such as aged, infant, and handicapped.

(3) Technology concerning Global Environment

Protection of global environmental is important all over the world. Japan has the responsibility to lead the environmental conservation. The subjects required to study at PWRI are;

(a) Construction and planning methods for energy conservation
(b) Analysis on the influence of heat island
(c) Analysis on the impact of green-house on climate and natural disaster
(d) Preservation of global ecosystem
(e) Treatment of construction waste
(f) Methods for reuse and recycling of construction waste

(4) Efficiency and Safety in Construction Works

Lack of skilled workers and aging of labors caused various problem in safety of construction. The following studies are required in future ;

(a) Simulation system of construction which provides the designers with simulation of site before initiating construction.
(b)Construction machines and construction methods with easy operation.
(c)Construction machines with energy-saving and reduction of emission gases.

(5) New Construction Materials

New materials used for space station, communication technology and marine technology could be applied for civil engineering. The new material which are expected to be studied are;

(a) Utilization of biology, high polymer material, petro-chemistry, and electronics
(b) Materials which realize free maintenance.
(c) Materials with higher strength and durability than concrete, steel and rock.

(6) Infrastructure Management and Maintenance

Next step required to Japan is pursuing artistic quality of structures. Administration and maintenance methods are becoming important to keep life cycle. The followings will need to be studied ;

(a) Free maintenance and more durability for infrastructure
(b) Construction management and maintenance
(c) Reduction of structural life cycle cost
(d) Designing and maintenance methods of artistic structures

(7) New Frontier of Construction Fields

The universe and undersea space have many unknown space for development as the "New Frontier". New frontier development will contribute to not only solving the population problem and shortage of food but also the conversion of military industries to construction. The following studies are required to be conducted ;

(a) Method for human living
(b) Design methods of space structures
(c) Robotics construction
(d) Construction materials

(8) Construction Management Engineering

Estimating systems for new technology are required to be developed for implementing to construction. Following researches are requested to be made ;

(a) Systematization of construction management
(b) Evaluation and information systems for

new-developed technology
(c) Efficiency in whole processes of construction work

(9) International Research Cooperation

Basic and initiative researches are strongly requested from other countries. It is required to develop much more original technology in PWRI, and open such technology to the world. The world-wide researches such as disaster mitigation and global environmental problem demands the research network extending to all over the world. PWRI needs to promote for formulating such networks. For the technical cooperation with other countries, PWRI promotes to study the planning and construction methods which are consistent with the natural and environmental condition of the countries. Dissemination of technical information needs to be made more effectively.

4.3 Research Needs in Wind and Seismic Effects

The above Research Theme for Needs of Time may be break down in the wind and seismic effects area as :

(1) Technologies which enables construction of super-long span bridges

Research and developments which have been so far made for long-span bridges were compiled for constructing the Honshu-Shikoku Bridge Projects. In facts, the researches and developments made at PWRI were the core of technologies which enabled the construction of Honshu-Shikoku Bridges. They were also effectively used for constructing other long-span bridges, and for formulating codes and standards for ordinary bridges.

For effectively using national land, there are many projects in which super-long span bridges are included as the core structures. Because the Honshu-Shikoku Bridges are constructed at the most moderate sites in wind and seismic effects in Japan, design and construction methods which enables to withstand the bridges against more strict wind and seismic environment are required. More technical development for wind and seismic effects to those structures is required for realizing those projects.

In wind engineering, reduction in deformation due to wind load and increase in flutter speed are most important. In order to reduce the deformation, stiffening deck with small drag coefficient should be selected or developed. New cable arrangement might be necessary to carry some part of drag force on stiffening deck.

In order to increase flutter speed, cross section of stiffening deck should be improved in view point of aerodynamics and torsional rigidity. Arrangement of cables and hangers should be improved to increase torsional natural frequency. New active control devices, which change flow pattern around the bridge deck so that flutter may not take place, might be required.

In seismic design, more rational design methods taking nonlinear dynamic response of foundation into account are required. Because the foundations need to be constructed at deep sea and on faults with the earthquake magnitude as large as 8, proper evaluation of seismic safety is essential. Seismic design considerations for new type of foundations needs to be developed.

Research and development for new and advanced technologies which enable to introduce the progress of science and technology are required in earthquake engineering. Those will include the passive and active control technology.

(2) Technologies for mitigating urban disasters

Concentration of population in urban areas is increasingly progressing. Significant progress of the information and computer systems have changed economic and social systems. Industrial structures have already shifted from 1st and 2nd to 3rd. New types of structures which are of buildings, bridges and underground structures are being increasingly constructed. Water-front developments require construction of many artificial lands vulnerable to soil liquefaction. Propagation of fire and inundation due to damage of river dykes are serious problems. Those developed high risk and vulnerability against an extreme earthquake in urban areas.

Comprehensive researches are required for decreasing such new type of risk in urban areas. The core researches may include ;

(a) Main transportation network
Transportation and utilities are the most critical lifelines in urban area against earthquake disaster. Researches are required for mitigating suspension of traffic and evacuation at road network. Countermeasures to utility systems are also important. Technologies of seismic strengthening for overcrossings and high road embankments in urban areas are critically important. Technologies for strengthening cut and filled slopes, river and coastal dykes and road slopes are indispensable.

(b) Improvement of seismic safety of ground
Technologies for upgrading seismic safety of soft alluvial deposits, reclaimed land and boundary zone from soft to hard soils are required. Special attention needs to be paid to soil liquefaction because many water-front projects are being executed on reclaimed land constructed

by filling weak saturated sand vulnerable to liquefaction.

(c) New type of structures
New types of structures which have not yet experienced damage in the past earthquakes are increasing in urban areas. Research for such new types of structures is indispensable.

(d) Tsunami
Tsunamis developed a large number of loss of lives. Further investigations are required for tsunami water pressure, height and propagation.

(e) Warning, evacuation and disaster information systems
Appropriate warning and evacuation systems using advanced technologies are required. Disaster information systems which enables to notice the danger prior to the failure is required. Because number of aged residence and foreigners who do not understand primary language is increasing, an appropriate measure for such new change is required.

(f) Social and economic effects of disasters
Social and economic impact of disasters require more attention, especially in urban areas. Indirect economic damage sometimes far exceeds the physical property damage in urban areas. Spreading mechanism of the physical damage and interaction of indirect effects between lifeline facilities are expected to be investigated.

4.4 System for Efficient Research and Development

For conducting research effectively various systems are implemented in PWRI. The first is the establishment of 5-years Research Program for clarifying research goal and scopes with priority of the technical developments in a period of next five years. The re-evaluation of the 5-year Research Program is made sat an appropriate interval.

The second is the encouragement for original researches. In addition to the problem-oriented researches, basic researches which are free from the restriction of time and budget are also encouraged. Great discovery in the field of basic research is expected.

The third is the appropriate modification of the research systems and organizations in accordance with the change of social and economical needs. It is important that the organizations and systems be flexible for the change of "needs of time".

The fourth is the expansion of research networks. In Japan, researches are being made not only in universities but at private companies. Researches for practical subjects are made in private companies while researches for more basic subjects are made in universities. Therefore, it is required at PWRI to make a research network with the university and private companies so that overall research including from fundamental to problem-oriented researches be made with collaboration with various organizations. The research network needs to be expanded all over the world. The Panel on Wind and Seismic Effects, UJNR, has been the most important channel with U.S.A. as the research network. PWRI wishes to become one of centers for implementation of international cooperation in Public Works Research and Development.

5 CONCLUDING REMARKS

The role of the Public Works research Institute was overviewed in the scope of the progress of civil engineering and its contribution to economic and social development in modern Japan. Future perspectives of the research required at the Public Works Research Institute based on the recent trend of Japanese economic and social changes was also presented with emphasis on the research requirements on wind and seismic engineering.

The Public Works Research Institute has been leading technical development for infrastructures improvement. Because it seems to have more siginificant changes in the future in various areas including environmental and urban problems, it is significantly important to initiate new and advanced technical developments with clear priority based on the needs of the time. This is believed to be the way for contributing to the technical developments required for improving quality of life all over the world.

REFERENCES

Sumiyoshi, Y., Suzuki, K. and Hirabayashi, K. : Progress of Civil Engineering and Its Contribution to Economic and Social Development in Modern Japan, Technical Memorandum, No. 3188, Public Works research Institute, 1993

Table 1 Large Projects and Projects for Stimulating Local Districts

PROJECT	CONTENTS
Ring Roads Around Tokyo Metropolitan Area	includes Tokyo Bay Road, Trans-Tokyo Bay Road
New Kansai International Airport	at offshore of Osaka Bay
Honshu-Shikoku Bridges	connects Honshu and Shikoku by 3 routes Akasi Strait Bridge becomes the longest suspension bridge in the world
Seikan Tunnel	connects Hokkaido and Honshu the longest undearsea tunnel in the world
Tohoku Shinkansen	connects Tokyo and Tohoku region
Joetsu Shinkansen	connects Tokyo and Japan Sea across the Honshu Inland by Shinkansen
Kan-Etsu Expressway	connects Tokyo and Japan Sea across the Honshu Island
Tohoku Expressway	connects Tokyo and Tohoku region

Table 2 .Effect of Social and Economic Development by Constructing New Expressway

Access from an Interchange of New Expressway	Area within 30 minutes	Area More Than 30 Minutes
Increase of Population	3.7%	0.9%
Customable Production	44.6%	37.8%
Manufactured Shipment	38.5%	31.0%
Retail Selling Price	48.4%	42.1%

Table 3 Five Stages of Technical Development in Civil Engineering in Japan

1st stage	1st Introduction of Foreign Technology (1868～1887)
2nd stage	Reform of the Introduced Technology (1888～1912)
3rd stage	Technological Stagnation (1913～1945)
4th stage	2nd Introduction of Foreign Technology (1946～1964)
5th stage	Developement of Original Technology (1965～)

Table 4 Invited Engineers and Their Contribution

INVITED ENGINEERS	ACHIEVEMENTS
J.England (U.K.) J.England (U.K.) T.Gray (U.K) Engineer From Holland	Ishiyagawa Tunnel Sumiyoshigawa Tunnel Ashiyagawa Tunnel Kuriko Tunnel
Vogel (Holland) Branton (U.K) Holt (U.S.A.) Paul, White (U.K)	Kurogane bridge Yoshida bridge Toyohira bridge Mukogawa bridge
Engineers of American company Engineers of American company	Ooi Dam (Kisogawa river) Komaki Dam (Syokawa river)
C. J. Van Doorn (Holland) J. De Rijke (Holland) H. L. R. (Holland) I.A.Lindow (Holland)	Imp. of Tone river, Asaka Canal Imp. of Kiso, Yodo river, etc. Tone Canal Imp. of Shinano river

Table 5 MOC Support Systems for Encouraging Research in Private Companies

Comprehensive R&D Prject for Construction Technology with Private Sectors
Government / Private Sector Joint R&D Project
PWRI R&D Program for Private Sectors to Join PWRI's Research
PWRI Program to Accept Researchers of Private Sector
Evaluation System for Advanced Technology Developed by Private Sectors
Pilot Construction Works Program to Implement Developed Technology

Table 6 Main Natural Disasters Developed in 20 Years after the World War II

DATE	NAME OF NATURAL DISASTER	NUMBER OF KILLED AND MISSED
1946	Nankai Earthquake	1330
1947	Catherine Typhoon	1930
1948	Fukui Earthquake	3769
1948	Iona Typhoon	838
1958	Kanogawa Typhoon	1269
1959	Isewan Typhoon	5041
1964	Niigata Earthquake	25

Table 7 History of Seismic Design Codes of Bridges in Japan

Year	Name of Regulations	Seismic Design Methods	Other Stipulations for Seismic Effects	Major Earthquakes
1886	Order No. 13, Ministry of Internal Affairs	Not Considered	Not Considered	1881 Nohbi (M8.4) 1923 Kanto (M7.9)
1926	Details of Road Structures (Draft), Road Law, MIA	Seismic Coefficient Method k_H=0.15~0.4 ($k_H \geqq 0.3$ advised in Tokyo and Yokohama)	Not Considered	
1939	Design Specifications of Steel Highway Bridges (Draft), MIA	Seismic Coefficient Method (k_H=0.2, k_V=0.1)	Not Considered	1946 Nankai (M8.1) 1948 Fukui (M7.3)
1956 (and 1964)	Design Specifications of Steel Highway Bridges, Ministry of Construction	Seismic Coefficient Method (k_H=0.1~0.35)	Not Considered	1952 Tokachi-oki (M8.2) 1964 Niigata (M7.5)
1971	Specifications for Seismic Design of Highway Bridges, MOC	• Seismic Coefficient Method (k_H=0.1~0.24) • Modified Seismic Coefficient Method (k_H=0.05~0.3)	• Evaluation of Sandy Layers Vulnerable to Liquefaction • Device for Preventing Falling-off of Superstructure	1978 Miyagi-ken-oki (M7.4)
1980	Part V Seismic Design of Design Specifications of Highway Bridges, MOC	• Seismic Coefficient Method (k_H=0.1~0.24) • Modified Seismic Coefficient Method (k_H=0.05~0.3) • Check of Deformation Capability of RC Piers • Dynamic Response Analysis	• F_L-Method for Evaluation of Liquefaction • Device for Preventing Falling-off of Superstructure	1982 Urakawa-oki (M7.1) 1983 Nihon-kai-chubu (M7.7)
1990	Part V Seismic Design of Design Specifications of Highway Bridges, MOC	• Seismic Coefficient Method (k_H=0.1~0.3) • Check of Bearing Capacity of RC Piers for Lateral Force • Dynamic Response Analysis	• F_L-Method for Evaluation of Liquefaction • Device for Preventing Falling-off of Superstructure	

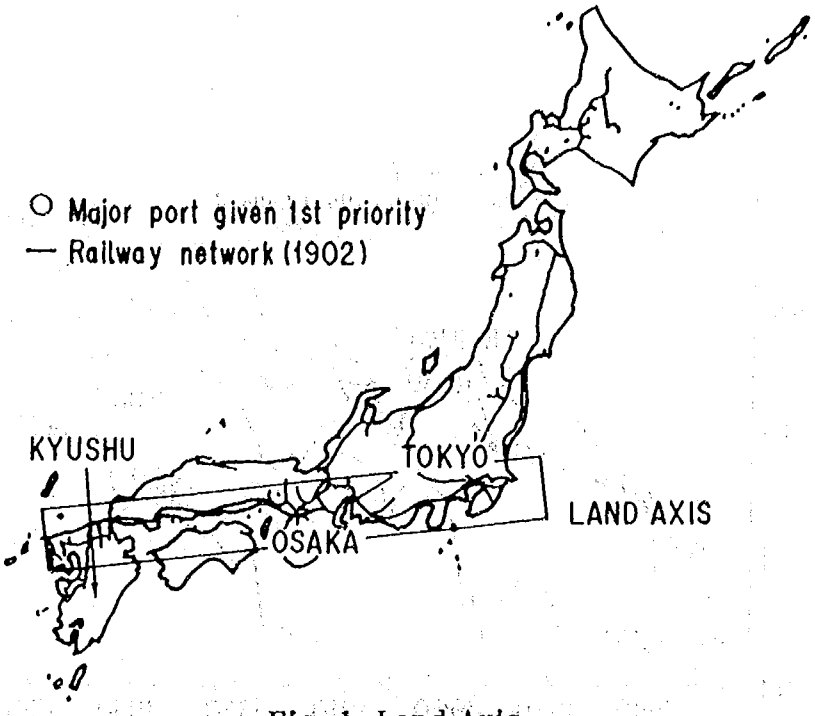
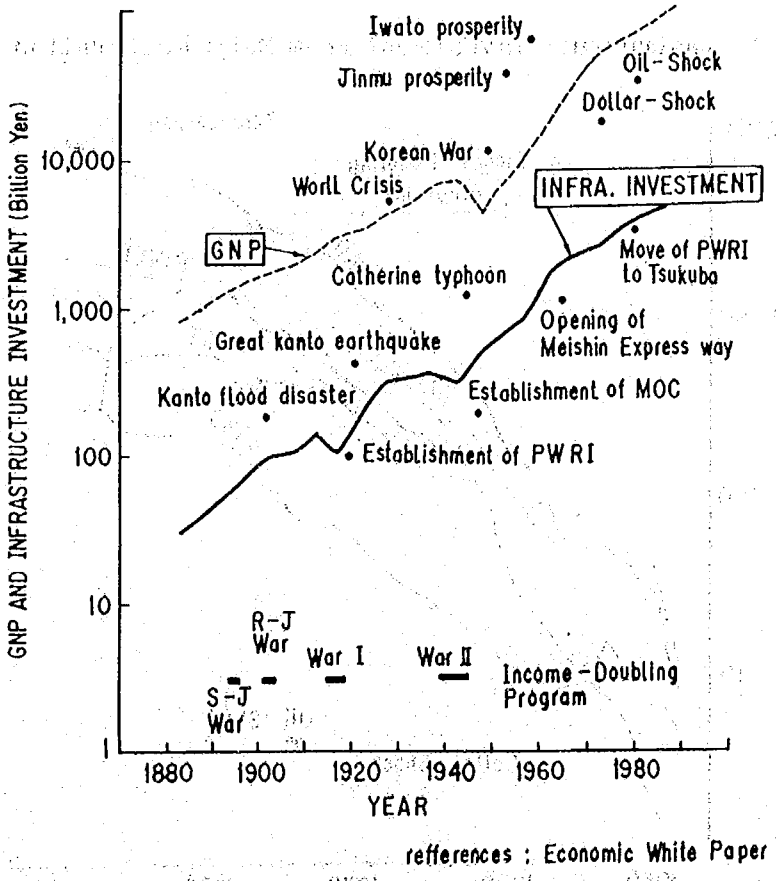


Fig. 1 Land Axis



refferences : Economic White Paper

Fig. 2 Growth of GNP and Infrastructure Investment

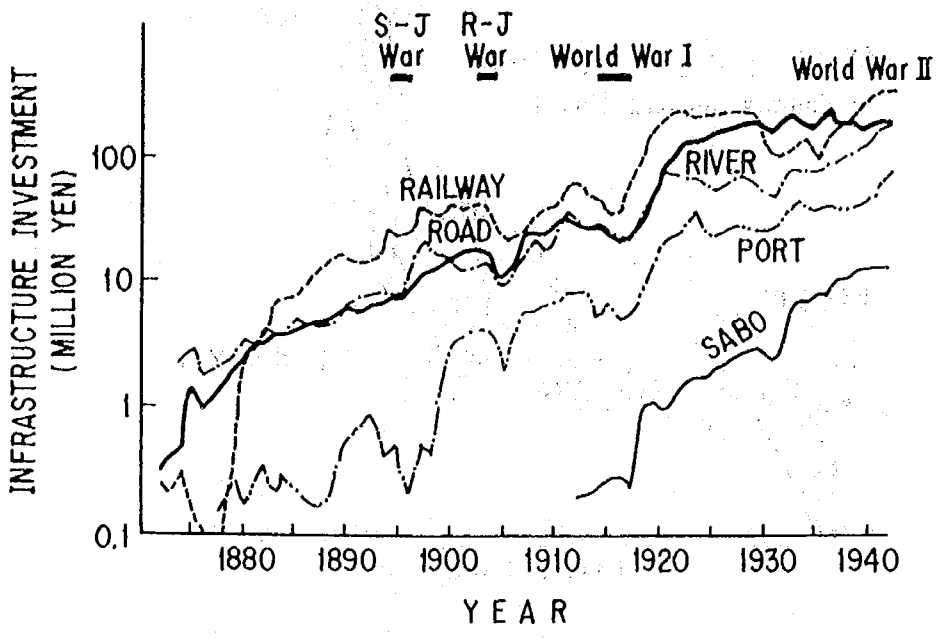


Fig. 3 Growth of Infrastructure Investment from Meiji Restoration to World War II

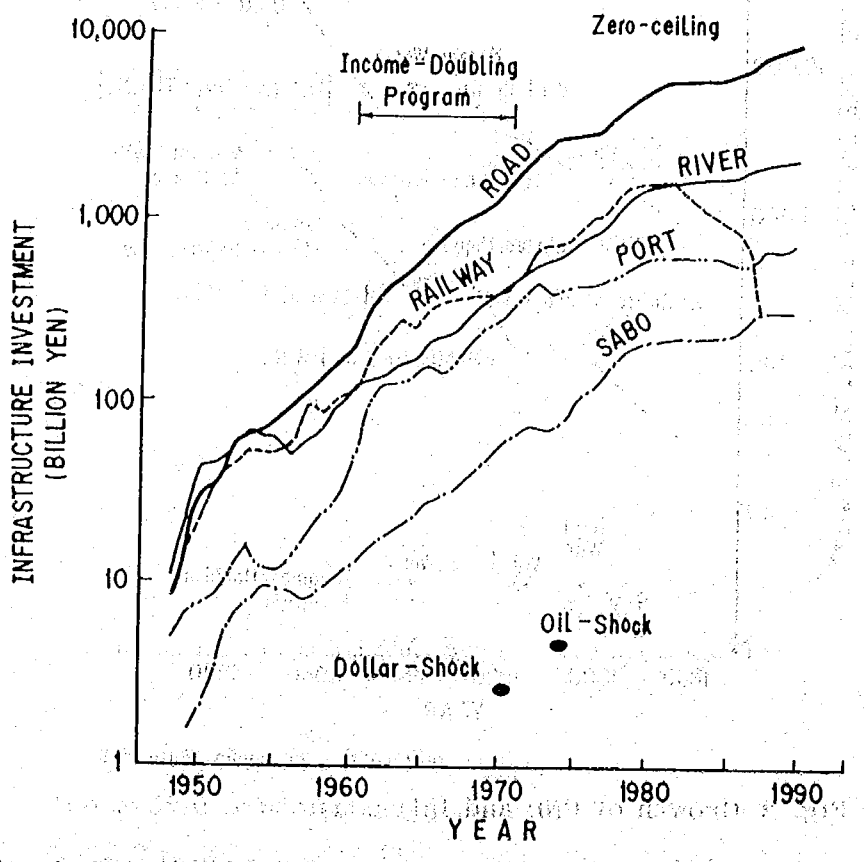


Fig. 4 Growth of Infrastructure Investment after World War II

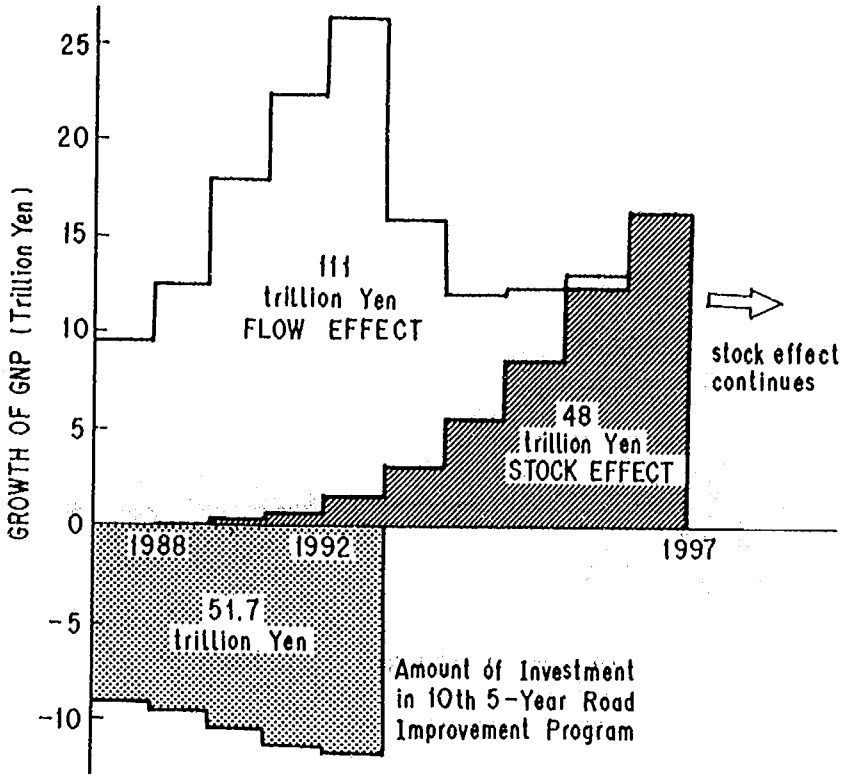


Fig. 5 Growth of GNP by 10th 5-Year Road Improvement Program

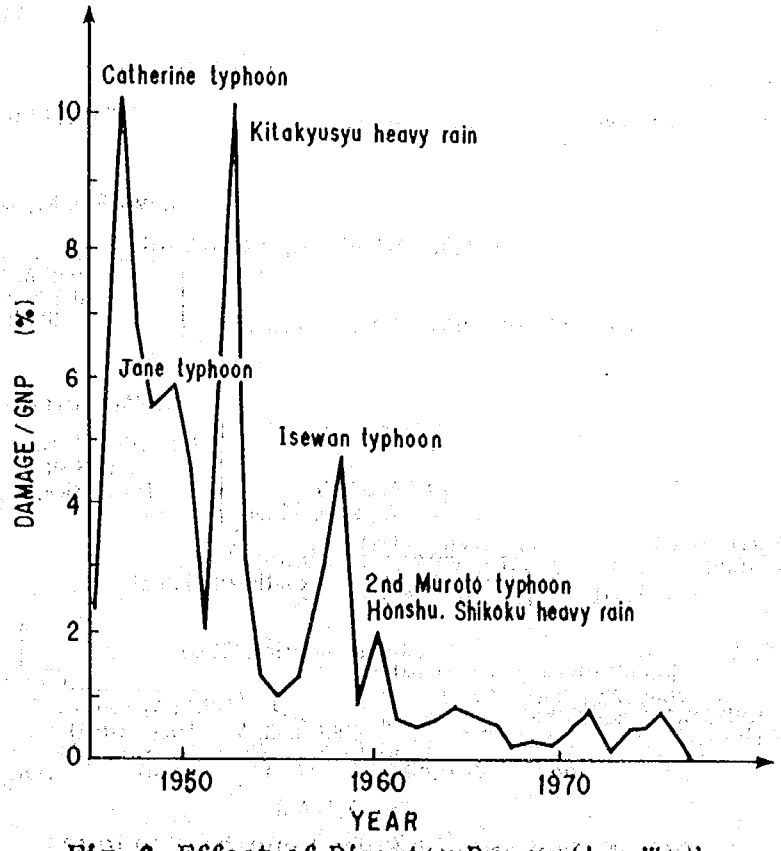


Fig. 6 Effect of Disaster Prevention Works

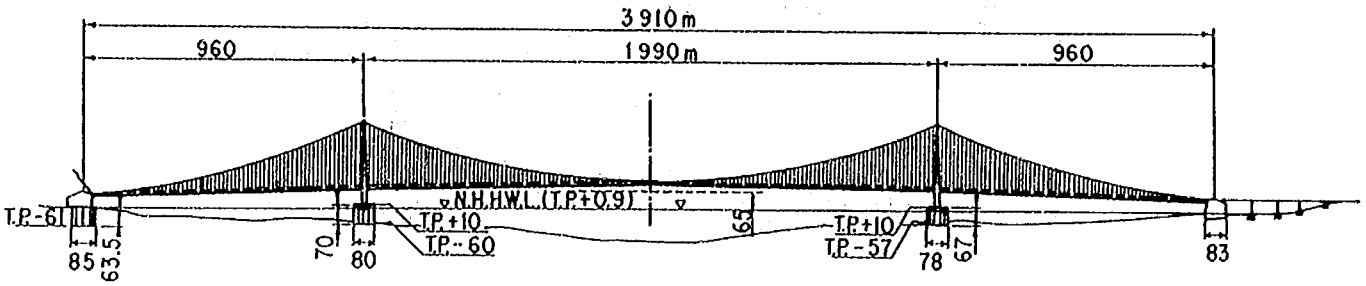


Fig. 7 Akashi Strait Bridge

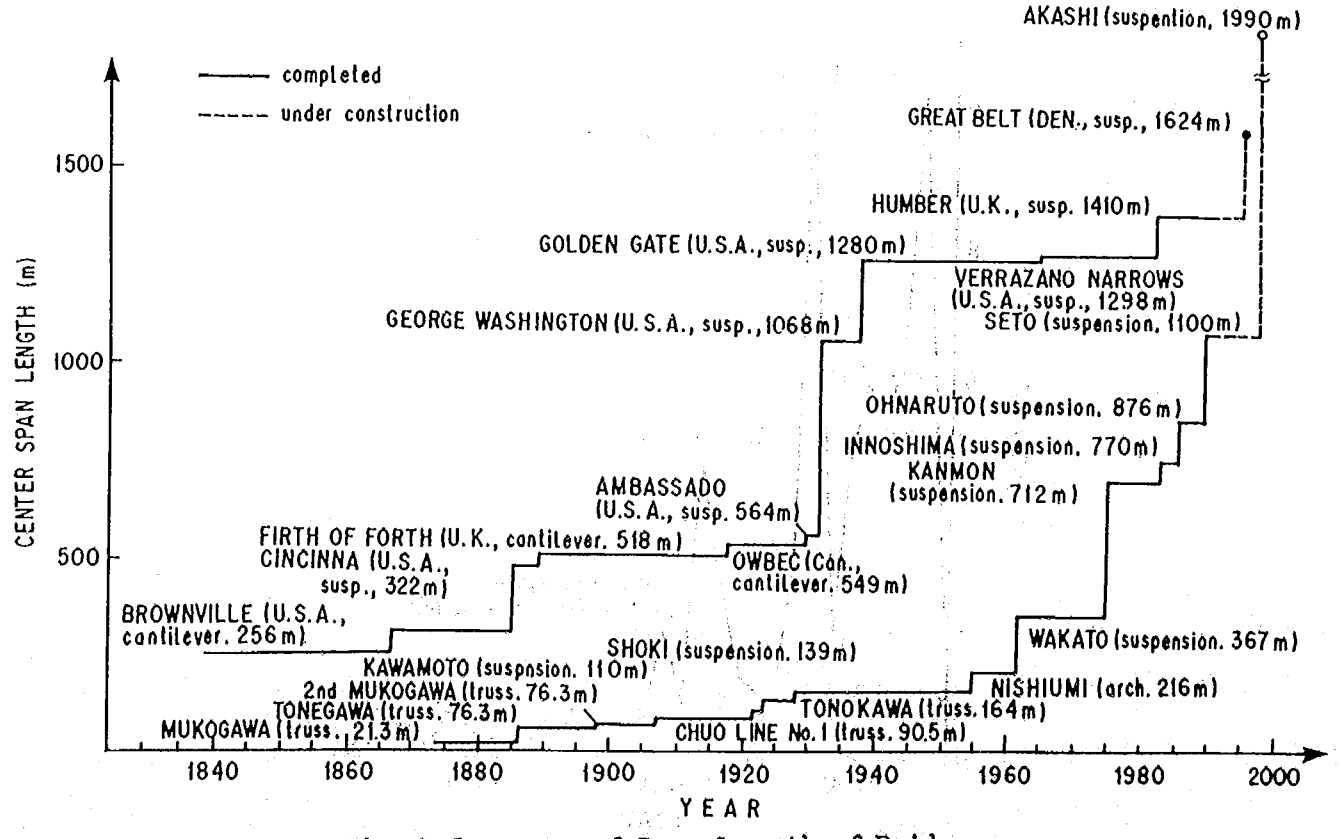


Fig. 8 Increase of Span Length of Bridges

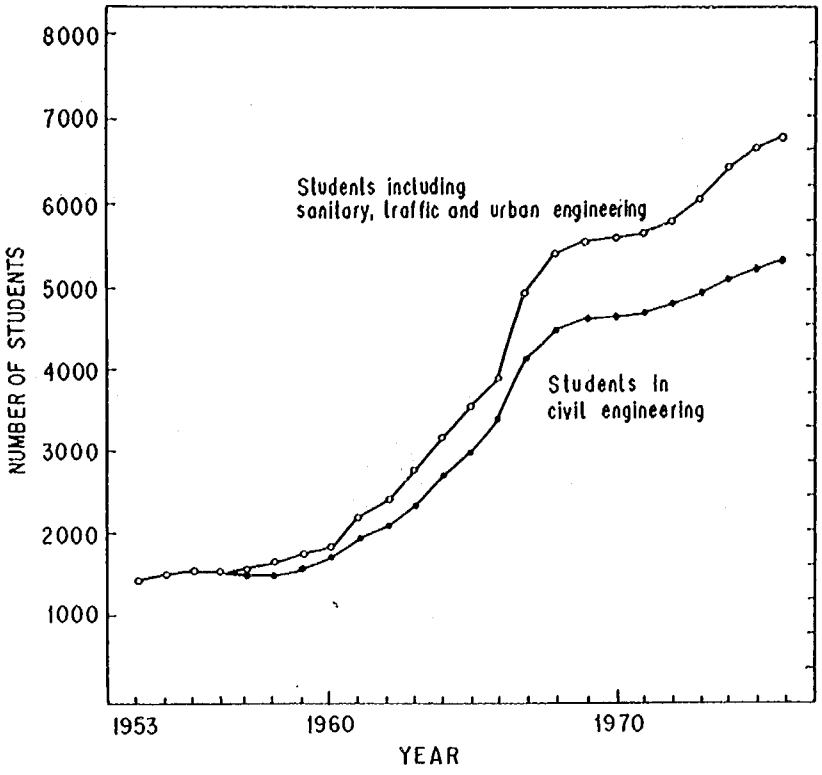


Fig. 9 Number of Students in Civil Engineering

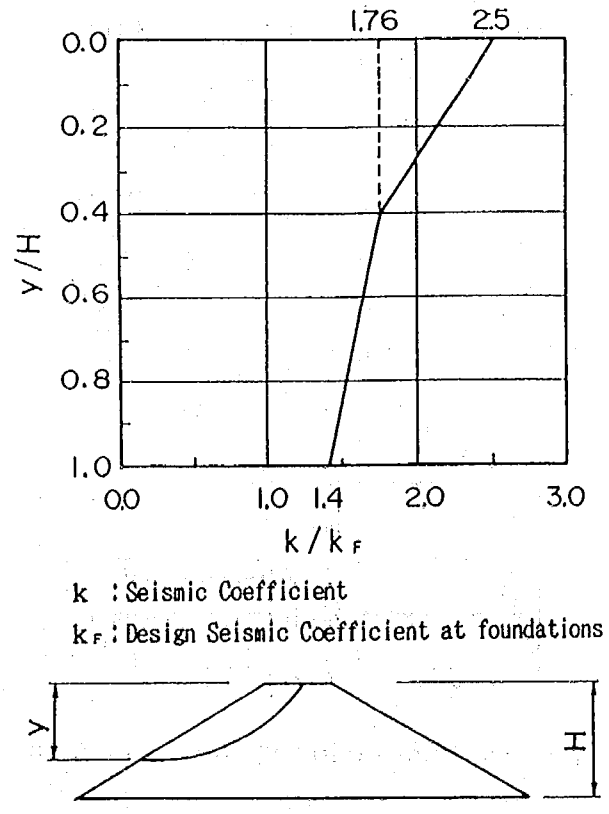


Fig. 10 Seismic Coefficient

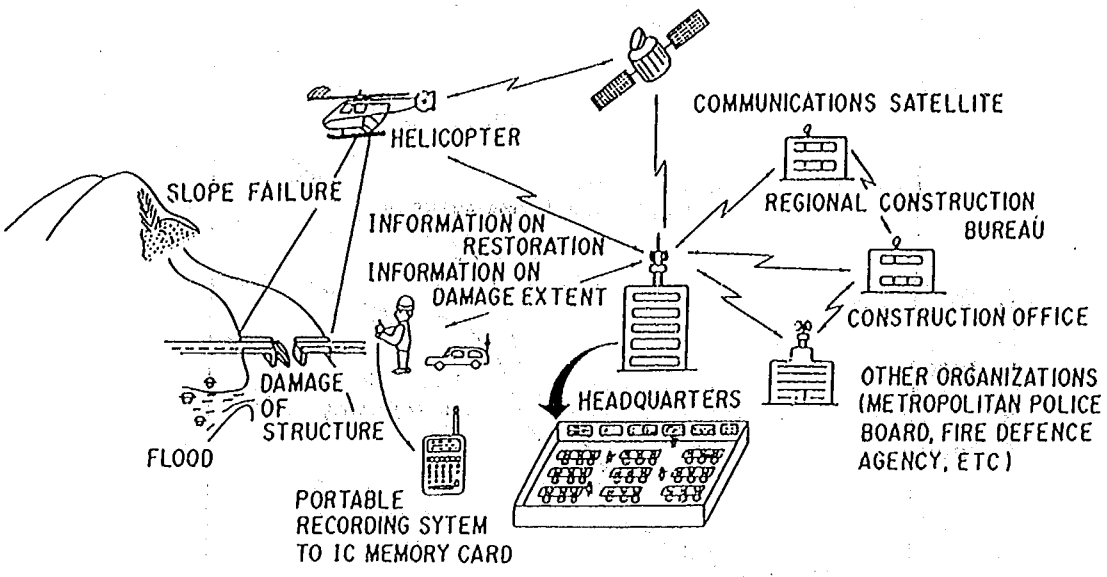


Fig. 11 Disaster Information Systems

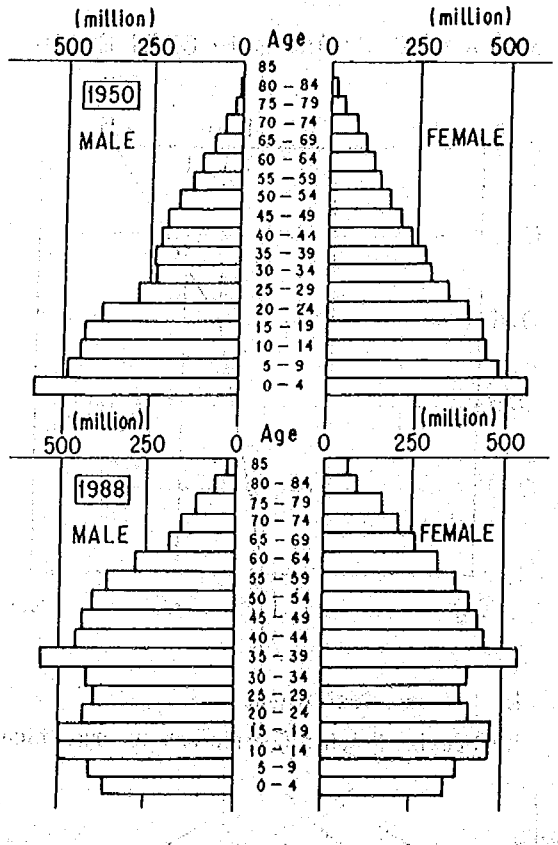
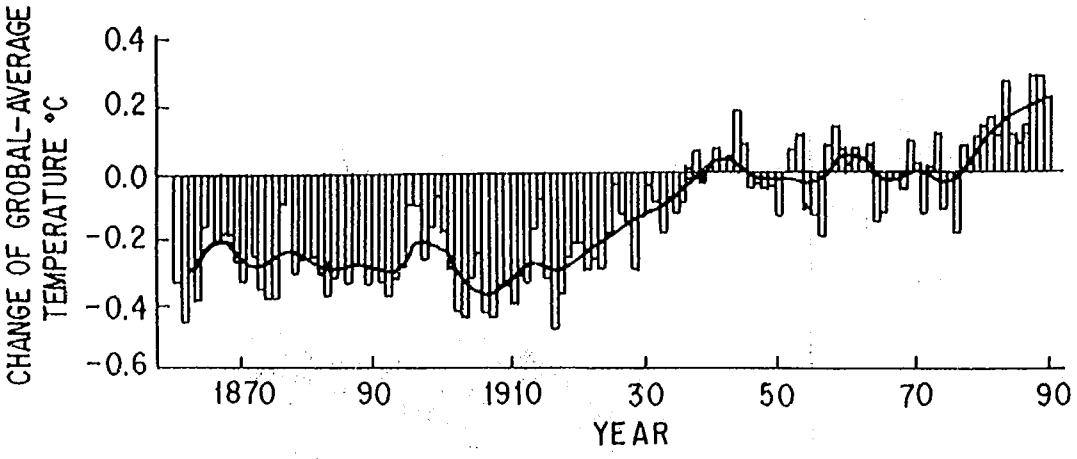


Fig. 12 Population Pyramid in Japan



refferences : Proceedings of IPCC
written by deflection from average of 1951-1980

Fig. 13 Fluctuation of Global Temperature

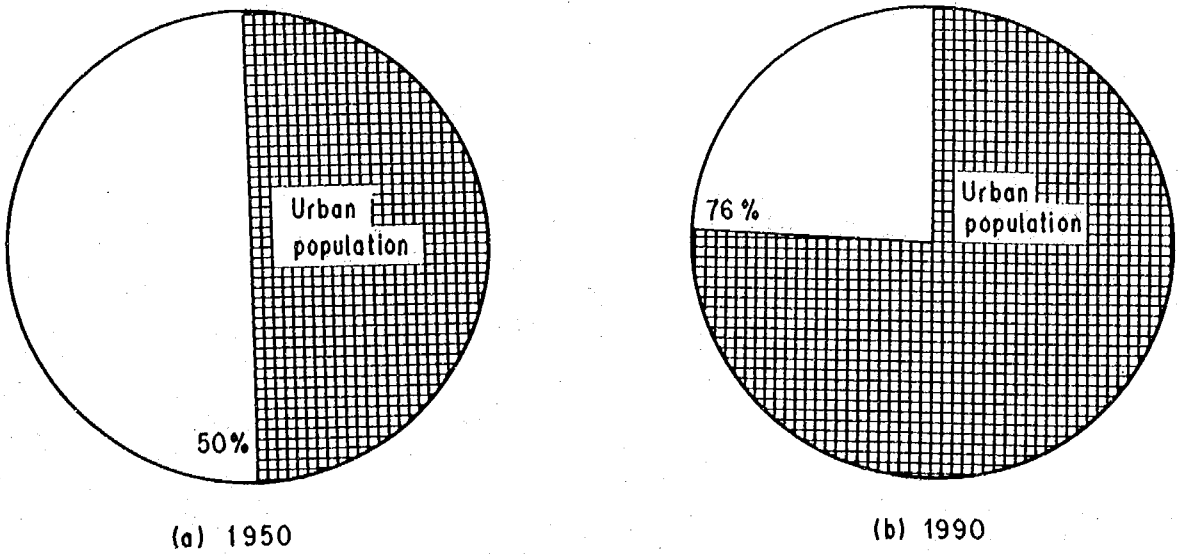


Fig. 14 Urban Population

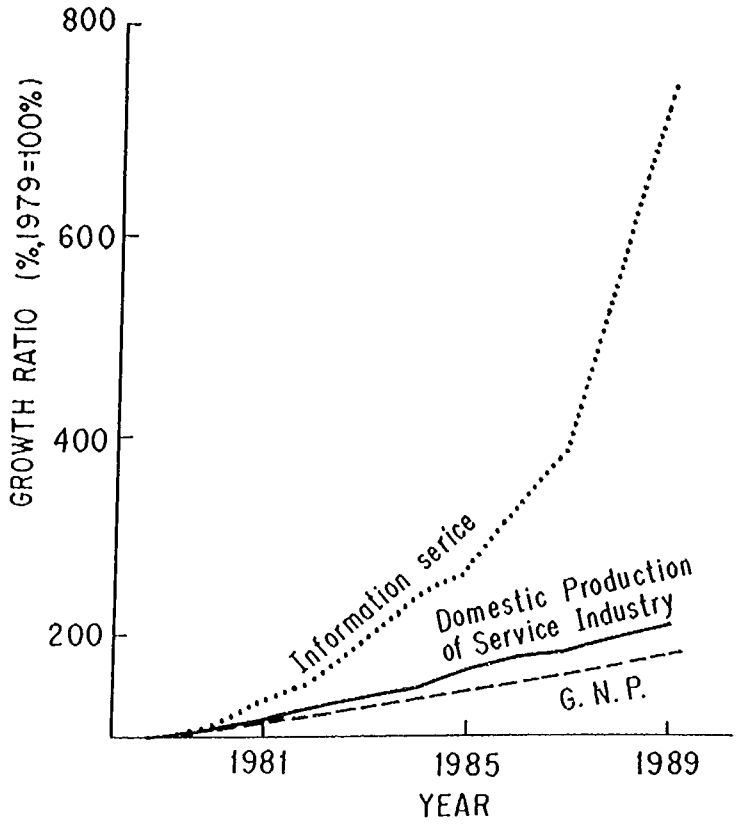


Fig. 15 Sales Amount of Information Service Industry

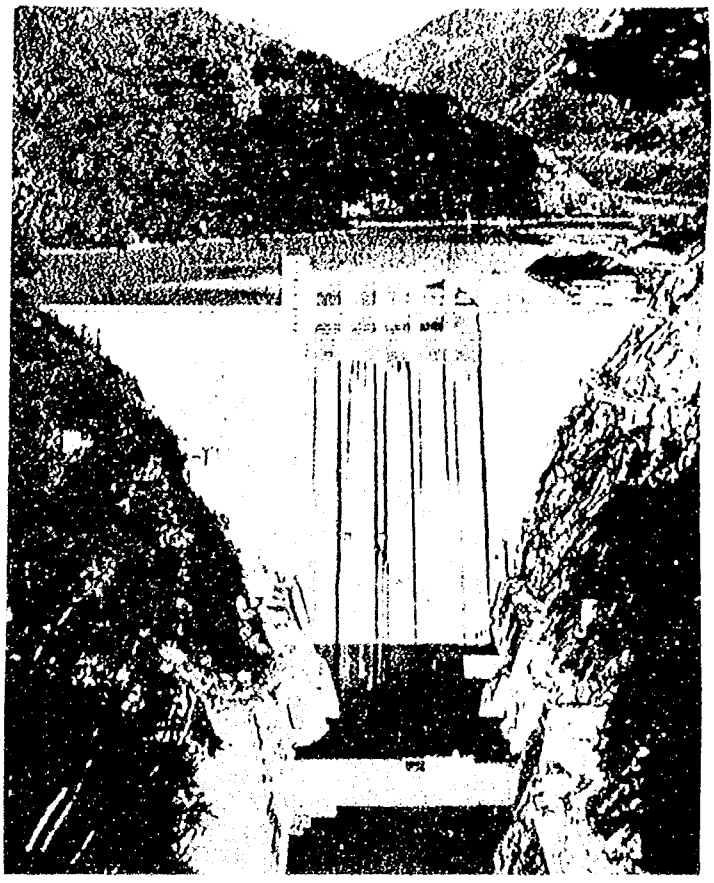


Photo 1 Sakuma Dam

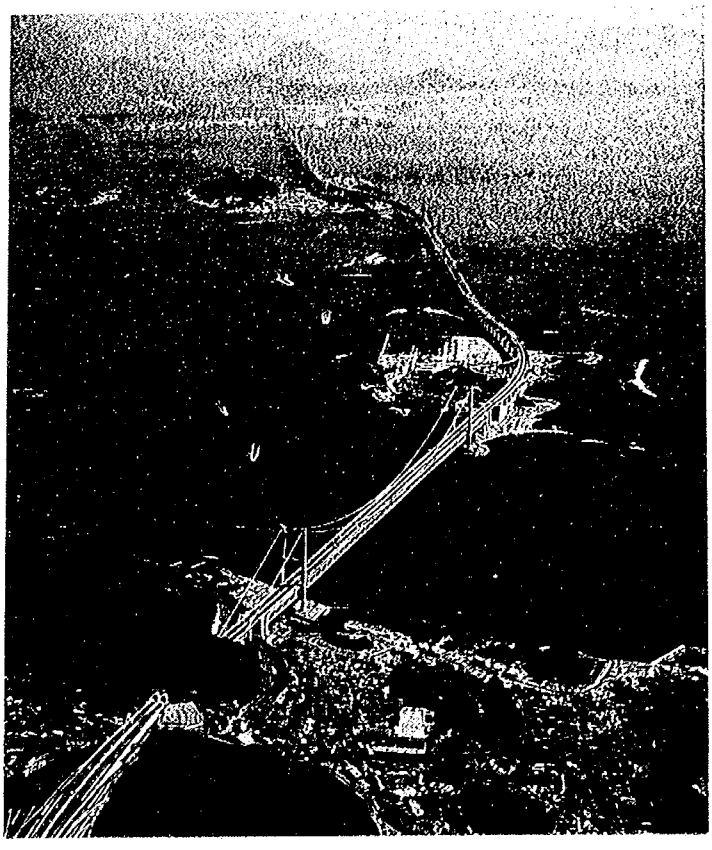


Photo 2 Honshu-Shikoku Bridge (Seto Bridge)

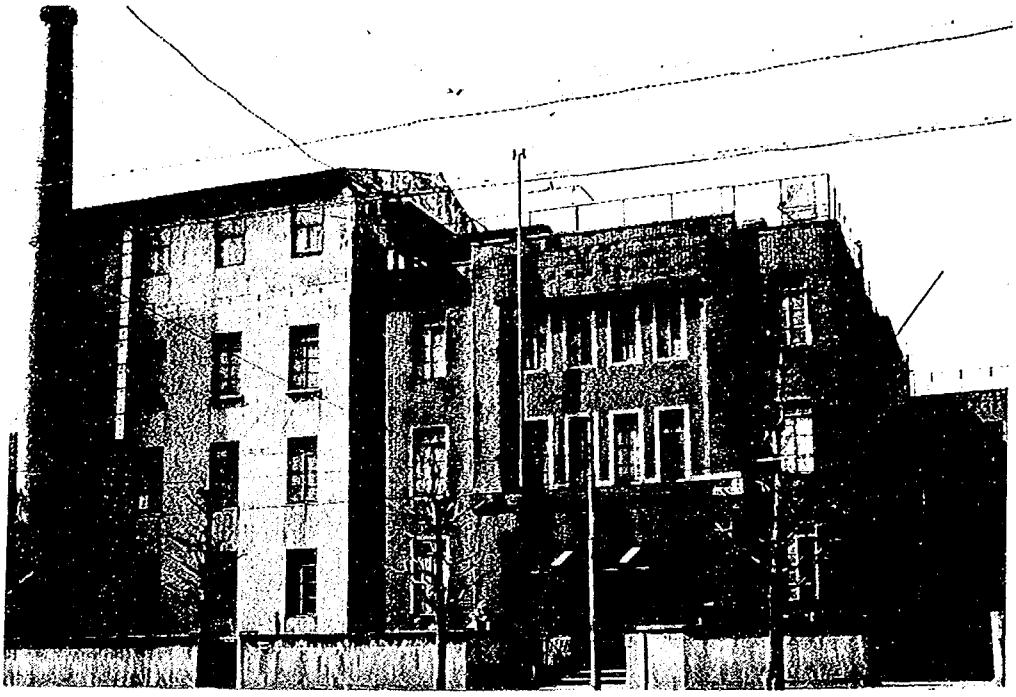


Photo 3 Main Building of PWRI (Komagome, Tokyo)

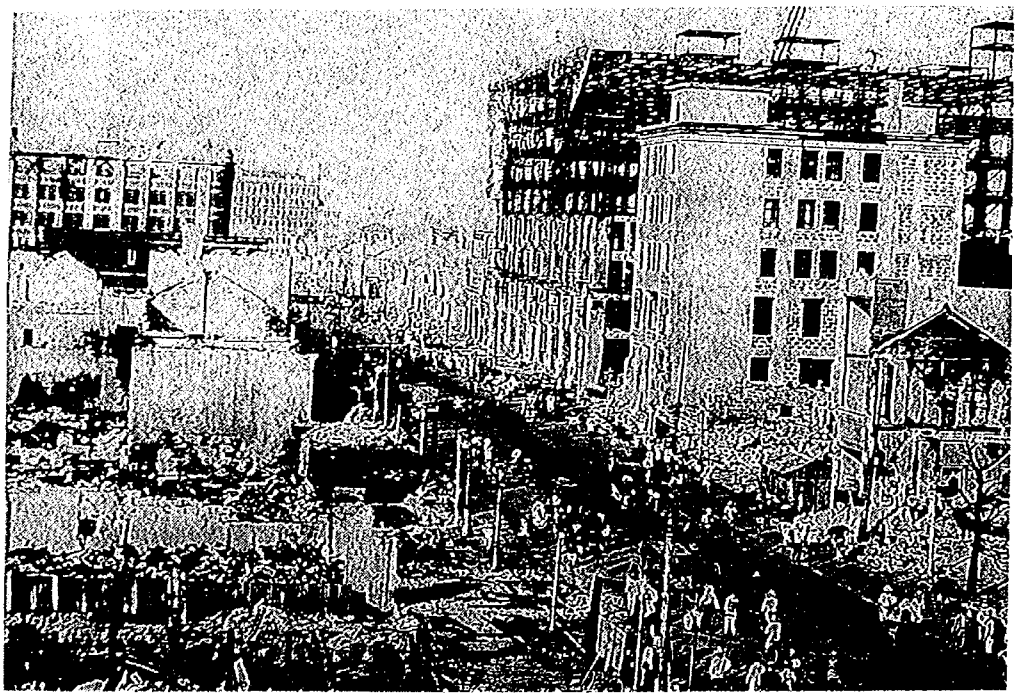


Photo 4 Great Kanto Earthquake (Ginza, Tokyo)



Photo 5 Damage of Showa Bridge by Niigata Earthquake in 1964

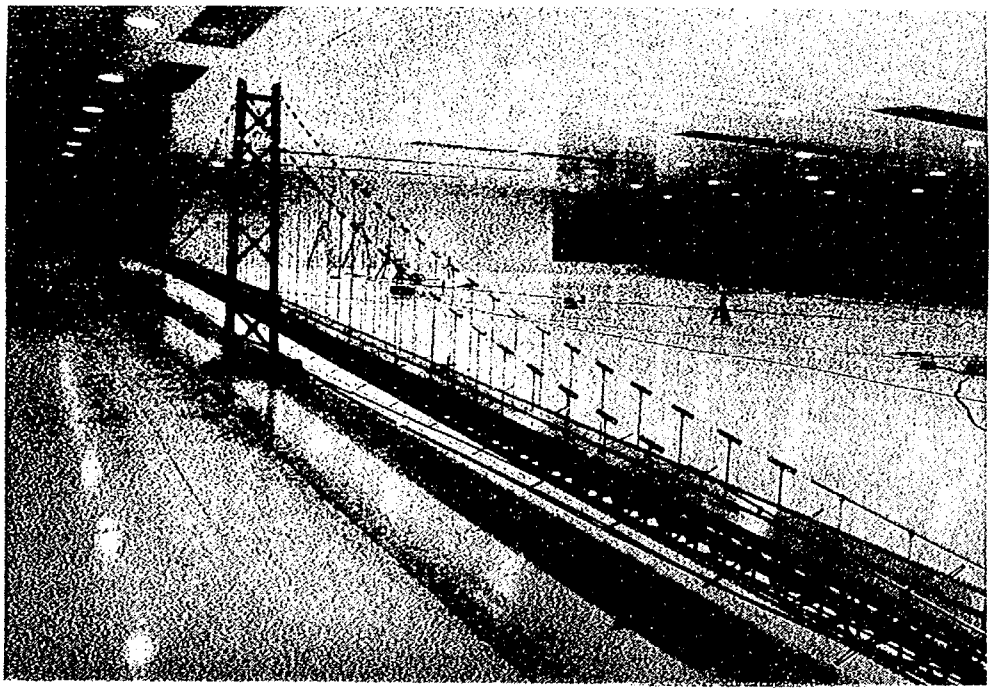


Photo 6 Wind Tunnel Model of Akashi Strait Bridge

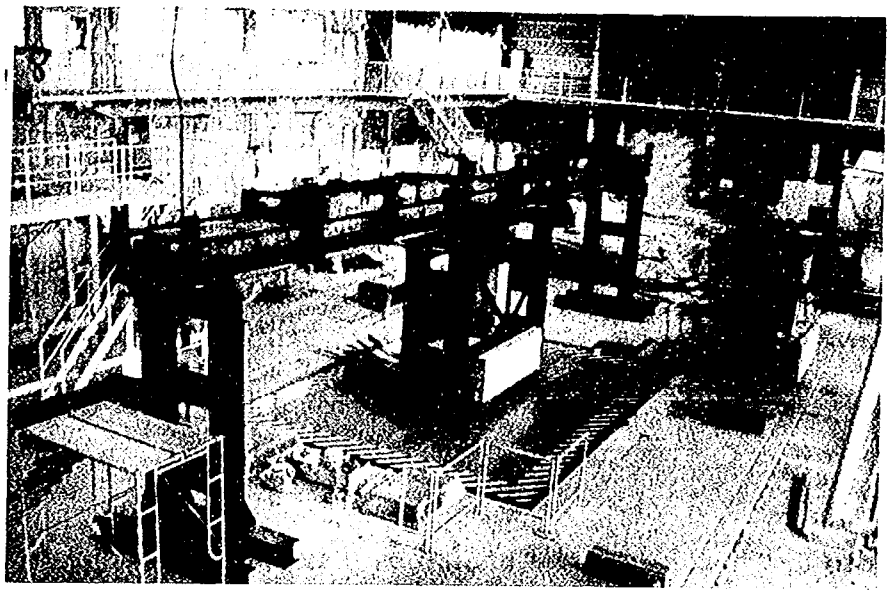


Photo 7 Shaking Table Test for Reinforced Concrete Columns

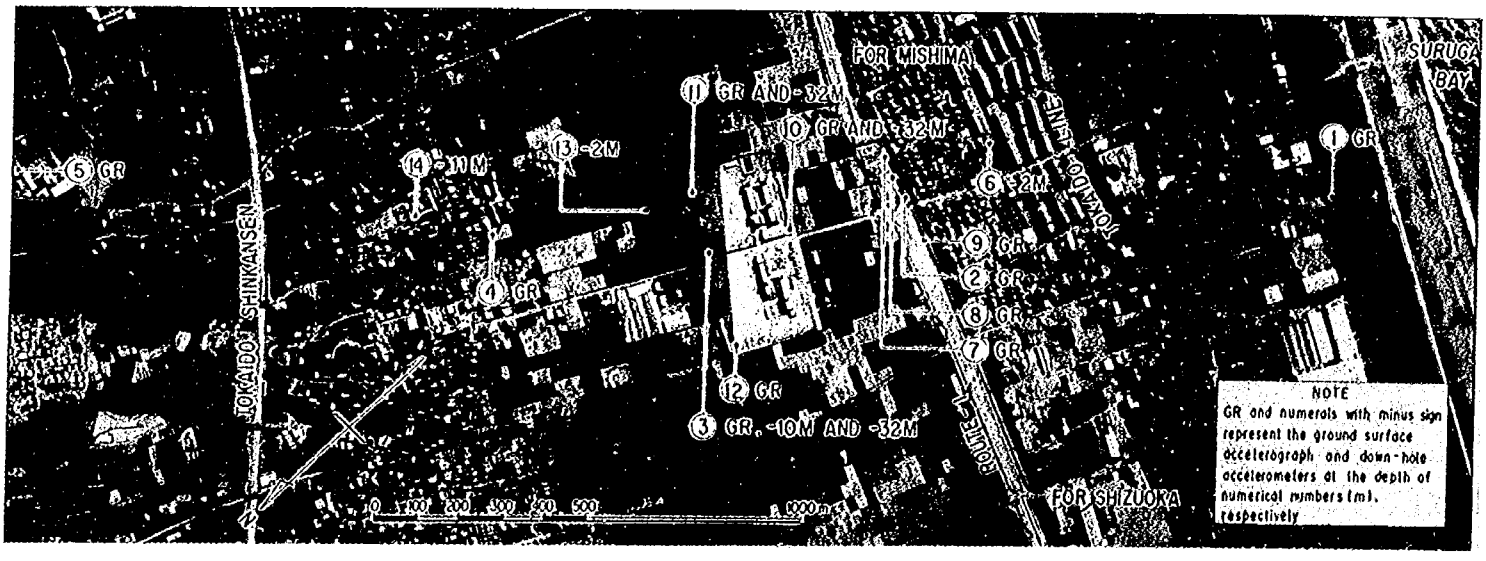


Photo 8 Array Observation at Sagara, Shizuoka Ken



Photo 9 Shaking Table Test for Behavior of Foundation in Liquefying Sandy Soils

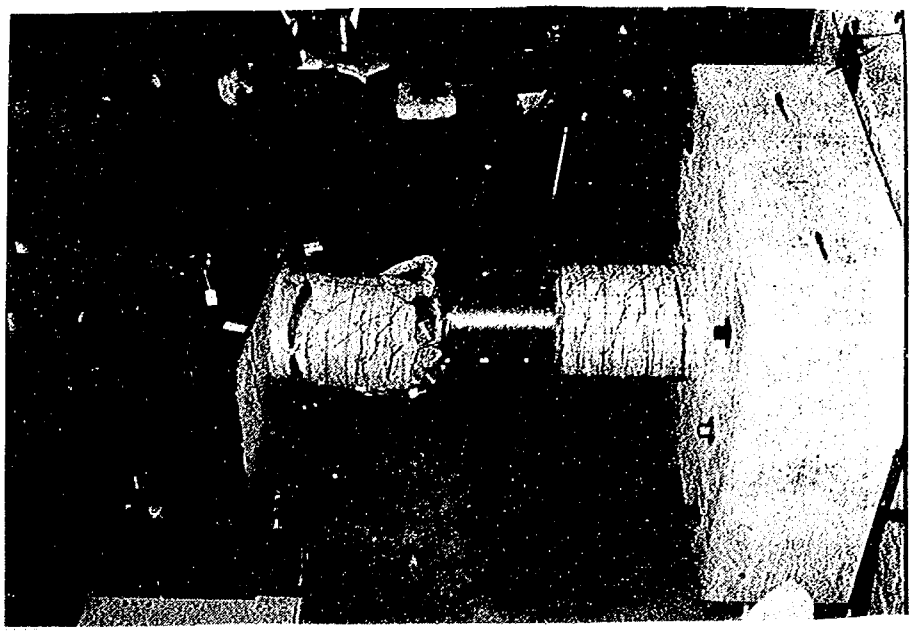


Photo 10 Dynamic Loading Test for Strengthening of Bridge Columns by Means of Steel Jacket

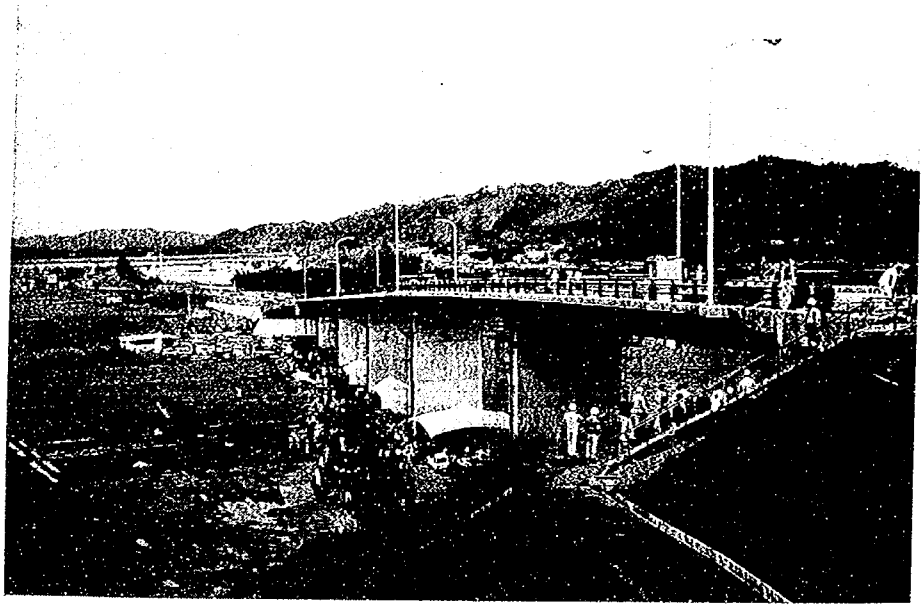


Photo 11 Forced Excitation Test of Menshin Bridge
(Yama-Age Bridge, Tochigi-ken)

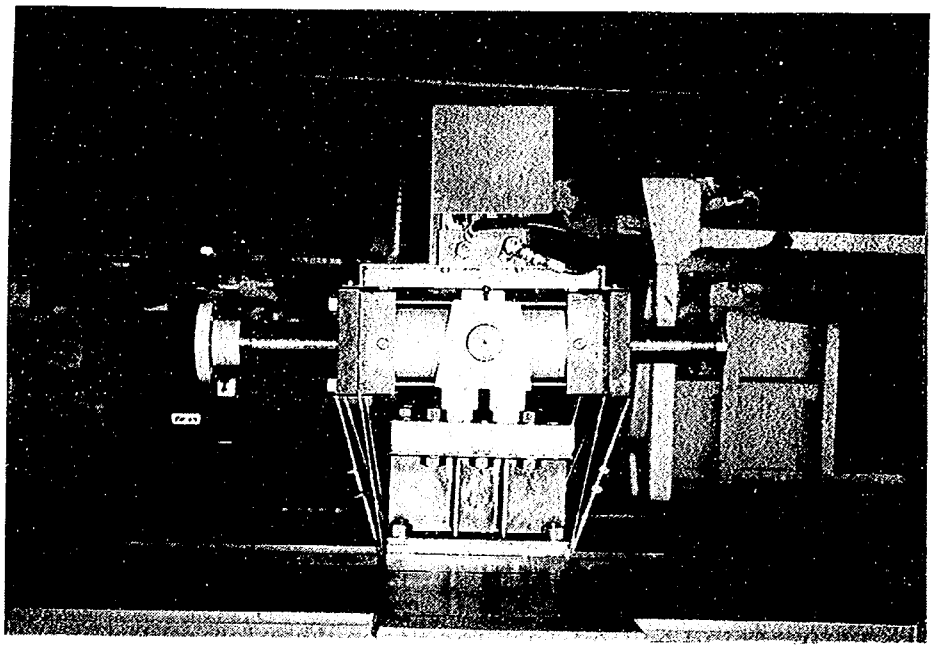


Photo 12 Variable Damper

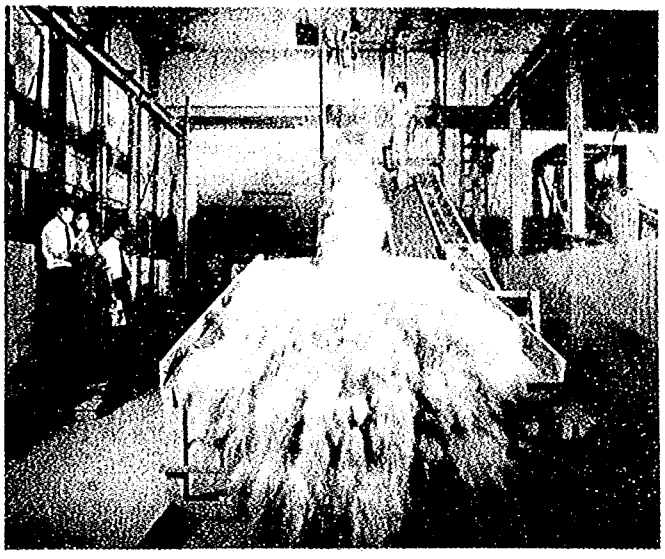


Photo 13 Experiment of Pyloclastic Flow



Photo 14 Deposition Area of the Pyroclastic Flow on June 3



Photo 15 Scattered Concrete Blocks at Minehama Coast
(Nihon-kai-chubu Earthquake)

Performance Based Seismic Design and Evaluation Criteria

by

Jim Hill*
Robert P. Kennedy**
Stephen A. Short***
Thomas A. Nelson and Robert C. Murray****

ABSTRACT

Seismic design and evaluation criteria are based on probabilistic performance goals for Department of Energy [DOE] facilities across the United States. These criteria, as given in UCRL-15910, "Design and Evaluation Guidelines for Department of Energy Facilities Subjected to Natural Phenomena Hazards" [1] utilize probabilistic seismic hazard curves for specification of earthquake loading combined with deterministic response evaluation methods and permissible behavior limits. Through the use of such a design/evaluation approach, it may be demonstrated that there is high likelihood that probabilistic performance goals can be achieved. These criteria have been described in previous technical papers. The purpose of this paper is to present proposed modifications to DOE seismic design and evaluation criteria. These modifications account for various slopes of seismic hazard curves, make corrections to earlier versions, and take advantage of an improved quantitative basis for the acceptance criteria.

1. INTRODUCTION

Design and evaluation criteria in UCRL-15910 are intended to apply equally to the deign of new facilities and to the evaluation of existing facilities. In addition, the criteria are intended to cover design and evaluation of buildings, equipment, piping, and other structures for earthquake, extreme wind, and flood. Only the seismic criteria from UCRL-15910 are discussed in this paper. These criteria are deterministic procedures that establish earthquake loadings from probabilistic seismic hazard curves; specify acceptable methods for evaluating response to these loadings; provide acceptance criteria to judge whether computed seismic response is acceptable; and provide detailing requirements. The criteria include specified earthquake hazard annual probabilities from which the design/evaluation basis earthquake (DBE) is established combined with response evaluation methods, acceptance criteria, and ductile detailing provisions with controlled intentional levels of conservatism based on the target probabilistic performance goals as illustrated in Figure 1.

2. PERFORMANCE GOALS AND CATEGORIES

There is a wide variety of DOE facilities ranging from normal industrial and office buildings to unique and expensive processing and testing facilities to facilities containing significant quantities of radioactive or toxic materials. Requirements for earthquake mitigation at DOE facilities are established within a graded approach in order to provide the appropriate level of seismic protection for:

1. Working in safe locations
2. Minimizing property loss
3. Assuring essential operations
4. Protecting the public and environment from hazardous materials.

A graded approach in one in which seismic design, evaluation, and construction requirements have varying conservatism and rigor. For DOE, the graded approach is implemented by defining four performance categories each with a qualitative performance goal for behavior (i.e., maintain structural integrity, maintain ability to function, maintain confinement of hazardous materials) and a quantitative target probabilistic performance goal, P_F (expressed as an annual probability of exceedance of acceptable behavior limits [i.e.,

* U.S. Department of Energy, Washington, D.C. 20585
** RPK Structural Mechanics Consulting, Yorba Linda, California 93686
*** EQE Engineering Consultants, Irvine, California 92715
**** Lawrence Livermore National Laboratory, Livermore, California 94550

behavior limits beyond which damage/failure is unacceptable]). Performance goals for each performance category are presented in Table 1.

One of the proposed modifications to UCRL-15910 is to use performance categories for individual structures, systems, and components (SSCs) which replace usage categories for facilities. This change has been made such that all categorization guidance and criteria is removed from UCRL-15910 and placed in a performance categorization criteria DOE Standard. General Use, Important or Low Hazard, Moderate Hazard, and High Hazard usage categories have been replaced by Performance Categories 1, 2, 3, and 4, respectively. In addition, performance goals and the associated criteria apply to individual SSCs rather than entire facilities.

UCRL-15910 provides four sets of NPH design and evaluation criteria, one for each performance category. These criteria range from those provided by model building codes for Performance Category 1 to those approaching nuclear power plant criteria for Performance Category 4. Table 2 illustrates how UCRL-15910 seismic criteria for these performance categories compare with seismic design and evaluation criteria from other sources. DOE seismic criteria for Performance Categories 1 and 2 are similar to that from the Uniform Building Code (UBC) [2]. DOE seismic criteria for Performance Category 3 is similar to that from the Department of Defense seismic criteria for essential buildings [3] and also to that used for the evaluation of commercial plutonium facilities licensed by the Nuclear Regulatory Commission [4]. DOE seismic criteria for Performance Category 4 is similar to that used for the evaluation of commercial nuclear power plants [5] UCRL-15910 was reissued in 1993 as a DOE Standard, DOE-STD-1020-92.

3. DOE SEISMIC CRITERIA

The annual probability of exceedance of structure, system, or component (SSC) damage as a result of earthquakes (i.e., performance goal) is a combined function of the annual probability of exceedance of the earthquake, factors of safety introduced by the seismic design/evaluation procedures and other sources of conservatism. The ratio of the earthquake hazard annual probability of exceedance and the performance goal annual probability of exceedance is called the risk reduction ratio, R_R in UCRL-15910. This ratio establishes the level of conservatism to be employed in the seismic design or evaluation process. For example, if the performance goal and earthquake hazard annual probabilities are the same ($R_R = 1$), the seismic design or evaluation approach should introduce no conservatism. However, if conservative design or evaluation approaches are employed, the earthquake hazard annual probability of exceedance can be larger (i.e., more frequent) than the performance goal annual probability ($R_R > 1$). The seismic design or evaluation criteria for a specific SSC are established in three steps:

Step 1 Establish an acceptable approximate seismic performance goal, P_F, for the components being designed or evaluated.

Step 2 Establish a set of conservative seismic acceptance criteria which introduce a significant reduction, R_R, in the risk of unacceptable seismic performance below the annual frequency of exceedance of the DBE.

Step 3 Establish DBE at an annual frequency of exceedance, P_H, equal to R_R (from Step 2) times P_F (from Step 1), i.e.:

$$P_H = R_R (P_F) \qquad (1)$$

Table 3 provides a set of seismic hazard exceedance probabilities, P_H and risk reduction ratios, R_R for Performance Categories 1 through 4 required to achieve the seismic performance goals specified in Table 1. Note that different structures, systems, or components may have different specified performance goal probabilities, P_F.

The seismic hazard exceedance probabilities, P_H, shown in Table 3 produce ground motion levels which are: (1) consistent with UBC levels for Performance Category 1; (2) consistent with NRC P_u facility evaluation levels for Performance Category 3; and (3) consistent with nuclear power plant safe shutdown earthquake (SSE) levels for Performance Category 4. The risk reduction ratio, R_R, resulting from the prescribed conservative seismic acceptance criteria depends on the slope of the seismic hazard

curve. If all seismic hazard curves had the same slope, it would be sufficient to have a single specified seismic hazard exceedance probability, P_H, and single set of conservative seismic acceptance criteria corresponding to risk reduction ratio, R_R, in order to meet target seismic performance goals, P_F. However, to account for the range of potential seismic hazard curve slopes and to utilize a single set of conservative seismic acceptance criteria, a definition of the DBE using both hazard and performance goal probabilities, P_H and P_F, has been employed for DOE seismic criteria. By this definition, the DBE is defined from probabilistic seismic hazard curves as the larger of the value at the hazard exceedance probability, P_H, or a specified coefficient F_a, times the value at the performance goal probability, P_F.

DOE seismic design and evaluation criteria are summarized in Table 4. By these criteria, Performance Category 1 or 2 SSCs may be seismically evaluated using the simplified approaches specified in the UBC seismic provisions since these provisions achieve an R_R ratio of about two or greater. However, for the Performance Category 3 or 4, the seismic evaluation must be performed by a dynamic analysis approach. In either case, the design detailing provisions from the UBC, which provide ductility, toughness, and redundancy, are also required such that SSCs can fully realize potential inelastic energy absorption capability. A dynamic analysis approach requires that:

1) the input to the SSC be defined by either a design response spectrum, or a time history input motion.

2) the important natural frequencies of the SSC be estimated, or the peak of the design response spectrum be used as input.

3) the resulting seismic induced inertial forces be appropriately distributed with the SSC and a load path evaluation be performed.

The words "dynamic analysis approach" are not meant to imply that complex dynamic models must be used in the evaluation. Often equivalent static analysis methods are sufficient so long as the above listed three factors are incorporated. This dynamic analysis approach should comply with the seismic response analysis provisions of American Society of Civil Engineers Standard 4-86 [6].

For Performance Category 1 and 2 SSCs, DOE seismic design and evaluation criteria employ the UBC provisions with the exception that site-specific information is used to define the earthquake input excitation used to establish seismic loadings. Maximum ground acceleration from probabilistic seismic hazard curves and site-specific ground response spectra are used in the appropriate terms of the UBC equation for base shear. Use of site-specific earthquake ground motion data is considered to be preferable to the general seismic zonation maps from the UBC. UBC provisions require a static or dynamic analysis approach in which loadings are scaled to the base shear equation value. In the base shear equation, inelastic energy absorption capacity of structures is accounted for by the parameter, R_W. Elastically computed seismic response is reduced by R_W values ranging from 4 to 12 as a means of accounting for inelastic energy absorption capability in the UBC provisions and by these criteria for Performance Category 1 and 2. This reduced seismic response is combined with non-seismic concurrent loads and then compared to code allowable response limits (or code ultimate limits and code specified load factors).

For Performance Category 3 and 4 SSCs, DOE seismic design and evaluation criteria specify that seismic evaluation be accomplished by dynamic analysis. The recommended approach is to perform an elastic response spectrum dynamic analysis to evaluate elastic seismic demand on SSCs. However, inelastic energy absorption capability is recognized by permitting limited inelastic behavior. By these provisions for Performance Category 3 and 4, inelastic energy absorption capacity of structures is accounted for by the parameter, F_u. Elastically computed seismic response is reduced by F_u values ranging from 1 to 3 as a means of accounting for inelastic energy absorption capability for more hazardous facilities. F_u values are much lower than R_W resulting in larger values of the risk reduction ratio, R_R. the Same F_u values are specified for all Performance Categories of 3 and higher. In order to achieve different risk reduction ratios, R_R appropriate for the different performance categories, the reduced seismic response is multiplied be a seismic load factor, L_S. Seismic load factors L_S are specified for

Performance Category 3 and 4. The resulting factored seismic response is combined with non-seismic concurrent loads and then compared to code ultimate response limits.

4. DESIGN/EVALUATION BASIS EARTHQUAKE (DBE)

Seismic design/evaluation criteria based on target probabilistic performance goals requires that DBE motions be based on probabilistic seismic hazard assessments. The deterministic acceptance criteria has been established with sufficient conservatism so as to achieve approximately or slightly greater than the specified risk reduction ratios for seismic hazard curves in which an approximate doubling of the ground motion corresponds to an approximately ten-fold reduction in the annual exceedance probability. However, the slope of actual site-specific probabilistic seismic hazard curves may differ substantially from this idealized situation. Figure 2 represents two representative probabilistic seismic hazard curves expressed in terms of mean annual probability of exceedance versus peak ground acceleration. One curve represents a seismic hazard estimate for a western higher seismic site. The other curve represents a typical seismic hazard estimate for an eastern lower seismicity site. For western higher seismicity sites the ground motion increase factor corresponding to a ten-fold reduction in annual exceedance probability may drop as low as 1.5, and for eastern lower seismicity sites, this factor may become as high as 3.75 within the 10^{-3} to 10^{-5} annual probability range of greatest interest. To conservatively accommodate such a wide variation in slopes, the DBE must be defined as the larger of:

$$DBE \geq a_{PH} \qquad (2a)$$

$$DBE \geq f_a a_{PF} \qquad (2b)$$

where a_{PH} and a_{PF} are the mean ground motions at the seismic hazard probability, P_H, and performance goal probability , P_F, respectively, and f_a is a DBE factor specified in Table 4 as a function of the specified risk reduction ratio, R_R.

The DBE probabilistic definition is used to account for the potential wide variation in site specific seismic hazard curve slopes while utilizing a single deterministic acceptance criteria for the range of all potential hazard curve slopes. DOE seismic criteria encourages obtaining modern site-specific probabilistic seismic hazard assessments [7 and 8], especially for facilities with Performance Category 3 and higher SSCs. For sites in which the seismic hazard curve has a slope for which there is larger than a two-fold increase in acceleration for a ten-fold increase in probability (this is typical of modern site-specific seismic hazard curves at eastern U.S. sites), the DBE defined by coefficient f_a times the ground motion value at the performance goal probability will govern.

The DBE ground motion at the site shall be defined in terms of smooth and broad frequency content response spectra in the horizontal and vertical directions defined at a specific control point. In most cases, the control point should be on the free ground surface. However, in some cases it might be preferable to define the DBE response spectra at some other location. One such case is when a soft (less than 750 feet/second shear wave velocity), shallow (less than 100 feet) soil layer at the ground surface is underlain by much stiffer material. In this case, the control point should be specified at the free surface of an outcrop of this stiffer material. Wherever specified, the breadth and amplification of the DBE response spectra should be either consistent with or conservative for the site soil profile, and facility embedment conditions.

Ideally, it is desirable for the DBE response spectrum to be defined by the mean uniform hazard response spectrum (UHS) associated with the seismic hazard annual frequency of exceedance specified in Table 3 over the entire frequency range of interest (generally 0.5 to 40Hz). However, considerable controversy currently exists concerning both the shape and amplitude of mean UHS.

First, many existing mean UHS shapes are not consistent with response spectrum shapes derived from earthquake ground motion recordings. The DBE response spectrum should be consistent in shape with response spectrum shapes from ground motion recorded at similar sites for earthquakes with magnitudes and distances similar to those which dominate the seismic hazard at the specified annual frequency. Unless it can be demonstrated that the mean UHS shape is consistent with the response spectrum shapes

obtained from appropriate ground motion records, the mean UHS should not be used.

Second, even for a specified ground motion parameter such as peak ground acceleration (PGA) or peak ground velocity (PGV), the mean estimate for a given hazard exceedance probability tends to be unstable between different predictors and tends to be driven by extreme upper bound models. Mean estimates should be used only when such estimates are stable. Mean estimates outside the range of 1.3 to 1.8 times the median estimate are likely to suffer from the above problems.

Because of these issues with regard to both mean estimates and UHS, the Department of Energy has published a standard on the use of probabilistic seismic hazard estimates [9]. The following recommendations have been adapted from this draft standard:

1) When a stable mean estimate of the PGA and PGV does not exist, then a surrogate mean DBE PGA and PGV set at an appropriate factor times their median estimates at the appropriate seismic hazard annual frequency of exceedance should be used. The DOE Standard defines an approach which may be used to obtain an acceptable median estimate from existing eastern U.S. seismic hazard study results and defines the surrogate mean to median factor.

2) The DBE response spectrum is then defined by a deterministic smooth and broad frequency content median response spectrum shape scaled so as to be anchored to the surrogate mean DBE PGA and PGV values defined in Step 1.

Preferably, the median deterministic DBE response spectrum shape should be site-specific and consistent with the expected earthquake magnitudes, and distances, and the site soil profile and embedment depths. The DOE Standard provides an acceptable approach for estimation of the earthquake magnitudes and distances to be used in defining this median deterministic site-specific response spectrum shape. When a site-specific response spectrum shape is unavailable then a median standardized spectral shape such as the spectral shape defined in NUREG/CR-0098 [10] may be used so long as such a shape is either reasonably consistent with or conservative for the site conditions. The median site-specific response spectrum shape may be derived from any combination of the following:

1) the median response spectrum shape from a suite of actual ground motion records associated with reasonably similar magnitudes, distances, and site soil profiles.

2) regression equations defining median spectral amplifications at various natural frequencies as a function of the magnitude, distance, and site soil profile.

3) band-width limited random vibration models benchmarked against response spectra from actual ground motion records associated with magnitudes, distances, and soil profiles as similar to the site as practical.

5. MEETING PERFORMANCE GOALS BY DOE SEISMIC CRITERIA

A new report entitled "Basis for Seismic Provisions of UCRL-15910" [11] demonstrates that performance goals are achieved when: (1) DBE is defined from probabilistic seismic hazard curves as the larger of the value at the hazard exceedance probability or a specified coefficient, f_a, times the value at the performance goal probability and (2) conservatism in acceptance criteria results in less than about 10% probability of unacceptable performance at a scaled DBE equal to a factor of safety, F_R, times the DBE. The required factor of safety, F_R, to achieve a desired risk reduction ratio, R_R is function of:

1) Seismic hazard curve slope represented by A_R (A_R is the ratio of ground motions corresponding to a ten-fold reduction in exceedance probability)

$$1.5 < A_R < 3.75$$

2) Seismic capacity variabilities (uncertainties) defined by logarithmic standard deviations ß.

$$0.3 \leq \beta \leq 0.5$$

This range of ß values is known from past probabilistic risk assessments (PRAs). The large the value of ß, the larger the uncertainty in seismic capacity. For example, at ß = 0.3

the ratio of 90% confidence to median seismic capacity ranges from about 0.6 to 1.65, while at $\beta = 0.5$ the ratio of 90% confidence to median seismic capacity ranges from about 0.45 to 2.30. Over this range of slopes, A_R, and seismic capacity uncertainties, β required F_R values have been evaluated which achieve risk reduction ratios, R_R, of 2, 10, and 20. The results of this evaluation are shown in Table 5. For Performance Categories 1 and 2, the risk reduction ration R_R of 2 is achieved by F_R of unity which, in turn, is judged to be achieved by following seismic acceptance criteria in accordance with recent editions of the Uniform Building Code. For Performance Categories 3 and 4, at risk reduction ratios, R_R of 10 and 20 the required F_R values are 1.5 and 1.7, respectively. The required F_R values for these values of R_R are achieved in the seismic acceptance criteria by specifying conservative material strengths, structural capacities, inelastic energy absorption factors, and a seismic load factor.

In particular, DOE seismic design and evaluation criteria will only have intentional conservatism introduced which achieve the required safety factor, F_R, by:

1) establish material strength properties at the 95% exceedance strength associated with the time during the service life at which such strengths are minimum;

2) basing capacities upon code-specified minimum ultimate or limit-state capacity levels with the appropriate capacity reduction factor (e.g., standard for concrete - American Concrete Institution ACI-318 or ACI-349 ultimate strength approach; structural steel - American Institute of Steel Construction (AISC) limit-state strength approach or AISC plastic design approach, American Society of Mechanical Engineers (ASME) components - ASME Service Level D);

3) permitting limited inelastic behavior by specifying inelastic energy absorption factors, F_u by which elastic response may exceed capacity (F_u values are provided or may be estimated as the value associated with a permissible level of inelastic distortion specified at about the 5% failure probability level);

4) using a seismic load factor, L_S, of 1.0 for Performance Category 3 and 1.15 for Performance Category 4; and

5) requiring equipment qualified by test to be tested at the required input spectrum scaled by a factor of $1.4L_S$.

To summarize load combinations and acceptance criteria by the DOE seismic design and evaluation provisions, the elastic-computed seismic demand D_S should be modified by the appropriate inelastic energy absorption factor F_u and by the appropriate seismic load factor L_S to obtain an inelastic-factored seismic demand D_{SI} by:

$$D_{SI} = L_S \frac{D_S}{F\mu} \qquad (3)$$

The total inelastic-factored demand D_{TI} is then given by:

$$D_{TI} = D_{NS} + D_{SI} \qquad (4)$$

where D_{NS} represents the best-estimate of all non-seismic demands expected to occur concurrently with the DBE. Equation 4 represents the DBE load combinations equation. The seismic capacity is adequate when the capacity C_C determined as defined above exceeds D_{TI}, i.e.:

$$C_C \geq D_{TI} \qquad (5)$$

Equation 5 represents the seismic acceptance criterion appropriate for the DBE. No load factors are needed on D_{NS} in Equation 4. The non-seismic demand D_{NS} should be defined at its best-estimate level as opposed to an unlikely to exceed or conservative level. The conservatism embodied in defining C_C, F_u, and D_S are sufficient to achieve the specified R_R ratios without additional sources of conservatism being required.

New DOE seismic provisions will differ from editions of UCRL-15910 in that a single value of inelastic energy absorption factor, F_u will be specified for both Performance Categories 3 and 4 and a seismic load factor will be specified which differs from Performance Category 3 to 4. This change was needed because the UCRL-15910 specified F_u of 1.0 for brittle failure modes from both Moderate

and High Hazard categories. As a result, different performance goals for each category were not achieved for these brittle failure modes. In the new DOE seismic criteria, performance goals will be met for brittle failure modes by introducing a seismic load factor, L_S, which has a larger value for Performance Category 4 with a lower performance goal probability than for Performance Category 3 with a higher performance goal probability. F_u specified in the new DOE seismic criteria will be about the same value as the Moderate Hazard values from the UCRL-15910. By this change, seismic criteria for Performance Category 3 SSCs is not affected (i.e., they will be the same as the Moderate Hazard seismic criteria). For Performance Category 4, this change results in slightly more liberal criteria for ductile failure modes and slightly more conservative criteria for brittle failure modes.

New DOE seismic criteria will also include damping levels provided at several response levels to be used in structural evaluations for the purpose of determining in-structure response spectra or interaction displacements. In the new DOE seismic criteria, seismic interaction will be explicitly addressed.

6. SUMMARY AND CONCLUSIONS

The Department of Energy utilizes deterministic seismic design/evaluation criteria developed to achieve probabilistic performance goals as provided in UCRL-15910. By these criteria, seismic hazard probabilities are specified which are consistent with UBC ground motion for Performance Category 1, with Department of Defense (DOD) ground motion for Performance Categories 2 and 3, and with SSE levels for Performance Category 4. The specified earthquake hazard probabilities are appropriate if seismic design or evaluation is conservatively performed.

In the DOE seismic criteria, a conservatism level is introduced which is sufficient to achieve the performance goals. This conservatism increases from Performance Category 1 to 4. For Performance Categories 1 and 2, conservatism should be consistent with the Uniform Building Code. For Performance Category 3, conservatism should be consistent with that of the DOD seismic design of essential buildings manual or with that used for evaluation of commercial plutonium facilities. For Performance Category 4, conservatism should approach that used for nuclear power plants. For analytical evaluations, conservatism has been introduced through the use of conservative inelastic demand-capacity ratios combined with ductile detailing requirements, through the used of minimum specified material strengths and conservative code capacity equations, and through the use of a seismic load factor. For evaluation by testing, conservatism has been introduced through the use of an increase scale factor which is applied to the prescribed design/evaluation input motion.

The DOE seismic design and evaluation criteria follow the philosophy of : (1) gradual reduction in hazard annual exceedance probability; and (2) gradual increase in conservatism of evaluation procedure as one goes from a Performance Category 1 to a Performance Category 4 structure, system, or component. Four separate sets of seismic design/evaluation criteria have been presented in UCRL-15910 each with a different performance goal. In all these criteria, earthquake loading is selected from seismic hazard curves on a probabilistic basis but seismic response evaluation methods and acceptable behavior limits are deterministic approaches with which design engineers are familiar.

7. REFERENCES

1. Kennedy, R.P., S.A. Short, J.R. McDonald, M.W. McCann, R.C. Murray, J.R. Hill, **Design and Evaluation Guidelines for Department of Energy Facilities Subjected to Natural Phenomena Hazards**, Lawrence Livermore National Laboratory and U.S. Department of Energy, Report June 1990.

2. **Uniform Building Code**, 1991 Edition, International Conference of Building Officials, Whittier, California.

3. **Seismic Design Guidelines for Essential Buildings, a supplement to Seismic Design for Buildings**, February 1986, Army TM5-809-10.1, Navy NAVFAC P-3551.1, Air Force AFM 88-3, Chapter 13.1, Departments of the Army, Navy and Air Force, Washington, D.C.

4. Bernreuter, D.L., et.al., **Seismic Evaluation of Commercial Plutonium Fabrication Plants in the United Sates,** October 1, 1979, UCRL-52705, Lawrence Livermore National Laboratory.

5. **Standard Review Plan for the Review of Safety Analysis Reports for Nuclear Power Plants, LWR** Edition, 1989, NUREG-0800, U.S. Nuclear Regulatory Commission.

6. **Seismic Analysis of Safety-Related Nuclear Structures and Commentary on Standard for Seismic Analysis of Safety-Related Nuclear Structures,** September 1986, Standard 4-86, American Society of Civil Engineers (ASCE).

7. **Seismic Hazard Characterization of 69 Nuclear Power Plant Sites East of the Rocky Mountains,** January 1989, NUREG/CR-5250, U.S. Nuclear Regulatory Commission, Volumes 1-8

8. **Probabilistic Seismic Hazard Evaluation at Nuclear Plant Sites in the Central and Eastern United States: Resolution of the Charleston Issue,** April 1989, EPRI NP-6395-D, Electric Power Research Institute, Palo Alto, California.

9. U. S. Department of Energy, Guidelines for use of Probabilistic Seismic Hazard Curves, DOE-STD-1024-92, December 1992.

10. Newmark, N.M. and W.J. Hall, 1978, **Development of Criteria for Seismic Review of Selected Nuclear Power Plants,** NUREG/CR-0098, U.S. Nuclear Regulatory Commission.

11. Kennedy, R.P. and S.A. Short, **Basis for Seismic Provisions of UCRL-15910,** September 1992 Draft, UCRL-CR-111478 DR, Lawrence Livermore National Laboratory.

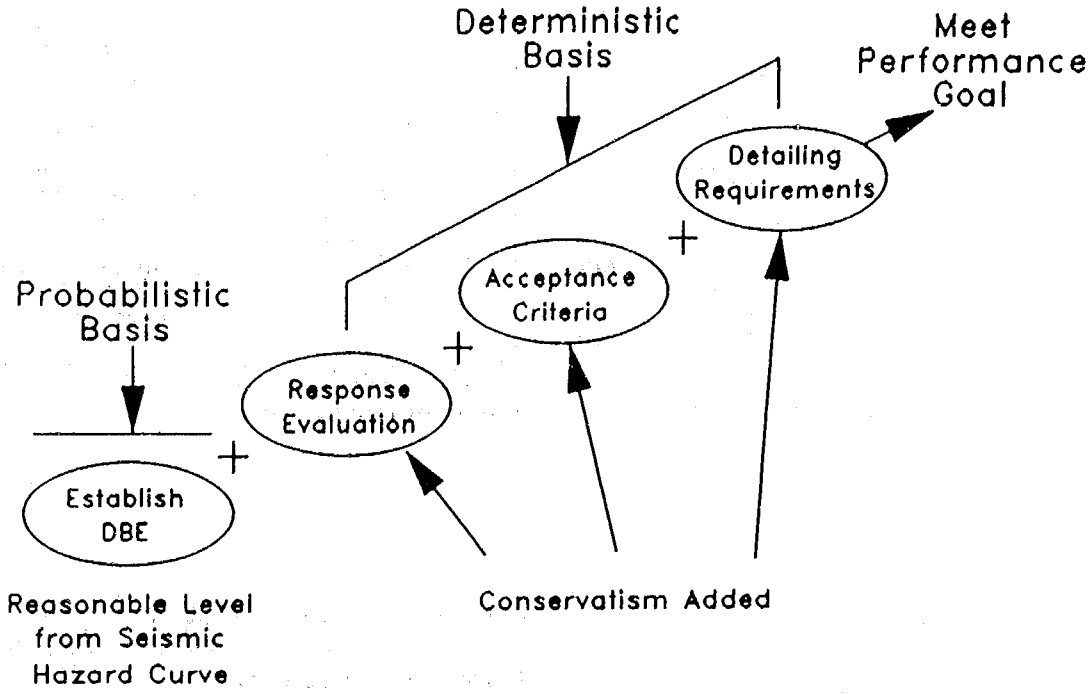


Figure 1 DOE Seismic Criteria Combines Probabilistic and Deterministic Methods to Achieve Performance Goals

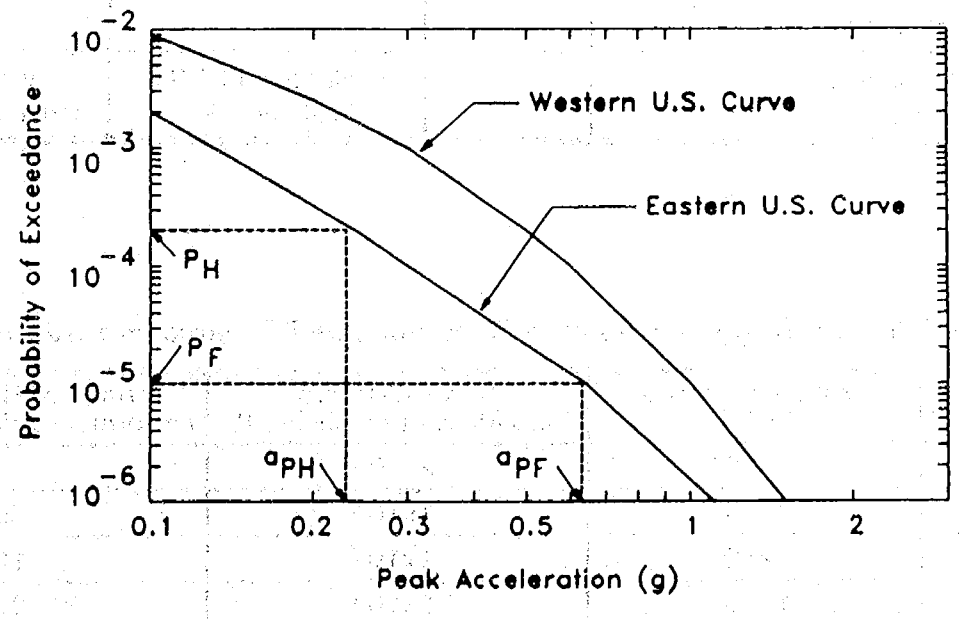


Figure 2 Representative Probabilistic Seismic Hazard Curves

Table 1 Structure, System, or Component (SSC) Seismic Performance Goals for Various Performance Categories

Performance Category	Performance Goal Description	Seismic Performance Goal Annual Probability of Unacceptable Performance, P_F
1	Maintain Occupant Safety	$\simeq 10^{-3}$ of the onset of SSC(1) damage to the extent that occupants are endangered
2	Occupant Safety, Continued Operation with Minimum Interruption	$\simeq 5\times10^{-4}$ of SSC damage to the extent that the component cannot perform its function
3	Occupant Safety, Continued Operation, Hazard Confinement	$\simeq 10^{-4}$ of SSC damage to the extent that the component cannot perform its function
4	Occupant Safety, Continued Operation, Hazard Confinement	$\simeq 10^{-6}$ of SSC damage to the extent that the component cannot perform its function

(1) SSC refers to structure, distribution system, or component (equipment).

Table 2 Comparison of Seismic Criteria by Various Sources

Source	Performance Category			
UCRL-15910	1	2	3	4
Uniform Building Code	General Facilities	Essential Facilities	-	-
DOD Tri-Service Manual for Seismic Design of Essential Buildings	-	-	High Risk	-
Nuclear Regulatory Commission		-	Evaluation of NRC Fuel Facilities	Evaluation of Existing Reactors

Table 3 Seismic Performance Goals & Recommended Seismic Hazard Probabilities

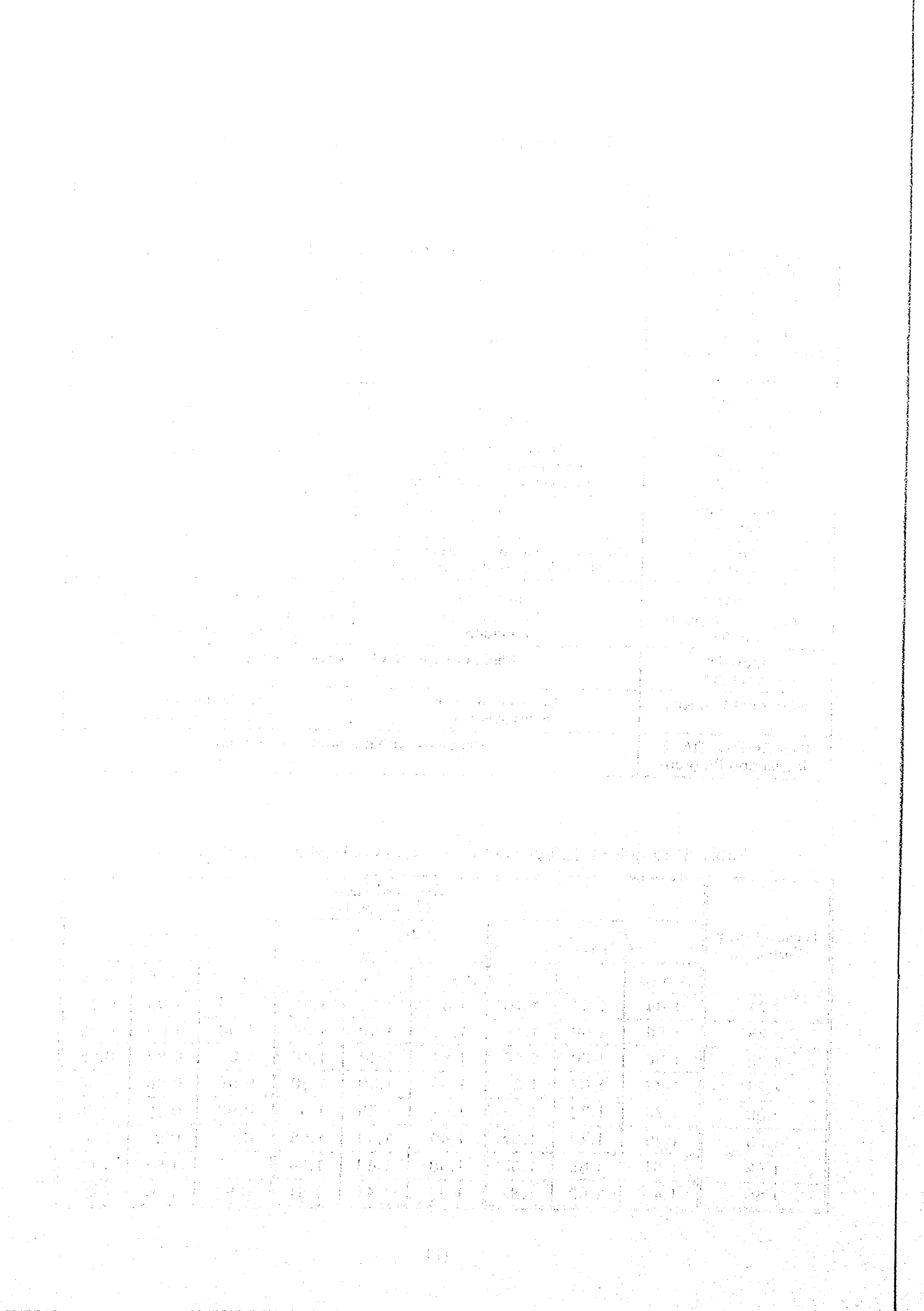
Performance Category	Seismic Performance Goal, P_F	Seismic Hazard Exceedance Probability, P_H	Ratio of Hazard to Performance Probability, R_R
1	1×10^{-3}	2×10^{-3}	2
2	5×10^{-4}	1×10^{-3}	2
3	1×10^{-4}	1×10^{-3}	10
4	1×10^{-6}	2×10^{-4}	20

Table 4 Summary of Earthquake Evaluation Provisions

	Performance Category			
	1	2	3	4
Hazard Exceedance Probability, P_H	$2x10^{-3}$	$1x10^{-3}$	$1x10^{-3}$	$2x10^{-4}$
Risk Reduction Ratio, R_R	2	2	10	20
DBE factor accounting for hazard curve slope	Not Used		$f_a = 0.5$	$f_a = 0.45$
Response Spectra	Median amplification (no conservative bias)			
Damping	5%		Post yield levels	
Acceptable Analysis Approaches	Static or dynamic force method normalized to code level base shear		Dynamic analysis	
Importance Factor	I = 1.0	I = 1.25	Not used	
Load Factors	Code specified load factors appropriate for structural material		$L_s = 1.0$	$L_s = 1.15$
Inelastic Energy Absorption Ratios	Accounted for by R_w in UBC base shear equation		F_μ value by which elastic seismic response is reduced to account for permissible inelastic behavior	
Material Strength	Minimum specified or known in-situ values			
Structural Capacity	Code ultimate or allowable level		Code ultimate or limit-state level	
Peer Review, QA, & Inspection Program	Required within a graded approach			

Table 5 Required Safety Factors to Achieve Desired Risk Reduction

Hazard Curve Slope, A_R	Required Factor of Safety, F_R								
	$R_R = 20$ $f_a = 0.45$			$R_R = 10$ $f_a = 0.5$			$R_R = 2$ f_a not used		
	$\beta = .3$	$= .4$	$= .5$	$\beta = .3$	$= .4$	$= .5$	$\beta = .3$	$= .4$	$= .5$
3.75	1.64	1.53	1.46	1.47	1.38	1.31	1.10	1.03	0.98
3.25	1.65	1.56	1.49	1.49	1.40	1.34	1.06	1.00	0.96
2.75	1.68	1.60	1.56	1.51	1.44	1.40	1.02	0.97	0.95
2.25	1.72	1.67	1.67	1.55	1.50	1.50	0.99	0.96	0.96
2.05	1.75	1.72	1.75	1.57	1.55	1.57	0.98	0.96	0.98
1.85	1.79	1.79	1.87	1.49	1.49	1.56	0.97	0.97	1.01
1.65	1.61	1.66	1.80	1.38	1.43	1.54	0.97	1.01	1.09
1.50	1.49	1.60	1.82	1.32	1.41	1.61	0.99	1.07	1.21



GUIDELINES FOR DISASTER INFORMATION SYSTEMS FOR IMPORTANT INFRA-STRUCTURES

By Kazuhiko KAWASHIMA*, Kenichi TOKIDA**, Hideki SUGITA***, Tomoru NAKAJIMA*** and Hideo MATSUMOTO****

ABSTRACT

This paper outlines the "Guidelines for Disaster Information Systems for Infra-structures". This is a part of the "Guidelines for Disaster Information Systems" which was compiled in March 1992 as a final accomplishments of a comprehensive five year research project on Development of Disaster Information Systems. Description is given to proposed seismic damage information systems for the Ministry of Construction. Emphasis is placed on the Damage inspection with use of video cameras from helicopters and visual information systems for seismic zonation of ground hazard.

KEYWORDS: Disaster, Information, Earthquake, Damage Inspection, Ground Hazard

1. INTRODUCTION

When a destructive earthquake occurs, it is of significant importance to immediately collect accurate information on the extent of damage in the area affected by the earthquake. Road transportation is likely to be interrupted in urban area such as Tokyo as a direct result of damage of not only transportation facilities but buildings and lifeline facilities along roads. Confusion caused by people in evacuation and automobiles left on roads are anticipated, and they would also cause considerable disruption of transportation. It is required therefore to develop a new information collecting and processing systems which enable the extent of damage to be recognized immediately after an earthquake for formulating the repair and restoration strategy promptly.

A comprehensive 5 year research program entitled "Development of Information Collecting and Processing Systems for Disaster Mitigation" was initiated in 1987 by the Ministry of Construction, Public Works Research Institute, Building Research Institute and Geographical Survey Research Institute are involved in the research. The objectives of this research project were to develop new information collecting and processing systems, using advanced new technologies, for various disasters such as earthquakes, floods and debris flows. As shown in Fig.1, key items of the research development were :

a) bird's eye information collecting systems from helicopters,
b) on-line information processing systems, and
c) real-time digital mapping systems.

For this purpose, measuring and assessing technology of damage degree of structures using moving picture information detected from helicopters and new media oriented high-grade disaster prediction methods as well as planning systems for repair and restoration in damaged areas was developed. To avoid distortion of information during transferring from regional offices to headquarters, it was aimed to adopt visual motion picture systems.

This paper presents the outline of "Guidelines for Disaster Information Systems for Infra-structures", which is a part of the "Guidelines for Disaster Information Systems".

2. SCOPES AND CONTENTS OF THE GUIDELINES

The Guidelines is of five parts as :

Part I General Remarks and Proposals
Part II DEvelopment of Principal Technology for Disaster Information Systems
Part III Damage Information Systems for Important Infra-structures
Part IV Damage Information Systems for Urban Disaster

In Part I, summary of the 5 year project is presented with the background and needs of the project. Details of the program is presented in Parts II, III and IV. In Part II, various new and advanced technology for disaster information systems are presented. They include utilization of GPS positioning system, thermal image sensors, aero photo and video image camera. In Part IV, governments is presented. Data base required for disaster information systems, real time simulation of fire spreading and evacuation systems are included. GSI, PWRI and BRI are in charge of making Part II, III and IV, respectively.

In the Part III, which will be briefly introduced in this paper, the following issues are described :

---

* Head, Earthquake Engineering Division, Public Works Research Institute
** Director, Kanazawa Construction Office
*** Research Engineer, Earthquake Engineering Division, Public Works Research Institute
**** Hilgawa and Kandogawa Construction Office, Ministry of Construction

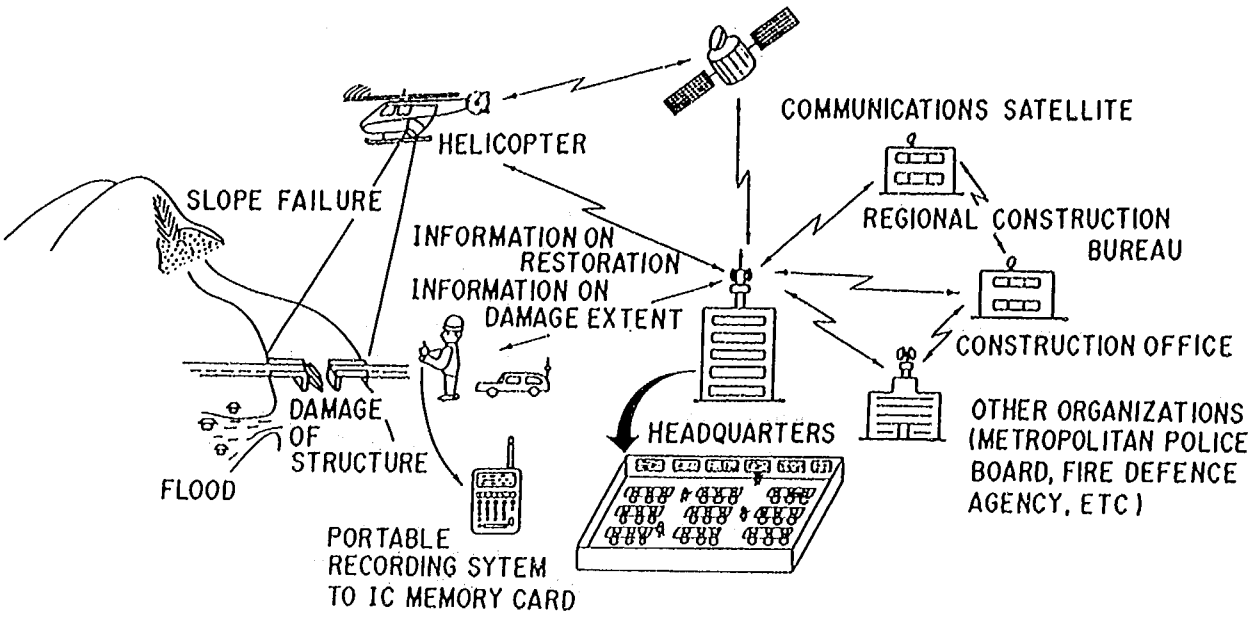


Fig. 1 Disaster Information Systems for Important Infra-structures

1 Common Part
- 1.1 General
- 1.2 Information Required during Disasters
- 1.3 Information Collecting and Processing before an earthquake
- 1.4 Damage Information System with use of Electric Still Cameras and Electric Handy Recorders
- 1.5 Outline of Damage Information Systems Common System Required for Various Disasters
- 1.6 Application to Normal Work
- 1.7 Organization Required for Application of Damage Information Systems

2 Damage Information Systems for Earthquakes
- 2.1 Damage Information Collecting Systems
- 2.2 Damage Information Transferring Systems
- 2.3 Damage Information Processing Systems

3 Damage Information Systems for Ground Failure during Earthquakes
- 3.1 Estimation of Ground Movement
- 3.2 Damage Inspection of Embedded Underground Structures
- 3.3 Damage Inspection of Road Facilities
- 3.4 Information Processing System for Ground Hazard

4 Damage Information Systems for Flooding
- 4.1 Damage Information Collecting Systems
- 4.2 Damage Information Processing Systems
- 4.3 Damage Information Transferring Systems

5 Damage Information System for Land Slide
- 5.1 General
- 5.2 Damage Information Collecting Systems
- 5.3 Damage Information Processing Systems Required for Restoration
- 5.4 Damage Information Processing Systems Required for Management of Construction Materials, Driftwood and Sand

3. PROBLEMS OF CURRENT DAMAGE INFORMATION COLLECTING SYSTEMS AND BASIC REQUIREMENTS FOR DEVELOPING NEW SYSTEMS

Although there were not destructive earthquakes which seriously hitted urban area in the last 40 years in Japan, it has been repeatedly pointed out from the experience of seismic damage in local areas that information collection and dissemination are the most important but difficult issue for central and regional governments in charge of control of public facilities[2)3)]. This was also pointed out at the Loma Prieta, U.S.A., Earthquake in October 1989[4)5)]. From the past experiences, various obstacles for collecting damage information are anticipated[2)3)]. The most important one is unexpectedly long time required for collecting damage information due to interruption of roads and damage of information transferring media such as telephone. Even if telephone could survive an earthquake, disruption of communication repeatedly happened due to concentration of call to a specific region.

Inadequate accuracy of the collected information is the second problem. Unconfirmed and sometimes uncorrect information were sent. Only a part of total information arrived. It is difficult to know the accuracy and correctness. Sometimes the same information arrived through different routes, and they were misunderstood as different information. Confirmation of source of information is very important. When a series of

events occurred, information on subsequent event sometimes arrived earlier than the information of the preceding event. There are examples that this caused significant misunderstanding on what were going on the events and the repair.

Because most of information is transferred by a voice and letters, correct evaluation on the information is difficult. Distortion of information always occurs. Therefore it is required to send information in a form of visible information. Still picture and moving picture information are quite effective.

Basic requirements for solving the problems of the current damage information collecting systems are:

(1)Prompt Information Collection

Collection of damage information in wide areas has to be made at not only day time but night time. Because accuracy of the damage information required changes in accordance with time following an earthquake, it is important to be able to collect damage information with reasonable accuracy depending on the time after an earthquake. Visible information through video cameras is quite important.

(2)Delivery of Updated and Same Information for All Bodies Involved in Repair and Restoration

Although quality of the information required depends on the task of individuals involved in repair and restoration, it is essentially important that the same and updated damage information is able to be delivered for all individuals from site engineers to decision makers. The real-time damage information has to be displayed in the form of not only letters but moving pictures. Because it is important for site engineers involved in inspection and emergency treatment to know real-time progress of damage and repair even in other area for which they are not in charge of, the systems should have capability to display the damage information of not only inside but outside of the controlled area.

(3)Data Processing Systems for Repair and Restoration

The data processing systems has to be capable to control all the damage information in a system, and can be used from the first stage (immediately after an earthquake) to third stage (stage of permanent repair and restoration) [2)3)]. It should also have a capability to execute various simulation for studying restoration strategy.

4. PROPOSED SEISMIC DAMAGE INFORMATION SYSTEMS

For enabling the requirements presented in the preceding chapter, Seismic Damage Information Systems was proposed for collecting and processing seismic damage information for repair and restoration of roads and river facilities. The Seismic Damage Information Systems is to be operated at the Main Headquarters for Disaster Countermeasures (Headquarters Office at the Ministry of Construction), the Headquarters for Disaster Countermeasures (Headquarters Office at Regional Construction Bureaus) and the Branch for Disaster Countermeasures (Regional Construction Offices).

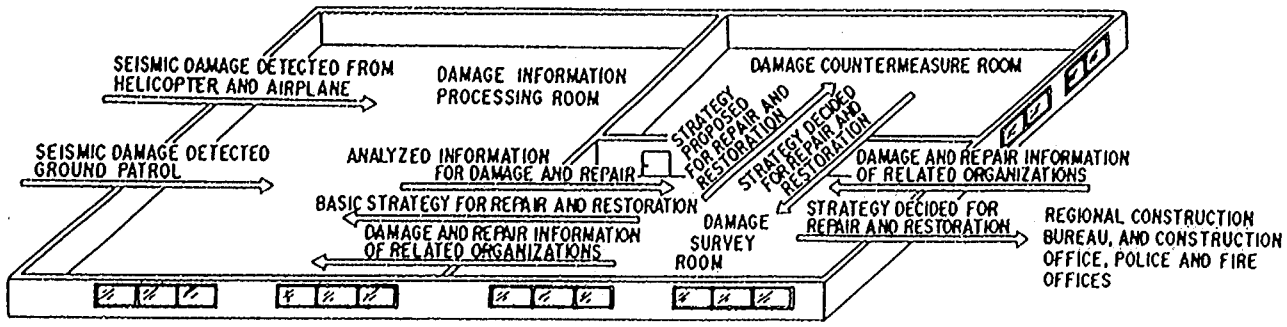
Fig.2 shows layout and role of three sub-sections of the Seismic Damage Information Systems. At Damage Information Processing Room, all damage information are collected from various sources such as ground patrol teams, helicopter patrol teams, other organizations and public. From such information from various sources, important information required for repair and restoration of roads and river facilities are identified. Preliminary statistical analysis of the damage are made. At Damage Survey Room, repair and restoration plan based on the damage information compiled at the Damage Information Processing Room are formulated. Communication and adjustment for restoration with related organizations such as police, fire departments and local governments have to be made at this stage. At Damage Countermeasure Room, basic policy and strategy for repair and restoration based on the information compiled at the Damage Survey Room is decide.

Fig.3 shows an image of the Damage Survey Room and the Damage Information Processing Room which should be placed at the Headquarters Office at Regional Construction Bureaus.

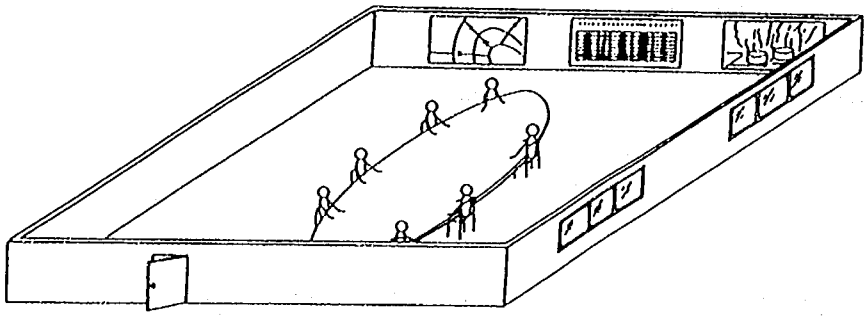
The Seismic Damage Information Systems is of four sub-systems for collecting, transferring, processing and maintenance of the damage information. The outline of the sub-systems are as follows.

(1) Seismic Damage Information Collecting Systems

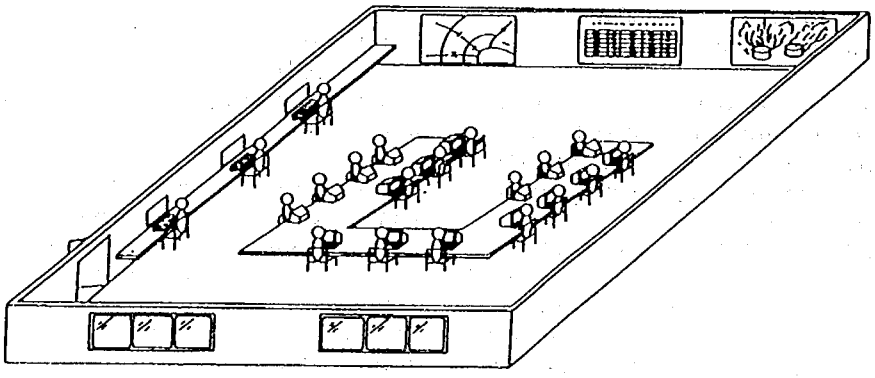
Information on seismic damage detected by helicopter patrol teams and ground patrol teams is collected and processed in this systems. The damage information is of moving picture, still picture and letters. They have to be detected by video cameras, electric still cameras and electric hand notes. The electric hand notes are specially designed man-machine handy type personal computers for exclusive use for recording seismic damage. When the electric notes are operated by field engineers, the notes automatically display and ask important items for identifying the damage situation such as



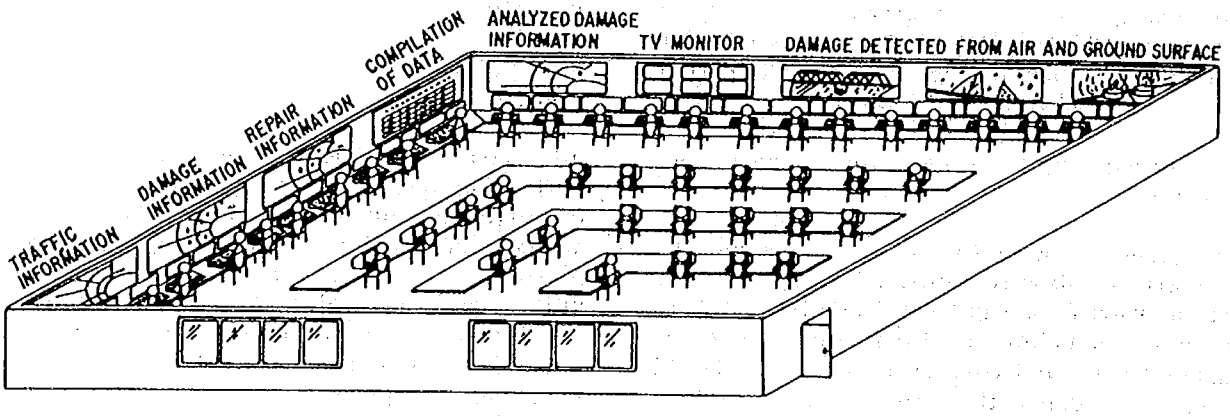
(a) FLOW OF INFORMATION



(b) DAMAGE COUNTERMEASURE ROOM

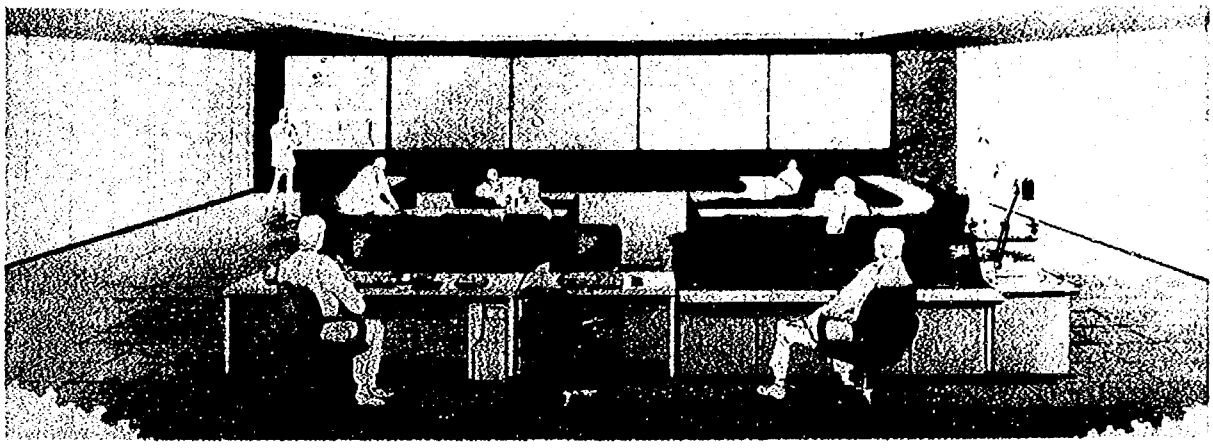


(c) DAMAGE SURVEY ROOM



(d) DAMAGE INFORMATION PROCESSING ROOM

Fig. 2 Layout and Role of Headquarters



(a) Damage Survey Room (Regional Construction Bureau)



(b) Damage Information Processing Room (Regional Construction Bureau)

Fig. 3 Image of Damage Information Processing Room and Damage Survey Room

location, size, type and degree of damage. The data are stored on floppy disk, and they can be sent to a host computer at the Headquarters by cables or radio communication systems.

(2) Data Transferring Systems

Fig.4 shows an image of the Data Transferring Systems for transferring the damage information between Headquarters, Regional Construction Bureaus, Regional Construction Offices, patrol helicopters and ground patrol teams. The information to be covered by the systems includes;

a) moving picture motion detected by video cameras on helicopters
b) moving picture motion by video cameras of ground patrol teams
c) still picture motion by still cameras of ground patrol teams
d) character and mapping data used in the Seismic Damage Information Processing Systems
e) telemetered data on earthquake and meteorology
g) Information through telephone and faximile

Main facilities required for the Data Transferring Systems are presented in Fig.5. Main facilities included in the systems are of satellite communication systems and ground communication systems. The satellite communication systems includes satellite, fixed receivers, portable receivers and moving picture transmitting systems. The fixed receiver and portable receivers were already installed at two and five of eight Regional Construction Bureaus, respectively. The ground communication systems are of radio network for exclusive use of the Ministry of Construction and picture motion communication systems. The radio network of the Ministry of Construction covers about 800 locations including Regional Construction Offices and local governments throughout the country.

(3) Seismic Damage Information Processing Systems

Fig.6 shows ten sub-systems for operating the Seismic Damage Information Processing Systems. Whole seismic damage data, repair and restoration data, mapping information, and

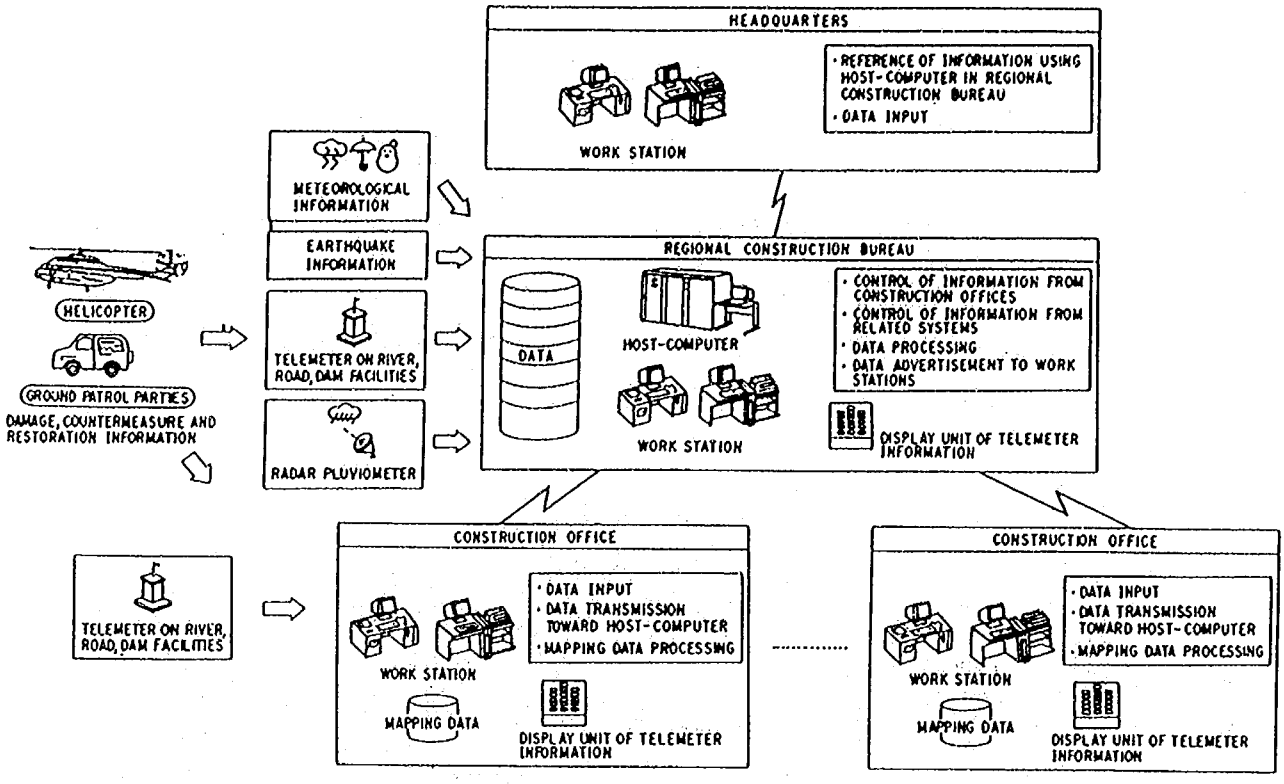


Fig. 4 Image of Data Transferring Systems

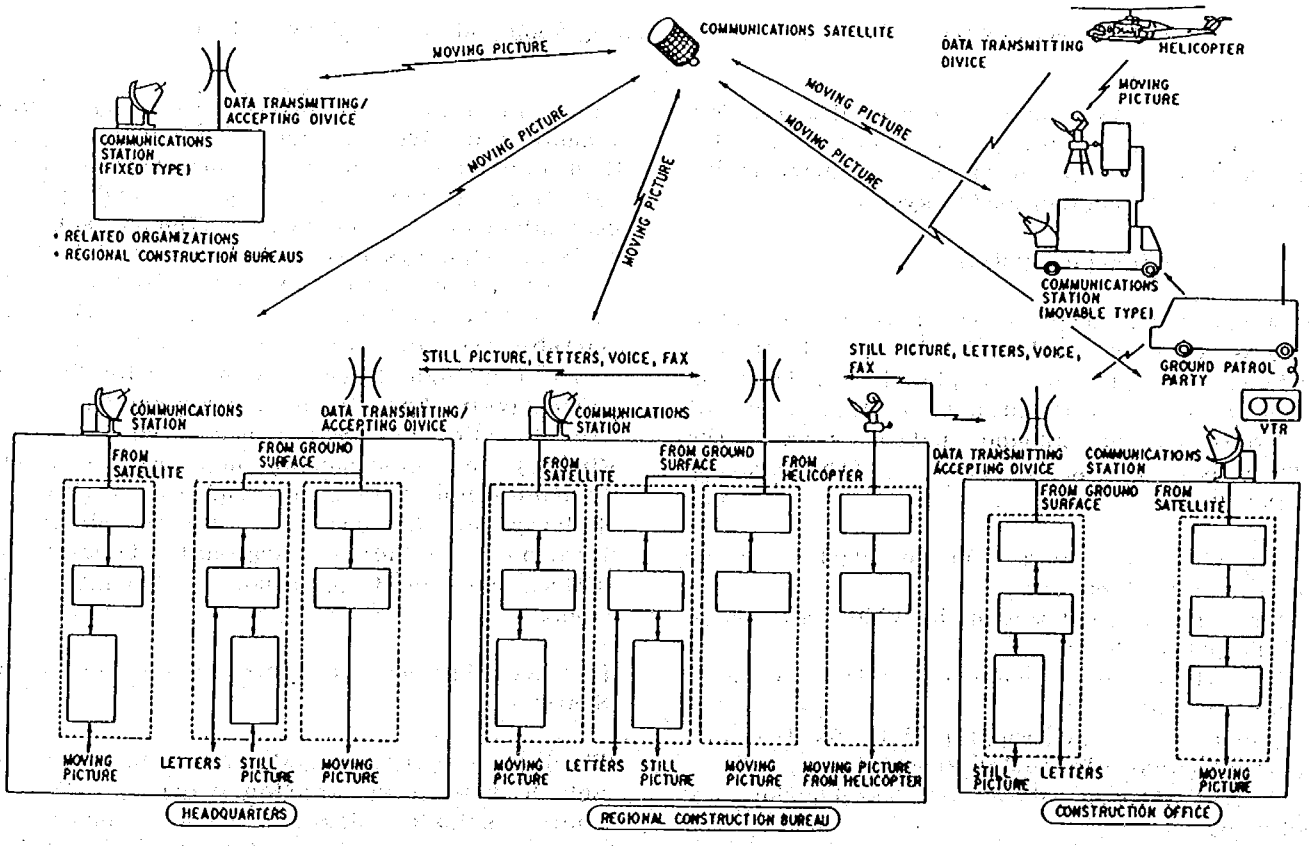


Fig. 5 Main Facilities for Data Transferring Systems

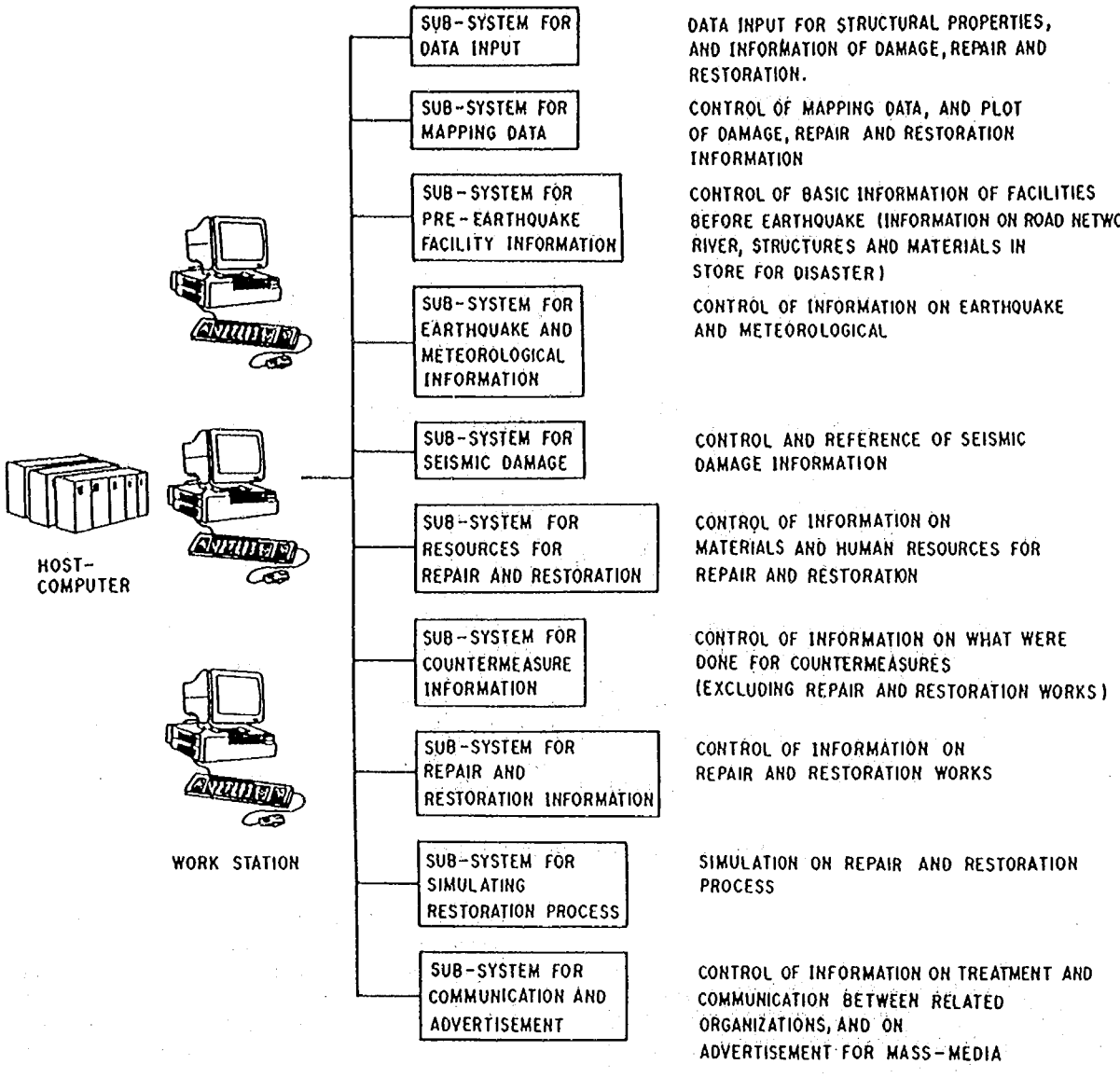


Fig. 6 Sub-systems of Seismic Damage Information Processing Systems

facilities information prior to an earthquake are compiled and controlled in this systems. Simulation of restoration strategy can be made for clarifying the most appropriate way of restoration. Control of information on adjustment with other organizations are made. Notice and announcement on damage and repair to mass-media is also controlled by this systems. It is of host computer for data processing and work-stations for data input and output. Analyzed data should be displayed on monitor in a well organized form for deciding repair and restoration strategy.

(4) Audio Visible Systems

Fig.7 shows an image of the Audio Visible systems. It includes screens with 200 inches and 70 inches, monitor of telemeters, projectors and electric black boards. The Audio Visible Systems should have the capability to monitor the damaged area through large screen, to understand the damage feature by comparing the still and moving pictures taken prior to the earthquake, and to conduct TV conference.

5. DAMAGE INSPECTION FROM HELICOPTERS

Damage inspection from helicopter seems attractive to collect damage information promptly because it is not interrupted by traffic congestion and road suspension. To investigate the effectiveness of the damage survey from helicopter, model damages were intentionally placed on various road and river facilities. A helicopter owned by the Ministry of Construction was used for this test. It is for exclusive use for disaster prevention as shown

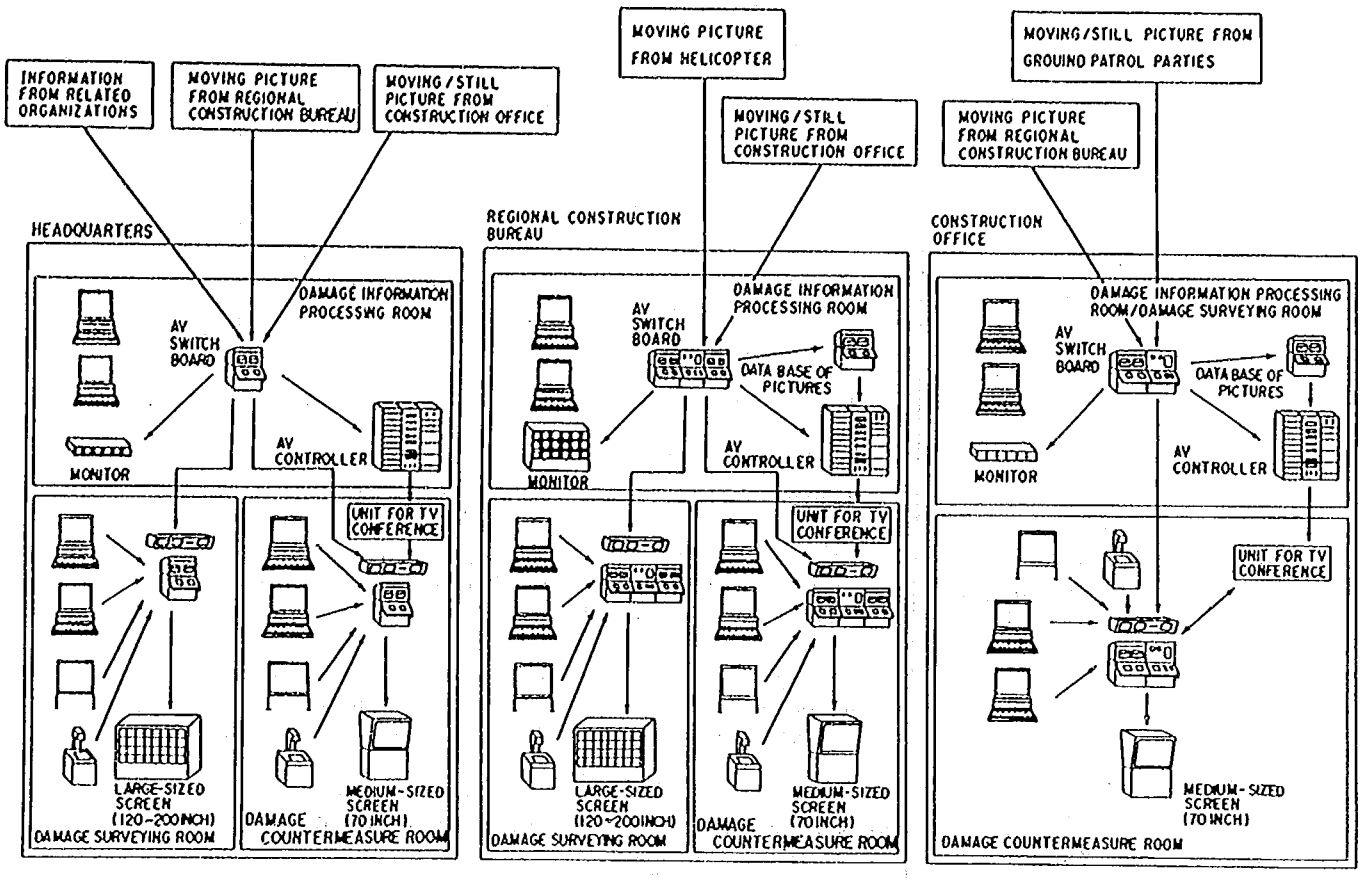


Fig. 7 Image of Audio Visible Systems

in Photo 1.

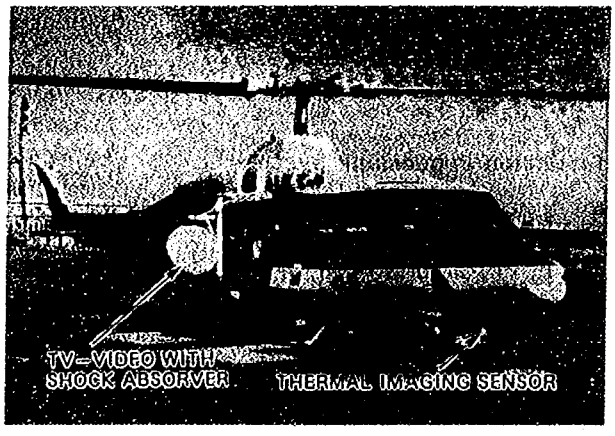


Photo 1 Helicopter for Disaster Prevention Owned by Ministry of Construction

A video camera which is set in a specially designed camera case for isolating the camera from vibration of the helicopter was used to detect artificial damage. The focal distance of the video camera is from 12.5 mm to 550 mm. By using the focal distance of 550 mm, a flame of 4.8 m by 3.6 m can be recorded when the height of the helicopter is 300 m which is regulated minimum height at city area. Real time transferring of the picture from the helicopter to the ground receiver can be made. A thermal image sensor is also provided on the helicopter. It can detect the difference of temperature with the resolution of 0.25 degree in Centigrade. Because zoom as large as 4 times is provided in the thermal image sensor, a flame with 37 m by 21 m can be recorded.

Various seismic damage was intentionally developed on bridges, pavement, road embankment and river structures. Photo 2 shows cracks which were made by placing white vinyl tape with width of 5 cm for aiming to represent a damage developed at mid-height of reinforced concrete pier and a damage of prestressed concrete deck. The former damage is likely to be developed when reinforcing bars are terminated at mid-height with inadequate anchoring length[3] and the latter damage tends to be developed on the concrete near the bearing supports[7] when the deck is pulled laterally. Photo 3 shows how such damages are detected from helicopter flying 321 m above the ground surface with velocity of 60 km/h[8]. The focal distance was 550 mm. It is apparent that the cracks at pier and deck can be clearly detected. The test was made by varying the velocity and height of flight.



Photo 2 Cracks Placed on Mid-height of Pier and Girder

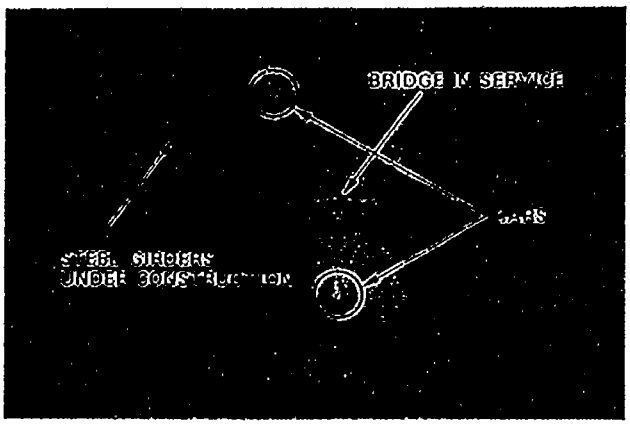


Photo 4 Bridges Detected by Thermal Image Sensor at Night (Height is 338m)

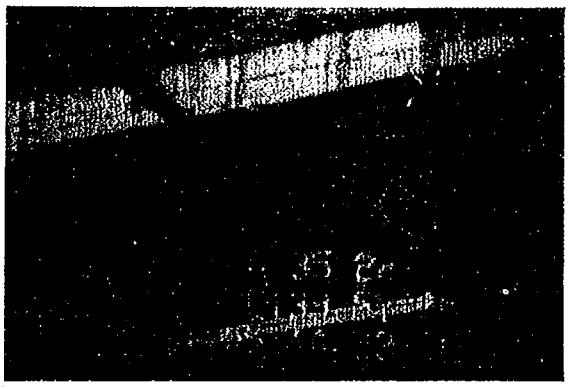


Photo 3 Damage Detected by Video Camera Placed on Helicopter (Height is 321m, Focal Distance is 550mm)



Photo 5 Slop Failure at Nashimoto District of Izu Peninsula Detected by Video Camera from Helicopter

Photo 4 shows picture representing a new bridge construction along an existing bridge in use for traffic. This was detected by the thermal image sensor at night. Flight height was 338m from the ground surface. Automobiles driving on he existing bridge and four girders under construction can be apparently seen[3]. The thermal image sensor is effective to detect large damage of steel and concrete structures.

Photos 5 and 6 show the seismic damage of road along natural slope , which was caused by the Izu Ohshima-kinkai Earthquake[2] with the Richter magnitude of 7.0 in January 1978. Extensive slope failure was developed along the road with total distance of about 125 m and height of 30 to 50 m , and this embedded a public bus with three being killed. Photo 6 shows the repairing job by a crane. Because this is a part of video taken by a TV company for broadcasting, the flight information such as height and velocity is unknown. By carefully examining the video record, length, depth and soil volume were surveyed by three geologists with different professional careers[3]. The geologist with 17, 10 and 5 years professional career is designated herein as A, B and C geologist, respectively.



Photo 6 Repair Work Detected by Video Camera from Helicopter

Table 1 compares the accuracy of the estimation by three geologists based on the video film. It is interesting to note that the geologist A gives the most appropriate estimation, and that the geologists with shorter professional career tends to give 30 to 50 % smaller estimation. Because estimation was made through video picture which is, of course, much smaller in size

than the actual damage, the surveyors tend to give smaller estimation in size.

Table 1 Accuracy of Estimation by Three Geologists with Different Professional Career

DAMAGE	GEOLOGISTS			MEASURED
	A	B	C	AT SITE
AVERAGE WIDTH	70(CRANE(10m)x7)	60~80	10~30	100m
AVERAGE DEPTH	10(AVERAGE WIDTHx 1/7~1/10)	5~10	•	5m
FAILURE AREA	•	320~480	•	-
SOIL VOLUME	20,000(30mx70mx10m)	20,000	•	26,500
LENGTH OF ROAD INTERRUPTED BY SLOPE FAILURE	100(AVERAGE WIDTH +α)	80	•	125

1. • MEANS THAT IT WAS UNABLE TO ESTIMATE FROM VIDEO TAPE
2. ( ) REPRESENTS HOW GEOLOGISTS EVALUATED LENGTH, DEPTH AND DISTANCE

Fig. 8 shows the geological feature detected by the geologist A based on the video film. Various information which is useful to judge the cause of failure and probability to cause further progress of the failure can be obtained if the video picture is carefully evaluated by a person with enough professional knowledge.

It was found from the study that estimation of the volume and length of failure is easier when artificial goods and facilities such as car, gird rails, house are found in the moving picture because they can be used as a reference to measure the distance[10] On the other band, it was found difficult to estimate the distance and length when the failure is enormously large as compared with the size of such artificial goods and facilities.

The study presented here is now being extended for studying the maximum flight velocity to detect a certain size of damage[11], effect of temperature and wind velocity for detecting damage by thermal image sensor[12], and the most appropriate way of flight[13].

6. DEVELOPMENT OF GRAPHIC SYSTEMS FOR EARTHQUAKE DAMAGE INFORMATION

Graphic display with use of a computer system is effective for realizing various information and data. However development of a graphic system for disaster information system includes various problems such as in core memory and computer time required. Therefore a pilot-system for earthquakes disaster information system was developed to study the feasibility and display method.

The pilot system can display information on seismic ground motion and hazard which are required immediately after an earthquake as the

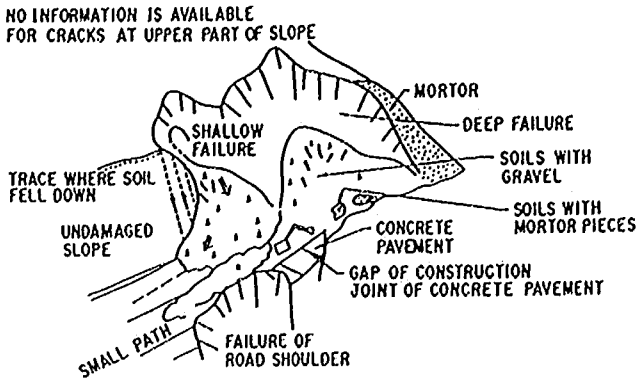


Fig. 8 Geological Feature Detected by Geologist A based on Video Film

basic disaster information for damage evaluation and restoration. The system can display an epicenter, magnitude of earthquake, ground motion records and ground failures.

As a case study, a pilot model was formulated for southern Kanto district around Tokyo-Bay. The system can display a monitor with three different scales. Map A indicates wide area of 158km × 130km with 14 × 14=196 cells. Map B indicates middle areas of 11.3km× 9.25km with 20 × 20 = 400 cells. A whole Map B corresponds to one cell of the Map A. Map C represents small area of 566m × 466m scale, and a whole Map C corresponds to one cell of the Map B.

The hardware of the pilot system is of a memory, a display, a keyboard with a mouse, a printer and a mainframe computer as shown in Photo. 7. Photos 8 and 9 show the graphics on peak acceleration and liquefaction potential.

7. CONCLUDING REMARKS

When the Kanto Earthquake which resulted in about 120 thousands of death occurred in September 1923, there were only about 4,500 vehicles in Tokyo City. People evacuated by either walking or bicycle. This clearly indicates the great difference of anticipated damage situation, between in 1923 and current time, in urban area hitted by a destructive earthquake. It is important to note that there have not be destructive earthquakes which hitted badly urban areas in the last 40 years, and during this time the size, structures of living, lifelines and techniques completely changed. It is therefore anticipated to face a new situation when a large event happens near urban area. It is quite important to develop and introduce a new systems for collecting and processing seismic damage information.

Because the proposed systems would become a large systems consisting of a number of hardwares and softwares, further study needs to

be made for an integrated architecture so that they can be used even after a destructive earthquake. Special training for operating the systems is inevitably important. Because sudden operation immediately after an earthquake can not be made, it has to be used as a part of the comprehensive systems for dally use. Appropriate form of the emergency operation systems in normal time has to be well examined.

Although the thermal image sensors are effective to detect large damage at night, they can be used for surveying more detailed damage if the camera with longer focus distance was developed. The use of new technology such as the high vision camera is promising.

ACKNOWLEDGEMENTS

In executing the project, the Technical Research Center for National Land Development established the Committee for the Development of Disaster Information Systems, which is chaired by Dr. H. Umemura, Professor Emeritus of the University of Tokyo, with the commitment of the Ministry of Construction. The reports presented in this paper are being executed with the supervision by the Subcommittee for the Development of Supporting Systems for Disaster Restoration Plan (Chairman : Professor Emeritus K. Kubo).). The authors express their sincere thanks to all committees members for their invaluable suggestions and guidance. Special thanks go to Professor E. Kuribayashi, T. Katayama and Prof. H. Kameda for their invaluable suggestions.

REFERENCES

1) Ministry of Construction : Guidelines for Disaster Information Systems, March 1992
2) Public Works Research Institute: Guidelines for Disaster Information Systems for Important Infra-structures, Technical Note of Public Works Research Institute, Vol.58, March 1992
3) Public Works Research Institute : Manuals for Repair Methods for Civil Engineering Structures Damaged by Earthquakes, Technical Note of the Public Works Research Institute, Vol. 45, December 1986 (in Japanese). Translated version is available from the National Center for Earthquake Engineering Research, University of New York, Buffalo, U.S.A.
4) Japan Road Association Guide Specifications for Earthquake Hazard Mitigation for Transportation Facilities - Repair and Restoration -, February 1987
5) Public Works Research Institute: Report on the Disaster Caused by the Izu-ohshima-kinkai Earthquake, Report or the Public Works Research Institute, Vol.158, March 1982
6) Kawashima, K., Sugita, H. and Kanoh, T. : Survey of Seismic Damage by Video Tapes Taken from Helicopter, Civil Engineering Journal, Vol. 33-1, January 1991
7) Kawashima. K., Sugita, H. and Kanoh, T. : Maximum Flight Velocity of Helicopter for Surveying Seismic Damage With Use of Audio Visual Picture, Civil Engineering Journal, Vol.33-9, 1991
8) Kawashima, K., Sugita,H., Kanoh, T. and Iida, H. : Application of Thermal Image Sensor for Survey of Seismic D,,Image, Civil Engineering Journal, Vol. 33-1,
January 1991
9) Kawashima, K., Sugita, H. and Kanoh, T. : Flight Method of Helicopter for Surveying Damage Information Immediately After An Earthquake, Civil Engineering Journal, Vol.33-9. 1991

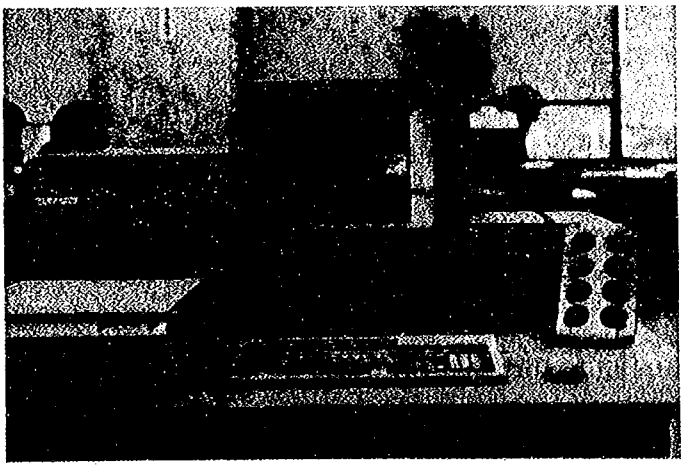


Photo 7 Visual Information Pilot System

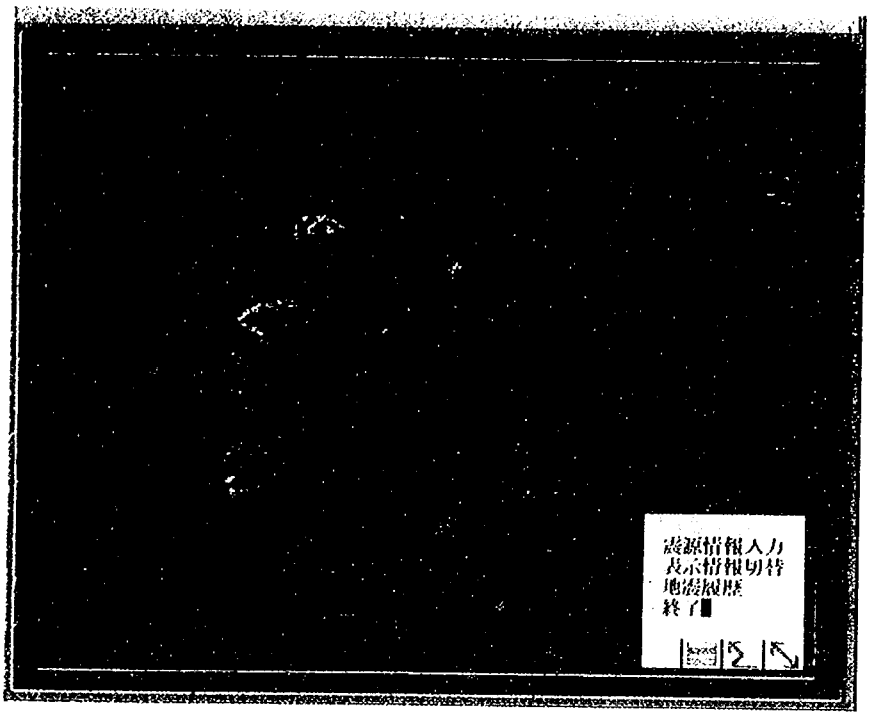


Photo 8 Maximum Acceleration of Ground Surface and Seismic Intensity

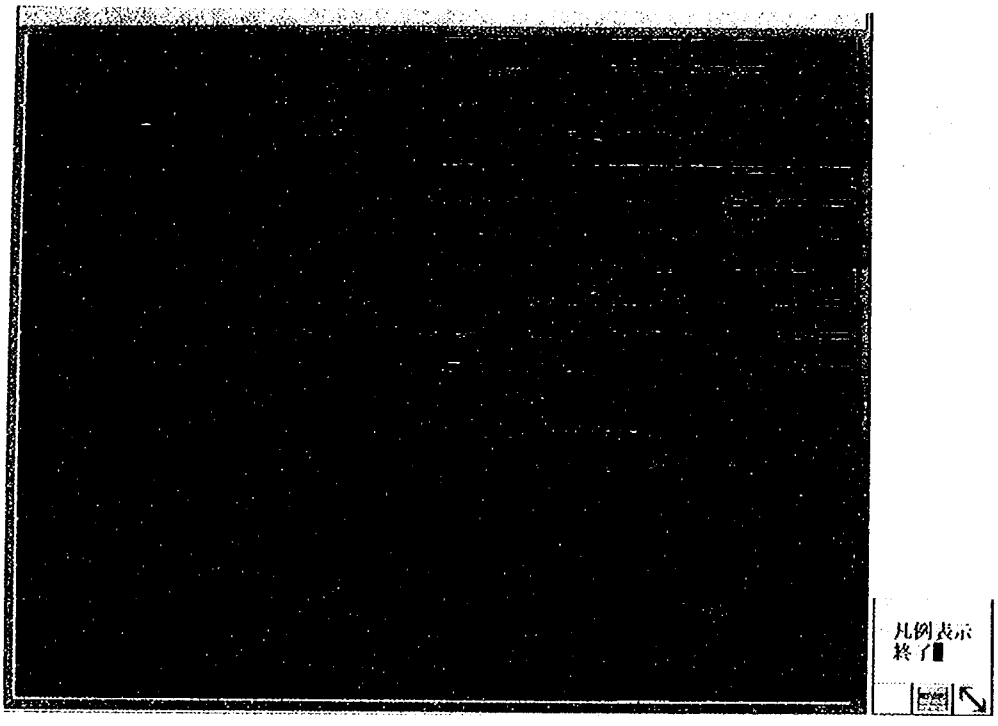


Photo 9 Liquefaction Potential Estimated for Each Cell

CIVIL INFRASTRUCTURE SYSTEMS RESEARCH: INTELLIGENT MATERIALS AND NATURAL HAZARD MITIGATION

S.C. Liu and K.P. Chong[1]

ABSTRACT

This paper describes the recently developed Civil Infrastructure System (CIS) Research Program by NSF and reports the concept and a proposed program framework of continuous research. Two important underlying components, i.e., the development of intelligent materials for CIS applications and the CIS implications in natural hazard mitigation, are highlighted.

KEYWORDS: civil infrastructure; intelligent materials; natural hazard; structural control

INTRODUCTION

In 1992, following an intensive program development effort including a special workshop in April 1991 (NSF, 1992), a program concept and framework was developed for a broad-based CIS research which will be conducted on a continuous, interdisciplinary basis (NSF, 1993) . In these reports, NSF is recommended to establish a multidisciplinary initiative to conduct basic research on materials, and infrastructure components, to integrate systems, and to transfer research results into industrial applications.

PROGRAM CONCEPT AND FRAMEWORK

The initiative calls for the establishment of a national focus of continuous CIS research to (1) quickly put existing knowledge about civil infrastructure to work and (2) generate new engineering and scientific knowledge. The approach should be scholastic, targeting optimal system performance and innovative techniques and methods. Further, the program should seek to

1. Promote proof-of-concept research, knowledge transfer,
education and training, human resource development, and federal, state, and private-sector partnerships.

2. Systematically address issues of deterioration science, assessment technologies, and renewal engineering.

3. Strengthen research programs at infrastructure-related academic research centers.

4. Encourage university and other investigators to pursue
critical civil infrastructure systems research needs.

A CIS research effort should be developed with two thrusts: one for performing basic research, and another for addressing knowledge diffusion-enabling research results to be turned into products and services for industry. In this effort, NSF should target three elements of infrastructure renewal:

- **Deterioration Science**

A fundamental issue in understanding why

[1] Program Directors
National Science Foundatin
Washington, DC 20550
U.S.A

constructed facilities decay is to understand better the science of deterioration. A major component of this research will be materials science and mechanics. Other components are studies in failure processes; risk and reliability; materials processing, fabrication, manufacturing, and assembly; corrosion, fatigue, and environmental hazards; performance criteria; extension of service life; and strength and durability.

- **Assessment Technologies**

A major problem in repairing and upgrading infrastructure is an inability to assess accurately the state of health of a constructed facility. Current methods for assessing constructed facilities are relatively primitive and unreliable, prompting conservative, often costly decisions. Research in this area will focus on nondestructive evaluation, smart materials, damage processes, advanced instrumentation, evaluation of service life and long-term monitoring; system evaluation; characterization of performance under extreme events; acceptable risk; interdependence of infrastructure systems; geographical information systems; and social and economic effects.

- **Renewal Engineering**

Constructed facilities - the nation's largest, tangible resource - include facilities for transportation, energy, waste collection and treatment, water supply and protection, environmental protection, and for living, working, playing and performing functions of education and government. These physical underpinnings of society need renewal, modification, and upgrading, and research will emphasize new design and construction methods. Other important studies include using new or modified materials, trenchless technology (e.g. micro-tunneling), batch manufacturing techniques in construction, simulation, innovative repair and modification, and modified construction techniques suited to robotics applications. Innovative electrical and communication systems could play a role in intelligent highways. Other research topics include performance criteria and repair strategies; demolition, disposal, and recycling; preservation of national resources; information theory, expert systems, and artificial intelligence; and integrating structural design, processing, and fabrication.

Each element addresses cross-cutting research in materials science, mechanics, social sciences, geotechnical and structural engineering, fluid mechanics and water resources, environmental engineering, chemistry, and mathematical, computer, and information science. This broad-based, multidisciplinary program emphasizes system integration and builds on NSF strengths in engineering and science.

It is interesting to note that, shortly after the completion of the NSF development of CIS initiative, President Clinton said in his message on America's technology for economic growth, called for investment in establishing an integrated research program designed to enhance the performance and longevity of the nation's existing infrastructure (President Clinton and Vice President Gore, 1993). Specifically it is directed, quote, "...this program would systematically address issues of assessment technology and renewal engineering," unquote.

CIS AND NATURAL HAZARD MITIGATION

Earthquake engineering research-aggressively conducted over the last two decades-has help laid the knowledge and technological foundation of CIS. Earthquake engineering and other natural hazard research will continue to play a major role in the CIS research program.

The infrastructure is affected by natural phenomena such as wind, earthquakes, and landslides. While research in these areas has been common in the past, much remains to be done. There is a need to refine predictive capabilities so movement levels can be determined and controlled, and design techniques for new technologies (such as reinforced earth) can be developed. Foundations for existing structures may prove inadequate during extreme loads imposed by natural hazards; methods are needed to identify and correct deficiencies.

Some of the important CIS research needs as related to natural hazard mitigation include:

- Develop effective and economical methods that can be implemented in the field to evaluate and retrofit existing hazardous infrastructure systems and components subject to natural and man-made hazards, including earthquake, wind and flood.

- Develop technologies to diagnose and assess the condition of, and risk inherent in, individual infrastructure systems and components (for use in pre-and post-disaster situations).

- Develop outage engineering management technologies to lessen facility down time and to develop rapid rehabilitation and construction methods.

- Develop innovative repair and replacement techniques through system integration of passive, active and hybrid control technology and use of advanced materials.

- Establish the knowledge needed to set system performance standards, evaluation procedures, codes and criteria under seismic and other natural hazard conditions for major lifeline systems including public and private utilities.

- Develop high-tech systems to facilitate infrastructure maintenance and operations, such as emergency damage control, quick recovery and service restoration following a natural disaster.

CIS RESEARCH IN SMART MATERIALS

The key to successfully integrating material science and structural mechanics is in the development of intelligent systems that connect microscopic properties to the macro level functional behavior of structures. Intelligence can be introduced at the microscopic level (shape memory alloys, piezoelectric materials, magnetostrictive materials, electrorheological fluids) or at the macro level (passive, active, adaptive vibration controls). The latter requires state of the art dynamic sensing, processing, and control. CIS applications should be explored.

One continuing long-range goal of infrastructure systems research is to learn how living systems function, adapt, and transfer this understanding into smart materials and optimal structural design. The challenge for CIS is optimal (Chong and Liu, 1992) performance of systems in terms of safety as well as functionality, rather than the behavior of individual system components.

The demand to understand and control the dynamic characteristics of structures and their components has generated many new developments in smart materials and devices, primarily in aerospace and mechanical engineering fields. But such advances cannot yet be readily applied to distributed mass or multiple-degree-of-freedom systems such as many typical civil infrastructure systems. This area is a critical research frontier in structural performance and safety and in natural hazard mitigation.

Academic and industry research in intelligent control systems over the recent years has spurred advances in three key elements: sensor technology, control theory, and actuator dynamics. A challenge exists to integrate such existing techniques, while developing new ones, for broad applications in safety control of CIS-including both existing and new structures.

One critical component in transportation infrastructure systems is the bridge structure. Bridge research for seismic and non seismic loads has been ongoing for many years. Most of this research is of an applied nature, and address immediate needs. Little attention has been paid to fundamental research and longer-term issues of future loads and new structural forms, and more research is needed. For existing bridges, the major goals are the indefinite extension of remaining life, and the maintenance-free bridge. For future construction, new configurations using smart materials, structural control, new coating systems, and improved foundation techniques need attention.

Some infrastructure research topics in this area include:

- Develop advanced materials which have added energy-absorbing or variable damping property, and those having varying stiffness, strength, and self-healing capability under conditions of changing stress, pressure or temperature.

- Develop smart materials such as superalloys, electrorheological fluids, and piezoelectric material which possess the appropriate degree of sensing, data and information processing, and control capabilities for infrastructure applications.

- Design and test manufacturing and construction processes of new and smart materials for possible commercial mass production.

CONCLUDING REMARKS

Academic and industrial research over the last decade has spurred advances in ne materials, structural systems, automated construction, ground enhancement, prefabricated assemblies, electrokinetic geotechnology, corrosion inhibition, electro-optical communication, understanding of public decisions, management, location and siting, and public finance. Yet barriers still exist to transferring this basic knowledge into civil infrastructure practices. Today, it generally takes 5 to 20 years to move such knowledge from research institutions to the marketplace.

Basic research in natural hazard mitigation and in smart materials and structures, and developing research results, have great potential for prolonging the life and enhancing the capacity of our civil infrastructure systems and for improving our economic productivity and quality of life as well.

REFERENCES

"Civil Infrastructure Systems Research", Report of a workshop by National Science Foundation, Washington, D.C. 1992.

"Civil Infrastructure Systems Research, Strategic Issues", a report by the Strategic Planning Committee, National Science Foundation, Washington, D.C. 1993.

Chong, K.P., and Liu, S.C., "Engineering Research on Smart Materials", NSF Directions, vol.5 (5), 1992.

"Technology for America's Economic Growth, A New Direction to Build Economic Strength", by President Clinton and Vice President Gore, February 22, 1993.

Evaluation of Ground Displacement and Its Effect on Lifeline Performance

by

Steven Glaser*

ABSTRACT

This paper examines the state-of-the-art of liquefaction-induced ground displacement estimation with special attention to lifelines. The state-of-the-art for estimating permanent ground displacements is purely empirical. Several methods are examined, and they all appear to have comparable predictive abilities. The recommended method takes into account geological, geotechnical, topographical, and seismological parameters.

KEYWORDS: building technology; earthquakes; liquefaction; material properties; permanent soil displacements.

1. INTRODUCTION

Damage resulting from liquefaction is especially costly for lifelines. Damage to roads, rail, telecommunications, power, and pipelines of all types is always harmful, especially so during time of emergency. One of the most striking examples of the effect of lifeline damage on public safety was the 1906 San Francisco earthquake, following which over 490 city blocks were totally destroyed by one of the largest and most deadly fires in U.S. history (O'Rourke et al., 1991). Little could be done to stop the spread of the fire since the pipelines carrying water were broken due to liquefaction-induced ground displacements. The same areas that suffered liquefaction-induced ground displacements in 1906 suffered similar displacements during the 1989 Loma Prieta earthquake.

This review considers significant technical papers presenting methods for estimating horizontal ground displacements due to liquefaction. This paper serves as a thorough overview and evaluation of where the profession is today. This paper takes a "critical" point of view when examining proposed methods in order to examine the underlying suppositions of a given approach, conditions which define the validity and applicability of that method.

2. ESTIMATING HORIZONTAL DEFORMATIONS

The major hazard of liquefied soils is the occurrence of horizontal displacements. Almost all the alarming photographs of wide-spread destruction from an earthquake are for damage done by large horizontal movements of the soil surface (e.g. NRC, 1985; Steinbrugge, 1982) The body of work which has developed in the attempt to estimate horizontal ground displacements will be examined.

In order for ground displacement to take place, a driving force must be present. If a loose sand liquefies, the driving shear stresses are the "static stresses required for static equilibrium....correspond(ing) to those one would calculate in a stability analysis." (Castro, 1987). This situation involves three general geometries. Liquefaction of a sloping stratigraphy leads to a general flow failure or slope failure, such as at the Lower San Fernando dam in 1971. A sloping lower boundary leads to lateral spreads when the sand liquefies and looses shear strength. The lateral displacements of soil towards a river or open cut is illustrated by the large-scale damage done by the 1964 Niigata earthquake. The amount of slope needed to drive the movement is very small — 0.1 to 3 degrees if there is a nearby free face.

Driving shear stress can also be provided by man-made structures such as buildings and earth embankments. A railroad embankment caused large (> 1.5 m) displacements above a liquefied layer in Niigata (Ishihara, 1985). A very through analysis of this problem, based on several

* National Institute of Standards & Technology, Gaithersburg, MD 20899, U.S.A.

shake table tests, was reported by Ishihara and Takeuchi (1991). The paper is especially useful for its qualitative description and conceptual evaluation of the displacement problem.

In the case of cyclic mobility, where the soil maintains some shear strength and the static forces are less than the steady-state strength, the earthquake excitation itself drives the soil displacement. This is a stable situation, rather than one leading to catastrophic failure. A mechanistic solution is generally used for this situation, although constitutive models are being written to solve for the displacements directly. Whether soil liquefies or undergoes cyclic mobility, the displacements will be a function of the steady-state strength of the soil, although the "shear strength" of a loose, liquefied sand might be better described as its viscosity.

2.1 SIMPLE EMPIRICAL APPROACHES

The most straightforward approach to estimating horizontal displacements due to liquefaction is to compile a database of known displacements, and to correlate the displacements with measurable parameters. A difficulty is choosing parameters, since so many geotechnical, topographical, and seismological variables affect the results. The accurate measurement and compilation of in situ displacements, and the relevant parameters, is also a formidable task.

The first important study of this kind was done by Hamada (Hamada et al., 1987, 1986). Detailed mapping was done in Noshiro City, Japan, after the 1983 Nihonkai-Chubu temblor. The displacements were scaled from before and after air photographs. Over 2,000 points were analyzed, with maximum lateral displacements of three to five meters noted. Hamada combined this data with information from Niigata (1964) and San Fernando (1971) for a regression analysis. The parameters chosen as relevant were thickness of the liquefied layer and the steepest slope angle of either the bottom of the liquefied layer or ground surface, in percent. The result of the regression is given by

$$D = 0.75 \sqrt[2]{H} \sqrt[3]{q} \qquad (1)$$

where D = displacement
H = thickness of liquefied soil layer, from Japanese Bridge Code procedure
θ = greater of the slope of bottom layer or ground surface (in percent).

The fit between the actual data and the regression equation is shown in Fig. 1, with the factor of two range indicated by the dashed lines.

Finn (1988) points out that the database is biased by several factors. There is strong influence from Noshiro City, which had shallow slopes and displacements, and the large displacements from Niigata. The estimates of slope are unreliable at areas of rapid change, such as near river banks. The included temblors were all close in magnitude, and the soils very similar, so Hamada's equation does not represent general conditions. Finn recommends separating extreme topographies into specific studies.

Other researchers looked at the same case studies as Hamada, and derived different regression equations based on what they though were the controlling parameters. Miyajima et al. (1988) focused on the permanent ground displacement after the 1983 Nihonkai-Chubu earthquake. Miyajima broke the areas showing displacement into three categories: non-liquefied areas, liquefied areas without sand boils, and liquefied areas with sand boils. These three categories relate to aspects of the buildup and dissipation of excess pore water pressures (Dobry, 1989).

From the field data, and from shaking table tests to evaluate the correlation of the width of displaced zone with permanent lateral displacement, Miyajima found that "The maximum value [displacement] seems to be directly proportional to the width of the loose sand deposit." There was also a good correlation with the slope of the ground. Note, however, that this approach is inherently flawed. There is no way that this analysis can lead to a predictive equation since the width of the mobilized zone is an a posteriori variable. This fallacy is carried further in Miyajima et al. (1991), where the duration of liquefaction is added as a controlling variable, another a posteriori parameter.

Jian and Lianyang (1991) apply a rational technique in choosing the physical parameters by which to estimate displacement. The authors use a Fibonacci search method of optimization. Five factors were chosen to represent the in situ condition and excitation. They are (1) earthquake magnitude, (2) distance from earthquake hypocenter, (3) depth of water table, (4) depth of sand, and (5) average SPT blow count. A database of forty data points was compiled from the literature based on thirteen different earthquakes, where liquefaction did or did not occur.

The model was trained on twenty randomly selected data points, which included calculating weightings for the various factors. When the system was tested on the remaining twenty points, the authors were able to predict the actual displacement quite well, claiming a correct rate of 95%. The analysis shows that the SPT blow count and temblor moment magnitude were the most important factors, with depth to the water table the least important. The results are promising, and as the authors point out, more field data is needed to strengthen the analysis. Further detail about the analysis and approach is also needed.

2.2 ADVANCED EMPIRICAL APPROACHES

Through a review of case histories, Youd appraised the amount of damage structures undergo for different amounts of ground displacement (Youd, 1976). The severity or damage potential of the displacement was expressed by the liquefaction potential, S (Youd and Perkins, 1987), defined as the amount of permanent ground displacement in millimeters divided by 25 (i.e. maximum displacement in inches). The relation between displacement, liquefaction severity, and damage is indicated in Table 1. Youd lists fifteen different factors that affect the severity of liquefaction-induced displacement, covering seismological, geological, topographical, and geotechnical factors.

The factor S will vary throughout a region which undergoes liquefaction. A metric called the Liquefaction Severity Index, LSI, was formulated to give the general severity of ground displacement over a region. Avoiding the over-generalization of Hamada et al. (1986, see Finn, 1988), Youd and Perkins insist that the LSI be evaluated for distinct topographic and geologic environments. In general, the LSI was derived for "wide active flood plains, deltas, or other areas of gently-sloping late Holocene fluvial deposits." LSI ranges from one to one hundred, with anomalously large displacements given the maximum value of one hundred. Also note that the LSI is the conservative, *maximum* severity in an area, with other lesser displacements also present.

Displacements and parameters associated with six earthquakes in the western United States and Alaska were analyzed. Youd's analyses showed that most of the geological, topographical, and geotechnical factors were not relevant variables since the comparisons were done for roughly equivalent regions. For instance, the SPT blow counts ranged from two to ten, and only failures more than ten meters in extent were included. The final regression equation of Youd and Perkins is given by:

$$log(\mathrm{LSI}) = -3.491 - 11.86 log(\mathrm{R}) + 0.98\mathrm{M_w} \qquad (2)$$

where R = epicentral distance in km
$\mathrm{M_w}$ = moment magnitude.

Youd and Perkins argue that the quality of the data available to users does not warrant the inclusion of second order terms. This equation is valid for the western U.S., and possibly Alaska. Application to other regions is dangerous because attenuation is higher in the western portion of the U.S., and the impedance contrast is greater between bedrock and the soil, leading to much higher accelerations in the eastern U.S..

Recent work has been conducted using a multiple linear regression analysis to take into account a great number of variables in a predictive equation for horizontal displacements (Bartlett, 1992; Bartlett and Youd, 1993). This analysis examined 43 detailed factors, from eight different earthquakes, in order to account for seismological, topographical, geological, and geotechnical effects on the permanent displacement of ground due to liquefaction. Bartlett's database comprised 448 horizontal displacement vectors, SPT blow counts from 270 bore holes, and nineteen observations from Ambraseys (1988).

Since the temblors at Niigata and Noshiro City were so similar, the analysis could initially be run for these two sites independently of the seismological factors. This analysis showed that the two types of spreading — towards a free face and down gentle slopes — would need separate predictive equations. The free face equation was derived for Niigata, the sloping ground equation for Niigata and Noshiro City. The U.S. temblors were included to account for seismic and other site-specific conditions.

The final analysis resulted in two lengthy equations based on six parameters. The free face relation is given by

$$Log(D_H + 0.01) = -16.366 + 1.178M - 0.927Log(R) - 0.013R + 0.657Log(W) + 0.348Log(T_{15}) + 4.527Log(100 - F_{15}) - 0.922D50_{15} \quad (3)$$

and the sloping ground relation is given by

$$Log(D_H + 0.01) = -15.787 + 1.178M - 0.927Log(R) - 0.013R + 0.429Log(S) + 0.348Log(T_{15}) + 4.527Log(100 - F_{15}) - 0.922D50_{15} \quad (4)$$

where **M** = earthquake moment magnitude
R = epicentral (horizontal) distance to earthquake (km)
W = Ratio of free face height to distance to free face (%)
S = ground slope (%)
$(N_1)_{60}$ =Corrected blow-count of the liquefiable layer, (60% hammer energy and 1 tsf overburden pressure).
T_{15} = cumulative thickness of saturated sandy layers with $(N_1)_{60} < 15$ (m)
F_{15} = average fines content of saturated granular layers in T_{15} (%)
$D50_{15}$ = average mean grain size of layers included in T_{15} (mm)

There are limitations to the use of these formulae, based on the data set used to derive the correlations. Until final development of correction factors, the method is not suitable for the eastern U.S.

The Bartlett and Youd correlations are a definite improvement over past attempts to estimate liquefaction-caused displacements empirically since they take into account information from all major areas of controlling factors: seismological, topographical, geological, and geotechnical parameters. This inclusion lends a certain degree of intellectual grounding to the empirical relationships, since it begs common sense that soil properties, for instance, did not enter into Hamada's relationship. What is now needed is application of the improved relationships to areas not included in the data base in order to fully evaluate their efficacy.

3. ESTIMATING DISPLACEMENTS IN STABLE SITUATIONS

Liquefaction of a sandy soil is not the only, or most common, behavior due to earthquake excitation. If the sand is moderately dense, it will behave in a dilative manner when cyclically loaded and strain harden. The cyclic stress-strain curve for this material is monotonically increasing and the steady-state strength is the maximum strength of the sand. Earthquake loading reduces the strength of the susceptible layer, allowing some small displacement, but the steady-state strength is always greater than the driving shear stress. Makdisi and Seed (1978) say that the accumulated strains will be very small due to the almost elastic behavior of the soil in this condition.

Another form of non-catastrophic "controlled" displacement is termed lateral spreading. In this case, the driving shear stresses alone are less than the steady-state strength of the soil. Lateral spread caused severe damage to Juvenile Hall during the 1971 San Fernando earthquake (Youd, 1973). Conditions leading to lateral spreading involve shallow slopes, or flat terrain close to an open face such as a river. In all these cases the added force that causes motion from the earthquake acceleration is the force over-and-above static stress.

There are two very different approaches to estimating lateral displacements. The most commonly accepted method is a mechanistic approach first put forth by Newmark (1965),

which makes use of the steady-state strength of the liquefaction susceptible sand. This method has been accepted by virtually all members of the geotechnical community (e.g. Baziar et al., 1992; Mabey, 1992; Marcuson et al., 1990; Castro, 1987), and will be described in this major section. The other approach is a full nonlinear finite element approach, and will be described in the next major section.

3.1 NEWMARK'S METHOD

Newmark visualized blocks of solid soil overlaying liquefied material. A pictorial example of this scenario is given in Fig. 2 The inertial forces induced by the earthquake cause the blocks to move on the weakened soil towards a free face (e.g. incised river channel) rather than towards the fixed boundary in the opposite direction. It can be assumed further that loose soil and debris will fill the fissures formed in the firm material so that the block will move only towards the unsupported (free face) side.

The force needed to initiate motion for a given block of soil is calculated just as for the static case of a block on an incline. The horizontal force that is required to initiate block movement is called the yield acceleration, and is equal to the product of the mass of the block and the mobilized soil shear strength. In reality, the shear strength of the interface is the strength of the weak, potentially liquefied layer. Newmark chose to model the soil as rigid-plastic in order to ease computation. For the case where the sand is very loose and contractive, the shear strength would be the steady-state strength, leading to a slope or flow failure.

For earthquake horizontal accelerations below the yield acceleration, there is no relative movement of any part of the soil profile. When the acceleration is greater than the yield acceleration, the block of soil will move from the time the acceleration exceeds the threshold, until the velocity of the block becomes zero. Note that the motion is only assumed to take place in the down-hill (or free face) direction, since a tremendous amount of acceleration would be needed to move the block either uphill, or against the passive earth pressure in the flat ground case. Castro notes that displacements greater than one hundred millimeters are usual only for peak accelerations more than five times greater than yield acceleration (Castro, 1987)

An in-depth analysis of the Newmark method is given in Baziar (1991), including a derivation for the case of a fully submerged block excited by sinusoidal acceleration. The essence of the analysis is given by Fig. 3. When ground acceleration exceeds the yield acceleration at t_1, the block begins to move until its velocity returns to zero at time t_3. The displacement for that cycle is found by twice integrating the acceleration curve for the time of motion (from t_1 to t_3). The cumulative displacement, d_c is the sum of all cycles, as shown in Fig. 3.

Baziar derives an equation for estimating the cumulative amount of lateral displacement, involving peak acceleration, period of acceleration, and the number of cycles exceeding the yield acceleration. The displacement is a function of the ratio of yield to peak acceleration, and is inversely proportional to the square of the frequency of excitation (Baziar, 1991). The same conclusion was reached independently by Yegian et al. (1991). This result appeals to common sense, since if the frequency of acceleration is very high, there is little time for the block to move.

The frequency dependent behavior, hence the validity of the Newmark method, was tested experimentally and found to hold true only for contractive (loose) sands (Baziar, 1991). The experiments, specialized cyclic triaxial tests, showed that the frequency of acceleration had no effect on displacement for dilative materials. In addition, dilatant materials, which have no constant-strength plateau, do not obey a rigid-plastic model. Castro (1987) implies that, for a low number of cycles (stress path below the yield envelope), the sliding block analysis is correct for dilative sands, although the amount of displacement involved is insignificant. It would seem possible to derive an expression for applying a Newmark-type analysis for the dilative case, with permanent displacement being a function of cumulative cyclic displacement. In addition, Baziar's modeling of the Newmark situation in an axial cyclic triaxial test might not be strictly accurate, in the sense that the cyclic simple shear test might model the in situ motions more accurately.

Baziar applied his combined method (Baziar and Dobry, 1991) to the Wildlife Site, Imperial Valley, CA, and to the standard soil conditions used by Youd and Perkins (1987) in developing the LSI. The analytical results were comparable, but indicated that predictions would not be better than a factor of two or three (i.e., no better than Hamada et al., 1986). Finally, Baziar combined his approach with a regional attenuation relation, in a manner similar to Youd and Perkins (1987). Comparison with the conclusions of Youd and Perkins show the two different approaches giving much the same results.

Mabey (1992) combined the Newmark sliding block analysis with a stochastic ground motion scheme. The method also integrates a correlation between steady-state strength and corrected SPT blow count. This was done by incorporating a large data base of historical lateral spread displacements. Estimates would be predicted by using the lowest $(N_1)_{60}$ value to assess residual strength, and then subjecting the modeled system to a suite of simulated ground motions. Mabey compiled a large variety of such results and formulated a crude regression relation to allow preliminary estimates to be done by hand, although actual sliding block analysis was recommended for serious work. At this time, the accuracy and usefulness of this approach is not known.

An approach similar to Newmark's method was developed by Yegian et al. (1991). The application was geared towards estimating the permanent displacements of earthen dams and large embankments due to earthquake excitation. Yegian et al. use actual acceleration histories to estimate displacements, taking into account the magnitude of the temblor in the predictive model. Error theory is then used to model the uncertainties involved in the prediction. A computer code was developed that "provides the probability that the permanent deformation of a critical sliding mass will exceed a specified value." The probabilistic approach is especially useful for planners, but it is unclear whether the resulting prediction accuracy is sufficient to warrant the effort.

Makdisi and Seed (1978) customized the application of Newmark's method to the evaluation of earthquake-induced deformations of earthen dams. The concept's assumptions remain the same as Newmark's, but a rational approach to estimating the actual embankment accelerations due to the shaking was incorporated. The yield acceleration — that needed to just force the embankment to move — was calculated as a function of the geometry of the soil "block" and cyclic strength of the weak layer. A two-dimensional finite element analysis utilizing an equivalent linear strain-dependent soil model was used to calculate the earthquake-induced average accelerations to which a given block would be subjected. This step rationalized the application of the sliding-block procedure to large embankments that will have a dynamic response of their own, different from the free field. The final calculation of displacement was done with the double-integration method described above, and illustrated in Fig. 3.

A recent "improvement" to the Newmark sliding block method was proposed to incorporate a more thorough description of the post-liquefaction behavior of sand (Byrne et al., 1992; Byrne, 1991). Byrne claims that the rigid-plastic model used by Newmark "...cannot in its present form account for the large strains and displacements that occur within the zone of liquefaction." Byrne notes that the post-liquefaction stress-strain response of a loose sand is not rigid-plastic, but rather strain hardening up to a limiting strain, whereupon the liquefied sand takes on the steady-state strength.

Byrne proposes a soil model where the stiffness of the soil varies linearly until limiting strain. However, Byrne uses the same variable (SPT blow count) to calculate the supposedly independently measured quantities of stress and strain (which he uses to calculate his stiffness, and displacements), residual strength, and limit displacement. The method seems to be a step forward from Newmark's approach by accounting for actual soil behavior, and N-degree of freedom systems. However, due to lack of the necessary input data, the examples given become empirical correlations based on the corrected SPT blow count, and the method looses its theoretical uniqueness.

4. AN ATTEMPT AT DIRECT CALCULATION

An attempt has also been made to derive a simplified analytical expression for lateral spread based on a minimum energy principle (Tokida et al., 1992; Towhata et al., 1991, 1989). The work was based on shake table tests conducted to determine the effect of the length of slope on flow due to liquefaction. Due to interaction with the end of the tank, specimens with shorter slopes showed less strain. It was also found that a dense overburden helps retard liquefaction.

For the analytical model, the soil is expected to deform with a quarter-sinusoid distribution — zero at bottom and maximum at the top of the layer. The soil will flow with constant volume, and as a liquid governed by the hydraulic gradient. The upper confining layer acts as a horizontal bar with a given Young's modulus. A value for displacement at the top of the liquefied stratum is derived by minimizing the potential energy of the ground using the variational principle. This is usually a complicated computation involving the entire strain tensor, but has been simplified by the authors.

The solution to the problem is formula comprised mostly of geometric factors describing the slopes and thicknesses of the firm sub-base, liquefied layer, and unsaturated cover layer. The only material parameters involved are the unit weights of the liquefied layer and overburden, and the Young's modulus of the overburden. In fact, the material properties only serve as constants, since , arbitrary values rather than actual in situ properties are assigned when the analysis is applied to case histories. This observation is borne out by the lack of material properties in the simplified practical method suggested in the later paper (Tokida et al., 1992), where displacements are estimated using a regression equation derived solely from shake table tests.

The results of test analyses on twelve sites with lateral spread in Niigata and Noshiro City indicate that this method gives very acceptable results. It should be noted, however, that the length of slide was known a posteriori in these cases, and therefor the method will not work in a predictive mode.

5. AN ILLUSTRATIVE CASE STUDY

At this point, it is beneficial to present some details from a case study illustrating some of the concepts that have been discussed above. Egan and Wang (1991) provide a summary of liquefaction-related ground deformations at Treasure Island, CA, due to the 1989 Loma Prieta earthquake. Treasure Island is a small man-made island in the San Francisco Bay. It was constructed in the 1930's by pumping hydraulic fill behind a set of rock dikes set on the bay floor.

Reported large-scale lateral spreading, from 120 to 300 mm, took place over areas as large as 170 m (Egan and Wang, 1991). Witnesses reported that all displacements took place during the shaking, and that no visible deformations appeared after the earthquake. The effect on lifelines was considerable, with 44 utility line breaks have been reported. Many of the pipeline breaks were due to lateral spread, although some appeared to be due to differential settlement associated with soil blocks undergoing lateral displacement. Based on analyses after Newmark (1965) and Makdisi and Seed (1978), back-calculations indicate that the undrained residual cyclic stress was approximately 19 KPa (400 psf).

Vertical differential settlement was widely observed close to structures. The differential settlement was on the order of 50 to 150 mm, with the entire island appearing to subside by almost this amount. Some areas subsided by as much as 0.6 m, corresponding to the locations of the thickest deposits of liquefaction-prone fill (see Dobry, 1989). Application of the techniques of Tokimatsu and Seed (1987) was found to over-estimate the actual settlement by a factor of two. Better correlation was found using a hybrid method in which Egan and Wang combined elements of Tokimatsu and Seed, a probabilistic method of estimating liquefaction susceptibility, and the influence of grain size.

6. CONCLUSIONS

The current state-of-the-practice of the geotechnical approach to the problem of estimating liquefaction-caused horizontal displacement is empirical in nature. Simple formulae for estimating displacements, such

as Hamada's method, are examples of purely empirical solutions.

There are several reasons why this condition exists. Soils are a very complicated and non-linear material. Material properties can change by an order of magnitude over a very short distance. Soils were placed apparently erratically by nature when deposited, and then transformed through time in a very non-uniform manner. In addition, it is virtually impossible to measure in situ material properties of a soil without the very act of measuring contaminating the results. These factors serve to make constitutive modeling of these materials virtually impossible. An empirical approach is the selected alternative.

A variety of mechanistic and empirical approaches to estimating the extent of lateral spreading induced by earthquake excitation of saturated sands have been presented. It is obvious that no method models the actual physical behavior of the soil. This is the case because there is at present no generally agreed upon, detailed understanding of what happens after liquefaction, and no method exists to measure the relevant parameters even if there were agreement.

The obvious conclusion to be reached is that the only useful techniques currently available for estimating post-liquefaction deformations are the purely empirical correlations. This is true for both vertical and horizontal displacements,. It is difficult to choose one empirical technique over another, since they all seem to give results correct to within a factor of two or three. It is believed that the regression approach of Bartlett (1992) is more satisfying since it takes into account all the major physical concepts that control displacement.

A possible area of future improvement is the estimation of residual, or steady-state strength. Both the empirical SPT-based approach championed by Seed, and the laboratory-based approach advocated by Castro, are based on making very accurate guesses of the in situ void ratio of a sand (Marcuson et al., 1990).

Problems that remain to be solved include the accurate measurement of in situ residual strength of the liquefied sand, and actual in situ relative density. It is disappointing that at present there is not enough understanding of the liquefaction problem to lead to a good theory based on first principles. It is hoped that study of the problem in the field will soon clear our clouded vision.

7. REFERENCES

1. Ambraseys, N. N. (1988). Engineering Seismology. *Earthquake engrg. struct. dyn., 17*(1), 1-105.

2. Bartlett, S. F. (1992). *Emperical analysis of horizontal ground displcement generated by liquefaction-induced lateral spreads.* (CEG-92-01). Provo Utah: Dept. Civil Engineering, Brigham Young University.

3. Bartlett, S. F., & Youd, T. L. (1993). Emperical prediction of lateral spread displacement. T. D.

4. O'Rourke, & M. Hamada, *Proc. 4th Japan-U.S. workshop on earthquake resistant design of lifeline facilities and countermeasures for soil liquefaction.* (NCEER-92-0019) Honolulu, Hawaii.

5. Baziar, M. H., Dobry, R., & Elgamal, A.-W. (1992). *Engineering evaluation of permanent ground deformations due to seismically-induced liquefaction.* (NCEER-92-0007).

6. Baziar, M. H., & Dobry, R. (1991). Liquefaction ground deformation predicted from laboratory tests. S. Prakash, *2nd int. conf. recent advances in geotech. earthquake engrg. soil dyn.* I St. Louis, MO. 451-458. Rolla, MO: University of Missouri-Rolla.

7. Byrne, P. M. (1991). A model for predicting liquefaction induced displacement. S. Prakash, *2nd int. conf. recent advances in geotech. earthquake engrg soil dynamics. II* St. Louis, MO. 1027-1035. Rolla, MO: University of Missouri-Rolla.

8. Byrne, P. M., Jitno, H., & Salgado, F. (1992). Earthquake induces displacements of soil-structure systems. *Tenth world conference on earthquake engineering, 3,* Madrid. 1407-1412. Rotterdam: Balkema.

9. Castro, G. (1987). On the behavior of soilsduring earthquakes - liquefaction. in A. S. Cakmak, *Soil dynamics and liquefaction.* (Developments in geotechnical engineering 42). 1-36. Amsterdam: Elsevier.

10. Dobry, R. (1989). Some basic aspects of soil liquefaction during earthquakes. in K. H., and Turkstra, Carl J. Jacob, *Earthquake Hazards and the Design of Constructed Facilities in the Eastern United States, 558.* 172-182. New York: The New York Academy of Sciences.

11. Egan, J. A., & Wang, Z.-L. (1991). Liquefaction-related ground deformation and effects of facilities at Treasure Island, San Francisco, during the 17 October 1989 Loma Prieta earthquake. T. D. O'Rourke, & M. Hamada, *Proc.3rd Japan-U.S. workshop on earthquake resistant design of lifeline facilities and countermeasures for soil liquefaction.* NCEER-91-0001. 57-76. Buffalo:NCEER

12. Finn, W. D. Liam. (1988). Permanent deformations in ground and earth structures during earthquakes. *Proc. 9th world conf. earthquake engrg. VIII* Tokyo, Japan. 201-212.

13. Hamada, M., Yasuda, S., Isoyama, R., & Emoto, K. (1986). Study on Liquefaction Induced Permanent Ground displacement. Tokyo: Association for the Development of Earthquake Prediction.

15. Hamada, M., Towhata, I., Yasuda, S., & Isoyama, R. (1987). Study on permanent ground displacement induced by seismic liquefaction. *Computers and geotechnics, 4,* 197-220.

16. Ishihara, K. (1985). Stability of natural deposits during earthquakes. *11th Int. Conf. Soil Mech. Found. Engrg. 1* San Francisco, CA. 321-376.

17. Ishihara, K., & Takeuchi, M. (1991). Flow failure of liquefied sand in large-scale shaking tables. S. Prakash, *2nd int. conf. recent advances in geotech. earthquake engrg. soil dynamics. II* St. Louis, MO. 1753-1766. Rolla, MO: University of Missouri-Rolla.

18. Jian, D., & Lianyang, Z. (1991). Prediction of field sand liquefaction caused by earthquake by optimum seeking method. S. Prakash, *Proc. 2nd int. conf. recent advances in geotech. earthquake engrg. soil dynamics. I* St. Louis, MO. 431-436. Rolla, MO: University of Missouri-Rolla.

19. Mabey, M.A. (1992). *Prediction of displacements due to liquefaction induced lateral spreads.* (CEG-92-02). Provo Utah: Dept. Civil Engineering, Brigham Young University.

20. Makdisi, F., & Seed, H.B. (1978). Simplified prodecure for estimating dam and embankment earthquake-induced deformations. *J. geot. engrg., 104*(7), 849-867

21. Marcuson, W.F., Hynes, M.E., & Franklin, A.G. (1990). Evaluation and use of residual strength in seismic safety analysis of embankments. *Earthquake spectra, 6*(3), 529-572.

22. Miyajima, M., Kitaura, M., & Nomura, Y. (1988). characteristics of permanent ground displacement induced by soil liquefaction. *Memoirs of the faculty of technology, Kanazawa University, 21*(1), 1-10.

23. Miyajima, M., Kitaura, M., & Ando, K. (1991). Experiments on liquefaction-induced large ground deformation. T. D. O'Rourke, & M. Hamada, *Proc. 3rd Japan-U.S. workshop on earthquake resistant design of lifeline facilities and countermeasures for soil liquefaction.* NCEER-91-0001. 269-278.

24. NRC, (National Research Council committee on earthquake engineering). (1985). *Liquefaction of soils during earthquakes.* (CETS-EE-001). Washington, D.C.: National Academy Press.

25. Newmark, N.M. (1965). Effects of earthquakes on dams and embankments. *Geotechnique, 15*(2), 139-160.

26.O'Rourke, T.D., Gowdy, T.E., Stewart, H.E., & Pease, J.W. (1991). Lifeline and geotechnical aspects of the 1989 Loma Prieta earthquake. S. Prakash, *2nd int. conf. recent advances in geotech. earthquake engrg. soil dynamics. II* St. Louis, MO. 1601-1612. Rolla, MO: University of Missouri-Rolla.

27.Steinbrugge, K.V. (1982). Earthquakes, boils, and tsunamis. New York:Skandia America.

28.Tokida, K.-i., Matsumoto, H., Towhata, I., & Sasaki, Y. (1992). Study on prediction of lateral ground flow by soil liquefaction and its influence on piles. N. J. Raufaste, *Proc. 24th joint panel meeting of the U.S.-Japan cooperative program in wind and seismic effects. 24* Gaithersburg, MD. (paper 4-16). Gaithersburg, MD: NBS

29.Tokimatsu, K., & Seed, H. B. (1987). Evaluation of settlements in sands due to earthquake shaking. *J. geotech. engrg.*, 113(8), 861-878.

30.Towhata, I., Tokida, K., Tamari, Y., Matsumoto, H., & Yamada, K. (1991). Prediction of permanent lateral displacement of liquefied ground by means of variational principle. T. D. O'Rourke, & M. Hamada, *Proceedings from the third Japan-U.S. workshop on earthquake resistant design of lifeline facilities and countermeasures for soil liquefaction.* Technical Report NCEER-91-0001 San Francisco, CA. (pp. 237-251). Buffalo: National Center for Earthquake Engineering Research.

31.Towhata, I., Yamada, K., Kubo, H., & Kikuta, M. (1989). Analytical solution of permanent displacement of ground caused by liquefaction. T. D. O'Rourke, & M. Hamada, *Proc. 2nd Japan-U.S. workshop on earthquake resistant design of lifeline facilities and countermeasures for soil liquefaction.* NCEER-89-0032. 131-144.

32.Yegian, M.K., Marciano, E.A., & Ghahraman, V.G. (1991). Earthquake-induced permanent deformations: probabilistic approach. *J. geotech. engrg., 117*(1), 35-50.

33.Youd, T.L. (1973). Ground movements in the Van Norman Lake vicinity during the San Fernando, CA earthquake of Feb. 9, 1971. in *Report on the San Fernando earthquake of February 9, 1971.* (3). Washington, D.C.: U.S. Dept. Commerce, National Oceanic and Atmospheric Administration.

34.Youd, T.L. (1976). Ground failure displacement and earthquake damage to buildings. *Proc. conf. civil eng. nuc. pow.* 2 Knoxville, TN. 761-766. New York: ASCE.

35.Youd, T.L., & Perkins, D.M. (1987). Mapping of liquefaction severity index. *J. geotech. engrg., 113*(11), 1374-1392.

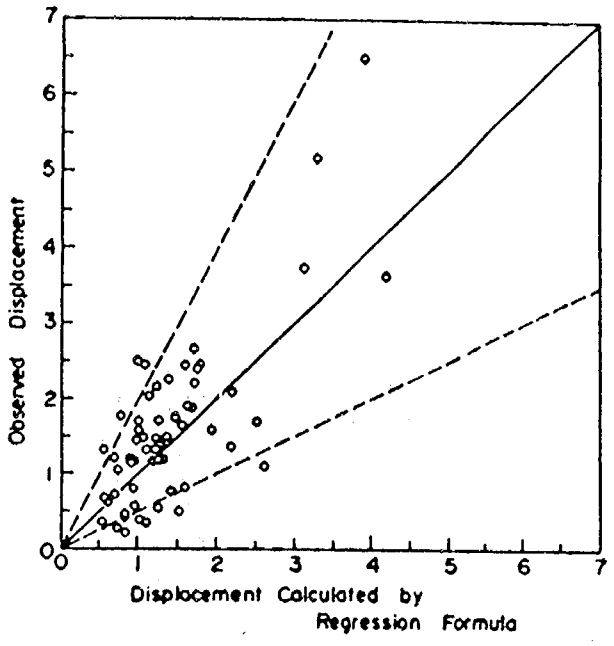


Fig. 1 Comparison between actual permanent horizontal displacements in meters and those calculated by Hamada (from Hamada et al., 1986).

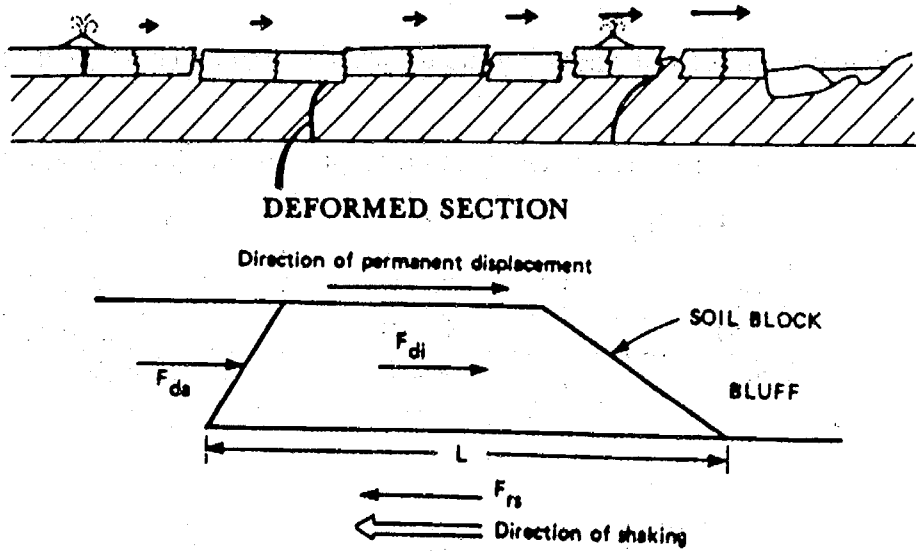


Fig. 2 Geometries leading to lateral spread during earthquake strong shaking (from NRC, 1985).

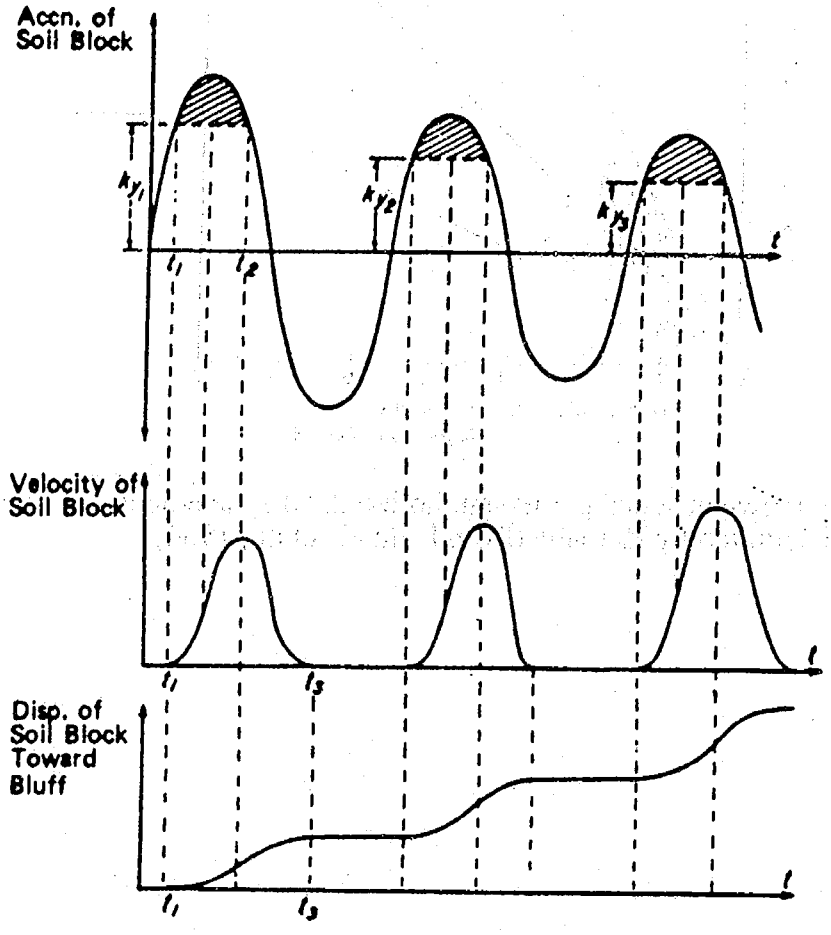


Fig. 3 Ground displacement calculated using the Newmark method (NRC, 1985).

TABLE 1 Estimated damage associated with ground displacements (after Youd, 1976).

DISPLACEMENT, mm	S	DAMAGE
50 - 100	< 5	minor
120 - 600	5 - 20	intermediate
> 760	> 30	major

New Developments in Analyzing Ground Motion and Structural Recordings: Site Amplification and Soil-Structure Interaction

by

*Erdal Şafak**

ABSTRACT

Advanced techniques from signal processing and estimation theories can be utilized to develop new methods for analyses of seismic recordings. These methods can increase significantly the accuracy and the amount of information that can be extracted from records. In this paper we present two sets of such methods, one set to characterize site amplification, and the other to investigate the effects of soil-structure interaction. The methods introduced for site amplification use a range of models, from the simple constant amplification model to the time-varying filter model. The methods introduced for soil-structure interaction permit the detection of the presence of the soil-structure interaction, and the identification of the natural frequency of the fixed-base building. Examples for the methods are given by using real-life and simulated recordings.

KEYWORDS: Seismic recordings; data analysis; site amplification; soil-structure interaction; dynamic response.

1. INTRODUCTION

As the volume of ground motion and structural response data increases, the need for more accurate and powerful methods for data analysis becomes more imperative. Modern methods of signal processing and estimation theories provide the necessary tools to develop such methods. The goal in developing new methods is to improve the accuracy and the amount of information that can be extracted from records.

In this paper we present two sets of such methods, one set to analyze site amplification, and the other to analyze soil-structure interaction. The methods introduced for site amplification use a range of models, from the simple constant amplification model to the time-varying filter model. The methods introduced for soil-structure interaction permit the detection of the presence of the soil-structure interaction, and the identification of the natural frequency of the fixed-base building. Examples for the methods are given by using real-life and simulated recordings.

2. SITE AMPLIFICATION

The standard method to estimate site amplification from recorded motions has been to use the spectral ratio, the ratio of the FAS (Fourier amplitude spectrum) of a soil-site recording to that of a nearby rock-site recording. Spectral ratios do not provide a robust measure of site amplification. Although they might show the correct resonance frequencies, spectral ratios rarely give the correct amplitudes of site amplification, because the amplitudes are

* *Research Structural Engineer, U.S. Geological Survey, 922 National Center, Reston, VA 22029, USA.*

very sensitive to the noise in the records, selection of time windows, and the type of smoothing applied (Şafak, 1991). Moreover, spectral ratios cannot be represented by simple analytical expressions. In practical applications, the ratios are averaged over selected frequency bands, and the resulting constant values are taken as the site amplification.

In this paper, we introduce five new alternatives to spectral ratios to describe site amplification. The methods are based on the following models: (1) constant amplification models, (2) damped oscillator, (3) weighted-averaged spectral ratio, (4) equivalent one-layer model, and (5) time-varying filters. An example for the application of each method is given by using a pair of rock- and soil-site recordings from the Loma Prieta earthquake. The rock- and soil-site recordings used in the examples are the transverse accelerations, with respect to the epicenter, from the Oakland Outer Harbor Wharf and the Piedmont Junior High School, respectively (CDMG, 1991). These accelerations and their spectral ratio, calculated by using three different triangular smoothing windows, are given in Fig. 2.1.

2.1 Constant amplification models

The simplest approach to describe site amplification is to approximate it by a constant for a specified frequency band. If $X(f)$ and $Y(f)$ denote the complex Fourier spectra of rock- and soil-site accelerations, respectively, the constant amplication factor, S, is defined for all frequencies in the frequency band $f_1 \leq f \leq f_2$ as $S = |Y(f)|/|X(f)|$. The amplitude error $\epsilon(f)$ at frequency f, of this approximation is $\epsilon(f) = |Y(f)| - S \cdot |X(f)|$. By using the least squares error criterion, and minimizing the total squared error from f_1 to f_2, we obtain the following expression for S:

$$S = \frac{\sum_{f=f_1}^{f_2} |X(f)| \cdot |Y(f)|}{\sum_{f=f_1}^{f_2} |X(f)|^2} \qquad (2.1)$$

For records that are believed to have outliers (i.e., large erroneous peaks), the least absolute value sum might be a more appropriate error criterion than the least squares sum.

Using the pair of accelerations given in Fig. 2.1, we calculate the constant amplification factors for four different frequency bands. The FAS of the rock- and soil-site recordings, and the frequency bands used in the calculations are shown in Fig. 2.2. Calculated S values for the least squares and the absolute value error criteria are given in Table 2.1 for each frequency band. Also given in the table for comparison are the averaged spectral ratios in each frequency band for three different smoothing windows. For a given frequency band, it can be shown analytically that the constant site amplification calculated from Eq. 2.1 has smaller variance than that calculated by averaging spectral ratios, and therefore is more accurate (Şafak, 1993*b*). In fact, if the noise in the records is Gaussian, Eq. 2.1 gives the optimal (i.e., minimum variance, maximum likelihood) estimate of the constant site amplification.

An alternative approach to estimate constant site amplification can be developed by using the ground motion model given in Şafak et al. (1988). The model is developed based on the observations that the cumulative squared FAS of accelerations can be approximated with a straight line. This approximation corresponds to a

a band-limited white-noise process for accelerations. The slope and the end points of the straight line fitted to the cumulative FAS give the constant amplitude and the effective frequency band, respectively, of the band-limited white-noise process. The ratio of the constant spectral levels of white-noise processes for soil and rock sites gives the site amplification and the effective frequency band for the amplification. The advantage of this approach over the preceding approach (Eq. 2.1) is that there is no need to select a frequency band.

This approach is presented in Fig. 2.3 for the sample pair of accelerations. The calculated site amplification is 5.75, and the effective frequency band is 0.4 to 2.2 Hz.

2.2 Damped oscillator

A popular method of modeling site amplification has been to approximate the soil layer as a damped linear oscillator (Kanai, 1957). For a damped linear oscillator with natural frequency f_f and damping ratio ξ_f, the transfer function $H(f)$ relating the input (rock-site) and the output (soil-site) accelerations is given by the following equation:

$$|H(f)|^2 = \frac{1 + 4\xi_f^2 \left(\frac{f}{f_f}\right)^2}{\left[1 - \left(\frac{f}{f_f}\right)^2\right]^2 + 4\xi_f^2 \left(\frac{f}{f_f}\right)^2} \tag{2.2}$$

The parameters f_f and ξ_f can be estimated in the frequency domain by matching the spectral ratios via least squares approximation. They can also be estimated in the time domain by first determining the parameters of a second order discrete-time filter, where the rock- and soil-site accelerations are the input and output of the filter (i.e., by fitting an ARX model), and then calculating f_f and ξ_f from the filter parameters (Şafak, 1989). The relationship between the numerator and the denominator in Eq. 2.2 should be noted when determining the filter parameters. Figure 2.4 shows the spectral ratio (smoothed by a 7-point triangular running window) of the records given in Fig. 2.1, and the matched transfer function of the damped oscillator. The frequency and the damping ratio of the oscillator are 1.28 Hz and 0.02, and the peak amplitude is 25.

2.3 Weighted-averaged spectral ratio

An alternative, and theoretically more accurate, method of calculating spectral ratios is to take the weighted average of the raw spectral ratio according to its inverse variance at each frequency (Ljung 1985). This approach results in the following equation for the spectral ratio $R(f)$:

$$R(f) = \frac{\left| \sum_{j=1}^{2k+1} W(j) Y(f-k-1+j) X^*(f-k-1+j) \right|}{\sum_{j=1}^{2k+1} W(j) \left| X(f-k-1+j) \right|^2} \tag{2.3}$$

where $W(j)$ is the smoothing window and the superscript $*$ denotes the complex conjugate. It can be shown analytically that for any specified smoothing window this spectral ratio has a smaller variance at all frequencies than the spectral ratio calculated by the standard method (Şafak, 1993*b*). For the sample pair of records, the comparison of the spectral ratios calculated from Eq. 2.3 and by the standard method using 7-point smoothing window are given in Fig. 2.5. The

weighted averaged spectral ratio gives smaller site amplification than the standard spectral ratio.

2.4 Equivalent one-layer medium

The relationship between soil-site and rock-site records can be represented by an equivalent one-layer system with a specific travel time (i.e., depth/velocity), the reflection coefficient at the rock-soil interface, and the attenuation factor Q. Consider the one-layer system schematically given in Fig. 2.6, where $x(t)$ and $y(t)$ denote the rock and soil-site recordings on the surface, respectively, and $u(t)$ and $d(t)$ denote the upgoing and downgoing shear waves at the top and the bottom of the layer, respectively. Assuming, for the moment, that there is no attenuation (i.e., $1/Q = 0$), we can write the following equations from Fig. 2.6 (Şafak, 1993*b*):

$$u(t) = -rd(t-\tau) + 0.5(1+r)x(t-\tau) \qquad (2.4a)$$

$$d(t) = u(t-\tau) \qquad (2.4b)$$

$$y(t) = 2u(t) \qquad (2.4c)$$

where τ is the one-way travel time of the shear waves in the layer, and r is the reflection coefficient at the soil-rock interface for upgoing waves. Note that since the reflection coefficient for the free surface is one, the incoming wave amplitudes at the rock-soil interface should be $x(t)/2$. It is assumed that the downgoing waves transmitted to the rock layer do not return. By solving $y(t)$ from Eqs. 2.4, we can write

$$y(t) = -ry(t-2\tau) + (1+r)x(t-\tau) \qquad (2.5)$$

or, by using the time-shift operator q (i.e., $q^{-j}y(t) = y(t - j \cdot \Delta)$ where Δ is the sampling interval,

$$y(t) = \frac{(1+r)q^{-\tau/\Delta}}{1+rq^{-2\tau/\Delta}} \cdot x(t) \qquad (2.6)$$

The coefficient of $x(t)$ on the right-hand side is the discrete-time filter representing site amplification. The transfer function $H(f)$ of the filter is obtained by putting $q = e^{i(2\pi f)\Delta}$, where $i = \sqrt{-1}$; that is:

$$H(f) = \frac{(1+r)e^{-2i\pi f\tau}}{1+re^{-4i\pi f\tau}} \qquad (2.7)$$

Seismic waves are attenuated while travelling through the soil layer. This reduction is defined by the attenuation parameter Q, and is commonly accounted for by using complex velocities, such that v is replaced by $v + i/2Q$, and reducing the amplitudes by the filter:

$$A(f) = e^{-\pi f\tau/Q} \qquad (2.8)$$

To incorporate this attenuation in the above formulation, upgoing and downgoing waves in Eqs. 2.4 should be filtered with $A(f)$. When this is done, the transfer function $H(f)$ takes the following form:

$$H(f) = \frac{(1+r)e^{-2\pi f\tau(i+1/2Q)}}{1+re^{-4\pi f\tau(i+1/2Q)}} \qquad (2.9)$$

The derivation of the above equation can be found in Şafak (1993*b*).

Equation 2.9 represents the exact transfer function for a linear one-layer medium with frequency-independent Q, and has only three parameters, r, τ, and Q. For a given pair of rock- and soil-site records, we can estimate the parameters of $H(f)$

by matching the spectral ratio and using nonlinear curve-fitting algorithms.

The site amplification model given by Eq. 2.9 is superior to other models (e.g., the damped oscillator model), because it can account for multiple reflections and uses the physical parameters of the soil layer. Equation 2.9 also provides a convenient model to simulate ground motions at soil sites. Assuming a white-noise or an omega-squared model for rock-site accelerations, one can easily simulate the soil-site accelerations from Eq. 2.9 for given site characteristics. The simulation can be done in the frequency domain by using $H(f)$ directly and Fourier transforms, or in the time domain after converting $H(f)$ into a time-domain recursive filter (Şafak, 1993*b*).

To give an example, we determined the parameters r, τ, and Q of the equivalent one-layer medium that relates the sample rock- and soil-site records of Fig. 2.1. The values of parameters and the match of the transfer function amplitude with the spectral ratio is presented in Fig. 2.7.

2.5 Time-varying filters

In real life, since ground motions are nonstationary and the site response is generally nonlinear, the relationship between rock- and soil-site recordings are time and frequency dependent. Such a relationship can best be modeled by an adaptive, time-varying filter. The details of the theory and the formulation of the adaptive filtering approach to site amplification can be found in Şafak (1989). Here, we will only present, in Fig. 2.8, the time-varying amplitude of the estimated filter for the sample pair of records. The filter used is of second order. Higher order filters would give more detail on the peaks and valleys of the filter amplitude (Şafak, 1991).

3. SOIL-STRUCTURE INTERACTION

SSI (soil-structure interaction) can significantly alter the interpretation to be placed on the seismic recordings obtained in buildings. Although SSI is always present to some degree, it is generally assumed when SSI is small that the recorded motions at foundation level are not influenced by the motions of upper stories. Therefore the building can be assumed to be fixed-based and the foundation level recordings can be taken as the base excitation.

In this paper, we investigate the effect of SSI on recorded frequencies of the superstructure, and present methods to detect and identify SSI from recorded accelerations. An example for the application of the methods is given for a model building.

3.1 Effect of SSI on frequencies

The effect of SSI on the frequency content of the building records can be shown by studying the response of a 2-DOF system as shown in Fig. 3.1. A 2-DOF system is a simple model for soil-structure interaction. The lower mass-spring-dashpot (m_f, k_f, and c_f) represents the soil-foundation system, whereas the upper mass-spring-dashpot (m_b, k_b, and c_b) represents the building. The model is based on the assumptions that both systems are linear, their motions are dominated by fundamental modes, and rocking motions are negligible. The two natural frequencies of this coupled system are:

$$\omega_{1,2}^2 = \frac{1}{2}\left[\omega_f^2 + (1+\mu)\omega_b^2 \mp \sqrt{[\omega_f^2 + (1+\mu)\omega_b^2]^2 - 4\omega_f^2\omega_b^2}\right] \quad (3.1)$$

where $\mu = m_b/m_f$ is the mass ratio, and $\omega_f = \sqrt{k_f/m_f}$ and $\omega_b = \sqrt{k_b/m_b}$ are the natural frequencies of the foundation when no building is present, and of the building with non-moving foundation, respectively. The parameter ω denotes the radial frequency, and will be used interchangeably with the corresponding cyclic frequency f (i.e., $\omega = 2\pi f$).

We can write the following equations for the ratios of the natural frequencies of the coupled system to the frequencies of the building and the foundation:

$$\left(\frac{\omega_{1,2}}{\omega_b}\right)^2 = \frac{1}{2\eta^2}\Big[1 + (1+\mu)\eta^2 \mp \sqrt{[1+(1+\mu)\eta^2]^2 - 4\eta^2}\Big] \quad (3.2)$$

$$\left(\frac{\omega_{1,2}}{\omega_f}\right)^2 = \eta^2\left(\frac{\omega_{1,2}}{\omega_b}\right)^2 \quad (3.3)$$

where $\eta = \omega_b/\omega_f$. Note that the ratios are functions of μ and η only. Variations of these ratios for η varying from 0.1 to 10, and three values of μ are plotted in Fig. 3.2. The figure shows that for the lowest natural frequency, ω_1, the ratios are always less than one. In other words, the fundamental frequency with SSI is always lower than the frequencies of the fixed-base building and the foundation with no building. For the second natural frequency ω_2, the ratios are always greater than one. It can be shown, by studying the limits of Eqs. 3.2 and 3.3 for extreme values of η, that if $\eta << 1$, then $\omega_1 \approx \omega_b$, $\omega_2 \approx \omega_f$, and if $\eta >> 1$, then $\omega_1 \approx \omega_f/\sqrt{1+\mu}$, $\omega_2 \approx \sqrt{1+\mu}\cdot\omega_b$. The first limit corresponds to flexible buildings and stiff soil conditions, where SSI is negligible, and the frequencies of the coupled system converge to those of the fixed-base building and the foundation, respectively, for all values of μ. The second limit corresponds to rigid buildings and soft soil conditions, where SSI is significant, and the frequencies of the coupled system converge to two values, one smaller than the frequency of the foundation, and the other larger than the frequency of the fixed-base building.

In general, the recorded response component in buildings is acceleration. We can see the effects of SSI on the frequency content of recorded accelerations by investigating the frequency response functions H_f and H_b of $\ddot{x}_f$ and $\ddot{x}_b$ for the model in Fig. 3.1. To calculate frequency response functions, we take $\ddot{x}_0 = e^{i\omega t}$, where $i = \sqrt{-1}$, and let $\ddot{x}_f = H_f e^{i\omega t}$ and $\ddot{x}_b = H_b e^{i\omega t}$. This results in the following equations for the frequency response functions (Şafak, 1993*a*):

$$H_f = \frac{1}{\Delta}\Big[-i\omega^3 2\xi_f\omega_f - \omega^2(\omega_f^2 + 4\xi_f\xi_b\omega_f\omega_b) + i\omega(2\xi_f\omega_f\omega_b^2 + 2\xi_b\omega_b\omega_f^2) + \omega_f^2\omega_b^2\Big] \quad (3.4)$$

$$H_b = \frac{1}{\Delta}\Big[-\omega^2 4\xi_f\xi_b\omega_f\omega_b + i\omega(2\xi_f\omega_f\omega_b^2 + 2\xi_b\omega_b\omega_f^2) + \omega_f^2\omega_b^2\Big] \quad (3.5)$$

with

$$\Delta = \omega^4 - i\omega^3[2\xi_f\omega_f + 2(1+\mu)\xi_2\omega_2] - \omega^2[\omega_1^2 + (1+\mu)\omega_b^2 + 4\xi_f\xi_b\omega_f\omega_b] + i\omega(2\xi_f\omega_f\omega_b^2 + 2\xi_b\omega_b\omega_f^2) + \omega_f^2\omega_b^2 \quad (3.6)$$

where ξ_f and ξ_b are the damping ratios defined as $\xi_f = c_f/2\omega_f$, $\xi_b = c_b/2\omega_b$.

Figure 3.3 shows the transfer functions for four values of μ ($\mu = 0.1$, 1, 5, and 10), and for $f_f = \omega_f/2\pi = 0.7\,Hz$, $f_b = \omega_b/2\pi = 0.5\,Hz$, $\xi_f = 0.20$, and $\xi_b = 0.05$. For low μ values (i.e., $\mu < 0.1$) the SSI is negligible, and transfer functions have

peaks near their respective frequencies, f_f and f_b. As the μ value increases, the effect of SSI becomes significant, and both transfer functions have a peak at the same frequency which is lower than the individual frequencies of the foundation and the fixed-base building. Figure 3.4 shows the transfer functions for various combinations of f_f and f_b, and for $\mu = 5$, $\xi_f = 0.20$, and $\xi_b = 0.05$. The figure and further studies show that, except for $f_f >> f_b$, both transfer functions have a peak at a frequency which is lower than the smaller of f_f and f_b. For $f_f >> f_b$, which corresponds to stiff soil, flexible building condition and negligible SSI, the transfer functions have peaks at their respective natural frequencies (i.e., H_f at f_f, and H_b at f_b). These observations are in parallel to those concluded from Fig. 3.2.

The foregoing discussions, and Figs. 3.2, 3.3, and 3.4 clearly show that SSI has significant influence on the frequency content of the motions recorded at the foundation level and the superstructure. Depending on the magnitude of SSI, the dominant frequencies of the recorded motions can be completely different from those of the fixed-base building, or the foundation when no building is present. The observed narrowband characteristics of the foundation transfer function (H_f) for soft soils and large buildings (i.e., small $\eta = f_f/f_b$ and/or large $\mu = m_b/m_f$) suggest that recordings from basements of such buildings cannot be taken as the free-field ground motions.

3.2 Detection of SSI

Since SSI alters the frequency characteristics of the recorded motions, it is important to determine, prior to analyses of the records, if the building is subjected to SSI. Normally, the motion of the building is recorded at the foundation level, top story, and several intermediate stories. If there is no SSI, we can identify the building by taking the recordings at the foundation level as the input, and the recordings at upper stories as the output. A building with no SSI represents a causal system, because the input at time t_i can only influence the output at times $t \geq t_i$. When the building is subjected to SSI, the motions of upper stories influence the motion of the foundation, i.e., the input and the output of the system are coupled. Such systems are termed closed-loop systems. It can be shown that the impulse response function of closed-loop systems is non-causal (Akaike, 1967).

The causality condition provides a convenient tool to detect the SSI. For causal systems the impulse response of the system is zero for $t < 0$, whereas for non-causal systems it is not. Therefore, we investigate the impulse response of the building from the records of the foundation and the upper stories. If the impulse response shows significant amplitudes at negative times in comparison to those at positive times, we conclude that there is SSI.

Another method to detect SSI is first to identify the building as if there were no SSI, and then investigate the cross-correlation of the input with the residuals (i.e., the difference between the recorded output and the output of the identified model) of the identification. If there is SSI, the cross-correlation would show large amplitudes at negative time lags. A more detailed discussion of this method can be found in Şafak (1988).

We will give an example for detection of SSI from the impulse-response function by using calculated responses of a 10-story building shown in Fig. 3.5. The

frequencies and response time histories to two-directional base excitation of the building were calculated twice, one assuming a fixed-base condition, and the other assuming SSI represented by horizontal springs at the foundation level. The base excitation is the two horizontal components of the accelerations recorded at Piedmont Junior High School, a rock site, during the magnitude 7.1 Loma Prieta earthquake (CDMG, 1991). For each direction and each case, dominant frequencies of the building are given in Fig. 3.5; time histories of the excitation (i.e., ground acceleration), and calculated acceleration responses at the top story and the foundation level are given in Fig. 3.7. Note that for no SSI, foundation and ground accelerations are identical.

We calculate the impulse response functions by taking the foundation accelerations as the input, and the top-story accelerations as the output, and using the method given in Ljung (1987). Figure 3.6 shows calculated impulse response functions (solid lines) in the x and y directions for the fixed-base and the SSI cases. The y direction represents the weaker direction. To see the effects of measurement noise on the results, impulse response functions were re-calculated after adding Gaussian white noise sequences to calculated accelerations. The RMS (root-mean-square) values of noise are assumed to be 50-percent of those of the original accelerations (i.e., the signal to noise ratio= 2). The impulse response functions corresponding to noisy data are also shown in Fig. 3.6 (dashed lines). It is clear from the figure, especially in the weaker y direction, that when there is SSI, the impulse response function has amplitudes for $t < 0$ comparable to those for $t > 0$. For no SSI, the amplitudes for $t < 0$ are significantly smaller than those for $t > 0$. Although the preceeding comments are based on visual inspection of Fig. 3.6, various statistical confidence tests can also be used to decide on the significance of the impulse response amplitudes for $t < 0$ in comparison to those for $t > 0$. Figure 3.6 also shows that the noise in the records has very little influence on the impulse response functions.

3.3 Identification of SSI

The term "identification of SSI" will refer to extracting dynamic characteristics of the fixed-base building, and the foundation (when no building is present) from the recordings of the foundation and upper stories. We will address this problem again by using the simple 2-DOF model of the SSI given in Fig. 3.1. Let us first calculate the ratio $R = H_b/H_f$ of the transfer functions for accelerations $\ddot{x}_b$ and $\ddot{x}_f$. From Eqs. 3.4 and 3.5, and by defining the nondimensional frequency ratios $r_f = \omega_f/\omega$ and $r_b = \omega_b/\omega$, we can write:

$$R = \frac{-4\xi_f\xi_b r_f r_b + i(2\xi_f r_f r_b^2 + \cdots}{-i2\xi_f r_f - r_f^2 - 4\xi_f\xi_b r_f r_b + \cdots} \cdots \frac{\cdots + 2\xi_b r_b r_f^2) + r_f^2 r_b^2}{\cdots + i(2\xi_f r_f r_b^2 + 2\xi_b r_b r_f^2) + r_f^2 r_b^2} \quad (3.7)$$

Note that R is independent of $\mu = m_b/m_f$. Also, note that if $\xi_f = \xi_b = 0$, then $R = r_b^2/(r_b^2 - 1)$, which is independent of r_f (or ω_f) and has a peak at $r_b = 1$ (or at $\omega = \omega_b$). It can further be shown, analytically or numerically, that the amplitude of R is independent of r_f and ξ_f, and always has its peak at or near $r_b = 1$ for small values of ξ_b. In other words, $|R|$ is not influenced by the dynamic characteristics of the foundation, and always

peaks at or near the fixed-base building frequency for buildings with small damping. To show this graphically, we plot $|R|$ in Fig. 3.8 for r_b varying from 0.5 to 1.5, and for four values of ξ_b. Variations in r_f and ξ_f do not change the curves. Also given in the figure is the r_b value corresponding to the peak of each curve. As the figure shows, $|R|$ has a peak at $r_b = 1$ (or $\omega = \omega_b$) for realistic values of building damping ratios (i.e., $\xi_b < 0.20$). Even at $\xi_b = 0.50$, the shift of the peak frequency from the frequency of the fixed-base building is only 17 percent.

Considering the definitions of H_f and H_b, $|R|$ can be calculated as the ratio of the Fourier amplitude spectrum (FAS) of the top story accelerations to that of the foundation accelerations. The dominant peak of this ratio gives the fundamental frequency of the building for the fixed-base case. The fundamental frequency of the foundation can be estimated from Eq. 3.1. For this, we first determine ω_1, the dominant frequency of the top story records, and make an assumption for the value of μ based on the design specifications for the building. We then put the values of ω_1, ω_b, and μ in Eq. 3.1, and solve it for ω_f.

To give an example, we calculate $|R|$ for the simulated building with SSI of Fig. 3.5, by taking the ratio of the FAS of the top-story acceleration response to that of the foundation acceleration response. The amplitudes of R are shown in Fig. 3.9 for each direction, along with the FAS of top-story and foundation accelerations. Note that for both directions the peaks of $|R|$ are at the natural frequencies of the fixed-base building, $1.15\,Hz$ in the x direction and $0.71\,Hz$ in the y direction. These frequencies differ from the dominant frequencies of the top story response, which are $0.60\,Hz$ in the x direction and $0.52\,Hz$ in the y direction. Thus, the results confirm that the spectral ratio gives the fixed-base natural frequency. The mass ratios (μ), calculated considering only the first modes, are 0.80 and 0.83 for the x and y directions, respectively. Using these values for μ, the frequencies of the top-story response for ω_1, and the calculated fixed-base frequencies for ω_b, we can calculate the foundation frequencies ω_f from Eq. 3.1. The calculation confirms that the foundation frequencies when no building is present are $0.87\,Hz$ for both directions, as originally assumed in the model. For a real-life building, we have to estimate the mass ratios (using recorded motions and structural drawings) in order to use Eq. 3.1.

4. CONCLUSIONS

Advanced techniques from signal processing and estimation theories can provide useful tools to develop methods that improve the accuracy and the amount of information that can be extracted from seismic records. In this paper, we develop two sets of such methods, one to analyze site amplification, and the other to analyze soil-structure interaction.

We introduce five methods, alternative to spectral ratios, for modeling site amplification. The methods vary in complexity, ranging from a constant amplification to time-varying adaptive filtering. An example for each method is presented. The methods are superior to the commonly used spectral ratio method in terms of robustness, accuracy and/or practicality of use.

For soil-structure interaction, we show that the dominant frequency of a structure with SSI is always smaller than that of the fixed-base structure and of the foundation with no structure present.

The relationship between the foundation response and the upper-story response of a building with SSI results in a non-causal impulse response function. This causality condition provides a convenient tool to detect the existence of SSI. If the amplitudes of the impulse response function at negative times are comparable to those at positive times, we conclude that the building is affected by SSI. The ratio of the Fourier amplitude spectrum of an upper-story acceleration to that of the foundation acceleration gives the dominant frequency of the fixed-base building. Once this frequency is determined, the dominant frequency of the foundation with no building can be estimated from simple analytical relations. An example given for a 10-story model building confirms the validity of the methods.

5. REFERENCES

1. Akaike, H. (1967). Some problems in the application of the cross-spectral method, in *Spectral Analysis of Time Series* (Ed. by B. Harris), John Wiley & Sons, New York, N.Y.

2. CDMG (1991). The Loma Prieta (Santa Cruz Mountains), California Earthquake of 17 October 1989, *Special Report 104*, California Division of Mines and Geology (CDMG), Sacramento, California.

3. Kanai, K. (1957). Semi-empirical formula for the seismic characteristics of the ground, *Bulletin of the Earthquake Research Institute*, Tokyo University, Vol.35, pp.308-325.

4. Ljung, L. (1985). On the estimation of transfer functions, *Automatica*, Vol.21, pp.677-696.

5. Ljung, L. (1987). *System Identification. Theory for the user*, Prentice-Hall Inc., Englewood Cliffs, New Jersey.

6. Şafak, E., Mueller, C., and Boatwright J. (1988). A simple model for strong ground motions and response spectra, *Earthquake Engineering & Structural Dynamics*, Vol.16, No.2, pp.203-215.

7. Şafak, E. (1988). Analysis of recordings in structural engineering: Adaptive filtering, prediction, and control, *Open-File Report, 88-647*, U.S. Geological Survey, Menlo Park, California.

8. Şafak, E. (1989). Optimal-adaptive filters for modeling spectral shape, site amplification, and source scaling, *Soil Dynamics & Earthquake Engineering*, Vol.8, No.2, pp.75-95.

9. Şafak, E. (1991). Problems with using spectral ratios to estimate site amplification, *proceedings*, Fourth International Conference on Seismic Zonation, Aug. 26-29, Stanford University, Stanford, California, Vol.2, pp.227-284.

10. Şafak, E. (1993*a*). Analysis of soil-structure interaction in buildings from vibration recordings, *Earthquake Engineering & Structural Dynamics*, submitted for publication.

11. Şafak, E. (1993*b*). Analysis of seismic site amplification, *Journal of Engineering Mechanics*, ASCE, will be submitted for publication.

TABLE 2.1

Comparison of constant amplification factors for four different spectral bands.

	Band 1 (0-5 Hz)	Band 2 (0-4 Hz)	Band 3 (0-3 Hz)	Band 4 (0.5-2 Hz)
Least squares sum (Eq.1)	2.9	2.9	3.1	4.2
Absolute value sum	2.3	2.5	2.5	4.3
Averaged spectral ratio (3-point smoothing)	5.0	5.0	5.6	8.6
Averaged spectral ratio (7-point smoothing)	4.2	4.5	5.1	7.8
Averaged spectral ratio (11-point smoothing)	4.0	4.3	4.9	7.5

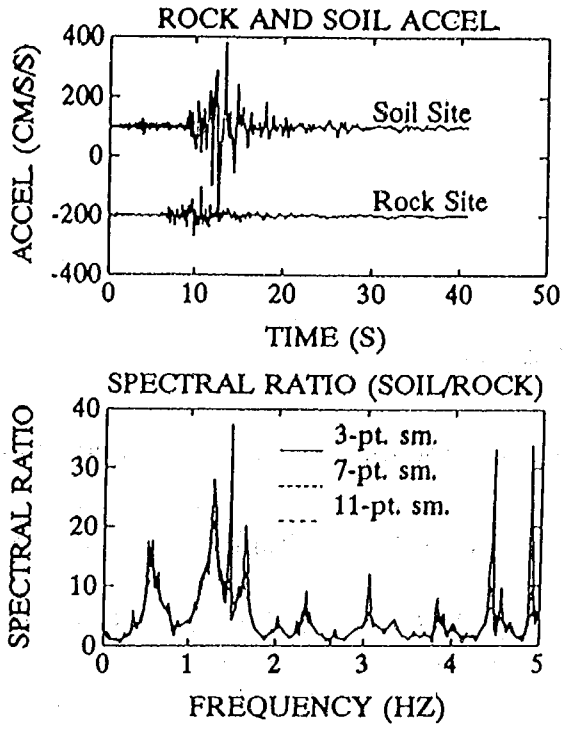


Figure 2.1. Rock- and soil-site accelerations used in the examples, and their spectral ratio for three triangular smoothing windows.

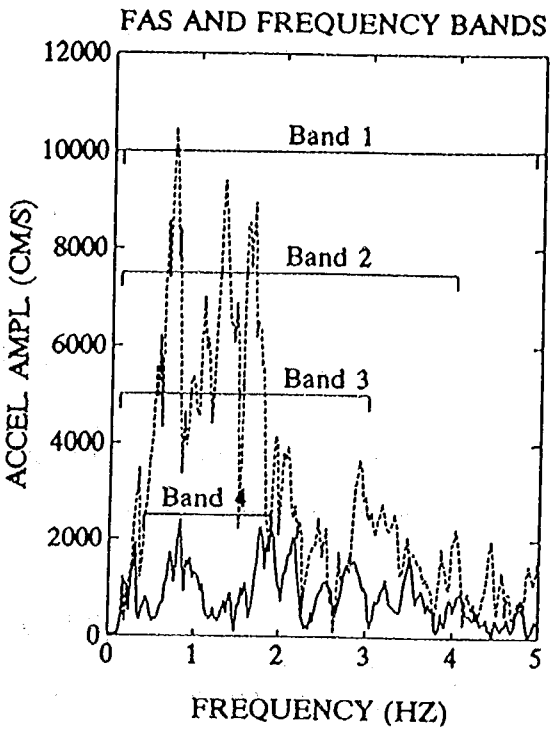


Figure 2.2. FAS of rock- (solid line) and soil-site (dashed line) recordings and the four frequency bands.

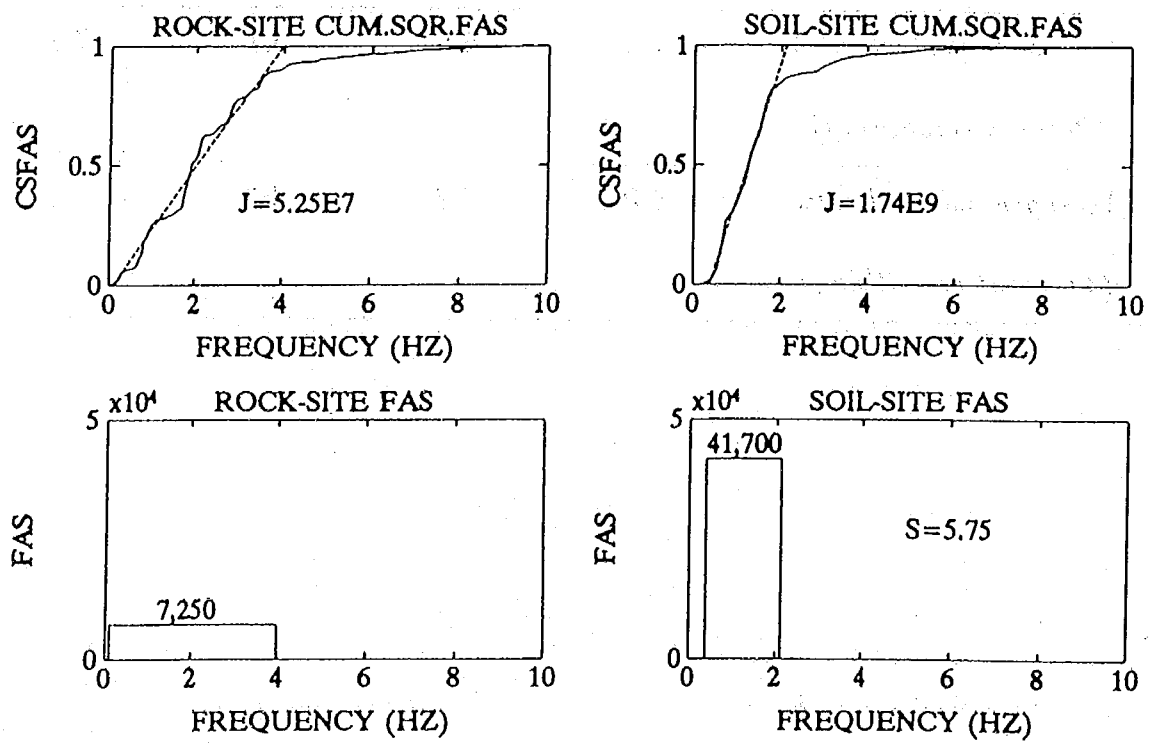


Figure 2.3. Estimation of site amplification by matching the cumulative squared FAS with a straight line.

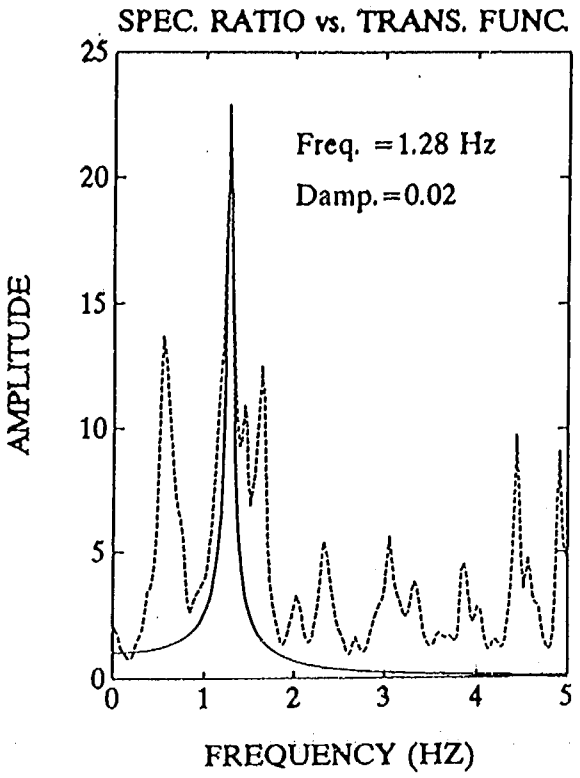


Figure 2.4. Comparison of the spectral ratio with the transfer function of the damped oscillator.

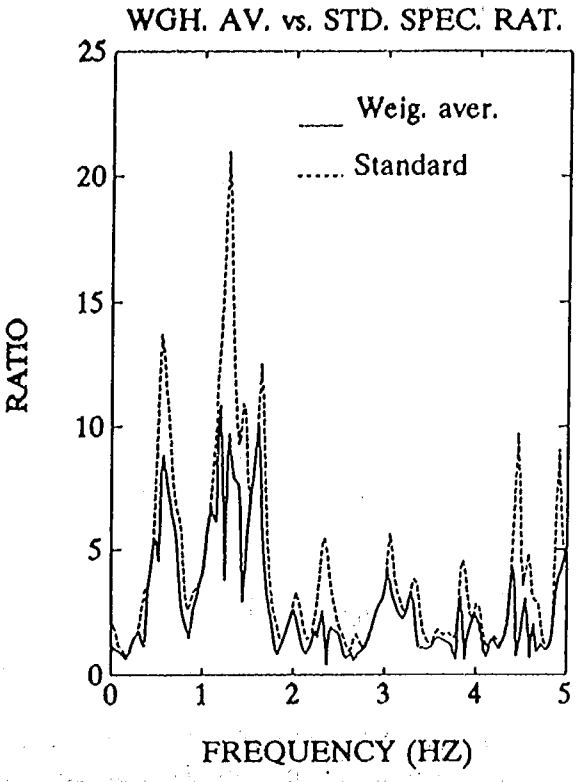


Figure 2.5. Comparison of the standard spectral ratio with the weighted averaged spectral ratio (both smoothed by a 7-point triangular window).

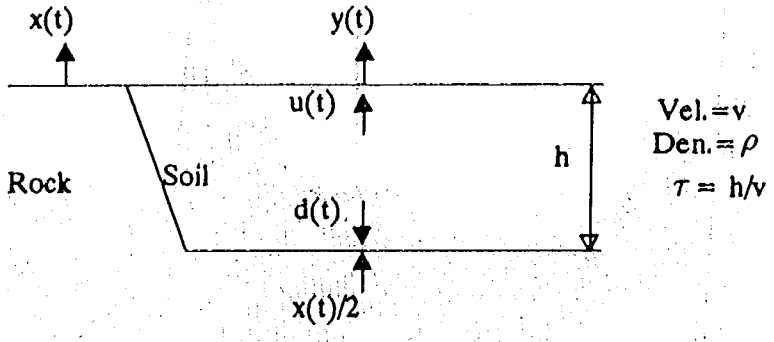


Figure 2.6. Model for one-layer soil medium with rock- and soil-site surface recordings, and upgoing and downgoing waves.

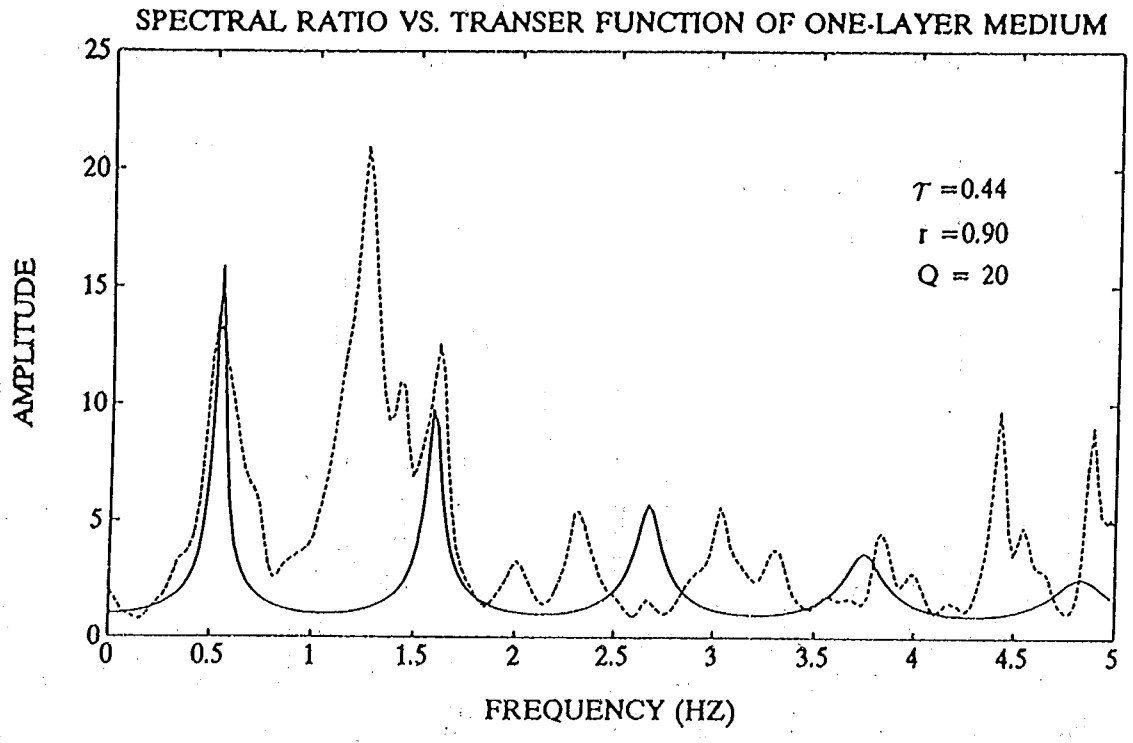


Figure 2.7. Match of the transfer function of the equivalent one-layer soil medium with the spectral ratio, and estimated parameters of the layer.

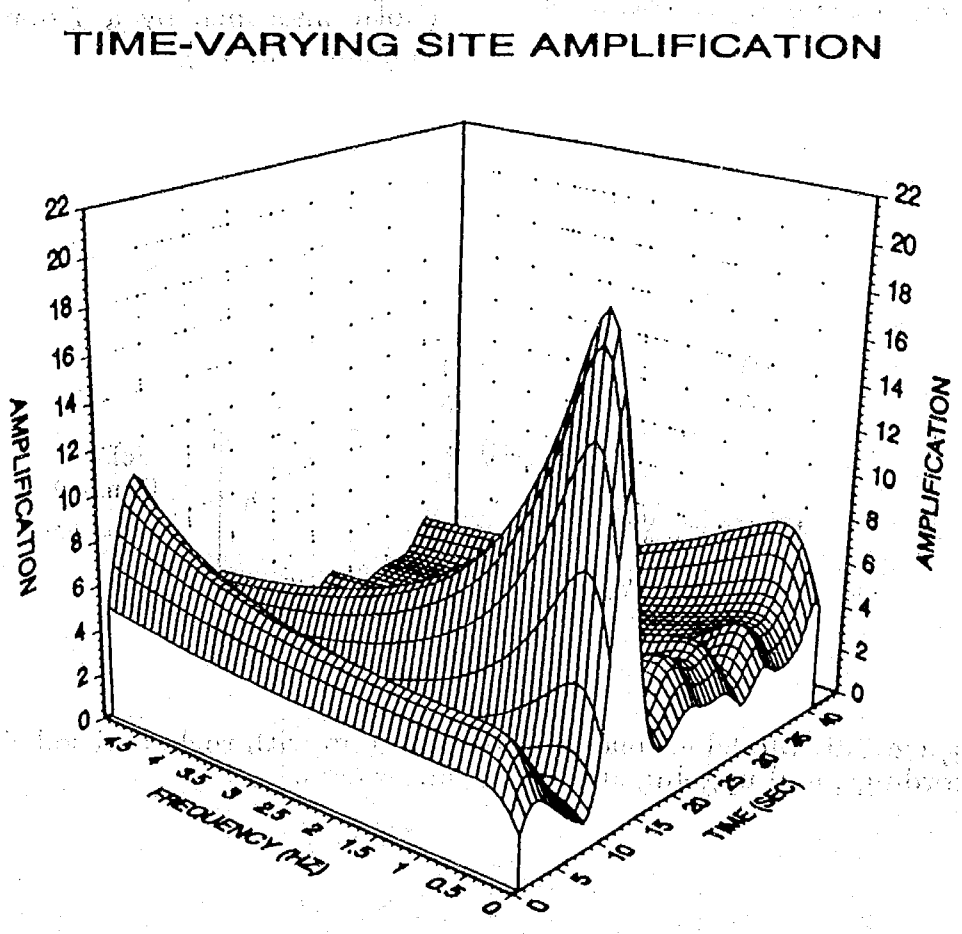


Figure 2.8. Time-varying site amplification calculated by using adaptive filtering method.

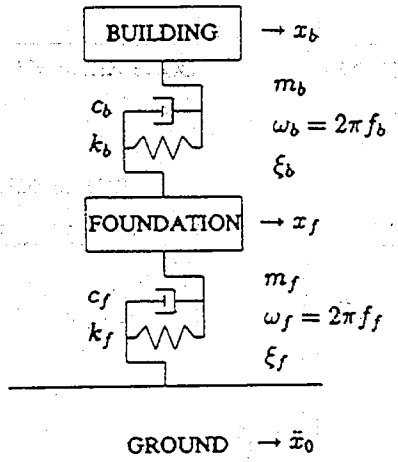


Figure 3.1. Two-degrees-of-freedom system representing soil-structure interaction.

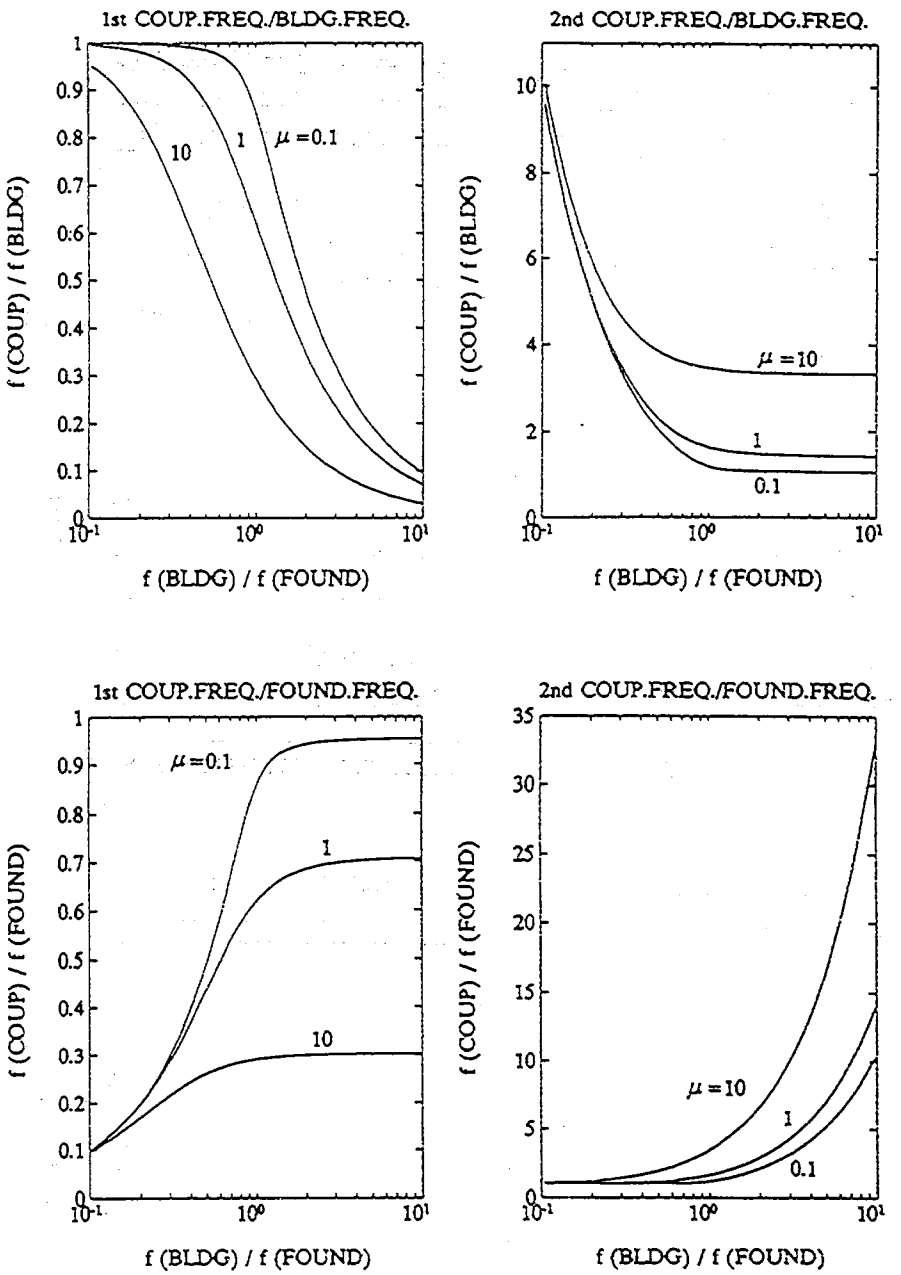


Figure 3.2. Variations of f_1/f_b and f_2/f_b (top figures), and f_1/f_f and f_2/f_f (bottom figures) with $\eta = f_b/f_f$ for $\mu = 0.1$, 1, and 10.

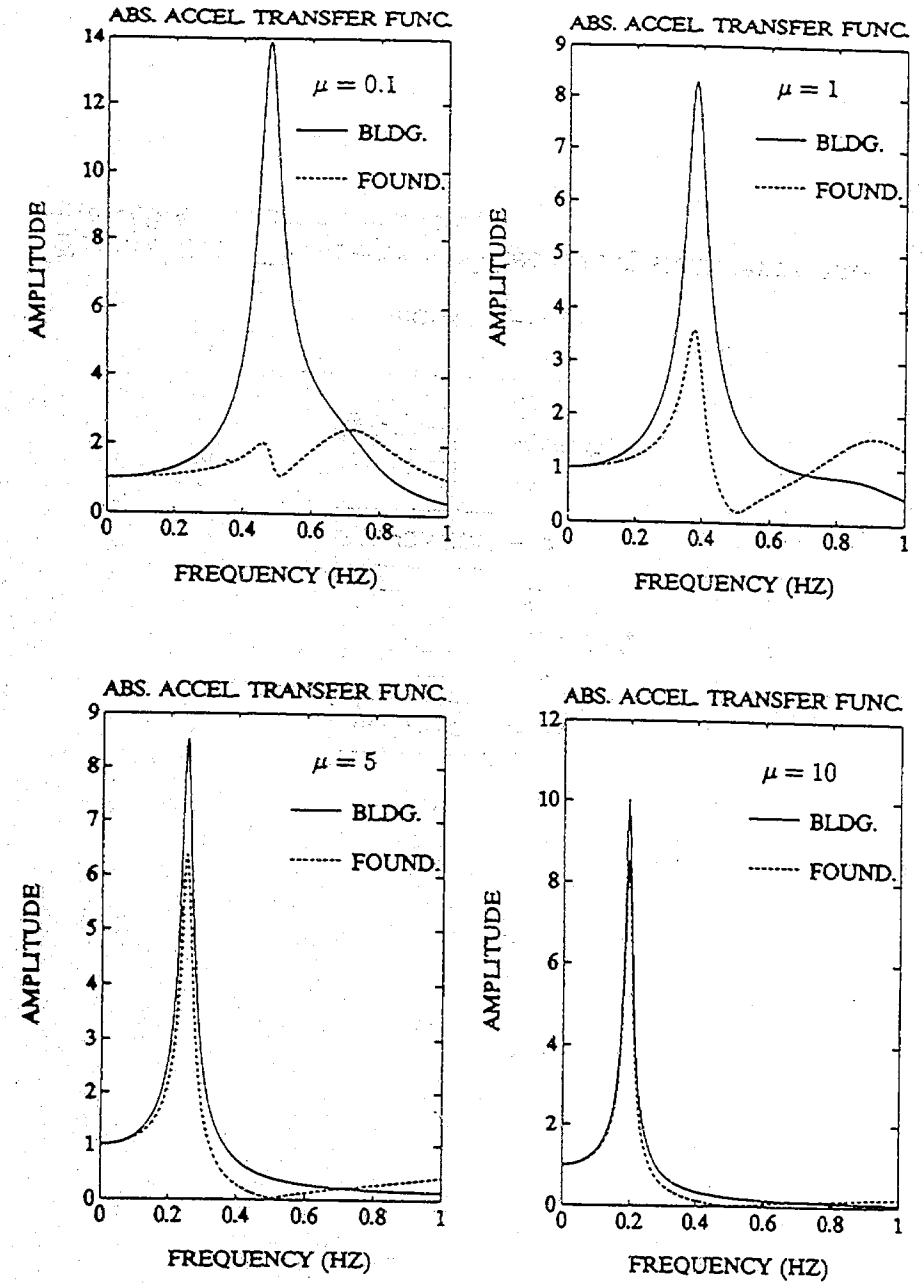


Figure 3.3. Transfer functions of the building (H_b) and the foundation (H_f) for four values of μ (μ = 0.1, 1, 5, and 10), and for $f_f = 0.7\,Hz$, $\xi_f = 0.20$, $f_b = 0.5\,Hz$, and $\xi_b = 0.05$.

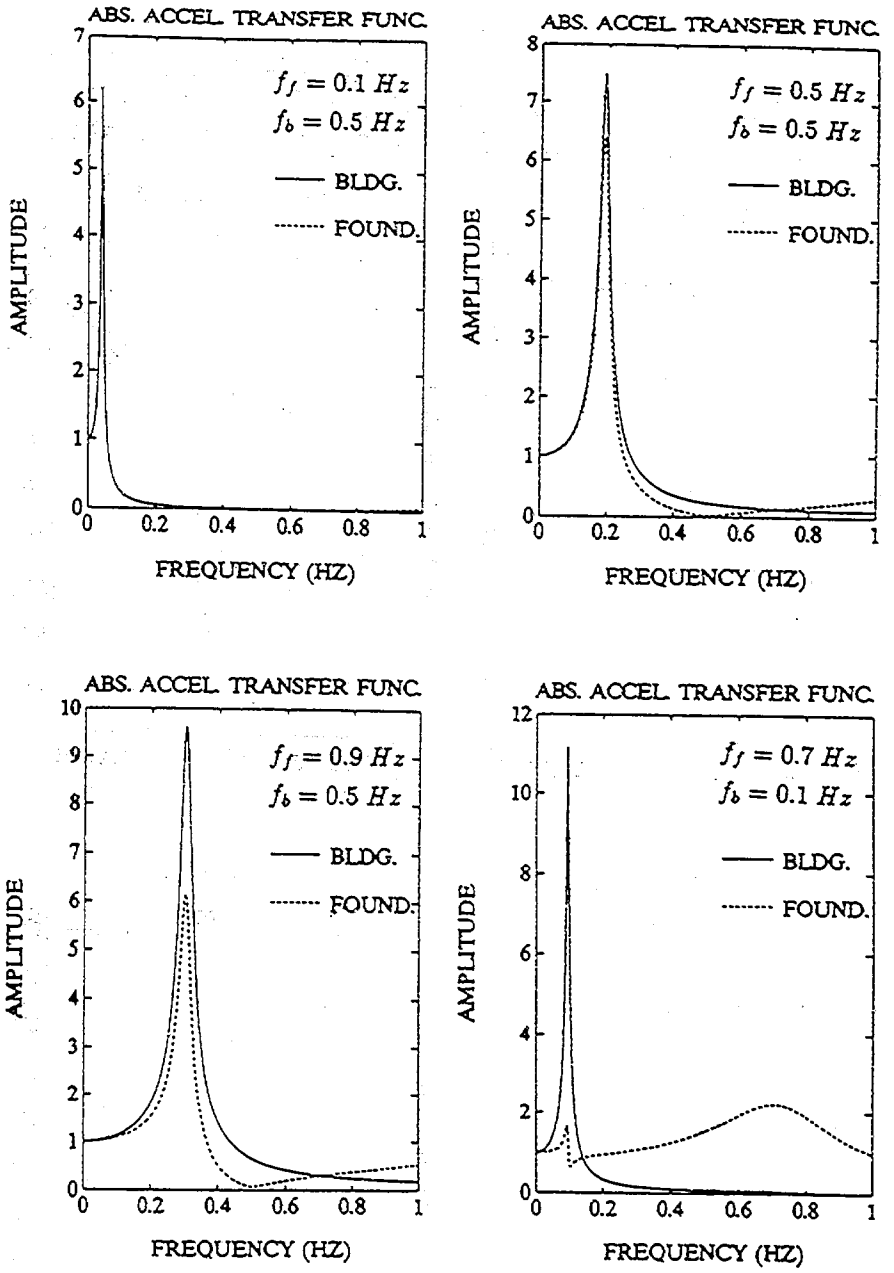
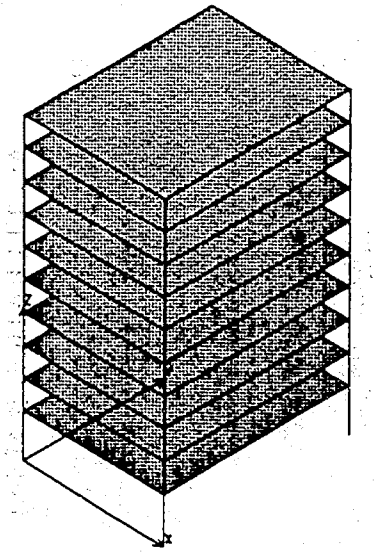


Figure 3.4. Transfer functions of the building (H_b) and the foundation (H_f) for four pairs of f_f and f_b, and for $\mu = 5$, $\xi_f = 0.20$, and $\xi_b = 0.05$.



NO SSI : $f_x = \omega_x/2\pi = 1.15\,Hz$

$f_y = \omega_y/2\pi = 0.71\,Hz$

WITH SSI : $f_x = \omega_x/2\pi = 0.60\,Hz$

$f_y = \omega_y/2\pi = 0.52\,Hz$

Figure 3.5. 10-story model building and its fundamental frequencies in the x and y directions with and without SSI.

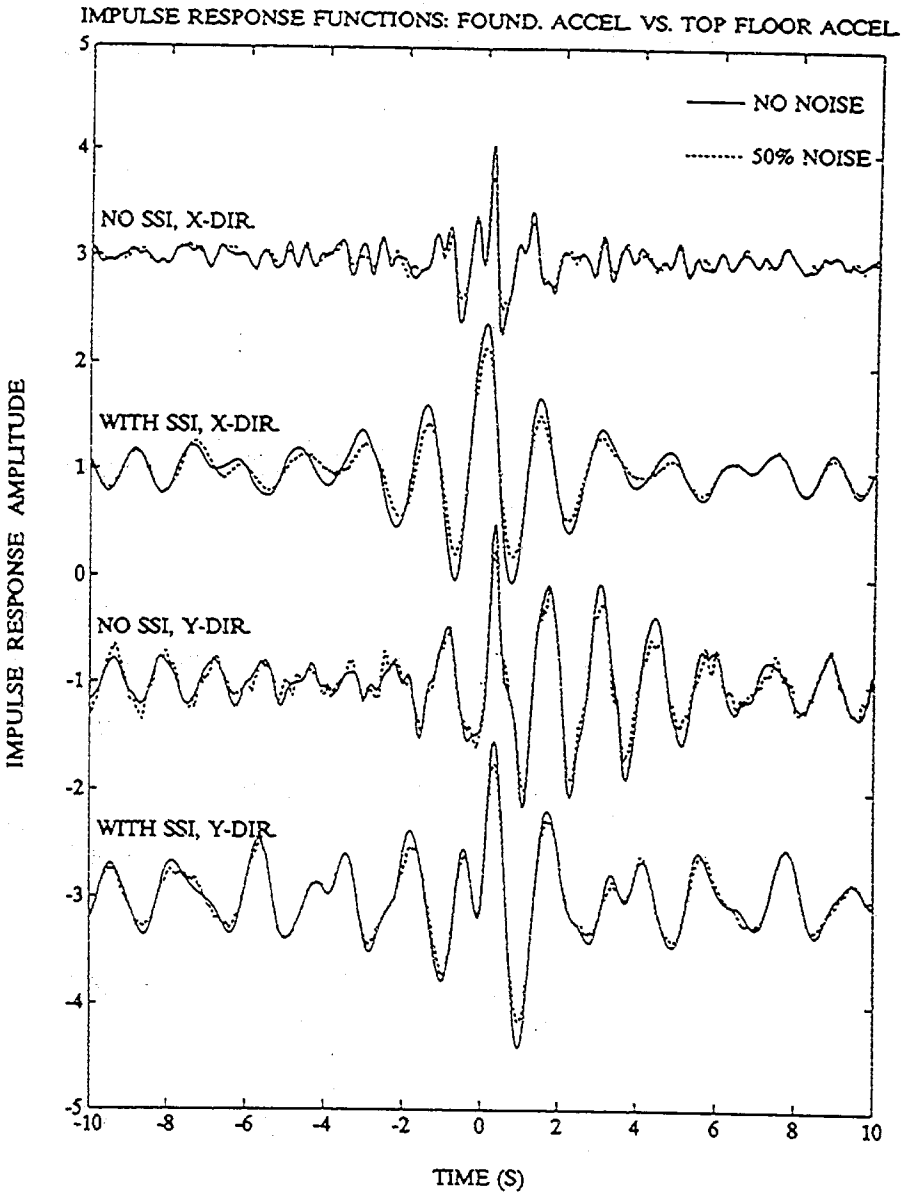


Figure 3.6. Impulse response functions in the x and y directions obtained from the top story and foundation accelerations for no SSI and SSI, and no noise and 50% noise cases.

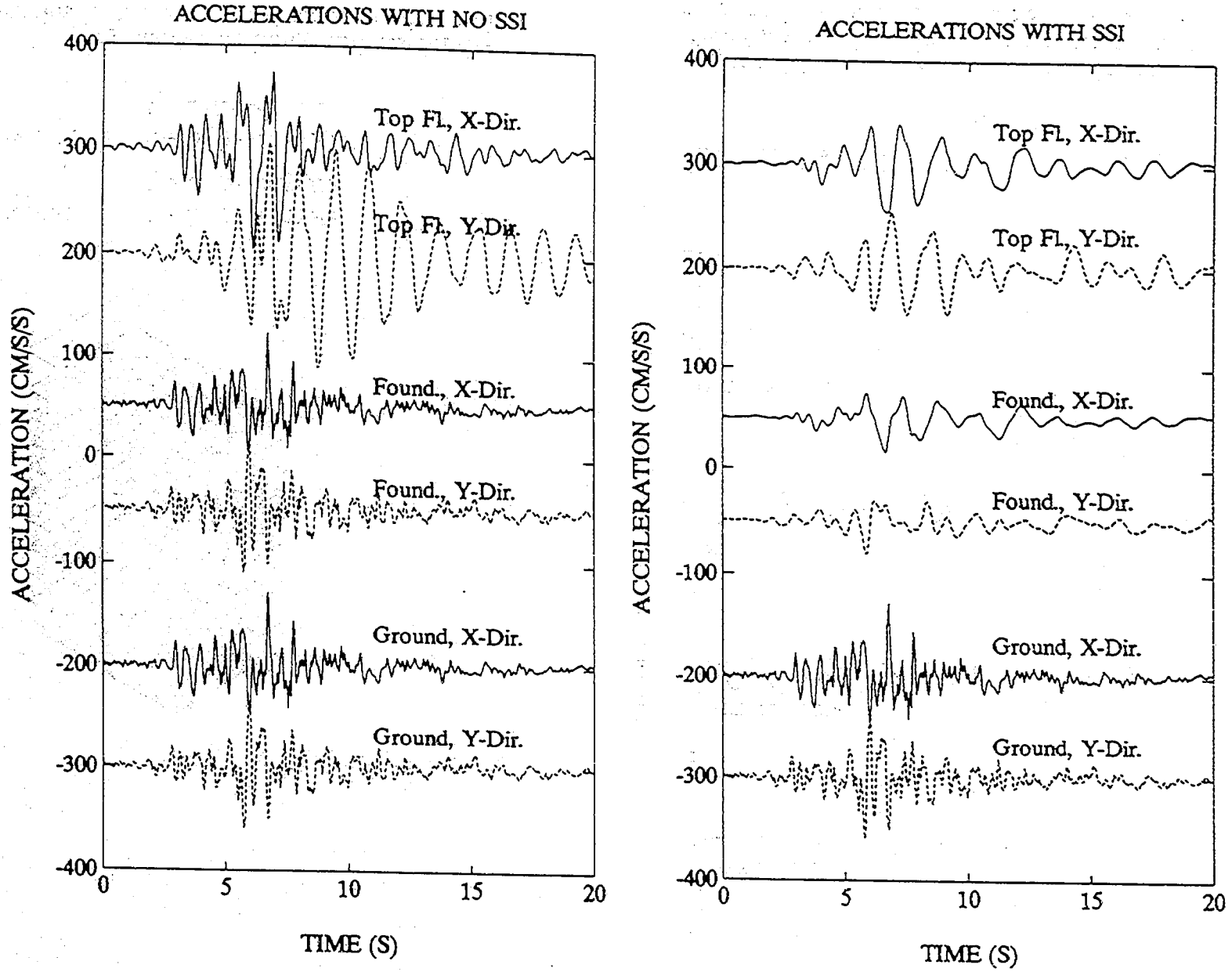


Figure 3.7. Ground accelerations and calculated acceleration response at the top story without (left figure), and with SSI (right figure).

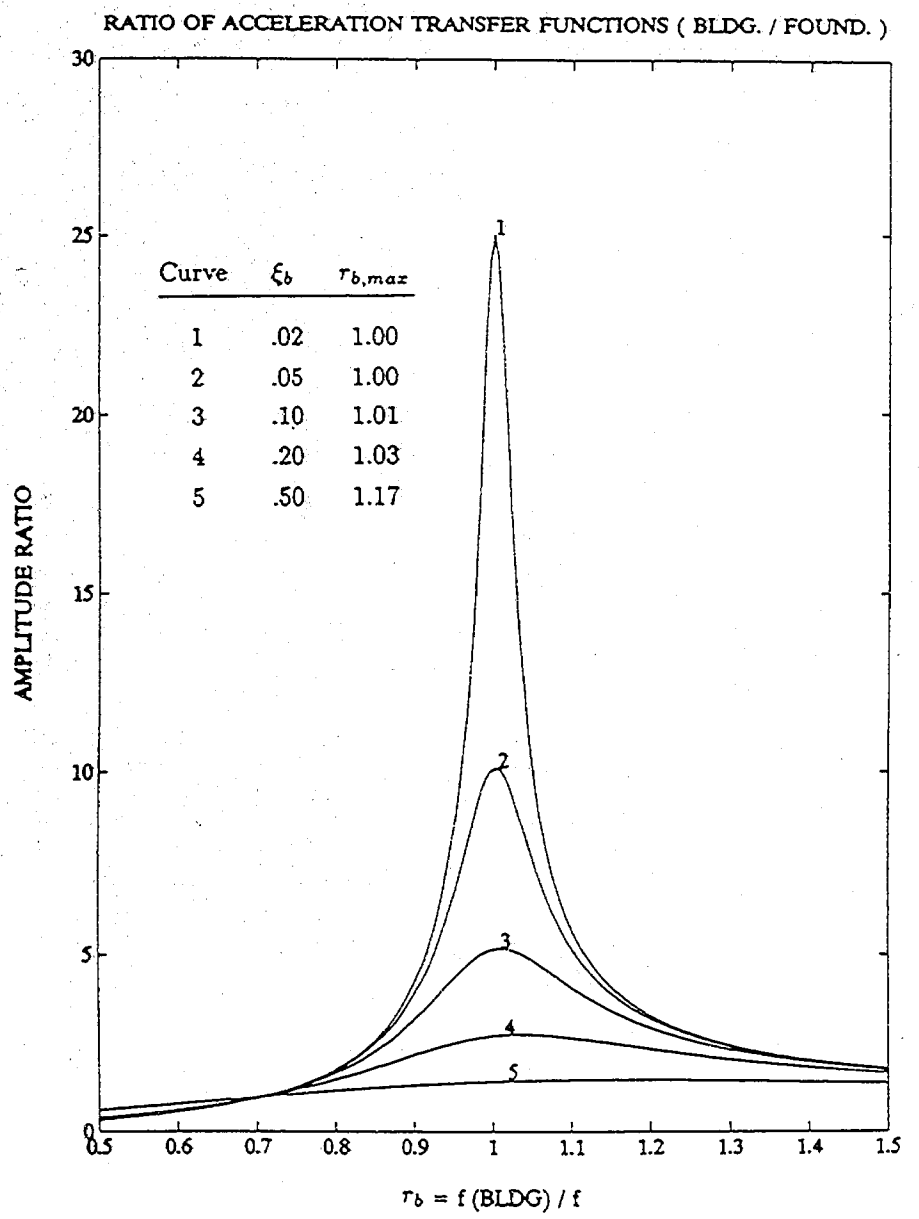


Figure 3.8. Variation of $|R|$ with $r_b = f_b/f$ for four values of ξ_b, and r_b values corresponding to the peaks (r_f and ξ_f do not affect the curves).

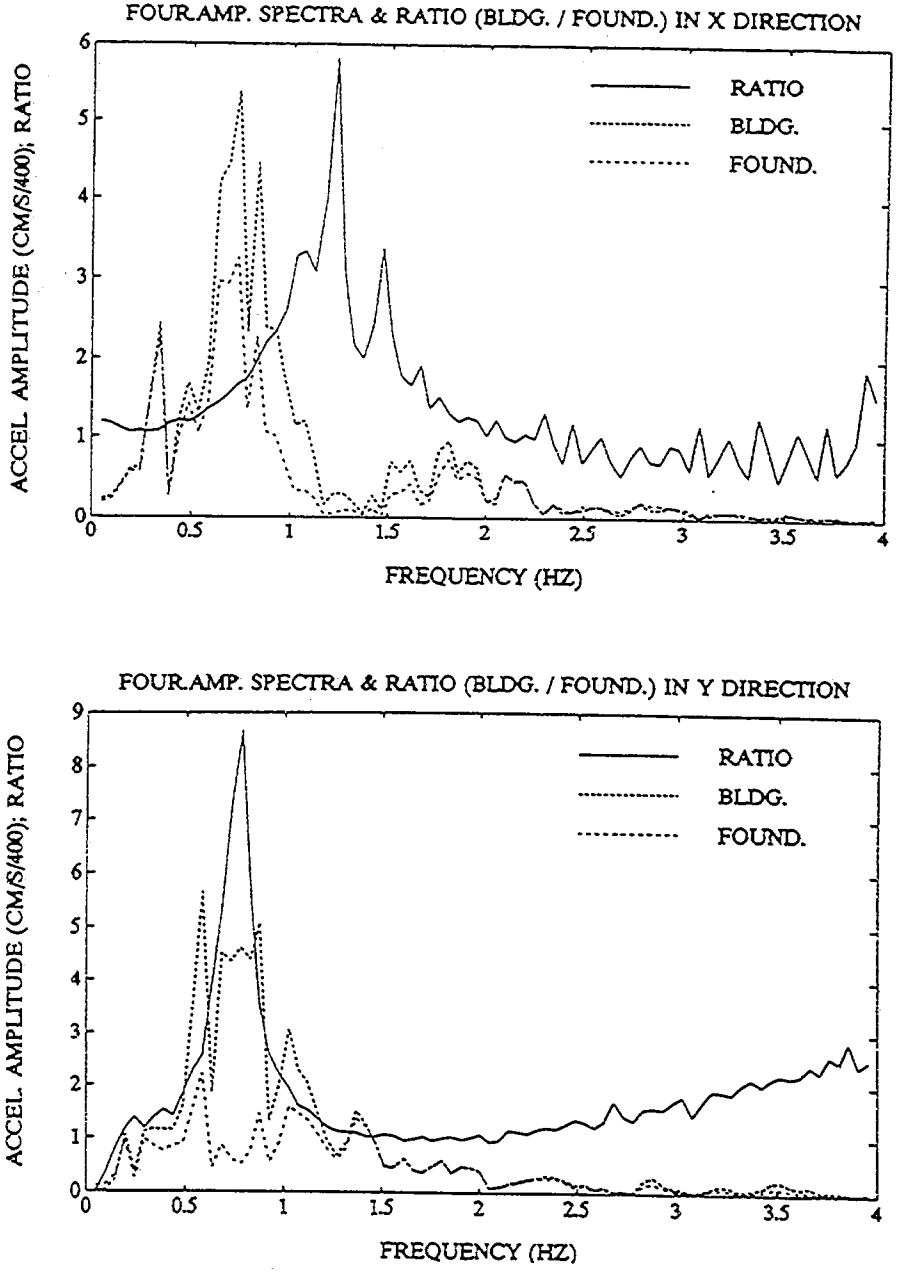
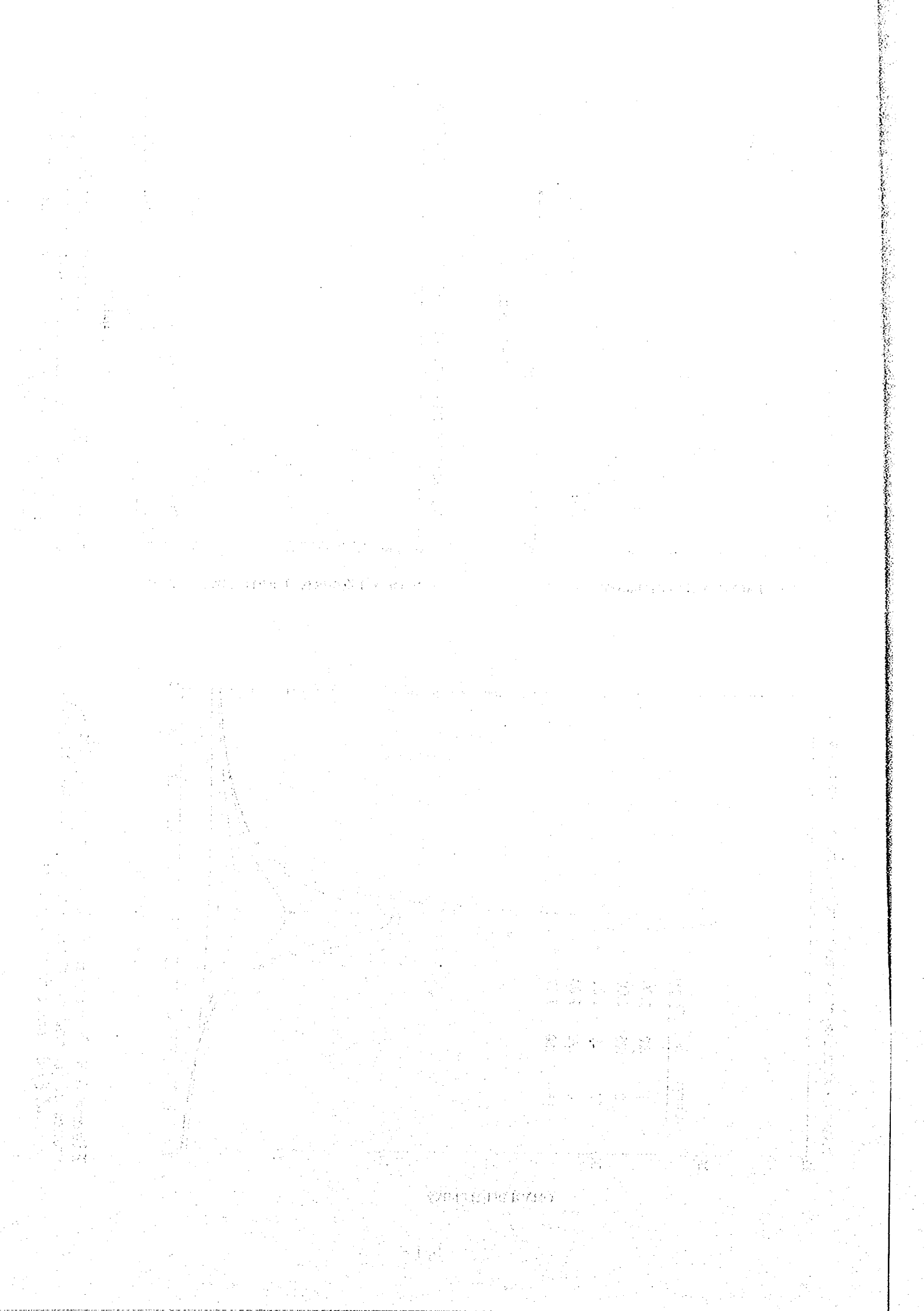


Figure 3.9. Fourier amplitude spectra (divided by 400) of the top story and foundation accelerations and their ratio ($|R|$) in the x (top figure) and y (bottom figure) directions for the SSI case.



Present Situation and Possibility of Constructing Bridge Foundations in Deep Water in Japan

Michio Okahara*, Jiro Fukui** , Tomohiro Fujimura ***

ABSTRACT

In addition to offering results of past achievements and possible applications of bridge foundations constructed in deep water, including the Honshu-Shikoku Bridge, the results of an estimation of the possibility of constructing bridge foundations in the deep water, for example, the Tokyo Bay Bridge and Ise Bay Bridge, which exceed the Honshu-Shikoku Bridge in scale.

KEYWORDS: bridge foundation, laid caisson, caisson, bell type foundation, multi-column foundation

1. INTRODUCTION

The Akashi Kaikyo Bridge is at present under construction and will be the longest suspension bridge in the world when completed. This bridge with its expansive superstructure is considered to be one of the largest structures in the world in terms of substructure. The foundation, which bears a 300 meter-high main tower, is being constructed in water 50 meters deep. Such bridge foundations constructed in deep water are found on bridges such as these on the roads surrounding Tokyo Bay, Ise Bay and Osaka Bay and show the marked progress of technology.

On the other hand, in the large-scale projects following the Honshu-Shikoku Bridge, there has been a strong tendency to construct roads across Tokyo Bay, Ise Bay and straits in all parts of Japan. Since construction of bridge foundations in deep water in these areas occur under severe conditions, it is necessary to overcome new technological problems. This paper shows the present situation and possibility of constructing bridge foundations in deep water under such circumstances in Japan.

2. DEEP WATER FOUNDATIONS CONSTRUCTED IN THE PAST

Recent construction technology has advanced greatly, leading to the development of new forms and methods appropriate for deep water, as well as larger-scale construction and mechanization. The following are representative forms or methods :

(1) Laid caisson
This foundation method is used when hard ground (bearing layer) lies close to the surface of the sea bottom. The method consists of first excavating the surface and exposing the bearing layer; laying a steel or reinforced concrete box-shaped body which was made on land and then casting concrete inside the body (Fig. 1). It is a type of spread foundation.

(2) Open-caisson
The foundation method of laying a cylindrical reinforced concrete body, which was made on land, in a fixed place; excavating the ground just under the body underwater using a grab bucket; sinking the body to the fixed bearing layer, and then casting concrete on the bottom.

(3) Pneumatic caisson
A foundation similar to the open-caisson. The foundation method of installing an operation room near a body point; preventing water entering the body by increasing atmospheric pressure; excavating ground by man power or machines under the visible ground; sinking the body to a fixed bearing layer; and then casting concrete on the bottom

(4) Diaphragm wall foundation
The foundation method of inserting a steel bar cage into a hole excavated in a channel shaped to the bearing layer, combining concrete cast members (diaphragm wall) in a closed area formed by a special joint, and constructing a body on them. There is also the method of excavating ground surrounded by a diaphragm wall to a bearing layer and casting concrete on

*Head, Foundation Engineering Division, Structure and Bridge Department, Public Works Research Institute, Ministry of Construction, Japan
**Senior Research Engineer, ditto.
***Research Engineer, ditto.

the bottom (Fig. 2).

(5) Bell type foundation
The foundation method of cutting a pile head on the sea bottom, laying a steel body made on land on it, then casting concrete inside the body (Fig. 3). This is a kind of pile foundation.

(6) Multi-column foundation
The foundation method of lifting a pile head above the water up above the water surface, and combining heads by members in a slab-shape (top slab)(Fig. 4). This is a kind of pile foundation.

By means of a case investigation of past types of bridge foundations constructed in deep water in Japan, the positive achievements and the applicability of each method were investigated. However, the foundations investigated do not include all such bridge foundations constructed in Japan.

Fig. 5 shows the relation between water depth and construction depth (the depth from the water surface to the foundation point) in the typical foundation methods. The positive achievements of each foundation method are shown in Table 1-6. From the above, the characteristics of each foundation method are as follows:

(1) Laid caisson
A bearing layer of a foundation is laid on a strong rock mass, such as soft rock and hard rock. The excavation depth of the surface layer is not so deep, except for the Akashi Kaikyo Bridge and the South Bisan Seto Bridge. However, the load scale has a maximum of 125,000 tf which is the biggest of all foundation methods.

(2) Caisson foundation
The positive achievements of construction depth by both open and pneumatic methods are less than 15 meters. The pneumatic method is divided into a filled coffer dam type and a floating type. The construction depth for a filled coffer dam type is less than 10 meters. This is because construction is impossible in deeper water or this method is not economical as the construction cost is higher in water deeper than 10 meters. Construction depth by the pneumatic method has a maximum depth of 52 meters (combined with the deep well method), in deeper water than that, the open method, whose maximum depth is 60 meters, was used. The load scale differs greatly between the open and the pneumatic method, whose maximum loads are 4,000 tf and 60,000 tf respectively. It is considered because reliability (anchorage to a bearing layer) of construction by the open method will decrease if the load scale exceeds this value; the pneumatic method, under which confirmation of a bearing layer is certain, will then be chosen.

(3)Diaphragm wall foundation
This foundation method is still new, there existing only two examples of its use in underwater construction. Its maximum water depth is 12 meters. As a filled coffer dam is required when this foundation is constructed in deep water, a large scale coffer dam and the construction of a filled coffer dam disadvantage this method economically. The construction depth is at a maximum of 60 meters because deep excavation is possible. The structure of the joint splice, which causes a construction problem, has been devised and developed; however, in the case of deep water construction, it is supposed that the structure of the joint splice, as well as accuracy of wall excavation, leave much room for improvement.

(4) Bell type foundation
The efficacy of this method in underwater construction can be judged from the fact that are six bridges which used it, however, the construction depth is 10-25 meters, except for two bridges. In terms of the type of pile and construction method, when the surface and intermediate layer are relatively soft and the bearing layer is sandy ground, a driving steel pipe pile is used. When the intermediate layer is relatively hard and the bearing layer strong too, a cast-in-place pile is used. In the case of this foundation, the method of combining a pile head with a footing is important at the design level. Therefore, in the case of every bridge it is supposed that a certain length of a pile head is inserted into a footing and concrete and mortar are cast around it, some are expected to transmit shearing by putting a shear connecter steel strip around a steel pipe pile.

(5) Multi-column foundation

Multi-column foundations mostly utilize the steel pipe pile method or the steel pipe pile/ a concrete inside filled method. A precast concrete pile was used only on the Yokohama Bay Bridge. The pile of the Yokohama Bay Bridge is 10 meters in diameter, which is bigger than an average precast concrete pile. The construction depth ranges from 5-20 meters. The embedment depth of the piles was almost always less than 20 meters, which was relatively shallow, except for the Yokohama Bay Bridge with 70 meters embedment depth. It is considered that because lateral displacement amounts become higher at the pile head (the top slab) and in the design ground surface when the intermediate layer is thicker, it is difficult to design.

As a result of the above, the major factors in determining the method of constructing bridge foundations in deep water are considered to be the water depth to the sea bottom, the depth from the sea bottom to the bearing layer (ground bearing load from the foundation), and load scale.

When the depth from the sea surface to the bearing layer is shallow, the spread foundation (laid caisson), which lays foundation on the bearing layer directly, is the likeliest types, regardless of the water depth.

3.INVESTIGATION OF THE APPLICABILITY OF THE PAST FOUNDATION METHODS

3.1 Conditions for Calculations

In this section, calculations are carried out to investigate the applicability of the laid caisson foundation, the caisson foundation, the bell type foundation in deep water from the construction achievements given in 1. Conditions for calculations are as follows:

(1) Superstructure load
Supporting a main tower of a suspension bridge of the Akashi Kaikyo Bridge class, the conditions are set up as follows:
*Vertical load V: 130,000 (tf)
*Horizontal load H: 3,800 (tf)
(Horizontal seismic coefficient k_H:0.2)
*Moment M: 380,000 (tf·m)

(2) Location condition
*Water depth : 20, 50, 80 m
*Thickness of intermediate layer: 0, 25, 50 m

(3) Ground Condition
*Intermediate layer : dilluvial sandy layer with N value approximately 20
*Bearing layer: supposing tertiary soft rock (C_L-D_H class), ground constants at design have the following values
c=10tf/m^2, ϕ= 35°, γ = 2.1 tf/m^3,
E_0=3,000 kgf/cm^2
*Bearing capacity: allowable bearing capacity (q) of the laid caisson foundation and the caisson foundation at ordinal time are 100 tf/m^2 and 150 tf/m^2 respectively, the ultimate bearing capacity (q_d) of the pile point is 1,000 tf/m^2, given that the depth of embedment is sufficient.

3.2 Results of Calculations

(1) Laid caisson
Every past laid caisson is cube or pillar shaped and a 100 % fill-up section, however, because self-weight is heavier in deeper water, the required plane shape can be bigger. Therefore, as shown in Fig. 6, calculations are conducted for a cube-shape 50% hollow section as well as cube-shape 100% fill-up section, and an inverted-T-shaped hollow section whose upper part is narrowed down. In the case of the inverted-T-shaped 50% hollow section, the upper plane shape is minimized 30 x 70 m which is required to lay an anchor frame of a main tower.

As a result of the calculations, the dimension of the foundation is determined by the vertical bearing capacity in every case. Fig.7 shows the relation between the plane dimension and the subgrade section. In a water depth of 50 m or in the cube 100% section, because self-weight is heavy, subgrade reaction will not be smaller even if the plane dimension is bigger; therefore, in order that allowable bearing capacity is kept within its limit, footing is required to be 175 x 175 m, thus rendering it impractical. On the other hand, in the case of the cube 50% section and the inverted-T-Shaped 50% section , designs are possible on a plane dimension of approximately 60 x 70 m. Both cases require almost the same dimension; however, from the point of construction, the cube 50 % has an advantage. Next, in a water depth of 80 m, even if the plane dimension of the cube 100% is bigger, the subgrade reaction will no longer

decrease below the allowable bearing capacity; therefore, it cannot be constructed in terms of the structure. On the other hand, the cube 50% section of 125 x 125 m is kept within the allowable bearing capacity. However, sliding safety factor becomes less than 1.0. The inverted-T-shaped 50% section of 90 x 90 m is kept below the allowable bearing capacity, and the sliding safety factor is kept at 1.7.

(2) Caisson foundation
As a result of the calculations of the laid caisson, it has been proved that the cube 100% section is unrealistic at the design level; therefore, both the cube 50% section and the inverted-T-shaped 50% section are calculated at the caisson foundation (Fig. 8).

As a result of the calculations of the caisson foundation, the foundation dimension is determined by the vertical subgrade reaction at the base of the foundation, the horizontal displacement and the horizontal subgrade reaction in front of the foundation have the required space at the design ground surface. Fig. 9 shows the relation between plane dimension and vertical subgrade reaction at a water depth of 50 m. Regarding the cube shape, because self-weight is great even in the 50% hollow section, the intermediate layer thickness has a slight influence on the required plane shape. On the other hand, the inverted-T-shaped 50% section requires a smaller plane shape than the cube shape; moreover, if the intermediate layer thickness is bigger, the required plane shape will not be that much bigger. The 80 m water depth shows the same trends described above (Fig. 10). Thus, it is assumed that the caisson foundation requires that the upper section be turned into an inverted-T-shape by being narrowed down. It becomes further investigations in structural planning and construction necessary.

(3)Bell type foundation
There are two methods, one of which reduces the number of piles by using piles of large diameter, while the other increases it using an ordinary size pile in an underwater steel pier. However, a large diameter RC pile is used and limited to a 4 x 4 arrangement in the calculations, because the method of reducing RC piles has an advantage in the view point of construction work, and the positive achievement that RC piles with a diameter of 10 m were used in the Yokohama Bay Bridge. Moreover, the calculations are conducted supposing the body is limited to the inverted-T-shaped section and footing is 100 % fill-up (Fig. 11).

As a result of the calculations, the foundation plane dimension and the pile diameter are determined by the pile head reaction (vertical bearing capacity), and horizontal displacement is a rather small 10 cm, causing few structural problems. Moreover, regarding a reinforcing bar arrangement of the pile, the ordinary area of reinforcement makes the design possible.

Fig. 12 shows the relation between plane dimension and (pile head reaction/allowable bearing capacity), regardless of the thickness of an intermediate layer, the design is possible by using 72 x 72 m (ø 9 m) in a water depth of 50 m, and 80 x 80 m (ø 10 m) in a water depth of 80 m. In the future, investigation of the pile driving method, and the design and construction of connection between pile heads and footing are necessary.

(4) Multi-column foundation
In the multi-column foundation, using a big diameter of RC pile, the calculations are conducted in 4 x 4 arrangement. A footing, with reference to the past construction examples, is applied to an 80% fill-up section (Fig.13).

As a result of the calculations, in a water depth of 50 m, footing dimension and pile diameter are determined by the pile had reaction (vertical bearing capacity). Fig.14 shows the relation between plane dimension and (pile head reaction/ allowable bearing capacity), regardless of the thickness of the intermediate layer, a 48 x 70 m (ø 6 m) footing is required in design. However, at the top slab, the displacement amounts to more than 25 cm. Moreover, the bending moment occurring at the pile itself is also so great that the requiring area reinforcement amounts to more than 10% of the pile section area. In a water depth of 80 m, the horizontal displacement of the design ground surface is not so lower than the allowable values (50 mm) that it is impossible to construct. Therefore, the adoption of a inclined pile and one with high rigidity are required.

4. CONCLUSION

In this paper, the present situation was clarified by investigating the positive achievements of foundations constructed in deep water in the past, and calculations were carried out to investigate the potential of conventional foundation methods.

As a result of investigations into the positive achievements of foundations constructed in deep water in the past, water depth, construction depth and load scale are proved to be the most important conditions governing the choice of foundation methods. As a result of the calculations, 1) the laid caisson foundation is easily influenced by water depth, therefore, in deeper water it is necessary to lighten its self-weight by hollowing the section or turning the section into an inverted-T-shaped section. 2) As a result of investigations into the three methods, namely the caisson foundation, the bell type foundation and the multi-column foundation, if an intermediate layer exists it was proved that in terms of construction and economy, the multi-column foundation has an advantage, and in terms of structure, the bell type foundation is advantageous.

In the future, we will investigate the potential of conventional foundations constructed in deep water continuously. As clarified by the results of the calculations carried out in this study, each foundation has limits on structure. Therefore, it is also necessary to develop a completely new foundation method appropriate for deep water areas. The potential of bridge foundations whose structure is the same as the oil rig in a submarine oil field, shown in Fig. 15., is now under investigation. The results of this current study will be reported when the project is completed.

References

1)A special issue featuring articles on the Honshu-Shikoku Bridge: The Bridge and Foundation Engineering, 1984. 8

2)Kashima Satoshi, Narui Shin, Yasuda Masahiko, Hirahara Nobuyuki: Outline of the Design of the Akashi Kaikyo Bridge, The Bridge and Foundations Engineering, 1990 .1

3)Mitsuse Jun : The Foundation Work of the Hiroshima Bridge, The Foundation Engineering & Equipment, 1978.4

4)Arita Takeo : The Substructure Work of the Kaida Bridge in the important port of Hiroshima Bay -The Open-Caisson Suspended Method-, Civil Engineering, 1987.9

5)Kojima Yuji: The Construction Situation of Metropolitan Expressway 12 and the Tokyo Bay Bridge, Bridge Engineering, 1988.6

6)Kogo Makoto: Ise Road around Bay, The Bridge and Foundation Engineering,1990.8

7)Matsuda Dairoku, Otsubo Masayuki, Yamagishi Akira : The Construction of Substructure of Kitaurako Bridge, Honshi Technical Report, 1987.7

8)Nosaka Ryuichi, Ishihara Masaru, Sato Kenji, Taguchi Fumio : The Diaphragm Wall used for the Main Tower Foundation of the Hakucho Bridge, The Foundation Engineering & Equipment, 1989.1

9)Motoyama Toshi, Tsunomachi Hiroshi, Tsuji Hideki, Ota Hiroshi, Maruyama Tadaaki : The foundation of Kansai International Airport Bridge, Foundation Work, 1988.2,3

10)Kagawa Yuji, Nakamura Shunichi, Momiyama Yoshiyuki : Planning and Design of a Multi-Span Continuous Bridge and Sub-Structures of the Trans-Tokyo Bay Highway Bridge, The Bridge and Foundation Engineering, 1991.1,2

11)Wada Katsuya, Ogasawara Masafumi : The Design and the Construction of the Substructure of the Yokohama Bay Bridge, Bridges and Foundations, 1988.10

Table 1 Construction achievements of the laid caisson

No	Name of Bridge (Substructure)	Plane scale (m)	Bearing layer	Load Rd(tf)	Total amount excavated(m^3)
1	Wakamatsu Bridge (P1)	15.0×20.0	hard rock	12,000	5,200
2	Iwagurojima Bridge (1B2P-4P)	22.0×45.0	soft rock	25,000	10,500
3	South Bisan Seto Bridge (5P,6P)	27.0×59.0	medium hard rock	78,000	22,500
4	Akashi Kaikyo Bridge (2P, 3P)	φ80.0	hard rock	125,000	73,500
5	Second Amakusa Bridge (P_1, P_2)	φ12.0	soft rock	800	200
6	Third Amakusa Bridge (P_1, P_2)	φ17.0	hard rock	4,000	650
7	Fourth Amakusa Bridge (P_1-P_4)	φ17.0	soft rock	4,000	750
8	Oyashirazu Beach Elevated Bridge (5 bridges)	13.0×21.0	hard rock	4,000	3,400
9	Kurohime Bridge (P_1-P_5)	10.0×12.0	soft rock	1,500	1,520
10	Ikutsuki Bridge (Hirado side P6 pier)	22.0×25.0	hard rock	10,000	490
11	Kurono Seto Bridge (P_1,P_2)	10.0×22.0	soft rock	5,000	530

Table 2 Construction achievements of the open-caisson

No	Name of Bridge (Substructure)	Plane scale (m)	Bearing layer	Load scale Rd(tf)
1	Hiroshima Bridge (A_1-P_9)	φ10.0	gravel	4,000
2	Kanazawa Seaside Line Bridge (P211)	φ11.0	hard pan	2,000
3	Muya Bridge (4P)	φ16.0	gravel	3,500
4	Kiso Sansen Bridge (total 29 bridges)	φ11.0	gravel	3,000
5	Kaida Bridge (P_6-P_{28})	φ16.2	medium hard rock	6,000
6	Nitta Bridge (P_6-P_8)	φ9.0	gravel	1,000
7	Sakashiro Bridge (P_{14}.P_{15})	φ10.0	soft rock	3,000
8	Kasumigaura Bridge (P_{28},P_{21})	φ3.5	soft rock	500

Table 3 Construction achievements of the pneumatic caisson

No	Name of Bridge (Substructure)	Plane scale (m)	Bearing layer	Road Rd(tf)
1	Lake Kawaguchi Bridge (P_1-P_4) ①	10.0×12.0	medium hard rock	2,000
2	Keihin Channel Bridge (P_{402},P_{403}) ①	26.0×26.0	medium size sand	5,000
3	Arakawa Tailrace Bridge (A_1-A_2) ①	φ13.0	silt, mixed sand	2,000
4	New Tokachi Bridge (P_2, P_3) ②	27.0×32.0	soft rock	10,000
5	Tomazaki Miyamae Bridge (P_{180}, P_{181}) ②	φ11.0×2	soft rock	1,500
6	Rokko Island Bridge (P_6, P_7) ②	22.0×32.0	gravel	8,000
7	East Kobe Bridge (main tower foundation) ①	32.0×35.0	gravel	20,000
8	Oshima Bridge (5P) ②	13.0×35.0	medium hard rock	25,000
9	Shimotsui Seto Bridg (SP2P) ②	19.0×56.0	medium hard rock	60,000
10	Kameura Viaduct L4P, 5P) ②	20.0×29.5	medium hard rock	8,000
11	Monzaki Viaduct (T2P-T7P) ②	28.0×30.0	medium hard rock	11,500
12	Meiko West Bridge (P_2, P_3) ①	33.0×25.0	medium size sand	8,000
13	Minato Bridge (P_2, P_3) ②	40.0×40.0	gravel	25,000
14	Hamanako Bridge (P_1-P_5) ①	19.0×25.0	soft rock	5,000
15	Tsurumi Waterway Bridge (P_2, P_3) ①	40.0×40.0	gravel	20,500
16	Tokyo Harbour Bridge (A_1-P_{12}) ①	25.0×49.0	soft rock	20,000

17	Nadahama Bridge ① (P_1, P_2)	16.0×28.0	gravel	8,000
18	Wakato Bridge ① (P_{23}, P_{24})	17.1×40.1	soft rock	8,000
19	Iwa Bridge (P_2) ②	φ14.0	hard rock	15,000
20	Senjyu Shim• Bridge② (P_4-P_7)	φ8.0	gravel	3,000
21	Sumida River Bridge ① (P_8, P_9)	18.0×22.0	gravel	3,000
22	Aratsu Bridge ②	20.0×20.0	gravel	5,000
23	Shimousa Tone Bridge ② (P_{10}-P_{13})	12.6×13.1	gravel	1,000
24	Shin Kawa Oto Kawa② Bridge (P_1)	5.0×15.5	gravel	5,000
25	Kurujima First Bridge (3P) ①	35.0×46.0	soft rock	20,000
26	Eitai Bridge ② (P_1, P_2, A_2)	15.0×16.5	gravel	1,500
27	Rinku Town North Bridge (P_6) ②	29.0×30.0	gravel	20,000
28	Meiko Central Bridge ① (P_2, P_3)	30.0×34.0	soft rock	30,000
29	Meiko East Bridge ①	28.0×34.0	soft rock	20,000

Notes) ① floating type
② filled coffer dam type

Table 4 Construction achievements of diaphragm wall foundation

No	Name of Bridge (Substructure)	Plane scale (m)	intermeadiate layer	Bearing layer	Load Rd(tf)
1	Kitaurako Bridge (2P-5P)	9.0×10.0	alluvial gravel	grevel	5,000
2	Hakucho Ohashi Bridge (side tower 2P)	φ37.0	soft silt	soft rock	5,000

Table 5 Construction achievements of bell type foundation

No	Name of Bridge (Substructure)	Plane scale (m)	Bering layer	Load Rd (tf)	Kind of a pile	Pile diameter (mm)	Number of piles
1	Arakawa Wangan Bridge	37.6×22.6	gravel	8,000	steel pipe pile	φ1,500	60
2	Kansai International Airport Bridge (P1-P30)	28.8×24.8	an alternate clay and sand layer	5,000	steel pipe pile	φ1,500	56
3	Hitsuishijima Bridge (3P)	46.0×29.0	soft rock	20,000	cast-in-place pile	φ4,000	32
4	Daikoku Bridge (P4-P6)	34.0×30.0	soft rock	12,000	steel pipe pile	φ1,422	72
5	Trans-Tokyo Bay Bridge (P1-P12)	28.0×28.0	sand		steel pipe pile	φ1,600	49
6	Kishiwada Bridge (KP3)	49.0×27.0	gravel	10,000	cast-in-place pile	φ1,500	78

Table 6 Construction achievements of multi-column foundation

No	Name of structure (Substructure)	Plane scale (m)	Bearing layer	Load Rd(tf)	Kind of a pile	Pile diameter (mm)	Number of piles
1	Yokohama Bay Bridge (P_2, P_3)	56.0×54.0	soft rock	15,000	cast-in-place pile	φ10,000	9
2	Kojima Bay Bridge (P_7-P_{13})	16.0×20.0	gravel	3,000	steel pipe pile	φ1,500	20
3	Oshima Bridge (P_3-P_5)	23.0×33.3	medium hard rock	4,700	double steel pipe pile	φ3,500	12
4	Onaruto Bridge (3P, 4P)	25.5×60.0	soft rock	25,000	steel pipe pile	φ7,000	21
5	Kosan Bridge (P_2-P_6)	31.4×25.0	soft rock	7,000	steel pipe pile	φ2,500	20
6	Haneda Movable Bridge P8, P11, P12)	5.0×5.0	gravel	200	PHC pile	φ1,000	4
7	Ikarajima Bridge (P_2-P_5)	30.0×30.0	soft rock	8,000	steel pipe pile	φ3,300	16

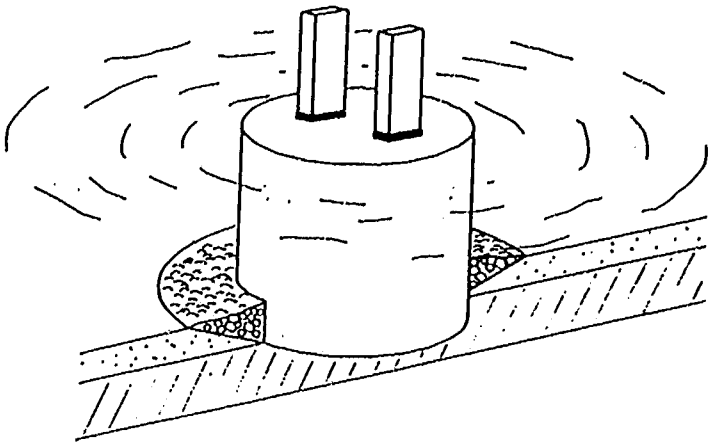


Fig. 1 Laid caisson foundation

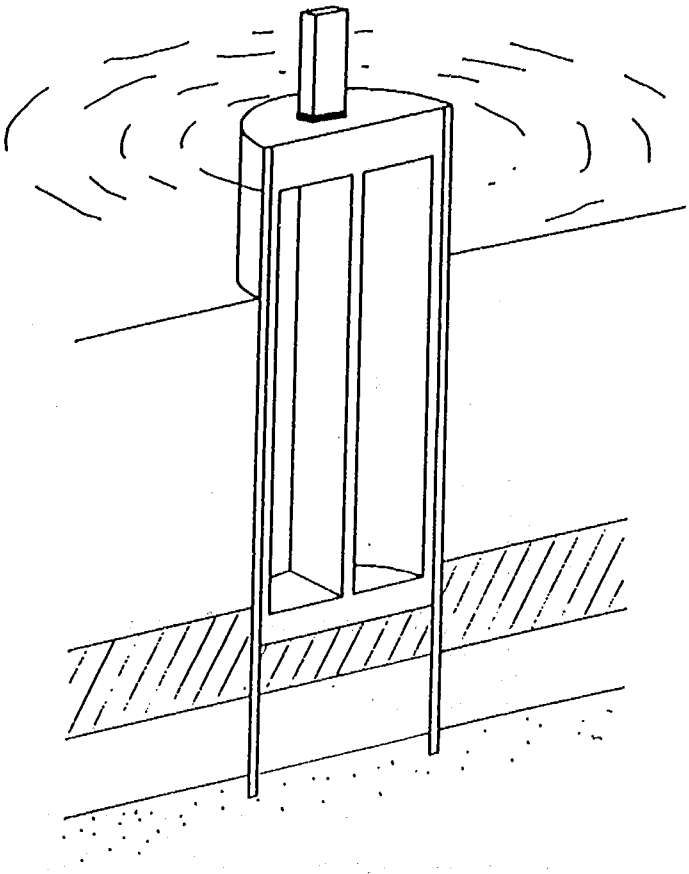


Fig. 2 Diaphragm wall foundation

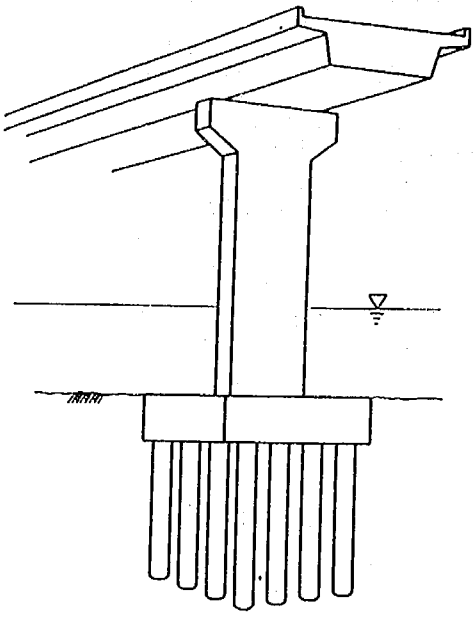


Fig. 3 Bell type foundation

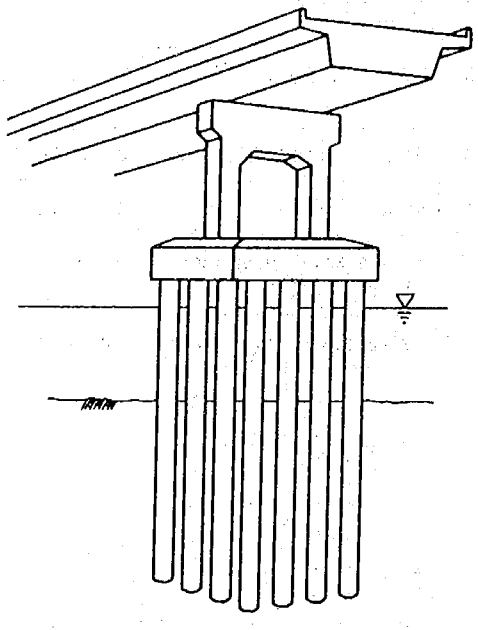


Fig. 4 Multi-column foundation

Fig. 7 Resalts of the caluculation (1)

Laid caisson

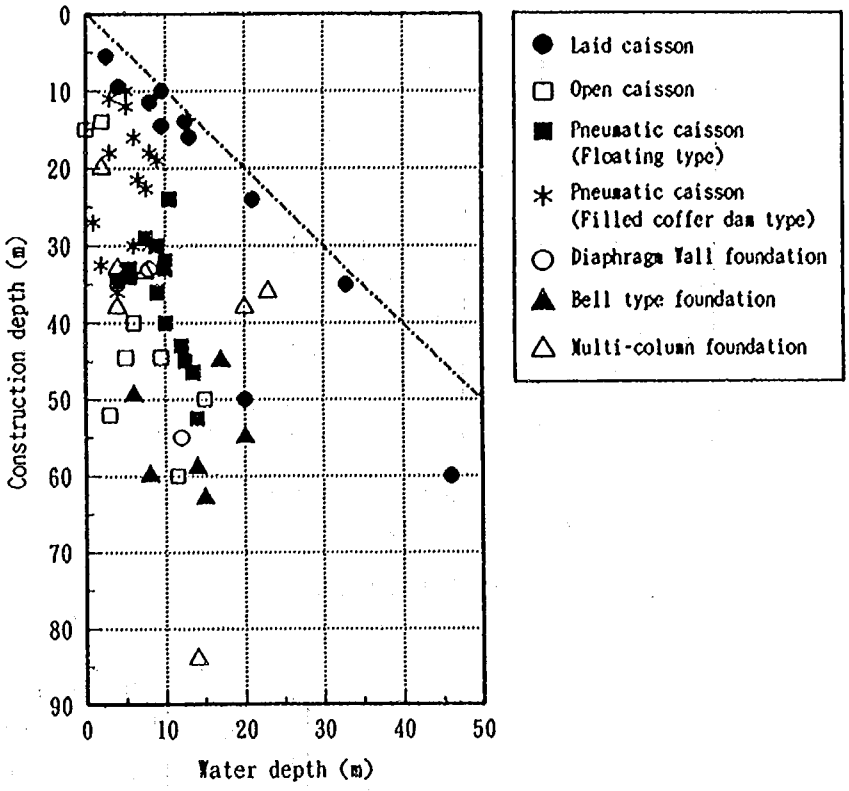


Fig. 5 Construction achievements of under water foundations

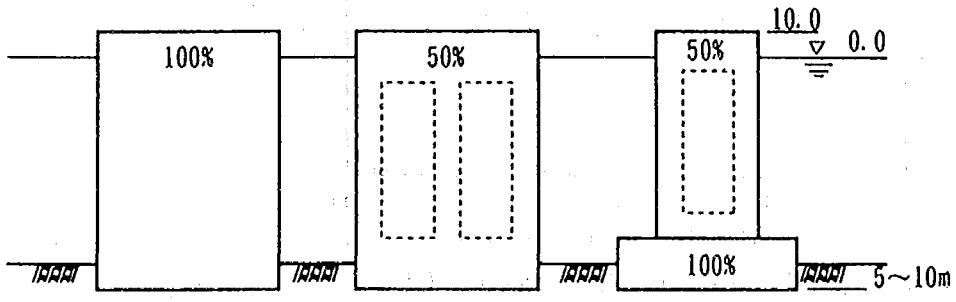
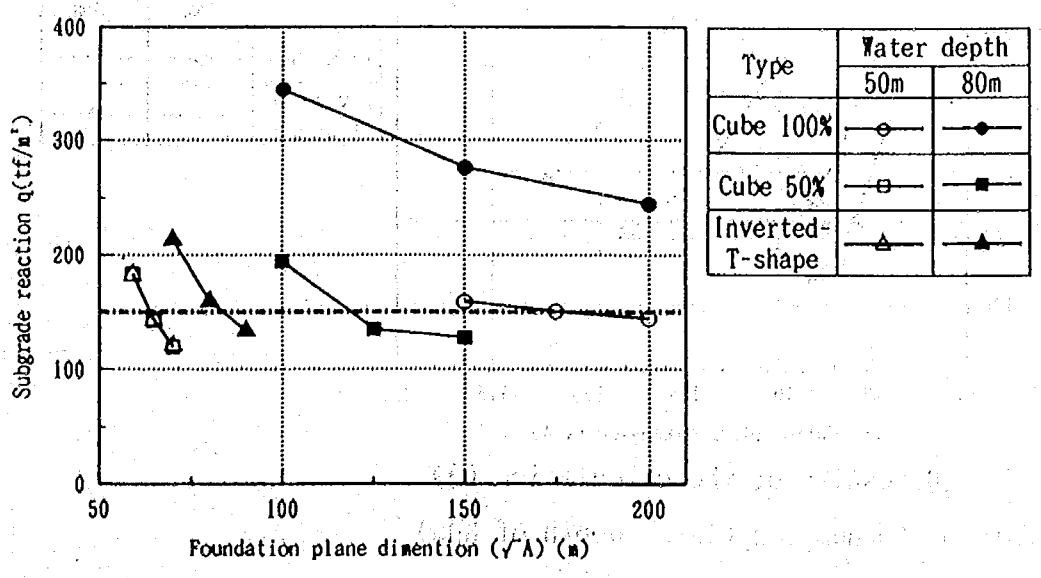


Fig. 6 Laid caisson



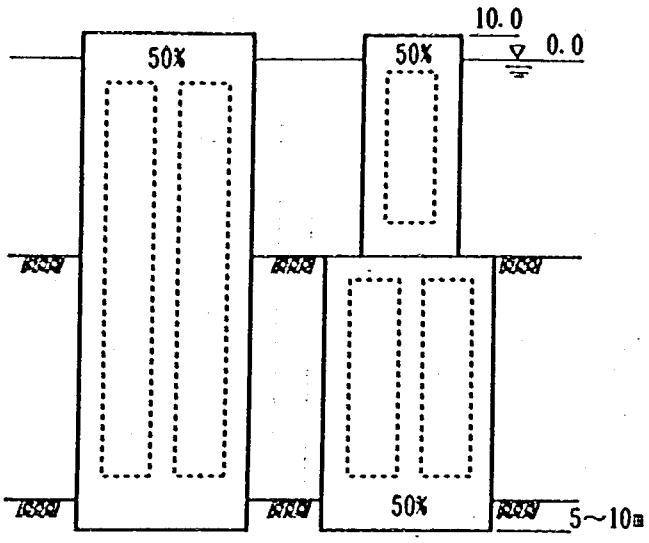


Fig. 8 Caisson foundtion

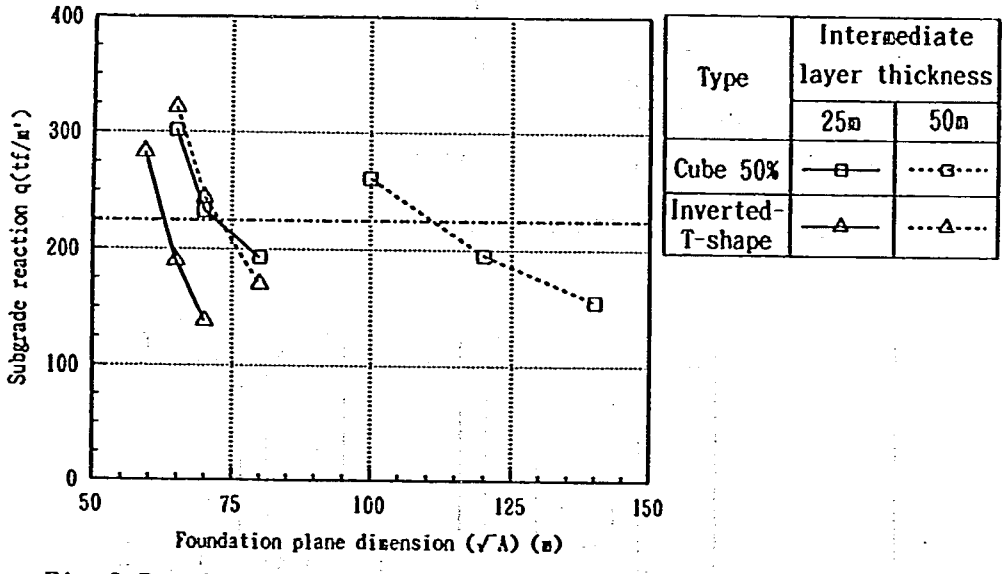


Fig. 9 Results of the calculation (2)
Caisson foundation (Water depth of 50m)

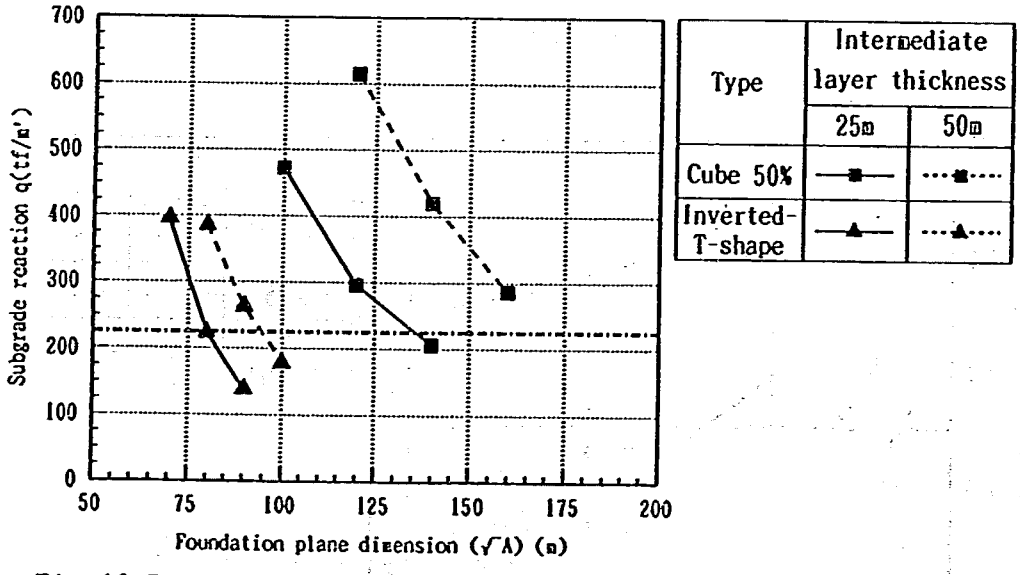


Fig. 10 Resalts of the calculation (3)
Caisson foundation (Water depth of 80m)

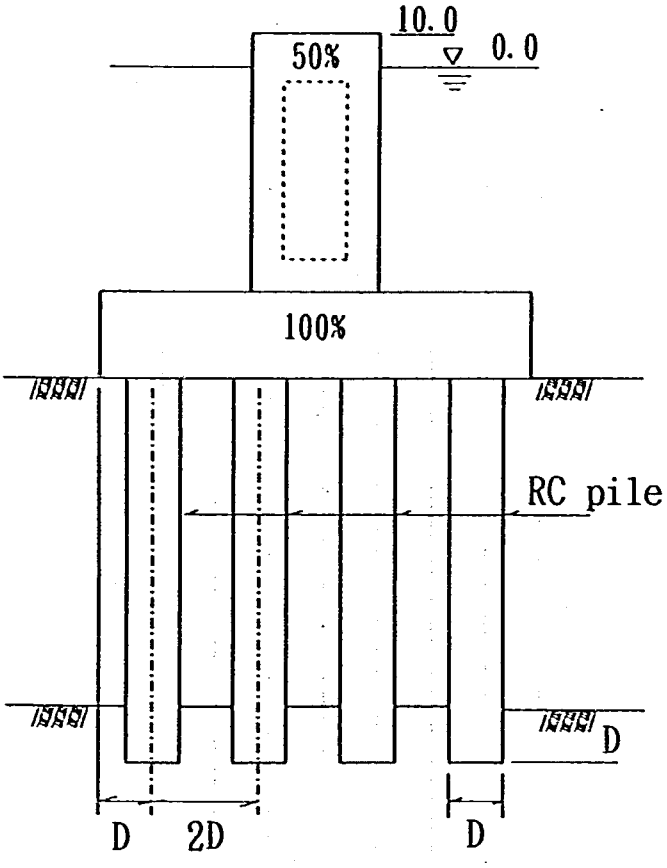


Fig. 11 Bell type foundation

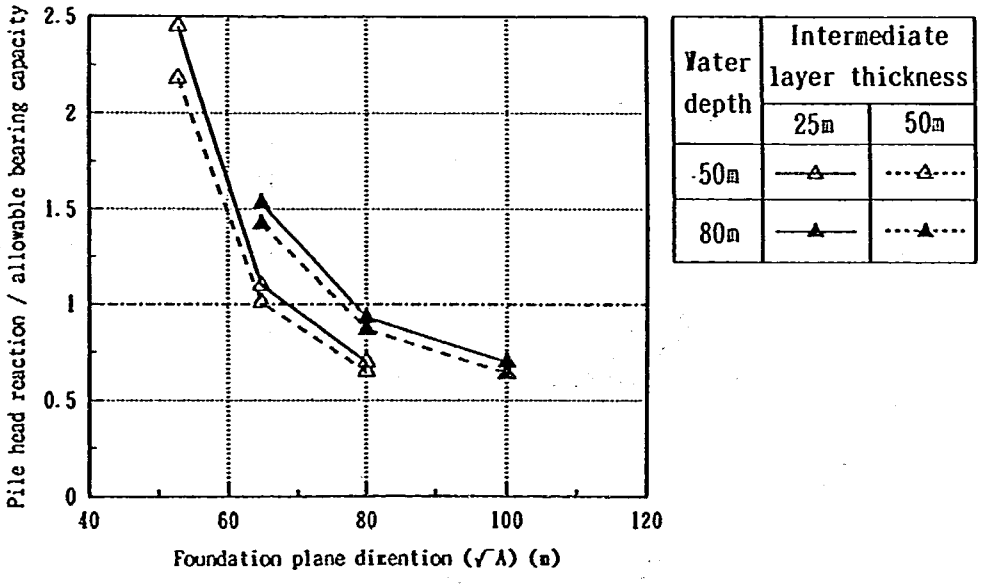


Fig. 12 Resalts of the calculation (4)
Bell type foundation

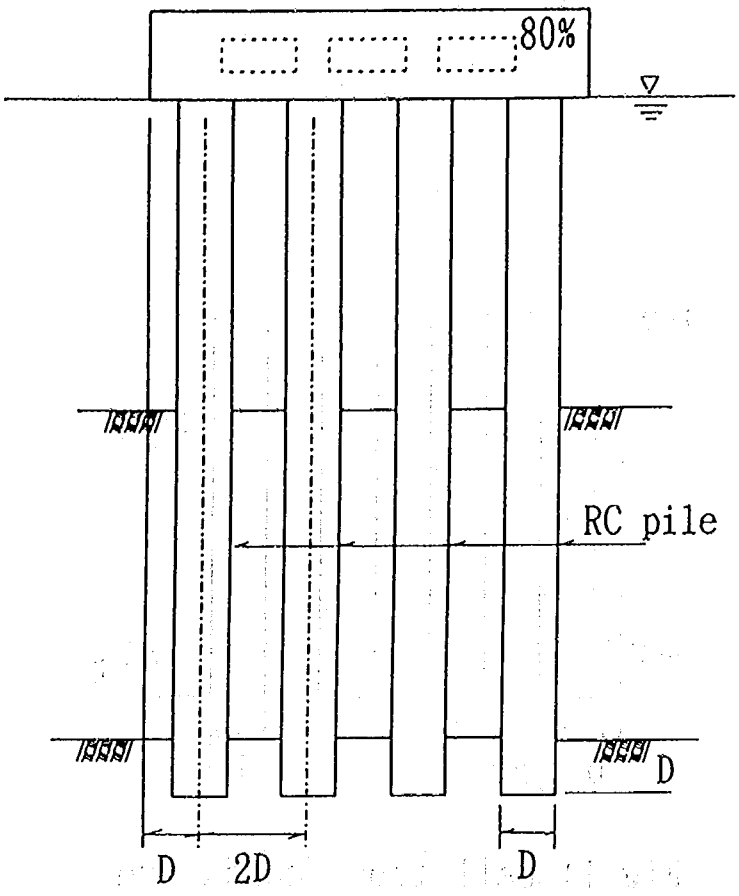


Fig. 13 Multi-column foundation

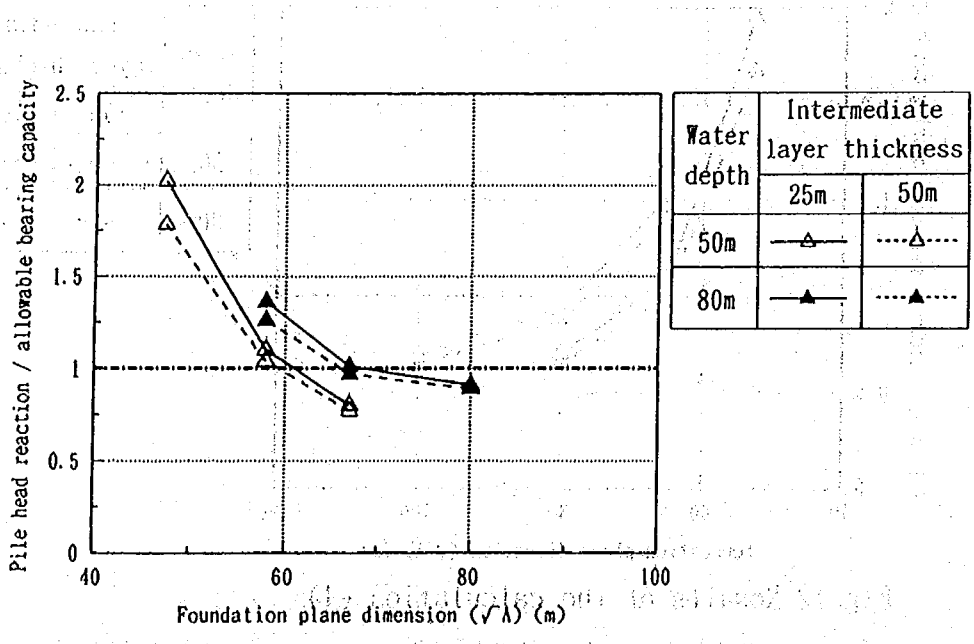


Fig. 14 Resalts of the calculation (5)
Multi-column foundation

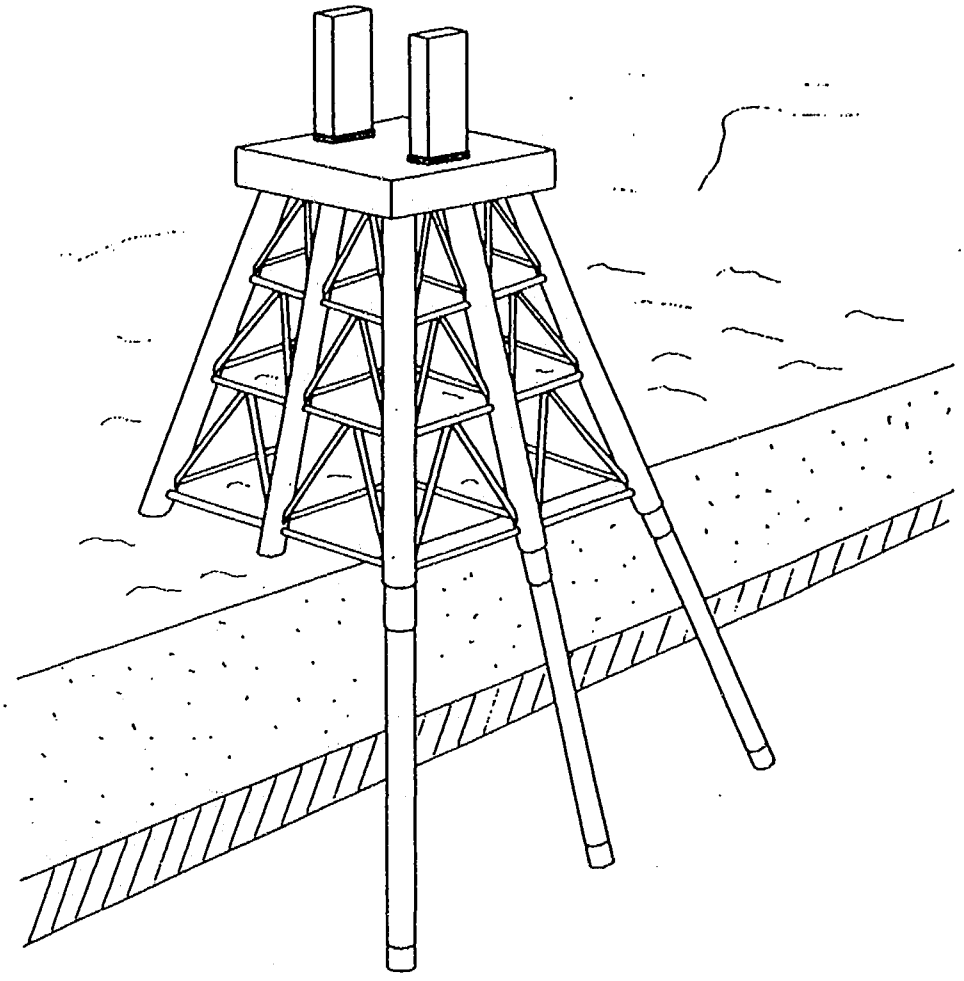


Fig. 15 New type foundation in deep water

Theme 4

Numerical Simulation by Multi-Level Model for Storm Surge Generated by Ise-wan Typhoon

Chiaki Goto, Hidenori Shibaki* and Tomotsuka Takayama**

Abstract

In order to obtain an accurate water elevation by storm surges, a new numerical simulation method by multi-level model is developed. In this paper, some results from a fundamental study for numerical simulation of storm surge are reported. It is clarified that multi-level model should be adopted for numerical simulation of storm surge to get accurate results.

Keywords : storm surge; multi-level model; Ise-wan typhoon

1. Introduction

It is well known that the storm surge due to tropical cyclone is a meteorologically forced long water wave motion resulting in a sustained superelevation of the sea surface above that produced by the normal periodic astronomical tide. From a dynamic point of view, the storm surge is caused mainly by the suction of sea water due to the pressure drop over the sea surface as well as by the strong wind drift of sea water toward down-wind.

In these two effects to generate storm surge, the wind driven flow has a character with that flow velocity is the fastest at the water surface and decreases in proportion to water depth.

Usually, one-layer model with water velocity which averaged from the bottom to the surface is adopted to numerical simulation of storm surges. In the case, accuracy of water velocity near surface becomes worse, so that the discharge flux of sea water into bay from ocean would be underestimated. This can be considered as a serious problem for numerical simulation of storm surge.

In this paper, a numerical simulation method by multi-level model for storm surges is presented. If wind and pressure fields are calculated correctly, it is clarified that the multi-level model gives more accurate water elevation height distribution due to storm surges compared with the convensional one-layer model.

2. Convensional compuation of storm surge

2.1 Storm surge phenomena

The long period sea surface fluctuation caused by meteorological factors, such as strong wind and abrupt atmospheric pressure change, is called the meteorological tide. The storm surge is a meteorological tide with abnormal rise of sea water, and is mainly induced by tropical cyclone, especially typhoons in the case of Japan.

When a low pressure front passed over a sea area, a certain change in the sea level appears. This is caused mainly by the suction of sea water due to the pressure drop over the sea surface as well as by the strong wind drift of sea water toward down-wind. Such a rise of sea water, accompanied by the propagation of the low pressure front, becomes a kind of forced progression of waters in the unbounded sea water region. The suction of sea water due to low pressure is independent of water depth, but the rise of sea water above still water due to wind drift is inversely proportional to the water depth. Because of this latter fact, storm surge in general has a tendency to be large in a shallow water region.

When the forced progressive wave mentioned above approaches the edge of the continental shelf, where the water depth is about 200 m, the storm surge increases in height due to the sudden decrease of water depth, and at the same time sufferes the effect of wave reflection due to the sea bottom configuration. In addition to the above, the storm surge induces edge waves which

* Ocean Energy Utilization Lab., PHRI

** Director, Hydraulic Engineering Div., PHRI

propagate along the continental shelf, and other oscillations on the shelf. All of those combine with the forced progressive waves in producing a complicated pattern of sea water fluctuations.

When the storm surge progresses into the shallower region and enters a bay, wave reflection will occur at the head of the bay. Thus a part of the wave energy will escape, but most of the energy will be confined to the bay for a long time. Thus natural osillation of the bay water is developed by the above processes. The above induced oscillation is named the secondary oscillation of harbour, or sometimes called a seiche, and is maintained for many hours.

2.2 Empirical formula

To express the height of a storm surge at a particular point, the value obtained by subtracing the predicted astronomical tide from actually record sea level is used and called the meteorological tide anomaly. The correlation between the maximum anomaly and meteorological conditions such as maximum wind velocity, wind direction, and lowest atmospheric pressure at a particular location is attempted, and is applied to predict the storm surge there.

It is possible to consider that a storm surge is basically generated by the combined effect of suction due to low atmospheric pressure and water mass compilation at the shore due to wind drift; therefore the following equation can be used for practical purpose,

$$\eta_{max} = a\Delta P + bU^2 \cos\theta + cH_{1/3} \qquad (1)$$

where η_{max} is the maximum meteorological tide anomaly, ΔP the difference between the spatial mean pressure over the sea surface and the lowest atmosperic pressure on thre sea surface, U the maximum wind speed, θ the angle between the optimum wind direction to produce the maximum anomaly and the directions of maximum wind speed, $H_{1/3}$ the significant wave height and a, b and c the constants determined empirically.

2.3 Numerical simulation

The empirical method mentioned above is applicable only to locations where the observation data have been compiled over many years. Recently, numerical simulation of storm surges has been developed. The numerical simulation method gives not only the maximum meteorological tide anomaly distribution for extended area but also time history of water elevation. Moreover the method has the possibilty of advancement to use more realistic atmospheric pressure distribution which may changes its pattern with time.

After many numerical models have been tried, the leap-frog and ADI methods by one-layer model became the most common in numerical simulations of storm surges for practical use. Accuracy of numerical results depends on the kind of equations, the scheme of the finite difference method, and grid sizes in space and time.

Usually, motion of storm surges can be described by the depth integrated long wave equations. In deep sea until it arrives at a water depth of about 50 m, following the linear equations of long waves including the Coriolis and the other external forced terms is adopted.

$$\frac{\partial \eta}{\partial t} + \frac{\partial M}{\partial x} + \frac{\partial N}{\partial y} = 0 \qquad (2)$$

$$\frac{\partial M}{\partial t} + gD\frac{\partial \eta}{\partial x} + \frac{D}{\rho_w}\frac{\partial P}{\partial x} = fN + \frac{\tau_{sx}}{\rho_w} - \frac{\tau_{bx}}{\rho_w} \qquad (3)$$

$$\frac{\partial N}{\partial t} + gD\frac{\partial \eta}{\partial y} + \frac{D}{\rho_w}\frac{\partial P}{\partial y} = -fM + \frac{\tau_{sy}}{\rho_w} - \frac{\tau_{by}}{\rho_w} \qquad (4)$$

where (M, N) indicates horizontal mass transport in the direction of (x, y), η the water elevation height, D the total depth, ρ the density of water, P the atmospheric pressure, f the Coriolis coefficient, τ_s the momentum transfer from wind and τ_b the bottom shear stress. Wind and bottom stresses are supposed to be proportional to the square of wind velocity and square of the mean flow velocity respectively as follows,

$$\tau_{sx} = \rho_a C_d U_x \sqrt{U_x^2 + U_y^2}$$

$$\tau_{sy} = \rho_a C_d U_y \sqrt{U_x^2 + U_y^2}$$

$$\tau_{bx} = \frac{\rho_w g n^2}{D^{7/3}} M \sqrt{M^2 + N^2}$$

$$\tau_{by} = \frac{\rho_w g n^2}{D^{7/3}} N \sqrt{M^2 + N^2}. \qquad (5)$$

where (U_x, U_y) is the wind speed in the direction of (x, y), ρ_a the air density, n the Manning's roughtness coefficient and C_d the drag coefficient for air-sea interface.

In a sea shallower than 50 m, following nonlinear shallow-water long wave equations including the Coriolis and the other external forced terms are used.

$$\frac{\partial \eta}{\partial t} + \frac{\partial M}{\partial x} + \frac{\partial N}{\partial y} = 0 \qquad (6)$$

$$\frac{\partial M}{\partial t} + \frac{\partial}{\partial x}\left(\frac{M^2}{D}\right) + \frac{\partial}{\partial y}\left(\frac{MN}{D}\right) + gD\frac{\partial \eta}{\partial x} + \frac{D}{\rho_w}\frac{\partial P}{\partial x} = fN + \frac{\tau_{sx}}{\rho_w} - \frac{\tau_{bx}}{\rho_w} \qquad (7)$$

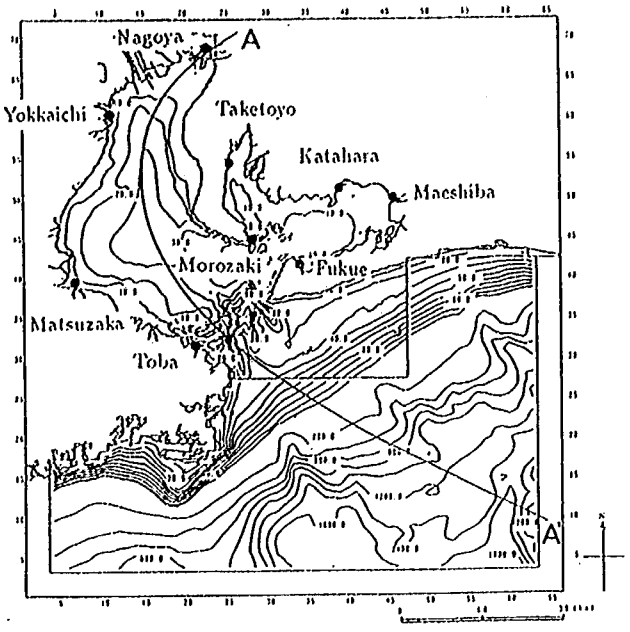


Fig.1 Water depth distribution of Ise Bay

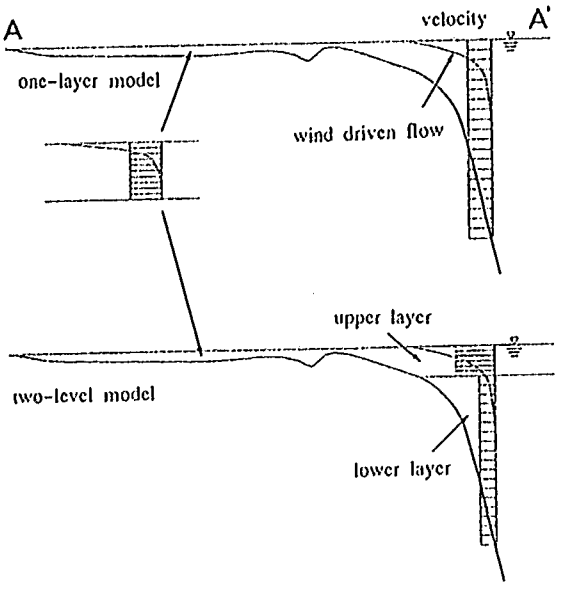


Fig.2 Approximation of wind driven flow

$$\frac{\partial N}{\partial t} + \frac{\partial}{\partial x}\left(\frac{MN}{D}\right) + \frac{\partial}{\partial y}\left(\frac{N^2}{D}\right) + gD\frac{\partial \eta}{\partial y} + \frac{D}{\rho_w}\frac{\partial P}{\partial y} = -fM + \frac{\tau_{sy}}{\rho_w} - \frac{\tau_{by}}{\rho_w} \quad (8)$$

Figure 1 shows water depth distribution of Ise Bay. Ise Bay is located center of Honsyu Island in Japan and faced on the Pacific Ocean. The averaged water depth at bay mouth is 30 meters and Ise Bay connected to the ocean with relatively steep bottom slope. In the figure, the numerials indicate water depth and the lines is the equi-water depth. Figure 2 shows a sectional bottom profile along A and A' line in Fig. 1 and the comparison of approximation of water velocity distribution in the numerical simulation between one-layer and two-level models. In the figure, thick lines indicates actual distribution of wind driven flow and thin line is velocity distribution approximated in numerical simulation.

In the one-layer model computation, water velocity of vertical distribution is approximated as uniform, so that water enters into the bay is calculated as small valume and reflected water volume toward the ocean is calculated as large. This is a reason that the accurate result could not be obtained by the conventional numerical simulation. On the other hand, two-level model gives relatively good approximation for vertical distribution of wind driven flow. Therefore, it is expected that an accurate numerical simulation of storm surge could be carried out by use of two-level model.

3. Two-level model for storm surge

3.1 Estimation of wind field

As the estimation of pressure and wind field, the following axi-symmetric cyclone model by Myer's is adopted.

$$P = P_\infty - \Delta P \exp\left(-\frac{r}{r_0}\right) \quad (9)$$

In the formula, P_∞ is the peripheral pressure of the cyclone which is fixed as 1,010 hPa. The symbol ΔP the depression of the central pressure, r the distance from the center of the cyclone and r_0 the emperical constant.

For the wind distribution, the Miyazaki's formula,

$$W = C_1 G + C_2 V_t \exp\left(-\frac{r}{r_0}\right)$$
$$G = -\frac{rf}{2}\sqrt{\left(\frac{rf}{2}\right)^2 + \frac{\Delta P}{\rho_a}\frac{r_0}{r}\exp\left(\frac{r_0}{r}\right)} \quad (10)$$

is adopted. In the formula, W is the estimated wind vector, G the gradient wind vector, V_t the movement speed vector of the cyclone, and C_2 the emperical constant which are fixed as 0.66.

3.2 Governing equations of storm surge

The nonlinear long wave theory including terms of Coriolis force, bottom friction and momentum trasfport from air is used as the governing equations as following.

For upper level of water:

$$\frac{\partial \eta}{\partial t} + \frac{\partial M_1}{\partial x} + \frac{\partial N_1}{\partial y} + \frac{\partial M_2}{\partial x} + \frac{\partial N_2}{\partial y} = 0 \quad (11)$$

$$\frac{\partial M_1}{\partial t} + \frac{\partial}{\partial x}\left(\frac{M_1^2}{D_1}\right) + \frac{\partial}{\partial y}\left(\frac{M_1 N_1}{D_1}\right) - \frac{M_1 w}{D_1} + gD_1\frac{\partial \eta}{\partial x} + \frac{D_1}{\rho_w}\frac{\partial P}{\partial x} = fN_1 + \frac{\tau_{sx}}{\rho_w} - \frac{\tau_{ix}}{\rho_w} \quad (12)$$

$$\frac{\partial N_1}{\partial t} + \frac{\partial}{\partial x}\left(\frac{M_1 N_1}{D_1}\right) + \frac{\partial}{\partial y}\left(\frac{N_1^2}{D_1}\right) - \frac{N_1 w}{D_1} + gD_1\frac{\partial \eta}{\partial y} + \frac{D_1}{\rho_w}\frac{\partial P}{\partial y} = -fM_1 + \frac{\tau_{sy}}{\rho_w} - \frac{\tau_{iy}}{\rho_w} \quad (13)$$

For lower level of water:

$$w + \frac{\partial M_2}{\partial x} + \frac{\partial N_2}{\partial y} = 0 \quad (14)$$

$$\frac{\partial M_2}{\partial t} + \frac{\partial}{\partial x}\left(\frac{M_2^2}{D_2}\right) + \frac{\partial}{\partial y}\left(\frac{M_2 N_2}{D_2}\right) + \frac{M_2 w}{D_2} + gD_2\frac{\partial \eta}{\partial x} + \frac{D_2}{\rho_w}\frac{\partial P}{\partial x} = fN_2 + \frac{\tau_{ix}}{\rho_w} - \frac{\tau_{bx}}{\rho_w} \quad (15)$$

$$\frac{\partial N_2}{\partial t} + \frac{\partial}{\partial x}\left(\frac{M_2 N_2}{D_2}\right) + \frac{\partial}{\partial y}\left(\frac{N_2^2}{D_2}\right) + \frac{N_2 w}{D_2} + gD_2\frac{\partial \eta}{\partial y} + \frac{D_2}{\rho_w}\frac{\partial P}{\partial y} = -fM_2 + \frac{\tau_{iy}}{\rho_w} - \frac{\tau_{by}}{\rho_w} \quad (16)$$

where (M_1, N_1) and (M_2, N_2) are the mass transport of upper and lower layers in the direction of (x, y), w the vertical velocity at interface, D_1 and D_2 the total depth of upper and lower layers, τ_i the shear stress on interface between upper and lower layers. The interface shear stress are also supposed to be proportional to the square of the mean flow velocity as follows,

$$\tau_{ix} = \frac{\rho_w f_d}{D^2}(M_1 - M_2)\sqrt{(M_1 - M_2)^2 + (N_1 - N_2)^2}$$

$$\tau_{iy} = \frac{\rho_w f_d}{D^2}(N_1 - N_2)\sqrt{(M_1 - M_2)^2 + (N_1 - N_2)^2} \quad (17)$$

where f_d is the empirical coefficient of shear stress at interface.

3.3 Boundary condistion

At the open boundary, storm surges are assumed to satisfy barometric balance and to pass through outwards waves. At the land boundary, zero discharge is assumed at a fixed shore.

4. Discussion for numerical results

4.1 Computation area

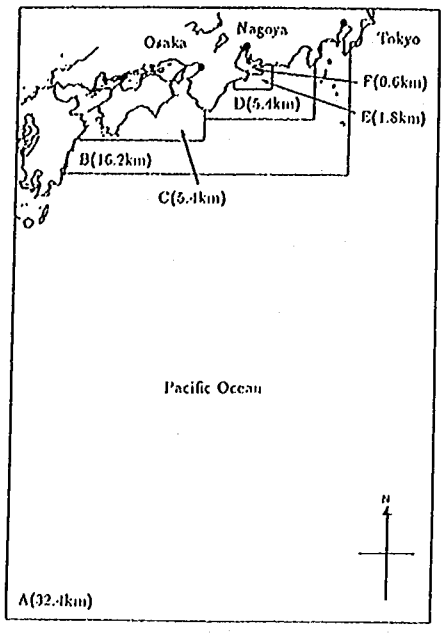


Fig.3 Numerical region

Computation areas are divided six regions, region A to region F. The grid size in deepest area is set as 32.4 km and is made small in shallow sea area down to 16.2 km, 5.4 km, 1.8 km and 0.6km. Numerical grid areas are shown in Fig 3.

4.2 Computation results

As an examination of numerical simulation, the storm surge in Ise Bay generated by Ise-wan typhoon is carried out. Japan was attacked many times by typhoon storm surges. This is due to the location of the islands which coincide with the track of typhoons. Among typhoons, Ise-wan Typhoon was the biggest typhoon which attacked the central part of Japan in September 1959. The storm surge results in considerable damage to exposed coastlines, the flooding of low lying land and loss of life.

Figure 4 shows the distribution of the maximum water surface elevation by one-layer model. We can see well that the water surface elevation increase gradually from bay mouth to inner part of bay. Figure 5 shows water velocity vectors at 30 minutes before the time when the maximum water surface elevation at Nagoya port.

Figure 6 shows the distribution of the maximum water surface elevationby two-level model. In the computation by two-level model, depth of the upper layer is set as 100 m. The water surface elevation by two-level model is simulated as higher than that by one-layer

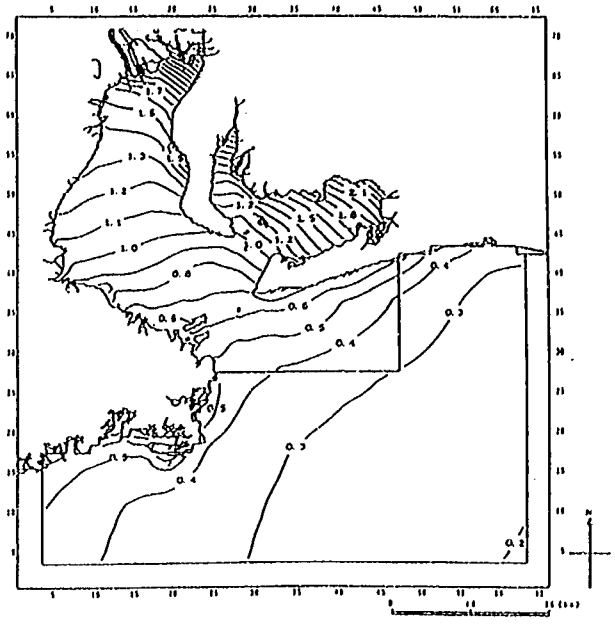


Fig.4 Maximum water elevation by one-layer model

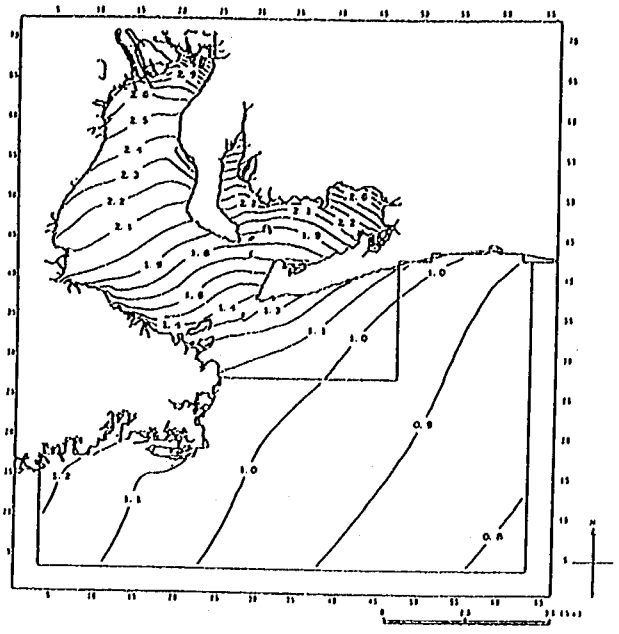


Fig.6 Maximum water elevation by two-level model

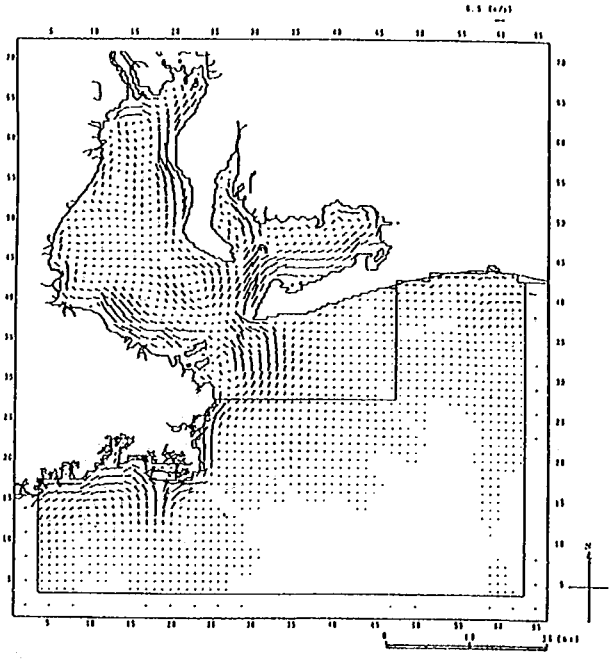


Fig.5 Velocity vector by one-layer model

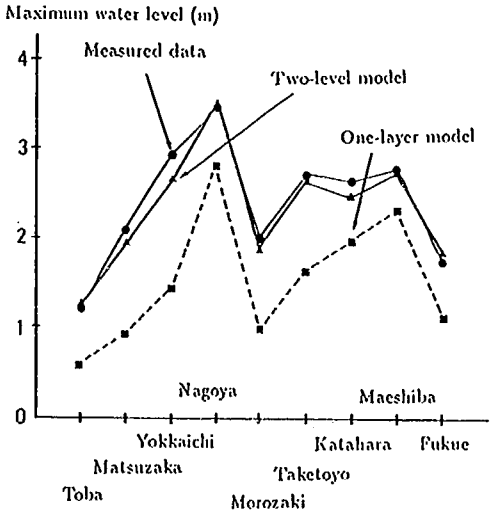


Fig.7 Comparison the maximum water height between measured data and numerical results

model.

Figure 7 shows the comparison of maximum water surface level between observed and computed ones. From the figure, we can understand that two-levels model gives an accurate result. On the other hand, one-layer model gives underestimated results.

5. Conclusion

In order to obtain an accurate result, we have to adjust emperical coefficients of wind speed and water level at bay mouth in numerical simulation by convensional one-layer model. This is the reasion why water velocity of vertical distribution approximates as constant, so that water enters into the bay is calculated

as small valume and refrected water volume toward the ocean is calculated as large. But these ajustment cannot be considered as an improvement from physical point of view for growing mechanisum of storm surge. This study presents the numerical simulation method by two-layers model as a method can be sloved this difficulty.

In addition to expression of wind driven flow, there may be many problem for numerical simulation of storm surges, so that we have to continuously investigate numerical models with high accuracy.

References

1) Murakami, K, M. Morikawa and T. Horie : Numerical simulation of storm surges by alternating direction implicit method, Technical Note of PHRI, No.529, 35p., 1985.

2) Konishi, T. : Numerical forecast of storm surges on real time basis, Oceanogr. Mag., Vol.39, Nos.1-2, 1989.

Storm Surge Assessment for Hurricanes Andrew and Iniki

by

William E. Roper[1] and Andrew W. Garcia[2]

ABSTRACT

Storm conditions at land fall are summarized for Hurricane Andrew on the Florida and Louisiana coasts and for Hurricane Iniki on the Kauai coast. Storm surge and water run up limits are presented for all three events in terms of observed high water line and tide gage readings. Field observations and instrument data are assessed to estimate storm surge conditions at time of land fall. For the Florida coast, the performance of several beach and storm protection projects are assessed and damage prevention estimates are given.

KEYWORDS: Storm surge, Hurricanes, beach erosion, storm protection, high water lines, water levels, Andrew, Iniki.

1. INTRODUCTION

Between 25 August and 11 September of 1992, hurricane Andrew and Iniki hit the southern U.S. and Hawaii with devastating force. Andrew and Iniki have been ranked as the first and third most costly hurricanes in United States history. Although the majority of damage was caused by high winds, storm surge and flooding damage was also imparted by both storms. Storm surge and flooding was a more significant factor in hurricane Iniki than Andrew. Because of the Corps of Engineers mission in storm surge protection and the design and construction of coastal and harbor entrance projects as well as beach protection systems, the Corps has a direct interest in collecting post storm data on storm surge and flooding. This information is used to improve prediction models for evacuation purposes and project design parameters, as well as assist in recovery operations, and develop damage estimates. This paper presents a summary of the storm surge information collected by the Corps of Engineers in cooperation with a number of other organizations and agencies for hurricane Andrew and Iniki.

2. ANDREWS IMPACT ON FLORIDA COAST

This section summarizes the cooperative actions of the US Army Corps of Engineers (USACE), Jacksonville District (SAJ), the Florida Department of Natural Resources (DNR), Division of Beaches and Shores, and the US Army Engineer Waterways Experiment Station's Coastal Engineering Research Center (CERC) with respect to determining the impacts of Hurricane Andrew on the beaches of Florida.

---

[1] Assistant Director, Directorate of Research and Development, Civil Works Program, Headquarters, U.S. Army Corps of Engineers, Washington, DC 20314-1000

[2] Research Oceanographer, Coastal Engineering Research Center, U.S. Army Engineer Waterways Experiment Station, Vicksburg, MS 39180-6199

Storm Summary

The Center of the eye of Hurricane Andrew made landfall near Florida City, 25 miles south of downtown Miami, at approximately 0500 on 24 August 1992 with winds at the eye wall of 145 miles per hour (mph) and gusts up to 175 mph (Figure 1). Surge distributions generated by the hurricane are presented.

Impacts to Florida's Coast

The Corps' Jacksonville District performed an aerial inspection and videotaped the coastal areas of Florida from Anna Maria island south to Marco Island on the gulf coast, and from West Palm Beach to Key Biscayne on the east coast on 25 August 1992. Ground inspections were made on 31 August 1992 in Dade and Broward Counties.

A coast of Florida (COF) study for Dade, Broward, and Palm Beach Counties. The feasibility coast sharing agreement for the study calls for post storm monitoring of the beaches in all three counties following the storm. As a part of this study effort, direct digital aerial images of Dade, Broward, and Palm Beach Counties were flown on 29 and 30 August 1992. Additional data collection efforts funded by the COF study were accomplished as work-in-kind by the Florida DNR. As apart of the COF study monitoring efforts, DNR performed on-the-ground and helicopter inspections for both coasts on 25 August 1992. DNR survey crews surveyed the beaches in Dade and Broward County at 1,000 ft intervals from each DNR survey monument. Broward County performed some of the survey work for its county. As part of the COF study effort, DNR performed controlled aerial photography of Dade and Broward Counties at a scale of 1" = 100 ft. CERC then also went to Dade County to document still water levels (SWL). The surge elevation of 16.9 ft at the Burger King Corporate Headquarters was the highest surge of record. The water mark locations were reported to DNR survey crews to determine elevation. The data from the tide gage located at Bakers Haulover Inlet, which was operational during the storm were also retrieved. An overview of storm surge records for the Biscayne Bay area is illustrated in Figure 2. The radius of maximum winds occurred 11 miles north of the eye landfall at Kings Bay with a surge level of 14.5 ft above National Geodetic Vertical Datum (NGVD). Peak storm surge at the location of eye landfall was 8.5 feet above NGVD. Aerial inspections of the Florida gulf coast was also made at the time of high tide. Waves at the time of the inspections were between 2 to 4 ft in height. In general, the beaches along the gulf coast were not impacted by the hurricane to any appreciable degree. A minor scarp of one to two feet was observed in the beach or dune along much of the area.

Hardcast data were used with the SLOSH/NOS model to calculate estimated storm surge tide heights along the western shore of Biscayne Bay for Hurricane Andrew during landfall. Figure 3 shows a preliminary comparison of these predicted levels with observed high water marks. The model analysis followed actual levels closely though consistently over predicting water levels except for the maximum location. The maximum occurred at the Burger King Corporation building where the predicted level was about .7 meters less than actual. Further studies are underway to better understand the differences between predicted and actual storm surge water levels.

The Jacksonville District was requested by Dade and Broward Counties to perform rehabilitation studies for specific shore

protection project segments under authority of Public Law 84-99. One hundred ninety five thousand dollars ($195,000) was provided to the District to accomplish this mission. There rehabilitation reports were completed by 20 October 1992. The results of the rehabilitation reports are summarized as follows:

a. Key Biscayne. The shore protection projects for Key Biscayne were constructed to an elevation of +7 ft relative to mean low water (MLW). Surge levels for the island were reported up to 9.3 ft NGVD. The island was overtopped by the storm surge. The beach appeared unaffected.

b. Virginia Key. The shore protection project for Virginia Key was constructed to an elevation of +6 ft relative to MLW. Surge levels for the island to the south (Key Biscayne) were reported at 9.3 ft NGVD. The island was overtopped by the storm surge. The beach appears unaffected.

c. Fisher Island. A privately constructed shore protection project was constructed and consists of several nearshore breakwaters with an arragonite beach fill. The structures appeared intact based on aerial inspections, but the arragonite beach fill was somewhat eroded.

d. Dade County Hurricane and Storm Damage Reduction Project. The 9.3 mile project from Government Cut to Bakers Haulover Inlet was generally in good condition. The project is designed to protect against a hurricane with a central pressure of 27.5 inches (931 mb), a radius of maximum winds of 37.5 miles, a forward speed of 13 mph, and maximum overwater wind speed of 104 mph. These parameters result in a design SWL of 8.9 ft. This tide, combined with expected wave run-up, resulted in a design dune height of 11.5 ft for a no-overtopping condition. the dune appeared to be intact along the entire project. The debris line was generally at the seaward foot of the dune.

e. Haulover Park. The portion of the Dade County project is 1.2 miles in length and is located north of Bakers Haulover Inlet, and was generally in good condition. he beaches appeared to be intact along the length of the park. The debris line was generally at the seaward edge of the project, indicating some overtopping.

f. Dade County North of Haulover (Sunny Isles). This portion of the Dade County project is 2.5 miles in length and is located north of Bakers Haulover, and ws generally in good condition. The beaches appears to be intact in this area. The debris line was generally at the berm elevation of the project.

g. Broward County - Hillsboro Inlet to Port Everglades (Segment II Pompano, Lauderdale by the Sea). Over the 5.2 miles of constructed project, 178,000 cy yds was eroded from the upper beach face. Accretion $143,000 cu yds was measured by MLW to -4 ft, indicated a net loss beyond 14 ft of 35,000 cu yds. The loss is equivalent to a net change of -0.7 cu yds per ft of shoreline.

h. Broward County - Port Everglades to the South County Line (Segment III - J. U. Lloyd, Hollywood and Hallendale). Over the 6.8 miles of constructed project, 163,000 cu yds was eroded from the upper beach face. Accretion of 95,000 cu yds was measured by MLW to -4 ft, indicating a net loss beyond -4 ft of 68,000 cu yds. The loss is equivalent to a net change of -1.9 cu yds per ft of shoreline.

Damages Prevented

The Federal shore protection projects

prevented an estimated $24.6 million in damage during Hurricane Andrew. Their projects were located in both Broward and Dade County, the shore protection projects prevented $5 million in damages for the Hollywood/Hallendale project segment. The Sunny Isles portion of Dade County was spared $7.6 million in damages. The coastal areas south of Bakers Haulover Inlet to Government Cut which includes Bal Harbour, Surfside and Miami Beach would have experienced an additional $12 million in damages had the Dade County hurricane and storm damage reduction project not been in place.

3. ANDREWS IMPACT ON LOUISIANA

After clobbering southern Florida as a category 4 Hurricane, Andrew proceeded westward into the Gulf of mexico with somewhat diminished strength. He raced across the gulf on a nearly straight track moving to the west northwest at about 15 knots and made land fall along the Louisiana coast as a category 3 hurricane.

Storm Summary

The National Weather Service predicted immense damages in southern Louisiana and high storm surges. Fortunately for those of living in metropolitan New Orleans area, Andrew tracked 100 miles west of New Orleans before turning northward over Atchafalaya Bay and moving inland west of Morgan City, LA (Figure 1). This track caused the maximum hurricane winds of Andrew to blow offshore as the eye approached and alongshore as the eye passed. Hours after the eye passed a point on the coast, the trailing winds blew toward the land.

Impact to the Louisiana Coast

The National Weather Service was correct about the wind damage which Andrew would cause, but apparently overstated the storm surge. Winds and tornadoes associated with Andrew damaged homes, businesses, and government facilities as well as doing massive damage to crops, trees, and the ecosystem. The moderate storm surge along the Louisiana coast eroded hundreds of acres of barrier island, uprooted and destroyed thousands of acres of marsh and killed millions of fish.

No Corps of Engineers flood control project was overtopped by the storm surge brought ashore by Hurricane Andrew. Some minor damage was experienced along the Bayou Sale' levee southwest of Morgan City, LA. At Grand Isle, LA the beach and dune performed very well. Less than 20 percent of the length of the project has been damaged and the worst erosion is only half way through the sand dune. No Corps project was subjected to stages that even came close to design conditions. Minor wind damage was experienced at several Corps of Engineers Navigation Projects.

Comparing state hydrographs with Hurricane Andrew's track shows good agreement for the water level response we expected during this storm. The open coast storm surge caused backwater in the Mississippi and Atchafalaya Rivers.

4. HURRICANE INIKI'S IMPACT ON KAUAI

The coastal areas of the Hawaiian Islands are vulnerable to infrequent but potentially sever storm wave attack as a result of North Pacific hurricanes passing near or over the islands. Hurricane Iniki generated wind and wave action over the shallow reefs of Kauai, creating high storm surge levels which flooded

inland areas and contributed significantly to shoreline property damage. Shoreline properties along the southern coast (Poipu to Kekaha) of Kauai suffered extensive damage due to high coastal flood levels.

Storm Summary

Hurricane Iniki was the strongest and most destructive hurricane to affect the Hawaiian Islands this century. It was a small but relatively intense hurricane as it made landfall during the afternoon of 11 September 1992 near Port Allen on the south coast of Kauai. The track of Iniki on 11 September 1992 is shown in Figure 4. During the 24 hours prior to landfall on Kauai, Iniki came under the influence of a large extra-tropical system centered near 40 degrees north latitude, 165 degrees west longitude. The circulation of this system caused Iniki to accelerate rapidly toward the north during the 12 hours prior to landfall. Based upon best track positions, the forward speed of Iniki increased from about 12 mph to 25 mph during this period.

As Iniki passed over the island of Kauai, the highest sustained wind recorded was 97 mph at Lihue with estimates to 130 mph and gusts to 160 mph. Minimum central surface pressure was estimated at 945 millibars (mb). The topography of Kauai is quite mountainous with several peaks exceeding 4000 ft and two exceeding 5000 ft in elevation. Steep valley slopes and sharp peaks undoubtedly produced localized areas of very high winds. Damage estimates are expected to exceed 1.8 billion dollars, making Iniki the third most costly hurricane in the United States history behind Andrew of 1992 and Hugo of 1989. The only other hurricane to make landfall on a Hawaiian Island this century was Dot of August 1959, also on Kauai Hurricane Iwa of November 1992 affected Kauai, but the eye passed to the west of the island. Moreover, both Dot and Iwa weakened and were minimal hurricanes as they approached Kauai.

Impacts to Kauai's Coast

Although coastal damage occurred on the southwest and east shores of the island, the most severe coastal effects were along the southwest shore to the east of Port Allen. A general map of the island of Kauai is shown in Figure 5. Figure 6 shows hourly values of sustained wind speed and direction as obtained at the NOAA National Ocean Service (NOS) Next Generation tide station at Port Allen. Even though the eye of Iniki passed close to Port Allen, the maximum wind speed recorded was 58 mph (25.8 m/s), less than half the estimated peak of 130 mph. The low recorded speed at Port Allen is certainly due in part to the instrument system sampling only two minutes each hour. Because Iniki was moving at over 20 mph as it made landfall, passage of the eye probably occurred in about half and hour; continuous sampling would have more accurately depicted the wind history. Similarly, the barograph presented in Figure 7 shows a minimum surface pressure of approximately 962 mb, substantial above the estimated minimum of 945 mb. Again, the recorded values are undoubtedly affected by the sampling scheme of the instruments.

Wave Effects

No near-shore wave data were acquired during Iniki's passage over Kauai. The nearest wave measurements were acquire at the NOAA National Data Buoy Center (NDBC) station 51003 located at 19.3 degrees north latitude, 160.9 degrees west longitude, or approximately 195 miles south-southwest of Port Allen, Kauai. The greatest significant wave height observed at this location during

Iniki's passages was approximately 18 feet (5.5m) with a dominant period of about 14 seconds. Figure 8 presents the sustained wind speed, significant wave height, and dominant wave period acquired at station 51003.

A second NDBC station, 51002, was located at 17.2 degrees north latitude, 157.8 degrees west longitude, or approximately 345 miles south-southeast of Port Allen. The greatest significant wave height of 19.5 feet (6m), was just slightly higher than observed at station 51003. Maximum sustained windspeeds were 36 mph and 44 mph at stations 51002 and 51003, respectively. Figure 9 presents the sustained wind speed and significant wave height acquired at station 51002.

The southwest shore of Kauai is predominantly rocky with only limited stretches of beach. Estimates of wave heights along this reach of shore ranged from about 10 ft to 30 ft and are based largely upon eyewitness accounts. At the mouth of Waikomo Stream (just west of Poipu) there is a channel through the reef into the open ocean. Debris lines at elevations up to 22 feet above Mean Lower Low Water (MLLW) were present a short distance upstream from the stream mouth. Eye witnesses reported that waves 10 to 15 ft high moved into the stream mouth from the open ocean during the peak of the hurricane.

Just west of Waikomo Stream, severe wave action was evidenced by large rocks (2-3 ft diameter) being moved into dwellings located landward of the coast road. Slightly farther to the west along Lawai Road, all that remained of several homes were the foundation slabs. These homes were located on the seaward side of the coast road with direct exposure to the open ocean. No significant debris from the remains of these homes was founded in the immediate vicinity and no eyewitnesses were available that could provide information on wave heights. At Port Allen there was some wave damage to the head and seaward face of the breakwater. At Kekaha, near the southwest end of the island, there was substantial overwash with sand being moved from the beach and deposited on the shore road to depths of 1 to 2 feet. Eyewitnesses in the vicinity estimated the wave heights at about 10 ft. On the west side of the island, near the Barking Sands Pacific Missile Test Facility, there were no significant signs of wave effects.

Inundation Effects

Inundation effects were determined by water-level data obtained at NOS tide gages and high-water marks recovered shortly after Iniki's passage. As with the wave effects, the greatest heights were along the southwest coast of Kauai although there was evidence of significant inundation along the east shore of the island as well. The highest inundation levels were observed in the Poipu vicinity and diminished with distance in both east and west directions. Figure 10 presents the elevations as a function of distance along the coast starting near Kekaha. Along most of the shoreline, the elevations were in the interval of 10 to 15 ft above MLLW. At Poipu, however, there were several marks at elevations greater than 15 ft MLLW, with the highest (a debris line) at 22.5 ft above MLLW. The highest still-water level was at 16.2 ft MLLW elevation. A debris line at elevation 13.6 ft MLLW at the mouth of the Wailua River indicated substantial inundation effects along the eastern shore of Kauai.

The elevation and distance from the shore of debris lines at Polpu were consistent with the elevation of water marks recovered in the vicinity. The greater elevation of water

makers at Poipu as compared with adjacent stretches of coast are likely due to the maximum surface winds at landfall occurring in this vicinity. Poipu is approximately 10 miles east of Port Allen and the eye of Iniki is passed just to the west of Port Allen. This indicates a radius of maximum winds (RMW) of about 12 to 15 miles, a relatively small value for the RMW but consistent with the small eye diameter depicted in the satellite imagery.

For comparison purposes, Figure 10 also shows the profile of inundation elevations acquired following passage of Hurricane Iwa of 1982 taken from the Federal Emergency Management Agency's Flood Insurance Rate Map. In general, the surge elevations associated with Iwa are comparable to those of Iniki except in the Poipu vicinity. At Poipu, the envelope of surge elevations is 5 to 10 ft higher for Iniki than for Iwa, a consequence of the higher windspeeds along this reach of coastline.

The NOS operates two tide stations on Kauai, one at Port Allen and the second at Nawiliwili Harbor. Figure 7 shows the hydrograph acquired at Port Allen during Iniki. A record water level of 6.2 ft above MLLW as observed at approximately 1530 local time. The predicted high tide at Port Allen was 1.5 ft above MLLW at 1506 local time, vary close to the time of Iniki landfall. The storm surge (total water level minus the predicted tide) was therefore about 4.7 ft. Figure 11 presents the NOS hydrograph acquired at Nawiliwili where a record high water level of 5.8 ft above MLLW was observed. The predicted high tide at Nawiliwili was 1.7 ft above MLLW at 1515.

The peak water-level values observed at the tide gages were substantially lower than high-water marks acquired along open reaches of coastline. Several factors can contribute to these differences. First, both tide gages were located in harbors protected by breakwaters where wave action presumably was less. Second, both gages were located on piers extending into the harbors away from the shoreline, therefore removed from wave run-up effects. Third, both gages were equipped with filters to minimize wave effects on measurements. In short, the tide gages were measuring what they were designed to measure, the still water level minimally affected by waves. Where high-water marks were located in physical settings similar to those of the tide gages, as at Nawiliwili Harbor, the elevations were comparable.

5. FUTURE STUDIES

The use of hydrodynamic computer models to determine total storm surge elevations and inundation, normally require calibration and verification with observed events. Previous hurricane studies conducted in Hawaii used data obtained from Hurricane Iwa in 1982. The high-water marks data left by Hurricane Iniki will be used to verify model results and enable future hurricane studies to accurately predict surge levels for evacuation and planning purposes.

6. REFERENCES

1. Preliminary Report, HURRICANE INIKI, September 5-13, 1992 National Weather Service, NOAA, in press

2. Haraguchi, Paul; "Hurricanes in Hawaii", Special Report prepared for Pacific Ocean Division, U.S. Army Corps of Engineers, March 1984

3. Schmidt, David V., and Garcia, Andrew W., "Impacts of Hurricane Andrew on the

Beaches of Florida", Coastal Engineering Research Board Proceedings, October 29, 1992

4. Combe, Adrian J., "Hurricane Andrew '92 in Louisiana", Coastal Engineering Research Board Proceedings, October 29, 1992.

5. Garcia, Andrew W., "Coastal Effects of Hurricane Iniki on Kauai, Hawaii", Proceedings, National Conference on Beach Preservation Technology, St. Petersburg, Florida, February 1993.

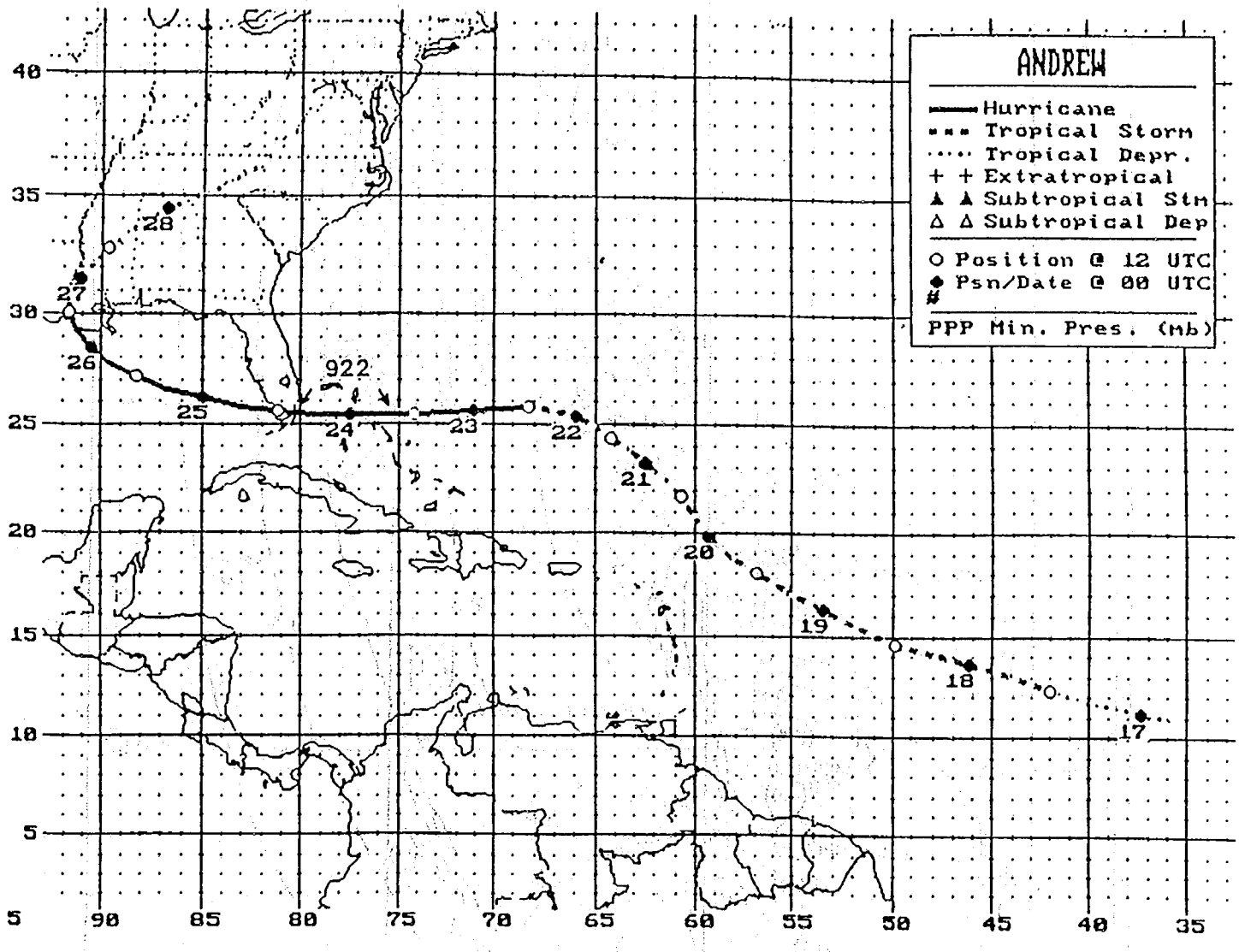


Figure 1. Best track positions for Hurricane Andrew

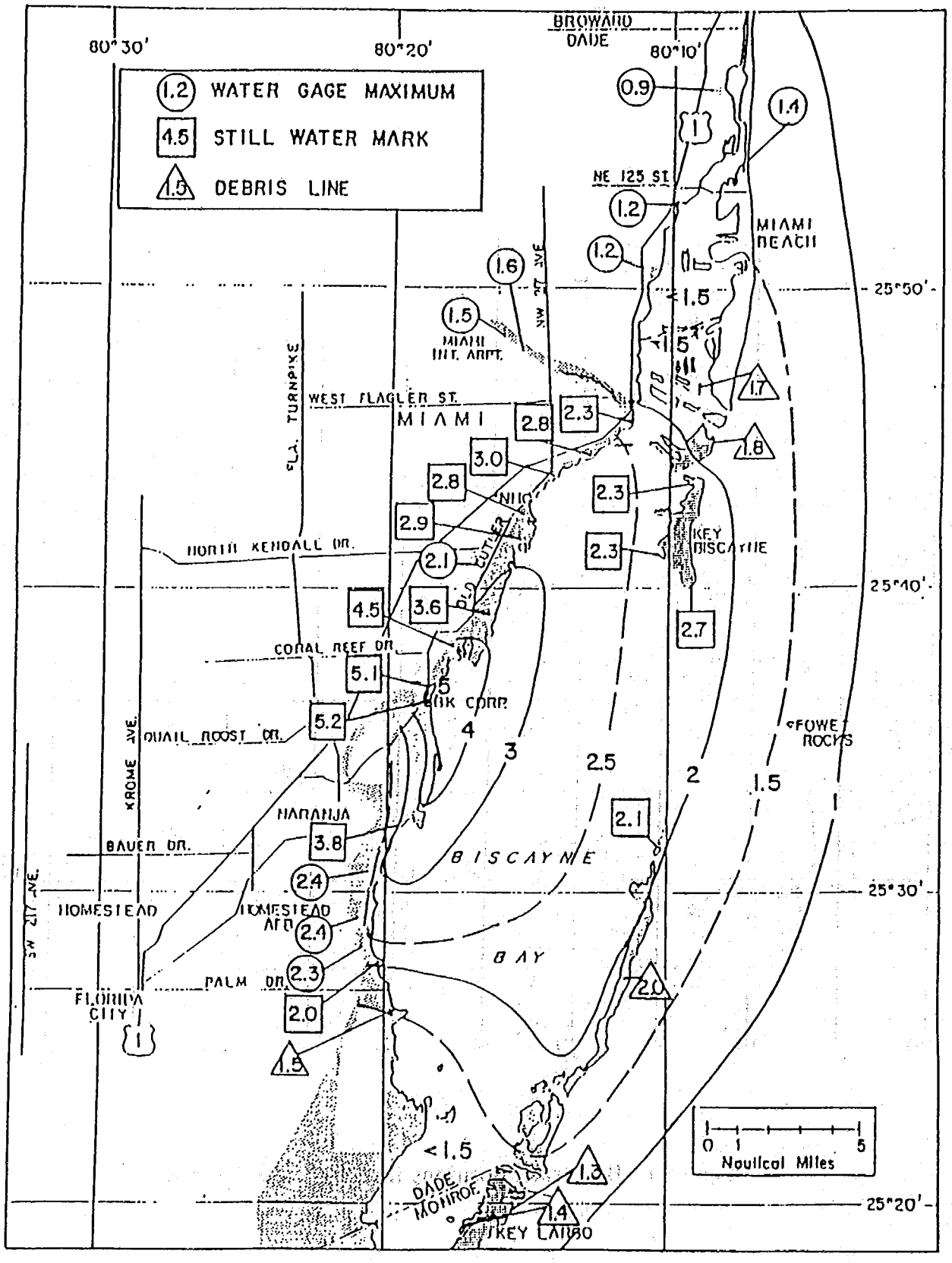


Figure 2. Analysis and representative observations of the maximum storm tide during Hurricane Andrew's landfall in Florida, labelled in meters above 1929 mean sea level (1 meter = 3.28 ft). Shading indicates inland inundation.

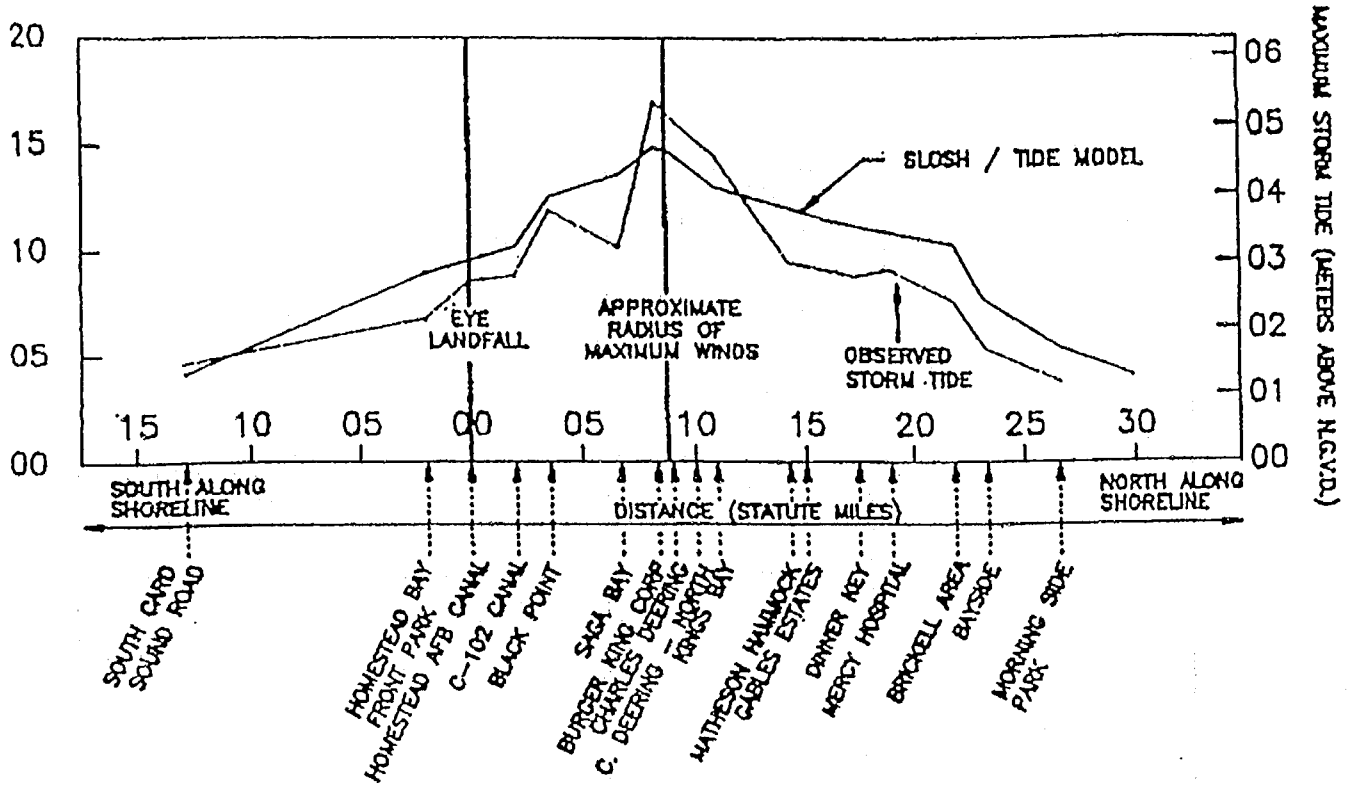


Figure 3. Comparison of Profiles of Observed versus Slosh/NOS Model Calculated Storm Tide Heights along Western Shore of Biscayne Bay for Hurricane Andrew August 24, 1992. (Heights in Feet above NGVD- National Geodetic Vertical Datum - Zero Elevation - i.e. Mean Sea Level of 1929)

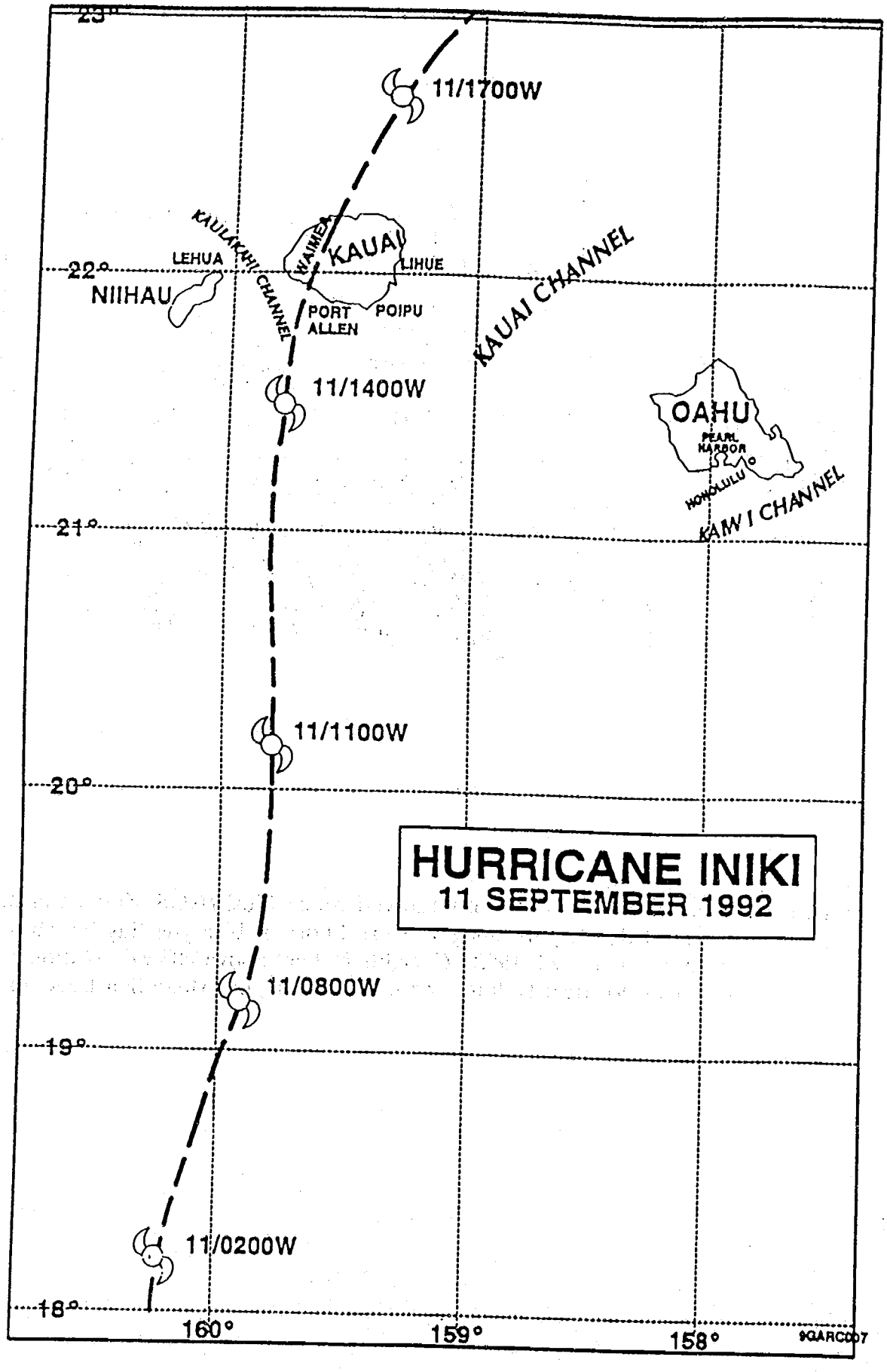


Figure 4. The track of Hurricane Iniki, 11 September 1992

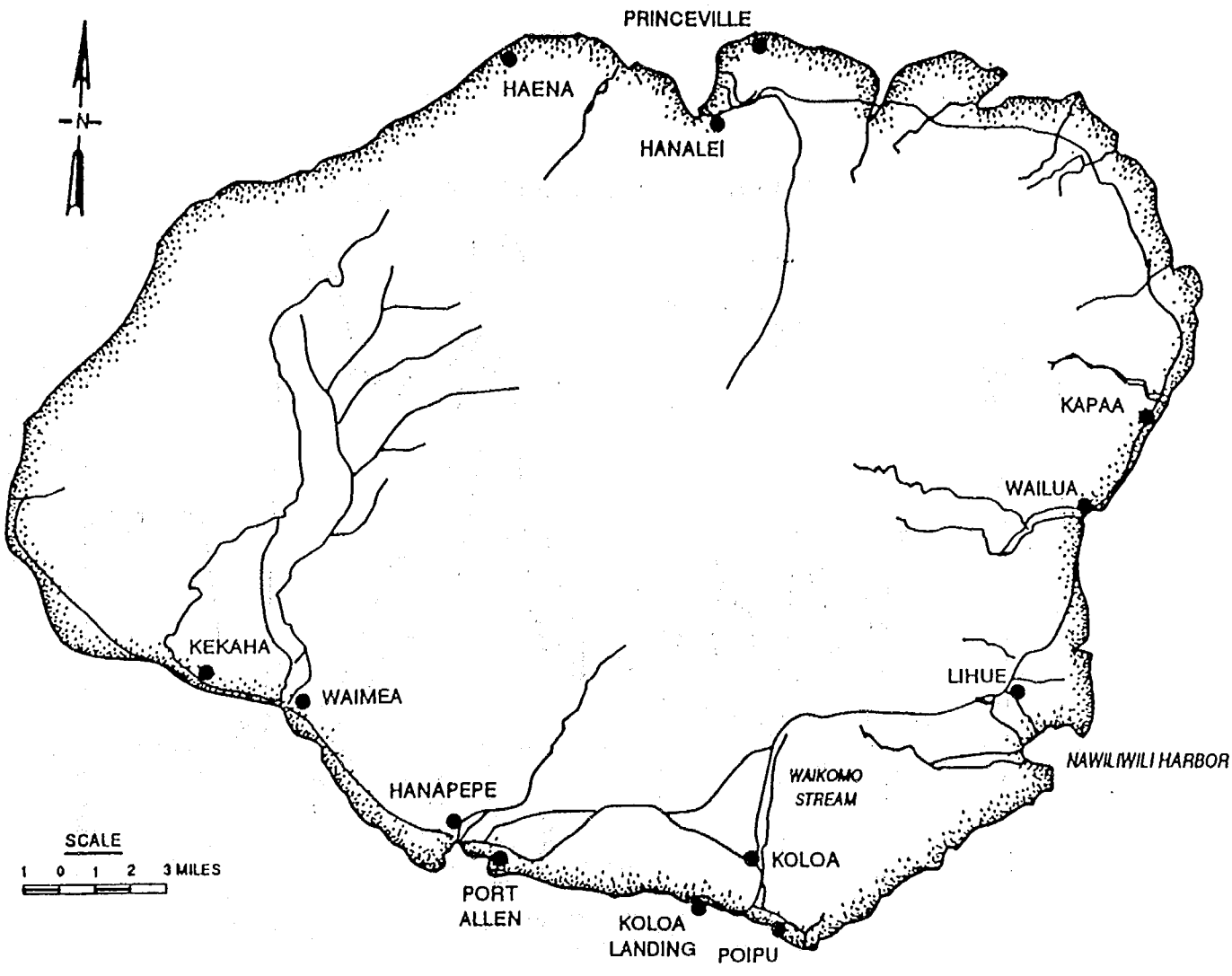


Figure 5. ISLAND OF KAUAI

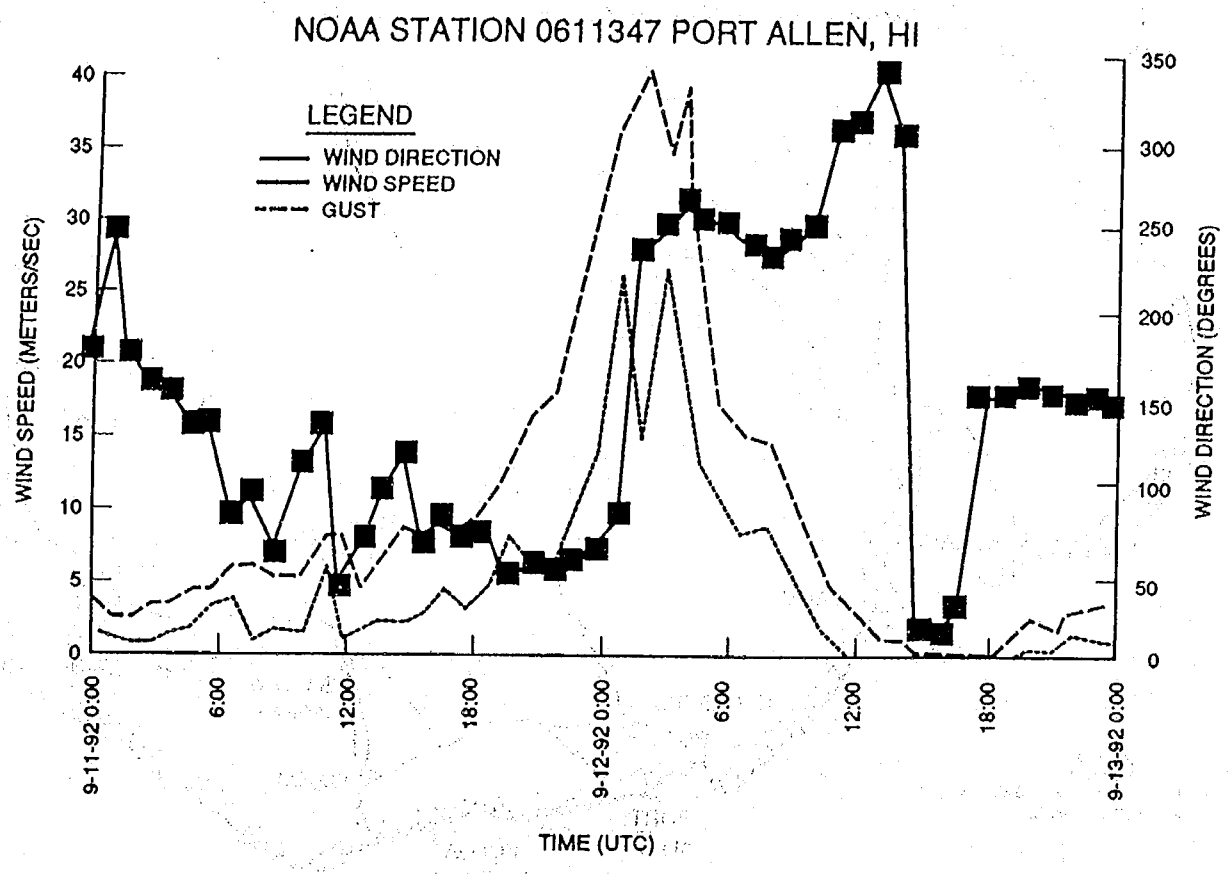


Figure 6. Sustained wind speed, wind direction, and gusts recorded during Hurricane Iniki at NOS station 0611347 Port Allen, Kauai

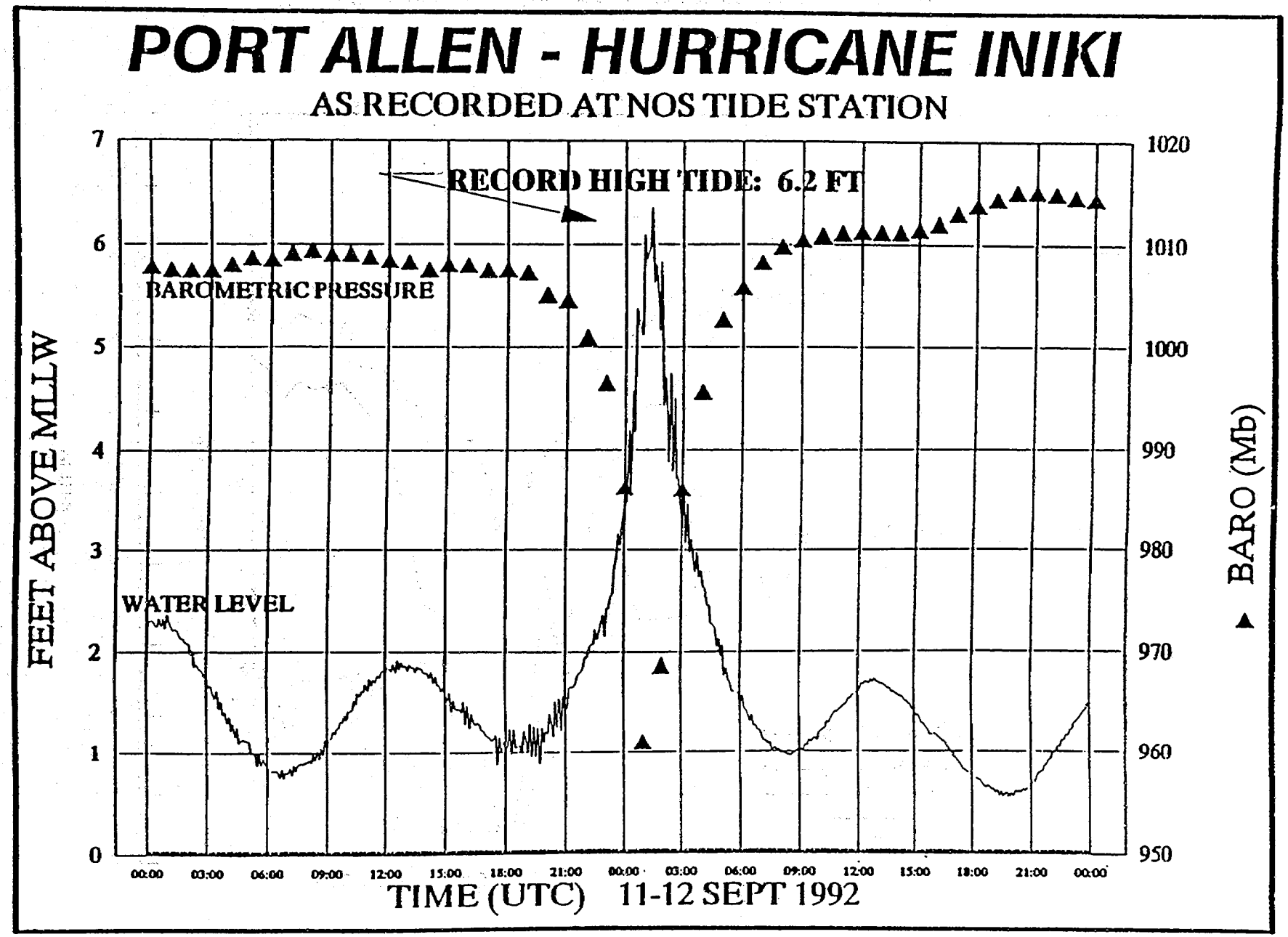


Figure 7. Water level and barometic pressure recorded during Hurricane Iniki at NOS tide station Port Allen, Kauai

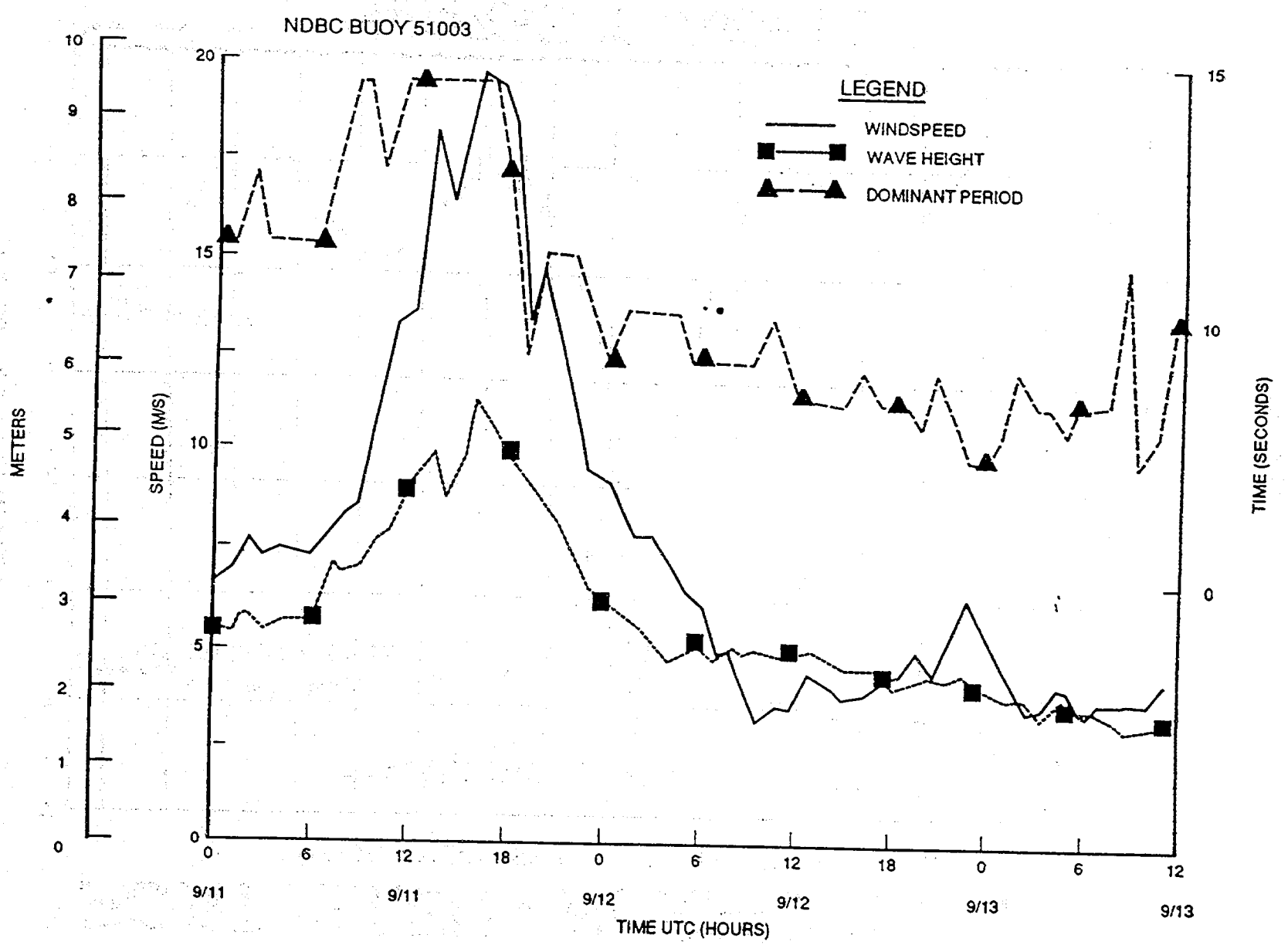


Figure 8. Windspeed, significant wave height, and dominant wave period recorded during Hurricane Iniki at NDBC station 51003

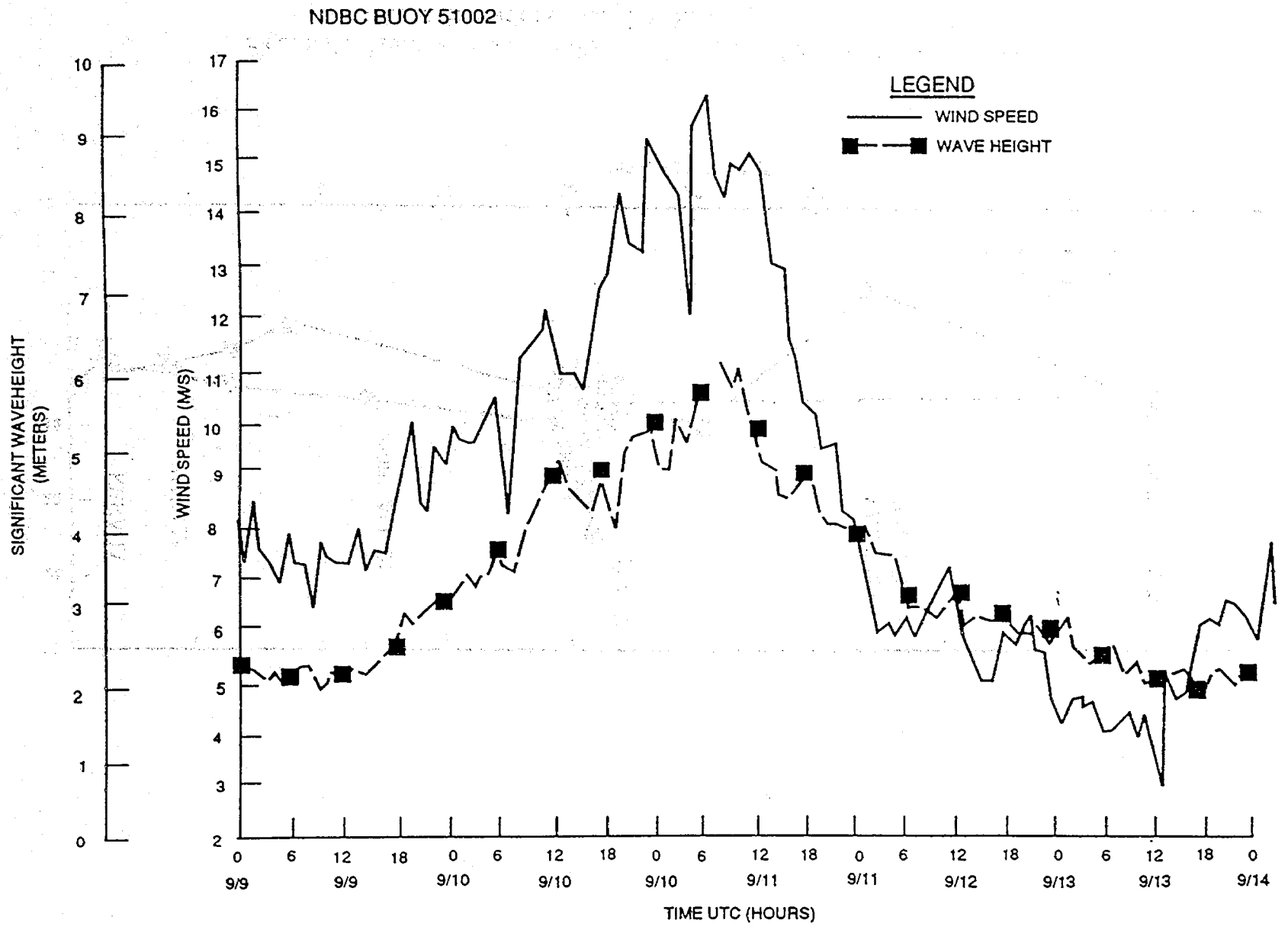


Figure 9. Windspeed and significant wave height recorded during Hurricane Iniki at NDBC station 51002

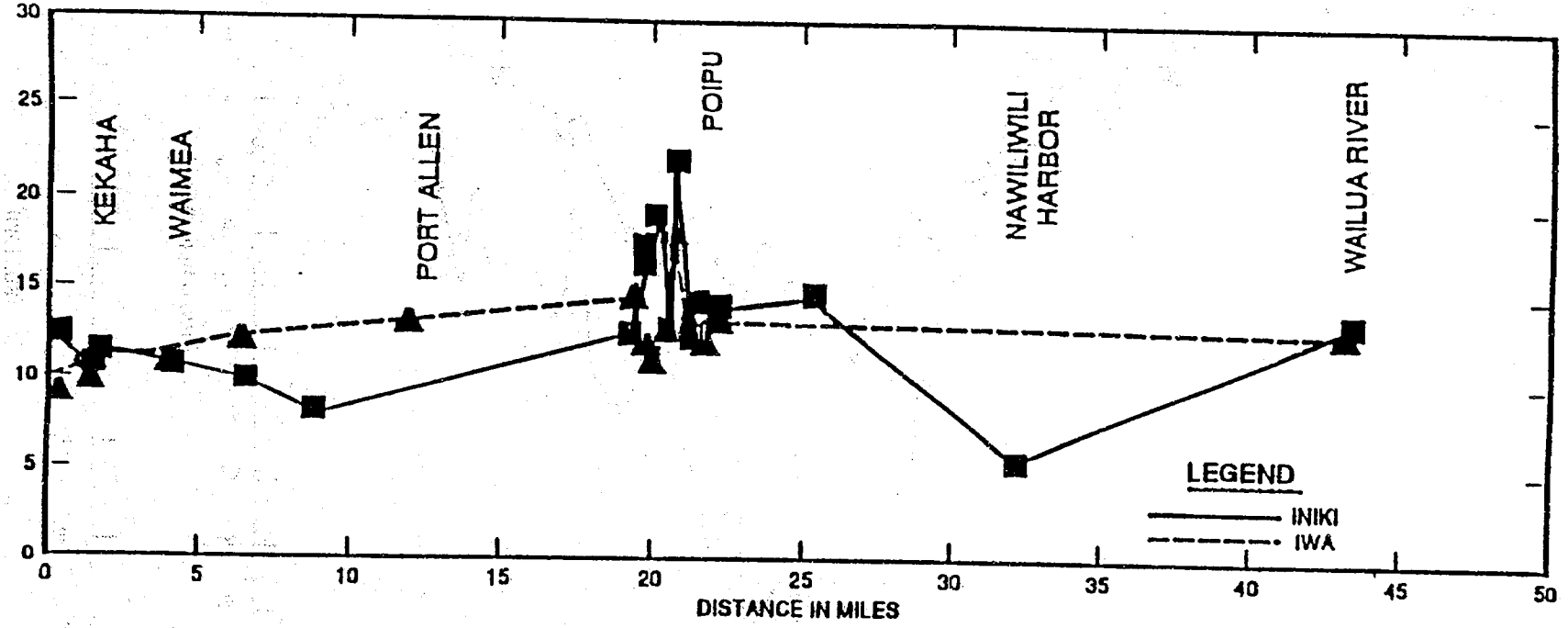


Figure 10. Hurricane Iniki (1992) and Hurricane Iwa (1982) comparison of Flood Elevations, Island of Kauai

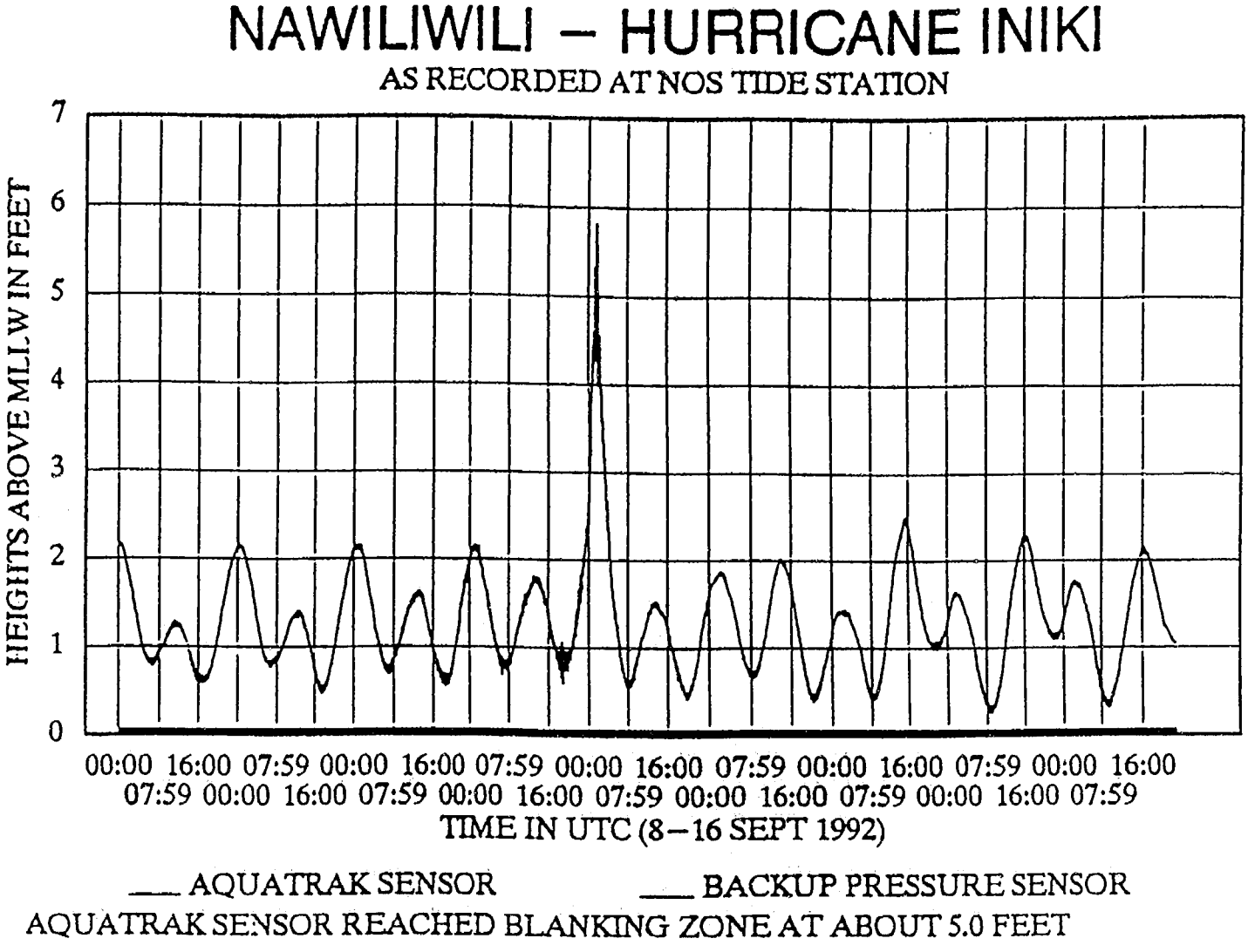


Figure 11. Water level recorded during Hurricane Iniki at NOS tide station Nawiliwili Harbor, Kauai

Theme 5

General Concept of Japan Connection Design Manual for Precast Seismic Structural Systems

by

Fumio Watanabe[1], Hitoshi Shiohara[2] and Sinsuke Nakata[3]

Abstract

Since 1989, the Japanese Connection Task Group has been engaged in PRESSS. At the first PRESSS meeting in San Diego, the classification of connections, typical examples of equivalent monolithic connections and connection elements to be designed were discussed. After that, the Connection Task Group again classified the precast concrete connections into several connection labels according to performance criteria. Classified labels were reported at the second PRESSS meeting in Tsukuba. In addition to these works, the Connection Task Group prepared the first draft of connection data base (connection book) of Japan side and it was submitted to the Tsukuba meeting. The purpose of it was the mutual exchange of information on precast connection details used in Japan and U.S.A. The Connection Task Group of Japan side have been working to prepare the Design Manual for Connection Details. However, it could not be completed due to several difficulties such as delay of tests and tough discussions. The Design Manual for Connection Details is still under examination so that the contents in this report should be treated as tentative until this work has been carried out.

1. Introduction

After the first PRESSS meeting in San Diego, the Connection Task Group had started the preparation of connection data base (connection book) which is to include practically used or experimentally verified precast connection systems in Japan. The purpose of it was the mutual exchange of information on precast connection details used in Japan and U.S.A. The first draft of connection data base (connection book) of Japan side was then submitted to the second PRESSS meeting in Tsukuba.

On the other hand, those connection systems in the connection data base are required to meet the design criteria such as stiffness, strength, ductility, durability, fire resistance and so on. This means that each connection system must be evaluated experimentally or theoretically whether it satisfies the design criteria or not. From such viewpoint, the Connection Task Group again classified the precast concrete connections into connection labels in accordance with performance criteria. Following 6 labels were listed up as the equivalent monolithic connections.

- Moment Resisting Ductile Connection
- Moment Resisting Non-ductile Connection
- Diaphragm Connection
- Composite Member Connection
- Wall Connection
- Non-earthquake Resistant Connection

For each connection label, the required items to meet the design criteria were discussed at the second PRESSS meeting in Tsukuba 1991.

Since Tsukuba meeting, the Connection Task Group of Japan side have been working to prepare the Design Manual for Connection Details. However, it could not be completed due to several difficulties such as delay of tests and tough

1) Associate Professor, Department of Architectural Engineering, Faculty of Engineering, Kyoto University
2) Senior Researcher, Building Research Institute of Japan, Tatehara, Tsukuba, Ibaragi-ken, Japan
3) Director, Department of Testing and Evaluation, building Research Institute

discussions. Several problems to be solved still remain so that only the outline of the Design Manual for Connection Details is introduced in this report.

Main forces of discussion are placed on equivalent monolithic connections because other types of connections have not yet been discussed in the Connection Task Group.

2 Connection Design Manual

In chapter 1, the purpose of this manual, contents, history, present condition and future development of precast concrete in Japan are described.

Main purposes of this manual are to give consulting engineers 1) fundamental concept for the design of connection in precast seismic structural system, 2) practical design method of equivalent monolithic connection. Definition of equivalent monolithic connection is described in chapter 3.

This Design Manual consists of seven chapters as 1) Precast concrete, 2) General principle of connection design, 3) Demand to connection performance, 4) Modeling of connection, 5) Strength and deformation of connection element, 6) Design example and 7) Drawing of connection details and construction works.

Brief history, present condition and future development in Japan were reported by Dr. Yoshizaki (Taisei Cooperation) at the first PRESSS meeting in San Diego. His report will be adopted in this chapter.

3 General principle of connection design

In the chapter 2 , the general principle for the design of connection in precast system are described.

3.1 Loading effects

An appropriate load combination is chosen for the structural design of a precast system as same as for in monolithic system.

For service load condition:

- Allowable stress design (WSD-S)
  D+L
  Commonly used for reinforced concrete

- Ultimate strength design (USD-S)
  $\alpha D+\beta L$
  Not common excepting prestressed concrete

For earthquake load condition:

- Allowable stress design (WSD-E)
  $D+L+E_1$
  First phase seismic design

- Ultimate strength design (USD-E)
  $D+L+E_2$
  AIJ Design Guidelines

- Capacity design (CPD-E)
  $D+L+E_3$
  Second phase seismic design

D=dead load, L=live load, a and b =load factor, E_1=design seismic load for moderate earthquakes which corresponds to base shear coefficient of 0.2, E_2=design seismic load for ultimate strength design specified in the AIJ Design Guidelines, which corresponds to base shear coefficient of 0.25, and E_3=required lateral strength which depends on the ductility of a building. For ductile frames, E_3 corresponds to base shear coefficient of 0.30.

If necessary, wind loading and/or snow loading are to be considered in addition to above load combinations. Temporary loading during erection is also considered.

For dynamic response analysis, earthquake waves recorded in the past and/or artificial waves are used.

3.2 Design moment and/or forces for connections and precast elements

Design moment and/or forces for connections and precast elements are obtained from structural analysis for the load combination given in Chapter 2.

In allowable stress design (WSD-S) for service load condition, ultimate strength design (USD-S) for service load condition and allowable stress design for moderate earthquake load (WSD-E), linear frame analysis is applied based on full section stiffness regardless of cracking.

In ultimate strength design (USD-E, in accordance with AIJ Design Guidelines), Linear frame analysis is carried out to obtain the design moment for intended plastic hinge regions based on reduced section stiffness due to cracking, and the reinforcement arrangement in plastic hinge region is decided. Non-linear frame analysis or equivalent ones is then carried out to obtain member moment and forces at collapse mechanism, where over strength at plastic hinge regions should be considered. Obtained moment and forces are increased to take into account the effects of higher mode of vibration and two way frame action.

In capacity design (CPD-E, second phase seismic design), non-linear frame analysis or equivalent ones is carried out on a building designed according to (WSD-E, First phase seismic design) to verify the required lateral strength at each story of a building.

In the structural analysis, floor slab is generally assumed to behave as a rigid diaphragm so that it should be designed to have enough rigidity.

When a precast building is designed by allowable stress design for earthquake loading (WSD-E), each connection and precast element should be designed to have reserve strength and ductility in certain extent. Because the ultimate limit state of connections and precast elements which might occur during an earthquake is not clear.

If the connection element has a possibility to give higher strength of the connection than predicted in design, it should be taken into account. When a large and stiff joint of longitudinal reinforcement is arranged in hinge region or near hinge region, for example, maximum moment at hinge region might be larger than the predicted over strength due to large strain hardening.

Equilibrium torsion of main beams due to loading from secondary beams and slabs should be considered. Compatibility torsion is not necessary to consider.

4 Connection performance criteria

4.1 Strength

Each connection and precast element should have enough strength to withstand design moment and forces calculated according to clause 2.2.2 under given load combination. When a precast building is designed based on ultimate strength design concept (USD-E) or capacity design concept (CPD-E), connections at critical portion (potential plastic hinge region) should reach their yield strength within the expected deflection situation of the building under given load combination.

In the design for service load condition, resisting moment and forces at connection should reach the design moment and forces within the expected deflection situation

4.2 Restoring force characteristics

Structural performance of precast connection should be evaluated based on the restoring force characteristics of a building, not based on the connection itself.

In most precast systems, some slip deformation in connection are unavoidable. If additional deflection δ_s due to slip at connection element was expected in building response, the extent of it should be restricted within the allowable limit. This concept is illustrated in figures 1-1 and 1-2 schematically. Figure 1-1 indicates elastic inter story drift responses of precast system and equivalent monolithic system in same load situation, respectively. Figure1-2 also indicates inelastic responses for both systems in same deflection situation. The ratio of ds to dt should be within an certain limit to assure that the maximum inter story drift angle of precast system is comparable to the value specified for monolithic system. The maximum allowable value of ds/dt is determined from the dynamic response analysis on the precast system which has the restoring force characteristics as shown in figures 1-1.b) and 1-2.b). The ratio of δ_s/δ_t in precast system is evaluated in terms of inter story drift angle of a beam column sub-assemblage subtracted from a building as shown in figure 2. For the estimation of δ_s and δ_t, both

analytical approach (mathematical modeling of precast system) and experimental approach are available.

On the other hand, the member to member connection in plastic hinge region should show ductile behavior without significant decrease in load carrying capacity until a precast system reaches the intended collapse mechanism or the maximum deflection situation predicted in the design.

Plural number of connections usually exist in a member so that the contribution of all connections to restoring force characteristics has to be taken into account when evaluating the value of ds.

4.3 Redundancy in stress transfer mechanism

If there was a possibility of brittle failure of connection due to accidentally higher load than design load, a member should sustain at least vertical dead and live load by another stress transfer mechanism even if the primary stress transfer mechanism disappears.

4.4 Serviceability

Serviceability under service load condition should be assured as same as in monolithic system. Deflection, crack width , strain of concrete and so on are to be estimated.

During a moderate earthquake, precast building should response in elastic manner and maximum inter story drift angle has to be comparable to the value specified for monolithic system.

4.5 Miscellaneous

Durability and fire resistance have to be assured for precast system as same as for monolithic system.

Durability: Same specifications to monolithic system are applied for crack width, concrete cover thickness, corrosion protection of metallic devices and so on. :

Fire resistance: Same specifications to monolithic system are applied for concrete cover thickness and surface protection of metallic devices. Especially, mechanical properties of connection materials against high temperature are to be checked, i.e., plastic and rubber materials.

Stability of a precast system during erection is also checked.

5 Manufacturing

In New Zealand guidelines for precast construction, three different types of tolerances are described, i.e., product tolerance, erection tolerance and interface tolerance. In equivalent monolithic system, the effect of product tolerance to the structural performance of connection may be negligible after cast-in-situ concrete has hardened. However, when the design of connection is largely influenced by the value of a small dimension which is sensitive to variation caused by tolerance, then tolerance should be allowed for the design. Such situation may occur during erection and construction even in equivalent monolithic system.

6 Demand to connection performance

In this chapter, required connection performances are described. Connections in precast construction are classified into equivalent monolithic connection, dry connection and others.

In this design manual, equivalent monolithic connection is defined as follows.

i) Design moment and/or forces for connections and precast elements can be predicted by the structural analysis generally used for in monolithic system.

Connection should have enough stiffness to assure this requirement.

ii) Connections are strong enough to transfer the design moment and/or forces.

If the connection failure or yielding occurred in early stage of loading, unexpected failure or yielding mode of precast system will take place. To avoid such change of structural performance of precast system, connections should have at least

comparable strength to equivalent monolithic system.

iii) Serviceability, durability and fire resistance are as same as in monolithic system.

Specified conditions for monolithic system are also applied to precast system. Items to be considered are deflection, crack width, creep and shrinkage of concrete and mortar, concrete cover thickness, corrosion protection, fire protection, mechanical properties of connection materials under high temperature

iv) Structural performance of precast system under earthquake loading is comparable to that of monolithic system.

Precast system should have at least comparable deformation capability and same collapse mechanism to equivalent monolithic system for lateral loading. Maximum inter story drift angle of precast system during an earthquake should be within the limit specified for monolithic system even if some slip deformation take place at connection interface. Allowable limit of slip deformation is given in terms of the ratio of the additional inter story drift angle due to slip to the total inter story drift angle as described for Chapter 2.

Equivalent monolithic connection is classified into two categories of ductile connection and strong connection.

6.1 Ductile connection

When a member to member connection is situated at the critical portion in a precast system and the formation of plastic hinge is expected, it should be designed as a ductile connection. Requirements for ductile connections are as follows.

Cracking load:

Flexural cracking in precast system may occur in early stage of loading at the interface between precast element and cast-in-situ concrete so that the stiffness of precast system near cracking load is slightly smaller than that of monolithic system. However, this stiffness reduction seems to have no any significant effect on the structural performance of a precast system. In figure 3, load deflection curves of monolithic and precast systems are illustrated.

Flexural strength:

Bending moment at connection must attain both its yield strength and over strength in post yield range of deformation without any premature brittle failure. In composite members, shear stress transfer across the connection interface should be assured

Stiffness at yielding:

Tangential stiffness of precast system at yielding should be comparable to monolithic system as shown in figure 3.

Prevention of brittle failure:

Brittle failure such as shear failure and bond splitting failure should be avoided both in connection and precast element.

Limitation of slip deformation in connection:

Deformations due to slip at concrete to concrete or concrete to mortar interface, slip at joint of reinforcement (grout filled sleeve joint, lap splice joint and so on), should be limited within a certain extent. As described in clause 2.3.2, maximum allowable slip is given as a percentage of them in the inter story drift angle of a precast system. When there are plural connections in a story, all of possible slips in connections should be taken into account. For the estimation of slips, both analytical approach (mathematical model of connection and mechanical behavior of connection element) and experimental approach are available.

Safety assurance for damage concentration:

If there is a possibility of damage concentration to reinforcing bars and/or concrete, safety against it should be assured. When a stiff reinforcing bar joint is used, for example, strain concentration

must occur in adjacent reinforcing bars in post yield range of deformation. These phenomena are indicated in figure 4 schematically. In case of figure 4 a), reinforcing bar must have enough elongation capacity. In case of peripheral columns, there are no perpendicular beams and surrounding slabs at the column bottom part so that the crushing of foundation concrete likely to occur as shown in figure 4 b). To avoid such unfavorable phenomena, concrete strength in foundation should be at least equal to that of column concrete.

Redundancy:

Fracture and sudden decrease of carrying force of tension element in a connection is not allowed. To satisfy this requirement, experimentally verified joint of reinforcement must be used.

Estimation of beam elongation due to load cycling in post yield range of deformation:

Inelastic elongation during load cycling in post yield range of deformation occur at plastic hinge region. The extent of elongation should be predicted to avoid the drop down of connected precast elements. Evaluation method of beam elongation is described in New Zealand Guidelines for Precast Construction.

Torsional strength:

If a ductile connection is subjected to equilibrium torsion, it should be designed so as to sustain the torsional moment.

Peeling of peripheral shell element:

Peeling of thin peripheral concrete shell element in composite member should be prevented.

Durability, serviceability and fire resistance: Serviceability, durability and fire resistance are required as same as in monolithic system.

6.2 Strong connection

No any inelastic deformation are expected to the connection, it is designed as a strong connection. Strong connection should have enough stiffness and strength to transfer safely the design moment and/or forces, and behave in elastic manner under any types of loading. In this design manual, beam-to-column joint is assumed to be strong connection because required energy dissipation should be achieved by the inelastic deformation of beam plastic hinge region. Requirements for strong connections are as follows.

Stiffness:

Connections, i.e., member to member connections and composite effect connections, should have enough stiffness under the design load condition. Because design moment and/or forces for connections and precast elements are predicted by the structural analysis generally used for in monolithic system.

In the structural analysis, floor slab is assumed to be a rigid diaphragm. To assure this assumption, floor system should have enough rigidity. If the small deformation of floor system due to diaphragm stresses is predicted it should be less than 20 % of maximum inter story drift at corresponding story.

Significant degradation of stiffness should not occur even if a precast system is responding to a severe earthquake.

Strength:

Connection has enough strength to transfer design moment and/or forces, any types of failure modes are allowed such as shear failure and concrete crushing excepting tensile fracture of tensile elements. However, any significant degradation of strength should not occur even if a precast system is responding to a severe earthquake.

Cracking load:

Flexural cracking in precast system may occur in early stage of loading at the interface between precast element and cast-

in-situ concrete so that the stiffness of precast system near cracking load is slightly smaller than that of monolithic system. However, this stiffness reduction seems to have no any significant effect on the structural performance of a precast system.

Load transfer:

Design moment and/or forces should be transferred through the connection without yielding of tension element excepting beam to column joint.

Limitation of slip deformation in connection:

Deformation due to slip at concrete to concrete or concrete to mortar interface, at joint of reinforcement (grout filled sleeve joint, lap splice joint and so on) and at reinforcing bar to concrete interface, should be limited within a certain extent. As described in clause 2.3.2, Maximum allowable slip is given as a percentage of it in the inter story drift of a precast system.

Redundancy:

If there is a possibility of brittle failure of connection due to accidental load higher than design load, a connection should sustain the design load by another mechanism even if the primary mechanism disappear.

Durability, serviceability and fire resistance: Serviceability, durability and fire resistance are required as same as in monolithic system.

7 Modeling of connection

The purpose of connection design is to assure the required connection performance under given load combination. Generally, following process is adopted in the design of connection details.

1) Choice of appropriate stress transfer mechanism in connection which can properly transfer the design moment and/or forces, where designer have to consider several conditions such as stress level, deformation behavior, creep and shrinkage, thermal stresses, tolerance and so on.

2) Computation of connection element stresses due to design moment and/or forces.

3) Confirmation of the strength of connection elements, which should be greater or equal to the computed element stresses.

4) Confirmation of additional deflection due to slip of connection element, which should be within a allowable limit.

7.1 Stress transfer model

a) Friction

If normal stress is acting on the concrete to concrete or concrete to mortar interface, shear stress can be transferred by friction. This concept is illustrated in figure 6. In figure 6, + marks indicate the experimentally observed maximum strength. From those test results, friction coefficient m is obtained, which depends on the condition of the interface. To assure the stress transfer across the interface, the combination of shear stress and normal stress acting on the interface should be within a hatched area. Normal stress acting on the interface is estimated from the equilibrium condition.

b) Shear friction

When the normal stress is not acting on the interface or very small , shear stress can be transferred by shear friction. In shear friction, certain amount of well anchored transverse reinforcement is necessary to produce the normal stress at the interface. The normal stress is generally estimated by assuming the tensile yielding of transverse reinforcement. However, we should pay attention the fact that 1) when maximum shear strength is achieved a certain amount of shear slip occurs, and 2) transverse reinforcement does not yield when high strength steel is used. From such view point, shear friction theory can not be

applied for the design of connection where no any shear slip is permitted.

c) Dowel action

Dowel action can also be expected for the transmission of shear stress across the interface. In the design, both the dowel strength of transverse reinforcement and bearing strength of surrounding concrete should be considered. If there is a possibility of spalling of cover concrete, additional transverse reinforcement should be arranged near the interface. Maximum dowel strength is associated with a certain amount of slip deformation along the interface as same as in shear friction. This characteristics should be taken into account in connection design.

d) Free body diagram

Design force of tension and compression element can be estimated from the equilibrium condition using free body diagram.

e) Strut and tie

Strut and tie model is very useful tool for estimating the design stresses at connection element. One example of strut and tie model is illustrated in figure 9. When there is a design element at the interface between beam and column like figure 8, this interface can be easily designed according to friction concept given in clause 4.2.1. If the ratio of shear force Q to normal force C is smaller than the friction coefficient m, no any slip deformation occurs at the interface. On the other hand, if this condition is not satisfied, we have to arrange other shear transfer mechanism like shear key. This strut and tie model also can be used for the design of beam to column joint as same as for in monolithic system.

f) Truss analogy

Truss analogy is also a useful tool for the design of precast connections.

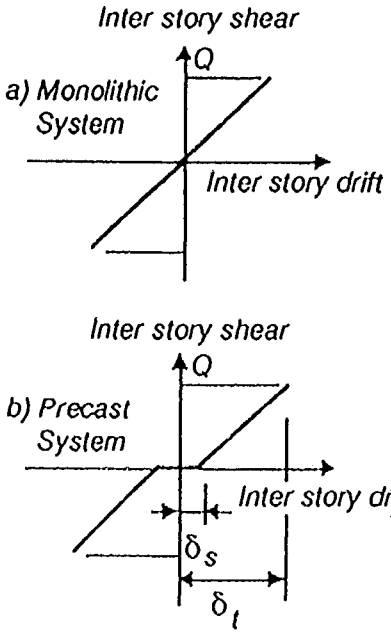


Fig.1-1 Slip evaluation (elastic response)

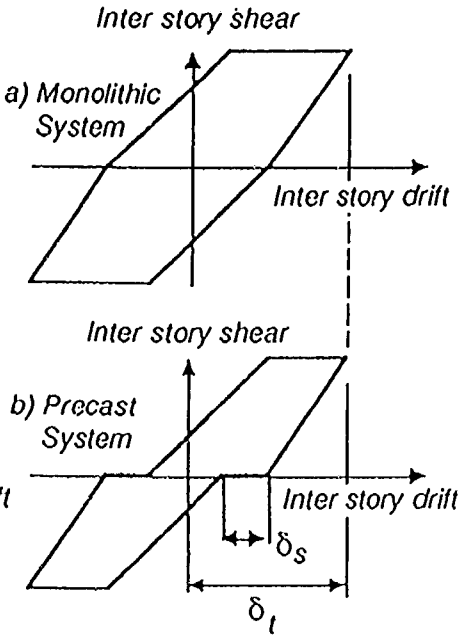


Fig.1-2 Slip evaluation (inelastic response)

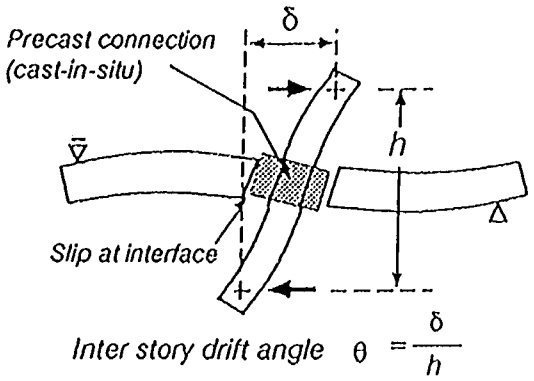


Fig.2 Beam column assemblage

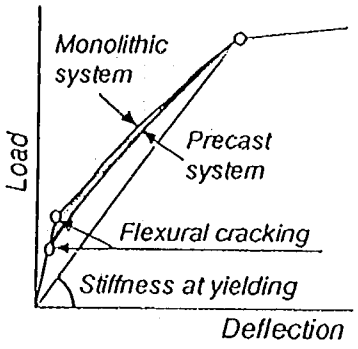
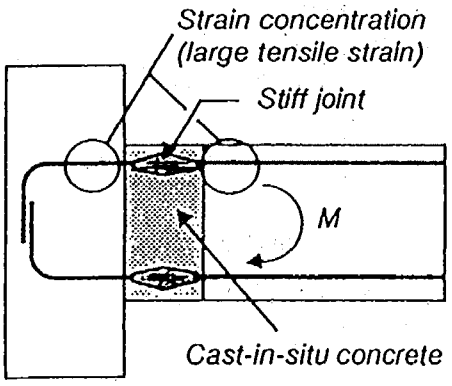
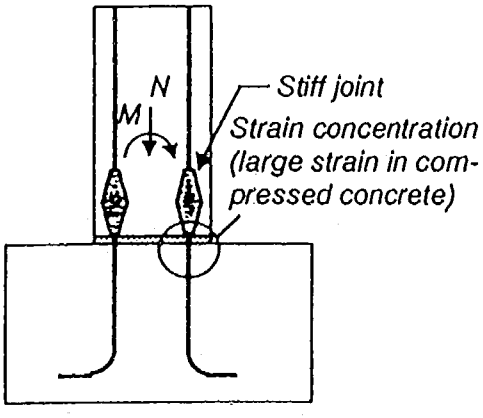


Fig.3 Effect of cracking



a) Beam to column connection



b) Column to foundation connection

Fig.4 Damage concentration

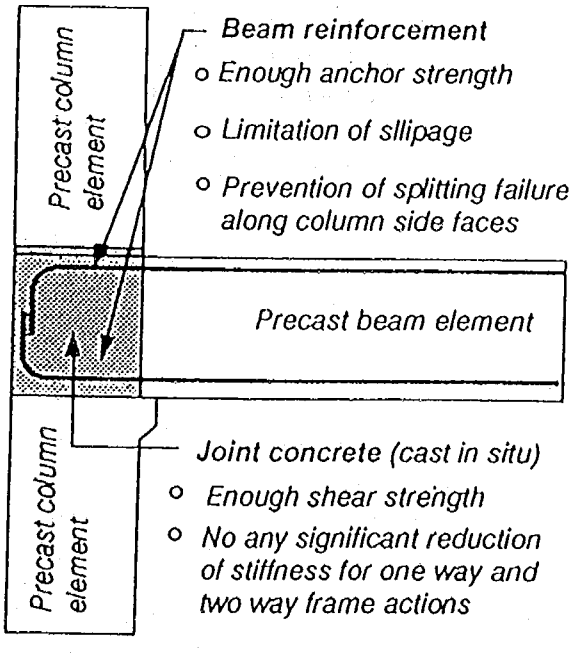


Fig.5 Example of strong connection (beam to column joint)

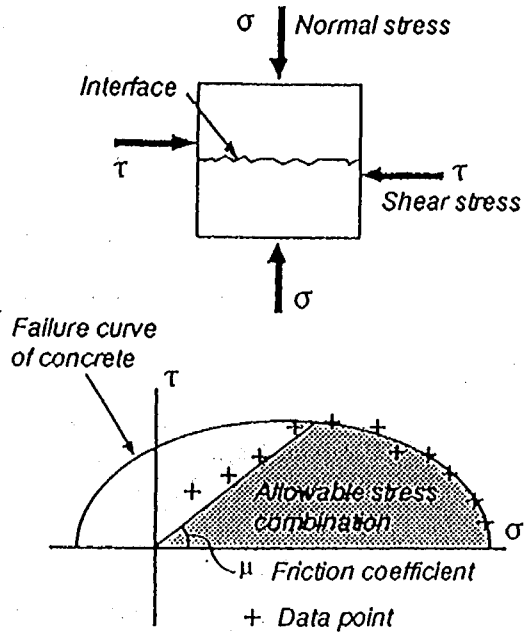


Fig.6 Stress transfer by friction

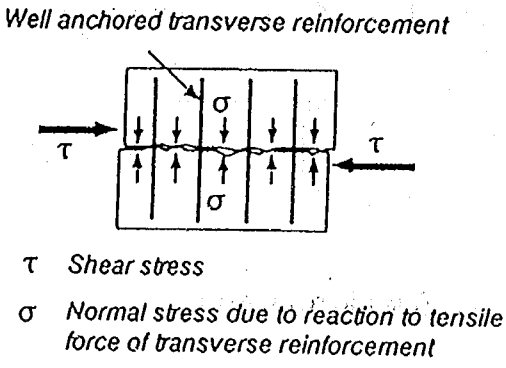


Fig.7 Shear friction

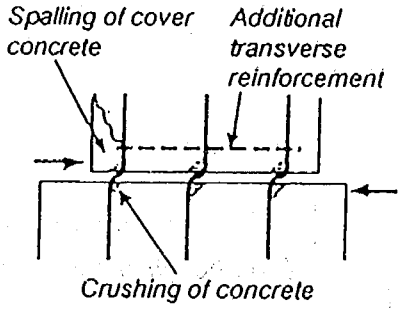


Fig.8 Dowel action

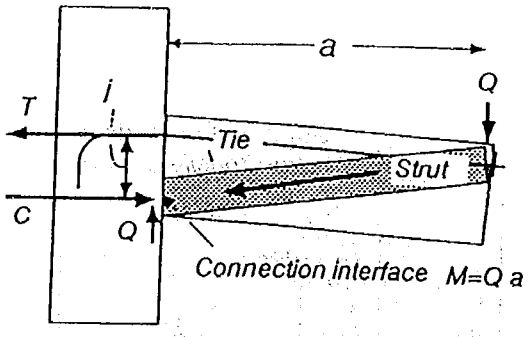


Fig.9 Strut and tie model

PRESSS - A Coordinated U.S./Japan Research Program on the Design of Precast Seismic Structural Systems

by

M. J. Nigel Priestley[1]

and

H. S. Lew[2]

ABSTRACT

A coordinated research program on precast seismic structural systems is described. The program, which is being carried out in conjunction with a parallel Japanese effort under the auspices of the United States/Japanese Natural Resources (UJNR) program has been active for three years and is expected to continue for a further three years. Aims of the program are to develop new structural systems for precast structures in seismic regions, and to produce the necessary design guidelines based on extensive experimental and analytical research to enable such structures to be accepted by regulatory authorities.

KEYWORDS: building technology; building code requirements; elastic connections; precast structural systems.

1. INTRODUCTION

Precast structural systems for buildings are rarely constructed in the more seismic regions of the United States. This is primarily due to restrictive building code requirements, which demand that it be shown that a proposed precast system has strength, deformation and energy absorption characteristics equal to an equivalent reinforced concrete structure. This reinforced concrete emulation forces the designer into connection details which are often not the most economical, not necessarily the best technically, and generally requires proof by testing, which can result in delays in regulatory approval, and hence in construction, which are unacceptable to the client.

Three years ago, a coordinated research effort was initiated by the National Science foundation (NSF), in conjunction with the precast Prestressed Concrete Institute (PCI), and the Precast Concrete Manufacturers Association of California (PCMAC), with the aim of developing new concepts for precast concrete building construction, and performing the necessary experimental and analytical research to provide a basis for seismic design recommendations. It is expected that this research will enable the designer to take advantage of the special attributes of precast concrete,

[1]University of California San Diego, La Jolla, CA 92093

[2]National Institute of Standards and Technology, Gaithersburg, MD 20899

without the need for testing, or for reinforced concrete emulation. The research is being carried out in cooperation with a similar Japanese effort.

2. PHASE 1 RESEARCH

The initial phase of the U.S. PRESSS (Precast Seismic Structural Systems) program has been concentrated on concept development, review of existing research, development of special analytical tools, and consideration of the appropriate framework for design recommendations. There has also been considerable interaction with the Japanese side. Brief notes on the individual projects follow.

2.1 Concept Development

A major task of the phase 1 research has been the identification of suitable precast structural system for both frame and panel structures that would be expected to perform well under seismic response, and also be economical and suitable for construction. This has involved interaction between consultants, precasters, contractors and researchers. A key element in this task has been information obtained from Industry Regional Workshops, held at four different U.S. locations during 1991, where different structural concepts were discussed and evaluated by a wide spectrum of the precast industry and professional [1].

The emphasis in the concept development project has been on what is termed ductile connections. Conventional precast design based on reinforced concrete emulation has traditionally provided connections which are stronger than the connected elements, so that inelastic action is forced to occur away from the connections. Since there is a large body of existing research relevant to this philosophy, it has not been considered in the concept development project, which has concentrated on systems where inelastic deformation occur in the connection.

A second task of this project relates to the design and analysis of a 15-story "test-bed" building being subject to parallel design effort by the U.S. and Japanese teams. Analysis of the expected performance of this building under a number of different precast bracing systems have provided valuable insight into advantages of different concepts, and have facilitated discussion and comparison of differences between the U.S. and Japanese design philosophies.

3. CONNECTION CLASSIFICATION AND EVALUATION

The considerable body of existing information on connections has been collated and assessed. This has been summarized in the form of connection evaluation forms [2]. A similar exercise has been carried out by the Japanese side related to their very large connection data base. A second task of this project has been to develop hysteretic rules for the inelastic response of different connection categories that have been identified for testing in

Phase 2. These include the following:

(i) **Elastic connections:** In some cases of low rise buildings in regions of moderate seismicity it will be economical to design for purely elastic response, where strength exceeds maximum expected seismic forces. A more interesting alternative of non-linear elastic response is being considered for both panel and frame connections, where the connection between elements is made by unbonded prestressing tendons. These allow large rotations to develop at connections with the tendon remaining within the elastic range. In frame structures significant economies can be achieved by this procedure, particularly in the beam/column joint region. Preliminary testing of the concept has confirmed its viability. Although initial stiffness was high, drift angles approaching 3% were achieved with the structure still responding in the elastic range [3].

ii) **Connections relying on axial tension and compression yield of connecting elements:** Connections involving yield of either (but not both) of the top or the bottom connection element at a beam/column intersection are favored. The non-yielding connection element would be an integral part of the erection connection process, deliberately made strong, with the secondary, yielding element added later. This concept also seems to hold considerable promise.

iii) **Connections involving shear yield:** These are particularly appropriate for midspan beam connections where the structural ductility and energy dissipation are provided by relative vertical displacement of the connected beam elements, and also for panel-to-panel vertical connections.

iv) **Connections involving added damping:** This could be achieved by special friction-grip bolted connections, by dissipating energy through coulomb damping, or by the addition of special proprietary damping materials or elements.

4. ANALYTICAL PLATFORM DEVELOPMENT

Special inelastic time-history analysis programs are being developed to act as basic analysis tools for PRESSS Phase II. These are based on the well known DRAIN 2DX program, and have been extended in terms of element modeling (particularly connection modeling) and the ability to cope with 3D configurations [4].

5. DESIGN RECOMMENDATIONS

An early task has been making design recommendations for required strength of different connections in strong-joint (i.e. reinforced concrete emulation) designs. Draft recommendations based on structural evaluation of the performance criteria for different connection details, based on capacity design principles have been developed.

6. PHASE II PROGRAM

The Phase 2 program is just commencing, with a series of tests planned on ductile connectors for both panel and frame structures. All test units will be tested in accordance with a standard test pattern, designed to enable tests carried out at different institutions to be compared. For frame tests, the design limit state will be a lateral drift of 2%. For the tests to be considered satisfactory, the test units must sustain a drift of 3% - i.e, 50% higher than the design limit state without significant strength loss. For panel tests, a test limit drift of 2% is adopted, corresponding to a design limit state of 1.33%. At the time of writing this paper, details for the Phase 2 tests had not been finalized. Examples will be presented at the conference.

7. CONCLUSIONS

The U.S. PRESSS research program is entering into the crucial second phase where experiments and analyses are carried out to prove the viability of different ductile connectors, and to provide the necessary basis for determining lateral strength of different systems to satisfy the design limit states drift. The conclusion of this phase of testing should provide the design profession and the precast industry with a series of precast structural options for seismic regions that are structural competent, and economically competitive with structural systems of alternative materials.

8. ACKNOWLEDGEMENTS

The financial support of the National Science Foundation, the Precast/Prestressed Concrete Institute, and the Precast Concrete Manufacturers Association of California is gratefully acknowledged. Any opinions expressed in this paper are those of the authors alone, and should not be construed to be official policy of the NSF, PCI, PCMAC or NIST.

8. REFERENCES

1. Stanton, J.F. and S. Dow Nakaki, "PRESSS Industry Seismic Workshops." Edited by M. J. Nigel Priestley, Report No. PRESSS - 91/02, October 1991, 185 pp.

2. Stanton, J.F., T. R. Hicks and N. M. Hawkins, "PRESSS Project 1.3 Connection classification and Evaluation." Edited by M. J. Nigel Priestly, Second Meeting of the Joint Technical Coordinating Committee on Precast Seismic Structural Systems (PRESSS). Report No. PRESSS - 92/01, Tsukuba, Japan, January 1992.

3. Priestley, M. J. Nigel and Greg MacRae, "Tests on Unbonded Prestressed Precast Beam/Column Joints." (PRESSS Report 93/01) May 1993.

4. Powell, G. H. and F. C. Filippou, "Project 1.4 Analytical Platform Development." Edited by M. J. Nigel Priestley, In Report on the Third U.S. PRESSS Coordinating Meeting, Report No. PRESSS - 92/02, August 1992.

U.S.-Japan Cooperative Earthquake Research Program on Composite and Hybrid Structures

by

Hiroyuki Yamanouchi *1, Stephen A. Mahin *2, Subhash C. Goel *3 and Isao Nishiyama *4

ABSTRACT

A five-year research program on Composite and Hybrid Structures as the Phase 5 of the U.S.-Japan Cooperative Earthquake Research Program has been recommended to be initiated in 1993 in both countries. Presented in this report is a recommended research program which is based on a number of technical meetings of the U.S. and Japan Planning Groups and a Joint Planning Workshop. Because of diverse and broad scope of the subject area, the research program is organized into the following four groups: New Materials, Elements and Systems; Concrete Filled Tube Column Systems; Reinforced Concrete (RC) and Steel Reinforced Concrete (SRC) Column Systems; and RC/SRC Wall Systems. A theme structure with well selected layout, geometry and design loads for the research is also presented, which will provide a common focus for various systems to be studied, and will provide a common prototype structure from which the components and sub-assemblages will be drawn.

KEYWORDS: composite and hybrid structures; recommended research program; theme (focus) structure.

1. INTRODUCTION

The U.S.-Japan Cooperative Earthquake Research Program began in 1979 following the recommendations as outlined in the final report of the U.S.-Japan Planning Group for the program (Ref.1). The overall objective of the total program is to improve seismic safety practices in both countries through cooperative studies to determine the relationship among full-scale tests, small-scale tests, component tests, and related analytical and design implication studies. First four phases of the program are: Reinforced Concrete (RC) Structures, Steel Structures, Masonry Structures, and Precast Concrete Structures. Phase 4 of the program on Precast Concrete Structures is currently in its final stages. Research on Mixed Steel/RC Structures was identified as an important phase of the program as recommended in the planning group report.

It is widely recognized that innovative uses of two or more different materials in a structure leads to more efficient system for resisting seismic forces. During the past ten years the use of composite and hybrid structures has increased in the U.S. and Japan. In spite of some research and development work by Japanese construction companies, not enough is known at present regarding their seismic behavior or performance. Design procedures and codes for use in typical design offices are currently non-existent.

Considering the importances of developing design guidelines (a unified code development) for typical composite and hybrid structures that are used in current practice, and of developing new and innovative composite structural elements and hybrid systems using advanced new materials and/or devices, a five-year research program on Composite and Hybrid Structures is recommended as the fifth phase of the ongoing U.S.-Japan Cooperative Earthquake Research Program. The research program on Composite and Hybrid Structures includes that on Mixed Steel/RC Structures listed in the planning group report. The recommendations are based on a number of technical meetings of the U.S. and Japan Planning Groups and a Joint Planning Group Workshop held in Berkeley on September 10-12, 1992 (Ref.2).

---

*1 Program Director, International Standard and Technology Development Program, Research Planning & Information Department, Building Research Institute (BRI), Ministry of Construction (MOC), Tatehara-1, Tsukuba, Ibaraki 305, Japan.

*2 Professor, Department of Civil Engineering, University of California at Berkeley, 777 Davis Hall, Berkeley, CA 94720, U.S.A.

*3 Professor, Department of Civil and Environmental Engineering, University of Michigan, Ann Arbor, MI 48109-2125, U.S.A.

*4 Senior Research Engineer, International Institute of Seismology & Earthquake Engineering, BRI, MOC.

Because of diverse and broad scope of the subject area, it is recommended that the research program be organized into the following four groups: New Materials, Elements and Systems; Concrete Filled Tube (CFT) Column Systems; RC/Steel Reinforce Concrete (SRC) Column Systems; and RC/SRC Wall Systems. A theme structure is recommended for the program to facilitate cross comparison between various system types identified and to derive structural elements and sub-assemblages for detailed studies.

2. THEME STRUCTURE

It is recommended to have a theme (focus) structure with well selected layout, geometry and design loads for the research. The theme structure will provide a common focus and a strong link between various components of the research program, facilitate cross comparisons between various systems to be studied, and will provide a common prototype structure from which the structural elements and sub-assemblages for detailed studies will be drawn. The following criteria were used for selection of the theme structure:

- The building plan should be selected so as to reflect the benefits that the hybrid structures provide over non-hybrid structures.
- The basic plan should be common to various types of hybrid structures. The number of stories and the make-up and combination of structural components and details can be varied.
- Rules to determine dead load, live load and seismic forces to be used in design simulation should be common to the U.S. and Japan Groups.

The basic plan selected for the program is representative of typical office buildings. As shown in Figure 1, it provides office space of 12.8 meters in span length outside the central core. The central core is used as utility space for elevators, stairs, etc. Floor area of the central core is determined on the basis of a twenty story office building. The core area may be changed with the number of stories, if desired. Six types of theme structures are selected as shown in Table 1. The reasons for selecting numbers of stories as 3, 6, 9, 10, 12, 24 or 40 for different structure types are as follows:

- Six, twelve and twenty four stories have been used frequently in Japan for RC, SRC and steel construction, respectively.
- Six is selected as the standard (key) number of stories for RC(OPEN)-06 structure. Three and nine are selected for comparison.
- Twelve is selected as the key number for (S-SRC)+W-12 and (S-RC)+W-12 structures.
- Twenty four is selected as the key number for CFT(OPEN)-24 structure. Ten and forty will be necessary for comparison.
- Buildings more than forty stories may be investigated under 3.1 New Materials, Elements and Systems.

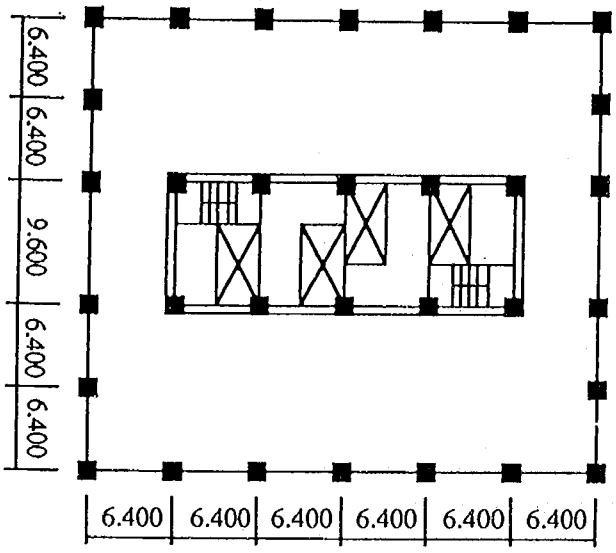


Figure 1 Prototype Plan of Theme Structure

Plan dimensions and layout for the above six structure types are shown in Figures 2-7. The efforts to get more desirable attributes of the theme structures is being made in the U.S. (Ref.3).

Table 1 Six Types of Theme Structures

Name	Number of Stories	Exterior Column	Interior Column /Beam	Wall and Misc.
RC(OPEN)-06	3-6-9	RC	RC/S	-
RC+W-06	6	RC	RC/RC	Wall
(S-SRC)+W-12	12	S	SRC/SRC	Wall
(S-RC)+W-12	12	S	RC/RC	Wall
CFT(OPEN)-24	10-24-40	CFT	CFT/S	-
CFT+B/HD-24/	24	CFT	CFT/S	brace/hinge-device

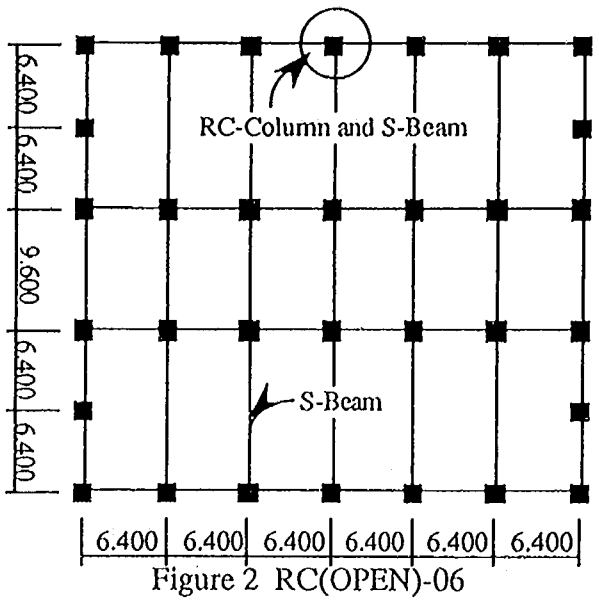


Figure 2 RC(OPEN)-06

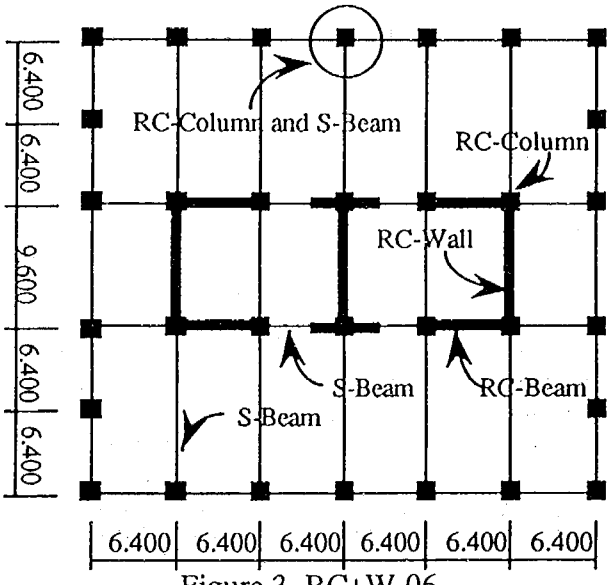


Figure 3 RC+W-06

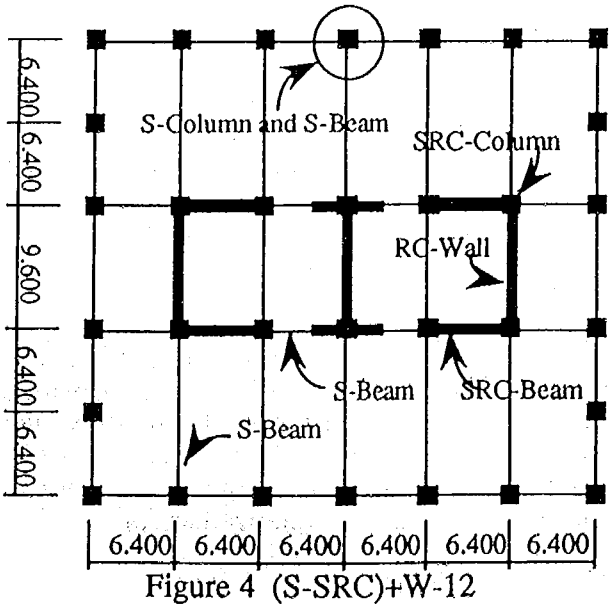


Figure 4 (S-SRC)+W-12

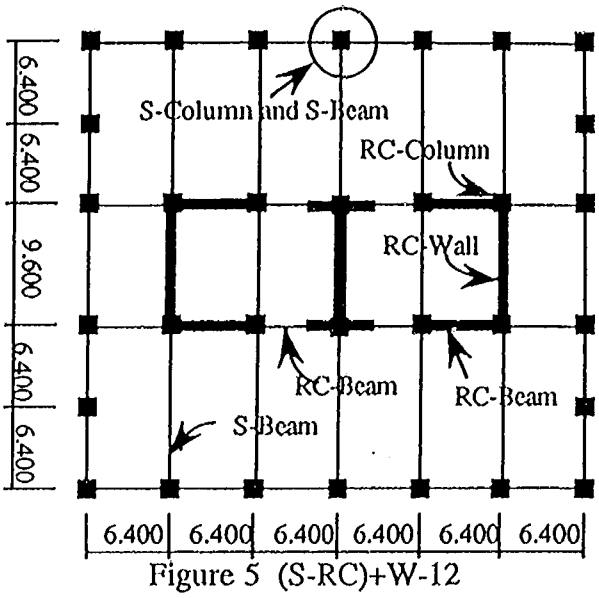


Figure 5 (S-RC)+W-12

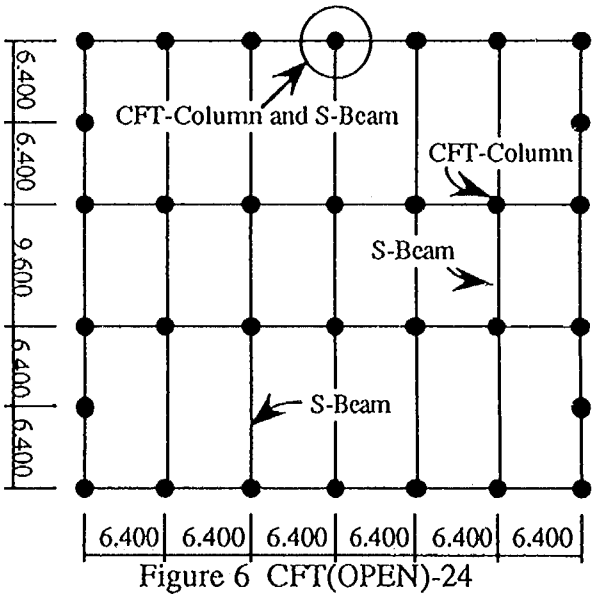


Figure 6 CFT(OPEN)-24

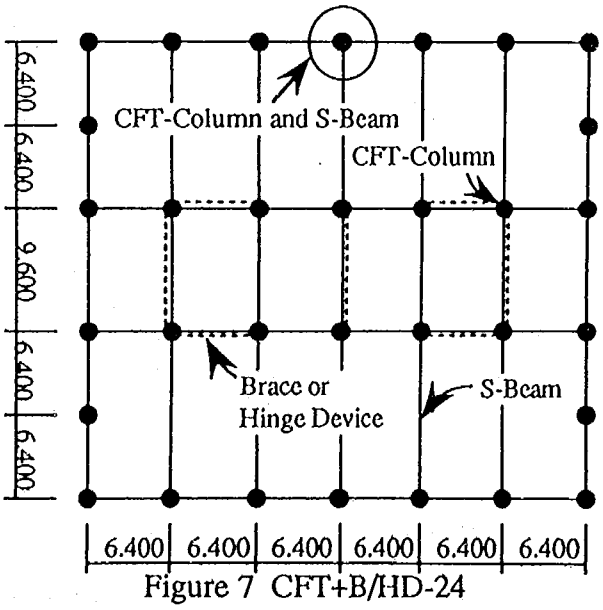


Figure 7 CFT+B/HD-24

3. RESEARCH PROGRAM

Since the subject area of the Composite and Hybrid Structures is diverse and broad, it is recommended that the research program should be organized into the following four groups: New Materials, Elements and Systems; CFT Column Systems; RC/SRC Column Systems; and RC/SRC Wall Systems. The first group aims at developing new and innovative composite structural elements and hybrid systems using advanced new materials and/or devices. The other groups rather practically aim at developing design guidelines (a unified code development) for typical composite and hybrid structures currently used. The research needs, formulation of recommended research plan and priorities of research topics in each group are summarized as follows:

3.1 New Materials, Elements and Systems

(1) New Materials

Improvement in structural systems are driven by improvements in materials, or by improvements in the understanding of how existing materials respond to complex loads which will occur at various locations in buildings. The following are the lists of the materials-related research which is carefully focused on composite and hybrid structures among wide variety of materials.

- Establishment of a thorough data base on existing materials.
- Definition of ideal material properties.
- Evaluation of ductility under reversed loadings, brittleness effects in members under axial or shear loadings, creep and shrinkage, and confinement effects of concrete and high performance concrete.
- Modifications of strength, stiffness and ductility properties; and those of geometries and surface treatments of structural steel and high performance steel.
- A detailed and critical survey of the application of fiber reinforced concrete (FRC) in critically stressed regions.
- Research on interface bond, durability and standardized testing methods of fiber reinforced plastic (FRP), and feasibility studies on suitable application and development of more effective FRP.

(2) New Elements

Elements are defined as those of a composite and hybrid structure that act in conjunction with the primary building structural components. They may modify the behavior of ordinary connections, provide innovative bracing actions and offer special behavioral characteristics such as reduction of seismic forces and damping action. Specific examples of such elements that have already received some research and development are mentioned below. Other new elements need to be conceived and developed.

- Development and definition of properties and behavior under reversed loadings of bracing elements such as unbonded steel bars embedded in concrete members or panel with unbonded and embedded thin linear steel elements.
- Development of dampers and connectors which provide beneficial damping such as damped pinned connections for steel beams to concrete walls and visco-elastic dampers installed into or onto structures.

(3) New systems

Development of new composite and hybrid structural systems that go beyond those currently in use or under study is a natural evolutionary process that takes place primarily in the design office. It is suggested that this process can be strengthened and accelerated with research efforts that involve carefully structured teams of researchers, practicing engineers, and industrial materials experts. The following are the specific topics identified, but it is important to realize conceptual breakthroughs which will make new topics in addition to the following, which cannot be identified at present.

- Feasibility studies on innovative systems.
- Studies on optimal geometries and materials for members.
- Development of precast or prefabricated elements and connections.
- Development of composite frames with "fuse" connections.
- Re-evaluation of existing systems.

3.2 CFT Column Systems

A number of research topics related to CFT Column Systems were raised and prioritized based on their importance. Then, they were grouped into several categories. Highly prioritized research topics which are categorized into six groups are summarized as follows:

(1) Beam - Columns

- Determination of the effect of confinement versus composite action.
- Determination of methods for evaluating axial, shear and flexural stiffness; and ductility and resistance under monotonic and cyclic loadings.
- Determination of bond stress and shear transfer mechanisms between the steel tube and the concrete.

(2) Columns

- Evaluation of creep and shrinkage effects on CFT columns in high rise buildings.

(3) Connections

- Determination of force and moment transfer mechanisms and design models for FR (fully restrained), PR (partially restrained) and pinned connections at connections between braces, beams and columns.
- Determination of panel zone deformation effect on the seismic performance of CFT columns.

(4) Frames

- Analytical studies combining the above connection and member behavior to evaluate the seismic performance of moment resisting frames with CFT columns, which should be directed toward determination of Ds and Rw and the seismic design forces.
- Analytical studies combining the above connection and member behavior to evaluate the seismic performance of braced frames with CFT columns, which should be directed toward determination of Ds and Rw and the seismic design forces..

(5) Very High Strength Concrete

- This is a general topic related to all composite or hybrid structures, but it has particular impact on CFT columns.

(6) Literature Review

- Complete a literature review related to CFT construction with a complete list of publications and brief abstracts of individual papers and reports to facilitate the exchange of information between the U.S. and Japan.

3.3 RC/SRC Column Systems

In Japan, RC column - steel beam moment frames have been used in low-rise office and shopping center buildings with long floor spans. The economic advantage of this system is achieved replacing steel columns with RC columns. The RC columns also offer increased stiffness compared to the steel columns. In the U.S., such systems have been used in mid- to high-rise construction, which are usually constructed by first erecting a steel frame with light steel erection columns which are later encased with concrete. The application of such systems has been advanced in Japan through experimental research and development programs at some large construction companies. However, many of these previous tests were "proof tests" to demonstrate adequacy of such new systems. On the other hand in the U.S., practice on such systems has been limited to regions of low to moderate seismicity.

The following is a summary of the research recommendations which are given high priorities.

(1) Moment Connections between RC Columns and Steel Beams

- Database and Evaluation of Previous Research; There is an urgent need to develop a database and summary of tests which have been conducted in the U.S. and Japan including a comparison and evaluation of the data in light of proposed design models.
- Experimental Tests; The following parameters should be considered in the planning of tests, those are, basic configuration or geometry of joint, 2D and 3D geometries and loading conditions, presence of axial loads, effect of composite floor slabs, difference in details depending on the construction sequence, type of cyclic loading regime, and design philosophy.

(2) Evaluation of Hybrid System Response

- Nonlinear Analysis; One objective of the analytical studies is to help guide and establish priorities for connection and sub-assemblage tests by offering information on the local ductility requirements and loading effects on connections. Another objective of the analyses are to sort out questions related to inelastic loading response factors such as Ds and Rw and other design requirements.

(3) Connections between RC/SRC Columns and Concentric Steel Braces

- Connection Tests; There is need in the U.S. for research and tests to develop design models and detailing requirements for transferring axial forces between the concentric braces and columns.

3.4 RC/SRC Wall Systems

For the purposes of discussion on the issues of the RC/SRC Wall Systems, the theme structure shown in the figure 8, which is similar to the theme structures shown in the figures 3 to 5, is focused, in which the core wall system is four bays by one bay with walls all around the perimeter and a central web creating in plan a double box. For shorter buildings, the core wall would probably provide the entire lateral force resistance. As the building becomes taller, the core would work with a perimeter moment frame with no moment connections between the two. As the building becomes even taller, moment connections would be added between the core walls and perimeter frame. For the tallest building, the core walls and perimeter moment frame would be coupled by a roof-top hat or the equivalent at appropriate levels of the building.

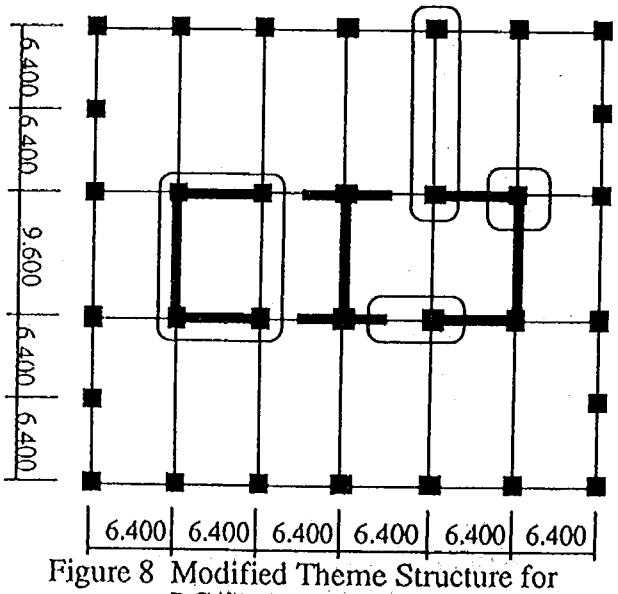


Figure 8 Modified Theme Structure for RC/SRC Wall Systems

The issues raised were prioritized and grouped into four categories based on the degree of the interaction between the core wall and the perimeter frame as follows: Interaction Between Core and Frame; Issues Related to Core Wall; Topics Related to Boundary Elements; and Topics Related to Coupling Beams. The highly prioritized research topics are summarized as follows:

(1) Interaction Between Core and Frame

- Develop and test connections that transmit "shear only" between the steel/composite floor beams and the core wall.
- Develop and test connections that transmit shear and moment between the steel/composite floor beams and the core wall.

(2) Issues Related to Core Wall

- Investigate the behavior of 2D core walls under 2D horizontal loads.

(3) Topics Related to Boundary Elements

- Investigate shear transfer between steel column and the concrete in the boundary elements.

4. SUMMARY

A recommended research program is presented in this report on a five-year research program on composite and hybrid structures which will be carried out as the Phase 5 of the U.S.-Japan Cooperative Earthquake Research Program.

REFERENCES

1. "Recommendations for a U.S.-Japan Cooperative Research Program utilizing Large-Scale Testing Facilities", Report No. UCB/EERC 79-26, September 1979.
2. "Recommendation for U.S.-Japan Cooperative Research Program -Phase 5 Composite and Hybrid Structures", Report No. UMCEE 92-29, November 1992.
3. Personal communication from S. A. Mahin to H. Aoyama & H. Yamanouchi dated on February 24, 1993.

APPENDIX: Resolutions Adopted at the Joint Planning Workshop

(1) In view of the advantages and opportunities for innovation that composite and hybrid structures provide for earthquake resistance and the urgent need for analysis methods, design procedures and code development, and final report of the planning workshop should be completed and distributed to appropriate government agencies, to industries, and to researchers and practitioners as soon as possible.

(2) It is recommended that the program of cooperative research in this phase, as set forth in the report, be initiated in 1993 in both countries.

(3) The level of funding for the recommended program should be sufficient to permit fulfillment of the goals and objectives defined in the report.

(4) To ensure successful execution of the recommended cooperative research program, full coordination of all research activities carried out in both countries is essential. Therefore, formation of the following committees is recommended:

   (a) Joint Technical Coordinating Committee (JTCC) to provide scientific and technical advice to participating institutions in the program. This committee should meet at least once a year during the program; and

   (b) Joint Technical Subcommittees (JTSC) to provide advice and coordination, as needed, in carrying out research in the areas identified in the report. The Co-Chairs of each JTSC should also be members of the JTCC. These sub-committees should meet as often as needed.

(5) Active participation of practitioners and industry representatives in planning, coordination and execution of the recommended research program is strongly recommended.

(6) To assure and enhance the cooperative effort in this joint research program, adequate exchange of personnel involved in both countries is essential.

(7) To assure that exchange of information and coordination activities continue until the research effort in both countries is fully implemented, meetings between the groups involved in both countries are required.

(8) It is recommended that U.S.-Japan Panel on Wind and Seismic Effects of U.J.N.R. Program endorse the research program in this phase.

(9) To enhance the objectives of this research program exchange of information on related research efforts in other countries should be encouraged.

(10) Future plans should include the possibility of carrying out research on composite and hybrid structures, other than buildings, under the overall U.S.-Japan Cooperative Earthquake Research Program.

SEISMIC RESPONSE CONTROL OF HIGHWAY BRIDGES BY VARIABLE DAMPER

by

Kazuhiko Kawashima[1], Shigeki Unjoh[2] and Hidetoshi Mukai[3]

ABSTRACT

This paper presents experimental studies on the effectiveness of a variable damper developed at the Public Works Research Institute. A prototype model of the variable damper is developed and the dynamic characteristics and the controllability through the dynamic loading tests are presented. The shaking table tests of a model bridge to verify the effectiveness of the variable damper for reducing seismic response of highway bridges are also presented. Furthermore, the variable stiffness concept in which the natural period of highway bridges is shifted to avoid resonance using the variable damper is formulated, and the effectiveness is analytically studied.

KEY WORDS : Seismic Response Control, Highway Bridges, Variable Damper, Prototype Model, Shaking Table Test, Variable Stiffness

1. INTRODUCTION

The variable damper is a viscous damper in which the viscous damping force is variable depending on the response of highway bridges so that the variable damper have the advantages of an usual viscous damper stopper, a passive energy dissipator and a stopper with a shock absorber function. Because integration of functions of a damper-stopper and a energy dissipator is effective for increasing seismic safety of highway bridges, the applicability and practicability of the variable damper has been studied at the Public Works Research Institute.[1)-4)]

This paper presents experimental studies on the effectiveness of the variable damper developed. A prototype model of the variable damper is fabricated and the dynamic performance and the controllability is verified through dynamic loading tests. Shaking table tests of a model bridge to verify the effectiveness of the variable damper for reducing seismic response of highway bridges are also presented. Furthermore, an application of the variable damper to the variable stiffness control is presented. In the variable stiffness control, the natural period of highway bridges is shifted for avoiding resonance.

2. DEVELOPMENT OF A PROTOTYPE MODEL OF THE VARIABLE DAMPER

2.1 Outline of A Prototype Model of the Variable Damper

Fig.1 and Photo 1 show a design plan and a view of a prototype model of the variable damper developed. The model is designed so that the maximum damping force is 20tf, maximum stroke is within ± 13cm. The control of the damping ratio is arbitrarily made by a personal computer depending on relative displacement and/or velocity developed between deck and substructures.

The piston-cylinder has total length of 118.4cm, and the pressure area of the piston is 137.4cm^2. A steel pipe by-pass with servo valves is installed between the cylinder-cells divided by the piston.

The servo valve is a D.C. proportional relief valve and the oil pressure through the valve is adjusted. The servo valve relieves the pore oil pressure over a certain value. This pressure is defined hereafter as the control pressure. Since the damping force of the piston is caused due to the difference of the pressure between the two cells in the cylinder, it increases up to the control pressure, and then becomes constant over the control pressure. Therefore, the damping force is dependent on neither displacement nor velocity of the piston.

The input voltage from a servo amplifier to the servo valve is designed to be in the range of 0 to 5V. The control pressure is 0 at the input voltage of 0V and increases with increase of the input voltage. The viscous material used for the variable damper is an usual oil for a dynamic loading actuator. The variable damper also has a fail-safe function for emergency conditions such

1) Head of Earthquake Engineering Division, Earthquake Disaster Prevention Department, Public Works Research Institute, Ministry of Construction
2) Senior Research Engineer, ditto
3) Assistant Research Engineer, ditto

as power failure. The control pressure can be preset at arbitrary pressure in such case.

2.2 Dynamic Loading Tests of the Prototype Model of the Variable Damper

In the controlling algorithm, it is the most important critical point to assure the relation between the input voltage and damping force of the variable damper. For verifying the algorithm, a dynamic loading test are made.

Fig.2 shows the set-up of the dynamic loading test. Loading was applied to the piston by a dynamic actuator under the displacement control. The control pressure of the servo valve was kept constant. The input voltage to the servo valve, reaction force and stroke of the piston were measured. Ten cyclic loading was made for each loading displacement.

Two tests as shown in Table 1 was made. In Case 1, the friction force of the damper piston was measured. Because loading rate is not important for measuring the friction force, loading frequency was 0.05Hz with loading displacement of ± 10cm. The input voltage of the variable damper was assumed to be 0V so that the control pressure be 0. In Case 2, the relation between the input voltage to the servo valve and damping force of the variable damper was tested. Combination of loading frequency, loading displacement and input voltage were varied. All loading were made with the peak loading rate less than 7cm/s because of the capability of the loading apparatus.

2.3 Performance of the Prototype Model of the Variable Damper

(1) Friction Force of the Damper Piston

Fig.3 shows hysteresis loops of the load-displacement relation in Case 1. The hysteresis loops show almost rectangular shape, i.e., typical friction type load-displacement relation. The hysteresis is stable for a number of loading cycles. The average friction force is about 1tf.

(2) Hysteresis Loops of the Load-Displacement Relation

Fig.4 shows hysteresis loops of the load-displacement relation with loading frequency of 0.1Hz in Case 2. Variation of the hysteresis loops with the input voltage are also shown. Although overall shape of hysteresis loops are rectangular, some distortion is seen at the instance when the direction of movement of the piston changes at peak displacement. This is because of time-lag for increasing the oil pressure from 0 to the control pressure. But this effect becomes less as the loading stroke increases. This may be resolved by adopting servo valve with large capacity. Turbulence is also found at the instance when the damping force reaches the preset peak force. This may be because of the pressure wave motion by sudden increase of the pressure.

(3) The Relation between the Input Voltage and Damping Force

Fig.5 shows the relation between the damping force and the input voltage. The damping force varies as a power function of the input voltage in the range of 0V and 1.8V. When the input voltage is greater than 1.8V the relation becomes almost linear. An empirical equation was obtained by a least square method as

$$F = \begin{cases} 0.42V^{3.7} + 1.0 & (0 \leqq V \leqq 1.8) \\ 8.14V - 9.95 & (V > 1.8) \end{cases} \qquad (1)$$

where, F and V represent the damping force (tf) and the input voltage (Volt), respectively. In Eq.(1), the constants are determined as averaged values of those obtained in each loading case.

2.4 Controllability of the Prototype Model of the Variable Damper

The controllability of the variable damper using Eq.(1) was tested. The control of the variable damper is made by controlling a signal from a personal computer depending on the measured displacement. Since digital control is made by the computer, sampling time to detect displacement is preset.

Fig.6 shows hysteresis loops of the load-displacement relation thus obtained. The commanded damping force and the measured one are compared in Fig.6. The damping force is perfectly found to be controlled. Some corrugation in the sampling time of 0.1 sec. Therefore, in order to control accurately, it is required to determine the appropriate sampling time in consideration with the loading velocity.

3. SHAKING TABLE TESTS OF A MODEL BRIDGE CONTROLLED BY THE VARIABLE DAMPER

3.1 Model Bridge

In order to verify the effectiveness of the variable damper, shaking table tests of a model bridge were made. The tests were made using the shaking table at the Public Works Research Institute.

Photo 2 and Fig.7 show the set up of shaking table test and the model bridge. The model bridge is an elastically supported single span girder. It has a pier height of 1.6m, deck length of 7.6m and deck weight of 39.8tf. The deck is supported by 4 rubber bearings as shown in Fig.8. The stiffness of the rubber bearings are designed so that the fundamental natural period of the model bridge be 1sec. Therefore, the stiffness of rubber bearing is designed as 160tf/m at 50% shear strain. Total thickness and shear modulus of the rubber is 10cm and 6kgf/cm^2, respectively.

The variable damper is installed between the deck and the top of left pier as shown in Photo 3.

Fig.9 shows the control algorithm of the variable damper.[3)4)] The displacement dependent damping was assumed and the variable damper is controlled by the displacement of deck relative to the pier top.

3.2 Dynamic Response Characteristics of A Model Bridge

Because the rubber bearings have some nonlinearity, the stiffness and energy dissipation depend on the shear strain (shear displacement). For clarifying these characteristics, the model bridge was firstly excited by a series of harmonic motions without controlling by means of the variable damper.

Fig.10 shows the frequency response function of deck displacement. Peak deck displacement increases from 2.8cm to 9.8cm by increasing the peak acceleration of harmonic table motion from 20cm/s^2 to 40cm/s^2. The predominant frequency of the deck also shifts from 1.15Hz to 1.0Hz by doubling the table motion.

From the harmonic excitation tests, the load-displacement hysteresis of the bearing as shown in Fig.11 was evaluated. The equivalent stiffness and equivalent damping ratio was computed as :

$$h_e = \frac{1}{2\pi}\frac{\Delta W}{W} \qquad (2)$$

$$K_e = \frac{F(u_{max}) - F(u_{min})}{u_{max} - u_{min}} \qquad (3)$$

where,

h_e : equivalent damping ratio
K_e : equivalent stiffness
W : strain energy
ΔW : energy dissipation
u_{max} : maximum displacement developed in bearings
u_{min} : minimum displacement developed in bearings
$F(u_{max})$: force developed at displacement u_{max}
$F(u_{min})$: force developed at displacement u_{min}

Fig.12 shows the equivalent stiffness and the equivalent damping ratio of the rubber bearings by Eqs.(2) and (3). The equivalent stiffness decreases with increase of displacement. The displacement dependence of the equivalent damping ratio is less significant.

3.3 Earthquake Response Characteristics of the Model Bridge Controlled by the Variable Damper

In order to verify the effectiveness of the variable damper, the model bridge was excited by an earthquake motion. An acceleration ground motion, which recorded on the ground around Hachirogata during the Nihon-kai-chubu Earthquake of 1983, was used as an input acceleration by reducing the time axis one half so that the predominant frequency of the record matches with the fundamental natural frequency of the bridge model. Peak acceleration was modified to be 200cm/s^2 and 500cm/s^2.

Three cases in total were made. In Case A, the model bridge was not controlled by the variable damper and the peak acceleration was assumed as 200cm/s^2. In Case B, the model bridge was controlled by the variable damper and the peak acceleration was assumed as 200cm/s^2. In Case C, the model bridge was controlled and the peak acceleration was increased to 500cm/s^2.

Figs.13 to 15 show the measured responses of above three cases, respectively. The displacement and acceleration of the model bridge and the damping force of the variable damper are shown. The simulation results described later is also shown.

Fig.13 shows the input acceleration and the deck responses of the Case A (no control). The deck responses with the period of about 1sec which is the fundamental natural period of the model bridge. The peak displacement and peak acceleration of deck are 376cm/s^2 and 9.2cm, respectively. The deck acceleration is amplified to 2.2 times the input acceleration. Fig.14 shows those in Case B (with control). The deck responses contain the faster frequency

components and the peak displacement and peak acceleration of deck decrease to 203cm/s^2 and 1.3cm, respectively. The amplification of the deck acceleration is 1.1 times the input acceleration. Fig.15 shows those in Case C (with control). The peak displacement and the peak acceleration of deck are 412cm/s^2 and 3.5cm, respectively.

Table 2 summarizes the peak responses of the model bridge and the variable damper. Comparing Cases A and B, the peak acceleration and peak displacement of deck controlled by the variable damper decrease to 54% and 14% of those with no control, respectively. The peak damping force of the variable damper in Case B is 7.2tf.

3.4 Simulation of the Shaking Table Tests

In order to simulate the tests results, a computer program "VDAM" which can analyse earthquake response of a multi-degree-of-freedom system with the variable damper developed at PWRI was used.[3] The simulation results are shown in Fig.13 to 15 described in the above. Equivalent stiffness and equivalent damping ratio of the rubber bearing obtained through the harmonic excitation in the above were used for the simulation.

In case A (no control), fair agreement between measured and computed responses are found in displacement and acceleration responses.

In case B and C (with control), computed deck displacements are larger than the measured ones. On the other hand, the measured damping force is greater than computed one. The difference between measured and computed peak displacements is about twice. This is because of the over-shooting of the damping force of the variable damper. Therefore, the servo valve which has quick response capability should be adopted so as to decrease the over-shooting of damping force. However, the computed and measured responses in Cases B and C show the fair agreement.

4. SEISMIC RESPONSE CONTROL OF HIGHWAY BRIDGES BY VARIABLE STIFFNESS

4.1 Algorithm of the Variable Stiffness

Most of bridges with usual size have the natural period ranging from 0.3 to 1.5 second, and this natural period range corresponds to the predominant period of earthquake-induced ground motions. Thus the resonance of the bridges response with the ground motion tends to be developed during an earthquake. The bridge response could be reduced provided the resonance of bridge response with the ground motion could be avoided.

Although it is hard to predict the predominant period of ground motion prior to an earthquake, it can be evaluated time by time during an earthquake. The moving window analysis may be used for evaluating the instantaneous predominant period of ground motion T^*. The resonance of bridge response with the ground motion may be avoided if the instantaneous natural period of bridges T be shifted from the instantaneous predominant period of ground motion T^* during an earthquake.

There are various methods to shift the instantaneous natural period of bridges during an earthquake. Flexibility of bearings may be changed, and active tendons/bracings may be adopted.

If one provides the variable dampers for a bridge which is elastically supported by rubber bearings, the natural period of the bridge can be varied by changing the damping coefficient of the variable dampers. If one makes the damping ratio of the variable damper very large, the variable damper would acts as the damper stopper. On the other hand, if one makes the damping ratio small, the natural period of the bridge takes the value computed from the stiffness of the rubber bearings and piers. The variable dampers have various advantage for controlling the instantaneous natural period of bridges because it is more stable for long term use than the active tendons/bracing systems.

Fig.16 shows the algorithm of the variable stiffness control. The instantaneous predominant period of ground motion T^* at time t_i is computed by the moving window Fourier Spectrum. The damping coefficient of variable dampers is varied so that the instantaneous natural period of the bridge T be shifted to prevent the resonance with the ground motion.

Although several algorithm can be considered, the period shift is assumed here as

$$T = \alpha T^* \qquad (4)$$

where,

T : instantaneous natural period of a bridge at time t_i

T^*: instantaneous predominant period of an earthquake ground motion at time t_i

α : control coefficient

The coefficient α has to be determined depending on the undamped natural period of the

bridge T and the instantaneous predominant period T^* of an ground motion. It is proposed that α is set as

$$\begin{aligned} \alpha &< 1/2 \quad (T < T^*) \\ \alpha &> 2 \quad (T \geqq T^*) \end{aligned} \tag{5}$$

4.2 Earthquake Response Analysis Method of Multi-Degree of Freedom System with Variable Stiffness Control

The equations of motion for a linear multi-degree-of-freedom system with the variable stiffnesses control may be written as

$$\underline{M}\ddot{\underline{X}} + (\underline{C} + \underline{C_v})\dot{\underline{X}} + \underline{K}\underline{X} = -\underline{M}\ddot{X_0} \tag{6}$$

in which $\underline{M}$, $\underline{C}$ and $\underline{K}$ represent mass, damping and stiffness matrices of the system, respectively. $\underline{X}$ and X_0 denote displacement vector of the system and an earthquake ground motion, respectively. $\underline{C_v}$ denotes a damping matrix of the variable dampers and is assumed as

$$\underline{C_v} = \sum_{k=1}^{n_v} \underline{c_{ij}}^v \tag{7}$$

where

$$\underline{c_{ij}}^v = \begin{bmatrix} V & -V \\ -V & V \end{bmatrix} \tag{8}$$

in which $\underline{c_{ij}}^v$ and n_v represent damping matrix of the variable dampers, which is installed between the i-th node and the j-th node, and a number of the variable dampers installed, respectively. V is the damping coefficient of an each variable dampers and is given according to the control algorithm as shown in Fig.16.

Although there are various methods to prescribe the damping matrix $\underline{C}$ of the structure, it is assumed here to be written as Eq.(9) assuming that the damping matrix $\underline{C}$ can be diagonalized by the modal matrix.

$$\underline{C} = (\underline{\Phi})^{-1}\,\mathrm{diag}[2h_k\omega_k]\,(\underline{\Phi}^T)^{-1} \tag{9}$$

in which, $\underline{\Phi}$ denotes a modal matrix of the system and $\mathrm{diag}[2h_k\omega_k]$ denotes a diagonal matrix with elements of $2h_k\omega_k$ (k=1,2,3,$\cdots\cdots$; mode number).

Since $\underline{C_v}$ is time-varying, Eq.(6) has to be solved by a direct integration method. According to the above analytical method, a computer program "VSTIFF," which can analyze earthquake response of a multi-degree-of-freedom system with the variable stiffnesses, was developed.

4.3 Highway Bridge Analyzed and Analytical Conditions

In order to analytically investigate the effectiveness of the variable stiffness, a three-span continuous girder bridge, as shown in Fig.17, with a span length of 90m is analyzed. The response in longitudinal direction is considered. The superstructure of the model is supported by elastic isolators in longitudinal direction and the 4 same variable stiffnesses are assumed to be installed between the superstructure and each pier top.

The weight of the superstructure and spring stiffness of the isolator are assumed as 481.2tf and 637tf/m, respectively. The flexural stiffness of piers is assumed so that the fundamental natural period of the model be 0.5sec when the 4 bearing supports are hinged. The stiffness of isolators result in the fundamental natural period of 1 sec for the model with elastic isolators. When the variable damper is not provided, the modal damping ratio of the bridge is assumed to be 2% of critical.

An acceleration ground motion as shown in Fig.18(a) is used as an input acceleration. The acceleration, recorded on the ground around the Tsugaru Bridge during the Nihon-kai-Chubu Earthquake of 1983, was modified so that the response spectrum matches with the target spectrum. The acceleration spectrum, which is specified in "Part V Seismic Design" of the "Design Specifications for Highway Bridges", for the check of bearing capacity of reinforced concrete piers on soft soil site (ground condition Ⅲ), is assumed as the target spectra.

Fig.18(b) shows the intantaneous predominant frequency ($1/T^*$) of the input acceleration. Because the predominant period of ground motion is about 1 sec., α in Eq.(4) was assumed as 1/2.

4.4 Effectiveness of Variable Stiffness Control

Figs.19 shows how the natural period of the bridge change depending on the damping coefficient of the variable dampers. At the damping coefficient C of about 430 tf·sec/m, the fundamental natural period of bridge take very large value, because this corresponds to the critical damping of the structure. Although the period shift may be made in the damping coefficient range of 0 to over 800 tf·sec/m, it is assumed here that the period shift be made in the range of damping coefficient C over 430 KN·sec/m.

Fig.20 compares the deck acceleration and

displacement of the bridge with and without control. The peak displacement and peak acceleration of deck decreases to 17% and 50% of those without control. The bending moment of pier bottom decreases to 52% of the one without control. The peak damping force required for the four variable dampers is 77.6 tf × 4 = 310 tf and peak stroke is 3.1cm.

5. CONCLUDING REMARKS

The effectiveness of the variable dampers was experimentally studied. A prototype model of the variable damper was developed and the performance was studied through the dynamic loading tests and shaking table tests. The variable stiffness control in which the natural period of bridges is shifted to avoid resonance with the ground motion was proposed, and its effectiveness was analytically studied. According to the investigations presented herein the following conclusions may be deduced:

1) Based on the dynamic loading tests of the prototype model developed, the damping force of the variable damper can be controlled as commanded.

2) Based on the shaking table tests of the model bridge, the peak acceleration and peak displacement of deck controlled by the variable damper decreases to 54% and 14% of those with no control, respectively. The peak damping force of the variable damper is 7.2tf.

3) The measured responses in 2) can be predicetd by the analytical model presented herein.

4) By the variable stiffness control, the peak displacement and peak acceleration of the deck decreases to 17% and 50% of those without control, respectively. The bending moment of pier bottom decreases to 52% of that without control. The peak damping force required for the four variable dampers is 77.6tf × 4 = 310tf and peak stroke is 3.1cm.

REFERENCES

1) Taguchi, J., Iwasaki, T., Adachi, Y., Sasaki, Y. and Kawashima, K. : U.S.-Japan Cooperative Research Program on Hybrid Control of Seismic Response of Bridge Structures, 22nd Joint Meeting, U.S.-Japan Panel on Wind and Seismic Effects, UJNR, Gaithersburg, Maryland, USA, May, 1990

2) Kawashima, K., Unjoh, S., Nagashima, H. and Shimizu, H. : Current Research Efforts in Japan for Passive and Active Control of Highway Bridges Against Earthquakes, 23rd Joint Meeting, U.S.-Japan Panel on Wind and Seismic Effects, UJNR, Tsukuba, May, 1991

3) Kawashima, K., Unjoh, S. and Shimizu, H. : Seismic Response Control of Highway Bridges by Variable Damper, 24th Joint Meeting, U.S.-Japan Panel on Wind and Seismic Effects, UJNR, gaithersburg, May, 1992

4) Kawashima, K., Unjoh, S., Iida, H. and Mukai, H. : Effectiveness of the Variable Damper for Reducing Seismic Response of Highway Bridges, Proc. of the 2nd U.S.-Japan Workshop on Earthquake Protective Systems for Bridges, Tsukuba, Dec. 7-8, 1992

5) Liu, S., C., Lagorio, H., J. and Chong, K., P. : Status of U.S. Research on Structural Control Systems, 23rd Joint Meeting, U.S.-Japan Panel on Wind and Seismic Effects, UJNR, Tsukuba, May, 1991

6) Kawashima, K., Unjoh, S. and Shimizu, H. : Earthquake Response Control of Highway Bridges by Variable Damper, Proceedings of Colloquium on Control of Structures, Japan Society of Civil Engineers, Part. B, pp.221-224, July, 1991 (in Japanese)

7) Feng, Q. and Shinozuka, M. : Use of A Variable Damper for Hybrid Control of Bridge Response Under Earthquake, U.S. National Workshop on Structural Control Research, University of Southern California, CA., U.S.A., October, 1990

8) Shinozuka, M., Feng, Q. and Kawamura, S. : New Perspectives for Sliding Base Isolation Systems, Proceedings of International Workshop on Recent Developments in Base-Isolation Techniques for Buildings, Tokyo, Japan, 27-30 April, 1992

9) Kawashima, K., Unjoh, S. and Shimizu, H. : Earthquake Response Control of Highway Bridges by Variable Damper, Transactions of the Japan National Symposium on Active Structural Response Control, Japan Science Council, pp.311-317, March, 1992 (in Japanese)

10) Kawashima, K., Unjoh, S. and Shimizu, H. : Experimental Study on Dynamic Characteristics of Variable Damper, Transactions of the Japan National Symposium on Active Structural Response Control, Japan Science Council, pp.311-317, March, 1992 (in Japanese)

Table 1 Test Cases

Case	Objective	Loading Frequency (Hz)	Loading Displace-ment (cm)	Input Voltage (Volt)
1	Measurement of Friction Force of Damper-Piston	0.05	±100	0
2	Relation between Damping Force and Input Voltage	0.1～1.0	±2～±100	0～5

Table 2 Peak Responses of A Model Bridge and Variable Damper

Test Cases	Peak Accel. of Shaking Table (cm/s^2)	Measured			Computed		
		Deck	Variable Damper		Deck	Variable Damper	
		Accel. (cm/s^2)	Force (tf)	Stroke (cm)	Accel. (cm/s^2)	Force (tf)	Stroke (cm)
A No Control	172	376	---	---	361	---	---
B With Control	185	203	7.2	1.3	148	5.2	2.5
C With Control	413	412	13.8	3.5	442	13.5	6.2

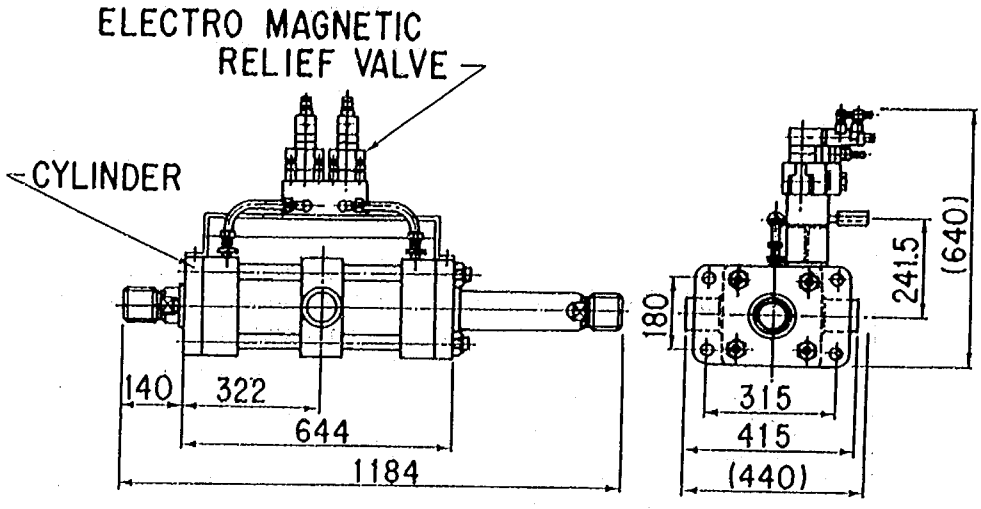


Fig.1 Prototype Model of Variable Damper Developed

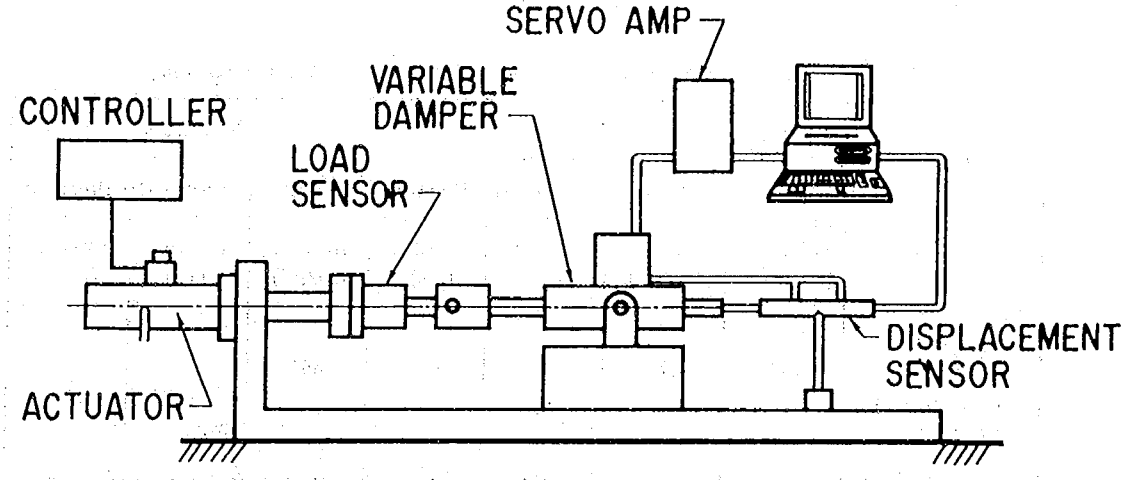


Fig.2 Set up of Dynamic Loading Tests of Variable Damper Developed

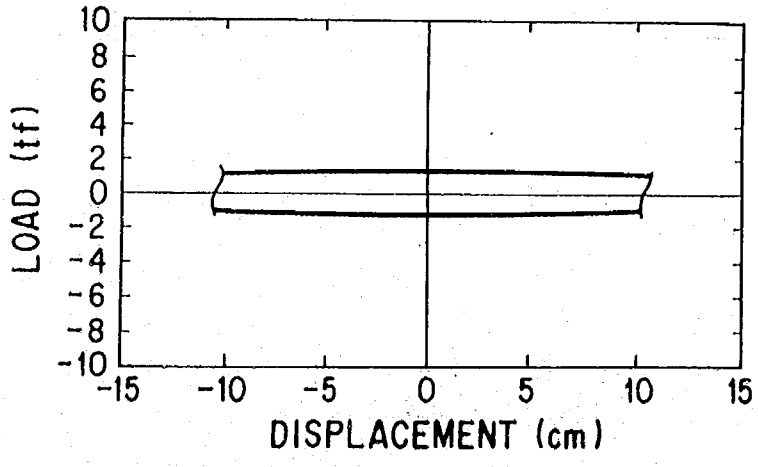
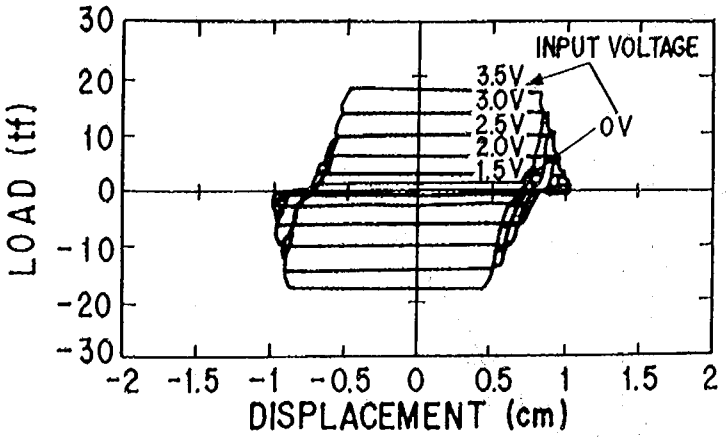
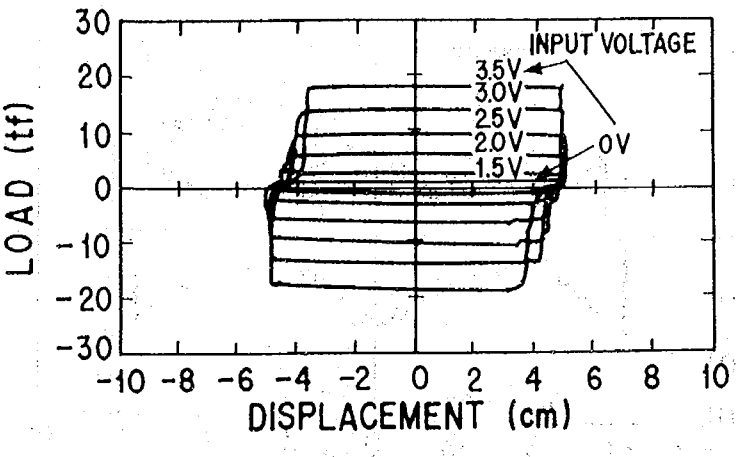


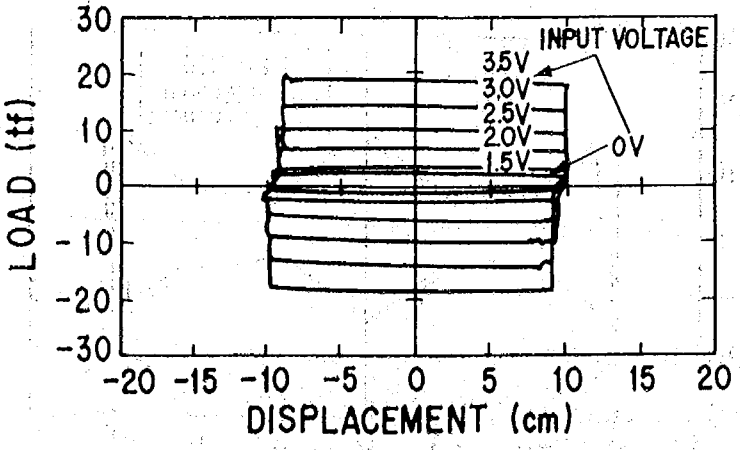
Fig.3 Hysteresis Loops of Load-Displacement Relation
(Displacement = 10cm, Frequency = 0.05Hz)



(1) Displacement 1cm



(2) Displacement 5cm



(3) Displacement 10cm

Fig.4 Hysteresis Loops of Load-Displacement Relation (Frequency = 0.1Hz)

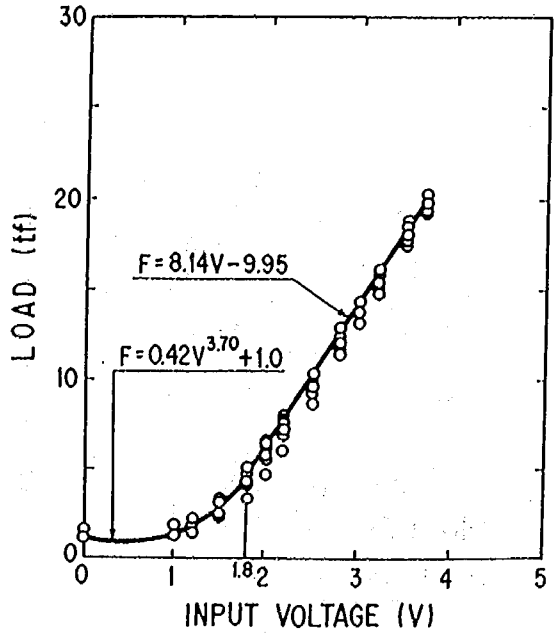
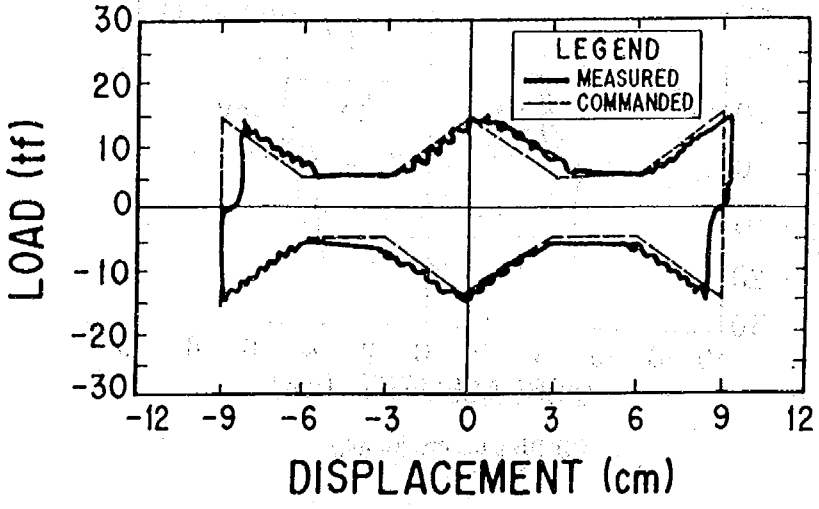
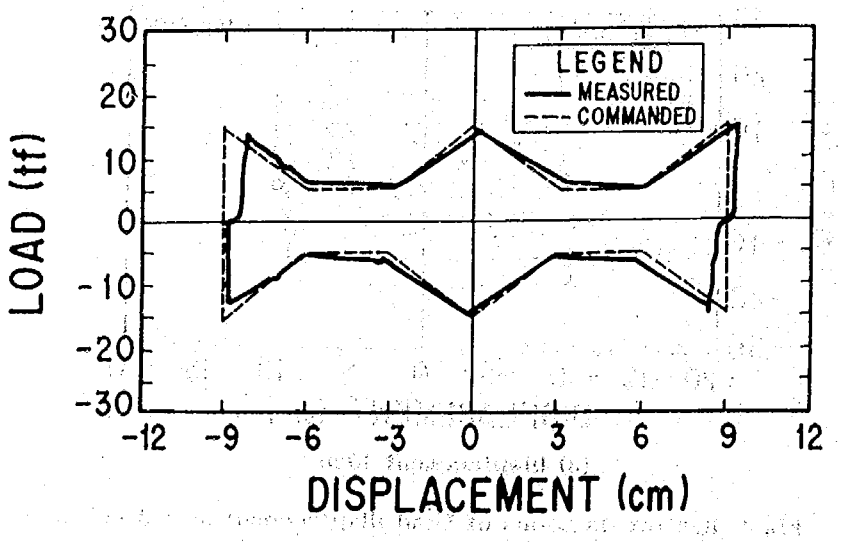


Fig.5 Damping Force vs. Input Voltage Relation



(1) Sampling Time 0.1sec



(2) Sampling Time 0.01sec

Fig.6 Controllability of the Variable Damper Developed

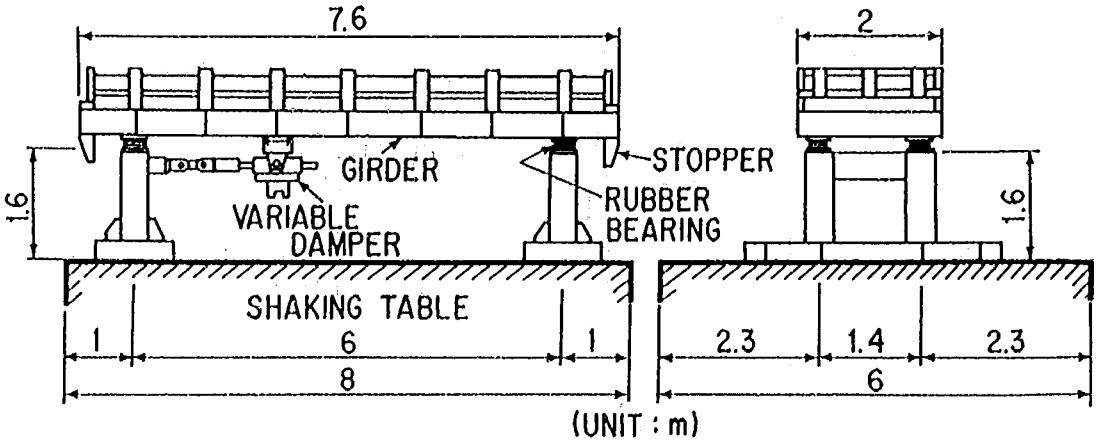


Fig.7 Model Bridge Studied

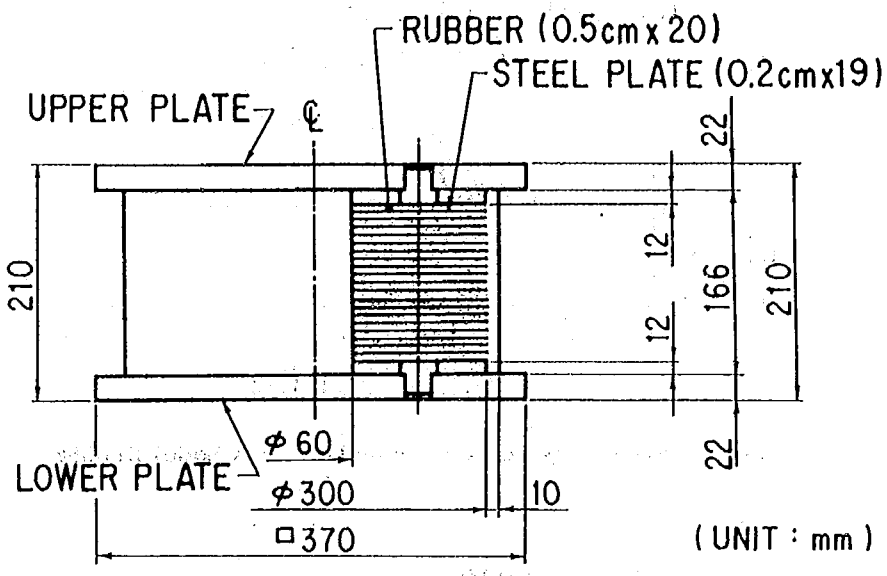


Fig.8 Rubber Bearing used for A Model Bridge

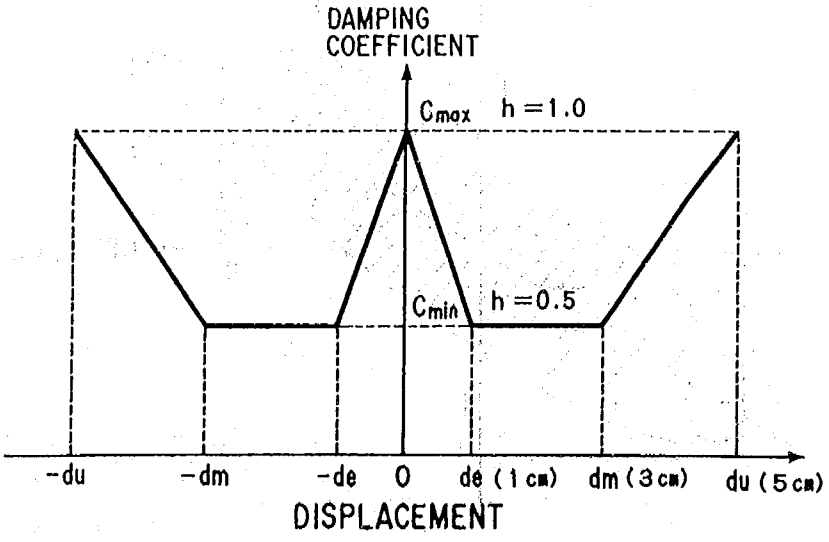


Fig.9 Control Algorithm of Variable Damper (Displacement Dependent Damping)

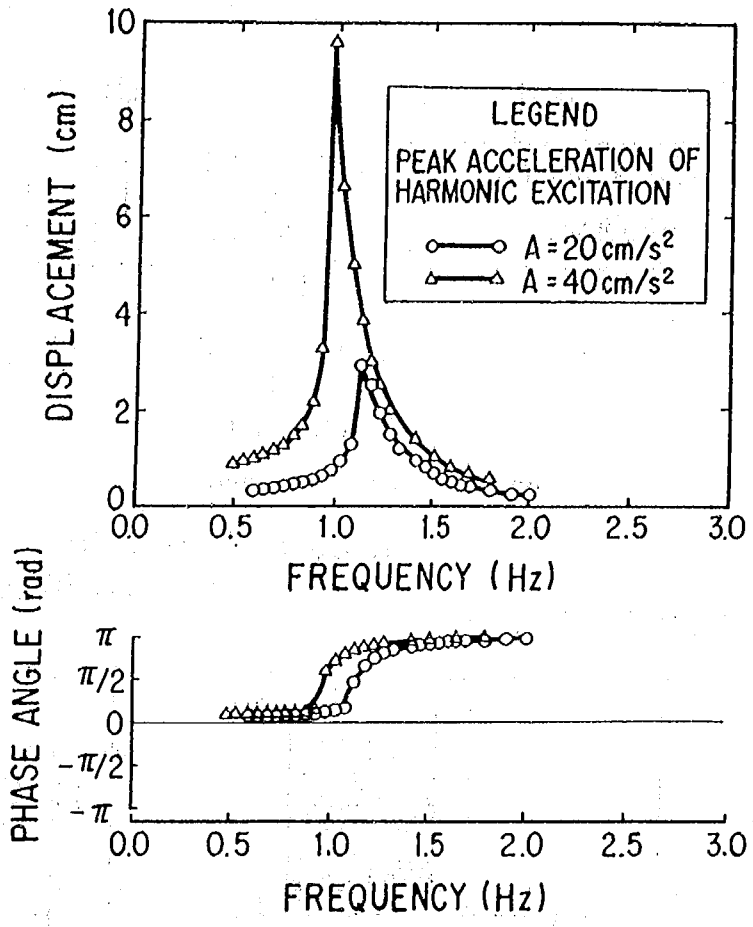


Fig.10 Frequency Response Function of A Model Bridge

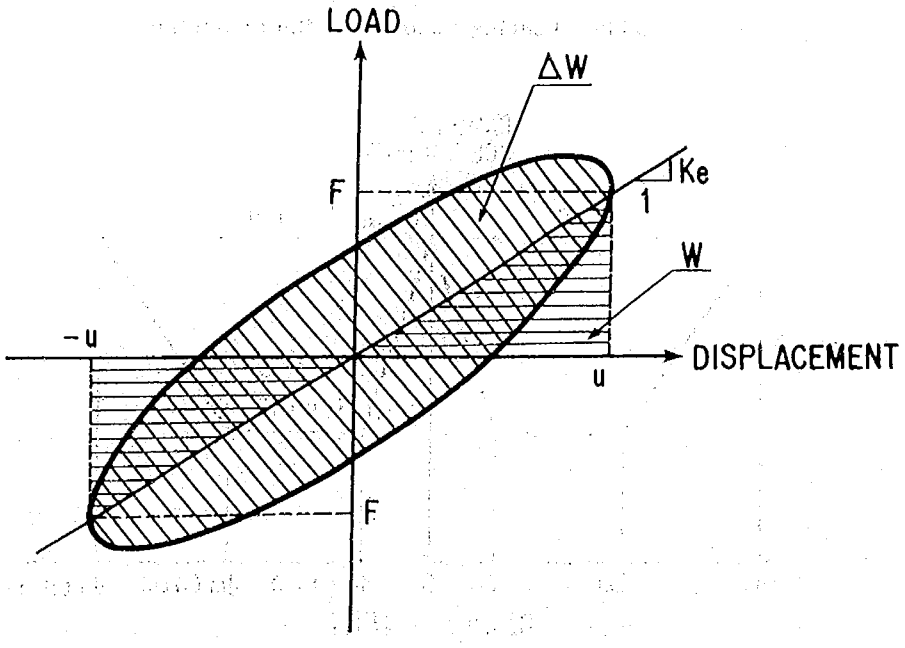
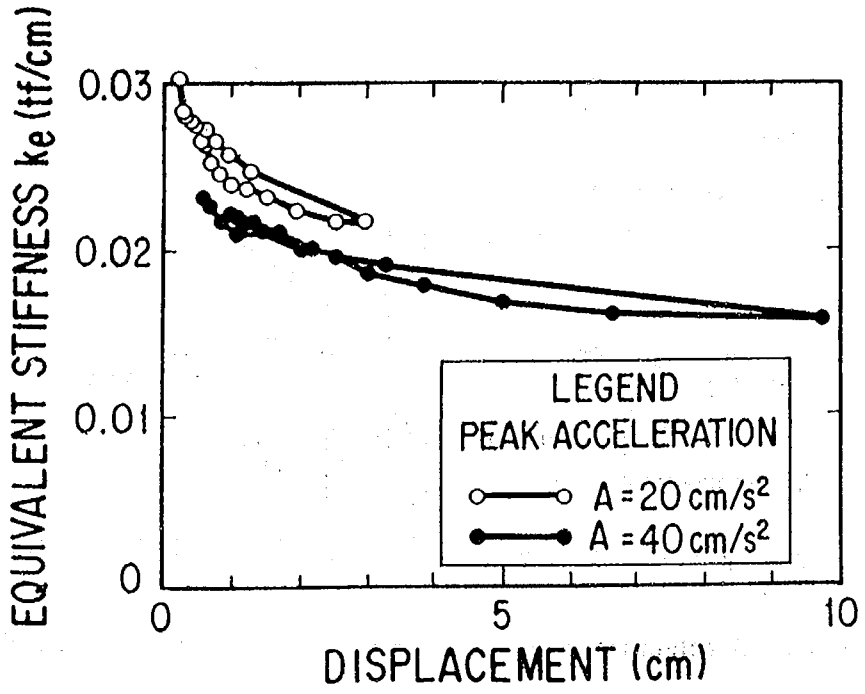
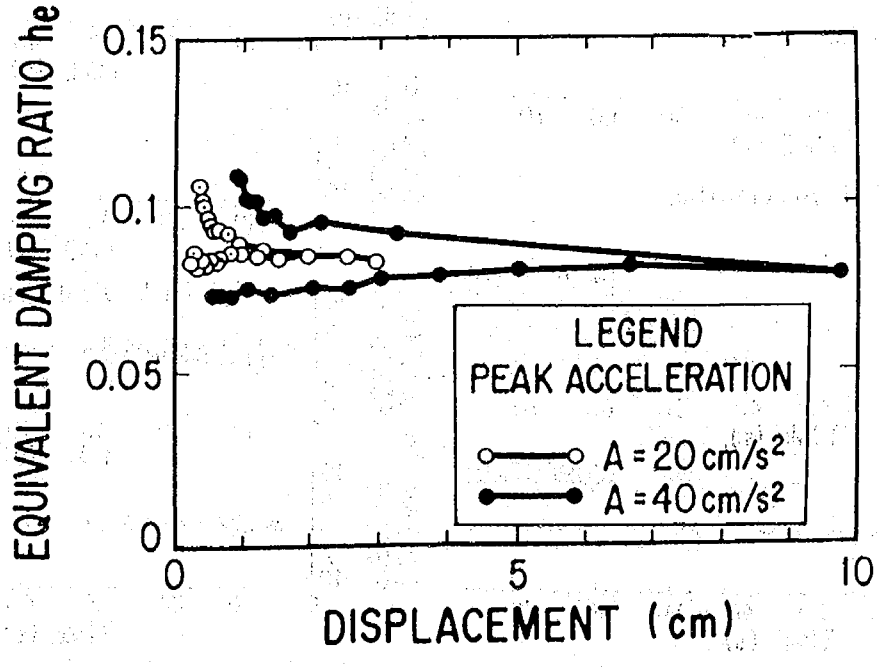


Fig.11 Hysteresis Loop of Load-Displacement Relation of Rubber Bearing



(1) Equivalent Stiffness



(2) Equivalent Damping Ratio

Fig.12 Equivalent Stiffness and Equivalent Damping of Rubber Bearing obtained through Harmonic Excitation Test

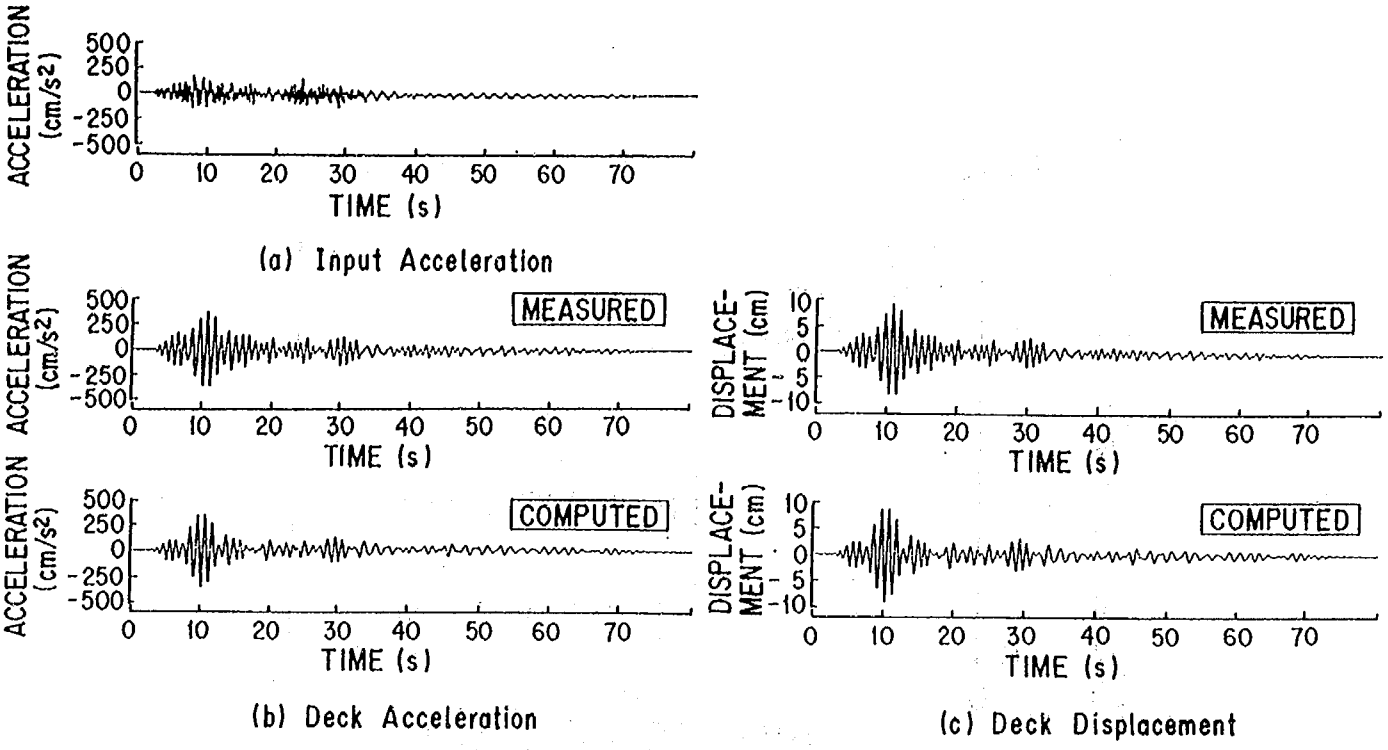


Fig.13 Responses of the Model Bridge without Control

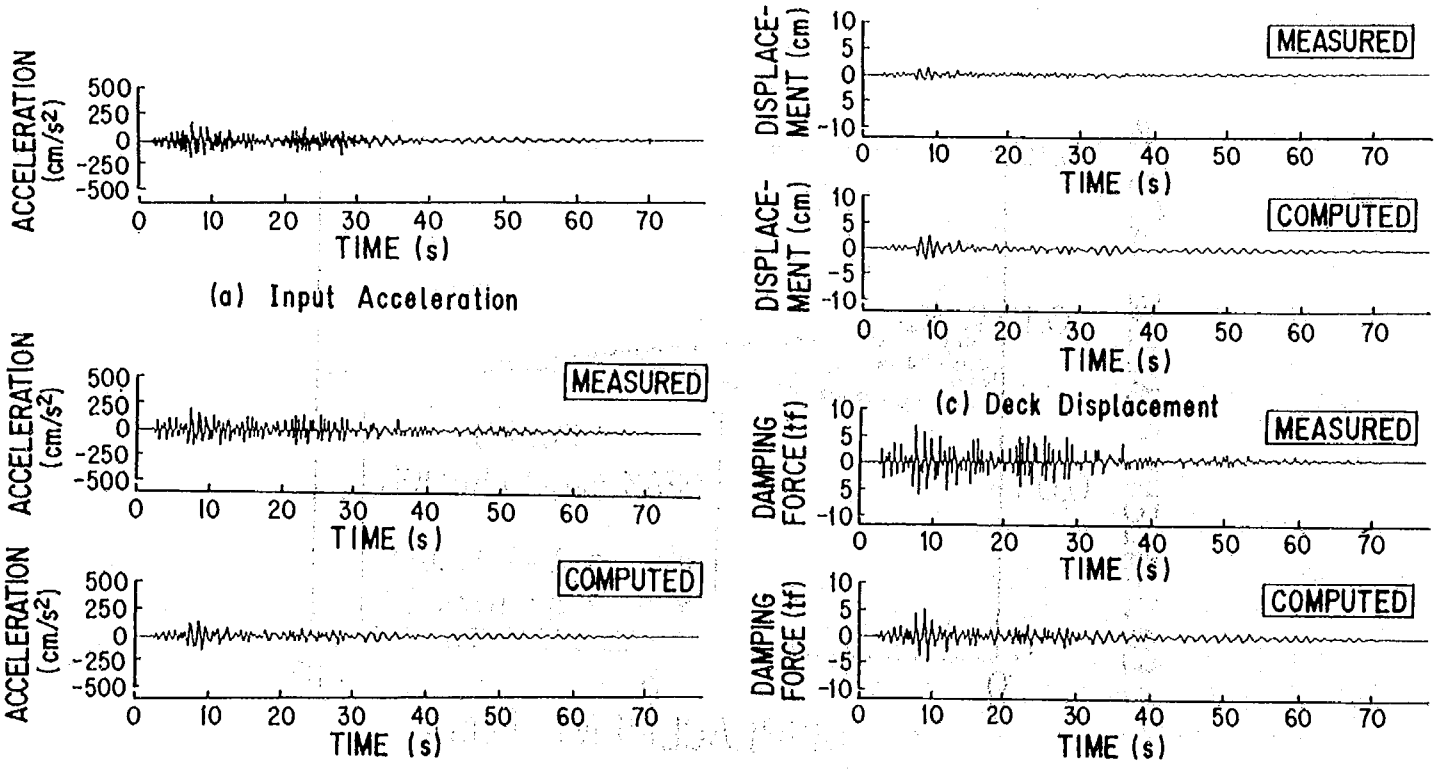


Fig.14 Responses of the Model Bridge with Control against a Table Motion with Peak Acceleration of 200cm/s²

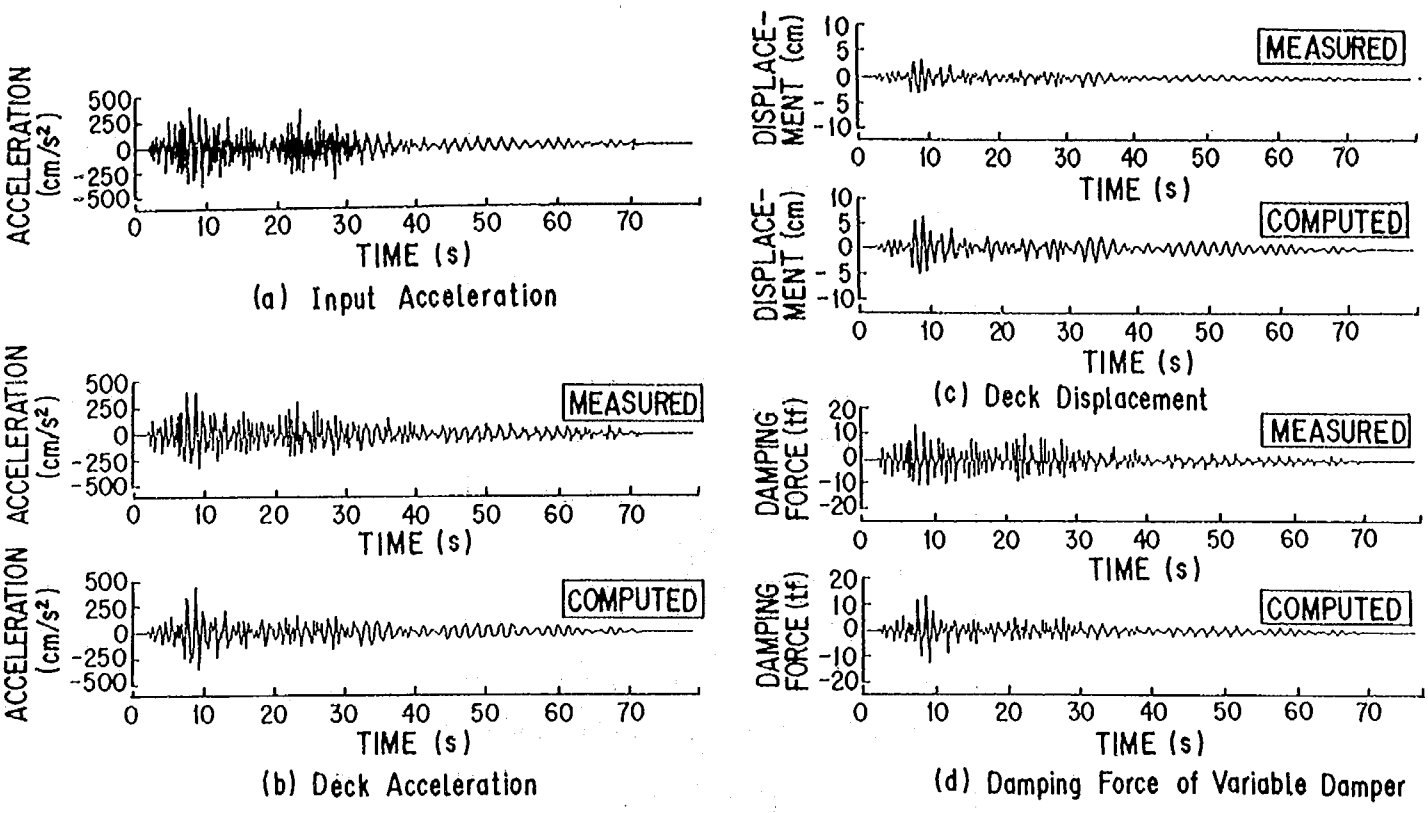


Fig.15 Responses of the Model Bridge with Control against a Table Motion with Peak Acceleration of 500cm/s^2

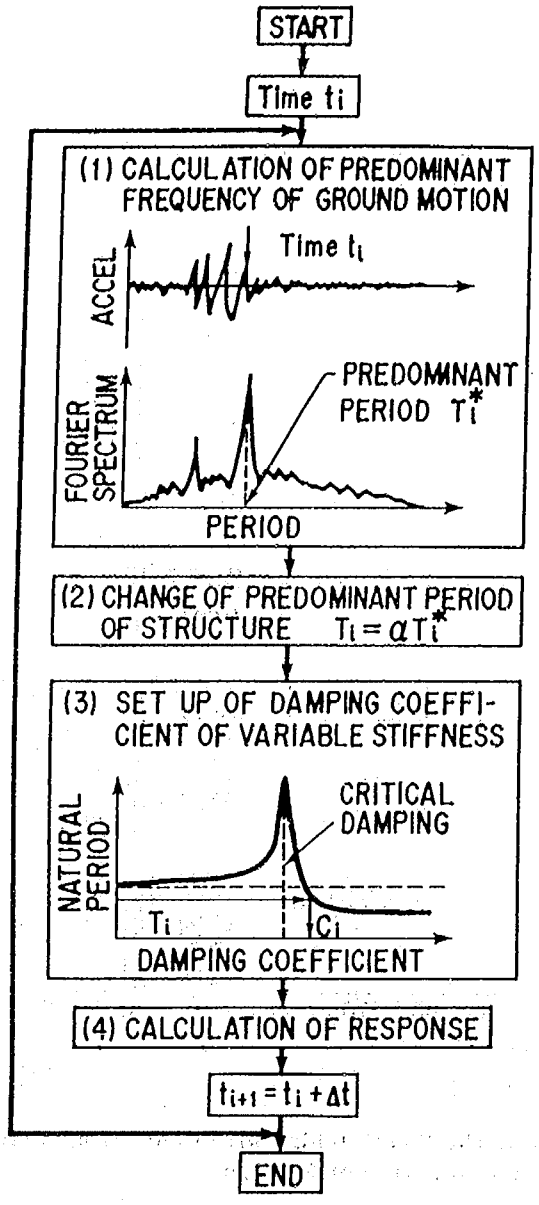


Fig.16 Control Algorithm of Variable Stiffness

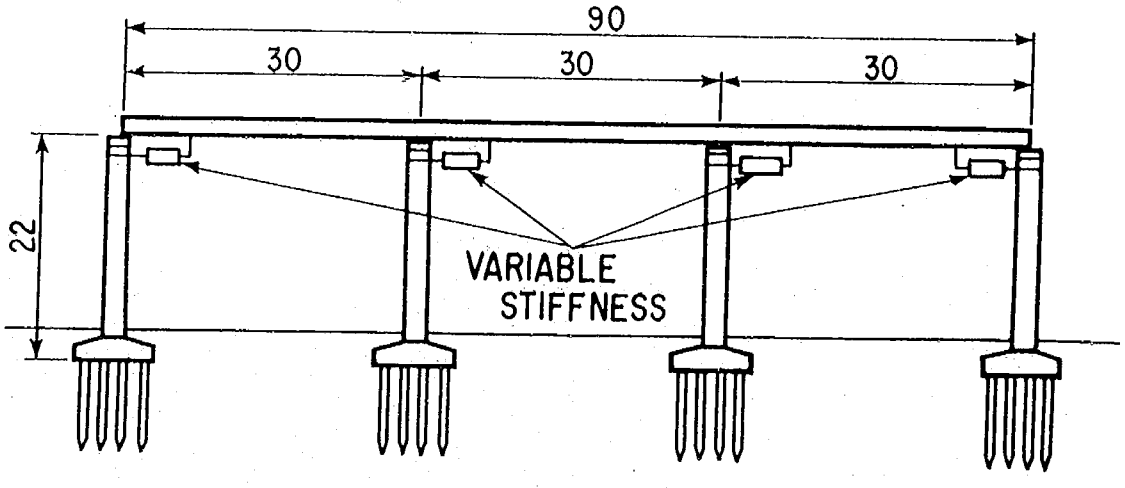


Fig.17 Model Bridge Analysed

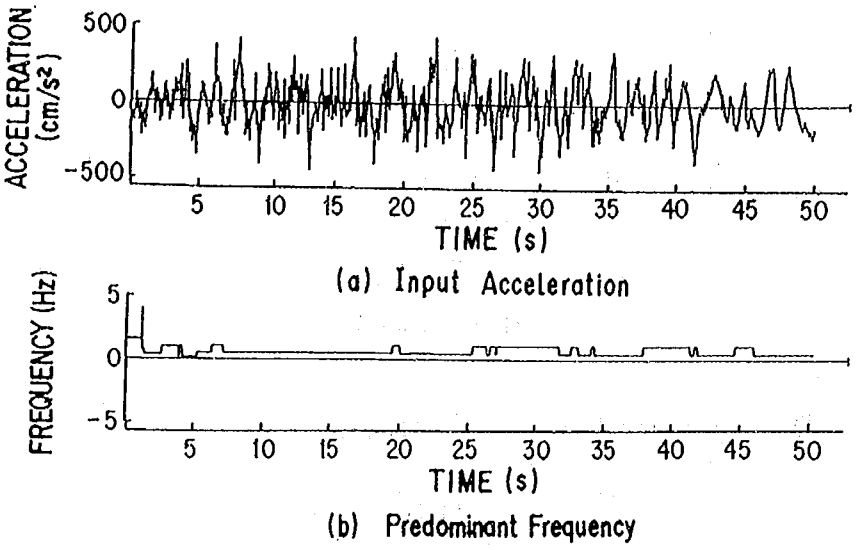


Fig.18 Input Acceleration and the Predominant Frequency

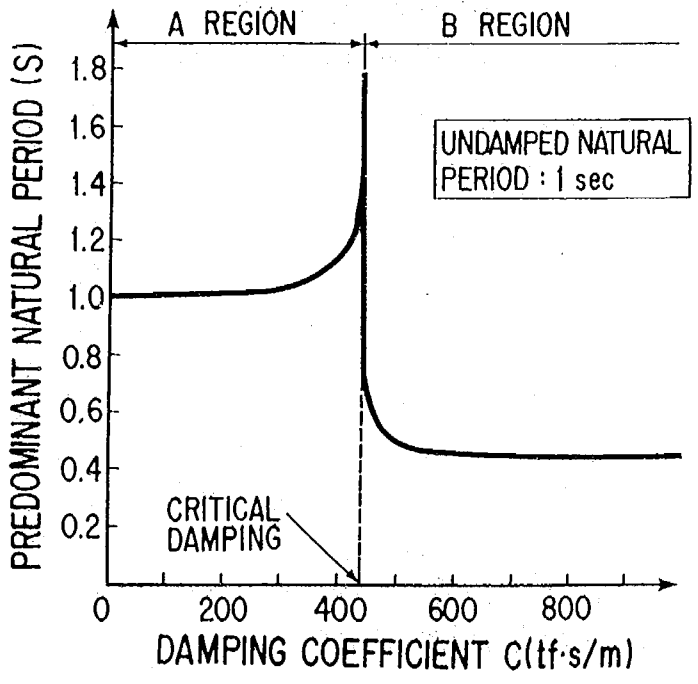


Fig.19 Relation between Damping Coefficient of Variable Stiffnesses and Predominant Natural Period of the Bridge

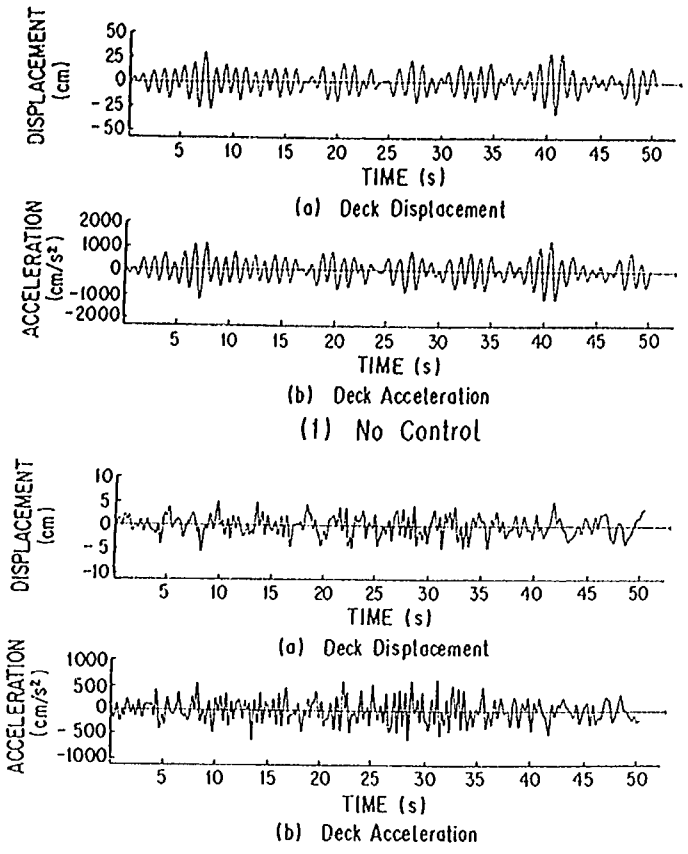


Fig. 20 Comparison of Deck Responses

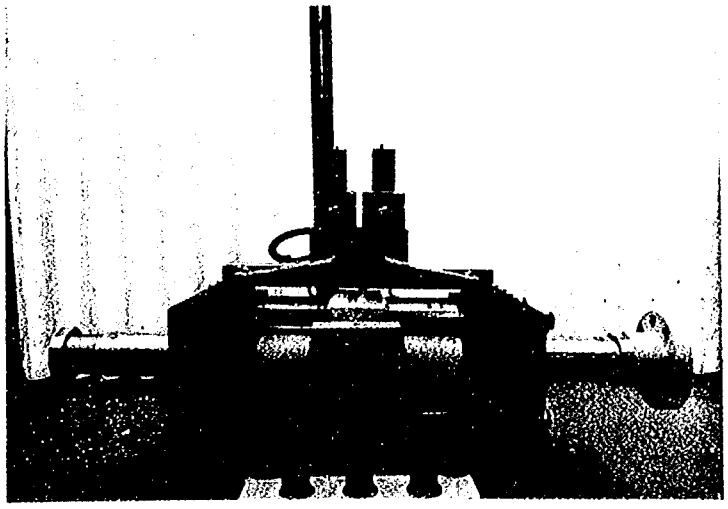


Photo 1 Prototype Model of Variable Damper Developed



Photo 2 Set up of Shaking Table Test

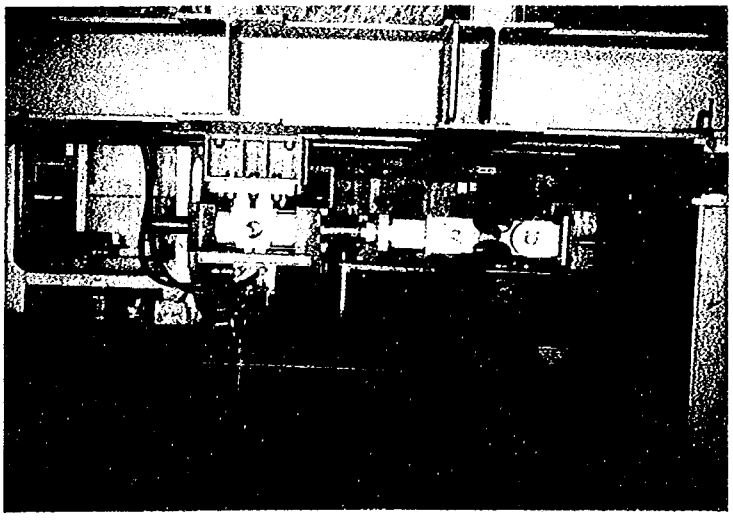


Photo 3 Set up of Variable Damper

Manuscripts Authored for Panel Meeting But not Presented Orally

Wind Resistant Design of Light-Frame Buildings

by

Ronald W.Wolfe[1]

ABSTRACT

Evidence strongly suggests that the extent of damage due to Hurricane Andrew was not due to an inherent weakness in light-frame wood construction. There is still some question as to the magnitude of wind forces that accompanied this storm, but there is general agreement, that with few exceptions, fastest mile wind speeds were within 5% of the design wind, giving wind forces within 10% of design load. Failures were due primarily to misapplication of connections and missile damage.

Damage surveys suggest the need for critical review of light-frame building design and construction methods. Improved performance of roofing and roof sheathing connections would have a significant impact on reducing the $13.4 billion of insurance claims. Other common problems included failures due to roof overhangs, missile damage, and inadequate interaction between internal and external wall systems.

KEYWORDS: design,; light-frame buildings; Hurricane Andrew; wind damage.

1. INTRODUCTION

Insurance statistics show that in the United States hurricane damage to buildings occurs at a rate of 0.1% of the assessed value of insured structures per year. Tornados account for 0.05% of assessed value and severe wind (less than 64 knots; 33 m/s) for 0.0006%. Thus, while hurricanes are confined to coastal regions of southern and eastern states bordering the Gulf of Mexico and the Atlantic Ocean, they do twice the damage of tornados and over 160 times the damage of severe winds.

---

[1] Research Engineer, United States Forest Service, Forest Products Laboratory, Madison, WI53705-2398 USA

As the population density along the these coastal regions of the U.S. increases, the probability of a storm that tests the limits of the design codes hitting a heavily populated area also increases. Hurricane Andrew is a good example of such an event.

Andrew hit southern Florida in August 1992. Despite the fact that the Southern Florida Building Code (SFBC) was recognized at the time as having the most stringent wind load provisions in the U.S.(CLRB, 1991), this storm did extensive damage to a heavily populated area. Fastest mile winds for this storm, in the range 49-56 m/s (110 to 125 mph), were not substantially beyond the design wind for the area. However, the winds heavily damaged 115000 homes, left ¼ million people homeless and resulted in $13.4 billion in insurance claims (Edmondson, 1992).

It is important that every effort be made to determine why damage was so extensive and what can be done to prevent it from happening again. Projecting to future events of this magnitude makes justification of costs involved with policy review and research and development to improve wind resistance seem trivial.

The objective of this paper is to review the damage to light-frame structural assemblies observed following Hurricane Andrew's pass through southern Florida in August of 1992, provide some assessment as to why the damage was so costly, and summarize recommendations of the light-frame construction industries regarding design and construction methods to minimize the effects of similar occurrences in the future.

2. LIGHT-FRAME BUILDINGS

The term light-frame is generally applied to assemblies framed using dimension lumber with a nominal thickness of 51 mm (2 inches). Most residential structures and a large portion of the light commercial buildings in the U.S. fall in this category. In the region of Dade County, Florida, where Hurricane Andrew hit, most of the houses built over the past 20 years are light-frame. Houses in this region built prior to 1970 appear to have been built mostly using concrete block walls with light-frame truss roof assemblies. The majority of these structures had aspect ratios of height to least width less than 2 with pitched (gable or hip) roofs having slopes in the range from 18° to 30°. Some of the older single story houses had lower slopes around 10° to 14°.

3. WIND PRESSURE

Design wind pressure, as described in the ASCE7 standard and model codes (ASCE 1988), is derived using basic wind speeds, characterized as "fastest mile" winds, having a 50 year recurrence interval or a 2%

chance of being exceeded in any 1 year period. Figure 1 shows the 50-year recurrence wind speeds for various areas of the continental U.S.. This map does not include any tornado force winds because tornados have a recurrence interval of 700 years for any square mile area within "tornado alley". Building codes do not include special design considerations for tornados due to their low frequency of occurrence.

Along the Atlantic coast, hurricanes of the size of Hurricane Andrew are considered to have a recurrence of once every 100 years for an area the size of Miami. Data compiled by FEMA (Edmonson,1992), (figure 2) shows that the occurrence of such winds in heavily populated areas of southern Florida is a common enough occurrence to warrant an exception to the 50 year recurrence. ASCE7 incorporates an importance factor (I) to adjust design (50 year) wind speeds to 100 year speeds for regions within 100 miles of a high wind coastal area. The SFBC, however, requires a design basic wind speed of 53 m/s (120 mph), roughly equal to the 100 year recurrence wind (figure 1) with no importance factor. This is noted as being the largest design wind speed in the U.S. (Edmondson,1992).

This basic wind speed, measured at 9m (30 ft) above the ground, is converted to a velocity pressure (q_z) using the dynamic pressure formula derived from Bernoulli's equation for ideal fluids (ASCE7).

$$(a)\quad q_z = 0.00256 K_z (IV)^2 \qquad (1)$$

$$(b)\quad q_z = 0.61334 K_z (IV)^2$$

where

q_z = velocity pressure (a =lb/ft^2, b= Pa)
V = basic wind speed (a=mph, b=m/s)
K_z = velocity pressure exposure coefficient evaluated at height z
I = importance factor

For the main wind resisting system, the wind pressure p is

$$p = qG_hC_p - q_h(GC_{pi}) \qquad (2)$$

where

q = velocity pressure q_z for windward walls at height z
q_h= velocity pressure for leeward wall and roof elevated at mean roof height
G_h = gust response factor at mean roof height
C_p = external pressure coefficient
GC_{pi}= internal pressure combined with gust response factor

For components and cladding, the wind pressure P is

$$P = q_h(GC_p) - q_h(GC_{pi}) \qquad (3)$$

In the case of components and cladding, q_h is the pressure at mean roof height under exposure condition C, (Appendix) regardless of terrain roughness.

Gust factors (G) account for the additional loading effects

of wind turbulence over the fastest mile wind and dynamic amplification of structures. Values applicable to low-rise buildings (ASCE,1988) range from 2.36 for 0-4.5 m (0- 15 ft) above ground in large city centers (exposure A) to 1.12 for 9 m (30 ft) above ground in unobstructed coastal areas (exposure D).

Accounting for a factor of safety of 2 on the wood design value, the wind gust velocity accounted for by the ASCE7 gust factors would range from 1.5 to 2.17 ($(2*1.12)^{.5}$ to $(2*2.36)^{.5}$) times the basic wind speed, depending on design exposure conditions. This suggests that even in the surge zones, buildings designed and constructed to meet requirements of the SFBC should have withstood gusts up to 80 m/s (180 mph).

The shape of low-rise buildings also gives rise to stress concentrations resulting from turbulence and wind shedding along edges and sharp transitions between adjacent surfaces. The ASCE7 code provides pressure coefficients to adjust for surface pressures on the roof and walls as a function of building aspect and roof slope.

Pressure coefficients, combined with gust response factors (figure 3) in equations (2) and (3), are used to account for local pressures at wall corners, eaves, roof corners, and ridges. For roof pitches in the range commonly used for residential structures in the Miami area, wind forces oriented normal to the ridge of the roof will cause uplift over both windward and leeward surfaces (figure 4).

Given the conservative nature of the SFBC, the news media (Pauley, 1992) have focused attention on issues of code enforcement. In looking at the causes of damage, it does seem that enforcment of the codes may be partially to blame, but there is also some need for standards revision.

4. COMMON CAUSES OF DAMAGE

A major portion of the damage due to Hurricane Andrew resulted from one or more of four basic weaknesses in the building construction. These weaknesses involved the attachment of roofing to the roof sheathing, the sheathing attachment to the roof framing, rake overhang details, and attachment of internal partitions to the external walls. Damage resulting from flying debris or missiles that penetrated the outer shell of many buildings also contributed significantly to the extensive damage and to system failures.

a. Roofing

Most houses surveyed (Meeks, and others, 1992, Keith and Rose,1992) had roofing either partially or totally stripped from the roof. This loss, accompanied by 25 cm (10 inches) of rain that fell in the storm and rain that fell in the weeks following the storm, left many buildings extensively water-damaged. Water seeping through the gaps between the sheathing saturated insulation and ceiling drywall, causing it to collapse. Damage to interior finish materials was extensive, even for houses that lost nothing other than the roofing.

In many cases, composition shingles (asphalt or fiberglass) were fastened to the roof over "15-lb" (.73 kg/m^2) felt using pneumatic staple guns. Once the wind managed to lift one layer of shingle tabs, the shingles act as a sail, bending at the attachment and tearing it away. In a number of cases, the shingles were completely stripped from a roof while the felt, fastened with a nail or staple through a light gauge sheet metal plate 5 cm in diameter remained in place (Figure 5). Staples left in the sheathing attest to the fact that the staples pulled through the shingles.

Asphalt shingles were not the only form of roofing removed from buildings (figure 6). The clay or cement tiles of some houses were also either partially or totally stripped. These types of roofing were applied using cement mortar on an 80-lb (3.89 kg/m^2) felt which was "hot mopped" to the roof. While these roofs still functioned to shed most of the water, the missiles they released did extensive damage to neighboring houses.

b. Roof Sheathing

The second most common problem was the loss of roof sheathing. In the majority of cases, the loss of sheathing coincided with high pressure areas such as eaves and ridges. Several reports (Meeks, and others,1992; Keith and Rose, 1992) attributed this to inadequate nailing. The SFBC required 6d common nails spaced 15 cm (6 inches) on center along panel edges and 30 cm (12 inches) on the interior. In some cases, this pattern was not followed; in other cases, there was some evidence for nail-head pull-through. Some nail-head pull-through may have been due to the smaller nail- head common on pneumatically driven nails.

Openings in the building shell also contributed to sheathing losses. Openings on the windward side of a building will result in pressurization (figure 7). Internal pressure, coupled with external suction, adds to the withdrawal force on sheathing fasteners. This is accounted for in equation (3) provided the correct combined gust and pressure coefficients (figure 3) are applied. When the

openings are on the leeward side of the building, the result is a drop in pressure on the interior, which can pull ceiling materials away from the framing.

Openings commonly found were due to missile damage as well as failure of garage and patio doors. In most cases, holes made by missiles were on a windward roof slope. However, unprotected windows were also a prime target. Steel garage doors were often knocked out of their tracks or the tracks were detached from the building frame. Some patio doors were apparently installed with an insufficient number of fasteners, causing the doors to be blown out of the wall frame. In all cases, such breaches of the external shell opened the buildings to wind-blown debris and pressurization.

c. Roof Overhangs

A roof configuration detail that often led to extensive damage was the overhang along a gable end on the windward end of the building. Such overhangs often range from 23 cm (9 inches) to 0.61 m (2 ft). In addition to serving an aesthetic function, the overhangs shade the building windows and finish from the sun and rain. Heavy winds, however, apply uplift force on these overhangs and in some cases tear the overhang off. When this happens, the first row of roof sheathing is normally taken off, opening the building to wind-blown debris and rain. The end sheathing often serves as bracing for the gable end as well. When it is removed the gable end may fall.

Two types of overhang configurations are commonly employed in gable end roofs (figure 8): the "ladder" and the "lookout" detail. The ladder, commonly used for overhangs less than 0.30 m (<1 ft) in length, consists of two rails face-nailed to the ends of dimension lumber "rungs" to form what looks like a ladder. This is then face- nailed along the upper edge of the gable end to form the "rake" overhang. The lookout detail, commonly used for overhangs >0.30 m (>1 foot), consists of "lookout rafters" end-nailed to the first rafter or truss top chord and extended across the top of the gable end. In this case, the top plate of the gable end is lower than the top of the rafters by the depth of the lookout. For this reason, some contractors call this a drop gable detail. The lookout rafters are fastened to the gable end using steel straps or wind clips and a "fly rafter" is face-nailed to the ends of the lookout rafters.

d. System Interactions

System interaction is an important factor when evaluating the performance record of light-frame residential structures. Despite the fact that interior walls are often considered to be nonstructural, they do provide lateral support for the exterior "structural" shell. A 10-m (30-ft)-long

127-mm (5-inches)- thick by 2.4-m (8-ft)- high shear wall that is connected only at its ends has insufficient lateral stiffness to resist an outward or inward thrust caused by wind pressure.

A number of the newer buildings surveyed in southern Florida had steel studs for interior partition framing. These partitions had gypsum wallboard attached to the steel frames, which consist of 20-gauge steel studs screwed to light-gauge steel top and bottom plates. A number of houses that had walls blown out had steel stud partitions that were apparently not attached to the outside wall (Figure 9). These buildings lacked the system redundancy traditionally relied on for structural resistance to wind pressures.

5. CONSTRUCTION RECOMMENDATIONS

The roofing industry has responded to criticism about the performance of composition shingles by pointing out proper application methods for heavy wind areas. In these areas, they recommend that roofing cement be used to seal the edges at the roof eaves and rakes (figure 10). They recommend the use of six roofing nails/ shingle rather than four nails or staples.

As for sheathing attachment, a recent study conducted by the American Plywood Association (Cunningham, 1993) suggests that the current nailing recommendation of the SFBC needs to be modified to resist the forces of a 53 m/s (120 mph) wind. These results appear to be substantiated by data collected in Dade County as well as by tests of panels over a vacuum chamber. The results of this study support changing recommended nailing schedules to require 8d nails spaced 15 cm (6-inches)on center throughout the panel with nails 10 cm (4-inches) on center over the gable end and 15 cm (6-inches) on center over 2x4 girts used to tie the two end trusses to the gable (figure 11). The result of this change will be about a 50% increase in the cost of nails.

To help prevent pressurization caused by missiles breaking through windows, it is recommended that houses be built with shutters that can be locked shut over the windows in the event of a hurricane. Taping windows before the storm hit helped alleviate the problem of shattered glass, but it did not prevent breakage. Some people who put plywood over their windows did not fasten it adequately, thus adding to the problem of flying debris. It is important to have a dependable shield over windows.

Patio doors should be properly nailed to the wall frame to prevent them from being blown in. A patio door with an area of 3.7-m^2 (40 ft^2), under a pressure of 2.4kPa (50 lb/ft^2) (windspeed = 53 m/s) must resist a force of 276-N (2000 lbs)

(NFPA,1991). Patio doors are normally installed in an opening which is 12 mm larger than the door frame, by nailing through wood wedges placed between the door jamb and the framing to compensate for a slightly out of square opening. Using a 16d casing nail with a design lateral resistance of 26 N (192 lbs) in southern pine, nail/wedge connections spaced 50 cm (20 inches) apart around the perimeter of the door jamb would be needed to adequately resist the lateral pressure.

Interior partitions should be attached to exterior walls to provide lateral support against outward pressure. Gypsum wallboard attached to wood framing has been shown to have a racking resistance in the range of 4.53-N/m (100-lbs/ft) (Wolfe,1983). This may not be applicable to steel framing, which is more prone to twisting and buckling, but it should be evaluated. If gypsum on steel framing does not provide adequate diaphragm stiffness, the steel frames should be built with diagonal bracing and rigidly attached to exterior walls.

6. FUTURE DEVELOPMENT

Other topics that may require further research deal with aerodynamic designs of buildings in heavy wind areas. Many people feel that the hip roof is better suited to these areas than a gable end because the framing at the end of the building is tied together better and the form of the hip does not incur the turbulence encountered by a gable end. Rounded structures such as Geodesic Domes generally perform better than rectangular pitched roof structures in heavy wind areas. It may be advantageous to develop arched roof shapes with continuous membranes or to explore further development of foam roofing which rigidly adheres to the roof sheathing, offering few discontinuities in the surface.

7. CONCLUSIONS

In light of the individual as well as societal costs incurred as a result of Hurricane Andrew and future projections regarding population growth in coastal areas, it is important that we act now to correct and rigidly enforce design and construction standards for light-frame structures in high wind zones.

Problems that have received the greatest attention can be fixed fairly easily with minor increase in the cost of construction relative to the cost of repair. Improvements include better attachment of roofing and sheathing materials, overhang connections that are more resistant to uplift forces, increased awareness of the potential for poorly attached components to become damaging missiles, and better details for attaching interior partitions to exterior walls.

APPENDIX A

Exposure A: Large city centers with at least 50% of the buildings having a height in excess of 70 ft.

Exposure B: Urban and suburban areas, wooded areas or other terrain with numerous closely spaced obstructions having the size of single family dwellings or larger.

Exposure C: Open terrain with scattered obstructions having heights generally less than 30 ft.

Exposure D: Flat, unobstructed coastal areas directly exposed to wind over a large body of water.

References

ASCE, Minimum Design Loads for Buildings and Other Structures, ASCE 7-88, American Society of Civil Engineers. New York, NY 1988.

CLRB, Guidelines for Design of Low Rise Buildings Subjected to Lateral Forces, Council on Low Rise Buildings, North Carolina State University, 1991.

Cunningham, T.P. Jr, Roof Sheathing Fastening Schedules for Wind Uplift, APA report T92-28, 1993.

Chow,P., McNatt, J.D., Lambrechts,S.J. and Gertner,G.Z., Direct Withdrawal and Head Pull-Through Performance of Nails and Staples in Structural Wood-Based Panel Materials, Forest Products J., Vol.38(6), 19-25, 1988.

Douglas, B.K. Hurricane Andrew: Part 2. Wood Building Analysis and Recommendations, Report of the National Forest Products Association, Nov. 1992.

Edmondson, S.C. Hurricane Andrew, The Building Official and Code Administrator, Nov./Dec. 1992, pp. 40-51.

Fujita, T.T., Tornados Around the World, Weatherwise, Vol. 26(2), 56-83, April 1973.

Keith,E.L., and J.D.Rose, Hurricane Andrew: Structural Performance of Buildings in Southern Florida (August 24, 1992), American Plywood Association, Report T92-21, Sept. 1992.

Meeks, J.E., Riba, R. and Triche, M.H., Performance of Metal Plate Connected Wood Truss Roof Structures During Hurricane Andrew, Truss Plate Institute, 1992.

National Forest Products Association, National Design Specification for Wood Construction, NFPA, Washington, D.C. 1991.

Pauley, J. Design for Disaster, NBC Date Line, Oct. 6, 1992, Burrelle's Information Services, Box 7, Livingston, NJ, 07039.

Wolfe, R.W., Contribution of Gypsum Wallboard to Racking Resistance of Light-frame Walls, USDA Forest Service, Forest Products Lab, FPL 439, 1983.

Figure Captions

Figure 1 Wind speed maps from ASCE7 showing fastest mile wind speeds in mph for 50- and 100- year recurrence intervals.

Figure 2 Summary of hurricanes with winds exceeding 45 m/s (120 mph) along the Atlantic coast from 1886 to 1970.

Figure 3 Gust factor and external pressure coefficients (GCp) from ASCE7 code.

Figure 4 Wind force applied normal to the roof ridge ($\theta \leq 30°$) causes uplift pressure on both the windward and leeward surfaces. Highest pressures occur along the ridge, eaves, and rake.

Figure 5 Shingles were stripped from the roof while felt remained over 60% of surface. Sheathing pulled from high pressure area over rake.

Figure 6 Tiles blown from this roof became air-borne missiles with the potential to damage neighboring buildings.

Figure 7 Openings may cause pressurization or depressurization of a building. Pressurization will push wall panels and roof sheathing out. Depressurization may pull ceilings down.

Figure 8 Common roof rake overhang details. The ladder detail (a) is normally used for overhangs of no more than 30 cm (12 inches). The lookout or "drop gable" detail (b) is used for overhangs extending to 0.61m (2 ft).

Figure 9 Building end wall,9 m (30 ft) long, fastened to the front wall of the building and to a stairway header on the back end. None of the steel-stud interior partitions that framed into the wall was rigidly connected to it.

Figure 10 Shingle attachment recommendations for wind-prone areas.

Figure 11 The American Plywood Association proposed roof sheathing nailing schedule for heavy wind areas.

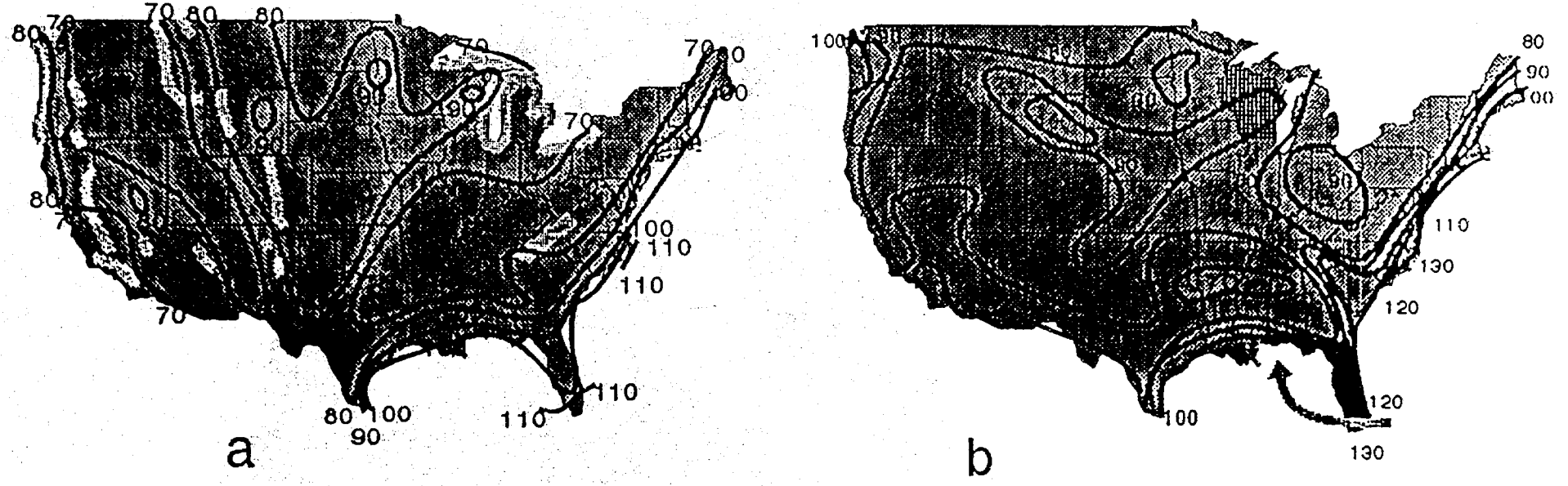


Figure 1 U.S. Wind-speed maps showing fastest mile wind speeds for (a) 50 year and (b) 100 year recurrance

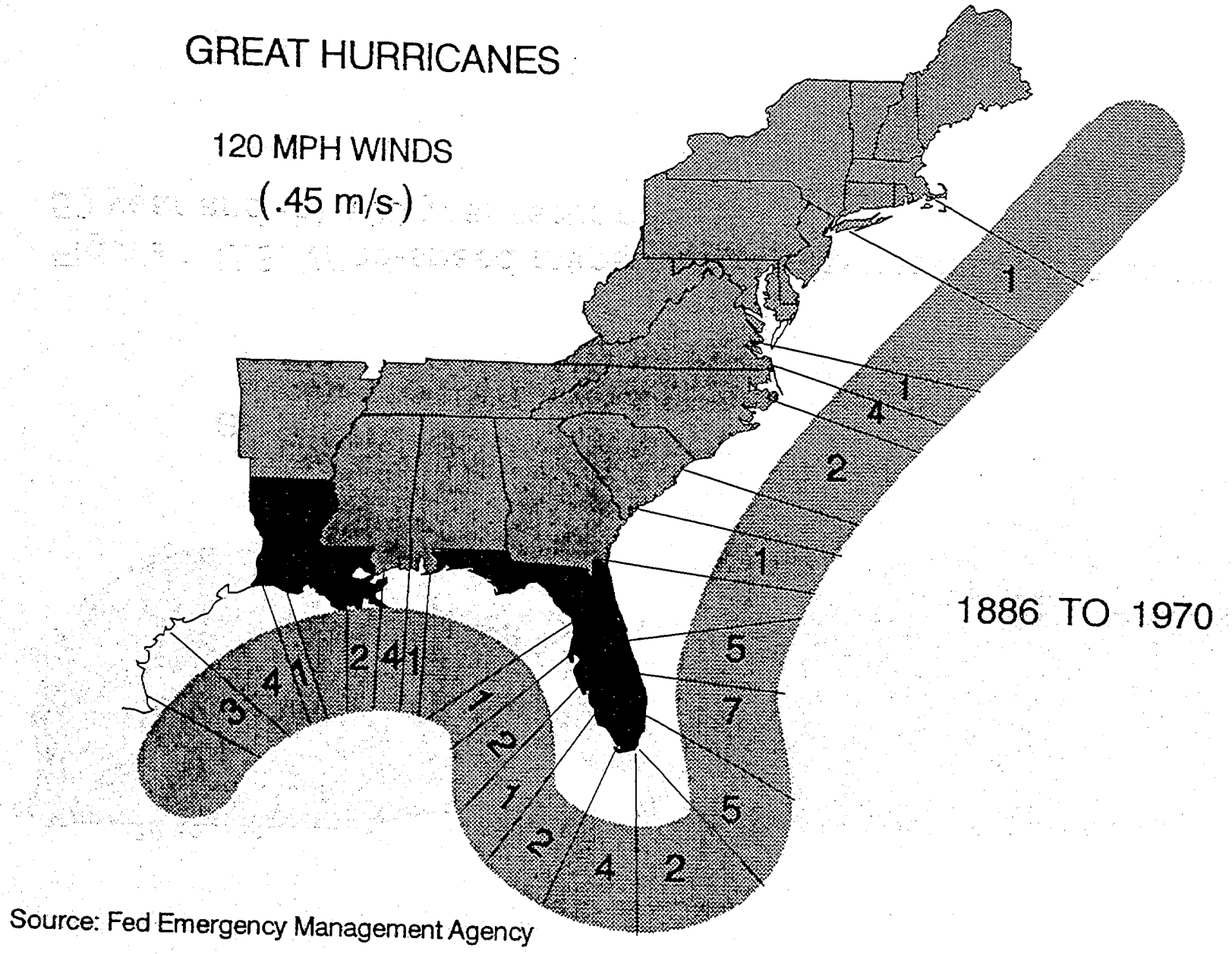


Figure 2 Hurricanes recorded from 1886 through 1992 which had wind speeds greater than 45m/s (120 mph)

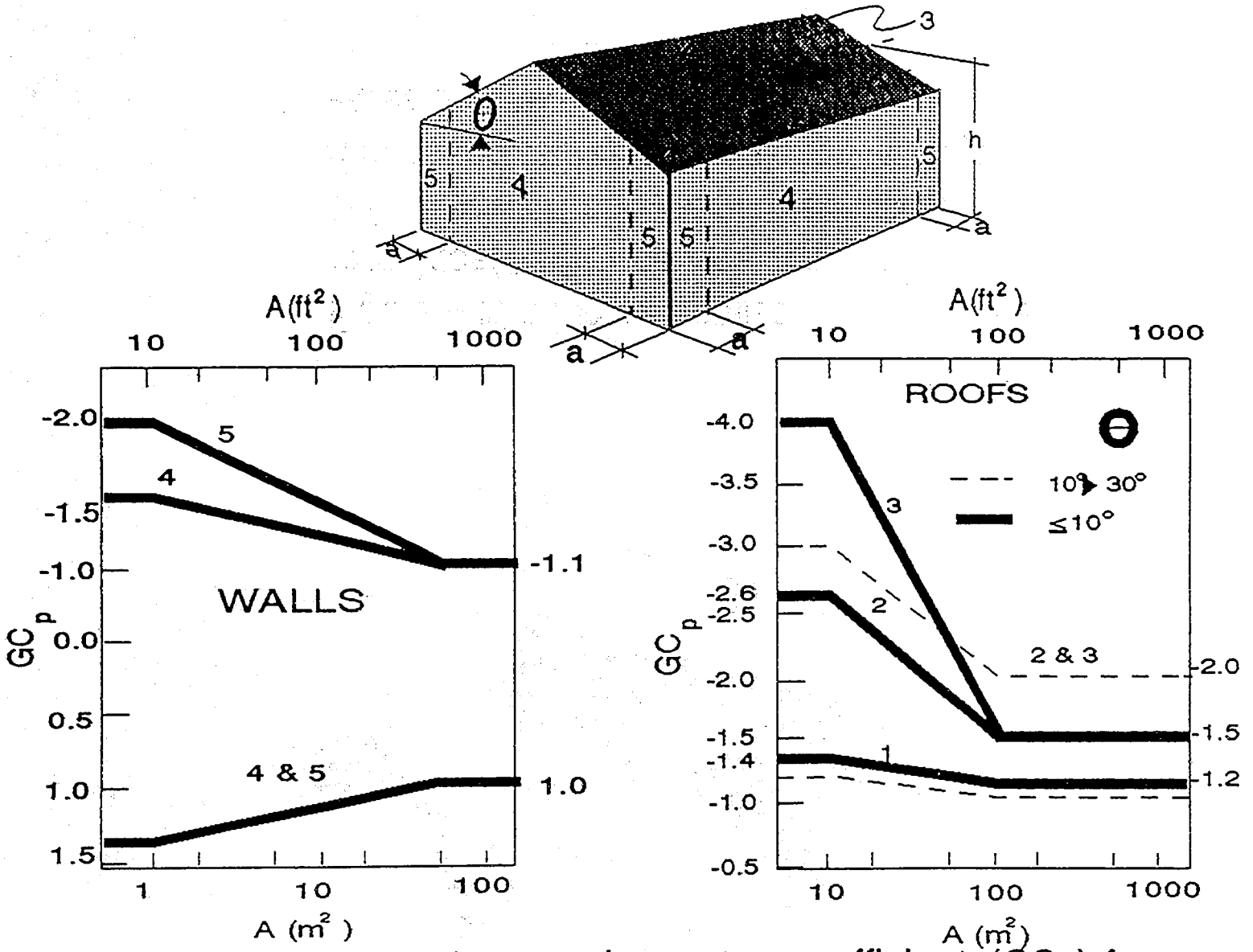


Figure 3 Gust factor and external pressure coefficients(GCp) from ASCE7 code.

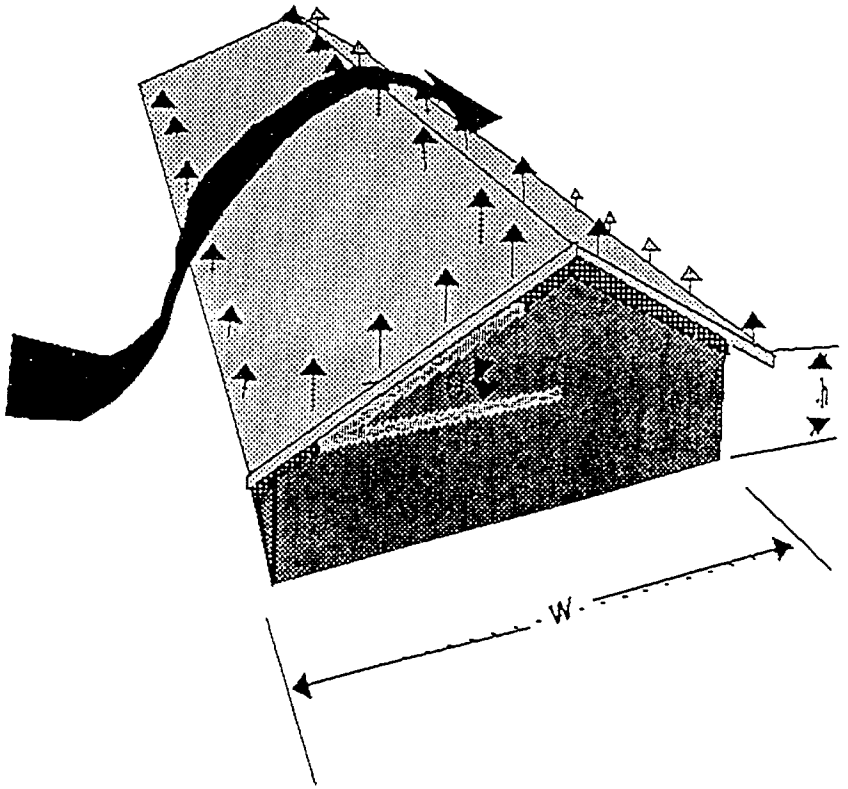


Figure 4 Wind force applied normal to the roof ridge($\theta \leq 30°$) causes uplift pressure on both windward and leeward surfaces. Highest pressures occur along the ridge, eaves and rake.



Figure 5 Shingles were stripped from the roof while felt remained over 60% of the surface. Sheathing was pulled from the high pressure area over the rake.



Figure 6 Tiles blown from this roof become air-borne missiles with the potential to damage neighboring buildings.

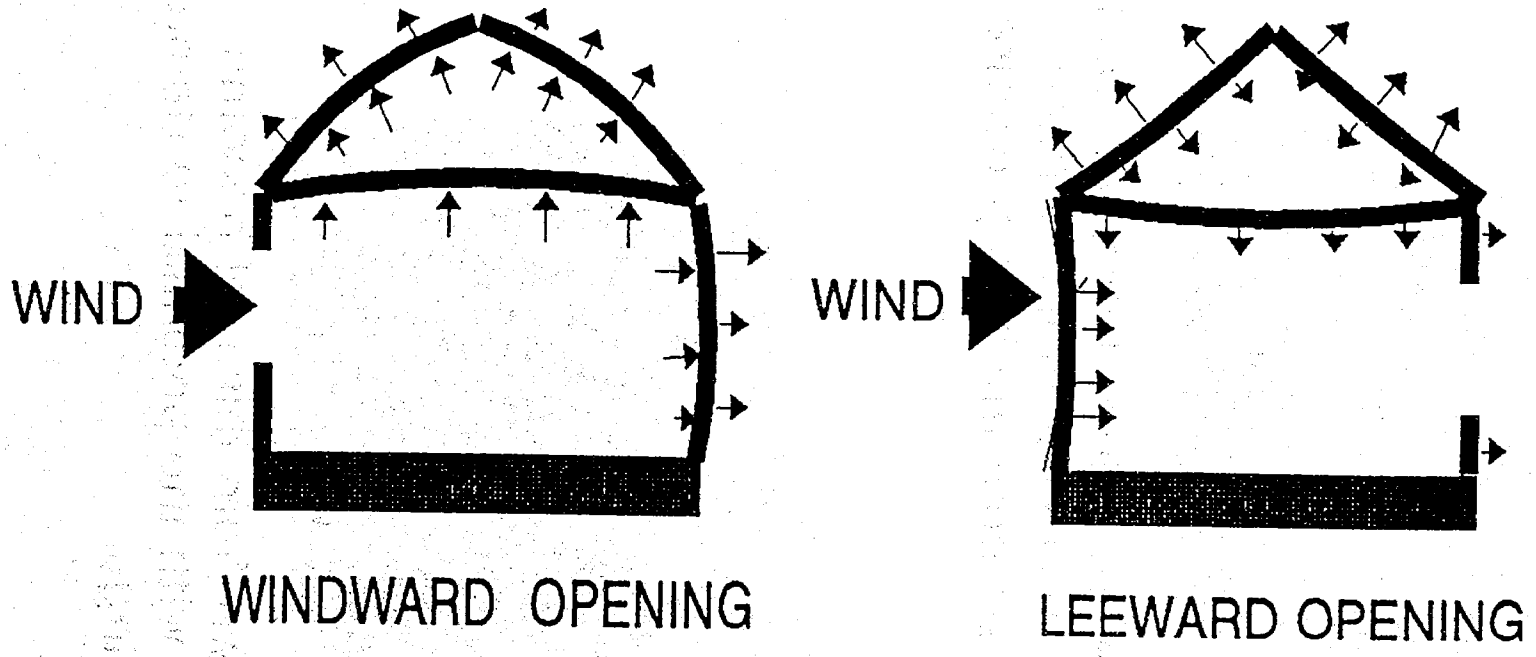
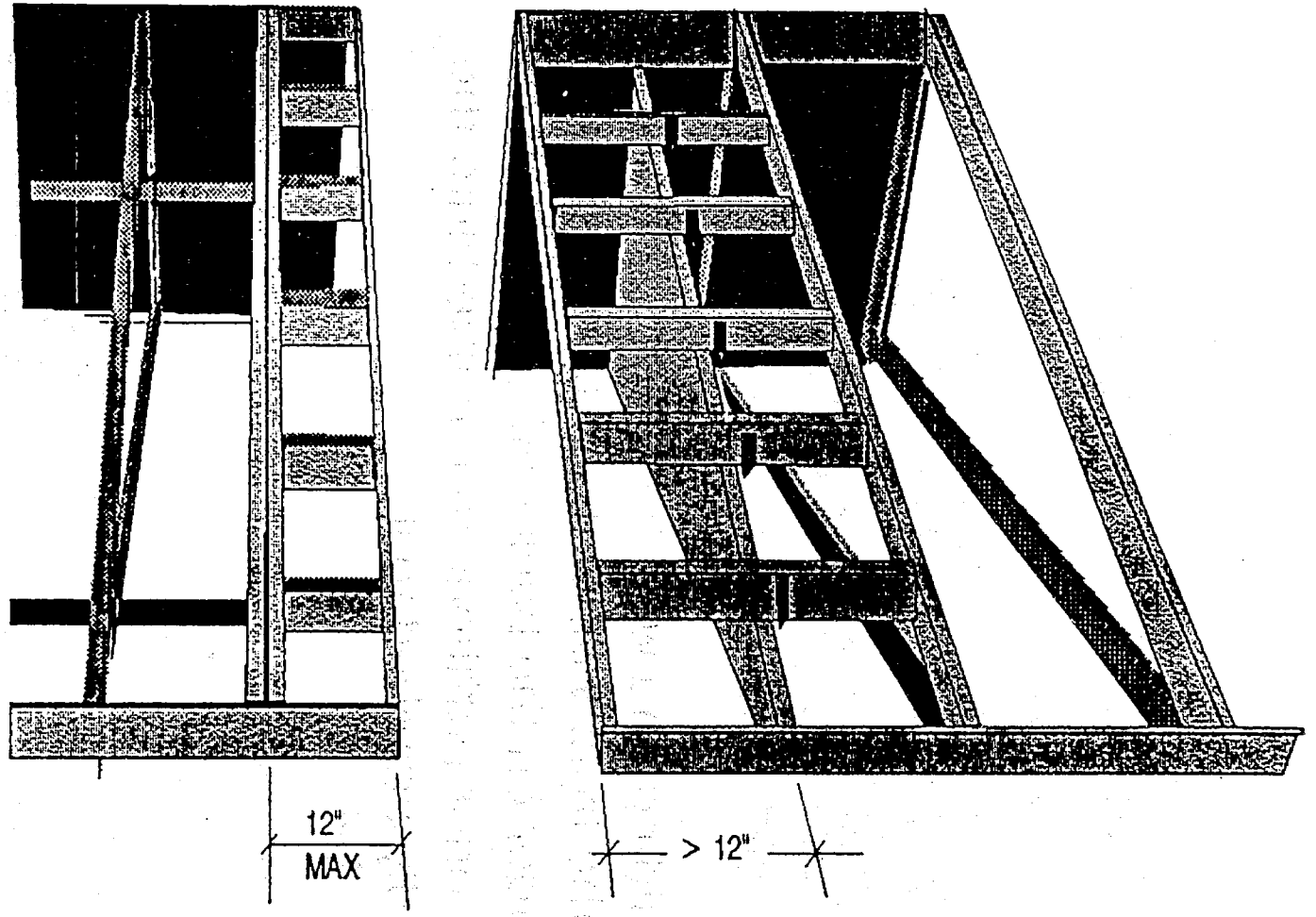


Figure 7 Openings may cause pressurization or depressurization of a building. Pressurization will push wall panels and roof sheathing out. Depressurization may pull ceilings down.



a b

Figure 8 Common roof rake overhang framing details. the ladder detail (a)is normally for overhangs of no more than 30cm(12 inches). The lookout or "drop gable" detail (b)is used for overhangs extending to .61 m (2 ft).

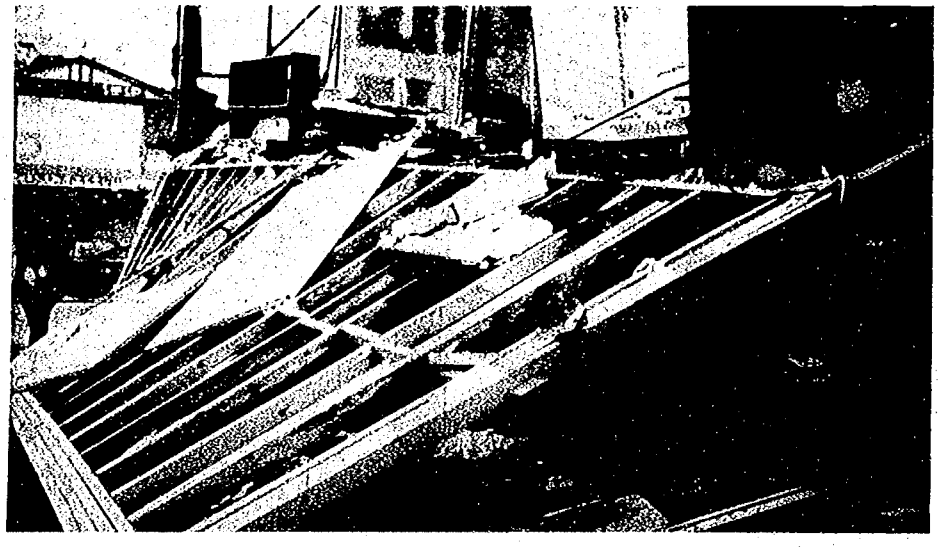
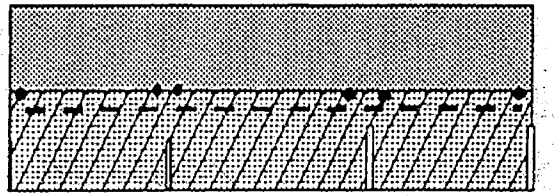


Figure 9. Building end wall, 9 m (30 ft) long, fastened to the front wall of the building and to a stairway header on the back end. None of the steel-stud interior partitions that framed into the wall was rigidly attached to it.



6 NAILS / SHINGLE

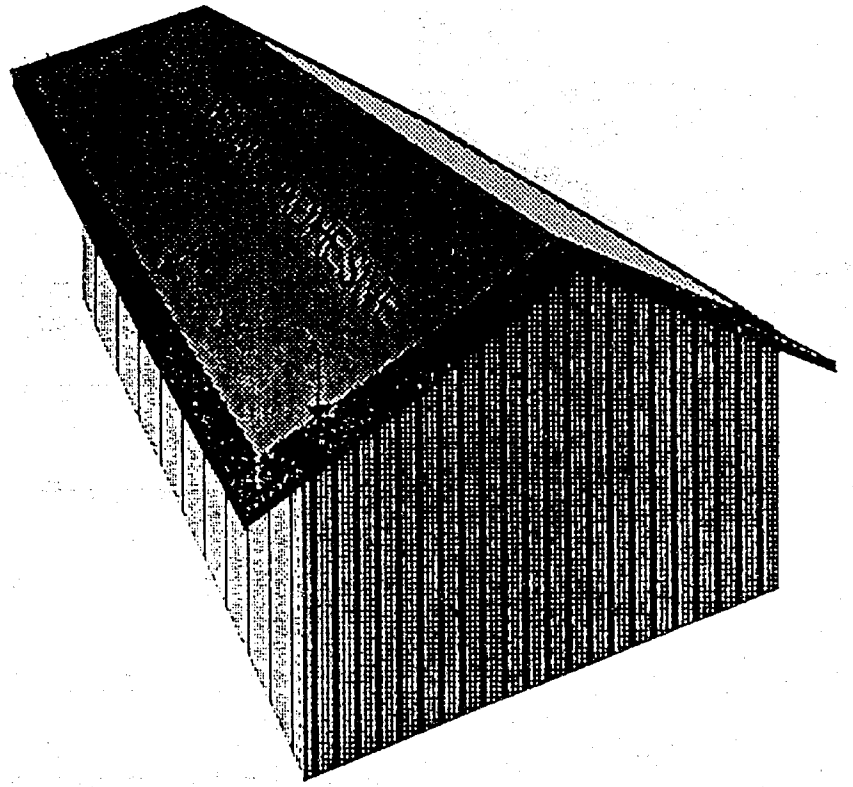


Figure 10 Shingle attachment recommendations for wind-prone areas

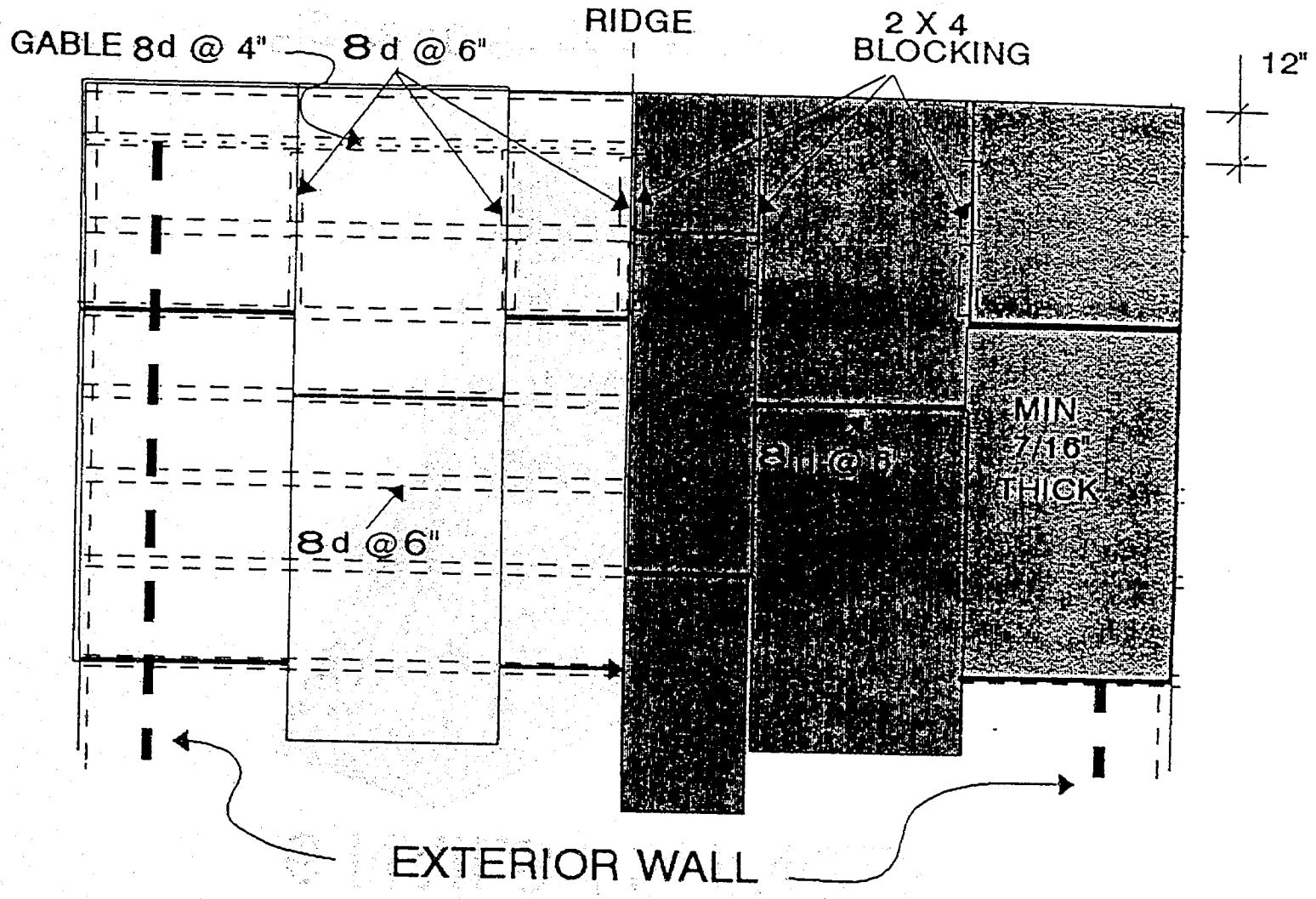


Figure 11 The American Plywood Association proposed roof sheathing nailing schedule for heavy wind areas

LOSS EXPERIENCE FROM WIND AND EARTHQUAKES IN THE DEPARTMENT OF ENERGY

(50 years of Natural Phenomena Hazard Losses)

by

James R. Hill

ABSTRACT

This paper presents a historical perspective on losses due to natural hazard incidents (1943-1993) at Department of Energy (DOE) and predecessor agencies including the Atomic Energy Commission (AEC) and the Energy Research and Development Agency (ERDA). This paper also demonstrates how an existing DOE resource can be used to gain valuable insight into injury or property damage incidents. That resource is the Computerized Accident/Incident Reporting System (CAIRS) module of DOE's Safety Performance Measurement System. CAIRS data selected the 1981-1991 DOE injury/illness reports, from all CAIRS property damage or loss reports, and the accident reports of the AEC that cited a natural phenomena hazard as either the direct or indirect cause of the injury/property damage. Specifically, injury or property damage reports were selected for analysis if they had a causal factor link to severe weather or natural phenomena hazard categories. Natural phenomena hazard categories are injury/property damage caused by hurricane/tornado, earthquake, lightning, or flood. Severe weather categories are injury/property damage associated with other than normal weather conditions.

Approximately 3,500 CAIRS and AEC injury or property damage reports were considered to have either a direct or an indirect causal link to at least one of the severe weather or natural phenomena hazard categories. These reports, which represent 1 to 2 percent of the total DOE injury or property damage reports, documented nine deaths (1981-1991) 2,600 injuries (1981-1991), and more than $30,000,000 in reported losses (1943-1993).

The lessons learned, as a result of reviewing case histories, are presented, as are suggestions on how to reduce the likelihood of future injuries/property damage as a result of similar events. A significant finding, is that most injuries and property damage were the result of an indirect causal link to a natural phenomena hazard and thus, may be more preventable than previously thought possible. The primary message, however, is that CAIRS and other incident data bases are valuable resources and should be considered for use by those interested in identifying new ways of protecting the health and safety of the worker and for reducing building losses due to the effects of natural phenomena hazards.

INTRODUCTION

This paper presents a historical perspective on losses due to natural phenomena hazard incidents (1943-1993) at DOE and predecessor agencies including the AEC and the ERDA. Historical information on life and property losses from natural phenomena hazards can provide an insight into the opportunities for reducing the impacts of future losses[1]. Efforts to mitigate natural phenomena hazards have been ongoing for thousands of years, but the complex infrastructure of our current world

requires creative and cost-effective mitigation strategies. This historical view has and continues to support planning for: 1) loss reduction strategies for DOE; and 2) participation in the International Decade for Natural Hazard Reduction[2] and in the United States (U.S.) Decade for Natural Disaster Reduction[3,4].

Another purpose of this paper is to demonstrate how an existing DOE resource, the Computerized Accident/Incident Reporting System (CAIRS)[5] module of the DOE Safety Performance Measurement System (SPMS) can be used to gain insight concerning how and why DOE personnel have been injured or how buildings and property have become damaged as a result of specific natural hazards. Though any number of hazards (e.g., excessive noise, radiation, confined spaces, or toxic materials) could have been selected for this demonstration, we chose to study those DOE injury or property damage cases that were considered to be, either directly or indirectly, attributable to a natural phenomena hazards. For the purpose of this paper, natural phenomena hazards will refer to injury or property damage associated with the traditional categories of natural phenomena (hurricane/tornado, earthquake, lightning, flood, volcano) and will also include injury or property damage associated with severe weather. Severe weather is taken to mean weather conditions other than normal weather conditions for the area (i.e., a 100 year storm is a severe weather condition).

METHODOLOGY

Traditionally, natural phenomena hazards are thought of as catastrophic events, ranging from tornadoes and hurricanes to earthquakes and volcanic eruptions. As indicated, the scope of this study was expanded to include severe weather related events that caused reportable injury or property damage or loss. The focus of the study was on property damage and losses due to natural phenomena hazards. A manual search of records was required for the period 1943-1973[6] and a computerized search was available for records for the remaining years. The injury records were searched for the period 1981-1991, only, to gain an insight into the contribution to total impacts. Note that costs related to (e.g., medical and hospital treatment or lost work days) injury/death and illness are not assigned or maintained for incidents caused by natural phenomena hazards.

Approximately, 3,500 injury or property damage reports from CAIRS and AEC were considered to have a direct or indirect causal link to catastrophic or weather natural hazards categories. These reports, which represent 1-2 percent of the total DOE injury or property damage reports, documented 9 deaths (1981-1991), 2,600 injuries (1981-1991), and more than $30,000,000 in property damage and loss (1943-1993).

For comparison, another DOE study[7] on injury/illness incidents for the period 1981-1991 found 3100 reports with direct or indirect causal links to natural as well as environmental (plant and animal) hazards categories. These reports, representing about eight percent of the total DOE injury/illness reports, documented nine deaths and more than 30,000 lost work days (the equivalence of some $40,000,000). Most of the injuries were caused by weather phenomena.

FINDINGS

DOE property damage for incidents due to natural phenomena hazards reported during the past 50 years (1943-1993) totaled $30 million. Losses due to all phenomena are tabulated by state in Table 1. Losses due to specific natural phenomena hazard are shown in Table 3. The largest incident loss for various natural phenomena hazards are provided in Table 2. Loss data for the DOE power administrations was not readily available;

however, informal estimates indicate annual costs of $500,000 to $1,000,000 per year for retrofit of electric transmission systems due to the effects of wind and other natural phenomena for the Western U.S. Much of the loss occurs in relatively few incidents. A listing of the 31 largest losses to occur in DOE is shown in Table 3, where some losses exceeded $5,000,000 annually. It is felt that the losses reported herein underestimate the real losses to DOE. Some reasons for the underestimate are as follows:

1) dollar values have not been corrected to today's dollar;

2) reporting system leads to some severe weather or natural phenomena injury or property damage events to be reported as other than damage due to the above;

3) over the 50 year period, many older losses were not reported;

4) DOE, as an Agency, has grown over the 50 year period so older reports don't reflect all the facilities currently under DOE responsibilities; and

5) no cost has been allocated to loss of use of a facility.

Looking at just the natural phenomena hazard losses in Table 3 for the years of 1989-1992, the minimum annual cost of injury/property damage to DOE is calculated to be $3.0 million annually. Based upon reported and estimated loss information and the above reasons for underestimate of losses, natural phenomena incidents cause $2-5 million annually in damage to DOE property.

Information is also collected on injuries caused by natural phenomena hazard, but no dollar loss is assigned even where medical treatment and lost work is involved. A comparison of the number of injuries caused by various natural phenomena hazards during a ten year period is given in Table 4. Nine fatalities were reported that were directly attributed to severe weather conditions for the period 1981-1991.

Hurricane damage to DOE facilities is minor compared to the overall U.S. statistics. However, six of the eight hurricanes that damaged DOE sites (Table 5) were among the 31 largest DOE natural phenomena incidents.

The DOE Computer Assisted Incident Reporting System (CAIRS) maintains records of reported incidents caused by fire and other accidents and annual[8] and quarterly[9] statistical reports are compiled for incidents including natural phenomena. Special investigations are conducted for incidents involving fatalities and large property damage.

The DOE manages or operates research, production, oil reserves, and power distribution facilities valued at over $120 billion. These activities are carried on in over 10,000 buildings (>10 sq. meters) in nearly all states. Total new construction averages $1 to $2 billion annually[10].

Losses due to natural phenomena hazards account for about 5 percent of all losses reported from 1943 to 1975. For the period 1984 to 1988 natural losses were one percent of the total incidents but accounted for 20 percent of the total dollar loss. For the period 1990-1993, natural loss damage increased an order of magnitude over all previous years.

A few comments on DOE's upgrading program for natural phenomena should provide a perspective on past losses. The Lawrence Berkeley Laboratory was one of the first DOE sites to complete a site-wide earthquake mitigation program[11]. Including other facilities that would have suffered structural damage, upgrading substandard buildings at LBL saved over $50 million during the Loma Prieta Earthquake[12]. The total cost to upgrade these buildings since 1971 is $4 million. LBL will spend another $10 million over

the next few years to complete its seismic upgrade program in preparation for the great earthquake that is sure to come. In the meantime, the work accomplished thus far has produced large cost savings for the DOE. The LBL experience in the implementation of its seismic upgrading program served as a basis for the development of the Seismic Safety Guide that was prepared for the Office of Safety and Quality Assurance, DOE. This Guide provides managers of facilities with practical guidelines for administering a comprehensive earthquake safety program.

CONCLUSIONS

This presentation provides a perspective of DOE losses during the past 50 years even though loss data was not readily available for all DOE operations. As such, this paper is considered as the starting assessment needed to provide an informed view on key damaging events. Review of the reported historical losses has provided an opportunity to create an awareness of the extent and location of a wide variety of natural phenomena hazards that have caused damage at most DOE sites.

Some observations to consider are:

- Mitigation strategies including design change can achieve reductions in wind damage.
- The cost of repair, upgrade, and related activities after the 1980 Livermore, California earthquake was approximately $60 million, but only $4 million in damage was reported.
- Most damage occurred to conventional construction.
- Lightning damage review may provide insight for design standards change.
- Flood storm water damage occurred where least expected.

The DOE has, and continues to, seek ways of reducing losses that can result from specific acts of nature. Many buildings and other structures have been upgraded, several standards and guidelines have been developed, using "lessons learned" from earthquakes, wind, tornadoes, floods, lightning, and volcanic ash. To date, losses from such acts have resulted primarily in property damage, loss of facility use, in personnel injuries, or death. While death is certainly possible from catastrophic acts of nature, they are much more likely to occur in DOE as a result of one of the less spectacular acts of nature, such as snow, ice, or wind storms.

Other earthquake, flood and wind upgrading programs at several DOE sites were reported at the 1985, 1989, and 1991 DOE Natural Phenomena Conferences[13,14,15] and seismic mitigation activities for DOE have been reported annually to Congress beginning in 1983[16]. The information presented in this paper has assisted in determining upgrading priorities as well as in recommending changes to design standards.

ACKNOWLEDGMENTS

The author wishes to acknowledge the support of Janet Macon for researching DOE's Computerized Accident/Incident Reporting System and other Occupational Injury and Property Damage Reports and to Charles Miller for developing the injury data.

REFERENCES

1. J. H. Wiggens Company, Building Losses from Natural Hazards: Yesterday, Today and Tomorrow, National Science Foundation, 1977.
2. Confronting Natural Disasters: An International Decade for Natural Hazard Reduction, National Academy Press, 1987.

3. National Academy Press, A Safer Future – Reducing the Impacts of Natural Disasters, 1991.

4. United States Geological Service, Reducing the Impacts of Natural Hazards – A Strategy for the Nation, 1992.

5. Department of Energy, Computer Assisted Incident Reporting System (CAIRS), EG&G Data Base, 1993.

6. Division of Operational Safety-USAEC, Operational Accidents and Radiation Exposure Experience with the U.S. Atomic Energy Commission, Wash 1192, fall 1975.

7. Hill, J. R. and Miller, C. F., Personnel Injuries/Illnesses Associated with Natural Environment Hazards, Reported in the Proceedings of the 1991 Hanford Annual Conference on Health and Environmental Effects, 1991.

8. Office of the Deputy Assistant Secretary for Safety, Health and Quality Assurance-DOE, Department of Energy Safety and Health Highlights - Fiscal Year 1992 (prepared by the System Safety Development Center, EG&G Idaho, Inc., 1993).

9. Office of the Deputy Assistant Secretary for Safety, Health and Quality Assurance, Occupational Injury and Property Damage Summary - January-March 1993 (prepared by the Systems Safety Development Center, EG&G Idaho, Inc., 1989).

10. Department of Energy, Real Property Inventory System (data base current - 1992).

11. Eagling, D. G., Seismic Safety Guide, Lawrence Berkeley Laboratory, 9143 (NTIS No. DE 84000542), 1983. (Currently being revised and expanded.)

12. Eagling, D. C. and Hill, J. R., "Benefits Realized from Upgrading the Lawrence Berkeley Laboratory," pg. 225-238 of the Proceedings of the 23rd Joint Meeting of the UJNR Panel on Wind and Seismic Effects, National Institute of Science and Technology, NIST SP 820, 1991.

13, 14, 15. Lawrence Livermore National Laboratory, Proceedings: DOE Natural Phenomena Hazards Mitigation Conference, CONF-851D118, 1985, CONF-8910192, 1989, CONF-9110122, 1991.

16. Hill, J. R., "Department of Energy" in Natural Earthquake Hazards Reduction Program: Fiscal Years Activities (Annual Report to the United States Congress, Congress of Federal Agency activities compiled by FEMA and issued annually beginning in 1983.

TABLE 1
LOSSES DUE TO TYPES
OF NATURAL HAZARDS BY STATE
DOE 1943 - 1993

DOLLAR LOSS ($000)

STATE	SEISMIC	WIND	FLOOD	HAIL, SLEET SNOW, RAIN	LIGHTNING	FREEZING	SUBSIDENCE	TOTAL
California	3429*	246	258	-	7	5617	370	9927
Colorado	-	1097	1347	87	21	161	-	2713
Florida	-	237	231	-	39	-	-	507
Hawaii		210						210
Idaho	**	120	66	12	69	54	-	321
Illinois	-	510	14	36	50	88	-	698
Kentucky	-	-	-	-	-	-	23	23
Louisiana	-	415	-	-	33	-	-	448
Maryland	-	-	188	-	-	-	-	188
Missouri	-	42	478	4	5	11	-	540
New Mexico	-	384	299	38	112	74	-	907
Nevada	1000	40	9	8	76	-	-	1133
New York	-	64	-	20	295	50	-	429
Ohio	-	292	-	-	9	43	19	363
Pennsylvania	-	12	-	-	33	3	-	48
Pacific	-	399	-	-	-	-	-	399
South Carolina	-	1604	110	597	135	182	-	2628
Tennessee	-	523	-	250	45	17	-	835
Texas	-	3000	-	2380	25	54	-	5459
West Virginia	-	40	-	-	-	-	-	40
Washington	-	337	66	8	335	106	-	852
Wyoming	-	10	16	-	34	-	-	60
TOTALS	4429	9582***	3082	3440**	1323	6460	412	28728

(Estimated losses for the 50 years that were not categorized for hazard types totaled 1680)

* Doesn't include research outage due to Loma Prieta.
** Mt. Borah earthquake of 1985 resulted in minimal damage.
*** Losses with both wind and hail damage allocated between wind and hail.

TABLE 2
DEPARTMENT OF ENERGY
LARGEST LOSS BY TYPE OF NATURAL HAZARD
($000)

YEAR	DESCRIPTION	LOSS ($000)
1990	SAN FRANCISCO BAY AREA FREEZE	5,600
1980	LIVERMORE, CALIFORNIA, EARTHQUAKES	3,416
1980	AMARILLO, TEXAS, WIND AND HAIL STORM	2,546
1967	AMARILLO, TEXAS, WIND AND HAIL STORM	1,872
1986	GOLDEN, COLORADO, FLOOD	1,174
1993	OAK RIDGE, TENNESSEE, TORNADO	500
1973	AIKEN, SOUTH CAROLINA, SLEET	393
1973	BERKELEY, CALIFORNIA, LANDSLIDE	370
1983	BAYOU CHOCTAW, LOUISIANA, HURRICANE	268
1976	ARGONNE, ILLINOIS, TORNADO	285
1993	OAKRIDGE, TENNESSEE, SNOW	250
1952	PACIFIC TYPHOON	250
1989	BROOKHAVEN, NEW YORK, LIGHTNING	240
1984	PINELLAS, FLORIDA, RAIN	231
1980	WASHINGTON AND IDAHO, VOLCANIC ASH	*

* LOSSES NOT REPORTED.

TABLE 3
MAJOR DOE LOSSES
DUE TO NATURAL PHENOMENON

1943 - 1993

HAZARD	$ LOSS (000)	YEAR	STATE	LOCATION	DESCRIPTION
Earthquake	3416	80	California	Livermore	0.25G, 2 major shocks
Wind/Hail	2546	84	Texas	Amarillo	106 MPH wind, baseball-size hail
Freeze	2000	90	California	Stanford	Damage Klyston cooling systems
Freeze	2000	90	California	Livermore	Damaged piping systems
Wind/Hail	1872	67	Texas	Amarillo	Damage to buildings and equipment
Wind/Tornado	1600	89	So. Carolina	Aiken	Damaged pine trees at Savannah River Site
Freeze	1500	90	California	Tupman	Compressors damaged
Flood	1174	86	Colorado	Golden	Runoff flooded equipment
Earthquake	1000	92	Nevada	Mercury	Earthquake damaged buildings
Wind	658	89	Texas	Amarillo	101 MPH wind, gravel broke glass
Wind	650	90	Colorado	Rocky Mountains	Strong winds crashed helicopter
Tornado	500	93	Tennessee	Oak Ridge	Damaged buildings
Flood	449	61	Missouri	Kansas City	Hurricane Carla
Sleet	393	73	So. Carolina	Aiken	Damaged pine trees
Landslide	370	73	California	Berkeley	6 weeks of heavy rain
Tornado	285	76	Illinois	Argonne	Damaged equipment and buildings
Wind/Rain	268	83	Louisiana	Bayou Choctow	Hurricane Alicia
Flood	258	83	California	Santa Barbara	Spread contamination
Typhoon	250	52		Pacific	Damage
Snow	250	93	Tennessee	Oak Ridge	Transformers and roof damage
Lightning	240	89	New York	Long Island	Ignition of gases
Rain	231	84	Florida	Clearwater	Rain caused electrical short
Wind/Flood	224	80	New Mexico	Albuquerque	Hurricane Allen, flooding
Wind	221	88	Ohio	Fernald	Damage to trailer and equipment
Wind	210	80	California	Tupman	Building burned
Hurricane	210	92	Hawaii	Hawaii	Damaged 22 buildings
Flood	200	83	Colorado	Golden	Damage transmission lines
Flood	188	72	Maryland	Baltimore	Explosion from water/calcium reactions
Hail	174	77	Texas	Amarillo	Damaged buildings and vehicles
Wind	166	80	Colorado	Golden	Loosened bolts on equipment
Earthquake	*	89	California	Stanford	Research out of service for over 6 months

*Costs not available

TABLE 4
DEPARTMENT OF ENERGY
INJURY INCIDENTS DUE TO NATURAL HAZARDS
1981 - 1991

WEATHER RELATED

ICE/SNOW/RAIN/WET/MUD	1578
SLIP/FALL/TRIP	1562
WIND	587
VISABILITY (FOG & OTHER)	67
HOT/COLD TEMPERATURES	17

TOTAL CASES = 2560

(Some cases are reported in more than one category.)

ACTS OF NATURE EVENTS*

HURRICANE/TORNADO	7
EARTHQUAKE	12
LIGHTNING	9
FLOOD	12

TOTAL CASES = 40

*Includes direct event, pre-event, and post-event injuries.

TABLE 5
DEPARTMENT OF ENERGY
HURRICANE LOSS SUMMARY

YEAR	($000)	HURRICANE	LOCATION
1961	449	CARLA	KANSAS CITY, MISSOURI
1983	268	ALICIA	BAYOU CHOCTAW, LOUISIANA
1952	250	TYPHOON	PACIFIC
1980	224	ALLEN	ALBUQUERQUE, NEW MEXICO
1992	210	INIKI	HAWAII
1972	188	AGNES	BALTIMORE, MARYLAND
1986	95	Not Named	BAYOU CHOCTAW, LOUISIANA
1959	50	GRACIE	AIKEN, SOUTH CAROLINA
1943 - 1993	1734	8 EVENTS	7 STATES

RECONSTRUCTION OF ERZINCAN (TURKEY) FOLLOWING THE 13 MARCH 1992 EARTHQUAKE

by

Mehmet Çelebi[1]

ABSTRACT

Extensive and speedy reconstruction efforts following the 13 March 1992 Erzincan, Turkey earthquake are described. Both existing and new techniques are applied to retrofit and repair existing buildings to improve their capabilities to resist future earthquakes and in turn prevent loss of lives. New construction shows vast improvement in quality, both in design and implementation.

KEYWORDS: buildings; damage; repair; retrofit; strengthening.

1. INTRODUCTION

This report covers observations, made between October 19-October 30, 1992, related to post-earthquake recovery, research and reconstruction efforts following the 13 March 1992 Erzincan, Turkey earthquake. An overview of the effects of the earthquake was presented in an earlier paper (Çelebi, 1992).

The final statistics for damage to buildings during the 13 March 1992 earthquake (as reported by the Ministry of Public Works and Reconstruction, Republic of Turkey) is as follows:

	Units
Collapsed, Heavily Damaged	**7007**
Medium Damage (Reparable)	**9227**
Light Damage (Reparable)	**15042**

The definition of a "unit" herein is a condominium, single-family house or a business (store or office).

As a consequence of the earthquake, approximately 40 percent of the population of the Erzincan region was displaced and all of the population was deprived of essential services (such as medical care requiring hospitals since all three hospitals had collapsed). Thus, half-a-year after the earthquake, the entire town of Erzincan had the appearance of one large construction site. Approximately $700 M (in public funds) have been earmarked to rebuild the city and surrounding towns and villages. Roughly a third of this amount is borrowed from the World Bank. Approximately 4000 new single-family homes and 2500 new condominium units are under construction, all to be completed by December 31, 1992. More units will be built during the next two summers. The goal of the massive reconstruction, repair and retrofit efforts is to bring most of the region back to normalcy before the severe winter season starts.

[1] USGS (MS977), 345 Middlefield Rd., Menlo Park, Ca. 94025

Unique repair and strengthening methods are being implemented on those buildings deemed repairable and/or requiring strengthening. Approximately 70 faculty members from three major universities (Istanbul Technical University [ITU], Middle East Technical University [METU-Ankara], and Bosphorus University [BU-Istanbul]) are heavily involved in all phases of planning, development of criteria, review and/or design of new and retrofit or repair construction. This effort resembles that of faculty members from UC Berkeley and UC San Diego following the Loma Prieta (1989) earthquake.

Repairs and retrofitting are being monitored by two main groups:

a. ITU Group: responsible for low-cost (social) housing buildings constructed with public funds even though the ownership may have been private during the earthquake. This effort involves 2000 units (from 36 different types of social housing construction).

b. METU Group: responsible for repair and retrofit of 36 public buildings (schools, government buildings, *etc.*). They have adopted a seismic coefficient of 0.3 for their calculations in retrofitting the buildings.

This report highlights the rebuilding efforts.

2. INVESTIGATIONS

All three university groups (ITU, METU and BU) are involved in all aspects of investigations related to defining the geotechnical environment of Erzincan and defining design response spectra for specific site conditions. Furthermore, each group has established laboratories for geotechnical investigations and separate materials laboratories to test, on site, the samples taken from damaged buildings or from buildings to be retrofitted as well as to carry out tests related to quality control of new construction.

Many boreholes have been made. The ITU Group has drilled approximately 35 boreholes with depths of 35 meters or so. Most of these have been cased for conducting cross-hole and related tests during the summer of 1993. Approximately 300 dynamic penetration tests have also been carried out. They found that the stratification varies a lot in each case. The METU group drilled approximately 20 boreholes with larger depths (100-200 meters). They have also carried out specific site-characterization efforts in the vicinity of the public buildings earmarked for retrofitting. BU Group has carried out microtremor measurements.

3. TEMPORARY CONSTRUCTION (Prefabricated Units)

These units are publicly financed and owned. They were erected immediately (within two weeks) following the earthquake, mainly to provide temporary housing and to replace tents. These units are normally stored in Ankara and trucked quickly to areas of natural disaster. Each unit usually has between 40-60 m^2 of living space. If weather conditions in the areas of natural disaster are favorable, these temporary units are also used to provide permanent housing. In such cases, sufficient land is provided with each unit to allow the new owners to enlarge their living spaces, if they so desire.

4. REBUILDING EFFORTS

Rebuilding efforts in Erzincan and vicinity can be classified into 2 major groups (as new construction and repair and/or

retrofitting of existing structures):

4.1 New Construction.

A significant point related to new construction was the observable improvement in the quality of design, materials and construction. New construction should be categorized into two groups (differentiated by public or private financing):

4.1.1 *Government Owned or Financed Housing and Public Buildings*

New low-cost (social) housing construction is mainly of four different types all of which resemble the general architectural plans that existed in Erzincan prior to the 13 March 1992 earthquake:

a. Single-story brick masonry with reinforced concrete tie-beams and ceilings.
b. Two-story reinforced concrete framed buildings with infill walls.
c. Three-story reinforced concrete frames with infill walls and reinforced concrete shear walls.
d. Four-story reinforced concrete tunnel-formed shear wall buildings.

Typical four-story tunnel formed buildings are shown in Figure 1.

Large construction companies have been contracted to construct the new low-cost housing structures. Similarly, new construction of other buildings such as hospitals and schools is being carried out by large construction companies.

4.1.2 *Privately Owned Buildings*

There was clear evidence of better design and construction of new, privately owned buildings. A new construction is shown in Figure 2 which exhibits better proportioned lateral force resisting elements as well as improved construction quality.

4.2 Repair and Retrofit of Pre-earthquake Inventory of Structures

Several methods and techniques are being used in repairing and retrofitting of structures to enhance their earthquake resistance capabilities.

(1) Reducing the number of floors and reducing dead loads.
(2) Capping of columns.
(3) Addition of shear walls.
   a. ITU method
   b. METU method
(4) Epoxy repair of cracks.
(5) Combination of two or more of the above.
(6) Special cases related to industrial structures.

These methods are being applied for both public and privately owned buildings.

For some buildings, both the number of floors and the dead loads were reduced, following the Mexico City example after the 1985 Michoacon earthquake. Figure 3 shows an example: the Kizilay (Red Crescent) Building in the center of Erzincan. Two of the four floors from one of the two wings of the building were removed, and selected columns were strengthened by capping. The balconies, which had been closed completely with floor to ceiling walls and used for heavy storage space, were reconverted as balconies.

Capping of reinforced concrete columns is a well known method and universally applied. In most cases in Erzincan, column capping was combined with the addition of shear

walls. Figure 4 shows the repair and strengthening at Unsan Flour Mill (also covered in earlier paper [Çelebi, 1992]). The figure shows shear walls being added to the corners of the building and columns being capped in the central section of the building.

Repairing and retrofitting for earthquake resistance of social housing buildings are being achieved mainly by addition of reinforced concrete shear walls. Figure 5 shows the addition of shear wall in one of the social housing buildings. The shear transfer between the floors and the new walls are being achieved by HILTI (Swiss patented) dowels. This approach has been initiated, designed and is being implemented under the direction of the Istanbul Technical University (ITU) Group.

Repairing and retrofitting for earthquake resistance of public buildings (schools and governmental buildings) are being carried out by a new method initiated, designed and being implemented under the direction of the METU Group. Application of this method is seen in Figures 6a and 6b. The building is strengthened by shear walls cast within a bay frame (of channel members) between two columns; the bay frame, in turn, is attached to the columns by a standardized jacket comprised of four longitudinal corner angles and plate strips between them (Figure 7). The channel at the top of the frame is anchored by a bolt system to the bottom frame channel of the floor above. This is the basic shear transfer mechanism. Once the new shear wall is cast after addition of the shear wall reinforcing bars, the columns are considered as not contributing to the lateral force resisting capability. During casting, a "cement board" is used as vertical form and left in with the concrete. This board is later painted.

Addition of shear walls, capping of columns, and epoxy repair of beams and columns were applied in the repair and retrofit of Officer's Club Building in Erzincan. This building is comprised of two structures separated by an expansion joint. Figure 8 shows one wing of the building and the added shear walls at the corners of the building. The original openings at the four corners of each wing of the building are now shear walls, eliminating the windows of those rooms, which were converted into larger suites using the adjoining rooms at each floor. Both injection and cosmetic surface epoxy repair techniques have been applied to some of the internal members.

The majority of the private buildings have been repaired and retrofitted by replacing the masonry infill with reinforced concrete shear walls. In this application, shear walls were constructed along both axes of the buildings.

The repair and retrofitting of industrial buildings utilizes several methods. In one pre-cast prestressed industrial building, the column ends were capped with a proper jacket both to strengthen those ends and to provide anchorage. An identical adjacent building under construction during the earthquake had collapsed and was re-erected to be retrofitted similar to the other.

The sugar refinery had lost the stack of the calcination unit and had suffered damage to some of its walls during the earthquake (Figure 9a). By October, it was completely repaired, equipped with a new stack and was already in production (Figure 9b).

5. CONCLUSIONS

In this cursory report, highlights of reconstruction efforts following the 13 March 1992 Erzincan (Turkey) earthquake

are presented. The reconstruction covers both new construction and the repair and retrofitting of existing building inventory. Some of the repair and retrofitting methods are new. These methods may be useful for mitigation efforts in central and eastern United States as well as in other parts of the world where there are large inventories of deficient masonry and reinforced concrete buildings.

It is observed in Erzincan that when strict quality control procedures are followed, it is possible to improve the earthquake resistant construction, thus decreasing the risk during future events. It is important to document the implementation of the repairing and retrofitting methods applied to existing structures as well as the improvements of new structures so that their effectiveness can be assessed during future earthquakes. This report partially serves that purpose on a small scale.

6. REFERENCES

1. Çelebi, M., 1992, Highlights of the 13 March 1992 Erzincan (Turkey) earthquake, PROC., 24th Joint Meeting of Panel on Wind and seismic Effects, the US-Japan Cooperative Program in Natural Resources, NIST-SP-843, September 1992, pp. 397-410.

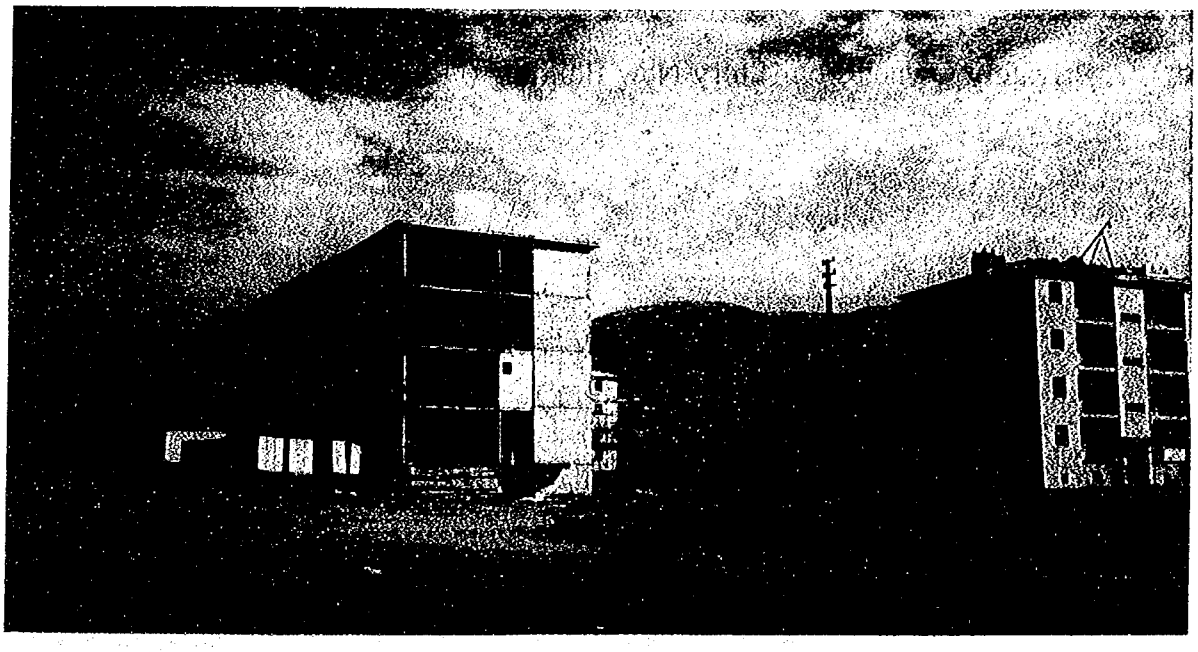


Figure 1. Four-Story Tunnel-Formed Reinforced Concrete Shear Wall Buildings (New Construction)

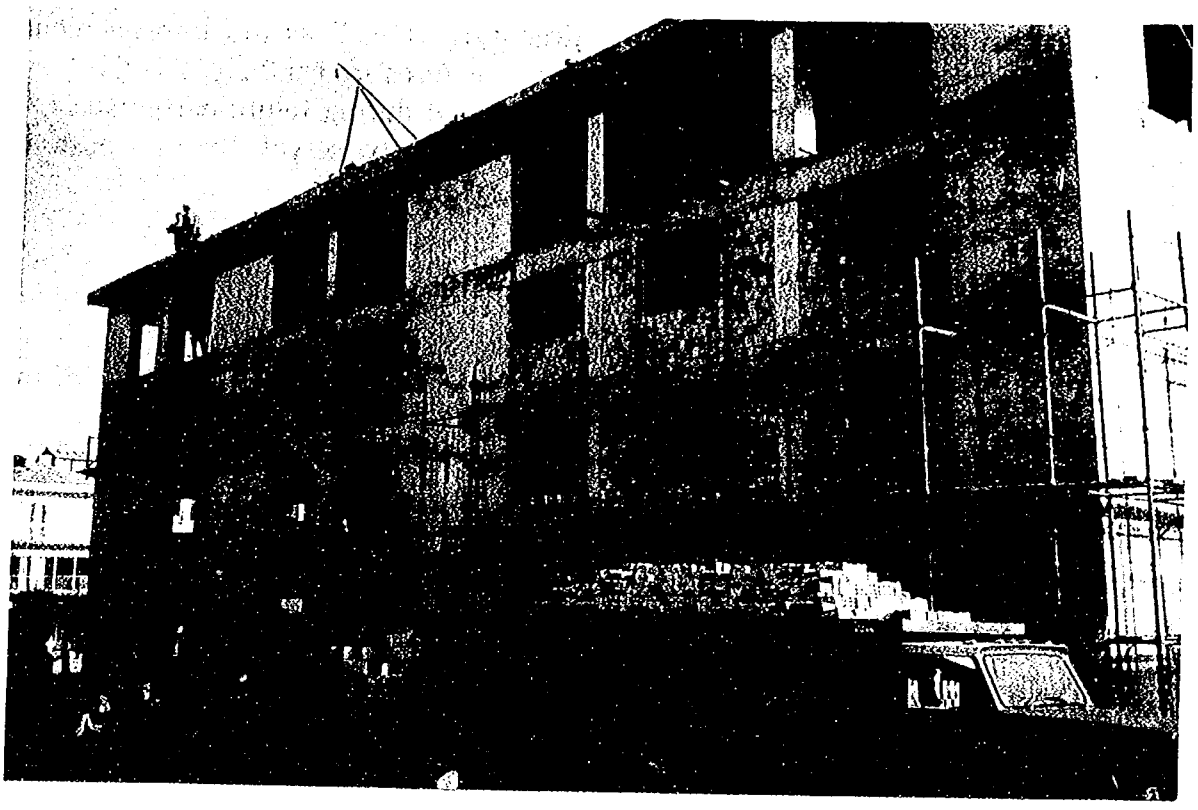


Figure 2. A Privately Owned Four-Story New Building (Note Corner and Central Shear Walls)

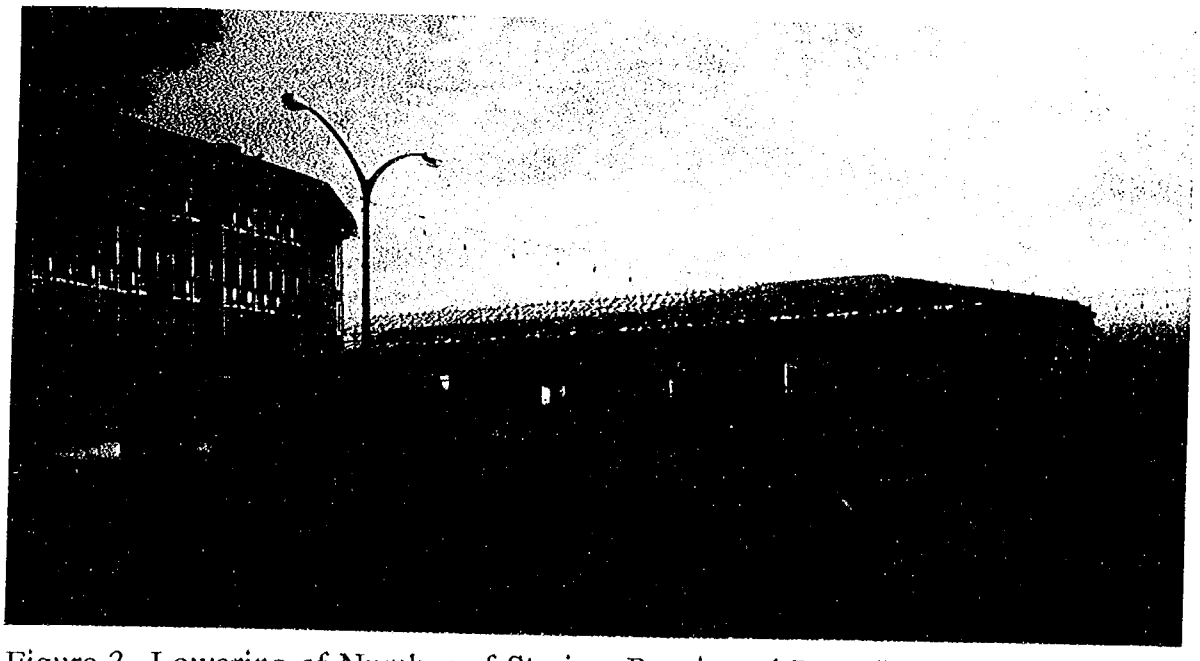


Figure 3. Lowering of Number of Stories, Repair and Retrofit of Kizilay Building

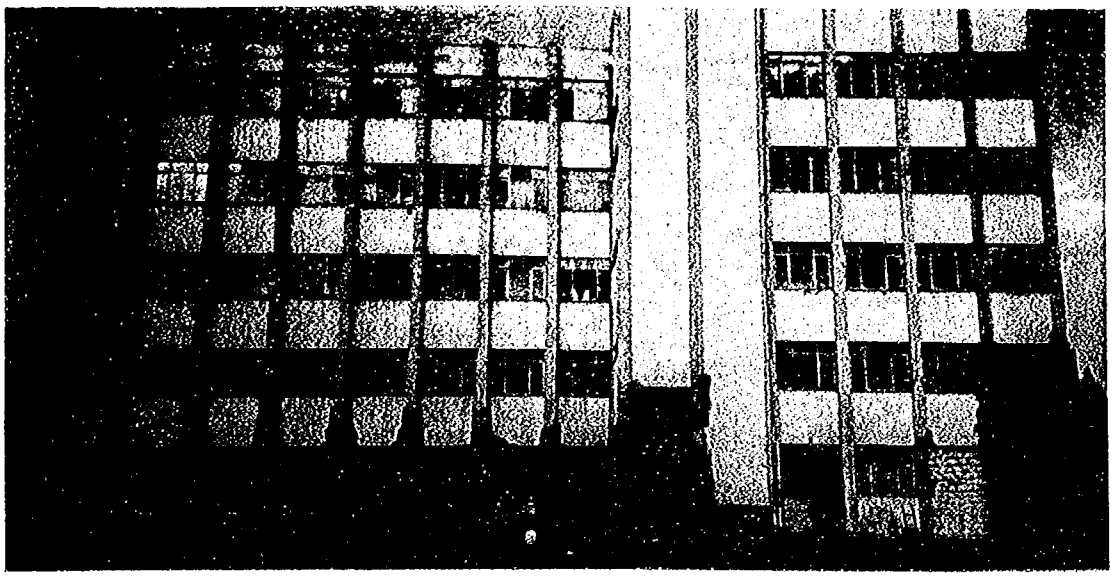


Figure 4. Unsan Flour Mill (During Repair and Retrofit)

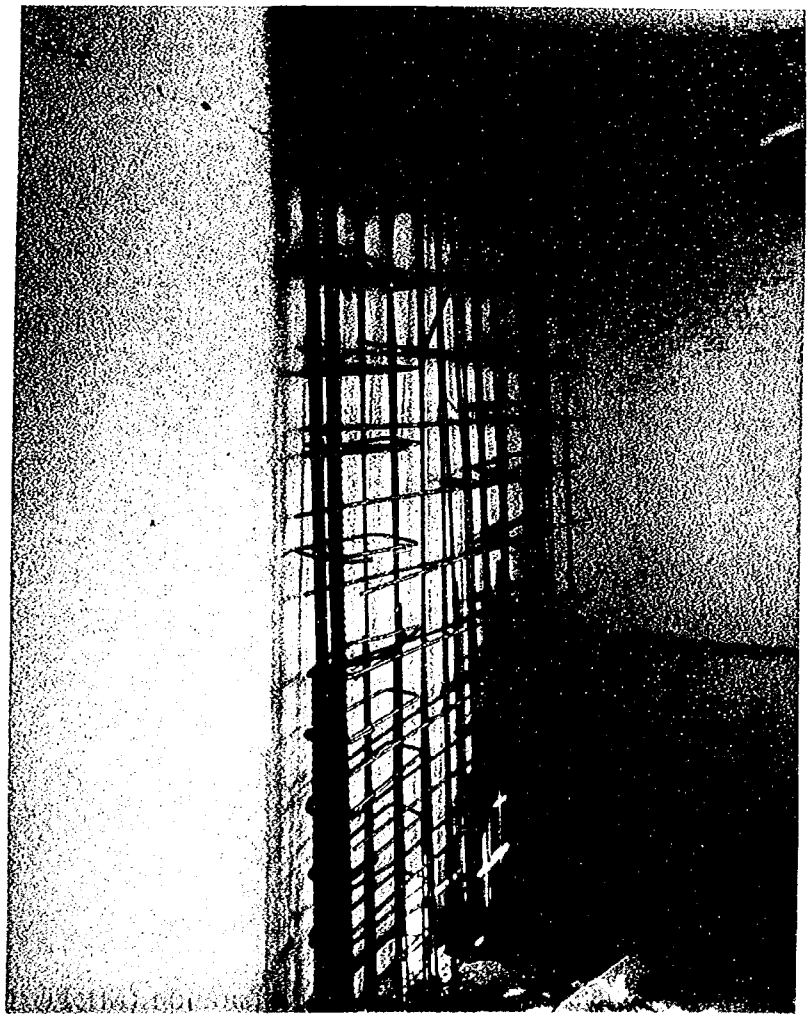


Figure 5. Reinforcement of Shear Wall Being Added



Figure 6a. A School Building Being Retrofitted (METU Method)



Figure 6b. A Shear Wall Retrofit In Preparation (METU Method)

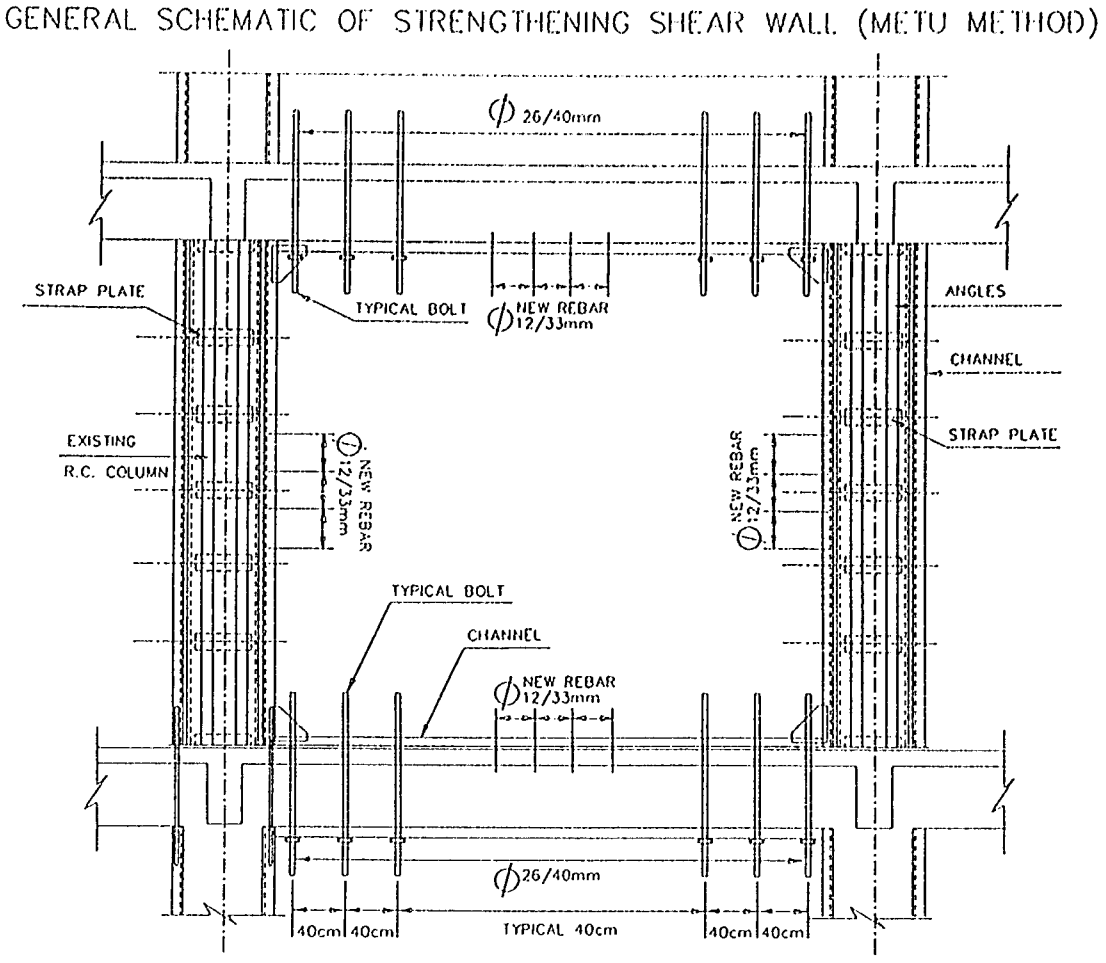


Figure 7. Details of Retrofit (METU Method)

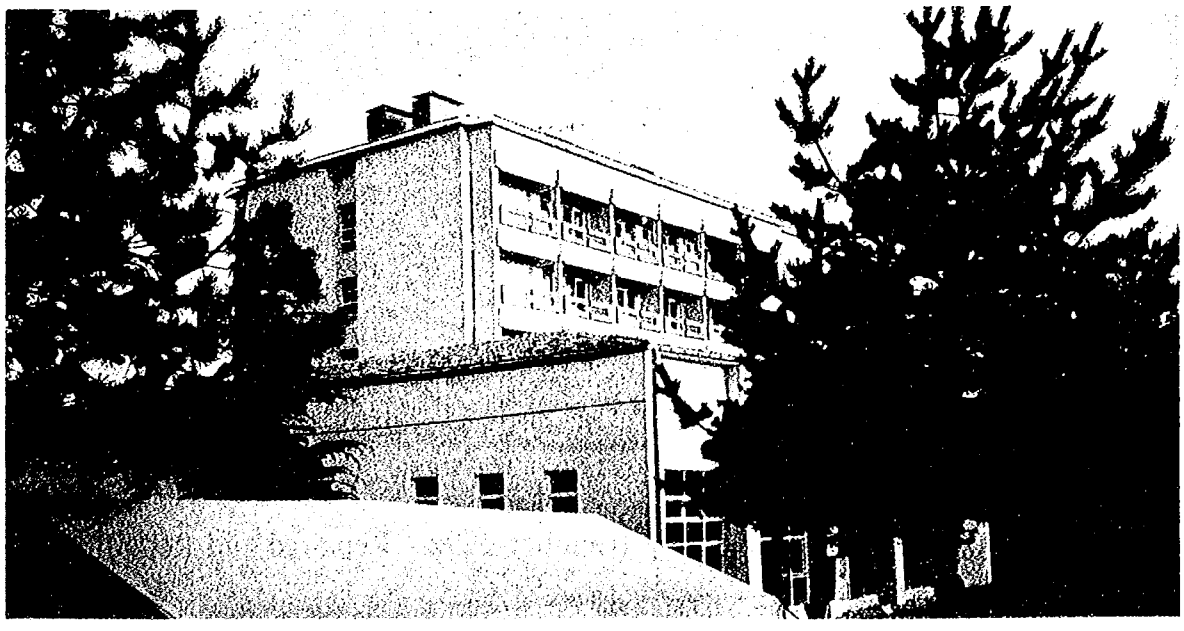


Figure 8. Retrofitted Officers Club Building



Figure 9a. Sugar Refinery (March 1992 -- Damaged Condition)

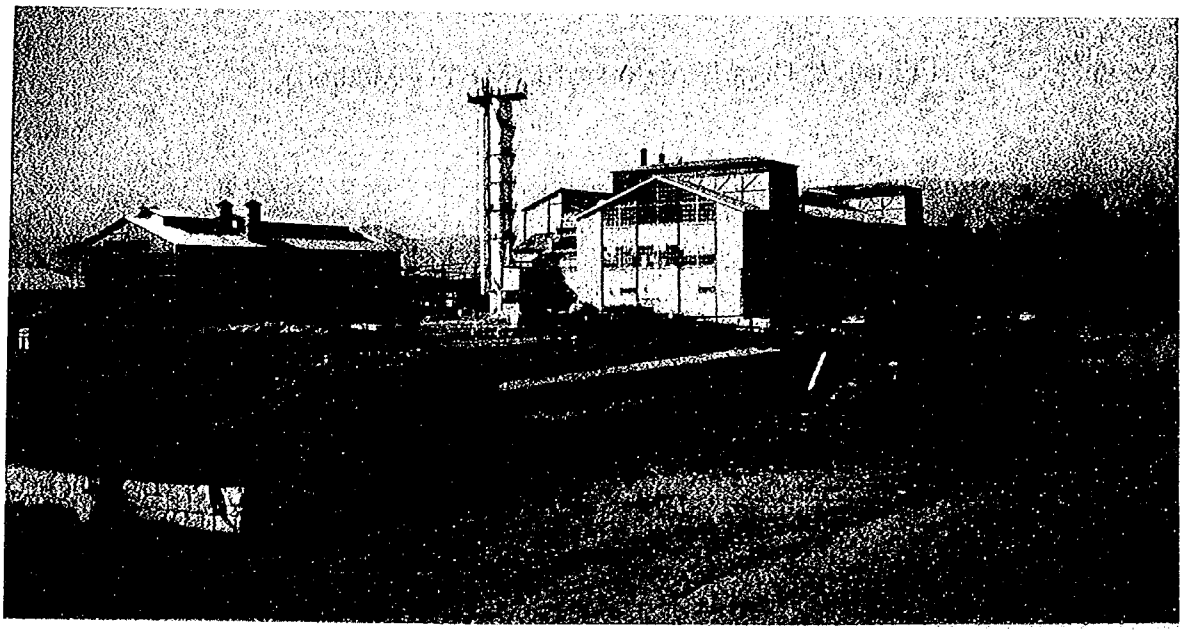


Figure 9b. Sugar Refinery Operating (October 1992 - Repaired and Retrofitted)

DOE NPH Mitigation Policy and Standards Program

by

James R. Hill*
Robert C. Murray**

ABSTRACT

This paper outlines a program to establish policy and develop standards and guidance for systematically evaluating the behavior of structures, systems, and components (SSC) in all Department of Energy (DOE) facilities located across the United States when subjected to natural phenomena hazards (NPH) of which the focus is on wind and earthquakes.

The policy were established in "Natural Phenomena Hazards Mitigation", Order DOE 5480.28. Criteria are summarized for those standards which implement the order. This paper summarizes the NPH Policy and Standards Program.

1. NATURAL PHENOMENA POLICY ORDER

As part of a coordinated effort to ensure proper performance of DOE facilities subjected to natural phenomena hazards (NPH), the Natural Phenomena Hazards Mitigation Order DOE 5480.28 was developed and approved. This order establishes (1) policy requirements for mitigation of NPHs at DOE facilities, (2) consistent requirements for all NPHs and for all DOE facilities, and (3) NPH requirements appropriate for facility characteristics and objectives within a graded approach. The order embodies the principles established by the DOE "General Design Criteria" Order, DOE 6430.1A, and NPH Design and Evaluation Guidelines UCRL-15910, which have been in use at DOE facilities for more than seven years. In addition, it establishes as requirements good practices that have been used at many of the DOE sites. The requirements cover the following:

- Assessment of NPHs for new and existing sites
- Natural phenomena effects to be considered
- Design of new facilities
- Evaluation and upgrade of existing facilities
- Design of additions and modifications
- Target performance goals
- Graded approach and performance categories
- Interactions and common cause effects
- Instrumentation
- Evaluation of NPH events - lessons learned.

The goals of the order are to (1) provide for safe workplaces, (2) protect against property loss or damage, (3) provide for continued operation of essential facilities, and (4) protect public health and the environment against exposure to hazardous materials-all in a cost-effective manner. To assist in implementing the new policies, a series of DOE standards is being developed.

The six standards required to implement the order are summarized in the next section. The first, DOE-STD-1020-92, is based on UCRL-15910, "NPH Design and Evaluation Guidelines". A draft of DOE-STD-1021-92, "Natural Phenomena Hazards Performance Categorization Criteria for Structures, Systems, and Components," is currently in the review process. Standards 1022 and 1023 will provide criteria for site characterization and hazard assessment; they will be available by mid-1993. The order also draws on other DOE standards as well as national codes and standards. (See Figure 1.)

* Department of Energy, Washington, DC 20585
** Lawrence Livermore National Laboratory, Livermore, CA 94550

For new facilities, the order becomes effective on the date of issuance. For existing facilities, implementation is planned over several years because of resource constraints and programmatic mission considerations. To start the process of evaluating and upgrading existing facilities, the order requires contractors/operators to establish an implementation plan that contains a prioritized evaluation schedule and identifies current and future NPH mitigation actions.

This plan is to be submitted to the DOE Headquarters Program Office within one year after the standards have been issued. Workshops are planned to cover the requirements of the order and the guidance on its implementation.

The issuance and implementation of DOE Order 5480.28 provides the framework for meeting Presidential Executive Order 12699 for seismic-hazard mitigation of new federal facilities and an Executive Order under development, which will require evaluation of existing facilities. In addition, it will form the basis for a DOE NPH rule for nuclear facilities to be developed this fiscal year as part of the Code of Federal Regulations.

2. NATURAL PHENOMENA HAZARDS DESIGN AND EVALUATION CRITERIA STANDARD

Design and evaluation criteria to implement the order are provided in the Standard DOE-STD-1020-92. UCRL-15910 provides the technical basis for this standard. The standard is undergoing extensive review.

The DOE policy established a graded approach for NPH requirements by defining performance categories (numbered 0 through 4), each with a qualitative performance goal for behavior (i.e., maintain structural integrity, maintain ability to function, maintain confinement of hazardous materials) and a quantitative target probabilistic performance goal (expressed as an annual probability of exceedance of acceptable behavior limits [i.e., behavior limits beyond which damage/failure is unacceptable]). DOE-STD-1020-92 provides four sets of NPH design and evaluation criteria (explicit criteria are not needed for performance category 0). These criteria range from those provided by model building codes for performance category 1 to those approaching nuclear-power-plant criteria for performance category 4. Table 1 illustrates how DOE-STD-1020-92 criteria for the performance categories defined in DOE 5480.28 compare with NPH criteria from other sources.

Design and evaluation criteria in DOE-STD-1020-92 are deterministic procedures that establish SSC loadings from probabilistic NPH curves; specify acceptable methods for evaluating SSC response to these loading; provide acceptance criteria to judge whether the computed SSC response is acceptable; and provide detailing requirements such that behavior is as expected, as illustrated in Figure 2. These criteria are intended to apply equally to the design of new facilities and to the evaluation of existing facilities. In addition, the criteria are intended to cover buildings, equipment, piping, and other structures combines probabilistic and deterministic methods to achieve performance goals.

The annual probability of exceedance of SSC damage as a result of NPH event (i.e., performance goal) is a combined function of the annual probability of exceedance of the event, factors of safety introduced by the design/evaluation procedure, and other sources of conservatism. The ratio of the hazard annual probability of exceedance and the performance goal annual probability of exceedance is called the risk-reduction ratio, R_R in DOE-STD-1020-92. This ratio establishes the level of conservatism to be employed in the design or evaluation process. For example, if the performance goal and hazard annual probabilities are the same ($R_R = 1$), the design or evaluation approach should introduce no conservatism. However, if conservative design or evaluation approaches are employed, then the hazard annual probability of exceedance can be larger (i.e., more frequent) than the performance-goal annual probability ($R_R > 1$). Seismic criteria are provided in DOE-STD-1020-92 that achieve risk-reduction ratios, R_R, of 2, 10, and 20.

The required factor of safety, F_R, to achieve risk-reduction ratios, R_R, of 2, 10, and 20 is a function of the hazard curve slope and uncertainties in seismic capacities of SSCs. For the potential range of hazard curve slopes and capacity variabilities, values of F_R have been evaluated for each desired R_R. For

performance-categories 1 and 2, the risk-reduction ratio, R_R, of 2 is achieved by F_R of unity which, in turn, is judged to be achieved by following a seismic-acceptance criterion in accordance with recent editions of the International Conference of Building Officials, Uniform Building Code (UBC). For performance-categories 3 and 4, risk-reduction ratios, R_R, are 10 and 20, respectively. The required F_R values for these values of R_R are achieved in the seismic-acceptance criteria by specifying conservative material strengths, structural capacities, inelastic energy-absorption factors, and a seismic load factor.

DOE-STD-1020-92 seismic provisions differ from past additions of UCRL-15910 Design and Evaluation Guidelines in that a single value of inelastic energy absorption factor, F_u, will be specified for both performance-categories 3 and 4, and a seismic-load factor that differs from performance categories 3 to 4. This change was needed because UCRL-15910 specified F_u of 1.0 for brittle modes for both moderate and high hazard categories. As a result, different performance goals for each category were not achieved for these brittle-failure modes. In the DOE standard, performance goals will be met for brittle-failure modes by introducing a seismic load factor, L_S, which has a larger value for performance-category 4. F_u specified in DOE-STD-1020-92 will be about the same value as the moderate-hazard values from the UCRL-15910. By this change, seismic criteria for performance-category 3 SSCs are not affected (i.e., they will be the same as the moderate-hazard seismic criteria). For performance category 4, this change results in slightly more liberal criteria for ductile-failure modes and slightly more conservative criteria for brittle-failure modes.

Another change incorporated into DOE-STD-1020-92 includes damping levels provided at several response levels to be used in structural evaluations for the purpose of determining in-structure response spectra or interaction displacements. In the DOE standard, seismic interaction is explicitly addressed.

3. STANDARD ON PERFORMANCE CATEGORIZATION FOR NATURAL PHENOMENA HAZARDS

Engineers and plant managers responsible for the design or evaluation of structures, systems, and components (SSCs) need to select the level of natural phenomena hazard (NPH) and corresponding amount of conservatism in NPH design and evaluation criteria that are appropriate for the SSC design. The design criteria are selected on the basis of the failure-consequences of the SSC. For example, if the failure of a large dam may wipe out a city, it is likely to be designed for a large recurrence-period precipitation. In contrast, because far fewer potential fatalities would result from the collapse of a warehouse roof, that roof may be designed for a much smaller recurrence-period precipitation. Still, if both designs are optimally performed members of the public would be exposed to the same level of risk.

To attain similar uniformity in risk from the potential failure of various SSCs that are present in DOE facilities, the new DOE order on NPH mitigation requires the placement of all SSCs in one of the five performance categories (PC); performance goals for these categories are specified in terms of "target" annual failure probabilities. A standard (DOE-STD-1021-92), has been prepared to provide guidelines and methods for placing SSCs into these performance categories. The basic categorization process presented in this standard (excluding system interaction effects) is outlined in the flow chart in Figure 3.

The standard uses the results of SSC safety classification, facility hazard classification, and accident analyses that are performed in conformance with DOE Orders.

Performance Category 4 (PC-4) SSCs have been defined as the safety class SSCs in facilities with sufficient quantities of radioactive/hazardous materials and energy that, if released, can potentially result in offset prompt fatalities. The dose criteria for prompt fatality have been specified as follows:

- Radiological Criterion: 100-Rem Effective Dose. Equivalent receive over seven days at the site boundary.
- Hazardous Chemical Criterion: American Hygiene Association's Emergency Response Protection Guide (ERPG)-3 concentration limits at the site boundary.

Performance Category 3 (PC-3) SSCs have been defined as the safety class SSCs in facilities with sufficient quantities of

radioactive/hazardous materials and energy that require on site emergency planning.

Performance Category 2 (PC-2) SSCs will include the safety class SSCs in facilities with sufficient quantities of radioactive materials to be reportable to the Environmental Protection Agency. Additionally, PC-2 SSCs must perform their emergency functions to preserve the health and safety of workers and co-workers.

Building structures or components with potential human occupancy and SSCs whose failure can potentially cause a life-threatening situation to workers or co-located workers will be placed in Performance Category 1 (PC-1) SSCs that are not important from safety, mission, or cost considerations need not be designed to withstand NPH loads and should be placed in Performance Category 0 (PC-0).

DOE-STD-1021-92 places special emphasis on considering system interaction effects while performing NPH categorization. Simple-to-use, but conservative, rules have been provided to preclude adverse effects of lower category SSCs (sources) interacting with higher category SSCs (targets). These rules satisfy the basic requirement that the performance goal of the target SSCs must not be compromised. Several examples have been provided to illustrate the use of the interaction rules.

4. NATURAL PHENOMENA HAZARDS SITE-CHARACTERIZATION CRITERIA STANDARDS

The purpose of this standards is to provide criteria for developing site characterization and identify site-specific information needed for design and evaluation of DOE facilities subjected to natural phenomena hazards.

The standard will cover geological, seismological, geotechnical (GSG), hydrological, and meteorological aspects of site characteristics. The seismic-related hazards include site earthquake ground shaking; tectonic site deformation; ground failure induced by ground shaking including liquefaction, differential compaction, and land sliding; and earthquake-induced flooding.

Considerations of geological and seismological aspects include identifying and characterizing seismic sources and resulting site ground motions, evaluating the potential for tectonic and other site deformation and earthquake-induced flooding, and evaluating volcanic hazards. Major considerations of geotechnical aspects involve defining site soil properties needed for hazard evaluation and seismic engineering analyses, evaluating site soil-amplification effects on ground motions, conducting seismic soil-structure interaction analyses, and evaluation the potential for site ground failure induced by ground shaking.

Hydrological and meteorological aspects of site characterization criteria are also important. Site studies of hydrological aspects include determination of ground-water conditions, flood runoff, drainage, and other hydrological characteristics that could influence the design or operation of DOE facilities. Ground-water conditions include ground-water levels, flow pattern, permeability, porosity, and gradients at the site, as well as the chemical analysis of the ground water. Site studies on meteorological aspects should be performed to provide sufficient information for the design and evaluation basis of wind and tornado hazards. Seasonal weather conditions of the local site and region, including temperature, precipitation, relative humidity, and prevalent wind direction need to be indicated. The occurrences and intensity of heavy rain, snow, ice storms, and thunderstorms, as well as strong wind, tornadoes and hurricanes, need to be provided.

The scope and degree of detail of investigations to address these natural hazards depend on several factors, including the hazard classification of the facilities; the subsurface conditions at the site; the seismologic, hydrologic, and meteorologic environments of the site region; and the extent of prior knowledge, investigations, and data regarding the site and site region. An appropriate scope of investigation should be developed for a particular facility considering these factors. For example, although more detailed investigations are generally appropriate for facilities having higher hazard classifications, investigations of lesser scope and detail may be appropriate when existing knowledge of the site and region is high. Similarly, although less-detailed investigation would generally be commensurate with lower-hazard facility classification, more comprehensive investigations may be needed if investigations to define the hazards have not

previously been conducted.

5. NATURAL PHENOMENA HAZARDS ASSESSMENT CRITERIA STANDARD

DOE Order 5480.28 requires a probabilistic assessment of the likelihood of future NPH occurrence. The level of probabilistic NPH assessment to be conducted is appropriate for the performance categories being considered in a manner consistent with the graded approach. For sites containing facilities with SSCs in performance-categories 3 and 4, a site-specific probabilistic NPH assessment shall be conducted. For sites containing facilities with SSCs only in performance-categories 1 and 2 and having no site-specific probabilistic NPH assessment, it is sufficient to utilize NPH maps from model building codes or national consensus standards.

The purpose of DOE Standard DOE-STD-1023-92 is to provide criteria for NPH assessments to ensure that adequate design-basis loadings are established for design and/or evaluation of DOE facilities. DOE-STD-1023-92 will provide general assessment criteria for all NPHs, as well as specific criteria for the assessment of seismic hazard, wind, tornado, and flood. The emphasis will be on the site-specific probabilistic NPH assessment, i.e., the development of NPH curves. Criteria for the development of design-response spectra to define the seismic input motion will also be provided by DOE-STD-1023-92.

6. GUIDELINES FOR USE OF PROBABILISTIC SEISMIC HAZARD CURVES STANDARD

This standard provides guidance in the use of probabilistic seismic hazards curves, developed by the Lawrence Livermore National Laboratory (LLNL) and the Electric Power Research Institute (EPRI) the Eastern United States. Several studies were completed to document an understanding of the differences in the LLNL and EPRI methods and in how they are being used and to provide an interim position on the DOE use of the recently developed information. The standard provides recommendations that result in more stable estimates of the seismic hazard.

7. SUMMARY

The overall program has currently established a foundation by developing the NPH Order and implementing standards. Further development of the methodology for screening evaluation and retrofit of existing facilities will continue over the next few years in collaboration with the effort of the National Hazards Reduction Program.

8. ACKNOWLEDGMENTS

Many people have been involved in the current program. We would like to acknowledge: Jeff Kimball and V. Gopinath of DOE for their assistance and the team at LLNL consisting of Tom Nelson, J. C. Chen, Joe Ueng, Steve Lu, and Mark Eli, and our consultants Bob Kennedy, RPK/SMC, Jim McDonald, Texas Tech., Marty McCann, J.R. Benjamin and Associates, and Steve Short and Steve Eder, EQE Engineering Consultants.

9. REFERENCES

1. U.S. Department of Energy, Natural Phenomena Hazards Mitigation, DOE Order 5480.28, Washington, D.C., January 15, 1993.

2. U.S. Department of Energy, Natural Phenomena Hazards Design and Evaluation Criteria for Department of Energy Facilities, DOE-STD-1020-92 Draft, February 28, 1993. (Formerly UCRL-15910.)

3. U.S. Department of Energy, Performance Categorization Criteria for Structures, Systems, and Components at DOE Facilities subjected to Natural Phenomena Hazards, DOE-STD-1021-92, December 1992.

4. U.S. Department of Energy, Natural Phenomena Hazards Site Characterization Criteria, DOE-STD-1022-92 Draft, April 1. 1993.

5. U.S. Department of Energy, Natural Phenomena Hazards Assessment Criteria Criteria, DOE-STD-1023-92 Draft, April 1. 1993.

6. U.S. Department of Energy, Guidelines for Use of Probabilistic Seismic Hazard Curves, DOE-STD-1024-92, December 1992.

7. Lawrence Livermore National Laboratory

and EQE Engineering Consultants, Program Plan for the Evaluation of Systems and Components in existing DOE facilities subject to Natural Phenomena Hazards, Draft Lawrence Livermore National Laboratory Report, November 1992.

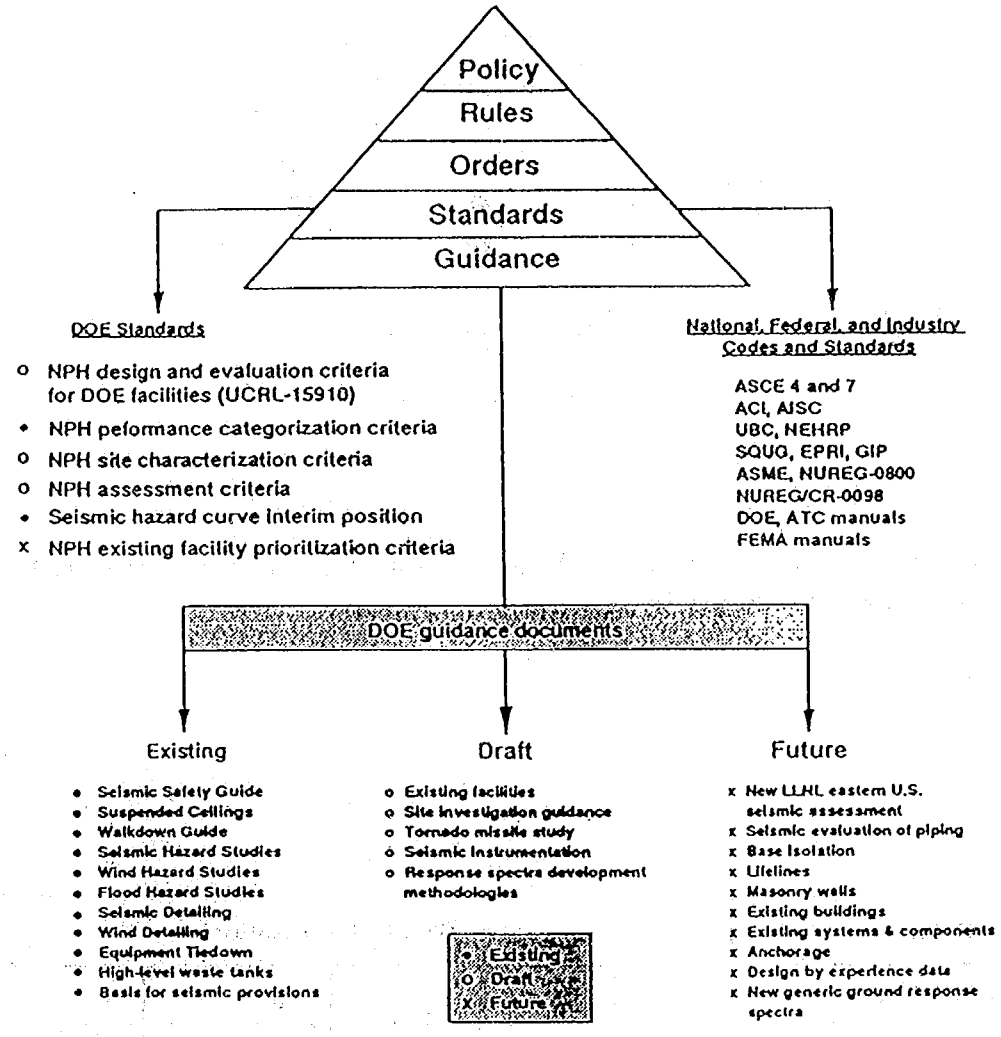


Figure 1. Overall DOE NPH mitigation program.

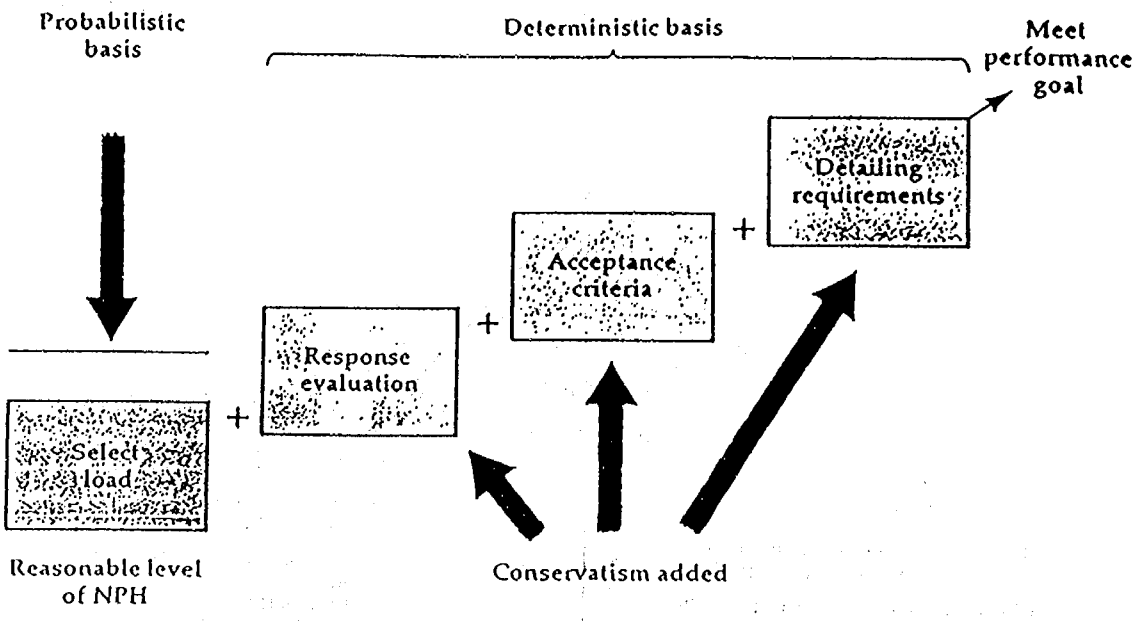
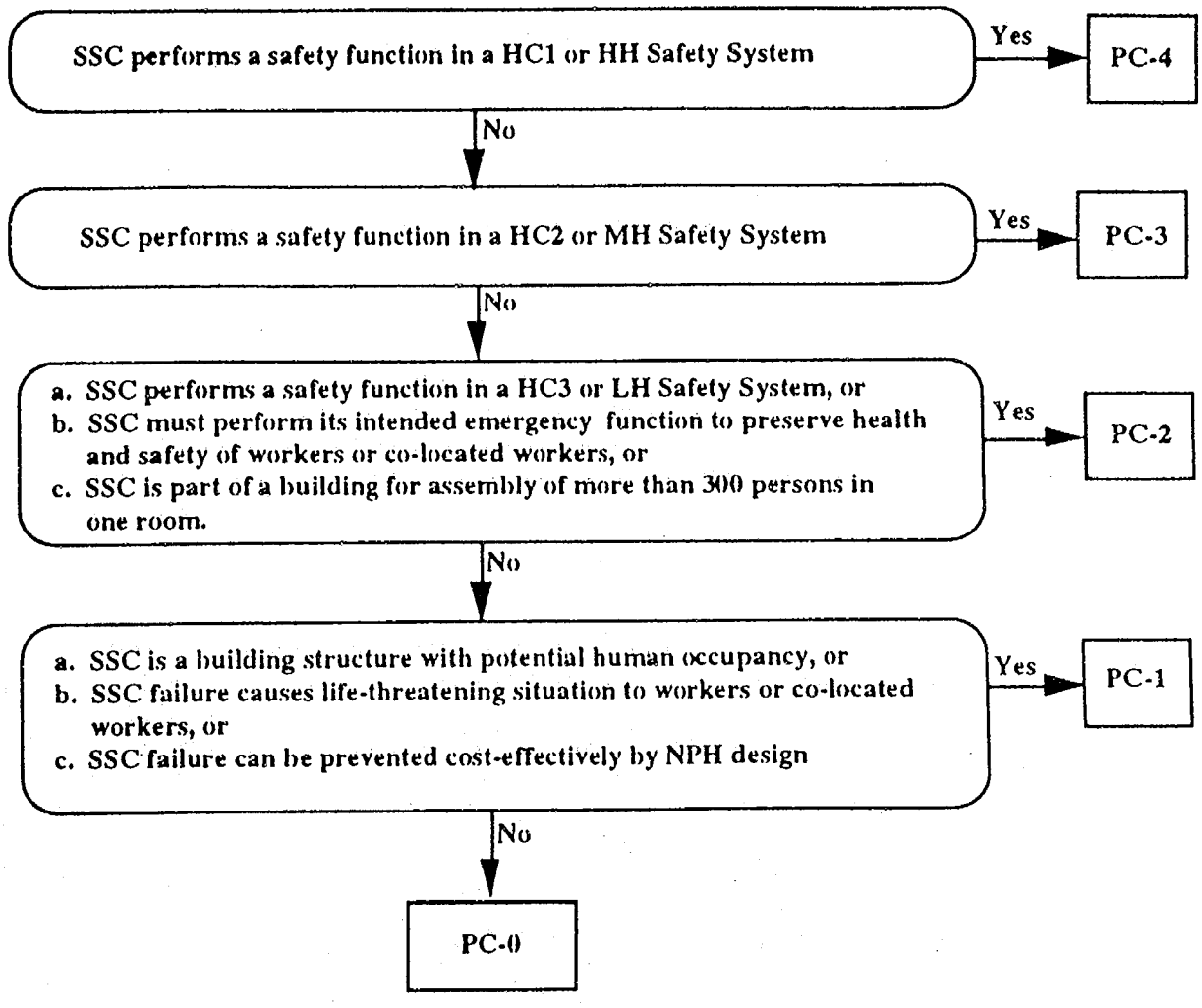


Figure 2. DOE-STD-1020-92 combines probabilistic and deterministic methods to achieve performance goals.

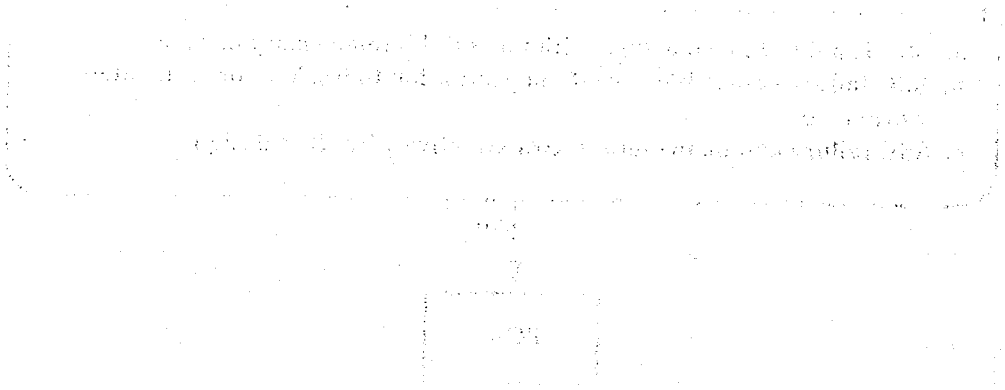
Reference	SSC Categorization				
DOE-STD-1020-92	0	1	2	3	4
Uniform Building Code	No life Safety	General Facilities	Essential Facilities		
DOD Tri-Service Manual for Seismic Design of Essential Buildings				High Risk	
Nuclear Regulatory Commission				Evaluation of NRC fuel facilities	Evaluation of existing reactors

Table 1. Comparison of performance categories from various references.

Figure 3 Basic Criteria for Preliminary NPH Performance Categorization of Structures Systems, and Components



Notes:
SSC = Structure , System and Component
HC = Hazard Category
HH = High Hazard Facility
MH = Moderate Hazard Facility
LH = Low Hazard Facility



Effect of Dynamic Loads on Lateral Strength of Nail Connections for the Manufactured/Modular Housing Industry

by

Steve G. Winistorfer and Lawrence A. Soltis*

ABSTRACT

Current methods used in the design of nailed connections do not directly relate to the types of joints found in modular and manufactured housing. These methods do not take into account the types of equipment used in current construction practices, the fact that many joints are built with filler materials separating main wood members, or the possibility of these joints undergoing dynamic forces during their lifetime.

A total of 240 joints were tested to investigate the effects of several variables: the use of hand-driven, uncoated nails compared to power-driven, coated nails; low- compared to high-humidity environments; particleboard compared to gypsum board filler material; and level of dynamic frequency. A preliminary test determined a critical frequency for the joints, which was the frequency that diminished connection stiffness and strength most compared to static (nondynamically loaded) joints.

The preliminary tests found that joint strength and stiffness became relatively stable at frequency levels more than 5 Hz. Dynamic forces were found to affect lateral joint stiffness but not joint strength. Similarly, moisture content level appeared to affect the stiffness, but not the strength, of static lateral joints. After the joint underwent dynamic loads, moisture content affected neither joint stiffness nor strength. In almost all cases, the strength and stiffness of joints with particleboard filler material were higher, by as much as 40 percent, than that of joints with a gypsum board filler.

KEYWORDS: connections; dynamic; lateral; modular; nails; wood.

1. INTRODUCTION

Connections in the manufactured/modular building industry are designed using fastener properties contained in the National Design Specification for Wood Construction (NDS) (NFPA, 1991). However, because many of these connections, specifically those with fillers, are not addressed in the NDS, designers must use judgment in modifying NDS methods and values to provide adequate connection designs. These NDS values were established before manufactured/modular manufacturing standards and practices were developed and before the manufactured/modular put-in-place environment became known.

Current NDS lateral design values are derived from yield equations based on mechanics of materials theory and are calibrated to match former values that were established using static, hand-driven test specimens. However, current manufacturing practices in the manufactured/modular industry take advantage of efficiencies gained using power-driven nails and staples. Manufacturing is also made more efficient by applying a plywood subfloor to the entire floor joist system before setting wall panels in place or applying gypsum board to the

* Research Engineer and Project Leader, respectively, of the Forest Products Laboratory, U.S. Department of Agriculture, Forest Service. Madison, Wisconsin, U.S.A. 53705-2398

roof truss system before it is set on the wall partitions.

Recent earthquake catastrophes in the western United States have also brought the concern of seismic loading to the forefront in the building design and construction industries. Although high-rise concrete and steel structures attract most of the public's attention, the need for information regarding the seismic performance of low-rise wood buildings is critical.

There is a need to identify fastener characteristics and performance in the manufactured/modular building environment. This need includes determining moisture content effects on fastener strength, the effects of dynamic loads on connection strength, how fastener characteristics (such as nail coatings and driving method) affect connection strength, and how filler materials between wood members of a joint affect its lateral strength.

2. BACKGROUND

Previous research conducted at the USDA Forest Service Forest Products Laboratory (in cooperation with the U.S. Department of Housing and Urban Development (HUD)) has determined that static connections modeling typical modular/manufactured joints compare favorably with current NDS lateral design values (Soltis & Nelson, 1990). The same study had a number of other conclusions, namely that the type of filler material separating wood members in a joint can have a significant effect on the strength of the connection and that compressive strength of connections is independent of fastener type.

The Soltis & Nelson study provides an in-depth presentation of and partial basis for design practices in use when the study was completed, which will not be repeated here. This project, which is a continuation of the study conducted by Soltis & Nelson, investigates connection properties that involve various combinations of materials under more stringent conditions than was done earlier. Another report, completed under the same cooperative agreement as this study, investigates the lateral and withdrawal strength of nailed connections similar to the joints tested here (Winistorfer & Soltis, 1993).

A limited amount of research has been conducted on the relative strength of power-driven and hand-driven nails. Two such studies (Youngquist & Scholten, 1951; Stern, 1952) investigated holding properties of proprietary fasteners specifically for use by the manufacturers.

An early German study (Gaitzsch, 1934) attempted to quantify several characteristics relating to nail-holding properties, one of which had to do with the influence of the speed of nailing. Although the results were applicable for nailing equipment of the day, the penetration rates studied were much too slow to provide a practical comparison with equipment and methods currently in use.

Studies referenced by Soltis et. al (1981) characterize vibrational responses of one- and two-story wood structures as having natural frequencies between 4 and 18 Hz. With respect to duration of perceptible motion for strong earthquakes, Rosenblueth and Bustamante (1962) documented that recorded earthquakes along the western coast of the United States have an average duration of 25 seconds.

The effects of moisture content on wood strength are well documented (Forest Products Laboratory, 1987). However, because of variations in nail type, wood species, and cyclic environmental conditions, moisture content effect in connector withdrawal and lateral resistance is not as completely defined. The Wood Handbook and other studies (Borkenhagen and Heyer, 1950; Heck, 1950; Lawniczak, 1956) have reported that cyclic moisture conditioning can reduce lateral and withdrawal resistance of certain types of nails and staples. In one case, a reduction of 25% from seasoned wood lateral loads is

recommended to avoid excessive deformation when fasteners will be used in unseasoned wood or in conditions where the wood will remain wet. Also, the NDS provides a 25% wet service factor reduction of lateral design loads when nailed connections are either partially seasoned or wet at time of fabrication but dry when in service.

3. EXPERIMENTAL METHODS

A total of 240 joints were tested. Figure 1 shows the wood/gypsum board/wood and wood/particleboard/wood joints used in the laterally loaded dynamic tests.

The wood/gypsum board/wood joints simulate a joint typical of those found in roof construction in the manufactured/modular building industry. As the upper schematic in Figure 2 shows, the top piece of wood represents a roof joist or bottom chord of a prefabricated roof truss; the gypsum board represents the material that is attached to the roof system before it is placed on the rest of the structure; and the bottom wood piece represents the top plate of the wall sections that support the roof.

The wood/particleboard/wood joints simulate a joint typical of those found in floor construction in the manufactured/modular building industry. The bottom piece represents the rim joist of the floor system, and the particleboard represents the subfloor deck applied with glue and nails to the floor joists. The top piece of wood represents the bottom wall plate of a prefabricated wall panel that is placed on the floor system and attached to the floor joists through the subfloor. The bottom schematic in Figure 2 illustrates the location of these joints in a typical manufactured/modular building.

The selection of these joint types and materials for testing provided continuity and comparability with a previous test sample (Soltis & Nelson, 1990). Although these joint types have not been identified as being susceptible to dynamic loads, they are representative of those used in manufactured and modular housing construction.

The dynamic study was divided into 2 sets of tests; the first was a preliminary study of 200 tests that determined the effect of dynamic frequency on connection residual lateral strength. A plot of residual stiffness in the initial portion of the load-deformation curve (compared to the static baseline test at 0 Hz) identified critical frequency. This critical frequency was used to complete the dynamic study in which an additional set of 40 specimens was tested.

3.1 Materials

The 240 dynamic test specimens were fabricated from No. 2 Douglas-fir nominal 2- by 4-in. (standard 38- by 89-mm) dimension lumber, which is listed in the NDS as having an average specific gravity of 0.51.

Nails, obtained through the International Staple, Nail, and Tool Association, had an 0.131-in.-(3.3-mm-) diameter shank and were 3-1/4 in. (83 mm) long. The HUD department identified nails of this size as being characteristic of those used in manufactured/modular construction. The nails were produced during a single production run. Half of the nails were coated with a thermosetting plastic, whereas the second half remained uncoated. The coating was applied to the point end of the nail and to approximately 50% of the length. The plastic coating was formulated to conform with Federal Standard FF-N-105B (GSA, 1971). This plastic coating melts from the heat generated when driven at high speeds with pneumatic nailers, then resolidifies, affecting a bond between the nail shank and wood fibers. As in the Soltis and Nelson study and contrary to American Society for Testing and Materials (ASTM) D1761 methods (ASTM, 1988), uncoated nails were not degreased prior to embedment to provide "as-built" data. (During the process of manufacturing nails, die lubricants and other materials can coat the finished nail. Nails that are coated with the types of thermosetting plastic coatings used in this test are degreased to assure

adhesion of the coating to the nail shank.)

The nail coating used in this study was produced specifically for this study in response to a desire to provide a coating typical of those used in construction. Fastener manufacturers provide a broad range of coated fasteners to manufactured and modular housing builders. The manufacturers supply a variety of proprietary coatings that range from less than 50% shank coverage to full shank coverage. The percentage of the shank that is coated and the specific coating formulation are only two of the many factors that can determine the effect of coatings on connection performance.

National Particleboard Association Class D-2 Mobile Home Decking particleboard (5/8 in. thick) (15.9 mm) and 5/16-in.- (7.9-mm-) thick gypsum board panels with a prefinished side, both typical of those used in the manufacturing/modular industry, provided filler material between wood members of the joint. A polyvinyl acetate (PVA) structural adhesive was applied to all joints prior to fabrication, with the adhesive joining the filler to the wood main member (member holding nail point). This is representative of the way PVA adhesives are used in the field to join the subfloor or ceiling covering to the floor joists or ceiling rafters, respectively. Care was taken to have the adhesive contact the facing surfaces of the wood main member and filler (and not coat the nails during penetration).

3.2 Procedures

3.2.1 Preliminary dynamic test

A 2^3x5 factorial experiment was designed to provide data regarding several variables involving nailed connections under dynamic load conditions. The following test matrix shows the combination of variables.

Variable	Quant.	Description
Frequency	5	0, 1, 5, 10, 20 Hz
Connections	2	Wood/gypsum board/wood, wood/particleboard/wood
Assembly method	2	Hand-driven uncoated nail, power-driven coated nail
Moisture content	2	6% EMC, 19% EMC
Replications	5	
Total Tests	**200**	

After lumber was cut, cross-matched, and labeled, all pieces were stored in environmentally controlled rooms to stabilize the equilibrium moisture content (EMC). Two different environments were used: low humidity (6% EMC: 80°F at 30% relative humidity) and high humidity (19% EMC: 80°F at 90% relative humidity), in accordance with the experimental design. Specimens were assembled and then returned to their respective conditioning rooms for at least 2 weeks prior to testing. This allowed adhesives to set before tests were conducted and also ensured that specimens were assembled and later tested in the same EMC-level environment. A piece of waxed paper was placed between the side wood member and the rest of the joint material to reduce initial friction (this helped to smooth out the initial portion of the load-deformation curve). Of course, this friction-reducing effect would not be present in actual construction. To the contrary, large friction forces caused by normal forces of system dead load do exist in the field.

The gypsum board and particleboard filler material was cut to size and placed in either the low- or high-humidity environment rooms, corresponding to respective joints.

The specimens with an uncoated nail were assembled using a standard, 16-oz (0.45-kg) construction hammer and took approximately five blows to obtain full nail embedment. The

specimens with a coated nail were assembled with a Duo-Fast compressed-air nail tool. The pressure on the air compressor was set to drive the nails completely with one drive.

Pilot holes half the diameter of the nail were drilled in the solid wood members to ensure that the nail penetrated perpendicular to the lateral plane of the connection. The pilot hole penetrated all 1-1/2 in. (38 mm) of the side member and penetrated the main member approximately ¼ in. (6.4 mm). Joints where the nail was power-driven did not require pilot holes in the main member. All specimens were assembled by the same technician to limit assembly variability.

Lateral tests were conducted to compare the static and residual static strength after dynamic loading of two types of connections at five different frequencies. Testing was conducted in accordance with ASTM D1761 (ASTM, 1988) procedures, with variations for dynamic loading.

Variations in the lateral set-up were necessary to minimize the eccentric loads applied through use of standard ASTM D1761 methods. Figure 3 shows the test set-up for the lateral dynamic tests. A frame, attached to the dynamic load head, loaded the wood side member while the filler material and wood main member were held stationary. A set of frictionless rollers held the wood side member perpendicular to the main wood member during dynamic and subsequent static loading.

Dynamic loading consisted of five frequencies ranging from 0 to 20 Hz (corresponding to the natural frequency range of 4 to 18 Hz of one- and two-story wooden structures) at an amplitude of 0.015 in. (0.38 mm) or peak-to-peak displacement of 0.030 in. (0.76 mm). The 0.015-in. (0.38-mm) displacement was chosen to coincide with the historical measure of the proportional limit of nailed connections. Sinusoidal dynamic load duration was 25 s, corresponding to the duration of an average earthquake. The number of cycles at each frequency differed based on test duration and frequency.

Deformation control was used in testing because load control was not possible with the equipment available given these dynamic parameters. After the dynamic loading was completed, the linear variable differential transducers (LVDTs) used for displacement measurement were reset to zero and specimens were tested to failure following ASTM D1761 lateral static test procedures, with the lateral load being applied in compression, that is, downward. No adjustments of the specimens or loading apparatus were made between the dynamic and static portions of the test. Deflections were measured with LVDTs accurate to +/- 0.00125 in. (0.032 mm). Load-deflection data were recorded digitally until failure occurred.

A section was cut from one specimen of each group of 10 replicates and specific gravity and moisture content were determined in accordance with ASTM D143 (ASTM, 1983a).

3.2.2 Critical-frequency dynamic test

Results from the preliminary dynamic tests were analyzed to provide information for the critical-frequency dynamic test. Comparison of load-deformation parameters from the baseline test of 0 Hz with similar parameters of dynamically loaded joints yielded a critical frequency. This frequency was used to test the additional 40 specimens.

Specimens were assembled as in the preliminary test, except that all 40 specimens had power-driven, coated nails. The following test matrix shows the combinations used for the critical-frequency test specimens.

Variable	Quant.	Description
Connections	2	Wood/gypsum board/wood, wood/particleboard/wood
Moisture content	2	6% EMC, 19% EMC
Replications	10	
Total Tests	**40**	

4. PRELIMINARY RESULTS

4.1 Materials

Moisture content and specific gravity were determined from one specimen of each group of replicates; values are contained in Table 1. Actual values, with specific gravity adjusted to 12% EMC using methods in ASTM D2395 (ASTM, 1983b), are compared with those found in the NDS. Douglas-fir dimension lumber used in this test had a specific gravity that agreed closely with the 0.51 value listed in the NDS.

Specific gravity was also determined for the two filler materials used, and this is also contained in Table 1.

4.2 Dynamic Loading

The load measured during the 25-s loading period dropped off quite abruptly, then leveled until dynamic movement was completed. Particleboard and gypsum board filler materials had a significant effect on the amount of load carried in the joint. Particleboard joints had a mean initial load of 402 lb (1,788 N), then dropped off approximately 13% to 352 lb (1,566 N) after 25 s of loading. Gypsum board carried an initial load of 223 lb (992 N), then dropped off 19% to 180 lb (800 N) after 25 s of loading. Comparing filler materials, the mean initial load for particleboard was 80% higher than that for gypsum board, and the mean final load for particleboard was 95% higher than that for gypsum board.

The frequency level affected how much the load decreased during dynamic loading. Table 2 shows the comparison between the decrease in loads carried by joints with particleboard and those with gypsum board fillers over the frequency range tested. For example, the load carried by joints subjected to a 1-Hz frequency with a gypsum board filler dropped off 13.7% from the first to the last cycle of dynamic load. This decrease in load is illustrated in Figure 4, which is a typical time compared to load curve for a specimen dynamically loaded at 1 Hz. Notice that most decrease in load occurs within the first few cycles.

4.3 Preliminary Dynamic Tests

Load-deformation curves obtained during preliminary tests were fitted to a hyperbolic tangent curve, using points up to 75% of maximum load. This curve-fitting procedure provided a consistent, repeatable method of analyzing the load-deformation data and provided a computerized method of obtaining slope and strength data. Figure 5 illustrates the three response variables that were used to compare values among different loading frequencies: the initial slope of the load-deformation curve, load at ¼-in. (6.4-mm) deformation, and the 5%-nail-diameter offset yield load. Tables 3, 4, and 5, respectively, contain mean and coefficient of variation results of replicate groups of these three response variables. Table 6 contains grouped statistical data for each response variable at each frequency.

Some joints failed abruptly; nails pulled completely out of the main wood member very suddenly. However, most joints did not fail abruptly. After these joints lost their initial stiffness, the load-deformation curve flattened out; that is, the connection maintained a relatively constant load while continuing to deform. After ¼-in. (6.4-mm) deformation, it was judged that test loading went from lateral to withdrawal resistance; therefore load at ¼-in.

(6.4-mm) deformation was chosen as a measure of ultimate lateral load. In cases where the joint failed before reaching ¼-in. (6.4-mm) deformation, the ultimate load was used.

Included in Table 6 are the ratios of the response variables to the baseline 0-Hz (nondynamically loaded) values. Figure 6 shows these ratios and illustrates that both the offset yield load and load at ¼-in. (6.4-mm) deformation gradually increase as frequency increases, then levels off after a frequency of 5 Hz. Conversely, the initial slope of the load-deformation curve for the 5-Hz group is only about 75% of the baseline value but levels off at about 95% of the baseline value after 10 Hz.

The relative values of the dynamically loaded to baseline value ratios can be understood by viewing Figure 7. Typical curves from static loading are shown for the nondynamically and dynamically loaded joints. The nondynamically loaded joints were relatively stiff at initial load, resulting in higher initial slopes than those for the dynamically loaded joints. In dynamically loaded joints, the fastener is worked loose, which creates a less stiff joint, providing for a low slope in the initial section of the load-deformation curve. (The initial portion of this curve is similar to that obtained from bolt testing, where an oversized hole creates initial sloppiness in the joint.) The resulting slopes from these two curves result in a higher offset yield load in dynamically loaded than in nondynamically loaded joints. Also, because the difference between curves decreases as the test progresses, it follows that load at ¼-in. (6.4-mm) deformation is nearly the same for both groups, as the respective ratio in Table 6 illustrates.

This analysis shows that dynamic loads affect joint stiffness but not necessarily joint ultimate strength. A dynamic frequency of 5 Hz was judged to be the point where frequency effect stabilized. This value was chosen as the critical frequency for the remaining group of 40 joints to complete the dynamic tests.

4.4 Critical-Frequency Dynamic Tests

Forty additional tests were conducted in accordance with the test matrix detailed previously, using 5 Hz as the critical frequency during dynamic loading. Table 7 compares values obtained from the preliminary tests with those from the critical-frequency test for the three response variables. Because of the effects of the EMC level and filler material used, the values in Table 7 are presented to show that the values from both tests compare very favorably, illustrating that the methods used in this study for dynamic loading provide repeatable results.

5. OVERALL TEST RESULTS

Statistical analysis was conducted on the two groups of data. Because the 5-Hz values were judged to be the level at which frequency effect stabilized with respect to the baseline (0 Hz) data, discussion will be limited to a comparison of these two levels: 0 Hz and 5 Hz. That is, when references to dynamically loaded specimens are made, they will refer specifically to 5-Hz values but generally to the 5- to 20-Hz frequency range tested. Also, because of the nature of the tests, effects of the main factors will be addressed separately using the initial slope as a measure of joint stiffness and load at ¼-in. (6.4-mm) deflection as a measure of joint strength.

Tables 8, 9, and 10 provide results comparing the main effects of initial slope of the load-deformation curve, load at ¼-in. (6.4-mm) deflection, and 5%-diameter offset yield load, respectively.

5.1 Effects of EMC

Analysis-of-variance (ANOVA) results show that EMC level has a highly significant effect on joint strength but not on joint stiffness. Because of several two- and three-factor interactions that show some significance of EMC, breaking the ANOVA analysis further for joint strength is

necessary.

When the ANOVA is broken into sections to determine the interaction effects, results show that joint stiffness is affected by EMC only in the nondynamically loaded (0 Hz) specimens; that is, after a specimen undergoes a dynamic load, the effect of EMC level is not significant. Further, joint stiffness of nondynamically loaded specimens was not significantly affected by the type of filler material at 6% EMC but was at 19% EMC. That is, at 19% EMC, nondynamically loaded specimens with a particleboard filler had a mean initial slope (51,170 lb/in. (8,960 N/mm)) more than four times higher than that for similar specimens with a gypsum board filler (11,750 lb/in. (2,058 N/mm)).

Results from Table 9 show that joint strength (load at ¼-in. (6.4-mm) deformation) was not significantly affected by differences in dynamic frequency. Regardless of the main effect considered, load at ¼-in. (6.4-mm) deformation remains relatively constant (not deviating more than 10%) over the frequency range tested.

5.2 Effects of Filler Material

Overall, joint stiffness was affected by type of filler material only in nondynamic joints at 19% EMC; specimens with a particleboard filler had a mean initial slope more than four times higher than that for specimens with gypsum board filler, as described previously in Effects of EMC.

However, specimens with particleboard filler had significantly higher joint strength than those with gypsum board fillers. Table 11 shows mean values observed for load at ¼-in. (6.4-mm) deformation. A ratio of gypsum board to particleboard values is also shown. These values illustrate an average decrease of approximately 25% in joint strength when a gypsum board filler is used rather than a particleboard filler.

The effects of filler material were similar throughout the dynamic frequency range. That is, observed differences in both joint stiffness and strength were a result of the type of filler material used and not the level of dynamic frequency.

5.3 Effects of Driving Method

In both nondynamic and dynamic joints, there were no differences in joint stiffness or strength attributed to the type of driving method and fastener coating (hand-driven, uncoated shank or power-driven, coated shank) used. The differences found between groups were shown to be caused by either EMC level or type of filler material used.

6. DISCUSSION

From the lateral strength data found in these tests, it appears that dynamic loading affects only the relative stiffness of nailed joints. When a joint undergoes a dynamic, cyclic load, a certain amount of sloppiness is added that causes the joint to lose its initial stiffness. It also appears that the majority of the loss of joint stiffness occurs during the first few cycles of dynamic loading.

Considering that transportation loads may exert similar dynamic loads on joints in mobile housing, a similar loss of stiffness may occur during transportation. Also, because most stiffness is lost in the first few cycles, short over-the-road trips used to transport mobile homes may induce as much loss of joint stiffness as longer trips would.

Moisture content effects were only found to be significant in the stiffness of nondynamic joints. After a joint is loaded dynamically, moisture content level is no longer a factor for either joint stiffness or strength. (This information, however, should not be misunderstood. Joints in this study were fabricated and tested in identical environments; that is, low-humidity joints were fabricated at low humidity, then stored and later tested under the same conditions. Reduction of

lateral design loads required in the NDS apply to joints for which fabrication and in-service environments are **different.**)

Although joint stiffness is significantly affected by dynamic loads, joint strength is not. This test program found no evidence that the ultimate strength of nailed joints is affected when those joints are subjected to dynamic loads.

In most cases, particleboard filler provided a stiffer and stronger joint than did gypsum board fillers. Joints with particleboard were up to 28% stronger than joints with gypsum board fillers when the moisture content level was high (19% EMC).

Driving method and the presence of a thermosetting plastic coating on the nail shank made no significant difference in joint stiffness or strength. Any differences in these methods or materials would more likely be seen in withdrawal values than lateral values, as observed in the companion study to this report (Winistorfer & Soltis, 1993). Lateral nail values tend to be most dependent on material properties of the components used in a connection (wood, fastener, and filler material).

7. CONCLUSIONS

The lateral resistance of timber connections depends not only on the properties of the fasteners and wood members used but also on the filler materials that separate those wood members and the fabrication and in-service environments of the connection. This study attempted to determine the effects of dynamic forces on nailed joints with two types of filler materials separating wood members, in two different humidity environments, and with different types of construction practices.

Conclusions from these tests include

1) that dynamic forces reduce the lateral stiffness of nailed joints but not their ultimate lateral strength,

2) that 5 Hz is the frequency level where joint stiffness and strength begin to stabilize, within the tested range of 0 to 20 Hz,

3) that the majority of stiffness reduction in a nailed joint subjected to dynamic loads occurs in the first few cycles,

4) that after a joint undergoes dynamic loading, the level of moisture content of the wood members is not a factor in lateral stiffness or strength (when the fabrication and in-service environments are the same),

5) that joints with particleboard filler materials have much higher lateral stiffness and strength levels than do similar joints with gypsum board filler material, and

6) that no differences in lateral strength are evident between coated, power-driven and uncoated, hand-driven nails.

8. ACKNOWLEDGMENTS

This test program was funded cooperatively by the USDA Forest Service, Forest Products Laboratory and the United States Department of Housing and Urban Development (HUD) under Interagency Agreement Number DU-100I91-0000029 and by support from member companies of the International Staple, Nail, and Tool Association (ISANTA). The guidance and advise of David Kirkman and William Freeborne, HUD, and of John Kurtz, ISANTA, are appreciated.

9. REFERENCES

ASTM (1983a). Standard Methods of Testing Small Clear Specimens of Timber. ASTM D143. American Society for Testing and Materials. Philadelphia, PA.

ASTM (1983b). Standard Test Methods for Specific Gravity of Wood and Wood-Base Materials. ASTM D2395. American Society for Testing and Materials. Philadelphia, PA.

ASTM (1988). Standard Test Methods for Mechanical Fasteners in Wood. ASTM D1761. American Society for Testing and Materials. Philadelphia, PA.

Borkenhagen, E.H., and Heyer, O.C. (1950). Resistance to Direct Withdrawal of Various Types of Nails Driven Into Green and Dry Wood and Subjected to Cycles of Wetting and Drying. USDA Forest Products Laboratory. Not for publication.

Forest Products Laboratory (1987). Wood Handbook: Wood as an engineering material. Agriculture Handbook 72 (Rev.). Washington, D.C.; U.S. Department of Agriculture. 466 p.

Gaitzsch, F. (1934). Die Festigkeit maschineller Nagelverbindungen (The Strength of Machine-Nailed Joints). Forschungsberichte Holz, No. 3. Translation by Fleischer, H.O.

Heck, G.E. (1950). Effect of Atmospheric Changes on Wall-Panel Fastenings. USDA Forest Products Laboratory. Not for publication.

Lawniczak, M. (1956). Influence of Variations in the Moisture Content of Wood on Its Nail Holding Power. Commonwealth of Australia, Commonwealth Scientific and Industrial Research Organization (Translation No. 3303).

NFPA (1991). National Design Specification for Wood Construction. National Forest Products Association. Washington, D.C.

Rosenblueth, E., and Bustamante, J.I. (1962). Distribution of Structural Response to Earthquakes. Proceedings of ASCE, 88(EM3), 75-106.

Soltis, L.A., Gromala, D.S., and Tuomi, R.L. (1981). Seismic Performance of Low-Rise Wood Buildings. American Society of Civil Engineers, p. 78-91.

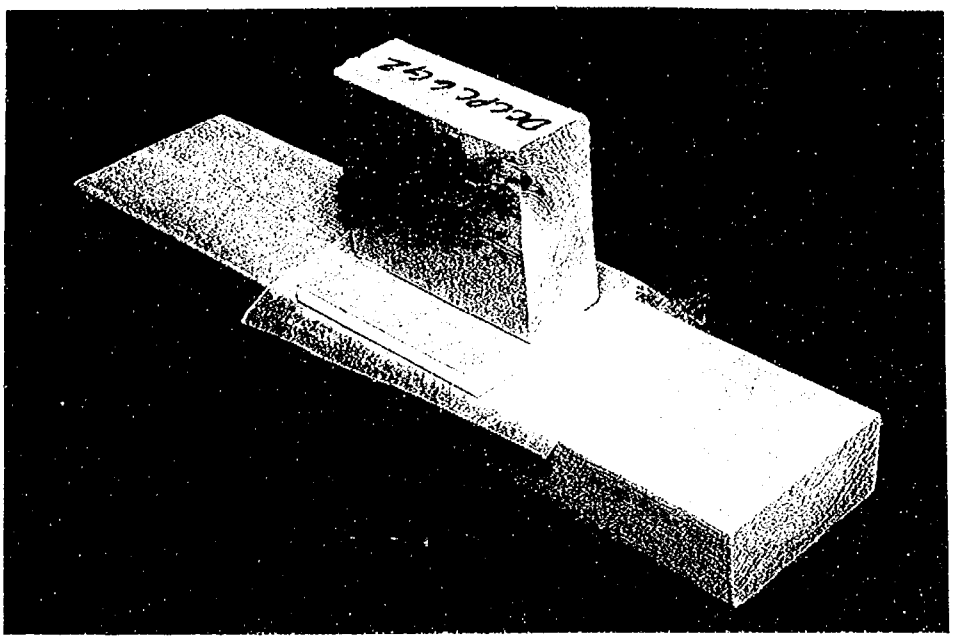
Soltis, L.A., and Nelson, W. (1990). Static Strength of Simulated Ceiling/Floor Connections in Modular/Manufactured Housing. Report submitted to the U.S. Dept. of Housing and Urban Development.

Stern, E.G. (1952). Strength of Auto-Nailer Assembled Skids. VPI Wood Research Laboratory Report No. 10. Blacksburg, VA.

GSA (1971). Federal Specification FF-N-105B: Wire, Cut and Wrought Nails, Staples and Spikes. United States General Services Administration.

Winistorfer, S.G., and Soltis, L.A. (1993). Lateral and Withdrawal Strength of Nail Connections for the Manufactured/Modular Housing Industry. Report submitted to the U.S. Dept. of Housing and Urban Development.

Youngquist, W.G., and Scholten, J.A. (1951). Comparative Holding Power of Common Wire Nails and New Type Powernails Manufactured by the Powernail Company. USDA Forest Products Laboratory report (not for publication).



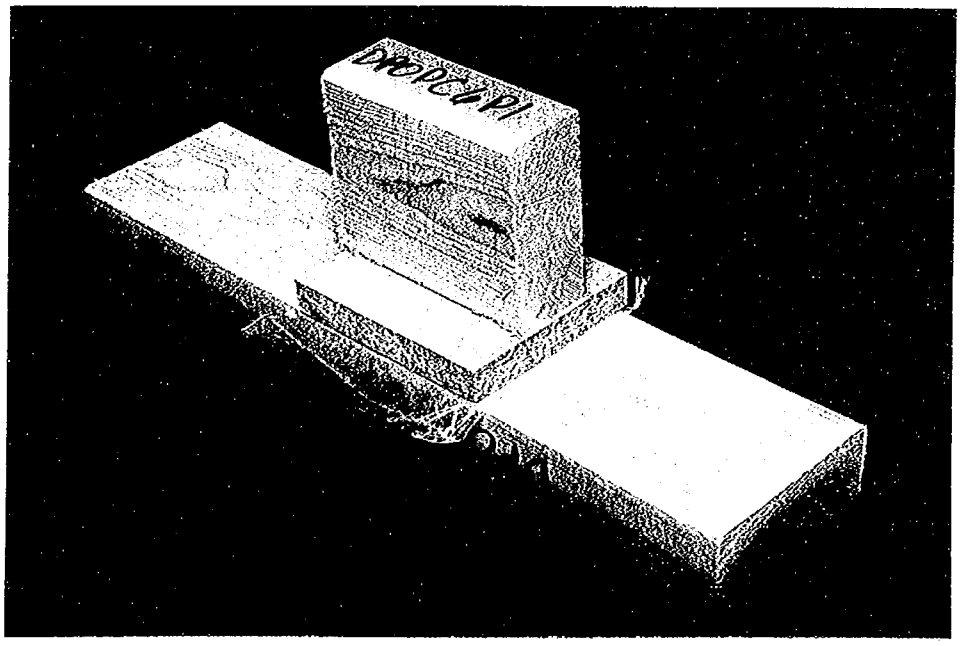


Figure 1. Joints with gypsum board (top) and particleboard (bottom) filler material for lateral tests.

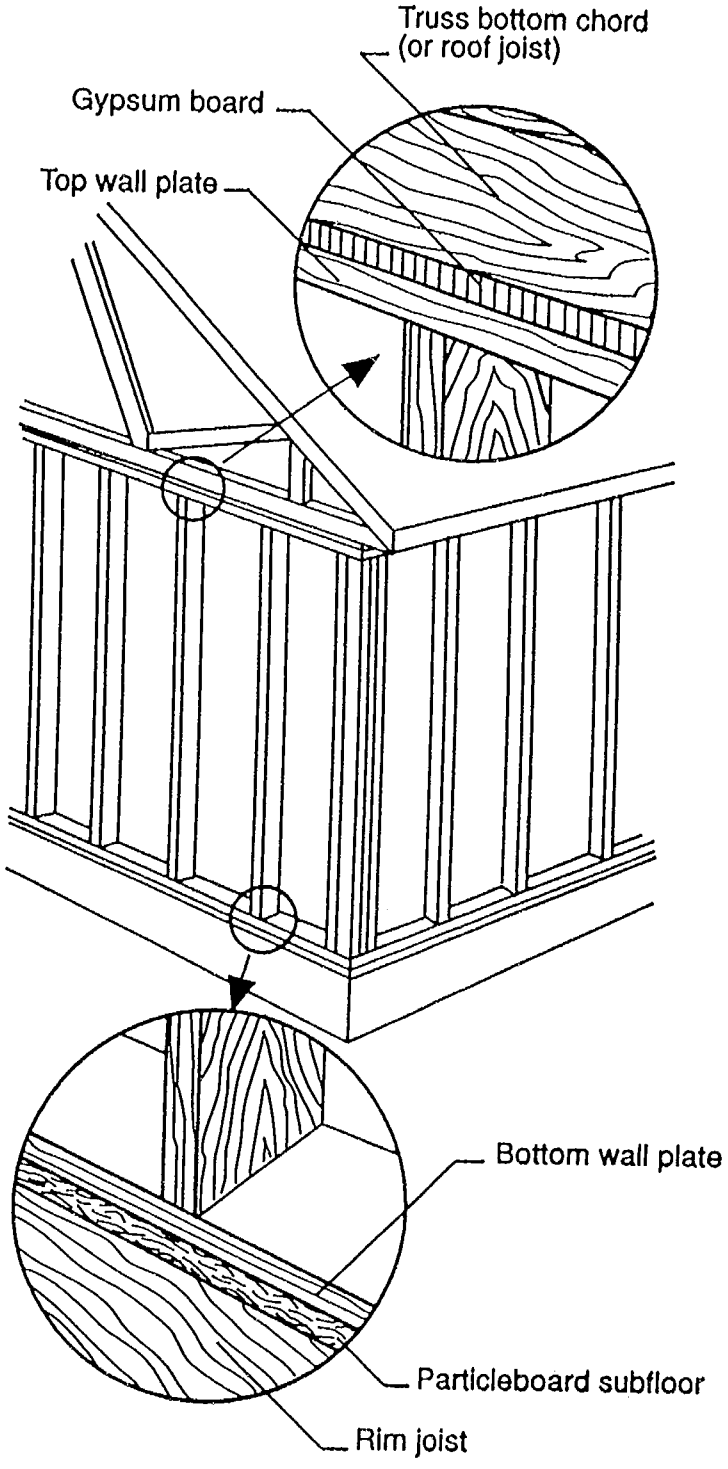


Figure 2. Construction in typical modular and manufactured housing. Particleboard subfloor is attached to floor joists before wall section is put in place, creating joint where particleboard is filler between main wood members. Similar section is created with gypsum board at roof section.

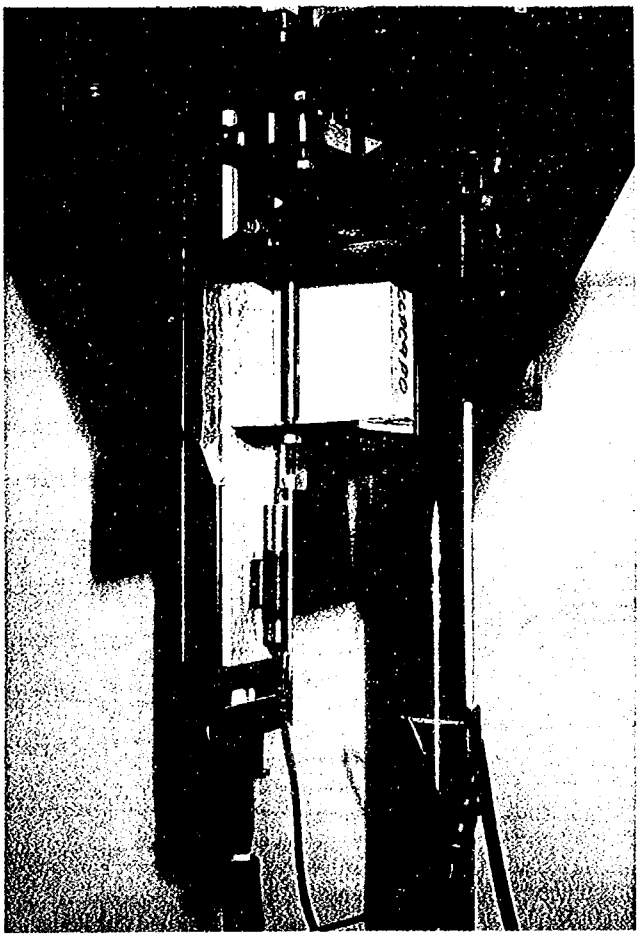


Figure 3. Lateral test set-up. Metal frame, attached to dynamic load head, oscillates vertically and applies load to wood side member, while filler material and wood main member are held stationary.

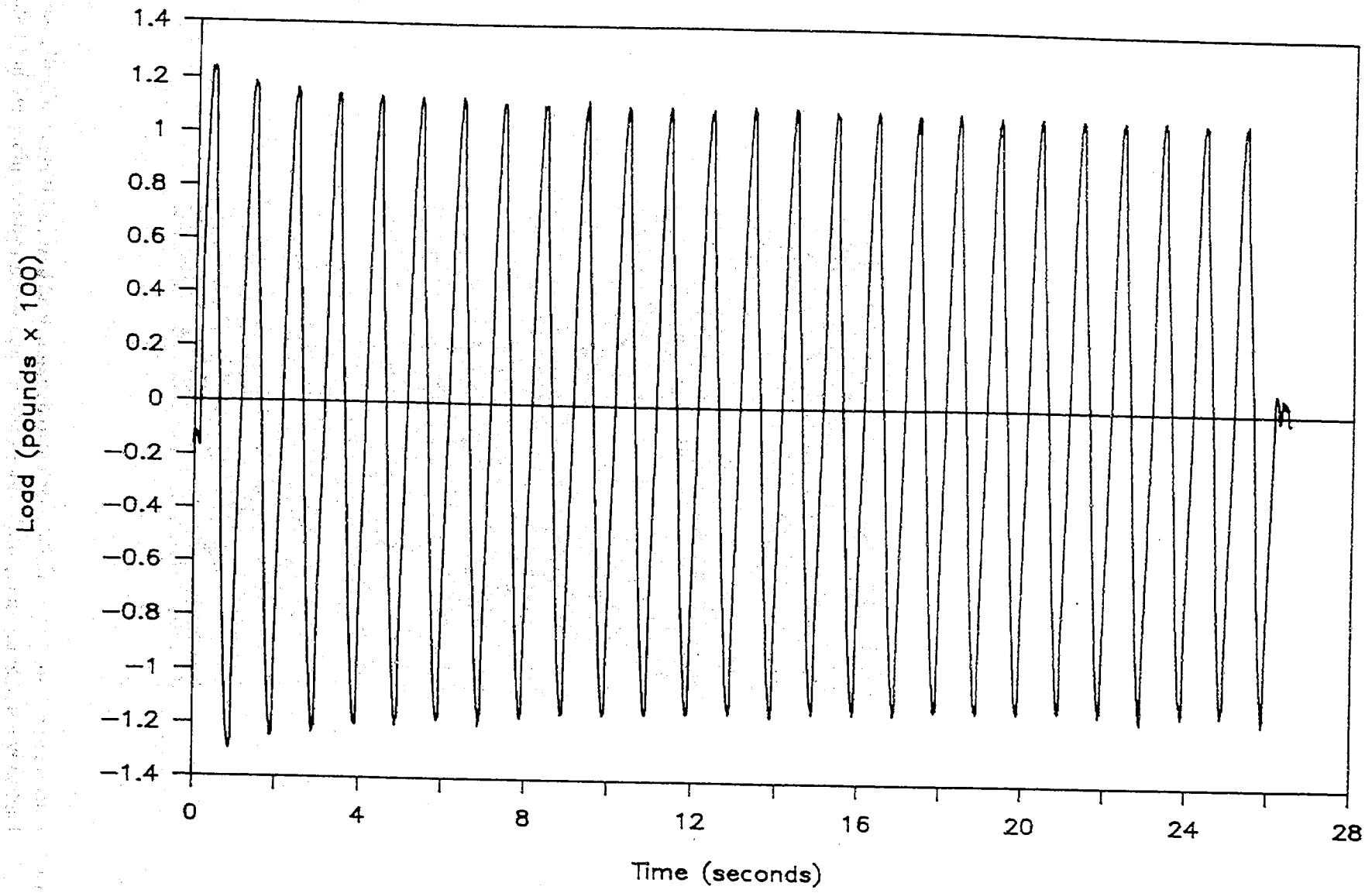


Figure 4. Load compared to time for the dynamic loading of lateral test specimen in preliminary dynamic group, at 1-Hz frequency.

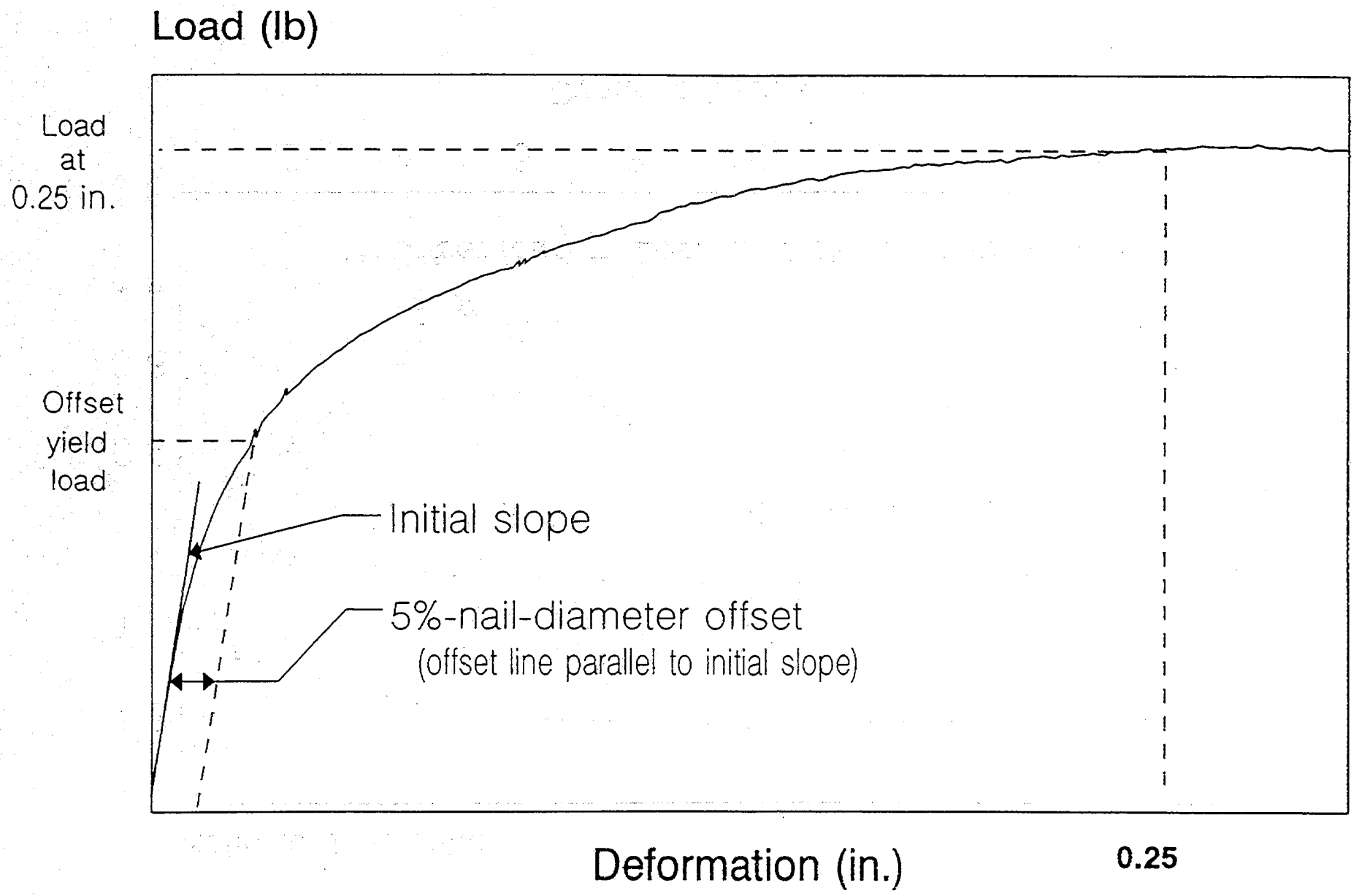


Figure 5. Three response variables used for comparison of load-deformation data.

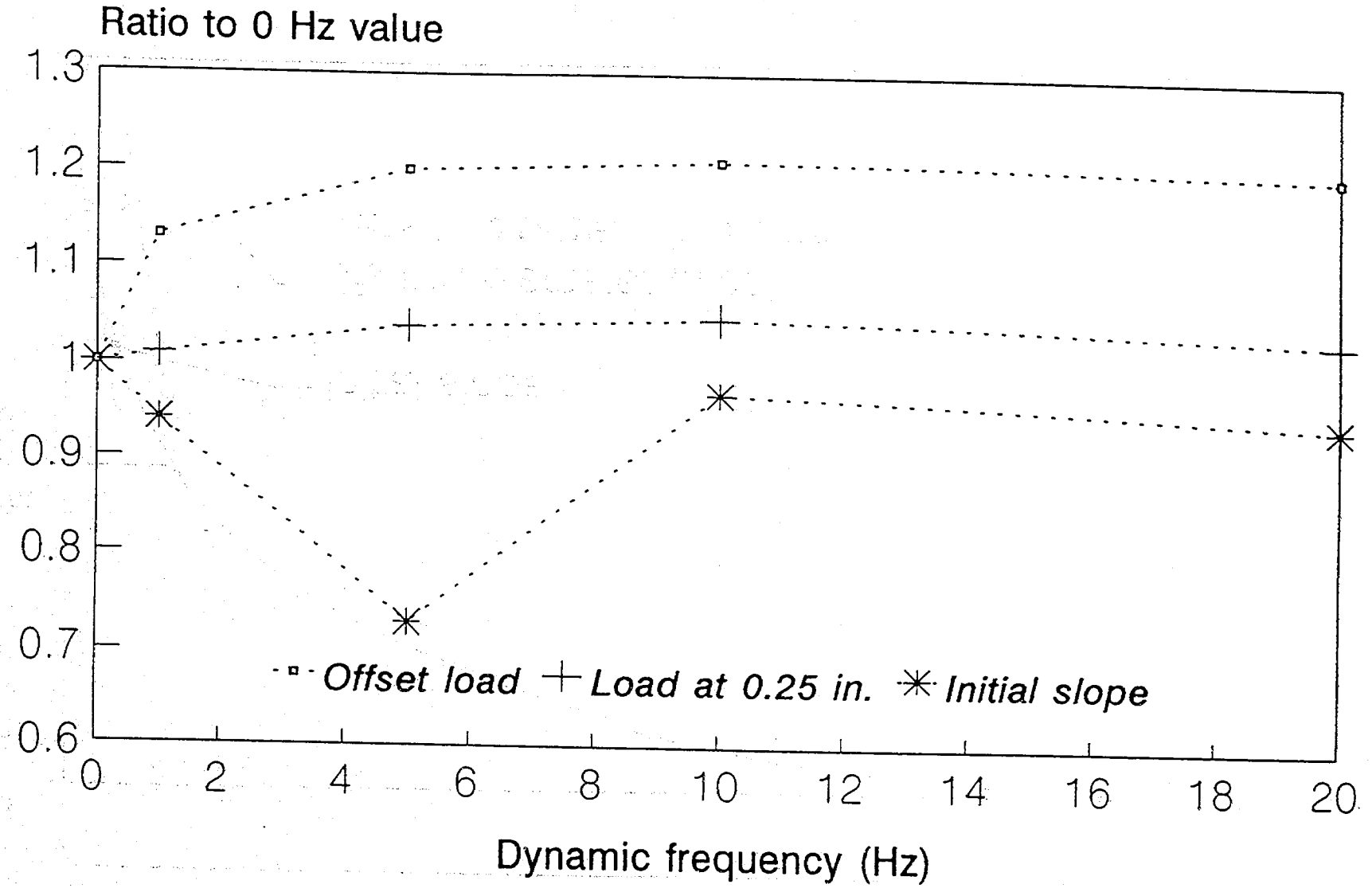


Figure 6. Comparison of dynamic frequency effect on three response variables from preliminary test (40 joints were tested at each frequency level).

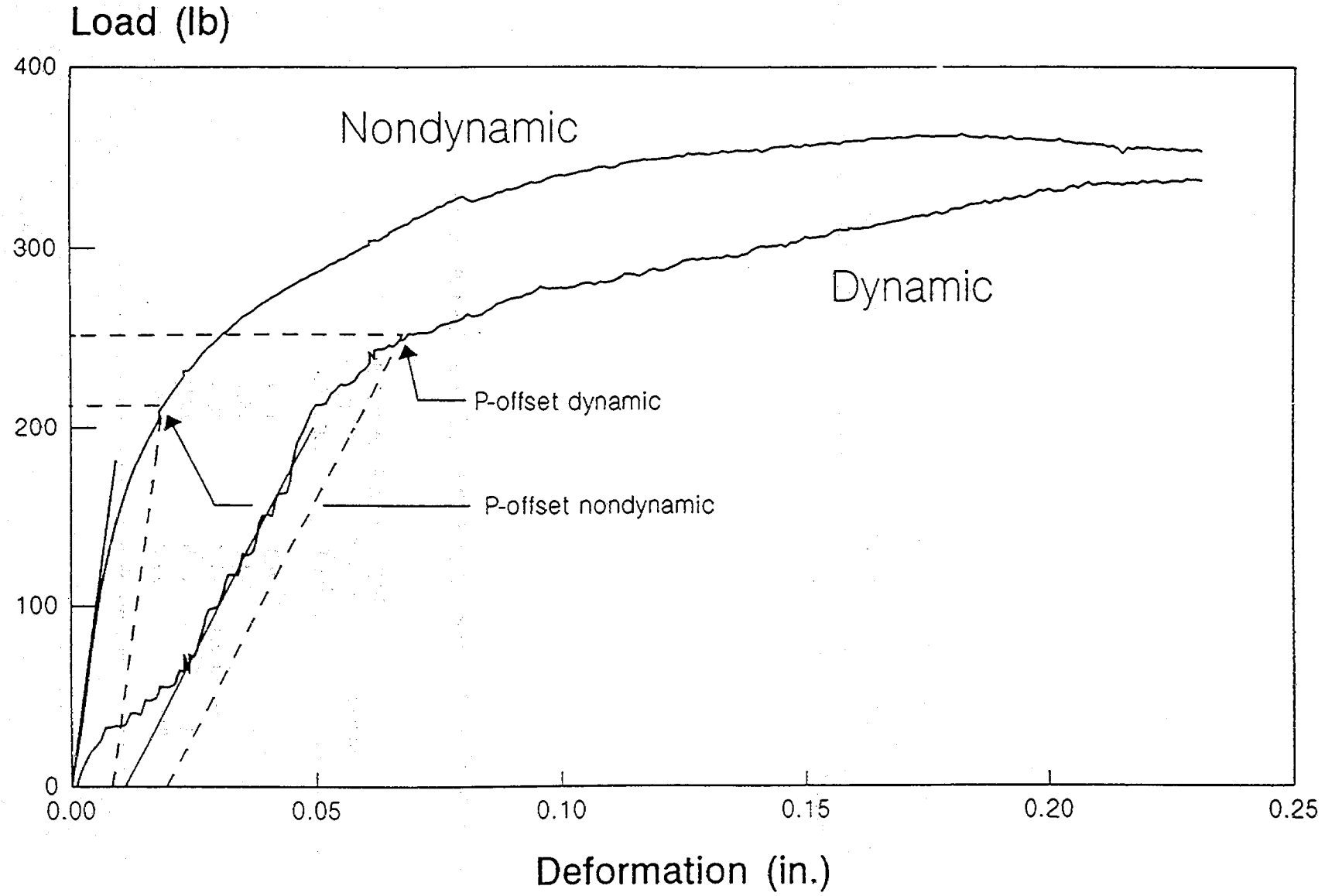


Figure 7. Typical load-deformation curves for lateral nail joints. Curves are of static tests, where dynamic group was subjected to dynamic loading prior to static testing.

Table 1. Wood and filler material properties

Material	Low EMC		High EMC	
	EMC[a]	SG[b]	EMC[a]	SG[b]
Douglas-fir	6.4	0.51	23.9	0.51
Particleboard[c]		0.70		
Gypsum board[c]	17.8	0.64[d]		

[a] EMC = equilibrium moisture content.
[b] SG = specific gravity, adjusted to 12% EMC.
[c] Specific gravity of filler material in different EMCs was not determined.
[d] Specific gravity of gypsum board could not be adjusted to 12% EMC since ASTM D2395 applies only to wood and wood-base materials.

Table 2. Comparison of percentage drop in load during dynamic loading

Frequency (Hz)	Percentage decrease in load	
	Particle board	Gypsum board
1	6.8	13.7
5	11.5	18.4
5 (Critical)	11.8	18.5
10	14.8	19.0
20	17.2	25.8

Table 3. Averages and COV of replicate groups: Initial slope

Frequency (Hz)	Assembly method	EMC[a] (%)	Filler	Initial slope Mean (lb/in)[b]	Initial slope COV[c]
0	Hand/uncoated	6	Gypsum	15,510	0.88
			Particle	16,030	0.26
		19	Gypsum	13,520	0.28
			Particle	47,090	0.39
	Power/coated	6	Gypsum	10,640	0.33
			Particle	17,530	0.20
		19	Gypsum	9,980	0.27
			Particle	55,250	0.35
1	Hand/uncoated	6	Gypsum	29,720	0.41
			Particle	19,050	0.56
		19	Gypsum	22,310	0.31
			Particle	22,300	0.70
	Power/coated	6	Gypsum	26,370	0.32
			Particle	22,680	0.47
		19	Gypsum	22,210	0.14
			Particle	9,510	0.10
5	Hand/uncoated	6	Gypsum	21,620	0.29
			Particle	22,100	0.17
		19	Gypsum	17,230	0.34
			Particle	20,900	0.62
	Power/coated	6	Gypsum	13,530	0.13
			Gypsum	15,410	0.22[d]
			Particle	17,350	0.23
			Particle	20,950	0.15[d]
		19	Gypsum	10,100	0.14
			Gypsum	12,890	0.17[d]
			Particle	11,950	0.19
			Particle	10,710	0.17[d]

[a] EMC = equilibrium moisture content.
[b] Each mean is calculated from a replicate group of five specimens; 1 lb/in = 0.18 N/mm.
[c] COV = coefficient of variation (of sample standard deviation).
[d] Groups are from final 5-Hz tests, with 10 replicates per group.

Table 3. Averages and COV of replicate groups: Initial slope (cont.)

Frequency (Hz)	Assembly method	EMC[a] (%)	Filler	Initial slope Mean (lb/in)[b]	Initial slope COV[c]
10	Hand/uncoated	6	Gypsum	19,340	0.20
			Particle	21,950	0.23
		19	Gypsum	26,750	0.38[d]
			Particle	27,990	0.72
	Power/coated	6	Gypsum	22,890	0.12
			Particle	21,690	0.18
		19	Gypsum	20,420	0.17
			Particle	18,150	0.29
20	Hand/uncoated	6	Gypsum	22,500	0.29
			Particle	25,400	0.31
		19	Gypsum	23,890	0.40
			Particle	28,620	0.36
	Power/coated	6	Gypsum	23,780	0.29
			Particle	19,120	0.31
		19	Gypsum	19,940	0.59
			Particle	11,670	0.09

[a] EMC = equilibrium moisture content.
[b] Each mean is calculated from a replicate group of five specimens; 1 lb/in = 0.18 N/mm.
[c] COV = coefficient of variation (of sample standard deviation).
[d] Only four test specimens available; equipment failed during one test.

Table 4. Averages and COV of replicate groups: Load at ¼-in. (6.4-mm) deformation

Frequency (Hz)	Assembly method	EMC[a] (%)	Filler	Load at ¼-in. deformation Mean (lb)[b]	COV[c]
0	Hand/uncoated	6	Gypsum	256	0.05
			Particle	324	0.06
		19	Gypsum	282	0.07
			Particle	377	0.05
	Power/coated	6	Gypsum	291	0.06
			Particle	373	0.10
		19	Gypsum	246	0.08
			Particle	343	0.08
1	Hand/uncoated	6	Gypsum	254	0.08
			Particle	312	0.05
		19	Gypsum	296	0.07
			Particle	379	0.06
	Power/coated	6	Gypsum	287	0.06
			Particle	375	0.10
		19	Gypsum	247	0.08
			Particle	379	0.04
5	Hand/uncoated	6	Gypsum	270	0.07
			Particle	324	0.05
		19	Gypsum	303	0.10
			Particle	422	0.04
	Power/coated	6	Gypsum	281	0.02
			Gypsum	283[d]	0.06
			Particle	389	0.06
			Particle	354[d]	0.06
		19	Gypsum	251	0.03
			Gypsum	249[d]	0.07
			Particle	353	0.05
			Particle	341[d]	0.06

[a] EMC = equilibrium moisture content.
[b] Each mean is calculated from a replicate group of five specimens; 1 lb = 4.448 N.
[c] COV = coefficient of variation (of sample standard deviation).
[d] Groups are from final 5-Hz tests, with 10 replicates per group.

Table 4. Averages and COV of replicate groups: Load at ¼-in. (6.4-mm) deformation (cont).

Frequency (Hz)	Assembly method	EMC[a] (%)	Filler	Load at ¼-in. deformation Mean (lb)[b]	COV[c]
10	Hand/uncoated	6	Gypsum	277	0.08
			Particle	331	0.07
		19	Gypsum	299	0.08[d]
			Particle	424	0.07
	Power/coated	6	Gypsum	298	0.05
			Particle	368	0.09
		19	Gypsum	257	0.03
			Particle	383	0.08
20	Hand/uncoated	6	Gypsum	254	0.05
			Particle	328	0.08
		19	Gypsum	291	0.12
			Particle	386	0.11
	Power/coated	6	Gypsum	290	0.05
			Particle	392	0.04
		19	Gypsum	256	0.04
			Particle	365	0.05

[a] EMC = equilibrium moisture content.
[b] Each mean is calculated from a replicate group of five specimens; 1 lb = 4.448 N.
[c] COV = coefficient of variation (of sample standard deviation).
[d] Only four test specimens available; equipment failed during one test.

Table 5. Averages and COV of replicate groups: Load at 5%-diameter offset yield

Frequency (Hz)	Assembly method	EMC[a] (%)	Filler	Load at 5%-diameter offset Mean (lb)[b]	COV[c]
0	Hand/uncoated	6	Gypsum	131	0.09
			Particle	176	0.10
		19	Gypsum	109	0.10
			Particle	204	0.09
	Power/coated	6	Gypsum	123	0.19
			Particle	164	0.14
		19	Gypsum	89	0.12
			Particle	161	0.10
1	Hand/uncoated	6	Gypsum	135	0.14
			Particle	167	0.07
		19	Gypsum	138	0.06
			Particle	212	0.06
	Power/coated	6	Gypsum	133	0.04
			Particle	194	0.14
		19	Gypsum	98	0.06
			Particle	229	0.05
5	Hand/uncoated	6	Gypsum	128	0.13
			Particle	177	0.05
		19	Gypsum	133	0.06
			Particle	271	0.05
	Power/coated	6	Gypsum	131	0.05
			Gypsum	123	0.11[d]
			Particle	197	0.14
			Particle	191	0.07[d]
		19	Gypsum	111	0.03
			Gypsum	102	0.10[d]
			Particle	243	0.10
			Particle	187	0.12[d]

[a] EMC = equilibrium moisture content.
[b] Each mean is calculated from a replicate group of five specimens; 1 lb = 4.448 N.
[c] COV = coefficient of variation (of sample standard deviation).
[d] Groups are from final 5-Hz tests, with 10 replicates per group.

Table 5. Averages and COV of replicate groups: Load at 5%-diameter offset yield (cont.)

Frequency (Hz)	Assembly method	EMC[a] (%)	Filler	Load at 5%-diameter offset Mean (lb)[b]	COV[c]
10	Hand/uncoated	6	Gypsum	136	0.09
			Particle	190	0.14
		19	Gypsum	129	0.13[d]
			Particle	264	0.13
	Power/coated	6	Gypsum	126	0.08
			Particle	197	0.11
		19	Gypsum	111	0.09
			Particle	245	0.15
20	Hand/uncoated	6	Gypsum	131	0.09
			Particle	191	0.10
		19	Gypsum	121	0.10
			Particle	244	0.09
	Power/coated	6	Gypsum	134	0.07
			Particle	216	0.09
		19	Gypsum	111	0.08
			Particle	237	0.14

[a] EMC = equilibrium moisture content.
[b] Each mean is calculated from a replicate group of five specimens; 1 lb = 4.448 N.
[c] COV = coefficient of variation (of sample standard deviation).
[d] Only four test specimens available; equipment failed during one test.

Table 6. Results of preliminary dynamic tests

Dynamic frequency (Hz)	Initial slope			5%-diameter offset yield load			Load at ¼-in. deformation		
	Mean (lb/in.)[a]	COV[b]	Ratio to 0 Hz Value	Mean (lb)[c]	COV[b]	Ratio to 0 Hz Value	Mean (lb)[c]	COV	Ratio to 0 Hz Value
0	23,200	0.84	1.00	145	0.27	1.00	312	0.17	1.00
1	21,800	0.48	0.94	163	0.27	1.13	316	0.18	1.01
5	16,900	0.41	0.73	174	0.33	1.20	324	0.18	1.04
10	22,400	0.64	0.97	175	0.34	1.21	327	0.19	1.05
20	21,900	0.44	0.94	173	0.32	1.20	320	0.18	1.03

[a] Each frequency has 40 replicated tests; 1 lb/in = 0.18 N/mm.
[b] COV = coefficient of variation (using sample standard deviation).
[c] Each frequency has 40 replicated tests; 1 lb = 4.448 N.

Table 7. Comparison of 5-Hz values from preliminary and critical-frequency tests (power-driven, coated specimens)

Test	Initial slope		5%-diameter offset yield load		Load at ¼-in. deformation	
	Mean[a] (lb/in.)[b]	COV[c]	Mean (lb)[d]	COV	Mean (lb)[d]	COV
6% EMC with gypsum board						
Preliminary	13,530	0.13	131	0.05	281	0.02
Critical frequency	15,410	0.22	123	0.11	283	0.06
6% EMC with particleboard						
Preliminary	17,350	0.23	197	0.14	389	0.06
Critical frequency	20,950	0.15	191	0.07	354	0.06
19% EMC with gypsum board						
Preliminary	10,100	0.14	111	0.03	251	0.03
Critical frequency	12,890	0.17	102	0.10	249	0.07
19% EMC with particleboard						
Preliminary	11,950	0.19	243	0.10	353	0.05
Critical frequency	10,710	0.17	187	0.12	341	0.06

[a] Preliminary test data are 5 replicated tests; critical-frequency test data are of 10 replicated tests.
[b] 1 lb/in = 0.18 N/mm.
[c] COV is the coefficient of variation (using sample standard deviation).
[d] 1 lb = 4.448 N.

Table 8. Comparison of main effects: Initial slope (lb/in x 1,000)[a]

Main effect	Mean dynamic frequency (Hz)[b]				
	0	1	5	10	20
Particleboard filler	34.0	18.4	17.0	22.4	21.2
Gypsum board filler	12.4	25.2	14.9	22.4	22.5
Hand-driven/uncoated nail	23.0	23.3	20.5	24.0	25.1
Power-driven/coated nail	23.4	20.2	14.4	20.8	18.6
Low humidity (6% EMC)	14.9	24.5	18.4	21.5	22.7
High humidity (19% EMC)	31.5	19.1	13.4	23.3	21.0

[a] 1 lb/in = 0.18 N/mm.
[b] Each mean is calculated from group of 20 specimens with main effect characteristic, except 5-Hz groups, which are calculated means from 30 specimens.

Table 9. Comparison of main effects: Load at ¼-in. (6.4-mm) deformation (lb)[a]

Main effect	Mean dynamic frequency (Hz)[b]				
	0	1	5	10	20
Particleboard filler	354	361	360	377	368
Gypsum board filler	269	271	271	282	273
Hand-driven/uncoated nail	310	310	330	335	315
Power-driven/coated nail	313	322	311	327	326
Low humidity (6% EMC)	311	307	317	319	316
High humidity (19% EMC)	312	325	314	343	325

[a] 1 lb = 4.448 N.
[b] Each mean is calculated from group of 20 specimens having main effect characteristic, except 5-Hz groups, which are calculated from 30 specimens.

Table 10. Comparison of main effects: Load at 5%-diameter offset yield (lb)[a]

Main effect	Mean dynamic frequency (Hz)[b]				
	0	1	5	10	20
Particleboard filler	176	201	206	224	222
Gypsum board filler	113	126	119	126	124
Hand-driven/uncoated nail	155	163	177	180	172
Power-driven/coated nail	134	164	157	170	175
Low humidity (6% EMC)	149	157	158	162	169
High humidity (19% EMC)	141	169	167	187	178

[a] 1 lb = 4.448 N.

[b] Each mean is calculated from group of 20 specimens having main effect characteristic, except 5-Hz groups, which are calculated from 30 specimens.

Table 11. Comparison of mean load at ¼-in. (6.4-mm) deformation

EMC (%)	Filler material	Mean (lb)[a]	Ratio[c]
6	particleboard	352[b]	1.00
6	gypsum board	276	0.78
19	particleboard	381	1.00
19	gypsum board	273	0.72

[a] 1 lb = 4.448 N.

[b] This value, and others in this table, can be calculated from those found in Table 4 by averaging appropriate means. For example, 352 lb is average of load at ¼-in deformation means from Table 4 for 6%-EMC groups with particleboard filler material:
(324 + 373 + 312 + 375 + 324 + 389 + 331 + 368 + 328 + 392)/10 = 352 lb.

[c] Ratio of mean values (of similar EMC levels) using particleboard value as baseline.

THE OFFSHORE NICARAGUAN EARTHQUAKE AND TSUNAMI OF SEPTEMBER 2, 1992

by

Mehmet Çelebi[1] and David Harlow[1]

ABSTRACT

This paper highlights the Nicaraguan earthquake and tsunami of September 2, 1992 and its effects. The tsunami, rather than the shaking, caused extensive damage and loss of lives along the Nicaraguan coast.

KEYWORDS: earthquake; tsunami; damage; tidal gage; run-off height.

1. INTRODUCTION

A destructive tsunami caused by an offshore earthquake (M_s=7.2) struck the Pacific coast of Nicaragua on September 2, 1992 at 00:16:01 UTC (local time September 1, 1992 at 7:16 PM). The National Earthquake Information Center (NEIC) located the earthquake epicenter at 11.8°N and 87.4°W (Figure 1) and the depth at 33 km. Numerous smaller magnitude earthquakes followed.

Very little structural damage was inflicted by the September 2, 1992 earthquake. However, the destructive tsunami generated by that event reminded Nicaraguans of the damage potential from offshore earthquakes. The tsunami caused widespread loss of property and cost approximately 200 lives along the coast of Nicaragua. In addition, approximately 500 injuries requiring treatment were reported. Tsunami wave heights reported in the press ranged from 6-10 meters. The tsunami undermined the economic base of coastal villages that rely on fishing, tourism and harbor activities for livelihood. An ancillary impact of the tsunami was an outbreak of cholera in villages where the water supply (wells) was contaminated.

Earthquake hazards and volcanic activity in Nicaragua are severe (White, 1991). The Pacific Coast of Central America is an active tectonic environment where the Cocos plate is subducting north eastward beneath the Caribbean plate at a rate of about 8 cm/year and consequently the large earthquakes and tsunamis are recurring. The two main sources of destructive earthquakes in Nicaragua are *(1)* shallow intra-plate earthquakes up to magnitude 6.2 along the volcanic chain and *(2)* inter-plate earthquakes up to magnitude 7.5 in the Pacific Ocean associated with the plate subduction. The interplate earthquakes can inflict structural damage over a wide area. A magnitude (M_s) 6.2 intra-plate earthquake devastated central Managua, the capital city of Nicaragua on December 23, 1972 (EERI, 1973, Brown *et.al.*, 1973). More than 11,000 people lost their lives during that event. The resulting destruction has had long term economic, social, and political impacts. The September 2, 1992 earthquake provides some insight into the rapid increase with time of earthquake risks due to the rapid increase in population. A similar earthquake struck Managua in 1931 killing 2,500 people out of a much smaller population. A magnitude 7.5 earthquake in 1898 was the

[1] USGS(MS977), 345 Middlefield Rd., Menlo Park, Ca. 94025

most recent inter-plate earthquake to cause significant damage onshore (Kanamori and Abe, 1983). That earthquake caused widespread destruction in Corinto, Chinandego and Leon.

During the two decades since the 1972 Managua earthquake, the population of Nicaragua has increased by at least 60% and the population of Managua has increased by an even faster rate. Thus, the number of homes, buildings, and public utility structures that are vulnerable to inevitable future earthquakes and tsunamis are also increasing.

The tsunami wave amplitudes are deemed (Satake, *et.al.*, 1993) to be significantly larger than would have been expected from an earthquake of magnitude 7.2. Understanding the mechanism of this particular tsunami has important implications for evaluating earthquake hazards along the coast of Central America. Earthquakes that produce such abnormally large tsunamis are called "tsunami earthquakes"; examples by Satake, *et.al.*, (1993) include the 1896 Sanriku, Japan, 1946 Aleutian and 1960 Peru earthquakes. Although catastrophic tsunamis are not frequent in Central America, a large earthquake in 1859 off the coast of El Salvador generated a tsunami that caused destruction in El Salvador and Guatemala. There is limited information about past tsunami experience dating back to 1859, 1919, 1950 and 1956 earthquakes. The tsunami generated by off-shore earthquakes in Nicaragua may also have implications for the Pacific Northwest in the United States where paleoseismic evidence indicates tsunamis have occurred in any area that currently shows low seismic activity.

There is a critical need for a well focused earthquake hazard reduction program in Nicaragua. In particular, the areas that need rebuilding and development include a country wide deployment of instruments to record and analyze earthquakes, drafting and upgrading building codes, civil defense planning and public education. This paper provides highlights of this event and the observations during post earthquake surveys.

2. OBSERVATIONS

The central and southwest coast of Nicaragua was affected mainly by the tsunami. Most residents of the coastal towns (Corinto, Poneloya, Les Penitas, Salinas, Salinas Grandes, Puerto Sandino, Miramar, El Velero, Il Transito, Masachapa, Pochomil, Montelimar, La Boquita, Caseras, Astillero, Salinas Grandes, Popoyo and San Juan Del Sur) reported no shaking but did report a "flashing light" before the tsunami struck. Those who felt the earthquake said they saw the "flashing light" after the earthquake occurred.

The level of inundation and height of waves were clearly visible to varying degrees in most coastal areas. Eyewitness reports of wave heights varied from 3-4 meters to 15 meters. However, in several locations, it was possible to locate how high the waves reached by marks on the trees and by the salt-water dried limbs and leaves of the trees. Tidal wave gages in Corinto recorded the arrival of the tsunami (Figure 2).

Figure 3 shows the result of a tsunami run-up wave height survey (Satake *et. al.*, 1993).

3. STRONG-MOTION AND SEISMIC NETWORKS

There are no strong-motion records from the Nicaraguan earthquake. A network deployed in the early 1970's with the United States Geological Survey (USGS) cooperation was disassembled during the 1980's, and the

accelerographs are stored in the offices of Instituto Nicaragüense de Estudios Territoriales (INETER). This is certainly a loss and shows the vulnerability of such programs to interruptions in maintenance. As a consequence, the whole strong-motion network will have to be re-established.

Data from a national network of seismic stations was used to identify a zone of seismic quiescence off the coast of Nicaragua that was considered to be the likely location for a future large earthquake (Harlow, White, Cifuentes and Aburto, 1981). That location appears to be the source of the September 2, 1992 earthquake and, therefore, offers some hope for the usefulness of such data for long term forecasting of earthquakes in this area.

4. STRUCTURAL RESPONSE AND DAMAGE

The typical construction on the coast consists of single or two-story buildings, in general, of timber construction or a mixture materials including unreinforced brick or stone masonry, lightly reinforced, concrete, framed construction and masonry infill walls. Some steel construction existed particularly in port facilities. However, timber construction dominates. On the coastal towns, parallel to the beachfronts, a row of buildings used either for sea-side hotels and restaurants or fishing facilities almost always had some stronger wall perpendicular to the beachfront while the resistance and stiffness parallel to the beachfront was less. It appeared that some of these buildings were specifically designed or evolved over the years with unusual wave heights during high-tides. Many of these buildings had large openings on the beachfront and continuous courtyards extending from the beachfront face to the streetfront face at the other end. Significant numbers of these buildings, particularly in Il Transito (approximately 300), Caseres and other centers, collapsed. Most of these buildings were built on approximately 1 meter high concrete (lightly-reinforced or unreinforced) continuous footing. The condition of one of the many buildings that collapsed is shown in Figure 4. The better built structures of this type survived with only doors and windows being damaged.

It is quite clear that the shaking damage is not very extensive for an event with a magnitude as large as the September 2, 1992 event (M_s=7.2) and the resulting tsunami which delivered waves as high as 6 meters (or 10 meters according to some estimates). One reason for the relatively small shaking damage is the distance from the coast to the off-shore earthquake epicenter (approximately 74 km) ans the other reason is that the coast of Nicaragua is not densely populated and most of the structures that were damaged were relatively substandard and not engineered. Well-built homes and planned resorts, on the coast, constructed with better quality material were either not damaged or lightly damaged. On the other hand, well built planned resort areas on the coast such as El Velero, Montelimar and Pochomil Nuevo (all in close proximity to San Juan del Sur), experienced little or no damage.

During the earthquake/tsunami, port and harbor facilities, in general, fared well. A conveyor belt and part of a building at Puerto Sandino, which is a major port for importing oil, suffered minor damage. The largest port, Corinto, was not damaged because of a barrier island and the shape of the bay. Topographical setting played a major role in the distribution of run-up heights and the damage in most locations including the port of San Juan del Sur, at the southern coast of Nicaragua. The port facilities on the southern part of the unique half-moon shaped bay of San Juan del Sur

are considerably on higher ground (on a cliff) than the beachead; therefore, the port facilities were spared while on the northern end of the bay, there was quite a lot of damage inflicted on the one and two story buildings. It is probable that this setting may have resulted in focusing of wave energy refracting off the cliffs.

5. CONCLUSIONS AND SUGGESTIONS

(1). Nicaragua needs a master emergency response plan to improve emergency response efforts following earthquakes and other related natural hazards. In future emergency response planning, the use of military helicopters should be given serious consideration in order to reach remote towns, villages, and other settlements. Furthermore, the road infrastructure should be improved. Additional land vehicles should be assigned for response efforts related to natural disasters.

(2). Strong(er) dialogue needs to be established between government, academics and practioners to improve codes and standards for building practices using local materials and encompassing earthquake and tsunami resistant design principles. A mechanism is needed to provide better guidelines for construction practices in the coastal areas where both seismic and tsunami effects must be taken into account. Also needed is a general policy for a "no-construction zone" along the shoreline. To insure local support, it may be desirable to provide for secure moorage and/or storage facilities for the fisherman whose livelihood depends on access to the sea.

(3). The strong-motion accelerograph network should be reestablished. The existing seismic network should be enlarged and activated. This should facilitate the acquisition of vital future data for engineering earthquake resistant design requirements, land-use planning and seismological studies. Furthermore, up-to-date sounding charts and a better tide-recording system should be established.

(4). Extensive public education through the print and broadcast media and training of technical personnel with respect to response should be undertaken. For example, posters could be prepared that exhibit in layman's terms what to do during an earthquake and tsunami, and how to build in rural areas. Some form of local warning system to mitigate future tsunami hazard should be established. In all communities, schools should be located outside of immediate coastal hazard zones and all schools should be built or strengthened to resist earthquake motions. Schools and churches in rural areas can be used to publicize "run-up height" and "inundation area" information to all people living on the coast. One means of such publicity would be to place memorials or markers at the upward boundaries. Signs or markers could be posted as to safe locations in the event of evacuation.

6. ACKNOWLEDGEMENTS

During the period between September 19-October 2, 1992, a U.S. scientific team visited Nicaragua. The authors were part of one of the US teams and thanks A. Aburto (University of Neveda), J. Bourgeois (Univ. of Washington and NSF, F. Gonzalez (NOAA), J. Preuss (Urban Regional Research), K. Satake (Univ. of Michigan), C. Synolakis (Univ. of Souther California) and H. Yeh (University of Washington). The authors also thank the officials and technical personnel of Instituto Nicaragüense de Estudios Territoriales (INETER) headed by Director Claudio Gutierrez and Vice-Director Emilio Soto, and Director Guillermo Guevara of Centro de

Coordinacion para la Prevencion de Desastres Naturales en America Central (CEPREDENAC).

7. REFERENCES

1. Brown, R., Ward, P., and Plafker, G., 1973, Geologic and seismologic aspects of the Managua, Nicaragua, earthquakes of December 23, 1973, U.S. Geological Survey Professional Paper 838, 34 pgs.

2. Earthquake Engineering Research Institute, Reconnaissance Report *on* Managua, Nicaragua Earthquake of December 23, 1972, May 1973.

3. Harlow, D. H., White, R. A., Cifuentes, I. L., and Aburto, Q. A., 1981, Quiet zone within a seismic gap near Western Nicaragua: Possible Location of a Future Large Earthquake, Science, vol. 213, pp. 648-651, 7 August 1981.

4. Kanamori, H., and Abe, Katsuyuki, 1979, Reevaluation of the turn-of-the-century seismicity peak, Journal of Geophysical Research, 84, pp. 6131-6139.

5. Satake, K., Bourgeois, J., Abe, Kuniaki, Abe, Katsuyuki, Tsuji, Y., Imamura, F., Iio, Y., Katoa, H., Noguera, E., and Estrada, H., 1993, Tsunami field survey of the 1992 Nicaraguan earthquake, in review, EOS, Transactions, American Geophysical Union.

6. White, R. A., 1991, Tectonic implications of upper-crustal seismicity *in* Central America, in Neotectonics of North America: Decade Map Volume 1, (D. B. Slemmons, E.R. Engdahl, M. D. Zoback, D. D. Blackwell, editors), Geological Society of America, Boulder, Colorado.

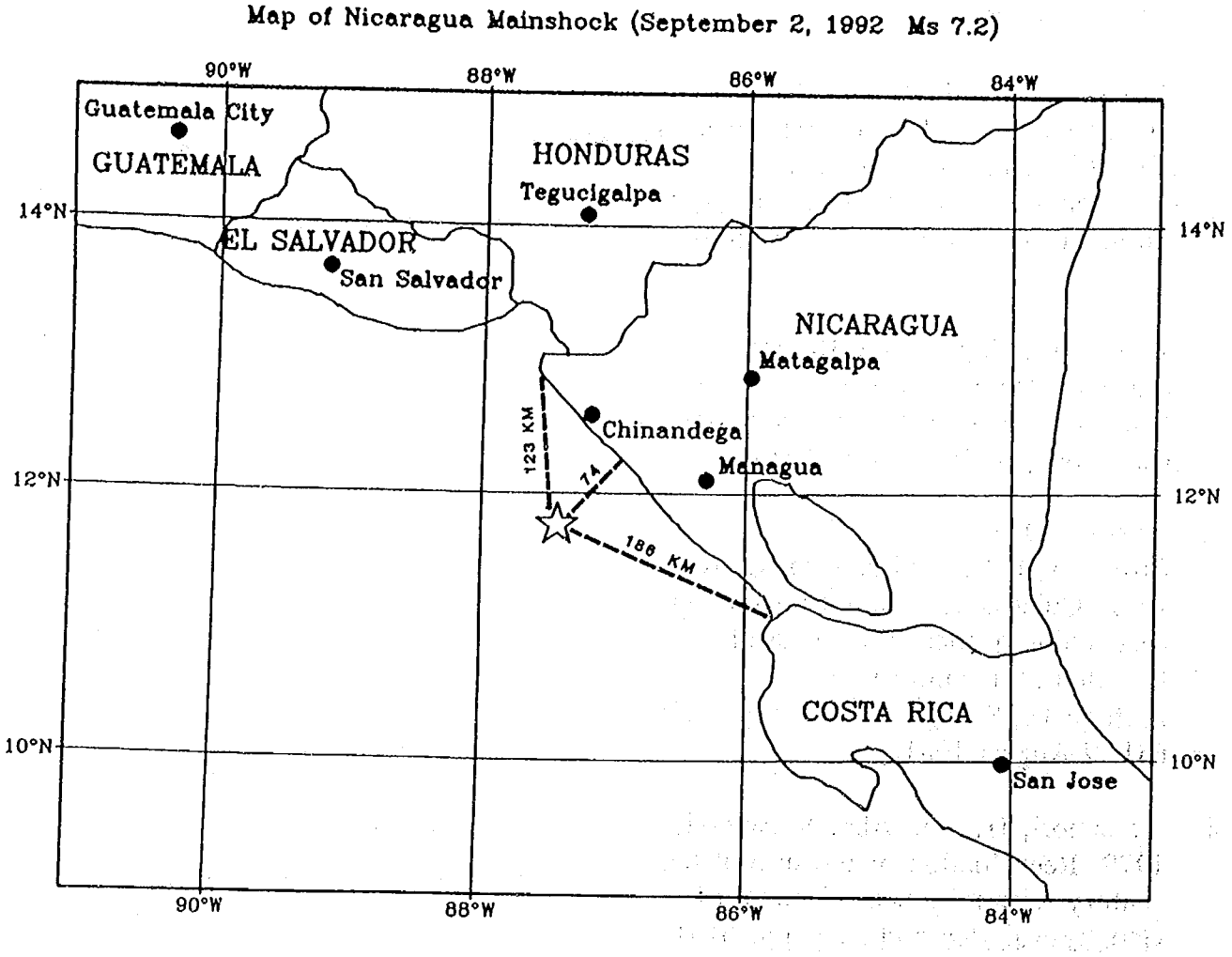


Figure 1. Map of Nicaragua and the Location of Epicenter (courtesy of NEIC)

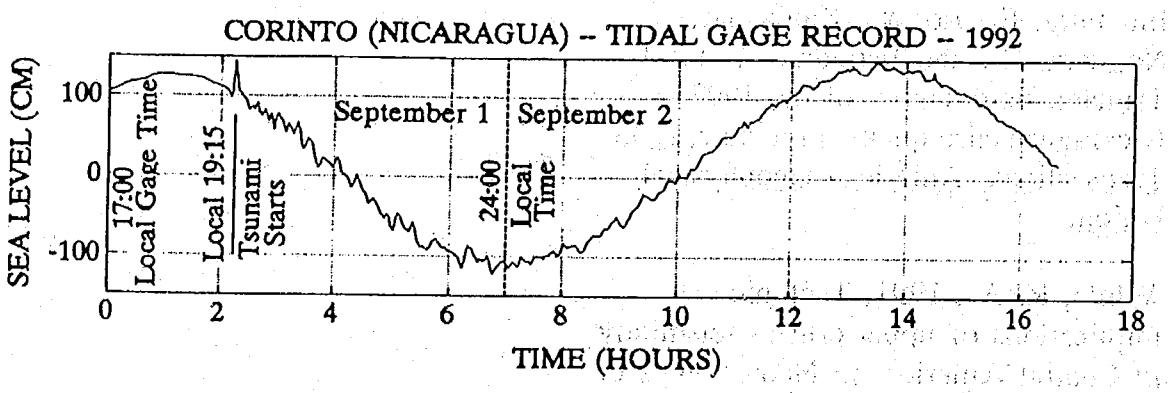


Figure 2. The digitized and replotted tidal gage record from Corinto.

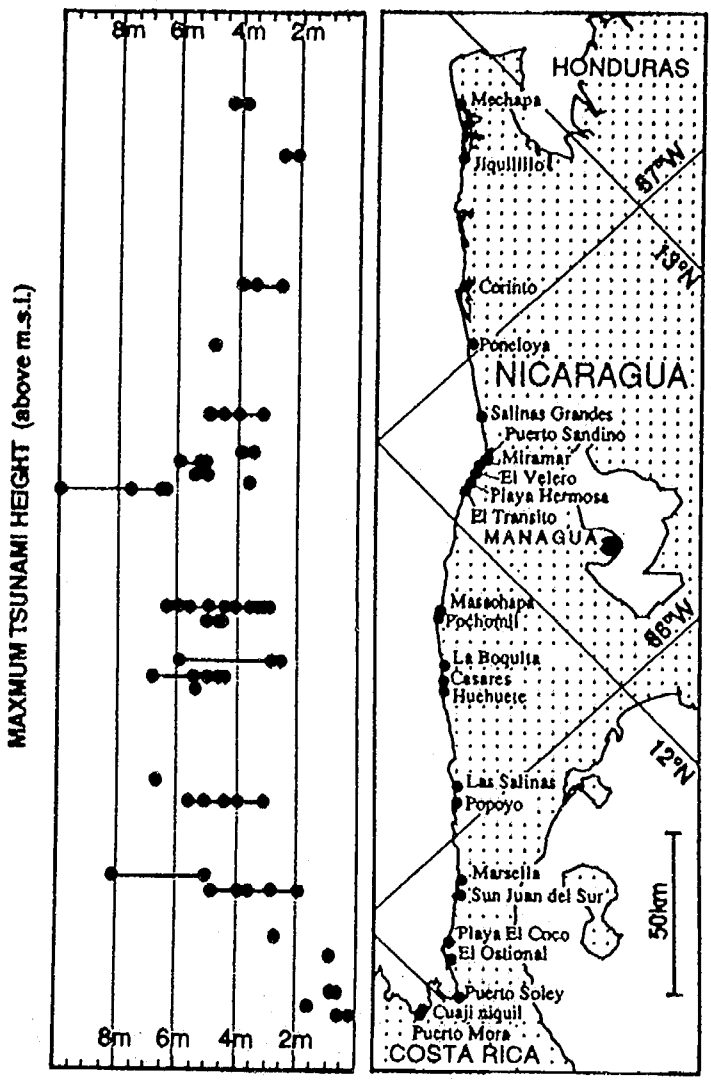


Figure 3. Tsunami run-up height map (adopted from Satake *et. al.*,1993).



Figure 4. Buildings completely washed away on the beaches of Il Transito.

U.S. Coordinated Program For Masonry Building Research: Eighth Year Status

by

James L. Noland[1]

March 9, 1993

ABSTRACT

The U.S. program, which consists of twenty-eight specific research tasks, is coordinated with a parallel program in Japan. Both are conducted under the auspices of the UJNR Panel on Wind and Seismic Effects. The primary purpose of the U.S. program is to support the development of a limit state design procedure for masonry as well as provide experimental data, analytical methods, etc. Several technical accomplishments have been realized in both modeling and experimental areas. The technology transfer plan includes dissemination of research reports, topical reports and a summary report on the specific research areas as well as by presentations and papers. Design and criteria recommendations will be an extremely important mode of technology transfer and are expected to support limit state design standard development. Current status of the program is presented. Completion is expected by July 1993.

KEYWORDS: masonry; progress; structures; technology transfer; UJNR

1. INTRODUCTION

The U.S. Coordinated Program for Masonry Building research is an integrated set of 28 specific research tasks being conducted by the U.S. Technical Coordinating Committee for Masonry Research (TCCMAR/US). The U.S. program is coordinated with a parallel program in Japan to exchange information and concepts for the mutual benefit of both countries. Both programs are conducted under the auspices of the United States - Japan Natural Resources Panel on Wind and Seismic Effects.

2. PROGRAM OBJECTIVES

Primary program objectives are:

1) Development of design and criteria recommendations for limit state design of reinforced masonry buildings and components.

2) Development of a consistent experimental database on the behavior of masonry materials, components and systems.

3) Development of analytical non-linear models for research and design office use for detailed analysis, system analysis, and dynamic loads determination.

4) Improved material and subassemblage experimental procedures for obtaining masonry properties.

5) Improved masonry fabrication procedures and standards.

6) Developing an increased awareness among engineers, architects, code bodies and the public of the capabilities of reinforced masonry in all seismic zones.

7) Interfacing with standards development groups to support development of a consensus limit state standard for masonry.

[1]Atkinson-Noland & Associates, Inc.
2619 Spruce Street
Boulder, CO 80302

3. APPROACH

With NSF support, the Technical Coordinating Committee for Masonry Research/U.S. (TCCMAR/U.S.) was formed in February 1984. TCCMAR/U.S. was and is comprised of researchers from academic and industrial organizations who have strong backgrounds in research into the properties and characteristics of reinforced masonry materials, structural components and systems, analytical techniques, structural dynamics, building codes, and earthquake engineering. TCCMAR researchers are listed in Table 1. TCCMAR participants defined the research program conducted, the research and will analyze and interpret the results.

The U.S. research plan is a phased step-by-step program of separate, but coordinated research tasks. Emphasis is being placed upon intra-task information exchange and consultations so the experimental and analytical efforts are mutually supportive. The research tasks comprising the coordinated program are listed in Table 2.

The program includes both experimental and analytical research tasks. The experimental and analytical efforts are conducted in parallel with each becoming more complex and sophisticated as knowledge and experience accumulate. The U.S. plan is thus a "building block" approach. The program began in October 1985 and will be completed by July 1993.

4. CURRENT STATUS

The program is approximately 95% complete. Remaining work consists of completing experimental tests on reinforcing bar bond and splicing, and continued development of limit state design and criteria recommendations, and final technology documentation. Work on research tasks pertaining to floor-to-wall intersections, limit state design methodology, and numerical reliability indices was not completed by the cognizant PIs. Information essential to the development of limit state design and criteria recommendations is being developed by a committee on that topic.

Construction of the five story research building was completed in August 1992. Testing was completed during September 1992. Performance of the building was successfully predicted by modeling routines developed during the program. A preliminary report has been distributed and a final report is in preparation.

Funding for the full scale research has been provided by the National Science Foundation, the Department of Energy, and the U.S. masonry industry (organizations such as the Council for Masonry Research, the Masonry Institute of America, the California-Nevada Concrete Masonry Association, and thirty regional masonry associations).

Work on Technology Documentation and Design and Criteria Recommendations began formally with a meeting on 10 April 1992. Several meetings have been held since, and supplementary studies conducted, to formulate recommendations. The work is being coordinated with the MSJC subcommittee on Limit State Design in order to implement research results into consensus standards as quickly as possible.

Technology Documentation will involve the preparation of a series of monographs on key topics to clarify and summarize research findings. The final number of such documents is being reduced because of budget reductions.

Funding for Technology Documentation and Design and Criteria Recommendations has been provided by the National Science Foundation and the U.S. Army Corps of Engineers.

TABLE 1

TCCMAR RESEARCHERS

Daniel Abrams
University of Illinois
Urbana, IL

Samy Adham
Agbabian Associates
El Segundo, CA

Richard Atkinson
Atkinson-Noland & Associates
Boulder, CO

Russell Brown
Clemson University
Clemson, SC

Robert Englekirk
Englekirk,Hart & Sabol
Los Angeles, CA

Robert Ewing
Ewing & Associates
Rancho Palos Verdes, CA

Ahmad Hamid
Drexel University
Philadelphia, PA

Mike Hammons
US Army Corps of Engineers
Vicksburg, MS

Gary Hart
Englekirk,Hart & Sabol/UCLA
Los Angeles, CA

Gilbert Hegemier
Univ. of CA-San Diego
La Jolla, CA

John Kariotis
Kariotis & Associates
South Pasadena, CA

Richard Klingner
Univ. of Texas-Austin
Austin, TX

Ronald Mayes
Computech Engin. Services
Berkley, CA

James L. Noland
Atkinson-Noland & Assoc.
Boulder, CO

Max Porter
Iowa State University
Ames, IA

M.J.N. Priestley
Univ. of CA-San Diego
La Jolla, CA

Freider Seible
Univ. of CA-San Diego
La Jolla, CA

P.B. Shing
University of Colorado
Boulder, CO

Leonard Tulin
University of Colorado
Boulder, CO

TABLE 2

RESEARCH TASKS

SUBJECT	RESEARCHER
Grouted Hollow-Unit Clay & Concrete Masonry in Compression	R. Atkinson
Grouted Hollow-Unit Concrete Masonry Under Combined Compression & Flexure	A. Hamid
Grouted Hollow-Unit Clay Masonry Under Combined Compression & Flexure	R. Brown
Masonry Test Methods for Limit State Design[2]	R. Atkinson
Nonlinear Force-Displacement Models of Reinforced Masonry Components & Systems	R. Englekirk
Nonlinear Finite Element Models for Analysis of Reinforced Masonry	R. Ewing
Nonlinear Lumped Parameter Models for Dynamic Response Analysis of Reinforced Masonry Systems	J. Kariotis
Nonlinear Models of Floor Diaphragms	M. Porter
Nonlinear Models of Reinforced Masonry Walls Acting Out-of-Plane	R. Mayes
Experimental Study of One-Story Reinforced Masonry Shear Walls	B. Shing
Experimental Study of Two-Story Reinforced Masonry Shear Walls	R. Klingner
Experimental Study of Three-Story Reinforced Masonry Shear Walls and Development of Automated Feed-Back Test Method for Stiff Structures	G. Hegemier F. Seible
Experimental Study, Static & Dynamic, of Out-of-Plane Behavior of Reinforced Concrete Masonry Walls	A. Hamid S. Adham

SUBJECT	RESEARCHER
Experimental Study, Static & Dynamic, of Out-of-Plane Behavior of Reinforced Clay Masonry Walls	R. Mayes
Experimental Study, Static & Dynamic, of Flanged Reinforced Masonry Walls	N. Priestley
Analytical Study Based on Prior Tests, of Wall-Floor Intersections[2]	G. Hegemier
Experimental Study (Preliminary) of Reinforcing Bar Bond & Splices in Grouted Masonry	L. Tulin
Experimental Study (continuation) of Reinforcing Bar Bond and Splices in Grouted Masonry[2]	R. Atkinson M. Hammons
Experimental Study, Static & Dynamic Behavior of Scale Model Three-Story Reinforced Masonry Buildings	D. Abrams
Development of Reliability-Based Limit-State Design Methodology for Masonry Buildings[2]	G. Hart
Development of Reliability Factors for Masonry Materials, Components, & Systems	G. Hart
Design of Five-Story Reinforced Masonry Research Building	J. Kariotis
Design and Construction of Large Specimen Research Building	G. Hegemier F. Seible
Experimental Study of Nonlinear Behavior of a Five-Story Building Under Cyclic Lateral Loads	G. Hegemier F. Seible
Design & Criteria Recommendation for Limit State Design and Documentation and Technology Documentation[2]	J. Noland
Overall Program Coordination[2]	J. Noland

[2]Research Tasks to be completed .

TASK REPORTS[3]

Task No.	Author/s - Title
1.1-1:	Atkinson and Kingsley, Comparison of the Behavior of Clay & Concrete Masonry in Compression, September 1985. 151 pgs.
1.2(a)-1:	Hamid A.A., Assis, G.F., Harris, H.G., Material Models for Grouted Block Masonry, August 1988. 67 pgs.
1.2(a)-2:	Assis, G.F., Hamid A.A., Harris, H.G., Material Models for Grouted Block Masonry, August 1989. 134 pgs.
1.2(b)-1:	Young, J.M., Brown, R.H., Compressive Stress Distribution of Grouted Hollow Clay Masonry Under Strain Gradient, May 1988. 170 pgs.
1.3-1:	Atkinson, R.H., An Assessment of Current Material Test Standards for Masonry Limit States Design Methods, June 1991. 38 pgs.
2.1-1:	Hart, G. and Basharkhah, M., Slender Wall Structural Engineering Analysis Computer Program (Shwall, Version 1.01), September 1987. 68 pgs.
2.1-2:	Hart, G. and Basharkhah, M., Shear Wall Structural Engineering Analysis Computer Program (Shwall, Version 1.01). September 1987. 75 pgs.
2.1-3:	Nakaki, D. & Hart, G., Uplifting Response of Structures Subjected to Earthquake Motions, August 1987. 200 pgs.
2.1-4:	Hart, G., Sajjad, N., and Basharkhah, Inelastic Column Analysis Computer Program (INCAP, Version 1.01), March 1988.
2.1-5:	Hong, W.K., Hart, G.C., Englekirk, R.E., Force-Deflection Evaluation and Models for University of Colorado Flexural Walls, December 1989.
2.1-6:	Hart, G.C. Jaw, J.W., Low, Y.K., SCM Model for University of Colorado Flexural Walls, December 1989. 31 pgs.
2.1-7	Hart, G., Sajjad, N., Basharkhah, M., Inelastic Masonry Flexural Shear Wall Analysis Computer Program, February, 1990. 41 pgs.
2.1-8	Hart, G., Englekirk, R., Srinivasan, M., Huang, S.C., Drag, D.J,., Seismic Performance Study, DPC Gymnasium, Elastic Time History Analysis Using SAP90, February, 1992.
2.1-9	Hart, G., Englekirk, R., Srinivasan, M., Huang, S.C., Drag, D.J., Seismic Performance Study, TMS Shopping Center, Elastic Time History Analysis Using SAP90, February, 1992.
2.1-10	Hart, G., Englekirk, R., Jaw, J.W., Srinivasan, M., Huang, S.C., Drag, D.J., Seismic Performance Study, RCJ Hotel February, 1992.
2.1-11	Hart, G., Englekirk, R., Jaw, J.W., Huang, S.C., Drag, D.J., Seismic Performance Study, 2-Story Masonry Wall-Frame Building, February, 1992.
2.1-12	Hart, G., Englekirk, R., Jaw, J.W., Huang, S.C., Drag, D.J., Seismic Performance Study, 2-Story Masonry Wall-Frame Building Designed by Tentative Limit States Design Standard, February, 1992.

[3]Task Reports are available through the Earthquake Engineering Research Library, Berkley, CA, and The Earthquake Engineering National Center, SUNY, Buffalo, NY.

2.2-1: Ewing, R., El-Mustapha, A., Kariotis, J., FEM/I - A Finite Element Computer Program for the Nonlinear Static Analysis of Reinforced Masonry Building Components, December 1987 (Revised June 1990).

2.2-2: Ewing, R.D., Parametric Studies on Reinforced Masonry Shear Walls Using FEM/I, A Nonlinear Finite Element Analysis Program, March 1992.

2.2-3: Ewing, R.D., Finite Element Analysis of Reinforced Masonry Building Components Designed by a Tentative Masonry Limit States Design Standard, March 1992.

2.3-1: Ewing, R.; Kariotis, J.; El-Mustapha, A., LPM/I, A Computer Program for the Nonlinear, Dynamic Analysis of Lumped Parameter Models, August, 1987. 200 pgs.

2.3-2: Kariotis, J., El-Mustapha, A., Ewing, R., Influence of Foundation Model on the Uplifting of Structures, July 1988. 50 pgs.

2.3-3: Kariotis, J., Rahman, M., El-Mustapha, A., Investigation of Current Seismic Design Provisions for Reinforced Masonry Shear Walls, January 1990. 48 pgs.

2.3-4: Kariotis, J., Rahman, A., Waqfi, O., Ewing, R., Version 1.03 LPM/I - A Computer Program for the Nonlinear, Dynamic Analysis of Lumped Parameter Models, February 1992.

2.3-5: Kariotis, J., Waqfi, O., Ewing, R., A Computer Program Using Beam Elements for the Nonlinear, Dynamic Analysis of Lumped Parameter Models, February 1992.

2.3-6 Kariotis, J., Waqfi, O., Comparison of the Dynamic Response of a Damped MDOF Nonlinear Beam Model With an Equivalent SDOF Hysteretic Model, April 1992.

2.3-7: Kariotis, J., Waqfi, O., Recommended Procedure for Calculation of the Balanced Reinforcement Ratio, February 1992.

2.4(b)-1: Button, M.R., Mayes, R.L., Out-of-Plane Seismic Response of Reinforced Masonry Walls: Correlation of Full-Scale Test and Analytical Model Results, March 1991. 65 pgs.

3.1(a)-1: Scrivener, J., Summary of Findings of Cyclic Tests on Masonry Piers, June 1986. 7 pgs.

3.1(a)-2: Shing, P.B., Noland, J., Spach, H., Klamerus, E., Schuller, M., Response of Single-Story Reinforced Masonry Shear Walls to In-Plane Lateral Loads, January 1991. 136 pgs.

3.1(b)-1: Seible, F. and LaRovere, H., Summary of Pseudo Dynamic Testing, February 1987. 46 pgs.

3.1(c)-1: Merryman, K., Leiva, G., Antrobus, N., Klingner, R., In-Plane Seismic Resistance of Two-Story Concrete Masonry Coupled Shear Walls, September 1989. 176 pgs.

3.1(c)-2: Leiva, G., Klingner, R., In-Plane Seismic Resistance of Two-Story Concrete Masonry Shear Walls with Openings, August 1991.

3.2(a): Hamid, A., Abboud, B., Farah, M., Hatem, K., Harris, H., Response of Reinforced Block Masonry Walls to Out-of-Plane Static Loads, September 1989. 120 pgs.

3.2(b)-1: Agbabian, M., Adham, S., Masri, S., Avanessian, V. Traina, Out-of-Plane Dynamic Testing of Concrete Masonry Walls, Volumes 1 and 2, July 1989. 220 pgs.

3.2(b)-2 Blondet, M., Mayes, R.L., The Transverse Response of Clay Masonry Walls Subjected to Strong Motion Earthquakes - Volume 1: General Information, April 1991, 172 pages.

3.2(b)-2 Blondet, M., Mayes, R.L., The Transverse Response of Clay Masonry Walls Subjected to Strong Motion Earthquakes - Volume 2: Walls No. 4 and 6 (Group 1), April 1991, 267 pages.

3.2(b)-2 Blondet, M., Mayes, R.L., The Transverse Response of Clay Masonry Walls Subjected to Strong Motion Earthquakes - Volume 3: Walls No. 8, 9, 10 and 11 (Group 2), April 1991, 310 pages.

3.2(b)-2 Blondet, M., Mayes, R.L., The Transverse Response of Clay Masonry Walls Subjected to Strong Motion Earthquakes - Volume 4: Walls No. 3, 5, and 7 (Group 3) April 1991, 256 pages.

4.1-1 Limin, H., Priestley, N., Seismic Behavior of Flanged Masonry Shear Walls, May 1988. 119 pgs.

4.1-2 He, L., Priestley, M.J.N., Seismic Behavior of Flanged Masonry Shear Walls - Final Report, November 1992.

4.2-1: Hegemier, G. Murakami, H., On the Behavior of Floor-to-Wall Intersections in Concrete Masonry Construction: Part I: Experimental

4.2-2: Hegemier, G., Murakami, H., On the Behavior of Floor-to-Wall Intersections in Concrete Masonry Construction: Part II: Theoretical

5.1-1: Porter, M., Sabri, A., Plank Diaphragm Characteristics, July 1990. 226 pgs.

5.2-1 Porter, M., Yeomans, F., Johns, A., Assembly of Existing Diaphragm Data, July 1990. 142 pgs.

6.2-1: Scrivener, J., Bond of Reinforcement in Grouted Hollow-Unit Masonry: A State-of-the-Art, June 1986. 53 pgs.

6.2-2: Soric, Z. and Tulin, L., Bond Splices in Reinforced Masonry, August 1987. 296 pgs.

7.1-1 Paulson, T., Abrams, D., Measured Inelastic Response of Reinforced Masonry Building Structures to Earthquake Motions, October, 1990. 294 pgs.

8.1-1: Hart, G., A Limit State Design Method for Reinforced Masonry, June 1988.

8.1-2: Hart, G., Expected Value Design in the Context of a Limit Sate Design Methodology, February 1990.

8.2-1: Hart, G., Zorapapel, G.T., Reliability of Concrete Masonry Wall Structures, December 1991.

8.2-2 Hart, G., Sajjad, N., Confinement in Concrete Masonry, December 1990.

8.2-3 Hart, G., Jang, J., Seismic Performance of Masonry Wall Frames, December 1991.

9.1-1: Kariotis, J.C., Johnson, A.W., Design of Reinforced Masonry Research Building, September, 1987. 42 pgs.

9.1-2: Kariotis, J.C., Waqfi, O.M., Trial Designs Made in Accordance with Tentative Limit States Design Standards for Reinforced Masonry Buildings, February 1992.

9.2-1: Seible, F., Report on Large Structures Testing Facilities in Japan, September 1985. 120 pgs.

9.2-2: Seible, F., Design and Construction of the Charles Lee Powell Structural Systems Laboratory, November 1986. 65 pgs.

9.2-3: Seible, F., The Japanese Five-Story Full Scale Reinforced Masonry Building Test, January 1988. 100 pgs.

9.2-4: Seible, F., Hegemier, G.A., Priestley, M.J.N., Kingsley, G.R., Kurkchubasche, A., Igarashi, A., The U.S. - TCCMAR Five-Story Full Scale Masonry Research Building Test - Preliminary Report, October 1992, 58 pages.

11.1-1: TCCMAR, Summary Report: U.S. Coordinated Program for Masonry Building Research, September 1985 to August 1986. 190 pgs.

11.1-2: Status Report: U.S. Coordinated Program for Masonry Building Research, November 1988. 170 pgs.

Mount Pinatubo Eruption: A Review

Celso S. Barrientos
Satellite Applications Laboratory
Office Of Research and Applications
National Environmental Satellite, Data and Information Service
National Oceanic and Atmospheric Administration
Washington, DC 20235 USA

Introduction

On June 15, 1991, Mount Pinatubo in the Philippines erupted after being dormant for over 600 years. The Philippines is affected by devastating natural disasters on a regular basis. The country lies in the most frequent path of tropical cyclones, averaging about 15 cyclones a year of various intensities passing within the Philippine Area of Responsibility. Of course, typhoons are accompanied by flooding due to storm surges, heavy rains, and devastating strong winds. Also, destructive earthquakes are not uncommon in the Philippines, since she is situated along the circum Pacific belt of fire. However, none of the most recent disasters in the Philippines compares with the Mount Pinatubo eruption. It has a devastating effect on the economy, politics, and most importantly the environment.

Political Impacts

The Mount Pinatubo event is politically comparable to the 1986 Peoples Power Revolution or the ensuing sequence of events after Admiral Dewey won the Battle of Manila Bay against Spain in 1898. One example of political impact which has various cascading effects on the economy, demography, and bilateral relations with the U.S., is the presence of military bases in the Philippines. For years there have been negotiations on the presence of American military bases in the Philippines, in particular, Clark Air Force Base and Subic Naval Base. These two bases are the biggest and the most visible. They have favorable effects in the economy but a sore point in the National pride of the Filipino people. To some Filipinos the presence of the bases is a blessing while to others it is a curse. Whatever it may be, Mount Pinatubo eruption and the ensuing consequences settled the political issue.

Mount Pinatubo immensely destroyed Clark Air Force base, such that it became prohibitively expensive for the United States to restore, even if it is strategically important. Subic Naval Base although also affected by Mount Pinatubo is basically intact and useable. Therefore, the negotiations narrowed to cover Subic only. Mount Pinatubo did what the negotiators could not accomplish during many years of dialog. After difficult negotiations between the U.S. and the Philippines, an agreement was reached. The agreement had to be ratified by the Philippine Senate, but they rejected it, even with the endorsement of then President Aquino.

Background

One of the key factors of assessing the effects of Mount Pinatubo is to estimate the amount and relative size compared to other eruptions. Recent eruptions are

Mount St. Helen in Washington, USA and El Chichon in Mexico. Mount St. Helen is in higher latitude while El Chichon is located in the tropics. The latitude of El Chichon is 17.33°N, while Mount Pinatubo is situated at 15.14°N latitude. Therefore, the two tropical region eruptions are ideal for comparison. Both eruptions spewed gases, dust, and debris causing sulfuric-rich particles to form in the stratosphere. Estimates of the amount of aerosols between the two volcanoes, showed that Mount Pinatubo introduced into the stratosphere almost double the amount (1.6 to 1.9) as El Chichon. The strong westerly winds in the stratosphere carried the aerosols around the globe in a little less than a month.

Local Impacts of Mount Pinatubo

Mount Pinatubo is on the island of Luzon about 60 km north of Manila. It lies in the region of the trade winds that spread the debris toward the West at low levels. However, the eruption was so big that the debris spread in all directions by kinetic energy. In the immediate vicinity of the volcano, rivers of lava formed. Farther away, the dust was so thick that the sun was completely blocked as if it was night. At Clark Air Force Base about 10 km from the eruption, the dust deposits were a foot deep or more, causing the collapse of airplane hangars and other buildings. The impacts around the vicinity of the volcano was severe that it devastated the environment. Rivers, rice paddies, roads, and communities were covered by so much dust that it will take many years to recover. To further aggravate the situation, an intense typhoon passed by two days after the first eruption. The typhoon rains mixed with the volcanic dust resulted in a muddy mixture called "lahar". The lahar produced a second wave of destructions unimaginable in extent.

Techniques in Assessing the Global Effects

The most effective way of looking at global effects of volcanic eruptions is by satellite observations. The Polar Orbiter Satellites (POES) carry an instrument system called the Advanced Very High Resolution Radiometer (AVHRR). AVHRR observations are used to compute Sea Surface Temperature (SST). Additionally, Aerosol Optical Thickness (AOT) can be estimated from the visible reflectance channel of the AVHRR to relate the discrepancy of the SST to aerosol concentration in the stratosphere.

Each Polar Orbiter satellite passed over a specific location on the globe twice a day providing global coverage. With two POES operating, sufficient observations are taken to examine some of the implications of the volcanic eruptions.

The Global Effects

What are the possible effects? With the sulfur-rich particles in the stratosphere, solar insolation is diminished. With the reduction of solar insolation it may cause a reduction in sea surface temperature. However, the opposite effect is also possible. The presence of stratospheric aerosols hinders the outgoing radiation, trapping the energy, and increasing the SST. Other esoteric effects are also plausible, such as, on the ozone layer. Studies for 1992 showed that the ozone thickness has diminished relatively more than the previous measurements particularly in the Northern Hemisphere and has been cautiously attributed to Mount Pinatubo.

Let us now look at the effects of Mount Pinatubo on SST. Algorithms have been developed using the multiple channels of the AVHRR to compute sea surface temperature (MCSST - Multi-Channel Sea Surface Temperature). Values of AOT and MCSST are both available routinely following the eruption of Mount Pinatubo. Only MCSST was available for the study of El Chichon. Comparative analysis therefore of the two events can only be made using MCSST data. A novel approach to study the effects of the eruption is to use the MCSST data after the event as compared to data taken without the volcano eruption (no stratospheric aerosols). This approach is called the 'MCSST Offsets'. After a volcano eruption, the MCSST has a pronounced negative bias (offset) compared to data when no volcanic dust is present in the stratosphere. This offset is used to quantify the aerosol effects. The negative offset resulted from the absorption due to sulfuric acid aerosol particles formed from gases in the original volcanic cloud. The MCSST algorithm is able to correct for atmospheric water vapor but not for volcanic aerosols. This is due to the difference in wavelength dependence between water vapor and sulfuric acid in the infrared bands used in the algorithm. The offset approach was also applied in the El Chichon event. The AOT values were used to support that the MCSST errors from Mount Pinatubo data are closely related to the presence of stratospheric aerosols.

MCSST data was collected over the oceans and averaged monthly over a 2.5° by 2.5° latitude/longitude grid. The data following the eruptions of El Chichon in 1982 and Mount Pinatubo in 1991 may be used to estimate the relative stratospheric loading. Comparing the first three months after the eruption, the data revealed ratios from 1.6 to 1.9, i.e. Mount Pinatubo is almost twice as big as El Chichon. The effect of stratospheric aerosols from Mount Pinatubo eruption is the lowering of the Earth's near-surface energy balance. Cooling of up to 0.5°C globally has been predicted to extend over at least the first two years following the eruption. Preliminary analysis of the data appears to confirm the prediction. This might be Nature's way of fixing the 'global warming'!

CONCEPT BEHIND ULTIMATE STRENGTH DESIGN GUIDELINES FOR REINFORCED CONCRETE BUILDINGS IN JAPAN

by

S. Otani*1)
M. Teshigawara*2)
S. Nakata*2)
T. Murota*2)

ABSTRACT

The paper briefly introduces Ultimate Strength Design Guidelines for Reinforced Concrete Buildings currently under development as a part of the U.S.-Japan PRESSS project. The design for gravity loading is based on traditional allowable stress design procedure. The design for earthquake loading is based on ultimate strength design procedure for serviceability limit state and ultimate limit state. This paper emphasizes the earthquake resistant design.

INTRODUCTION

It was reported [Ref. 1] in the previous meeting in Tsukuba (1991) that Japanese PRESSS design guidelines would be prepared in complete accordance with the existing Building Standard Law of Japan and accompanying Building Standard Law Enforcement Order [Ref. 2]. Otherwise, every building designed under the guidelines must be submitted to the Minister of Construction (Technical Appraisal Board for Concrete Buildings at Building Center of Japan) for approval that the building is equally safe or superior to those designed by Building Standard Law.

However, the guidelines would be useless if the guidelines simply compromises with the existing building regulations. It was further suggested that the guidelines should "violate" some requirements of the building regulations so that Ministry of Construction could issue a Notification stating that those buildings designed in conformance with the guidelines are equal or superior to those specified in Building Standard Law. The issuance of Notification is necessary to eliminate the technical appraisal.

Therefore, the guidelines is prepared to "violate" allowable stress design requirements in the earthquake resistant design. Instead, it introduces serviceability and ultimate limit state requirements both based on ultimate strength design procedure although the guidelines uses the working stress design for gravity, wind and snow loadings.

The guidelines provides the performance criteria of a designed building, and does not dictate the design method. The performance of the building is examined by either (a) static nonlinear analysis of the designed building under monotonically increasing lateral loading, or (b) static linearly elastic analysis and simplified limit analysis of the designed building.

The seismic design concept follows the one outlined in "Design Guidelines for Earthquake Resistant Reinforced Concrete Buildings based on Ultimate Strength Concept [Ref. 3]", published from Architectural Institute of Japan (AIJ) in November 1990. Namely, the earthquake resistant design procedure requires a structural engineer to plan a structure to form a specified mechanism of beam-yield type (flexural yield hinges to form at the end of all floor girders and at the base of first-story columns and structural walls). The region other than specified yield hinges would be provided with resistance sufficient to prevent flexural yielding, shear failure and bond failure even under a probable maximum earthquake excitation.

Two earthquake resistant design procedures are assumed in the guidelines; (a) complex design procedure requiring a nonlinear static analysis of a building structure under monotonically increasing lateral loading, and (b) design procedure using linear structural analysis and simple limit analysis.

SCOPE

The guidelines is intended to provide minimum requirements for the structural design of cast-in-situ reinforced concrete buildings with/without precast concrete elements. Precast concrete elements and their connections must be properly detailed to exhibit behavior as good as or superior to that of corresponding monolithic reinforced concrete assemblages.

A precast reinforced concrete building has been believed to be inferior to a cast-in-situ reinforced concrete building in earthquake resistance because the structural performance of connections of precast concrete elements was not proven to be as good as that of corresponding monolithic reinforced concrete assemblages. Therefore, a precast concrete building has been designed with an earthquake design load higher than that of a cast-in-situ reinforced concrete building. "PRESSS Connection Design Manual", however, will outline methods to design the connection of precast concrete elements to ascertain reliable performance as good as that of monolithic reinforced concrete assemblages.

*1)University of Tokyo
Bunkyo-ku,Tokyo 113
*2)Building Research Institute
Tachihara 1,Tsukuba,Ibaraki 305

(1) Structural Type and Height

The design guidelines is applicable to ductile moment resisting frame buildings with/without continuous structural walls, and of not more than 60 m in height. Structural walls and columns should be continuous from the ground floor to the top story. The performance of a building with structural walls discontinuous at certain level(s) or a building with setback has not been thoroughly investigated. Therefore, such a building will not be covered by the guidelines.

The height limit is introduced because some of design coefficients were examined for a limited number of bench-mark buildings of not more than 60 m in height. Building Standard Law will not be applicable to those buildings taller than 60 m. In practice, the design of buildings taller than 45 m must be reviewed by Technical Appraisal Board for Concrete Structures at Building Center of Japan in accordance with a Circular Notice (No. 96, 1981) of Building Guidance Division, Bureau of Housing, Ministry of Construction.

(2) Structural Regularity

The performance of a building with irregular stiffness or mass distribution has not been clearly understood at present, hence, the scope is limited to a building of regular structural configuration.

The structural regularity is judged by a stiffness ratio R_s and an eccentricity ratio R_e specified in Article 82-3 of Building Standard Law Enforcement Order; i.e., the stiffness ratio of each story should be equal to or greater than 6/10 and the eccentricity ratio of each story should not exceed 15/100 for a building to qualify as a regular structure. The requirement of eccentricity ratio is relaxed at the top story because a pent house sometimes cause a larger eccentricity at the floor althought the extra eccentricity is expected not to increase the response deformation of the structure during an earthquake.

The stiffness ratio R_s of a story is calculated as

$$Rs = r_s / \underline{rs} \qquad (1)$$

where r_s : reciprocal of the relative story displacement angle of the story, and $\underline{rs}$: arithmetic mean of all r_s's.

The eccentricity ratio R_e of a story is calculated by

$$R_e = e / r_e \qquad (2)$$

where e : distance of eccentricity from the center of stiffness to the center of vertical gravity loads, and r_e : elastic radius of gyration, defined as the square root of torsional stiffness divided by lateral stiffness.

A series of nonlinear earthquake response analyses have been carried out to confirm the adequacy of the requirements by an analysis sub-working group under Design Guideline Drafting Working Group.

(3) Yield Mechanism

Some yield mechanisms are more desirable for earthquake resisting behavior than other mechanisms. The performance of a building during an intense earthquake motion is believed to improve by forming the beam-yielding (weak-beam strong-column) type collapse mechanism in a moment resisting frame structure. Flexural yield hinges may be formed at the base of first-story columns and structural walls. Additional flexural resistance should be provided in regions other than specified yield hinges to assure the formation of the specified mechanism. Brittle failure in shear and bond should be prevented in any members.

The precast connection may be placed at a planned yield hinge because the connection is designed to ascertain reliable performance as good as monolithic reinforced concrete subassemblages.

STRUCTURAL MATERIALS

Materials and quality used for cast-in-situ concrete must conform to the requirements specified by "Japanese Architectural Standard Specification for Reinforced Concrete Work (JASS-5) [Ref. 4]", and materials and quality used for precast concrete elements must conform to "PRESSS Specification for Precast Concrete Work." Design concrete strength is limited to 210 to 360 kgf/cm^2 for normal concrete, and 210 to 270 kgf/cm^2 for light-weight aggregate concrete. The strength and quality of concrete specified in precast concrete elements and their connections must be as good as or superior to those specified for cast-in-place concrete.

Architectural Institute of Japan publishes JASS-5, which specifies (1) type and quality of concrete, (2) materials, (3) mix proportion, (4) production of concrete, (5) transportation and placing, (6) curing, (7) concrete finishing, (8) concrete cover, (9) fabrication and placement of reinforcement, (10) formwork, (11) quality control and inspection, (12) cold weather concreting, (13) hot weather concreting, (14) light weight concrete, and (15) special concrete.

Quality, shape and size of reinforcing bars must conform to the specifications prescribed in "Japan Industrial Standard (JIS) G-3112 "Steel Bars for Reinforced Concrete" [Ref. 5], which defines (1) sizes, (2) fabrication, (3) chemical contents, (4) mechanical properties, (5) shape, (6) mechanical testing, (7) quality control, (8) inspection, and (9) reports. The grades of reinforcing bars allowed in the guidelines are SR235, SR295 for round bars, and SD295A, SD295B, SD345, SD390 for deformed bars. The number in the steel grade indicates yield stress in MPa. The bar sizes are limited to 9 to 32 mm for round bars, and 10 to 41 mm for deformed bars.

Reinforcing bars may be jointed by (1) gas pressure welding, (2) flare welding, (3) lap splice, and (4) other methods approved by the technical appraisal boards at Building Center of Japan.

High-strength prestressing deformed bars (yield stress ranging from 7,000 to 13,000 kgf/cm^2) may be used as shear reinforcement if the use of specific products with their design method is approved by the Minister of Construction through the technical appraisal at Building Center of Japan.

WORKING STRESS DESIGN

The serviceability of a building under gravity loading (dead and live loads), wind and snow loading is examined by the working stress design procedure. Stresses in every part of structural members under the long term loading and the short-term loading must not exceed corresponding allowable stresses of materials for the long-term loading and the short-term loading, respectively. The long term loads include, in addition to gravity loads, soil pressure, water pressure, vibration, impact, temperature, shrinkage, uneven ground settlement, if applicable. The short-term loads, in addition to the long-term loads, include the wind pressure and the snow load.

The earthquake load is a typical short-term loading in Building Standard Law Enforcement Order, but this guidelines decides to examine the performance of a building under earthquake effect separately on the basis of ultimate strength of members. However, the ultimate strength of foundation and soil has not been clearly understood. Therefore, the earthquake resistant design of foundation is based on the working stress procedure.

Two levels of material allowable stresses are defined in Building Standard Law Enforcement Order; i.e., (a) allowable stress for the long-term loading (b) allowable stress for the short-term loading. The allowable stress of a structural material for the short-term loading is normally specified much higher than that for the long-term loading. The allowable stresses of concrete and reinforcing bars are listed in Tables 1 to 3. The allowable compressive stress of concrete for the long-term loading is one-third the specified concrete compressive strength, and that for the short-term loading is two-third the specified strength. The allowable tensile stress of reinforcing bars for the long-term loading is approximately two-third the yield strength, while that for the short-term loading is full yield strength. Note that a flexural moment corresponding to the short-term allowable stress of the reinforcement is close to the yield moment.

Deforamtion and damage caused by the design wind and snow are expected to be reasonably small as long as the stress in a member is limited to the allowable stress level for the short-term loading.

DESIGN EARTHQUAKE LOADS

Design earthquake story shear Q_i in the guidelines is calculated by multiplying the total of dead and live loads (for earthquake loading) W_i above story i by the seismic story shear coefficient C_i at the story:

$$Q_i = C_i W_i \quad (3)$$

The seismic story shear coefficient C_i is calculated by the following formula:

$$C_i = Z R_t A_i C_B \quad (4)$$

where, C_i: seismic story shear coefficient at a story i, Z: a value which reflects the extent of earthquake damage, seismic activity and other seismic characteristics (= 0.7 to 1.0, Fig. 1), R_t: a value representing vibration characteristics of buildings taking into account the natural periods of buildings and types of soil, A_i: a value representing a vertical distribution of seismic story shear coefficient considering the vibration characteristics of buildings, C_B: standard base shear coefficient, which is specified separately for serviceability limit state and ultimate limit state.

Values and expressions for Z, R_t and A_i are defined in Notification No. 1793 (1980) of Ministry of Construction.

Coefficient R_t (Fig. 2) is expressed as follows:

$$R_t = 1.0 \quad \text{for} \quad T < T_c \quad (5.1)$$

$$R_t = 1.0 - 0.2 (T / T_c - 1)^2 \quad \text{for} \quad T_c < T < 2 T_c \quad (5.2)$$

$$R_t = 1.6 (T_c / T) \quad \text{for} \quad 2 T_c < T \quad (5.3)$$

where, T_c: critical period of subsoil (0.4 sec for Type 1 soil of rock, stiff sand or gravel, 0.6 sec for Type 2 soil, and 0.8 sec for Type 3 soil of Alluvium mainly consisting of organic or other soft soil), T: period of a building. The period of a building may be calculated by

$$T = 0.02 h \quad (6)$$

where, h: total height of the building in m.

The vertical distribution factor A_i of story shear coefficients at story i (Fig. 3) is given by the following expression:

$$A_i = 1 + (1/\sqrt{a_i} - a_i)(2 T / (1 + 3 T)) \quad (7)$$

where,

$$a_i = W_i / W_1 \quad (8)$$

where, W_i: weight above story i.

The expression of design earthquake load is similar in Building Standard Law Enforcement Order.

EARTHQUAKE RESISTANT DESIGN CRITERIA

The performance of super-structure, basement and foundation structure of a building is examined for serviceability limit state under medium intensity earthquake motions and for ultimate limit state under an intense earthquake motion.

(1) Serviceability Limit State

A structure should be serviceable immediately after a medium intensity earthquake motion, which may be expected to occur several times during the use of the building. No member is allowed to yield under serviceability limit state. Non-structural element and mechanical facilities and equipments should not be damaged under serviceability limit state.

Standard base shear coefficient C_B for serviceability limit state is 0.2, the value of which is consistent with the existing building regulations. Story drift anagle at the design earthquake loading for the serviceability limit state is limited to a value, which varies with structural analysis methods under earthquake loading and the amount of structural walls in the building.

(2) Ultimate Limit State

A structure should not collapse during a high intensity earthquake motion, which may occur once in the lifetime of the structure. Extensive repair work of the structure may be necessary before reuse.

Maximum story drift angle during a high intensity earthquake motion, called design limit deformation R_{U1}, is limited for the safety; i.e., a design limit deformation is tentatively set to 1/100 for moment resisting frame buildings, and 1/100 to 1/150 for buildings with structural walls.

Yielding members must sustain the ultimate resistance to an expected maximum possible deformation, called design proof deformation R_{U2}. The design proof deformation is tentatively set to be twice the design limit deformation because the characteristics and intensity of probable maximum earthquake motions cannot be clearly defined and because the design procedure may involve much uncertainty.

Standard base shear coefficient C_B for the ultimate limit state varies from 0.3 to 0.4 depending on the amount of structural walls; i.e., base shear coefficient of 0.3 for moment-resisting frame structures, and 0.3, 0.35, and 0.4 for wall-frame structures in which structural walls resist up to 30 %, 30 to 70 %, and over 70 % of the base overturning moment at design limit deflection R_{U1}, respectively.

A designed structure should develop a lateral load resisting capacity not less than the design story shear for the ultimate limit state. The lateral load resisting capacity (retained horizontal strength) is defined as the sum of horizontal shear carried by columns, structural walls and braces at a formation of collapse mechanism under the action of earthquake loading (Circular Notice No.96, 1981, Building Guidance Division, Bureau of Housing, Ministry of Construction).

PERFORMANCE CRITERIA FOR EARTHQUAKE RESISTANCE

Two separate procedures are prepared to examine the performance of a designed building for earthquake resistance; i.e., (a) a procedure using static nonlinear analysis of a designed building under monotonically increasing lateral loads, and (b) a procedure using linearly elastic and simple limit analysis of a building.

(1) Procedure using Nonlinear Static Analysis

The guidelines requires a structural designer to perform nonlinear analysis of a building under monotonically increasing lateral loading taking into account realistic elastic and inelastic characteristics of constituent structural members. A building structure may be idealized as a series of plane frames in a principal direction if the effect of torsion and transverse frames can be neglected. The analysis may terminated when the maximum story drift angle of a story reaches a design proof drift angle of R_{U2}.

Modeling of Structural Members: A complete history of member deformation and structural resistance with structural deformation can be obtained by the analysis. The results, however, may be significantly affected by assumed force-deformation relations of constituent members. Therefore, the method of structural and member modeling and the resistance-deformation relation of members are specified in the guidelines; i.e., Inelastic deflection of a column and beam may be assumed to concentrate at the member end, represented by rotation of a rigid-plastic rotational spring. The stiffness characteristics of a column and beam under monotonically increasing load may be assumed to be of trilinear type with stiffness changes at flexural cracking of concrete and tensile yielding of longitudinal reinforcement.

Performance Criteria at Serviceability Limit State: At a load for the serviceability limit state, a building must not develop flexural yielding at any member end, and the story drift angle must be less than 1/200. The limit of story deformation is introduced to protect non-structural elements in a building during a medium intensity earthquake motion.

Performance Criteria at Ultimate Limit State: At a design limit deformation R_{U1}, the building must develop a story shear at any story not less than 0.9 times the design story shear for the ultimate limit state.

The design limit deformation is tentatively assigned to be 1/100 for a moment resisting frame, and 1/100 to 1/150 for a moment resisting frame with structural walls depending on the amount of structural walls. The values of design limit deformation do not have any logical ground, but the values are commonly used in the design of high-rise buildings in Japan.

At a design proof deformation R_{U2}, the building must develop a story shear not less than the design story shear for the ultimate limit state. The resistance beyond the design proof deformation will not be utilized in earthquake resistance.

The design proof deformation is tentatively selected to be 1/50 for a moment resisting frame structure, and 1/50 to 1/75 for a moment resisting frame structure with structural walls depending on the amount of structural walls.

A yield hinge specified for the yield mechanism must be provided with deformation capacity to a deformation amplitude calculated at the hinge at the design proof deformation.

A region other than the specified yield hinges must be provided with flexural, shear and bond resistances equal to corresponding amplification factors times the action calculated at the design proof deformation. The amplification factor should be determined to consider (a) the increase in material strengths from the specified value in design, (b) the lateral load distribution during an earthquake excitation different from the one assumed in the nonlinear static analysis, and (c) the concurrency of bi-directional earthquake loading. The amount of axial load acting in a column should be examined to be within an acceptable range.

Axial force in columns must be less than 2/3 N_u and 3/4 N_t, where N_u: ultimate compressive strength of the column, and N_t: ultimate tensile strength.

(2) Procedure using Linearly Elastic Analysis

This simple procedure uses a linearly elastic analysis of a designed building under lateral loading and a approximate limit analysis to define the lateral load resisting capacity (retained horizontal strength). The use of this procedure is limited to the design of a building not taller than 31 m.

Performance Criteria at Serviceability Limit State: At a load for the serviceability limit state, member actions calculated by a linearly elastic analysis of a designed building under combined gravity and earthquake loads must not exceed flexural yielding capacity at any member end.

In structural members, such as short-span beams, beams connected to a structural wall, and structural walls, subjected to high stresses in the linear analysis, the elastic stiffness may be reduced up to the secant stiffness at yielding.

Story drift angle calculated at a lateral load for the serviceability limit state must be not more than 1/600 for a moment resisting frame structure, and not more than 1/800 to 1/1000 for a moment resisting frame structure with structural walls. The values of drift angle were determined for trial design buildings.

Performance Criteria at Ultimate Limit State: The lateral load resisting capacity may be calculated by (a) limit analysis by virtual work method (upper bound theorem), or (b) approximate limit analysis method by distributing yield moment of yield hinges at a beam-column joint to elastic member ends (approximate method). Some of advantages and drawbacks of each method are briefly outlined below:

Limit analysis by virtual work method (upper bound theorem) : Yield hinges are inserted to form an intended yield mechanism, and the works done by the plastic moments and the external loads are equated under a set of virtual deformations. The calculation is simple. However, the method assumes infinite deformation capacity at each yield hinges. The analysis does not give any information about deformation; i.e., (1) possible concentration of plastic deformation at limited localities, and (2) a story drift at the formation of yield mechanism. For the drawbacks, the amount of moment redistribution may be limited from the action obtained by a linearly elastic analysis.

Yield moment distribution method (approximate method): A simple approximate analysis is often used to determine the moment distribution at a collapse mechanism, in which the sums of beam and column yield moments are compared at each joint to determine the possible location of yield hinges, and the sum of yield moments are distributed to elastic members at the joint. The story shears thus found do not correspond to the design seismic load distribution. The results of the method have the same short-coming as the limit analysis by virtual work method.

Flexural yield hinges must form at the end of floor beams and at the base of first story columns and structural walls to develop the specified yield mechanism of the structure.

A region other than the specified yield hinges must be provided with flexural, shear and bond resistances equal to corresponding amplification factors times the action calculated at the design assurance deformation. The amplification factors will be selected larger than those used for the procedure using nonlinear static analysis.

Axial compressive force N of interior, exterior and corner columns under unidirectiona and bidirectional earthquake loading must be limited.

CALCULATION OF ULTIMATE MEMBER STRENGTHS

The tensile strength of reinforcing bars may be taken to be 1.1 times specified yield stress and the compressive strength of concrete may be taken to be specified strength in calculating ultimate strength of members. Methods to evaluate ultimate strengths of structural members may be adopted from the AIJ Guidelines for Earthquake Resisting Design [Ref. 3].

Confining lateral reinforcement must be provided in a hinge region, defined as a region of length equal to 1.5 times the member depth from the member end. Special confining reinforcement must be provided in the first-story exterior column subjected to high axial load.

STRUCTURAL REQUIREMENTS

Size of longitudinal and lateral reinforcement is limited for practical construction and effectiveness. Minimum spacing of lateral reinforcement in a yield hinge region and a non-yield region is specified.

A special yield hinge region is defined as a yield hinge region where axial force N_c at the design proof deformation exceeds a limit. All longitudinal reinforcing bars in a special yield hinge region must be supported by a corner of rectangular lateral reinforcement or by a 135-degree bend of sub-ties except for a longitudinal bar within 20 cm from supported longitudinal bars.

A region equal to 1.5 times member depth from the orthogonal member face at a specified yield hinge is defined as a yield hinge region, where a closer spacing of lateral reinforcement is required. A region of a structural wall of height equal to 1/6 times the wall height or to the full wall width from the first story wall base is defined as a yield hinge region, however, the height of a yield hinge region may not be taken higher than the bottom face of the third floor beam.

In a yield hinge region of a structural wall, an opening must not be placed, and sub-ties must be placed at a closer spacing in the vertical and horizontal directions.

An expression for standard lead length l_{dh} for development of longitudinal reinforcement is proposed by AIJ [Ref. 6]:

$$l_{dh} = 16\ (1.9\ f_s / f_{do} - 0.9)\ d_b \quad (10)$$

$$f_{do} = 270\ k_1\ k_2\ k_3\ (F_c)^{0.5} \quad (11)$$

where, f_s: required development strength of reinforcement, d_b: diameter of longitudinal reinforcement, f_{do}: basic development strength, F_c: specified concrete compressive strength, k_1: coefficient for concrete type, =1.0 for normal concrete, and =0.85 for light-weight aggregate concrete, k_2: coefficient associated with side concrete cover depth of a hook, =1.0 for cover depth concrete cover depth more than 3 d_b, and =0.8 for cover depth less than above, k_3: coefficient associated with confinement of concrete around a hook, = 1.15 if lateral reinforcement of diameter not less than one-third anchored longitudinal bar diameter is placed at a spacing of not more than radius of bend along the full development length, =1.0 otherwise.

If the standard lead length l_{dh} is required more than 16 times bar diameter or the development length is calculated by other methods, the development strength f_{do}, specified in Eq. (12) must exceed the required design development force f_s#of the anchored longitudinal reinforcement.

$$f_{do} = 320\ k_1\ k_c\ k_h\ k_s\ (F_c)^{0.5} \quad (12)$$

where, k_c: a coefficient associated with side cover depth C, specified in Eq (13), k_h: a coefficient associated with lead length l_{dh}, specified in Eq. (14), and k_s: a coefficient associated with effectiveness of lateral confinement, specified in Eq. (15).

$$k_c = 0.1\ (C / d_b) + 0.43 \quad \text{but } k_c < 1.0 \quad (13)$$

$$k_h = 0.038\ (l_{dh} / d_b) + 0.544 \quad \text{but } k_h < 1.15 \quad (14)$$

$$k_s = 1 + (2/3)(d_s / d_b)^2 \quad \text{but } k_s < 1.4 \quad (15)$$

where, d_s: diameter of lateral reinforcement.

FOUNDATION STRUCTURES

Foundation and basement must be provided with rigidity and strength against gravity loading, during a strong wind, snow loading and medium intensity earthquake motions, sufficient to prevent excessive settlement, inclination and sliding for serviceability, and to prevent excessive cracking for durability.

Design stresses for basement structures include the effect of soil pressure and hydraulic pressure in addition to the effect of long-term gravity load and short-term snow, wind pressure and earthquake loads transmitted from the super-structure. Stresses caused by uneven settlement and lifting or deflection of the soil and piles must be considered if appropriate.

Design stresses due to the long-term gravity load and short-term snow load and wind pressure must not exceed allowable stresses of materials. Stresses at an earthquake load level for the serviceability limit state of the super-structure must not exceed the allowable stresses for the short-term loading; furthermore, the foundation must not be lifted. At an earthquake load level for the ultimate limit state of the super-structure, forces in the foundation structure must not exceed the ultimate strength of members and soil.

Foundation structure, such as foundation gierders, slab and piles, must be planned not to form a part of the specified yield mechanism. The properties of sub-structures are not clearly understood in relation to the behavior of super-structures. The sub-structure must be protected because it is often difficult to investigate the damage in the foundation after an earthquake and because the cost to repair the foundation damage is enormous.

ACKNOWLEDGEMENT

The guidelines is drafted and discussed by a working group with the following members; S. Otani, chairman, M. Teshigawara, Secretary, M. Hayashi, Y. Inoue, T. Kaminosono, I. Kawabata, M. Kinizuka, S. Nakata, K.Yagishita, K. Yoshikoka. The contribution of the working group members is deeply acknowledged.

The guidelines has been reviewed by Guidelines Committee of Japanese PRESSS with S. Otani, chairman, M. Teshigawara, secretary, M. Hayashi, H. Hiraishi, Y. Inoue, T. Kabeyasawa, T. Kaminosono, C. Kani, I. Kawabata, M. Kinizuka, S. Mochizuki, S. Nakata, S. Nomura, M. Ohkubo, K. Yagishita, K. Yatsushige, M. Yoshimura, and K. Yoshioka.

REFERENCES

1. Otani, S., "Proposed Structure of Seismic Design Guidelines for Precast Concrete Buildings in Japan," presented in the Second Meeting of the U.S.-Japan Joint Technical Coordinating Committee on Precast Seismic Structural Systems, Tsukuba, Japan, October 31-November 2, 1991.

2. Building Guidance Division and Urban Building Division, Housing Bureau, The Ministry of Construction, Ed., The Building Standard Law of Japan (in English), The Building Center of Japan, September 1990.

3. Architectural Institute of Japan, Design Guidelines for Earthquake Resistant Reinforced Concrete Buildings Based on Ultimate Strength Concept (in Japanese), November 1990, 337 pp.

4. Architectural Institute of Japan, Japanese Architectural Standard Specification for Reinforced Concrete Work (JASS-5) (in Japanese), eighth ed., 1986, 618 pp. (note: English translation available for sixth ed.)

5. Japan Industrial Standard: JIS G 3112 Steel Bars for Reinforced Concrete, 1985.

6. Architecural Institute of Japan, "Report of Ductility Design Sub-committee, Recent Research Development on Earthquake Resistant Design based on Ultimate Strength Concept (in Japanese)," August 1992.

Table 1: Allowable Stresses and Material Strength for Concrete (kgf/cm^2)

Type		Normal Concrete	Light-weight Concrete
Long-term Loading	Compression	Fc / 3	Fc / 3
	Shear	Fc / 30 and (5 + Fc / 100)	0.9 times the value for normal concrete
Short-term Loading	Compression	2 times the values for long-term loading	
	Shear	1.5 times the values for long-term loading	
Material Strength	Compression	Fc	Fc

Fc : Specified compressive strength of concrete

Table 2: Allowable Bond Stresses between Reinforcement and Concrete (kgf/cm^2)

Bar Type	Long-term Loading		Short-term Loading
	Top Reinforcement	Bottom Reinforcement	
Round	0.04 Fc and 9.0	0.06 Fc and 13.5	1.5 times the values for long-term loading
Deformed	Fc / 15 and (9 + 2 Fc / 75)	Fc / 10 and (13.5 + Fc / 25)	

Fc: Specified concrete compressive strength.

Table 3.4 : Allowable Stresses and Material Strength for Reinforcement (kgf/cm^2)

	Long-term Loading		Short-term Loading		Material Strength	
Steel Grade	Tension Compres	Shear Reinf	Tension Compres	Shear Reinf	Tension Compres	Shear Reinf
SR235	1,600	1,600	2,400	2,400	2,400 x 1.1	2,400
SR295	1,600	2,000	3,000	3,000	3,000 x 1.0	3,000
SD295	2,000	2,000	3,000	3,000	3,000 x 1.1	3,000
SD345	2,200	2,000	3,500	3,500	3,500 x 1.1	3,000
SD390	2,200	2,000	4,000	4,000	4,000 x 1.1	3,000
Welded Wire	2,000	2,000	3.000	-----	3,000 x 1.1	-----
High-strength Shear Reinf.	Values approved by Minister of Construction					

Note: Material strength is used to calculate ultimate strength of a member.

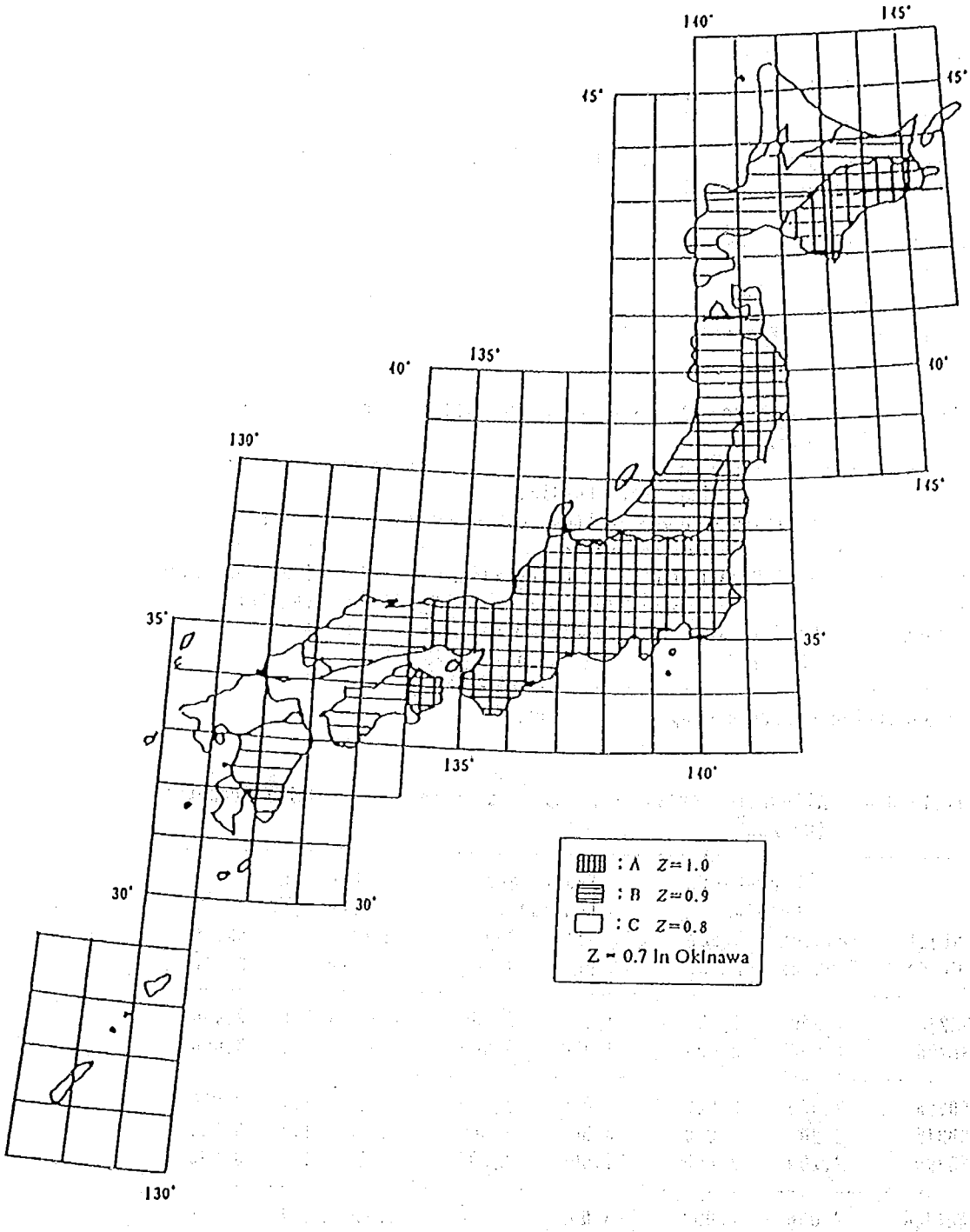


Fig. 1 : Seismic Zone Factor Z

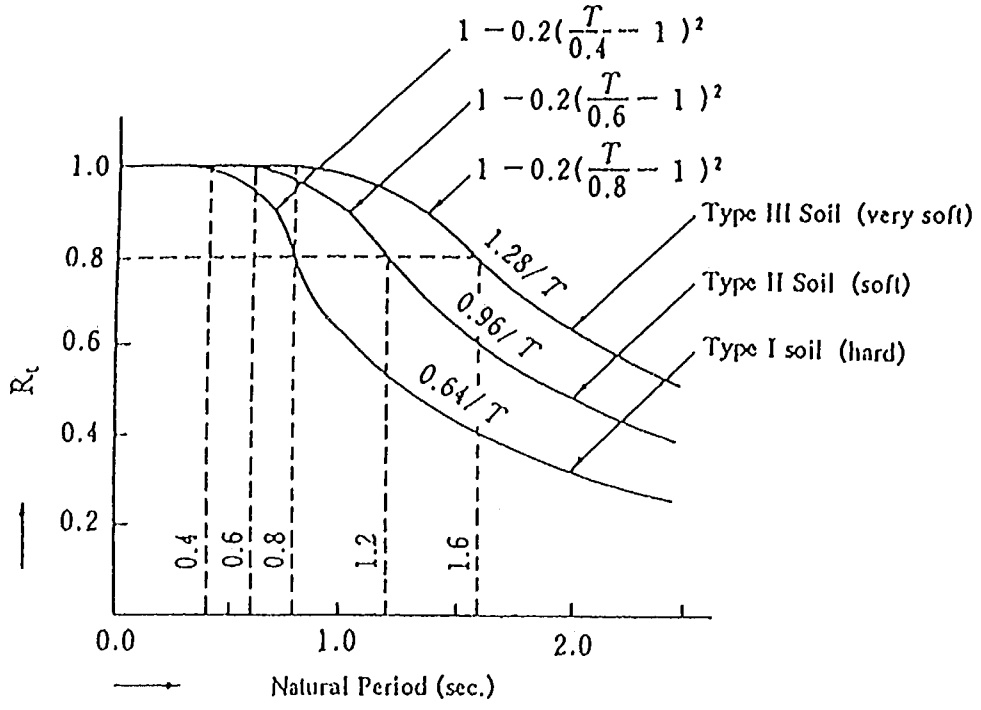


Fig. 2 : Value of R_t with Building Periods

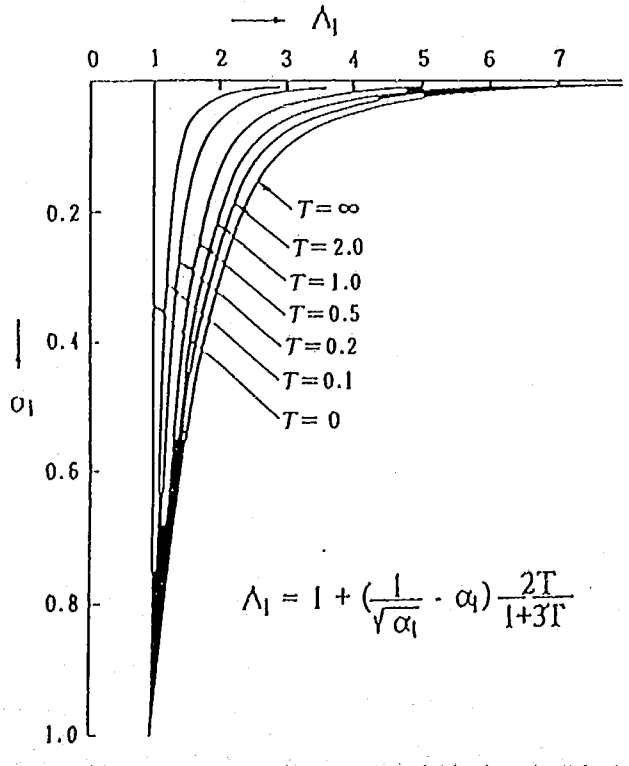
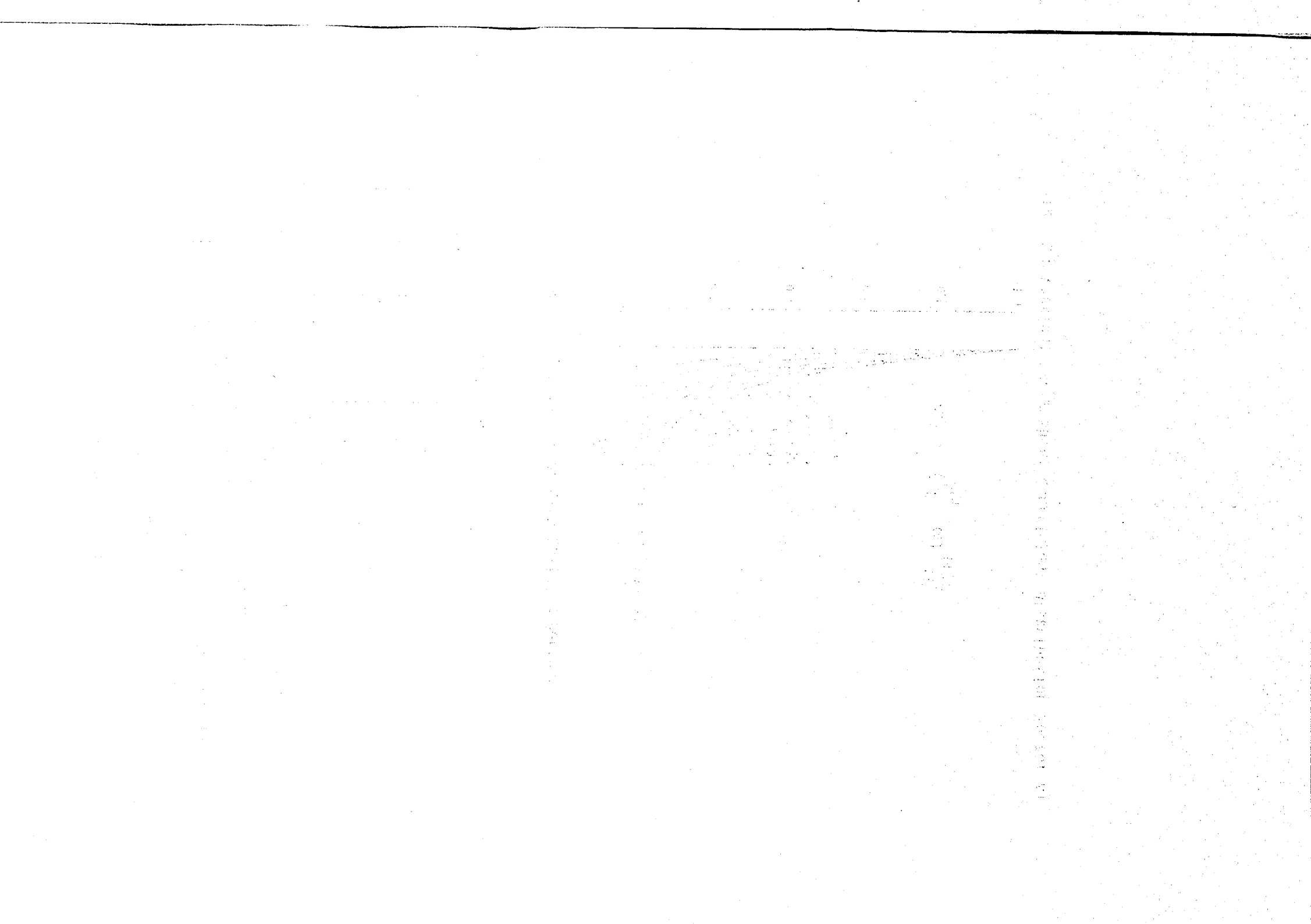


Fig. 3 : Vertical Story Shear Coefficient Distribution Factor A_i



IDNDR SYMPOSIUM

Earthquake Engineering – Stepping Into the Next Century

By: Keizaburo Kubo,
Professor Emeritus, Tokyo University

ABSTRACT

Earthquake engineering research work began with the Investigation Committee for Earthquake Disaster Prevention established officially in 1892, one year after the Nohbi earthquake of 1891. This year marks the 100th year anniversary for earthquake engineering in Japan. During the past 100 years, around 80 destructive earthquakes have occurred in earthquake-prone countries, resulting in considerable loss of human life and property damage. Earthquakes and the resulting seismic damage have proven to be valuable because they have yielded scientific data to earthquake engineers and other specialists and have taught many lessons.

This paper describes five typical earthquakes and what has been learned from their occurrence. In addition, major issues investigated in earthquake engineering are reviewed. They include: earthquake-proof design methods, strong motion observation dynamic analysis, vibration tests of models as well as actual constructions and technique and structural control systems. Finally, the author makes comments on investigation items which will be tackled in the field of earthquake engineering – stepping into the next century.

KEYWORDS: earthquake engineering; seismic damage; bridges; liquefaction; lifeline facilities

1. INTRODUCTION

As stated in the preceding section, this year marks the first year of the second century for earthquake engineering, and the fourth year of IDNDR activity (International Decade for Natural Disaster Reduction). In the following, the author tries to review the history of earthquake engineering, which includes seismic damages to different kinds of structures, lessons learned from past earthquakes and technical developments achieved so far.

During the past 100 years, there have been two major earthquakes in Japan: the Kanto earthquake of 1923 and the other is the Fukui earthquake of 1948. In the case of the former earthquake, the Japan Association of Civil Engineers established a study team to investigate seismic damage to civil engineering structures and housing. An excellent report was published which contains a large amount of seismic data, which has been quoted in many papers in the field of earthquake engineering. A reconnaissance team comprised of seismologists, building engineers, soil mechanics engineers and civil engineers was set up by the Science Council of Japan to study the seismic damage caused by the Fukui earthquake in 1948. Since that time, earthquake damage has been investigated by engineers of various fields. Research in these various fields has been widely promoted in Japan.

It should be emphasized that world conferences have been rendering remarkable services in the promotion of earthquake engineering. The first conference was held in San Francisco in 1956, in recognition of the 50th anniversary of the San Francisco earthquake of 1906. This was the first such conference in which distinguished experts gathered for the first time. Since then, every four years, the World Conference on Earthquake Engineering (WCEE) has been held in Japan and other countries around the world for the purpose of presenting papers on important topics and

exchanging technical knowledge. Last year, the 10th WCEE was held in Madrid, Spain, hosting more than 1500 participants.

The goal of earthquake engineering is, of course, to mitigate seismic damage to structures, lifeline facilities, and housing, all in the interest of human welfare. In order to be successful in these endeavors, the following issues have to be investigated:

1. Collection of data on structural damage in past earthquakes
2. Lessons learned from past events
3. Theoretical analysis of seismic damage data
4. The institution of anti-seismic codes or guidelines
5. Unification of construction techniques in each country

Issues to be discussed in this paper include: lessons learned from such major earthquakes as the Kanto, Niigata, that off the coast of Miyagi prefecture (Miyagi ken-oki), San Fernando, and Loma Prieta earthquakes, achievements made so far in the field of earthquake engineering and prospects for the future.

2. THE BIRTH OF EARTHQUAKE ENGINEERING RESEARCH

Nohbi Earthquake

In 1891, the central portion of Japan was hit by the Nohbi earthquake (M=8.0), and more than 140,000 houses were heavily damaged with the number of casualties over 7,000 total. The new Japanese government, established in 1867, which abolished the policies of the Shogun Era, was in a hurry to import new ideas and construction methods from the West. Over a 30 year period, Japanese engineers learned many modern technological means by which to construct railways, water supply facilities and bridges, all in the interest and hope of modernizing the nation. Several different kinds of structures, new to Japan at the time, were constructed during this period. Unfortunately, these new imported technologies were not designed to be earthquake-proof. Therefore, when the 1891 earthquake hit, several plain concrete bridge piers were sheared off and many modern buildings collapsed, damaging the reputation of foreign construction design and technology.

The Investigation Committee for Earthquake Disaster Prevention (ICEDP) was established by the Japanese government in 1892. Taking into consideration that Japan had been ravished by destructive earthquakes time and time again, it was concluded that construction within Japan must be, above all, earthquake-proof and that earthquake engineering research should be the key issue for reducing seismic damage to structures.

The first president of ICEDP was, at the time, the president of Tokyo University. The committee was also comprised of eleven other members. This committee became the distinguished experts on seismology and civil engineering. It came to an end in 1925, after publishing the "No. 100 Report" on seismic damages caused by the Kanto earthquake of 1923. Its primary responsibilities were taken over by the Earthquake Research Institute, Tokyo University.

The research activities of the committee, spanning 33 years, were outstanding, always functioning as a core for the promotion of seismology and earthquake engineering in Japan. Proposals for static seismic coefficient design method, dynamic analysis of buildings and civil engineering structures and dynamic earth-pressure during earthquakes are among the many contributions made by the committee.

The Progress of Earthquake Engineering During the Last Century

About 80 strong earthquakes hit Japan as well as other countries in the world, resulting in considerable loss to human life and property. Various lessons have been learned from past earthquake activity resulting in better methods for dealing with them now. During this century, UNESCO convened the Intergovernmental Conference on Seismology and Earthquake Engineering in 1964 and 1976, proposing several ideas for reducing the scale of seismic disasters. In the keynote lecture of the 8th WCEE in San Francisco in 1984, Dr. Frank Press, President of the US Academy, proposed the development of the action program of IDNDR, which has been accepted by the United Nations General Assembly, and in 1990, started implementation in earthquake-prone countries.

The progress of earthquake engineering was reviewed in two separate papers written by Dr. D. E. Hudson entitled, "Nine Milestones on the Road to Earthquake Safety", and "A History of Earthquake Engineering". Earthquake engineering progress has also been discussed by Dr. V. V. Bertero in his paper entitled "Major Issues and Future Direction in Earthquake Resistant Design". As stated in the three papers mentioned above, there has been remarkable progress in the field of earthquake engineering. Unfortunately the best that can be achieved to date is mitigation or reduction of the effect of earthquakes but not the eradication of the damage that results from seismic disasters. This is partially due to the high percentage of old structures which are vulnerable to earthquake activity. Additionally, we are not yet capable of perfectly analyzing seismological phenomena. Finally, structures are usually designed from a cost-benefits point of view. Many structures such as high-rise buildings, long suspension bridges and subway tunnels, have never been tested under earthquake conditions.

3. LESSONS LEARNED FROM PAST EARTHQUAKES

Seismic damage to constructions reveals precious data for developing earthquake engineering techniques which will be used to improve and revise interior design specifications in order to reduce seismic disasters during future earthquakes. So far useful lessons have been learned from almost all earthquakes in the past and many new anti-seismic countermeasures have been developed. In the following the author will introduce key issues obtained through analytical works from structural damage which have resulted from several major earthquakes.

Kanto Earthquake

This large seismic shock occurred in the Southern Kanto area, home to the population centers of Tokyo and Yokohama, on September 1, 1923. At about 150 sites, fires broke out after the M=7.9 earthquake occurred and about 40 of the larger fires spread throughout the region, taking with it 140,000 lives. Victims trapped under collapsed houses, or by other types of accidents were estimated to be less than 1% of the total casualty count. Property loss reached 40% of the total GNP of Japan at that time. Brick constructions, severely damaged by the Nohbi earthquake of 1891, showed similar poor performance in the Kanto earthquake of 1923. Reinforced concrete columns and girder buildings without any interior wall partitions were heavily damaged, while reinforced interior concrete buildings with interior stiff walls revealed good earthquake-proof performance, which increased horizontal resistance capacity and reduced the possibility of brittle failure.

For bridge girder supports without any restraint for vertical jumping motion, roller cylinders came out of the supporting lower shoes. At the hinged support, the upper shoe shifted and moved relatively against the lower shoe, thus unhinging the support. It should be noted that after this

event, design specification on girder supports was revised and the vertical restraint of hinged, as well as roller supports of bridges was specified.

It should also be mentioned that masonry arch bridges, such as Nihon Bridge and others as well, experienced little damage, exhibiting excellent performance during this high seismicity. This lesson was applied to restoration works of highway bridges over the Sumida River in Tokyo, where seven out of the ten rebuilt bridges were constructed as arch-type bridges. This technique was also applied to the Bandai Bridge (307.4 meters in length) in Niigata city in 1927. In 1964, Niigata city was shaken by the Niigata earthquake, M=7.5 and two modern steel girder bridges were heavily damaged, resulting in traffic flow over the two to be blocked. The Bandai Bridge, however, survived with virtually no damage and was very useful in the transportation of relief goods and reconstruction materials after the event. It is ironical that the seismic coefficient of 20% *g* was adopted to design computations for the former two girder bridges, but no percentage of *g* to the Bandai Bridge. Another example which displayed the high anti-seismicity of the masonry arch bridge type is that in Skopje which was constructed about 400 years ago and was "baptized" by the Skopje earthquake of 1963 (M=6.5) in the former Yugoslavia. There, as in Niigata, Japan, was minimal damage to the structure. It is clear, therefore, that the arch bridge construction is highly anti-seismic.

Niigata Earthquake

In 1964, an earthquake of M=7.5 hit Niigata City, the epicenter of which being 88 kilometers away from the city center. The sandy ground of the surrounding area became heavily liquefied, losing its bearing capacity. As a result, many heavy reinforced concrete buildings sank and tilted, while several story high apartment buildings on liquified ground overturned. In addition, the two girder bridges mentioned above over the Shinano River, the bridge with piers standing near the river and supporting railway plate girders, moved horizontally several meters down towards the water surface, causing the girder support to be forced out of the top of the pier.

In January of the same year, another earthquake occurred in Alaska, USA, resulting in large ground displacement in Anchorage as well, resulting from a liquefied sand layer. Both earthquakes became the motivating forces for developing mechanism research and countermeasures for liquefied sand both in the States and Japan as well. The condition for liquefaction of sandy soil are that the ground is, 1) sufficiently saturated, 2) loose and 3) shaken enough to change its volume. Papers on countermeasures concerning earthen work have been presented discussing two categories of sandy ground mitigation: consolidation work of sandy ground, in which a sand compaction pile method is employed, and the reduction of excessive pore water pressure by employing gravel drain.

As can be seen with the Bandai Bridge, its design gives us a good example of countermeasures in dealing with liquefied sandy ground in terms of structural design. It was resistant against lateral spreading of liquefied soil ground whose maximum displacement was 8.8 meters. It can therefore be concluded that the pier foundation of the Bandai Bridge will be useful for reducing seismic damage to civil constructions as well because of its stability.

Quantitative analysis of lateral spreading due to liquefaction started in the 1990's specifically for the purpose of investigating the relationship between seismic damage to buried gas pipes and ground movement near the breaking sites. The author's study group succeeded in measuring permanent ground displacement by comparing two aerial photographs taken before and after the

Nihonkai-chubu earthquake (M=7.0) of 1982. Maximum measured permanent displacement reached approximately 5.0 meters. This newly developed technique was also applied to measure the ground displacement in Niigata city in which it was found that the maximum displacement there was 8.8 meters at the measuring point near Bandai Bridge.

Another lesson was learned from this event as well. It comes from the collapse of the Showa Bridge, which was completed just one month before the earthquake in 1964. Several of the girders of this bridge fell. There has been no authorized report on the collapse mechanism of the bridge, but it is said that there are three major issues explaining the failure mechanism. The first issue is that in which the thickness of the ground layer supporting the pile foundations decreased by 10 meters, from an original 18 to 8 meters, due to soil liquefaction, reducing the horizontal resistance of the pile foundation. The second issue is that the support system in which hinged supports were installed on both sides of the bridge and the two girder supports of the two adjacent girders on the No. 6 pier were only roller supports. The dynamic response of the No. 6 pier was then different from that of the other piers on which one hinged support and one roller support were installed. The third issue is that the width of the top of the bridge piers was too narrow to prevent girders from dislodging. The collapse of the Showa Bridge not only caused serious traffic congestion but also significant economic loss resulting from reconstruction costs. Prevention devices against the collapsing of the bridge were recommended and these devices are now specified in the Earthquake-Proof Design Code and Regulations published by the Japan Highway Association.

Miyagi-Oki Earthquake

In 1978, Sendai city experienced an earthquake of M=7.4, the epicenter of which was 100 kilometers away from the city center. Housing on the rocky ground of the older part of the city was damaged slightly. However, some of the reinforced concrete buildings on soft ground in the newly developed area of the city were seriously damaged. It is similar to the example in which old brick railway bridge piers strengthened by reinforced concrete walls could survive, but plain concrete bridge piers standing near retrofitted piers were sheared off and dislocated.

The specific seismic damage was to the pipe joints of small diameter pipes whose diameter is 50 to 70 millimeters. In the Niigata earthquake of 1964, arc-welded steel pipes performed very well and survived without any damage. They are generally considered to be excellent under earthquake conditions if they possess sufficient ductility and strength. However, this concept proved to be less than satisfactory for doing any sort of comparison with other pipes as shown in Table-1 below.

Table-1 Damage Ratio of Buried Pipes

Gas Co. / Pipe	Sendai	Ishinomaki	Furukawa	Shiogama	Mean
Arc-welded Steelpipe	0	0	0	0	0
Cast Iron Pipe	0.02	0.17	0.04	—	0.08
Threaded Steel Pipe	0.84	1.07	0.23	0.40	0.51

It is clear that collar rings and threaded pipes can be easily deformed, causing loose connections in bending as can be seen in loading tests in the laboratory. Under the buried conditions, the threaded steel pipe with a small diameter is considered to show similar behavior as in laboratory tests. In the event of the Kushiro earthquake of 1993, damage ratios for threaded pipes of the Kushiro Gas Co. were very high in comparison with the ratios of the other kinds of pipe joints. It has been concluded through data damage ratios obtained in the above two earthquakes that threaded steel pipes are not earthquake-proof and should be retrofitted with other pipes or pipe joints.

San Fernando Earthquake

In 1971, the northern part of the cities of Los Angeles and San Fernando were strongly shaken by an earthquake of M=6.4. Many modern urban facilities in both cities were heavily damaged, just as in the Niigata earthquake. Olive View Hospital, constructed from reinforced concrete, Veteran Administration Hospital, constructed from brick, the overpass at the I-45 interchange, and an earth dam at Lower Van Norman reservoir sustained severe damage. In addition to these structural damages, seismic damage to buried pipes was especially heavy, causing water stoppage and power outages, raising havoc with people's lives. Power was out for more than 6 hours and as long as 30 hours in places. In Niigata, the power was out for three days, during which time 50% of the restoration work was completed. It also took as long as 15 days to restore only 50% of the water supply. It was then emphasized and recognized that lifeline facilities should be retrofitted and repaired much more efficiently than the Niigata example in the case of a future earthquake.

In the San Fernando earthquake, the impetus emphasized the necessity for earthquake-proof design of gas, electricity and water supply systems and thus a new technical term of "lifeline earthquake engineering" was proposed. The American Society of Civil Engineers established a new committee: the Technical Council on Lifeline Earthquake Engineering (TCLEE) in July 1974, for the purpose of elevating the level of engineering and technical practices in designing lifelines which could survive earthquakes. From November 8th~12th, 1976, the US-Japan Seminar on Earthquake Engineering with Emphasis on Lifeline Systems, was the first seminar for promoting research works in this field. Thirty papers were presented. Static anti-seismic design method for structures standing on the ground was proposed by Professor R. Sano in 1915. Earthquake-proof design method for such underground structures as water pipes, gas pipes and subway tunnels were not officially specified until the Oil Pipeline Business Bill of 1973.

It requires a great deal of time for lifeline engineers to determine the external loading conditions for the design of anti-seismic underground structures. Creative contributions of such design procedures came from two professors: Professor S. Okamoto and Professor G. W. Housner. In 1953, Professor Okamoto published his book on earthquake engineering, in which he compared damage intensities of housing and buried water pipes in Tokyo during the Kanto earthquake. He pointed out that the damages caused to buried pipes and that caused to housing is not the same. In 1960, Professor Housner proposed in his report the original idea of using wave length and amplitude for transmitting seismic waves in discussing the anti-seismicity of the Bay Area Rapid Transit (BART) system and the safety of the underground tunnel crossing San Francisco Bay. Design methods specified in the Oil Pipeline Business Bill and also the Guideline for Earthquake-Proof Gas Pipelines are based on the original ideas presented by Professor Housner. Both the Niigata and San Fernando earthquakes can be said to be the motivating forces that have been instrumental in establishing the anti-seismic design measures of buried structures.

Loma Prieta Earthquake

As with other strong earthquakes, many lessons have been learned from the Loma Prieta earthquake which hit the mountainous area between San Francisco and Los Angeles in October, 1989. In the case of the San Fernando earthquake, American civil engineers learned the importance of restraining the relative movement between neighboring bridge girders by investigating the damage from collapse of the I-45 overpass. The Japan Highway Association, in response to the Niigata earthquake outlined above, specified new issues and devices for preventing bridge girders from collapsing. There was a similar collapse, to what was seen on the Showa Bridge in Niigata and on the I-45 overpass, on the Cypress Viaduct of I-880 and the Bay Bridge as well. Both are located about 100 kilometers from the epicenter of the quake. In the case of the Bay Bridge, a length of the supporting seat of the damaged girder was 5" and the widening of span length from one support to another was 7". This caused a shear-off of the anchor bolts connecting the adjacent girder with the bridge pier. The Cypress viaduct is more complicated than the Bay Bridge example. The failure occurred by seismic damage to columns or column joints, which caused the collapse of upper girders and 67 passengers in cars below were crushed to death. Before the event, the Cypress viaduct had been strengthened by restraining neighboring girders using funding from the state budget. The Japanese practice currently in use was used as the model for this strengthening. The reason that the number of girder failures increased is said to be due to poor soil conditions, consisting of very soft bay mud. There was no collapsing of columns and girders on this viaduct in areas where the soil was more stable. Major lessons from the Cypress viaduct example are that soft ground clearly amplifies ground acceleration. Low ductility structures which are damaged by a shearing off of structural members or a shortage of supporting length, performs very badly allowing for little resisting capacity to withstand a earthquake.

Fires following the main shock of the San Francisco earthquake of 1906 spread due to the shortage of water which caused the main district of the city to be reduced to ashes. After this event, the city embarked on setting up an earthquake-proof water supply system for fire-fighting water, and a potable and auxiliary water supply which would be safe and highly reliable. In spite of all of the engineers' efforts, water distribution pipes were broken at various locations, especially in the Marina district. Four houses caught fire, which had to be extinguished by fire-fighting water from fire boats. The Loma Prieta earthquake thus tells us that it is not easy for all buried pipes to maintain equal anti-seismicity. The reason seems to be that water pipes are installed widely in urban areas, where various kinds of soil conditions exist. Soil conditions vary from very soft soil to very hard soil and a transition zone from hard to soft. Anti-seismicity for pipes is a function of soil conditions, their diameter and thickness, and the strength and physical conditions of the pipe joints, etc. The advantage of buried pipes is that they are installed deep in the ground, where seismic intensity is lower than on the ground. Lifeline earthquake engineering has been developing only for 20 to 30 years and the author believes that from now, many technical issues have to be addressed. Not only hardware but also software research must be made in order to reduce seismic damages to buried pipes as much as possible.

4. MAJOR ISSUES OF EARTHQUAKE ENGINEERING DURING THE LAST 100 YEARS

Improvement of Statical Design Method

Among 100 reports of the ICEDP, the most memorable report from the viewpoint of earthquake engineering is No. 83, that of Professor R. Sano, published in 1915. The behavior of houses when

shaken by an earthquake is not simple but the need to adequately design structures requires seismic input force and should use simplified static force. Professor Sano proposed in his paper that anti-seismicity of houses could be achieved by using the horizontal load of the weight of a structure multiplied by the so-called seismic coefficient and seismic coefficients would be the function of ground conditions and the potential level of seismic activity. The current standard seismic coefficient in Japan is 20% of the gravity force.

In 1952, the joint committee of the American Society of Civil Engineers and the Structural Engineers Association of Northern California recommended that the seismic coefficient be specified by the function of fundamental period of buildings. At present, the statical anti-seismic design method is the basic method ;used in all earthquake-proof design codes and regulations, which is specified by taking into consideration ground conditions and seismic activity at the construction site, fundamental period, and importance and ductility of the structure.

The concept of ductility is the key issue for earthquake-proof structures, and the main issue in modern earthquake engineering research. The ductile failure of a structure is achieved by the use of ductile construction materials and by preventing shear- or buckling- failures of structural elements.

Observation of Strong Earthquakes and Dynamic Analysis

The purpose of ground motion observation during earthquakes is to investigate earthquake source mechanisms and earth structures, and not to investigate the special characteristics of main shock for seismologists. Even though observation of strong ground motion and non-linear building vibrations are very important for earthquake engineering research work, ground motion observations had not been carried out prior to 1932. Dr. K. Suehiro, the first director of the Earthquake Research Institute of Tokyo University, lectured in the States in 1932 and talked about the necessity of measuring ground motion as well as building vibrations in his lecture on "Earthquake Engineering in Japan". His recommendation was soon accepted in the States, and strong ground motions were recorded at Long Beach in 1933 and at El Centro in 1940. The maximum acceleration recorded at El Centro was as high as 330 gal. Such recordings have not been observed for about 30 years. The time history curve of the El Centro record has been used so far for dynamic analysis of special structures so often that it looks like a standard input wave for dynamic analysis calculation.

In Japan, the first strong motion accelerograph of SMAC type was installed in 1953 and now about 2000 strong motion seismographs including SMAC type have been installed, dispersed widely at various places in Japan and recording very useful data for earthquake engineering. Recently observations of dense array networks, or in down-hole configurations have been carried out for investigating vibration amplification of surface layers.

Dynamic analysis of structural response has developed together with the progress of computer technology and the increase of the number of strong motion records. It has become an excellent tool for anti-seismic design after the second World Conference on Earthquake Engineering in Tokyo and Kyoto. Earthquake-proof high-rise buildings can be designed by using dynamic analysis, in which the input of seismic waves of three levels in acceleration level are used.

In 1968, the first high-rise building, Kasumigaseki Building was completed by developing the slit-wall device which shows high damping in the case of large amplitude vibration of the structure

and using a new design concept of the allowable relative drift of each floor, instead of allowable stress concept used in designing the general structures. So far, many high-rise buildings have been constructed in Japan, whose dynamic behaviors during earthquakes have been observed and those observed values are very similar to analytical ones for not so strong ground motions.

Model and Field Vibration Tests

Dynamic analysis techniques have made great progress recently and it is highly desirable for designers to investigate such vibrations characteristics for real structures as periods, vibrational modes and damping constants. For this purpose, model or field vibration tests should be carried out. Field observation of dynamic performance of special constructions has been limited to low level ground acceleration, because it is not easy to shake a prototype structure by actual earthquake ground motion of high acceleration. Therefore, shaking table tests are used for verifying analytical results of structural response of high stress level and for investigating the ultimate state and dynamic failure of the prototype structures.

In such situation, on-line testing techniques have been carried out in several institutes, in which large scale models can be tested, but testing is done very slowly compared with the dynamic performances of the prototype shook by a real earthquake.

In the following, one example of a full scale field test will be reviewed. The purpose of this test is to know the internal damping characteristics of bolted electricity transmission towers vibrating with small to large deformation range. The height of the tower tests was 143 meters and damping constants were measured by using damped free vibration. Damping constant of the tower is as low as that of steel material with small deformation and after slippage occurs between the bolted plates with deformation of the tower. Its damping constant increases. If the deformation of the tower increases over the limit state where the face of the bolts collide with the inside wall of the belt-hole and there is no slippage between the plates, the damping constant decreases with the amount of deformation of the tower. These characteristics obtained by field tests can be traced by numerical analysis with good accuracy, which was carried out under some assumptions. Generally speaking, flexible structures based on stable foundations have very low damping constants.

Aseismic Base Isolation and Structural Control Systems

Before 1967, structures had been designed to have enough horizontal resistance against seismic external forces and their seismic response amplitude was usually more amplified than that of structural foundation. In 1891 and 1909, new ideas for the separation of a building from its base foundation were proposed by a Japanese, Mr. S. Kawai and an English medical doctor. Their ideas were most likely formulated when they looked back upon the severe damage caused by the Nohbi earthquake of 1891 and the San Francisco earthquake of 1906. According to their ideas, building acceleration response may be reduced with its longer fundamental period. Unfortunately, it is very difficult to control building displacement caused by an earthquake because there were no restoring devices in their idea at that time. This fundamental problem was remedied by employing a laminated rubber bearing as a base-isolation device. The first base-isolated school building was thus completed in 1967 in Skopje, Makedonia. This three story building is supported by laminated rubber bearings whose horizontal rigidity is relatively low and therefore its fundamental period is much longer than that of buildings without base-isolation devices.

In Japan, the first four story base-isolated building was completed in 1986 and now about 60 base-isolated buildings have been constructed. Base-isolation systems are now so popular among

earthquake engineers that 33 papers were presented in the field of base-isolation at the 10th WCEE in Madrid, Spain. The fundamental periods for base-isolated constructions is 2 to 3 seconds, which is very effective for reducing seismic response due to input waves whose predominant periods are less than 0.5 seconds. In the event of the 1987 earthquake, the epicenter of which was located 100 kilometers southeast of Tokyo, five base-isolated buildings were shaken by it. The systems of two out of the five buildings were effective in reducing the response acceleration below that of ground level. However, the systems in the other three buildings were not successful. The fundamental period of one of the successful buildings was three seconds. That of the remaining four was two seconds, among which, one was successful. That is due to the fact that there were high frequency components predominant in its input wave types.

The modern trend for seismic control is changing from base-isolation systems to passive or active control systems in the building industry. Recent research on passive or active controls has been carried out with successful frequency. In Japan, the eleven story building with active control systems has already been completed and seismic response records have been obtained. Satisfactory results have been shown. Throughout the world about ten such buildings have been designed, some of which are now under construction. It cannot be denied that many building engineers around the world are not willing to apply active control systems for reducing the building vibration amplitude excited by severe earthquake activity. Most engineers are saddled with other problems such as reliability, energy problems in controlling the excited vibration amplitude, control algorithm of the system and, of course, cost-effectiveness issues.

In a special theme session of the 10th WCEE in Madrid, the establishment of the International Association for Structural Control (IASC) was proposed and accepted. During the 10th WCEE, the author discussed seismic control systems with other experts in attendance. Our conclusion was that for controlling seismic response of buildings, hybrid systems should be proposed: a technique in which a combination system of the active control system for wind excitation and weak or moderate earthquakes, and a passive control system for severe earthquakes would be introduced.

Automatic Supply-Shut Off Systems (ASS System)

At present, it is not feasible to imagine there being no damage to a structure which has undergone a severe earthquake. Because of this, an automatic supply-shut off system (ASS system) would be useful in reducing seismic damages to human lives and properties in the event of a severe earthquake. This paper outlines two examples of ASS systems: one for Shinkansen trains (Japanese bullet trains) and gas facilities.

For Shinkansen, electricity supply-shut off devices are installed at every substation, the interval distances of which are approximately 20 kilometers and if the peak ground acceleration at a substation is over the triggering acceleration of 40 gals, the shut off system comes into action and the electricity supply to Shinkansen trains stops immediately. The other detecting apparatus whose triggering acceleration is 80 gals is installed adjacent to the one of 40 gals. The use of two such apparatus allows for safe Shinkansen operation over the 40 gal limit. It is reasonable for over 40 gals of ground acceleration electricity supply to be automatically shut off. However, ground acceleration at substations might be less than 80 gals which is checked by a second seismograph of 80 gals. If so, electricity will be supplied and the train will be operable again.

Large gas companies are now installing ASS systems in which gas supply to main distribution pipes as well as for domestic use at the gas meter is stopped when the ground acceleration exceeds the

triggering acceleration point of 150 gals. There is another countermeasure for reducing seismic damage to gas facilities which would allow for the rehabilitation of damages facilities as quickly as possible. This is referred to as the blocking system. The primary purpose of this system is to reduce the area of no gas service to as small as possible. The whole gas supply area is divided into several blocks, each of which can shut off gas individually, when gas pipes are heavily damaged.

5. PROBLEMS RELATED TO EARTHQUAKE ENGINEERING IN THE NEAR FUTURE

Diagnosis of Anti-Seismicity of Existing Structures

Outlines of progress of earthquake engineering during the last 100 years have been reviewed in the above and now earthquake engineers have enough knowledge to classify structures and public facilities into two groups. One area is structures and facilities of high vulnerability to earthquakes. The other is earthquake-proof construction and has already seen the development of useful tools to diagnose the anti-seismicity of existing structures. In the first group, there are old structures designed before enactment of modern design specifications and construction made of brittle or low quality materials. Diagnosis technology and retrofitting work has been already applied to existing reinforced concrete buildings in Shizuoka Prefecture, which is under the threat of a large-scale earthquake.

Strengthening and Retrofitting Technology

Generally speaking, retrofitting work of existing vulnerable structures is not cheap and therefore is not applicable to all parts of the world. In this sense, cost-benefit issues must be taken into consideration when researching retrofitting technology. In the case of the IDNDR International Symposium on Earthquake Disaster Reduction Technology held in Tsukuba in December, 1992, Professor J. Kuroiwa of Peru presented his papers on studies to improve adobe construction reinforced with cane and wood and for new housing using local material of wood and bamboo, materials which are inexpensive and useful for construction of earthquake-proof housing. Both ideas are good examples of earthquake engineering research, which can save money and are usable for many different economic classes. The former technique will be contributing to the improvement of the seismic resistance of vulnerable adobe constructions which are widely used even in earthquake-prone countries.

The eight story Marunouchi Building, located near Tokyo Station, was damaged to some extent by a low magnitude earthquake, which had occurred two years before the Kanto earthquake of 1923, requiring retrofitting by connecting columns and beams rigidly with reinforced concrete members. This building was only slightly damaged by the Kanto earthquake which was much more severe than the one two years earlier, owing to the superb retrofitting work.

Individual Preparedness for Mitigating Disasters

For mitigation of seismic disasters, special preparedness by corporations as well as by individuals is highly recommended because both individuals and corporations must be responsible for protecting human life and property in the event of an earthquake.

Preparedness works carried out by national or local governments are 1) countermeasures for the safety of such public facilities as transportation and water supply service, 2) development of early detection techniques to determine damage to construction parts, 3) rehabilitation techniques of damaged structures and, 4) preparation of public evacuation areas.

Tasks to be carried out by corporations are 1) preventative measures in dealing with hazardous materials in the vicinity of factories, 2) minimization of corporate economic losses caused by an earthquake, 3) preparation of contingency plans, 4) assessment of the structural integrity of buildings, 5) retrofitting vulnerable constructions and, 6) employee training.

Tasks to be carried out by the individual are 1) securing of movable objects and furniture, 2) stocking of drinking water, food, medical goods and portable radio and, 3) settlement of communication measures among family members.

The importance of employee training, repeated at appropriate intervals must be emphasized for mitigating human loss and property damage. It is best that employee training be carried out under the contingency plan based on the possible seismic hazards of good accuracy estimated by experts. Training and drills of the masses is especially important, because without good training, the masses will be thrown into utter confusion, causing panic and even greater loss.

Collection and dissemination of correct information concerning seismic hazards and social aspects are also key issues for both corporations and individuals after the main shock of a large earthquake is felt.

Damage Induced by Other Corporations

People who are living in modern large cities have modern conveniences and services such as television, elevators, refrigerators, etc. They are therefore at a loss when electric power supply is interrupted in the event of a large earthquake. Perishable items such as meat, produce, etc., would be tainted and non-edible due to lack of refrigeration. As might be stated in the case of New York City, the interruption of electricity supply would induce not only the perishing of foodstuffs but also shortages of water which rely on electrical pumps for supply. There would also be a suspension in the usage of sewage systems. This means that seismic damage to one lifeline system will affect the other lifeline facilities as well. In the case of the San Francisco earthquake of 1906, damage to water distribution pipes stopped water supply which could have been used to extinguish fires which followed the main shock, resulting in the main part of the city being gutted.

In recent earthquakes in Japan, telephone service has been disrupted even if there is no seismic damage to the telephone facilities, rendering emergency calls useless. This is because the lines become overwhelmed by calls inquiring about the safety of friends and relatives in the hit area.

6. CONCLUSIONS

Earthquake engineering has achieved a lot of remarkable goals over the past 100 years since the establishment of ICEDP in 1892. Anti-seismic design specifications have been instituted for on-ground structures as well as underground facilities and the dynamic response of the structures can be numerically calculated with good accuracy, if an appropriate input seismic wave is provided. In addition, new tools for diagnosis of existing structures and retrofitting techniques of old houses are now in common use in many countries. Reduction of building response is now successfully controlled by using base-isolation systems or by passive or active control systems. Unfortunately, loss of human life and property still persists with severe earthquakes. It is said that earthquake prediction can mitigate damage to human life caused by earthquakes but so far only one earthquake in China has been successfully predicted. Earthquake engineering research at present is not perfect and thus needs to be further developed, making clear dynamic performances of

various kinds of structures for reducing seismic damages to houses and civil constructions. Now, major items for earthquake engineering in many countries is earthquake-proof design and construction of houses and reinforced concrete buildings and lifelines which will sustain the effects of most major earthquakes. Research in these areas is due to the fact that houses are made of local materials or buildings were designed before modern design codes were. These sorts of constructions are the most vulnerable in an earthquake and many people are killed by their failure to withstand seismic activity.

When an earthquake hits a city and lifeline facilities are broken, the living condition of people who have enjoyed their civilized lives with electricity and water supply are sunk to a sort of misery level. There are still many technical problems to be solved, as shown in the following.

1. Lifeline earthquake engineering has not developed sufficiently.
2. Seismic damage to underground facilities cannot be easily detected.
3. Experimental works on dynamic behavior of buried pipes during earthquake conditions are extremely difficult to predict.

Taking into consideration the present situation of lifeline earthquake engineering, this field will be the major research item of the second century of earthquake engineering.

The majority of lifeline earthquake engineers have been trying to develop new kinds of hardware techniques such as new types of pipe joints, strengthening pipes made of brittle materials and countermeasures for pipe deformation, as a result of sustained lateral spreading of surrounding liquefied soil layers. From now on, new fields of software techniques of lifeline facilities will be encouraged and developed around the following items:

1. Automatic shut off systems (ASS)
2. Blocking system in which the supplying area is divided into several blocks, some of which will survive earthquake damage and others will be supplied continuously even after a strong earthquake
3. Employee training

There are many research items to be solved in the field of earthquake engineering: retrofitting work of existing buildings, soil interaction problems, lifeline earthquake engineering, training individuals and employees, liquefaction of sandy ground and induced lateral spreading, etc. Paying attention to the present situation, in which the number of research staffs for earthquake engineering may be limited, international cooperation is very much needed and appreciated. This is the key concept of IDNDR — exchange of technological information between nations.

ASCE'S CONTRIBUTIONS TOWARD TECHNOLOGY FOR DISASTER MITIGATION

by

Edward O. Pfrang, Ph.D., P.E.*

It is truly an honor to have the opportunity of addressing this distinguished audience on the occasion of the UJNR Panel on Wind and Seismic Effect 25th Anniversary Meeting. Having participated in the panels' activities for the first 17 years of its existence, I greet this occasion with a sense of both happiness and sadness, as well as with an overwhelming sense of pride in our accomplishments. I am happy to have the opportunity of once again visiting with old friends such as Dr. Fukuoka, my mentor and the first Chairman to the Panel from the Japan Side; I am sad to note the passing of other friends such as Dr. Okubo, the first Secretary and later Chairman. But we can all take great pride in the enormous accomplishments of this panel. The Panel was originally formed to help mitigate the affects of natural disasters by utilizing the vast engineering and technical capabilities of our two peoples. Both of our countries have all too frequently shared the grief from losses inflicted by natural disasters, and as a result have developed engineering capabilities second to none in dealing with these calamities. By combining these two resources through the activities of this Panel, we have truly served our two great nations and all of humanity in contributing to the mitigation of the effects of natural disasters.

Today I have been asked to speak on the role of the American Society of Civil Engineers as its programs relate to disaster mitigation. But first, it might be well to tell you just a little bit about the American Society of Civil Engineers.

ASCE was founded in 1852, and is therefore the oldest professional engineering society in the United States. ASCE currently has over 110,000 members, of whom over 8,000 are international members, representing 130 countries around the world. ASCE is organized into 78 domestic sections, five international sections, and 11 international groups, as well as 246 student chapters and clubs. The first international section to be formed outside of the western hemisphere was established in Japan in 1988. ASCE is the world's largest civil engineering organization and also its most prolific in terms of the amount of technical

* American Society of Civil Engineers
345 East 47th Street
New York, New York 10017

and professional material produced. Each year the Society publishes over 65,000 pages in the form of journals, its magazine, standards, proceedings, monographs, and books. The technical work of the Society is carried out through a vast array of 500 technical committees, with currently over 6,700 committee members, who are organized into 25 technical divisions and councils. Thus, the main technical work of the Society is conducted by these committees through their technical division structure.

In recent years, the Society has been building upon the outstanding contributions of its technical divisions through the development of consensus standards. Because of the strength of our Structures Division, currently chaired by Dr. Richard Wright, who will be your next speaker, much of our earliest standards activities was in the structures area. More recently, the Society has been developing standards in a number of other areas such as transportation and the environment. We also have particular expertise and interest in the area of seismic lifelines, which I will discuss later.

Less than a month ago we held our 11th Annual Structures Congress, in Irvine, California. The theme for this congress was "Structural Engineering Leadership in Natural Hazards Mitigation." It had an outstanding program, with more than 50 presentations. The program also included technical tours on base-isolated buildings and seismic retrofit of concrete highway bridges. I was extremely pleased to see entire sessions organized and presented by colleagues from Korea, China, Taiwan, Mexico, and, of course, Japan. The sessions on seismic design and on performance and response of structures under various loading systems are illustrative of the material being accomplished by our technical committees and their members.

At the Congress, one of the major topics was the "Hurricanes of 1992." This topic is, of course, of vital interest to us in the United States because of the unprecedented damage suffered last year. As a result, we have now finalized plans for a major follow-up conference to be held in Miami, Florida, this December 1-3. This conference, like a similar one three years ago reporting on a 1989 hurricane that struck Charleston, South Carolina, will try to evaluate what happened, what went right, what went wrong and what can be done in the future to avert or to minimize further recurrences of damage.

We do not hold such conferences on each disaster but only when we feel that there is new information to be presented and discussed, due to a unique or distinctive occurrence. We really would prefer not to have need for such meetings, but, regretfully, extreme events of this sort still result in more damage than is tolerable. The conference in Miami will cover two

storms: Hurricane Andrew, which struck both Florida and Louisiana, and Hurricane Iniki, which devastated part of the Hawaiian island chain. Each of the three areas struck had its own unique damage. We are pleased that the three ASCE Sections involved are joining with our national committees to organize and present their combined experiences. After these events, we will publish the papers presented so that a permanent record is available enabling others to access the information and apply them.

Most of you have already seen photographs of the aftermath of Hurricane Andrew in Florida, and I recognize that Mr. Fuller will be discussing the lessons learned; however, I would like to show a few slides to set the stage for my next remarks. One of the recurring issues that surfaced following Andrew was the adequacy of the South Florida building code and also the degree to which the code was followed and enforced. I am pleased that ASCE received many excellent comments about our national standard ANSI/ASCE 7-88, which had formed the basis for wind loadings for the South Florida area. The standard, formerly known as A58.1, is entitled Minimum Design Loads for Buildings and Other Structures and has been one of our most frequently referenced standards. More importantly, it reflects the utmost care, concern and knowledge of our engineering community in establishing proper loadings for structural design.

I am pleased to announce we will soon be publishing an updated version of ASCE-7 that significantly modernizes the seismic loading provisions. These new seismic loading criteria have been based upon the 1991 National Earthquake Hazards Reduction Program provisions, which were developed by the Building Seismic Safety Council of the National Institute for Building Science under contract to the U.S. Federal Emergency Management Agency (FEMA).

We are expanding the scope of ASCE-7 as new information and research becomes available. For example, ASCE is completing a contract with FEMA on flood loadings on structures. We expect to include the results of that effort in a future version of ASCE-7. We also have established a new task committee to investigate the effects of ice loads on structures and, in due course, we expect that that too will become part of the standard.

A similar program we are participating in with the Building Seismic Safety Council and the Advanced Technology Council (ATC) under a contract with FEMA, is the development of a consensus-based report on the seismic rehabilitation of existing buildings. This follows upon a similar ATC report, in which we participated, on the Social and Economic Considerations of the Seismic Rehabilitation of Existing Buildings. We expect that this will

become a part of, or a companion document to, our existing ASCE standard entitled Guideline for Structural Condition Assessment of Existing Buildings (ASCE 11-90). The same group is also developing a standard to be entitled Condition Assessment of the Building Envelope (roofing, siding, etc.), which will address many of the Hurricane Hugo (which struck the Carolinas in 1989) and the Hurricane Andrew (Florida and Louisiana) findings.

One of the stronger parts of the ASCE-7 standard is the wind-loadings portion. However, as we have seen from the slides, there are still immense economic losses that result from damage caused by wind. We are very pleased with the proposed legislation now before the U.S. Congress for a Wind Engineering Research Program within NIST. We favor the legislation, and we intend to participate in development of the plan for a national wind-engineering research-and- development program. We need a reliable and consistent monitoring network for wind velocities; we need to acquire full-scale data on structural performance during extreme wind events. We need wind tunnel modeling tests to validate our models and to develop enhanced models for predicting the response of structures to wind loading. Finally, models must be translated into usable building code provisions to complete the process. Perhaps we can find analogies in damping for wind effects similar to those being applied to buildings for countering seismic effects. An additional ASCE effort in this area, now nearing completion, is a manual to be entitled Wind Damage Investigation.

I had earlier mentioned the task we had under way on flood loadings on structures. We want to disseminate the current state of the art in flood-resistant design and construction to engineers and architects and to incorporate these practices into building design and into land use planning in our nation's floodplains. We will also look at the protection of utilities and mechanical systems and the appropriateness of the use of various materials. This will augment the work underway in coastal zone management and coastal engineering research. We have also started the development of a standard on the design of shore-protection structures to preserve and protect shorefront properties. The scope of this activity is extensive and will address continued deterioration by erosion as well as the more violent attack by storms. Fluctuations in river, lake, and ocean levels over the life of protected structures will be considered, as will wave and other dynamic water-transmitted forces and the movement of sand during and after storms.

An additional activity in the water area is the work of a group preparing guidelines for inspection of dams. Our Geotechnical Engineering Division has

just sponsored a very successful conference on Dam Rehabilitation, which followed a Stability and Performance of Slopes and Embankments Conference that attracted well over 800 participants. We know that Japan has long had a comprehensive program of landslide control with land use planning and construction measures that are designed to prevent slope failures. In a number of areas in the United States we have the same concerns.

An additional area in which we are working is that of expansive soils and the construction of structures, particularly housing, on these materials. It is estimated that the damage to residences each year from expansive soils exceeds several billion dollars. It is our intent to produce criteria for the design of different types of residential foundations in areas of differing expansive soil and moisture conditions to minimize the problems with future construction. Although the direct hazard to people from these effects is relatively low, the economic costs are high, and we seek to adapt our design and construction practices to work effectively within these conditions.

Earlier, I noted that ASCE had a particular interest and expertise in the area of seismic lifelines. We have produced five specific monographs on such topics as Seismic Loss Estimates for a Hypothetical Water System; Seismic Risk Studies; which presents earthquake hazard and vulnerability analysis models for lifeline systems; and Lifeline Earthquake Engineering, which includes studies by investigators who have analyzed and evaluated the effects of earthquakes on lifelines. The latter volume includes a history of lifeline earthquake engineering. One monograph addresses lifelines in the central and eastern United States, where major earthquakes have been rare but are potentially devastating. We have produced a Guide to Post-Earthquake Investigation of Lifelines, which was written as a training guide to aid the process of post-earthquake investigation of lifelines. Our active investigation group aids government and private entities in affected areas in analyzing the reasons for lifeline failures. Active efforts by this group include the development of investigation procedures and the design of systems that will preclude or minimize system failures and outages. Finally, we have a monograph in preparation on Seismic Risk Analysis of Highway Transportation Systems.

An area of great interest -- and, indeed, need -- is the availability of standards for seismic lifelines. We anticipate that the development of these standards will become a major activity for ASCE. We felt so strongly about this subject that we proposed the establishment of a Lifeline Seismic Safety Council (LSSC), somewhat similar to the Building Seismic Safety Council (BSSC), which is well known to most of you. We believe that a

LSSC, affiliated with ASCE, could draw upon the expertise of our Technical Council on Lifeline Earthquake Engineering, our Structural Division, and other technical groups to provide a forum for the development of lifeline seismic standards and seismic planning, and for the design, construction, retrofit, and operation of lifeline systems.

In a nontechnical area, I would like to talk about some work being accomplished by our Committee on Natural Disaster Reduction (CNDR). We established this group a few years ago to develop goals and to guide actions for ASCE's role in natural hazard mitigation and disaster reduction. We specifically identified CNDR to serve as a focal point for activity contributing to the International Decade for Natural Hazards Reduction. This cuts across several disciplines, and its leaders represent each of the primary civil engineering disaster areas: earthquakes, landslides, floods, and wind. An important task they have under way is the development of a computer data base of ASCE members who are able to participate in response studies to future natural disasters. In previous emergency-response situations, our staff has normally pieced together an ad hoc group of knowledgeable ASCE members who respond to press inquiries and support requests from local government bodies. Our staff procedures to respond to natural disasters have been in existence and utilized successfully several times. The work by CNRD will provide us ready and instant access to qualified technical experts. We look forward to the completion of this task.

Not all of the disasters ASCE addresses are of natural origin; and if I may depart from that theme for a moment, I would like to mention what ASCE has planned to address with regard to man-made disasters. First, let me show a few slides. At our national convention in Dallas, Texas, this coming October, a plenary session will feature the bombing of the World Trade Center in New York City. ASCE Member, Gene Fasullo, is the Chief Engineer for the Port Authority of New York and New Jersey, which owns the World Trade Center. Gene was trapped in an elevator following the blast and dug his way out with an ordinary key. Gene will talk about the episode and be will joined by structural engineer Leslie Robertson, the designer of the World Trade Center, who will talk about the damage and retrofit that has been required. They will be joined by a member of our Structural Committee on Shock and Vibratory Effects, which expects to complete the draft of a report entitled Structural Design for Physical Security later this year. We hope that many of you will be coming to Texas in October to hear this and the other fine sessions at our convention.

I am pleased to have had the

opportunity to report on ASCE's programs and accomplishments in this important area and to provide you with some insight into our present and future activity involving disaster mitigation.

In closing, I wish to salute you on this your 25th Anniversary Meeting. The strong bonds of technical cooperation that have been fostered through the UJNR Panel on Wind and Seismic Effects have been of enormous significance in reducing the suffering of the people of our two great nations and of improving the well-being of mankind worldwide. I wish you well on the next 25 years.

COOPERATION ON RESEARCH AND TECHNICAL DEVELOPMENT IN WIND AND EARTHQUAKE ENGINEERING BETWEEN U.S.A. AND JAPAN IN THE LAST 25 YEARS
----ACTIVITIES OF THE PANEL ON WIND AND SEISMIC EFFECTS, UJNR---

Yukihiko SUMIYOSHI*

ABSTRACT

This paper introduces the cooperation on research and development in the field of wind and earthquake engineering between U.S.A. and Japan through the Panel on Wind and Seismic Effects of the U.S. - Japan Conference on Development and Utilization of Natural Resources (UJNR). The past accomplishments in the last 25 years and the future perspectives are presented.

KEYWORD: Wind Engineering, Wind Resistant Design, Earthquake Engineering, Seismic Design, Storm Surge, Tsunami, International Cooperation

1. INTRODUCTION

In 1964, the U.S.-Japan Conference on Development and Utilization of Natural Resources (UJNR) was founded as one of the three programs which comprise the U.S.-Japan Cooperative Science Program with the object of exchanging research personnel and information in the fields of technology for the benefit of both countries.

In 1967, the Panel on Wind and Seismic Effects was established as a new cooperative activities on the occasion of the 3rd UJNR Plenary Meeting in Tokyo. This Panel is one of the 17 UJNR Panels as shown in Fig. 1. Principal objectives of this Panel are to give opportunities for exchanging and presenting the research results on wind and seismic effects on structures in view of the fact that both the U.S. and Japan are prone to suffer from natural disasters.

The activity of the Wind and Seismic Effects Panel has been expanded every year since the 1st Joint Meeting in 1969. Exchange of the research results related to the revision of design criteria and developing comprehensive measures and technical efforts to mitigate loss of lives and properties from extreme wind, earthquake, storm surge and tsunami has been made.

The Panel has been established jointly in each country. Presently the Japan Panel consists of 33 members from 7 organizations as shown in Table 1 and is chaired by the Director-General of the Public Works Research Institute, Ministry of Construction. U.S. Panel is chaired by the Director of Building and Fire Research Laboratory, National Institute of Standard and Technology of Department of Commerce, and includes 52 members from 17 organizations as shown in Table 2.

The Joint Panel Meeting has been organized every year alternatively in U.S.A. and Japan since the 1st Joint Meeting in 1969, and the 25th Joint Meeting was held at Tsukuba, Japan, in May 1993.

This paper reviews the accomplishments of the Panel in the last 25 years and shows its future roles for contributing for reducing loss of lives and properties due to extreme wind, earthquake, storm surge and tsunami effects.

2. PROGRESS OF THE PANEL ON WIND AND SEISMIC EFFECTS, UJNR

Since the 1st Joint Panel Meeting which was held in Tokyo in 1969, activities of the Panel have been expanded for actively contributing to the exchange of technical information and research personnel. Although its scope was only for wind and seismic effects in early days, it was extended to include the storm surge and tsunami effects on the occasion of the 10th Joint Panel Meeting in 1978. New members joined the Panel.

Task Committees were formulated firstly in 1975 for effectively promoting the Panel program by exchanging technical information through not only the Joint Meeting but workshops sponsored by the Task Committees on the relevant subjects. Six Task Committees from "A Strong Motion Instrumentation Arrays and Data" to "F Earthquake Disaster Prevention of Lifeline Systems" were formulated in 1975. At present, 11 Task Committees as shown in Table 3 are actively continuing their activities. The Task Committees greatly contributed to the success of the Panel activities.

In 1977, the exchange of researchers was initiated. The U.S.-Japan cooperative research program was also initiated in this year. The following six U.S.-Japan Cooperative Research Programs have been conducted:

a) Cooperative Research on Reinforced Concrete Structures (1979-1987)
b) Cooperative Research on Steel Structures (1985-1987)
c) Cooperative Research on Lifeline Facilities (1982-1989)

*) Director-General, Public Works Research Institute, Ministry of Construction

d) Cooperative Research on In-situ Testing Methods for Soil Liquefaction (1983-1986)
e) Cooperative Research on Masonry Structures (1984-1988)
f) Cooperative Research on Precast Seismic Structural Systems (1991-continued)
g) Cooperative Research on Hybrid Control (1990-continued)

The cooperative research programs have facilitated exchange of researchers and technical information between both countries. The programs also have contributed to improve codes and standards of buildings, bridges and soil structures in both countries.

In 1979, 4 member organizations in Japan side, i.e., Public Works Research Institute, Building Research Institute, Geographical Survey Institute and Meteorological Research Institute, moved to Tsukuba Science City. On this occasion, advanced and large experimental facilities were equipped so that new experimental studies could be initiated. Those facilities have been effectively used for U.S.-Japan Cooperative Research Programs.

In 1987, a Charter of the Panel was formulated to clarify the aims of the Panel activity.

Recognizing that the 20th Joint Meeting signifies a major milestone in the history of the Panel on Wind and Seismic Effects, both sides developed and presented papers on their many accomplishments and proposed future directions. They were compiled published in the form of a report entitled "Two Decades of Accomplishments and Challenges for the Future" (Ref. 1).

A grandson of the Newton's apple tree, that is famous for the story that Sir Isaac Newton discovered the law of gravitation by observing a falling apple, was presented in 1987 from National Institute of Standards and Technology, U.S.A. to Public Works Research Institute, Japan in spirit of the continued strong cooperation between two institutes. It was planted as shown in Photo 1 at the front garden of PWRI.

Both U.S. and Japan sides published "A List of Panel Publications from 1969 to 1991" (ref. 2) for distribution to international organizations, especially those in developing countries as well as to U.S.A. and Japan domestic organizations.

3. ACCOMPLISHMENTS OF THE PANEL

The annual Joint Meeting and the Workshops provided the mechanism for interaction between the U.S. and Japanese researchers in wind and seismic engineering which provided opportunities to gain valuable information and to engage in cooperative research programs. Through these opportunities the Panel member organizations have realized important advances in building and structures technology. The Panel's activities have resulted in improving building and structures codes and standards in both countries.

The following activities were effective for contributing the technical exchange between the two countries :

(1) Joint Meetings and Workshops
Up to now, 25 Joint Panel Meetings were held as shown in Table 4. Photo 2 shows the latest 25th Joint Meeting held in May 1993 at PWRI, Tsukuba Science City, Japan. 32 Workshops were also held as shown in Table 5 under the auspices of the Task Committees of the Panel. Photo 3 shows the 9th Bridge Workshop held in May 1993.

Over 1300 technical papers have been presented from the U.S. side and Japan side at the Joint Panel Meetings and the Workshops. Proceedings of the Joint Meetings and the Workshops were printed, distributed and utilized to develop wind and earthquake engineering in both countries. Photo 4 shows the Proc. of the 24th Joint Meeting published by NIST.

(2) Exchange of Researchers
More than 200 U.S. and Japanese researchers have been exchanged to join cooperative research programs, earthquake survey and other activities in the counterpart country.

(3) Coordinated Damage Survey
The Panel's coordinated post-earthquake fact finding teams visited the sites of damaged structures from the Izu-Peninsula Earthquake of February 1978, Miyagi-ken-oki Earthquake of June 1978, Nihon-kai-chubu Earthquake of May 1983, and Loma Prieta Earthquake of October 17, 1989. The damage survey by the Japan side members to the Hurricane Andrew of 1992 was supported by U.S. members.

The Panel recognizes the importance of using these findings and experiences and encourages similar exchanges of information from future post-disaster investigations. Information transfer includes reports, seminars and special Panel sessions.

Furthermore, in regard to cooperation with developing countries, damage information was exchanged. Especially, the U.S. and Japanese investigation of damage due to Mexico Earthquake of 1985 , Chile Earthquake of 1985 and Armenia Earthquake of 1989 and support of aid were reported at the Joint Panel Meetings.

(4) Special Seminar and Symposium
A two-day seminar where Panel members

participated was held as shown in Photo 5 in Charleston, South Carolina during the Panel's technical study tour after the 22nd Joint Meeting in May 1990.

A one day International Symposium on the International Decade for Natural Disaster Reduction was held for commemoration of 100 years from the Nobi Earthquake in 1892. It was held in Gifu City, Japan on May 20, 1991 to increase the awareness about the disastrous effects from strong winds and earthquakes. The International Symposium was organized by the Chubu Regional Bureau of the Ministry of Construction and other organizations. The Panel provided three of the five presentations. As shown in Photo 6, more than 600 persons attended. The Nobi Earthquake had the magnitude of about 8 and caused destructive damage to structures. Damage was especially significant for those structures constructed by the newly imported technologies from European countries. It revealed the fact that the direct import of the construction technologies from European countries was not adequate in Japan because of seismic vulnerability. The Nobi Earthquake was an important turning point for initiating the technical development of seismic design method in Japan.

(5) Translation of Research Reports
The Japanese MOC document on "Manual for Repair Methods of Civil Engineering Structures Damaged by Earthquake" and the Japanese MOC reports on "Base Isolation Systems for Buildings" were translated into English, published, and disseminated to appropriate U.S. engineering community members.

(6) Exchange of Technical Data
Since strong motion records are valuable data for research on earthquake engineering, the strong motion record exchange system was built between U.S. and Japan. A strong motion records catalog is exchanged periodically, and wave records and digitized records of strong motion are distributed to the related agencies after publication.

Furthermore, records of strong wind and tsunami and data base have been also exchanged to be utilized for developing relevant research.

(7) Publication of List of Publications
The idea of creating List of Publications of the Panel's work first surfaced in 1988 for the occasion of its 20th anniversary. Three year later this idea was brought to realization in support of the IDNDR. The Japan-side Panel collected and categorized the papers published during the period April 1969 through May 1991 which make up the listings. These papers represent 23 years of collaborations between the United States and Japanese researchers. Over 1,200 papers were published during this period. Published papers are found in chronological order. The author's index is also presented in alphabetical order.

This List was published by PWRI and NIST (Ref. 2) and was distributed to U.S. and to Japanese domestic organizations and to international organizations in 1992. This List notifies the many organizations and individuals within IDNDR countries about the availability of this Panel's technologies. Collectively, they make a valuable contribution to the literature and is an important resource for international cooperation.

4 MAJOR RESEARCH COOPERATION THROUGH THE PANEL

4.1 Cooperative Research on Reinforced Concrete Structures

U.S.-Japan Cooperative Research on Reinforced Concrete Structures started as a Research Program Utilizing Large Scale Testing Facilities on August, 1979. The testing of a seven-story reinforced concrete building as shown in Photo 7 was initiated on March 1981 at Building Research Institute.

Based on the research, ultimate strength and deformation of the 7 story building with shear walls was confirmed through the full-scale test. The building behavior during a significant earthquake was made clear by the pseudo dynamic testing . The test result provided excellent information for improving seismic design method of reinforced concrete buildings in both countries.

4.2 Cooperative Research on Steel Frame Structures

A full-scale pseud dynamic testing of a 6-story steel frame building was conducted as shown in Photo 8. The effect of moment resistance of braced frame and the joint effect between the steel beam and the composite reinforced concrete slab were confirmed.

4.3 Cooperative Research on In-Situ Testing Methods for Soil Liquefaction

In-situ test for assessing the soil liquefaction needs to provide the same soil parameter whenever or wherever in the world it is conducted. However, it was noticed that there was some discrepancy in the standard penetration testing (SPT) method in both countries. Also, it was required to clarify whether the number of blow counts (N) of SPT is the same or not at the same sites.

A cooperative investigation was conducted to acquire the SPT data at the sites where the liquefaction apparently took place during the past earthquakes. The N values obtained by the popular manners in both countries were compared.

It was concluded that although there is some difference in the energy ratio, number of the blow count normalized for the same energy level is practically the same between the two countries.

4.4 Research of Lifeline Facilities

In the cooperative research, hysteretic behavior of reinforced concrete bridge columns subjected to a significant earthquake was investigated from 1982 to 1989. Scale effect was studied in U.S. side using large scale specimens as shown in Photo 9. Effect of loading rate and loading hysteresis were studied as shown in Photo 10 in Japan side using medium size specimens. The large static loading machine at NIST and the high loading-rate dynamic actuators at PWRI were used in the test.

The research results were effectively used for improving seismic design methods of bridge columns in both countries.

4.5 Research on Hybrid Control of Structures

Joint effort for developing active and hybrid control technologies for bridges is being made between Public Works Research Institute, National Science Foundation, National Center for Earthquake Engineering Research and Federal Highway Administration. Hybrid control algorithm which requires less energy for controlling bridge response is being studied. Photo 11 shows a shaking table test made for verifying the implementation of the variable damper.

4.6 Research on Masonry Structures

Both the U.S. and Japan side worked since 1984 on a coordinated research program on masonry structures in seismic zone. Based on a detailed understanding of the structural behavior of reinforced masonry buildings derived from analytical and experimental research programs on material, components, sub-assemblages and a five story full-scale prototype building which were carried out in both countries, the design guidelines was developed. The full scale tests were carried out in 1987 in Japan side as shown in Photo 12 and in 1922 in U.S. side.

5. FUTURE PERSPECTIVES OF THE PANEL

5.1 Change of Economical and Social Condition around the Panel and Progress of Technology

Because the technical cooperation requested to be made through the Panel is significantly increasing, it is requested to decide the Panel's future activities taking account of recent trend. The new trends which are required for creating new technical cooperation between both countries are as :

[1] Changes of Social Structures

(1) Aging
Aging problem may be more serious in Japan than in U.S.A. Population of younger generation under 30 years old is decreasing, and the labors are getting older. Shortage of 1.6 million labours will take place in 2000 in Japan. Women labors are required to increase .

(2) Urban Problems
Concentration of population in urban areas is increasing. High land cost is another serious problem in urban areas. This develops high risk and vulnerability against disasters. This also made the environmental conditions worth. On the other hand, number of population in local areas where only agriculture and fishery industries are the main industries is decreasing. Appropriate measures for promoting other industries in such local areas are required.

(3) Economic and Social Structures
Significant changes in economic and social structures took place in the last 30 years. For example, industrial structures have already shifted from 1st and 2nd to 3rd in both countries. Every systems are well formulated so that the most efficient economic and social activities be made with the redundancy being minimum. This increased the vulnerability in the society against disasters including an extreme earthquake.

(4) Information and Computer Dependent Society
Significant progress of the information and computer systems is the key issue for highly industrial society. But this produces new type of disasters which have not yet experienced when disruption of information and damage of computer systems are developed.

(5) Environmental Problems
The global temperature is clearly increasing in recent years. Development of clean energy is required for reducing the Green-House effect. The disappearance of forests and the expansion of desert areas are one of the most serious problems. This would cause shortage of rainfall and abnormal climate. Disaster prevention projects need to be made under strict environmental restrictions so that they match with the environmental conservation concept.

(6) Internationalization

Because U.S.A. and Japan are the two major countries leading the world in the technical development in wind and seismic effects, more efforts are required for effectively disseminating technical information and technology for developing countries.

[2] Progress of Science and Technology

(1) Observation Systems
Sensor technologies for observing and measuring behavior and damage of facilities and structures are considerably progressing. It is becoming possible to forecast and monitor failures based on such data. More efforts are required for developing monitoring and warning systems which are closely linked up with new sensor technologies.

(2) Remote Sensing Technology
Remote sensing technologies are also promising for forecasting and observing damages. More appropriate utilization of the remote sensing is expected.

(3) Computer Technology
Advanced analytical simulation highly depends on the progress of computer technology. Nonlinear simulation made it possible to predict sophisticated simulation. Further utilization of progress of computer technology including the development of appropriate analytical procedures is expected.

(4) Communication Systems
Progress of communication systems provides many new research areas for implementing them to disaster prevention.

5.2 Future Research Needs against Extreme Wind, Earthquake, Storm Surge and Tsunami Effects

[1] New Technologies Development for Structures

(1) Advanced technologies
Research and development for new and advanced technologies which enable to introduce the progress of science and technology are required in disaster mitigation. Those will include the passive and active control technology.

(2) Standardization and codes for ordinary structures
More efforts are required to standardization of normal type of facilities and structures so that appropriate design codes and standards be developed to mitigate damage by disasters.

(3) Improvement of seismic safety of ground
Technologies for upgrading seismic safety of soft alluvial deposits, reclaimed land and boundary zone from soft to hard soils are required. Special attention needs to be paid to soil liquefaction because many water-front projects are being executed on reclaimed land constructed by filling weak saturated sand vulnerable to liquefaction.

(4) Large structures projects
There are many projects in which large structures such as super long-span bridges, super long tunnels and skyscrapers are included as the core structures. More technical development for wind and seismic effects to those structures is expected for realizing those projects.

(5) New type of structures
New types of structures which are of buildings, bridges and underground structures are being increasingly constructed in urban areas. Research for such new types of structures is indispensable.

(6) Tsunami
Tsunamis caused a large number of loss of lives. Further investigations are required for tsunami water pressure, height and propagation.

[2] Disaster Prevention in Urban Areas

(1) Main transportation network
Transportation and utilities are the most critical lifelines in urban area against earthquake disaster. Researches are required for mitigating suspension of traffic and evacuation at road network. Countermeasures to utility systems are also important. Technologies of seismic strengthening for overcrossings and high road embankments in urban areas are critically important. Technologies for strengthening cut and filled slopes, river and coastal dykes and road slopes are expected.

(2) Earthquake disaster prevention for urban areas
Urban disaster prevention technologies are very important. Those will include failure of soils and ground, propagation of fire and inundation due to damage of river dykes. Hazard map for potential risk and vulnerability is required.

(3) Warning, evacuation and disaster information systems
Appropriate warning and evacuation systems using advanced technologies are required. Disaster information systems which enables to notice the danger prior to the failure is required. Because number of aged residence and foreigners who do not understand primary language is increasing, an appropriate measure for such new change is required.

(4) Social and economic effects of disasters
Social and economic impact of disasters require

more attention. Indirect economic damage sometimes far exceeds the physical property damage in urban areas. Spreading mechanism of the physical damage and interaction of indirect effects between lifeline facilities are expected to be investigated.

[3] Cooperation to Developing Countries

(1) Research on the Process from R/D to code standardization in U.S. and Japan
Experiences in U.S. and Japan on how research and development were managed and codes and standards were developed are valuable for developing countries. Realistic case study should be made to show consistent management from technical developments to standardization.

(2) Appropriate disaster countermeasures for developing countries
Cooperation of technical development which matches with the natural, economical and social conditions of developing countries is required. It is critically important that the cooperation should be made for those technologies which are consistent with the technology level and restrictions in developing countries. Developing appropriate construction technologies using the materials available in developing countries is the core of the technical cooperation.

(3) Code enforcement and construction management
In developing countries, critically important facilities such as hospitals, school buildings and highway bridges often suffer destructive damage due to an earthquake. Because it is always point out that inadequate code enforcing systems and construction management systems caused such damages, technical cooperation for those issues may be significantly important.

6. CONCLUDING REMARKS

The past Panel activities have greatly contributed in both countries to develop and improve design methods and countermeasures against extreme wind, earthquake, storm surge and tsunami effects, and further continuation of the exchange of research information and research personnel is essentially important for both countries.

Since cooperative research programs facilitated excellent results, cooperative research programs should be promoted actively in the future as well. To facilitate this goal, the Panel will continue to encourage them and provide sponsorship.

The International Decade for Natural Disaster Reduction (IDNDR) is closely related to the Panel's activities. Attention should be paid to the IDNDR program so that the Panel could contribute to it. Because there are many developing countries which suffer from natural disasters, efforts are required for conducting the research in order to provide technical information relevant to criteria for design of structures and disaster mitigation programs.

ACKNOWLEDGEMENTS

The Panel on Wind and Seismic Effects has been highly evaluated at the UJNR Plenary Meetings as one of the most active Panels among the 17 UJNR panels because of the active contribution to valuable information exchange and cooperative research programs. The accomplishments depend upon enthusiasm and leaderships of the successive chairmen of the U.S. and Japan Panels as well as the efforts made by all Panel members and supporting staffs. Variable supports from various organizations including the Science and Technical Agency of Japan and personnel who supported for the Panel activities are greatly appreciated.

REFERENCES

1) Narita, N. (Editor) : Two Decades of Accomplishments and Challenges for the Future, Panel on Wind and Seismic Effects, UJNR, Technical Note of Public Works Research Institute, No. 50, May 1988
2) PWRI and NIST : A List of Publications 1969-1991, Panel on Wind and Seismic Effects, UJNR, Technical Memorandum of PWRI, No. 3095 and NIST Special Publication 835, March 1992
3) Sumiyoshi, Y., Suzuki, K. and Hirabayashi, K. : Progress of Civil Engineering and Its Contribution to Economic and Social Development in Modern Japan, - PWRI's 70 Years and Perspective -, Technical Memorandum of the Public Works Research Institute, Vol. 3188, 1993

Table 1 Member Organizations of the Panel in Japan Side

Ministry	Member Organization
Ministry of Construction	Public Works Research Institute
	Building Research Institute
	Geographical Survey Institute
Japan Meteorological Agency	Meteorological Research Institute
Ministry of Transport	Port and Harbour Research Institute
Hokkaido Development Agency	Civil Engineering Research Institute Hokkaido Development Bureau
Science and Technology Agency	National Research Institute for Earth Science and Disaster Prevention

Table 2 Member Organizations of the Panel in U.S. Side

Department	Member Organization
U.S. Department of Agriculture	Forest Products Laboratory
U.S. Department of Commerce	National Institute of Standards and Technology
	National Oceanic and Atmospheric Administration
U.S. Department of Energy	Office of Safety Health and Quality Assurance
U.S. Department of Housing and Urban Development	Manufactured Housing and Construction Standards Division
U.S. Department of the Interior	Bureau of Reclamation
	Geological Survey
	Minerals Management Service
U.S. Department of State	Office of Foreign Building Operations
	Office of Foreign Disaster Assistance
U.S. Department of Transportation	Federal Highway Administration
U.S. Department of Veterans Affairs	Structural Engineering Service
U.S. Department of the Air Force	Air Force Civil Engineering Support Agency
U.S. Department of the Army	U.S. Army Corps of Engineers
U.S. Department of the Navy	Naval Civil Engineering Laboratory
Nuclear Regulatory Commission Commission	Office of Nuclear Regulatory Research Branch
Federal Emergency Management Agency	Policy Manager for Seismology
National Science Foundation	Directorate of Engineering
California Department of Transportation	Structures Division
State University of New York	National Center for Earthquake Engineering Research

Table 3 Task Committees of the Panel on Wind and Seismic Effects

Task Committee	
A	Strong-Motion Instrumentation Arrays and Data
B	Large-Scale Testing Programs
C	Repair and Retrofit of Existing Structures
D	Evaluation of Structural Performance
E	Ground Motion and Seismic Design Forces Programs
F	Disaster Prevention Methods for Lifeline Systems
G	Passive, Active, and Hybrid Control Systems
H	Soil Behavior and Stability during Earthquakes
I	Storm Surge and Tsunamis
J	Wind and Earthquake Engineering for Transportation Systems
K	Wind and Earthquake Engineering for Offshore and Coastal Facilities

Table 4 Joint Panel Meeting

No.	Place	Date	Number of Participants		Number of Papers Presented	
			U.S. Side	Japan Side	U.S. Side	Japan Side
1	Tokyo	April 23 - 26 1969	10	14	10	8
2	Washington	May 13 - 15 1970	10	6	6	12
3	Tokyo	May 10 - 12 1971	8	14	10	12
4	Washington	May 13 - 15 1972	16	9	7	12
5	Tokyo	May 14 - 16 1973	8	17	10	16
6	Washington	May 15 - 17 1974	20	7	17	12
7	Tokyo	May 20 - 23 1975	9	19	13	19
8	Washington	May 18 - 21 1976	30	9	22	18
9	Tokyo	May 23 - 27 1977	8	23	9	22
10	Washington	May 23 - 26 1978	23	8	22	16
11	Tsukuba	Sep. 4 - 7 1979	14	25	18	24
12	Washington	May 19 - 22 1980	14	5	15	19
13	Tsukuba	May 19 - 22 1981	15	26	20	27
14	Washington	May 17 - 20 1982	18	6	17	22
15	Tsukuba	May 17 - 20 1983	12	27	16	28
16	Gaithersburg	May 15 - 18 1984	28	7	19	25
17	Tsukuba	May 21 - 24 1985	12	27	19	28
18	Gaithersburg	May 12 - 15 1986	22	9	18	20
19	Tsukuba	May 12 - 15 1987	13	28	15	19
20	Gaithersburg	May 17 - 20 1988	37	9	15	20
21	Tsukuba	May 16 - 19 1989	11	30	18	15
22	Gaithersburg	May 15 - 18 1990	37	12	20	18
23	Tsukuba	May 14 - 17 1991	18	28	25	22
24	Gaithersburg	May 19 - 22 1992	40	14	20	17

Table 5(1) Workshops held under the Auspices of the Panel on Wind and Seismic Effects

Task Committee	Date	Place	Workshop
A	1987 Aug	San Francisco	Workshop on Strong-Motion Instrumentation Arrays and Data
B	1978 May	San Francisco	2nd Committee for the Joint Research Program on Large-Scale Testing of Structures
	1978 Dec	Tokyo	3rd Committee for the Joint Research Program on Large-Scale Testing of Structures
	1979 Jul	San Francisco	4th Committee for the Joint Research Program on Large-Scale Testing of Structures,
	1984 Mar	Tsukuba	1st Workshop on U.S.-Japan Masonry Program
	1985 Aug	Tokyo	Joint Research Program on Large-Scale Testing of Masonry Structures, 1st Joint Technical Coordinating Committee
	1987 Oct	Hokkaido	3rd Meeting of the Joint Technical Coordinating Committee on Masonry Structures
	1988 Oct	San Diego	4th Meeting of the Joint Technical Coordinating Committee on Masonry Structures
	1989 Oct	Tsukuba	5th Meeting of the Joint Technical Coordinating Committee on Masonry Structures
	1989 Oct	Tsukuba	Preparatory Meeting of the Joint Technical Coordinating Committee on Precast Reinforced Concrete Seismic Systems
	1990 Nov	San Diego	1st Meeting of the Joint Technical Coordinating Committee on Precast Reinforced Concrete Seismic Systems
	1991 Nov	Tsukuba	2nd Meeting of the Joint Technical Coordinating Committee on Precast Reinforced Concrete Seismic Systems
	1992 Nov	San Diego	3rd Meeting of the Joint Technical Coordinating Committee on Precast Reinforced Concrete Seismic Systems

Table 5(2) Workshops held under the Auspices of the Panel on Wind and Seismic Effects

Task Committee	Date	Place	Workshop
C	1980 May	Los Angeles	1st Seminar on Repair and Retrofit of Structures
	1981 May	Tsukuba	2nd Seminar on Repair and Retrofit of Structures
	1982 May	San Francisco	3rd Seminar on Repair and Retrofit of Structures for Earthquake Resistance
	1985 May	Tokyo	3rd Workshop on Evaluation of Performance of Existing Buildings
	1987 May	Tsukuba	Workshop on Repair and Retrofit of Existing Structures
	1990 May	Gaithersburg	Workshop on Repair/Retrofit and Evaluation of Performance of Structures
	1993 May	Tsukuba	Workshop on Smart and High-Performance Materials / Systems, jointly with Task Committee D and G
D	1983 May	Tsukuba	1st U.S.- Japan Joint Workshop on Evaluation of Performance of Existing Buildings
	1984 Jul	San Francisco	2nd Workshop on Evaluation of Performance of Existing Buildings
	1987 July	Tokyo	Meeting of the Joint Technical Coordinating Committee on Steel Reinforced Structure
E	1991 May	Tsukuba	Workshop on Risk, Hazard and Seismic Design Force
F	1984 May	Washington	1st Workshop on Lifeline Systems
	1984 Dec	Tsukuba	2nd Joint Workshop on Seismic Behavior on Buried Pipelines and Telecommunication Systems
	1986 Aug	Charlston South Carolina	Planning Conference on Disaster Prevention for Lifeline Systems held in conjunction with 3rd US National Conference on Earthquake Engineering
	1989 May	Tsukuba	3rd Joint Workshop on Earthquake Disaster Prevention for Lifeline Systems
	1991 Aug	Los Angeles	4th Joint Workshop on Earthquake Disaster Prevention for Lifeline Systems
	1992 Oct	Tsukuba	5th Joint Workshop on Earthquake Disaster Prevention for Lifeline Systems

Table 5(3) Workshops held under the Auspices of the Panel on Wind and Seismic Effects

Task Committee	Date	Place	Workshop
G	1991 Sep	Buffalo	1st Workshop on Earthquake Protective Systems for Bridges
	1992 Dec	Tsukuba	2nd Workshop on Earthquake Protective Systems for Bridges
H	1985 Aug	San Francisco	Joint Workshop on In-Situ Test Methods for Evaluation of Soil Liquefaction Susceptibility
	1988 May	Jackson Hall	Joint Workshop on Countermeasures for Soil Liquefaction
	1991 Jan	Tsukuba	International Workshop on Remedial Treatment of Liquefiable Soils
I	1983 May	Tsukuba	1st Joint Workshop on Storm Surge and Tsunami
	1983 Nov	Honolulu	2nd Joint Workshop on Storm Surge and Tsunami
J	1984 Feb	Tsukuba	1st Workshop on Bridge Structures
	1985 Aug	San Francisco	2nd Joint Workshop on Bridge Structures
	1987 May	Tsukuba	3rd Workshop on Performance and Strengthening of Bridge Structures
	1988 May	San Diego	4th Workshop on Bridge Engineering
	1989 May	Tsukuba	5th Workshop on Bridge Engineering
	1990 May	Lake Tahoe	6th Workshop on Bridge Engineering
	1990 Dec	Tsukuba	1st Workshop on Seismic Retrofit of Bridges
	1991 May	Tsukuba	7th Workshop on Bridge Engineering
	1992 May	Chicago	8th Workshop on Bridge Engineering
	1993 May	Tsukuba	9th Workshop on Bridge Engineering
K	1993 May	Yokosuka	Joint Meeting on Wind and Earthquake Engineering for Offshore and Coastal Facilities

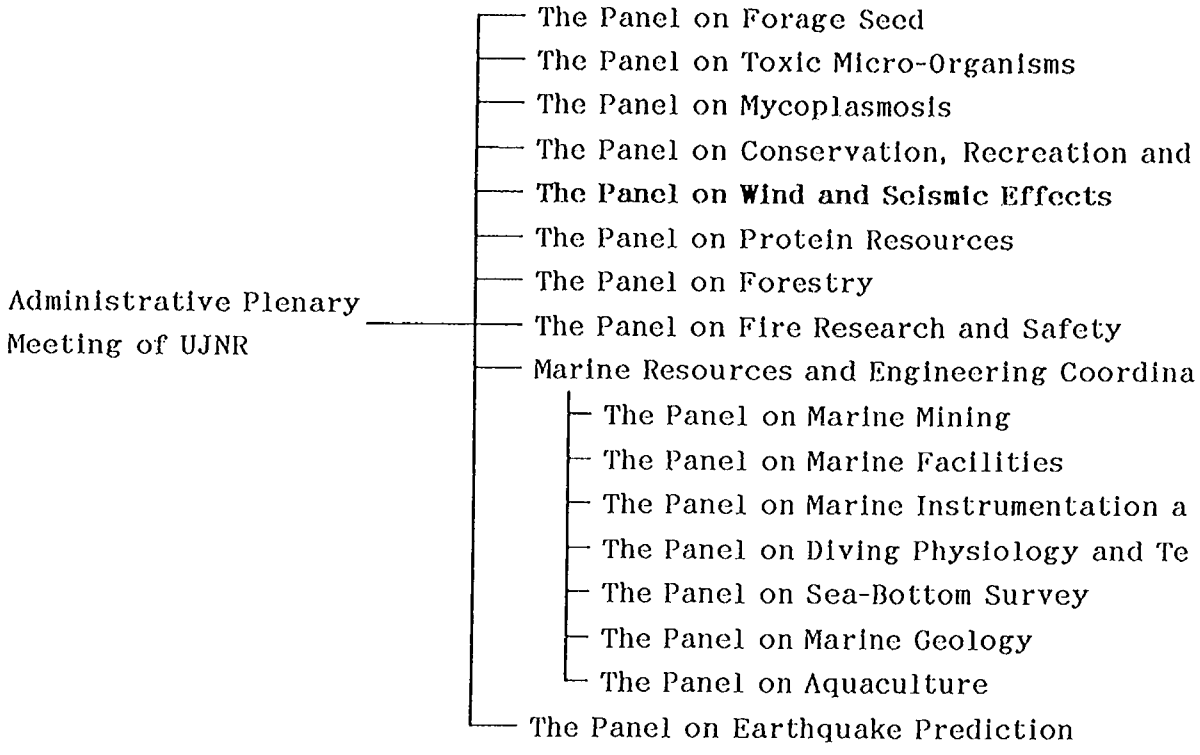


Fig. 1 Organization of the UJNR Panel



Photo 1 Planting of Newton Apple Tree at PWRI



Photo 2 25th Joint Meeting held in May 1993
at International Conference Room, PWRI



Photo 3 9th Bridge Workshop held in May 1993 at PWRI

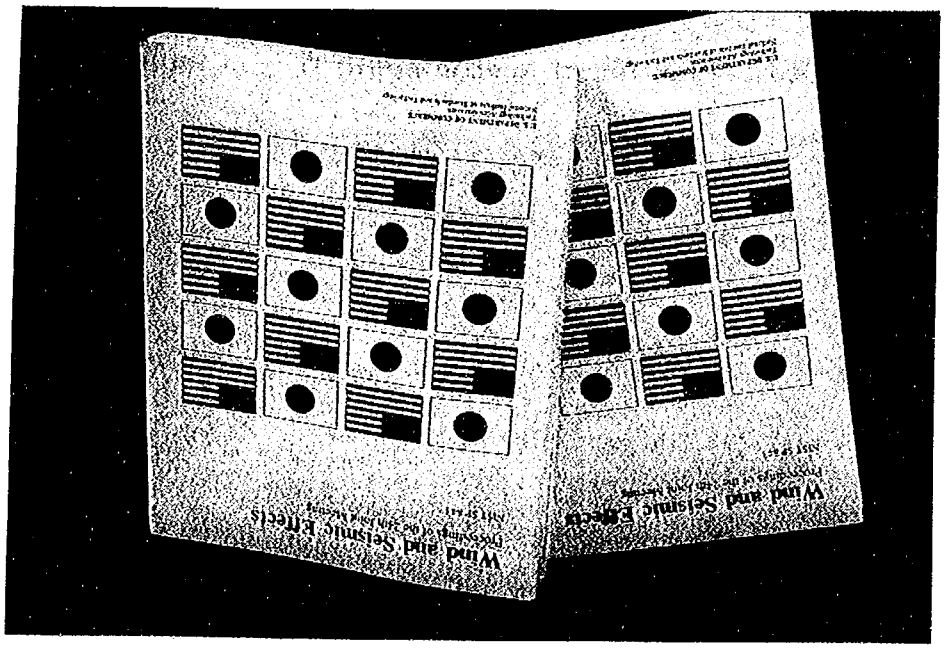


Photo 4 Proc. of the 24th Joint Meeting Published by NIST

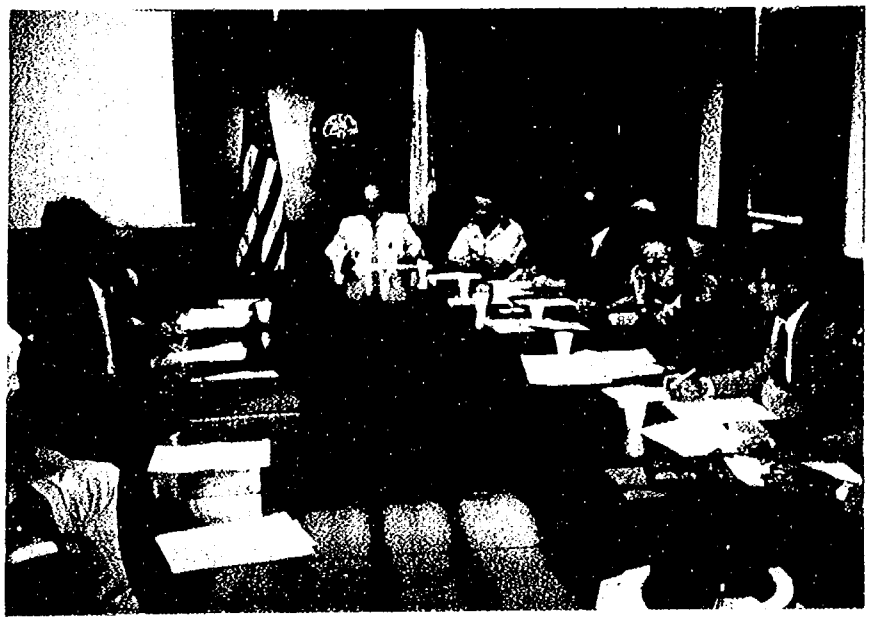


Photo 5 Seminar held at Charleston, South Carolina during the Technical Study Tour after the 22nd Joint Meeting in 1990



Photo 6 IDNDR Gifu International Symposium held during the Technical Study Tour after the 23rd Joint Meeting in 1991

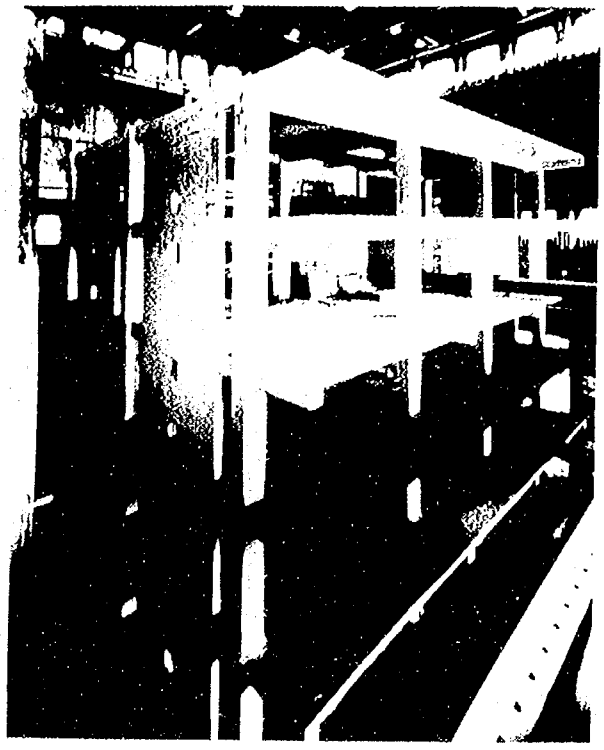


Photo 7 A Seven-story Reinforced Concrete Building Tested at BRI

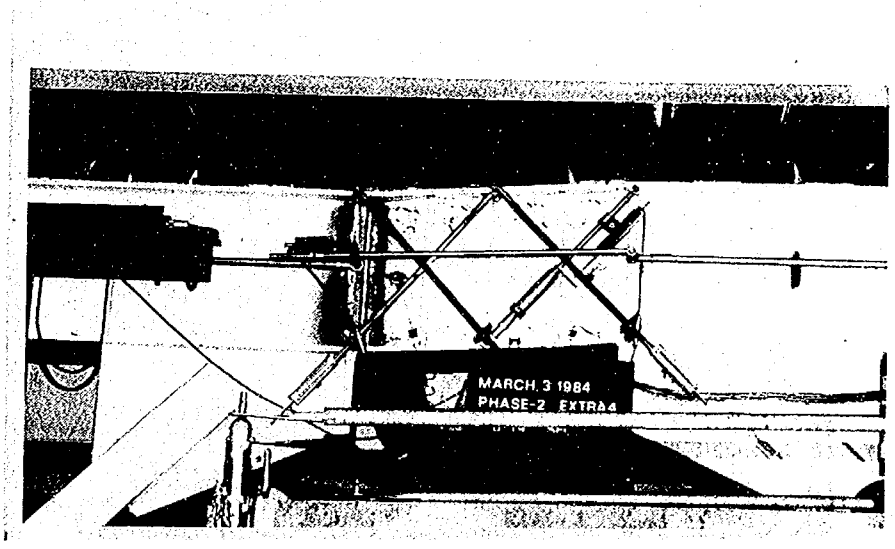


Photo 8 A Six-story Steel Frame Building Tested at BRI

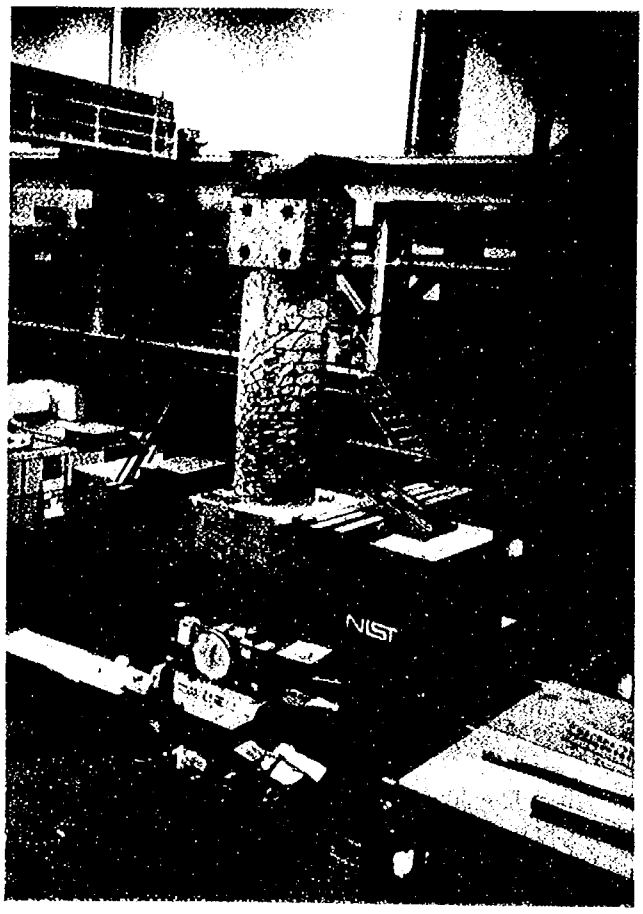


Photo 9 Large Scale Test for Reinforced Concrete Bridge Column at NIST

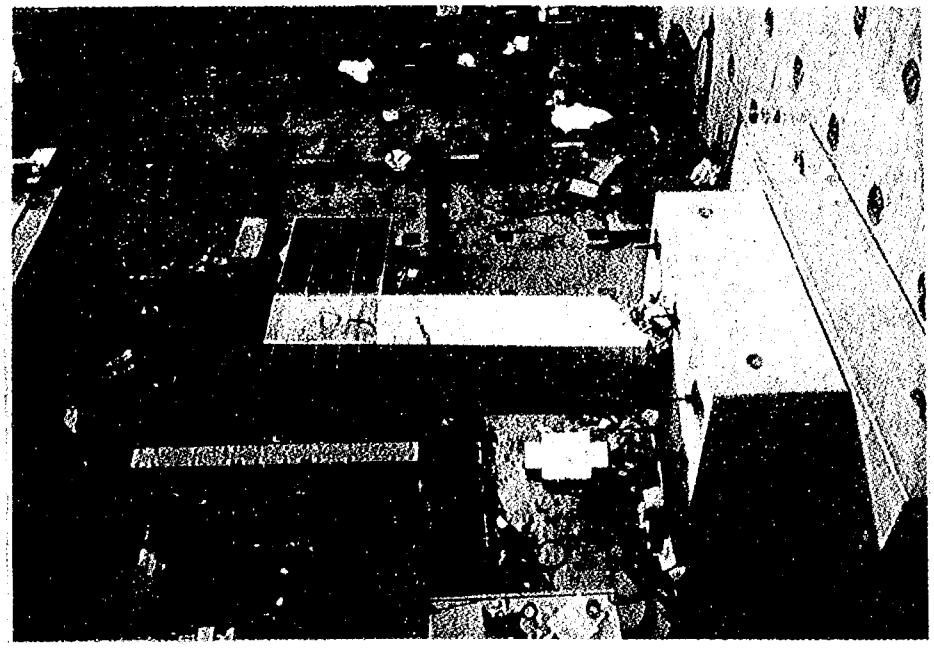


Photo 10 High Loading Rate Test for Reinforced Concrete Bridge Columns at PWRI

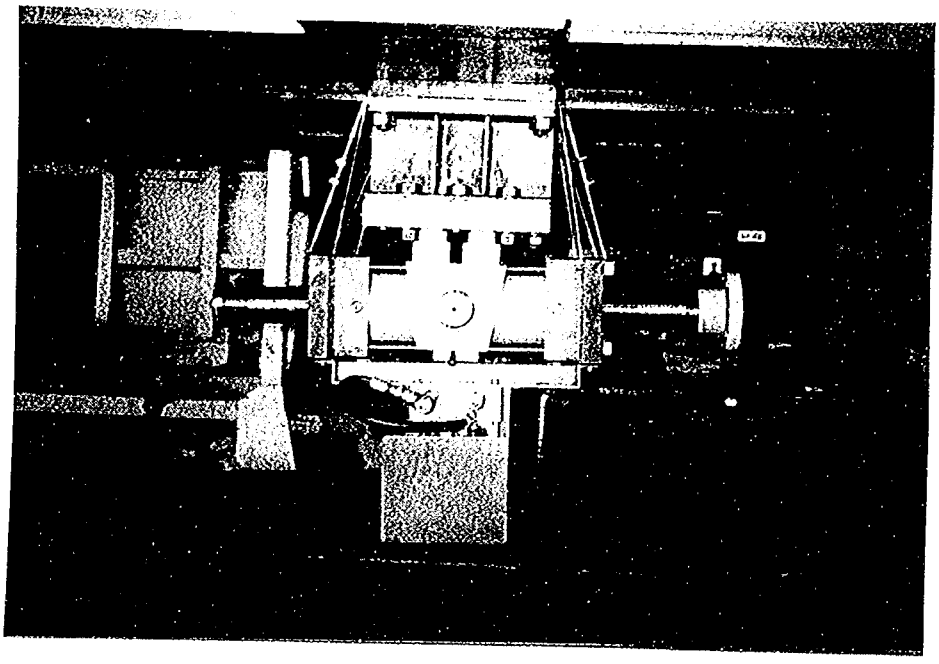


Photo 11 Shaking Table Test for Variable Damper at PWRI

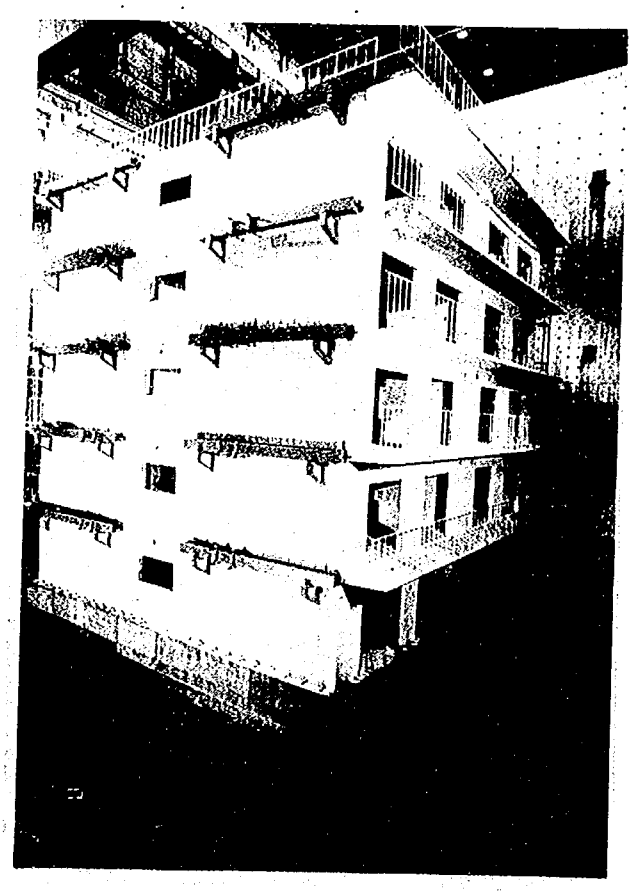


Photo 12 Full Scale Test of Masonry Structure

Lessons from the Loma Prieta Earthquake

by

Richard N. Wright*

ABSTRACT

The Loma Prieta, California earthquake (LPE) of October 17, 1989, has had profound influence on both policies and practices for earthquake hazards reduction in the United States. Special Federal funds were allocated for studies to learn from the earthquake how to improve policies and practices for earthquake hazards reduction. The President issued an Executive Order requiring Federal agencies to apply appropriate seismic design and construction practices for new Federal buildings and new Federally-assisted or regulated buildings. The Order also provided impetus for improvement of the State and local government building codes that govern non-Federal construction. Major changes were made in the legislation governing the National Earthquake Hazards Reduction Program (NEHRP); research, development and technology transfer activities in NEHRP responded to the legislation. Thus, this paper describes lessons in public policy as well as those in earth, engineering and social sciences and practices resulting from the earthquake.

KEYWORDS: buildings; earthquake; earthquake engineering; earthquake hazard reduction; geotechnical engineering; lifelines; public policy; seismology; structural engineering

1. INTRODUCTION

1.1 Damages of the Earthquake

At 5:04 p.m., Pacific Daylight Time, on October 17, 1989, an earthquake with a surface-wave magnitude of 7.1 occurred with its epicenter located about 15 km northeast of Santa Cruz and 95 km south-southeast of San Francisco, California. According to the U.S. Geological Survey, the earthquake ruptured a segment of the San Andreas fault below the Santa Cruz Mountains. The hypocenter was about 18 km beneath the Earth's surface, and the rupture propagated about 40 km both northwest and southeast within a 10-second period. The earthquake was felt over an area of 1,000,000 sq km, from Los Angeles to the south, Oregon to the north, and western Nevada to the east (Figure 1). This earthquake, named the Loma Prieta earthquake, was the largest on the San Andreas fault since the great San Francisco earthquake of 1906 (M = 8.3) when a 440 km stretch of the fault ruptured.

Strong shaking lasted only about 10 to 15 seconds. Even so the destructive effects of the Loma Prieta earthquake were extensive. Wood-frame dwellings and unreinforced masonry buildings in communities near the epicenter (Figure 2) and in isolated locations in San Francisco and Oakland (Figure 3) sustained substantial damage. In Santa Cruz, Watsonville, and Los Gatos, there was extensive damage to old buildings in the downtown areas where small business are located. Elevated highway structures sustained severe damage in the Bay area, including the collapse of a section of Interstate 880 in Oakland which claimed 42 lives (Figure 4). The collapse of a 15 m link span of the San Francisco-Oakland Bay Bridge (Figure 5) caused the bridge to remain closed for about a month. The Bay Area Rapid Transit System was in service immediately after the earthquake. However, damage to arterial

*National Institute of Standards and Technology, Gaithersburg, MD 20899

As of December 28, 1989, the following statistics had been compiled by the California Governor's Office of Emergency Services:

- 62 confirmed deaths; 3,757 injuries.
- Over $6 billion property damage.
- Over 12,000 people displaced from their homes immediately following the earthquake.

1.2 Sources of Data

This paper has drawn from many studies related to the LPE and the public policy activities it stimulated. Limited references are provided for readers who seek greater detail, but this is not an effort to review the literature. Early investigations of the LPE [1,2,3] provided much background on the subject. The NRC/EERI publication from the symposium "Practical Lessons from the Loma Prieta Earthquake" [4] provides many, recent references to the literature from the various concerned disciplines. In addition, under leadership of the United States Geological Survey, a definitive collection of papers on the LPE is in preparation as the Loma Prieta Earthquake Professional Paper Series.

1.3 Organization of Paper

The main sections of the paper deal with:

Policy Issues in Earthquake Hazard Reduction

Earthquake Mechanisms and Effects

Building Performance

Lifeline Performance

Post Earthquake Scientific and Engineering Activities

Summary and Conclusions highways and the bridge caused severe impacts on commuters and regional commerce.

2. POLICY ISSUES IN EARTHQUAKE HAZARD REDUCTION

2.1 Public Awareness and Public Policy

Executive Order 12699, "Seismic Safety of Federal and Federally Assisted or Regulated New Building Construction," was issued by the President on January 5, 1990 [5]. It requires that buildings constructed or lease-constructed for Federal use be designed and constructed with adequate seismic provisions. Provisions equivalent to the " NEHRP Recommended Provisions for the Development of Seismic Regulations for New Buildings" [6] have been determined to be appropriate for the Order's implementation. Federally assisted and regulated new building construction, such as new buildings sold with Federal mortgage insurance, also must comply with the Order.

In part because of the desire of State and local governments to be eligible for Federal assistance, the model building codes, which are the basis for most State and local building codes, have adopted seismic provisions equivalent to the NEHRP Recommended Provisions [5]. As State and local building codes adopt and enforce the current versions of the model codes, most new building construction in the U.S. should conform with up-to-date seismic provisions within the next few years.

However, strong advocacy efforts are needed to achieve policy decisions by governments, industry and individuals for earthquake hazard reduction. Needs remain for developing and implementing standards for existing buildings and new and existing lifelines, and for planning and implementing needed disaster mitigation, preparedness and response programs [7,8]. Information making the needs and benefits clear to policy makers and to the general public must be developed as part of NEHRP

to support the advocates.

As a result of the LPE and subsequent severe losses in Hurricane Andrew [9], the U.S. insurance industry has become convinced that Federal reinsurance is necessary if insurance companies are to survive a major earthquake or hurricane, and that strong mitigation requirements are a legitimate part of such an insurance program. The national organization of State emergency management officials endorses this position. These influential interests are likely stimulate major strengthening of Federal disaster mitigation programs, including NEHRP.

2.2 Improvement of NEHRP

The NEHRP Advisory Committee (AC) was called for in the reauthorization legislation for NEHRP [10] following the LPE. The AC has recommended major strengthening of NEHRP [8]:

> Improvements in management for prioritization in the planning and conduct of NEHRP.
>
> Stronger incentives for implementation of hazard reduction practices.
>
> Strengthened problem-focused engineering research to provide timely technical bases for improvements of practices.
>
> Improved methods for vulnerability assessment, and conduct of vulnerability assessments so that the benefits of earthquake hazard mitigation can be made evident to policy makers.

2.3 Vulnerability Assessments and Reductions

Epidemiology of injuries in earthquakes is an important element of improved technology to predict vulnerability. Injuries and deaths must be related rationally to the physical performance of constructed facilities. This knowledge also will guide improvement of new and existing structures to reduce casualties from earthquakes.

Indirect economic costs of earthquake damages are ill defined [11]. Can a physically catastrophic earthquake cause nationally catastrophic economic consequences (as the insurance industry believes)? Whether nationally catastrophic or not, these consequences must be predictable to define cost effective mitigation measures, such as standards for lifelines.

Physical vulnerabilities are better defined, at least for construction practices in California, but physical damage prediction capabilities need to be improved as part of the development of systematic techniques for vulnerability assessment.

Hazards of fire following earthquakes are dependent on physical damages, environmental conditions such as drought and wind, and the emergency preparedness of the community at risk. Damages from the LPE caused fires in San Francisco and disabled the water systems intended for fire fighting (Figure 6). San Francisco was extraordinary in having a backup water system for fighting post-earthquake fires, but this system also failed. Fortunately, there was an unusual lack of wind and fires did not spread rapidly, the site of the fires was close to the Bay, and a fireboat was available in about one and one-half hours to provide fire fighting water. Improved fire hazard predictive capability is an important aspect of vulnerability assessment and improved post-earthquake fire fighting capability is essential to earthquake hazard reduction.

2.4 Development of Design, Assessment and Retrofit Practices

The LPE has given impetus to development of practices for assessment and strengthening of existing buildings, and for the design,

construction, assessment and strengthening of lifeline systems. With enhanced funding from post LPE appropriations, the Federal Emergency Management Agency (FEMA) has supported preparation of guidelines for assessment and strengthening of existing buildings [12,13]. Work is underway to prepare national consensus standards based on these guidelines and the results of ongoing research.

With FEMA funding, and technical support from the National Institute of Standards and Technology (NIST), the Interagency Committee on Seismic Safety in Construction is working with the private sector to prepare a standard for the assessment and enhancement of the seismic resistance of existing Federal buildings [14]. The reauthorizing legislation of NEHRP calls for the standard to be issued by the President in December 1994.

The reauthorization of NEHRP also called for planning to develop and implement seismic design and construction standards for lifelines. With FEMA and NIST funding and collaboration from the private sector [15], a plan is being prepared for development and application of seismic guidelines and standards for lifelines. The plan is expected to emphasize hazard mitigation for existing lifelines, to use existing standards organizations to implement the recommended provisions to be developed, and to test proposed provisions in demonstration projects.

Practitioners and researchers involved in studies for the improvement of practices, or in their use, have made a number of recommendations for fundamental improvements in practices [4]. These include:

- Define acceptable risk as a basis for acceptable resistance in an existing structure, and the levels of resistance for which strengthened or new structures are to be designed.

- Account for the duration of strong shaking in considering the earthquake loading on a structure. This may require developing simulations of earthquake time history for use in design or review of resistance.

- Formulate design standards for functionality and reduction of property loss.

- Formulate standards in ways that improve users' understanding of behavior of the structure in earthquakes.

- Provide for safety from falling debris of persons or other structures outside of the damaged structure.

A recently reported integrated seismic design procedure [32] accounts for the first four of these requirements (Figure 7).

2.5 Implementation of Design, Assessment and Retrofit Practices

Experience has shown [4] that seismic design, assessment or retrofit for major structures requires review capabilities beyond the skills and financial resources of most building code enforcement agencies. Seismic safety standards and codes should call for peer review (engagement of a second source of earthquake engineering expertise) of design, assessment or retrofit of major or complex structures.

Assessment and strengthening of seismically inadequate existing buildings or lifelines is more expensive than design of seismically safe new buildings or lifelines. Therefore organizations responsible for many buildings or a lifeline system need risk based procedures to establish priorities for assessment and retrofit. The experiences of the California Department of Transportation before and after the LPE show the need for and value of risk based

priorities. Restrainers to prevent bridges from sliding off their piers or abutments were installed following the 1971 San Fernando earthquake and prevented hundreds of bridge failures in the LPE.

2.6 Emergency Response

Emergency response procedures were planned and exercised prior to the LPE by San Francisco Bay area local governments, the State of California and Federal government agencies. The plans and training were very valuable in the LPE. Building on this experience, the State of California has continued planning and training, developed rapid damage assessment techniques, and prepared a standardized emergency management system based on the management system of fire services.

News media can be a valuable resource or a great problem in a disaster. A constructive media policy should be developed. Planning should include working with the media for effective public information in the emergency period.

The general public needs to be educated to take appropriate actions before and during the emergency period. For instance, what actions can be taken in advance to reduce earthquake vulnerability of a home, and what actions should occupants of a building take when an earthquake occurs?

Volunteers can provide valuable assistance to emergency managers. Where the earthquake hazard is high, volunteers can be identified and trained in advance. In addition, whether the hazard is high or ordinary, emergency management organizations should plan to train and employ effectively volunteer services during the emergency.

2.7 Emergency Shelter

Emergency shelters are needed for persons displaced from their homes, but have been rejected by persons concerned about potential failure of the shelter during aftershocks. Careful assessment of the safety of shelters and education of occupants can alleviate this problem.

Emergency shelters should be planned to deal with persons homeless before the earthquake and persons unable to find alternative housing when their low cost residences are made unsafe by an earthquake. These circumstances lead to substantial, long term demands for shelter.

2.8 Urban Search and Rescue

Experiences in the 1985 Mexico City and 1988 Armenia earthquakes showed the needs to prepare for extraordinary efforts to rescue people from collapsed structures. For LPE, there was need for search and rescue only for the Interstate 880 structure in Oakland, CA. With support from FEMA, the U.S. has identified 25 task forces to serve as the nucleus of the National Urban Search and Rescue program. Two of the task forces were deployed to Hawaii in 1992 following Hurricane Iniki [16].

2.9 Dangerous Buildings Procedures

Just prior to the LPE, a recommended practice had been developed on Postearthquake Safety Evaluation of Buildings [17] and training had been provided on its use. This work was sponsored by the State of California and the Federal Emergency Management Agency. The technique was found very useful in assessing buildings damaged by the LPE, and the experience is leading to improvements in the practice. Following a rapid evaluation, buildings were labeled: inspected (apparently safe), limited entry (questionable), or unsafe.

Problems arose with buildings labeled limited entry. Businesses needed entry to obtain

information to continue their business; residents needed entry to obtain personal belongings. Property was lost by vandalism of illegal entrants while legitimate access to the damaged building was denied by authorities. The name of the intermediate status is being changed to restricted entry; owners will be allowed brief reentry to gather belongings subject to guidance of a consulting engineer and a waiver of responsibility for hazards of reentry.

Experience was gained in dealing with unsafe buildings. San Francisco's building regulatory department followed "due process" in determining whether to demolish an unsafe building. An owner was advised to hire a consulting engineer and obtain legal advice on whether to brace or remove a hazardous building. Disputes have arisen between Federal, State and local governments as to whether the Federal government should pay for repairs to damaged public buildings beyond restoration of conditions prior to the earthquake. Of course, such strengthening would mitigate future losses. Oakland, California, has established an ordinance requiring strengthening when repairs exceed 50% of the value of the building. Further work is needed to develop recommended practices responsive to the special needs of historic buildings for assessment and strengthening.

2.10 Recovery

The LPE showed the benefits of planning in advance of the earthquake for postearthquake recovery. This is being done in California, but may be difficult where damaging earthquakes are less frequent. Perhaps, a model plan can be developed. Early attention is needed to criteria for reconstruction. The general sense is that mitigation of losses from future earthquakes should be part of the rebuilding process - rebuilding to adequate levels of seismic resistance. As a practical note, local officials noted that records of recovery expenditures should be kept in the format required by FEMA for reimbursement.

3. EARTHQUAKE MECHANISMS AND EFFECTS

3.1 Mechanisms

The LPE occurred on an identified seismic gap - a region of the San Andreas Fault that had not slipped since 1906. The fault broke from a epicenter near the center of the zone that slipped and breakage spread both north and south. As a result, the duration of strong shaking was less than usual for magnitude 7.1: 10 - 15 seconds rather than twice that duration. Longer duration for the same amplitude would have produced more severe damages, particularly for structures of longer periods.

3.2 Attenuation and focusing of ground motions.

Ground motions were more intense at distances to the northwest of the epicentral area - precisely, the San Francisco Bay area. Studies [18] have explained this focusing in terms of reflections of seismic waves. Topographic effects were evident in motions of bedrock outcrops [19].

3.3 Effects of overburden on ground shaking.

Most of the damages in the San Francisco Bay area occurred on soft soil sites where ground motions were greatly amplified. Many damages in the epicentral area also occurred on sites underlain by soft soils. The amplifications of ground motions are well predicted by one-dimensional models except where bedrock configuration in non-planar [18,19]. Notably, amplification of ground motion occurs even for short period structures (Figure 8) and should be reflected in design criteria.

3.4 Stability of soils and embankments.

Liquefaction was associated with many pipeline failures [20]. It is a major threat to water systems; water losses, in turn, create severe fire hazards (Figure 9). Techniques for prediction of liquefaction were confirmed by liquefactions observed in LPE [4]. However, the amount of lateral spreading caused by liquefaction is an important parameter for design or assessment of pipelines. As yet there are no reliable methods for predicting the amount of lateral spreading [21].

4. BUILDING PERFORMANCE

4.1 Response of buildings.

In general, buildings responded as expected to the ground motions of the LPE [22]. Pounding damages were extensive for closely-spaced buildings. Remarkably, damages to non-structural systems, such as lighting and storage cabinets, did not cause casualties, but this may have been due to the timing of the earthquake [23] when few people were at work or in school. Because of conservative design, base isolation systems did not substantially reduce the shaking of the isolated structures in recent earthquakes [24].

4.2 Assessment and strengthening of buildings.

A study was made of buildings retrofitted prior to the LPE to determine whether they performed better than unretrofitted buildings. Results showed that completely retrofitted unreinforced masonry buildings performed substantially better than partially or unretrofitted buildings [25]. Post earthquake analyses of a number of buildings showed that many buildings have greater resistance than accounted for by current practices for analysis and assessment [4].

5. LIFELINES PERFORMANCE

5.1 Response of lifelines.

Lifeline failures in the LPE produced both severe losses of life in the collapse of the I-880 elevated highway structure in Oakland and major interruptions of economic activity, for example, as a result of the failure of the Oakland Bay Bridge.

Lack of redundancy and lack of ductility caused many of the failures of transportation structures [26]. Batter piles attracted high forces and often failed near similar foundations supported only on vertical piles which were undamaged.

Buried pipes performed generally well in stable soils, but suffered much damage from liquefaction. Ductile steel gas pipes performed well even when deformed in failures of surrounding soils.

Interactions of lifeline systems are important to performance. Telecommunication, water and other lifelines carried on bridges were cut by bridge failures. The loss of electrical power in San Francisco prevented closing valves to prevent drainage of water storage when liquefaction produced water pipe breaks. Therefore, fire fighting capability was lost, too. Water sloshing produced damages in tanks for water and waste water treatment. Incidentally, computer simulations of water distribution lifelines responses to damages agreed well with observed behavior.

High voltage (500 KVA) electrical substations suffered extensive damages, while lower voltage equipment performed well. In general, seismically-anchored equipment behaved well [23].

5.2 Assessment and Strengthening of Lifelines

Planning for the development and adoption of seismic guidelines and standards for lifelines, stimulated by the LPE, led to clear guidance from the lifelines community [15] and the NEHRP Advisory Committee [8] to give priority to assessment and strengthening of

existing lifelines. Because of interactions of lifelines and the needs for their services in the emergency period and during recovery, good performance of existing lifelines is essential to success. Use of controls for limiting damages to existing lifelines and protection of control centers are seen as an important means to reducing their vulnerability.

Retrofits of existing lifelines were shown to be successful. For instance, the installations of restrainers for bridges (ties to keep decks from sliding off abutments) saved hundreds of bridges from serious damages in the LPE. Research stimulated by the LPE has led to important techniques for strengthening bridges [27] and new analytical techniques for predicting behavior of damaged bridges [28]. Additional studies are needed to reduce the costs of retrofits.

Assessment of strength and planning of retrofits are challenging assignments requiring high professional expertise. Guidelines and standards are not sufficient guidance; expert peer review is needed, too. The California Department of Transportation's post LPE studies for retrofit of damaged bridges have provided valuable insights into both technical practices and procedures for assessment and retrofit [4].

6. POST EARTHQUAKE SCIENTIFIC AND ENGINEERING ACTIVITIES

Post earthquake investigations have growing importance for gaining knowledge needed to mitigate effects of future earthquakes [29]. Experiences from the LPE investigations show the importance of aerial reconnaissance capabilities for early identification of targets for investigation, value of video cameras for gaining detailed data, instrumentation of aftershocks to assess intensities on previously uninstrumented sites, and needs for collaboration between emergency management authorities and groups of investigators to gain timely access and avoid duplicative efforts.

The traditional Modified Mercalli Intensity scale is incapable of describing damages to the variety of modern buildings. It appears that two scales are needed: one for short period buildings (about 0.3 sec) and one for medium period buildings (about 1.0 sec).

Casualty and socio-economic post earthquake studies are needed particularly to provide the understanding of earthquake vulnerability needed to develop cost-effective measures for mitigation. These will include the epidemiology of injuries and deaths from earthquake effects, documentation of the inventory of structures and the direct damages suffered, assessment of direct and indirect losses from interruptions of services of buildings and lifelines, and analyses of the effectiveness of preparedness and emergency management activities.

7. SUMMARY AND CONCLUSIONS

The Loma Prieta earthquake of October 17, 1989, provided significant lessons for public policies and design and construction practices throughout the United States. While it was the largest earthquake to strike Northern California since the great San Francisco earthquake of 1906; earthquakes of similar or larger size are expected to affect 46 of the 50 states, Puerto Rico and the Virgin Islands [6]. Thus, lessons of structural performance and seismology, which can be learned from the Loma Prieta earthquake, can be used to reduce earthquake hazards throughout the United States and the rest of the world.

Performance of All Structures

1. The Loma Prieta earthquake caused substantial human losses of 62 lives and 3,757 injuries. But for fortunate circumstances, human losses would have been much greater. The unusual event of coincidence with a Bay Area World Series baseball game reduced traffic far below normal levels on the I 880 viaduct which

collapsed to cause most of the life losses. Although water supplies for fire fighting were lost over much of the Bay Area, unusually calm winds avoided uncontrolled spreading of fires. The areas affected by the earthquake are among the few best prepared in the United States. Clearly, earthquakes remain the United States' greatest single-event natural hazard threatening losses of life and injuries.

2. Direct property losses are estimated to exceed $ 6 billion, but these are modest compared to losses projected for earthquakes closer to major metropolitan areas, for instance $40 billion for a magnitude 7.5 earthquake on the Eastern Bay Area's Hayward Fault, [30] or $37 billion for a magnitude 7.6 earthquake in the New Madrid area of the Central U.S. [31]. Unless actions are taken to reduce earthquake hazards, nationwide, earthquake property losses may be sufficiently large to threaten U.S. financial stability [9].

3. Consequent economic losses were apparent in the major disruptions of transportation in the month that the San Francisco - Oakland Bay Bridge was out of service. Dislocations continue with segments of the Bay Area highway system still not functioning. The potential for consequent economic, national security and societal losses arising from earthquake damages add to the status of earthquakes as the Nation's greatest single-event natural hazard.

4. Most building and lifeline structures in the epicentral and Bay areas performed well. Californian efforts to develop, adopt and enforce up to date seismic design and construction practices for buildings and lifelines deserve great credit for this. However, much structural damage and most losses of lives and property occurred in the Bay Area far from the earthquake faulting. At such distances, for this sized earthquake, current seismic design and construction practices were considered to be capable of preventing structural damages. Thus, the seismology and structural performance in the Loma Prieta earthquake provide important opportunities for the assessment and improvement of national seismic design and construction practices.

5. Most structural damages in the Bay Area, 80 to 120 kilometers from the epicentral area, occurred to structures sited on deep deposits of overburden soils above the bedrock. Such sites are common in other areas of the Nation that also are subject to earthquake hazards. Also, the intensity of bedrock ground shaking was much higher in the Bay Area than in other directions from the epicentral area. Because many records of strong ground motions are available from the main shock and aftershock measurements, there are important opportunities to develop and verify seismological and engineering practices for prediction of the effects of geological and overburden soil conditions on the intensity of earthquake ground motions.

6. Structural damages and failures in both epicentral and Bay areas indicate amplification of ground motions on soft soil sites even for structures with natural periods less than that of their sites. Indepth studies of responses of damaged and undamaged structures can assess the needs, if any, for revisions of current seismic standards which allow reduced design forces for structures of low natural period sited on deep, soft soil deposits.

7. Ground failures, including landslides and liquefaction, were frequent in both epicentral and Bay areas. These attest to the potential of ground failures to produce earthquake losses of lives and

property and provide opportunities to assess the needs to improve existing criteria for the stability of soils in earthquakes.

Building Performance

1. Buildings designed and constructed in accord with modern seismic design and construction practices generally performed well in both epicentral and Bay areas. This shows the value of adopting and enforcing modern seismic design and construction practices in building codes and for Federal construction. However, examples of successful performance in areas of strong shaking and of failures in areas of moderate shaking provide opportunities to assess needs to improve modern seismic design and construction practices.

2. Widespread failures of older buildings, such as collapses of unreinforced masonry buildings, failures of cripple stud walls, and losses of chimneys and parapets, reemphasize the needs to assess the safety of existing buildings and to correct excessive hazards. It is sobering to note that many modern buildings also have these vulnerabilities in seismically hazardous areas of the U.S. which have not yet, or only recently have, adopted and enforced seismic design and construction provisions in their building codes.

3. Many older buildings in the epicentral and Bay areas had been retrofit to improve seismic resistance prior to the earthquake. Some performed well; some failed. Indepth studies of the performance of retrofit measures can reveal opportunities to affirm or to improve standards for assessment and strengthening of existing buildings that currently are being developed.

4. Many buildings in urban areas were damaged by pounding against adjacent buildings. Indepth studies of occurrences and non-occurrences of pounding can provide improvements, where needed, in standards for design of new buildings, and in standards for assessment and strengthening of existing buildings.

Lifeline Performance

1. The severe losses of lives in the collapse of the I-880 viaduct, which were fortuitously far less than the losses would have been under more normal circumstances, show the importance of successful performance of lifelines for life safety.

2. The disruptions of economic activities in the Bay area caused by failures of highway structures, and in the epicentral area caused by the landslides that closed State Highway 17, show the importance of successful performance of lifelines for the avoidance of property losses and consequent damages.

3. Water distribution system failures in the Bay Area show the vulnerability of U.S. cities in areas of seismic hazard to fires following earthquakes. Gas distribution system failures in the Bay and epicentral areas show a significant potential for ignition of fires following earthquakes. These failures were predominately in areas of unstable soils.

8. REFERENCES

1. Lew, H.S., editor, 1990, "Performance of Structures During the Loma Prieta Earthquake of October 17, 1989," Special Publication 778, National Institute of Standards and Technology, January 1990.

2. Benuska, Lee, editor, 1990, "Loma Prieta Earthquake Reconnaissance Report,"

Earthquake Spectra, supplement to volume 6, May 1990.

3. "Putting the Pieces Together: The Loma Prieta Earthquake One Year Later," 1990, The Bay Area Regional Preparedness Project, October 1990.

4. "Symposium on Practical Lessons from the Loma Prieta Earthquake," 1993, National Research Council and Earthquake Engineering Research Institute, publication pending.

5. Todd, Diana and Bieniawski, Ann, editors, 1992, "Guidelines and Procedures for Implementation of the Executive Order on Seismic Safety of New Building Construction," NISTIR 4852, National Institute of Standards and Technology, June 1992.

6. "NEHRP Recommended Provisions for the Development of Seismic Regulations for New Buildings," 1988, Federal Emergency Management Agency, FEMA 95.

7. "Improving Earthquake Mitigation," (1993), Federal Emergency Management Agency.

8. "Report of the Advisory Committee of the National Earthquake Hazards Reduction Program," 1993, Federal Emergency Management Agency.

9. "Earthquake Update," 1992, National Committee on Property Insurance, September, 1992.

10. "National Earthquake Hazards Reduction Program Five Year Plan for 1992-1996," 1991, Federal Emergency Management Agency, United States Geological Survey, National Science Foundation, National Institute of Standards and Technology, September 1991.

11. "Indirect Economic Consequences of a Catastrophic Earthquake," 1992, Federal Emergency Management Agency, July 1992.

12. "NEHRP Handbook for the Seismic Evaluation of Existing Buildings," 1992, Federal Emergency Management Agency, FEMA-178, June 1992.

13. "NEHRP Handbook for Seismic Rehabilitation of Existing Buildings," 1992, Federal Emergency Management Agency, FEMA-172, June 1992.

14. "Proceedings: ICSSC Issues Workshop, Development of Seismic Evaluation and Rehabilitation Standards for Federally Owned and Leased Buildings," 1992, National Institute of Standards and Technology, NIST GCR 92-617, October 1992.

15. "Proceedings of a Workshop on Developing and Adopting Seismic Design and Construction Standards for Lifelines," National Institute of Standards and Technology, publication pending.

16. "NEHRP Biennial Report to Congress," 1993, Federal Emergency Management Agency.

17. "Postearthquake Safety Evaluation of Buildings," 1989, Applied Technology Council, ATC-20.

18. Borcherdt, R.D. and Glassmoyer, G., 1992, "On the Characteristics of Local Geology and their Influence on Ground Motions Generated by the Loma Prieta Earthquake in the San Francisco Bay Region," Bulletin of the Seismological Society of America, 82, 2.

19. Yokel, Felix Y., 1993, "Effect of Subsurface Conditions on Earthquake Ground Motions, National Institute of

Standards and Technology, NISTIR 4769.

20. O'Rourke, T.D.,Pease, J.W.,and Stewart, H.E., 1992, "Lifeline Performance and Ground Motion During the Earthquake," The Loma Prieta, California Earthquake of October 17, 1989 - Marina District, U.S. Geological Survey Professional Paper 1551-F.

21. Glaser, Steven, 1993, "Estimating In Situ Liquefaction Potential and Permanent Ground Displacements Due to Liquefaction for the Siting of Lifelines," National Institute of Standards and Technology, NISTIR 5150, March 1993.

22. Cole, E.E., and Meehan, J.F., editors, 1991, "Reflections on the October 17, 1989,Loma Prieta Earthquake," Structural Engineers Association of California.

23. "The October 17, 1989, Loma Prieta Earthquake: Effects on Selected Power and Industrial Facilities." Electrical Power Research Institute, September 1991.

24. Kelly, J.M., Aiken, I.D., and Clark, P.W., 1991, "Response of Base-Isolated Structures in Recent Earthquakes," SMIP91: Seminar on Seismological and Engineering Implications of Recent Strong-Motion Data, California Division of Mines and Geology.

25. "Evaluation of the Performance of Seismically Retrofitted Buildings," 1992, Applied Technology Council.

26. Housner, George W., et al, 1990, "Competing Against Time," Report to Governor George Deukmejian from the Governor's Board of Inquiry on the 1989 Loma Prieta Earthquake.

27. Priestly, M.J.N., Seible, F., and Chai, Y.H., 1992, "Design Guidelines for Assessment, Retrofit and Repair of Bridges for Seismic Performance," University of California, San Diego.

28. Gross, J.L, and Kunnath, S., 1992, "Application of Inelastic Damage Analysis to Double Deck Highway Structures," National Institute of Standards and Technology, NISTIR 4857.

29. "Postearthquake Investigations," 1993, National Earthquake Hazards Reduction Program.

30. "Earthquake Planning Scenario for a Magnitude 7.5 Earthquake on the Hayward Fault in the San Francisco Bay Area," 1987, California Department of Conservation, Special Publication 78.

31. "An Assessment of Damage and Casualties for Six Cities in the United States Due to Earthquakes in the New Madrid Seismic Zone," 1985, Central United States Earthquake Preparedness Project.

32. Stone, W.C., and Taylor, A., 1993, "Seismic Performance of Circular Bridge Columns Designed in Accordance with AASHTO/CALTRANS Standards," National Institute of Standards and Technology, Building Science Series 170.

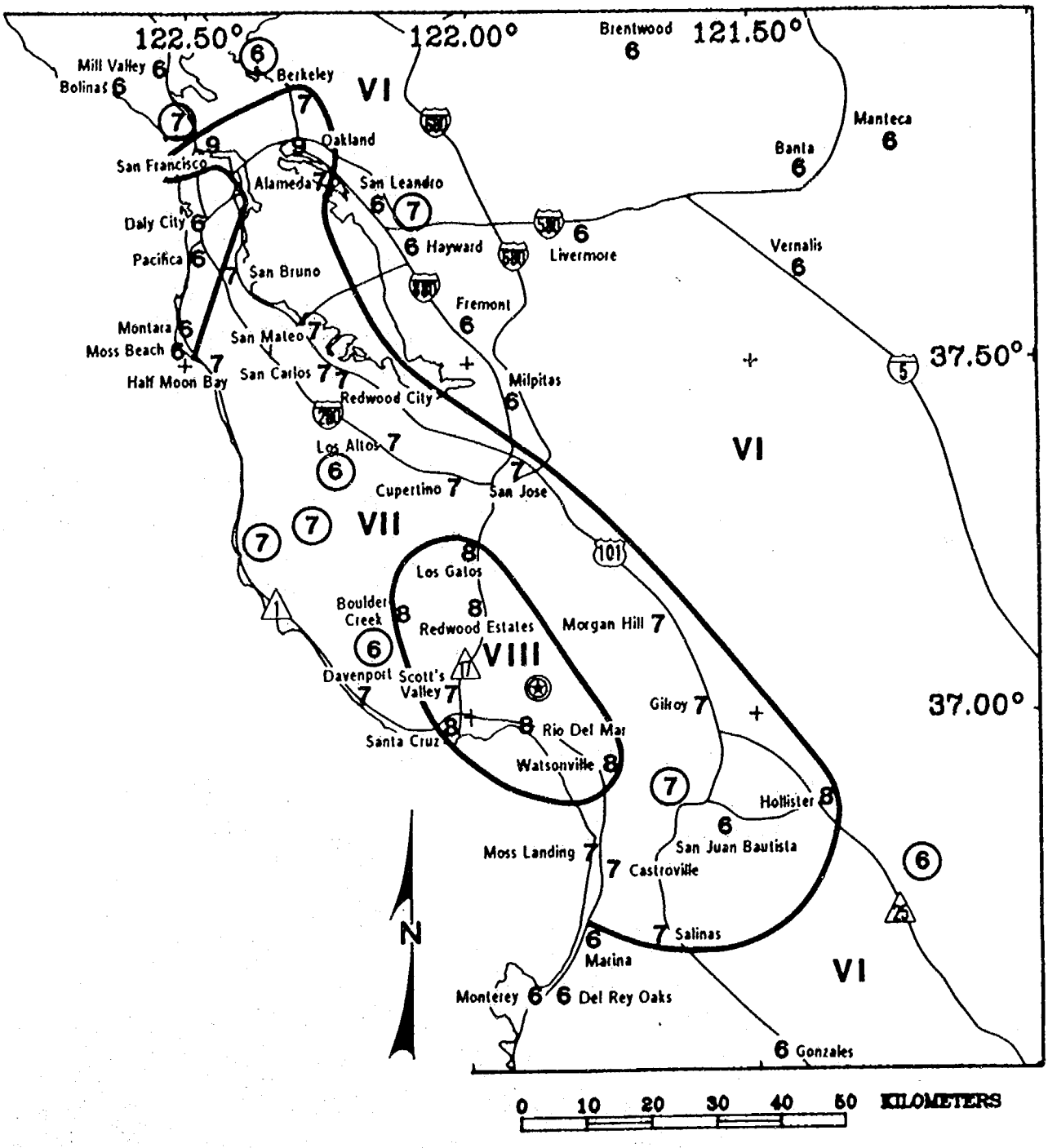


Figure 1. Modified Mercalli Intensity



Figure 2. Structural Damage, Los Gatos



Figure 3. Structural Damage, Marina Area

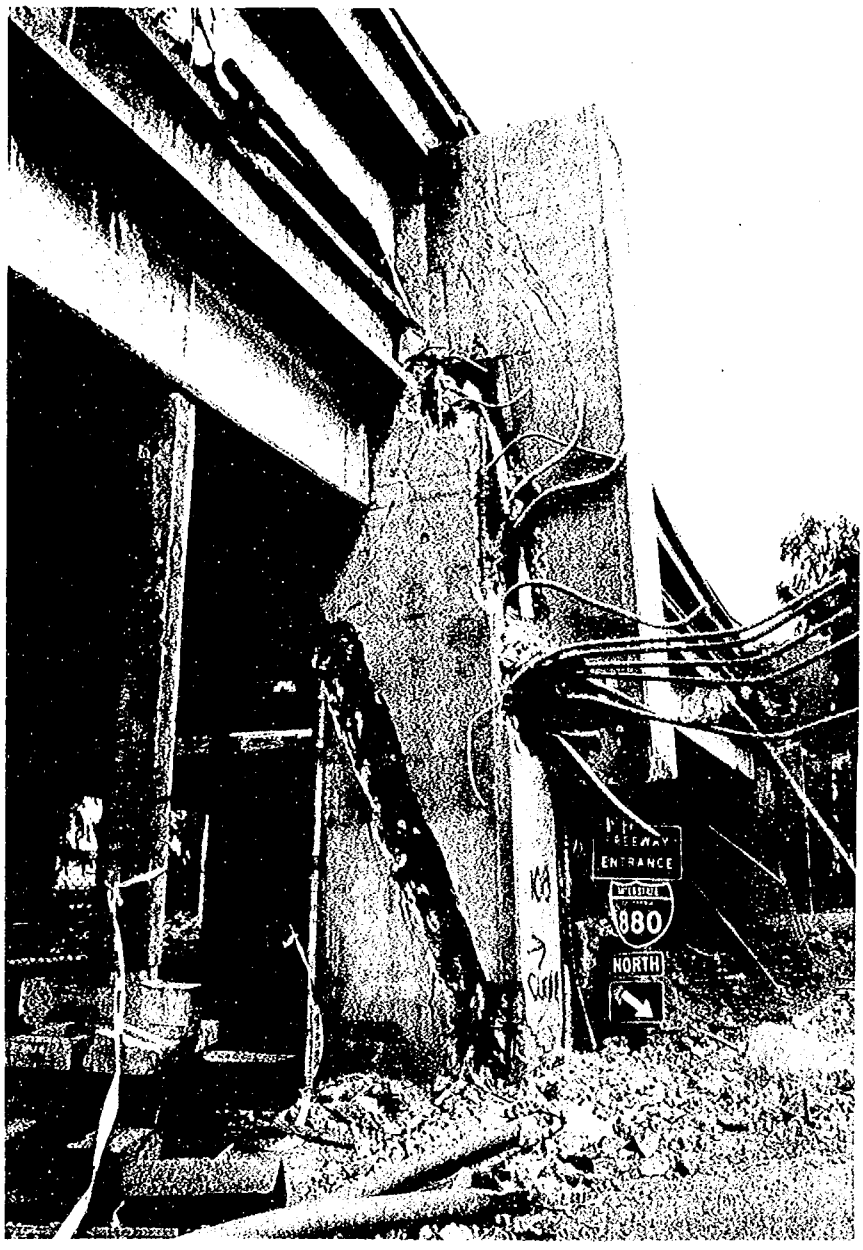


Figure 4. Failure of I-880 Viaduct, Oakland



Figure 5. Failure of Bay Bridge

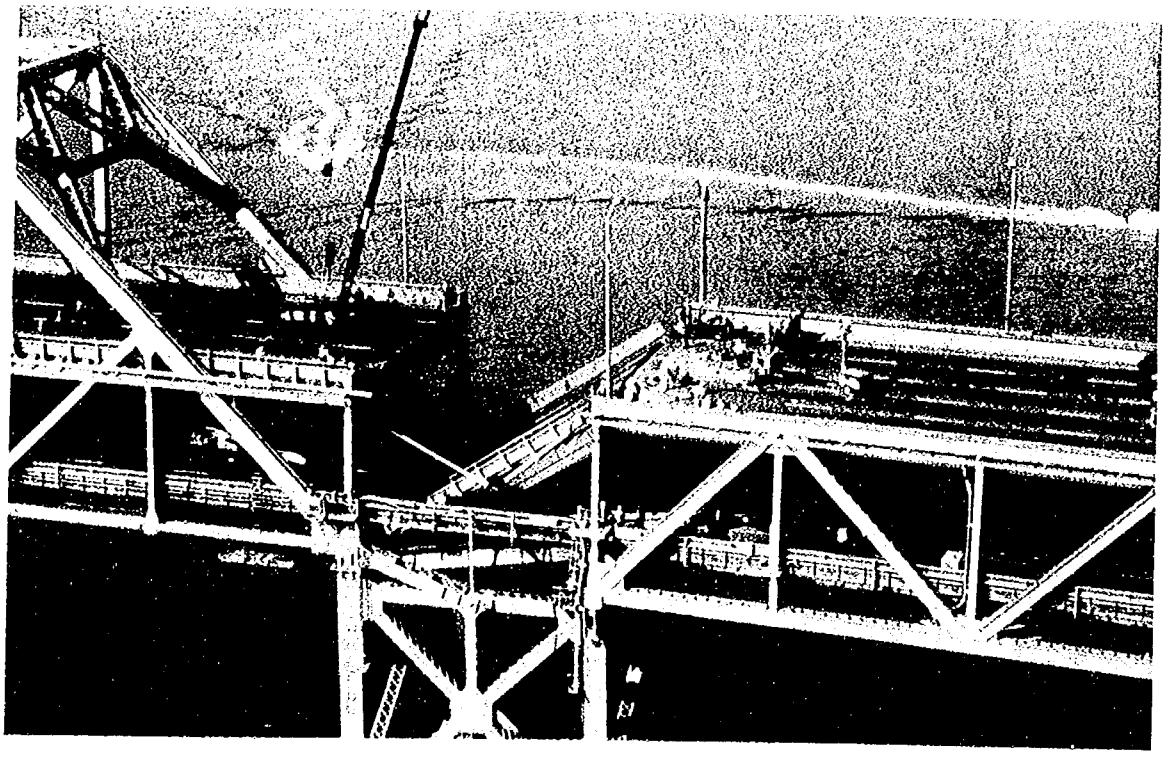


Figure 6. Fire Damage, Marina Area

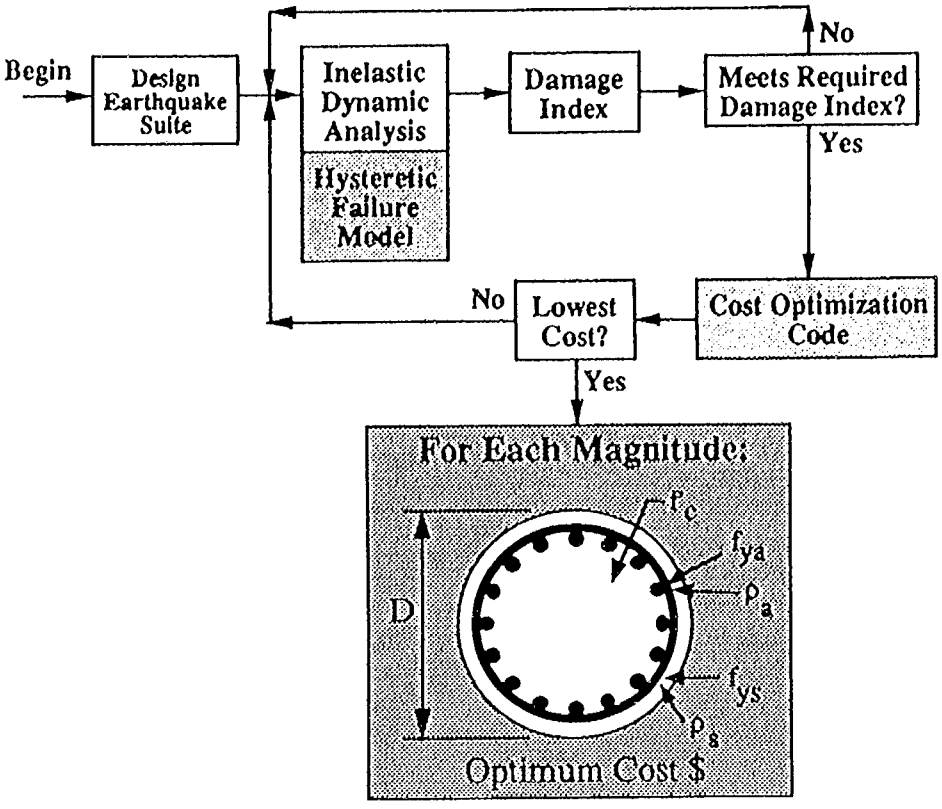


Figure 7. Integrated Seismic Design Procedure

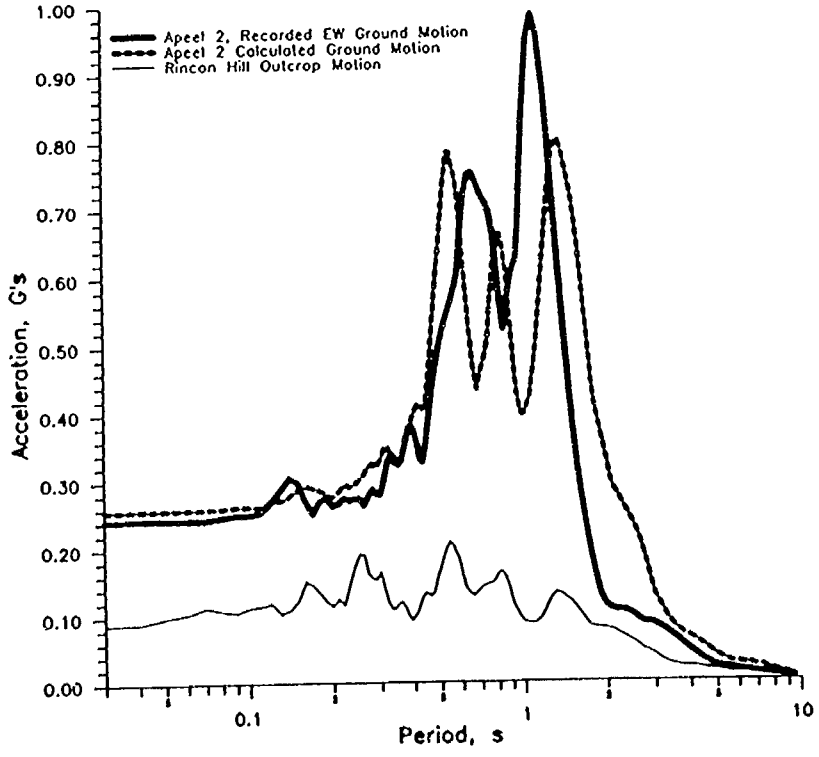


Figure 8. Amplification of Ground Motions



Figure 9. Liquefaction Damage, Marina Area

Damages and Lessons Learned from Hurricanes Hugo and Andrew

by

G. Robert Fuller, P.E.[1]

ABSTRACT

Hurricane Hugo evolved of the west coast of Africa and crossed the Caribbean Sea making landfall in the U.S. on September 22, 1989 at Charleston, South Carolina. The destruction that Hurricane Hugo left was greater than damage in any past North American hurricane. Damage estimates exceeded $10 billion, and there were 49 directly-related storm fatalities in the U.S. and Caribbean islands. Tropical Storm Andrew formed as a tropical depression on August 17, 1992, 850 miles (1370 km) southwest of the Cape Verde Islands. On August 24, Hurricane Andrew struck southern Florida, then passed through the Gulf of Mexico and hit Louisiana on August 25. The damages inflicted by Hurricane Andrew (over $30 billion) make it the costliest disaster in United States history. Within days after each hurricane, several investigative teams were assembled by Federal and State agencies and private insurance, professional and technical organizations. This report will summarize damages and lessons learned, along with recommendations for hurricane hazard mitigation, derived from several of the investigation reports.

KEYWORDS: anchorage, buildings, building code, coastal zone, damage assessment, design standard, disaster response, hazard mitigation, hurricane, infrastructure, manufactured housing, residential construction, shelters, structural, wind, wind pressure, wind velocity.

1. INTRODUCTION

1.1 Hurricane Hugo

Hurricane Hugo was the strongest storm to strike the U.S. since Camille pounded the Louisiana and Mississippi coasts in 1969.[1] At one point east of Guadeloupe, a NOAA research aircraft measured winds of 160 mph (256 km/h) and a central pressure of 918 mb, which rated Hugo as a Category 5 (See Saffir/-Simpson Scale, **Table** 1). When Hugo made landfall at Sullivans Island near Charleston, South Carolina on September 22, 1989, it was classified as a Category 4. It had sustained wind speeds of 135 mph (217 km/h); equivalent to 105 to 109 mph (169 - 175 km/h) at 10 meters elevation.[2]

Storm tides of approximately 20 feet (6 meters) were experienced along the South Carolina coast. Although the highest storm surges struck sparsely populated areas north of Charleston, damage was extensive and several lives were lost.[3]

From September 17th to 18th in Puerto Rico, Hugo destroyed or badly damaged 55,000 homes and left 37,000 homeless and at least five persons dead. In the U.S. Virgin Islands, it left four dead and 45,000 homeless. Then from September 21st to 22nd in South Carolina, 18 more were killed, and 24 Counties were declared disaster areas; in North Carolina there were four dead and 29 Counties declared disaster areas.[4]

[1] U.S. Department of Housing and Urban Development Washington, DC 20410-8000

Table 1 - Saffir/Simpson Intensity Scale

Classification	Wind Speed mph (km/h)	Storm Surge ft. (m)
Category 1	74-95 (119-152)	4-5 (1.2-1.5)
Category 2	96-110 (153-177)	6-8 (1.6-2.5)
Category 3	111-130 (178-209)	9-12 (2.6-3.7)
Category 4	131-155 (210-249)	13-18 (3.8-5.5)
Category 5	> 155 (> 249)	> 18 (> 5.5)

1.2 Hurricane Andrew

In the early morning hours of August 24, 1992, Hurricane Andrew made landfall on the southeast coast of Florida, ravaging South Dade County and the communities of Homestead and Florida City. It continued across the Florida peninsula, causing extensive damage as it moved through the Everglades National Park, before exiting the State near Naples on the southwest coast of Florida. Although rainfall in excess of 7 inches (18 cm) caused minor flooding, the significant damage was the result of Category 4 (Saffir/Simpson Scale) hurricane force winds.[5]

Within hours, President Bush declared Florida a major disaster area and designated the Counties of Broward, Dade, Collier and Monroe eligible for Federal disaster assistance. Additionally, a full response effort was activated by representatives of several Federal agencies and the military to support State and local response efforts.

The $30 billion estimate of damages resulting from Hurricane Andrew in Florida and Louisiana makes it the costliest natural disaster in United States history. Over 55 deaths were also attributed to the storm, and over 200,000 people were left homeless.

An estimated 80,000 single family homes, manufactured (mobile) homes, and apartments in Florida, and 10,000 in Louisiana, were destroyed or received major damage. Another 72,000 homes in Florida and Louisiana received moderate damage. Over 8,000 businesses were destroyed or damaged, and approximately 86,000 people became unemployed. Approximately 1.4 million people were without electricity and 3000 water mains were damaged.

About 1,900 traffic lights in Dade County needed repair or replacement, as did 100,000 traffic signs and 2,200 street lights. Fifty-nine hospitals and health facilities were damaged, and seven Post Offices were badly damaged. According to the Miami Herald newspaper, the Turkey Point Power Plant suffered an estimated $90 million in damages.

There were an estimated 280 Kindergarten through 12th Grade schools damaged; 19 with major damage, and the rest with moderate damage, for a total loss of about $300 million. Universities and colleges suffered another $60 million in damages.

Agriculture, with annual sales of $540 million, and supporting 23,000 jobs, is the mainstay of the economy of south Dade County. Nearly 80% of the 3,700 farms in Dade County suffered damage from Hurricane Andrew, for a total loss to agriculture of more than $1 billion. This was the second greatest agricultural loss in U.S. history, exceeded only by a previous drought in the Midwestern States.[5]

2. ESTIMATED WIND SPEEDS

2.1 Hurricane Hugo

The hurricane was a September Cape Verde storm, originating off the coast of Africa and traveling across the North Atlantic until it became a hurricane 1100 miles (1770 km) east of the Leeward Islands on September 13, 1989. The eye went over Guadeloupe and the storm continued on a west northwesterly path over the extreme eastern tip of Puerto Rico, and finally made landfall near Charleston, SC on September 22nd.[2]

The eye then continued in a northwesterly direction into North Carolina, weakening very slowly.

Some of the measured maximum surface wind speeds in miles per hour (km/hr) are as follows:

	One Min. Average	Peak Gust
Roosevelt Roads, P.R.	92 (148)	117 (188)
San Juan, P.R.	75 (121)	90 (145)
Charleston, SC	86 (138)	105 (169)
Sumter, SC	67 (108)	109 (175)
Charlotte, NC	60 (097)	87 (140)

2.2 Hurricane Andrew Wind Speeds

Andrew reached hurricane strength on Saturday, August 22, 1992. The eye formed, the storm strengthened, and within 36 hours Andrew reached the borderline between a Category 4 and 5 hurricane (**Table 1**). The central pressure fell rapidly from 1014 mb to 922 mb during this 36-hour period.

Andrew initially weakened over the Florida Straits, but then rapidly intensified during the last few hours preceding landfall on the southeastern shore of Florida. The eye came ashore on August 24th at 5:05 a.m., directly east of Homestead Air Force Base. During the next four hours, Andrew proceeded slightly north of west across the Florida peninsula. Although it weakened about one category during its transit over land, Andrew was still a major hurricane when it hit the southwestern Florida coast.

Modest intensification began again when the eye reached the Gulf of Mexico and began a northward trend toward Louisiana. The hurricane struck a sparsely populated area with Category 3 intensity on August 25th, and then weakened rapidly to tropical storm strength in about ten hours as it proceeded inland in a northerly direction through Louisiana.[5]

In its preliminary report, the National Hurricane Center (NHC) stated, "The maximum sustained surface wind speed (one minute average at 10 meters elevation) during landfall over Florida is estimated at 120 knots (about 140 mph), with gusts at that elevation near 150 knots (about 175 mph)."[5]

However, the number of reliable wind speed records obtained in Hurricane Andrew is limited. The reasons include: poorly designed anemometer masts which fail before maximum wind speeds, failure to maintain equipment, and lack of recording systems with backup electrical power. Therefore, wind speed records following the hurricane provide only a small part of the information needed to reconstruct the event.

Two independent models were used by the NHC to estimate the sustained wind speed. A standard pressure-wind relationship applied to 930 mb (storm pressure) yielded approximately 150 mph (240 km/hr) sustained winds.

In addition, a special TSAF unit Dvorak technique classification at landfall provided an estimate of sustained wind speed at 147 mph (237 km/hr).[5]

In the months following Hurricane Andrew, considerable effort has been expended in locating records of wind speed or barometric pressure to reconstruct the wind field over the areas of heaviest damage. Records obtained to date are summarized in **Table 2**. These observations are "raw data," and have not been corrected to standard conditions (anemometer height of 33 ft (10 m) in flat, open terrain).

In an attempt to reconstruct the wind field, Reinhold et al. used an analytical model calibrated with the limited wind speed data available. The model adjusts the surface wind speeds to account for the development of an internal boundary layer and the change in central pressure during and following landfall. The wind speeds generated by the model are fastest-mile speeds at a height of (33 ft) 10 m in flat, open terrain.[6]

Powell used a model in which the wind speed observations are composited in a storm-relative coordinate system over a period of several hours. In this model, aircraft observations also are included with adjustments made either to over-water or over-land exposures using empirical relationships.

Results of the two models, which are in reasonably good agreement for the northwest sector of the storm, are shown in **Table 3**. For the southwest sector, the normalized speeds obtained by Reinhold et al. are higher than those obtained by Powell. It should be noted that all values are subject to revision as additional surface wind speed data becomes available.**[6]**

3. SITE INVESTIGATIONS

3.1 After Hurricane Hugo

Shortly after Hurricane Hugo struck South and North Carolina, The Federal Emergency Management Agency (FEMA) organized an Interagency Hazard Mitigation Team (IHMT), made up of representatives of FEMA, DOT, HUD, and U.S. Army Corps of Engineers.**[3]** The purpose of an IHMT is to visit the disaster sites to assess causes of damage, to develop post-disaster hazard mitigation plans for the affected States, and to recommend to Federal, State, and local governments appropriate mitigation strategies.

Additionally, the Wind Engineering Research Council (WERC), under the auspices of the National Research Council of the National Academy of Sciences and Engineering, and with the support of NSF, FEMA, and NOAA, sent teams to Puerto Rico and South Carolina to assess hurricane damage.**[2]**

At the same time, HUD had Structural Engineers from its monitoring contractor for manufactured (mobile) home construction visit the area to analyze damage to single-family site-built and manufactured housing, to determine if designs or standards needed to be revised.**[7]**

3.2 After Hurricane Andrew

During the week of September 7, 1992, HUD dispatched two Structural Engineers from HUD's Monitoring Contractor to Florida to investigate causes of failure of manufactured (mobile) homes.**(Figure 1, 3, & 4)** They, with a renowned wind engineer, and also a representative of the State of Florida Bureau of Mobile Homes inspected seven manufactured housing parks. A Final Report was submitted to HUD on October 1, 1992.**[8]**

On September 9, 1992, after receiving initial reports of mass destruction of manufactured housing, the Secretary of HUD, Jack Kemp ordered a full-scale review of the Federal Manufactured Home Standards on wind design, to ensure protection of residents during hurricanes. Immediately, HUD engineers began a review, and HUD's Office of Policy Development and Research (PD&R) contracted with the National Institute of Standards and Technology (NIST) to evaluate all wind standards and building code provisions.**[6]**

Based upon these evaluations, on September 18, 1992, HUD engineers began drafting an Interim Rule to revise the Manufactured Home Standards to require wind design to comply with ASCE Standard 7-88, a consensus standard referenced by all major building codes.

The Federal Emergency Management Agency (FEMA) convened an Interagency Hazard Mitigation Team on September 15, 1992 in Miami, and HUD staff participated. Conclusions from this team effort are summarized later in this paper and are contained in a FEMA Interagency Hazard Mitigation Team Report (FEMA 955-DR-FL, August 1992), printed in January 1993.**[5]**

FEMA also organized a Building Performance Assessment Team in September 1992 to survey the performance of buildings in the storm's path.

This team of FEMA Headquarters and Regional staff, professional consulting engineers, and local building officials, observed successes and failures of buildings in withstanding Hurricane Andrew's wind forces, commented on failure modes of damaged buildings, and recommended measures for minimizing similar damage in the future. Their report, "Summary of Damages to Conventional Residential Structures," was published by the Florida Department of Community Affairs (FDCA) in September 1992.**[9]**

In cooperation with the Damage Assessment Team organized by FEMA and FDCA, the American Plywood Association (APA) and Florida Concrete Products Association conducted an assessment of performance of wood systems used in residential and commercial construction. APA Report T92-21, "Hurricane Andrew - Structural Performance of Buildings in Southern Florida," summarizes the observations of the APA team, and concentrates on wood-framed buildings, including modular and manufactured homes.**[10] (Figures 2 & 6)**

Florida's DCA also assembled wind engineers and experts for a "Workshop on Hurricane Building Code Provisions" on October 19, 1992. Engineers from HUD participated. This Workshop resulted in a January 31, 1993 Report: "Recommendations for Building Codes and Building Code Enforcement."**[11]**

In November, the Department of HUD investigated probable causes of failures of manufactured housing, to identify specific components and systems vulnerable to high wind forces. HUD's contractor also conducted in-plant inspections of manufacturing plants producing homes for Florida, to identify violations of standards which could weaken wind resistance of homes.

At the same time, HUD engineers began to review and analyze designs of manufactured homes to determine if there were areas of weakness with respect to resistance to high wind forces.

4. DAMAGE ASSESSMENT

4.1 Hurricane Hugo

4.1.1 Wind Engineering Research Council

The WERC reported that in Puerto Rico, the major type of structural damage was extensive glass and window damage in highrise condominiums. In Vieques Island, offshore of P.R., residential damage was severe.**[2]**

In South Carolina, many buildings, including schools, hospitals, condominiums, hotels and commercial structures, had extensive roof and glass failures which led to serious rain damage. Most cladding did not appear to be designed for hurricane wind forces.

On Sullivans Island, Isle of Palms, and Folly Beach - all adjacent to Charleston - one and two story residential construction was severely damaged or destroyed, often by a combination of wind and storm surge. Many beachfront properties had inadequate foundations, poor connection details to foundations, or insufficient cladding strength. Many piling foundations remained, while houses were moved several hundred feet away. Generally everything on those islands within 500 ft. (152 m) of water had major damage or complete loss.

Several large "pre-engineered" steel industrial buildings failed. Failures involved extensive cladding damage to sidewalls and roofs, and door damage. End bays of post and beam construction on some rigid-frame buildings failed from wind forces.

In Charleston's historic district, a few older buildings suffered partial structural collapse. There was much glass, porch, chimney, facade, and roof damage. However most newer structures performed satisfactorily.

Finally, as reported by WERC, electrical transmission and distribution lines in Puerto Rico, Virgin Islands, and South Carolina fared poorly.

4.1.2 HUD Manufactured Housing

Shortly after Hurricane Hugo, an investigation of damage to manufactured housing was initiated by HUD through a contractor, the National Conference of States on Building Codes and Standards (NCSBCS).**(Figures 1, 3, & 4)** Several areas were examined to determine causes of failure: 1) whether the design met the Federal Manufactured Home Construction and Safety Standard, 2) adequacy of manufacturer's installation instructions, 3) compliance with installation instructions, and 4) adequacy of Federal construction standards.**[7]**

Results of the investigation revealed the following weaknesses with manufactured housing:

Tie-downs, Anchors, and Foundations: The most severe damage resulted from overturning or homes shifting off their piers. This was generally caused by failure of ground anchors due to weakness of anchors in saturated soil or improper installation of the anchoring device. Anchor designs and installation instructions are provided by the home manufacturer, and are enforced by State and local building officials.

Negative Wind Pressure (Suction): The most common damage was the loss of siding at ends of homes, or the loss of metal roofs or roof shingles.**(Fig. 8)** The standards only require a positive wind design pressure of 25 psf (1200 Pa) on walls, and 15 psf (720 Pa) uplift on the roofs. Connections of metal roofs and fastening of asphalt roof shingles were inadequate to resist hurricane wind forces.

4.1.3 FEMA Hazard Mitigation Team Report

On October 16-20, 1989, a FEMA Region IV Interagency Hazard Mitigation Team (IHMT) of Federal and State representatives convened at the Disaster Field Office to identify immediate and long range opportunities for hazard mitigation. This IHMT was not able to visit sites in each of the 24 Counties affected by the hurricane, but they did visit areas representative of damages. Video recordings and photographs were also used to assess the magnitude and details of damage.**[3]**

Primary damages from Hurricane Hugo were caused by storm surge flooding, surge related erosion, wave action, and high winds, with rainfall and freshwater flooding of lesser consequence. Surveys indicated that newer construction complying with local building codes and National Flood Insurance Program (NFIP) regulations withstood hurricane forces better than older structures.

According to the U.S. Department of Agriculture, Soil Conservation Service (SCS), watercourses in 20 counties were clogged with fallen trees and debris from destroyed homes and properties. To prevent additional damage, SCS indicated immediate work was needed on 2,385 miles (3838 km) of stream banks, culverts, roads, and public and private property.

Forest areas, including private, Federal, and State lands, lost in excess of 6.7 billion board feet of timber valued at over $ 1.0 billion. Damaged timber was concentrated on about 4.5 million acres (1.8 million ha), representing 36% of the State's woodland. Due to the amount of timber on the ground and inaccessibility to affected areas, the threat of fire was significant.

The Department of Education estimated $56 million in damages to 368 primary and secondary schools. Thirty-five of 48 school districts in the affected counties reported damage.

A report by Clemson University stated that the agricultural industry suffered damages in excess of $336 million: $97 million for crops, $208 million for buildings, $14 million for machinery, $4 million for animal losses, and $10 million for on-farm conservation practices.

4.2 Hurricane Andrew Damage Assessment

4.2.1 HUD Manufactured Housing

During the week of September 7, 1992, a team composed of one State of Florida official, two

representatives from HUD's Monitoring Contractor, and Herb Saffir, P.E., a renowned wind engineering expert, conducted an investigation into the nature and causes of failures sustained by manufactured housing in Florida. The same two contractor representatives and one State of Louisiana official continued the investigation in Louisiana later that week.**[8] (Figures 1 & 3)**

The purpose of this investigation was to assess the:

* appropriateness of the current HUD standard requirements for wind-load design;
* performance of manufactured homes and identify patterns of failure of components; and
* effectiveness of local installation rules, practices, and enforcement.

In order to collect a broad base of data on performance of manufactured housing in the path of Hurricane Andrew, the team visited and videotaped seven manufactured home parks in Florida and eight in Louisiana.

According to information provided by Dade County, approximately 97% of the manufactured homes in the County were destroyed, while 11% of single-family homes were destroyed and 43% sustained major damage. **Table 4** summarizes the damage to dwellings in both Florida and Louisiana, as reported by the American Red Cross.

In areas where the investigative team found that many manufactured homes had been completely destroyed, the damage pattern appeared to be different from that of site-built housing. Connections of various segments of manufactured homes failed. In some manufactured homes, segments of roof blew away. In other homes, the floor system remained intact while the rest of the home turned to debris. The resultant flying debris then caused substantial damage to adjacent property.

In comparison, site-built homes usually sustained extensive damage to roof sheathing and trusses, while the remaining structure remained intact. Because many site-built homes had concrete block walls, their mode of failure cannot be compared to that of manufactured homes. However, site-built homes with wood wall construction in general remained intact, sustaining damage only to siding and roof sheathing.

Anchoring Systems: In Florida, virtually all homes observed had been anchored, but the anchoring systems had failed in most of the homes destroyed. Some of these systems included anchors embedded in only two feet (0.6 m) into soil; these anchors were pulled out of the ground. Other systems included short anchors embedded in concrete; these too were pulled out of the ground.

Many of the manufactured homes seen in Louisiana had no anchoring systems at all, or had only two or three anchors - less than the number required for hurricane zones. Where anchors had been installed, most were installed incorrectly, and many were only partially embedded in the ground with as much as 12" (0.3 m) of anchor protruding. An anchor installed in this manner can readily bend, allowing the home to move and fall off its piers.

While the majority of anchor system failures appeared to have resulted from improper installation, in several cases the holding capacity of the anchors was reduced because the soil was saturated.

Wind Uplift Straps: In many homes whose roofs had separated from the sidewalls, uplift straps failed when staple fasteners pulled through the light gage steel strap material. Staples were often found to have been over driven during construction, damaging the straps.

Siding: The team saw significant damage to siding of homes; in many cases, siding had pulled away from the walls. Damage of this type was more prevalent at gable ends of

homes, indicating significant negative wind load (suction). The typical failure appeared to be the result of fasteners, used to attach siding, pulled out of the wall studs or sheathing.**(Figure 8)**

Additionally, interlocking seams of both vertical and horizontal metal or vinyl siding were not capable of resisting the suction wind load. Once the seam failed the wind blew the siding off. Since most manufactured homes do not have sheathing installed behind the siding, once the siding is lost, wall insulation and interior wall board or panelling are exposed to wind and rain. Such exposure resulted in major damage to interiors of many homes.

Roof Metal: The team observed homes where metal roof seams also failed as a result of negative wind load. Joints between sections of roof metal located near the roof fasteners at the connection to the sidewall failed first. Joints between sections of roof metal opened along the length of the roof edge and wind entered the roof cavity.

Shingles: In manufactured homes, shingles are generally to roof decking with staples. Most shingles are tested for either 60 mph (96 km/hr) or 90 mph (145 km/hr) wind velocity. However, those tested for 90 mph are rarely used on manufactured housing. Roof shingles simply tore away from the staples used to fasten them to the sheathing.**(Figure 9)**

Roof Sheathing: In some homes, staples used to hold plywood roof sheathing to roof trusses pulled out, allowing the roof sheathing to blow off. However, in some homes where the sheathing remained in place, several staples missed the trusses either partially or completely, reducing the effectiveness of the connections. The team also saw homes where the staple crowns protruded above the surface of the sheathing up to 1/2 inch (13 mm), probably as a result of moving up and down from the wind.**(Figure 10)**

Edges, Corners, and End Walls of manufactured homes were particularly vulnerable to high winds. Many homes sustained damage from wind and rain when the exterior finish material was blown off.

4.2.2 Building Performance Assessment

The Florida Department of Community Affairs prepared a report on "Summary of Damages to Conventional Residential Structures,"**[9]** which provided the following summary of observations by FEMA's Building Performance Assessment Team:

Roofing Materials (Tile, Shingles,Membrane): The loss of roofing material was the most costly aspect of damage. An estimated 90% of residential structures lost roofing materials. Not only did it allow weather penetration into the affected building, it also contributed to a significant portion of wind blown debris that led to destruction of weather envelopes of other buildings.**(Figure 7)**

Doors and Windows: The loss of doors (primarily garage and sliding glass doors) and windows was the second most important and costly aspect of the storm. Flying debris contributed to much of this damage. The loss of windows and doors, along with roof coverings, caused major damage to many building interiors and contents. In most cases, structural damage was minimal, but the buildings were uninhabitable due to effects of rain water, i.e., collapsed ceilings and interior partitions.

Roof Sheathing: The loss of plywood or oriented strand board sheathing resulted in collapsed ceilings and partitions, and collapse of gable ends. In the majority of cases, the loss of roof sheathing was caused by inadequate nailing, which consisted of nails spaced further apart than required by the building code, or nails which missed trusses or rafters. A large portion of sheathing failures occurred along eaves or near ridges of gable roofs.**(Figures 2 & 7)**

Gable-End Failures were precipitated by the loss of roof sheathing support caused by inadequate fastening, lack of gable-end bracing, or inadequate attachment of the gable end to the top of the end wall.**(Figure 5 & 11)**

Connection Failures: Overall, failure of connections between individual elements in the lateral load path occurred in a relatively small percentage of conventional residential structures. In some cases, wall failure occurred with hardboard siding without plywood backing. This type of cladding without sheathing has insufficient strength to function properly, particularly if water is absorbed into the siding material.

4.2.3 American Plywood Association Report

In September 1992, the American Plywood Association published their investigative report, APA Report T92-21, "Hurricane Andrew: Structural Performance of Buildings in Southern Florida." **[10]** This report describes the structural performance of residential and low-rise commercial buildings in Southern Florida, and primarily concentrates on wood systems.

Conclusions are presented, dealing with roofing attachment; wood roof sheathing - both plywood and oriented strand board (OSB) - and its attachment to framing and gable-end roof systems; walls and connections of components; manufactured home construction and installation with tiedowns to ground anchors; attachment of metal roof deck panels to steel framing; connections between concrete and metal roof decks and concrete or masonry walls; and attachment of cladding for pre-engineered metal buildings.

Wood Construction: By far, the majority of wood structural failures due to Hurricane Andrew can be attributed to improper connection details. Inadequate detailing of several types of connections was evident. **(Figures 5 & 6)**

One of the major deficiencies was the connection of walls to adjacent walls, roofs and floor structures. Top plates occasionally were not lapped at corners, and wall sections were attached to walls with as little as three nails. Inadequate nailing of bottom plates to the floor structures at exterior walls also occurred.

The most common type of structural failure was the loss of gable-end walls. **(Figures 5 & 11)** This phenomena was almost always accompanied by the loss of 4 to 12 feet (1.2 - 3.7 m) of roof sheathing immediately adjacent to the gable end. Once the roof sheathing was blown off, the gable-end truss and adjacent trusses collapsed in domino fashion. Diagonal bracing of end trusses was rarely observed in these failed roofs.

Gable-end truss framing was also infrequently or inadequately fastened to the top plate of the wall below. Toe-nailing, if used, was often spaced at 4 to 6 feet (1.2 - 1.8 m) on center.

One of the most costly nonstructural failures was the loss of gypsum board ceilings. Often, rain with and subsequent to the hurricane was driven in through gable-end vents or directly into the roof cavities when roof systems failed. Rain would saturate the insulation and the ceiling board, causing widespread collapse of ceilings. This would also reduce the lateral support of the gable-end roof trusses and walls.

Much interior damage to buildings was also caused by loss of doors and windows, as reported elsewhere. Failures occurred because of inadequate fastening of door and window frames to the structure, and also low strength window glazing. When the doors and windows failed, interior pressures increased and often caused failure of interior non-loadbearing partitions, roof systems, or even exterior walls.

Very often, plywood or OSB roof sheathing was not adequately nailed to the primary structural gable-end truss. During the hurricane, when the roof overhang was exposed to the wind, the overhang lifted and "peeled" the roof sheathing off back to the second or third truss. **(Fig. 4)**

Another weakness occurred with tiedown straps connecting roof systems to walls and walls to floor systems. In some cases, straps were bent out of the way to avoid trusses, or straps were only lightly nailed to roof framing or not attached at all. Often this slight error led to total failure of the roof system, and in some cases, complete loss of the structure below.

Masonry/Wood Construction: There were a number of failures of masonry exterior walls with wood gable-end walls, and also masonry first floor with wood framed second floor walls. All collapsed gable ends observed were attributed to improper attachment of the wood gable end to the masonry wall below, or loss of lateral bracing of the wall due to loss of the roof diaphragm.**(Figure 6)**

As previously discussed, improper gable-end overhang details and the subsequent loss of roof sheathing at the end wall caused a domino type collapse of the gable end, roof trusses and adjacent wall.

One connection detail seen in a number of heavily damaged multifamily dwellings concerned inadequate attachment of shed-roof trusses to masonry fire walls. While the bottom ends of the trusses were placed in saddle-type connectors, the tops were inadequately anchored to the masonry wall. Lack of anchorage at the roof level prevented the transfer of lateral loads to the fire wall.

Wood Panel Roof Sheathing: Almost all roof decking for masonry, masonry/wood, and wood frame residential structures was plywood or OSB. Sheathing failures, where they occurred, were similar in all three building types.

As reported previously, most failures occurred at gable-end walls, because of inadequate or improper fastening of the roof sheathing panels. Typically, nails were spaced too far apart, or there was an erratic fastening pattern.

When staples were used, crowns of staples were often improperly placed perpendicular to the panel edge. This would locate one staple leg too close to the edge of the panel or the support framing, thus reducing the staple capacity by one-half.

The recurring loss of roof sheathing at gable ends is consistent with generally accepted wind load theory. Model building codes and the ASCE Standard 7-88 indicate that applied wind loads are greater at these locations.

Roof Coverings: Failure of roof covering material was observed on almost every damaged structure in Dade County. Almost all roofing types were included.**(Figure 7)**

Asphalt shingle roofing failures were usually related to "tear through" of shingles at staple fasteners. Shingle roof fasteners consistently remained imbedded in the plywood or OSB roof sheathing after shingles were blown off. **(Figures 9 & 10)**

Flat concrete tiles appeared to have better wind resistance than barrel-shaped tiles. However, both types failed in the same manner, showing no adhesion of cement mortar bedding to the tile back. The mortar would stick well to the roof deck, indicating that the mortar had partially set before tiles were placed. Some concrete or clay tile roofs that did survive were fully embedded in mortar. While concrete tile roofing had holes for mechanical fasteners, none were used.

Due to the weight of concrete and clay tile roofing pieces, they caused considerable projectile damage to neighboring structures, and probably caused most of the window failures.

Other Structures: Steel roof decking systems were often used for roofing in lowrise commercial buildings. These roofing systems suffered much damage from the hurricane. While many of the metal roof systems appeared to be attached in accordance with the building code, they still failed. Failure modes were pull-through of welds or fasteners attaching the metal to framing. Many of the failures of lowrise commercial buildings appeared to have been caused by loss of diaphragm action and subsequent collapse of supporting walls.

Several commercial buildings with long-span precast concrete roof T-beams and masonry bearing walls also failed. Welded connections at the end support to steel plates in walls, and connections to parallel nonbearing side walls, appeared to be inadequate.

In addition, there were commercial buildings which failed that had inadequate vertical reinforcement or connections between intersecting walls, lack of sufficient joint reinforcement, or inadequate bonding systems to attach brick veneers to the backup wall.

Several examples of failed pre-engineered metal commercial buildings were observed. Generally, the steel siding and its attachment to steel framing were not capable of resisting the shear and uplift wind forces and impact forces from wind-blown debris. When the building envelope was breached, the steel roofing or siding panels were blown off the framing. Then the unbraced steel framing collapsed under the intense wind forces.

5. LESSONS LEARNED

5.1 Measurement of Wind Speed

Both Hurricanes Hugo and Andrew revealed weaknesses in documenting actual wind speed records and in estimating surface design wind speeds after storms. Anemometers or their supports often failed before maximum winds speeds are reached, and there was an inadequate number of measuring devices located in the paths of the storms.

In addition, various agencies, building organizations, engineering groups, and professionals, using different assumptions and technologies, determined the wind speeds, with differing results. Because of a general lack of understanding by the media and the public of wind speeds and their effect on structural design, preliminary values were often blown out of proportion.

Such differences also profoundly affect future design standards and legislation, and complicate the development of building code provisions to mitigate future damage from hurricane winds. **[5]**

5.2 Building Codes and Wind Standards

Hurricane Andrew more than Hurricane Hugo revealed the importance of upgrading the wind design requirements of the building codes. Although both hurricanes did reveal inadequacies in the Federal Manufactured Manufactured Home Construction and Safety Standards maintained by U.S. Department of Housing and Urban Development (HUD).

Evaluations after Hurricane Andrew led to several recommendations to the American Society of Civil Engineers (ASCE), Southern Building Code Congress International (SBCCI), South Florida Building Code, State of Florida, and HUD to revise standards and building code provisions to be equivalent to ASCE 7-88.

Most of the recommended revisions pertained to increased wind uplift and negative (suction) pressures for cladding (siding and roofing materials), anchor and tiedown systems for manufactured housing, connections between structural components, window and door design pressures, and greater roof eave, ridge, and overhang design loads. **[5,6,8, & 11]**

5.3 Design, Details, and Construction

As indicated in most of the investigation reports, inadequate design and detailing led to a major segment of the damage and failures. However, in many cases lack of attention to detail during construction caused failures. Inadequate inspection and enforcement during the construction process, poor workmanship, and inattention to quality also resulted in buildings less resistant to high wind forces.

The majority of lowrise residential building and some commercial structures are not designed by structural engineers or other design professionals. Empirical and prescriptive requirements are generally provided by building codes for these structures. In addition, standard designs and details are prepared by builders, contractors, fabricators, or suppliers of many of the building components.

Therefore, the majority of the failures in connections, fasteners, gable-end walls, cladding, windows, doors, and anchorage cited in the investigative reports, could be contributed to the resultant lack of adequate design and detailing, or improper construction practices.

6. CONCLUSIONS

Natural hazard mitigation is an essential activity of Federal, State, and local governments, working cooperatively with nongovernmental organizations and the private sector, to reduce the fatalities and property losses from future events. The use of Interagency and Intergovernmental Building Performance Assessment Teams and Hazard Mitigation Teams by the Federal Emergency Management Agency (FEMA) provided an effective mechanism for post-disaster investigations and mitigation planning.

They were able to incorporate the background and expertise necessary to promote a comprehensive approach to hazard mitigation. The recommendations provide a framework for hazard mitigation activities, and guide Federal and State agencies involved in the recovery and reconstruction process.

7. REFERENCES

[1] National Oceanic and Atmospheric Admin. (NOAA), Hurricane: A Familiarization Booklet, National Weather Service, Weather Service Forecast Office, Miami, FL (1990).

[2] Saffir, Herbert S., Hurricane Hugo: With Total Damage Over Ten Billion Dollars, The Wind Engineer, Vol.4, No.1, Jan. 1990, Wind Engineering Research Council, Lubbock, TX.

[3] Federal Emergency Management Agency (FEMA), Interagency Hazard Mitigation Team Report, Hurricane Hugo, FEMA 843-DR-SC, Oct. 1989, Region IV, Atlanta, GA.

[4] Federal Insurance Admin. (FIA), Learning from Hurricane Hugo: Implications for Public Policy, June 1992, Federal Emergency Management Agency, Washington, DC.

[5] Federal Emergency Management Agency (FEMA), Interagency Hazard Mitigation Team Report, Hurricane Andrew, FEMA 955-DR-FL, Aug.1992, Region IV, Atlanta, GA.

[6] Marshall, Richard D., Preliminary Analysis of Hurricane Andrew Wind Velocities and Pressures, for U.S. Dept. of Housing and Urban Devel., National Inst. of Standards and Tech. (Unpublished).

[7] National Conference of States on Building Codes and Standards (NCSBCS), Preliminary Report - Disaster Site Investigations of Manufactured Homes, for U.S. Dept. of HUD, Dec. 28, 1989, Herndon,VA.

[8] NCSBCS, Hurricane Andrew's Effect on Manufactured Housing in Florida and Louisiana, for U.S. Dept. of HUD, Sep. 1992, Rev. Oct.1992, Washington, DC.

[9] Cook, Ronald A., Hurricane Andrew: Summary of Damages to Conventional Residential Structures, Florida Dept. of Community Affairs, Sep.24, 1992, Univ. of Florida, Gainesville, FL.

[10] American Plywood Association (APA), Hurricane Andrew: Structural Performance of Buildings in Southern Florida, APA T92-21, Sep.1992, Tacoma, WA.

[11] Cook, Ronald A., Hurricane Andrew: Recommendations for Building Codes and Building Code Enforcement, Florida Dept. of Community Affairs, Jan.31,1993, Univ. of Florida, Gainesville, FL.



FIGURE 1
Manufactured home park, Homestead, Florida



FIGURE 2
Damage to site-built homes, Homestead, Florida



One of the thousands of manufactured homes destroyed by Hurricane Andrew

FIGURE 3



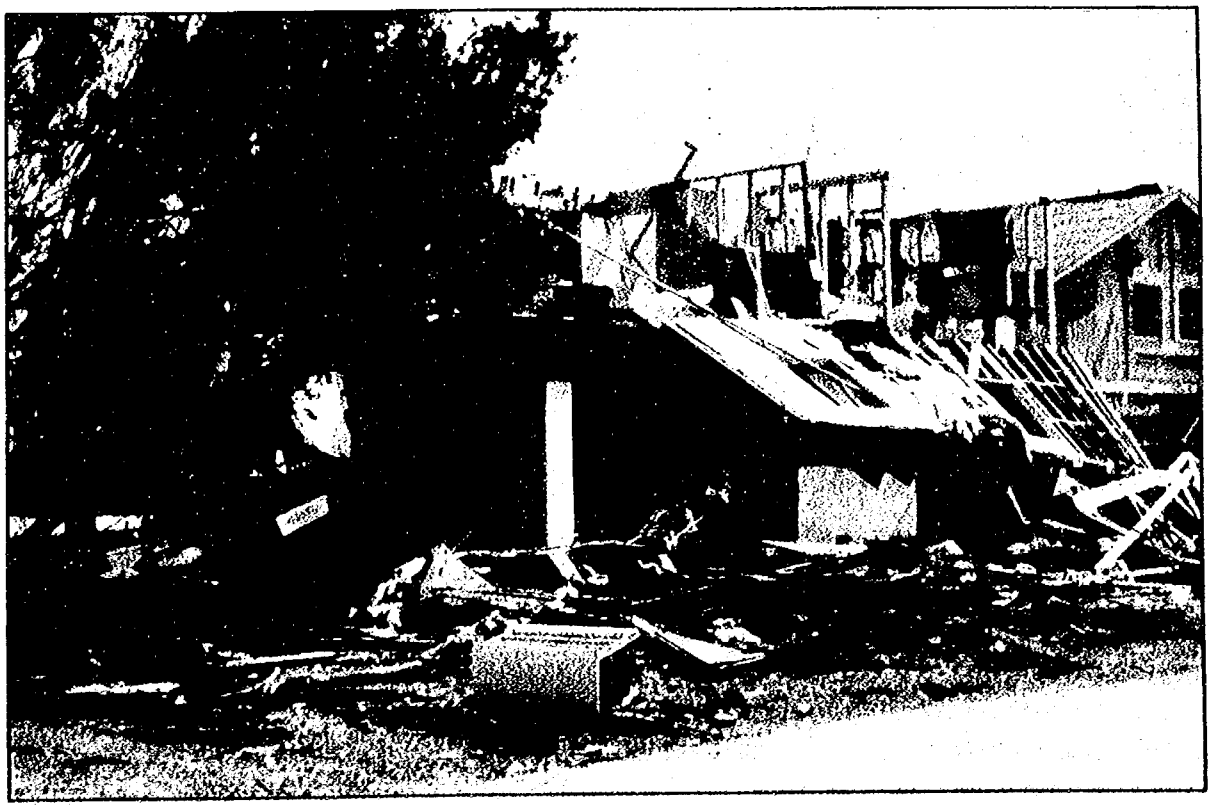
Destroyed manufactured homes contributed significantly to the amount of debris left by the storm

FIGURE 4



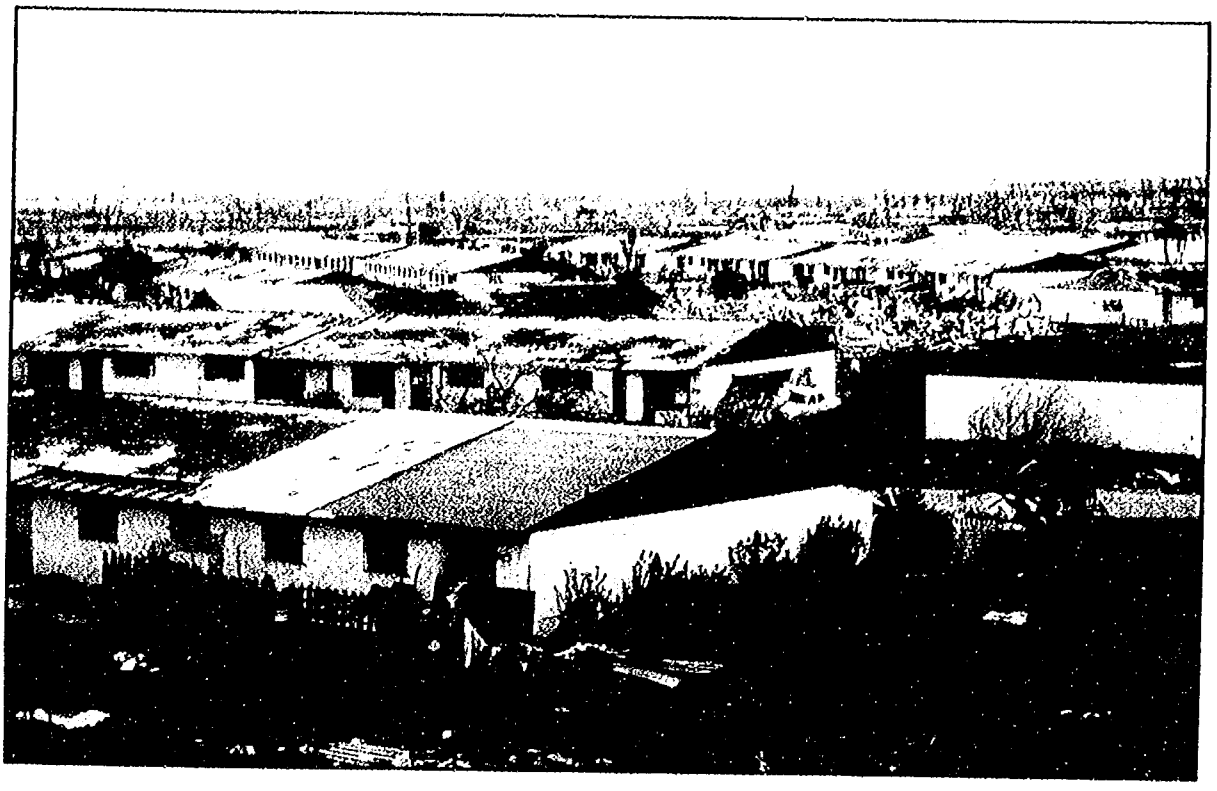
Structural damage similar to that found at many homes

FIGURE 5



The 140-plus mile-per-hour winds of Hurricane Andrew left very few homes in the area unscathed

FIGURE 6



Most of the homes in the disaster area had extensive roof damage
FIGURE 7

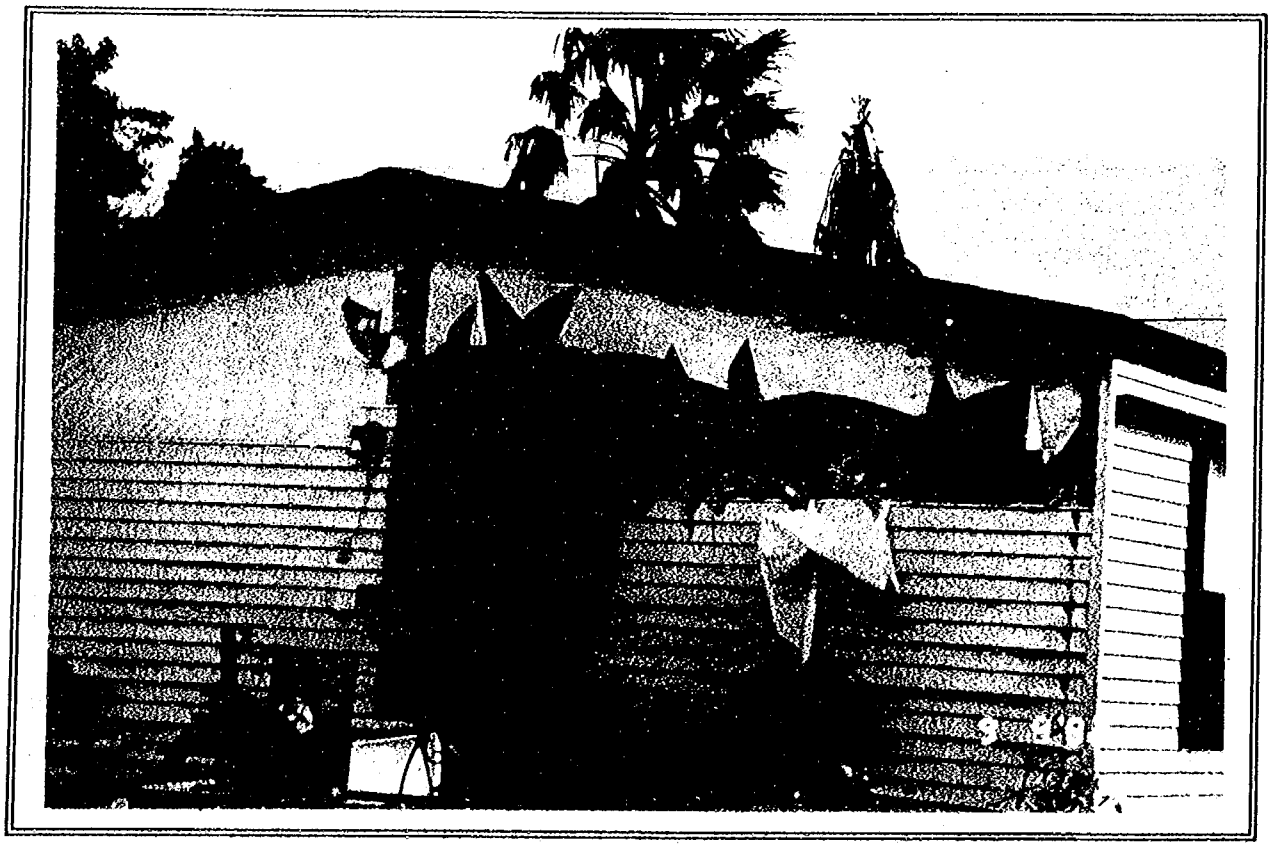


FIGURE 8 Failure of siding connections at end wall of home

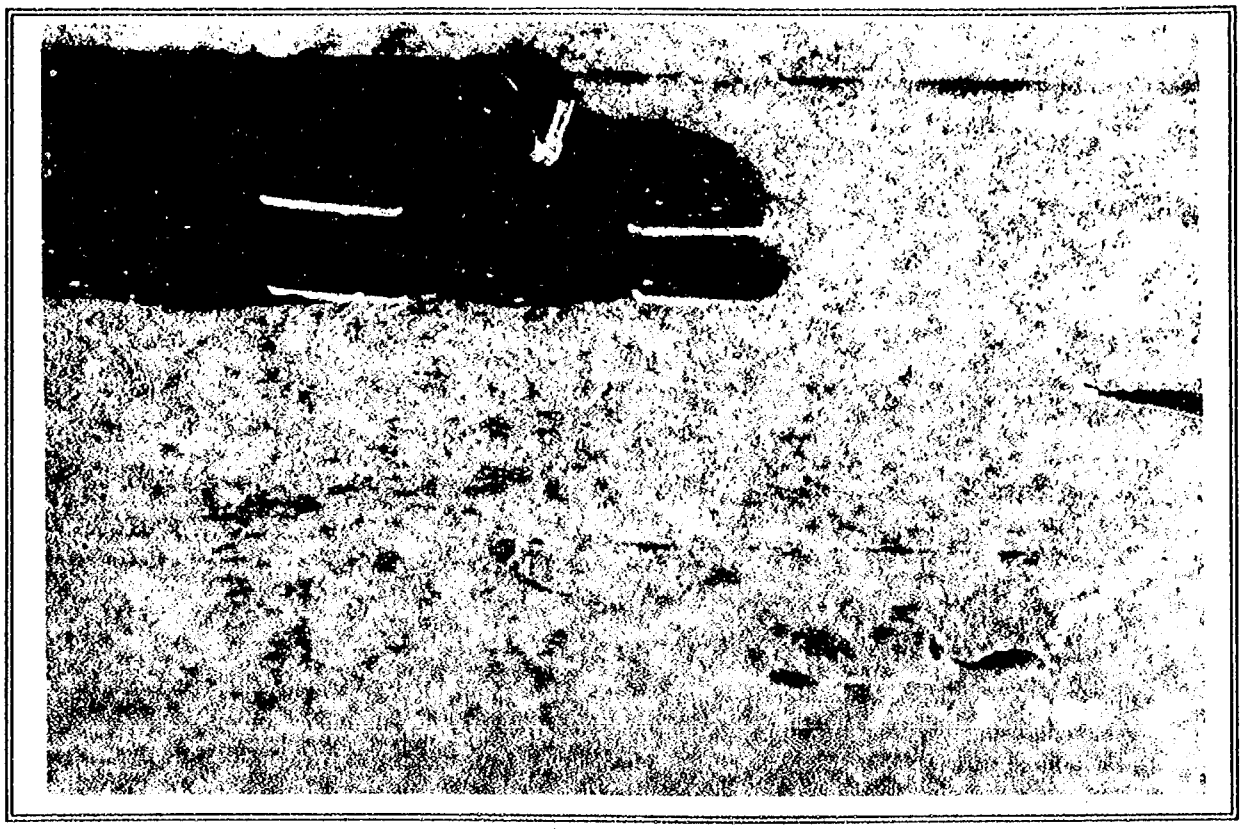


FIGURE 9. Roof, showing damaged and missing shingles

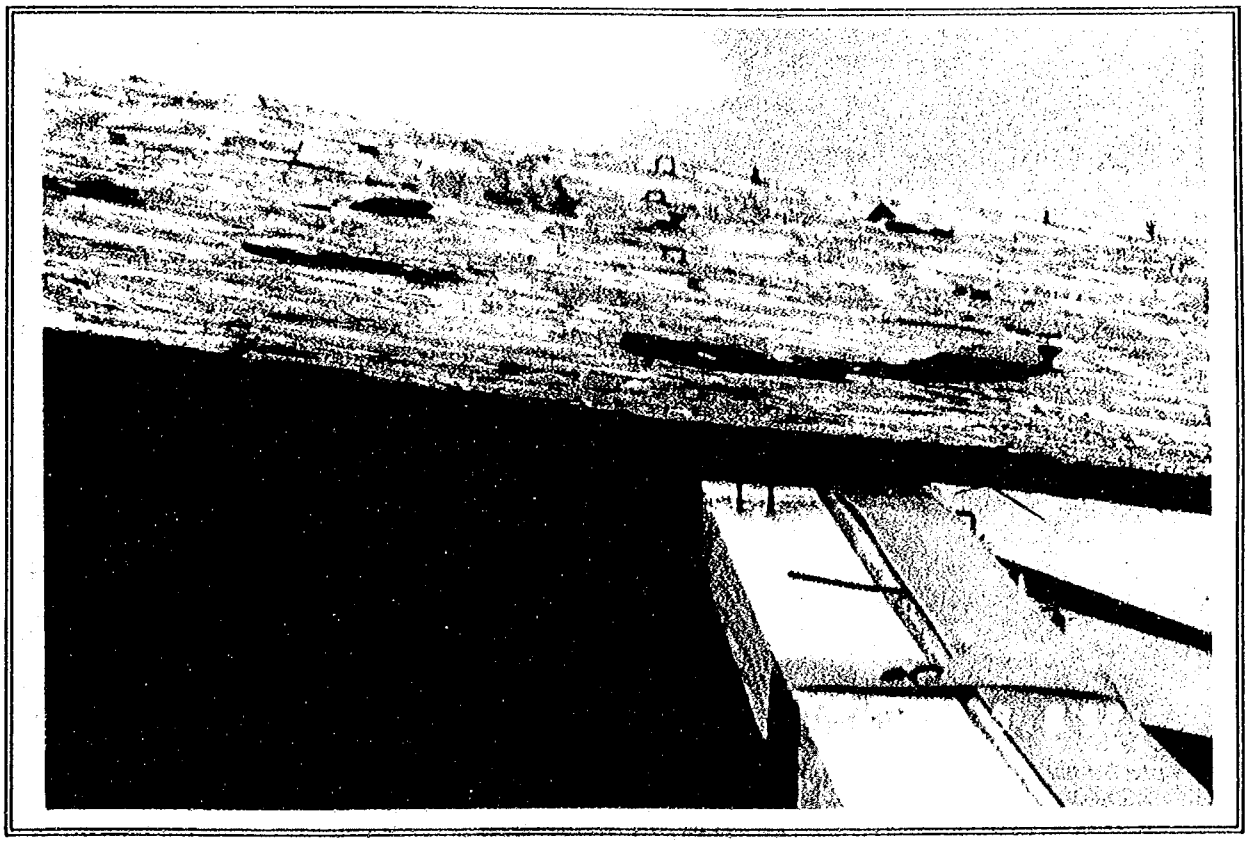
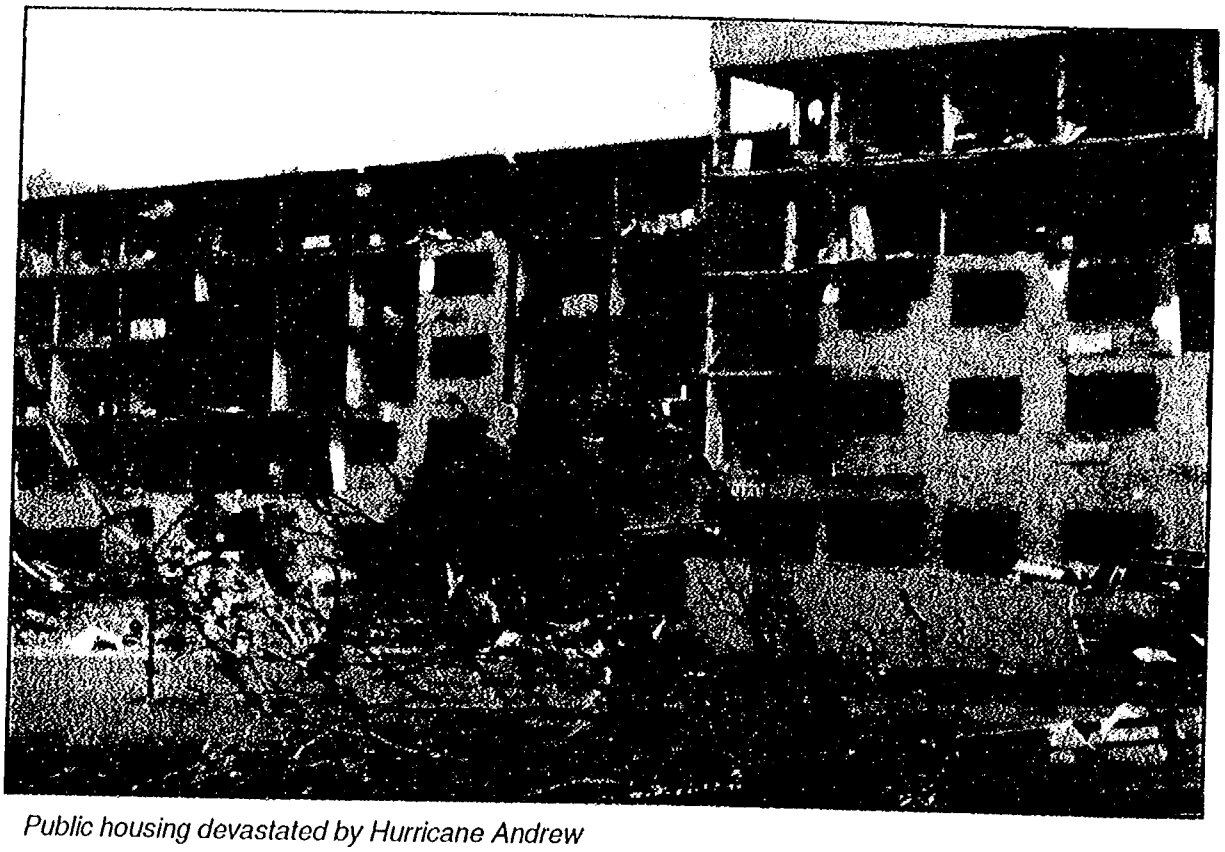


FIGURE 10. Staples protruding from surface of roof sheathing



Figure 11. Typical gable-end wall failure. Roof sheathing blown off adjacent to gable-end wall, resulting in failure of gable-end wall framing and "domino" collapse of adjoining trusses.



Public housing devastated by Hurricane Andrew

FIGURE 12.

TABLE 2. SUMMARY OF WIND SPEED OBSERVATIONS IN HURRICANE ANDREW

ID No.	Station	Sustained (knots)	Peak Gust (knots)	Direction (degrees)	Anemometer Height (m)	Time (GMT)	Pressure (mb)	Time (GMT)
1	Fowey Rocks C-MAN (25.59 N 80.10 W)	123 (2-min)	147 (1)	23	43.9	0800	967.5	0800
2	Miami WSFO/NHC	100	142 (2)		46	0850	982	0900
3	Miami International (MIA)	75	100 (3)		6.1	0950	992.6	0900
4	Virginia Key (25.79 N 80.25 W)	85	98	109	15	0930	992	0830
5	Miami Beach DARDC	65	92			0816		
6	Haulover NOS NGWLMS (25.90 N 80.12 W)	58	85	100	10	0900		
7	Turkey Point FLP (10 m) (25.40 N 80.34 W)		85 (1)	35	10	0820		
8	Turkey Point FLP (60 m) (25.32 N 80.38 W)		83 (1)	290	60	0825		
			64 (1)	280	10	0848		
9	Fort Lauderdale	66	76					
10	Tamiami Airport (TMB)	50	70 (1)		6.1	0833	988	
11	Molasses Reef C-MAN (25.01 N 80.38 W)	48 (2-min)	60	209	15.8	1000	998.5	0900

Notes: (1) Equipment failed shortly after observation - subsequent speeds probably higher.
(2) Anemometer mounted on mast atop 13-story building.
(3) Estimated values - equipment inoperable at time of Hurricane Andrew.

TABLE 3. ESTIMATED WIND SPEEDS FOR SELECTED LOCATIONS IN HURRICANE ANDREW

Location	Estimated Fastest-Mile Speed (mph)	
	Reinhold et al.	Powell
Key Biscayne (south tip)	135	145
Cutler Ridge Office Building	140	
Country Walk	133	130
Tamiami Airport	130	127
Homestead AFB	132	
Homestead	125	
Florida City	120	
Turkey Point	132	110

Appendix

Task Committees Reports

Report of Task Committee on

(A) STRONG MOTION DATA AND APPLICATIONS

(Consolidated Task Committees A and E)

Date : May 17, 1993

Place : Public Works Research Institute, Tsukuba, Japan

Attendees :	Japan Side	S. Noda (Chairman)	(PHRI)
		K. Kawashima	(PWRI)
		S. Iai	(PHRI)
		H. Ohtsuka	(PWRI)
		T. Hoya	(GSI)
		H. Mizuno	(BRI)
		Y. Kitagawa	(BRI)
	U.S. Side	A.G. Brady (Chairman)	(USGS)
		A.G. Franklin	(CORPS-WES)
		J.R. Hill	(DOE)
		C.E. Smith	(MMS)
		S.D. Markwell	(BuRec)

The Consolidated Task Committees A and E recommend
(1) merging of the Task Committees A and E,
(2) the election of Dr. Setsuo Noda as Chairman for the Japan side and Dr. A.G. Brady as Chairman for the U.S.side , and
(3) the adoption of the name of the new Task Committee as "Strong Motion Data and Applications".

The new Task Committee adopts the following objective and scope of work.

MISSION STATEMENT

1. Objective and Scope of Work

The objective of the Task Committee is (1) to coordinate and promote sharing of strong motion earthquake data among researchers and practicing engineers and (2) to develop techniques and exchange information for evaluating the destructive effects of earthquake motions.

The scope of work includes
(1) instrumentation,
(2) recording, processing and analyzing of strong-motion data,
(3) engineering characterization of ground motion,
(4) design applications, and
(5) seismic zonation.

The activities of the Task Committee include

(1) regular exchange of data and publications,
(2) creating procedures for the dissemination of significant strong-motion digital data with regard for the rights and expectations of (a) owner, (b) the users of data and (c) the earthquake engineering community,
(3) planning and conducting T/C workshops and meeting, and
(4) coordinating relevant research activities.

2. Accomplishments

(1) Catalogs of strong-motion earthquake records both in the U.S. and Japan were exchanged. U.S. data are published in the "Seismic Engineering Program Report" and the Japanese data are published in the "Strong Motion Records in Japan." Many other publications were also exchanged.

(2) Extensive planning and preparation have been made for a Japan - U.S. Workshop on Strong Earthquake Motion to be held in December 1993.

3. Future Plans

(1) The (new) Task Committee A will organize a Workshop on Strong Earthquake Motion in December of 1993, co-sponsored by the Science and Technology Agency of Japan and various U.S. funding agencies.

(2) A digital version of a earthquake motion recovered by the Building Research Institute, japan, during the 1993 Kushiro-Oki Earthquake of magnitude 7.8 will be made available to the U.S. side.

Report of Task Committee on

(B) TESTING AND EVALUATION PROCEDURES FOR BUILDING SYSTEMS

Date: May 17, 1993

Place: Public Works Research Institute, Tsukuba, Japan

Attendees:

Japan Side -	K. Ohtani (Chairman)	(NIED)
	H. Yamanouchi	(BRI)
	S. Nakata	(BRI)
	S. Okamoto	(BRI)
	Y. Yamazaki	(BRI)
	T. Murota	(BRI)
	H. Sato	(PWRI)
U.S. Side -	H. S. Lew (Chairman)	(NIST)
	N. Raufaste	(NIST)
	G. R. Fuller	(HUD)
	R. D. Hanson	(UM)
	J. D. Cooper	(FHWA)
	C. Rogers	(VPISU)
	M. Shinozuka	(PU)
	R. C. Murray	(LLNL)

To reflect its expanded role, Task Committee B proposed to change its title and the scope of work. The Task Committee adopts the following objective and scope of work.

MISSION STATEMENT

1. Objective and Scope of Work

The objective of the Task Committee is to develop rational test procedures and to collect performance data of dynamic response

of structures through both laboratory testing of prototype structures and field testing of structures in situ.

The scope of this Task Committee includes the following:

(1) Plans and conducts workshops and joint meetings to identify research topics and develops joint research programs.

(2) Coordinates research projects carried out by various laboratories in the U.S. and Japan. Facilitates publication of research results and implementation of findings in codes and standards.

(3) Facilitates exchange of research personnel, technical information and available testing facilities.

(4) Develops uniform testing procedure including test loading history for ease of comparison of results of tests carried out by various researchers, and for establishment of data base.

(5) Develops guidelines for interpretation of test results in consideration for design of structures.

(6) Develops methodology for evaluation and interpretation of physical test results.

2. Accomplishments

(1) The third U.S. Technical Coordinating Committee meeting on Precast Seismic Structural Systems Program (PRESSS) was held in October 1992 at San Diego, California.

(2) The third U.S.-Japan Joint Technical Coordinating Committee meeting on PRESSS was held in November 1992 at San Diego, California.

(3) The Japan PRESSS Research program was completed in March 1993.

(4) The joint U.S.-Japan workshop on composite and hybrid structural systems was held in September 1992 at Berkeley, California. The program recommendation has developed and has been forwarded to the Task Committee B for its endorsement.

(5) The second U.S. planning meeting on composite and hybrid structures was held in February 1993 at Seattle, Washington. Several Japanese researchers participated in the meeting.

3. Future Plans

(1) The second phase of the U.S. PRESSS research program is in progress and is expected to complete in 1994. The third phase will begin in 1994. The U.S. Technical Coordinating Committee meeting will be held in the fall of 1993.

(2) The fourth U.S.-Japan Joint Technical Coordinating Committee meeting on PRESSS will be held in Japan in November 1993.

(3) With the endorsement by the Panel of the joint research program on composite and hybrid structures, Phase V of the U.S.-Japan Joint Research Program will initiate in 1994.

(5) In support of the International Decade for Natural Disaster Reduction (IDNDR) Program, techniques will be explored to disseminate findings of the Joint Research Projects carried out under auspices of T/C "B" to countries with high seismic risks.

Report of Task Committees on

(C) DESIGN, EVALUATION AND IMPROVEMENT OF STRUCTURES
(Consolidated Task Committees C and D)

Date: May 17, 1993

Place: Public Works Research Institute, Tsukuba, Japan

Attendees: Japan Side:	H. Yamanouchi (Chairman)	(BRI)
	Y. Yamazaki	(BRI)
	T. Murota	(BRI)
	S. Nakata	(BRI)
	S. Okamoto	(BRI)
	H. Sato	(PWRI)
	K. Ohtani	(NIED)
U.S. Side:	G.R. Fuller (Acting Chairman)	(HUD)
	R.D. Hanson	(Univ. of Michigan)
	C. Rogers	(VPI)
	R.C. Murray	(DOE)
	M. Shinozuka	(Princeton U.)
	J. Cooper	(FHWA)
	H.S. Lew	(NIST)
	N. Raufaste	(NIST)

MISSION STATEMENT

Members of Task Committees "C" and "D" agreed that a new T/C on Design, Evaluation and Improvement of Structures shall be established by combining present T/Cs "C" and "D". This decision was based on the eliminating the duplication of both Task Committees.

1. Objective and Scope of Work

The objective of this Task Committee is to develop disaster mitigation policies and programs which will improve the performance of new structures and the capacity of existing structures in resisting wind and seismic forces. In order to establish adequate evaluation of performance, each country will coordinate development of condition assessment, screening, and structural analysis and design methodologies. Enhanced performance can be obtained by the intelligent renewal, repair and retrofit of existing buildings and other structures. Structures will be analyzed and instrumented, and then evaluated after disasters. Also, effective utilization of new advanced materials and structural systems, associated with appropriate design methods, will provide excellent structural performance in the life cycle.

The scope of work includes:

(1) Exchanging information, planning, and hosting workshops on new design technologies, evaluation technologies, and repair and retrofit techniques.

(2) Developing a uniform system for screening and analyzing wind and seismic resistance capacity of structures in each country.

(3) Developing sensor technology, instrumentation, and "expert" systems to provide condition assessment of existing structures.

(4) Evaluating masonry, precast concrete and composite/hybrid building structures; and providing documentation for post-disaster evaluation of performance.

(5) Studying new materials and methods for repairing and retrofitting existing structures and for new construction.

(6) Coordinating research projects in the U.S. and Japan to minimize duplication and maximize benefits.

2. Accomplishments

(1) BRI sent to the U.S. side the BRI Report No. 132 which compiles "Design and Construction Guidelines of Medium-Rise RM Buildings" developed by TCCMAR-Japan under the U.S.-Japan Coordinated Program on Masonry Research.

(2) Continued U.S. research sponsored by NSF has developed several reports on seismic rehabilitation and retrofit strategies, including innovative techniques for strengthening existing buildings.

(3) Supported the first U.S. "Workshop on Smart and High Performance Materials and Structures" jointly with T/C "G," in May 1993.

(4) U.S. members provided copies of "Damage Assessment Reports for Hurricane Andrew and Hurricane Iniki," published by the Flood Insurance Admin. (FIA) of the Federal Emergency Management Agency (FEMA).

(5) Japanese members provided copies of a "Guidebook for Home Buildings," developed by the Building Center of Japan after Typhoon 9119, September 1991. The guidebook provides valuable information on design and construction of housing to resist strong winds.

3. Future Plans

The following plans were made to work on Design, Evaluation and Improvement of Structures under the new T/C.

(1) Develop a uniform system for screening and analyzing wind and seismic resistant capacity, and improve sensor/inspection technology, instrumentation and expert systems to provide condition assessment of existing structures.

(2) Compile a database of advanced materials/systems that have potential for improving structural performance of new construction, as well as for use in rehabilitating and strengthening existing buildings.

(3) Investigate new design methodologies based on required structural performance, which will also be able to deal with advanced materials and systems. In order to effectively take this new approach, it is recommended that each country should make an effort to establish a U.S./Japan joint study group of members of appropriate institutions in each country.

(4) Develop design guidelines for applying advanced structural and materials systems to be used for Composite and Hybrid Structures under the joint U.S./Japan Cooperative Research Program.

(5) Participate in activities of the International Decade for Natural Disaster Reduction (IDNDR), including the "World Conference on Natural Disaster Reduction," to be held in Yokohama, Japan in May 1994.

(6) Continue to encourage participation by private industry, consulting engineers, universities, State and local government agencies, and other Federal agencies involved in instrumentation, evaluation, condition assessment, and retrofit and strengthening of existing buildings for seismic and wind resistance.

(7) The second workshop on "Structural Control and Intelligent Material Systems" was discussed to be held in the U.S. during 1994, in coordination with T/C "G."

Report of Task Committee on

(D) DAM EARTHQUAKE ENGINEERING

Date: May 18, 1993

Place: Public Works Research Institute, Tsukuba Japan

Attendees: Japan Side–	A. Nakamura	(PWRI)
	I. Nagayama	(PWRI)
	T. Tomaru	(PWRI)
	M. Tamura	(PWRI)
	H. Nishida	(PWRI)
	N. Yasuda	(PWRI)
U.S. Side–	W. E. Roper	(COE)
	S. D. Markwell	(BR)
	N. J. Raufaste	(NIST)

MISSION STATEMENT

1.Objective and Scope of Work

The Objective of this Task Committee is to develop technical insights into better understanding of the response of dams to seismic effects. The Task Committee will plan, promote, and develop research initiatives to assist in assuring seismic safety and economical protective against earthquake loadings for these structures. Its scope of work includes:

(1)Methods of Analysis for seismic design of dams.
Comparison of design methods between U.S. and Japan.
Investigation of dynamic analysis methods as tools (modeling, calculation codes).

(2)Dynamic Characteristics of Dams Materials.
Strength and deformation characteristics during earthquakes (concrete, soil and rock).

(3)Analysis of observed behavior of dams during earthquake.
Investigation of the mechanism of damages against earthquake loading.
Application of the analysis of the observed behavior during earthquake to the earthquake–resistant design.

Scope of work, membership and other details of the Task Committee will be coordinated between U.S. and Japan sides.

Report of Task Committee on

(F) DISASTER PREVENTION METHODS FOR LIFELINE SYSTEMS

Date: May 17, 1993

Place: Public Works Research Institute, Tsukuba City, Japan

Attendees: Japan Side	Y. Iida	(Chairman)	(PWRI)
	K. Kawashima		(PWRI)
	O. Nakano		(HDB)
	H. Sugita	(Observer)	(PWRI)
	J. Hoshikuma	(Observer)	(PWRI)
U.S. Side	J. D. Cooper	(Acting Chairman)	(FHWA)
	N. J. Raufaste		(NIST)
	H. S. Lew		(NIST)

MISSION STATEMENT

1. Objective and Scope of Work

The objectives of Task Committee "F" are to improve: 1) the behavior of lifeline systems during earthquakes and 2) the engineering and other seismic countermeasures such as damage estimation techniques and inspection procedures. The scope of work includes planning to conduct workshops on lifeline systems, facilitating exchange of technical information and promoting development of standards for lifeline systems.

2. Accomplishments

(1) Conducted the 5th Joint Workshop on Earthquake Disaster Prevention for Lifeline Systems on October 26 and 27, 1992, at PWRI in Tsukuba, Japan.
The workshop was attended by 16 U.S. and 44 Japanese participants.

(2) The Proceedings of the 4th Workshop on Earthquake Disaster Prevention for Lifeline Systems, which was held in Los Angeles, U.S.A, August 1992, was published and distributed by the U.S. side (NIST).

(3) The Japan side provided the U.S. side with copies of the "Guidelines for Disaster Information Systems for Important Infrastructures" and "Guidelines for Seismic Design Methods of Large Underground Structures." These documents were developed as the final accomplishments of the research projects of the Ministry of Construction.

3. Future Plans

(1) Publish the Proceedings of the 5th Workshop on Earthquake Disaster Prevention for Lifeline Systems.

(2) The 6th Joint Workshop on Earthquake Disaster Prevention for Lifeline Systems is proposed to be held before the 26th Joint Meeting.

(3) Encourage current efforts in both countries to establish seismic design guidelines and standards for lifeline systems. Existing UJNR channels should be fully utilized to facilitate the exchange of relevant information concerning standards development. Possible collaboration of joint development of guidelines and standards for lifeline systems should be pursued.

Report of Task Committee on

(G)STRUCTURAL CONTROL AND INTELLIGENT MATERIAL SYSTEMS

Date: May 18,1993

Place: Public Works Research Institute, Tsukuba, Japan

Attendees:	Japan Side	Y. Kitagawa(Chairman)	(BRI)
		S. Unjoh	(PWRI)
		T. Murota	(BRI)
		H. Yamanouchi	(BRI)
		Y. Yamazaki	(BRI)
		S. Nakata	(BRI)
	U.S.Side	R.D.Hanson(Acting Chairman)	(UM)
		M. Shinozuka	(UP)
		C.A. Rogers	(VPI & SU)
		H.S. Lew	(NIST)
		R.C. Murray	(LLNL/DOE)

MISSION STATEMENT

The members of T/C "G" at the 25th Joint UJNR Panel meeting, PWRI, Tsukuba, Japan, 1993, adopted the new title for its Task Committee to be "Structural Control and Intelligent Material Systems," based on its evolving objectives and scope.

Objective and Scope of Work

The objectives of the Task Committee are to: (1)develop research plans in control of equipment as well as structures; and in high performance structural and material systems; (2)implement control techniques for motion reduction or modification; (3)implement use of advanced materials in actual design and construction of buildings and other infrastructure systems under seismic or wind environments; (4)promote U.S.-Japan cooperation in structural control and intelligent material systems research; (5)bring together governmental, academic, and industrial participants in joint pursuit of these efforts; and (6)contribute to IDNDR by organizing joint research and other technical activities in structural control and intelligent material systems research on the basis of international cooperation.

T/C "G" works closely with other organizations to provide the leadership in this emerging research by facilitating the exchange of technical data and information through UJNR mechanisms. Work includes:

(1)Providing technical assistance, consultation and coordination to UJNR affiliated research organizations in the initiation, development, and execution of their programs in research area.

(2)Promoting joint government-university-industry collaborative

efforts to facilitate technology transfer and practical implementation.

(3)Sponsoring and conducting inter-disciplinary workshops and meetings to identify key areas of research and opportunities for cooperation, and to exchange new knowledge and experience in practice.

(4)Developing promotional and demonstrative activities to stimulate public awareness and interest in this field of research.

(5)Providing information useful for the establishment of performance standards, design specifications, guidelines and code recommendations for application in new construction as well as retrofit/rehabilitation of existing structures.

(6)Initiating research in intelligent material systems, sensors, actuators, optimal control system design, and encourage laboratory and field experiments of prototype and full-scale structures.

2. Accomplishments

(1)With the encouragement of the Task Committee co-chair, the U.S. Panel on Structural Control Research worked closely with its counterpart Japanese Panel in exchanging technical information and developing joint research plans.

(2)The "2nd U.S.-Japan Workshop on Earthquake Protective Systems of Bridges" was held at PWRI, Tsukuba, Japan, on December 7 and 8, 1992. A technical tour to visit base-isolated bridges across Japan was conducted by participants following the Workshop. I. Buckle of NCEER and UJNR Panel members S.C.Liu, M. Shinozuka, K.Kawashima, and about 120 researchers from the U.S., Japan, and New Zealand participated in the technical activities. Proceedings of the Workshop is being prepared for publication by PWRI.

(3)Under the NSF initiative on "Structural Control Research for Safety, Performance, and Hazards Mitigation," sixty seven(67) proposals were submitted by the U.S. research community. Twelve grants were made in FY 92 of the 5-year program, and additional proposals are currently under review for funding in FY 93. These research efforts will form the foundation for Task Committee "G" cooperative research activities.

(4)In cooperation with Task Committees "C" and "D", a U.S.- Japan Workshop on Smart and High Performance Materials and Structures was held at BRI, Tsukuba, Japan on May 14 and 15, 1993. The workshop recommended that appropriate UJNR Task Committees encourage appropriate governmental organizations of both countries in collaboration with academic and private sector to take initiative for development of new cooperative research in this field of research.

3. Future Plans

(1)Planning efforts for U.S.-Japan cooperative research project on seismic response control are continuing. Research cooperation between the U.S. and Japan will be pursued using such channels as the UJNR and other inter-governmental mechanisms. Specific plans to promote "The U.S.-Japan Cooperation Research Project" on active and hybrid control systems are considered to be set by NSF, BRI, and PWRI.

(2)Joint research projects on active and hybrid control of buildings are being developed by BRI and NCEER.

(3)At BRI, research programs on structural control of buildings have been developed and implemented under the direction of UJNR member. Collaborative research programs involving possible organizations and private companies are being developed.

(4)Joint Research Program for Hybrid control of Bridges is being performed through T/C "G" by PWRI, NSF, FHWA, NIST, NCEER, and UC Irvine. Under this program, experimental studies are planned at PWRI and at NCEER (SUNY and Buffalo). The experiment at PWRI will test and confirm the effectiveness of the sliding base-isolation systems developed at NCEER. The experiment at NCEER similarly will test and confirm the effectiveness of variable damper system developed at PWRI. These experiments will begin in or after October 1993.

(5)In cooperation with T/C "J", A 3rd U.S.-Japan Workshop on Earthquake Protective Systems for Bridges is scheduled for February 1994, in the U.S.A. A technical tour to visit base-isolated bridges across U.S. is being planned for participants following the Workshop.

(6)A Workshop entitled "Structural Control and Intelligent Material Systems" will be held in the U.S.A. during 1994, in cooperation with appropriate Task Committees of the UJNR.

4. Other(Information Items)

(1)The NSF Research on Structural Control will hold its coordination meeting in Ann Arbor, on June 4 and 5, 1993.

(2)International Workshop on Structural Control will be held in Honolulu, Hawaii on August 4 and 5, 1993, with major participation by Japan and U.S.A.

(3)The First World Conference on Structural Control will be held in Pasadena, California in 1994.

(4)The Second International Conference on Intelligent Materials will be held in Williamsburg, Virginia in June 1994.

Report of Task Committee on

(H) SOIL BEHAVIOR AND STABILITY DURING EARTHQUAKES

Date: May 18, 1993

Place: Public Works Research Institute, Tsukuba, Japan

Attendees:	Japan Side –	H. Ohtsuka (Chairman)	(PWRI)
		A. Nakamura	(PWRI)
		O. Matsuo	(PWRI)
		S. Iai	(PHRI)
		H. Mizuno	(BRI)
		Y. Iida	(PWRI)
		Y. Koga	(PWRI)
	U.S. Side –	A.G. Franklin (Chairman)	(WES)

MISSION STATEMENT

1. Objective and Scope of Work

Government agencies responsible for public works must assure their seismic safety and provide for economical protection against earthquake hazards.

The objective of Task Committee(H) is to assist in meeting these needs by enhancing the available technology for predicting the dynamic behavior of soils, analyzing dynamic soil–structure interaction, and modifying the earthquake behavior of foundations and earth structures to assure their safe performance during earthquakes.
In accordance with the objective, the scope of activities of T/C(H) are:

(1)to present technical papers at annual joint panel meetings on technological developments and on state–of–the–art and practice related to soil behavior and stability during earthquakes,

(2)to exchange information and technical data relating to field performance, research, and methods of practice,

(3)to plan and conduct programs of cooperative research and/or workshops in

coordination with the proposed or ongoing programs, and

(4)to make other needed efforts including exchange of researchers between U.S. and Japanese research institutions, publication of research results and recommended practice.

2. Accomplishments

(1)The U.S. side provided to the Japan side copies of a new report of the U.S. Army Corps of Engineers and the U.S. Navy on seismic design of waterfront structupres.

(2)The U.S. side provided to the Japan side a recent report on liquefaction occurrences in the New Madrid area of the central United States.

3. Future Plans

(1)The Waterways Experiment Station has initiated a new research project "Repair, Evaluation, Maintenance, and Rehabilitation Research (REMR)" (for the U.S. fiscal years 1992 – 1996).

(2)The Public Works Research Institute and the Building Research Institute have initiated a new research and development project "Research and Development on Earthquake Disaster Prevention in Large Urban Area" (for the Japanese fiscal years 1992 – 1996).

(3)The National Research Institute for Earth Science and Disaster Prevention, the Building Research Institute and Wayne State University have initiated the cooperative research "Research on Earthquake Pile Resistance in Liquefied Soils."

(4)In view of the recently started three research projects in both countries, and other research programs which may be initiated, T/C(H) will identify research tasks on soil behavior and stability during earthquakes that are of common interest, and will seek to promote cooperative research on those tasks.

(5)T/C(H) tentatively plan to hold the next (third) U.S.–Japan Workshop on Remedial Treatment of Potentially Liquefiable Soils in Japan in summer 1994.

Report of Task Committee on
(I) STORM SURGES AND TSUNAMI

Date: May 20, 1993

Place: Public Works Research InstituteTsukuba, Japan

Attendees:	Japan Side ---	S. Tanaka(Chairman)	(PWRI)
		M. Okada	(MRI)
		T. Konishi	(MRI)
		T. Takayama	(PHRI)
	U.S. Side ---	W. E. Roper(Acting Chairman)	(COE)

MISSION STATEMENT

1. Objective and Scope of Work

The objective of Task Committee(I) is to mitigate damages from storm surges and tsunamis through shared technologies, research, information sharing, and cooperative work. Storm surges are caused by hurricanes and typhoons. Tsunamis are caused by underwater earthquakes, volcanic activities and land slides. Both hazards may cause serious disasters along coastal region.

The scope of work of this T/C is as follows:

(1) Exchange results of research on storm surge and tsunami occurrence, generation, propagation, and coastal effects. This includes observations on historical, current, and theoretical tsunamis. Of particular interest is the effort by U.S. and Japan to acquire deep ocean tsunami measurements.

(2) Exchange results and status of countermeasure against storm surge and tsunami activities including analysis of the problem, planning, warning, and engineering approaches.

(3) Exchange information on development of technologies such as computer programs to predict travel times, land-fall locations, run-up heights, and wave characteristics, improved instrumentation, and use of satellite communications for detection and warning.

(4) Facilitate dissemination through exchanges of literature, technical reports at joint meetings, special workshops, joint projects, and direct interaction among participants.

2. Accomplishments

(1) The 2nd tsunami workshop was held in Honolulu on November 5 and 6 1990.

(2) Field Observation Damages due to Flores Island Earthquake Tsunami of December 12, 1992, Numerical Simulation by Multi-layer Model for Storm Surge Generated by Ise-wan Typhoon, and Storm Surge Assessment for Hurricanes Andrew and Iniki were reported in this joint meeting.

3. Future Plans

(1) The 3rd tsunami workshop is planned to be held at Osaka on August 28, 1993. The numerical simulation model, deep sea gauge technology and mitigation of tsunami will be discussed in the workshop. A summary workshop report will be prepared.

(2) Planning is underway to conduct a joint workshop on Wind and Earthquake Engineering for Offshore and Coastal Facilities with Task Committee (K) in the United States during the fall of 1994. The focus of the workshop will be on storm surge issues.

(3) Exchanges of data and information on activities concerning to tsunami measurements including deep ocean measurements.

(4) 1996 will be the centennial anniversary of the great Sanriku Earthquake and Tsunami in Japan and the 50th anniversary of the April 1, 1946 Aleutian Earthquake and Tsunami. These events led to the establishment of warning system and much of the current activity in this field.
Task Committee (I) will plan a Joint Commemorative Symposium or other observance in memory of these events.

4. Other

(1) The Storm surge research community is less well organized and lacking the specialty societies, journals, and international organizations to define and stimulate work in the field. The Task Committee (I) can help fill this gap.

(2) The tsunami problem is less severe in the U.S. than in Japan which leads to a smaller community of researchers. There are few U.S. researchers focusing on tsunamis at any specific location; thus highlighting the importance of T/C periodic meetings and workshop.

Report of Task Committee on

(J) WIND AND EARTHQUAKE ENGINEERING FOR TRANSPORTATION SYSTEMS

Date: May 18, 1993

Place: Public Works Research Institute, Tsukuba Science City, Japan

Attendeess:	Japan Side	M. Fujiwara	(Chairman)	(PWRI)
		Y. Iida		(PWRI)
		O. Nakano		(HDB)
		K. Nishikawa		(PWRI)
		H. Sugita	(Observer)	(PWRI)
		J. Murakoshi	(Observer)	(PWRI)
	U.S. Side	J.D.Cooper	(Chairman)	(FHWA)

MISSION STATEMENT

1. Objective and Scope of Work

The objectives of this Task Committee are to plan, promote, and foster research on the behavior of highway bridges when subjected to wind and seismic forces and to disseminate research results and provide specifications and guidelines based on the Task Committee's finding. Surface transportation systems play a vital role in the movement of goods and people. Highway bridges are especially influenced by the forces of wind and earthquakes because of their open exposure to those forces. The scope of work is focused on highway bridges without limitation on their size and function. Existing bridge and new bridge designs and the behavior of whole bridge systems and/or single components of a bridge will be investigated.

2. Accomplishments

(1) In cooperation with Task Committee(G), the Japanese side hosted the second U.S.-Japan workshop on the Earthquake Protective Systems of Bridges at Tsukuba Science City, Japan in December 1992. A study tour followed to view bridge construction and base isolated bridges.

(2) Conducted research studies on seismic performance of bridge piers and columns. Details of this work involved determining the performance of steel and reinforced concrete piers and columns subjected to dynamic cyclic loading, performing model tests on the failure of reinforced concrete piers, testing full and large-scale concrete columns and for

the behavior of concrete filled steel tubes.

(3) Held the ninth bridge workshop in Tsukuba Science City, Japan in May 1993 which was followed by site visits to review construction progress of the Akashi Kaikyo Ohashi suspension bridge, the Higashi Kobe Ohashi cable stayed bridge, the Kansai international Airport bridge, the Tsurumi Fairway cable stayed bridge, and the Rainbow suspension bridge. 68 participants representing government, academia, industry and private practice presented 31 papers in 10 technical sessions.

3. Future Plans

(1) Conduct the 10th bridge workshop in Lake Tahoe, Nevada in conjunction with the 26th Joint Panel meeting in Gaithersburg, Maryland in May 1994.

(2) Continue to plan to host a Second U.S.-Japan Workshop on Seismic Retrofit of Bridges in the U.S. The workshop will focus on practical seismic retrofit measures.

(3) Continue to investigate and exchange technical information on improved seismic retrofit and strengthening procedures for highway bridges based on experimental, analytical, and field studies. This exchange should include information on maintenance of existing bridges.

(4) Continue experimental research on the seismic performance of bridge piers and columns, and encourage research on base isolation and hybrid control of bridges in cooperation with Task Committee(G).

(5) Develop a coordinated research study on seismic, aeroelastic, and aerodynamic response of cable-supported bridges with emphasis on cable inspection, vibration control, and corrosion protection.

(6) Continue the coordinated research study to compare the seismic design criteria for bridges in Japan and the U.S. and discuss the method and analysis procedures for bridge column design. Information on application of limit state design method continues to be exchanged.

(7) Encourage a coordinated research study on seismic response and control, system identification techniques, nondestructive evaluation of bridge structures, use and performance of structural materials including new materials, and performance of jointless bridges.

Report of Task Committee on
(K) WIND AND EARTHQUAKE ENGINEERING FOR OFFSHORE AND COASTAL FACILITIES

Date: May 18, 1993

Place: Public Works Research Institute (Tsukuba Science City)

Attendees: U.S. Side - C. Smith (Chairman) (MMS)
G. Brady (USGS)
W. Roper (CORPS)
Japan Side - T. Uwabe (Chairman) (PHRI)
S. Noda (PHRI)
S. Tanaka (PWRI)
S. IAI (PHRI)

MISSION STATEMENT

1. Objective and Scope of Work

Criteria for the design of offshore and coastal facilities may differ greatly from their onshore counterparts. These differences can arise due to their unique design or mass distribution, to the fluid/structure or wind/structure interaction, to the placement of foundation elements in or on soft, fully saturated soils that can be subject to large hydrodynamic pressures, and to the lack of specific environmental data or the engineering experience that has been developed for most onshore sites.

The objective of this Task Committee is to develop technical insights necessary to mitigate damage to offshore and coastal facilities due to extreme wind and seismic effects. The Task Committee will plan, promote, and develop research initiatives to meet this objective, and will disseminate the results of their research for incorporation into future specification or design guidelines. Items of specific interest include the following.

(1) Sponsoring and conducting workshops and meetings to identify key area of research, opportunities for cooperation, and the exchange of knowledge.

(2) Predicting strong ground motions for offshore and coastal sites including assessing the effects of basin geometry, linear, and nonlinear local geological effects using actual seafloor response measurements.

(3) Determining the dynamic response and the interaction of structure/foundation/soil systems to seabed motions and/or extreme wind forces.

(4) Assessing the dynamic response and behavior of various operational facilities mounted on offshore and coastal structures.

(5) Developing assessment methodologies for seismicity and other characteristics of potential seismic sources (e.g.faults) for offshore and coastal sites in regards to how these conditions relate to structural design criteria.

(6) Promoting the implementation of new research results into current design and construction

processes.

(7) Developing research efforts to include laboratory and field programs to obtain data on the response of offshore and coastal facilities to extreme wind and seismic forces.

(8) Creating performance standards, design specifications, guidelines, and code recommendations for application to new construction as well as remedial action for existing facilities.

2. Accomplishments

The U.S./Japan Workshop on Wind and Earthquake Engineering for Offshore and Coastal Facilities was held at the PHRI, Yokosuka, Japan on May 12 and 13, 1993.

3. Future Plans

(1) Hold a U.S./Japan Workshop on Wind and Earthquake Engineering for Offshore and Coastal Facilities in the U.S. in the fall of 1994. This will be a joint workshop with Task Committee (I) Storm Surge and Tsunami

(2) Develop workshop agenda and finalize list of speakers from both the U.S. and Japan Side.

(3) The first Workshop Proceedings will be published, and made available for distribution by NIST.

(4) Coordinate, where possible, on-going research on wind and earthquake engineering for offshore and coastal facilities of interest to the members of the Task Committee.

Technical Site Visits

Technical Site Visits 22-28 May 1993

by
Noel J. Raufaste
Secretary-General, U.S.-side Panel on Wind and Seismic Effects
Building and Fire Research Laboratory
National Institute of Standards and Technology

Introduction

Japan is composed of four main islands; Hokkaido, Honshu, Shikoku, and Kyushu and further south the small island of Okinawa (lining north to south respectively). The islands are divided into 8 Districts or Regions: Hokkaido; Tohoku, Kanto, Kinki, Chubu, Chugoku, Shikoku, and Kyushu. These regions in turn are divided into 47 Prefectures. Regions are analogous to States and Prefectures to Counties. Each of the eight regions has a Regional Construction Bureau which reports to the Ministry of Construction (MOC). These Bureaus construct and maintain highways, flood control works, dams, and bridges. Prefectures' design and construction work is funded by the National Government and by their own jurisdictions.

In addition, there are several public corporations responsible for specific construction projects. The corporations participating in the technical site visits include the Japan Highway Public Corporation, Honshu-Shikoku Bridge Authority, and the Housing and Urban Development Corporation. They report to the MOC. Each receives a small percent of funding required for their construction projects as direct funding from the National Government. Loans from the National Government and Prefecture Governments and from private sources make up the remaining 90 to 95 percent of construction monies needed for each project. These loans must be repaid with interest within 30 years.

To gain a perspective of the MOC's public works construction funding; in 1991 their budget was $190 billion (21,000 B yen). For the same year, Japan's National Budget represented $640 billion (70,347 B yen). MOC receives about 30 percent of the National Budget for public works construction.

During the 25th Joint Panel Meeting 14 technical sites were visited. They are identified in figure 1.

Technical Site Visits

1. Miyagase Dam Construction Site. This site is on the Nakatsu River about 50 km southwest of Tokyo. The dam is under construction by the Ministry of Construction (MOC) through their Miyagase Dam Construction Office. When completed the dam will be the largest roller compacted concrete (RCC) dam in the world and sixth largest dam in Japan. It is a concrete gravity dam 155 m high, 400 m long with a concrete volume of 2 million m^3. The reservoir's capacity is 193 million m^3 with a catchment area of 214 km^2. The total construction cost is $2.5 billion (280 B yen); about 36 percent is funded by the National

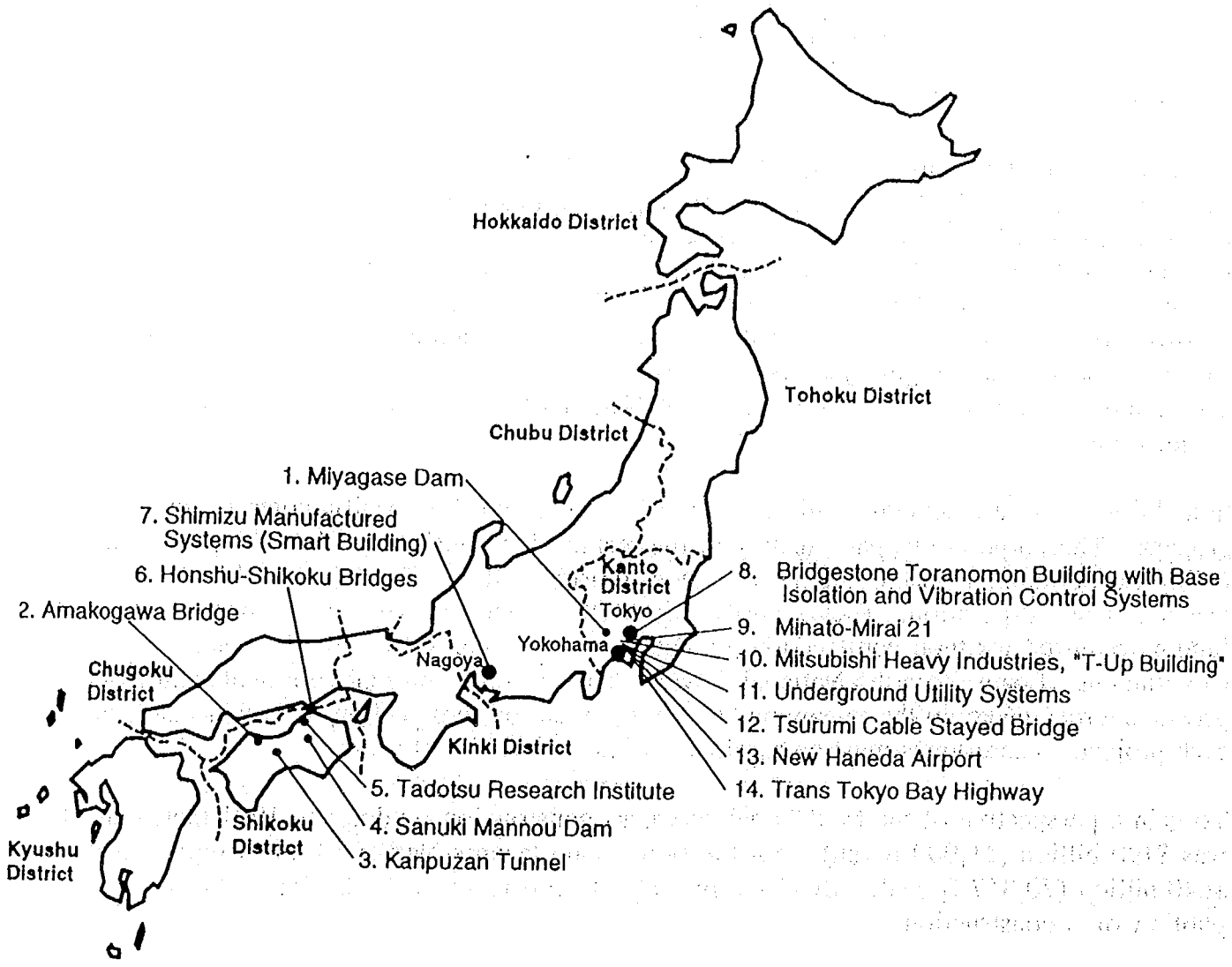


Figure 1. Sites visited during 25th Joint Meeting of Panel on Wind and Seismic Effects

Government, the remainder through loans.

Unique features of this construction project include:

- dam is designed for maximum earthquake of M7.8,
- guideway ramp system used to raise and lower 20 ton trucks with the RCC for the main structure,
- base rock material is high quality welded volcanic tuff,
- construction of 33 km of new road, 16 tunnels, and 100 bridges,
- two resettlement areas for 286 families were constructed on higher ground and local cemeteries in the flood area were relocated.

The construction sequence involves placement of 75 cm layers sequentially across the main structure in four equal sections in a four day cycle. In total, 4,500 m^3 of concrete are placed daily. Next vertical stainless steel joints, placed by a vibrating joint cutter, assist in water seepage control and structural strength. After placement of the joints, RCC is compacted by a 10 ton vibrating roller compactor for five cycles (10 passes) and 1 cycle (2 passes) with a seven-ton vibrating roller finishing compactor.

The compacted RCC cures for 2-3 days before placement of the next lift. Very careful surface cleaning, polishing, and wetting is completed before placement of the next lift.

Planning for the project started in 1971; construction will be completed in 1995. Full pool is expected to be achieved by 1999. Areas of controversy that delayed the overall project centered on the relocation of local residences and the preservation of cemeteries.

The Miyagase Project is part of an integrated water supply, flood control, and power generating system on the Doushi, Nakatsu, and Sagami River system. The Miyagase Project is connected above and below the dam structure by headraces to the Doushi River and Doushi Reservoir.

2. Amakogawa Bridge. The Amakogawa Bridge is part of the new Shikoku Longitudinal Expressway (Matsuyama Expressway) in the northwestern part of Shikoku in the Ehime Prefecture. This route is a succession of tunnels and bridges through a mountainous region. Tunnels are drilled and blasted. Along a 9 km stretch of this Expressway are five bridges under construction. The delegation visited one of these bridges, the Amakogawa Bridge.

The bridge is a Langer type reinforced concrete arch bridge with prestressed concrete stiffening girders spanning a 65 m- deep V-shape valley. The construction method uses a balanced cantilever attached to a buttress on both sides of the valley using temporary stay cables. Overall, the bridge will be 176 m long; with an arch of 116 m. The arch rib is connected to the stiffening girder by vertical columns. The rib consists of linear members whose gradients change at the vertical column. The stiffness of the arch rib is less than that of the stiffening girder. Bending moments in the linear arch rib member are small so the ribs act as axial force members. Taisei Corporation is the contractor.

The construction cost of the expressway is $36 million (4 B yen) per km. This cost includes the construction and land acquisition. The latter represents 1/3 of the total cost. About 5% of the costs are provided directly from the National Government, the remainder is borrowed with interest during its 30 year repayment period.

This expressway is managed by the Japan Highway Public Corporation (JHPC). JHPC constructs and operates toll roads including national expressways since it was created in 1956. Over 11,000 km of national expressways have been constructed in Japan. New expressways are generally traversal routes passing through mountainous regions and ring roads around large cities. JHPC reports to the Roads Bureau of the MOC. The MOC approves JHPC's management and its Board.

Expressway tolls, parking lot fees, and rent from expressway associated facilities repay the borrowed money used for construction and operation for all National Highways. A toll of about $0.21 (23 yen) is charged for each km. Research and testing is performed at the JHPC Engineering Department in Tokyo.

3. Kanpuzan Tunnel Construction. This tunnel is part of the over 100 km National Highway 194 that connects the northern coast of Shikoku with its southern coast. The highway traverses through steep mountains and valleys. Highway 194 often is closed during December through March due to inclement weather. This tunnel is designed to eliminate the road closing due to snow and ice. With this 6.4 km tunnel, the highway is expected to be open throughout the year.

Tunnel excavation is performed by the drill and blast method using four drill cuts. A 4.7 m diameter working tunnel first was excavated to map the geology and to dewater the tunnel. The 9 m diameter main tunnel is being constructed 25 m on center following the working tunnel. The main tunnel is cut by the Austrian tunnelling method. First the upper section is cut then the lower section. Support is provided by rock anchors and by steel ribs on 1-meter centers followed by shotcrete. The concrete liner is 30 cm thick. About 4 m of the tunnel is drilled and blasted each 20 hour day (2-10 hour shifts). Ventilation is provided from the top. The cost of the tunnel is $200 million (22 B yen).

4. Sanuki Mannou Arched Embankment Dam. The Sanuki Mannou National Government Park contains the Mannou Lake, the Prefecture's oldest and biggest reservoir. It was originally constructed in 821. In this part of Japan, rainfall averages 1.6 m per year. Water shortages for domestic use and agriculture necessitated construction of reservoirs. Over 16,000 ponds, some small, are in the island of Shikoku. The reservoir is adjacent to an 350 ha park being developed into a recreation area.

Mannou Lake is retained by an earth fill embankment 32 m high and 150 m in length. The outlet works consists of a control structure tunneled through the left abutment. A spillway (uncontrolled overflow) is located in the right abutment. At first glance this looks like a typical arched embankment dam; however, the uniqueness lies in the history of the site. Dam construction at this site was first initiated prior to the 14th century for the same purpose it serves today.

In the early 1300s, Chinese dam technology was introduced to Japan. It featured arched dam construction and a multi-level control structure which allowed the release of surface waters of the reservoir required by the rice fields. The waterways through the structures and the inclined multi-level outlet works were made of wood. Replacement of the structures were required about every 14 years. Previous structures although lower than the present embankment suffered overtopping and replacement many times in past history. Today's embankment is a modern structure that was built downstream of the previous structures.

5. Tadotsu Research Institute. This institute is part of the Nuclear Power Engineering Test Center (NPETC). Tadotsu operates the largest shake table in the world. The welded-steel vibration table is 15 x 15 x 3.5 meters; it was completed in 1982 at a cost of $230 million (25 B yen). The table has two degrees of freedom in the x and y directions and maximum excitation force of 3,000 ton and 3,300 ton respectively. It is set in a concrete foundation, 90 m in length and 43 m in width weighing about 150,000 tons.

Funding for construction of this facility was provided by the National Government (50%) and by the Japanese Power (electric) Company (50%). The facility's prime function is to test the effects of earthquake ground motion on large scale models of nuclear plant containment structures and components. An electric hydraulic servo system is used to apply the excitation force. With its 1000 ton loading capacity it can exert a maximum of 2.72 g horizontal and 1.36 g vertically. The facility's data analysis room is air suspended to avoid vibrations during routine testing. Tests have been conducted at a steady rate of one per year since its completion 11 years ago.

To demonstrate to the public the safety of nuclear power plants, the Institute performed two-stage tests on a two-story fully-furnished home built to the Japanese building code. A video tape was made and distributed to the media and to local public interest groups. The film showed damage experienced by the residential home based an a Kanto type earthquake of magnitude 7.9 and even greater damages sustained after more severe loadings. The latter are loads applied to nuclear power plant components. While this series of tests convinced the public that nuclear power plants were receiving sufficient design safety attention, the public may question the safety of their housing during a similar earthquake since this test home suffered considerable structural damage to render it unlivable.

Tadotsu's current schedule of tests shows work for another 5 years. As fewer reactors are expected to be constructed in Japan, future work of this type will begin to decline by the end of this decade. The facility is available for use by private firms. Costs per test range between $2.4-3.3 million (270-360 million yen).

6. Honshu-Shikoku Bridges. The Honshu-Shikoku Bridge Project consists of three major routes. From east to west they are the Akashi-Kaikyo Bridge (world's longest suspension bridge with center span of 1990 m when completed in 1998). The middle route, the Kojima-Sakaide Route, also known as the Seto Ohashi Route which means honorable bridges over the Seto Sea, consists of seven bridges; 3 suspension, 2 cable stayed, a truss, and viaduct. This route was completed in 1988. The western route is the Onamich-Imabari Route planned only for highway traffic. The Route consists of nine bridges; it is scheduled for completion

in 1999.

The delegation visited the 13.1 km Kojima-Sakaide Route over the Seto Inland Sea. Its construction costs were $10.3 billion (1,130 B yen). A four lane highway is on the upper level and a double track for conventional trains and a future Shinkansen (bullet) train is on the lower level. At the Honshu side of the bridge complex, is the Washuzan Tunnel. It was constructed to accommodate the highway traffic traveling above the railroad in the same configuration as on the double deck bridges.

The cross section of the suspension bridges are 35 m, the towers are 137 m above sea level. The twin cable stayed bridges are 27 m wide and 148 m high. The suspension bridges traversing the navigation lanes are 65 m above sea level. The deepest foundation is 50 m below sea level. These bridges were designed to withstand an earthquake of magnitude 8. Over 200 construction contractors were involved in the project; a large number considering each firm worked with three or more organizations and this was one of the three largest construction projects of the late 1980s.

The management of this project was performed by the Honshu-Shikoku Bridge Authority (HSBA) who reports to MOC for highway planning and construction and to the Ministry of Transport (MOT) for planning and constructing the railroad. In addition, agreements had to be made with the Ministry of Finance. HSBA was created in 1970. It is responsible for all toll highways and railways which link Honshu and Shikoku Islands. HSBA is responsible for the design, construction, management, maintenance and operation, and research and development of these three Routes.

Funding for this project relied on 55 percent [$5.7 billion (621 B yen)] from National and local governments with highway construction responsibilities and 45 percent of the total construction costs [$4.6 billion (509 B yen)] from railroad counterpart organizations. In both cases, the National Government provided direct funding of 4.8%. Local Governments contributed 2.5 percent to construct the highways. Borrowed money came from governmental accounts, from guaranteed bond and government guaranteed loans for a little more than 50, percent and private bonds and bank loans for a little over 40 percent of the overall construction costs.

7. Shimizu Manufactured System by Advanced Robotic Technology (SMART). This commercial office building is under construction in Nagoya by the Shimuzu Construction Engineering Corporation. As an experiment, Shimizu is integrating research, development, and engineering of advanced construction technologies. Twelve stories of the building's 20-story steel structure were completed. The building's dimensions are 24 m x 30 m and 88 m high. The construction technique includes installing prefabricated structural columns and beam system, curtain walls, and piping, and interior wall units. Following completion of site preparation, foundation, and 2-story basement, the roof and "top hat" section were constructed complete with computer control, lifting cranes and bridges, and enclosed construction areas. The "top hat" section (38 m high) included a jacking and lift system that uses four towers each with 300 ton lift capacity (each tower has 3-120 ton hydraulic jacks). The "top hat" becomes a 'manufacturing plant', a control room with two operators who

maneuver the cranes and hoists bringing prefabricated material into the first floor area, transferring it by another crane across and up the building exterior to the work floor and set in place with precision. Welding connections is accomplished by a robot welder completing three passes of full penetration as a continuous weld. Curtain walls and HVAC systems are installed and the unit jacked to the next story. Construction of each story is performed in eight days. Total completion time for the building including site and foundation is 24 months (14 months for underground and 10 months for the superstructure).

Building construction is performed in an enclosed environment protecting the building from the weather. Once the building is complete the "top hat" and jacking/lift system is removed and the roof lowered to the top story to complete the building.

While costly for using the new installation techniques, development of the procedures and first time acquisition of the manufacturing system including jacking/lifting systems, the technologies has application in construction areas where laydown and queuing of materials isn't possible.

This construction site was clean and orderly. The new procedure provides:

- an all weather enclosed work environment,
- automatic and controlled transportation and erection of steel members, prefabricated curtain wall, and some interior wall and piping units,
- automatic welding of column joints and other connections,
- building a complete floor system from the first story up,
- prefabrication techniques that provide and assure precision mating and connection surfaces,
- computer integrated and automatic total construction system with control of construction and recording of as-built connections,
- comprehensive system of worker and material protection that minimizes construction workforce,
- eliminates much of the use of typical construction waste and waste handling demands,
- enhanced safety from fixed safety systems,
- prefabrication enhances repair and replacement of unit systems.

Safety considerations include:

- workers are protected from weather and can work in an indoor-like atmosphere,
- minimal handling of materials is expected to reduce injury,
- safety systems for preventing falls and working areas remain in place from start to finish, e.g., scaffolding, netting, walk ways, ladders, lighting,
- work areas are easy to monitor,
- work areas are less cluttered.

8. Bridgestone Toranomon Building. The Bridgestone Toranomon eight story office building in Tokyo was constructed by Shimizu Corporation in 1988. The building is a steel and reinforced concrete, eight story structure incorporating base isolation devices of

laminated rubber bearings, steel dampers, and viscous oil dampers. Seismic design and response analysis used input motions of the 1940 El Centro Earthquake (N-S), the 1952 Taft Earthquake (E-W), the 1968 Hachinoke Earthquake (N-S), and the 1964 Tokyo 101 Earthquake (N-S).

Eight accelerators are installed in the structure; one at the base, three in the basement (x,y,z; y,z; x,z); one at the 5th floor (x,y); and three at the roof (x,y; x; y). They were activated by the February 2, 1992 Tokyo Bay M5.7 Earthquake (JMA Intensity of V); and the May 21, 1993 Ibaraki M4.2 Earthquake. Ground motion for the Tokyo Bay Earthquake was 0.27 m/s^2(x), 0.30 m/s^2(y), and 0.22 m/s^2(z). For the Ibaraki Earthquake the readings were 0.11 m/s^2(x), 0.10 m/s^2(y), and 0.07 m/s^2(z). Although the Ibaraki 1993 Earthquake was a moderate earthquake, horizontal acceleration below 1st floor was 1.7 times ground motion.

The 24 x 21 m building is supported by 12 laminated rubber bearings, 25 steel dampers, and 8 oil dampers. The steel dampers provide resistance to moderate winds and provide assurance that the rubber bearings function as backup.

The building is on reinforced concrete piles 20 meters in length. This moment resistant frame was designed for an earthquake shear coefficient of 0.150 at the base and 0.298 at the top of the building with a maximum displacement of 23 cm at an earthquake load of 0.15 to 0.20 percent gravity.

While the Japanese building code does not give credit for incorporating seismic base isolation systems, the design-builder, Shimizu Corporation felt the system would provide higher performance with less damage to structure and content and it will better insulate the occupants. The cost of this added quality and performance is estimated at about 10 percent over conventional design.

This is one of about 70 buildings in Japan that are designed and constructed with some form of seismic isolation or reduction systems. The Building Research Institute, MOC approves all base isolated building designs.

9. Minato-Mirai 21 Construction Site. The name 'Minato-Mirai' means 'future port area'. This site is a planned commercial and residential community along the water front in central Yokohama. The site is being developed by the Housing and Urban Development Corporation (HUDC) of MOC. HUDC's role is to develop 110 ha of existing land and reclaim an adjourning 76 ha from the bay into a master plan that accommodates needs of buyers of commercial and residential properties. Developed land is sold to private corporations to construct facilities. Land preparation started in 1983; completion is expected by the year 2000. HUDC hopes this project, and others, will begin to decentralize some of Tokyo's businesses.

The site is expected to accommodate 190,000 working population and 10,000 residences. While care was given to stabilizing the earth to resist earthquakes better; even greater attention was given to soil stabilization against liquefaction in the port facility area. History has shown that port areas often sustain greater damage from earthquakes.

As part of this redevelopment effort, HUDC will design:

- transportation networks for highways and ramps, rail and subway lines, and pedestrian spaces;
- urban facilities for service tunnels (3.7 km, the longest in Japan), refuse and sewer systems, district heating and cooling systems;
- infrastructure waterfront land reclamation, port facilities, and parks.

Several buildings have been constructed on this redeveloped site including the 296 m tall Landmark Tower (tallest building in Japan). Several buildings are under construction including the 34 floor Mitsubishi Heavy Industries Building (site visit report follows). Much attention has been given to providing a sense of scale, generous distances are between buildings, a variety of textures complement the buildings visual appearances, and integrated pedestrian walkways facilitate flow of pedestrians throughout the new spaces.

The cost of this redevelopment project is about $18 billion (2,000 B yen). Funding was provided by the National Government through the MOC and Yokohama City. Yokohama is expected to increase its revenues through increases in taxes.

10. Mitsubishi Heavy Industries "T-UP" Building. The Taisei Corporation is designing and constructing this 34-story building for the Mitsubishi Heavy Industries. This totally mechanized construction system for high-rise building is 52 m high, basement is 18 m, and the footprint is 6,200 m^2. This project is a joint venture with 14 building construction companies.

The construction concept is based on the jack climbing guide column concept. The jack system raises a 2000 ton "hat", which includes the building's roof and the cranes. Floors are fabricated under the "hat" and jacked using a hydraulic jack with clamp pins on eight guide columns. Five stories are raised before jacks are demounted and reattached under the hat to repeat the process. Overhead cranes in the lower portion of the hat are used to assemble the floor and exterior wall panels; the jib cranes build the core that jacks the completed floor assembly. A laser measurement system scans the position of the structural steel and plumbs the steel columns. An information system is used to control the operation system. The system has not been expanded to an 'integrated information system' which stores erection/placement information for use later during the maintenance of the building. Each floor is completed in three-days; floor finishing including some curtain wall erection requires additional time. Twenty thousand tons of steel will be used in the structure.

Building design analysis was based on earthquake loading not on wind loads. The building is designed with tuned mass dampers. It is not instrumented with accelerometers since data may be acquired from neighboring buildings.

Taisaei Corporation expects to save over 30 percent of normal construction costs using this method, after it is perfected. Expectations are to save six months of time from a normal 24-month project. Construction costs for this project are estimated at $550 million (60 B yen).

11. Underground Utility System Tunnel. This 7.6 m diameter utility system tunnel will house electricity, telephone, water, sewage, and gas lines. The tunnel will be 2.5 km in length. It is one of several links planned to have utilities underground. Tunnel diameter is determined based on the needs of the utilities required by the neighborhood being served. Branches stemming from the tunnel will service that particular neighborhood area.

The tunnel excavation method was determined based on soil conditions. The strata changes from a hard rocky bed with N value over 50 to soft alluvial soil with N value of about 2. A pressurized slurry shield tunneling method was selected to excavate the tunnel. It is computer operated; lasers make measurements for each cut. Soil is excavated by rotary blades and high pressure water. Soil and water are pumped to the surface. The soil is used as fill for reclaimed land elsewhere.

After cutting the tunnel, a 30 cm thick liner 7.6 m in diameter is installed, followed by a 20 cm thick concrete liner separating the space into four zones for the services identified above. Five persons install the liners. Four meters are excavated and lined per two-8 hour shifts.

This service tunnel runs parallel to a river and will be under a National Highway. The construction site is surrounded by noise absorbing panels. The concern for noise reduction is important in these highly dense neighborhoods in most Japanese cities.

The project is financed by the Yokohama Work Office and the Kanto Regional Construction Bureau (MOC). Its costs are projected at $64 million (7 B yen) per kilometer. Project costs are shared by the National Government who provide 30 percent of the costs, while 70 percent is provided by the municipality.

The MOC encourages such projects to stimulate use of underground spaces for utilities. Here, the utilities have greater protection from earthquakes and the unsightly appearance of hanging telephone and electric lines are eliminated.

12. Tsurumi Fairway Bridge. This bridge is one of many bridges and tunnels under construction that will create the 185 km Tokyo Bay Ring Road. As part of the Ring Road there is a 50 km section called the Bay Shore Route. This Route runs from the top of Tokyo Bay south towards Yokohama. The site addressed here is known as Section 4 of the Bay Shore Route, a 12 km stretch of highway between the double deck cable stayed Yokohama Bay Bridge and Haneda Airport. The U.S. Panel members visited the Yokohama Bay Bridge at the occasion of the 21st Panel meeting, May 1989.

About 2 km north of the Yokohama Bay Bridge is the site of the Tsurumi Fairway Bridge. It is a single plane center cable-stayed bridge with inverted Y-shaped towers. Its main span is 510 m and total length of 1,020 m and 50 m above mean water level. The bridge will be the largest center cable stayed bridge in the world. A second and identical bridge to the Tsurumi Bridge will be constructed in the near future to help relieve traffic in this highly congested area.

The Tsurumi Bridge design complements the design of the Yokohama Bay Bridge. It is a

steel frame reinforced concrete structure using octagonal steel cross sections. The bridge was designed to withstand an earthquake of the magnitude of the 1923 Kanto Earthquake (M7.9). The end piers and foundations, all underwater, are approximately 12 m in depth. Steel sheathed pneumatic caissons are used. They are embedded 28 to 44 m below the water surface. The tower foundations which will be subjected to large forces are built with caissons of large plane dimensions -- 40 m by 40 m. They are embedded below the design bearing surface by 1/2 of their width. The lower parts of the towers are steel-frame reinforced concrete. The top of this section, supporting the girder and tower column, is concrete and steel multi-cell.

The lower part of this section is reinforced concrete. The basis design concept is for the compressive force of the steel multi-cell to be completely transferred to the concrete by the bearing plate attached to the steel cell-plate, and for tensile force to be borne by the steel frame. Adhesion between the steel-plate and the concrete was realized by installing steel dowels.

The girder section is composed of a flat single box of 5 cell sections. Fairings are installed on both outside edges every 3 m for wind-resistant stability. The cables are prefabricated zinc-plated steel wire strands, 7-mm in diameter. Fifteen of the 34 cables attached to the main tower will be composed of 499 wires. The upper cables will be smaller in diameter and tension adjustments will be performed to disperse concentrated dead load tension to the lower levels. Vane-type damper mechanisms are used to prevent cable slack and to help dampen longitudinal oscillation of the girder. Two pendulum supports and wind shoe are placed at the ends of the girder. The girder was installed using a 3500 ton floating cranes using two temporary vents set 80 m apart.

The steel frames for the lower parts of the towers were assembled into a single unit on land and transported to site by a 700 ton floating crane. They were installed in the top slab of the caisson. The top section was installed in a similar manner.

This project is under the supervision of the Metropolitan Expressway Public Corporation. Its costs are $700 million (77 B yen).

13. New Haneda Airport Construction. Haneda Airport serves 40 million persons annually -- 40 percent of all Japan's air traffic. To meet future needs, the airport has expanded onto land reclaimed from the Tokyo Bay. The airport is located about 10 km north of the Tsurumi Fairway Bridge.

The expanded airport is on 650 ha of reclaimed soil originally having the consistency of mayonnaise. Cementitious materials first were dumped over the existing soil then agitated. This operation was followed by dumping soil from a variety of construction sites and compacting it. Sand piles, mats, and paper drains were installed to drain the land. Sand piles and prepacked sand piles (in netting) are spaced every 2-3 m and drilled to 30-40 m depth. Paper drains are spaced every meter and drilled to 30-40 m depth. Seventeen sand piles are installed daily per pile driver. Over 70 percent of Japan's pile drivers are on this site. In addition, a dry jet mixing method is used to stabilize the soil. Cement is poured

into the ground using compressed air to mix the it with the soil. The cost of draining these 650 ha is about $9 million (1.3 B yen) per ha.

The new terminal building "West Building" is a joint venture of Taisaei, Kajimia, Shimizu, Bechtel Corporation, and six other constructors. Construction started in August 1990 and is expected to be completed in September 1993. The overall airport area is 8 million m^3. The terminal is constructed using precast concrete mats on 3,000-800 mm diameter pile foundations driven to 81 m depths. The below ground structure is reinforced concrete. The above ground structure is a composite steel frame and reinforced concrete and steel. It is 840 m long, has five stories, and floor space of 290,000 m^2.

The potable water supply consists of 4-380 m^3 wooden tanks. The added expense of wood was justified because wood enhances the flavor of water.

The Tokyo-Haneda Monorail has been lengthened by 6.4 km to service the West Terminal and later will be extended to serve a second new terminal "East Terminal Building" soon to be under construction contract.

The Bay Shore Drive and National Highway and airport access roads are in an open tunnel running parallel to the new terminal building. Seven bridges ranging from 100 m to 298 m in length cross the 12 lane highway and access roads. The two center bridges, 103.4 m long, are suspended from an archway consisting of seven segmented cable stayed sections. The arch, painted red, was designed to make a statement for the new terminal building. The length of the arch is 160 m by 44.5 m high.

At both ends of the terminal, the roads enter prefabricated tunnels that are under construction. Tunnels were selected because bridges would have hindered ship passage and bridge towers pose a threat to aircraft.

The financial management and supervision of the airport is under the Ministries of Construction and Transport.

14. Trans-Tokyo Bay Highway. This highway is a 15 km tunnel-bridge complex. The highway traverses the central part of Tokyo Bay connecting Tokyo with Chiba. The project consists of two 5-km long tunnels starting at the Tokyo side (Kawasaki City) then rising through a man-made island serving as a transition to a 5-km long bridge to Kisarazu City, Chiba Prefecture. Two-2 lane highways will be excavated with space for a future third lane. This work is under the supervision of the Trans-Tokyo Bay Highway Corporation (TTBHC) and the Japan Highway Public Corporation (JPHC) of the MOC. Construction for the highway commenced in 1989; it is expected to be completed in 1996.

The delegation visited the two man-made islands and the bridge by boat. The first island, the Kawasaki man-made island, is 4.6 km from the Tokyo shore line. It is in 28 m of water. Since the sea bed is extremely soft to a depth of 30 m, the soil had to be stabilized by sand compaction. The construction of the island consists of a 98 m diameter diaphragm wall extending 117 m to the sea bottom. Its thickness in 2.8 m. This structure will ultimately

serve as the ventilation tower. The ventilation tower's base dimensions are: wall thickness, 4 m; height, 75 m; and bottom slab thickness, 6 m. Its first purpose is to serve as two of the four locations to begin excavating the highway tunnels (both sides of this tower base, at the Tokyo shore line, and at the second man-made island).

A 50 m steel trestle structure protects the main island's ventilation tower. It was towed to site by a crane-barge as 14 sections, sunk, and secured to steel piles. The steel jacket accommodates the working crew's quarters (daily), is a base for the construction equipment, work quarters, and serves as a shield against a wayward ship. After excavating the tunnels, the ventilation tower will be divided into seven floors on the inside to accommodate tunnel ventilation equipment, tunnel cross overs, and fire fighting equipment.

The second island, the Kisarazu Tunnel-bridge Interface Island, is oblong in shape. It will be 650 m in length and 100 m wide. A 750 m ramp will rise from the sea bottom. The soil at this site were replaced with sand and gravel. A retaining wall of 48 sheet steel piles 37 m high were towed, filled with sand, and sunk to form the edges of the island. Fill work will be similar to that performed at the Kawasaki man-made island. Steel moles are constructed on either side of the descending ramps. It will be filled with improved soil to make the tunneling work easier. Armored riprap, rubble stones, and wave dissipating concrete blocks will protect the embankment.

Tunneling will be done using a pressurized slurry shield tunneling machine. It will excavate 100-150 m per month. The tunnel diameter will be 14.1 m. The tunnels are designed to be 28 m apart and 60 m below the water surface. It will be the longest tunnel for vehicle traffic in the world.

The bridge exiting the Kisarazu man-made island will be 4.4 km in length. The bridge's superstructure sits on 42 Y-shaped piers, 12 are in deep water. The height of the bridge at this point is 29 m above mean water height. These piers were assembled at fabrication yards and transported to the work site where a floating crane set them into place. The footings were anchored to steel piles. The 12 deep water piers are made of steel. They contain a 5 m strip of titanium-cladded steel in the splash zone. Its base is reinforced concrete set on steel pipe piles. Cathodic protection is installed in the reinforced concrete. Dolphins will be constructed on both sides of six of the 12 piers in the shipping lanes. The remaining 30 piers are reinforced concrete with steel-pipe sheet pile foundations.

The 4.4 km bridge-girder is separated into 5 sections. The longest is 1630 m which spans 10 piers. The girder is 29.9 m wide. Rubber bearings with high damping are used for 11 spans; rubber bearings for 10 spans, and roller bearings for the remaining 21 spans.

Much attention was given to designing the highway against earthquakes. The elbows at each of the horizontal ends of the tunnels are potential weak points. They were given special attention by the designers.

The construction costs of the highway is $10.5 billion (1,150 B yen) split 81 percent paid by the TTBHC and 19 percent by the JHPC. Of the 81 percent from TTBHC: 6.3 percent is

from capital; 41.4 percent from government guaranteed bonds; 25.6 percent from private loans and loans by the Japan Development Bank; and 26.6 percent by official loans.

The expected traffic flow per day is estimated at 33,000 vehicles with a growth to 64,000 vehicles after 20 years. Tolls cost $45.50 (5000 yen) one way. Will the TTBHC experience a lower than predicted vehicle rate as recorded at the Seto Ohashi Route? Are toll rates too high?